SPONSORED BY:

American Institute of Aeronautics and Astronautics
in Cooperation with:
Institute of Electronics & Communications Engineers of Japan
Deutsche Gesellschaft für Luft-und Raumfahrt E.V. of Germany
Association Aeronautique et Astronautique de France

A COLLECTION OF TECHNICAL PAPERS

AIAA 8th COMMUNICATIONS SATELLITE SYSTEMS CONFERENCE

April 20-24, 1980/Orlando, Florida

For permission to copy or republish, contact the American Institute of Aeronautics and Astronautics-1290 Avenue of the Americas, New York, N.Y. 10019

SPONSORED BY:
American Institute of Aeronautics and Astronautics
in Cooperation with:
Institute of Electronics & Communications Engineers of Japan
Deutsche Gesellschaft für Luft-und Raumfahrt E.V. of Germany
Association Aeronautique et Astronautique de France

A COLLECTION OF TECHNICAL PAPERS

AIAA 8th COMMUNICATIONS SATELLITE SYSTEMS CONFERENCE

April 20-24, 1980/Orlando, Florida

For permission to copy or republish, contact the American Institute of Aeronautics and Astronautics·1290 Avenue of the Americas, New York, N.Y. 10019

Digitized by the Internet Archive
in 2024 with funding from
Amateur Radio Digital Communications, Grant 151

https://archive.org/details/aiaa8thcommunica00unse

CONFERENCE COMMITTEE

General Chairman
WALTER L. MORGAN
Comsat Labs

Vice Chairman
A. JACK SCHIEWE

Secretary
JERRY WAYLAN
Naval Electronic Systems

Technical Program Committee

East
THOMAS SEAY
MIT Lincoln Labs

West
GEORGE J. GLEGHORN
TRW Defense & Space Systems Group

Europe
RENE C. COLLETTE
ESA/ESTEC (The Netherlands)

and

DIETRICH E. KOELLE
MBB (Germany)

Japan
TADAHIRO SEKIMOTO
Nippon Electric Co., Ltd.

Financial Chairman
DENIS CURTIN
COMSAT Labs

Local Arrangements
ROBERT A. SYLVIA
Martin Marietta - Orlando

Publicity
O. GENE GABBARD and LINDA COONEY
Digital Communications Corp.

Members-at-Large

URIEL DOMB
Tele-Space Information Ltd. (Canada)

ALBERT R. GIDDIS
Ford Aerospace and CommunicationsGroup

DAVID M. NEWLANDS
Hughes Aircraft Co.

DELBERT D. SMITH
Satellite Communications

TABLE OF CONTENTS

PAPER NO. PAGE NO.

80-0471 Present and Future Aspects of Japanese "CS" Program - K-i TSUKAMOTO, H. FUKETA, Y. ICHIKAWA 1

0472 A Satellite Communications System for Electric Utilities - A. VAISNYS and L. BERGEN 10

0473 Salient Design Features of INSAT-1 Space Segment System - M. K. SAHA 18

0474 Anik C Space Segment for Telsat Canada - W. ZATYCHEC 32

0477 The KDD Yamaguchi Shore Station for the MARISAT System - K. KOMURO, S. ENDO, M. YOKOYAMA, Y. KATASE, K. TSUNODA, T. TERASHIMA 41

0478 Innovative Services in Use Over the MARISAT Satellites - S. ENGELMAN, J. F. PARKER, J. L. BEAUCHAMP 51

0479 Direct Mechanical Stabilization of Mobile Microwave Antennas - R. J. MATTHEWS 58

0481 Numbering Principles for Automatic Maritime Mobile Services and Maritime Mobile Satellite Services - R. J. MANTERFIELD 65

0483 Microwave Components and Technology Developments in the European Space Agency - D. R. MADDEN, M. H. GIBSON, P. H. MONIER 72

0484 Linearizing T. W. T. Amplifiers in Satellite Transponders - System Aspects and Practical Implementation - C. BREMENSON, M. PALAZO, R. NEYER 80

0485 A New Generation of Satellite Traveling-Wave Tubes for TV Broadcasting and telecommunications - J. COLLOMB, P. GOSSET, H. RAYE 90

0486 Past and Present Intelsat TWTA Life Performance - R. STRAUSS, J. R. OWENS 98

0487 EHF Solid State Transmitters for Satellite Communications - J. E. RAUE 107

0488 High Power Satellite Travelling Wave Tubes with 200 W and 450 W Output Power - D. DEML 112

0489 Demand Assigned TDMA System for Digitally Integrated Service Network - K. KOHIYAMA, Y. WATANABE, S. SAMEJIMA, S. KATO 117

0491 Digital Earth Stations for Satellite Networks - J. H. TILLEY, D. M. FRALEY, J. J. HANGEN, P. J. FREEDENBERG, S. B. SALAMOFF 125

0492 Scanning Spot Beam Satellite for Domestic Service - Y. S. YEH 134

0493 The NATO Digital Satellite Communications System - M. CELEBILER, J. MUNNS, E. TURNER 140

0494 An Advanced Mixed User Domestic Satellite System Architecture - H. G. RAYMOND and W. M. HOLMES, JR. 148

0498 Public Service Satellite Application After WARC-79 - P. McMANAMON 154

0499 Satellite Broadcasting After WARC-79 - R. R. BOWEN 156

0501 Flight Performance of the LES-8/9 Three-Axis Attitude Control System - F. W. FLOYD, C. H. MUCH, N. P. SMITH, J. R. VERNAU, J. P. WOODS 159

0503 The Thermal Control System of the German Direct Transmitting Communication Satellite TV-SAT - H. KREEB and W. SCHWARZOTT 171

0504 Widebody Bus Extends Shuttle Economy to Synchronous Orbit - T. C. EAKINS and G. W. DURLING 178

0505 The GEO-SPAS Platform -- A Third Generation Communication Satellite Concept - D. E. KOELLE and W. KLEINAU 185

PAPER NO.		PAGE NO.
80-0506	Developing the Concept of a Geostationary Platform - W. T. CAREY, R. M. BOWMAN, G. R. STONE	192
0507	Longitude-Reuse Plan Doubles Communication Satellite Capacity of Geostationary Arc - D. v. Z. WADSWORTH	198
0508	European Multipurpose Telecommunication Satellite: Development Plans - B. L. HERDAN	205
0509	The Effects of Geography on Domestic Fixed and Broadcasting Satellite Systems in ITU Region 2 - P. H. SAWITZ	216
0510	In-Orbit Measurements of OTS Payload Performance - C. D. HUGHES and R. A. GOUGH	224
0513	Overview of Digital Satellite Communication Networks - P. KAUL	234
0515	AT&T/GSAT Domestic Satellite Operational Network - R. F. LATTER	242
0516	Network Organization and Operation of the Western Union Digital Exchange System (DES) - J. BAER, F. R. HANVEY, JR., G. PAROWSKI	246
0517	The Digital Network of American Satellite Corporation - T. D. BREEDEN and E. J. HABIB	253
0518	Network and Control for Tactical Satellite Communications System - R. W. BRICKER, JR. and J. P. LEIPHART	257
0519	19 and 28 GHZ Propagation Considerations Affecting Satellite Communications System Design - H. W. ARNOLD, D. C. COX, H. H. HOFFMAN, R. P. LECK	261
0520	Rain Attenuation Over Earth-Satellite Paths: A Seasonal, Oceanic Model - N. E. FELDMAN, H. H. BAILEY, R. E. HUSCHKE	267
0521	A New Adaptive Control System for Compensating Cross-Polarization-Couplings on the UP and/or Down Path in Frequency Reuse Satellite Communication Systems - H. MAKINO, Y. ORINO, S. ORUI, H. FUKETA, T. INOUE	280
0522	Microwave Filters and Multiplexing Networks for Communications Satellites in the 1980s - C. M. KUDSIA, K, R. AINSWORTH, M. V. O'DONOVAN	290
0523	Crossbar Switching Requirements for Future Multibeam TDMA Communications Satellites - M. HOFFMAN	302
0524	Development Status of Low Noise Amplifiers - M. KAJIKAWA, I. HAGA, S. FUKUDA, W. AKINAGA	309
0527	TDRSS Multiple Access Telecommunications Service - R. BLYTH and D. HALDEMAN	317
0528	Landsat D Telecommunications Payload: Earth Imaging Data via TDRS - H. B. POZA	328
0529	TIROS-N -- The Operational Environmental Satellite of the 80's -A. SCHNAPF	337
0530	Emergency Response Communication Satellite Systems of the 80's - L. C. McCOY	347
0531	The Earth Station for TV-Relay from the Antarctic Continent - M. TAKAHASHI, S. MIZUARAI, E. MIYATA, K. TSUNODA	353
0532	Design and Performance of 30/20 GHZ Band Earth Stations for Domestic Satellite Communication System - H. FUKETA, M. KURAMOTO, T. INOUE, H. KATO	361
0536	Highly Mobile Ground Station for the OTS Experimental Program - H. FROHLICH and G. BOMMAS	370
0537	Packet Communications in Satellites with Multiple-Beam Antennas and Signal Processing - R. DAVIES, F. CHETHIK, M. PENICK	378

AIAA NO. PAGE NO.

80-0538 A Two-Level Multiple Access Scheme for a Packet Satellite System of Many Terminals - S. L. KOTA and B. E. WHITE ---------------------------------- 386

0540 Digital Phase Modulation Methods Giving a Band-Limited Spectrum for Satellite Communications - D. MUILWIJK and J. NOORDANUS ------------------ 391

0541 A New Approach to the Encoding of Multiple Data Sets - M. HANKAMER ------- 399

0542 Multi-Spectral Data Compression Using Hybrid Cluster Coding - J. R. MacCALLA and M. U. CHANG -- 404

0543 Is There a Space Platform in Intelsat's Future? Facing the Institutional Challenges of the 1980's and 1990's - J. N. PELTON ----------------------- 408

0544 A Projection of the Development of High Capacity Communications Satellites in the 1980's - R. J. RUSCH and C. L. CUCCIA ----------------- 412

0546 The Present Status and Future Development of The INTELSAT Leased System - T. M. KELLEY -- 419

0547 Evolution of Fixed Service Communication Satellite Systems in the 1980's - G. BERRETTA -- 425

0548 Satellite Communication Technology Challenges for the '80's - D. K. SACHDEV 433

0549 Operational Experience with ANIK A - P. N. WADHAM ----------------------- 445

0551 Facsimile Transmission Utilizing TDMA Satellite Service - W. L. DUNN and G. C. JENKINS -- 450

0552 Users - The Second Phase - R. E. BUTTON --------------------------------- 453

0553 A Medium Rate Integrated TDM/TDMA Satellite System - S. N. VERMA and S. SALAMOFF -- 457

0554 Improving Future Communications Satellite Antenna Designs - W. J. ENGLISH 464

0555 System Trade Off on 20-30 GHZ Multispot Beam Antenna Requirements for a Domestic Communication Satellite - G. MANONI and G. PERROTTA ----------- 471

0556 L-Band Phased Array Transmitter for Communication Satellites - R. COIRAULT --- 484

0557 K_a-Band Multibeam, Contiguous Coverage Satellite Antenna for the USA - P. FOLDES --- 490

0559 Antennas Aboard the INSAT-1 Communication Satellite - T. M. SMITH, D. F. FORD, R. W. LeMASSENA, R. D. BRUNO ------------------------------ 500

0561 EHF Systems for Mobile Users - D. R. McELROY and R. E. EAVES ----------- 509

0562 Fleet Satellite Communications (FLTSATCOM) Program - P. S. Melancon and R. D. SMITH -- 516

0563 Navy Military Satellite Considerations - R. E. CONLEY and C. J. WAYLAN -- 523

0566 Satellite Distributed Broadcast Services at Western Union - J. T. RAGAN-- 529

0567 The Intelpost System - H. RAAG --- 534

0568 Digital Facsimile Communication Over Satellite Links - N. HATTORI ------- 538

0569 Experiment Results of Japanese BSE Program in the First Year - N. IMAI, S. SONODA, Y. ICHIKAWA -- 546

PAPER NO. PAGE NO.

80-0570 System Design and Technology of the German Direct TV Broadcasting Satellite - H. KELLERMEIER and D. E. KOELLE ---------------------------- 557

0571 French Satellite Broadcasting System - J. F. ARNAUD, C. DERIEUX, A. POUZET -- 568

0573 Performance of the Telesat Real-Time State Estimator - F. C. KES, R. G. LAGOWSKI, A. J. GRISE --- 577

0574 Three-Axis Attitude Control Acquisition Results and Regular Operational Status of BSE - S. SHIMOSEKO, K. ARAI, H. MATSUMOTO -------------------- 584

0575 Multiple Satellite Operations and Management - R. W. WEBER ------------- 592

0577 Operational Experience on OTS-2 - A. S. FAGG and J. B. MacLAUCHLAN------ 599

0578 Hermes Satellite (CTS): Performance and Operations Summary - H. R. RAINE and J. S. MATSUSHITA -------------------------------------- 606

0580 30/20 GHz Fixed Communications Systems Service Demand Assessment - M. WESTHEIMER, R. B. GAMBLE, K. M. SPETER, H. R. SELTZER --------------- 615

0583 Multigigabit Satellite On-Board Signal Processing - W. M. HOLMES, JR. -- 623

0584 Direct Access Satellite Communications Using SS-FDMA - J. D. KIESLING -- 627

0585 20/30 GHZ Satellite Business System in Germany - D. OTTO, W. KRIEGL, H. M. BRAUN -- 634

0586 An Experimental 20/30 GHz Communications Satellite Conceptual Design Employing Multiple-Beam Paraboloid Reflector Antennas - A. M. GOLDMAN,JR. 640

0588 Ariane Performances and Cost for Communication Satellite Launches - B. STOCKWELL -- 651

0589 IUS - A Key Transportation Element for Communication Satellites - D. R. HANFORD -- 655

0592 Ascent Propulsion Study for INTELSAT VI - M. H. KAPLAN and W. W. DORSEY 665

0593 Forward Error Correction for Satellite TDMA in the INTELSAT V Era - J. S. SNYDER and T. MURATANI --------------------------------------- 674

0594 A High Performance Processor Controlled BPSK/QPSK Modem for Data Rates Up to 4 MBPS - W. PAIK, L. A. WEAVER, I. GURANTZ, I. PEER ------------ 684

0595 Prefiltered QPSK - A Bandwidth Efficient Modulation - M. U. CHANG and M. C. AUSTIN --- 690

0596 Digital Chirp Modulation: Opportunities for Lower Cost and Higher Performance in Mobile-Satellite Communication - P. K. LEE, J. M. RUDDY, B. E. WHITE -- 696

0597 Application of Satellite Demand Assignment in Telephone Networks - J. M. FRASER --- 703

LATE PAPERS

0480 High-Speed Satellite Data Transmission of Maritime Seismic Data - T. O. CALVIT and L. B. HEITMAN -------------------------------------- 714

continues........

LATE PAPERS

PAPER NO.		PAGE NO.
80-0525	RCA Satcom System Expansion - W. BRAUN and J. E. KEIGLER ---------------	723
0535	Experiments in Satellite Communications With Small Earth Terminals - J. KAISER --	730
0560	Space Laser Communications Systems for the Eighties - M. ROSS, J. D. WOLF, R. M. F. LINFORD, J. L. ABERNATHY ----------------------------------	739
0558	Shaped-Beam, Frequency-Reuse Feed Arrays for Offset-Fed Reflectors - E. C. NYGREN --	746
0526	The Impact of Satellite Technology on Rural Telephone System Planning - B. B. LUSIGNAN, M. M. MOUSA, M. K. SAMARKANDY, C. C. HAN ---------------	755
0495	International and Mobile Satellite Systems After WARC-79 - D. J. WITHERS	759
0514	Trends in Military Satellite Communication Networks - I. M. JACOBS, E.V. HOVERSTEN, C. R. MOORE --	762
0539	Cryptographic Techniques for Satellite Networks - LEE ------------------	766
0591	An Italian Upper Stage to Inject Low toMedium Weight Satellites in Orbit - G. BARRESI and C. CARNEBIANCA -----------------------------------	772
0496	Satellite Systems for Industrialized Nations - After WARC '79 - P. G. ACKERMAN --	776
0502	The INTELSAT V Nickel-Hydrogen Battery System - G. VAN OMMERING, C. W. KOEHLER, D. C. BRIGGS ---	781

80-0471

PRESENT AND FUTURE ASPECTS ON JAPANESE " CS " PROGRAM

Ken-ichi TSUKAMOTO
Radio Research Laboratories, MOPT
Koganei-shi, Tokyo 184, Japan
Hiroaki FUKETA
Yokosuka Electrical Communication Laboratory, NTT
Yokosuka-shi, Kanagawa 238-03, Japan
Yoh ICHIKAWA
National Space Development Agency of Japan
Hamamatsu-cho, Minato-ku, Tokyo 105, Japan

Abstract

The Japan's CS spacecraft was launched successfully in December 1977 and placed at 135 degrees east longitude on a geostationary orbit. After initial on-orbit performance checkup, substantial communication and operation experiments have been conducted as scheduled starting in May 1978.

Spacecraft attitude and position are being kept precisely, and on-board mission equipments including the despun antenna and C-band(6 GHz/4 GHz) and K-band(30 GHz/20 GHz) transponders are working well except two K-band transponders which had been excluded from the articles of experiments due to malfunctions occured during the checkup period. Confidence was obtained, after one year experiments, that the present CS-like system would be suitable for future operational domestic satellite system in Japan. The paper will present typical experiment results obtained in the first one year.

I. Introduction

CS is the first experimental communication satellite in Japan planned by Ministry of Posts and Telecommunications(1). The spacecraft was developed by National Space Development Agency of Japan(NASDA) and launched successfully from ETR of USA on December 14, 1977. Nine days after the lift-off, the spacecraft was placed at 135 degrees east longitude on a geostationary orbit. The performances of the spacecraft were checked using NASDA's and RRL's ground facilities, and making assurence that all functions of the spacecraft are normal except the two K-band transponders, the spacecraft was offered to be used in communication experiments which are being conducted by Radio Research Laboratories(RRL) in cooperation with Nippon Telegraph and Telephone Public Corporation(NTT).

The CS is a spin-stabilized spacecraft weighing about 340 kg on orbit, and has two C-band(6 GHz/4 GHz) and six K-band(30 GHz/ 20 GHz) transponders, named G_1, G_2 and F_1 through F_6 as shown in Figure 1, and a shapwd beam mechanical despun antenna commonly used in the both frequency bands. TT&C operations are carried out either in S-band(2.1 GHz/ 2.3 GHz) or C-band. NASDA provides S-band TT&C ground facilities, and RRL and NTT provide various kinds of ground facilities for C- and K-band communication experiments and C-band TT&C operation.

In Japan, C-band satellite communications are severely restricted becaure of potential interference problems against heavily distributed terrestrial networks and it is quite important to solve the frequency sharing problems between space and terrestrial communications in this frequency band. Therefore, K-band was positively adopted in the CS system notwithstanding difficulties such as rainfall attenuation, necessity of hardware development and so forht in this new frequency region. Throughout the first one year of experimental period, valuable technical and operational data have been acquired.

II. Launch and Initial Check of CS Performance

Launch

The CS was launched by use of No.137 Delta 2914 vehicle from Kennedy Space Center, NASA, at 7:47 pm on Dec. 14, 1977, and the spacecraft was accurately injected into the transfer orbit. After injection into the transfer orbit, Tsukuba Space Center conducted determination of the spacecraft attitude, orbit and functions using the telemetry and ranging data which were gathered by the ground stations of NASDA and NASA.

Maneuvers for the spacecraft attitude change were carried out three times before the apogee motor firing which was taken place at near 133.8 degrees east longitude over the equator near the 3rd apogee at Dec. 16, 12:25(JST). Then, the CS was injected into the drift orbit of which orbital parameters were very close to the planned values. On the drift orbit, the satellite attitude was changed twice for setting the spin axis normal to the orbital plane and the despun antenna towards the south.

Finally, the CS was placed at the geosyncronous orbit position of 135 degrees east longitude on Dec. 24. It was about 9 days after the lift-off.

Initial checkup

The initial operation and checkup of the CS system were carried out by NASDA with support of RRL. The results of the bus equipments checkup were satisfactory in all functions and performances. At the first checkup, all communication subsystem, which consists of six K-band, two C-band transponders, K-band beacon oscillator and despun antenna, functioned normally and satisfied all the requirments.

Two months after the launch, spurious signals were found in the down link signal of one of the K-band transponders(F2). The cause of this failure was investigated by means of simulation test, which was conducted on the ground. A presumable cause of the failure was due to a change of charac-ter-istics of a resistance which was used in the frequency multiplier of the receiver local oscillator.

Another failure occurred after three months from the launch in another K-band transponder(F6) of which transmitting power suddenly vanished. From the telemetry data, it was found that the protection

Copyright © American Institute of Aeronautics and Astronautics, Inc., 1980. All rights reserved.

circuits in the TWT power supply tripped due to some trouble in the high voltage circuit.

III. Characteristics of the Antenna and Transponders

The bandwidth of each communication transponder is about 200 MHz, and the nominal output powers are 4 dBW in K-band and 4.5 dBW in C-band respectively. The AGC function of the first K-band transponder(F1) can be deactivated by command, and the C-band transponder(G2) has command-controlled step attenuators which range from 0 dB to 10.5 dB with 1.5 dB step. Owing to the troubles in two K-band transponders(F2 and F6), only four K-bnad transponders have been used in various experiments.

The CS communication antenna was designed so as to cover Japan mainlands with 33 dB gain in K-band and whole Japan territory with 25 dB gain in C-band.

Antenna pattern for the communication

The communication antenna system consists of a shaped beam horn-reflector and waveguide assemblies to transmit and receive signals of circular polarization in both C- and K-bands.

The azimuth pattern only was measured by means of the despun antenna bias off-setting in order to save the fuel consumption.

Figure 2 shows the K-band downpath antenna pattern data measured at several places in the mainland of Japan, and Figure 3 shows the C-band down path antenna pattern data at Kashima in the mainland and remote Miyako-jima island.

The measured values are a little lower than the calculated ones based on the antenna Acceptance Test(AT) data obtained at ground before the launching. These results may depend on the beacon output level degradation. In K-band, there is a spin modulation from 2 to 4 dB depth at the antenna bias of 0 degree, and all measured data show the average gain.

Characteristics of the transponders

Figure 4 shows the input-output characteristics of the K-band transponder(F1). The values of input power to the transponder was given from telemetry data and the output power was calculated using link-budget data. Figure 5 shows the frequency amplitude and delay responses. The data shown in Figures 4 and 5 are close to those of the prelaunch data, and there are no secular degradations.

Assuming that the transponder nonlinearity is expressed as AM/PM conversion and suppression factors of input-output characteristics, these parameters are obtained by the unbalance two tones method. Table 1 shows these values. They are nearly equal to those of the pre-launch data.

Figure 6 shows the input-output characteristics of the C-band transponder(G2) when the ground transmitter power changes. The input power of the the transponder ranges from -94 dBW to -104 dBW to get the saturated output power of 4.8 dBW. They are the same ones as the pre-launch data. Also, it is indicated that the seven steps attenuators are operating normally.

The amplitude and delay variations were measured as within 0.8 dB/±50 MHz and within 3ns/±50 MHz respectively at saturation region. When the ground transmitter output level decreases(to +10 dBW) for the transponder to be operated at linear region, the linear first order frequency response becomes within 1 dB/±50 MHz though the delay-characteristics is the same as saturated operation case. In either case, they meet to the specification values.

IV. General Signals Transmission Characteristics

Telephone and TV signals transmission in FM(2)(4)

The FM modem of RRL has wide-band characteristics suitable for modulating FDM telephony signals(24 to 1872 channels) or a composite color TV signal. Experiments have been conducted in both C- and K-band links, changing transmission parameters such as frequency deviation, channel frequency, emphasis on/off, receiver BPF bandwidth and C/N_0(carrier to noise power density ratio). Especially, effects of spin modulation and rainfall attenuation in K-band links have been investigated.

Figure 7 shows the results of K-band noise loading test of 1872 channels with emphasis. Though the optimum loading level is about 6 dB above the nominal loading level(419 KHz rms/channel), 1872 channels of FDM telephony signals can be transmitted over the K-band links with signal quality better than 50 dB of S/(N+D), (signal/thermal and intermodulation noise), at Kashima station. On a clear day, total link C/N_0 better than 100 dB-Hz can be kept for an EIRP of 86 dBW from the ground, and rain attenuation margins for uplink and downlink are measured as 11 dB and 7 dB respectively when the lower limit of S/(N+D) is assumed to be 43 dB. Comparing with the modem back-to-back test, degradation of S/(N+D) within 0.5 to 2.5 dB is measured in the satellite links due to nonlinearities of the satellite-borne TWTA. Furthermore, it is found that the threshold C/N_0 in the K-band satellite link is about 1 dB larger than that in the modem back-to-back case. This effect seems due to the spin modulation and the TWTA nonlinearities.

Figure 8 shows S/N vs C/N_0 characteristics of the FM-TV signal transmission at Kashima station through the K-band transponder. For a C/N_0 of 102 dB-Hz, unweighted S/N's of 59 dB and 53 dB are obtained for 50 MHz and 20 MHz(p-p) frequency deviation respectively. The threshold C/N_0 is also measured as 94 dB-Hz and 88 dB-Hz for each frequency deviation. Differential gain and differential phase were measured and almost same values were obtained compared with the modem back-to-back cases.

Studies of the degradation of S/N due to rainfall attenuation in K-band satellite links are quite important, and long term measurements of S/N, C/N_0, received beacon signal level and other radio wave propagation data are being carried out during the rainy swason. From the propagation data, a relation between downlink(20 GHz) and uplink(30 GHz) rainfall attenuation, Ld and Lu, was determined statistically as follows.

$$\log Lu = 2.1 \log Ld$$

Figure 9 shows S/N versus downlink rainfall attenuation characteristics in the case of satellite loop-back test where uplink attenuation also occurs simultaneously. The figure shows that the experiment results agree with the calculated values.

PSK signals transmission

PSK signals transmission tests have been conducted at Kashima station for various kinds of digital signals such as PCM multiplexed telephony signals, DPCM television signals and others with various transmitting parameters such as bit rate, modulation phase, energy dispersal and so forth. The bit error rate(BER) performance is affected by rainfall attenuation, spin modulation and transponder nonlinearities. The variation in E_b/N_0(energy per bit/ noise power density) due to spin modulation in K-band is observed to be 3 to 4 dB at Kashima station in the worst case. Bit errors occur mostly at the bottom portion of periodic spin modulation, and BER performance is degraded when referred to the E_b/N_0 value averaged over the spin modulation period. Figure 10 shows an example of BER performance in the K-band satellite link(F1) when the ground station transmitting power is changed within the range of transponder's AGC function. BER performance in K-band is worse by 1 to 2 dB than those in C-band. Table 2 shows the degradation in BER performance compared with the modem back-to-back test, and the uplink and downlink margins when the threshold signal quality is taken as 1×10^{-4}.

Figure 11 shows S/N vs BER characteristics of the PCM-TV and PCM-Telephone signals. In the PCM-Telephone signal transmission, weighted S/N increases with increasing E_b/N_0 up to 1×10^{-4} in BER, and it saturates at 42 dB because of quantization noise which satisfies CCITT REC G712. In the PCM-TV signal transmission, 50 dB of unweighted S/N is obtained at a BER of 1×10^{-4}, and the quality of the TV picture is estimated as excellent (5th grade in five point scale of CCIR REC 500).

SCPC and SSRA signals transmission

SCPC(Single Channel Per Carrier) and SSRA(Spread Spectrum Random Access) equipments have been developed by RRL(3) for small taffic multiple access communications(between a main earth station and small-sized stations through the CS K-band transponders. The small sized K-band station consists of a 2 meter dish Cassegrain type antenna of XY mount and indoor modem units. The antenna gains are 53.5 dB in 30 GHz and 50.0 dB in 20 GHz, and an IMPATT diode transmitter with 2 watt output power and a GaAs FET receiver with 800 degrees K noise temperature are mounted in the back structure of the antenna. The SCPC system can transmit and receive 64 Kbps, 4-phase, DPSK voice signals or equivalent multiplexed data signals. The voice signal is encoded with bit rate of 48 Kbps or 64 Kbps in an adaptive delta modulator. A 3/4 error correcting coding can be applied to any baseband signal of bit rate lower than 48 Kbps. Figure 12 shows the BER characteristics of this system. On a clear day, C/N of about 25 dB could be obtained at the small station. The figure shows that a coding gain of about 2.8 dB can be expected at BER of 10^{-3}.

Application of the spread spectrum techniques to the satellite communication systems is a quite attractive matter because of their excellent characteristics such as interference insensitiveness, code division muliple access, information security, ranging capability and so forth. Especially, it will provide powerful means to solve frequency sharing problems. Reflecting the experiences of ATS-1 communication experiments, RRL has developed a new SSRA system which would exhibit superior performances to the former one. Improved items are as follows.

(a) Increase of the number of coexisting channels by adopting coding techniques in the baseband.
(b) Quick initial synchronization by applying supplemental FSK signals during acquisition period.
(c) Increase fo identification number of user stations by alloting carrier frequencies of the FSK signals.
(d) Channel multiplexing by use of the delayed PN codes.

Experiments in the satellite links have not yet started, but preliminary in-house test results promise the expected good performances.

V. Propagation Characteristics

Rainfall Attenuation

At Kashima station, various kinds of propagation data such as K- and C-band beacon levels, cross-polarization component level, rainfall rate, reveiving system noise temperature, radar reflectivity of rain and telemetry data of the CS are collected and processed by a mini-computer system. Figure 13 shows the cumulative distributions of the K-band beacon(19.45 GHz) attenuation and the rainfall rate at Kashima. The beacon signal attenuation and rainfall rate are 12 dB and 40 mm/h respectively for 0.01 % of the time.

NTT is measuring site diversity effect between Yokosuka station and Sugita station which are aligned in north-south direction with about 21 Km separation. Figure 14 shows the cumulative distribution of rainfall attenuation on 19.45 GHz beacon signal at these stations and the diversity effects.

Excess noise temperature due to rain

At Kashima staion, receiving system noise temperature is being measured continuously at 18.40 GHz which is outband frequency of the transponders. When it rains, system noise temperature increases along with the attenuation. Figure 15 shows the relation between the excess noise temperature beyond the clear day's system noise temperature and the rainfall attenuation. There is a very good correlation between them as expected.

Other propagation effects

Cross polarization discrimination, XPD, is degraded by the rainfall. Figure 16 is a sample of XPD and attenuation records of the K-band beacon signal on a rainy day. Of course, there exists some correlations between degradation of XPD characteristics and rainfall attenuation, but the relation is not so simple to be explained by assuming some raindrops structure model. Analysis of the accumulated data are being made.

Weak scintillations have been often observed in the C-band beacon. The scintillation phenomena are believed to be due to electron density irregularities in the ionosphere.

Relative propagation delay between C- and K-band satellite links has been measured precisely, and it was recognized that the daily changes of the delay agreed well with the change of the total electron content along the path through the ionosphere. These relative propagation delay between different frequency bands would have to be taken into consideration when some communication system is designed with requirement to keep time synchronization between links of different frequency bands.

VI. Communication System Operation Experiments

Experiments by the C-band Small Transportable Earth Station(6)

Small Transportable Earth Station(STES) can be tramsported to any place in our country, and can make a satellite link between STES and the Fixed Earth Station(FES). Fundamental STES-FES satellite link characteristics were obtained between STES and FES located at Yokosuka Laboratory of NTT. After the initial experiments, STES was transported to Miyako-jima, southern most remote islands, located at the fringe of the CS C-band antenna pattern in order to affirm transmission capability all over Japan.

Two-way STES-FES satellite link is made through a single transponder, and required transponder output power to FES is far less than to STES. Figure 17 shows the C/N_0 of satellite link measured at Yokosuka and Miyako-jima island.

In this case, transmitting power of STES has a fixed value of 20 dBW and transmitting power of FES was changed from 0 to 17 dBW. Then, FES transmitting power was adjusted to the value in order to take same C/N_0 values in the two ways.

Figure 18 shows the threshold characteristics of the satellite link. Differences from the modem characteristics at 16 kHz is due to the noise of the earth station up/down converters. From this figure, it is understood for 132 telephone channels transmission, required C/N_0 is about 76 dB-Hz at threshold(S/N = 43 dB). Therefore, Figure 17 shows that the threshold margin at Miyako-jima island is about 4 dB for 132 telephone channels transmission.

Experiments by the K-band Small Transportable Earth Station(7)

At the beginning of the CS experiments, K-band STES was located at Yokosuka and fundamental STES-FES satellite link characteristics were obtained. Then, STES was transported to Kyoto, Owase, Nagoya, Tokyo and Aomori, covering central to northern part of Japan, for experiments. Initial tracking of CS at each place was made easily using a magnetic compass.

For the K-band STES-FES communication, a new FES transmitting power control method was developed to reduce unavailable time of the satellite link caused by precipitation. Figure 19 shows the controlled FES transmitting power as functions of downpath rain attenuation. By this control method, C/N_0 improvement effects of about 3 to 4 dB for rain at FES and about 1.5 to 2 dB for rain at STES were obtained. The two way communication link C/N_0 was about 87 dB-Hz, which agreed well with the predicted value.

Experiments in TDMA systems

There are two different TDMA burst synchronization techniques in CS experimental system. One is noncoherent system developed by RRL, the other is clock coherent system developed by Yokosuka ECL of NTT(5). In this paper, some results of K-band and C-band TDMA system of NTT are described.

The TDMA-100M system, whose bit rate is 106.88 Mbps, was designed for communications between the mainland of Japan and some remote islands. It has the simultaneous transmission capacity of 384 oneway telephone channels and two 32 Mbpa color TV channels.

The TDMA-60M system has the bit rate of 64.136 Mbps and transmission capacity of 960 one-way telephone channels. This system was designed for communications among K-band fixed earth stations which will be constructed in several main cities in Japan.

Figure 20 and Figure 21 show K-band TDMA and C-band TDMA BER performances respectively which were measured through the CS satellite links. Both performances are almost same as the predicated values except for the K-band spin modulation dagradation.

The equivalent E_b/N_0 at BER of 1×10^{-4} was 1.8 dB from the theoretical value. This is the sum of the IF loop degradation of 1 dB and the satellite transmission path degradation of 0.8 dB. The IF loop degradation is mainly caused by intersymbol interference due to band limiting effect of filter.

Figure 22 shows the relation between BER and spinning time. BER changes with the satellite spin period and depends on the antenna pointing azimuth bias value. Therefore, the average BER versus average C/N_0 during the spin period shifts to the worst BER. If the degradation is improved, the BER performance will be close to IF loop characteristics of the earth station.

Figure 23 shows the error correction performance in C-band TDMA. This uses rate 7/8 convolutional coding and threshold decoding with two errors correction capability within its constraint length. The measured values are very close to the calculated value and the coding gain of the forward error correction(FEC) codec was 3.8 dB in E_b/N_0 at BER of 1×10^{-7}.

The phase ambiguity of the recovered carrier is removed by the carrier recovery circuit by detecting the unmodulated carrier phase, which is transmitted at the top of TDMA burst. The measured cycle slipping occurrence of the recovered carrier phase was negligible small, and finally the full capacity of the FES codec was obtained.

These K-band and C-band TDMA systems adopted the network clock synchronization system through clock coherent operation. In this system the transmitting symbol's clock timing of non-reference stations is synchronized in phase on the satellite transponder to the timing of the reference station. The burst time position can be synchronized within one symbol accuracy. Figure 24 shows the phase error of the transmitting clock timing of non-reference station. The phase jitter is within 10 deg_{p-p}. It is possible for the automatic phase control to compensate the phase error caused by the frequency variation of the transmitting clock timing oscillator. This result satisfies the design value of ±6 deg.

The lower level transmitting PN synchronization is used for the initial acquisition. The transmitting power of acuisition signal is decided by the allowable interference level to the normal signal and the acquisition probability. Figure 25 shows the range of the trasmitting power in C-band TDMA. The allowable acquisition range is between 11 dB and 18 dB lower than the normal signal level. In this case, the BER of normal signal is better than 1×10^{-4} against the interference caused by acquisition and the detection miss probability of the acquisition is less than 1×10^{-2}.

VII. Spacecraft Operation and Control

The regular operation and control of the CS spacecraft have been performed by NASDA CS operation and control system. The system is composed of Okinawa and Katsuura Tracking and Control Stations which are linked to Tsukuba Space Center, Tracking and Control Center.

The orbital position and attitude of the CS have been kept within an accuracy of ±0.1 degrees, and the beam pointing of despun antenna for communication has also been kept within ±0.3 degrees. The attitude control is executed every about 3 weeks,and east-west and north-wouth orbital control are executed every about 3 weeks and 10 weeks respectively.

Through about two years period wihch includes three eclipse seasons, the CS has been smoothly operated functions and performances.

VIII Future Experiment Plans

Fun experiments have been conducted according to experiments have been conducted according to the predetermined schedule based on the three years spacecraft designed life. At present, however, it is anticipated that the experiment period could be extended at least one year longer, and RRL and NTT are now planning additional experiment items and preparing necessary equipments for them.

Typical new experimental items of RRL are as follows.

(1) Experiments on satellite K-band computers network; transmission of random burst signals and evalutation of link-level protocol

(2) Experiments on K-band FM-SCPC communication system using very small sized earth terminal of 1 meter dish antenna

(3) Experiments on K-band MCPC(Multiple Channels Per Carrier) communication system using small sized earth terminals of 2 meter dish antenna with digital multiplexed voice channels

NTT has also following new plans.

(1) Total system experiment connected with terrestrial communication network

(2) Small capacity communication experiments between many C-band small stations and the fixed station

(3) High speed data, facsimile, television conference and packet switching experiments using the new type K-band small earth station

Furthermore, many organizations other than RRL and NTT will join the experiments for cultivating their communication means via satellite under the technical supports of RRL and NTT.

XI Conclusion

During the first one year experiments, quite usefull results have been obtained in the CS program. Fundamental technical oriented experiments including K-band propagation studies will be continued further. With the expections of satellite life extension, some applications or social oriented experiments will be added in the latter half experiment priod.

Responding to the proposal of Ministry of Posts and Telecommunications, the Space Activities Commission had decided last year that an operational communication satellite, CS-2, should be launched in 1983 from Tanegashima Space Center by N-2 type rocket. The CS-2 will be similar to the present CS in results of development and experiments in the CS program will be sully reflected on the CS-2 program.

The authers wish to thank staffs of Radio Regulatory Bureau of the Ministry for their general promotion of the CS program and many colleagues of RRL, NTT and NASDA for their efforts in experiments and operations in the program.

Reference

(1) H. Kaneda, K. Tsukamoto and H. Fuketa "Experiments in the Japanese CS program" AIAA 7th Communication Satellite Conference. 1978 76-616

(2) K. Tsukamoto, Y. Otsu, K. Kosaka, T. Shiomi and H. Sasaoka "Experimental Program and Performance of Japan's Communication Satellite(CS) and its First Results" IEEE Trans on Communications, Oct., 1979 Vol. COM-27 No.10

(3) M. Yokoyama, H. Sasaoka, S. Yoshimoto, K. Sasaki and M. Shiojima "Development of the Mutiplexed-SSRA Equipment & Experimental Results" National Telecommunications Conference in USA, Nov. 1979

(4) Y. Otsu, A. Iso and M. Okazaki "Fundamental Characteristics of CS Communication System" 1979 Joint Convention of Four Insitutes of Electrical Engineers, Japan.

(5) S. Egamim Y. Watanabe and K. Kosaka "Operation Techinique Experiments of CS Communication System" 1979 Joint Convention of Four Institues of Electrical Engineers, Japan.

(6) T. Okamoto and M. Oguchi, "Design and Performances of Microwave Small Transportable Earth Station for Satellite Communication. "Review of Electrical Communication Laboratory of NTT. Vol. 26, Nos. 9-10, 1978

(7) S. Egamim T. Okamoto, H. Fuketa, "K-band Mobile Earth Station for the Domestic Satellite Communication System." IEEE Trans on Communication, to be published in Feb, 1980

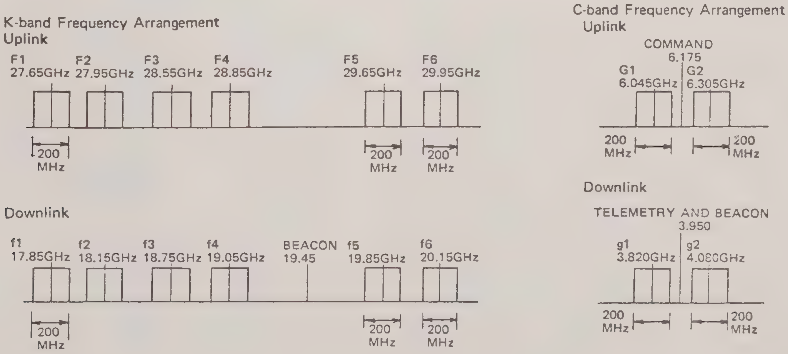

Fig. 1 Frequency arsignment in the CS system

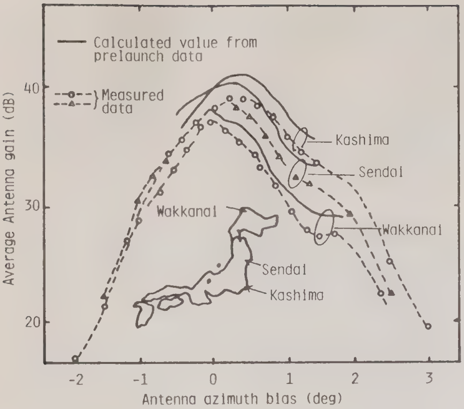

Fig. 2 Satellite K-band antenna pattern

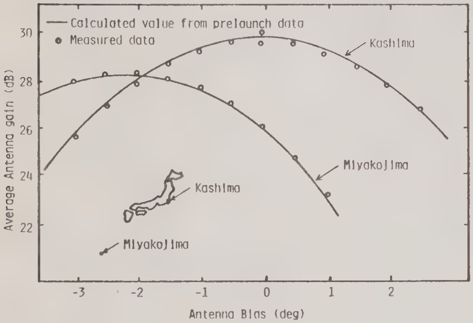

Fig. 3 Satellite C-band antenna pattern

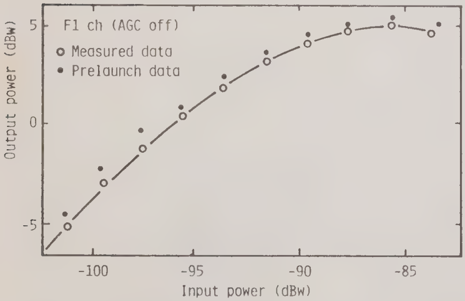

Fig. 4 Input-output characteristics of K-band transponder

Table. 1 Transponder characteristics by the unbalanced 2 tones method

Item \ channel	F1	F3	F4	F5	G1	G2
Suppression factor	1.0	0.9	0.9	1.0	0.9	1.0
AM/PM conversion coefficient (deg/dB)	2.9	4.7	3.2	4.0	2.1	3.3

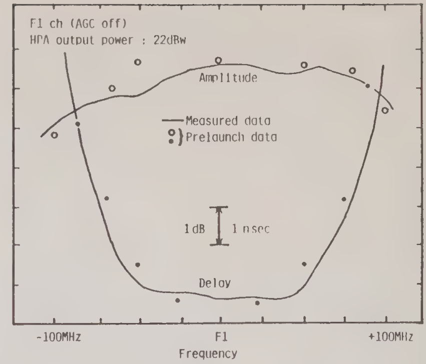

Fig. 5 Frequency-response and delay characteristics of K-band transponder

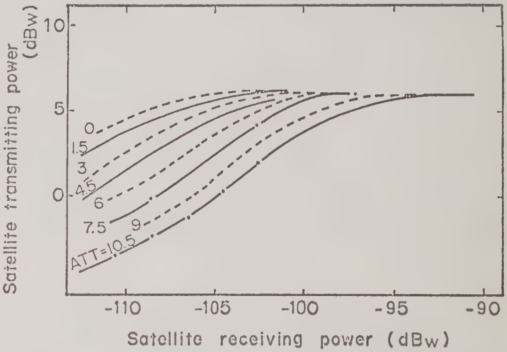

Fig. 6 Input-output characteristics of C-band transponder

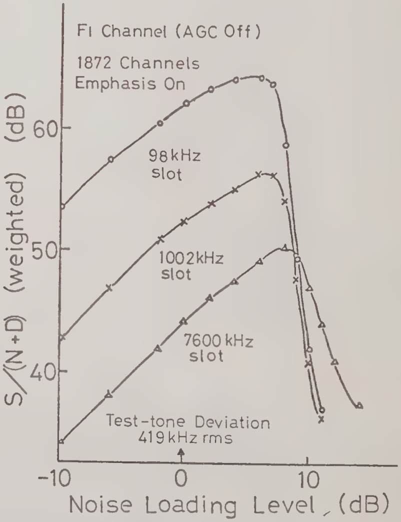

Fig. 7 Noise loading characteristics

Fig. 8

S/N vs. C/N_0 characteristics of FM-TV

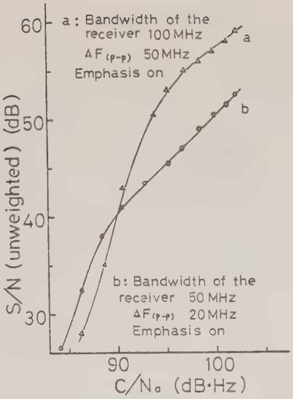

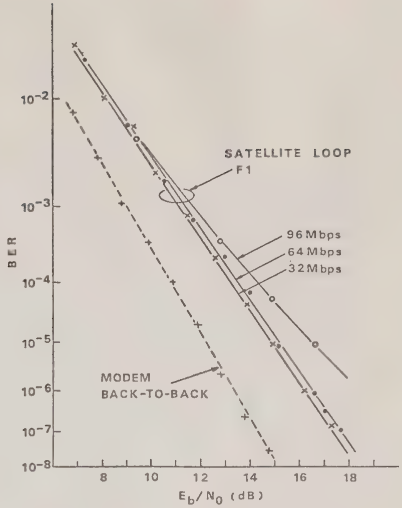

Fig. 10 BER performance of 4-phase PSK(F_1 with AGC)

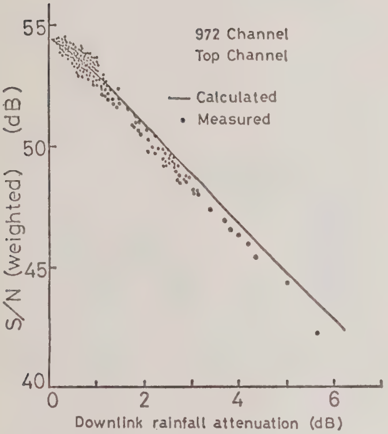

Fig. 9 S/N vs. rainfall attenuation

Fig. 11

S/N vs. BER characteristics of PCM-TV (unweighted) and PCM-Telephone (weighted)

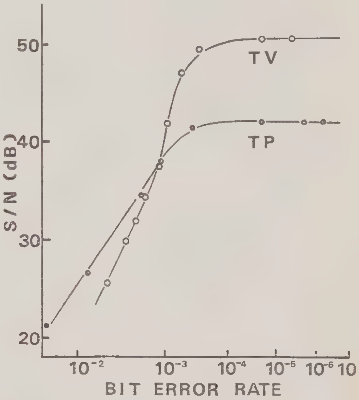

Table. 2 Degradation from modem back-to-back test and link margin

Item / Link / Band / modem	Degradation from modem back-to-back test at a BER of 1×10^{-4} (dB)				Link margin (dB)			
Link	uplink*		downlink**		uplink		downlink	
Band	K	C	K	C	K	C	K	C
32Mbps 2-phase	-***	0.9	-	-	-	17.0	-	-
4-phase	2.7	0.9	2.1	-	18.4	16.6	16.8	-
8-phase	-	1.9	-	1.1	-	11.4	-	13.1
64Mbps 4-phase	3.0	2.0	2.1	0.8	14.1	12.6	13.9	14.7
96Mbps 4-phase	3.2	-	2.1	-	9.9	-	8.7	-

* corresponds to uplink degradation of C/N_0 by varying transmitting power.

** corresponds to downlink degradation of C/N_0 by adding noise at earth station receiver.

*** not measured.

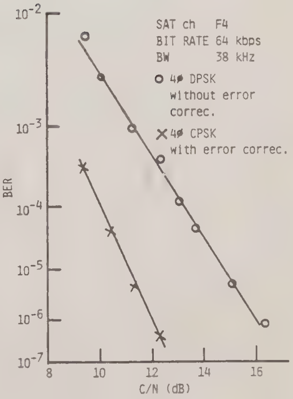

Fig. 12 BER characteristics of SCPC system

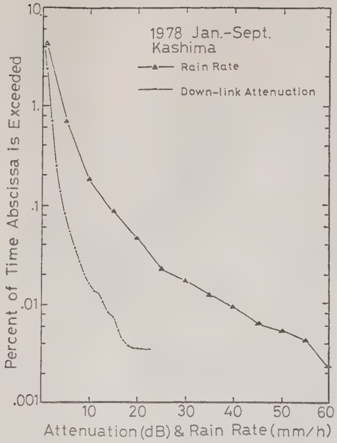

Fig. 13 Cumulative distribution of downlink (19.45 GHz) attenuation and rainfall

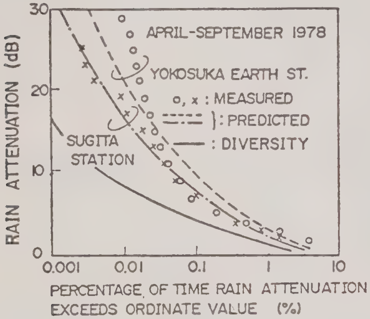

Fig. 14 Cumulative distribution of rain attenuation and diversity effect

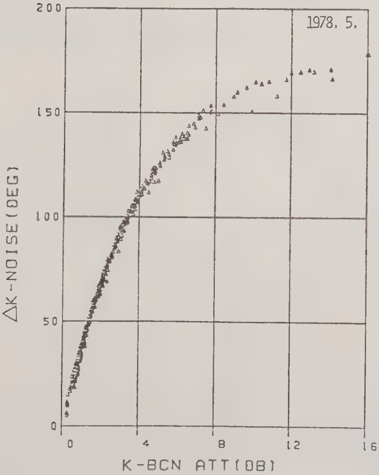

Fig. 15 K-band excers noise temperature vs. K-band beacon attenuation

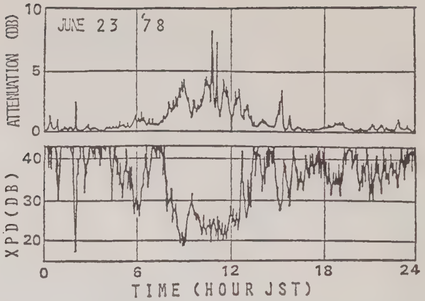

Fig. 16 Degradation of XPD characteristics and rain attenuation

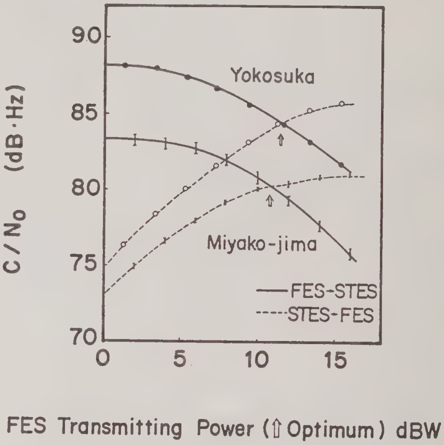

Fig. 17 C/N_0 as function of FES's TX power (STES's TX power : 20 dBW const)

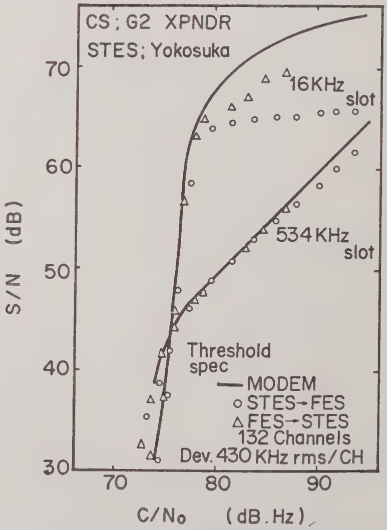

Fig. 18 Satellite link threshold characteristics

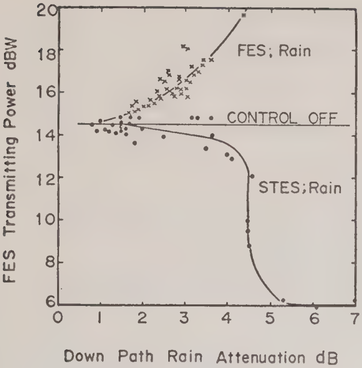

Fig. 19 Controlled FES TX power as function of down path rain attenuation

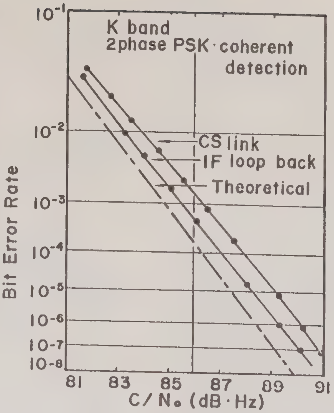

Fig. 20 BER performance (TDMA-60M system)

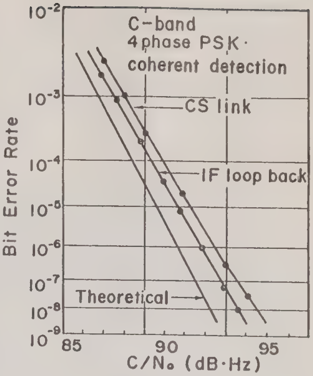

Fig. 21 BER performance (TDMA-100M system)

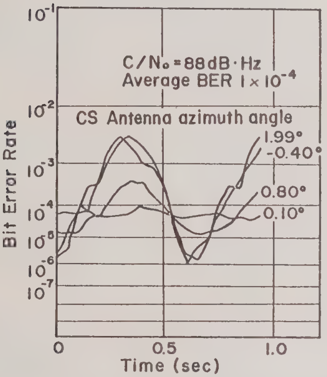

Fig. 22 BER performance vs. CS antenna spinning time

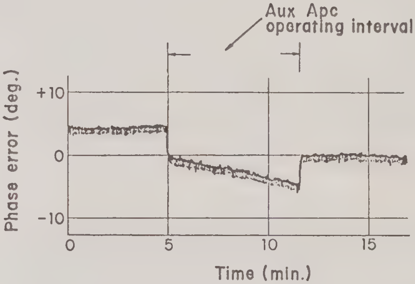

Fig. 24 TX clock timing phase error performance

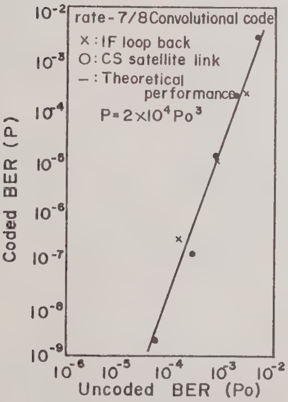

Fig. 23 FEC performance

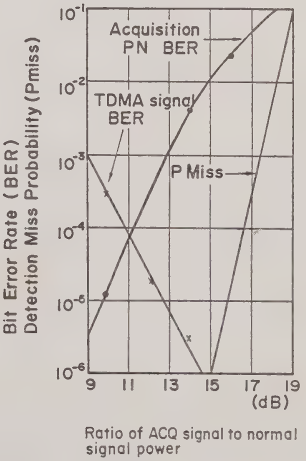

Fig. 25 Acquisition performance

80-0472

A SATELLITE COMMUNICATIONS SYSTEM FOR ELECTRIC UTILITIES*

ARVYDAS VAISNYS
Jet Propulsion Laboratory
4800 Oak Grove Drive
Pasadena, California 91103

LAYTON BERGEN
Boeing Aerospace
PO Box 3999
Seattle, Washington 98124

Abstract

This paper presents the results of a study into the feasibility of using satellite communications for a country-wide system of electric distribution system monitoring and control. The concept selected for study involves the use of a geostationary satellite with a large multi-beam antenna to provide a major part of the communications and control network between participating utilities and various elements of their power distribution networks, including customer loads. Electric utility communications requirements are projected through 1995 in order to size the required capacity of the system. Two basic systems are examined: a one-way system for load control, and a two-way system for distribution system monitoring and control, including customer meter reading. An operating protocol is proposed for each system. Preliminary cost estimates are identified element by element. Finally, expansion of the basic system to include a set of ancillary communications functions is briefly discussed.

INTRODUCTION

The United States has entered an era of rapidly increasing energy cost. High fuel costs, increasing demand for electricity, and environmental restrictions require that electric energy generation and distribution systems become as efficient as possible.

An important aspect of system efficiency is the smoothing out of daily and seasonal load demand in order to reduce requirements for generation and transmission capacity. Efficient distribution requires close monitoring and control of the distribution system. Both demand control and distribution system monitoring require a reliable flow of control signals and information between the utilities and various segments of their distribution networks.

The United States Department of Energy (DOE) is involved in the evaluation of communications systems for electric utilities. This study was sponsored by the DOE and was intended to evaluate space communications as an alternative to terrestrial communications systems. The study was carried out by the Boeing Aerospace Company under the direction of the Jet Propulsion Laboratory. This paper presents a summary of the results of this study.

DISTRIBUTION SYSTEM MONITORING AND CONTROL

Distribution system (including customer loads) monitoring and control can be subdivided into three functional categories, as listed in Table I.

Demand control can be achieved either through incentives to customers or direct discretionary control of the load by the utility. Incentives include imposing variable rates according to time of use, i.e., charging higher rates during peak demand periods. The demand created by some types of electricity usage, such as residential air conditioners and water heaters, may not lend itself to control through incentives alone. In such cases, a more direct means of demand control is required, such as discretionary switching of these loads. This is accomplished by cycling groups of appliances off for short periods (5-10 minutes) during peak demand hours.

Control of time-of-use meters can be accomplished with clock driven timers, but discretionary load switching requires a means of sending control signals from the utility to the customer. Once such a network is established, time-of-use metering can also be integrated into it and made more effective by allowing adjustment of the meters for weekly and seasonal demand fluctuations.

Remote meter reading involves the flow of communications in both directions. Requests for meter readings go out to the customer terminal and information comes back to the utility. Once a two-way flow is implemented, it can also be used to monitor the effects of demand control activity.

Network operational management involves the control of certain elements in the distribution network, as well as monitoring of operational parameters. It also requires a two-way communication system to perform all of its functions.

COMMUNICATIONS ALTERNATIVES

Distribution system monitoring and control is under experimental investigation in several areas of the United States and a number of installations are in commercial use. The types of communications systems for demand control currently being tested or in commercial use include terrestrial radio, power line, and telephone systems.

---

*This paper is based on research conducted by Boeing Aerospace under contract with the Jet Propulsion Laboratory, California Institute of Technology, for the U.S. Department of Energy under an interagency agreement with the National Aeronautics and Space Administration.

Copyright © American Institute of Aeronautics and Astronautics, Inc., 1980. All rights reserved.

TABLE I

FUNCTIONAL CATEGORIES FOR DISTRIBUTION SYSTEM MONITORING AND CONTROL

1. DEMAND CONTROL	
Discretionary load switching	Direct remote control of residential, commercial, industrial, or agricultural loads.
Time-of-use pricing	Remote switching of meter registers for time-of-day metering.
Load shedding	Rapid disconnect of blocks of load.
2. REMOTE METER READING	
Automatic customer meter reading	Remote reading of total power consumption, peak demand, or time-of-day consumption.
3. NETWORK OPERATIONAL MANAGEMENT	
Network re-configuration	Remote control of switches and breakers for shifting loads among feeders.
Voltage regulation	Remote control of selected voltage regulators within the distribution network.
Transformer load management	Monitoring transformer load, core temperature, etc., to prevent overload, burnout, or abnormal operation.
Feeder load management	Monitoring of feeder loads.
Capacitor control	Remote switching of capacitor banks.
Fault detection location and isolation	Automatic location and isolation of faults within the distribution network.
Cold load pick-up	Controlled pick-up of dropped load.
System studies	Special real-time data gathering for off-line analysis.

1. Terrestrial Radio

Communications by terrestrial radio requires an extensive network of radio transmission-reception stations strategically distributed throughout the service area. These stations must be tied to the utility's Master Control Station (MCS) through leased telephone lines or radio links.

2. Power Line System

An alternative communication technique makes use of the electric power lines for signal propagation. Three basic systems exist [1]. These are power line carrier, and ripple control, which utilize modulated carriers injected into the power line; and power waveform modification, which involves direct modification of the 60 Hz power wave form.

In the power line carrier system outgoing messages are converted to curent signals at each substation and injected into the power lines (feeders) emanating from that substation. Incoming carrier current signals are picked-off the feeders and forwarded to the MCS via leased telephone lines or radio. Because of the high frequency of the carrier (5 KHz - 300 KHz), the power distribution system can produce significant attenuation of the signals. Feeders over a few miles in length can require communication repeaters for signal enhancement. Provisions may also be required to reduce signal attenuation caused by transformers and power-factor correction capacitors.

Ripple control systems use pulses of a lower frequency carrier (100 Hz - 1000 Hz). Coding is usually accomplished by the relative timing of information pulses with respect to a start pulse. Since the carrier frequency is relatively close to 60 Hz, propagation characteristics are better than for power line carrier systems. For this same reason, however, signaling power required is higher, typically 0.1 - 0.5 percent of the system power level. Because of the high power requirements and low data rate capability, ripple systems have generally been limited to one-way, outbound signaling.

An example of a power waveform modification system is a system currently undergoing field trials, which uses shifts in the zero crossing of the 60 Hz power waveform for outbound signaling. An advanced zero crossing represents a data "one", while a retarded zero crossing represents a "zero". Communications inbound from remote locations is accomplished by generating short, 50 amp pulses with a resistive load at precise time locations in the power waveform.

3. Telephone Systems

Leased telephone lines connect the MCS to appropriate Telephone Switching Centers. From each Switching Center messages are routed to the addressed remote terminals via dial-up lines under the control of a special signal injector located at the Center. Lines are used on a non-interference basis with normal telephone traffic. Pole-top terminals, and other remote sites may require installation of telephone service.

4. Satellite System

The elements of a satellite communications system are illustrated in Figure 1. A satellite in geostationary orbit offers a unique advantage as a means for relaying signals between a utility and all parts of its distribution system, including individual customers. Because of the satellite's position in space, direct line of sight communications can be maintained to almost every point on

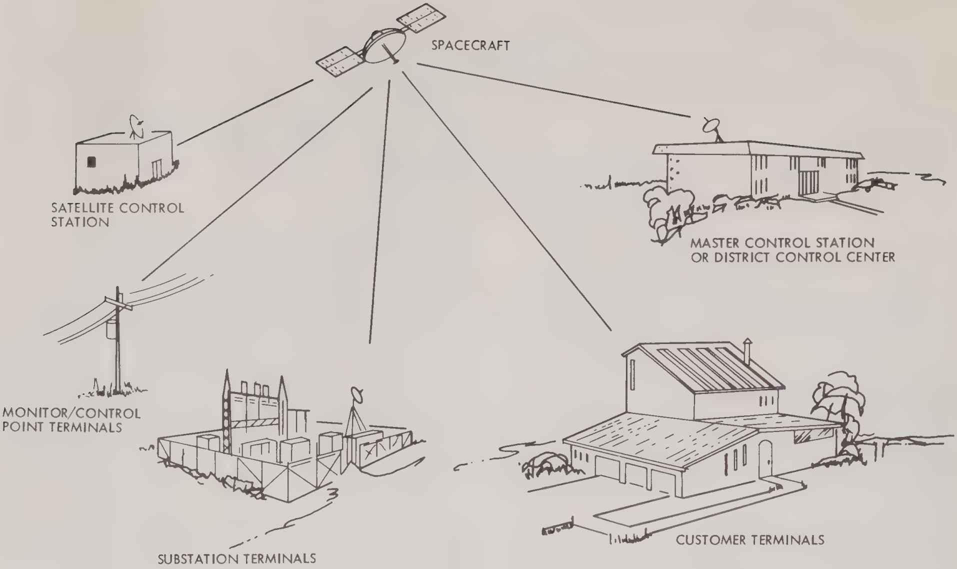
SPACECRAFT
SATELLITE CONTROL STATION
MASTER CONTROL STATION OR DISTRICT CONTROL CENTER
MONITOR/CONTROL POINT TERMINALS
CUSTOMER TERMINALS
SUBSTATION TERMINALS

Figure 1. Elements of the Space Communication System

the ground. This avoids the requirement of the signal distribution network associated with terrestrial systems.

SIZING THE SYSTEM

Since the design, fabrication, and launch of a communications satellite represents a significant investment, its operation should be shared by as many users as possible. For this study it was assumed that one satellite would satisfy the communications requirements of all utilities in the Continental United States that might elect to participate in such a system by the year 1995.

In order to size the required communications capacity of such a satellite, the size and operational requirements of the United States electrical distribution system was determined by means of a survey of the number of utilities in the country, their geographical distribution, and various statistics on their customers. A projection was then made to the year 1995[2]. Table II shows a country-wide summary of utilities, electric meters, and residential loads amenable to discretionary switching. An estimate was made of the percentage of participation by year for the residential demand control, meter reading and the operational management functions[2]. These results, giving bounds on minimum and maximum expected participation are illustrated in Figure 2.

For operational requirements, estimates were made of the frequency, as well as time criticality of each monitoring and control function. On the basis of system size and operational requirements, it was established that the overall communications requirements are modest in terms of data rate. No time critical functions were found. Even load shedding allows response times of tens of seconds. This means that the communications system can be designed with a fairly uniform data rate.

Table II

A PROFILE OF THE ELECTRIC UTILITY INDUSTRY IN THE YEAR 1995

The year 1995

Total United States population	250×10^6
Number of electric utilities	3100
Number of electric meters	110×10^6
Number of residents with:	
Central Air Conditioners	33×10^6
Electric water heaters	24×10^6
Electric space heaters	7×10^6

SYSTEM TRADE-OFFS

The basic system trade-off is satellite versus ground terminal complexity. From a total system cost standpoint, in a system with many ground terminals, it generally pays to minimize ground terminal cost while allowing greater complexity in the satellite. Low cost terminals imply small antennas, simple receivers, and low power transmitters. The required gain must be made up in the satellite antenna. In this study it was decided to use a multiple beam antenna, which not only provides the required gain, but tends to reduce satellite signal spill-over outside of the boundaries of the United States.

Within each beam, access must be provided to each utility using the satellite. The possibilities range from time division multiple access (TDMA) systems where each utility is assigned a time slot in a single frequency channel, to frequency division multiple access (FDMA) systems

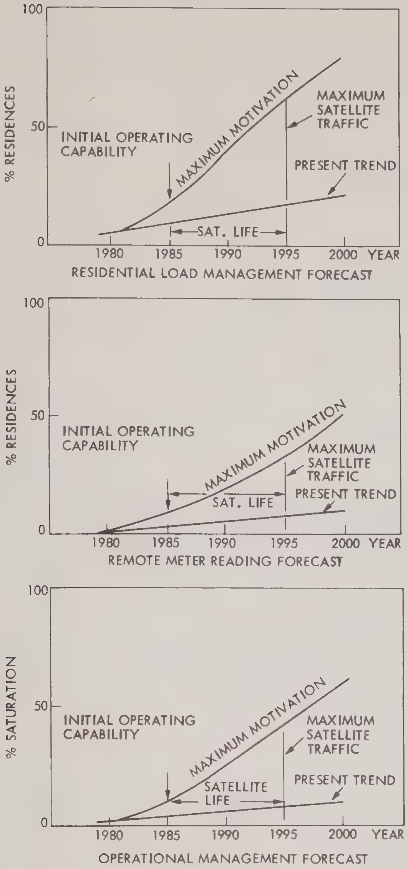

Fig. 2. Projected Participation

where each utility is assigned one or more exclusive frequency channels.

The TDMA approach requires a higher data rate at each customer terminal as well as a control station to assign time slots. The FDMA approach makes each utility operationally independent, but results in many very low data rate channels. This makes the practical implementation of an FDMA system less spectrum efficient. TDMA was chosen for the baseline design because of its smaller bandwidth requirement.

Another trade off to be made in the evaluation of a baseline system is the selection of the operating frequency. There are both technical and regulatory aspects involved. The lower the frequency, the larger both spacecraft and ground antennas have to be. At frequencies above approximately 10 GHz, weather related propagation phenomena become significant. Receiver technology is also not as mature as at lower frequencies and is therefore more costly.

A broad system cost minimum was found in the region of 1 GHz, so this frequency was chosen for the baseline design. System costs were also projected on either side of this frequency range.

In addition to technical and cost aspects of frequency selection, the requirements of the International Radio Regulations must be met. These regulations specify bands that may be used for certain purposes, as well as such technical matters as allowable power flux density (PFD).

A system using small ground terminals with essentially omnidirectional antennas and low cost receivers requires a high space-to-earth power flux density. Some space communications frequency bands have space-to-earth PFD limits set by international law. These set a lower limit on the quality, usually expressed in terms of antenna gain to system temperature ratio (G/T), of the ground terminals. For example, PFD limits in some of the fixed and broadcasting satellite service bands are 10 dB or more lower than required by this system. The satellite to remote terminal link portions of the system would therefore be excluded from these bands on this basis.

Because of the incompatiblity with the fixed and broadcasting satellite service some other frequency band must be found for this service. The fact that the bandwidth required is relatively small means that there is a reasonable chance of accommodating such a system even in the already crowded UHF portion of the frequency spectrum. Particular attention must be paid, however, to any PFD limits in each candidate band. A sharing study is also required to demonstrate compatability with other services authorized to use these bands.

BASELINE SYSTEM CONCEPT

The baseline concept for an electric utility communications system involves a geostationary satellite with about 6 regional beams. Two uplink and two downlink channels are required per beam for the two-way system, for a total of 24 channels. Some frequency reuse is possible due to the spatial separation of the beams and possible use of polarization diversity.

All the utilities in a given region would share each channel by means of Time Division Multiple Access (TDMA). A central controlling agency would assign each utility a certain number of time slots in proportion to their communications traffic requirements.

The six regions were chosen to be of approximately equal population. This resulted in beam diameters in the range of 3.4 degrees to 1.2 degrees, depending on the population density of the region. The boundaries and statistics for one low density and one high density region, including the number of utilities and electric meters per state, are shown in Figures 3a and 3b. The communications traffic was estimated on the basis of both messages per month and messages per hour during peak activity periods. The results for the western region outlined in Figure 3a are shown in Table III. Figure 4 illustrates the amount of time required to transmit some number of messages N, given the message length and data rate. On the basis of predicted communications traffic, the data rate required to provide all the communications for a given region is fairly low, in the

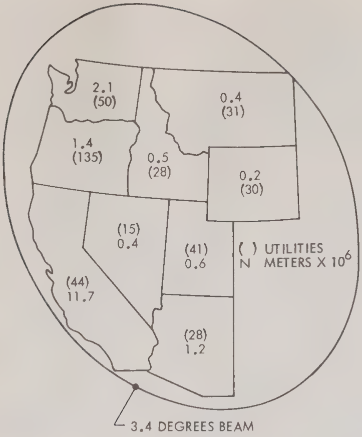

IN THE YEAR 1995

402 UTILITIES/REGION
  100 SUBSCRIBING UTILITIES
18.5 x 10^6 METERS/REGION
  3.7 x 10^6 TOTAL CONSUMPTION REMOTED
  0.4 x 10^6 MAXIMUM DEMAND REMOTED
  1.9 x 10^6 TIME-OF-DAY REMOTED
2.0 x 10^6 AIRCONDITIONERS (CENTRAL)
  1.2 x 10^6 UNDER LOAD MANAGEMENT
3.5 x 10^6 WATER HEATERS
  2.1 x 10^6 UNDER LOAD MANAGEMENT
1.7 x 10^6 SPACE HEATERS
  1.0 x 10^6 UNDER LOAD MANAGEMENT

Fig. 3a. A Typical Low Population Density Region

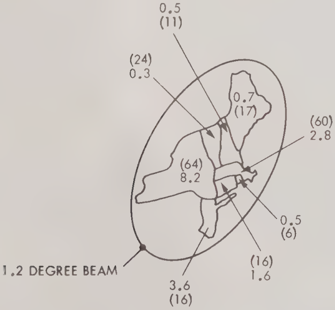

IN THE YEAR 1995

214 UTILITIES/REGION
  120 SUBSCRIBING UTILITIES
18.2 x 10^6 METERS/REGION
  3.5 x 10^6 TOTAL CONSUMPTION REMOTED
  0.3 x 10^6 MAXIMUM DEMAND REMOTED
  3.2 x 10^6 TIME-OF-DAY REMOTED
3.0 x 10^6 AIRCONDITIONERS (CENTRAL)
  2.0 x 10^6 UNDER LOAD MANAGEMENT
3.6 x 10^6 WATER HEATERS
  2.5 x 10^6 UNDER LOAD MANAGEMENT
4.4 x 10^6 SPACE HEATERS
  2.9 x 10^6 UNDER LOAD MANAGEMENT

Fig. 3b. A Typical High Population Density Region

TABLE III

COMMUNICATIONS TRAFFIC, WESTERN REGION

	MONTHLY TRAFFIC MESSAGES/MONTH	PEAK TRAFFIC MESSAGES/HR
DEMAND CONTROL	4.2×10^6	19.2×10^3
AIR CONDITIONERS	2.3×10^6	9.4×10^3
WATER HEATERS	1.5×10^6	8.2×10^3
MISCELLANEOUS	$.4 \times 10^6$	1.6×10^3
NETWORK OPERATIONAL MANAGEMENT	3.1×10^6	70.5×10^3
LOAD RECONFIGURATION	$.2 \times 10^6$	3.4×10^3
TRANSFORMER MANAGEMENT	1.1×10^6	14.0×10^3
FEEDER MGT.	$.6 \times 10^6$	40.0×10^3
VOLTAGE REGULATION	$.8 \times 10^6$	8.0×10^3
CAPACITOR CONTROL	$.3 \times 10^6$	4.5×10^3
FAULT DETECTION, ISOLATION	$.1 \times 10^6$	0.6×10^3
REMOTE METER READING	9.8×10^6	N/A*
TOTAL CONSUMPTION	3.7×10^6	
MAXIMUM DEMAND	$.4 \times 10^6$	
TIME-OF-DAY	5.7×10^6	
TOTAL	17.1×10^6 MESSAGES/MONTH	89.7×10^3 MESSAGES/HOUR

* Accomplished during low activity periods.

order of 1000 to 2000 bps. An estimate of 5000 bps was chosen for the baseline system.

The operating protocol would differ somewhat between the demand control and meter reading functions. During daylight hours when demand control activity is at a peak, each utility would be given access to its customers on at least a once per minute basis. The command word length would be standardized at around 50 bits to allow for synchronization, message bits, and sufficient address bits to address each individual load under demand control. Certain addresses would be reserved for addressing groups of customers or even the entire utility service area. While each individual customer load could be addressed individually, demand

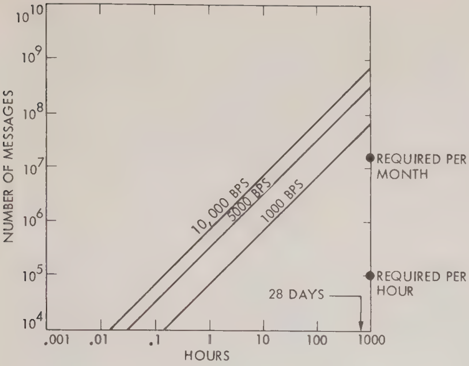

Fig. 4. Time to Transmit N 50 Bit Messages

control would be by groups of loads, thereby saving considerable time.

A possible protocol implementation for meter reading would be to assign each utility a monthly exclusive use of the channel for about 1 hour per 10^5 customers. This could be done at night when demand control traffic is at a minimum.

In most cases, customer transceivers will be located outside of the customer's building. Electric loads may be remote from the transceiver location. In this study it was assumed that the link between the transceiver and the load control associated parts of the customer terminal will be over the power line, using a simple power line carrier scheme. In most cases this is a lower cost alternative to hard wiring. Use of a power line carrier system on the customer side of the power transformer presents few of the problems of using power line carrier over the entire power distribution system. It also allows a simple method for several customers to share a transceiver. There are no anticipated problems with this portion of the link.

SYSTEM PERFORMANCE

At 1 GHz the spacecraft antenna size for the narrowest beam (1.2°) would be 20 meters in diameter. A 15 cm x 15 cm microstrip array antenna with around 3 dB gain was chosen for the customer terminal. Table IV gives the link budget for a satellite to customer link. A receiver with a noise figure of 14 dB, T = 7000 K, is assumed. The noise figure and the customer antenna gain will ultimately be determined by the power flux density (PFD) limits imposed upon this type of service.

Transmission from customer terminals requires power levels of less than one watt, which is easily handled by solid state devices in this frequency range. The power levels associated with customer terminal transmitters do not produce any microwave exposure hazards even at distances of less than one foot from the antenna.

TABLE IV

LINK BUDGET FOR SATELLITE TO CUSTOMER TERMINAL LINK

	Low Density Area	High Density Area
Transmitter Power	10 dBw (10 watts)	0 dBw (1 watt)
Spacecraft Antenna Gain	34 dB (3.4° BW)	43 dB (1.2° BW)
Path Loss (1000 MHz)	- 184 dB	- 184 dB
Receiving Antenna Gain	3 dB	3 dB
Received Power	- 137 dBw	- 138 dBw
N_0 (t_s = 7000 K)	- 190 dBw	- 190 dBw
Data Rate 5000 bps	37 dB	37 dB
E_b/N_0	16 dB	15 dB
Threshold E_b/N_0	11 dB	11 dB
Margin	5 dB	4 dB

RELIABILITY CONSIDERATIONS

Reliability is ordinarily defined as "the probability of a device performing its intended purpose adequately for the period of time intended under specified environmental conditions."

A high level of reliability can be achieved in a spacecraft through the use of both block and functional redundancy. This redundancy can be employed such that no single-point failure can have a catastrophic effect on the mission. In block redundancy two identical elments are provided to perform the same function, either in an active mode wherein both elements are powered online simultaneously, or in a standby mode wherein the redundant element is switched on only in the event of failure of the primary element. Functional redundancy provides the capability to perform the same, or nearly the same, function in two different ways. The overall mission reliability of a single spacecraft, of the design examined in this study, is estimated to be .744 for ten years of full-up operation. This value increases to over .93 with one standby unit.

Ground terminal reliability does not affect system operation in the same critical sense as does satellite reliability. The impact of a terminal failure manifests itself in terms of possible customer complaints, a potential loss of revenues, and in maintenance, repair, or terminal replacement costs.

The reliability objective for customer terminals is to keep failures below 2-3% per year (which is akin to replacing the entire population of terminals every 50 or 30 years).

The estimated overall failure rate for a two-way customer terminal (most complex configuration) with one transceiver unit serving five customers, each having three load devices under control, is less than 1% per year.

SYSTEM COST ESTIMATES

The major thrust of the cost estimating effort was in the area of customer terminals. Terminal component costs were derived through a combination of vendor surveys and internal estimation. Figure 5 shows block diagrams of dedicated one-way and two-way customer terminals. Table V lists the estimated manufacturing costs for the various components of these terminals. Costs were estimated on the basis of high volume production.

Terminal costs can be significantly lowered by sharing receive/transmit equipment among several customers. One neighborhood transceiver can serve as many customers as are tied to the secondary of a single distribution transformer.

Estimated costs for the rest of the system are shown in Table VI. Terminal costs reach half of the total system cost at about a one million terminal system. For the projected system of 25 million terminals country-wide, terminal costs will predominate.

ANCILLARY COMMUNICATIONS FUNCTIONS

Once a satellite communications system which can reach practically all households in the country is in place, it can also be used for communications functions other than those described so far in this paper. Without an appreciable increase in bandwidth requirements, a one-way system can provide such functions as maintenance personnel paging and various public service messages such as severe weather warnings or civil defense alerts. A two-way system can provide meter reading for other utilities, environmental monitoring and data gathering, and a means of receiving citizen generated messages such as emergency assistance request or public polling responses.

CONCLUSIONS

A satellite communications approach was investigated for country-wide electric distribution system monitoring and control. The system would provide electric utilities the capabilities for electric demand control, network operational management and meter reading. Most of the communications traffic in such a system is not time critical and therefore allows many utilities to share a single, modest bandwidth, channel. A single geostationary satellite with about 6 regional beams can satisfy the estimated 20 year communications requirements of electric utilities for distribution system monitoring and control.

A satellite system offers the advantage of a direct signal path between a central control station and all customer or network terminals. Given sufficient participation, satellite costs become small on a per terminal basis. Country-wide participation in this system would lead to high production, standard terminals, thus minimizing costs. The terminals can be designed to include other low data rate communications functions with minimal cost impact.

System questions remaining to be resolved are the organization of an operating authority to manage the system, and the determination in which frequency band this system can be accommodated.

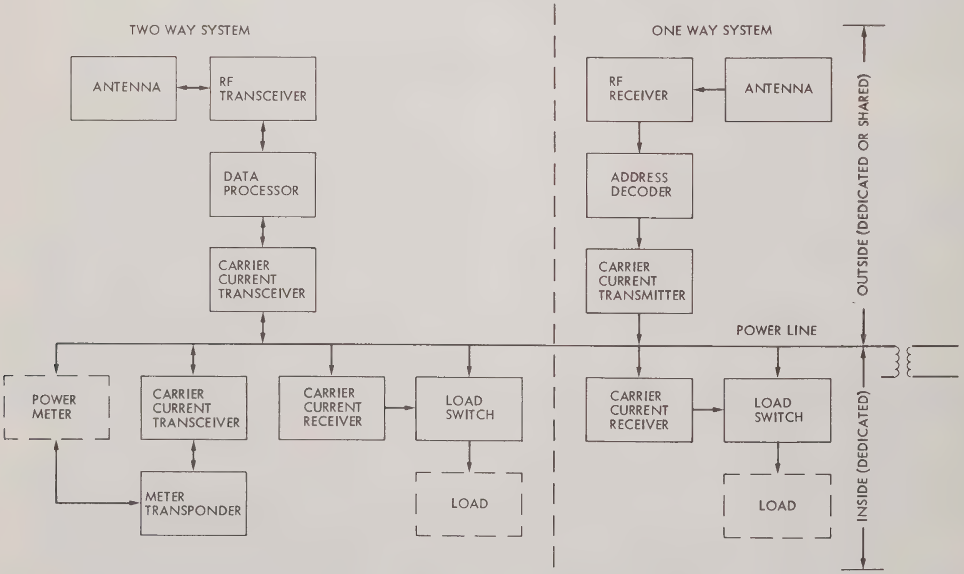

Fig. 5. Customer Terminal Block Diagrams

TABLE V

ESTIMATED CUSTOMER TERMINAL MANUFACTURING COSTS

Dedicated 2-Way System		Dedicated 1-Way System	
Antenna	$ 15	Antenna	$ 15
RF Transceiver	$200	RF Receiver	$ 60
Data Processor	$ 50	Address Decoder	$ 25
Carrier Current Transceiver (outdoor)	$ 50	Carrier Current Transmitter (outdoor)	$ 20
(OUTDOOR* EQUIPMENT)	($315)	(OUTDOOR* EQUIPMENT)	($120)
Carrier Current Receiver (indoor)	$ 15	Carrier Current Receiver (indoor)	$ 15
Load Switch	$ 5	Load Switch	$ 5
Carrier Current Transceiver (indoor)	$ 40		
Meter Transponder	$100		
TOTAL	$475	TOTAL	$140

* Can be shared among several customers.

TABLE VI

ESTIMATED SYSTEM COSTS - EXCLUDING CUSTOMER TERMINAL PURCHASE COSTS

Satellite costs	$ 40 M
Launch cost	$ 41 M
On-Orbit Spare	$ 81 M
Satellite control Station	$ 10 M
Utility Ground Station	$ 125 M (1000 stations)
Design and Development	
Satellite	$ 105 M
Customer Terminal	$ 5 M
Ground Station	$ 12 M
Total Investment	$ 419 M
Investment per Terminal	$ 16.76 (based on 25 M terminals)

REFERENCES

1. M. G. Morgan and S. N. Talukdar, "Electric Power Load Management: Some Technical, Economic, Regulatory and Social Issues," Proceedings of the IEEE, Vol. 67, NO. 2, February 1979.

2. C.H.M. Saylor, "Data Estimates by State to Help Establish Communications Requirements for: Remote Meter Reading, Customer Load Management, Distribution Automation," Report prepared by Systems Control, Inc. for Boeing Aerospace, May 8, 1979.

80-0473

SALIENT DESIGN FEATURES OF INSAT-1 SPACE SEGMENT SYSTEM

M.K.Saha*
Dept. of Space, Govt. of India
Bangalore, India

Abstract

The Space Segment of INSAT-1 system expected to be operational by 1981 comprises of two multipurpose geostationary spacecrafts and a Master Control Facility(MCF). Direct TV broadcast, Meteorological and Telecommunications services are integrated in each 3-axis stabilised spacecraft having dual compatibility for launch by either expendable launch vehicle or Space Transportation System(STS). This paper brings out the salient design features with an overall description of the entire INSAT-1 Space Segment.

1. Introduction

Presently planned Indian National Satellite System (INSAT-1) will provide three services:

- Long distance telecommunications
- Meteorological data
- Direct TV broadcast to community receivers.

The key feature of INSAT-1 system concept as shown in figure-1 is the integration of 3 services in a single spacecraft. While the integrated multipurpose INSAT-1 spacecraft system design approach optimizes launch cost, it still provides adequate spare capacities for all the three services for future growth. Among the various factors which were taken into consideration for INSAT system design are primarily cost effectiveness, maximal use of proven technology and reliability.[1] The Space Segment of INSAT-1 System comprises of two geostationary satellites configured for launch by either DELTA 3910 or NASA's Space Transportation System(STS) for location at 74 deg.E & 94 deg.E and also a ground based Master Control Facility (MCF) located at Hassan near Bangalore. The Master Control Facility design provides the support for the transfer orbit, drift orbit and positioning phases of INSAT-1 spacecraft with adequate system margin and availability. It also provides the capability of on-orbit control of two geostationary satellites simultaneously. The INSAT-1 spacecraft and the ground based equipments for the Spacecraft Control Centre (SCC) of MCF are being built by Ford Aerospace and Communications Corpn.(FACC) of USA while the ground Antenna and other electrical equipments for MCF upto 70 MHz interfacing SCC equipments are being fabricated by Space Applications Centre, India.

Service requirements and its impact on the spacecraft subsystem design, some of the problems of integrating three services in a single spacecraft and dual compatibility of launch by either STS/PAM or DELTA 3910/PAM are brought out in this paper. The design of Master Control Facility for INSAT-1 mission is also outlined.

2. Service Requirements

Two Satellites are to be positioned in the geostationary orbit at 74 deg.E ± 0.1 and 94 deg.E ± 0.1. The one at 94 deg.E±0.1 will be active inorbit spare. Figure 2 and 3 corresponding to locations at 74 deg.E and 94 degE respectively show the areas to be covered for the following services:

a. Fixed Satellite Services (FSS):

- 12 channels with 5935-6425 MHz receive and 3700-4200 MHz transmit capabilities.
- Each channel with 36 MHz usable Bandwidth shall have 32 dBw(min.) as the Equivalent Isotropic Radiated Power (EIRP) over the primary coverage area-the mainland areas within the Indian subcontinent.

b. Broadcast Satellite Service (BSS):

- Two active channels with 5855-5935MHz receive and 2555-2635 MHz transmit capabilities.
- Each channel with 36 MHz usable bandwidth shall have 42 dBw (min.) as the EIRP over the primary coverage area.

Receive G/T for the entire band (5855-6425 MHz) should be -6dB/°K min. Antenna pointing error limits for Telecommunication and TV broadcast services are:

Pitch ±0.2°, Roll ± 0.2°, & Yaw ± 0.4°

c. Meteorological Service:

- A Data collection (DCS) channel with receive G/T of -19 dB/°K (min.) in the band 402.65-402.85 MHz and transmit EIRP -2 dBw (min.) per carrier in the band 4038-4038.2 MHz.
- A visual and Imaging (VIS) channel with transmit EIRP of 8.5 dBw at 4034.55 MHz shall have
  - * Spectral bands (μm):
    Visible 0.55-0.75, Infrared 10.55-12.5
  - * Ground resolution (KM)better than:
    Visible 2.75x2.75, Infrared 11.0x11.0
  - * Frame:
    Size &Time:20°x20°, 30 minutes. Sector scan- full frame in east-west and 5° in North-South direction with provision to be

---

*Assistant Project Director
INSAT-1 Space Segment Project

Released to AIAA to publish in all forms.

set within 1° step.

- Imaging stability:
  - The registration accuracy of two sequential lines within a frame shall be within 0.2 visible resolution element.
  - Pixel elements of two sequential frames shall have an R.M.S. error less than 1.3 visible resolution element.

3. Spacecraft System Design

The spacecraft system for INSAT-1 consists of the transfer orbit injection propulsion stage (Perigee motor), Apogee motor and the satellite. Transfer orbit injection is accomplished by the Payload Assist Module (PAM) of MDAC (McDonnel Douglas Astronautics Company USA) compatible for STS and DELTA 3910 flight operations.

The satellite is designed for a minimum operating life of 7 years. Adequate redundancy in component/sub-system level is provided and also appropriate test plan has been devised to ensure the overall mission reliability requirement of

a) 0.75 for 10 out of 12 C-band (4/6 GHz)R.F. channels.

b) 0.75 for both TV direct broadcast (6/2.5GHz) RF channels

c) 0.8 for Data Relay Channel (400 MHz/4 GHz) and
d) 0.6 for VHRR functions including data transmission channel.

3.1. Launch Vehicle and Mission Sequences:

Flight history of expendable launch vehicle suitable for INSAT-1 mission, the time frame of INSAT-1 launch in 1981 and the subsequent launch costs generated the dual compatibility requirements of spacecraft for either DELTA 3910 or STS flight operation. Considering the maximum capability of DELTA 3910, the spacecraft including PAM is designed to have a nominal mass of about 3347Kg. Only in the case of STS launch an Active Nutation Control (ANC) system is to be provided in view of the fact that prior to PAM separation the spacecraft inclusive of PAM is likely to be in parking orbit for about 45 minutes after separation from STS. Unfavourable moment of inertia ratio during this phase results in the building up of the nutation angle which is kept within the limits by the ANC system.

To create a benign environment for spacecraft inside cargo-bay of STS, a thermally controlled protective cover weighing about 60.8 Kg (41.4 Kg for Sunshield and 19.4 Kg for Cradle mounted blankets, heaters, structural and electrical interfaces) capable of being opened and closed by command from STS crew cabin currently under development by MDAC will be provided.

After completion of PAM burn, the transition from spinning mode to 3-axis stabilisation takes place instead of conventional spin stabilisation for the entire transfer orbit of about 27.5° inclination, 36,161 Km. apogee and 167 Km. perigee (~296 Km. perigee for STS launch). This mission plan, apart from reduction in equipment complexity leading to an inherent improvement in mission success probability and a corresponding reduction in equipment and propellant weight, enables the spacecraft to be better controlled even though it has unfavourable moment of inertia ratio . The major mission sequence for DELTA launch is outlined in figure-4.

3.2. Configuration:

The 3-axis stabilised satellite has the main body dimension of 1.55x1.40x2.2 meters (approx.) with a single suntracking solar array designed to generate a B.O.L.power output of about 1200 watts at Autumnal equinox.

The configuration of the spacecraft in launch, transfer orbit and on-orbit conditions is shown in figure 5, 6 and 7.

The principal features of the configuration other than the dual compatibility for DELTA and STS are:

- Bipropellant (MMH & N_2O_4) for Apogee motor burns in transfer orbit and other thrusters for various phases of the mission utilising the common tankage and pressurant system (Two propellant tanks and one pressurant tank).
- A single deployed solar array on the south side of the spacecraft providing an unobstructed view of space for the radiation cooler of the Radiometer.
- A deployable solar sail consisting of an aluminised Kapton covered cylinder at the end of a 9.4 meter extendable mast mounted on the north face to balance the solar torque due to solar array.
- Deployable C-band (1.37 meters dia.) and C/S band (1.52 x 1.62 meters) antennas located at East and West faces respectively.
- 3 axis stabilisation of satellite with momentum bias system consisting of two skewed momentum wheels with momentum vectors in pitch yaw plane and a reaction wheel along yaw axis forming 3 for 2 redundancy. For the imaging stability requirements, solar array movement and thruster firings are inhibited during the picture taking process of one full frame (about 23 minutes).

The majority of the high power dissipating equipments such as S-band TWTAs, AOCS electronics, VHRR electronics and communication amplifiers are mounted on the inside surface of the north and south panels, allowing radiation of dissipated heat to free space.

Earth viewing panel contains an annular slot array UHF antenna for the DCS at 402.75MHz, TTC omni antenna, Earth Sensors, coarse analog sun sensors and optical port of VHRR. On the internal face of the panel are the communication receiver equipments and co-axial cables/ waveguides for antenna feed.

The solar array when deployed extends to about 5 meters from the south face and a solar sail is extended to 9.4 meters from the north face. Both north and south faces have their external surfaces partially covered with optical solar reflectors (OSR).

C and C/S band reflectors held to the east panel and earth face respectively, solar array held against south and earth panels in folded condition, and solar sail/boom coiled and retracted into a cannister are the fully stowed components during launch, ascent and solar array is partially stowed in transfer orbit phases.

3.3 Spacecraft Subsystems

A functional schematic diagram of the satellite is given in figure-8 showing the primary elements of the payload and the bus systems with their interrelations.

3.3.1 Communication Payload

The multifunction communication transponder as shown in figure 9 includes the FSS C-band transponder, the BSS C to S band transponder, the DCS UHF to C band transponder, the VIS C-band transmitter, C band receive transmit and C/S band transmit antennas and UHF receive antenna. The transponder is designed to operate in the following modes:

- On-orbit noneclipse mode:
  Simultaneous operation of up to 12 FSS channels (6 GHz to 4 GHz), the DCS channel (402.75 MHz to 4 GHz), both BSS and the VHRR data transmission.
- On-orbit eclipse mode:
  Operation of 4 of the 12 FSS channels, the DCS channel & VHRR transmission (IR channel only)
- Transfer orbit/Any other phases:non-operating excepting two FSS TWTAs for Telemetry functions.

The transponder receives all the 6 GHz uplink signals via C band receive/even transmit antenna. In the maximum gain setting condition input flux density -92 dBw/m^2 gives a saturated output of 32 dBw EIRP for a single carrier. Although a gain setting capability of about 22 dB maximum in steps of about 2.5 dB has been provided in the transponder, the input flux density for single carrier operation is not to exceed -75 dBw/m^2 for saturation of the transponder.

Receive system G/T of -4.5 $dB/^{o}K$ has FET transistors as 6 GHz preamplifier. Input and output multiplexers for both C & S bands are made of GFRP. Use of non-contiguous multiplexers in C-band system simplifies the filter design and eliminates the requirements of on-board group delay equaliser except for channels 8 and 9.

AGC provided dynamic range of the C/S band system is nearly 15 dB. The input flux density from -92 dBw/m^2 to -77 dBw/m^2 saturates the 50 watt S-band TWTA to give an EIRP of min 42 dBw for each channel of usable bandwidth 36 MHz.

The DCS transponder with a bandwidth of 200 KHz has receive Earth coverage antenna with G/T of -19 $dB/^{o}K$ at UHF and transmit C band EIRP 21 dBw and 0 dBw corresponding to input flux density of -132 dBw/m^2 and -153 dBw/m^2 respectively.

VHRR transmit system consists of BPSK modulator modulated by 400 Kbs VHRR data stream, frequency translator and power amplifier coupled to the output multiplexer of even-channel C-band system. EIRP is about 8.5 dBw with usable bandwidth of 800 KHz.

Wide C-band receiver, C/S receiver, VHRR transmit system and DCS transponder, each one of these has one out of two redundancy while S-band TWTAs and amplifiers have two out of 3 redundancy. The redundant one is kept inactive.

C and C/S band reflectors have receive gain about 27.6 dB and transmit gain about 27.1 dB over the primary coverage area. Beyond 4.5° from the peak, the roll off is about -20 dB with respect to the peak. 4 individual feed horns provide the beam corresponding to the required coverage. UHF antenna for DCS transponder has an array of 4 slot radiating elements with gain better than 11 dBi. TTC has two horn pairs mounted on earth and anti-earth faces. Only during synchronous on-orbit operations the low power telemetry transmitters will be connected to C and C/S band reflectors. Some features of spacecraft antenna are shown in Table-1.

Table 1 - Spacecraft Antenna Characteristics

Band	Polarisation			Beam width
	Receive	Transmit	Ortho.with Axl.ratio	
C-band includes VHRR X'mtr	5.35-6.43: GHz. LIN Yaw Pitch: Plane	3.71-4.2 GHz. LIN Roll yaw Plane	Transmit ⊥ Rcv > 20 dB	4.5°
C/S Band	-do-	2.55-2.64 G Hz. LHCP	-- <3 dB	4.5°
UHF(DCS X'ponder	402.75 MHz. LHCP	4038.1MHz. LIN Roll Yaw Plane	-- < 3 dB > 20dB	38°Earth coverage with annular rings
TTC Omni Ant.	TC_1 6258 MHz. TC_2 6262 MHz. CP	TM_1 4031 MHz. TM_2 4039 MHz. CP	-- < 3 dB	30°cone around Yaw axis

3.3.2 Very High Resolution Radiometer (VHRR)

The VHRR instrument package weighing about 39 Kg and dissipating nearly 23 watts consists of scanner, optics, detector, radiation cooler to maintain the infrared detector temperature at about 105°K and the processing electronics package.

Scanning mechanism provides a scanning capability of frame size 20° which has about 1137 lines in N-S direction. Each line scanning in E-W direction (20°) takes one second followed by 0.2 second to step about one IR IFOV in the N-S direction. Time taken to complete the full frame scan is about 23 minutes. Sector scan capability with a width of 5° in North-South direction is also provided in increments of 1° by ground command. After completion of one full framethe scan mirror retraces back to the original position. The next scanning operation starts after a lapse of another 7 minutes during which house keeping operations like thruster firing and or solar array forward movement by 7.5° are completed.

The resolution requirements dictate that the IFOV of Visible and Infrared channels shall not exceed 76.8 and 307 micro radians respectively. Mercury-Cadmium-Telluride detectors and silicon detectors are used for IR and Visible channels respectively. The geometric center of the Visible and IR channels shall be aligned initially such that the full frame registration of the IR and Visible channels shall be concurrent spatially. The salient detector characteristics are shown in Table-2.

Table - 2 - Detector characteristics

	Infrared	Visible
Type	HgCdTe	Si photodiode
Size of sensitive area	0.0018" x 0.0018"	0.0040" x 0.0033"
No. of elements	2	8 element array
Avg.Detectivity (@ 500Hz & 105^{o}K)	$2x10^{10}$ Cm--Hz$^{\frac{1}{2}}$W^{-1}	--
Responsivity (Avg.Spectral)	20,000 V/W	0.35 amp/W (0.55 to 0.75 μm)
Spectral Response (11.2 - 12.8 μm)	80% of peak	--
Spectrl.Response (10.2 - 11.2 μm)	70% of peak	--
Operating temp.	105^{o}K	20^{o}C to 50^{o}C
Bias power	$1.2 x10^{-3}$W	15 V

Passive Radiation cooling system comprising of sunshield, radiator (1st stage)& patch (2nd stage) mounted on the north panel of the spacecraft is used for cooling the patch temp. on which infrared detectors are mounted. The passive thermal cooler and heater control system design shall maintain the IR detector temperature within ± 0.25°K of the operating temperature 105°K over any portion of the 7 year life time.

VHRR Electronics Package:

Figure 10 is a block diagram of the VHRR instrument. The output signals from the visible detectors and the infrared detector are amplified by amplifiers (separate amplifier for each of the ten detectors) and filtered to the appropriate bandwidth by low-pass filters. Each channel signal after digitization is combined with redundant PN noise generator followed by signal drivers which provide the digital data output to the spacecraft.

During operation, #1 power supply is operative and it powers the normal set of detectors, amplifiers and data processing circuits. Power supply #2 powers the redundant set of detectors, amplifiers and data processing circuits. An additional redundancy feature has been included in that the output from any one from each of the four pairs of visible detectors can be selected. In order to operate in this redundant mode both power supplies must be powered.

On-board instrument calibration in the IR channels provides a cold space reference that occurs at the end of each scan line and the second calibration point when the scan mirror observes the black body surface in the instrument optical cavity once during each normal scan sequence. To ensure the linearity and accuracy of the electronic data channels, an electronic calibration circuit has also been included in the system.

3.3.3 Structure

The structural design takes care of all direct and cumulative load combinations occuring during spacecraft testing, transportation and handling, launch and orbital maneuvers. Both Delta and STS environments have been considered. The structural elements for INSAT-1 spacecraft are shown in figure-11. Central thrust tube cylinder and cone are of Berrylium and supports two horizontal and three vertical honeycomb panels. Lower cone and ring configuration is dictated by PAM interface. The single pressurant tank is supported on a truss arrangement mounted on the cylindrical portion of the tube assembly and laterally supported by a strut connected to an adjacent equipment panel.

The mechanisms used to deploy the C, C/S band reflectors and solar array are based on already qualified designs. The boom is packaged into a cylindrical container and mounted on the North equipment panel. In the stowed configuration, the solar sail will be collapsed flat against the side of the satellite and be restrained during launch. The ground command will uncage the boom and sail from the satellite and a motor driven system will release the sail at a controlled rate.

3.3.4 Attitude & Orbit Control System (AOCS)

Three axis stabilisation system has been chosen for INSAT-1. The overall requirements for AOCS from mission point of view are

1) VHRR imaging stability:
    - Short term stability of 0.2 visible pixel for line to line registration in a period of 2.2 seconds i.e. 0.0008°/2.2 seconds.
    - Long term stability of 1.3 visible pixel between a frame and the next subsequent frame in a period of about 30 minutes i.e. 0.0044° for half an hour duration.
2) Communication Antenna pointing accuracy:
    - Pitch ± 0.2°, Roll ± 0.2°& Yaw ±0.4°
3) Orbital positional error in geostationary orbit:
    - Longitudinal ± 0.1°, Latitudinal ±0.1°

Longitudinal and latitudinal errors directly translate into Roll and Pitch errors of 0.017° each, and a worst case yaw error of 0.1° at nodal crossings . Excluding satellite alignments and thermal distortion effects, the net pointing accuracy requirements during normal and station keeping mode of AOCS operations for communications mission must not exceed Pitch ± 0.14°, Roll ± 0.1°&Yaw ± 0.32°.

Obviously of the two requirements i.e. communication and VHRR missions, the stability requirements for the later are more demanding. The VHRR overall requirements also include the scan repeatability. The present implementation scheme of the AOCS systems predicts a frame to frame stability of 1.3 visible pixel achievable by inhibiting the movement of the solar panel and any thruster firing during the picture taking process for one full frame (23 minutes).

Temperature constraints on the VHRR cooler dictate one sided solar array. For compensation of solar torque in order to meet attitude stability and to avoid excessive propellant usage a solar sail with long boom (9.4 m) is incorporated. Unbalance in torque due to seasonal variation andthe degraded surface properties of the sail over the life time has been compensated by a magneto-torquer comprising of a current carrying single coil maintained inside the spacecraft and oriented normal to Z axis.

AOCS operating modes are

- o Nutation damping:
  - * Only for shuttle launch prior to PAM burn.
- o Transfer orbit mode including three axis acquisition and apogee boost operations:
  - * Provide automatic despin after PAM separation using ARA(Angular Rate Gyro Assembly)
  - * Provide automatic sun acquisition with -X Roll axis pointed towards the sun and continue Roll rate of 0.75°/sec till earth acquisition.
- o Normal on-orbit:
  - * Attitude control using earth sensor and wheel. Provides stable on-orbit control of satellite attutude for VHRR imaging and communication antenna pointing. Also unloads wheels using magnetotorquer and thrusters as required and steps solar array between VHRR frames.
- o Station keeping:
  - * Attitude control using earth sensor, sun sensors & thrusters. Performs north-south and east-west orbit maneuvers while maintaining satellite in earth centroid pointing.

The AOCS scheme showing various operating modes is shown in figure 12.

3.3.5 Propulsion

The choice of bi-propellant propulsion system for INSAT-1 over the solid propulsion apogee motor and hydrazine auxillary propulsion system has resulted in:

- reduction in total propulsion fuel (in view of higher specific impulse)
- Flexible configuration resulting from ability to store propellant for the different mission phases in common tankage.
- Reduced loading environment, i.e. peak acceleration on spacecraft component resulting from increasing time of apogee burn (approx.50 minutes vs. typical solid apogee motor burn of less than one minute).
- Capability to restart apogee motor;

Two titanium propellant tanks pressurised with Helium regulated from 3000 psi during apogee burn and then operating in a "blow down" mode during the remainder of the mission contain N_2O_4 and MMH as propellant. One 445N thruster and twelve 22N attitude and orbit control thrusters provide all necessary incremental velocities and reaction torques for all phases of the mission. The elements of propulsion subsystem are shown in figure 13.

3.3.6 Telemetry, Tracking and Command (TT&C)

The TTC subsystem shall operate in C band (6/4 GHz) in all phases of the mission. The normal on-orbit telemetry operation shall be through communications subsystem antenna while command functions for all phases and Telemetry operations in Transfer orbit phase shall be exercised through two separate horn antenna mounted on Earth viewing and Anti-Earth viewing faces of the satellite. Capability is also provided to receive selected commands from and Telemetry baseband data to STS data processing equipments when the spacecraft is installed in the STS bay.

Link design performance analysis give ranging error below 50 m, command BER of 10^{-6} and Telemetry BER of 10^{-4} (Considering MCF, Hassan station will have receive G/T ≈31.7dB/°K and transmit EIRP Max 85 dBw).

Table-3 INSAT-1 TTC characteristics

Command	
Frequency (MHz)	
Channel 1	6258
Channel 2	6262
Modulation	PCM-FSK-FM
Carrier dev.(KHz)	± 400
Data Rate (b/s)	100 ± 2%
RF Bandwidth (MHz)	1.5
G/T (dB/K) (Min.)	-44
Telemetry	
Frequency (MHz)	
Channel 1	4031
Channel 2	4039
Modulation	PCM-PSK-PM
Carrier dev.(radians)	1 ± 0.1
Subcarriers(KHz)	
PCM/PSK	32.0
Data Rate (b/s)	1000
Main frame rate	0.512 sec/frame with Dwell mode cap.
Frame format	64 words (8 bits word length)
EIRP (dBw)	11 dBw max. for sync.orbit.

Ranging	
Modulation	
Uplink	FM
Downlink	PM
Range Tones (KHz)	
No.1	27.777 or 19.000
No.2	3.968
No.3	0.2834
Carrier dev.	
Uplink (KHz)	± 400
Down link (radians)	1 ± 0.1

3.3.7 Electrical Power Subsystem

A single axis sun oriented solar array of 5 panels, two 12 AH (28 series connected cells) Nickel-cadmium batteries, Power Control and Integration electronics, and DC/DC converters are the major elements of the electrical power subsystem shown in figure 14.

Battery supplies the load requirements prior to partial deployment of solar panels, during eclipse periods occuring at all phases of mission life and supports partial load during transfer orbit phase (from about To + 4hrs. to To + 6 hrs.), if it is near winter solistice launch as shown in Power Profile figure 15.

Some design features of solar array and its predicted performance and battery assembly characteristics are shown in Table-4 and Table-5 respectively.

Two independent primary buses are provided and each out of solar array main circuits is independently limited to 42 ± 0.5 V.d.c. by use of sequential linear, partial shunt regulators controlled by Power Control and integration electronics (Table-6). The DC/DC converters located in subsystem modules provide regulated, isolated output voltages as required by individual spacecraft subsystems.

Table-4 Design Features of Solar Array

Total Array Area	$11.3\ m^2$
Number of panels	5
Solar cell	1.85x4.1x0.02 cm. K 4.75 Si n/p, shallow junction withBSR
Main array circuits provide:	2 primary bus.
o Primary bus (1)	48 parallel by 127 series cells.
o Primary bus (2)	55 parallel by 127 series cells.
o Total power at the end of 7 years	903 w at summer solstice.
Charge array circuits provide	Charging current for two battery sets.
o For each battery	6 parallel by 11 series cells.
o Current at 7 years	1.55 Amps at summer solstice.

Table-5 Battery Assembly Design Characteristics

No. of batteries	1 per bus
No. of Ni-Cd cells	28 per battery
Cell capacity @ +20°C	12 AH
Max DOD @ +20°C	55%
Nominal discharge current at 33.6V	5.5 Amp.
Continuous charging current (Equinox)	1.23 to 1.29Amp. (Charge). 0.31 to 0.26Amp. (Trickle charge).
Operating temp. range	1° to + 5°C

Table-6 Primary Bus Characteristics

Power output	150 to 1050w (total) divided between two buses.
Bus voltage range	Voltage limited to 42±0.5V DC(sunlight); Battery voltage 26 to 42.0 V dc(durg.eclipse)

3.3.8 Thermal

Temperature control of the INSAT-1 satellite accomplished by conventional passive technique augmented with flight-proven heater elements for components having relatively small allowable temperature ranges meets component performance requirements from launch through a 7 year mission life.

A summary of the thermal control subsystem design key features is as follows:

* Passive thermal control augmented by redundant heaters resulting in low mass and high reliability.
* The design employs optical solar reflector (OSR) radiators, multilayer insulation , and selected finishes for internal radiative coupling and energy sharing, resulting in the smallest satellite internal temperature variation with the change in mainbody energy dissipation from sunlight to eclipse conditions.
* The thermal protection system employed for the C-band and C/S band antenna reflectors is white paint.

Thermal loads at various mission phases:

Pre-launch conditions for either DELTA or STS are airconditioning with temperature range 22° to 28°C and humidity less than 60%.

Delta Launch to Fairing Jettison:

Fairing interior is limited to a max. wall temp. of 160°C with an emittance ≤ 0.1

Fairing Jettison to Spacecraft Separation:

Following fairing jettison, the spacecraft is subjected to solar, earth albedo, earth emission heating and aerodynamic heating. Earth albedo may be considered to have 0.3 ± 0.02 avg. reflectivity. The earth emission is equivalent to a 288°K black body with a value of $237 \pm 7 w/m^2$. Aerodynamic heating shall be below 0.028 $cal/s/cm^2$. The heating rate from the PAM rocket motor case and plume to the spacecraft shall be below 0.1 $cal/s/cm^2$.

Transfer Orbit:

Sun angles measured from east/west axis in north/south plane are restricted from 0° to ±48° with no eclipse periods allowed until past initial apogee burn.

Synchronous orbit:

In the sync. orbit, the spacecraft is subjected to yearly variations in the spacecraft-sun angle between +23.5° (at summer solstice) to -23.5° (at winter solstice). At angles between ± 8°, the spacecraft is subjected to eclipses of the sun with a max. eclipse duration of 1.2 hours at equinox.

STS Launch

Satellite is protected from orbiter cargo wall environment by PAM and a heater controlled protective cover. The design takes care of the thermal load on the spacecraft spinning about its east/west axis for about 45 minutes after STS insertion of the spacecraft with PAM in parking orbit.

Solar Sail:

The thermal design of the solar sail was constrained by three major considerations.

a) Maximise specular reflective surface for max. solar pressure effectiveness.
b) Minimise incident energy on VHRR cooler aperture.
c) Minimise incident energy to north panel of spacecraft from solar sail.

A closed cylinder constructed essentially of aluminised teflon with a Kapton(Polymide) backing for constraint 'a'.

Constraint 'b' was taken care of by geometry, i.e. the conical bottom of sail and the supporting boom which is placed far enough away present a small view factor to the cooler aperture. The total energy to the cooler under worst case conditions is about 40 mw.

Constraint 'c' was handled by placing sail in such a position that minimum solar energy is reflected from sail to north panel, providing a low emittance source of IR energy from sail bottom and by constructing sail bottom as a cone so that no IR energy emitted from north panel can reflect back to panel. The solar sail benefits the spacecraft during transfer orbit by covering a major portion of the north panel OSRs radiating areas thereby attenuating energy loss to space.

4. Master Control Facility

Master Control Facility(MCF) for INSAT-1 is to be located at Hassan near Bangalore which will be the major element of the Ground Control System to support INSAT Satellite operations. INTELSAT network will provide TT&C support during transfer orbit phases when satellite is not in view of Hassan. MCF will consist of two Satellite Control Earth Stations (SCES) with fully redundant systems and Spacecraft Control Centre (SCC) co-located with SCES having two computers and other equipments for supporting transfer orbit operations and two satellites in orbit simultaneously.

The interface between SCES and SCC will be through 70 MHz IF signal. Within MCF Complex which is on about 31.5 acres of land, there is Power Complex, Air-conditioning Plant, 2 antenna mount for 14M dia. steerable antenna and buildings for housing SCC and SCES equipments. The entire MCF system as shown in figure 16 has adequate redundant equipments and is designed for an estimated availability of 0.9999.

Each SCES will include a fully steerable 14M dia parabolic antenna dish with Cassegrain mono-pulse feed, Low Noise Amplifiers, Up and Down converters, Transmitters, Switching and combining networks, SCC interface equipments, Test loop translators, SCES control console and test equipments. In addition to the above, one of the SCES will include 6.1M dia. parabolic antenna with S-band receive system only and also a reference Data Collection Unit.

The SCC will include Computers, Command generators, Telemetry processors and ranging subsystems. In addition, recording, timing subsystems with SCC Control console and status display system, VHRR quick look evaluation equipments, test equipments and communication facilities will be part of SCC. Most of the SCC operations are carried out from a control console located within each SCC. Each control console contains CRT/ANK terminals which allow direct computer interface for the real-time operations control and monitor of satellite and ground equipment.

4.1 SCES - Satellite Interfaces

The SCES will interface with the satellite in the following frequency bands:

- C-band (4 GHz) reception of FSS, Telemetry, ranging, DCP data and VHRR data signals;
- S-band (2.5 GHz) reception of BSS, FM Broadcast TV channels;
- C-band (6GHz) transmission of FSS, BSS, command, ranging signals.
- UHF (400 MHz) transmission of data collection platform (DCP) signals.

C-band Downlink:

The characteristics of the C-band Down link RF signals are defined in Table-7.

S-band Downlink:

The characteristics of S-band Downlink RF signals are defined below:

Center Frequency	: 2575 MHz, 2615 MHz
Polarization	: LHCP, Axial Ratio < 3.0dB
EIRP	: 42 dBw min.
Required Ground Eqpt.	
Bandwidth(RF)	: 80 MHz (nominal)
Data Bandwidth	: 36 MHz(Usable per chan.)
G/T (SCES)	: 13.4 dB/°K
Modulation type	: FM
Modulation	: FM Dev. 18MHz pk.to pk.
Frequency Stability	: ± 60 KHz (Long term)

C-Band Uplink:

C-Band Uplink will comprise of 12 FSS channels, command and ranging signals. The characteristics of these RF signals are defined in Table-8.

DCP Uplink:

The DCP Uplink has RF characteristics as defined below:

Frequency	: 402.65 MHz to 402.85MHz
Polarization	: LHCP, Axl.ratio < 3.0 dB max.
Illum.levels at Satellite:	: a)-153 dBw/m^{2}min.(1DCP) b)-125 dBw/m^{2}min.(Saturation)
G/T (receive Satelt.)	: -19 dB/°K
Required Ground Eqpt.	
Bandwidth (RF)	: 200 KHz
Data Bandwidth	6 KHz
EIRP	: 20 dBw (approx.)

Modulation Type : PCM-(NRZ)-PSK(Biphase)
Modulation : Phase dev. 0° and 180°
Frequency stability : 1 in 10^7 per day

4.2 Antenna

Antenna system consists of

- One 6.1m dia. parabolic reflector with composite feed for S-band reception and transmission of UHF DCP signal.
- Two 14m dia. parabolic reflector for C-band operations.

C-band antenna:

The two solid parabolic reflectors each of about 14M diameter have mechanical steering capabilities. The drive system is servo controlled and backlash in the drive system is minimised by counter torque arrangement. The essential parameters are:

Mount	EL over AZ.
Antenna Dia.	14M parabolic dish.
Feed	Cassegrain with monopulse tracking capabilities.
Coverage	AZ$\pm$ 270°, EL 0°to 90°

Tracking:
a) Speed about each axis: 1°/sec.max.
b) Acceleration about each axis:$0.2^\circ/\mathrm{sec}^2$

Slew:

a) Speed about each axis : 2°/sec
b) Acceln.about each axis:$1^\circ/\mathrm{sec}^2$

Tracking error	0.04° rss peak
Pointing error	0.08° rss peak
Antenna gain	
a) Transmit	56.0 + 20 log f/6 dB.
b) Receive	53.0 + 20 log f/4 dB.
Receive G/T	31.7 dB/°K at 4GHz @ 5°EL.
Polarisation:	
a) Communication	Rotatable linear with option to circular of either sense.
b) Tracking	Circular.

DCP & S-Band Antenna

Antenna	6.1M dia. parabolic chicken mesh reflector.
Antenna mount	X - Y
Frequency	2555 to 2635 MHz & 400 MHz.
Gain	41.8 dB at 2.6GHz & 22 dB at 402.75 MHz.
Polarization	LHCP, axl.ratio <3 dB.
Receive G/T	13.4 dB/°K at 2.6 GHz.

4.3 MCF Power System

The Power Supply system for MCF is designed to cater for the power requirements of two SCES and one SCC. MCF shall operate on 3 phase, 4 wire, 415V, 50Hz. The corresponding single phase voltage of 240 volts is also available for equipments supply.

The load for power supply system has been divided into three categories.

No-break Load:

Comprising of the electric equipments for telecommand, telemetry, ranging and tracking including SCC computer, static inverters, lead acid battery banks and rectifiers which would not suffer any break even if the commercial supply fails. Total capacity provided in this category is 80 KVA in each SCES and SCC.

Short-break Load:

Antenna drive system, test equipments, airconditioning plant etc. have been included in this category. About 40 seconds will be lapsed for the Standby Diesel operated Generators to take over load in the event of failure of commercial power supply. SCES and SCC each will be provided with 310 KVA capacity standby diesel generating sets to meet short break load requirements.

Restoration Load

Comprising of Station utility loads which can be off till the main supply is restored.

4.4 Communication Network:

The telecommunication link facilities required for INSAT-1 Master Control Facility broadly fall under two categories:

1) Link on a permanent basis:
MCF-Network Operation and Control Centre (NOCC) of P&T (Delhi)- Bangalore.
2) Short-term requirements during the launch phase - for about one month before and after the actual launch.

The permanent link will have following facilities:

* Two dedicated voice channels between MCF and NOCC, Delhi
* Two dedicated voice channels between MCF and Bangalore (SSPO).
* Two dedicated 50 Baud Tele-type channels between MCF and NOCC, New Delhi.
* Two dedicated 50 Baud Tele-type channels between MCF and Bangalore.

INTELSAT Control Centre/ Washington will be connecting the Remote tracking stations to MCF, Hassan during Launch and orbit raising phases.

5. Acknowledgement:

The paper is based on the design efforts by the Ford Aerospace & Communications Corpn., of U.S.A. for the INSAT-1 Spacecraft and SCC related equipments of MCF and also on the design of SCES equipments by Space Applications Centre (SAC), ISRO, Ahmedabad, India. The author thanks Dr.K.P.M.Bhat, Mission Operations Manager and Mr.V.K.Kaila of INSAT-1 SSPO for valuable suggestions, and Mr.P.P.Kale, Project Director for the permission to publish the paper.

Reference

1. T.Parthasarathy and M.K.Saha "A Domestic Satellite for India" JBIS (UK), pp-801-810 Vol.27, No.11, Nov.1974.

TABLE 7 C-BAND DOWN LINK

	SIGNAL TYPE				
	TLM	RANGING	VHRR	DCP	FSS
Center Frequency (GHz)	CH #1 4.031 CH #2 4.039	CH #1 4.031 CH #2 4.039	4.03455	4.0381	3.73 to 4.18
Polarization	Transfer Orbit TX #1 +Yaw RHCP -Yaw LHCP TX #2 +Yaw LHCP -Yaw RHCP Synchronous Orbit TX #1 and TX #2 Linear (Horizontal Polarization) Axial Ratio >20 dB	Transfer Orbit TX #1 +Yaw RHCP -Yaw LHCP TX #2 +Yaw LHCP -Yaw RHCP Synchronous Orbit TX #1 and TX #2 Linear (Horizontal Polarization) Axial Ratio > 20 dB	Linear (Hozizontal Polarization) Axial Ratio >20 dB	Linear (Horizontal Polarization) Axial Ratio >20 dB	Linear (Horizontal Polarization) Axial Ratio >20 dB
EIRP	Trans Orbit - 11.1 to +1.9 dBW See note 3 Synch +5.0 dBW	Trans Orbit - 11.1 to +1.9 dBW See note 3 Synch +5.0 dBW	8.5 dBW min. 12.5 dBW max.	Composite Illum.: 19.0 dBW (minimum) Single DCP: -2.0 dBW (minimum)	32.0 dBW min 34.0 dBW max.
Ground Equipment Bandwidth (RF)	> 270 kHz	> 270 kHz	> 880 kHz	> 280 kHz	500 MHz
RF Data Bandwidth	68 kHz	68 kHz	800 kHz (First Spectrum Zero)	200 kHz	36 MHz (Usable per Channel)
SCES G/T (Receive)	31.7 dB/°K	31.7 dB/°K	31.7 dB/°K	31.7 dB/°K	31.7 dB/°K
Modulation Type Modulation	PCM-Bi0-PM 1.0 Mod. Index PCM 1.0 kb/s	FM 1.0 Mod. Index (2)	PCM-NRZ-L-Bi0 400 kbps	TBS (DOS)	FDM-FM Voice, FM Monochrome or Color TV, MA SCPC
Frequency Stability	Satellite: ±25 parts in 10^6 (long term) ±55 kHz Doppler (Transfer Orbit)	Satellite: ±25 parts in 10^6 (long term) ±55 kHz Doppler (Transfer Orbit)	Satellite: < ±40 kHz (Long term life & Temp) < ±6 kHz Drift (one month)	Satellite: < ±40 kHz (Long Term life & Temp) < ±6 kHz Drift (one month) < 30 Hz rms in 100 Hz to 12 kHz Band DCP: TBS (DOS)	Satellite: < ±40 kHz (Long Term life & Temp) < ±4 kHz Drift (one month) < 30 Hz rms in 100Hz to 12 kHz Band < 20 hZ rms in 300Hz to 3400 Hz Band

TABLE 8 C-BAND UPLINK

PARAMETER	SIGNAL TYPE			
	COMMAND	RANGING	FSS	BSS
Center Frequency (GHz)	CH #1 6.258 CH #2 6.262	CH #1 6.258 CH #2 6.262	5.935 to 6.425	5.875, 5.915
Polarization (Satellite Receivers)	Receiver #1 +YAW RHCP -YAW LHCP Receiver #2 +YAW LHCP -YAW RHCP	Receiver #1 +YAW RHCP -YAW LHCP Receiver #2 +YAW LHCP -YAW LHCP	Linear (Vertical Polarization) axial ratio >20 dB	Linear (Vertical Polarization) axial ratio >20 dB
Input Flux Density (at Satellite)	Operating -92 dBW/M^2 to -72 dBW/M^2 Max -50 dBW/M^2	Operating -92 dBW/M^2 to -72 dBW/M^2 Max -50 dBW/M^2	-92 dBW/M^2 to -70 dBW/M^2	-92 dBW/M^2 to -70 dBW/M^2
Satellite Equipment Bandwidth (RF)	> 1.6 MHz	> 1.6 MHz	> 570 MHz	> 570 MHz
Data Bandwidth	> 850 kHz	> 850 kHz	36 MHz (Usable per channel)	36 MHz (Usable per channel)
G/T (Receiver)	-44 dB/°K min	-44 dB/°K min	-6 dB/°K	-6 dB/°K
Modulation Type	PCM-FSK-FM	FM	FCM-FM Voice, FM Monochrome or color TV, MA SCPC	FM
Modulation	PCM Rate 100 b/s carrier deviation ±400 kHz Tones (kHz): One - 24.4 Zero - 25.2 (side 1) & 26.0 (side 2) Execute - 26.8	Carrier Deviation ±400 kHz Ranging Tones: 27.778 kHz 4.003 kHz 3.968 kHz 0.2834 kHz	TBS (DOS)	TBS (DOS)
EIRP	75 dBW to 85 dBW	75 dBW to 85 DBW	75 dBW to 85 dBW	75 dBW to 85 dBW
Frequency Stability	MCF: 1 part in 10^7/day ±85 kHz Doppler (Transfer Orbit)	MCF: 1 part in 10^7/day ±85 kHz Doppler (Transfer Orbit)	MCF: 1 part in 10^6/day	MCF: 1 part in 10^6/day

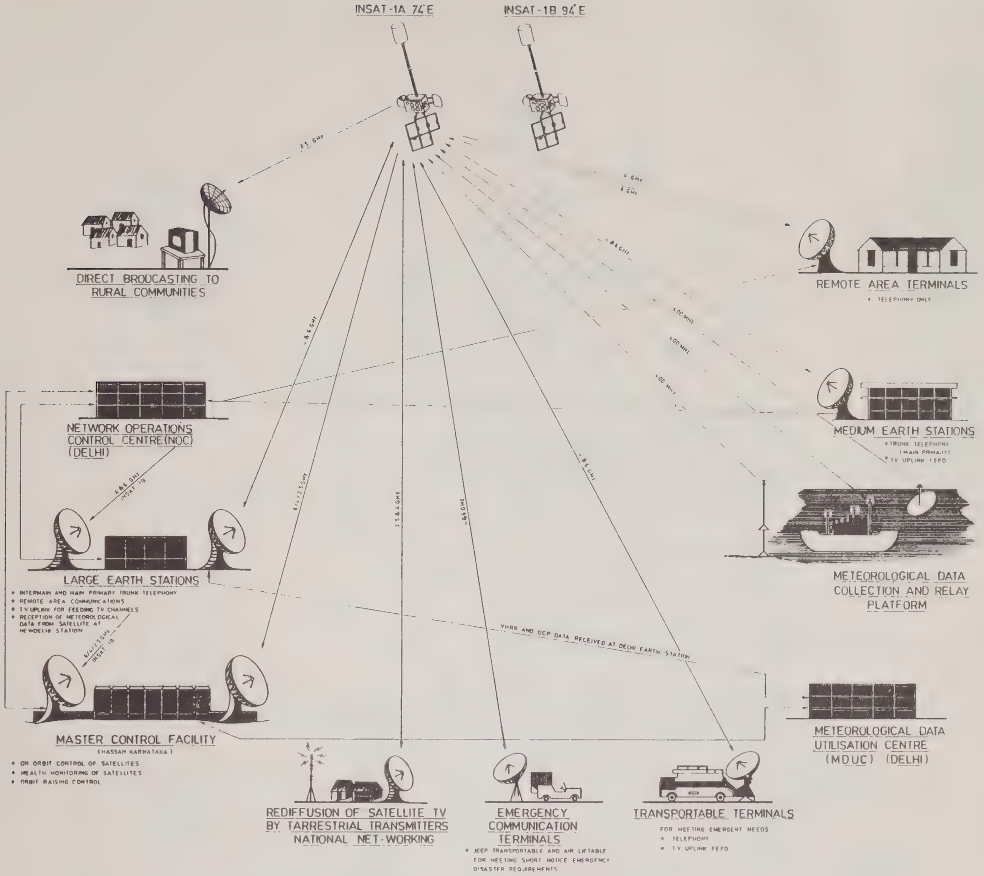
INSAT-1A 74°E
INSAT-1B 94°E
2.5 GHz
4 GHz
6 GHz
4 & 6 GHz
400 MHz
400 MHz
400 MHz
4 & 6 GHz
6/4/2.5 GHz
2.5 & 4 GHz
4 & 6 GHz
4 & 6 GHz
DIRECT BRODCASTING TO RURAL COMMUNITIES
REMOTE AREA TERMINALS
• TELEPHONY ONLY
NETWORK OPERATIONS CONTROL CENTRE (NOC) (DELHI)
MEDIUM EARTH STATIONS
• TRUNK TELEPHONY (MAIN PRIMARY)
• TV UPLINK FEED
4 & 6 GHz INSAT 1B
LARGE EARTH STATIONS
• INTERMAIN AND MAIN PRIMARY TRUNK TELEPHONY
• REMOTE AREA COMMUNICATIONS
• TV UPLINK FOR FEEDING TV CHANNELS
• RECEPTION OF METEOROLOGICAL DATA FROM SATELLITE AT NEWDELHI STATION
METEOROLOGICAL DATA COLLECTION AND RELAY PLATFORM
6/4/2.5 GHz INSAT 1B
VHRR AND DCP DATA RECEIVED AT DELHI EARTH STATION
MASTER CONTROL FACILITY
(HASSAN KARNATAKA)
• ON ORBIT CONTROL OF SATELLITES
• HEALTH MONITORING OF SATELLITES
• ORBIT RAISING CONTROL
METEOROLOGICAL DATA UTILISATION CENTRE (MDUC) (DELHI)
REDIFFUSION OF SATELLITE TV BY TARRESTRIAL TRANSMITTERS NATIONAL NET-WORKING
EMERGENCY COMMUNICATION TERMINALS
• JEEP TRANSPORTABLE AND AIR LIFTABLE FOR MEETING SHORT NOTICE EMERGENCY DISASTER REQUIREMENTS
TRANSPORTABLE TERMINALS
FOR MEETING EMERGENT NEEDS
• TELEPHONY
• TV UPLINK FEED

FIG-1 INSAT-1 SYSTEM CONCEPT

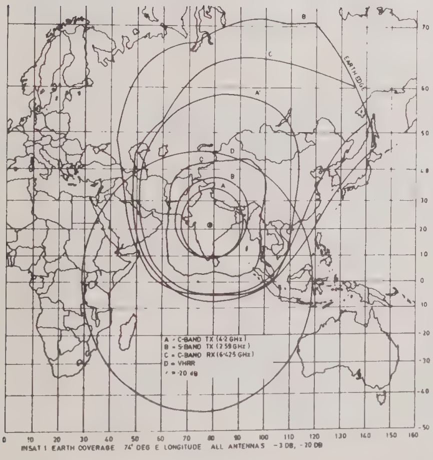
A
B
C
D
A'
EARTH EDGE
70
60
50
40
30
20
10
0
10
-20
-30
-40
-50
0
10
20
30
40
50
60
70
80
90
100
110
120
130
140
150
160
A = C-BAND TX (4.2 GHz)
B = S-BAND TX (2.59 GHz)
C = C-BAND RX (6.425 GHz)
D = VHRR
' = -20 dB
INSAT 1 EARTH COVERAGE 74° DEG E LONGITUDE ALL ANTENNAS -3 DB, -20 DB

FIG. 2. INSAT-1 EARTH COVERAGE (74° LONGITUDE)

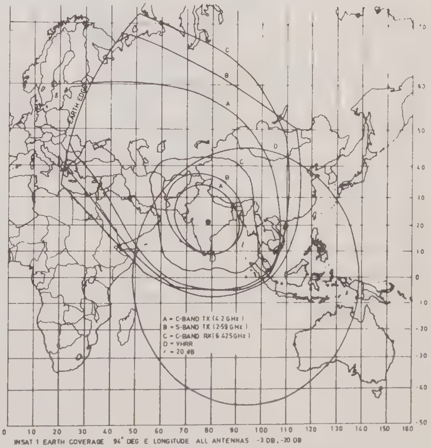
A
B
C
D
EARTH EDGE
70
60
50
40
30
20
10
0
10
-20
-30
-40
-50
0
10
20
30
40
50
60
70
80
90
100
110
120
130
140
150
160
A = C-BAND TX (4.2 GHz)
B = S-BAND TX (2.59 GHz)
C = C-BAND RX (6.425 GHz)
D = VHRR
' = -20 dB
INSAT 1 EARTH COVERAGE 94° DEG E LONGITUDE ALL ANTENNAS -3 DB, -20 DB

FIG-3. INSAT-1 EARTH COVERAGE (94°E LONGITUDE)

EVENT NO.	DESCRIPTION
1	LAUNCH (T_0)
2	JETTISON FAIRING (T_0+240 SEC)
3	TRANSFER ORBIT INJECTION (T_1)
4	SEPARATION (T_1+2 MIN)
5	SPIN DOWN TO 5°/SEC (T_1+2 MIN+2 SEC
6	RATE DAMPING AND SUN ACQUISITION (T_1+3 MIN)
7	ESTABLISH TT&C WITH BANGALORE (T_1+20 MIN)
8	VERIFY SUN ACQUISITION (T_1+30 MIN)
9	SOLAR ARRAY PARTIAL DEPLOYMENT C-BAND ANTENNA DEPLOYMENT (T_1+40 MIN)
10	EARTH ACQUISITION IN ROLL (T+120 TO T+195 MIN)
11	REORIENTANTION ACS STATION KEEPING MODE WITH SUN ANGLE BIAS (T_1+240 MIN)
12	ATTITUDE REORIENTATION (T_1-270 MIN
13	FIRST AMFIRING WITH 445N THRUSTER FOR 54 MIN (T_2=T_1+288 MIN.
14	END FIRING (T_2+54 MIN)
15	SOLAR ARRAY & SAIL DEPLOYMENT (T_2+60 MIN)
16	START WHEEL SPIN UP NORMAL 3 AXIS MODE (T_2+85 MIN)
17	ECLIPSE (< 73 MIN) (T_2+308 MIN)
18	ORBIT & ATTITUDE DETERMINATION (T_2+2 TO T_2+22 HRS
19	REORIENTATION ACS STATION KEEPING MODE WITH SUN ANGLE BIAS (T_2+23 HRS)
20	SECOND AMFIRING WITH 2 X 22N THRUSTERS FOR 20 MIN (T_3=T_2+23·5 HRS)
21	S BAND ANTENNA DEPLOYMENT (T_3+25 MIN)
22	STATION ACQUISITION (T_3+1 MONTH)

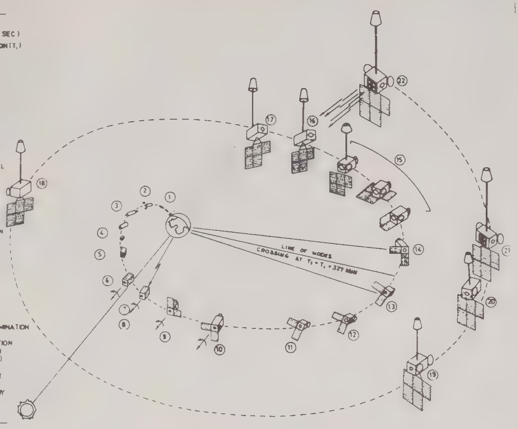
LINE OF NODES
CROSSING AT T_2 = T_1 + 327 MIN
①
②
③
④
⑤
⑥
⑦
⑧
⑨
⑩
⑪
⑫
⑬
⑭
⑮
⑯
⑰
⑱
⑲
⑳
㉑
㉒

FIG-4, INSAT-1 SATELLITE MAJOR MISSION EVENTS

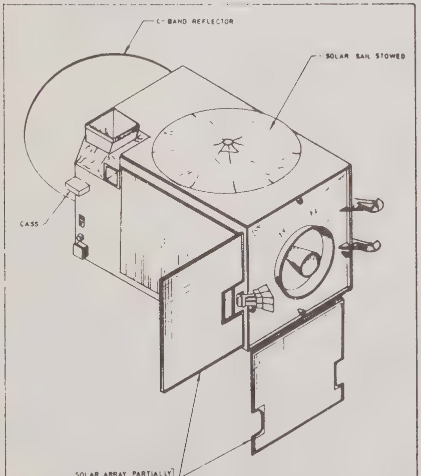
C-BAND REFLECTOR
SOLAR SAIL STOWED
CASS
SOLAR ARRAY PARTIALLY DEPLOYED

FIG-6, INSAT-1 TRANSFER ORBIT CONFIGURATION

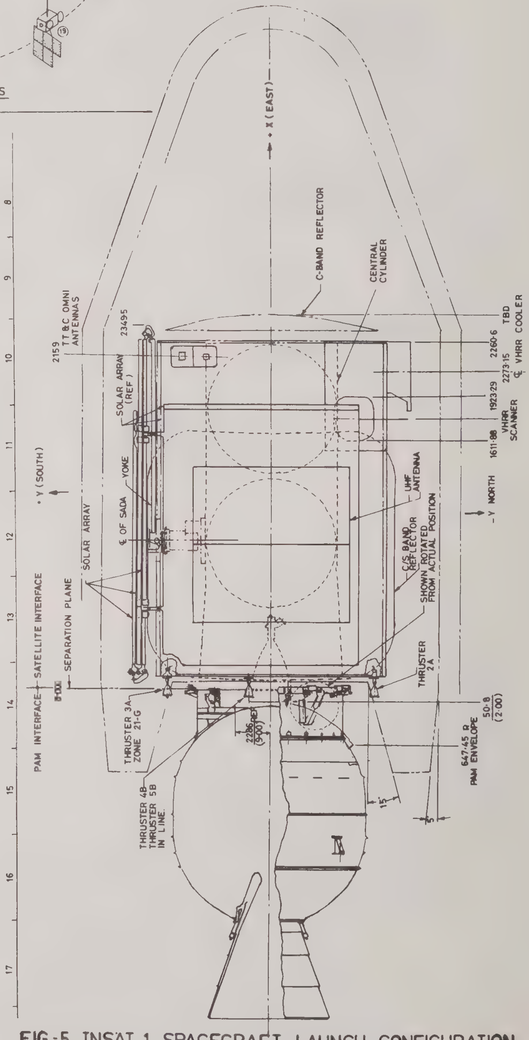
+X (EAST)
C-BAND REFLECTOR
CENTRAL CYLINDER
TBD
2260·6
2273·15 ℄ VHRR COOLER
1923·29
VHRR SCANNER
1611·88
UHF ANTENNA
-Y NORTH
C/S BAND REFLECTOR SHOWN ROTATED FROM ACTUAL POSITION
THRUSTER 2A
50·8 (2·00)
647·45 R PAM ENVELOPE
TT&C OMNI ANTENNAS
2159
23495
SOLAR ARRAY (REF)
YOKE
℄ OF SADA
SOLAR ARRAY
+Y (SOUTH)
PAM INTERFACE
SATELLITE INTERFACE
SEPARATION PLANE
THRUSTER 3A ZONE 21-G
2286 (9·00)
THRUSTER 4B THRUSTER 5B IN LINE
8
9
10
11
12
13
14
15
16
17

FIG-5, INSAT-1 SPACECRAFT LAUNCH CONFIGURATION (DELTA)

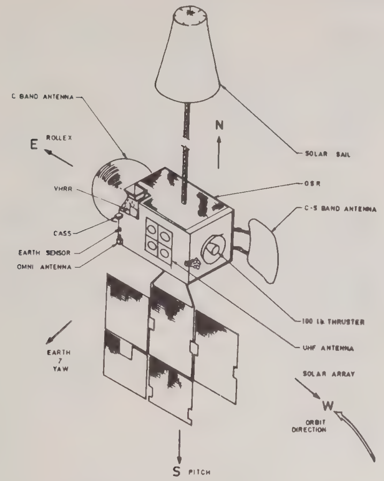
C BAND ANTENNA
ROLLEX
E
N
SOLAR SAIL
OSR
C-S BAND ANTENNA
VHRR
CASS
EARTH SENSOR
OMNI ANTENNA
100 lb THRUSTER
UHF ANTENNA
EARTH
YAW
SOLAR ARRAY
W
ORBIT DIRECTION
S PITCH

FIG-7 INSAT-1 ON ORBIT CONFIGURATION

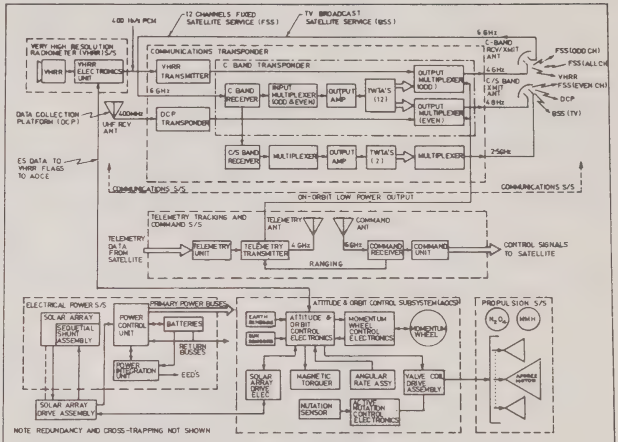
12 CHANNELS FIXED SATELLITE SERVICE (FSS)
TV BROADCAST SATELLITE SERVICE (BSS)
400 kb/s PCM
VERY HIGH RESOLUTION RADIOMETER (VHRR) S/S
VHRR
VHRR ELECTRONICS UNIT
COMMUNICATIONS TRANSPONDER
VHRR TRANSMITTER
C BAND TRANSPONDER
C BAND RECEIVER
INPUT MULTIPLEXER (ODD & EVEN)
OUTPUT AMP
TWTA'S (12)
OUTPUT MULTIPLEXER (ODD)
OUTPUT MULTIPLEXER (EVEN)
6 GHz
4 GHz
4.8 GHz
C-BAND RCV/XMIT ANT
C/S BAND XMIT ANT
FSS (ODD CH)
FSS (ALL CH)
VHRR
FSS (EVEN CH)
DCP
BSS (TV)
DATA COLLECTION PLATFORM (DCP)
400 MHz
UHF RCV ANT
DCP TRANSPONDER
ES DATA TO VHRR FLAGS TO AOCE
C/S BAND RECEIVER
MULTIPLEXER
OUTPUT AMP
TWTA'S (2)
MULTIPLEXER
2.5 GHz
COMMUNICATIONS S/S
ON-ORBIT LOW POWER OUTPUT
TELEMETRY TRACKING AND COMMAND S/S
TELEMETRY ANT
COMMAND ANT
TELEMETRY DATA FROM SATELLITE
TELEMETRY UNIT
TELEMETRY TRANSMITTER
4 GHz
6 GHz
COMMAND RECEIVER
COMMAND UNIT
RANGING
CONTROL SIGNALS TO SATELLITE
ELECTRICAL POWER S/S
SOLAR ARRAY
SEQUENTIAL SHUNT ASSEMBLY
POWER CONTROL UNIT
BATTERIES
PRIMARY POWER BUSES
RETURN BUSSES
POWER INTEGRATION UNIT
EED'S
SOLAR ARRAY DRIVE ASSEMBLY
ATTITUDE & ORBIT CONTROL SUBSYSTEM (AOCS)
EARTH SENSORS
SUN SENSORS
ATTITUDE & ORBIT CONTROL ELECTRONICS
MOMENTUM WHEEL CONTROL ELECTRONICS
MOMENTUM WHEEL
SOLAR ARRAY DRIVE ELEC
MAGNETIC TORQUER
ANGULAR RATE ASSY
VALVE COIL DRIVE ASSEMBLY
NUTATION SENSOR
ACTIVE NUTATION CONTROL ELECTRONICS
PROPULSION S/S
N_2O_4
MMH
APOGEE MOTOR
NOTE REDUNDANCY AND CROSS-TRAPPING NOT SHOWN

FIG-8, SATELLITE SIMPLIFIED BLOCK DIAGRAM

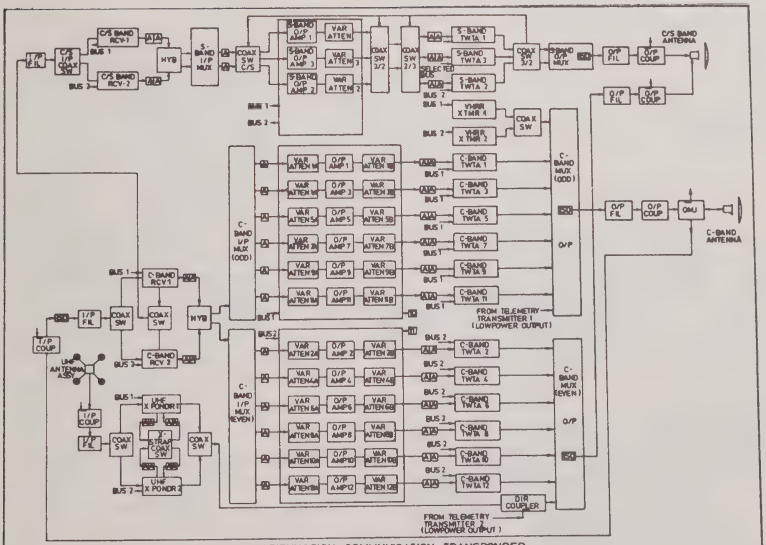
I/P FIL
C/S I/P COAX SW
BUS 1
BUS 2
C/S BAND RCV-1
C/S BAND RCV-2
HYB
S-BAND I/P MUX
COAX SW C/S
S-BAND O/P AMP 1
S-BAND O/P AMP 3
S-BAND O/P AMP 2
VAR ATTEN 1
VAR ATTEN 3
VAR ATTEN 2
COAX SW 3/2
COAX SW 2/3
SELECTED BUS
S-BAND TWTA 1
S-BAND TWTA 3
S-BAND TWTA 2
S-BAND O/P MUX
ISO
O/P FIL
O/P COUP
C/S BAND ANTENNA
VHRR XTMR 1
VHRR XTMR 2
COAX SW
C-BAND I/P MUX (ODD)
VAR ATTEN 1A
O/P AMP 1
VAR ATTEN 1B
C-BAND TWTA 1
C-BAND TWTA 3
C-BAND TWTA 5
C-BAND TWTA 7
C-BAND TWTA 9
C-BAND TWTA 11
C-BAND MUX (ODD)
O/P
OMJ
C-BAND ANTENNA
FROM TELEMETRY TRANSMITTER 1 (LOWPOWER OUTPUT)
C-BAND RCV 1
C-BAND RCV 2
COAX SW
HYB
I/P COUP
UHF ANTENNA ASSY
C-BAND I/P MUX (EVEN)
C-BAND TWTA 2
C-BAND TWTA 4
C-BAND TWTA 6
C-BAND TWTA 8
C-BAND TWTA 10
C-BAND TWTA 12
C-BAND MUX (EVEN)
UHF X PONDR 1
UHF X PONDR 2
X-STRAP COAX SW
DIR COUPLER
FROM TELEMETRY TRANSMITTER 2 (LOWPOWER OUTPUT)

FIG-9 MULTIFUNCTION COMMUNICATION TRANSPONDER

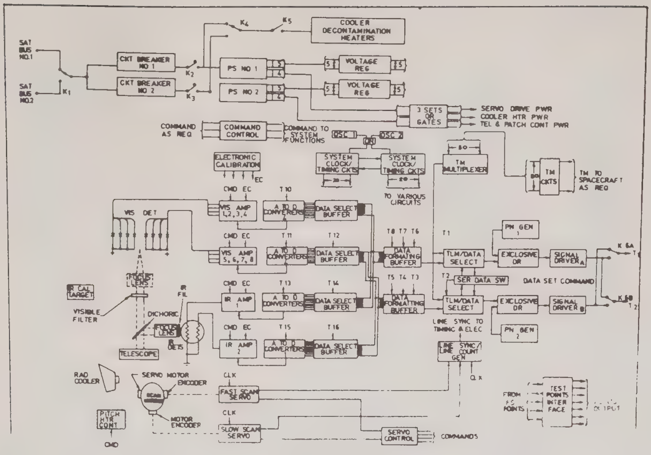
SAT BUS NO.1
SAT BUS NO.2
K1
CKT BREAKER NO 1
CKT BREAKER NO 2
K2
K3
K4
K5
COOLER DECONTAMINATION HEATERS
PS NO 1
PS NO 2
5
4
VOLTAGE REG
VOLTAGE REG
3 SETS OR GATES
SERVO DRIVE PWR
COOLER HTR PWR
TEL & PATCH CONT PWR
COMMAND AS REQ
COMMAND CONTROL
COMMAND TO SYSTEM FUNCTIONS
OSC 1
OSC 2
OR
ELECTRONIC CALIBRATION
EC
SYSTEM CLOCK/ TIMING CKTS
SYSTEM CLOCK/ TIMING CKTS
20
TO VARIOUS CIRCUITS
80
TM MULTIPLEXER
TM CKTS
TM TO SPACECRAFT AS REQ
CMD EC
T 10
VIS DET
VIS AMP 1,2,3,4
A TO D CONVERTERS
DATA SELECT BUFFER
T 11
T 12
VIS AMP 5, 6, 7, 8
T8 T7 T6
DATA FORMATTING BUFFER
T1
TLM/DATA SELECT
PN GEN 1
EXCLOSIVE OR
SIGNAL DRIVER A
K 6A
T
T2
SER DATA SW
DATA SET COMMAND
T5 T4 T3
DATA FORMATTING BUFFER
TLM/DATA SELECT
EXCLOSIVE OR
SIGNAL DRIVER B
K 6B
T 2
PN GEN 2
LINE SYNC TO TIMING & ELEC
LINE SYNC/ LINE COUNT GEN
CLK
FOCUS LENS
IR CAL TARGET
IR FIL
VISIBLE FILTER
DICHORIC
FOCUS LENS
IR DETS
TELESCOPE
T 13
T 14
IR AMP 1
T 15
T 16
IR AMP 2
RAD COOLER
SERVO MOTOR
ENCODER
SCAN
MOTOR ENCODER
FAST SCAN SERVO
SLOW SCAN SERVO
PITCH HTR CONT
CMD
SERVO CONTROL
COMMANDS
FROM S/C POINTS
TEST POINTS INTER FACE
OUTPUT

FIG-10 BLOCK DIAGRAM IVHRR

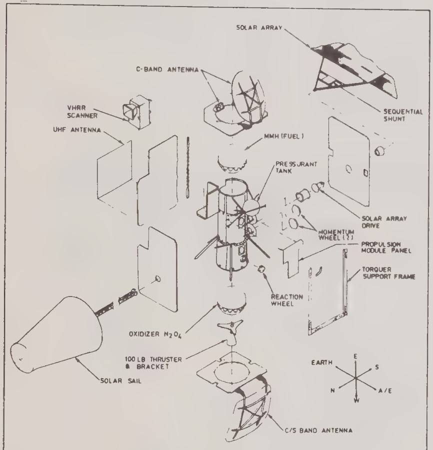
SOLAR ARRAY
C-BAND ANTENNA
VHRR SCANNER
UHF ANTENNA
SEQUENTIAL SHUNT
MMH (FUEL)
PRESSURANT TANK
SOLAR ARRAY DRIVE
MOMENTUM WHEEL (2)
PROPULSION MODULE PANEL
TORQUER SUPPORT FRAME
REACTION WHEEL
OXIDIZER N_2O_4
100 LB THRUSTER & BRACKET
SOLAR SAIL
EARTH
E
S
N
W
A/E
C/S BAND ANTENNA

FIG-11. INSAT-1 SATELLITE INTEGRATION COMPONENTS

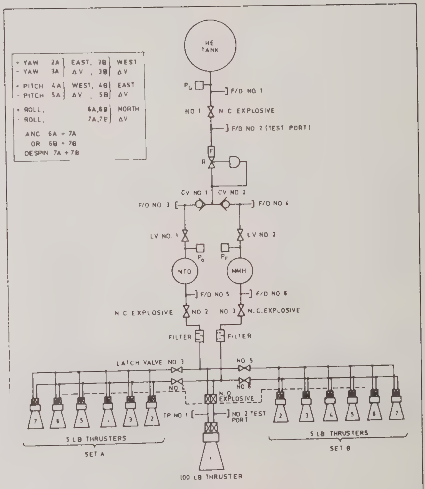
+ YAW 2A
- YAW 3A
EAST, ΔV
2B
3B
WEST ΔV
+ PITCH 4A
- PITCH 5A
WEST, ΔV
4B
5B
EAST ΔV
+ ROLL, 6A,6B
- ROLL, 7A,7B
NORTH ΔV
ANC 6A + 7A
OR 6B + 7B
DESPIN 7A + 7B
HE TANK
P_G
F/D NO 1
NO 1
N C EXPLOSIVE
F/D NO 2 (TEST PORT)
F
R
CV NO 1
CV NO 2
F/D NO 3
F/D NO 4
LV NO. 1
LV NO 2
P_O
P_F
NTO
MMH
F/D NO 5
F/D NO 6
N C EXPLOSIVE
NO 2
NO 3
N.C.EXPLOSIVE
FILTER
FILTER
LATCH VALVE NO 3
NO 4
NO 5
NO 6
N O EXPLOSIVE
TP NO 1
NO 2 TEST PORT
7
6
5
4
3
2
5 LB THRUSTERS
SET A
1
100 LB THRUSTER
2
3
4
5
6
7
5 LB THRUSTERS
SET B

FIG 13 ELEMENTS OF PROPULSION SUBSYSTEM

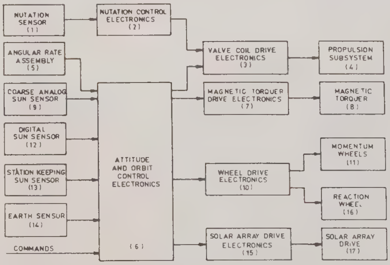
NUTATION SENSOR (1)
NUTATION CONTROL ELECTRONICS (2)
ANGULAR RATE ASSEMBLY (5)
VALVE COIL DRIVE ELECTRONICS (3)
PROPULSION SUBSYSTEM (4)
COARSE ANALOG SUN SENSOR (9)
MAGNETIC TORQUER DRIVE ELECTRONICS (7)
MAGNETIC TORQUER (8)
DIGITAL SUN SENSOR (12)
ATTITUDE AND ORBIT CONTROL ELECTRONICS (6)
MOMENTUM WHEELS (11)
STATION KEEPING SUN SENSOR (13)
WHEEL DRIVE ELECTRONICS (10)
REACTION WHEEL (16)
EARTH SENSOR (14)
SOLAR ARRAY DRIVE ELECTRONICS (15)
SOLAR ARRAY DRIVE (17)
COMMANDS

1 NUTATION DAMPING
ITEMS (1),(2),(3) & (4) ONLY ACTIVE

2 TRANSFER ORBIT INCLUDING THREE AXIS ACQUISITION AND APOGEE BOOST OPERATIONS .
- SUN ACQUISITION
  ITEMS (5),(9),(6),(3) & (4) ONLY ACTIVE
- EARTH ACQUISITION & APOGEE BOOST
  ITEMS (9),(12),(14),(6),(3) & (4) ONLY ACTIVE

3 NORMAL OR ORBIT
ITEMS (14),(6),(3),(7),(10),(15),(4),(8),(11) & (17) ONLY ACTIVE

4 STATION KEEPING
ITEMS (13),(14),(6),(3),(7),(10),(15),(4),(8),(11) & (17) ONLY ACTIVE.

FIG 12 AOCS OPERATIN SCHEME

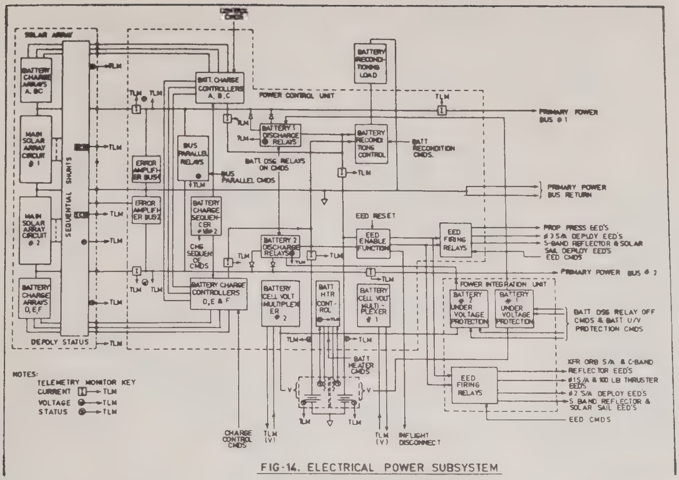
SOLAR ARRAY
BATTERY CHARGE ARRAYS A, B, C
MAIN SOLAR ARRAY CIRCUIT # 1
MAIN SOLAR ARRAY CIRCUIT # 2
BATTERY CHARGE ARRAYS D, E, F
SEQUENTIAL SHUNTS
DEPLOY STATUS
BATT. CHARGE CONTROLLERS A, B, C
POWER CONTROL UNIT
BATTERY RECONDITIONING LOAD
BATTERY 1 DISCHARGE RELAYS
BATTERY RECONDITIONING CONTROL
BATT RECONDITION CMDS.
PRIMARY POWER BUS # 1
ERROR AMPLIFIER BUS 1
ERROR AMPLIFIER BUS 2
BUS PARALLEL RELAYS
BUS PARALLEL CMDS
BATT. DSG RELAYS ON CMDS
PRIMARY POWER BUS RETURN
BATTERY CHARGE SEQUENCER # 1 & 2
CHG SEQUENCER CMDS
EED RESET
BATTERY 2 DISCHARGE RELAYS
EED ENABLE FUNCTION
EED FIRING RELAYS
PROP PRESS EED'S
# 3 S/A DEPLOY EED'S
S-BAND REFLECTOR & SOLAR SAIL DEPLOY EED'S
EED CMDS
PRIMARY POWER BUS # 2
BATTERY CHARGE CONTROLLERS D, E & F
BATTERY CELL VOLT MULTIPLEXER # 2
BATT HTR CONTROL
BATTERY CELL VOLT MULTIPLEXER # 1
POWER INTEGRATION UNIT
BATTERY # 2 UNDER VOLTAGE PROTECTION
BATTERY # 1 UNDER VOLTAGE PROTECTION
BATT DSG RELAY OFF CMDS & BATT U/V PROTECTION CMDS
BATT HEATER CMDS
XFR ORB S/A & C-BAND REFLECTOR EED'S
#1 S/A & 100 LB THRUSTER EED'S
#2 S/A DEPLOY EED'S
S BAND REFLECTOR & SOLAR SAIL EED'S
EED CMDS
CHARGE CONTROL CMDS
TLM (V)
INFLIGHT DISCONNECT
TLM
NOTES:
TELEMETRY MONITOR KEY
CURRENT
VOLTAGE
STATUS

FIG-14. ELECTRICAL POWER SUBSYSTEM

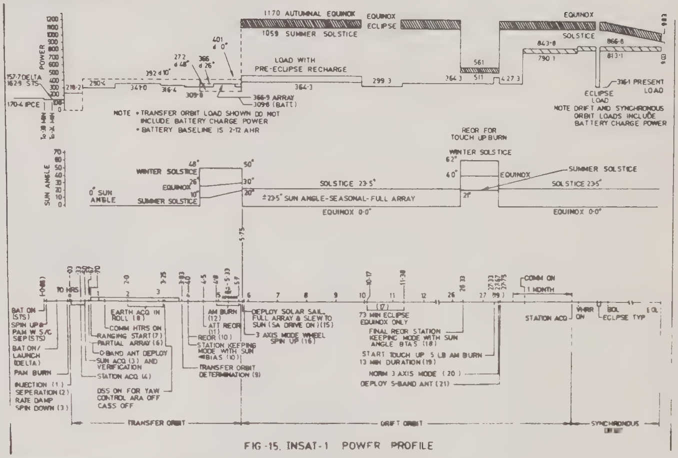

FIG-15. INSAT-1 POWER PROFILE

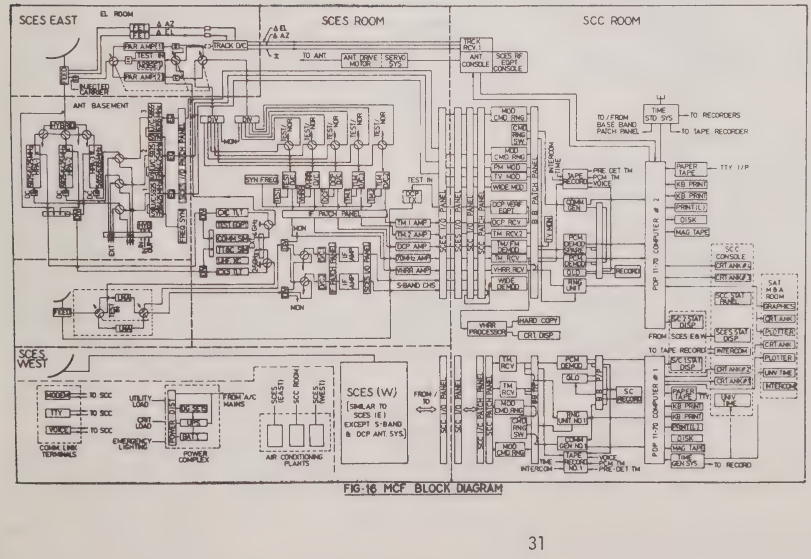
SCES EAST
EL ROOM
SCES ROOM
SCC ROOM
ANT BASEMENT
INJECTED CARRIER
TRACK D/C
TRACK RCV. 1
ANT CONSOLE
SCES RF EQPT CONSOLE
ANT DRIVE MOTOR
SERVO SYS
TO ANT
HYBRID
FEED
SYN FREQ
TEST IN
DCP TX
IF PATCH PANEL
TM 1 AMP
TM 2 AMP
DCP AMP
70MHz AMP
VHRR AMP
S-BAND CHS
MON
SCES I/O PANEL
SCC I/O PANEL
SCC PATCH PANEL
B B PATCH PANEL
MOD CMD RNG
CMD RNG SW
PM MOD
TV MOD
WIDE MOD
DCP VERIF EQPT
DCP RCV
TM RCV 2
TM/FM DEMOD
TM RCV
VHRR RCV
WIDE DEMOD
TAPE RECORD
COMM GEN
PCM DEMOD
SPARE
QLD
RNG UNIT
RECORD
TIME STD SYS
TO/FROM BASE BAND PATCH PANEL
TO RECORDERS
TO TAPE RECORDER
PDP 11-70 COMPUTER # 2
PAPER TAPE
KB PRINT
PRINT (L)
DISK
MAG TAPE
TTY I/P
SCC CONSOLE
CRT ANK # 4
CRT ANK # 3
SAT M & A ROOM
GRAPHICS
CRT ANK
PLOTTER
UNV TIME
INTERCOM
SCC STAT PANEL
S/C 2 STAT DISP
SCES STAT DISP
FROM SCES E & W
VHRR PROCESSOR
HARD COPY
CRT DISP
SCES WEST
MODEM
TTY
VOICE
TO SCC
COMM LINK TERMINALS
UTILITY LOAD
CRIT LOAD
EMERGENCY LIGHTING
POWER DIST
DG SETS
UPS
BATT
FROM A/C MAINS
POWER COMPLEX
SCES (EAST)
SCC ROOM
SCES (WEST)
AIR CONDITIONING PLANTS
SCES (W) [SIMILAR TO SCES (E) EXCEPT S-BAND & DCP ANT. SYS.]
FROM/TO
S/C 1 STAT DISP
TO TAPE RECORD
PDP 11-70 COMPUTER # 1
RNG UNIT NO. 1
COMM GEN NO. 1
TAPE RECORD NO. 1
SC RECORD
TIME GEN SYS
TO RECORD
PCM TM
PRE-DET TM
VOICE
INTERCOM
TIME

FIG-16 MCF BLOCK DIAGRAM

80-0474

ANIK C SPACE SEGMENT FOR TELESAT CANADA

W. Zatychec*
Telesat Canada
Ottawa, Canada

Abstract

The Anik C Space Segment is a unique high-capacity communications satellite system designed and optimized to augment terrestrial means of providing message and television distribution services, in the southern regions of Canada, in an economical manner. This paper reviews the communications capability of the Anik C spacecraft, considers the constraints on the space segment designs, and identifies the propulsion requirements. An overview of the communications payload and its operational features are presented. The high-capacity 16 RF channel transponder operates in the 14/12 GHz bands and fully reuses the available 500 MHz bandwidth. The communications antenna forms various spot beams with commandable beam switching available for each channel. Antenna beam coverage, frequency plans, communications capacity, and significant technical parameters are highlighted. The overall spacecraft configuration including the supporting subsystems are described briefly. Problems of adapting the spacecraft designs for compatibility with the Space Shuttle, with Delta backup, are discussed. The propulsion, launch, and orbital insertion problems are addressed and the selected approach is reviewed.

Introduction

Incorporated by Act of Parliament in 1969 as a commercial company, to provide communications services via satellite, Telesat Canada established its first operational system during early 1973 using the Anik A series of satellites. Three of these 12 RF channel satellites are currently in orbit and operate in the 6/4 GHz frequency bands. The fourth satellite, Anik B, launched in December 1978, features a dual band payload with 12 RF channels operating in the 6/4 GHz and 6 channels in the 14/12 GHz bands. The 6/4 GHz transponders are used to provide message and television distribution services to all parts of Canada, and the 14/12 GHz transponders are leased to the Canadian Department of Communications for implementation of various pilot projects.

In January 1977, Telesat Canada became a member of the Trans-Canada Telephone System (TCTS). As part of the membership agreement, Telesat has undertaken to provide a significant expansion of its satellite communications capacity. Using roof top antenna systems, 8.0 meters (26 ft) in diameter, at conveniently located downtown earth terminals and operating in the 14 and 12 GHz frequency bands, Telesat and TCTS plan to introduce in 1982 new communications services via satellite. The new series of satellites known as Anik C, specifically designed for this service, and built under contract with Hughes Aircraft, would form the Space Segment. The first two satellites would be located in geosynchronous orbit at 112.5°W and 116°W Longitude respectively. A third spacecraft would be retained initially as an on-ground spare. It would subsequently be launched to occupy the 109°W Longitude position when additional capacity or in-orbit backup support dictated the need.

Space Segment Communications Requirements

The satellite link is required to form part of the communications system designed specifically to provide the services listed in Table 1. These services are concentrated in the highly populated southern regions of Canada.

TABLE 1
Communications Service Requirements

- HEAVY ROUTE MESSAGE SERVICE
- MEDIUM ROUTE MESSAGE SERVICE
- HIGH QUALITY TELEVISION DISTRIBUTION

By using the 14 and 12 GHz bands, exclusively reserved for satellite communications, co-location of earth stations and customer facilities could be achieved. Costly backhaul links between the satellite earth terminal and the user facility, as used for 6 and 4 GHz services to avoid interference with terrestrial installations operating in these bands, are not required.

Service availability has to be extremely high and demands a near 100.00% availability of the satellite link typically 99.97%. Full operation during sun eclipse periods is therefore mandatory.

Spacecraft Constraints

Spacecraft designs are constrained, in terms of weight and size, by their respective launch vehicle payload capability and fairing envelope. Selection of the launch vehicle is limited by current availability of operational vehicles and their associated launch services costs. The more popular are listed in Table 2.

TABLE 2
Available Launch Vehicles

Launch Vehicle	Geosynchronous Orbit Payload	Fairing/Bay Diameter
DELTA 2914	375 kg (830 lb)	2.4m (8 ft)
DELTA 3910/PAM	580 kg (1280 lb)	2.4m (8 ft)
ATLAS CENTAUR	1000 kg (2200 lb)	3.0m (10 ft)
ARIANE	1000 kg (2200 lb)	3.0m (10 ft)
STS/SSUS-D	660 kg (1450 lb)	4.5m (15 ft)
STS/SSUS-A	1065 kg (2350 lb)	4.5m (15 ft)
STS/IUS	2270 kg (5000 lb)	4.5m (15 ft)

---

* Director, Satellite Systems Division

Copyright © American Institute of Aeronautics and Astronautics, Inc., 1980. All rights reserved.

The NASA Space Transportation System (STS) utilizes the Shuttle Orbiter which provides different degrees of freedom and is destined to displace the NASA unmanned vehicles. The Orbiter affords a 4.5m (15 ft) diameter cargo bay with a 18m (60 ft) usable length. User costs are proportional to the length/weight fraction occupied by this payload on a multiple payload flight.

Three classes of upper stages are being developed for use by payloads for transfer orbit insertion of the spacecraft from the low earth parking orbit provided by the Orbiter. The SSUS-D and SSUS-A (Spinning Solid Upper Stage - Delta Class and - Atlas Class), and the IUS (Inertial Upper Stage) are being developed and will provide payload capabilities of 660 to 2270 kg into geosynchronous orbit.

The above seemingly wide choices of launch vehicle size are rapidly diminished when one realizes that a communications satellite, in orbit on station, is valued at about $55,000 per kg. Also, it must be appreciated that additional space occupied by the spacecraft and its upper stage, as installed in the Orbiter during launch, is very much cost sensitive and is available at increments of about $20,000 per cm of bay length or $1,200 per kg.

Hence, the Anik C spacecraft was sized with these factors in mind. The Anik C is compatible with the SSUS-D class upper stage and occupies about 2.5 meters, or 1/7, of the Shuttle Orbiter cargo bay. The Anik C, with its upper stage, can also be launched on the Delta 3910, in the event that the Shuttle schedule cannot support the required launch date. This approach provides a cost effective solution which minimizes costs for either launch mode.

Communications Payload Features

The Anik C communications payload uses the concept of frequency reuse to achieve a capacity of 16 RF channels, each with a nominal usable bandwidth of 54 MHz. The frequency plan (see Fig. 1) provides an offset of 13 MHz between the centre frequencies of corresponding RF channels in the two repeaters to minimize interference between them (see Fig. 2). Initial channel operating modes include single access, four phase PSK digital message signals, and two access (FM/FDMA) TV signals. Other modes such as PSK/TDMA can be accommodated.

The uplink antenna coverage (Fig. 3), for both repeaters, uses single shaped antenna beams. Linear orthogonal polarization provides the necessary isolation between the two uplink beams.

The downlink antenna coverage area (Fig. 4) is divided into four regions across Canada, each region being approximately 2° wide E-W by 1° wide N-S as viewed from synchronous orbit. One repeater services the western two regions while the other repeater services the eastern two regions. Within each repeater, each RF channel has RF output switching to permit servicing either of its coverage regions individually or both simultaneously. The Variable Power Dividers are configured to provide three power split positions selectable by ground command which allow routing of the channel RF power to one spot beam horn array, the adjacent spot beam array, or splitting power equally to both. Hence, the downlink coverage requirements for each RF channel can be optimized for the type of traffic and service to be provided. Typically the broader area coverage is more appropriate for TV distribution while the narrower coverage is preferred for heavy route message service.

Two single frequency conversion repeaters are multiplexed into sixteen RF channels, eight per repeater (Fig. 5). Each channel has a Travelling Wave Tube Amplifier (TWTA) with a saturated RF output power of 15 watts. Thus the spacecraft total RF output power is around 240 watts.

The RF channel performance characteristics are optimized to allow transmission of two high quality FM TV signals through a single RF channel. This requires careful attention to RF transmission characteristics. The input multiplexers and TWTA's must be designed to minimize FM to FM cross-talk while the output multiplexer must be designed to reduce intermodulation products falling into adjacent RF channels. Alternatively, each RF channel is required to allow transmission of a 91 MBS data stream carrying a total of 1344 message circuits.

The communications payload is designed for high reliability within the practical constraints of weight, size and cost. The selected transponder configuration affords an optimum match of RF channel size for the expected communications traffic, provides maximum usable RF bandwidth, and uses the minimum amount of transponder hardware. Redundancy features have been incorporated where practical. Three spare communications receivers are available to replace the two main receivers, by ground command, in the event of malfunction. Similarly, four spare TWTA's are incorporated in a "Ring Redundancy" scheme, and by ground command are available to replace malfunctioning units. Furthermore, a total of 16 RF channels are available to provide a committed 14 channel minimum requirement. Detailed computerized reliability analysis has confirmed that the selected redundancy scheme has been optimized for the specified mission life.

The payload characteristics are summarized in Table 3.

Spacecraft Bus Features

The Anik C spacecraft features a spin stabilized cylindrical configuration with a despun section containing the communications payload (Fig. 6). The antenna dish and the aft cylindrical solar panel are both deployed in orbit to achieve the proper configuration for on-station operations. This approach allows a compact and efficient packaging of the spacecraft with its upper stage within the Shuttle Orbiter, and expanded dimensions in space necessary for solar energy collection and communications antenna orientation.

Attitude stability during the transfer orbit phase is achieved by virtue of favourable Moment of Inertia (MOI) ratio characteristics during this phase. On station, in the operational mode

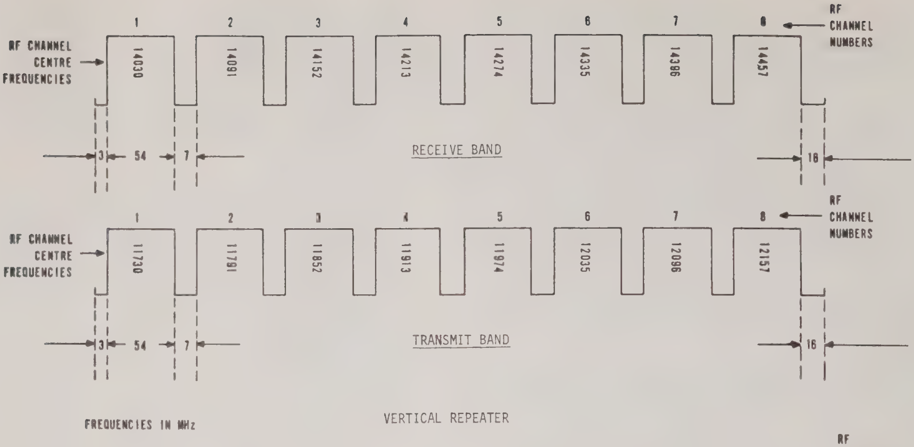
RF CHANNEL NUMBERS
RF CHANNEL CENTRE FREQUENCIES
1
2
3
4
5
6
7
8
14030
14091
14152
14213
14274
14335
14396
14457
3
54
7
16
RECEIVE BAND
11730
11791
11852
11913
11974
12035
12096
12157
TRANSMIT BAND
FREQUENCIES IN MHz

VERTICAL REPEATER

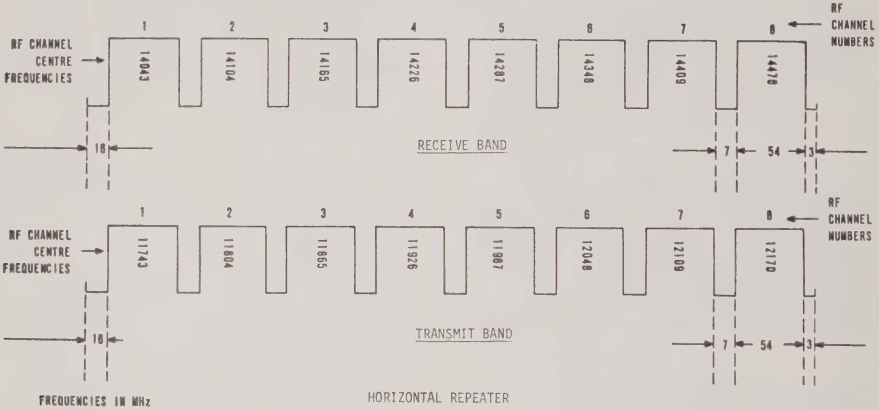
RF CHANNEL NUMBERS
RF CHANNEL CENTRE FREQUENCIES
1
2
3
4
5
6
7
8
14043
14104
14165
14226
14287
14348
14409
14470
16
RECEIVE BAND
7
54
3
11743
11804
11865
11926
11987
12048
12109
12170
TRANSMIT BAND
FREQUENCIES IN MHz

HORIZONTAL REPEATER

Fig. 1 Frequency plan.

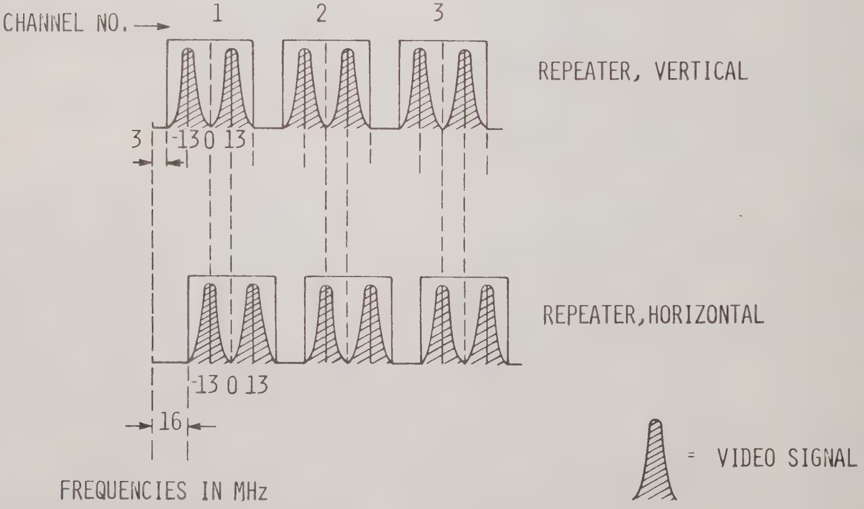
CHANNEL NO.
1
2
3
REPEATER, VERTICAL
3
-13 0 13
REPEATER,HORIZONTAL
-13 0 13
16
FREQUENCIES IN MHz
= VIDEO SIGNAL

Fig. 2 Typical two carrier per channel TV service.

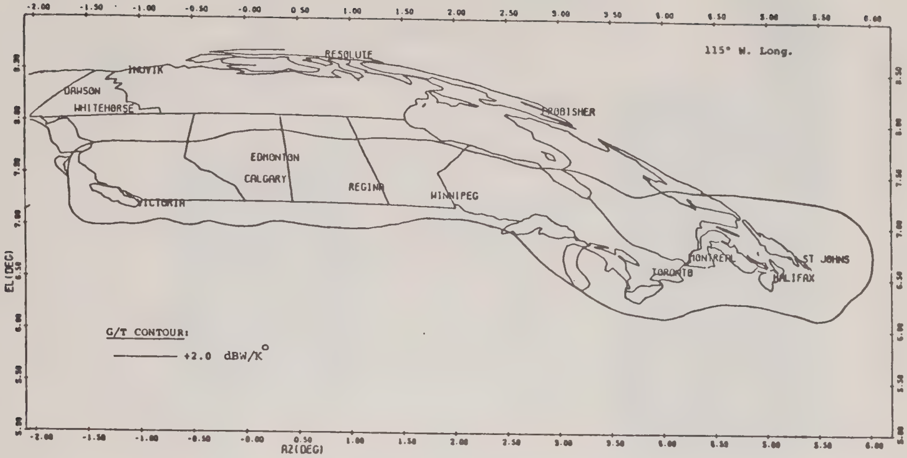

115° W. Long.
RESOLUTE
INUVIK
DAWSON
WHITEHORSE
FROBISHER
EDMONTON
CALGARY
REGINA
WINNIPEG
VICTORIA
MONTREAL
TORONTO
ST JOHNS
HALIFAX
G/T CONTOUR:
+2.0 dBW/K°
EL(DEG)
AZ(DEG)
-2.00
-1.50
-1.00
-0.50
-0.00
0.50
1.00
1.50
2.00
2.50
3.00
3.50
4.00
4.50
5.00
5.50
6.00
8.50
8.00
7.50
7.00
6.50
6.00
5.50
5.00

Fig. 3 Receive coverage.

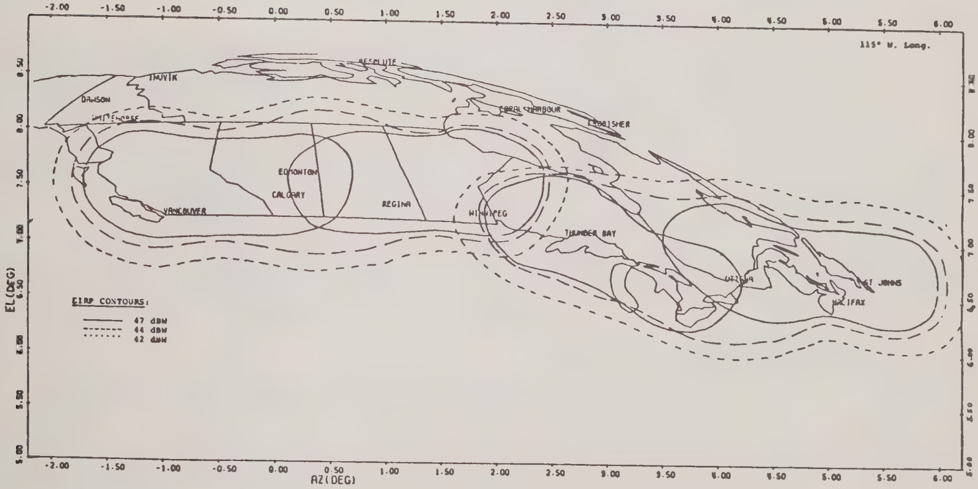

115° W. Long.
RESOLUTE
INUVIK
DAWSON
WHITEHORSE
CORAL HARBOUR
FROBISHER
EDMONTON
CALGARY
REGINA
VANCOUVER
WINNIPEG
THUNDER BAY
OTTAWA
ST JOHNS
HALIFAX
EIRP CONTOURS:
47 dBW
44 dBW
42 dBW
EL(DEG)
AZ(DEG)
-2.00
-1.50
-1.00
-0.50
0.00
0.50
1.00
1.50
2.00
2.50
3.00
3.50
4.00
4.50
5.00
5.50
6.00
8.50
8.00
7.50
7.00
6.50
6.00
5.50
5.00

Fig. 4 Transmit coverage.

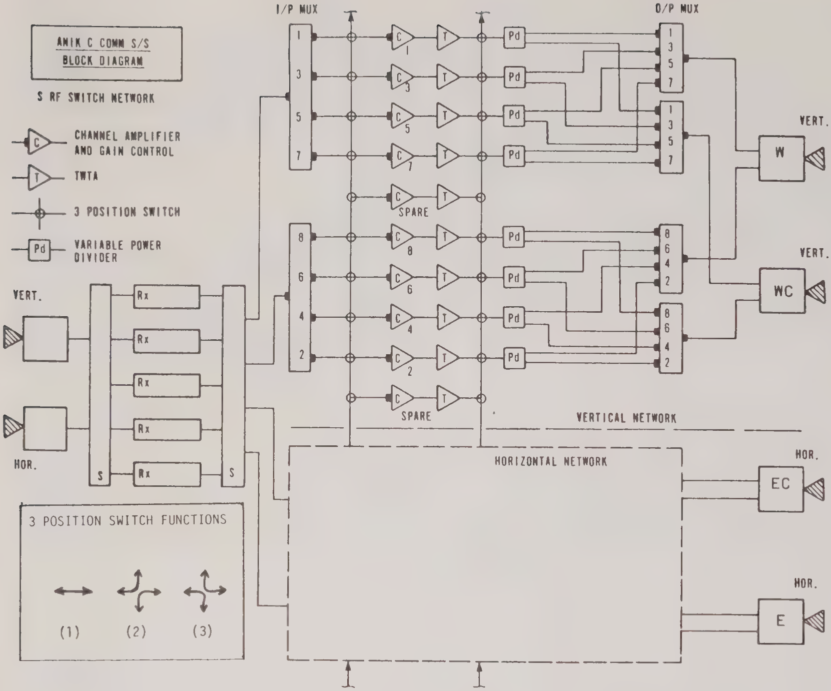

Fig. 5 Anik C communications subsystem block diagram.

TABLE 3
Anik C Spacecraft Characteristics

OPERATIONAL RF CHANNELS		16(1)
SPARE TWTA		4
ECLIPSE RF CHANNELS (AT 50% DOD)		16
RF CHANNEL SPACING (MHz)		61
USABLE RF CHANNEL BANDWIDTH (MHz)		54
RECEIVE COVERAGE (SOUTHERN CANADA)		$\approx 1^{\circ} \times 8^{\circ}$ (X-POL)
RECEIVE G/T BEAMEDGE (dB/K°)		+2.0
RECEIVE CARRIER POWER/NOISE TEMPERATURE(dBW/K)		-123.5(3)
CHANNEL GAIN CONTROL, 2 POSITION, RANGE (dB)		-2.5
TRANSMIT COVERAGE	- PRIMARY SPOT BEAMS $\approx 0.8^{\circ} \times 2^{\circ}$	4(2)
	- SECONDARY AREA BEAMS $\approx 1.2^{\circ} \times 4^{\circ}$	2
EIRP	- PRIMARY SPOT BEAM EDGE (dBW)	47
	- SECONDARY AREA BEAM EDGE (dBW)	42
ANTENNA POLARIZATION ISOLATION (dB)		33
WEIGHT (KILOGRAMS)		1080
DESIGN LIFE (YEARS)		10
MISSION LIFE (YEARS)		8
RELIABILITY (14 RF CHANNELS, 8 YEAR)		0.60
CALCULATED MEAN LIFE FOR 14 RF CHANNELS (YEARS)		8.1
UPPER STAGE		SSUS-D CLASS
LAUNCH VEHICLE		STS/DELTA

NOTES: (1) 8 EAST CANADA, 8 WEST CANADA
(2) 8 EAST-CHANNELS SWITCHABLE E, EC, E + EC
8 WEST CHANNELS SWITCHABLE W, WC, W + WC
(3) EQUIVALENT TO SATURATING FLUX DENSITY OF -81 dBW/m^2

with solar panel and the antenna dish deployed and with the communications platform despun, the MOI ratio drops below 1.0. Stability, during this phase, is based on the Gyrostat principle, and is achieved using active despin motor reaction torque control. Attitude control for all mission maneuvers is performed using a standard hydrazine fueled Reaction Control System which requires only 4 thrusters and 4 tanks arranged to achieve redundant operation (Fig. 7). During despun operation, on station, the antenna dish is controlled in the N-S and in E-W directions using RF beacon tracking systems to achieve extremely accurate antenna pointing control. Earth sensor tracking control is available as a backup.

The apogee motor is a standard solid motor design and has fuel onload capability consistent with the maximum expected spacecraft separated weight.

The solar array is sized to sustain all 16 RF channels at end of life. The batteries are also sized to support this full load during eclipse seasons at a 50% depth of discharge at beginning of life. Battery life is an upper limit on satellite operational life. The Anik C batteries incorporate the latest cell technological improvements, advantageous management techniques, and are sized with adequate reserves to assure achievement of at least an 8-year operational life. Provision has also been made to retrofit the third satellite with further improved cells, should they become available prior to a planned launch.

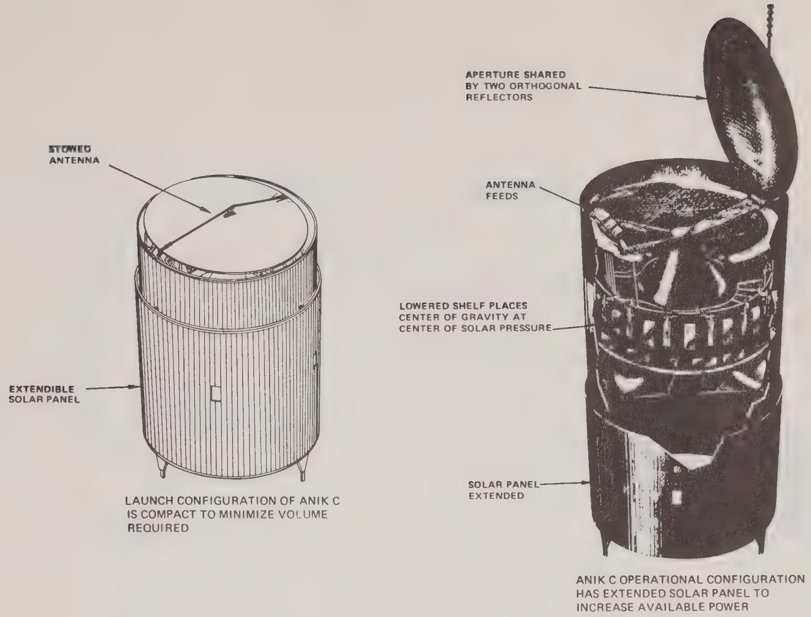
STOWED
ANTENNA
EXTENDIBLE
SOLAR PANEL
LAUNCH CONFIGURATION OF ANIK C
IS COMPACT TO MINIMIZE VOLUME
REQUIRED
APERTURE SHARED
BY TWO ORTHOGONAL
REFLECTORS
ANTENNA
FEEDS
LOWERED SHELF PLACES
CENTER OF GRAVITY AT
CENTER OF SOLAR PRESSURE
SOLAR PANEL
EXTENDED
ANIK C OPERATIONAL CONFIGURATION
HAS EXTENDED SOLAR PANEL TO
INCREASE AVAILABLE POWER

Fig. 6 Spacecraft configuration.

Thermal control is achieved by passive means augmented by thermostatically controlled heaters in critical areas.

The redundant Telemetry and Command systems provide adequate control of spacecraft functions and afford sufficient control and status information for proper satellite management.

The most challenging requirement in establishing the spacecraft bus configuration is achievement of a high reliability system within the constraints of allowable weight, size and cost. The selected configuration is intended to permit a full 10-year mission fuel load when launched on the STS. If this is achieved, the "Calculated Mean Life" for an Anik C satellite would be 8.1 years, a significant improvement over previous Telesat spacecraft programs.

Propulsion Requirements

Historically, Telesat spacecraft have been launched into orbit by NASA utilizing the three stage Delta series vehicles. The Delta launch vehicle has the capability of placing the spacecraft payload into an inclined transfer orbit. Telesat assumed from that point responsibility for the subsequent mission sequencies and, by utilizing the spacecraft's internal Apogee Motor, performed the apogee kick maneuver to achieve the near circular geosynchronous drift orbit. The on-board Reaction Control System was then utilized to complete the drift phase and perform the on-station positioning maneuvers.

The Anik C spacecraft is designed for launch on the STS. The mission implications of Shuttle flights and impact on spacecraft hardware are relatively severe. The Shuttle Orbiter mission delivers its cargo into a near earth circular orbit of 296 km (160 nmi)(Fig. 8). The user is required to provide his own upper stage (an equivalent to the Delta third stage) to propel his spacecraft into the desired transfer orbit. This upper stage must also incorporate the necessary avionics, structural and mechanical attachments to properly interface the payload with the Orbiter. Furthermore, both the upper stage and spacecraft are required to incorporate the necessary safety features required for flight on a manned vehicle. Telesat has placed a contract with Hughes Aircraft for the provision of a Perigee Kick Stage System (PKSS) using the Payload Assist Module (PAM) built by McDonnell Douglas to serve as the upper stage for Anik C.

The STS program, at the present time, is still in its development phase. The First Manned Orbital Flight (FMOF) has been rescheduled for late 1980. In the event that the STS program is unable to support the Telesat first launch requirement, provision has been made in the Anik C and PKSS designs to permit flight on the Delta 3910, a two stage vehicle (Fig. 9). In this flight mode, the spacecraft would have to be off-loaded to some extent and would be capable of a reduced mission life of approximately 7 years.

Conclusion

The Anik C Space Segment when established in 1982 will significantly extend Canada's communications capacity. This will mark the beginning of full integration of the communications satellite system with the advanced terrestrial

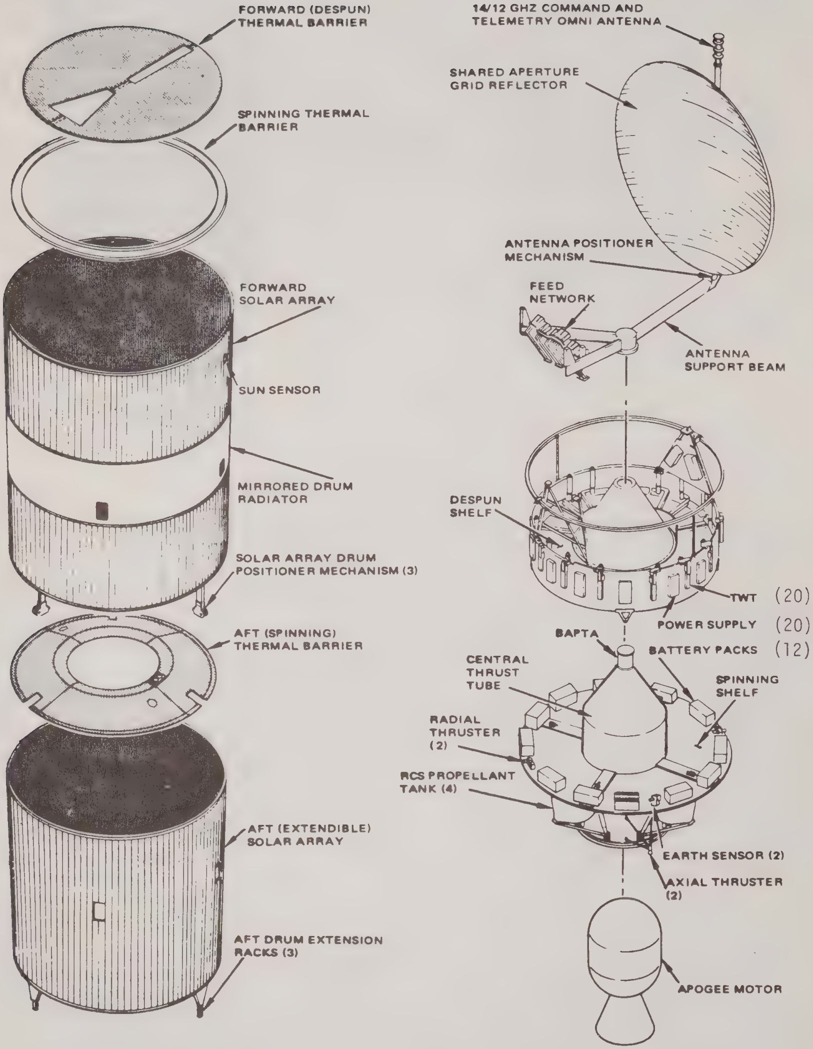
FORWARD (DESPUN) THERMAL BARRIER
SPINNING THERMAL BARRIER
FORWARD SOLAR ARRAY
SUN SENSOR
MIRRORED DRUM RADIATOR
SOLAR ARRAY DRUM POSITIONER MECHANISM (3)
AFT (SPINNING) THERMAL BARRIER
AFT (EXTENDIBLE) SOLAR ARRAY
AFT DRUM EXTENSION RACKS (3)
14/12 GHZ COMMAND AND TELEMETRY OMNI ANTENNA
SHARED APERTURE GRID REFLECTOR
ANTENNA POSITIONER MECHANISM
FEED NETWORK
ANTENNA SUPPORT BEAM
DESPUN SHELF
TWT (20)
POWER SUPPLY (20)
BAPTA
BATTERY PACKS (12)
CENTRAL THRUST TUBE
SPINNING SHELF
RADIAL THRUSTER (2)
RCS PROPELLANT TANK (4)
EARTH SENSOR (2)
AXIAL THRUSTER (2)
APOGEE MOTOR

Fig. 7 Spacecraft exploded view.

INITIAL PARKING ORBIT

	DELTA 3910	STS
PAYLOAD (kg)	2908	4197
PERIGEE (km)	157	296
APOGEE (km)	189	296
INCLINATION	28.7°	28.5°

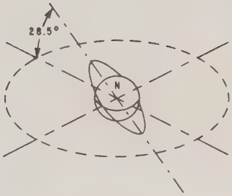

TRANSFER ORBIT (PKS)

PAYLOAD (kg)	1047	1128
PERIGEE (km)	185	296
APOGEE (km)	36620	36620
INCLINATION	27.0°	27.0°

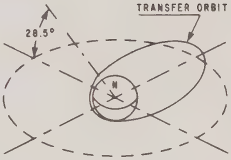

DRIFT ORBIT (AKM)

PAYLOAD (kg)	569	621
PERIGEE (km)	35786	35786
APOGEE (km)	36620	36620
INCLINATION	0°	0°

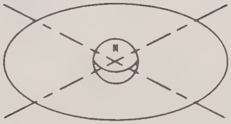

Fig. 8 Propulsion requirements.

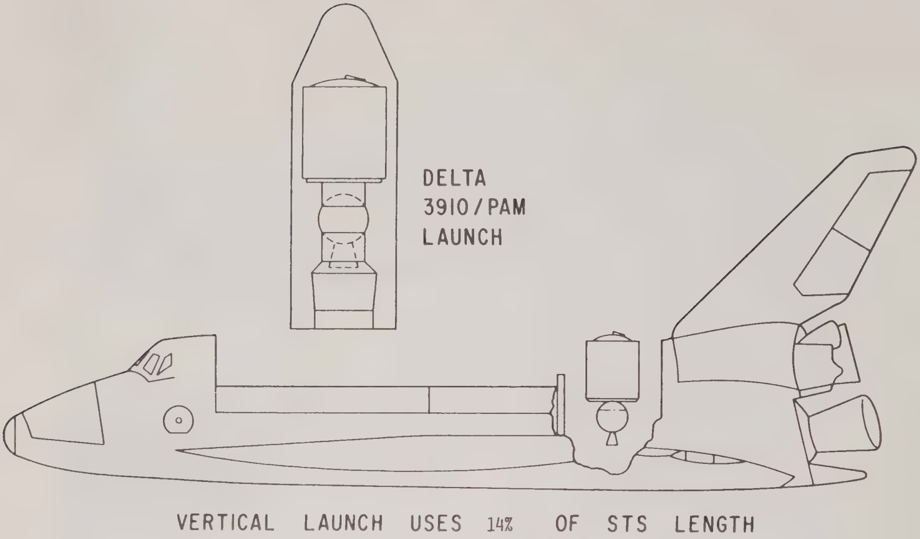
DELTA
3910/PAM
LAUNCH
VERTICAL LAUNCH USES 14% OF STS LENGTH

Fig. 9 Launch configurations.

systems currently being installed by the national telecommunications carriers in Canada.

The Anik C has presented a significant challenge to the Aerospace community and has required new solutions in a series of high technology areas. Canadian industry is participating fully in these developments and will be in a position to enter into future space programs demanding hardware solutions appropriate to the Space Shuttle area.

80-0477

THE KDD YAMAGUCHI SHORE STATION FOR THE MARISAT SYSTEM

K.Komuro, S.Endo and M.Yokoyama
Kokusai Denshin Denwa Co., Ltd. (KDD). Tokyo, Japan
Y.Katase, K.Tsunoda and T.Terashima
Nippon Electric Co., Ltd. (NEC). Yokohama, Japan

Abstract

The MARISAT system has since its inception in 1976 provided reliable service to ships at sea and off-shore platforms. With the completion of the Japanese shore station, the MARISAT coverage is worldwide. This paper describes the system configuration and typical features of the MARISAT Shore Station constructed in Yamaguchi, Japan in 1978. The features, that represent an improvement over the state-of-the-art, are: a) Reduction of L-band sidelobes by the use of a frequency selective subreflector, b) Improvement of tracking accuracy by a factor of 2 over conventional step-tracking systems, c) Prevention of loss of acquisition in the earth to satellite AFC loop, even for short switching periods, and d) Highly reliable software and hardware operation of the Network Control Processor (NCP) for call processing, statistic data recording, etc..

1. Introduction

Mobile maritime satellite communications have been provided by the MARISAT system through two U.S. shore stations, namely Santa Paula, California, for the Pacific Ocean region, and Southbury, Connecticut, for the Atlantic Ocean region, since August 1976. The communications service in the Indian Ocean region was commenced in November 1978 through the Yamaguchi Shore Station in Japan. The station was constructed and has been operated by Kokusai Denshin Denwa Co., Ltd. (KDD), and was manufactured by Nippon Electric Co., Ltd. (NEC). The MARISAT satellite communications system provides fast and reliable voice and telex communications services between ships at sea and shore-based subscribers. The system also has the capability of data and facsimile communications. The KDD Yamaguchi shore station has outstanding features as follows:

- Commonly used C-band and L-band 13-meter cassegrain antenna.
- Reduction of L-band sidelobes by the use of a Frequency Selective Subreflector.
- Improvement of tracking accuracy by a factor of 2 over conventional step-tracking systems.
- Stable, automatic frequency control operation.
- Identical IF frequencies at both transmit and receive in the 70 MHz band.
- In-station RF and IF loopback test capability without commercial service interruption.
- Software debugging capability during operation.

2. Shore Station Configuration

The Yamaguchi shore station consists of a 13-meter Cassegrain antenna, which is used simultaneously for L-band and C-band signals, tracking and servo subsystem, RF and IF equipment, modulation and demodulation equipment, network control processor (NCP), test ship terminal, supervisory and control equipment and peripheral equipment. The telephone and telex exchange equipment and the charging equipment are located at the gateway exchange center in Tokyo, Japan. A system block diagram of the station is shown in Fig. 1.

All major equipment in the station is fully redundant. Exceptions are the Antenna Subsystem, the Test Ship Terminal, and the Supervisory and Control Equipment. Furthermore, all equipment is designed for high reliability with solid state circuits, except the klystron tubes in the C-band High Power Amplifiers.

Transmit and receive IF frequencies for both the C-and L-bands are identical in the 70 MHz IF band. This permits in-station IF loop testing by connecting only test cables on the patch board.

In-station RF loop testing is also possible by push button control, using redundant equipment for the test loops. Various loop combinations are available.

The antenna is used simultaneously for both C-and L-band signals. A frequency selective reflecting surface on the periphery of the subreflector is used to improve the L-band sidelobe performance. Major parameters of the station are summarized as follows:

(1) Frequency Bands (MHz)

C-band	Reception	Transmission
Antenna	3700 - 4200	5925 - 6425
RF Equip't	4191.5 - 4200	6416.5 - 6425
L-band	1535 - 1543.5	1636.5 - 1645
IF of L-band	65.75 - 74.25	65.75 - 74.25
IF of C-band	64.25 - 74.25	64.25 - 74.25

(2) Receiver
C-band : 55 K Uncooled Low Noise Amplifier (Parametric Amplifier)
L-band : 230 K FET Amplifier

(3) Transmitter
C-band : 3 kW klystron High Power Amplifier
L-band : 10 W Transistor Amplifier

Copyright © American Institute of Aeronautics and Astronautics, Inc., 1980. All rights reserved.

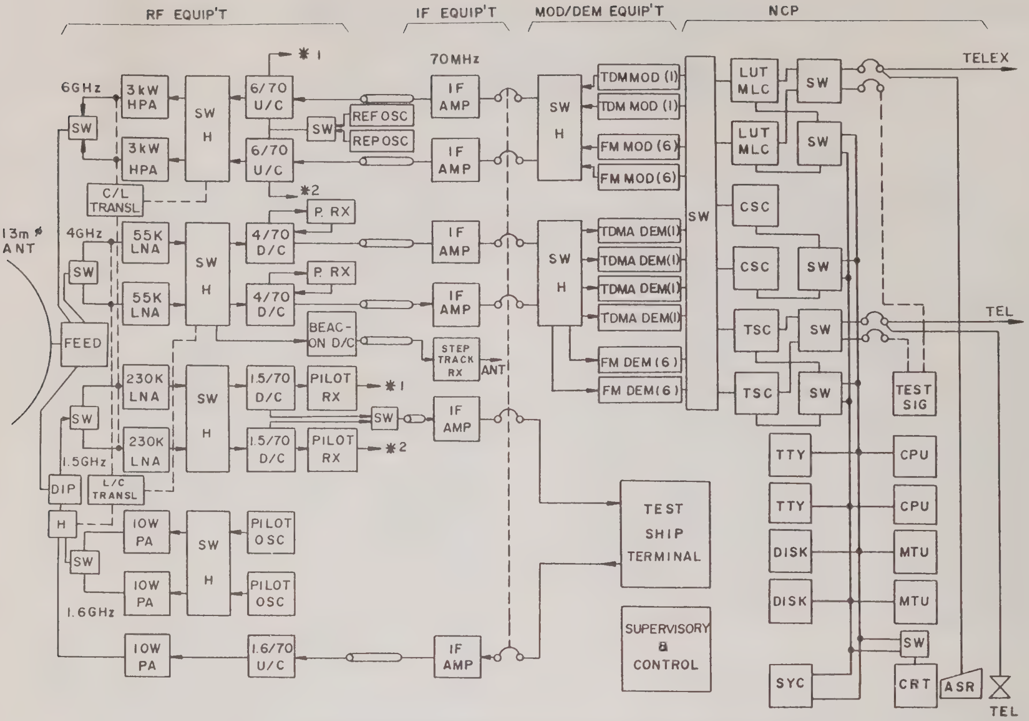
RF EQUIP'T
IF EQUIP'T
MOD/DEM EQUIP'T
NCP
6GHz
3kW HPA
3kW HPA
SW
SW H
6/70 U/C
6/70 U/C
*1
*2
70MHz
IF AMP
REF OSC
REP OSC
C/L TRANSL
P. RX
13m⌀ ANT
4GHz
55K LNA
4/70 D/C
BEAC-ON D/C
STEP TRACK RX
ANT
FEED
230K LNA
1.5/70 D/C
PILOT RX
1.5GHz
DIP
L/C TRANSL
H
10W PA
PILOT OSC
1.6GHz
1.6/70 U/C
TDM MOD (1)
FM MOD (6)
TDMA DEM(1)
FM DEM (6)
TEST SHIP TERMINAL
SUPERVISORY & CONTROL
LUT MLC
CSC
TSC
TTY
DISK
SYC
CPU
MTU
CRT
ASR
TEST SIG
TELEX
TEL

Fig. 1 Schematic Block Diagram of KDD Shore Station

Legend to Fig. 1

HPA : High Power Amplifier
LNA : Low Noise Amplifier
PA : Power Amplifier
DIP : Diplexer
H : Hybrid
TRANSL : Translator
U/C : Up-converter
D/C : Down-converter
P.RX : Pilot Receiver
LUT : Line Unit
MLC : Multiple Line Controller
CSC : Common Signalling Controller
TSC : Telephone Signalling Controller
CPU : Central Processor Unit
MTU : Magnetic Tape Unit
SYC : System Control Unit
CRT : Cathode Ray Tube Display Unit
ASR : Telex Terminal
TEL : Telephone Terminal

(4) Network Control Processor
Central Processor : NEAC 3200 Model 70
Instruction Execution Time : 1.7 micro-sec.
Number of Instructions: : 88
Memory Capacity : 64 K words

The equipment which was installed at Yamaguchi Shore Station is shown in the following photographs from Fig. 2 through Fig. 7.

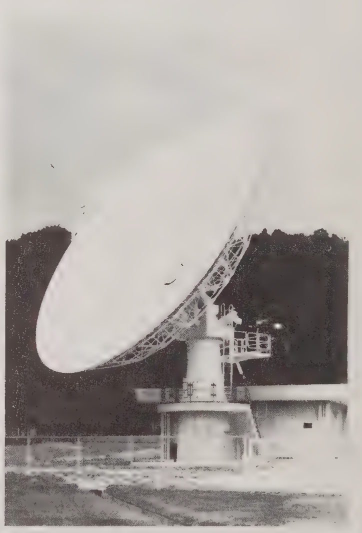

- 13-meter diameter cassegrain antenna
- C-and L-band LNAs are installed in the antenna center-hub

Fig. 2 Shore Station Equipment

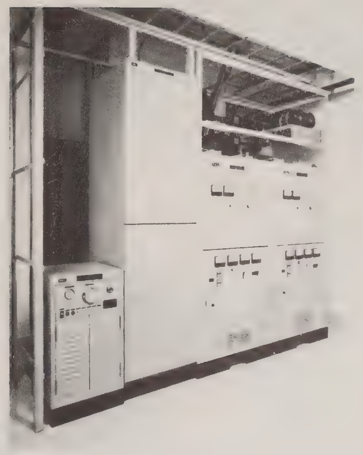

From left

- Dehydrator
- Control equipment for de-icing
- Redundant 6 GHz 3 kW klystron HPAs

Fig. 3 Shore Station Equipment

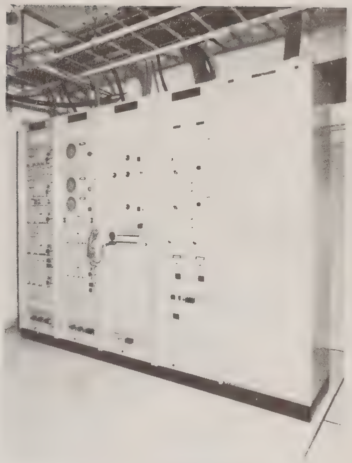

From left

- C-band transmitters and L-band receivers
- L-band transmitters and C-band receivers
- Test translators
- Antenna tracking and LNA control equipment
- Power distribution board

Fig. 4 Shore Station Equipment

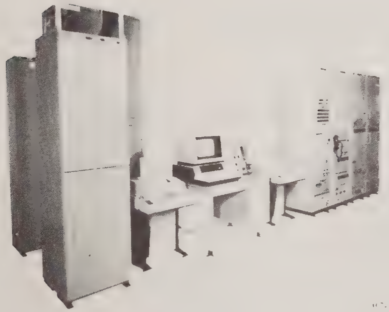

From left

- Power distribution board
- TTY
- CRT display
- Telephone set

(TTY, CRT display, Telephone set: for commissioning tests of ship terminals, supervising and control of satellite circuits, etc.)

- TTY for telex loopback test
- Network test rack for loopback test
- IF equalizing and switching rack
- MOD/DEM racks

Fig. 5 Shore Station Equipment

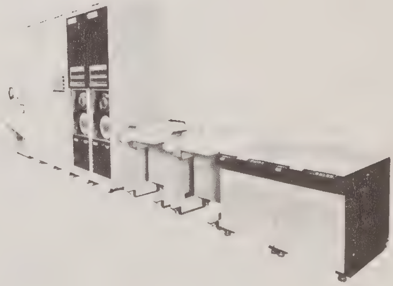

From left

- Test ship terminal
- Telephone interface bay
- Telex interface bay
- System controller
- CPUs (Central processor units)
- TTYs (Teletypewriters)
- Disks

Fig. 6 Shore Station Equipment

Supervisory and control equipment

Fig. 7 Shore Station Equipment

3. Subsystem Summary

3.1 The 13-meter Cassegrain Antenna

A cassegrain antenna is used for both L-and C-band applications with a frequency selective reflecting surface on the periphery of the subreflector to improve the L-band sidelobe characteristics. The shore stations are generally required to provide transmission and reception not only in the C-band for voice and telex channels, but also in the L-band for fully automatic frequency control (AFC). To fulfil these requirements two alternative methods can be considered. One is to install separate antennas for C-and L-bands and the other is to install a single antenna that can be used for both C-and L-bands. The latter scheme was adopted for the KDD Yamaguchi shore station in view of economic, operational ease and maintainability considerations. Several C-and L-band sharing schemes, as shown in Fig. 8, were investigated before finalizing the design of the common C-and L-band radiation system :

(i) Method of using a common primary horn, common main and subreflectors and combined C-and L-band feeds.

(ii) Method of installing separate C-and L-band feeds behind the main reflector. Between the L-band feed and the main reflector, a frequency selective reflecting surface (FSRS) is provided to direct the C-band signals to the subreflector after reflection. The L-band feed is located behind the reflecting surface, which is transparent to the L-band energy.

(iii) Method of a multifeed Cassegrain configuration, by installing several L-band primary horns around the periphery of the C-band primary horn.

(iv) Method of an offset antenna configuration by installing the L-band multi-feed at it's focal point. For C-band operation, the antenna works in a Gregorian configuration.

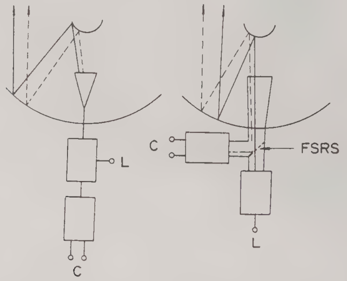

(i) Using a Common Primary Horn

(ii) Using a FSRS

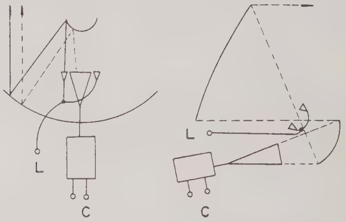

(iii) Using Several L-band Primary Horn

(iV) Combined Gregorian Configuration

Fig. 8 C-and L-band Sharing Schemes

In view of the present state of technical developments and performance improvement, it was concluded that method (i) would be the most appropriate. A 13-meter Cassegrain antenna with a C-band corrugated primary horn was designed to optimize the C-band characteristics, accordingly. The L-band signals are injected and extracted from couplers located at the neck of the horn (Fig. 9). It is difficult to obtain a good L-band sidelobe performance when optimizing the C-band characteristic. Furthermore, it should be taken into consideration that L-band interference caused by harmonic and spurious signals from TV relay terminals (UHF), radars, etc. might be present at the earth station. For improving the L-band characteristics, a subreflector with a frequency selective reflecting surface (FSRS) attached to its periphery, allowing the passage of C-band signals and reflecting L-band signals, was employed to reduce the L-band spill-over signals around the subreflector. This not only improves the receive G/T but also the transmit gain, with a corresponding reduction in output power of the L-band power amplifier.

Table 1 summarizes the major RF performance data of the antenna, and Fig. 10 shows the improvement in sidelobe reduction due to employment of the frequency selective surface around the subreflector.

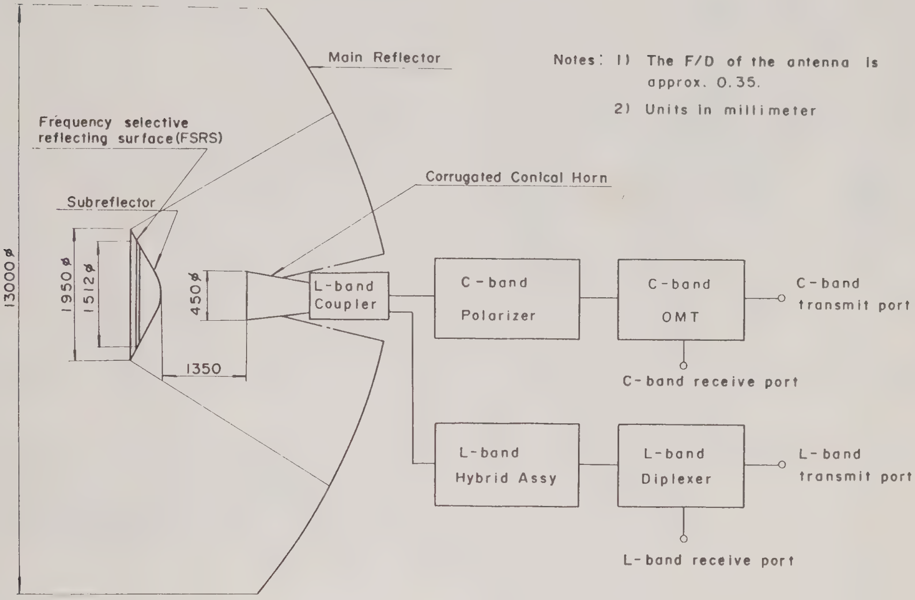
Main Reflector
Notes: 1) The F/D of the antenna is approx. 0.35.
2) Units in millimeter
Frequency selective reflecting surface(FSRS)
Corrugated Conical Horn
Subreflector
13000⌀
1950⌀
1512⌀
450⌀
1350
L-band Coupler
C-band Polarizer
C-band OMT
C-band transmit port
C-band receive port
L-band Hybrid Assy
L-band Diplexer
L-band transmit port
L-band receive port

Fig. 9 Configuration of Antenna Feed

Table 1 Measured RF Performance of the Shore Station Antenna

Item		4 GHz Band	6 GHz Band	1.5 GHz Band	1.6 GHz Band	Note
Measured Frequency (MHz)		4197.25	6422.50	1541.5	1640.52	
G/T (dB/K)	EL=5°	34.5		15.6		by radiometer method using Cas-A*1
	EL=17°	35.4		15.8		
Gain (dB)		54.3*2	57.4*3	40.5*2	42.0*4	same as above
Noise Temperature (K)	EL=5°	41.5		154		
	EL=17°	24.5		141		
Axial Ratio (dB): at Boresight		0.53	0.68	0.65	0.63	

*1 The radio star Cas-A parameters are taken from Report 390-3 of the C.C.I.R.
*2 at LNA input
*3 at OMT input
*4 at diplexer input

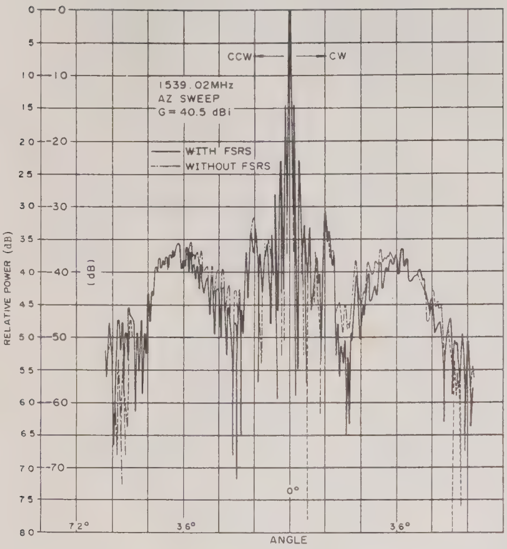

Fig.10 L-band Antenna Pattern

3.2 The Tracking System

A unique tracking system is adopted in the Yamaguchi shore station.

Fig.11 shows the schematic diagram of the step-tracking system. The antenna is moved continuously in the direction of the increment of a receive signal level, until it crosses the peak point. When the antenna has crossed the peak point back and forth several times, the logic circuitry decides that the peak has been reached. Such a tracking process is made around each axis of azimuth and elevation in turn at a preset time interval.

Fig.12 shows the voltage variations of each point in Fig.11. An antenna drive direction can be decided by comparing two signals, namely (a) the received signal level from the satellite at point A, and (b) a combined signal of a sample-hold signal level received just prior to (a), and an integration voltage proportional to the antenna velocity at point B. These two signals are summed at an Adder, and the combined signal at point C is compared to a reference voltage by two comparators. Comparator-1 outputs a pulse for sample-holding a new input signal. The other comparator-2 outputs a pulse for both sample-holding a new input signal and reversing the antenna drive direction.

For the continuous satellite tracking, a tracking accuracy of 0.011 degrees RMS can be achieved under light wind condition, which is an improvement by a factor of 2 over conventional step-tracking systems. Besides, implementation is simplified and economic advantages are gained.

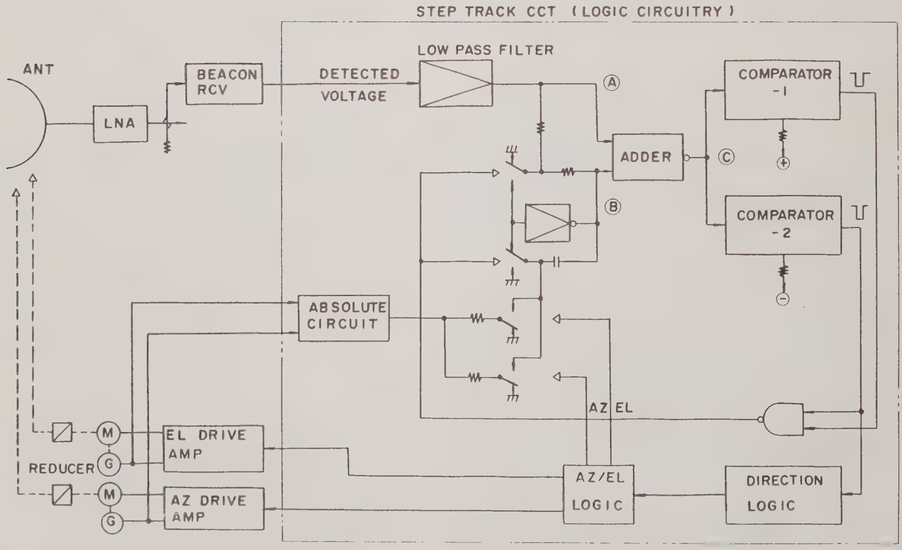
STEP TRACK CCT (LOGIC CIRCUITRY)
LOW PASS FILTER
ANT
BEACON RCV
DETECTED VOLTAGE
LNA
Ⓐ
COMPARATOR -1
ADDER
Ⓒ
Ⓑ
COMPARATOR -2
ABSOLUTE CIRCUIT
AZ EL
M
G
EL DRIVE AMP
REDUCER
M
G
AZ DRIVE AMP
AZ/EL LOGIC
DIRECTION LOGIC

Fig.11 Schematic Diagram of Step-tracking Circuit

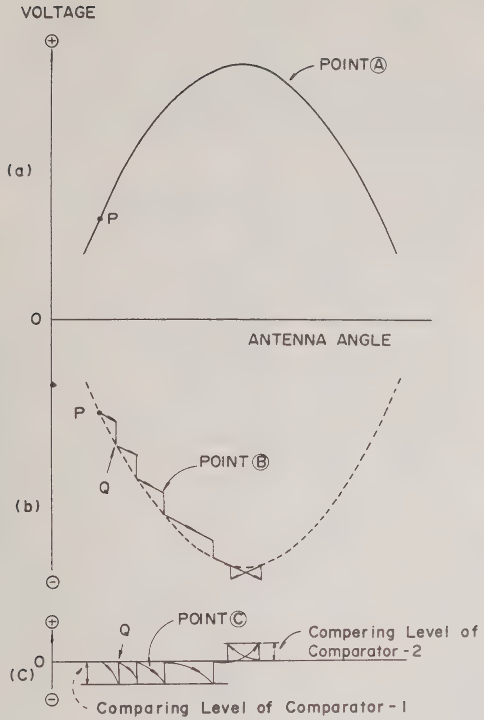

Fig.12 Voltage Variation of Each Point in Fig.11

3.3 The Automatic Frequency Compensation System

A newly developed design is applied to the automatic frequency compensation circuitry for compensation of the frequency translation error in the C-to-L band and L-to-C band satellite loops. This translation error is caused mainly by instability of the satellite local oscillators.

The automatic frequency compensation circuitry consists of an automatic phase control (APC) circuit, associated with an automatic frequency control (AFC) circuit installed in the AFC Panel and operates to compensate for the translation error. The AFC circuit is designed to operate at a lower threshold than the APC circuit, so that when acquisition of the APC circuit is lost by, for example, switching over from on-line to stand-by equipment, the re-acquisition of the APC circuit will be made automatically and immediately by the AFC circuit.

Fig.13 shows the schematic diagram of the C-to-L automatic frequency compensation loop. The received 1.5 GHz band including the pilot signal is converted to a 10 MHz band signal by the L-band Down-converter (L-D/C) and pilot Receiver (PIL RCV). The pilot signal passes through the crystal band-pass filter (BPF), and the level is controlled by an automatic gain control (AGC) circuit. When the pilot signal is outside the bandwidth of the BPF, the local oscillator (PLO in the PIL RCV) frequency is swept by a voltage controlled crystal oscillator (VCXO) until a BPF output signal is acquired. A pilot Detector (PIL DET) detects the signal acquisition and the sweep of the VCXO is stopped. After that, the frequency difference between the pilot

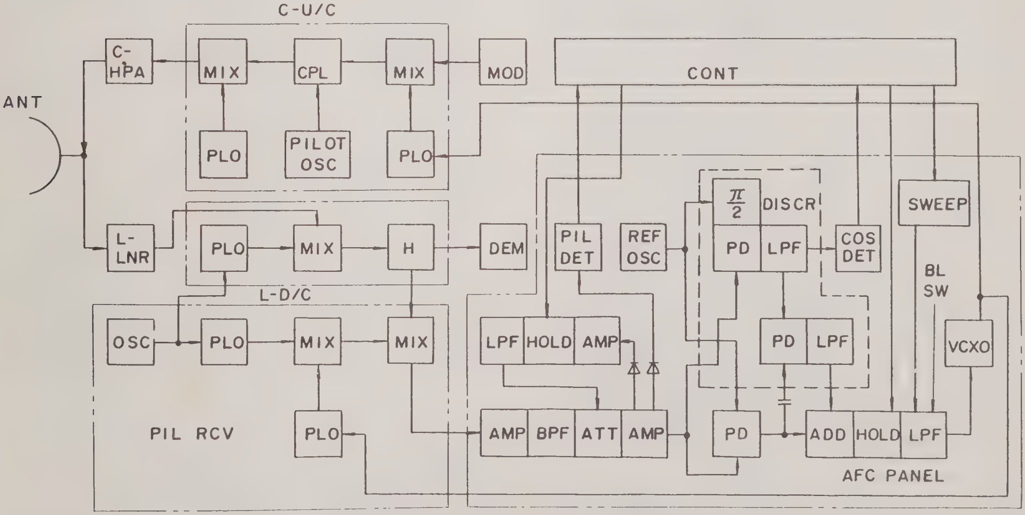
C-U/C
C-HPA
MIX
CPL
MIX
MOD
CONT
ANT
PLO
PILOT OSC
PLO
SWEEP
π/2
DISCR
L-LNR
PLO
MIX
H
DEM
PIL DET
REF OSC
PD
LPF
COS DET
BL SW
L-D/C
OSC
PLO
MIX
MIX
LPF
HOLD
AMP
PD
LPF
VCXO
PIL RCV
PLO
AMP
BPF
ATT
AMP
PD
ADD
HOLD
LPF
AFC PANEL

Fig.13 Schematic Diagram of C-to-L AFC Loop

signal and a Reference Oscillator (REF OSC) signal is detected by a Frequency Discriminator (DISCR), and the detected signal is then fed to the Adder (ADD), and is combined with the output of a sine phase detector, which has the pilot signal at one input port and the reference oscillator signal at the other input port. The combined signal controls the VCXO to achieve the frequency compensation loop, that is, the pilot signal frequency is controlled by the AFC loop within the lock-in range of the APC loop, and is thus automatically pulled in by the APC loop. The AFC loop is designed to turn-off automatically when the APC loop is achieved.

The frequency error produced at the output of the VCXO is proportional to the frequency drift produced by the satellite link. The output frequency of the VCXO is fed to the local oscillator (PLO) of the C-band Up-converter (C-U/C), and the received frequency of the ship terminal is therefore controlled so as to receive the correct frequency. Furthermore, this frequency compensation circuit is designed to maintain the previous frequency of the AFC circuit and hold the AGC voltage if the pilot signal is lost, in order to minimize the traffic loss. The approach described in the previous paragraphs has shown excellent results at the Yamaguchi shore station.

3.4 Network Control Processor

A network control processor (NCP), which is incorporated between the PSK/FM modem and gateway exchange center, is used to assign the communication line circuits, to supervise the communication line status, to analyze the request messages transmitted over the ship-to-shore request channel and to make the assignment messages for the ship terminals. It also performs interworking of the different signalling systems between satellite circuits and terrestrial circuits.

Fig.14 shows a configuration diagram of the NCP. The NCP employs stored program control and consists of a general purpose mini-computer as a central processor, input/output devices as peripheral units, telex and telephone interface units for the communication lines, common signalling controller for assignment and request messages, system control units for control and supervision of on-line/stand-by modes, and telex and telephone position terminals for operation and maintenance. Redundancy is provided for all units contained in the NCP except for supervisory equipment and position terminals, with automatic switch-over for operational reliability in case of equipment faults. Manual switch-over is also available. Switch-over causes no interruption to communication lines. Channel capacity and signalling systems between the shore station and the gateway station are as follows:

Telex : 22 channels ... type B signalling system
Telephone: 2 channels ... CCITT No.5 signalling system (extendable up to 6 channels)

The NCP is provided with call processing functions for telex and telephony, operation supervising functions, and maintenance and testing functions.

(1) Call Processing Functions

The NCP is capable of handling telex and telephone calls as listed below:

- Ship-originated and gateway-station-transit calls
- Ship-originated and shore-station-terminated calls
- Shore-station-originated and gateway-station-transit calls
- Gateway-station-originated and ship-terminated calls
- Gateway-station-originated and shore-station-terminated calls
- Shore station originated and ship-terminated calls
- Gateway-station-originated broadcast
- Shore-station-originated broadcast

The NCP is capable of handling a maximum of 30 telex and 5 telephone calls per minute. Telex and telephone distress services have the highest priority in processing. Even if all channels happen to be occupied with ordinary calls, the NCP can receive a distress call from a ship terminal. That is, one of the occupied channels will be disconnected and automatically allocated to the distress call.

(2) Operation and Supervision Functions

The NCP has the following operation and supervision functions:

- Capability of recording all processed information for telex and telephony, and channel status indication at all times
- Capability of establishing a channel to any ship terminal, and releasing the channel
- Capability of handling commissioning tests for any ship terminal

(3) Maintenance and Test Functions

The maintenance and test functions of the NCP are as follows:

- Out-of-band or inband signalling sequences and other channel tests can be conducted on a via-satellite or shore-station-loopback basis.

For the purpose of maintenance tests, the NCP is capable of checking the call processing function on a shore-station-loopback basis without affecting the operational system, using the stand-by units isolated from the operating units.

The features of the NCP are as follows:

(1) The NCP is fully duplicated for enhanced reliability, and the following two alternate operational modes are possible so that software debugging can be performed without affecting the traffic:

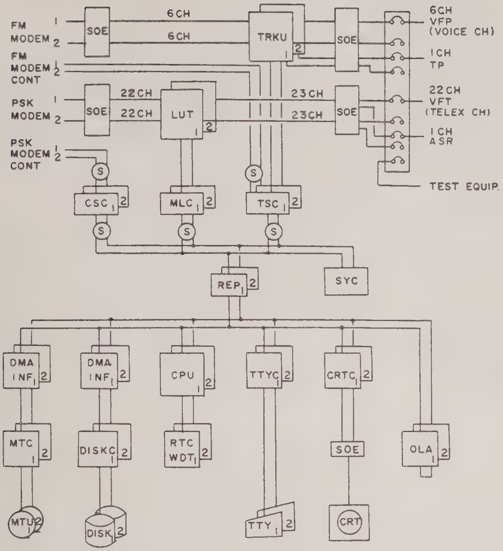

CPU : Central Processing Unit
RTU/WDT: Real Time Clock and Watch'dog Timer
DMA : Direct Memory Access
MTU : Magnetic Tape Unit
DISK : Magnetic Disk
TTY : Teletypewriter
CRT : Cathode Ray Tube Display Unit
OLA : On-line Adapter
REP : Repeater
SOE : Switchover Equipment
SYC : System Control Unit
LUT : Line Unit
MLC : Multiple Line Controller
CSC : Common Signalling Channel Controller
TSC : Telephone Signalling Controller
TRKU : Telephone Trunk Unit
TP : Telephone Terminal
ASR : Teletypewriter for Telex

Fig.14 Network Control Processor Configuration Diagram

a) Duplex Mode

This mode is the basic mode of the redundant NCP. With either one of the two central processing units (CPU) performing the on-line processing, such as network control, the other can be placed in a stand-by mode. If the on-line CPU stops operations either due to failure or upon receiving an instruction, the stand-by CPU will take over the on-line processing without affecting the traffic. The stand-by NCP checks its own status periodically, and receives necessary data from the on-line NCP likewise periodically, and performs switch-over if necessary.

b) Simplex Mode

This operational mode is for operating one of the two CPU systems independently, regardless of the other. Operation takes place in such case as if there was no stand-by CPU. The simplex mode operation may be further classified into the isolate and non-isolate modes, depending on whether the channel interface unit is isolated or not. The channel interface unit is usually operated under conditions in which switching control from the operational CPU is possible. However, it is possible by operation of the system control unit to isolate the stand-by channel interface unit from the operational one, so that two independent systems each including a CPU may be established. Under this condition, software debugging is possible during on-line operations. The former and latter are commonly referred to as "non-isolate" and "isolate" modes, respectively.

(2) Circuit information of all circuits such as call direction, ship terminal ID number, call sequence event number, are displayed on the color CRT display unit.

(3) If a failure has happened, detailed information is printed on the teletypewriter. Hence, quick repair may be achieved.

(4) Abundant and useful commands for switch-over of units, updates of ship terminal ID numbers, software amendments are provided for operation and maintenance.

(5) A micro-computer is used in the telex interface unit to reduce the load on the CPU.

Characteristics of the CPU and software are as follows:

(1) CPU
Memory capacity : 64K words (1 word = 16 bits)
Memory cycle time: 850 nano-sec.
Instruction execution time: 1.7 micro-sec.
Number of instructions: 88

(2) Software
Capacity for program: approx. 70K steps
Capacity for table : approx. 6K words

The NCP can operate in an isolate mode as stated in a previous paragraph. This mode is very powerful and very suitable for program debugging and for NCP functional amendments. In fact, the software amendments for functional extensions such as addition of time information to the carrier ID message of telex call, changing of alarm signal supply condition, permission of telex test messages (QBF message) transmission to un-authorized ship terminals waiting for commissioning tests, and other various addition of functions are performed in the Yamaguchi shore station by use of this isolate mode operation, without any interruption to the on-line traffic.

4. Conclusion

Extensive on-site testing of the Yamaguchi shore station has verified that substantial improvements over conventional designs have been obtained in the areas described in this paper, namely (1) reduction of sidelobes in the L-band, (2) greatly improved tracking accuracy, (3) stable operation of AFC and APC circuitry, and (4) reliable operation of the NCP. All items mentioned above are expected to be applicable in other fields of satellite communications.

5. Acknowledgement

Numerous people have contributed in one way or another to this project.

However, special thanks are due to Comsat General Corporation for cooperation in designing the shore station equipment, Messrs. M. Orima, N. Oyama, T. Satoh, K. Kobori of KDD Head Office, and Mr. J. Okamoto of KDD Yamaguchi Satellite Communication Center for invaluable suggestions and advice in the design and construction of this station, and to Messrs. I. Sato, H. Shimayama of NEC for the development of the shore station equipment.

References

(1) K. Komuro, S. Endo, M. Yokoyama, Y. Shigeyeda, M. Murata, K. Tsunoda and T. Terashima : MARISAT Shore Station Equipment for the MARISAT System. IECE (Japan) TG, SANE 78-31 (1978)

(2) S. Endo, M. Yokoyama, N. Matsunaka, K. Yamamoto, H. Shimayama, M. Ando and K. Yoshizumi : RF Equipment for the MARISAT System. 1979 Nap. Conv. IECE Japan

(3) N. Matsunaka, K. Yamamoto, H. Shimayama, K. Yano, K. Yokouchi and Y. Isoe : Automatic Frequency Compensation Circuit for the MARISAT System. 1979 Nap. Conv. IECE Japan

(4) M. Orima, et al : Construction of Yamaguchi Shore Station. KDD Technical Jornal, No.99, Jan. 1979

(5) T. Satoh : Trends in International Maritime Satellite Communication Systems. KDD Technical Jornal, No.99, Jan. 1979

80-0478

AIAA 8th

COMMUNICATIONS SATELLITE SYSTEMS CONFERENCE PAPER
FOR PRESENTATION APRIL 20-24, 1980

INNOVATIVE SERVICES IN USE OVER THE MARISAT SATELLITES

By

S. Engelman, J. F. Parker & J. L. Beauchamp
COMSAT General Corporation
950 L'Enfant Plaza, S.W.
Washington, D.C. 20024

Abstract

This paper describes the types of telephone and telegraph services presently available and the new services being planned for the Maritime Mobile Satellite Systems. The telephone, telegraph and data services available to the maritime mobile satellite users are described and the expected and measured transmission performance of these services are shown. New services, which have been developed for the maritime industry utilizing the Maritime Mobile Satellite System, will be described. In addition, future uses of maritime mobile satellites are presented.

1. Introduction

The MARISAT System of satellites for Maritime Mobile Satellite Services has now been in operation for nearly four years and is offering reliable service in the Atlantic, Pacific and Indian Ocean regions to mobile terminals installed aboard all types of vessels. Figure 1 shows the present shore stations and the coverage area of the satellites. The shore stations serving the Atlantic and Pacific are in Southbury, Connecticut and Santa Paula, California and are operated by COMSAT General Corporation. The shore station serving the Indian Ocean region is in Yamaguchi, Japan and is operated by KDD Co., Ltd. As can be seen in Figure 1, the coverage area of the MARISAT System covers the entire world with the exception of small areas located in the west part of the Gulf of Mexico and in the Southwestern Pacific. With the advent of INMARSAT, the next generation of satellites will provide full world-wide coverage. The applications of satellite service provided by these satellites and earth stations to ships at sea vary greatly depending on the type of vessel the terminal is installed upon.

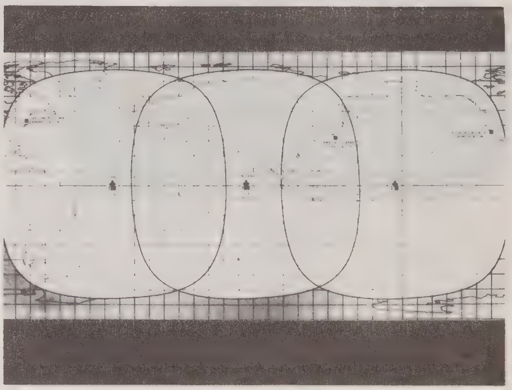

Figure 1.

Figure 2 shows an example of a MARISAT terminal as it is placed aboard a ship. As can be seen, the terminal has a teleprinter and a telephone associated with it. The telex teleprinter can be used to provide normal telex service. In addition, there are data jacks associated with the terminal. These jacks can be used to interconnect with a data modem to transmit data up to 2400 bps. The MARISAT System is interconnected with the U.S. domestic and the international telephone and telex networks as well as private networks. The services that are available now are almost exactly those which any business has in their office location. The only difference is that these services are now extended to ships at sea.

Copyright © American Institute of Aeronautics and Astronautics, Inc., 1980. All rights reserved.

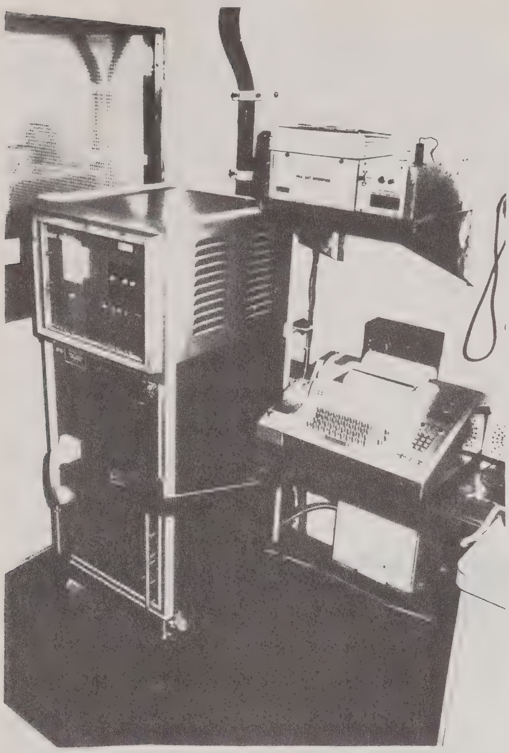

Figure 2.

2. Users

The MARISAT System was originally designed for ships on the high seas. The user population as of January 1, 1980 is shown in Table 1. The great diversity of users results in an equal diversity of their communications requirements. Cargo ships send manifests, seismic ships send data and passenger ships have personal calls. The drilling ships have extensive requirements to transmit large amount of data.

Table 1

Type of Ship	No. of Ships with Terminals
Construction	9
Drill Rigs	27
Cargo Container	58
Fishing	11
LNG	23
Passenger	16
Seismic, Survey	32
Tankers	88
Yachts	9
Other	19

Table 1 Continued......

MARISAT Telex Network

MARISAT telex, ship-to-shore and shore-to-ship, access methods closely resemble the standard worldwide telex/TWX network procedures. Both employ circuit and message switching to accomplish their purpose.

Figure 1 showed a nominal edge of coverage of 5^0 elevation. At this elevation the telex character error rate should be less than $6x10^{-5}$.[1] For telex particularly, because of our 5 dB margin, communication is frequently achieved well beyond the nominal edge of coverage with elevation angles down to 0^0.

In the ship-to-shore direction, upon request each MARISAT terminal is assigned a TDM/TDMA frequency which allows a telex connection to be extended from the mobile terminal via the satellite system to the desired Telex Switching Center.

Upon connection into the Switching Center. the calling party types, via keyboard, the proper CCITT destination code followed by the called number. This is accepted by the Switching Center, which in turn performs the necessary handshaking to extend the call to the called party.

At this point the connection is complete, conversation begins and chargeable time is calculated by the switch that originally processed the call.

TWX connections (North America only) are processed in a similar manner, except that it is necessary to convert, in real time, the 110 baud 7-level TWX code to 50 Baud 5-level Baudot code for telex compatibility.

Shore-to-ship access is accomplished by directing a call to one of the U.S. domestic, (WUD) or international carriers, CGC, ITT, RCA or WUI), keying in the proper IRC country codes, 805, Atlantic, 705 Pacific or 905 for the Indian Ocean followed by the mobile terminal number. The called number is then used to route the call to the individual ship. In the event the called terminal does not respond, each ocean area is then tried before the call is abandoned. Standard service codes, i.e., OCC, NC, etc., are returned to the sender in the event the call is not completed.

Ship-to-ship calls are similarly processed using standard CCITT F.69 destination codes, 581, Atlantic, 582, Pacific or 583 for the Indian Ocean. The type of call requires the use of two satellites on an ocean call or the use of one satellite twice in a same ocean call.

Incoming and outgoing MARISAT telex access is available from the following terminal types:

1. Domestic telex machines
2. Domestic TWX machines
3. International Record Carrier (IRC) private line machines
4. International telex terminals (participating countries)
5. MARISAT Mobile terminals

3.1 Standard Telex Services

A number of standard telex services are offered to the shipboard industry. Generally, any service available to terrestrial subscribers is also available aboard ship. Listed below are the various features available to MARISAT subscribers via the COMSAT General network.

*Standard Circuit Switched Telex Service

Point-to-point telex connection via the worldwide telex and TWX networks.

*Abbreviated Single Digit Dialling

Ordinary 7 or 10 digit telex or TWX numbers can be abbreviated to allow the calling party to dial only one digit to complete the call.

*Customer Mailed Telex Service

Telex messages transmitted to a central number will be forwarded to the addressee by ordinary mail.

*MARITRAN Store and Forward

Messages destined to busy or temporarily unavailable telex or TWX machines will be stored and delivered when the called machine becomes available, with time and date of delivery reported to the addressor.

*Multiple Address Common Text Messages

One common text message will be delivered to a multiple address list.

*Group Address Service

Message or messages will be delivered to a specified group of addresses at various locations.

*Departmental Billing

Each message transmitted may be charged to a specific department by using a special code in the address.

*News Service

News, sports, stock reports are available as requested by the MARISAT subscriber.

*Voice Access (Dictation)

Through agreement with another carrier.

*MARITEXT

Shore-to-ship telex service whereby a message may be filed by telephone to a MARISAT equipped ship or offshore facility.

3.2 Telex Innovative Services

The wide range of standard telex services which have now been discussed have led to customers aboard ships desiring additional types of services which are unique to the shipboard industry. Managers of ships especially want to obtain data from the ship while its at sea. Before, ships would be out to sea and when they were out of line of sight the communications to these ships would be very unreliable and not very current. Sometimes it would take days to reach a ship at sea via HF or MF frequencies. Now with MARISAT some new innovative services have come into being. The first of these is position indication. Interfaces have been developed for three types of electronic satellite navigational receivers. An example is shown in Fig. 3. As can be seen, a satellite navigational receiver can be interfaced directly through to the MARISAT terminals. These navigational receivers give the ship various types of data, such as the ship's latitude and longitude and time since last fix. Speed and heading are entered and microprocessors use this data to calculate other information: course made good, way point latitude and longitude, great circle and rhumb line distance. Course to steer, current set and drift can also be calculated, displayed and returned to shore. The navigational receiver not only gives the ship's captain very accurately his position and speed and direction but the same data can now be automatically obtained from any shore side telex machine. The interface device shown in the picture is called a Universal Telegraph Interface Unit (UTI). This UTI interfaces between

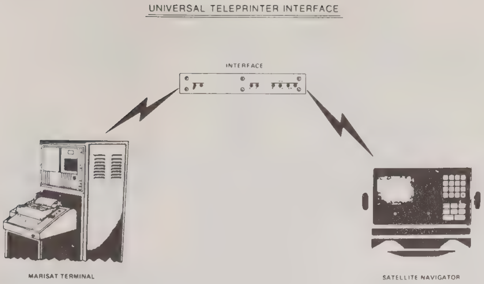

Figure 3.

the MARISAT terminal and the navigational receiver. The UTI is programmable to monitor the telex lines and look for a specific code. Upon reception of this code, it will interrogate the navigational receiver, obtain the data that is stored in the receiver's memory and convert it to be transmitted over the telex. Therefore, a ship owner can call its ship anywhere in the world via telex and automatically obtain the ship's position, heading, latitude and longitude; all the information that is available to the ship captain. This data is valuable to shipowners and management in order to calculate when a ship will arrive in port and how it is progressing on its course.

Another innovative service which is now being tested is the interfacing of a MARISAT terminal with an automatic weather collection device. The weather station automatically collects air temperature, sea water temperature, wind direction and speed, barometric pressure and other weather conditions. To obtain this information from ships in the middle of the ocean in real time and as often as needed is a real advance for forecasting weather in ocean areas where now very little weather data is obtainable. A UTI unit contains a microprocessor which can be programmed to interface with various devices and it is programmed, as shown before, to work with the navigational receivers and with automatic weather stations. The UTI converts speeds, codes and electrical interfaces. It will convert from an EIA interface to a 20 mil/neutral interface, and to most other common interface types.

The U.S. Maritime Administration (MARAD) has developed systems in which data may be sent from a ship and processed and forwarded on shore to assist shipowners. Such systems are now commercially available. They include automated data collection; from ships, as in the systems described above, and also include manual data sending from ships, computer processing of data input into and output from computerized data bases, and formatting and sending messages virtually anywhere in the world on land or sea.

This service is useful for:

Vessel Performance Monitoring

Voyage Reporting

Cargo Booking

Economic Planning

Personnel Administration

Scheduling in Ports and Repair Facilities

Accounting

Control of Cargo Containers

These systems frequently use computer time sharing networks and the automatic placing and reception of telex calls with ships provides shipowner a new tool for improving the profitability of his ships.

Table 2

MARISAT BASEBAND - BASEBAND STANDARD

Signal to noise ratio 29 dB at edge of coverage, for 0 dBr signal

Bandwidth: 300 - 3000 Hz

Group delay: 1000-2600 Hz ≤ 330 μsec.
600-2600 Hz ≤ 1000 μsec.
500-2800 Hz ≤ 2000 μsec.

Impulse noise: ≤15 counts/15 min.

Phase noise: ≤ 0.8 pp on a 1 KHz,
-4 dB signal

Clipping level: 0 dBr

Approximate speed level: 6-1/2 dBr, because of companding of 2:1, with 0 dBr unaffected

Nominal data level: 6 dBr (for -13 dBm0 carriers)

4. MARISAT Voice Service

4.1 General

MARISAT ship-to-shore and shore-to-ship voice service is provided on demand via a single channel per carrier (SCPC) using frequency modulation (FM). Each time a voice grade call is established, a frequency path is selected by the shore station and assigned to the particular mobile terminal for the duration of the call. Upon completion, the frequency is released and is available for another call.

At present, all voice calls are manually extended by the MARISAT shore station operator into the domestic or international telephone network. However, there are definite plans being implemented which permit automatic ship-to-shore operation and automatic shore-to-ship operation with the advent of INMARSAT by February 1982.

In setting up a MARISAT ship-to-shore voice call, the MARISAT operator, upon request, extends the ship satellite link to the AT&T telephone network via connection to one of AT&T's international operating centers or co-located domestic exchanges. From this point on, the MARISAT call is handled similarly to any domestic or international telephone call.

In the shore-to-ship direction, U.S. domestic calls are accepted by the MARISAT operator via a special line. The MARISAT operator then establishes the satellite link to the called party and subsequently extends the call to the calling party through a terrestrial line.

Incoming international calls are processed by the international operators and extended to the ship by the MARISAT operator.

4.2 Characteristics of the Voice Channel

The satellite voice channel meets or exceeds the standards shown in Table 2. These values exceed AT&T standards for C2 conditioning. The MARISAT channels use in-band signalling at 2600 Hz which creates the same limitations on transmission at this frequency as are found elsewhere. Upon request the satellite circuit may be operated without the companders in the circuit. The satellite circuit contains a half echo suppressor at the shore station, which is disabled by both CCITT and North American standard data carriers.

4.3 Data Transmission Via the MARISAT Network

Data calls are processed through the MARISAT System exactly as a voice call, except the calling party has a choice of retaining or removing compandors on each end of the satellite link prior to exchanging data.

As in the voice mode, data service is established on demand via a single channel per carrier, (SCPC) satellite channel using frequency modulation. Compandors are retianed in the satellite facility by selecting the voice operation mode at either the ship terminal or shore station end. Voice mode would be used when using the ship terminal telephone handset in conjunction with an acoustical coupler.

On one widely used type of terminal, when a non-compandored channel is used, data is introduced into the channel via two data jacks, located on front of terminal, which are enabled by selection of the 'data' mode (i.e., a non-compandored channel). Generally, asynchronous data at speeds up to 1800 bps is transmitted through the handset whereas the data jacks are used for higher speed (2400 - 4800 bps) synchronous data. This is not due to the satellite link design but depends on the operation and modulation scheme of a particular modem.

Tests have shown that, at the edge of coverage, using suitable modems, for a 2400 bps data rate, error rates of better than $2x10^{-5}$ are achievable. For 4800 bps error rates of better than $3x10^{-3}$ are achievable. Different types of modems were tested, with the best results being obtained from a modem that used 8 phase PSK modulation.

In the case of data transmitted to and from international points, the process is similar to establishing a domestic terrestrial call except that due to tariff restrictions, data must be transmitted and received via an international record carrier, i.e., RCA, ITT, WUI, or TRT. Therefore, all data calls must be routed to an IRC gateway in a gateway city and not via the international telephone network; however, a recent FCC decision may eliminate this restriction.

4.4 Facsimile Service Via the MARISAT Voice Channel

A number of different types of facsimile units have been tested and are used over the MARISAT System. Both acoustically coupled units and the more recently developed digitized facsimile units are used. These devices use various schemes, such as: AM, FM, PM and AM with vestigial sideband transmission in transmitting pictures.

Some of the Facsimile Units tested successfully through the MARISAT System are:

Unit	Coupling	Modulation
1. Xerox		
a) Teleconier III	- Acoustically Coupled	FM
b) Telecopier 400-1	- 2/4 Hybrid Coupled	FM
c) Telecopier 410	- Acoustically Coupled	FM

Unit	Coupling	Modulation
2. Graphic Science		
a) DEX Model 700	Acoustically Coupled	Choice of AM or FM
b) DEX Model 580	Acoustically Coupled	Choice of AM or FM
3. Qwip		
a) Model 2400	Acoustically Coupled	Choice of AM or FM
4. Muirhead		
a) Muirhead K-400	D/S transmitter and K401-D/5 Receiver	4 Wire Mode
5. RapiCom		
a) Model 100	Digital Fax	Speed up to 4800 bps
6. Panafax		
a) MUI200	2/4 Hybrid Coupled	
b) UF320	Digital 4800 bps - 2/4 Hybrid Coupled	

Scanning time on each unit varies from as low as 35 seconds to two, three, four and six minutes per 8-1/2" by 11" page. Horizontal and vertical resolution varies from 62 lines per inch to as high as 200 lines per inch depending on selected transmission speed.

Facsimile resolution, density, transmission time along with other factors such as line width, scan sweeps, tone shades and transmission line parameters all affect picture quality and cost.

In general, Facsimile transmission (picture quality), over the MARISAT Facility is equal to transmission over the telephone lines used in the U.S. domestic telephone system.

5. FUTURE USES OF THE MARISAT SATELLITE

Both COMSAT General and other organizations continue to investigate new uses for the MARISAT satellite. Recent suggestions have included:

Terminals aboard aircraft

Terminals of lower G/T (Gain to receive noise temperature ratio) for use aboard smaller vessels

Rescue beacons and terminals aboard lifeboats

Surveillance of coastal oil tankers and fishing craft.

Terminals aboard aircraft would use existing communications channels and would, therefore, have a G/T equal to ship terminals, or at least not much lower. This requires an antenna with a fully steerable beam. A manufacturer has developed a plan for fitting a Boeing 747 aircraft with a radome to contain a standard design of MARISAT antenna.

In addition to mechanically steered antennas. phased array antennas are possible. Discussions with manufacturers have shown that it would be possible to develop phased array antennas with a gain of about 19 dB, although probably 16 dB is a more reasonable target for practical costs. If 19 dB were achievable, it would be possible to use standard MARISAT communication channels, at least for elevations of above about 10°.

There may be demand for cheaper terminals to be used on smaller ships. INMARSAT Preparatory Committee has considered antennas of the so-called 'standard' and 'standard C'. These would have G/Ts of approximately -12 DBK and -19 DBK, respectively compared with G/T of -4 DBK for present terminals.

The choice of G/T was based upon the assumption that the major cost factor would be antenna steering. The two types would have the highest gain possible with either no steering, or else steering that did not require continuous compensation for vessel motion.

Before introducing such terminals many details, including modulation methods, and access and control methods, must be decided.

For the past four years experiments have been taking place in the use of 'EPIRBs', "Emergency Position Indicating Radio Buoys". These would be low powered beacons ejected by ships or aircraft in case of an accident. An EPIRB is constrained by having only a limited power supply, and by having to transmit while being tossed about in a probably rough sea. This results in a transmitter with an EIRP of probably less than 7 dBw transmitting through an essentially omnidirectional antenna, and therefore being very susceptible to multipath fading.

In the Federal Republic of Germany, the DFLVR, (Deutche Fersuchsanstaldt fur Luft & Raumfart) have developed a prototype, which can send a message of approximately 100 bits, using narrow band FSK. For adequate margin, if the existing maritime mobile satellite shore stations are used, this prototype will require a satellite transponder gain higher than provided by either MARISAT or the proposed INTELSAT MCS (Maritime Communications System) packages.

Experiments are now taking place with an alternative concept. This would use a spread spectrum PSK modulated signal. The wider bandwidth would allow a greater processing gain which, together with integration of successive repetitions of the signal, would permit reception of the message through existing satellites. Techniques usable with an EPIRB might also be usable with a similar transmitter in a lifeboat. The lifeboat transmitter would be able to change its canned message and might be able to use more power.

Another requirement that appears to be developing in the world is a means of monitoring possition of ships. In waters of concern to the U.S. such ships would incolude fishing boats, and vessels carrying dangerous cargoes, such as oil tankers and liquified natural gas ships. All these types of ships might be required to report their position, possibly with a considerable degree of accuracy.

MARISAT's primary role is communications and not navigation. However, MARISAT could be used to transmit data back to shore derived from other navigation equipment which ships would in any case carry. Ships are already transmitting navigation data back to shore, as indicated above, and such data could be transmitted using the low power terminals envisaged here instead of the MARISAT telex channel used today.

COMSAT General has been approached by customers seeking to use terminals on land. Except where necessary for control or development purposes such use is not permitted by the regulations of the International Telecommunications Union and the U.S. Federal Communications Commission.

The results of the WARC World Administrative Radio Conference have provided no dramatic changes that will affect Mobile Maritime Satellite service. The Maritime Mobile Satellite Band will be expanded from 7.5 MHz to 14 MHz. MARISAT satellites now use 4 MHz. However, the present growth in traffic[2] will clearly eventually make the extra bandwidth necessary.

In addition to the 14 MHz, available both to ship, and from ship, there is an extra 5 MHz in the ship to satellite direction only. This could be used for such purposes as the High Speed Data service discussed elsewhere at this conference.

The new maritime mobile satellite bands will be: ship receive, 1530 to 1544 MHz, and ship transmit, 1626.5 to 1645.5 MHz. In addition, 1 MHz will be shared with the aeronautical service for emergency purposes. This 1 MHz wide band was moved by 1.5 MHz and will be between 1544 and 1545 MHz for ship receive and 1645.5 and 1646.5 for ship transmit.

6. Conclusions

MARISAT's integration of ships communications with the world telephone and telex network has resulted in a number of uses beyond traditional speech and record communications. As with terrestrial systems these uses are continuing to grow. Such uses will continue to grow and although changes appear at first glance to be evolutionary rather than revolutionary, they are beginning to make major changes to world shipping.

References

1. D. W. Lipke et al - "MARISAT - A Maritime Satellite Communications System" COMSAT Technical Review Fall 77
2. D. W. Lipke - "An Overview of MARISAT Commercial Service" Conference Proceedings Intelcom 79
3. "Technical Requirements for MARISAT Shore Stations" published by COMSAT General Corporation 1 Feb. 78
   NOTE: With the coming into existence of INMARSAT, a corresponding INMARSAT document will supersede this document, probably in about mid-1980
4. Report 761 of the CCIR "Technical and Operating Characteristics of Distress Systems in the Maritime Mobile Satellite Service" CCIR Green Book, Kyoto '78, Vol. VIII.
5. Weinberg, Kaminsky and Keblawi, "A Novel Concept for a Satellite Based Maritime Search and Rescue System" IEEE Journal of Ocean Engineering Vol. OE-2 No. 3 July 77

80-0479

DIRECT MECHANICAL STABILIZATION OF MOBILE MICROWAVE ANTENNAS

R. J. Matthews, President
SeaTel, Inc.
Martinez, California

Abstract

Recent developments in direct mechanical stabilization (DMS) make this an attractive alternative to servo methods in common use. Advantages of cost, reliability, and serviceability are provided in DMS equipment. DMS operates on the principle of convertibility of angular impulse and gyroscope momentum. DMS gyros typically weigh several pounds, have low spin speeds, and have operating lives exceeding five years. Statically balancing the assembly about all motion axes eliminates the major source of stabilization disturbances occurring in earlier DMS designs. Means for providing a reference orientation to the balanced assembly are described. DMS is shown to have the potential for breaking the cost barrier to mass mobile satellite communications usage.

Introduction

Microwave antennas used in mobile applications ordinarily must provide substantial levels of gain, hence they are inherently directive, and must be aimed. In applications aboard ship, on airplanes, or in land vehicles, most microwave antennas must not only be initially aimed but also must be stabilized so as to maintain correct pointing in the presence of vehicle motions. This paper reviews briefly the stabilization requirements of microwave antennas used in mobile satellites communications service and presents an introduction to direct mechanical stabilization (DMS) for such use.

Even though DMS pre-dates servo technology, most stabilized equipment used over the years has been of the servo type. Historically, servo stabilization systems have been designed to provide increasingly accurate performance, but they have also become increasingly complex, costly, and difficult to service.

DMS is not new: patent literature describing DMS equipment exists which dates back to the early part of the century.[1] Full development of DMS technology did not occur over the long intervening period, however, probably because of the concurrent evolution and greater versatility of servo technology. For whatever reasons, certain basic DMS concepts have only recently been described in governmentally issued patents and patent applications and thus are still under patent protection.[2, 3]

In the present era of expanding commercial mobile satellite communications applications, obtaining exceptionally high levels of stabilization accuracy is much less important than obtaining exceptionally high levels of reliability from inexpensive equipment.[4] As will be shown below, direct mechanical stabilization offers both of the latter characteristics while still providing prudent performance margins. It therefore holds the key to several potentially large mobile satellite communications markets. In short, DMS is a technology whose time has come.

Antenna Stabilization Requirements

Well-designed plane aperature antennas typically have 3 dB beamwidths given by:

$$\psi = K \frac{\lambda}{d} \text{, degrees} \qquad (1)$$

where K is a constant ranging from 55 to 75 depending on sidelobe level, λ is the operating wave length, and d is the effective antenna aperature diameter expressed in the same units as are used for wavelength.[5] Equation (1) indicates that a 50-inch diameter antenna operating at 1650 MHz will have a half-power beamwidth of about 10 degrees. Since motions of most vehicles on which such an antenna would be mounted greatly exceed this value, antenna stabilization is usually required. Antennas used aboard ship in the MARISAT satellite communications system, for example, should be designed to[6] accommodate the range of motions listed in Table 1.

A diagram of accelerations which can exist at a masthead location as a result of the conditions listed in Table 1 is shown in Figure 1. It can be seen that a pendulum-supported antenna at that location would experience pointing errors up to 20 degrees, causing a signal reduction of more than 20 dB. Although this is only one example, it is illustrative of the magnitude of motion effects which can be expected in mobile microwave antenna applications.

Satellite communication links typically are designed with 10 to 20 dB received power contingency margins for atmospheric attenuation, multi-path effects, transmit power variations, receiver sensitivity and noise temperature degration, and other communications parameters. In that context an allowance of 1 dB for antenna mis-pointing from all causes is entirely reasonable since it amounts to only one fifth of the total communications link error (or uncertainty) budget. For a 50-inch diameter antenna operating at 1650 MHz the 1 dB half-beamwidth is about 3 degrees, an amount which realistically can be tolerated for antenna mis-pointing from all causes in terms of overall communications system performance. Analysis of the various factors which contribute to antenna pointing errors shows that assignment of half the allowable error to the stabilization system, and the other half to mis-pointing from all other causes is reasonable and in keeping with achieving a balanced design. For the example, then, a stabilization system accuracy requirement of 1.5 degrees would be appropriate.

The stabilization accuracy criterion described above, namely one half of the antenna's 1 dB half-beamwidth, is at variance with the commonly used one-tenth rule. Specifying equipment to be ten times as accurate as the desired accuracy of a measurement is generally appropriate for measuring equipment, but it leads to unneccessarily expensive equipment when applied to communications antenna steering systems.

Released to AIAA to publish in all forms.

Copyright © SeaTel, Inc. 1980
All rights reserved.

Table 1 Recommended Environmental Conditions
For MARISAT Ship Terminals (abbreviatd)

Motion	Amplitude	Period	Equipment Installation Distance From Motion Axis
Roll	± 25°	4π sec	30 m
Pitch	± 7½°	3π sec	76 m
Yaw	± 4°	100 sec	70 m
Surge	± 0.1 g		
Sway	± 0.1 g		
Heave	± 0.25 g		
Turning Rate	6°/sec		
Headway	30 knots		

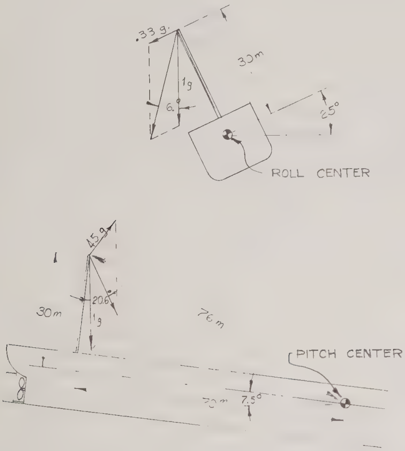

Fig. 1 Simplified Acceleration Diagram for MARISAT Ship Motions

This paper deals specifically with stabilization against vehicle pitch and roll motions, but it should be understood that in most applications stabilization against yaw/turning motions is also necessary. Typically this is accomplished by slaving the antenna's azimuth axis to a gyro compass using methods unrelated to direct mechanical stabilization.

Direct Mechanical Stabilization (DMS)

Direct mechanical stabilization, as the phrase implies, involves the application of direct mechamcal forces to a support platform so as to resist disturbing forces which tend to change the angular orientation of that support platform. The applied mechanical forces, or torques, are derived from simple gyroscopic assemblies. The gyro assemblies used in DMS equipment differ from instrument-type gyros used in servo applications mainly as regards size and speed, with important consequences regarding cost and reliability. Instrument gyros typically rotate at 20,000 rpm and higher, weigh only a few ounces, and have operating lives measured in hundreds of hours. In contrast, DMS gyros spin in the range of 1500 to 4,000 rmp, weigh several pounds, and have operating lives ranging beyond 50,000 hours. Complete, two-axis direct mechanical stabilization can be added to a basic four-axis antenna pedestal for less than the cost of the cheapest inertial sensors used in servo-stabilized pedestals. These advantages, which are discussed in subsequent sections, account for the currently increasing use of DMS equipment. It can be noted that even though maritime satellite communication ship terminals have been manufactured for less than five years, four major companies have already adopted DMS for their designs.[7]

As differentiated from servo-type systems, DMS uses no transducers, no signal processing, no amplification, and no mechanical-to-electrical-to-magnetic-to-mechanical conversions. Disturbing torsional impulses occurring to a support platform are resisted by gyro assemblies converting those impulses into equivalent changes in angular momentum. These angular momentum changes are manifested by gyro precession motion. The physical mechanism by which this occurs and the underlying theory are discussed in the following section.

The Magnavox Company manufactures a maritime satellite communication ship terminal which utilizes a direct mechanically stabilized antenna pedestal, Figure 2.

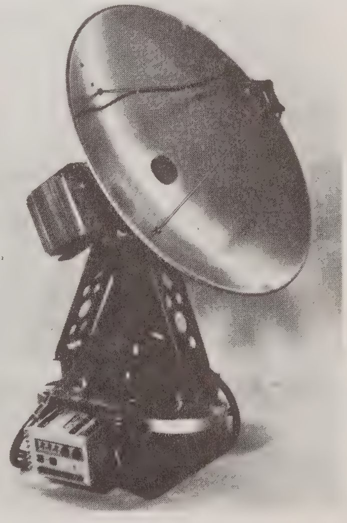

Fig. 2 Commercial DMS-Type Antenna Pedestal

Designated the Model MX 111, the Magnavox unit has an extensive history of satisfactory operation in the MARISAT system. The pedestal consists of an elevation-over-azimuth-axis assembly which is electrically steered to any desired direction, and which itself is mounted on a stabilized roll/pitch gimbal assembly. Two flywheels (gyros), each supported on its own precession axis, are mounted on the roll/pitch gimbal to provide individual stabilizing effect for ship roll and pitch motions, respectively. The third motion axis, azimuth (or train), is also stabilized in this equipment. Yaw/turning motions of the ship are decoupled from the antenna by virtue of the azimuth axis being slaved to the ship's gyro compass. In operation the antenna remains rotationally motionless in inertial space while the ship rolls, pitches, and yaws/turns under it.

Basic DMS Theory

DMS equipment operates on the well-known principles of gyroscopic action. Briefly stated those principles are: (1) when there is no moment of force acting on a gyroscope, the spin axis maintains a fixed direction in inertial space; (2) when some external moment of force is exerted at right angles to the spin axis, precession takes place, and (3) the gyroscope then exerts an equal and opposite reaction moment on the external moment; (4) a moment of force about an axis parallel to the axis of precession will cause a tilt of the gyroscope.[8] The manner in which these effects occur is illustrated in Figure 3.

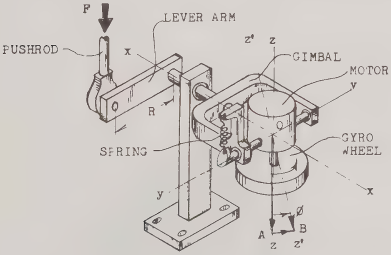

Fig. 3 Elementary Gyroscopic Mechanism

In Figure 3 a gyro wheel is attached to the shaft of a motor which rotates about spin axis z-z at an angular velocity ω. The wheel and motor combination is supported by a transverse axis on low friction bearings such that this gyro assembly can rotate at least over a limited range about axis y-y. Axis y-y is called the precession axis; it is substantially perpendicular to spin axis z-z. Power to the motor is provided through flexible conductors so as to avoid undesired precession motion restraint. A gimbal supports the gyro assembly and itself is supported on an axle which allows it rotation about torque axis x-x. In the steady state all three axes, x-x, y-y, and z-z, are mutuallly perpendicular.

In the absence of an external torque and with the wheel rotating, the gyro assembly will tend to remain at some initial orientation which has been established by external means. As will be shown later, the external reference orientation means used are critically important to the dynamic stabilization accuracy which is achieved. When a torque tending to rotate the gimbal is applied, as by a force F acting on the gimbal lever arm, an opposing torque will be developed by the gyro assembly in accordance with the principles for the convertibility of impulse and momentum. This can be illustrated as follows: Let I and ω be the rotational mass moment of inertia and the angular velocity of a gyroscope about its spin axis. Let L be the moment of an externally applied force, and let Ω be the angular velocity of precession. To find the simplified relationship between these quantities let the vector OA, Figure 4, represent the system's initial angular momentum, the magnitude of which is given by the product I x ω. After a short time t, during which a torsional impulse of magnitude L x t will have been applied, vector OA will have turned through a small angle Ø to position OB, where Ø = Ωt. For this to happen, angular momentum, represented by vector AB, must have been added, and this must equal L x t. Therefore:

$$\frac{L \times t}{I_g \times} = \frac{AB}{AO} = \Omega t, \text{ whence} \tag{2}$$

$$L = I_g \omega \Omega \tag{3}$$

Thus it can be seen that a gyro assembly converts disturbing torsional impulses into equivalent changes in angular momentum, by precession of its spin axis. Note that this change in angular momentum involves no changes whatever in spin speed.

In changing its spin axis orientation the gyro assembly actually undergoes two different motions: a continuing rotation about the precession axis y-y as described above, and a small, one-time angular off-set about torque axis x-x. When a torque is first applied a transient rotation occurs about the torque axis. After this transient motion dies out there is a final steady deflection caused by the imposed torque. Thus, the gyro assembly behaves as if it were a stiff spring opposing rotation about the torque axis. The transient motion may be analyzed by means of the general equations for rotation of a body about its mass center. The result is simple if the increment $e = \theta - \theta_o$ is sufficiently small, θ_o being the value of θ for no applied torque and no precession, where θ is defined as the angular orientation of the gimbal with respect to the support member about the torque axis x-x. The general equation is:

$$L = I_t \frac{d^2e}{dt^2} + B\frac{de}{dt} + \frac{I_g^2\omega}{I_t} \tag{4}$$

Here I_t is the mass moment of inertia of the combined gyro and gimbal assembly about the torque axis, B is a dampimg coefficient, and other symbols are as defined earlier. Solutions of (4) lead to simple harmonic motion when L is constant. When damping forces, represented by the coefficient B, have damped out the oscillations, the resulting deflection is:

$$e_{\text{final}} = \frac{I_t \times L}{(I_g \times \omega)^2} \tag{5}$$

Equation (5) describes, as a first approximation, the steady state error in platform orientation as the result of a constant disturbing torque. The system acts like there were a spring whose torsional stiffness is:

$$k_\theta = \frac{(I_g \omega)^2}{I_t} \qquad (6)$$

The total angular motion of the gyro assembly about the precession axis is an important design parameter because it establishes the required precession axis angular range. This angle, symbolized as $\emptyset$, depends on the time duration of the disturbing torsional impulses. If the disturbing torque acts a period of time t, and if $\frac{d\theta}{dt}$ is the same at the beginning and end of t, the total precession angle $\emptyset$ is given by:

$$\emptyset = \frac{1}{I_g \omega \sin \theta} \int_0^t L \, dt \qquad (7)$$

The preceding analyses show that a gyro assembly will maintain a gimbal (platform) close to its original orientation in the presence of disturbing torques of limited duration, provided it can precess. A continuously applied torque will of course produce continuous motion about the precession axis, and if precession proceeds to the point where a mechanical stop is reached the gimbal will become unstabilized. This is analogous to the condition of saturation in a servo stabilization system which, when it occurs, also results in platform destabilization.

Orientation References

As previously noted, means must be provided for establishing initial orientations to the gyro and gimbal assemblies and for returning them to those positions when displacements have occurred. One method is to make the several assemblies pendulous, thus using gravity as the basic orientation reference.[2] Although this method has been used in several commercial designs, it imposes several limitations on stabilization system performance. Other reference orientation means have therefore been developed in more recent designs which avoid those limitations. Each of these main types of reference orientation means is discussed below.

A pendulous assembly (pendulum) moves in response to the vector sum of all accelerations and other forces acting on it. Gravity is normally the predominant factor, but in mobile applications a pendulum can experience horizontal accelerations which cause large excursions from true vertical. This is indicated in Figure 1, which shows that an undamped pendulum will swing 20° degrees away from vertical in the indicated environment. Errors of a damped pendulum would be even larger. For equipment located some distance from a ship's motion center it can be shown that a ship's periodic motions cause horizontal accelerations which are approximately proportional to the product of the sine times the cosine of the motion amplitude. Thus the larger the motion amplitude, the larger are the horizontal accelerations acting to mis-orient a pendulous platform. Making a platform pendulous thereby creates the interesting, and undesirable, paradox that the pendular effect used to establish the basic orientation is the same effect responsible for the largest disturbances to that orientation!

As an example, consider a pendulous platform which weighs 150 pounds and has its cemter-of-gravity 0.5 inches below the support axes. In the static situation the pendulum effect will exert a torque of 1.3 inch-pounds per degree to return the platform to its equilibrium position whenever it is displaced from that position. That same pendulous characteristic will also create a disturbing torsional impulse on platform orientation of over 100 inch-pound-seconds per half-cycle of roll motion when operated in the dynamic environment described in Figure 1. For a typical pendulous DMS pedestal this will cause an antenna pointing error somewhere in the range of ½ to 1½ degrees during each half-cycle of motion.

As an alternative to making the platform pendulous, the supporting structure (ship) itself can be used as a basic orientation reference.[3] This is possible because, on the average, the support vehicle is upright. A ship, for example, may, and usually does, roll and pitch away from vertical in oscillating motions which typically have periods in the range of 8 to 30 seconds. The average orientation, however, is vertical. Thus the ship itself can be considered and used as a giant reference pendulum. Coupling the vehicle structure to the stabilized platform can be accomplished in various ways, but in all cases the platform itself should be statically balanced about its support axes. Balancing the platform has the very desirable effect of making it immune to horizontal accelerations.

Simple linear springs can be used to couple the support structure to the stabilized platform. This arrangement has the virtue of simplicity, but it can cause relatively large disturbing torsional impulses. A preferred arrangement involves the utilization of non-linear springs which develop increasing torque with increasing displacements for small displacements, and which maintains that torque at an essentially constant value for all larger displacements. This mechanization also lends itself to the inclusion of controlled viscous damping in the orientation restoration function. These effects can be obtained using combinations of simple mechanical elements. The same levels of restoration torque for small offsets as are developed in the pendulous case, but which create less than one-tenth of the disturbing torsional impulse, can be developed. Significant accuracy improvements will result.

A third reference orientation means, and the preferred method, utilizes a separately supported pendulum which is coupled to the platform by means similar to those described above.[3] This arrangement establishes a true vertical reference orientation even if the support structure takes some average position away from vertical (as occurs when a vessel lists) while retaining all of the advantages associated with the previously described method. Again, when an auxiliary pendulum is used, the platform itself should be statically balanced about its support axes.

Combined Motions

As in conventional servo-stabilized platforms, DMS equipment provides separate and independent stabilization for the two horizontal (roll and pitch) motion axes. This is achieved by using two gyro assemblies which are oriented in quadrature to each other. Simultaneously occurring roll and pitch motions therefore have no interactive effects since each gyro assembly stabilizes only its components of the combined resultant motions. Yaw/turning, or other motions about the vertical (azimuth) axis, however, can induce large disturbances to platform level when they occur at the same time as roll or pitch motions. These combined-motion effects result from coupling horizontal centrifugal accelerations with any horizontal components of angular momentum in the gyros. No horizontal angular momentum component exists when the gyro spin axis is exactly vertical, but this is not the usual situation. Usually the spin axis has precessed some angle away from vertical as a result of correcting for some disturbing torsional impulse. Any horizontal component of angular momentum in one gyro will couple with any horizontal centrifugal acceleration to create a platform disturbing torque which, because of the quadrature arrangement, the other gyro assembly must resist. This is an operating condition which is accommodated in some DMS designs simply by increasing the torsional impulse absorbing capacity of the gyros.

Another method for handling the problem of combined motions applicable in those designs where the gyro assemblies are mounted on structure which rotates in azimuth, is simply to limit the maximum allowable azimuth turning rate. This method, however, has large disadvantages in applications where communications continuity is important.

A third, and preferred, method for solving the combined-motion problem is to mount the gyro assemblies on their own free-floating azimuth structure. The gyros thereby never experience horizontal angular accelerations and consequently cannot create disturbing torques from them. This is the configuration which, when used in conjunction with the statically balanced arrangement described in the preceding section, produces the highest levels of stabilization accuracy from currently available DMS equipment.

Gyro Spin Speed

Angular momentum of the gyro assemblies is a primary design parameter in DMS equipment since it largely determines platform accuracy and torsional impulse absorbing capacity of the system. The angular momentum of a spinning assembly is defined as the product of mass moment of inertia times spin speed. From this and other basic definitions it can be shown that the ratio of momentums between two gyro wheels of the same diameter is simply the ratio of their respective weights times their spin speed. Thus the same angular momentum can be obtained in different designs using the same wheel diameter simply by keeping the product of weight times speed constant. This has important implications regarding equipment reliability because of the separate effects of load and speed on bearing life.

Standard design handbooks present information which shows that, in the speed range of interest, ball bearing life is inversely proportional to the cube of the load.[9] From this it follows that for a given bearing the ratio of operating life for two gyro designs having the same angular momentum and wheel diameter varies as the square of the speed ratio. As an example, consider two alternative designs where spin speed is 1500 rpm in one case and 3000 rpm in the other. The above criterion shows that, because of its lighter wheel, the 3000 rpm design will have four times the operating life of the 1500 rpm alternative. Thus, in the speed range of interest, DMS equipment which uses low speed gyros is not necessarily more reliable, and indeed may have a considerably shorter operating life than DMS equipment which uses higher speed gyros.

In this application grease lubrication of the gyro motor bearings is the only practical choice. The grease in such bearings must be replenished periodically, the frequency depending on operating speed. The higher the operating speed the shorter is the re-lubrication period, the relationship being exponential in form. These factors establish an upper practical limit on gyro spin speed which lies somewhere in the range of 3600 to 4000 rpm because higher speeds would necessitate unacceptably frequent servicing.

Within the desirable speed range, i.e. up to about 4000 rpm, use of higher spin speeds not only tends to produce longer operating life, it also results in lighter overall pedestal weight. By way of example, one commercially available DMS pedestal uses 1500 rpm gyros and weighs over 300 pounds, while another design uses 3200 rpm gyros and weighs less than 150 pounds. In both cases the pedestal is fitted with a 50-inch diameter parabolic antenna. The advantages of light weight equipment in mobile applications are obvious.

Contemporary DMS Equipment

Direct mechanical stabilization can be included as an original, integral part of an antenna pedestal, or it can be substituted for servo stabilization in an existing design. One example of the former was depicted and discussed earlier; a second example, and one which includes the latest developments in DMS technology, will be discussed later. Arrangements wherein DMS can be applied as a modification unit to existing pedestals are discussed next.

Figure 4 depicts a DMS modification unit intended to substitute for the servo system in an existing MARISAT antenna pedestal. In this design a support post attached to the radome baseplate supports a U-joint which serves as the roll/pitch gimbal. The U-joint is mounted such that it does not revolve and so that its two transverse axes are parallel, respectively, to the roll and pitch axes of the antenna pedestal, not shown. An azimuth spindle extends from the upper U-joint yoke and supports bearings which in turn support the gyro mounting frame. This frame is free to rotate as it will in azimuth. Electrical power to the gyro motors is carried across this axis via a rotary air gap transformer (not shown) or alternatively by slip rings. Attached to the gyro frame are two gyro assemblies, each mounted on its own precession axis and oriented 90° to each other.

Each gyro assembly is balanced about its precession axis but is restrained toward a vertical position by a spring. These two gyro springs are arranged to be in contact with an adjacent structural member so as to create a small, but important, damping effect.

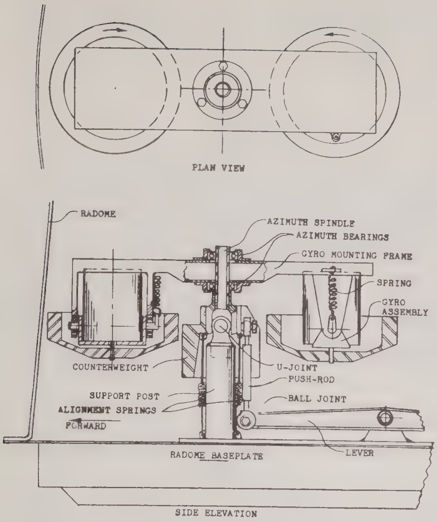

Fig. 4 DMS Modification Unit

The upper yoke of the U-joint carries brackets to which two ball-joint/push-rod assemblies are attached. One of these picks off roll motion and the other pitch motion. At their other ends these push-rods are connected to levers which, through a second pair of push-rods, control the roll and pitch orientation of the antenna pedestal gimbal.

The entire assembly is counter-weighted so as to be statically balanced about its support axes. Non-linear springs are connected between the support post and the upper U-joint yoke so as to urge them into alignment with each other in both directions. As with the gyro springs the gimbal alignment springs are arranged to provide a damping effect.

In operation the stabilizer unit will assume the orientations shown when no ship motions are present. When the ship rolls, pitches, or both, the system will tend to remain stable in this initial orientation in inertial space because of its mass moment of inertia and from being statically balanced. Nonetheless, disturbing torques will develop from push-rod bearing friction, residual imbalance, and from the alignment springs. These disturbances will be resisted by the gyros as they convert them into changes of angular momentum, manifested by precession. An observer could note that the gyro mounting frame remains horizontal while each gyro rocks back and forth on its precession axis as the ship rolls and pitches.

When the ship yaws, or turns, the gyro mounting frame does not turn with it but remains essentially motionless in azimuth by virtue of its being free-floating. Even when a gyro has precessed a large angular amount (as a consequence of having absorbed torsional disturbances) and thereby has a significant component of momentum in the horizontal plane, yaw/turning accelerations are not coupled to it, hence no gyro reaction torques are created. The system is therefore immune to the effects of yaw/turning combined with roll/pitch motions. The system is similarly immune to antenna cable rewrap operations because, again, the gyro mounting frame does not rotate. It can be noted in passing that some pedestals of both the servo- and DMS types are vulnerable to destabilization if a cable rewrap operation occurs simultaneously with large roll or pitch motions.

Two dimensions of the gyro mounting frame "motionless" (in inertial space) orientation are transmitted to the antenna pedestal gimbals through push-rods and lever linkages using geometry which provides faithful reproduction of motions (with respect to the ship) and which avoids cross-talk.

A DMS unit which incorporates all of the technical advances described in this paper is currently under development by SeaTel, Inc. When completed, this unit will combine high reliability, high accuracy, and light weight in a low cost, integrated pedestal. Central to obtaining these characteristics is use of a modified automotive U-joint as the gimbal assembly. In this statically balanced, four-axis pedestal the roll, pitch, and azimuth axes all mutually intersect, while the elevation axis is located so as to provide balance for other pedestal elements with minimum counterweighting.

Reliability

A simplified parts list for a DMS stabilization system and for a contemporary servo stabilization system are presented in Table 2.

Table 2 Simplified Parts Lists

I. DMS Sub-System

Item	Quantity
1. Drive motors	2
2. Flywheels	2
3. Precession bearings	4
4. Orienting springs	4
5. Gyro support frame	1
6. Support frame bearings	2
Total number of parts	15

II. Servo Stabilization Sub-System

Item	Quantity
1. Servo drive motors	2
2. Drive pulleys	4
3. Drive belts	2
4. Inertial rate sensors	2
5. Orientation sensors	2
6. Transistors	50
7. Integrated circuit modules	35
8. Potentiometers	6
9. Capacitors	81
10. Diodes	37
11. Resistors	156
12. Varistors	3
13. Transformer	1
14. Fuses	4
15. Inductors	18
16. RFI Filters	16
Total number of parts	419

It can be seen that more than 400 active components, not counting solder joints, cables, and connectors, are used in the servo system as compared to fewer than two dozen in the DMS design. It seems appropriate to repeat the somewhat facetious truism that all parts not used in a piece of equipment will never fail in that equipment. More scientifically, the MTBF for an equipment can never be greater than the worst (least reliable) component used in that equipment; further, the failure rate of equipment in which failure results from failure of any one of the constituent components can be computed simply by adding together the individual failure rates of all components. MTBF for the integrated equipment is then given as the reciprocal of that failure rate total.[10] Thus, confirmation is provided for the intuitive feeling that MTBF bears some kind of inverse relationship to the number of parts used.

A detailed reliability analysis of parts used in DMS equipment will show that, except for the gyro motor bearings, all parts can be designed to be so lightly stressed and to have such low duty cycles and such small individual failure rates, that the overall equipment failure rate is determined almost entirely by the bearings used in the gyro motors. Noting that DMS gyros typically operate in the range of 1500 to 4000 rpm, and that motor bearing loads are small, it can be shown that standard commercial quality (ABEC-1) bearings can be used to obtain an overall DMS equipment MTBF in excess of 40,000 hours at the 90% confidence level. Four out of five bearings will last even longer, with attendant trouble-free life for the complete DMS sub-system.

Cost

A four-axis antenna pedestal fitted with a DMS system utilizes only a few dozen more components and assemblies and is only slightly more complicated than a basic four-axis pedestal without any stabilization equipment. This is indicated by the simplified parts list shown in Table 2. Thus the parts cost for a DMS pedestal need be only a few hundred dollars more than the cost for the basic pedestal. From another viewpoint, the cost differential for adding DMS to a basic pedestal will be less than the cost for the cheapest inertial sensors which might be used to servo-stabilize that pedestal. The inertial sensors of course are only one small part of a complete servo stabilization system.

There is as much difference in maintenance expense between DMS and servo stabilized equipment as there is between their initial hardware costs. This is because DMS equipment has intrinsically high reliability (needs infrequent service) and because trouble diagnosis and repair in most cases is obvious and simple. In contrast, servo stabilization trouble diagnosis, which is needed more frequently, is subtle, involves sophisticated techniques, and is time-consuming, hence expensive.

DMS also has advantages in other categories of expense. As compared to servo equipment, DMS spare parts stocking requirements are fewer, service technician training is faster and easier, less supporting documentation is required, and much less testing is required to determine if a given unit is performing correctly. In summary, DMS has significant advantages over servo stabilization systems in every category of cost which goes into establishing the total cost of equipment operation and ownership.

Conclusions

Understanding the basic physics of direct mechanical stabilization has led to recent significant improvements in applied DMS technology. The intrinsic simplicity of DMS equipment is directly responsible for its characteristically high reliability, ease of service, and low initial cost. Comparisons between DMS and servo-stabilization show that DMS is the preferred method in applications where they both have adequate accuracy. Finally, DMS has the potential for breaking the equipment cost barrier to mass mobile satellite communication system usage.

---

[1] U. S. Patent No. 1,324,477, "Stabilized Gyroscopic Pendulum," H. L. Tanner, December 1919.

[2] U. S. Patent No. 4,020,491, "Combination Gyro and Pendulum Weight Passive Antenna Platform Stabilization System," Beezer et al, April 1977.

[3] U. S. Patent Application No. 8,066, "Mechanically Stabilized Platform System," R. J. Matthews, January 1979.

[4] Contract No. CGC-ES-108 between COMSAT General Corp. and Scientific-Atlanta Corp., filed with Federal Communications Commision, June 1974.

[5] Reference Data for Radio Engineers, 5th ed. (Howard W. Sams & Co., 1972), pp. 25-31.

[6] "Technical Requirements for MARISAT Mobile Terminals," published by COMSAT General Corp. as Manager for the MARISAT Joint Venture, August 1977.

[7] Letter from E. J. Martin, COMSAT General Corp., to R. J. Matthews, SeaTel, Inc., June 1979 (unpub.).

[8] Physics, 8th ed. (P. Blakiston's Son & Co., Inc., 1937), p. 87.

[9] SKF Engineering Data (SKF Industries, Inc., 1973), pp. 5-8.

[10] H. R. Henly, "Reliability" in Wireless World, February 1978.

80-0481

NUMBERING PRINCIPLES FOR AUTOMATIC MARITIME MOBILE SERVICES AND MARITIME MOBILE SATELLITE SERVICES

R. J. Manterfield
British Post Office, London

Abstract

Maritime communications are currently operated on a manual basis, but many administrations now wish to introduce automation such that through connections can be automatically established. The automation of the maritime services requires the use of national and international telecommunications networks and so international studies of numbering/routing techniques and numerical ship identification were necessary. This paper outlines the international standards recently agreed for the maritime mobile satellite services and describes how requirements for commonality with the maritime mobile VHF services affected the course of studies.

In the maritime mobile satellite services, land originated calls will be routed via international networks and hence international procedures (eg dialling) will be adopted. For ship originated calls, a prefix scheme will be used to identify the type of call required, thereby allowing standardisation of ship board procedures. All ships will be identified by unique 9 digit ship station identities, the first 3 digits indicating the registered nationality of the ship. Initially, only the first 6 digits will be significant, the last 3 digits being trailing zeros. This format allows transmission of the significant part of the identity through national networks whilst providing potential to evolve to a 9 significant digit scheme.

1. Introduction

Most current maritime communications are operated on a manual basis. However many countries now wish to introduce automation so that a through connection can be established automatically between land based terrestrial customers and customers on board ships. Due to inherent characteristics of the various maritime services, only automation of the maritime mobile satellite and VHF (coastal) services has been considered in detail. Automatic set up of telephone and telex connections are of immediate concern, but in future automatic operation of all other services (eg data) is being considered.

Any automation of maritime communications should be carried out to internationally agreed standards so that communication between ship and shore can take place on a worldwide basis: this is particularly important for distress purposes. Distress is a major function of maritime communications and matters relating to distress are regarded with the utmost importance throughout the world. To avoid any possible confusion relating to distress traffic, it has been agreed that as many numbering/routing aspects as possible should be standardised internationally. This standardisation would also reduce customer and administration confusion and provide evolutionary potential for future services. In particular, a ship identification scheme was required that could be applied to telephony and telex over maritime mobile satellite and VHF systems.

This paper is intended to describe recent provisional agreements at international meetings (CCITT, CCIR, etc) relating to the numbering/routing and ship identification principles for future automatic maritime mobile satellite services. Some proposals for automatic maritime mobile VHF services have been described in order to explain the impact of these services on the maritime mobile satellite services.

2. Numbering for Fixed Services

2.1 International Calls

World numbering plans currently exist for international telephone, telex and data calls. For telephony, a customer wishing to automatically call a customer in another country would dial an international prefix, the country code of the required country and the required customer's national significant number. For example, a customer in the United States calling a United Kingdom customer would dial the following format:

011 US international telephone prefix
44 UK telephone country code
1 London)
261 4256 Subscriber) national (signi-
number) number ficant)

Similarly, a UK customer calling a US customer would dial:

010 UK international telephone prefix
1 US telephone country code
202 Washington DC)
554 6838 Subscriber) national (signi-
number) number ficant)

The international prefix varies from one country to another but this code identifies to the national network the requirement for an international call. The country code indicates to the national and international networks the country or geographical area in which the required customer is located. For telephony, country codes consist of 1, 2 or 3 digits depending on the size of the telephone population of each country. The national significant number not only identifies the particular terminal required but also identifies the terminal's location.

The telex world numbering plan has a similar format to the telephone numbering plan, but the country codes (destination codes) consist of 2 or 3 digits. Data country codes consist of 3 digits only (the first 3 digits of the Data Network Identification Code), more than one country code being allocated to countries with large data requirements.

2.2 National Calls

National numbering plans for telephony, telex

Released to AIAA to publish in all forms.

and data vary throughout the world and no format is typical. However, as in 2.1, the national significant number identifies not only the required terminal but also its location.

3. Numbering for Maritime Services

Automation of the maritime services requires an extension of the principles described above. The set up of automatic connections in the maritime mobile VHF and satellite services can be initiated by land based customers (shore originated calls) or by customers on board ship (ship originated calls). Unlike the fixed services, the numbering/routing characteristics for setting up the two directions of traffic are different in some basic respects. In particular, for shore originated calls the identification of the ship does not inherently determine its location. This means that, in addition to providing sufficient numbering range for all ships, variable information concerning the ship's location must also be incorporated. The number of digits capable of being transmitted through national and international networks is limited and so the addition of location information poses a possible problem in all mobile systems. Hence, many of the principles described below can be applied to any mobile system (land, air, etc).

For ship originated calls, the general principles outlined in section 2 apply, in that variable location information is not required.

3.1 Shore Originated Calls

3.1.1 Maritime Mobile Satellite Services

Automatic maritime mobile satellite systems are international in nature and will be considered as part of the international network (eg the international telephone network), their introduction causing little or no impact on the existing network (see figure 1). During the course of studies it was found useful to regard the maritime mobile satellite system as a country in its own right, with ships participating in the system being analogous to customers in the satellite country (figure 1, section C). Hence, in general, the international telecommunications networks will be used to gain access to the satellite system whether or not the calling customer is located in the same country as the relevant shore station (figure 1, section B).

A series of international telephone country codes, 87S, has been allocated for use in the maritime services. Hence, to initiate a shore originated telephone call, a land based customer will dial an international prefix, a maritime country code and the ship identification, as follows:

+	International telephone prefix	
87	Maritime international code	maritime country code
S	Ocean area/ satellite system	
NIDXXX(000)	Ship identification (format described in section 4).	

Routing through the networks (figure 1, sections A and B) will be based upon the country code 87S. The relevant shore station will be determined by the value of the S digit, chosen by the customer to indicate the expected ocean area in which the ship is located (and satellite system if more than one system exists). When there is more than one shore station per ocean area, the choice of shore station will be made by the originating operating authority. The maximum significant number length currently permitted in the international telephone network is 12 digits and so, allowing for the 3 digit 87S code, 9 digits would be available for ship identification purposes.

As the world's major ocean regions can be served by 3 satellite coverage areas, the ship location information can easily be conveyed within the S digit. Three maritime telephone country codes are currently allocated: 871 indicates the MARISAT Atlantic Ocean satellite system, 872 indicates the Pacific Ocean satellite system and 873 indicates the Indian Ocean satellite system. Further specific codes may be allocated in the future.

FIGURE 1 - GENERAL NETWORK ROUTING FOR SHORE ORIGINATED MARITIME MOBILE SATELLITE CALLS

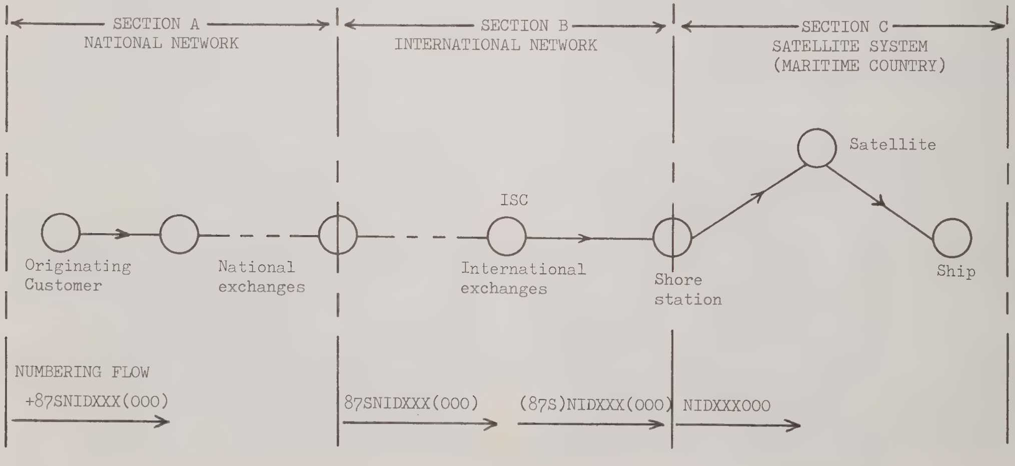

As an example of how the codes are used, a customer in the United States wishing to make a telephone call to a MARISAT ship in the Atlantic Ocean will dial:

011	US international telephone prefix
871	Maritime telephone country code for Atlantic Ocean
NIDXXX(000)	Ship identification (format described in section 4)

The numbering flow through the network for a general case is given in figure 1.

A corresponding series of telex destination codes (58X) has also been allocated (where X is equivalent to S for telephony). Hence, to initiate a shore originated telex call, a land based customer will dial or key the international prefix of the particular country, the destination code 58X followed by the ship identification.

In general, the shore station will act as the interface between the satellite system (country) and the international network (figure 1, interface between sections B and C). Hence, it is currently envisaged that the shore station will appear as, and have the status of, an international switching centre (ISC) as far as the international network is concerned. It follows that the network interface with the shore station will be provided via international procedures (signalling systems, etc). Each administration can decide whether the shore station should have full ISC status or whether only limited facilities would be provided.

In telephony, for transmission reasons (eg propagation delay) it is undesirable for two satellite links to be tandem connected. Hence for calls to or from the maritime mobile satellite service, satellite links in fixed services should be avoided. For shore originated calls, identification of the code 87S would provide sufficient information for this purpose, but application of this principle depends on the route selection capability of terrestrial ISCs. For ship originated calls, difficulty will be encountered in identifying maritime satellite service calls until future network techniques are available.

3.1.2 Maritime Mobile VHF Services

Maritime mobile VHF services are more localised in nature than the maritime mobile satellite services. Attempts were originally made to adopt similar dialling procedures for the two services, but after much study it was agreed to give access to the maritime mobile VHF services through national networks ie part of each national network numbering range would be allocated to the maritime mobile VHF services. Although it was agreed that the method of access to the VHF services would be different to that of the satellite services, the desire for a common ship identification scheme remained. Such a common ship identification plan is outlined in section 4. The decision to give access to the VHF services through national networks means that national network limitations become prominent and that methods of access to the VHF services will vary from country to country. Several methods of access have been identified and 3 levels of operation, relating to routing aspects of ship location registration have been agreed.

To illustrate the principle, an example of one method of access to maritime mobile VHF services has been identified for a customer in one country calling a ship off the coast of another country:

+	International prefix of originating country	
$I_1 I_2 I_3$	1, 2 or 3 digit country code	
ABC	Code to identify maritime mobile VHF services	national (significant) number
X_1-X_n	Ship identification	

National access methods require the allocation of a code (ABC) from the national numbering range (unlike access to the maritime mobile satellite services). As many national networks can only handle 9 digit national significant numbers, a 3 digit ABC code would only allow 6 digits for ship identification purposes. This limitation, and the desire for a common maritime mobile VHF/satellite ship identification scheme, imposed restrictions on the numbering for the maritime mobile satellite services (section 4).

The 9 digit national significant number length also causes difficulty for locating the ship. The ABC code may include ship location information, or the location information might be retrieved from maritime centre(s) performing a ship location registration function.

3.2 Ship Originated Calls

Some aspects of automatic maritime mobile satellite ship originated calls are similar to the shore originated calls outlined in section 3.1.1. In particular, it was found useful to continue regarding the maritime mobile satellite system as a separate country (figure 2, section 1) with the shore station acting as the interface between the maritime country and the international networks (figure 2, interface between sections 1 and 2).

As part of the separate country concept, it was agreed to adopt a scheme whereby a prefix would be dialled by the ship board customer to indicate to the shore station the type of call to be made. This technique allows a great deal of flexibility in that the maritime country can arrange its procedures completely independently of the international networks. Two prefixes were required initially for the maritime mobile satellite services, but others will be considered in the future. The prefixes used would be standardised internationally.

Prefix 0 would be used to inform the shore station that an operator is required. A second digit (following the prefix) could then indicate the type of operator requested. An example of the principle is given in table 1.

The digit values and types of operator given in table 1 are examples only and are not yet agreed, but the idea is to standardise such a table internationally in the future so that any customer on board ship may request an operator with the same OX codes irrespective of the ship's position. Codes 03 and 04 are primarily included for the maritime mobile VHF service, but it was considered desirable to standardise one table for all services.

Table 1: Example of Prefix 0 Principle

Numbering Sequence		Type of Operator
Prefix	Digit	
0	1	International operator
0	2	International information service
0	3	National operator
0	4	National information service

Each administration may decide which operators to provide, where they are to be located and how the call would be routed. If a request is received from a ship for a type of operator that the administration does not provide, then the call will be routed to an operator convenient for that administration.

Prefix 1 is used to inform the shore station that an automatic international call is required. The ship board customer will always use an international significant number following the prefix, whether or not the required customer is in the same country as the shore station. In this way standardised ship board dialling procedures are achieved on a worldwide basis.

For example, a customer on board a ship in the Atlantic Ocean making a telephone call to a customer in the United Kingdom via a US shore station would dial:

1	Prefix - automatic call
44	UK telephone country code
1	London) national
261 4256	Subscriber) (significant)
	number) number

Similarly, a customer on board a ship in the Atlantic Ocean making a telephone call to a customer in the United States via a US shore station would dial:

1	Prefix - automatic call
1	US telephone country code
202	Washington DC)national
554 6838	Subscriber)(significant)
	number)number

The numbering flow through the network for a general case is given in figure 2.

Satellite system ship to ship calls will be initiated by dialling the prefix 1, the country code 87S followed by the required ship identification. In the future, the use of a prefix to identify a ship to ship call may be desirable.

Prefix 2 has been allocated as an alternative to prefix 1 for use in the maritime mobile VHF services to identify national dialled calls (primarily for local shipping).

4. Ship Identification Plan

A ship identification plan was required whereby (a) each ship participating in the scheme would have a unique numerical identity, (b) the ship identity should be valid on a worldwide basis and (c) one identity could be used in the maritime mobile satellite and VHF services for telephony and telex. National telephony networks are generally more restricted than telex networks in terms of the maximum number of digits capable of being handled and so the numbering plan was devised on the basis of telephony and later applied to the telex service. Requirement (c) results in the numbering principles for the maritime mobile VHF and satellite services being inextricably associated, thereby restricting the flexibility of studying maritime mobile satellite services.

The development of a ship identification scheme depended on two major factors: (i) the characteristics of the maritime mobile satellite and VHF systems and (ii) the limitations of national and international telecommunications networks. International automatic maritime communications have not yet been established

FIGURE 2 - GENERAL NETWORK ROUTING FOR SHIP ORIGINATED MARITIME MOBILE SATELLITE CALLS

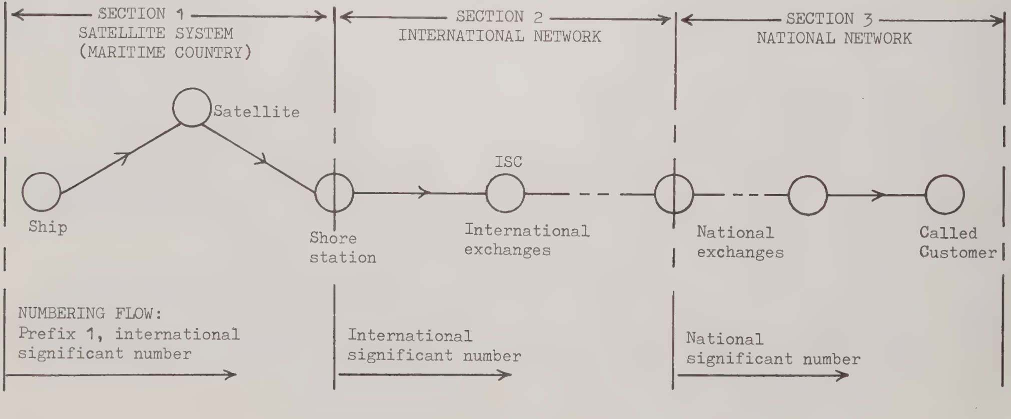

and so point (i) did not restrict the flexibility of developing a numbering plan. Opportunity was taken to achieve as much standardisation as possible in this area. The limitations of existing national and international networks, point (ii), did impose severe restrictions on the numbering plan.

Section 4.1 below outlines the studies that were undertaken concerning the numbering plan used over the radio path and section 4.2 describes how it was agreed to apply the radio path scheme to national and international telecommunications networks.

4.1 Ship Station Identities (Radio Path)

The ship population requiring automatic maritime mobile satellite and/or VHF communications in the future was studied at length. Although no definite figures for ship population could be derived, it was considered that 9 digits would contain sufficient capacity to allow for a reasonable number of ships (including small craft) based on current forecasts. Hence, each ship participating in automatic maritime mobile services and maritime mobile satellite services will be identified by a unique 9 digit ship station identity (where ship station identity is defined as the ship's identification transmitted on the radio path).

The content of the ship station identity was discussed and proposals to include information relating to ship nationality, accounting authority, owner, etc were considered. It was agreed that it was essential to include nationality information (country of registration) but that no other information should be included for practical purposes.

For the ship identification scheme to be truly international, the nationality code had to allow for over 100 countries (or geographical areas). Therefore, some nationality codes would need to be 3 digits in length. The capacity of the numbering scheme was critical and so it was agreed that all nationality codes would be 3 digits in length, countries with large numbers of ships being allocated more than one nationality code. Hence, it was agreed to allocate the first 3 digits of the ship station identity as nationality identification digits (NID). If possible, a country with a requirement for more than one NID would be allocated sequential NIDs, but this could not be guaranteed in the future when the numbering scheme became more fully used.

It was decided that the first digit of the NID should denote the geographical zone in which the ship's country of registration was located. This zoning was adopted to ease administration difficulties and allow for network techniques to improve the future capacity of the scheme. It was noted that international data country codes were also split into zones on the basis of the first digit and that it was desirable to use similar zoning for the maritime services. Hence, NIDs will begin with digits 2-7, the first digit indicating the zone in which the ship's country of registration is located, on the basis shown in Table 2. Initial digits 8 and 9 are used for network techniques (section 4.2), initial digit 0 is used for group calls (section 4.3) and initial digit 1 is reserved for future use.

Table 2: Relevance of the First Digit of NIDs

First digit of NID	Zone in which the ship's country of registration is located
2	Europe
3	North America
4	Asia (except South East Asia)
5	Oceania and South East Asia
6	Africa
7	South America

4.2 Application of Ship Station Identities (Networks)

4.2.1 Initial Stage

Ship station identities are transmitted over the radio path but, for automatic shore originated calls, the ship identification has to be transmitted through national and international networks. To help apply the numbering scheme in practice and increase the capacity of the scheme, three categories of ship were identified: ships requiring automatic shore originated coverage on (a) a worldwide basis, (b) a regional basis (up to 10 countries) and (c) a national basis. In addition, the term ship station number was adopted to indicate the ship identification dialled by the customer.

For worldwide roaming ships (satellite ships and ships using VHF on a worldwide basis) the 9 digit ship station identity will consist of a relevant NID followed by 6 digits. As common ship station identities are desirable in the maritime mobile satellite and VHF services and as many national networks can only handle 6 digits for ship identification purposes, a technique was applied whereby only 6 of the digits in the ship station identity were significant, the final 3 digits being trailing zeros. Hence, ships in the category would be allocated ship station identities of the form NIDXXX000 (where X may be 0-9). A capacity for up to 1,000 ships per NID would be available. In the maritime mobile satellite service all 9 digits could be dialled by a terrestrial customer whereas in the maritime mobile VHF services only the first 6 digits, the ship station number, would be transmitted across the network (the coast station adding the trailing zeros). This technique allows a minimum number of digits to be used initially in national networks but permits evolution of the scheme to cater for greater numbers of ships in the future.

To increase the capacity of the scheme for the maritime mobile VHF services, a form of short code dialling within terrestrial networks was developed. This relied on grouping ships into national and regional categories based on the required shore originated coverage area. In the regional scheme, up to 10 countries could agree to use a code 8 Y to indicate one of 10 NIDs and in the national scheme a code 9 would be used to indicate the particular national NID. These short code forms of NID effectively enable 7 digit or 8 digit ship station numbers to be passed across the national network. In both cases, the ship station identity is made up to 9 digits by the coast station by translating the abbreviated code into the relevant NID and adding trailing zeros.

The scheme is illustrated in table 3.

Table 3: Illustration of Numbering Plan

Shore Originated Automatic Coverage (Category)	Ship Station Number (Dialled by Terrestrial Customer)	Ship Station Identity (Over Radio Path)	Type of NID in Ship Station Identity
Worldwide	NIDXXX(000)	NIDXXX000	Any NID
Regional	8YXXXZ	NIDXXXZ00	NID of Country Y
National	9XXXXZ	NIDXXXXZ0	NID of Coast Station Country

X may take the value 0-9, Z may take the value 1-9.

A further group of ships could employ full 9 digit numbers on a manual basis for shore originated calls and on an automatic basis for ship originated calls.

4.2.2 Stages 2 and 3

When the number of ships requiring worldwide automatic shore originated services cannot be identified within the capacity of 6 significant digits, a second stage of the numbering plan will be implemented by extending the length of ship station number (dialled by the customer) to 7 digits. In this case, the ship station identities for worldwide ships will be of the form NIDXXXX00. The duration of the first stage of the plan will be extended by judicious assignment of ship station identities. This should allow national networks to develop numbering schemes capable of handling 7 digits for ship identification purposes. Similarly, future progression will be to 8 digit ship station numbers. The ultimate aim is to use ship station numbers identical to ship station identities for all ships (ie to use the full 9 digits).

Ships equipped with satellite communication equipment will be covered by the worldwide category of ships. The formats of the ship station identities during the 3 stages of the numbering plan are summarised in table 4. Eventually, the significant use of all 9 digits would be possible. The ship station number (dialled by the land based customer) of a ship participating in the satellite system may be identical to the ship station identity at each stage of the scheme, due to the ability of the international network to handle 9 digits for ship identification purposes (section 3.1.1).

Table 4: Format of Ship Station Identities

Stage of numbering plan	Format of satellite ship station identities
1	NIDXXX000
2	NIDXXXX00
3	NIDXXXXX0

X may take the value 0-9

4.3 Group Calls

Group calls are calls to groups of ships having a community of interest. Several types of group call have been identified so far, including an all ships call, calls of a particular nationality, calls to ships of a fleet and calls to ships in a particular area. Group calls are not considered to be suitable for use by the general public and so their use may be restricted to operators and/or authorised users over leased lines (or other restricted access arrangements). Group call identities will begin with digit 0 to facilitate easy recognition and, if necessary, barring of such calls in the public switched networks. The format of group call identities beyond the initial digit 0 has not yet been established.

4.4 Application of the Ship Identification Plan

The current maritime mobile satellite system (MARISAT) uses a ship identification scheme based on 7 digit octal ship station identities. It is desirable that future maritime mobile satellite systems operate on the basis of the ship identification plan outlined in 4.1 to 4.3 above. Hence, a period of transition will be necessary from the MARISAT scheme to the international scheme. Studies are currently being performed to investigate possible solutions that will allow an easy transition with minimum customer and administration confusion.

5. Summary

The paper outlines how numbering principles for international automatic maritime mobile satellite services were established and describes how requirements for commonality with maritime mobile VHF services played an important part in the development of the principles.

Shore originated maritime mobile satellite telephone calls will be initiated by dialling an international prefix, the maritime country code (87S) followed by the ship identification. Shore originated telex calls will be initiated in a similar manner, but using the destination code 58X.

For ship originated maritime mobile satellite calls, a prefix will be used to identify the type of call to be made. Prefix 0 followed by a second digit is expected to identify the need for a particular type of operator. Prefix 1 will identify a requirement for an automatic call to a terrestrial customer and will be followed by an international significant number.

Ships operating in the maritime mobile satellite service will initially be identified by ship station identities of the form NIDXXX000, where NID indicates the nationality of the ship registration. In the future, ship station identities of the form NIDXXXX00 and NIDXXXXX0 will be introduced. NIDs will begin with digits 2-7 (indicating the zone of the registered country), initial digit 0 being used for group calls, initial digit 1 being reserved for future use and initial digits 8 and 9 being used for network techniques.

Studies are currently being conducted to investigate how the current MARISAT octal numbering scheme will evolve into the international numbering plan.

6. Acknowledgements

The subject of this paper is based upon recent agreements of CCITT and CCIR. Co-operative enthusiasm at these meetings resulted in agreements allowing the design of new systems and evolution of existing systems towards international standards.

Acknowledgement is made to the Director of the Network Strategy Department of the British Post Office for permission to publish this paper.

80-0483

MICROWAVE COMPONENTS AND TECHNOLOGY DEVELOPMENTS IN THE EUROPEAN SPACE AGENCY

D.R. Madden, M.H. Gibson, P.H. Monier

European Space Research and Technology Centre,
Noordwijk, The Netherlands.

Abstract

Advanced microwave technological developments are pursued by the European Space Technology Centre of the European Space Agency (ESA), within an overall programme of Scientific and Communications spacecraft and payloads development and operation.

A selection of microwave hardware technology developments is presented, having particular relevance to next-generation communications satellite repeater designs. Items described include dielectric resonator materials evaluation for filter/MIC applications to 12 GHz; BAW-resonator stabilised bipolar oscillator at 1.5 GHz; geostationary-orbit radiation dose-depth experiment results; low-noise FETA performances at 12 GHz and 20 GHz; application of dual-gate FET in QPSK modulator.

A. Dielectric Resonator Materials for MIC Applications up to 12 GHz

Introduction

High dielectric-constant resonators offer potential size and cost advantages over waveguide alternatives for high performance microwave filters operating at frequencies at least up to 12 GHz. The unloaded Q's available from dielectric resonators are comparable with those of waveguide, whilst the corresponding resonator sizes are considerably reduced.

The small size of the resonators makes them compatible with microwave integrated circuits, thus permitting the realisation of high performance MIC filters impractical before now due to the low unloaded Q's of thin/thick-film resonators printed on quartz/alumina etc. substrates.

Resonator Materials

Four dielectric materials have been evaluated for ESA with ELECTRONIK/CENTRALEN (Denmark), for application to high Q resonators:

1. Ba-Ti — A Barium Titanate based ceramic of composition adjusted for a small temperature coefficient of K.
2. Zr-Ti(τ) — A Zirconium Titanate based ceramic of a composition optimised for minimum temperature coefficient of resonator f_0.
3. Zr-Ti(Q) — A ceramic similar to 2 but optimised for minimum dielectric losses, thus maximum resonator Q.
4. K49/Li-Nb — A sandwich structure resonator composed of Lithium-Niobate with a large positive temperature coefficient of K, and K49 - a specially developed sintered ceramic with large negative temperature coefficient of K.

The Barium Titanate and Zirconium Titanate based materials were supplied by Thomson CSF (France) and the K49/Li-Nb material was from a batch prepared for an earlier L-band evaluation contract with ELEKTRONIK CENTRALEN.

Materials Characterisation

The primary electrical and thermal/mechanical characteristics have been determined for the four materials, with a view to assessing their respective suitability for use as high Q resonators at 4,8 and 12 GHz, and at power levels up to 10 Watts at 12 GHz.

The testing jig used to measure f_0 and unloaded Q consisted of below cut-off waveguide with an E-probe in the narrow wall to excite the TE01δ mode in the resonator. The resonator under test was positioned in the waveguide by means of a polystyrene foam carrier. Fig. A1 shows the measured values of unloaded Q for all 4 materials as a function of frequency, and Table 1 gives a more detailed comparison of some of the electrical/mechanical/thermal characteristics.

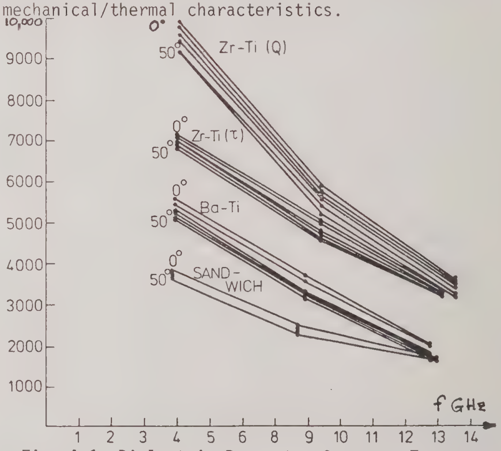

Fig. A.1 Dielectric Resonator Q versus Frequency

The power handling characteristics of the Ba-Ti and Zr-Ti based resonator materials were measured at 12 GHz up to 10W, with the resonators mounted on alumina and beryllia substrates, foam suspended in cut-off waveguide. Fig. A2 shows the measured values of unloaded Q versus power level.

The Zr-Ti (τ) based material has been selected to evaluate compatibility with MIC technologies and techniques, particularly due to its minimum τ,

Copyright © American Institute of Aeronautics and Astronautics, Inc., 1980. All rights reserved.

and to its Qu comparable with Zr-Ti (Q) at higher frequencies. This evaluation involves the measurement of unloaded Q, Fo, external Q, and coupling factor versus interresonator spacing using different substrate materials (fused silica, alumina, teflon, etc.) at 4, 8 and 12 GHz. Boron Nitride (good thermal conductivity) and quartz have also been evaluated as resonator support materials. (stand-offs).

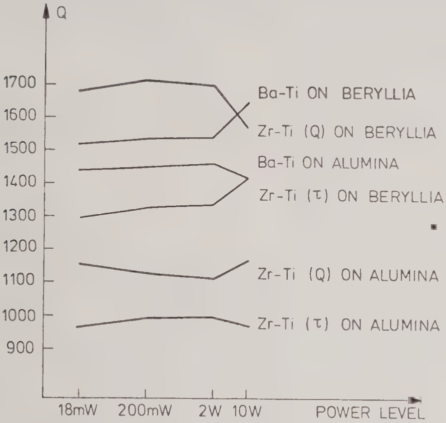

Fig. A.2 Unloaded Q versus Power Level

The 4 GHz coupling factor measurements (K) for Zr-Ti (τ) on teflon substrate are shown in Fig. A.3 with stand-off spacer material as a parameter.

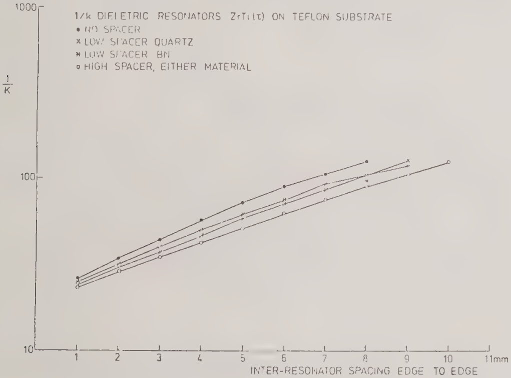

Fig. A.3 Inter-Resonator Coupling Factors

Discussion and Conclusions

Four High-K resonator materials have been characterised and evaluated at 4, 8 and 12 GHz for their potential use in space microwave hardware. Power-handling capabilities up to 10 Watts at 12GHz are demonstrated for three of the candidate materials. Measurements confirmed the high unloaded-Q's up to 12 GHz, and the Zirconium Titanate (τ)-based material was selected for further MIC-compatibility tests and coupling-factor measurements.

Additional work is proceeding on resonator-to-microstrip coupling measurements, and a high-performance 3-pole 12 GHz MIC bandpass filter using Zr-Ti (τ) resonator mounted in cut-off waveguide is under development for electrical and thermal performance evaluation over the 0-40°C temperature range. External-Q values for the materials indicate bandwidth limits of about 1% for filters on MIC, with an increase to about 1.5% in cut-off waveguide. Other applications under study include their use as stabilising resonators for FET microwave oscillators. This work shows high-K dielectric materials to be very promising for a number of space hardware applications.

Resonator Material / Parameter	Ba-Ti	Zr-Ti(τ)	Zr-Ti(Q)	K49/Li-Nb Sandwich
Density g/cm^3	4.48	6.06	5.24	
Coeff of * Thermal expansion (PPM/°C)	9.7	5.7	5.5	
Thermal conductivity W/MK	2.0	1.2	1.0	
τ 4 GHz ** (PPM/°C)	-8.7	-0.54	-20.9	6.8
τ 8 GHz (PPM/°C)	-8.0	-1.59	-18.1	1.6
τ 12GHz (PPM/°C)	-8.1	-1.61	-20.9	37.9

Table 1: Hi-K Dielectric Materials Characteristics

* Coefficient of thermal expansion is taken as the mean coefficient of linear thermal expansion between 23°C and 150°C.

** has usual definition i.e. $\frac{1}{f_{res}} \frac{d f_{res}}{dT}$

B. 20 GHz Low-Noise FET Amplifier

Introduction

The 20 GHz uplink frequency band is presently being examined for space communications applications such as, for example, a currently proposed 20/12GHz TVBS repeater in the European L-SAT programme.* Low-noise amplification at 20 GHz is becoming a firm requirement and sub-micron gate FET amplifiers are a strong candidate for the application. The best-non-degenerative parametric amplifier designs at this frequency should achieve a ~ 3 dB noise figure with around 600 MHz bandwidth capability, using an 80 GHz pump. When the higher NF of FETA's can be accommodated there are many advantages to be gained in the areas of bandwidth, stability, complexity, mass, drive-level tolerance, - and the need for an adequate 80 GHz pump source is avoided.

Amplifier Development

A low noise 20 GHz amplifier development is being performed for ESA by the Plessey Co, (UK), in which half-micron chip FET's of Plessey manufacture (GAT-6) are employed. Development includes: definition of suitable packaging technology to preserve box hermeticity and to ensure long-life space reliability of unpackaged chip FET's and circuitry; selection of preferred transmission media at 20 GHz to ensure reaslisation of available NF performance from the low-noise devices; definition of RF characterisation procedures for chip FET devices at 20 GHz to optimise circuit analysis and design.

---

* Uplink frequency allocation for this service now around 18 GHz (WARC 1979).

Chip devices are being used to avoid the excessive gain and noise performance degradation resulting from package parasitics. Each chip device is mounted onto a carrier and then wire-bonded to the input and output matching circuits fabricated on small alumina substrates. Alumina was found to be satisfactory for this application following comparative measurements on other transmission media such as quartz. The chip devices have been characterised for 'S' parameters and noise figure up to 18 GHz (measuring equipment limitation) using computer aided measurement techniques to remove the effects of connectors, bondwires etc. in the test jig. Device modelling techniques were then employed to extend their characterisation up to 20 GHz, for application to the present amplifier development.

Typical GAT-6 chip characteristics i.e. gain and noise figure as a function of frequency are shown in fig. B1. A typical device noise figure at 20 GHz is less than 4 dB with an associated gain of ~ 6.5 dB.

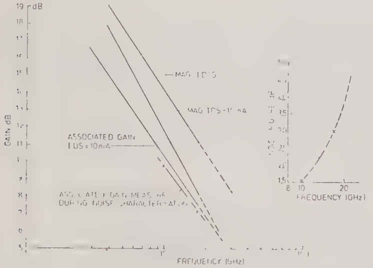

Fig. B.1 Full GAT-6 FET Characteristics

A block diagram of the complete amplifier including the voltage regulators is shown in Fig. B.2.

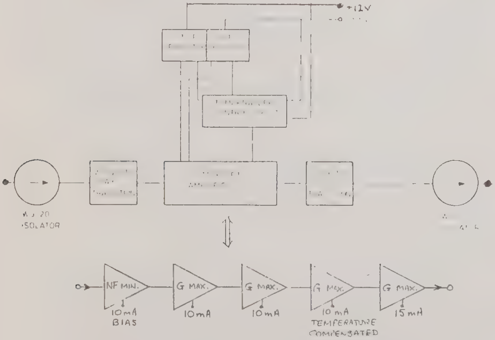

Fig. B.2 20 GHz FETA Block Diagram

Amplifier specifications include:

Centre frequency	19.8 GHz
Instantaneous bandwidth	800 MHz (minimum)
Noise Figure	7 dB
Nominal gain	25 dB
Gain variation in 350 MHz BW	< ± 0.25 dB
Gain variation in 800 MHz BW	< ± 0.5 dB(< ± 0.25 dB goal)
Group delay variation in 350 MHz BW	< ± 1 ns
I/p and O/p VSWR	< ± 1.3:1
Operating temperature range	0°C to + 40°C

Results and Conclusions

All specification requirements for the 20 GHz FET low noise amplifier have been met with comfortable margins. Continuing design optimisation is expected to result in an instantaneous bandwidth capability approaching 2 GHz, with NF around 6 dB over the band at operating temperatures of 0-40°C. The technologies employed ensure good compatibility with space equipment environmental requirements.

Further work on the amplifier will include the application of heat-pipe cooling techniques already developed and demonstrated in a parallel programme. Cooling the amplifier input stages to about - 50°C is expected to result in a 1 dB to 1.5 dB improvement in noise figure, giving a 2 GHz BW amplifier having an NF performance of 4.5 - 5.0 dB at 20 GHz.

C. Stable Microwave Source Using Bulk Acoustic-Wave Resonator

Generation of the local oscillator signal for a satellite-borne microwave communication repeater typically requires an HF quartz master oscillator followed by a multiplier/amplifier chain. Such circuitry is necessarily complex, calling for many stages and numerous filter elements to preserve an acceptable spectral purity free of parasitic signals and undesired harmonics (Fig C.1).

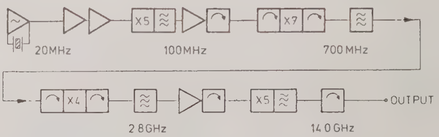

Fig. C.1 Typical Xtal-Osc./Multiplier Chain

A new frequency source (Fig. C.2) has been developed for ESA by TH/CSF (France) using a simple high power transistor oscillator (1.5GHz) phase locked to a quartz reflective bulk acoustic-wave (BAW) delay line. The BAW delay line length is optimised for frequency stability (1 us delay at 1.5 GHz). Mode spacing is increased by parallel coupling of a shorter 0.25 uS delay line (not shown in figure) whilst retaining the long line stability. The AT-cut quartz angle is slightly tilted to compensate for the known temperature drift of the transistor oscillator. The electro-acoustic transducer is a $\lambda/4$ lithium niobate crystal, 163° cut. Fine frequency setting is achieved by thinning (ion milling) of the BAW delay line after integration of the complete oscillator.

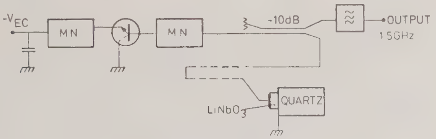

Fig. C.2 Bulk Acoustic-Wave Oscillator (BAWO)

This source provides a 1.5 GHz - 100 mW output signal having a stability similar to that of a crystal oscillator chain. Fig. C.3 shows the comparative phase noise measurements of the non-thermally stabilised BAWO and a conventional oven-controlled crystal oscillator (OCXO) with multiplier chain. By adding a single-device X12 Impatt multiplier developed at Lille Univeristy (France), a 10 mW - 17.5 GHz source is obtained. The phase noise curves of Fig. C.4 indicate no excess impatt multiplier noise above that due to the multiplication factor. Long term stability of the BAWO is mainly determined by the quartz delay line ageing, which is expected to be better than 10^{-6} /year.

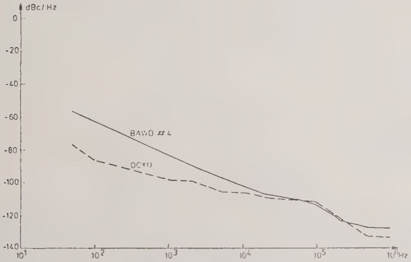

Fig. C.3 Comparative Phase-Noise Measurements at 1.46 GHz

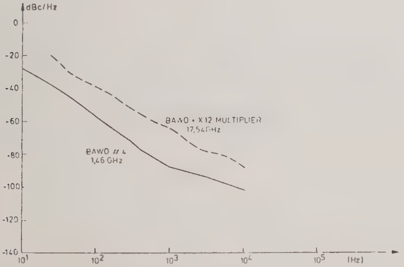

Fig. C.4 Phase Noise of BAW alone, and with added X12 Multiplier

To summarise, it has been shown that a BAWO provides a stable frequency source in the 1 to 3GHz range, of low complexity and small size. By adding a novel single Impatt multiplier stage any frequency in the X to K-band range may be generated, keeping the low noise and high stability of the BAWO. This combination offers a high quality L.O. source having excellent ruggedness and reliability together with low power consumption, making it very suitable for space equipment applications.

D. Low Noise 12 GHz FETA NF-Improvement Using Heat-Pipe Cooling

Introduction

A decrease in noise-figure and increase in gain as operating temperature is reduced are well-known characteristics of GaAs FET's. The performance of a satellite microwave communications repeater using an FET pre-amplifier could therefore be improved if suitable dedicated cooling were applied to the preamplifier unit. One way of implementing such cooling could be by means of heat pipes used in conjunction with a dedicated radiator positioned on the outside of the space-craft. Experimental tests performed upon a developmental GaAs FET low-noise amplifier using heat-pipe cooling are described and results presented.

FETA Description

The amplifier was developed for ESA by the Plessey (U.K.) company, and performance specifications include:

- Frequency range: 9.95 - 13.45 GHz
- Instantaneous BW (±0.7dB): 10.70 - 12.70 GHz
- Gain: 35 dB
- Noise figure: 5.3 dB max.
- Ambient Temp, range: 0 - 40°C
- I.M.3 Products at - 48dBm input: - 55 dB max.

Plessey ½-micron gate-length GAT-6 devices are used in the input stages to meet the specified noise figure requirements over the operational temperature range, and 1-micron GAT-5 devices are used in the later stages to meet gain and linearity requirements. The design incorporates bias regulation and thermistor/pin-diode attenuator temperature compensation, such that the performance is optimised for 0 - 40°C ambient, but the technologies used are compatible with environmental temperatures down to - 50°C. The preamplifier configuration is illustrated in Fig. D.1.

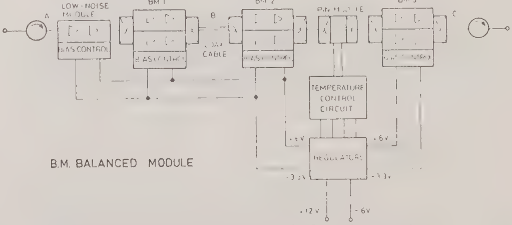

Fig. D.1 12 GHz FETA Overall Configuration

Heat Pipe Cooling System

Thermal analysis and design of the experimental heat-pipe system was based upon spacecraft environmental assumptions which included:

- FET amplifier thermally insulated from mounting plate;
- Constant ambient temperature + 20°C in vacuum;
- Amplifier dissipation plus parasitic heat leakage totalling 5.7 Watts;
- Heat pipes and radiator thermally insulated from spacecraft.

A pair of 3.2 mm diameter ammonia heat-pipes, 60 cm long, connected the amplifier to a 450 cm^2 radiator plate (Fig. D.2).

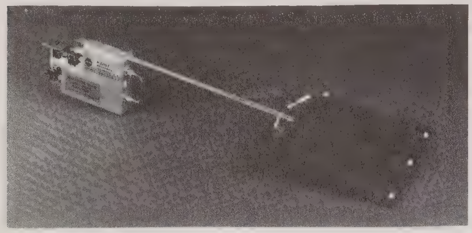

Fig. D.2 FETA, Heat-Pipe and Radiator Cooling Assembly

The amplifier and cooling system were mounted in a thermal/vacuum chamber, and were surrounded by a liquid nitrogen cooled shroud to simulate the space environment. The radiator plate was made isothermal by employing integral heat-pipes, to improve efficiency.

Test Programme

Ambient temperature performances of the amplifier were measured over the frequency range (noise figure, gain, power consumption, etc.) before cooling and evacuation of the vacuum chamber, to give reference data. The chamber was then evacuated ($< 10^{-5}$ torr) and the shroud cooled. Supplementary heating elements attached to the radiator permitted simulation of solar radiation incidence, and enabled amplifier performance measurements to be made at measured temperatures of - 15.7°C; - 33.0°C and - 41.4°C as monitored by thermocouples attached in the vicinity of the FET input stages. Amplifier operation was maintained for one hour at each temperature for full stabilisation to be achieved prior to measurements, and the chamber was then allowed to heat up to normal ambient temperature, with normal pressure restored. Amplifier characterisation was then repeated following one hour stabilisation operation under ambient conditions, to check the reference performance.

Results Achieved

Figure D.3 shows a plot of measured noise figure versus frequency at different temperatures. The reduction in noise figure ranges from 1.35 dB at 10.7 GHz to 1.80 dB at 12 GHz, for an operating temperature decrease from + 32°C to - 41.4°C (73.4°C differential).

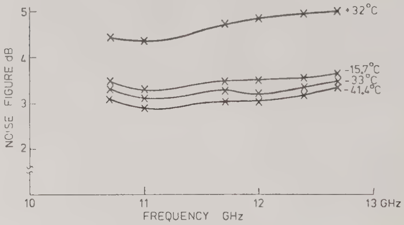

Fig. D.3 FETA NF Versus Frequency As A Function of Temperature

Gain versus frequency is plotted at the reference temperature of + 32°C in figure D.4, together with the gain curves at - 15.7°C and - 41.4°C. As expected, a large gain increase is observed at the lower temperature since amplifier temperature compensation was optimised only for the 0°C to + 40°C operational design range.

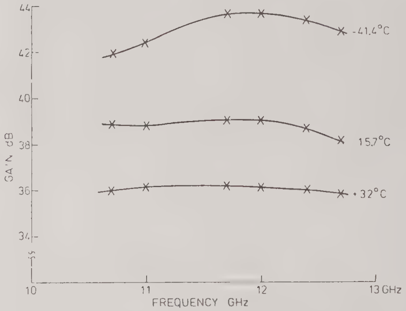

Fig. D.4 FETA Gain Versus Frequency As A Function of Temperature

No correction has been made in the measured data of figs. D.3 and D.4 for the possible effects of temperature change on coaxial cable insertion losses, but these are considered to be acceptably small (± 0.2 dB for N.F.).

Conclusions

The performance characteristics of a 12 GHz low-noise GaAs FET amplifier have been presented, and a heat-pipe cooling experiment aimed at improving the amplifier noise-figure has been described. Tests carried out under low temperature high-vacuum conditions have indicated a noise-figure improvement of up to 1.8 dB for an operational temperature reduction from + 32°C to - 41.4°C, with NF around 3.1 dB over most of the 10.7 GHz - 12.7 GHz operational bandwidth. These low-temperature functional tests have demonstrated the effectiveness of the heat-pipe system under simulated space conditions, and the compatibility of the low-noise FETA overall design with the cooling techniques and technologies. A considerable reduction in radiator dimensional requirements will be obtained in future work by thermally isolating the noise-figure determining input stages from the rest of the amplifier, and providing local cooling to these stages only.

E. 11.65 GHz QPSK Switching Modulator Using Dual-Gate FET's

Introduction

Direct carrier modulation at a satellite repeater final output stage would, if shown to be feasible, avoid the non-linearity distortion products typically generated in output power amplifiers. The FET constitutes an ideal device for direct modulation since the modulating signal may be applied directly via the gate terminal. In particular, the dual gate FET has the advantageous capability of signal modulation via its second gate, leaving the first gate for signal input.

Modulator Development

A joint ESTEC/Plessey (U.K.) development of a low-level QPSK modulator utilises the Plessey dual-gate FET type DUGAT 10/000, using alumina substrate MIC technology. A schematic of the switching modulator is shown in Figure E.1, in which the modulator operates as a "phase-shift inserter" by switching the relevant phase shift.

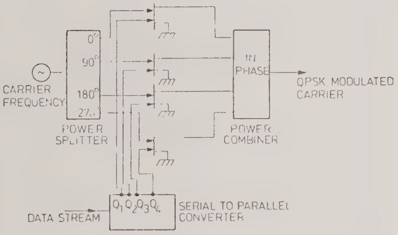

Fig. E.1 Dual-Gat FET QPSK Modulator

This configuration results in an efficient modulator of relatively simple design, and alleviates difficulties associated with signal and modulation separation and filtering. Additionally the FET provides signal gain, in contrast to mixer and pin-diode modulator alternatives. (fig. E.2). To minimise distortions and phase errors all FET modules must track to within 1°, and forward isolation of the modules must be better than 40 dB in the "off" state. Fine tuning for phase-tracking is effected by gate voltage adjustment of each device, and Figure E3 shows the typical phase shift versus gate voltage characteristic for the DUGAT 10/000 FET.

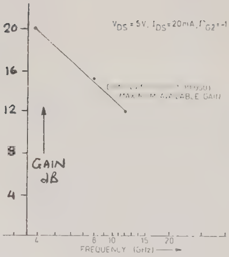

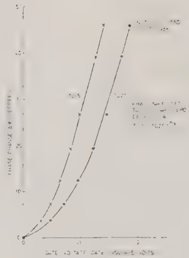

Fig. E.2 Dual-Gat FET Gain Versus Frequency

Fig. E.3 Dual-Gate FET 12 GHz Phase-Shift Characteristics

Specifications for the present modulator include:

Centre frequency:	11.65 GHz (OTS/ECS bands)
Instantaneous 3 dB bandwidth:	450 MHz min.
Nominal gain per state:	3 dB
Nominal output per state:	3 dBm
Nom. modulation port impedance:	200 ohm (10 MHz - 2 GHz)
Phase imbalance per state:	± 1° max.
Gain imbalance per state:	± 0.25 dB max.

Present and near-future bandwidth requirements of European systems (~ 360 M bits/sec) are easily met with this design, and its G bit/sec. capability may readily be implemented when needed.

Conclusions

The design and performance figures for a low-level QPSK switching modulator using a dual-gate GaAs FET have been presented, demonstrating the feasibility of the approach for communications satellite repeater applications. FET's capable of delivering several Watts at 12 GHz (compatible with existing system EIRP's and antenna gains) are not yet available, but promise to be available in the near future, and the experience gained with the present low-level modulator will be transferred to the higher power designs with the aim of achieving a directly-modulated output amplifier.

F. Radiation Sensitivity of Small-Signal Microwave Transistors. A Space Borne Experiment

Introduction

The radiation environment experienced by synchronous orbit communciations satellites can induce ionisation-damage effects in small-signal microwave bipolar transistors, resulting in d.c. current gain (h_{FE}) reduction and corresponding RF amplifier performance degradation. Radiation damage can be limited by amplifier box shielding, and the performance effects of h_{FE} degradation can be minimised by suitable amplifier circuit design, but a knowledge of actual radiation conditions in an orbital environment over extended periods is desirable in order to assess device survivability during typical mission lifetimes (refs. 1, 2, 3).

Experiment Description

A spaceborne experiment designed to measure the degradation of a commonly used small-signal microwave transistor (NEC2SC1268 device) in an actual space environment has been designed and built in ESTEC. Design details and operational results so far obtained are described. The specially designed "radiation damage monitoring unit" (RDMU) shown in fig. F.1 is incorporated into the OTS-2 communications satellite payload - launched in May 1978 - and consists of three separate and identical single transistor amplifier stages which are exposed to the orbital space environment. A calibrated MOS-type dosimeter is also included in the RDMU for measurement of the incident radiation levels. Each transistor amplifier stage is biased at 5 mA at "start of life", and radiation-induced changes in transistor h_{FE} result in corresponding changes in individual transistor bias currents. The associated incident radiation levels are monitored by the accompanying dosimeter, and the combined data are coded and telemetred to ground on a continuous basis to provide long-term radiation-level and associated ionisation damage information.

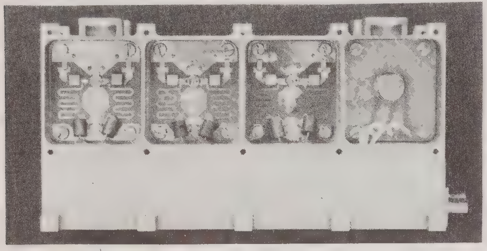

Fig. F.1 Radiation Damage Monitoring Unit (RDMU)

Experiment Results

Fig. F.2 illustrates the current 7-year dose-depth predictions at geosynchronous altitude versus aluminium shield thickness. An "OTS" point superimposed on the figure is based upon the first 12 months of orbital data, extrapolated out to a 7-year prediction. Similar dosimeters placed on board the GEOS II geostationary satellite are providing corresponding data for various thickness of shielding aluminium, to provide additional data-points for fig. F.2.

Fig. F.3 shows the typical h_{FE} versus radiation dose characteristics for the test microwave transistor type, and Fig. F.4 gives typical gain $|S21|^2$ and noise figure sensitivity to collector current and normalised h_{FE} (H).

Work is proceeding in parallel with a ground-based irradiation programme on microwave transistors using X-rays as a source of ionising radiation, correlating the ground-based X-ray levels and related device damage with the monitored space radiation levels and associated device degradation. The results can subsequently be used in the assessment of microwave equipment designs for space radiation hardness.

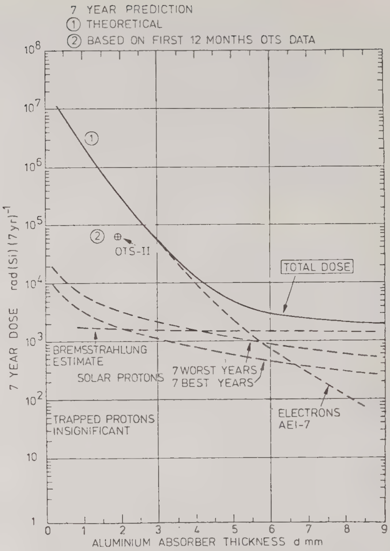

Fig. F.2 7-Year Accumulated Dose-Depth Versus Aluminium Shield Thickness, Geostationary Orbit.

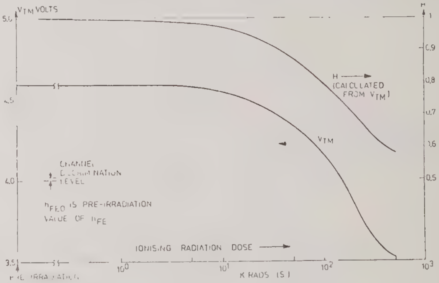

Fig. F.3 Typical Radiation Sensitivity of Telemetry Voltage (V_{TM}), and Normalised h_{FE} ($H \approx h_{FE}/h_{FEO}$)

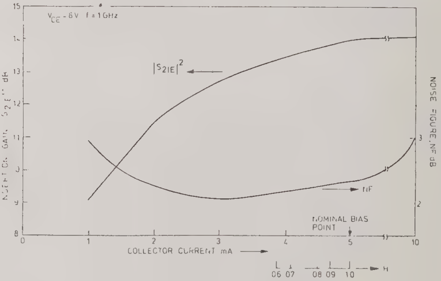

Fig. F.4 Typical Insertion Gain and Noise Figure Sensitivity to Collector Current and Normalised h_{FE}

The incident radiation dose versus time for the OTS RDMU is presented in Fig. F.5, and approximately 3 Kilorads are seen to have been logged to date. In the ground-based irradiation tests, first indications of microwave transistor h_{FE} degradation (1% - 2%) occurred at the 3 Krads does level, which corresponds to the cumulative dose so far measured in robit. Analysis of RDMU test-transistor h_{FE} data also indicates approximately 2% degradationat the present time, but greater accuracy will be possible as more orbital time is accumulated and measurement uncertainties are averaged out.

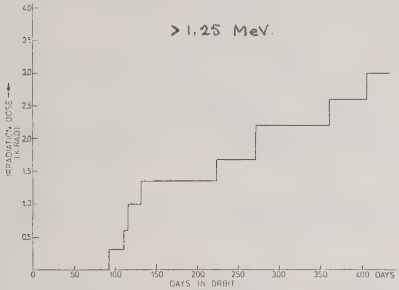

Fig. F.5 Incident Radiation Dose Versus Time in Orbit (OTS-2)

Conclusions

A radiation damage monitoring unit (RDMU) placed on board the OTS II communications satellite for the assessment of orbital dose-depth effects upon low-noise microwave transistors has been described, and results to date presented. Data collected so far are in fair agreement with 7-year dose predictions for the geosynchronous altitude, and microwave device radiation degradation effects - now becoming apparent - will be monitored throughout the orbital lifetime of the satellite.

The information gained from the RDMU will be correlated with that obtained from ground-based X-ray irradiation experiments as an aid to the radiation-hardened design of space equipments.

References

1. I. Thomson. "Effects of ionising radiation on small-signal microwave bipolar transistors". IEEE Trans. Electron Devices, Vol. ED.25, pp. 736-741, June 1978.

2. M. Gibson and I. Thomson. "Radiation considerations in design of linear microwave transistor amplifiers for space applications" IEEE Trans. MTT-26 No. 10, October 1978.

3. I. Thomson, M.H. Gibson, M.B. Christenssen, G.J.G. Janssens. "The sensitivity of microwave bipolar transistors and amplifiers to ionising radiation" IEEE Trans. NUCLEAR SCIENCE, Vol. NS-26, No. 3, June 1979.

80-0484

LINEARIZING T.W.T AMPLIFIERS IN SATELLITE TRANSPONDERS
SYSTEM ASPECTS AND PRACTICAL IMPLEMENTATION

C. BREMENSON
M. PALAZO
R. NEYER
THOMSON-CSF, Space and Radiolinks Division
BP.302, 92301 Levallois-Perret, FRANCE

Abstract

The paper discusses the advantages of a satellite transponder TWT predistortion network, both in FDMA and TDMA .

The advantages in transponder capacity for a given transponder power consumption, and in power consumption for a given capacity are calculated and found to be very similar to that of and ideally linear TWT .

Then the paper gives a description of a practical 4 GHz linearizer, including two carriers intermodulation ratio measurement results .

Introduction

Linearization of power amplifiers in earth stations and in satellite transponders does present many advantages for an overall system optimization. It has already been used for many years in earth stations at 6 GHz (multicarrier operation in FDMA) as well as at 14 GHz (e.g.TDMA operation in the OTS system) . But up to now is has not been used in satellites where its advantages would have a greater impact on system optimization .

Among various linearization methods, that of using a predistortion is characterized by the simplicity of its implementation and by the importance of its bandwidth; it consists in inserting at the input of the amplifier to be linearized a predistortion network presenting amplitude and phase shift responses in opposition to those of the amplifier .

Introduction of such a linearizing network in 6 GHz earth stations [1] allows the use of power amplifiers with 3 dB lower saturation levels . This paper presents an application of this method to linearize 4 GHz TWT amplifiers in satellite tranponders [2] ; it could also be applied to linearize 12 GHz amplifiers .

System aspects of linearization of power amplifiers aboard satellites

The purpose of such a linearization is :
- in FDMA (FDM/FM or PCM/PSK) to reduce the level of third order intermodulation products
- in TDMA -1) to reduce intersymbol interferences due to nonlinearity of the TWT amplifiers
  -2) to reduce spectrum spreading at the output of the TWT which does generate strong interferences in adjacent channels.

In both operations, linearization will reduce the TWT output back-off . This reduction shall be more important when the initial back-off (in the absence of a linearizer) is high i.e.:
- in FDMA when the number of carriers is larger than 2, or when modulation indexes are low (spot beam parameters)
- in TDMA when using a modulation with a high number of states (8 phases modulation, mixed amplitude/phase modulation, etc...) .

In this "system aspects" section we will refer to a standard "Intelsat TWT" [3] , similar to those used in Intelsat satellites .

The characteristics of this tube, associated or not with a linearizer, are given by figure 1 .

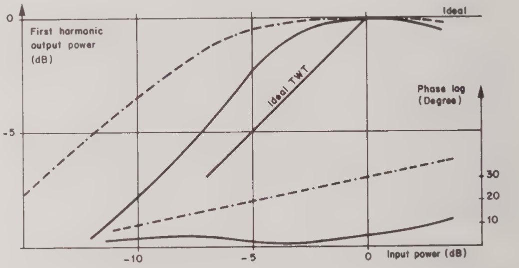

FIGURE 1. Single carrier characteristics of Intelsat TWT :
- with linearizer (solid lines)
- without linearizer (dotted lines)

Figure 1bis gives the carrier to intermodulation ratio versus the multicarrier output back-off computed from the data given by figure 1 . The linearizer has been computer optimized (c.f annexe I) in order to maximize the C/I for output back-offs ranging from 3 to 7 dB .

/...

Copyright © American Institute of Aeronautics and Astronautics, Inc., 1980. All rights reserved.

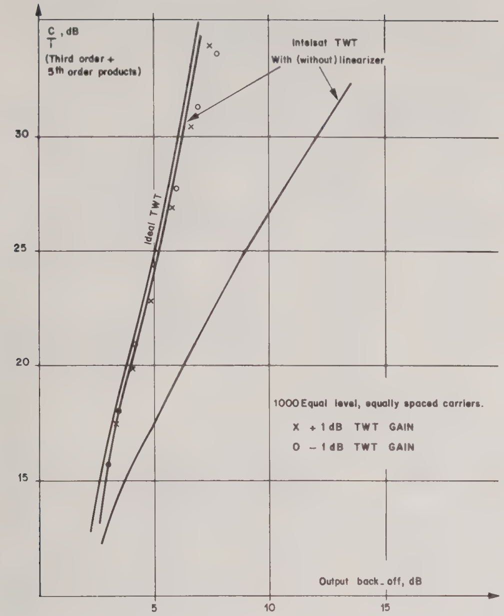

FIGURE 1 bis : Multicarrier intermodulation

FDM/FDMA - First approach

Figure 2 illustrates the method of optimization of the number of telephony channels that can be transmitted by a given transponder of a given satellite , in a bandwidth limited configuration (FM demodulators operating above the threshold).

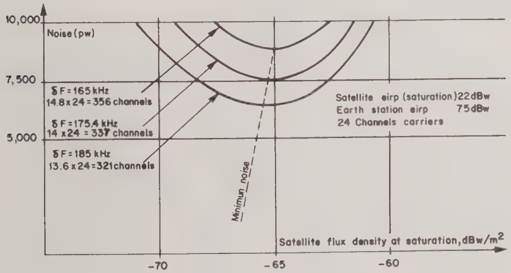

FIGURE 2. Optimization of the number of channels per transponder. FDM/FDMA operation – standard Intelsat TWT - bandwidth limited

Let us try to transmit in a 36 MHz repeater several carriers, of equal amplitude, each one modulated by a 24 channels telephony multiplex, with a 22 dBW transponder EIRP at saturation and a 75 dBW earth station EIRP per 24 channels carrier (Intelsat IV global beam parameters) .

For each value of δ F, RMS test tone frequency deviation per telephony channel, we can calculate the RMS and the 12 dB peak deviations of one 24 voices channel carrier, then the Carson bandwidth B, then the number of carriers 36/B that one transponder can handle, and the noise contribution of the up link in each voice channel . Then, for each value of the transponder flux density at saturation * , we can calculate the satellite EIRP per carrier and the global output back-off for the 36/B carriers, then the noise contribution of the down link and of the TWT intermodulation .

The sum of the three contributions versus the transponder flux density is plotted in figure 2, for each value of δ F, using a standard INTELSAT TWT. The locus of the minimums gives the trade off of number of voice channels versus channel noise . If the maximum noise is 7500 pW as in the INTELSAT network, we can determine the capacity of one repeater as 337 channels and the optimum satellite flux density as -65.3 dBW/m^2 .

* The transponder flux density at saturation is a decreasing function of the transponder gain . If the transponder gain increases, for a given input power, the noise contribution of the down link decreases and the TWT intermodulation increases .

Figure 3 gives the curves corresponding to a minimum of 7500 pW, with a standard INTELSAT TWT, a standard INTELSAT TWT associated with the described linearizer, and an ideal TWT (cf.figure 2).

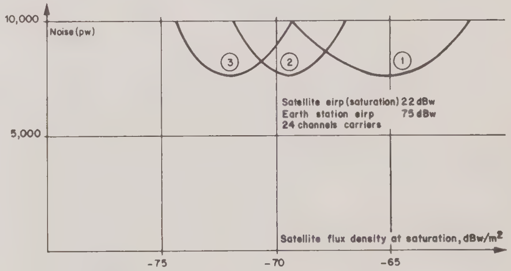

FIGURE 3 . : (See comments next page)

CURVE	1 without linearizer	2 with described linearizer	3 ideal TWT
δ F (kHz)	175.4	155.4	154.3
nb.of channels	14.0 x 24 = 337	15.7 x 24 = 376	15.8 x 24 = 378
optimum flux density (dBW/m2)	-65.3	-69.5	-72
optimum output back-off (dB)	-5.3	-4.7	-4.6
up-link noise (pW)	745	949	962
down link noise (pW)	4342	5350	5294
intermod.noise (pW)	2416	1201	1246
total noise (pW)	7504	7501	7503

FIGURE 3. : Advantage of a linearizer in FM/FDMA INTELSAT IV - Global beam

NOTA : In figure 3, for example, the transponder capacity of 376 channels is given by "15.7" carriers, each one modulated by a 24 channels multiplex . This notation is valid because the capacity does not depend much on the size of carriers .

The real operation could be with fifteen 24 channels carriers + one 12 channels carrier + two SCPC carriers .

Figure 4 gives the same data as figure 3 but with 60 channels carriers and SPOT beam parameters .

The advantage of a linearizer can then be summarized by the following table :

	TWT + DESCRIBED LINEARIZER (2)	IDEAL TWT (3)
GLOBAL BEAM	11.6 %	12.3 %
SPOT BEAM	26.8 %	27.5 %

Table I : Increase of transponder voice channel capacity given by a linearizer

As can be seen in TABLE I, the potential gain (ideal TWT) is higher in SPOT beam operation (high C/N and C/I, large back-off, and low δ F and FM advantage) than in global beam operation .

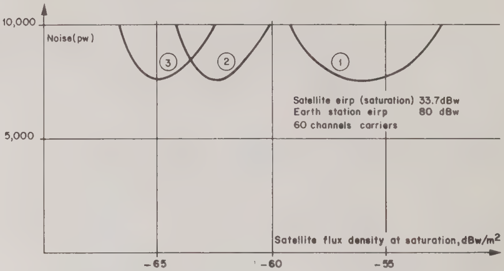

CURVE	1 without linearizer	2 with described linearizer	3 ideal TWT
δ F (kHz)	164.5	127.1	126.2
nb.of channels	11.4 x 60 = 685	14.1 x 60 = 847	14.2 x 60 = 852
optimum flux density (dBW/m2)	-56	-62.5	-65
optimum output back-off (dB)	-9.5	-6.9	-6.7
up-link noise (pW)	1458	2443	2478
down-link noise(pW)	3878	4362	4300
intermod.noise (pW)	2169	698	718
total noise (pW)	7506	7504	7497

FIGURE 4. : Advantage of a linearizer in FM/FDMA INTELSAT IV - SPOT beam

FDM/FDMA - Second approach

An other type of optimization can be made, illustrated by figure 5. The capacity per transponder, and then the δ F are defined, and we try to minimize the satellite EIRP at saturation, and the power consumption of a transponder .

Figures similar to figure 3 and 4 are not reproduced here, but only the optimized results (tables II and III) .

/...

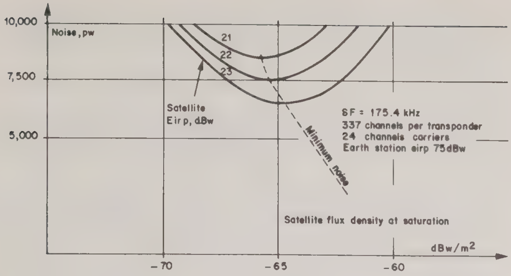

FIGURE 5. : Optimization of the satellite EIRP FDM/FDMA operation - Standard INTELSAT TWT - Bandwidth limited .

	without linearizer	with described linearizer	ideal TWT
EIRP (dBW))	22	19.95	19.82
optimum flux density (dBW/m2)	-65.3	-70.5	-73.1
optimum output back-off (dB)	-5.3	-4.3	-4.1
up-link noise (pW)	745	745	745
down-link noise (pW)	4342	5511	5452
intermod.noise (pW)	2416	1243	1304
total noise (pW)	7504	7500	7502

TABLE II : Advantage of a linearizer in FDM/FDMA INTELSAT IV Global beam - 24 channels carriers - δ F = 175.4 kHz - 337 channels per transponder

	without linearizer	with described linearizer	ideal TWT
EIRP (dBW)	33.7	29.05	28.95
optimum flux density (dBW/m2)	-56	-64.3	-66.8
optimum output back-off (dB)	-9.5	-6.0	-5.9
up-link noise (pW)	1458	1458	1458
down-link noise (pW)	3878	5083	5063
intermod.noise (pW)	2169	962	973
total noise (pW)	7506	7504	7495

TABLE III : Advantage of a linearizer in FDM/FDMA INTELSAT IV Spot beam - 60 channels carriers - δ F = 164.5 kHz - 685 channels per transponder

Table II et III are summarized in table IV .

	number of channels per transponder	TWT	described linearizer + TWT	ideal TWT
GLOBAL BEAM	337	0 dB	-2.1 dB	-2.2 dB
SPOT BEAM	685	0 dB	-4.6 dB	-4.7 dB

TABLE IV : Reduction of satellite EIRP given by a linearized TWT

The advantage of a linearizer is more important in table IV than in table I .

In particular, for the same total satellite power consumption, neglecting power consumption of subassemblies other than TWT, the 4.6 dB (ratio of 3) power saving of table IV gives a threefold increase of capacity if the number of spot beams is tripled .

PCM/PSK/TDMA

Let us consider, as an example, the simplified transmission block diagram of figure 6. The global filtering function is a Nyquist filter with 50% roll-off, constituted by two equal filters, one before and the other after the TWT . These filter may represent those located at the end of the transmission chain, in the transmitting and the receiving earth stations . The input and output multiplexers of the satellite are not taken into account .

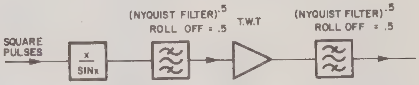

FIGURE 6. : TDMA link block diagram .

Figure 7 is the results of the simulation of figure 6 for three modulation schemes, four phases PSK, eight phases PSK, and 4 QAM * . It gives the impairment of the figure of merit E_{SAT}/N_0 , for a bit error rate of 10^{-9}, versus the input back-off, for various TWT. S. E_{SAT} is the energy per bit of information corresponding to the saturation of the TWT minus the output back-off .

N_0 is the noise power spectral density .

Back-offs are defined for an unmodulated carrier .

---

*For 4 QAM, the impairment includes the degradation of E/N_0 due to a residual carrier at a level 10 dB below the peak modulated level, necessary for carrier recovery in the particular simulation used .

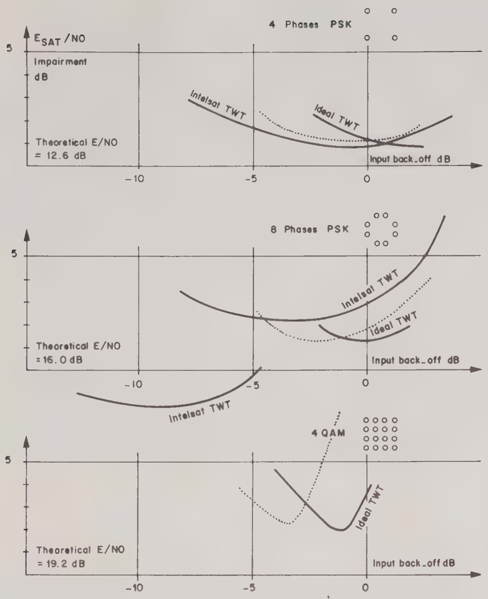

....dotted lines : described linearizer + intelsat TWT

FIGURE 7. : $E/_{SAT}/N_0$ impairment . BER = 10^{-9}

Figure 8 gives the same data, for BER = 10^{-4}

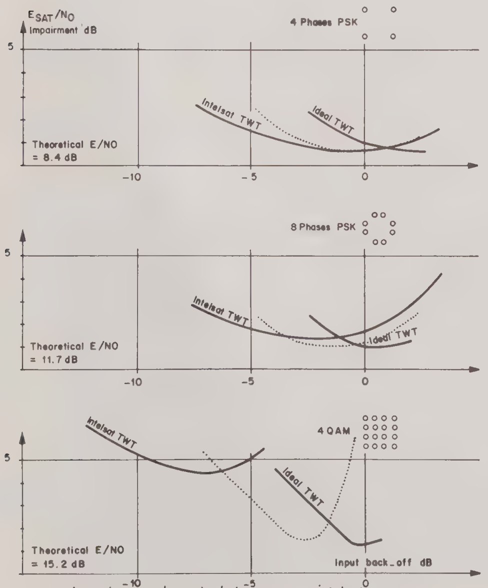

.....dotted lines : described linearizer + intelsat TWT

FIGURE 8. : E_{SAT}/N_0 impairment . BER = 10^{-4}

Tables V and VI summarize the results for the optimum back-offs .

	TWT	described linearizer + TWT	ideal TWT
4 PHASES PSK	0 dB	NOT SIGNIFICANT	
8 PHASES PSK	0 dB	.9 dB	1.0 dB
4 QAM	0 dB	4.2 dB	4.4 dB

TABLE V. : Reduction of satellite EIRP given by a linearized TWT - BER = 10^{-9}

	TWT	described linearizer + TWT	ideal TWT
4 PHASES PSK	0 dB	NOT SIGNIFICANT	
8 PHASES PSK	0 dB	.5 dB	.5 dB
4 QAM	0 dB	3.2 dB	3.3 dB

TABLE VI. : Reduction of satellite EIRP given by a linearized TWT - BER = 10^{-4}

When using a smaller roll-off, the improvement due to a linearizer would probably increase .

The above assumptions are very simplified : the contributions of up-link noise, multipath, up-link and down link adjacent carriers interference (A.C.I.) are not taken into account .

In a different approach, for given TWT saturation power, given frequency separation between transponders, and given satellite input multiplexer, a linearizer allows increasing the bit rate because :

- as seen previously, the intersymbol interference due to the TWT will be reduced, the Nyquist bandwidth may thus be increased (and the roll-off be decreased to ensure a sufficiently high up-link A.C.I.)
- the spectrum spreading of the TWT will be reduced. The selectivity of the satellite output multiplexer, which contributes to down link A.C.I. may thus be relaxed, leading to a decrease of its insertion losses .

PRACTICAL IMPLENTATION

This linearizer has been developped to compensate phase and amplitude non linearities of a traveling wave tube used in satellite transponder operating within the 3.7/4.2 GHz frequency band .

Technology and design have been choosen to minimize size and weight and to provide an easy adjustment of the linearizer

This study have been carried out under an INTELSAT contract and supported by French P and T administration .

The linearizer is made of :

- a predistortion network performing the compensation of phase and amplitude non linearities of the traveling wave tube,
- an amplifier compensating the insertion loss of the predistortion network
- an amplitude equalizer which compensated the gain variations within the frequency bandwidth .

Predistortion network

In order to compensate for the non linearity effects of the TWT, the linearizer produces :

- a phase advance increasing when the input level increases,
- an attenuation decreasing when the input level increases

through a linear and a nonlinear path and 3 dB couplers. Figure 9 shows the vectorial diagram of different components .

A = output signal from linear path
B = output signal from non linear path
C = A + B = output signal of linearizer .

When the input signal increases,

A increases from A to A'
B increases from B to B'
C gets a phase advance $\Delta \emptyset$ and an amplitude expansion ΔC .

Such a system therefore produces a correction of the TWT both in phase an in amplitude .

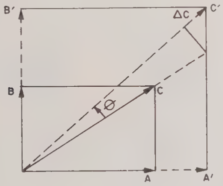

FIGURE 9. : Vector diagram of the linearizer

Figure 10 gives a block diagram of the predistortion network and figure 11 shows the predistortion network .

The predistortion network is made up of the following parts realised in MIC Technology using screen and fire process :

. a WILKINSON 3 dB coupler dividing the input signal in a linear path and a non linear path ,

. the non linear path is made up of two shottky diodes head to tail in series in a 50 ohms line, between two integrated circulators . The shottky diodes are represented in the diagram shown figure 12 .

For this type of beam lead diodes, typical values of the parameters are :

R_S : series resistance : 8 ohms
C_S : junction capacitance : 0.13 pF
L_p : case inductance : 0.1 nH
C_p : case capacitance : 0.07 pF

The current/voltage characteristic of the diode has the following form : $i = I_S (e^{Nv} - 1)$

The parameters I_S and N have been determined experimentally and found equal to :

$I_S = 18.5$ nA
$N = 25.5$ volt $^{-1}$.

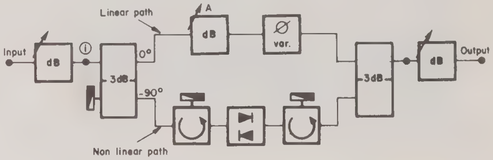

FIGURE 10. : Linearizer block diagram

FIGURE 11 . : Predistortion network

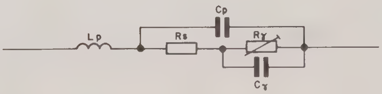

FIGURE 12. :Diode equivalent network

The mechanical characteristics of the diode are given in figure 13. These diodes are thermocompressed upon a 50 ohms line . The neutralizing inductance is made of a 38 microns wire thermocompressed in parallel with the diodes . Figure 14 shows the mounting of the diodes

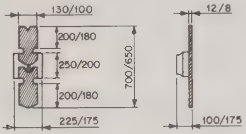

FIGURE 13. : Mechanical characteristics of the diode (dimensions in microns, max. and min.) .

FIGURE 14. : Diodes and compensating inductance mounting

The linear path is composed of an attenuator and of a phase shifter . The phase shifter is a circulator loaded by a short circuited line, the length of which can be adjusted .

The attenuator is made of a 200 ohms resistive film bonded on the 50 ohms line . The attenuation can be changed by adjusting the length of the resistive film .

A 3 dB WILKINSON coupler adds the signals coming from linear and non linear channels .

Input and output attenuators allow an easy adjustment of levels applied to the diodes and to the TWT A. These attenuators are also made with resistive film .

Amplifier

This amplifier is designed to provide 20 dB gain and a high intercept point (+33 dBm) within the 3.7 to 4.2 GHz bandwidth . Two stages of gallium arsenide field effect transistors NEC 695B are used . The amplifier is made in MIC Technology using screen and fire process on 1 mm alumina substrates . The substrates are soldered on carriers which are screwed in the case . Input and output circulators are integrated . The power supply providing the positive and negative regulated voltages is located in the lower part of the case . The amplifier is powered by a 12 V voltage . Figure 15 shows this amplifier .

The consumption of the amplifier is about 2 Watts and the size is 85 mm x 48 mm x 35 mm .

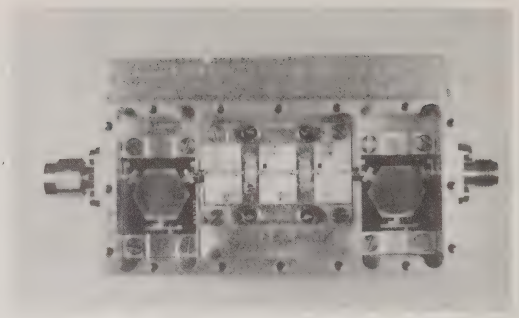

FIGURE 15. : 4 GHz Amplifier

Amplitude equalizer

In order to provide a good compensation of TWT non linearities within the 3.7 to 4.2 GHz bandwidth, the gain variations of TWT must be less than 1 dB . The TWT used to carry out this study having an important gain variation (3 dB) within the bandwidth, an amplitude equalizer was necessary . In the future, this amplitude equalizer will not be used if the TWT gain variations are less than 1 dB .

The equalizer is made in MIC Technology using screen and fire process on 1 mm alumina substrate having a size of 30 mm x 20 mm . Its configuration of three shunt stubs on a 50 ohms line allows signal attenuation at any frequency within the band . The frequency is selected by adjusting the stub length and attenuation is set by choosing the resistor value . Figure 16 shows the amplitude equalizer configuration .

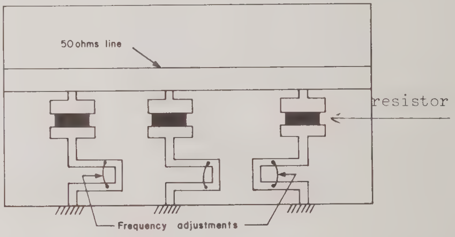

FIGURE 16. : Amplitude equalizer.

In the future, the amplifier and predistortion network will be in the same case and the foreseen dimensions are 140 x 45 x 35 mm . The maximum weight of linearizer will be 0.35 kg.

EXPERIMENTAL RESULTS

In order to check the improvement of linearizer on the TWT non linearities within the bandwidth, intermodulation tests have been performed with two input signals having frequencies F_1 et F_2 defined here after (these frequencies were specified in the Intelsat contract) .

TEST N°	1	2	3	4	5	6	7	8	9	10
F_1 (MHz)	3720	3820	3920	3750	3805	3860	3970	4070	4170	4000
F_2 (MHz)	3720	3830	3930	3790	3845	3900	3980	4080	4180	4040

The third and fifth intermodulation products versus output back-off have been measured with and without linearizer, using a 13 Watts TWT .

The characteristics of this tube are different of those of the "Intelsat TWT" described in the above "System Aspects" section .

The test set-up used to perform these measurements is shown in figure 17 .

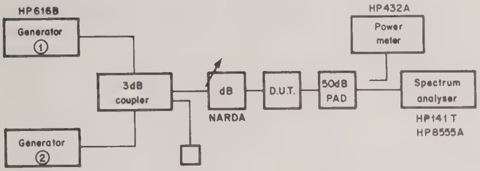
HP616B
Generator ①
Generator ②
3dB coupler
dB
NARDA
D.U.T.
50dB PAD
HP432A
Power meter
Spectrum analyser
HP141T
HP8555A

FIGURE 17. : Intermodulation measurement .

Figures 18, 19, 20 show the improvement obtained when the linearizer is optimized for an output back-off of 5 dB .

For a third order intermodulation products level of 25 dB, 3.8 dB are gained on the back-off within the 500 MHz bandwidth .

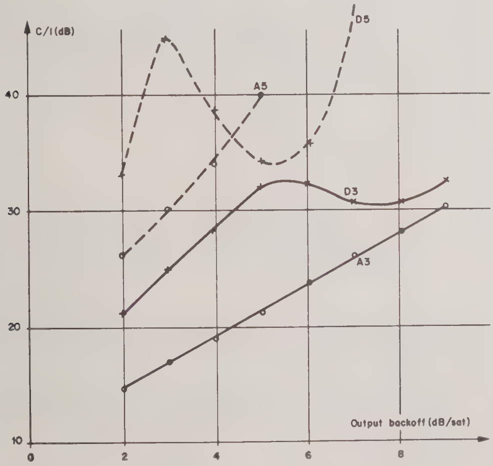

FIGURE 18. : Two tone intermodulation products
F_1 = 3720 MHz F_2 = 3730 MHz

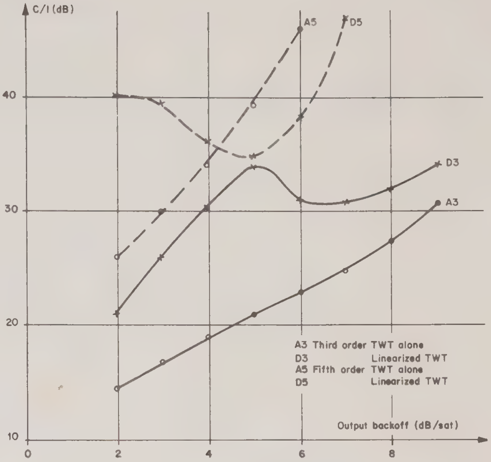

FIGURE 19. : Two tone intermodulation products
F_1 = 3970 MHz F_2 = 3980 MHz

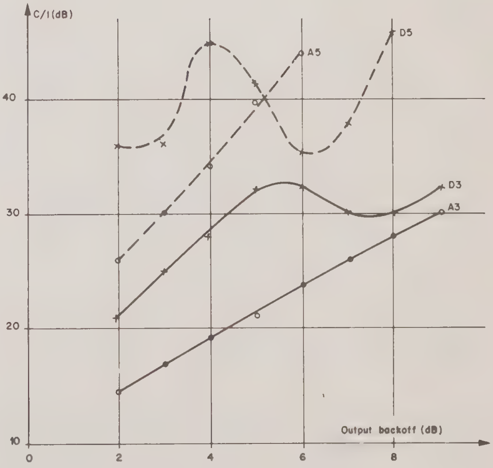

FIGURE 20. : Two tone intermodulation products
F_1 = 4170 MHz F_2 = 4180 MHz

Figure 21 shows the improvement on the phase lag obtained with the linearizer .

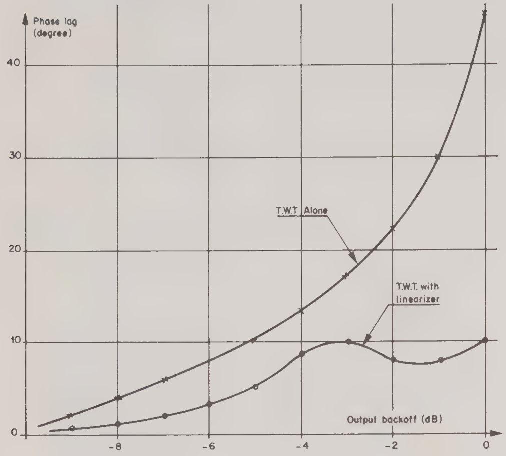

FIGURE 21. : Phase lag of TWT with and without linearizer .

ANNEX I

This annex gives the principles used in the calculations of the first section "system aspects".

- The Carson bandwidth is equal to :

$$B = 2 (\Delta Fp + f m)$$

$$20 \log \Delta Fp = 20 \log \Delta Frms + P + MA$$

$$20 \log \Delta Frms = 20 \log \delta F - 1 + 10 \log N$$

f m = multiplex maximum frequency

Δ Fp = multiplex peak deviation

Δ Frms = multiplex rms deviation

δF = test tone rms deviation per telephony channel

P = multiplex peak factor, 10 dB

MA = margin for over deviation, 2 dB

- The up link carrier to noise ratio is :

$$\frac{C}{N} \text{up} = \text{EIRP} \frac{\lambda^2 \text{up}}{4 \pi D} \left(\frac{G}{T} \right)_{SAT} \frac{1}{k\ B}$$

EIRP = earth station EIRP , per carrier

λ up = wavelength (4.82 cm for F = 6325 MHz)

$\left(\frac{G}{T}\right)_{SAT}$ = satellite receiver figure of merit - 17.6 dB/°K

k = Boltzmann constant, $1.38\ 10^{-23}$

D = earth satellite distance, 40,700 km

- The down link carrier to noise ratio is given by the same formula, with

$$\lambda_{down} = 7.5 \text{ cm } (F = 4.000 \text{ MHz})$$

$$\left(\frac{G}{T}\right)_{ES} = 40.7 \text{ dB/°K}$$

- The input back-off of the satellite TWT is given by :

$$BO = \frac{M \times \text{EIRP}}{4 \pi D^2 \phi_S}$$

EIRP = earth station EIRP, per carrier

M = number of carriers

ϕ_S = satellite flux density at saturation

- Knowing the input back-off, the intermodulation products of the TWT, with and without linearizer, can be computed .

The method used is due to DUROS (4) and is similar to the method of SHIMBO(5) .

It is based on a FOURIER-BESSEL development of the TWT characteristics :

$$z (r) = \sum_i Z_i J_i (K \lambda_i r)$$

Z (r) = complex (amplitude and phase) TWT characteristic

r = TWT input level (voltage)

$J_i(x)$ = BESSEL function of first kind

λ_i = i^{th} root of $J_1(x) = 0$

The linearizer simulation is given in reference (1).

The linearizer has been optimized by maximizing the sum of C/i (cf.Fig. 1bis) for output back-offs of 3, 4, 5, 6 and 7 dB .

The optimum parameters are then :

- A = 13 dB (cf.fig.10)
- level at point ⓘ (cf.fig.10) corresponding to the TWT saturation : 7.7 dBm
- Resistance in parallel with the diodes R_p = 480 ohms . 1

At this point, an equivalent flat intermodulation noise has been calculated .

In order to take into account the real non-flat intermodulation spectrum, assuming large index and gaussian modulation of carriers, the flat noise is multiplied by

$$\frac{x}{\sqrt{2 \pi}} \sum_{n=0}^{\infty} e^{-(nx)^2/8}$$

with :

$$x = \frac{B}{\sqrt{3}\ \Delta F_{rms}}$$

NOTA :

Two slightly pessimistic assumptions have been made :

The C/i has been calculated in the center of the repeater band, and for a very large number of carriers (1000 instead of 11/16) .

REFERENCES

1 "Predistortion network for travelling wave tube"
C. BREMENSON and J. JAUBERT
Revue Technique THOMSON. C.S.F vol.6 n°2, June 1974 - pages 529 to 548.

2 "Linearization of a satellite transmission medium in TDMA"
C. BREMENSON and D. LOMBARD
Third international conference on digital satellite communications
November 1975, KYOTO, pages 144 to 151.

3 Request for proposal IS-565
"Transponder linearizer", INTELSAT,
April 16, 1973

4 "Intermodulations créées par un tube à onde progressive",
by B. DUROS
THOMSON. C.S.F unpublished document

5 "Effects of intermodulation, AM-PM conversion ...."
by O. SHIMBO
Proc. IEEE, vol.59, N°2,
February 1971

6 "Linearisation d'un tube à onde progressive par prédistorsion en fréquence intermédiaire"
by D. POMMIER and J. RICHARD
Revue-Radiodiffusion-Télévision N° 56, 1979

80-0485

A NEW GENERATION OF SATELLITE TRAVELING-WAVE TUBES FOR TV-BROADCASTING AND TELECOMMUNICATIONS

J. Collomb* - P. Gosset** - H. Rayé***

THOMSON-CSF, Electron Tube Division
Paris, France

ABSTRACT

Presented are a series of advanced traveling-wave tubes (TWT's) for direct TV-broadcasting satellites. Operating in the 11.7 to 12.5-GHz frequency range, they are designed to deliver 100 to 120 watts, 150 watts and 200 to 230 watts of output power, respectively. By equipping them with a multistage direct-radiating collector, overall efficiency exceeding 50 % has been achieved.

Detailed are the main technologies relied upon in the design of these TWT's, including the brazed-helix slow-wave structure and the direct radiating collector, with its pyrolytic-graphite electrodes. A detailed picture of the test results to date will also be given, along with a scheme for operating these tubes in parallel, where necessary.

INTRODUCTION

The telecommunication satellite system is the most important development of the past decade in the field of applications satellites. Direct-to-the-home television broadcasting from space is one of the most exciting developments awaited in the coming decade, providing developed countries the solution for additional broadcast channels and developing countries a means of establishing national television coverage for much less expense and time than with a conventional terrestrial system.

Advanced system studies and the allowed radiated power figures set at the World Administrative Radio Conference (WARC-77) for the near-12 GHz broadcast-satellite frequencies imply an output power in the range of 100 to 400 W for the European countries. To cover France, for example, the level of power radiated from the antenna is 270 watts, which requires, due to losses, 340 watts maximum at the amplifier output.

After a review of the different high-power amplifier candidates: klystron, crossed-field amplifier, coupled-cavity traveling wave tubes (TWT) and helix TWT's, the last mentioned was finally selected because of its excellent fine characteristics (linearity, group delay, spurious signals, etc.), its capacity for cooling at high temperature, its weight and the long experience accumulated in the use of such tubes on other low-power satellites.

This paper describes the family of high-power helix TWT's under development by the Electron Tube Division of THOMSON-CSF for future television-broadcasting satellites (TVBS).

Support for this development program has been provided by the French National Space Research Center (CNES) and the French National Broadcasting Agency (TdF) since 1977.

The program covers the development of a series of tubes of unitary power ranging from 100 to 230 watts. In parallel operation, an RF output of up to 400 watts is achievable.

HIGHLIGHTS OF THE BROADCASTING-TWT DESIGN

This family of broadcast-satellite TWT's is characterized by advanced, proven technology and innovative design (see Figure 1). Three of its particularly interesting features are the electron gun, incorporating a long-life impregnated cathode, the all-brazed, tapered helix slow-wave structure and the four-stage depressed collector, cooled by direct radiation into space from its high temperature outer surface and incorporating pyrolytic-graphite electrodes.

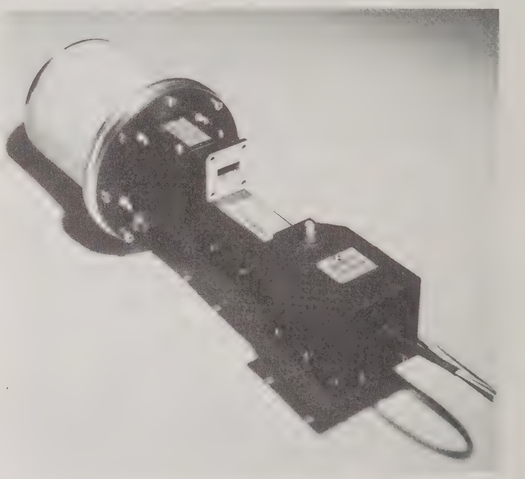

Fig. 1 - The TH 3579 TWT.

The Electron Gun (Figure 2)

The gun has an impregnated cathode loaded at 0.8 A/cm² for an extremely long operating life(1). The similarity of loading permits operating the cathode at the temperature selected for the 20 W/11 GHz OTS TWT, for which a successful demonstration of failure-free life of more than 1.8 million hours has already been completed.

This electron gun includes two anodes. A first one, to control the beam current, will maintain the RF output characteristics constant up to the end of life. A second one, raised to about 120 volts above the helix potential, acts as an ion barrier to protect the cathode from ion bombardment.

The Brazed-Helix Slow-Wave Structure (Figure 3)

The slow-wave structure is made using the brazed-helix technology developed at THOMSON-CSF, which has made possible a large increase in wideband output power over that achievable with conventional methods(2).

The helix, made of copper, is brazed to its beryllium-oxide support rods, which are themselves brazed to the envelope. This structure is characterized by a lack of contact

---

* Satellite Tube Marketing Manager
** Development Engineer, Space Activities Group
*** Manager, Space Activities Group

Copyright © American Institute of Aeronautics and Astronautics, Inc., 1980. All rights reserved.

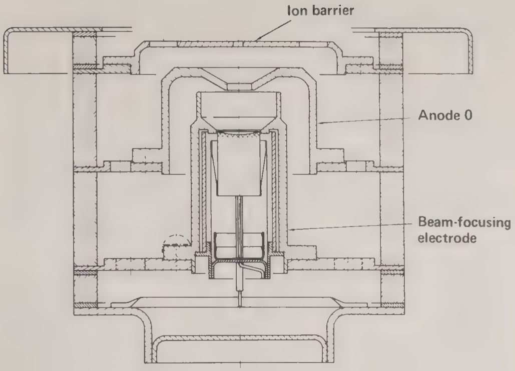

Fig. 2 - The TH 3579's electron gun.

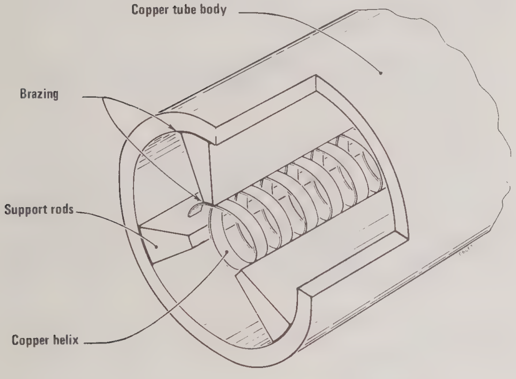

Fig. 3 - THOMSON-CSF brazed-helix technology.

problems, excellent heat transfer, and low RF losses resulting from the low temperatures of the helix, the lower electrical resistivity of copper as compared to tungsten and its low temperature coefficient of resistivity.

Measurements have shown that the average temperature gradient between the helix and the envelope, in vacuum, is less than 2 °C per watt of dissipated power per linear cm. This is some 10 times better than the value found for conventional force-fitted helix slow-wave structures as in our 20-W, 11-GHz TWT's.

Our long experience in the computation and manufacturing of tapered-pitch helixes[(3)] [(4)] has found here an excellent new application (Figure 4). In combination with the low-loss brazed-helix technology, it has led to the achievement of unusually high interaction efficiency. The electronic efficiency is nearly 19 %, which makes it possible to attain better than 51 % overall efficiency, with a four-stage depressed collector, and facilitates the beam design.

The RF output of the 100 and 150 W tubes is a coaxial feed-through. For the 230 W tube, to reduce the RF losses in the output window and improve the cooling of the last helix turn, the output uses a short coaxial section connected to a transformer and a brazed alumina waveguide window (see Figure 5).

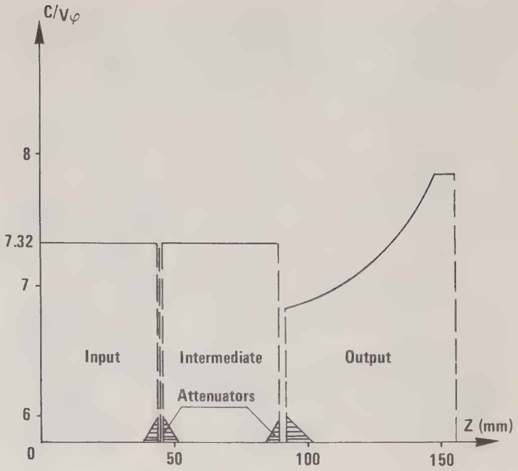

Fig. 4 - Profile of the helix pitch variations.

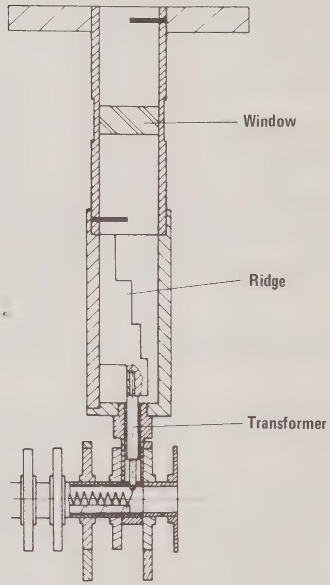

Fig. 5 - Details of the RF output of the TH 3619.

The Collector (Figure 6)

Even with over 50 % electrical efficiency, a new solution for dissipating the waste heat so as not to cause unmanageable thermal problems within the satellite was a mandatory requirement.

Consequently, the collector has been designed to project beyond the satellite's outer surface and to radiate its heat directly into space at high temperature. This solution also permits reducing the collector radiator's size and weight.

First, in a trade-off between collector efficiency and power-supply complexity, the optimum number of collector stages

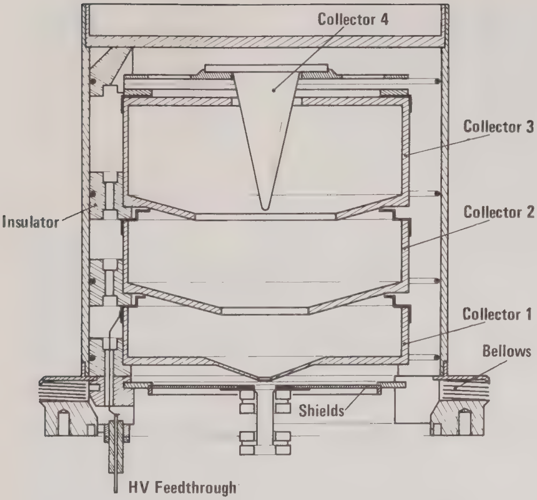

Fig. 6 - The TH 3579's collector.

was selected to be four. The final stage is operated in fact at the cathode potential.

Then, in designing the collector, the following guidelines were followed :

- The optimum shape of the electrodes was defined by computation of the electron trajectories, to collect the electrons with the best attainable efficiency.
- The materials used to make the electrodes were selected for their thermal properties to achieve good thermal heat transfer to the envelope and radiation into space.
- Materials having low secondary emissions and electron reflection were selected.
- The heat transfer between the collector operated at high temperature and the tube body cooled by conduction to a reasonable radiator temperature (< 70 °C) was to be minimized.
- The mechanical stresses during thermal cycling and vibrations were to be limited to low enough values to enable the tube to pass the qualification vibration and thermal cycling tests.

These guidelines have been followed by selecting pyrolytic graphite as the material to use for the collector electrodes. Pyrolytic graphite is characterized in particular by a very low secondary-emission coefficient(5), high thermal emissivity (approximately 0.9), excellent thermal conductivity, low density, and excellent mechanical strength. Because this material has long been used with success for the grids of our high-power tetrodes and triodes, THOMSON-CSF also has a wealth of experience in its production and processing.

The collector electrodes are cooled by conduction from their hotter parts to their relatively cooler parts, then by radiation to the collector envelope.

The collector envelope radiates directly into space. To hold down the weight, the collector's cylindrical envelope is operated at approximately 300 °C. For its thermal properties and its mechanical strength plus stability over the mission life, stainless steel was selected as the envelope material. To have a good emissivity at a temperature of 250-300 °C and a high reflectance in the visible-light spectrum, this envelope has been covered with a fine layer of alumina. Measurements at CNES have shown that the thermal emissivity of this coating is approximately 0.8 (Figure 7) and the visible-light reflectance is also near 0.8. Thermal cycling has confirmed the perfect adherence of this coating.

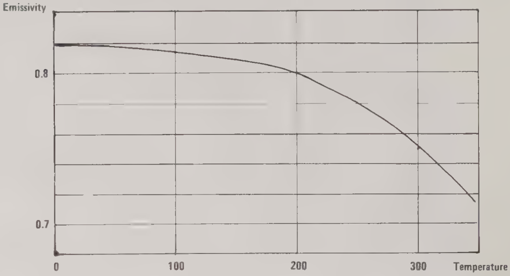

Fig. 7 - Thermal emissivity of stainless steel coated with alumina.

The inner surface is specially treated for low reflectance in the far infrared spectrum.

The temperature of the electrodes is calculated not to exceed 600 °C, which they can easily withstand.

To simplify tube manufacturing the same collector size is used for the 230 W and 100 W TWT's. The 100 W tube will operate at a lower temperature (200 °C for the external envelope and 450 °C for the electrodes).

To prevent the waste heat from returning to the main part of the tube body and causing beam-focusing problems, both heat shields inside the collector and an outer heat barrier are employed. This barrier takes the form of bellows around the collector where it mates with the rest of the tube and the internal heat shields consist of polished metal plates between the first collector electrode and the collector support ring.

These measures are highly effective and only about 10 % of dissipated power is transferred back to the tube body, under worst-case conditions.

The Housing (Figure 8)

The housing has been designed for easy fastening of the body to a radiator baseplate, ensuring efficient heat transfer from the electronic-interaction part of the tube. The housing also gives the TWT sufficient mechanical strength to withstand the vibrations that may occur and protects the tube from electromagnetic interference and radiation hazards.

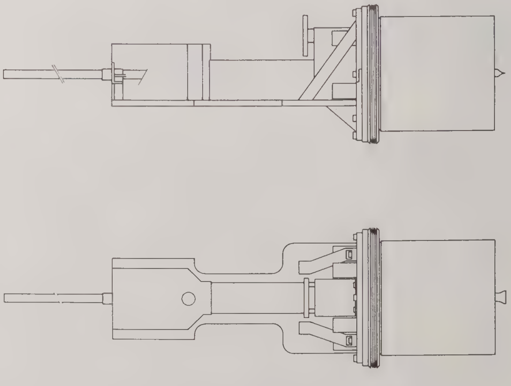

Fig. 8 - Outline drawing of the TH 3579.

TUBE TEST RESULTS AND PERFORMANCES

The TH 3579 150-W TWT

The base model of this family is the TH 3579.

With an overall length of only 370 mm, it weighs just 2.9 kg. Figure 8 shows a drawing of this tube.

Table I presents its principal electrical characteristics. An important fact to note is the relatively low high voltage of just 6 kV and the beam current of 130 mA giving a typical 19.2 % beam efficiency.

TABLE I - Electrical Characteristics of the TH 3579 TWT
(for P_o = 150 W)

Heater voltage and current	6 V/0.85 A
Cathode current	130 mA
Anode 0 voltage and max. current	4.2 kV/± 0.5 mA
Anode 1 voltage and max. current	6.1 kV/± 0.1 mA
Helix voltage and current	6.0 kV/4 mA
Collector stage 1 voltage and current	3.2 kV/44 mA
Collector stage 2 voltage and current	2.2 kV/48 mA
Collector stage 3 voltage and current	1.2 kV/24 mA
Collector stage 4 voltage and current	0 V/10 mA

The tube's typical RF performance characteristics (as measured) are given in Table II and illustrated by Figures 9 to 15.

In the first figure, the output power and the overall and electronic efficiencies across the operating band, at saturation are shown. Figure 10a represents the gain flatness in the operating band at saturation and Figure 10b the same characteristic for small-signal operation (P_o = 10 W). The small signal-to-saturation phase shift is shown in Figure 11 and the third-order intermodulation distortion in Figure 12. Output power and overall efficiency as functions of the drive power are given in Figure 13, along with the variation of the tube currents.

The measured cold and hot input and output SWR are shown in Figures 14a-14b. The noise figure is typically 33 dB.

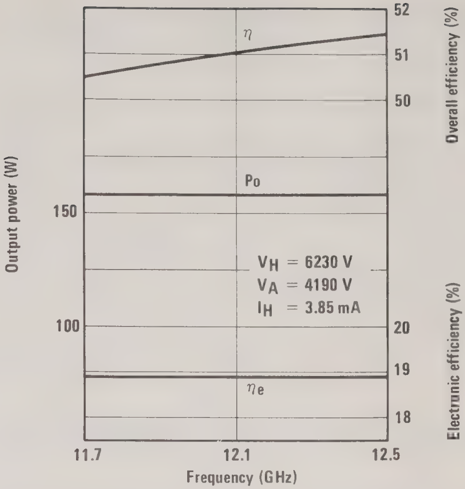

Fig. 9 - Output power and efficiency of the TH 3579 over the operating band.

The variation of the currents with the collector electrode voltages is not sensitive. For example, a decrease of the collector 1 voltage by 200 volts produces an increase of the helix current of only 1 mA. Collector stage 4, normally connected to the cathode, can be biased at up to 40 volts without impact on the collector stage 4 current at saturation.

The TH 3599 - a 100-120 W TWT

Easily derived from the base-model TH 3579, the TH 3599 is a 100 to 120 W tube. Development of the TH 3599 TWT will be limited to an optimization of the voltage and currents and an adjustment of the attenuation sections to achieve the desired gain of near 55 dB at saturation. The dimensions, housing technology and weight will be identical to those of the TH 3579. This will decrease the level of thermal stress on the tube, reduce the cathode loading below 0.6 A/cm² and actually increase the tube's reliability.

The performances of a TH 3579 operating at an output power of 120 watts are presented in Figure 15. Of special note is the

TABLE II - RF Characteristics of the TH 3579

Frequency range				11.7 - 12.5 GHz
Output power at saturation, min.				150 W
Power variation over the band				± 0.10 dB
Saturated gain				59 dB
Small-signal gain (10 W)				66 dB
Overall electrical efficiency, min.				50 %
Gain ripple in any 50-MHz channel :				
- at saturation, max.				± 0.1 dB
- small-signal, max.				± 0.2 dB
Gain slope :				
- at saturation, max.				± 0.01 dB/MHz
- small-signal, max.				± 0.02 dB/MHz
Noise figure				34 dB
Phase shift :				
- output power level below saturation	0 dB	−3 dB	−6 dB	−10 dB
- phase shift, max.	50°	30°	15°	9°
Third-order intermodulation :				
- level of each output carrier relative to single-carrier saturation		−6 dB	−9 dB	−13 dB
- intermodulation product level relative to either output carrier		−17 dB	−23 dB	−31 dB
AM/PM conversion coefficient, max.				5 °/dB
Harmonic power, relative to saturation, max.				−12 dB
Allowed overdrive				+10 dB
Input/output cold SWR, max.				1.5 : 1
Input/output hot SWR, max.				2.5 : 1

over-50 % overall efficiency achieved at this lower power level. The saturated gain is 55 dB and the other characteristics (gain variation, phase shift, SWR) are similar to those of the TH 3579. The cathode current is only 100 mA.

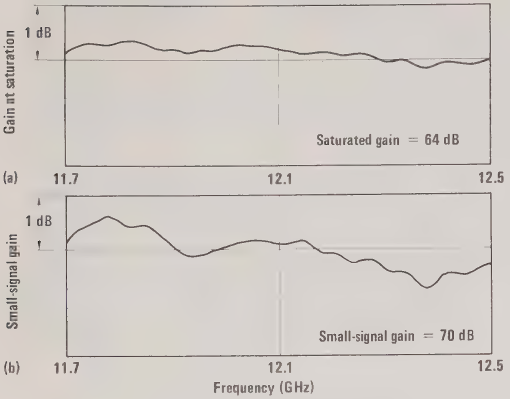

Fig. 10 - Gain flatness of the TH 3579 at saturation (a) and in small-signal operation (b).

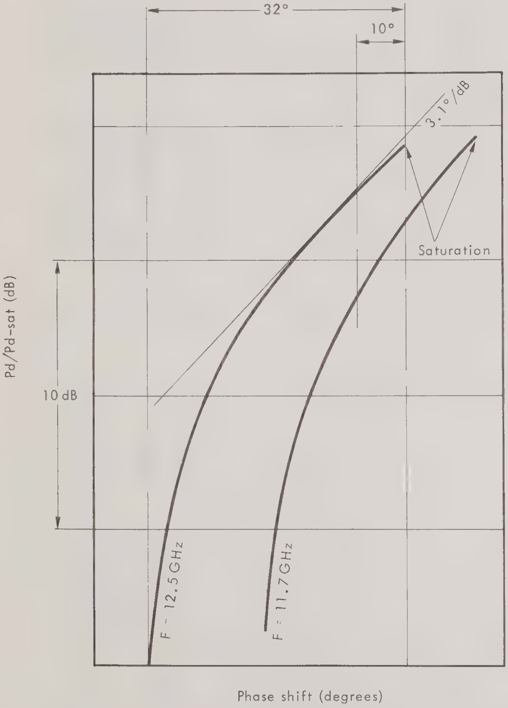

Fig. 11 - Small-signal-to-saturation phase shift at the two ends of the operating band (TH 3579).

The TH 3619 - a 200-230 W TWT

We are now developing a high-power version of the TH 3579, the TH 3619.

This tube is designed to deliver an output power of 200 to 230 watts in the same frequency band.

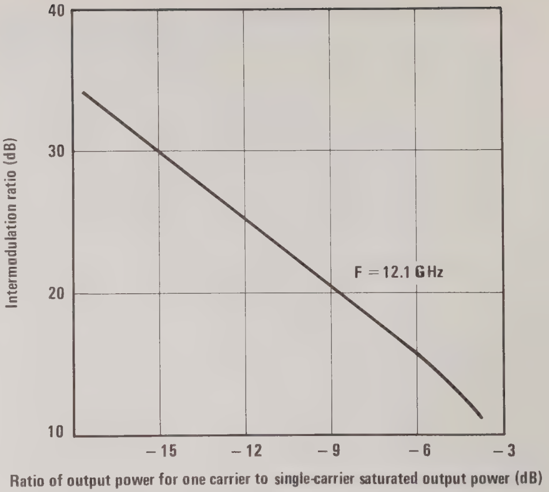

Fig. 12 - Intermodulation ratio for two carriers (TH 3579).

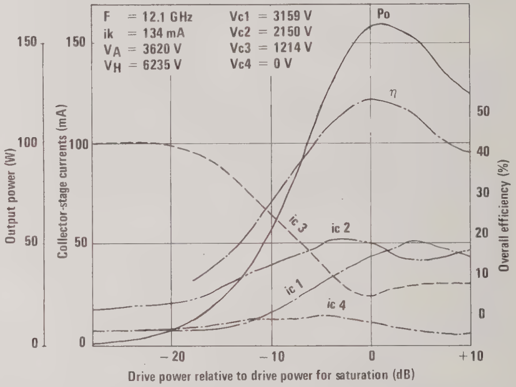

Fig. 13 - Output power, efficiency and current distribution among the collector electrodes as a function of tube drive.

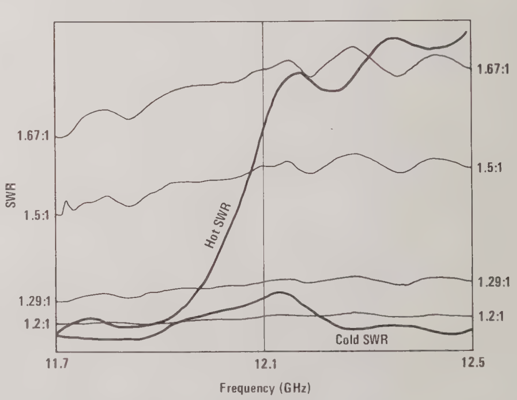

Fig. 14a - Input SWR of the TH 3579.

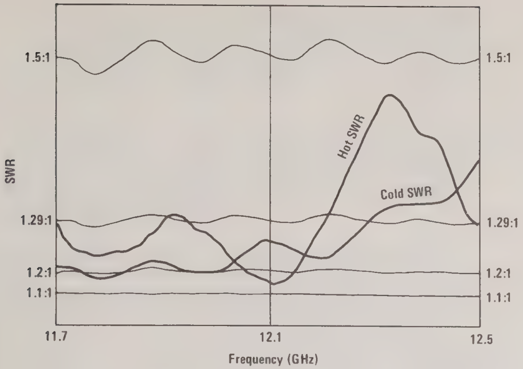

Fig. 14b- Output SWR of the TH 3579.

The TH 3619 will have the same concept and technology as the other tubes. The changes will mainly concern the cathode diameter, to maintain the cathode loading at a sufficiently low value for good reliability, and a scaling of the helix dimensions. To reduce the RF losses in the coaxial output feedthrough and improve the cooling of the last helix turn, the output will be made of a short coaxial line connected to a transformer and a brazed waveguide alumina window (see Figure 5). The design goals for the TH 3619 are given in Table III.

COMBINING HELIX-TWT OUTPUT POWER

For satellite applications, THOMSON-CSF today considers the 230 watts of the TH 3619 to be the practical limit for long-life helix TWT's. Beyond this level, at 250 W of output power and more, only coupled-cavity TWT's may be capable of providing sufficient per-unit power. However, it is well known that the fine transmission characteristics (linearity, group delay variations, load SWR, etc.) of coupled-cavity tubes are inferior to those of helix TWT's. Furthermore, beyond an output power per tube of 300 watts, it becomes more and more difficult to evacuate (under vacuum conditions) the heat generated by the power dissipated in the tube body, no matter what slow-wave structure is employed.

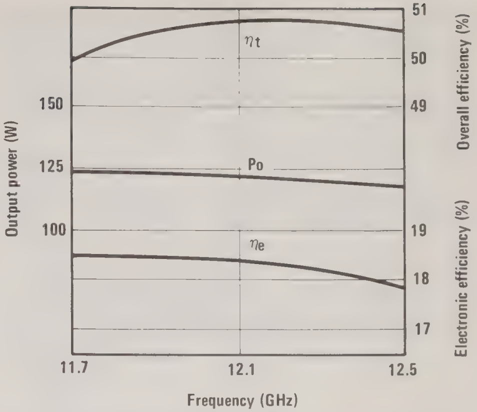

Fig. 15 - Output power and efficiency of the TH 3579 operated at the output power level of the TH 3599 (120 watts).

Faced with this limitation and with a requirement for 340 watts of amplifier output power in the TVBS application, the

TABLE III - Characteristics of the TH 3619 TWT

Electrical (for P_o = 230 W)				
Heater voltage and current	7 V/0.9 A			
Cathode current	156 mA			
Anode 0 voltage and max. current	5.4 kV/± 0.5 mA			
Anode 1 voltage and max. current	7.15 kV/± 0.5 mA			
Helix voltage and current	7 kV/6 mA			
Collector stage 1 voltage	4.1 kV			
Collector stage 2 voltage	2.9 kV			
Collector stage 3 voltage	1.45 kV			
Collector stage 4 voltage	0 kV			
RF				
Frequency in the range	11.7 - 12.5 GHz			
Bandwidth	340 MHz			
Output power at saturation	200 - 230 W			
Saturated gain, min.	50 dB			
Overall electrical efficiency, typical	50 %			
Small-signal gain	55 dB			
Gain ripple in any 190-MHz channel :				
- at saturation	± 0.25 dB			
- small-signal	± 0.5 dB			
Gain slope :				
- at saturation	± 0.01 dB/MHz			
- small-signal	± 0.02 dB/MHz			
Noise figure, max.	35 dB			
Phase shift :				
- output power level below saturation	0 dB	−3 dB	−6 dB	−10 dB
- phase shift, max.	50°	30°	15°	9°
AM/PM conversion coefficient	6 °/dB			
Harmonic power, relative to saturation, max.	−12 dB			
Allowed overdrive	+10 dB			
Input/output cold SWR, max.	1.5 : 1			
Input/output hot SWR, max.	2.5 : 1			

Electron Tube Division came up with the solution of paralleling two or more helix TWT's, to form, with the existing development tube, up to 400 W output amplifiers$^{(6)}$.

In fact, such power combining has already been done in space, but at a much lower power level. This was first done in the Pacific Ocean INTELSAT II satellite in 1967 and later in NASA's experimental ATS6 satellite.

Combining the output power of two or three tubes can present numerous important advantages. In particular :

1) Helix TWT's can be employed to extend the amplifier power range up to 400 watts.
2) The satellite heat-transfer problems are simplified, because the waste heat is radiated from several smaller tubes, physically separated, instead of from a single larger one.
3) The combined amplifier can be operated at half-power without sacrificing efficiency, by operating only one tube at a time.
4) Such characteristics as the small-signal gain variation and the noise figure are improved after power combining, the individual tube characteristics not being correlated.
5) And in a three-tube arrangement, there is the capability of "graceful output-power degradation" and higher intrinsic reliability, because there is more redundancy and each tube operates at a relatively low output-power level.

Shown in Figure 16 is the proposed arrangement for combining the output power from three THOMSON-CSF helix TWT's. This arrangement makes it possible to transmit using any pair of the three TWT's, or any single tube at a time. With three TH 3619's, a total output power of up to 400 watts can be obtained from any pair of tubes. The third tube is kept for redundancy and can be used to replace either of the two other TWT's as necessary.

Table IV summarizes the losses which can be expected with such an operating arrangement, with the losses experienced in the single power tube plus backup arrangement, for comparison.

Typically, the losses resulting from combining the output power of two tubes should never exceed 15 % of the sum of the output power of the two tubes, as compared to 8 % losses with a single high-power tube.

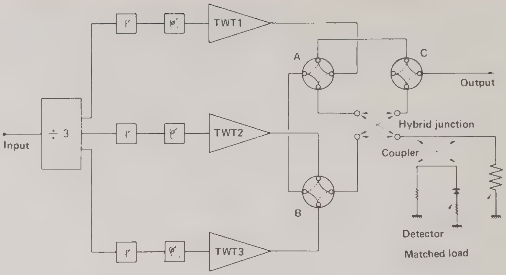

Fig. 16 - Scheme for combining the output power of three high-power helix TWT's.

The preliminary results of the study performed under CNES contract show :

- The RF phase shifter included in the input line, to compensate for the possible aging of the EPC's, can be advantageously replaced by two steps of commanded helix voltage per EPC.
- The attenuator in the input line is a fixed attenuator to compensate for tube to tube saturated gain differences.
- The mismatch combination results are better than the calculated values for the typical SWR values.
- We expect the same to hold true for the combined losses evaluation.

RELIABILITY

In designing these high-power TVBS satellite tubes, the parameters impacting reliability have been carefully evaluated. Every effort has been made to ensure an operating life on the orbital station of at least 7 years. In fact, the design goal for tube operation is 10 years.

All the technologies employed have been thoroughly proven by testing or long operational experience.

Filament

The potted-filament technology of the space-qualified 20 W - 11 GHz tubes yields high temperature cycling stability. After

TABLE IV - Estimated Losses

LOSS DESIGNATION	2 of 3 TWT's in parallel		1 of 2 TWT's	
	Typical values	Max. values	Typical values	Max. values
	dB	dB	dB	dB
• **Dissipation switches**	0. 16	0. 20	0. 08	0. 10
Power combiner	0. 05	0. 10	–	–
Waveguides	0. 10	0. 20	0. 05	0. 10
Sub-total	0. 31	0. 50	0. 13	0. 20
• **Phase difference** (max. = 17° typ. = 12.3°)	0. 05	0. 10	–	–
• **Mismatches**	0. 32	0. 76	0. 21	0. 52
TOTAL	0. 68 dB 15 %	1.36 dB 27 %	0.34 dB 8 %	0.72 dB 13 %

3000 temperature cycles, the cathode temperature variation does not exceed 5 °C, and 58 life-test tubes have shown no filament resistance variation after 1.8 million hours of operation. Thus the same technology is adopted for these higher-power tubes.

Cathode

The density of electron emission does not exceed 0.85 A/cm², making it possible to operate the impregnated cathodes at approximately the same temperature as in THOMSON-CSF's 20-W, 11-GHz space TWT's.

In the reliability-demonstration program for the 12 GHz space tubes, 58 of them have now operated for a cumulative grand total of 1.8 million hours, with not a single failure to date.

The variation of the TWT's main RF parameters recorded are :

- Output power	No variation
- Gain at saturation	No variation
- Helix current	+ 0.07 mA/10,000 hours
- Noise figure	+ 0.5 dB/10,000 hours
- Cathode current at constant anode voltage	−1.2 %/10,000 hours

Some similar microwave-link TWT's have operated continuously for more than 11 years, and their WEIBULL curve shows no wear-out phenomena.

Helix

The helix operates at a significantly lower temperature than in the 20-watt space tubes and the good electronic interaction efficiency of about 19 % makes a positive contribution to the tube reliability.

Other THOMSON-CSF tubes (250 W, 6 GHz) employing this same technology have demonstrated individual lives as long as 40,000 hours without problem. The same technology is employed for a 600-W, 14-GHz air-cooled earth-station TWT, illustrating clearly the wide margin of operating capability. THOMSON-CSF has operated brazed-helix TWT's up to a power level of 2,500 watts, in X-band, with liquid cooling.

Collector

Proven methods for manufacturing and processing pyrolytic-graphite electrodes and 15 years of company experience in producing Pyrobloc® pyrolytic-graphite grids for power-grid tubes are elements in our confidence in the reliability of this material.

Other positive factors for collector reliability are :

- The thermal decoupling allows during processing to increase the collector temperature for complete outgassing of the collector structure.
- The absence of brazes.
- The separation of the cooling function by radiation from the insulation of the electrodes, which are powered through independent potted feedthroughs kept at low temperature.

Environment

The TH 3579's design has been submitted with no failure to very severe environmental tests. As passage at the rate of 2 octaves/mn covering the spectrum from 5 to 2000 Hz as follows :

5 -	22 Hz -	6.35 mm -	0 to peak
22 -	130 Hz -	1.3 G's -	0 to peak
130 -	250 Hz -	1.8 G's -	0 to peak
250 -	400 Hz -	4.5 G's -	0 to peak
400 -	2000 Hz -	7.5 G's -	0 to peak

When a resonant frequency was discovered at 300 Hz, the test was prolonged for one-half hour at the resonant frequency following this vibration test ; there were absolutely no changes in the tube's electrical characteristics. Disassembly of the tube then followed, and no mechanical failures of any kind were found.

To verify the capability of the collector structure for supporting the frequent thermal cycling to which it will be subjected during the orbital life of the TWT, a thermal test consisting of 4000 thermal cycles will be conducted by THOMSON-CSF. This is equivalent to ten full years of operation in space.

In conclusion, the only wear-out phenomenon limiting the life of such a tube remains the cathode emission, and by similarity with the 20-W, 11-GHz tube family, the life expectancy exceeds 10 years and the demonstrated reliability figure is better than 600 F.I.T.*

DEVELOPMENT PROGRAMS

The qualification of this TVBS tube family is progressing, with the support of the French Administration, along three axes :

1) Preparation of the space-TWT manufacturing line for TH 3579, TH 3599 and TH 3619, including establishment of the procurement, manufacturing and testing procedures, qualification of each subassembly process, development and manufacturing of the tools and testing facilities. This task will be completed in October 1980.

2) Development of the TH 3619 Engineering model to be completed in March 1981.

3) Implementation of a life test demonstration to qualify the collector design by a thermal vacuum cycling life test demonstration accumulating 4000 temperature cycles of the collector under vacuum, with a liquid nitrogen cooled wall. This will be completed in July 1981.

*F.I.T. = failures per 10^8 hours.

REFERENCES :

(1) SHROFF A.M. ; PALLUEL P. ; "Dispenser Cathodes for Space Telecommunication" ; Tri-Service Cathode Workshop ; Washington ; DC ; 1978.

(2) FLEURY G. ; KUNTZMANN J.C. ; LAFUMA P. ; "Advantages of the Brazed-Helix Technology for High-Power TWT's" ; Satellite Communications ; October 1978.

(3) MALONEY E.D. ; "Foresight Made Tubes Available for 11-GHz Satcom" ; Microwave Systems News ; November 1979.

(4) STRAUSS R. ; "Demands on TWT's Tighten as Carrier Density Grows" ; Microwaves ; April 1978.

(5) FORMAN R. ; "Secondary Emission Properties of Conducting Surfaces for Use in Multistage Depressed Collectors" ; I.E.D.M. ; Washington ; 1977.

(6) PUJES J.P. ; "Combining High Power TWT's : an Original and Attractive Approach to Direct TVBS Amplifier Design" ; International Television Symposium ; Montreux ; 1979.

80-0486

PAST AND PRESENT INTELSAT TWTA LIFE PERFORMANCE†

R. Strauss*
COMSAT Laboratories, Clarksburg, MD

J. R. Owens**
INTELSAT, Washington, D.C.

Abstract

The traveling wave tube amplifier (TWTA) is a key element of microwave transponders used in communications satellites. In-orbit performance requirements demand stringent transmission characteristics and high efficiency as well as long and uninterrupted lifetimes. The primary performance limiting element is the cathode of the traveling wave tube (TWT). Considerable experience related to long life performance of tubes, power supplies, and cathodes has been accumulated. This paper reviews the TWTA life performance of the INTELSAT IV satellite series, the expected life performance and design concept incorporated into INTELSAT V, redundancy aspects, and the important considerations associated with the candidate cathodes (e.g., oxide and matrix types), particularly with regard to future communications satellite applications.

Introduction

An earlier paper by the authors[1] described the pertinent life design factors of commercial communications satellites. As indicated, TWTs are among the few major components which, by virtue of a degradation or "wear out" mechanism, limit the useful life of these satellites. In TWTs, the primary fundamental life limiting subelement is the cathode. The electron emission capability of the cathode is controlled by physio-chemical processes that proceed inexorably at a prescribed rate. The emission electron work function increases gradually. The initial cathode current, which is space charge limited, progresses toward a temperature limited condition and then noticeably decreases.

Since the TWT gain is directly related to the cathode current, it also decreases in time, followed eventually by a noticeable reduction in RF output power. This type of fundamental degradation mechanism occurs in all current TWTs regardless of cathode type. However, both the mechanisms and specific rates differ greatly depending on the cathode type, its environment, the operating temperature, the initial setting of the operating space charge limited current, and the emission activation procedures applied. Satellite TWTs have used both oxide and impregnated matrix dispenser type cathodes. With few exceptions, average cathode limited TWT lifetimes ranging from 50,000 to 80,000 hr either have been space demonstrated or are anticipated on the basis of ground life test data.

This paper will review the current expectations of TWT life performance in terms of space applications. The review will be based primarily on TWT life performance in operational INTELSAT IV satellites, the life expectancies of TWTs being designed into current satellite programs, and future TWT life expectations utilizing a newer class of cathodes. In addition, some aspects of TWT, or preferably TWTA (TWT + power supply), operating redundancy strategy will be discussed since this strategy directly depends on the TWTA failure patterns.

Commercial Satellite TWT Applications

More than 1000 TWTs are now in space.[2] The majority of these tubes operate at 4 GHz, and without exception have used oxide cathodes (see Figure 1). Oxide cathodes are typically set to operate at temperatures ranging from 650°C to 750°C with space charge limited cathode current densities (J_o) usually between 150 and 200 mA/cm^2. The saturation or fully temperature limited cathode current density is typically more than a factor of 10 greater than J_o at normal operating temperatures. Furthermore, an increase of 25°C in the actual cathode operating temperature generally will reduce the life of the oxide cathode by a factor of two.[3]

At output power levels above 10 W and at frequencies of 11 GHz or higher, all current or projected TWT applications utilize the impregnated matrix dispenser cathode. This cathode type can provide long life if its operating temperature is well controlled and near 1000°C (brightness temperature). At this temperature, the normal space charge limited cathode current density typically ranges from J_o = 650 to 700 mA/cm^2. The saturation current density is a factor of 5 to 6 times greater than J_o. Thus, compared with an oxide cathode, the matrix cathode operates significantly closer to its temperature limited condition and is therefore more temperature sensitive in the normal space charge limited region of operation.

To attain a constant cathode current during long-term life, the cathode temperature must be carefully controlled and maintained. However, as will be shown later, the matrix cathode unfortunately does not maintain a constant cathode current, although cathode temperatures are held to within ~±10°C of the preselected initial life temperature. In addition, experimental data indicate, for example, that an increase of 30°C to 40°C in the cathode operating temperature will increase the cathode current by about 1 to 2 percent at the start of life and possibly 4 to 5 percent toward end of life (~7 yr). Furthermore, such a temperature increase will also accelerate the physio-chemical process and reduce the life of the matrix cathode by a factor of two.

---

*Director, Reliability and Standards.

**Manager, Satellite Operations Department.

†This paper is based upon work performed at COMSAT Laboratories under the sponsorship of the International Telecommunications Satellite Organization (INTELSAT).

Copyright © American Institute of Aeronautics and Astronautics, Inc., 1980. All rights reserved.

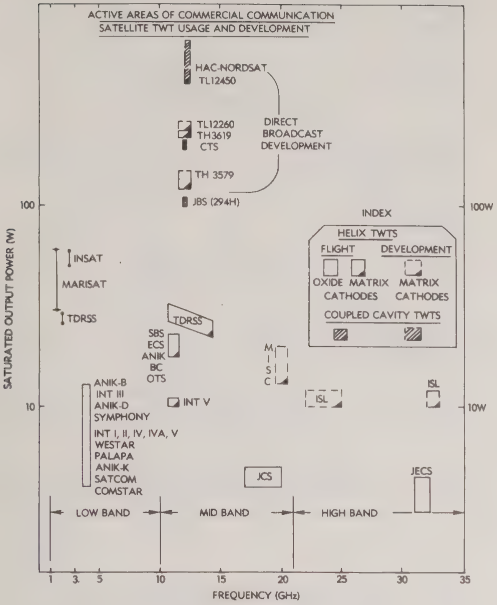

Figure 1. Active Areas of Commercial Communications Satellite TWT Usage and Development

Comparison of Oxide and Matrix Cathode Characteristics

Both oxide and matrix cathodes have been used commercially for many years.[4-7] Continuing interest exists in analyzing their characteristics and developing not only improved understanding but also improved performance.[8-11] Figure 2 shows the basic start of life and end of life cathode current (I_k) as a function of relative cathode temperature and with fixed electron gun anode voltages. These curves are sometimes referred to as underheating curves.

The well-activated oxide cathode, particularly at the start of life, has a relatively sharp "knee." A knee temperature (T_{kno}) can be clearly defined by the intersection of the two extrapolated linear portions of the curve . As shown in Figure 2, the knee of the curve distinguishes between the space charge limited region of operation and the temperature limited region. These two regions are separated in a well-activated cathode by a relatively narrow temperature transition region. As the cathode's physio-chemistry proceeds, the knee temperature (T_{knx}) progresses toward the cathode operating temperature. For this example, $\Delta T_{kn} = T_{kn0} - T_{kn1} = 60°C$. In some cases, ΔT_{kn} may be as high as ~100°C or or as low as ~50°C; however, the progression based on empirical results is between 0.5 to 1.0°C/1000 hr of life. End of life occurs when the TWT gain or output power decreases below some level set by system considerations. A typical number is 4-dB loss of small signal gain. The relationship between the loss of cathode current and small signal gain to a first approximation is as follows:

$$\Delta G_{ss}(\text{dB}) \sim K(G_{ss} + A) \frac{\Delta I_k}{I_k}$$

where G_{ss} = start of life TWT small signal gain (dB)

A = wave start-up loss in the TWT, which is typically ~ 15 dB for a 2-gain-section tube

$\Delta I/I_k$ = 0.08 in Figure 2 for normal and constant cathode temperature

K = 0.33 (theoretical) to 0.65 (Actual values of K can be determined for each tube type by plotting cathode underheating gain curves.)

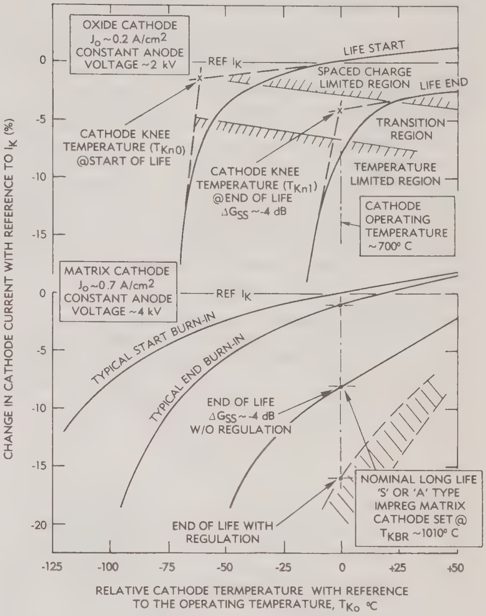

Figure 2. Comparison of Oxide and Matrix Cathode Characteristics as a Function of Cathode Temperature

The matrix cathode has a broad knee without a clear transition region. This is further substantiated by a greater current sensitivity as a function of cathode temperature in the space charge limited region. In addition, the impregnated matrix cathode, which is a surface metal film emitter cathode, depends on a bulk reaction, "Knudsen flow" transport feed mechanism within the matrix, and surface area coverage by migration that requires significant time (minutes to several hours) to achieve complete operational equilibrium at a given temperature. These factors lead to an interpretation that the matrix cathode has a small but persistent component of emission current which is always temperature limited. Therefore, the cathode operating temperature is chosen to be as low as possible, consistent with an essentially (but not completely) space charge limited mode of emission. As shown in Figure 2, a well-activated impregnated matrix (S or B type) dispenser cathode, when set at its operating temperature (e.g., 1010°C brightness), will change its I_k by approximately ± 2.5 percent for a $\pm 50°C$ ΔT_{BR} at emission densities near 0.7 A/cm^2.

As the matrix cathode ages, significant changes are observed. Even after a typical space TWT burn-in period of 1500 or 2000 hr, in which the cathode is kept at the normal operating temperature, an observable decay trend is usually noted (see Figure 3). Depending on factors such as the activation and the cathode, this "initial" decay may require 1000 to several thousand hours until a steady-state decay rate is obtained. The discovery of a "space charge limited" emission current decay, strongly dependent on the cathode operating temperature,[8,9,11] was initially reported a few years ago. The complete theoretical explanation for the decay is still lacking although experimentally all matrix type impregnated dispenser cathodes experience some characteristic decay. As indicated in Figure 3, some cathodes appear to stabilize at rates as low as −0.5 percent ΔI_k/10,000 hr (type A), while others decay more rapidly at rates of ~2 percent Δ_k/10,000 hr (type S) when operated at comparable temperatures such as 1010°C $\pm$ 10°C brightness without Joule cooling. A current decay concept is disconcerting to the TWT user who has been accustomed to the relatively constant current experienced with the oxide cathodes. As shown in Figure 3, the usual oxide cathode does not exhibit a decay characteristic until the latter stages of its life. Furthermore, there are other cathode types called reservoir dispenser cathodes (e.g., MK or L types) which have shown no gradual current decay until the reservoir (e.g., BaO) is depleted; then the current decreases rapidly, again toward the end of life (e.g., 50,000-70,000 hr).[12]

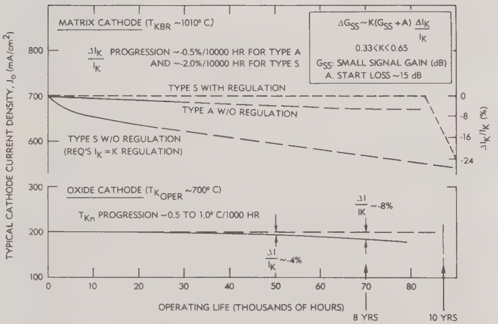

Figure 3. Comparison of Oxide and Matrix Cathode Characteristics as a Function of Life

During the past few years, extensive tests have been performed on TWTs and cathode testers (usually diodes) to determine the basic emission current life characteristics. Dispenser type cathodes in test diodes can be used effectively since they are capable of being operated at elevated temperatures to establish cathode life acceleration factors.[13] Figures 4 and 5 illustrate this for two types of cathodes tested. Both appear to be capable of reaching 8 years of emission life but with dramatically differing end of life current degradation. For the "S" cathode, a 20-percent cathode current degradation would result in an unacceptable TWT gain reduction.

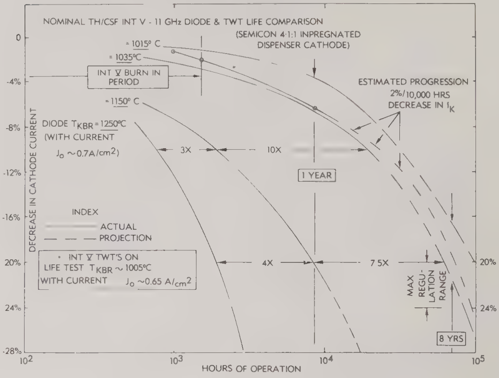

Figure 4. Nominal Thomson/CSF INTELSAT IV 11-GHz TWT Diode Life Comparison (Semicon. Corp. 4:1:1 impregnated matrix dispenser cathode)

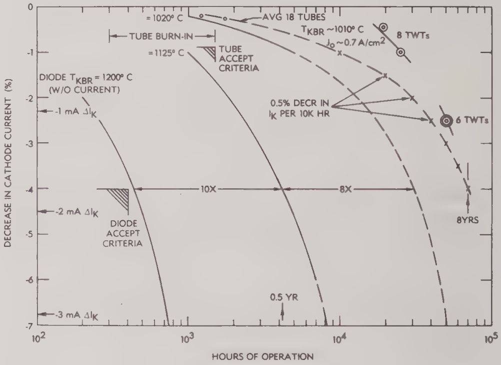

Figure 5. Nominal 12-GHz 20-W TWT and Diode Life Comparison (type A impregnated dispenser cathode)

Thomson/CSF, manufacturer of the INTELSAT V 11-GHz TWT, proposed the use of a double anode electron gun with the first anode (approximately at half cathode potential) serving as a beam current control element.[14] This anode (A_o) intercepts essentially no current and its voltage can be increased approximately 20 percent while constant cathode current conditions are maintained without deleterious defocusing effects; therefore it is the ideal control element in a constant cathode current sensing-feedback loop control network. Such a network was incorporated into the power supply associated with Thomson/CSF TWT's by Ford Aerospace Comm. Co. Figure 6 illustrates this concept with an electron gun. Figure 7, which shows the responses recorded in a recent dip test (removal of filament power for a prescribed period, which in this case was 2 s), indicates the effectiveness of the constant current control network. The estimated end of life current compensator capability allows an uncompensated current decrease of about 25 percent. Figure 3 illustrates the projected life characteristic for the "S" type matrix cathode, with and without regulation.

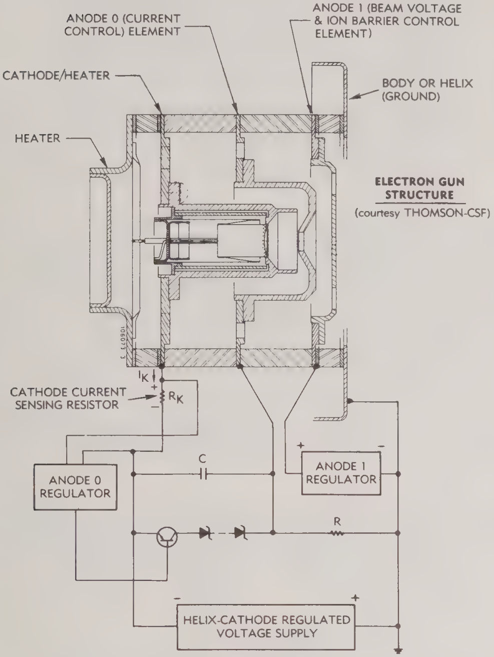
ANODE 0 (CURRENT CONTROL) ELEMENT
ANODE 1 (BEAM VOLTAGE & ION BARRIER CONTROL ELEMENT)
CATHODE/HEATER
BODY OR HELIX (GROUND)
HEATER
ELECTRON GUN STRUCTURE
(courtesy THOMSON-CSF)
I_K
CATHODE CURRENT SENSING RESISTOR
R_K
C
ANODE 0 REGULATOR
ANODE 1 REGULATOR
R
HELIX-CATHODE REGULATED VOLTAGE SUPPLY

Figure 6. Conceptual Illustration of the Dual Anode Electron Gun and a Feedback Sensing Network Which Regulates and Controls the Anode 0 Voltage for Maintenance of Constant Cathode Current

Performance of Oxide Cathode TWTs in INTELSAT IV

The largest and oldest "homogeneous" TWTA population in space is aboard the INTELSAT IV series.[15] There are seven satellites, each with four receivers and 24 transmitters arranged in 12 output channels (2 for 1 redundancy). Each receiver contains one driver TWT. The total population is therefore 28 driver TWTs (twenty-six 262H and two 272H) and 168 transmitter TWTs (261H).[16] Every TWT has its own dedicated power supply. Three commands per transmitter TWTA are possible: filament on, high voltage on, and all voltages off. As will be shown later, this permits both the usual "hot" and the occasional "cold" start. The usual start allows four minutes of filament warmup before high voltage is applied to the TWT. The driver TWTAs, on the other hand, could only be given a "cold start," in which all voltages are commanded "on" at the same time. Telemetry is not available except for the changes in bus current (ΔI_{BUS}) after the execution of commands, and temperatures from several judiciously located thermocouples on the despin platform near TWT collectors. Approximately 5,000,000 TWT operating hours have now been accumulated on INTELSAT IV satellites.

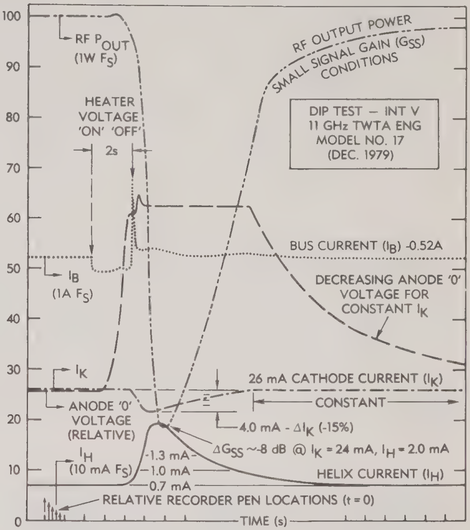

Figure 7. Dip Test of INTELSAT V 11-GHz TWTA Engineering Model #17 (December 1979)

Driver TWTA

The receivers are arranged in a quadruple redundancy configuration so that only one driver TWTA is operational at any time. The tube has a saturated output power capability of 1.5 W but typically operates in the small signal gain (linear) region with an output of several hundred milliwatts. Of the seven INTELSAT IV satellites in orbit, four have all receivers stored in an "off" condition to conserve the remaining cathode life. These are contingency or spare satellites. Table 1 shows the estimated remaining receiver life for each satellite, along with the life history of the driver TWTAs.

The oldest satellite (F-2) has approximately three months of remaining receiver life. Unfortunately, the average 262H lifetime was slightly less than two years. The gain degradation patterns were consistent (e.g., loss of cathode current emission and a reduction in linear gain), as shown in Figure 8. There were never any EPC (power supply) related problems with these tubes. The major factors pertinent to the limited life of this device are a higher than usual cathode current density (280 mA/cm^2), an associated elevated cathode temperature (740°C), and an exceptionally high ratio of anode aperture diameter to cathode diameter (1.05) required by the shallow angle gun for the attainment of an 18-dB noise figure . All the other TWT features were completely consistent with the typical long-life space tube technology

Table 1. INTELSAT IV Driver TWTA Life History
(as of December 1979)

Satellite	Launch Date	Months in Orbit	Rx Life Remaining (mo)	No. of TWTAs[a] Failed	No. of TWTAs Never in Service	Average Useful Life (mo) of Failures
F-1	May 1975	56	N/A	0	3	--[b]
F-2	Jan 1971	106	~3[c]	4	0	11
F-3	Dec 1971	97	~11[c]	3	1	24
F-4	Jan 1972	96	~24[c]	3	0	15
F-5	June 1972	91	~7	3	0	20
F-7	Aug 1973	77	21[c]	3	1	23
F-8	Nov 1974	62	24	2	1	21
				TOTAL 18 of 28		

[a] Failed means that the transponder gain has dropped below specification levels but that some useful performance is still possible. The gain loss has always been the failure indicator but cathode deactivation is the failure cause.

[b] The F-1 spacecraft was equipped with two-262H and two-272H TWTs. Only one 272H (Rx #4) has been in service. It now has satisfactorily accumulated about 40,000 hours.

[c] Receiver currently stored off.

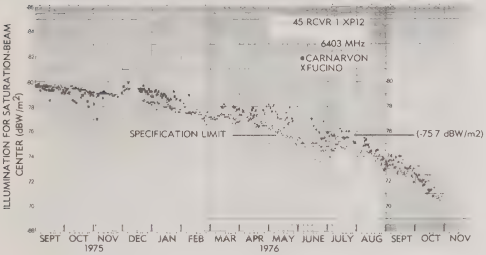

Figure 8. "Death" of a Receiver Due to Driver Tube Cathode Deactivation (INTELSAT IV F5, Rx #1)

that existed at that time (e.g., an ion-anode blocking voltage, depressed collector, long term burn-in, and selection criteria). Since these cathode deactivation patterns allowed time for receiver replacement, system communications services were never compromised in any spacecraft with quadruple redundancy.

The successor TWT (272H) does not appear to have a similar degradation problem. Two were used in the F-1 satellite (see Table 1) and twelve on the three COMSTAR satellites. Several of these 272H tubes have been operating for more than four years without any sign of deactivation. The 272H was virtually identical to the 262H (1500-V cathode voltage) except that its oxide cathode operated at a lower temperature (~700°C), the cathode current density was lower (200 mA/cm^2), and the anode aperture to cathode diameter was notably lower (0.88). Other driver TWTs such as the 233H (INTELSAT III), 276HA (Westar, Anik A), and the 263H (DSCS-III) have performed exceptionally well with many tubes whose lives are beyond the 50,000-hr mark, again without any indication of deactivation. In all of these cases, the cathode current density was below 200 mA/cm^2 with cathode temperatures of ~690°C.

Driver TWTs are now being replaced by solid-state driver amplifiers in the more recent series of communications satellites. Current experience with 4-GHz space-borne medium-power solid-state driver amplifiers has been uniformly excellent.

Transmitter TWTA

The seven INTELSAT IV satellites contain 168 transmitter TWTAs; of the initial 84 TWTAs (A units), 61 are still capable of satisfactory performance. The 23 failed A units have been replaced by standby TWTAs (B units) since the spacecraft transmitter is fully redundant (2 for 1). With the exception of one EPC failure (e.g., INTELSAT IV F-5, channel 2-B or as coded: 45-2B), all 24 "B" units have worked successfully after many years of "off" storage in space. In Figure 9, which shows the complete history of all 24 failed TWTAs, the relative start times of the "B" units can be determined from the failure time of the A units.

The total "operated" population (98 TWTAs) may be divided into two classifications: non-eclipse cycled and eclipse cycled TWTAs. The non-eclipse cycled TWTAs were never turned off for an extended period (2-3 months), but they may have occasionally been turned off for testing of the alternate unit. Eclipse "off" cycling on a modest scale did not start until 1977 when the satellite battery performance began degrading. More extensive cycling was started in the spring of 1978. Shortly thereafter, five of eight TWTAs which had been turned off during this eclipse season (2-3 months) failed with fairly rapid (several months) cathode deactivation. Prior to that, only six non-cycled TWTAs had failed; three of these failures are believed to be power supply related and three cathode related.

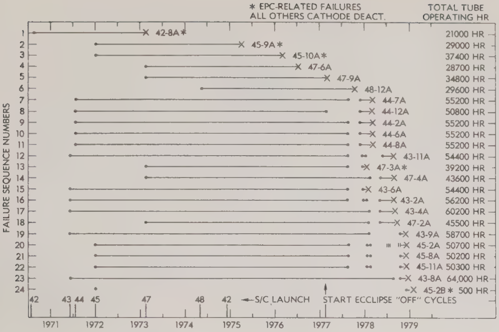

Figure 9. History of the Failed Tx TWTAs on the INTELSAT IV Spacecraft [total space population: 168 TWTAs comprising 84A and 84B (redundant) units]

Of the total cycled population ($N_C = 46$) there are now 16 cathode related failures. The operating life patterns for the uncycled and cycled populations are shown in Figures 10 and 11. Present estimates are for an average TWTA life of 8 years (non-eclipse cycled) and 6.9 years (eclipse cycled), respectively.

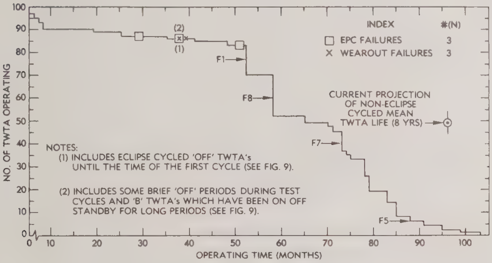

Figure 10. INTELSAT IV Transmitter TWTAs: Operated Continuously (September 1979)

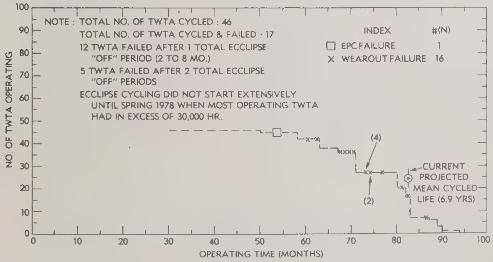

Figure 11. INTELSAT IV Transmitter TWTAs: Eclipse Cycled (total TWTA population eclipse cycled by June 1979)

In terms of operating history, the total TWTA population can be divided into four groups. Two groups represent early life failures (e.g., in the 20,000- to 40,000-hr range) comprising about 3 percent each of the total operated population (e.g., the "early" continuously operated cathode deactivation group and the EPC related failure group). The third group, comprising 16 percent of the operated population, consisted of TWTAs which deactivated after one or more long eclipse "off" periods. The cause for this behavior is still under investigation. The final group (78 percent) appears to be extremely healthy regardless of the type of operation (e.g., uncycled or cycled). The single EPC related failure of a backup TWTA is as yet unclassified. Additional life details, including some daily cycling test results, are reported in Reference 17.

Since 19 of the failures, excluding the EPC related failures, were attributed to cathode deactivation, it became necessary to obtain a more fundamental understanding of the detailed interrelationships (e.g., gain, cathode current, and bus current). There are basically only three measures available for analysis on each INTELSAT IV transmitter TWTA: change in bus current (ΔI_B) telemetry, transponder gain, and relative transmitter saturated output power. Furthermore, each of these measures could be determined with only limited resolution, e.g., 40 mA for ΔI_B and ~2 dB for gain and relative output power. Therefore, simulation tests were conducted at COMSAT Laboratories to analyze the deactivation characteristics. These tests revealed some interesting features of TWTA deactivation. Subsequent in-orbit tests could then be performed with confidence.

INTELSAT IV Transmitter TWTA Deactivation Characteristics

When all TWT supply voltages are kept constant and the cathode current gradually degrades, as in the case of cathode deactivation (transition from space charge limited to temperature limited operation), the tube's RF characteristics change. The exact changes can be closely approximated by simulating deactivation through reduction of the cathode temperature. The so-called underheating effects on the RF characteristics and helix interception of the 261H are shown in Figure 12 as a function of RF drive. Thus, for a reduction in I_k (e.g., $\Delta I_k = -2$ mA), the corresponding changes of gain, saturation drive, output power, helix current, and phase delay can be determined. A family of such curves can be established for most TWTs and life performance assessed if the change in cathode current with time is known. Although other performance factors such as noise figure, VSWR, and gain slope could also have been measured as a function of ΔI_k, this was not considered necessary.

In the INTELSAT IV satellite, the power supply was series regulated so that as a first-order approximation, the bus current (I_B) was directly proportional to I_k. Figure 13 shows the relative rise of helix, cathode, and bus currents and their correspondence to RF output power for a "cold start" (all voltages including normal 4.5-V heater voltage applied to the TWT simultaneously). The transient temperature rise of the cathode is superimposed on this figure. It should be noted that the cathode current becomes space charge limited when the cathode temperature reaches more than ~625°C. Figure 14 shows the effect of cathode deactivation. In that case the filament voltage has been reduced to 3.3 V and the cathode must reach ~700°C before the cathode current become space charge limited. Moreover, approximately 180 seconds are required as shown to reach 700°C. In an actual space TWT deactivation case where the filament voltage remains constant (e.g., $E_f = 4.5$ V), the same temperature is reached in less time (~150 s), but the phenomenon is the same: a more extended starting or stretched transient due to the increased knee temperature, T_{kn} (see Figure 1), for the aged TWT. This streching effect has frequently been clearly observed and measured in space TWTs by monitoring ΔI_B and RF output after a cold start turn on. Therefore, T_{kn} progression can be measured from the ground provided that the TWT can tolerate cold starts. Since some TWTs cannot survive a cold start due to excessive body current interception during the extended turn-on transient, this type of procedure cannot be universally applied.

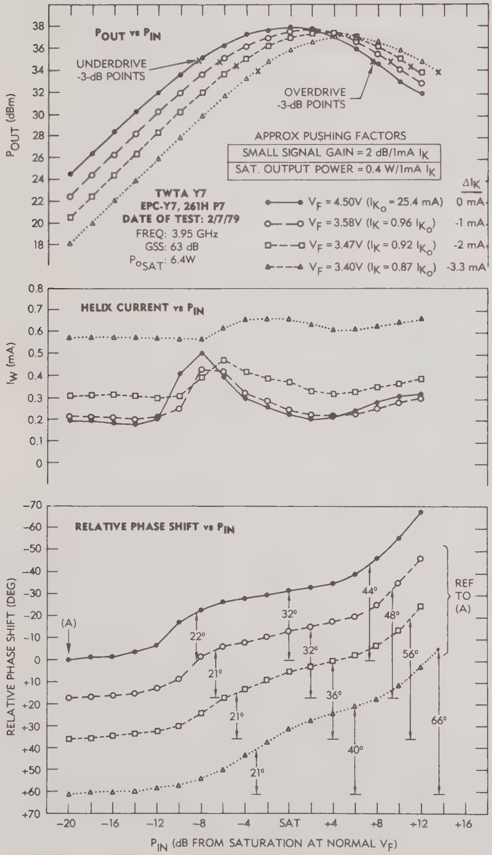

Figure 12. Effect of Reduced I_K by Filament Underheating (TWT 261H)

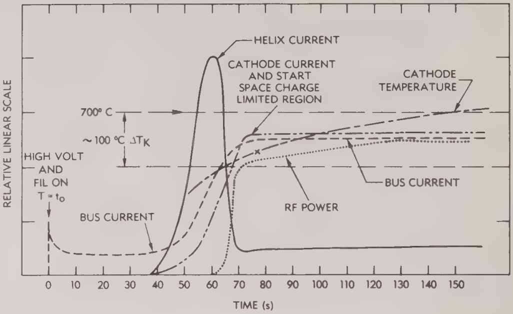

Figure 13. "Cold Start" Characteristic with Normal Filament Voltage (INTELSAT IV simulator TWTA E5, filament voltage = 4.5 V)

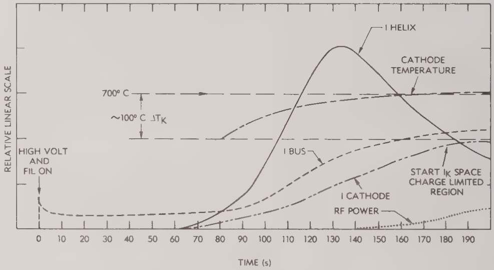

Figure 14. "Cold Start" Characteristic with Cathode Degradation Simulated by Reduced Filament Voltage (INTELSAT IV simulator TWTA E5, filament voltage 3.29 V)

A second method for determining deactivation progression is to observe the bus current and RF transient with a normal "hot" start (typically 4-min filament/cathode warm-up prior to applications of high voltages). A simulated case is given in Figure 15, which shows the normal start with $E_f = 4.5$ V and the underheated value ($E_f = 3.1$ V). The unexpected ~2-minute transient decay in I_k and output power for the latter case is due to the Joule cooling effect, which occurs with electron emission. That is, at the instant at which I_k is drawn, the cathode cools (~10°C in this case); since the emission is now temperature limited, the cooling results in a decrease of emission until the cathode reaches its new equilibrium temperature. Obviously, under space charge limited emission conditions, this effect is never observed. Therefore, in a seriously degraded TWT, the Joule cooling effect may easily be recorded on the ground, and plans for switching on a redundant TWTA made. A typical trace on a degraded space tube is shown in Figure 16. The techniques developed by simulation at COMSAT Laboratories and applied by INTELSAT in space have permitted a much better assessment of the state of the TWTs in space.

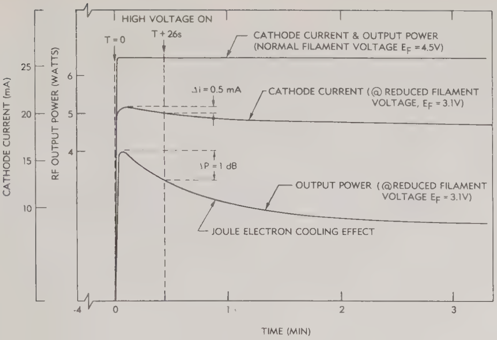

Figure 15. Cathode Current and Output Power Signature with "Hot" Turn On with Operation at Normal and Reduced Filament Voltage (simulator TWTA E5, E_F = 3.1 V and normal filament voltage E_F = 4.5 V)

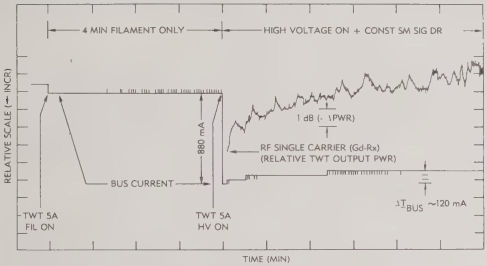

Figure 16. INTELSAT IV F2 TWTA 5A Turn on Sequence (February 1979, Andover, Maine)

Redundancy

Several TWTA transmitter channel redundancy concepts have been used in communications transponders. As previously mentioned, INTELSAT IV satellites used a 2 for 1 transmitter redundancy. Both INTELSAT IV-A and V have a considerable number of channels with 3 for 2 redundancy. More recent configurations use the concept conceived at COMSAT Laboratories[18] and currently designed into such spacecraft as SBS (two circuits, each with 8 for 5 redundancy) or Anik C (approximated by two circuits, each with 12 for 8 redundancy). There is also the zero redundancy concept (e.g., SATCOM and COMSTAR) in which a channel is allowed to die when a TWTA fails. Since failure is usually gradual, this allows time (weeks) to reconfigure the ground systems.

Until recently, the choice of a specific concept has perhaps been more subjective than objective. Now that the TWT life patterns are better understood (at least at 4 GHz) and the channel loading as a function of satellite lifetime is also firmer, a more objective TWT redundancy strategy may be chosen. One example of interest was the INTELSAT IV-A 3 for 2 redundancy case.

There are two basic TWTA utilization strategies: minimum switching or equal aging. The minimum switching strategy minimizes the number of on-off switching cycles, since units are left on until a failure occurs and then the redundant unit is turned on. This obviously is the best choice for channels with 2 for 1 redundancy. For channels with 3 for 2 redundancy, this same minimum switching strategy can lead to nonoptimum channel availability when wearout failure is strictly due to the length of time that a unit remains on. If both online units failed there would only be one backup unit available when two are needed, and channel capacity would decrease.

For the equal aging strategy, this problem is overcome by rotating the on-line assignment of the three units to equalize the accumulated life. This strategy does require switching and associated long-term storage of the units after they have accumulated substantial life. Based on the evidence gained on the INTELSAT IV program and the significantly higher failure rate of cycled as compared to uncycled TWTAs, it has been decided to use the minimum switching strategy on all channels of the INTELSAT IV-A satellite. Furthermore, current INTELSAT IV-A satellite transmitter TWTA experience with over 2,000,000 hours of operation on five satellites (20 transmitter channels per satellite) confirms the general early life pattern established on the INTELSAT IV series of satellites.

Future Life Expectations

Several significant developments have occurred during the past year. In terms of oxide cathodes, the most recent satellite TWTs have used a cathode loading density of 130 mA/cm^2 and cathode temperatures 20°C to 30°C lower than normally used for loadings of ~200 mA/cm^2. In principle, this should increase the TWT lifetime by perhaps a factor of two. That is, if all failures on INTELSAT IV, for example, were due to classic cathode deactivation (as in the case of uncycled population), the mean estimated life would be 16 years. This trend has been substantiated by 94,000 hours of successful transponder operation of the INTELSAT III F-3 satellite prior to its decommissioning during the fall of 1979. The two types of TWTs used (233H and 235H, two each per satellite) were both operated with a cathode current density of ~140 mA/cm^2.

The same order of lifetime could be estimated for matrix type cathodes operated with a constant cathode current regulator providing J_o ~300 mA/cm^2 at a brightness temperature near 980°C. Since matrix cathodes are more resistant to residual gas effects and can be evaluated with accelerated temperature tests prior to flight, they may be preferable to oxide cathodes. Furthermore, NASA (Lewis), ESTEC, and INTELSAT are continuing to develop improved matrix type cathodes, with the expectation that 100,000-hour cathodes with a capability of 2 A/cm^2 will evolve. This same cathode could, conversely, be operated at the present 0.7-A/cm^2 levels with temperatures 60°C to 80°C below those currently in use. The expected result would be cathode and in turn TWT lifetimes of the order of 200,000 hours. These candidate cathode types utilize either osmium or indium, properly incorporated with the Tungsten matrix, in impregnated or storage matrix dispenser type cathodes.

Conclusion

This paper has documented the past and present status of TWTA lifetimes, primarily in the INTELSAT satellite system. The characteristics of cathode degradation, both for oxide and matrix type cathodes, have been presented. Reliable and long-lived TWTA performance has been demonstrated which meets or even exceeds the expectations of the late 1960's. Furthermore, current work on newer types of matrix cathodes indicates that a factor of two improvement in lifetimes may be possible. Although space field effect transistor amplifiers (FETAs) are strong contenders for displacing space TWTAs at the low power levels (~1 W or less), they have not yet proven their ability at higher power microwave levels (~4 W or greater). Further proof must be established before system designers can with complete confidence elect to use power FETAs rather than TWTAs for long-term (>10-year) satellite appliications.

References

1. R. Strauss et al., "Design Factors Affecting Communiations Satellite Lifetime," 28th Congress of the International Astronautical Federation, Prague, September 1977.

2. R. Strauss, "Microwave Tube Requirements for Communication Satellite Systems," 1977 International Electron Devices Meeting, Washington, D.C., December 1977.

3. M. G. Bodmer, et al., "The Satellite Traveling Wave Tube," Bell System Technical Journal, July 1963.

4. G. Hermann et al., The Oxide Coated Cathode, London: Chapman & Hall Ltd., 1951.

5. W. B. Nottingham, "Thermionic Emission," Handbuch der Physik, 1956.

6. V. L. Stout, "Dispenser Cathodes," Proc. 4th National Conference on Tube Techniques, September 1958.

7. E. S. Rittner, "On the Mechanism of Operation of Ba Aluminates Impregnated Cathodes," Journal of Applied Physics, Vol. 28, No. 12, 1957.

8. R. Forman, "Surface Studies of Ba and BaO on Tungsten and its Application to Understanding Mechanism of Operation of an Impregnated Tungsten Cathode," Journal of Applied Physics, Vol. 47, No. 12, 1976.

9. R. T. Longo, "Long Life, High Current Density Cathodes, 1978 International Electron Devices Meeting , Washington, D.C., December 1978.

10. L. R. Falce and R. E. Thomas, "Controlled Porosity Density Cathodes," 1978 International Electron Devices Meeting, Washington, D.C., December 1978.

11. P. Palluel and A. M. Shroff, "Experimental Study of Impregnated-Cathode Behavior, Emissivity, and Life," to be published early 1980 in Journal of Applied Physics.

12. Private communication, European cathode workshop; Figure 8, "RW80 Life Test Results," Siemens TWT Data Book, 1977/78.

13. R. Strauss et al., "TWTs for Communications Satellites," IEEE Proceedings, Vol. 65, No. 3, March 1977.

14. D. Henry et al., "A Triple-Power-Mode Advanced 11-GHz TWT," 7th European Microwave Conference, Copenhagen, September 1977.

15. E. T. Jilg, Ed., "The INTELSAT IV Spacecraft," COMSAT Technical Review, Vol. 2, No. 2, Fall 1972.

16. "Summary of Space TWT and TWTA Experience," Hughes Aircraft Company, Electron Dynamics Division, Torrance, Cal., September 30, 1978.

17. Contribution of the Director General, "Report on the Status of TWTAs in Orbit," INTELSAT Document BG/T-29-18, 27 June 1979.

18. F. Assal et al., "Network Topologies To Enhance The Reliability of Communications Satellites," COMSAT Technical Review, Vol. 6, No. 2, Fall 1976.

80-0487

EHF SOLID STATE TRANSMITTERS FOR SATELLITE COMMUNICATIONS

Jorg E. Raue*
TRW Defense and Space Systems Group
One Space Park, M5/1426
Redondo Beach, CA 90278

Since 1970 TRW has been active in all phases of millimeter component, subsystem and system development, including passive high performance components and antenna systems, active semiconductor power and low noise receiver devices, and active circuits. The intense 1970-75 efforts led to a series of technological breakthroughs, including the first successful application of network analysis and computer aided design at millimeter wave frequencies, and resulted in a series of components that clearly advanced the state-of-the-art. (References 1-6). This work then formed the basis for subsequent successful millimeter wave subsystem and system development. One of these is an on-going concentrated effort to develop high power (greater than 1 watt CW) solid state amplifiers suitable for space applications. This paper describes these development efforts for 2 to 10 watt communication amplifiers in the frequency ranges near 35, 40 and 60 GHz.

The two technical challenges that have to be overcome in order to produce reliable multi-watt solid state amplifiers are: (1) solid state sources with reasonable output power and efficiency are required, and (2) diode combining circuitry with good combining efficiency and small size are essential. Significant progress has been made in both areas in the past two years. Hughes, Raytheon and TRW have produced IMPATT power sources with output power exceeding 1 watt at 40 GHz and 0.5 watt at 60 GHz with reasonable junction temperatures. In the circuits area, TRW is developing a 10 watt solid state amplifier at 41 GHz and a 2 watt amplifier at 60 GHz. Table 1 summarizes these and other recent developments.

The success of these technology development efforts, all of which are directed toward space communication applications, is primarily attributable to the successful application of advanced design techniques to millimeter wave frequencies. This includes detailed device and circuit analysis and modeling with heavy reliance on computer aided design. In addition, great strides have been made recently in advancing the state-of-the-art of EHF waveguide circulators - components of fundamental importance in the design of high performance reflection amplifiers.

This paper describes the aforementioned amplifiers, including device and circuit design aspects, design techniques, gain and bandwidth tradeoffs, efficiency and reliability considerations, etc. For example, two of these amplifiers are depicted in Figures 1 and 2.

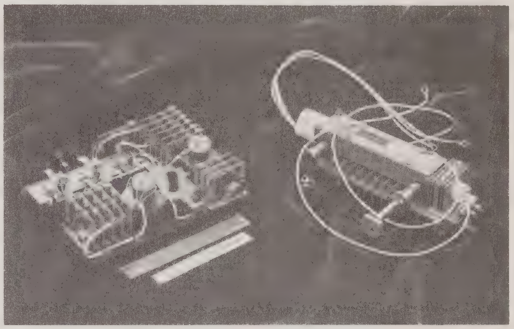

Figure 1. Comparison of 5-watt 37 GHz solid state amplifier with TWT. (TWT power supply not shown.) Both units have 30 dB of gain. Solid state amplifier is cigar box size and weighs 9 pounds.

Table 1. Summary of TRW's High Power EHF Solid State Amplifier Developments

Amplifier Description				
Frequency	Output Power	Gain	Bandwidth	Status
37.3 GHz	5 Watts	33 dB	700 MHz	Completed 1977
38.1 GHz	5 Watts	30 dB	700 MHz	Completed 1978
41 GHz	10 Watts	30 dB	100 MHz	Under Development
60 GHz	1 Watt	14 dB	600 MHz	Completed 1978
60 GHz	2 Watts	17 dB	200 MHz	Under Development

---

*The author is now with the California Polytechnic State University, San Luis Obispo, CA, 93407, as Head of the Department of Electronic and Electrical Engineering.

Copyright © American Institute of Aeronautics and Astronautics, Inc., 1980. All rights reserved.

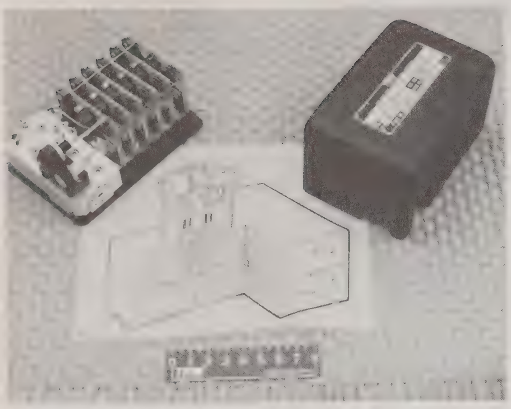

Figure 2. 1-Watt 60 GHz solid state power combining amplifier. Demonstration unit weighs 2 pounds

Our in-house developed line of breadboard laboratory network analyzers, which covers the 26 to 40, 33 to 50, 55 to 65 and 90 to 100 GHz band, each with 10 GHz instantaneous bandwidth,is typified by the V-band unit shown in Figure 3. These units, used together with the proper RF circuits, allow accurate device terminal impedance measurements and circuit evaluation. For example, the circuit impedance seen by a diode in a Ka-band circuit is shown in Figure 4. Of particular value here is the 10 GHz instantaneous bandwidth which eliminates the time consuming measurements typical of commercial units available up to 40 GHz. These units have an instantaneous bandwidth of 2 GHz.

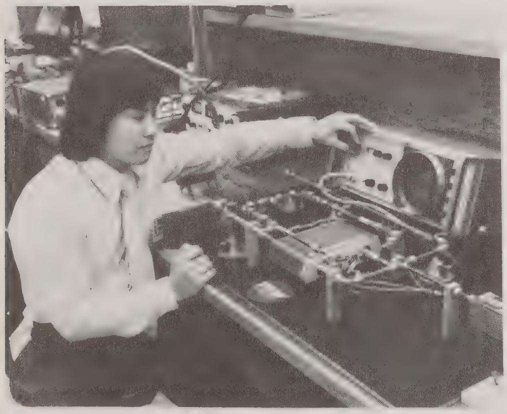

Figure 3. Broadband EHF network analyzer with 10 GHz instantaneous bandwidth (55 to 65 GHz).

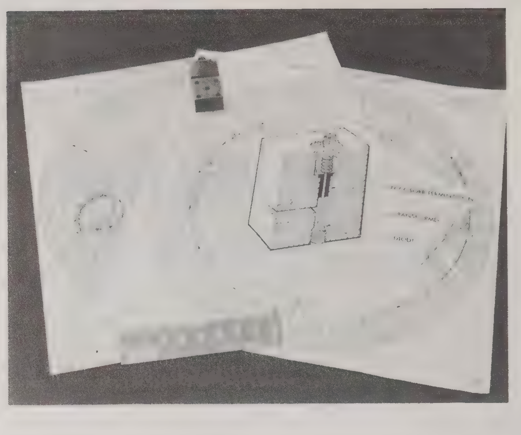

Figure 4. Single stage 41 GHz amplifier circuit. Impedance plots compare calculated and measured impedance seen by the diode for two different circuit conditions.

Also evident is the extraordinary simplicity of the RF circuit, which allows analytical treatment.

The starting point of the driver amplifier circuit design was the measurement of diode impedance. From this data and from the measured impedance of other diodes from the same lot, it was determined that the reactive component of the small signal impedance under bias, clustered principally around -j0.5 normalized to 50 ohms. Based on this assessment, the reactive component of the circuit impedance was targeted to +j0.5 ohms (normalized to 50) to complement the diode impedance.

A coupled coaxial circuit was selected as the primary circuit for development because of its potential for analytical characterization and because of its similarity to the combiner coaxial segment. Figure 4 depicts this circuit. Of particular interest are the thick iris coupling from the coaxial line to the waveguide port and the dumbbell type bias line. This type of circuit had previously been successfully employed with Gunn devices. The pin, however, has the drawbacks of being relatively difficult to modify and presents stability problems when implemented with an IMPATT device. As a consequence, a bias line similar to that used in the combiner, was implemented. This line consists of a pin extending from the diode package, past the waveguide coupling iris, through a lossy termination element to a spring tensioner and bias connection. In addition, a transformer may be attached to the end of the line to facilitate impedance matching to the diode. The advantages of this type of line are high ease of modification and the stable terminated environment presented to the diode to suppress out of band spurious oscillations. This circuit is characterized by exceptionally low Q's - typically less than 10.

Various forms of power combining at the circuit level were considered for the power stage. A previous successful effort at 37 GHz involving a circular TM_{010} cavity combining scheme provided for substantial impetus to employ the same technique at 41 GHz. Due to the increased frequency, the diameter of the basic TM_{010} cavity is restricted to a point where the maximum number of diodes that can be accommodated is reduced. A minimum of twelve diodes will be required on the assumption that 1 watt RF is available per device and a projected combining efficiency of 80% is realized. This large number of devices at a higher frequency dictates that a higher order mode be utilized, specifically the TM_{020} mode. The experimental breadboard combining circuit for the final power stage of the 10 watt, 41 GHz amplifier is seen in Figure 5, together with a schematic representation of the combining structure. All stages of these various amplifiers are designed and built in a fully deterministic fashion, i.e., no tuning elements are used.

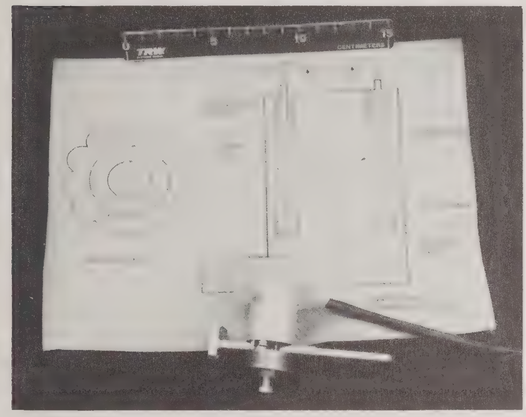

Figure 5. Experimental 12-watt 41 GHz IMPATT combining circuit.

High performance circulators are imperative for successful quality amplifier design. For this reason, we developed, from scratch, an entirely new line of exceptionally high performance circulators. The new design is compared with the well-known previous approach in Figure 6. The cylindrical junction, mechanically interlocked without the use of any adhesives within the waveguide housing, and consisting of simple shapes which are relatively easy to fabricate, inspect and assemble, results in excellent repeatability of performance and unlike the commonly used triangular, rigidly epoxy-bonded structures which are susceptible to thermal, shock and vibrational stresses, this junction is soft-mounted and impervious to these stresses. Similar junctions, constructed at lower frequencies for space applications, were thoroughly tested to spacecraft level specifications without a single failure. The ferrites of the junction are designed to operate with a high level of magnetic bias. This requires higher quality, more expensive, rare earth permanent magnets, but the added expense is easily justified considering that the need for a precise adjustment of the magnetic bias is eliminated saving labor, and that the thermal stability of the circulator and its power handling capability are significantly enhanced.

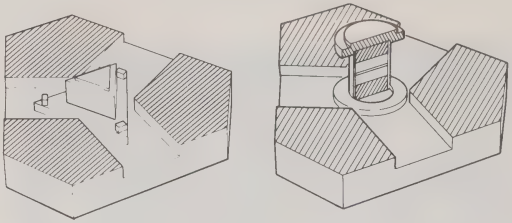

- TRIANGULAR GEOMETRY
- PARTS DIFFICULT TO FABRICATE AND INSPECT
- ASSEMBLY REQUIRES LOCATING FIXTURES, QUALITY CONTROL OF SIX EPOXIED INTERFACES, CURING OVEN
- ASSEMBLED CIRCULATOR REQUIRES POST-ASSEMBLY TUNING - NO TWO CIRCULATORS ALIKE
- DIFFICULT TO QUALIFY UNDER SHOCK AND VIBRATION
- EXPENSIVE, LOW RELIABILITY CIRCULATOR

- CYLINDRICAL GEOMETRY
- PARTS EASY TO FABRICATE AND INSPECT
- SIMPLE ASSEMBLY
- NO POST-ASSEMBLY TUNING, REPRODUCIBLE AND REPEATABLE
- CIRCULATOR SHOCK AND VIBRATION PROOF
- SIGNIFICANTLY LESS EXPENSIVE, HIGH RELIABILITY CIRCULATOR

Figure 6. Comparison of triangular and TRW's cylindrical circulator junction.

In the microwave frequency ranges below 30 GHz, the circulator designer may select the ferrite material from an available range of compositions to satisfy the specification requirements. Above 30 GHz, this freedom of choice vanishes; there is only one material suitable and even this ferrite with the highest saturation magnetization of 5250 gauss becomes marginal as we approach 50 GHz. This limitation of saturation magnetization poses difficult problems to the wideband junction design. Narrowband, or Faraday rotation components can be constructed, but the narrowband circulators are not suitable for use with solid state devices with wideband negative resistance characteristics, and the Faraday rotation circulators are characterized by prohibitively high insertion loss.

The wideband performance of the circulators is obtained by the design of the junction ferrites, which allow a simultaneous propagation of two adjacent dielectric resonator modes. With an adequate level of saturation magnetization for the given frequency range, this design approach insures good balance of the amplitude of the VSWR and isolation ripple. After a proper selection of the ferrite dimensions, the length of the matching dielectric spacer, the length and the diameter of the metallic transformer is calculated to complete the circulator design. The task is relatively simple and easy when the ferrite material has adequate magnetic properties and when a relatively narrow bandwidth is acceptable, or when the circulator is used in a system where the insertion loss is not a crucial consideration. The present design (patent issued in 1979) evolved from a thorough and logical consideration of the whole problem. A detailed evaluation of the electrical, environmental and manufacturing requirements pointed out the way to the cylindrical geometry, which combines the structural simplicity with the best potential for analytical optimization of the electrical parameters. A representative sample of the full line of circulators is shown in Figure 7.

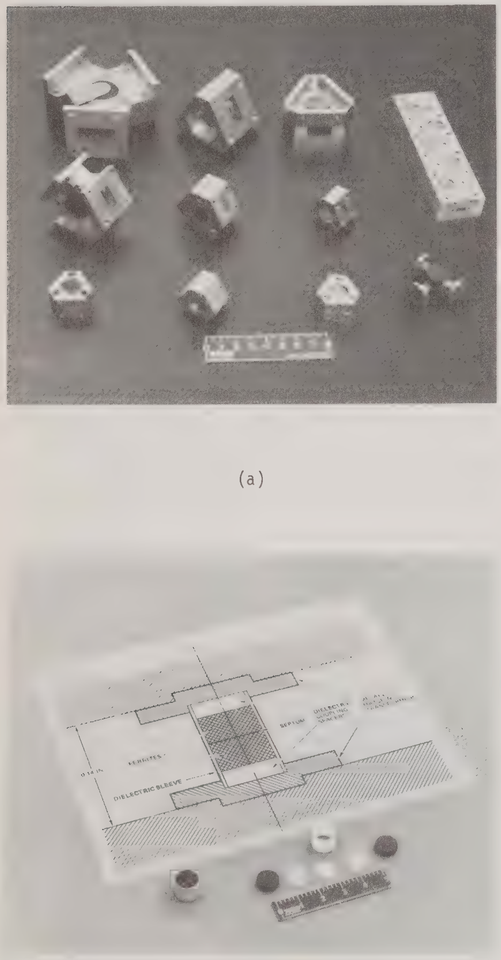

(a)

(b)

Figure 7. All circulators, X-band to 60 GHz, shown in (a) feature the simple cylindrical junction geometry and piece parts shown in (b).

Typical performance data for Ka- and Q-band circulators comprises Figures 8 and 9. Typical insertion loss per junction in the 7 to 40 GHz range is 0.07 dB to 0.1 dB per pass, with bandwidth of 25 to 30 percent, and CW power handling capability of 200 Watts at X-band and 20 Watts at 45 GHz.

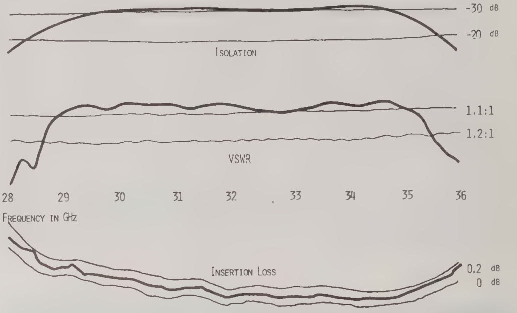

Figure 8. Ka-band Circulator.

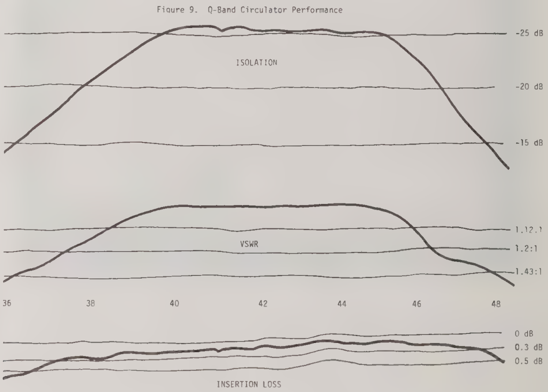

Figure 9. Q-band Circulator Performance

Acknowledgements

The author gratefully acknowledges the key contributions of Franklin Bayuk who is responsible for the power amplifier development, Wieslaw Piotrowski, who is responsible for the ferrite development, and Dale Mooney who has made significant contributions in the area of computer aided EHF amplifier design and development. This work was supported in part by the Air Force Avionics Laboratory, under contracts F 33615-77-C-1184 and F 33615-77-C-1185. R.T. Kemerly is the project engineer.

References

[1] Bayuk, F. J. and J. E. Raue, "Large Signal Device Characterization for Broadband Ka-Band Avalanche Diode Amplifier Design", IEEE-MTT International Microwave Symposium Digest, pp. 210-212, June, 1976.

[2] Bayuk, F. J. and J. E. Raue, "Ka-Band Solid State Power Amplifier", IEEE-MTT International Symposium Digest, June 1977.

[3] J. E. Raue, "High Performance Millimeter Wave Receiver and Transmitter Component Development", EASCON-77, pp. 24-4A-E, September, 1977 (invited paper).

[4] Yuan, L.T., et al, "A V-Band Network Analyzer/ Reflection Test Unit", IEEE-MTT International Microwave Symposium Digest, pp. 221-223, June, 1976.

[5] U.S. Patent No. 4,145,672, March, 1979.

[6] Piotrowski, W.S. and J. E. Raue, "Low Loss High Power Latching Waveguide Switch", International Symposium Digest, pp. 103-104, June 1978.

80-0488

HIGH POWER SATELLITE TRAVELLING WAVE TUBES WITH 200 W AND 450 W OUTPUT POWER

D. Deml
AEG-Telefunken, Engineering and Production Manager
Microwave Devices
Ulm, West-Germany

Abstract

For future TV broadcasting satellites as BS II, German TV-SAT, Nordsat etc., power amplifiers in X-band of a few hundred watts are required. At AEG-TELEFUNKEN helix tubes and coupled cavity tubes were developed for this application. Power levels of 100 W, 200 W and 260 W are covered by broadband helix tubes. Beyond 260 W coupled cavity tubes were developed with 450 W and 800 W output power. All tubes are equipped with multi-stage-self-radiating collectors for weight saving and efficiency improvement. Power weights of less than 15 g/W could be realized for the tubes.

General

Different television-broadcast-satellite- (TVBS) studies in Europe were performed which showed that for this application tubes in the power class of approx. 200 W and approx. 500 W were required. AEG-TELEFUNKEN started the development in 1972 under a feasibility contract of the German Space Agency (DFVLR) where a 800 W breadboard-model tube was built. More detailed studies finally led to power levels of 200/260 W and 450 W. AEG-TELEFUNKEN then started the development aiming for this power level. Engineering-models of the 200 W and the 450 W tube were delivered in 1979. A 260 W contract , awared in 1979, calles for flight-model tubes in late 1981 which will be used in the German TV-SAT. Within this contract a life test program is carried out where seven tubes will be tested under realistic environmental conditions. Besides that fifteen gun testers are included in this program to verify th the predicted cathode performance. The program is such that the results are direct applicable to any power level within the 100 W to 500 W range.

450 W Coupled Cavity Tube TL 12450

Concept

The tube consists of the following three main subassemblies

a) Electron gun with mod-anode and AC-heater

b) Delay line out of three section coupled cavities with direct heat transfer to a baseplate

c) Collector self-radiating with five stages.

Fig. 1 shows the 450 W tube TL 12450. The tube length is 500 mm at a weight of 6,700 g.

Electron Gun. The electron gun uses a modified "Pierce" optic for beam forming. The cathode used is of tungsten matrix type. Extended life tests performed at AEG-TELEFUNKEN show that with this type of cathode more than 100,000 hours can be achieved operating with a cathode loading of 0.75 A/cm^2. In this life test program we have now accumulated 1.3 million hours with tubes and diodes. Six tubes have now operated successfully for 48,000 hours. The longest sample run with diodes is more than 100,000 hours. Twelve samples have now reached 74,000 hours and ten others have passed the 50,000 hour point. Furthermore another life test program with 25 tubes was started. Fourteen tubes are operating between 5,000 and 34,000 hours so far.

Designing the gun for the 450 W led to a cathode loading of 1.1 A/cm^2 because of the beam area compression ratio of 50. We regard this as the upper limit for long life space tubes. Due to this, accelerated life programs were performed with different cathode loadings in order to find the relation between cathode loading and life.

Fig. 2 shows the result. It is seen that with a cathode loading of 1.1 A/cm^2 a cathode life of 90,000 hours is achievable which leaves enough margin for the required 7-year life (62,000 hours).

Copyright © American Institute of Aeronautics and Astronautics, Inc., 1980. All rights reserved.

Delay Line System. The tube uses a coupled cavity circuit as a delay line because of thermal considerations. The delay line is formed by copper resonators and iron pole pieces. The pole pieces are part of the vacuum envelope and extend right down to the electron beam. This integrated technique has two main advantages:

- Best use of the magnetic material $SmCo_5$, which means lowest possible magnet weight and
- Complete compensation of transverse magnetic fields and, therefore, excellent beam transmission.

The delay line itself consists of three sections which are separated by an internal sever. This gives high isolation between input and output beyond 100 dB. The sections are terminated by absorbers which are designed to withstand very high reflected power, for instance 100 W continuously, or total output power for a few seconds.

The system has excellent thermal properties, because each copper resonator is directly screwed to the baseplate which is part of the tube housing. The thermal gradient is such that the maximum temperature drop between baseplate and hottest point of the output resonator is only in the order of 30 °C. For the baseplate to which the tube is mounted the permissible temperature is - 30 °C to + 80 °C which means that the resonator is at 110 °C maximum. This is well below the maximum allowed copper temperature for long life tubes.

Collector. Because of the high overall efficiency required the collector is of 5-stage design. A special feature is that the collector is completely decoupled from the baseplate and radiates its dissipated power directly into space without any additional radiators. The radiator temperature will be at 300 °C to 350 °C. The mechanical design leads to very low collector weight, approx. 2.0 kg at a total tube weight of 6.8 kg because direct heat conduction, rather than radiation is used inside the collector from the electrodes to the outer envelope which is entirely on ground potential. Tests with elevated temperature have been performed which show that no degradation in isolation and heat transfer characteristics will occur within a 10-year life.

RF-Measurements

The tube is designed to operate between 11.7 GHz and 12.5 GHz. In order to cover the band four sets of parameters have to be used. Each set of parameters gives a 1 dB instantaneous bandwidth of 200 MHz.

Fig. 3 shows the saturated output power of the engineering-model for two sets of operating parameters. It can be seen from this figure that the 450 W output power is achieved over the total band.

Fig. 4 shows the measured instantaneous bandwidth of the engineering-model for a typical set of parameters. Optimizing the tube for the required 30 MHz channel leads to less than 10 W output power variation in a channel.

The gain of the tube is beyond 50 dB. Nonlinear phaseshift is typically around 50° and the AM-PM conversion factor measured was below 4.5 °/dB.

The overall efficiency recorded on the engineering-model is to be seen from fig. 5. The tube was optimized for this midband channel and it can be seen that overall efficiency is in excess of 50 %.

200/260 W Helix Tubes TL 12200/TL 12260[x]

Concept

As described in the section before the tube consists of three main subassemblies as well

a) Electron gun with mod-anode and AC-heater

b) Delay line out of two section tape helix. The output helix has a taper against backward wave oscillation. The envelope has an integral pole piece design which assures excellent focusing by optimum thermal properties

c) Collector self-radiating with three resp. five stages.

Fig. 6 shows the engineering-model 200 W tube TL 12200. The overall length is 400 mm. The weight with three stages is 2.6 kg and with five stages 3.3 kg. The difference is due to the collector which results in an efficiency improvement of approx. 4 % to 5 %.

---

[x] For the 200/260 W tubes an EPC is under development at AEG-TELEFUNKEN Backnang.

Electron Gun. The electron gun is of modified "Pierce" type. A tungsten matrix cathode with a 0.7 A/cm^2 current loading is used which operates near 1020 °C. This will result in an expected life of more than 100,000 hours (fig. 2). The mechanical design uses the so-called sandwich-technique where ceramic rings and electrodes stacked on top of each other form the vacuum envelope. The gun design allows final mechanical allignment during focusing for achieving excellent beam transmission. The beam area conversion is less than 50 what assures optimum entrance conditions.

Delay Line System. The delay line used for this tube is a two section tape helix. Both sections are tapered against backward wave oscillations. The output section has an efficiency taper on top. By means of special heat removal design 2.7°K/Wcm are achieved which keeps the helix within safe operating temperature limits. Under worst case conditions the helix of the 260 W tube stays below 200 °C. which is a safe limit for long life tubes. The tube is severed and internally terminated by carbon layers on the BeO-helix supporting rods. The vacuum envelope is formed by pole pieces and spacers out of copper. The inner diameter is honed after bracing what results in

- excellent thermal contact between supporting rods and pole pieces
- exact allignment between magnetic and beam axis what results in excellent and unproblematic focusing.

The pole pieces have two copper extensions which are in direct contact with the baseplate. This technique has a power handling capability for satellite application of up to 280 W rf-power. The power fading after "snap on" is less than 0.05 dB what demonstrates the excellent heat transfer properties. The magnetic material used is $SmCo_5$.

Collector. The collector is of the same basic design as for the 450 W tube. The 200 W tube is equipped with a three stage self-radiating collector while the 260 W tube has to use a five stage design because of efficiency requirements. The interface between three stage and five stage collector with the delay line is identical so that either tube can be equiped with either one of the different collectors. The weight difference of the two collectors is approx. 500 g which is the penalty for gaining 4 % to 5 % overall efficiency. The operating temperature of the collector is between 300 °C and 350 °C depending on drive conditions.

RF-Measurements

The tube is designed for an instantaneous bandwidth of 800 MHz (11.7 to 12.5 GHz).

In fig. 7 the output power for both tubes 200 and 260 W is shown versus frequency for constant conditions. It can be seen that the tubes have an excellent broadband performance. There is less than 0.5 dB power variation across the whole band.

Fig. 8 shows a typical transfer curve. The 200 W tube saturates with an input power of approx. 20 mW which corresponds to 40 dB gain minimum. The 260 W tube has a saturated gain of 42 dB minimum what means that less than 10 mW input power is required to saturate the tube.

The nonlinear phaseshift of the tube is approx. 45°. This is a typical figure across the whole 800 MHz band. Measured intermods give values which are typical for helix tubes (11 dB at saturation and 36 dB at 13 dB below 2 carrier saturation). The measured noise figure is below 35 dB. The second harmonic was measured 30 dB below the fundamental. This is due to the waveguide output which suppresses the coupling efficiency at these frequencies. The AM-PM conversion factor measured was 4 °/dB.

The overall efficiencies measured so far depend on the number of collector stages used. With two stages 40 % to 41 % was achieved under nominal conditions. Using a three stage design 43 % to 44 % could be measured. With the final five stage collector design 46 % to 47 % was achieved so far. These results show that even the three stage collector was not fully optimized. A five stage collector has to be used to guarantee 45 % efficiency minimum under worst case conditions with some design margin.

Fig. 9 shows the overall efficiency versus collector stages for the 200/260 W tubes. It can be seen that a relative good agreement between calculated resp. scaled data with actually measured data is achieved.

Conclusion

Four high power X-band tubes for TV-SAT application were developed at AEG-TELEFUNKEN. The status of these tubes is as follows

- 800 W tube TL 12800: breadboard status
- 450 W tube TL 12450: engineering-models delivered
- 200 W tube TL 12200: engineering-models delivered
- 260 W tube TL 12260: qualification and flight-models production contract awarded with flight model delivery in late 1981.

During the development a power limit for a helix tube in this frequency range could be established which is 280 W. Above this power level coupled cavity tubes have to be considered.

The test results available so far demonstrate that the tubes will meet their main specified parameters for use as power amplifiers in broadcasting satellites:

- Cathode design life of more than seven years
- Specific weight of less than 15 g/W
- Efficiency of 45 % for broadband helix tubes
- Efficiency of 50 % for coupled cavity tubes.

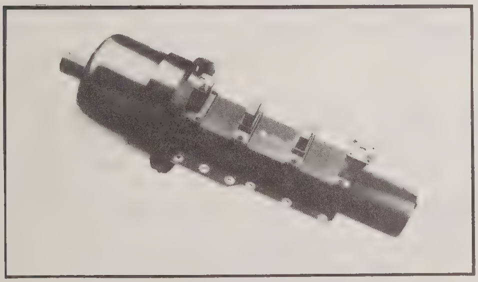

Fig. 1: 450 W Satellite TWT TL 12450

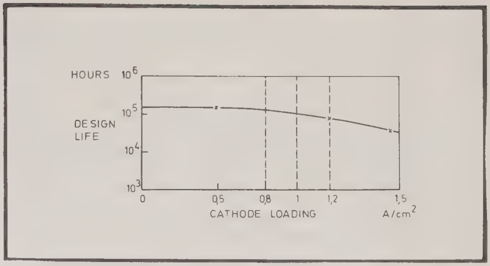

Fig. 2: Design life capability versus cathode loading

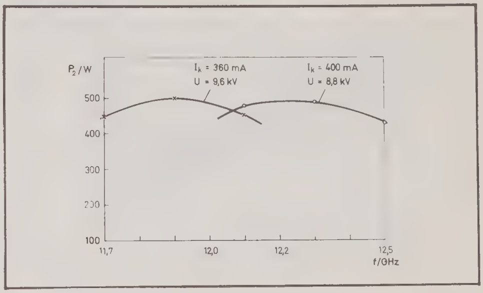

Fig. 3: Saturated output power versus frequency for the 450 W TWT TL 12450

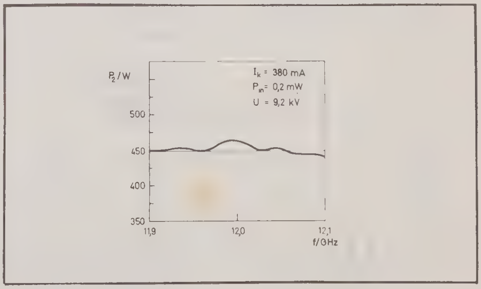

Fig. 4: Instantaneous bandwidth of satellite TWT TL 12450

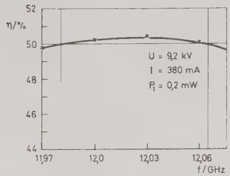

Fig. 5: Overall efficiency measured in a channel bandwidth of 80 MHz for the TWT TL 12450

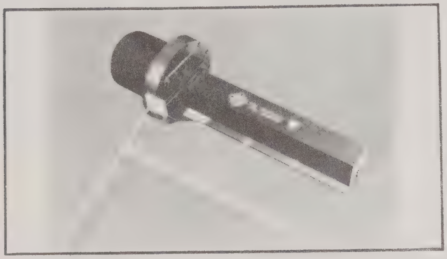

Fig. 6: 200 W Satellite TWT TL 12200

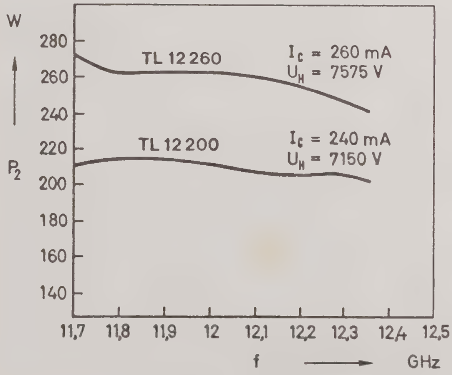

Fig. 7: Output Power P_2 versus frequency for the 200 W TWT TL 12200 and the 260 W TWT TL 12260

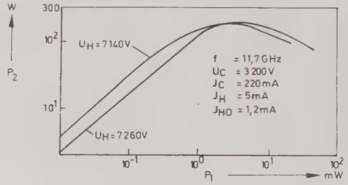

Fig. 8: Output power P_2 versus input power P_1 for the satellite TWT TL 12200

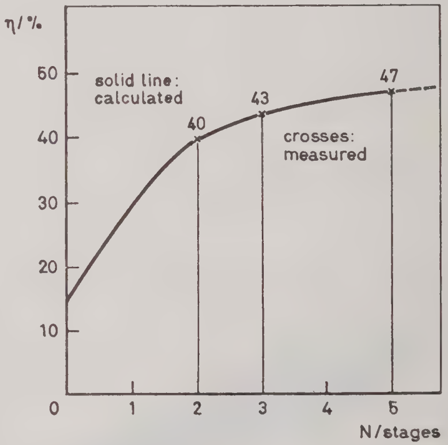

Fig. 9: Overall efficiency η versus collector stages N for the 200 W/260 W TWT

80-0489

DEMAND ASSIGNED TDMA SYSTEM FOR DIGITALLY INTEGRATED SERVICES NETWORK

Kenji Kohiyama, Yoshio Watanabe, Shuichi Samejima
and Shuzo Kato

Yokosuka Electrical Communication Laboratory, NTT
Yokosuka, Japan

Abstract

The demand assigned TDMA (DA-TDMA) system has remarkable advantages with regard to effective utilization of satellite traffic channels and network flexibility. The DA-TDMA system is one of key technological developments for application to integrated services satellite digital networks (ISSDN) which transmit digitally integrated information signals between earth stations. The exprimental DA-TDMA system designed for an ISSDN experiment has a 20 Mbps bit rate and operates in a fully variable demand assignment mode. The ISSDN experiment using the Japanese 30/20 GHz band "CS" satellite, which is planned as the first stage of ISSDN study in Japan, is scheduled to start in 1980. This paper describes the outline of the DA-TDMA system and the ISSDN experimental plan.

Introduction

The Nippon Telegraph and Telephone Public Corporation (NTT) has been actively engaged in the development of TDMA systems for domestic satellite communications. SMAX system,(1) an experimental demand assignment TDMA system with a capcity of 244 telephone channels, was developed and operated successfully in 1968 using the ATS-1 satellite.

In 1973 NTT started developing a medium capacity domestic satellite communications system which mainly uses 30/20 GHz bands. To date two types of preassigned TDMA systems, a 64 Mbps system for 30/20 GHz bands and a 107 Mbps system for 6/4 GHz bands, have been developed.(2) These systems have been successfully demonstrated by using the "CS"(3) satellite.

Moreover, NTT has also been doing research on a demand assigned TDMA system. The DA-TDMA system is used for an integrated services satellite digital network (ISSDN) experiment using the "CS" satellite. The DA-TDMA system operates in a fully variable demand assignment mode for various services information signals such as voice, data, facsimile and video signals, with bit rates ranging from 6.4 kbps - 6.3 Mbps.

This paper briefly describes the DA-TDMA system and presents an experimental plan using the "CS" satellite. This experiment is planned as the first stage of ISSDN study in Japan. The objective of this experiment is to confirm that various service networks can be possible with satellite communication in which various information signals are digitalized and integrated for communication between earth stations.

Integrated Services Digital Network via Satellite Communication

In recent years remarkable advances in satellite communications have expanded the service areas of regional and domestic satellite communications systems as well as international system.

As main satellite communications techniques which have promoted this extension of service areas, the following technological developments can be considered:

Digital satellite communications techniques such as TDMA

The development of communications satellites with higer EIRP and G/T,

Techniques for new frequency exploitation in frequency bands over 10 GHz.

By using TDMA systems and small earth stations, high quality and high speed digital communications networks have become possible. Furthermore, developments in frequency bands over 10 GHz make it possible to locate these small earth stations near terrestrial traffic centers. Therefore, high quality and wide band signal transmission networks between subscribers can be possible via satellite communication.

Recently, there has been a trend toward integrating services networks with digital transmission lines and time division switching systems in the terrestrial networks. One disadvantage of satellite networks in comparison with these terrestrial integrated services digital networks (ISDN) is propagation delay. On the other hand, satellite networks have the following advantages:

Quick construction of networks,

Wide band signal transmission between subscribers,

Multi-address broadcast mode communication,

Mesh-type switching networks.

In the aforementioned situations, satellite communications networks which offer integrated services by digital communications systems are called integrated services satellite digital networks (ISSDN) in this paper. This viewpoint is very important in satellite communications system research for the purpose of expanding satellite services in the future.

Outline of the DA-TDMA System

This experiment uses small earth stations installed on the roofs of buildings and operated in the 30/20 GHz bands. This arrangement provides direct access of wide band information signals from customer terminals to small earth stations without long transmission lines on the ground. Major characteristics of the small earth stations are shown in Table 1.

The major features of the DA-TDMA systems are:

Fully variable demand assignment,

A central network control system,

Copyright © American Institute of Aeronautics and Astronautics, Inc., 1980. All rights reserved.

Rate-1/2 convolutional encoding and Viterbi decoding with soft decision and CPSK coherent detection,

Open loop initial acquisition,

Synchronous interface between customer terminals and DA-TDMA equipment.

Table 2 shows the major featuers of the DA-TDMA system.

Frame and burst structure

Figure 1 shows the frame and burst structure of the DA-TDMA system. Primary frames whose time interval is 2 msec have one sync burst and 39 data bursts. The time positions of these bursts are fixed in the primary frame. The first super frame is composed of 40 primary frames. Sync bursts in the first super frame, which is arranged at top of each primary frame, are respectively transmitted from different small earth stations. The reference station which is assigned to the network control station (NCS) transmits five sync bursts in the first super frame once every eight frames. Therefore, maximum number of earth stations that can participate in this system are 35 small earth stations and one network control station.

The second super frame which consists of two first super frames becomes time interval of traffic channel assignment. When alloting the number of data bursts in identical time slots of the primary frame within the second super frame to an information signal, it is possible to assign a traffic channel to the information signal on a single channel per burst basis according to the bit rate of the signal.

Table 1 Major Characteristics of an Experimental Small Earth Station

Antenna	Type	Offset Cassegrain
	Frequency Band	
	Transmit	27.45 - 28.75 GHz
	Receive	17.45 - 18.95 GHz
	Size	4.7 x 2.9 m^2
	Gain Transmit	57.2 dB
	Receive	53.7 dB
	Tracking Mode	Fixed
HPA	Type	Klystron
	Output Power	1 kW (Peak,30% Duty Factor) 500W (Average)
	Bandwidth	80 MHz
LNA	Type	Parametric Amplifier
	Colling Mode	Uncooled
	Noise Temperature	270 K
	Bandwidth	1.5 GHz

In this manner, the DA-TDMA system operates in a fully variable demand assignment mode on a per-call basis. Each call from customer terminals is assigned to a traffic channel from the "pool" of the satellite capacity by the allotment of data bursts in the second super frame according to their bit rates. This assignment is maintained for the duration of communication between customer terminals and is released to the "pool" when the call is completed. Table 3 shows the bit rates of information signals which can be assigned in the second super frame.

Table 2 Major Features of the Experimental DA-TDMA System

System	Satellite	Japanese "CS"
	Frequency Band	30/20 GHz
	Bit Rate	19.968 Mbps
	Clock Rate	43.776 MHz
	Number of Stations	Network Control Station : 1 Small Earth Station : 35
	Network Control	Central Control System
CTTE&MODEM Subsystem	Modulation	2-phase CPSK, Coherent Detection
	Burst Synchronization	Storage Counter Method
	Initial Acquisition	Open Loop Prediction Method
	Foward Error Correction	Rate-1/2 Convolutional Encoding, Viterbi Decoding with 3-bit Soft Quantization
DAMA Subsystem	Traffic Channel Assignment	Fully Variable Demand Assignment (Preassignment available)
	Signaling	Common Signaling Channel Control

Table 3 Information Signal Bit Rates

Bit Rate	The Number of Data Bursts in the Second Super Frame
6.4 kbps	1
12.8	2
32	5
64	10
128	20
256	40
512	80
1536	240
6312	1040

The third super frame is composed of four first frames and has a time interval of 320 msec which covers the round trip delay time. It is used for the control time interval of burst time position correction.

Sync burst : The reference sync burst and non-reference sync bursts are transmitted from the network control station and small earth stations, respectively. These sync bursts include a unique word (UW) of 40 symbols. The reference UW represents the fixed position in TDMA systems. Each small earth station establishes transmitter timing by detecting reference UW and its own non-reference UW.

Preamble and postamble word : Preamble and postamble words are arranged at the beginning and end of each burst, respectively. Preamble word includes carrier recovery symbols, bit timing recovery symbols and UW. There are 40 all zero symbols used for carrier recovery. They are also utilized for removing carrier phase ambiguity in order to realize coherent detection of CPSK without differential encoding. Postamble word which comprises 16 symbols is used to complete FEC decoding within one burst.

Data burst : Each data burst has 1024 information bits and pre- and postamble words. Information bits are doubled by rate-1/2 FEC coding.

Common signaling channel (CSC) : CSC which is included in each sync burst is used as a signaling channel for connection and release of traffic channels. It is transmitted between NCS and each small earth station. The bit rate of this channel is 6 kbps from NCS to small earth stations and 1.2 kbps in the opposite direction.

Efficiency : The frame utilization efficiency of this frame structure is 91%, as there are 87,552 total symbols and 79,872 data symbols in the primary frame.

Description of the DA-TDMA System

The proposed DA-TDMA system operates in a fully variable demand assignment mode. This system provides a satellite traffic channel of full-duplex and multi-address broadcast circuits when requested by customer terminals. The provided traffic channel is created on time slots within a common TDMA frame under the control of the demand assigned signaling system. Information signals from customer terminals are directly connected to the DA-TDMA equipment in a small earth station. The NCS controls traffic channel assignments and signaling procedures when assignment requests from small earth stations are transmitted through a common signaling channel. If a traffic time slot is not available when assignment request is detected, the NCS does not assign a traffic channel; consequently the call is not completed.

This system partially operates in a preassignment mode to meet the requirement for fixed point-to-point or point-to-multipoint communications. In this case traffic channels are assigned to fixed traffic time slots by command inputs at the NCS, and are maintained until release commands are keyed in the NCS.

Figures 2 and 3 shows block diagrams of DA-TDMA equipment. The equipment is subdivided into CTTE & MODEM and DAMA subsystems, each having its respective functions.

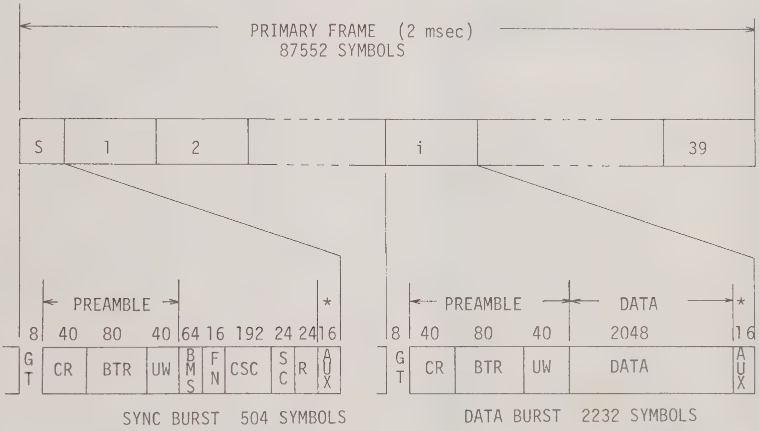

GT: Guard Time
CR: Carrier Recovery Symbols
BTR: Bit Timing Recovery Symbols
UW: Unique Word
BMS: BER Measurement Symbols
FN: Frame Number
CSC: Common Signaling Channel
SC: Supervisory & Control
R: Reserved Symbols
AUX: Auxiary Symbols for FEC Decoding
DATA: Data Symbols
*: Postamble

Figure 1 Frame and Burst Structure

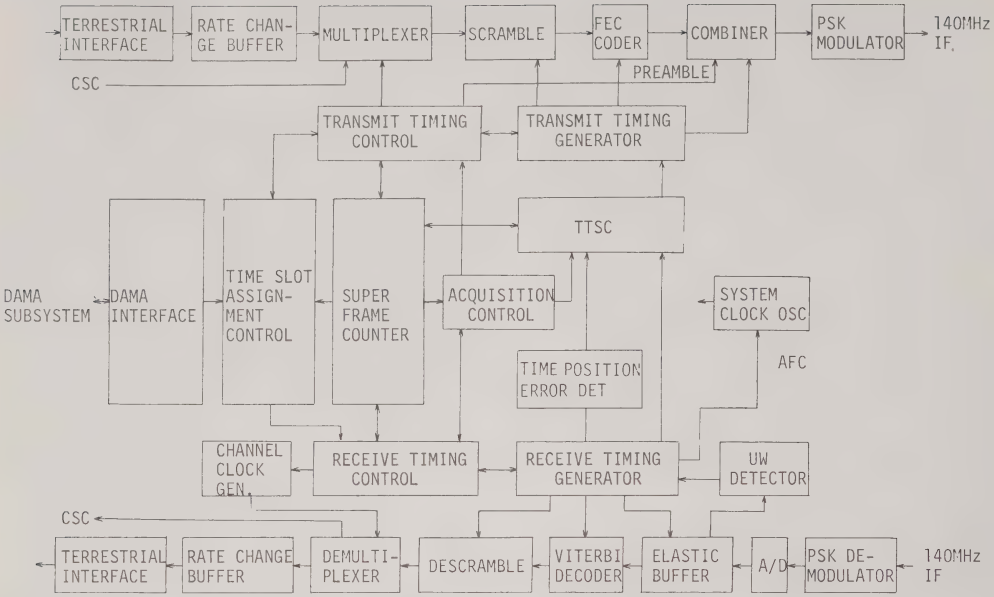
TERRESTRIAL INTERFACE
RATE CHANGE BUFFER
MULTIPLEXER
SCRAMBLE
FEC CODER
COMBINER
PSK MODULATOR
140MHz IF.
CSC
PREAMBLE
TRANSMIT TIMING CONTROL
TRANSMIT TIMING GENERATOR
TTSC
DAMA SUBSYSTEM
DAMA INTERFACE
TIME SLOT ASSIGNMENT CONTROL
SUPER FRAME COUNTER
ACQUISITION CONTROL
SYSTEM CLOCK OSC
AFC
TIME POSITION ERROR DET
CHANNEL CLOCK GEN.
RECEIVE TIMING CONTROL
RECEIVE TIMING GENERATOR
UW DETECTOR
CSC
TERRESTRIAL INTERFACE
RATE CHANGE BUFFER
DEMULTIPLEXER
DESCRAMBLE
VITERBI DECODER
ELASTIC BUFFER
A/D
PSK DEMODULATOR
140MHz IF

Figure 2 Blockdiagram of CTTE & MODEM Subsystem

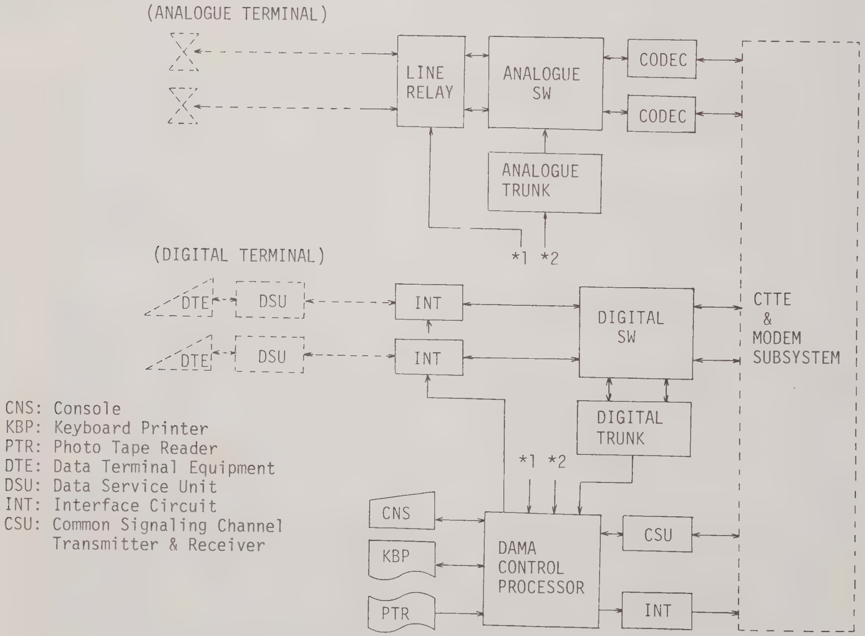
(ANALOGUE TERMINAL)
LINE RELAY
ANALOGUE SW
CODEC
CODEC
ANALOGUE TRUNK
*1 *2
(DIGITAL TERMINAL)
DTE
DSU
INT
DTE
DSU
INT
DIGITAL SW
DIGITAL TRUNK
CTTE & MODEM SUBSYSTEM
*1 *2
CNS
KBP
PTR
DAMA CONTROL PROCESSOR
CSU
INT
CNS: Console
KBP: Keyboard Printer
PTR: Photo Tape Reader
DTE: Data Terminal Equipment
DSU: Data Service Unit
INT: Interface Circuit
CSU: Common Signaling Channel Transmitter & Receiver

Figure 3 Blockdiagram of DAMA Subsystem

CTTE & MODEM subsystem:

- PSK modulation and demodulation
- Data compression and expansion
- Multiplexing
- FEC coding and decoding
- Synchronization
- Preamble word generation and detection
- Initial acquisition
- Data scrambling

DAMA subsystem:

- Interface with customer terminals
- Analogue / digital voice band signal conversion
- Signaling to/from customer terminals
- DAMA assignment control
- Initial acquisition control.

Digital voice, data and video signals of a demand assignment mode are connected to and processed at a digital trunk interface unit which includes a baseband signal transmission terminating circuit. Analogue voice band signals, such as telephone and voice band data signals, are processed at an analogue trunk interface and converted to digital signals by PCM codecs.

These signals are converted to data bursts by time compression at rate change buffers, and are then connected to a multiplexer. Time slot assignments of data bursts are established by the DAMA control processor at a small earth station. This assignment control is managed by the DAMA subsystem of the NCS through the common signaling channel via the satellite link.

The multiplexed data bursts are scrambled to disperse transmitting carrier burst energy density and ensure a stable bit timing recovery at the demodulator. They are also convolutionally encoded to provide forward error correction by means of Viterbi decoding at the receiving side.

CPSK-coherent detection is adopted for modulation and demodulation. Soft decision of the demodulator output is provided by a 3-bit A/D converter. The reference carrier is recovered by reverse modulation of the received PSK signal and by a single-tuned filter & limiter circuit with an AFC loop. Recovered carrier phase ambiguity is removed at the carrier recovery circuit by detecting the carrier phase of carrier recovery symbols arranged at the top of each burst. By adopting CPSK with soft decision and Viterbi decoding, 4.6 dB of coding gain at a decoded bit error rate of 1×10^{-4} is obtained where the parameters of the Viterbi decoder are K=7 and rate-1/2.

Frame and burst synchronization are maintained to effect receiving and transmitting frame and burst alignment, respectively. Frame and receive data burst synchronization are achieved by detecting the reference UW of the reference sync burst and data UWs of data bursts. Transmit burst synchronization is realized using the transmit timing storage counter method. In this method, a variable delay which covers range variations due to the movement of the satellite is controlled to correct the burst transmitting timing by comparing local sync UW receiving time position with a prediction time position.

An open loop prediction acquisition method is adopted for the initial acquisition. The range of the satellite is predicted by the DAMA subsystem at each small earth station using range data measured at the NCS. These range data are transmitted through the common signaling channel from the NCS. The NCS monitors the communication states at all small earth stations by detecting the UWs of each sync burst. When a loss of UWs is detected, the DAMA subsystem of the NCS assigns one data burst as an initial acquisition time window. The small earth station performs initial acquisition at this assigned time slot using the predicted timing.

A highly stable clock oscillator whose frequency is automatically controlled to eliminate frequency differences between the reference and non-reference stations performs the function of system clock timing. Clock timing of the receiving side is recovered from the bit timing recovery symbols of each burst. The recovered clock timing is used to regenerate the symbols of the demodulator output. Because clock timing recovered from individual bursts are non-coherent with one another, retiming of regenerated symbols is accomplished by the system clock timing using an elastic buffer. Variation of burst transmit and receive timing caused by the movement of the satellite are compensated for by providing another kind of elastic buffer which covers the round trip time variation. Rate change buffers which perform time compression and expansion also perform the function of this elastic buffer.

Clock timing of terrestrial interface is frequency-locked to channel clock timing which is generated from the system clock timing.

Figure 4 shows the DA-TDMA equipment.

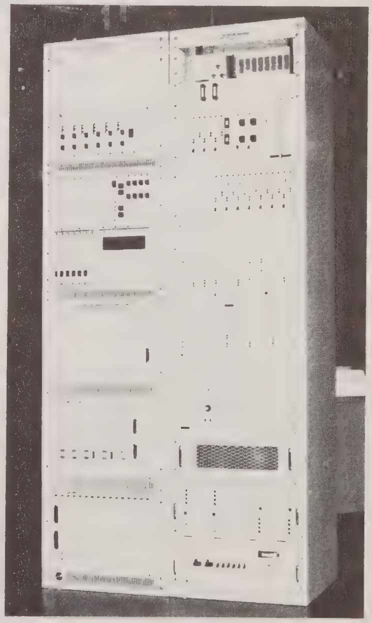

Figure 4 Experimental DA-TDMA Equipment

Experimental Plan

Figure 5 shows configuration of the experimental network. It has one NCS and two small earth stations with 30/20 GHz band. Communications between customer terminals, such as telephones, data terminals, high speed facsimiles and packet switching systems, are performed through the two small earth stations. The NCS, which is a large earth station with a 11.5-meter antenna, operates as a reference station in a TDMA synchronization system and also as the central station of a network control system.

This small earth station has an offset Cassegrain antenna with an equivalent aperture of 3.3 meter. This size was chosen by making trade-offs between off-beam power loss due to the movement of the satellite, high-power amplifier (HPA) output power and the transportability of the station on the condition that simple tracking is employed. Maximum up-link and down-link losses without tracking that are caused by nominal satellite station keeping of the "CS" satellite (±0.1° NS and EW) are estimated to be 2.2 dB and 1.0 dB, respectively. A larger antenna aperture would have more off-beam losses and adversely affect transportability. On the other hand, a smaller antenna aperture would require more output power of the 30 GHz band HPA which is more limited at the present time than the conventional 6 GHz band HPAs.

Table 4 Satellite Link Parameters

Up Link		Down Link	
Earth Station EIRP	86.7 dBW	Satellite EIRP	40.7 dBW
Antenna Offbeam Loss	2.2 dB	Propagation Loss	209.2 dB
Propagation Loss	213.2 dB	Earth Station G/T	28.5 dB/K
Satellite G/T	-3.2 dB/K	Antenna Offbeam Loss	1.0 dB
Up Link C/N	96.7 dBHz	Down Link C/N	87.6 dBHz

Table 4 shows the experimental satellite link parameters. Each 30/20 GHz band transponder of the "CS" satellite has a 200 MHz bandwidth and is automatically gain controlled against 16 dB input signal power fading due to up-link rainfall attenuation.

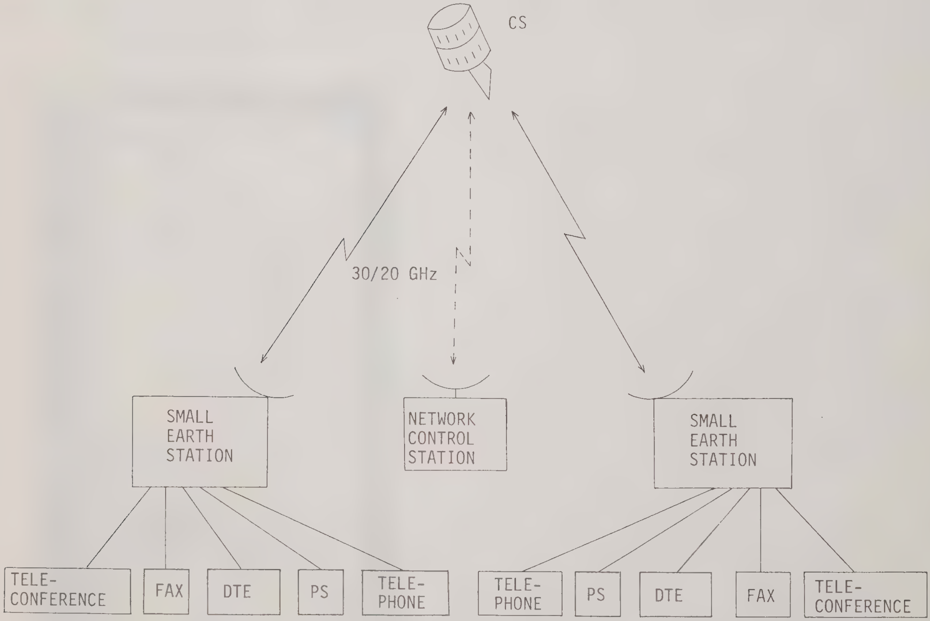

DTE : Data Terminal Equipment
PS : Packet Swithing System
FAX : Facsimile Equipment

Figure 5 Configuration of the Experimental Satellite Network

Figures 6 and 7 show up link and down link C/N margins vs. HPA output power or low-noise amplifier (LNA) noise temperature. Large HPA output power is required in order to realize sufficient earth station EIRP. In the case of 1 kW peak power HPA and 270 K noise temperature LNA, an up-link margin of 17 dB and a down-link margin of 7.5 dB are estimated at a signal quality of 10^{-4} bit error rate for a 20 Mbps bit rate. From these values and rainfall attenuation statistics in Japan, the link availability is estimated to be 99.5 % in the Tokyo region. This estimated value is sufficient for experiments, however, it may have to be improved for future commercial use.

The configuration and external appearance of the small earth station are shown in Figure 8. The transmitter and receiver are installed on an antenna mount. Therefore, rotary joints or a beam guided feed system for connection between the antenna and RF equipments is not necessary. The DA-TDMA equipment can be installed in a 2 x 4-meter shelter. This shelter and small earth station are easily transferred and installed on the roofs of buildings.

Because this system will operate in the 30/20 GHz bands, it will be feasible to locate these earth stations in cities. Interfaces to customer, terrestrial terminals will be simplified because of the small earth station affords easy installment.

The following communications services are being prepared in conjunction with this ISSDN experiment.

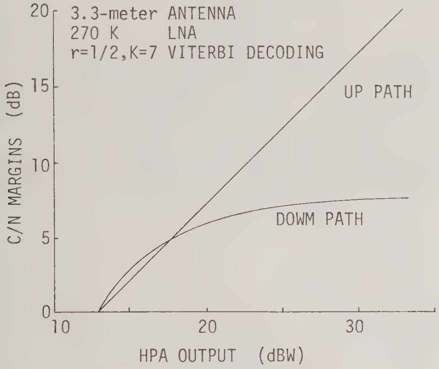

Figure 6 Up Link C/N Margins vs HPA Output Power

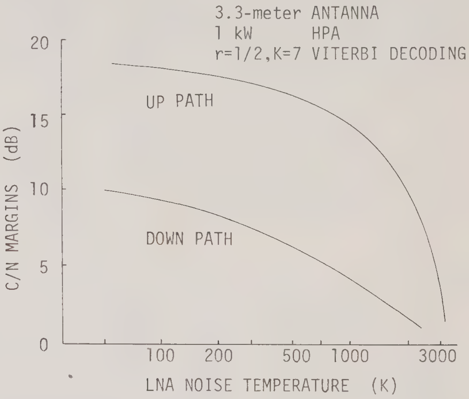

Figure 7 Down Link C/N Margins vs LNA Noise Temperature

Table 5 Major Experimental Communication Services

Communication Services	Terminal Equipment	Bit Rate	Mode	Remarks
Low Speed Data Communication	Data Terminals and Computers	6.4 kbps 12.8	DA	
Voice	Telephone	64	DA	PCM 8KHz Sampling 8bit Quantization
Facsimile-Computer	Analogue Facsimile	64	PA	1 minute/A4 Voice Band
Transport System	Computers	64	DA	HDLC
Packet Switching System	Packet Switching System	64	PA	HDLC
High Speed File Access	Computer	256	DA	HDLC
High Speed Facsimile	High Speed Facsimile	1536	DA	3 sec/A4
Video Conference				
(1)Moving Picture (A)	6.3 Mbps Codec	6312	PA	
(2)Moving Picture (B)	Inter Frame Codec	1536	PA	
(3)Still Picture	Still Picture Codec	1536	DA	
(4)Voice	Voice Codec	256		10 KHz Bandwidth

- Low speed data communication
- High speed data communication
- High speed file access
- Transport system experiment
- Facsmile-computer processing
- High speed facsimile
- Voice communication
- Video conference
- Packet switching signal transmission

Table 5 summarizes the major features of these communications services. These services include both demand assigned and preassigned modes. Supporting signaling procedures for both modes are shown in Table 5, for example, a digital DA signaling procedure is shown in Figure 9. In this digital DA signaling procedure, call set up time between small earth stations is estimated to be 1.5 sec.

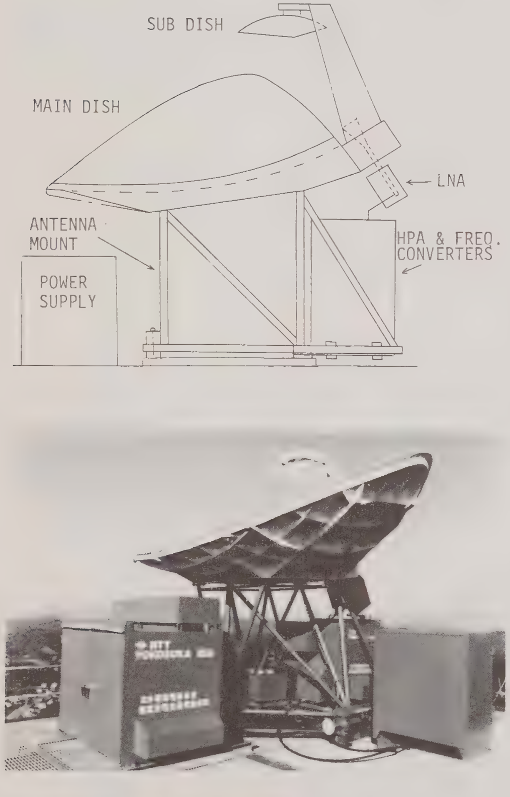
SUB DISH
MAIN DISH
LNA
ANTENNA MOUNT
POWER SUPPLY
HPA & FREQ. CONVERTERS

Figure 8 Configuration and External Appearance of the Small Earth Station

Conclusion

This paper describes the demand assigned TDMA system which is designed for an integrated services satellite digital network (ISSDN) experiment. This DA-TDMA system operates in a fully variable demand assigned mode for some kinds of services information signals with various bit rates.

The ISSDN experiment uses a 30/20 GHz band satellite network which consists of one network control station and two small earth stations. The experiment will start using the Japanese "CS" satellite from the begining of 1980.

Acknowledgements

The authors would like to acknowledge the continuing guidance and encouragement of Dr. Kazuhiro MIYAUCHI and Dr. Hiroaki FUKETA of Yokosuka Electrical Communication Laboratory, NTT.

References

(1) Y.Suguri, H.Doi and E.Metzger, "A TDMA/PCM experiment on applications technology satellite", IEEE Trans. Commun. Technol., vol.COM-19,Aug.1972
(2) K.Miyauchi, H.Fuketa and Y.Watanabe, "Digital Techniques for Domestic Satellite Communication Systems of NTT", 7th AIAA/CSSC, 1978
(3) H.Kaneda, K.Tsukamoto, H.Fuketa, "Experiments in the Japanese CS program", 7th AIAA/CSSC, 1978

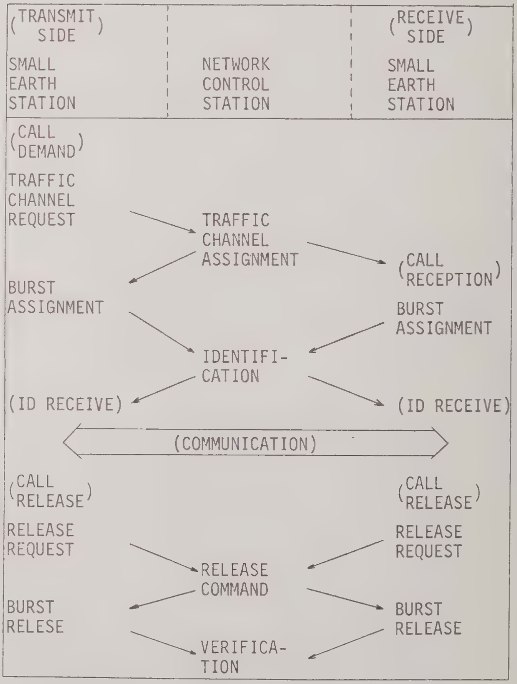
(TRANSMIT SIDE)
SMALL EARTH STATION
NETWORK CONTROL STATION
(RECEIVE SIDE)
SMALL EARTH STATION
(CALL DEMAND)
TRAFFIC CHANNEL REQUEST
TRAFFIC CHANNEL ASSIGNMENT
(CALL RECEPTION)
BURST ASSIGNMENT
BURST ASSIGNMENT
IDENTIFI-CATION
(ID RECEIVE)
(ID RECEIVE)
(COMMUNICATION)
(CALL RELEASE)
(CALL RELEASE)
RELEASE REQUEST
RELEASE REQUEST
RELEASE COMMAND
BURST RELESE
BURST RELEASE
VERIFICA-TION

Figure 9 Digital DA Signaling Procedure

80-0491

DIGITAL EARTH STATIONS FOR SATELLITE NETWORKS

J.H. Tilley, D.M. Fraley, J.J. Hangen, P.J. Freedenberg, and S.B. Salamoff
Digital Communications Corporation
Gaithersburg, Md. 20760

Abstract

Satellite communications systems have evolved from 30-meter heavy route stations to the well-publicized 4.5-meter TV receive-only stations in use by the cable TV industry. This paper discusses some of the major network design considerations and architectural solutions available using digital techniques. The significant economic issues are outlined, as are network protection and reliability. Various network applications and services are also discussed.

Introduction

Satellite communications networks to date have been utilized for SCPC voice communication, video distribution (i.e., point-to-multipoint) and for long haul trunking. Evolution of the technology has led in a relatively short time from 30-meter heavy route stations to the well-publicized 4.5-meter TV receive-only stations used by the cable TV industry. The use of small, inexpensive facilities for the distribution of TV to large numbers of users has grown enormously, but these facilities have not so far been extensively used for two-way data communications.[1] With the trend toward an all-digital communications system environment, more effective use of satellite communications resources is possible.

Types of Networks Considered

There is a growing market for communications systems which effectively connect such devices as teletype terminals, CRT terminals, facsimile machines and codecs such as are used for digitized voice or video. Of interest here are classes of networks interconnecting dispersed users of data terminals, generally operating at 9600 b/s or lower, but with some terminals operating at data rates as high as 56 kb/s. Rural communications applications for a few voice channels per terminal may sometimes fall in this class.

In present two-way satellite networks, voice or data channels are generally dedicated in fixed numbers between specific end points. This has been generally true both in heavy route FDM-FM systems and in SCPC systems. Except for SPADE, which is discussed below, Demand Assigned Multiple Access (DAMA) systems have found few practical applications. Traditionally, DAMA systems have been quite expensive, so that voice-actuated-carrier SCPC techniques are more economical. For small capacity users, even this combination is still comparatively expensive, and the need for versatile data communications between many ports further increases costs because of the proliferation of channel equipment.

Data Networks

Data networks serve to interconnect terminals to computers for such applications as remote job entry, time-sharing computation, and information exchange. A modern analog voice telephone channel, when properly conditioned, can provide data transmission service up to 9.6 kb/s. An entirely digital satellite network can achieve much greater data rates per station, can provide more operational flexibility, and can often perform more economically than a network configured from analog voice channels. Such satellite networks are typically configured in either a star or mesh configuration. The choice of configuration is driven by the dominant traffic flows in the network.

Star Network

The star configuration (see Figure 1) is the best network implementation when many small, low density users need to communicate with one or two larger central stations via satellite. Each remote user has a small amount of equipment for several channels of data and/or voice. The central station is larger and performs switching and temporary storage of traffic, if needed.

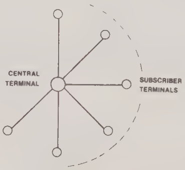

Figure 1. Star Network

The MARISAT ship-to-shore communications network is one example of a star network. Telesat's thin route voice system in Canada, which connects small northern villages to larger cities, is another.

SCPC/FDMA provides lowest cost solutions in this configuration, but TDMA is a very close second. Flexibility considerations

Copyright © American Institute of Aeronautics and Astronautics, Inc., 1980. All rights reserved.

tend to favor the TDMA approach. Since many commercial applications are operationally star networks, these tradeoffs are a potentially important consideration in network design.

Mesh Network

In a star network, all traffic which travels from one remote station to another must pass through the central station. This entails a double-hop utilization of the space segment and a 0.5 second delay. The former affects the economics of the system, while the latter makes the network unacceptable for speech to many users.

For these reasons and others, most medium and high capacity networks are best served by a MESH network when each station must communicate with many other stations in the network, particularly when communication is constrained to a single pass through the satellite. (See Figure 2.) TDMA affords a straightforward implementation of a mesh network, with extremely flexible reconfiguration capabilities.

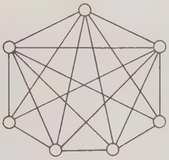

Figure 2. Mesh Network

Compared to the star configurations, mesh networks offer the potential advantage of alternate routing. By reducing the likelihood of a single failure affecting the viability of the entire network, the mesh configuration offers an inherently more reliable topology.

Evolution of Satellite Data Communication Equipment

SPADE (Single Channel Per Carrier PCM Multiple Access Demand Assigned Equipment)

To provide efficient utilization of its space segment, INTELSAT launched SPADE in 1970.[2] SPADE is a demand assigned multiple access system using a pool of Single Channel Per Carrier (SCPC) satellite channels on a demand basis. Since SPADE is a DAMA system with distributed control, it provides a politically palatable system to the INTELSAT members since the traffic is not controlled by any one country, even though they share a common space segment. The SPADE system has been supplied for almost a decade by DCC (see Figure 3), and has served well in the growth of the INTELSAT network. SPADE is now used in over 40 countries and provides demand access to channels made up of pairs of carriers selected from up to 800 per transponder. The cost of the SPADE equipment is in the order of $1 million per terminal for 16 channel ends.

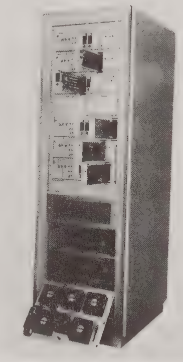

Figure 3. SPADE Terminal

SCPC (Single Channel Per Carrier)

With the growth of INTELSAT, a more economic SCPC approach has been largely adopted.[3,4] This 7-bit PCM 4ØPSK SCPC digital channel equipment is available for both data and PCM voice. (See Figure 4.) The success of SCPC is attributable to the cost effectiveness of the system, especially with the proliferation of Standard B earth stations. These lower (G/T) (gain over noise temperature) sites operate in a power-limited, rather than limited, space segment bandwidth-environment.

Figure 4. SCPC Terminal

A significant capacity gain is achieved through the use of voice activation in SCPC, which results in a savings in required transponder power. This mode of transmission is ideal for thin route applications. A 64 kb/s PCM voice channel, using 4ϕPSK modulation, uses a bandwidth of 45 kHz. Properly designed 32 kb/s Continuously Variable Slope Delta-Modulation (CVSD) codecs provide almost the same voice quality over half of the standard channel bandwidth, and are applicable in domestic thin route systems. Rate-3/4 coded 48 kb/s data, Rate-7/8 coded 56 kb/s and 64 kb/s data are often transmitted via SCPC carriers on INTELSAT links, and these rates, plus 1.544 Mb/s, are typical bit rates for domestic SCPC links.

Despite the effectiveness of SCPC from the standpoint of the G/T required, a heavy route station would require large numbers of individual channel units, each one consisting of codec, modem, frequency synthesizer and transmit/receive synchronizer. For links carrying large numbers of voice or data channels, wideband transmission systems such as TDMA are more cost effective, as the same modulator is time-shared by the many channels being carried at each site.

Wideband TDMA (Time Division Multiple Access)[5,6,7]

Wideband TDMA equipment specified by INTELSAT under technical specification BG 1-18 was delivered by DCC in the 1977-1978 period to TELESPAZIO of Italy and COMSAT, at a cost of $1 million for a nonredundant configuration. A domestic version of this terminal has been developed by DCC for American Satellite Corporation and other domestic users.[8] The fully redundant improved terminal now sells for approximately $300,000 in small quantities.

The domestic TDMA equipment is tailored to accept T1 ports (up to 28 typically) as a standard interface, with other rates provided as options. The satellite channel gross bit rate is 60 to 64 Mb/s using 4ϕPSK with full 36 MHz transponder occupancy; transponder hopping capability is also available. Microprocessor controlled auto-diagnostics and human engineering features are built into the equipment, and dynamic traffic reconfiguration of the overall TDMA system is now possible, thus optimizing the transponder utilization based on traffic variations while the equipment is in service.[9]

Wideband TDMA has a number of advantages over FDMA techniques. It allows sharing of one modem by a number of channels. It permits the operation of the transponder near saturation, overcoming the large back-off needed on SCPC transponders to avoid intermodulation problems. It is also intrinsically more flexible than FDMA, since no carrier frequency changes are required to accomplish traffic rearrangement. However, it has a disadvantage over FDMA since it requires that the G/T of all earth stations be capable of supporting the maximum burst rate, regardless of the actual volume of traffic being handled by the station. Figure 5 shows the impact of burst rate on G/T, with transponder EIRP as a parameter. When this G/T requirement is weighed against the EIRP gain due to transponder saturation, the result is that TDMA requires a certain minimum traffic per station before it becomes a cost effective alternative.

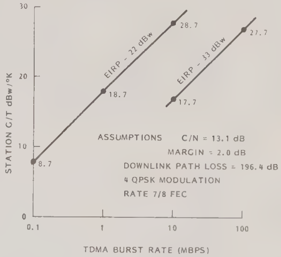

Figure 5. Station G/T vs TDMA Burst Rate

The choice of wideband TDMA versus SCPC depends primarily on the average number of channels per station. Figure 6 depicts the cost effectiveness of TDMA vs SCPC as a function of the total number of 64 kb/s voice channels (or equivalent data traffic) and the number of stations in the system. This figure shows a definite advantage of SCPC in thin routes, where many light traffic sites are being served, while wideband TDMA equipment is shown to be effective for systems with greater than 50 to 60 equivalent

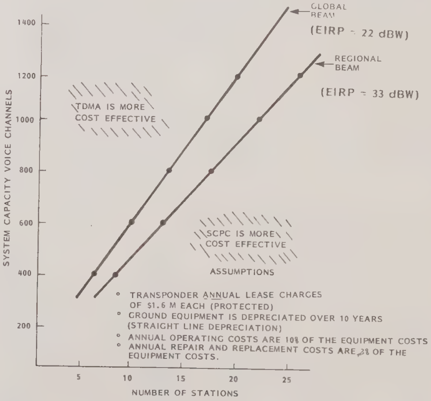

Figure 6. SCPC vs TDMA Cost Effectiveness

voice channels per station. Economics aside, it is also important to note that frequency clearances are usually easier to obtain for SCPC systems.

Intermediate-Rate TDMA Architectures

The MARISAT ship terminal, developed by COMSAT General utilizes a unique TDM/TDMA technique in the critical ship-to-shore data channel.[10] This very efficient link utilizes TDM transmission from the central terminal to the ship subscribers on one carrier frequency, while a TDMA carrier shared by many subscribers provides the return link to the central terminal. DCC has expanded on this principle with its new DYNAC[11] terminal. In addition to its use as a basic communication networking technique, DYNAC equipment may also be used to provide a data network overlay on an SCPC network. This combination provides a DAMA function in addition to an efficient data communications capability.

For low-to-moderate data capacity networks utilizing very low cost earth stations, the star network architecture and a single TDMA-carrier mesh network architecture offer unique economies and technical flexibility. These configurations provide solutions in cases where neither the thin-route SCPC or heavy-route TDMA systems are optimal, but may be designed for compatibility with either.

TDMA For Low Rate Systems

The DYNAC (Dynamic Network Assignment Communications) earth station terminal satisfies the requirements of many low-cost private communications networks. In a star configuration (Figure 7) the central site TDM transmission is broadcast to all remote sites, which are programmed to demultiplex information assigned to them. Frame durations are in the range of 50 to 250 milliseconds.

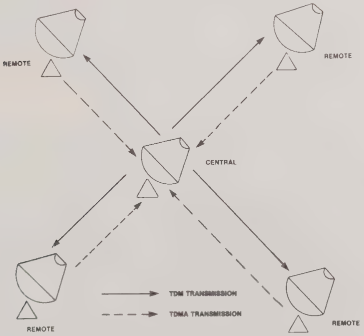
REMOTE
REMOTE
CENTRAL
REMOTE
TDM TRANSMISSION
TDMA TRANSMISSION
REMOTE

Figure 7. DYNAC Star Configuration

Any serial synchronous digital bit stream from 50 to 56 kb/s can be connected to individual compression/expansion data ports. Asynchronous interfaces[12] can feed a front-end statistical multiplexer, which can provide buffer occupancy information to the DYNAC terminal which, in turn, reassigns the bandwidth allocation of that individual port as a function of demand. (See Figure 8) The interface to the statistical multiplexer is thus a variable-rate port, which conserves network information capacity by allocating it upon demand, realizing a concentration factor of 2:1 or better.

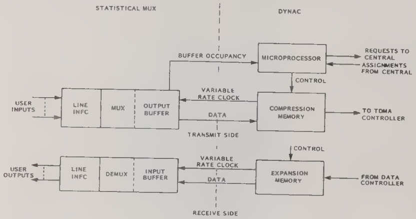
STATISTICAL MUX
DYNAC
BUFFER OCCUPANCY
MICROPROCESSOR
REQUESTS TO CENTRAL
ASSIGNMENTS FROM CENTRAL
CONTROL
USER INPUTS
LINE INFC
MUX
OUTPUT BUFFER
VARIABLE RATE CLOCK
DATA
COMPRESSION MEMORY
TO TDMA CONTROLLER
TRANSMIT SIDE
CONTROL
USER OUTPUTS
LINE INFC
DEMUX
INPUT BUFFER
VARIABLE RATE CLOCK
DATA
EXPANSION MEMORY
FROM DATA CONTROLLER
RECEIVE SIDE

Figure 8. Statistical MUX Connections To DYNAC

Channel ports of a fixed-assigned (selectable on demand) rate can be utilized for digitized voice (32 kb/s CVSD) or voice-quality and sound program PCM. Alternately, lower speed assignments for TWX/TELEX, DDS, FAX, computer-to-computer, or other interactive terminals can be assigned to a particular terminal on demand, or automatically, via time-of-day or operator control.

The network assignment is handled from the central site that communicates with all remote sites via an overhead signalling channel contained within the TDM/TDMA frame formats. The remote sites convey status, acknowledgements, and request messages automatically (under microprocessor control) to the Central site, which responds with remote commands and network assignments. The "down-line loading" of the network assignments contains burst position information, port connectivity and channel port rate assignments. The network plan is updated as often as necessary, and reconfiguration times of 2 to 5 seconds are typical for a 10 station network. Hourly traffic statistics for practical networks suggest that network configuration adaptability at this speed is sufficiently fast to provide adequate service. In addition, a significant savings is realized compared to call initiated DAMA systems.

The terminal is controlled by a local microprocessor, which, in addition to communicating status over the signalling channel, controls all terminal operations including reassignments and auto-switchover. Since the earth station is intended to be unmanned, provisions are made for remote control and diagnostics (by a central site operator) via the signalling channel or a telephone line.

Applications for a communications terminal as flexible as this, with distinct advantages over SCPC transmission yet at a competing cost, include corporate data networks, thin-route voice (DOMSAT), common-carrier backbone links, packet-switched value-added networks and shared-usage services. As an example, consider a thin-route voice network with limited data requirements.

In the star configuration, one TDM and one TDMA carrier each operates at a 2,048 Mb/s transmission rate. With 10 accesses and a 50 ms frame rate, the TDMA frame efficiency (remote-to-central) is 91 percent. Hence 58 full-duplex 32 kb/s channels can be accommodated, with 17.6 kb/s of additional capacity remaining for data traffic, which can be assigned in increments from 50 b/s to 9600 b/s. Since the 58 full-duplex circuits are reassignable, a greater number of VF connections can be accommodated at the terminal ends, since call statistics permit a concentration factor of 2.5 or better.

As the usage increases, a small percentage of calls will be "busied out" when bandwidth is not available. When this call blockage becomes unacceptable from a network operation standpoint, additional carriers can be added in the same transponder. The terminal equipment need not be changed, as the DYNAC controller is capable of Intermediate Frequency (IF) - Hopping. Under control of the microprocessor, transmit and receive modem local oscillators can be switched between two different frequency sources, allowing the station to transmit and receive two bursts per frame, each on a separate carrier. In this fashion, the total traffic capacity of the network is virtually doubled, without additional earth segment hardware, by means of a down-line loaded program change. Up to five separate local oscillator pairs can be accommodated on a channel select oscillator module.

The DYNAC system can also provide full single-hop connectivity among all sites in a mesh configuration. A single TDMA carrier is accessed by all sites including the reference (central) station. Overhead signalling and network reconfiguration is identical to that of the star network.

From a hardware standpoint, the star topology is the lower cost alternative, as one can take advantage of a larger central site earth station G/T, and use smaller, more economical, and easier-to-install (i.e. rooftop) remote site antennas. Transmission rates to 2 Mb/s can be accommodated using 5-meter installations, given an 11-meter central site. Additionally, since the remote sites are only transmitting one carrier (TDMA) at any instant of time, the remote site HPA requirements can be significantly reduced, as the amplifier can typically operate at 1 dB backoff. Solid-state devices are currently available at 5-watt saturated output power, but development is continuing toward higher power GaAs FET devices.

Hybrid TDMA/SCPC Networks for Data/Voice

The DYNAC concept of low cost, highly flexible TDMA transmission can be extended to various other network configurations employing SCPC, DAMA voice, telephony signalling and switching and local data distribution.

Consider Figure 9, in which several concentration nodes are connected using DYNAC as the backbone link. In this configuration, DYNAC performs a second level of concentration. Addressing (and demultiplexing) of transmit (and receive) data is done locally, while burst assignment and network control is handled by the central site. The node equipment consists of front-end communications processors (or other types of switches) tied into terrestrial microwave or cable distribution networks.

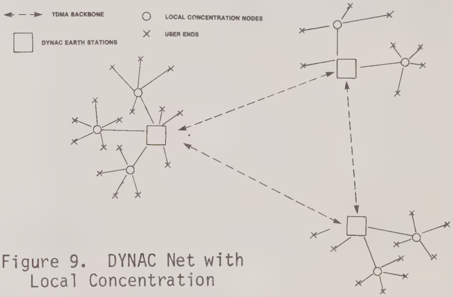

Figure 9. DYNAC Net with Local Concentration

A hybrid SCPC/TDMA scheme is depicted in Figure 10. The DYNAC network operates in a normal fashion and is used for interactive voice and data traffic. For fixed assigned, continuous wideband transmissions that would severely impact the total allowable information capacity of the DYNAC net, individual SCPC channel units can be remotely assigned via control signals sent from the central site to the applicable remotes. This control is identical to DAMA control information, and contains frequency assignment, carrier on/off, power level, and other required parameters. A single frequency assignment may be assigned as available, or multiple SCPC carriers can be used.

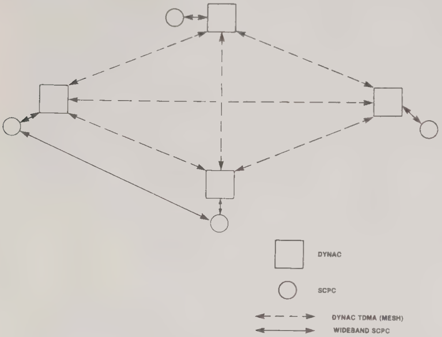
DYNAC
SCPC
DYNAC TDMA (MESH)
WIDEBAND SCPC

Figure 10. TDMA/SCPC Configuration

Extending the DAMA control concept one step further, one can envision the DYNAC system as the DAMA control (or signalling) channel of an SCPC voice network.[13,14] The TDMA carrier only need operate at 128 kb/s (or less, depending upon number of sites) and be connected at each SCPC earth station location as shown in Figure 11. DAMA control is centralized, reducing overall network hardware costs.

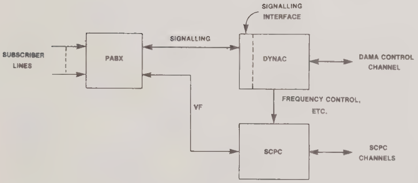
SIGNALLING INTERFACE
SUBSCRIBER LINES
PABX
SIGNALLING
DYNAC
DAMA CONTROL CHANNEL
VF
FREQUENCY CONTROL, ETC.
SCPC
SCPC CHANNELS

Figure 11. DYNAC Used As An SCPC DAMA Controller

For DOMSAT voice applications, the transfer of telephony signalling information into the central site is required, not only to process the calling site's request for a connection, but for toll recording and call statistics generation as well. The signalling information must be passed to the called site in order to complete the call. This is accomplished in a DYNAC mesh network as follows (see Figure 12): The calling party's off-hook signal is recognized by the DYNAC terminal as a Voice Frequency (VF) channel request to the central site. The channel is set up and signalling is forwarded in-band to the central site. The central switch determines the call destination, and instructs the central network controller to establish a VF connection from central to the called site. The signalling is forwarded to the called site, and upon receipt, the called and calling sites are reconfigured once again so that the previously assigned central-to-remote VF channels now connect the two remotes. On/off-hook is used to monitor the call duration for billing purposes at central. When the call is terminated, the VF channels can be reassigned.

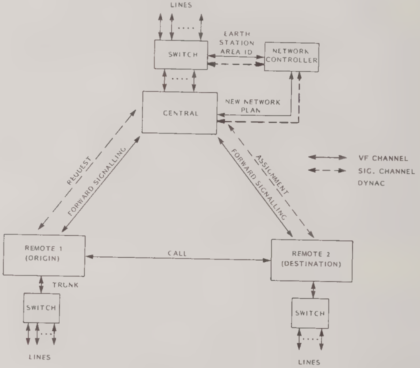
LINES
SWITCH
EARTH STATION AREA ID
NETWORK CONTROLLER
CENTRAL
NEW NETWORK PLAN
REQUEST
FORWARD SIGNALLING
ASSIGNMENT
FORWARD SIGNALLING
VF CHANNEL
SIG. CHANNEL
DYNAC
REMOTE 1 (ORIGIN)
CALL
REMOTE 2 (DESTINATION)
TRUNK
SWITCH
SWITCH
LINES
LINES

Figure 12. Call Processing for DYNAC Voice Networks

Network reassignment times during the signalling phase of the call are less than 1 second, and are done by individually updating the remote site network plans. Local on/off-hook handshaking and busy-back is provided by the DYNAC equipment to compensate for satellite delays.

Earth Station Size/Cost Considerations[15]

Each of the techniques described may prove cost effective under differing network assumptions. (See Figure 13.) Important parameters to consider include earth station data capacity, the number of earth stations and the relative space segment cost implied by a given architecture and earth station antenna size. The matrix shown in Table 1 illustrates the relative costs of various earth stations to illustrate the impact of TDMA techniques and small earth stations.

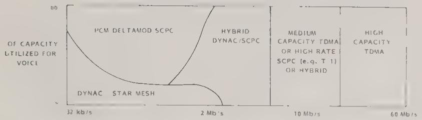

Figure 13. Earth Station Data Capacity

It is clear from Tables 1 and 2 that satellite systems utilizing large numbers of small earth stations for either voice or data may present cost-effective alternatives to existing network types.

Network Protection and Reliability

The simplest communications systems typically provide the best network availability. A small network of point-to-point SCPC links might appear to require less maintenance than a heavy route TDMA system. Table 3 shows that the MTBF (Mean-Time-Between-Failures) for SCPC equipment is three to four times greater than for TDMA equipment, for example. But the "per voice channel" maintenance rate of a fully loaded TDMA terminal is shown in Table 3 to be over three times greater than that of a fully loaded SCPC terminal.

Note that a comparison of maintenance requirements, as with cost efficiency, is related to traffic density per station. Figure 14 shows the rate of maintenance per voice channel for both SCPC and TDMA equipment as presently manufactured. The typical SCPC terminal, with less than 64 voice channels, requires less maintenance service than the corresponding TDMA equipment with similar channel availability (about 99.9997 percent). On the other hand, terminals carrying in excess of 100 voice channels should experience a lower maintenance rate per channel using TDMA than SCPC.

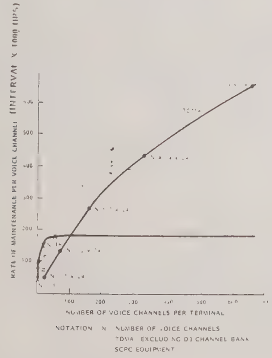

Figure 14. Per Channel Maintenance Requirements of SCPC and TDMA

To insure the indicated availabilities, the system designer must address those failure modes that can cause total network collapse. Fail-safe mechanisms must be built into the equipment regardless of the approach selected. In SCPC, loss of pilot (redundant) will cause a collapse of the network. In TDMA, loss of both reference bursts (from two separate redundant stations) will also shut down the network. Thus, such failure modes such as SCPC transmission that interferes with the pilot, or TDMA transmission that interferes with the reference bursts must be short lived via fail-safe controls.

The mean times to repair are also important to network availability. Self-test features should thus be addressed by the system designer. Current TDMA equipment, because of its complexity, has been designed with extensive auto-diagnostic features. A built-in microprocessor monitors all status and alarms, exercises the standby terminal to insure its availability, and provides the operator with a diagnostics print-out. The TDM/TDMA DYNAC equipment also has self test features originated by the colocated CP9100 processor/concentrator. Power-down features have been added to avoid failure modes that would interfere with other stations. The SCPC equipment, usually installed in thin routes, requires manual intervention for check out. Its high equipment availability makes this an acceptable approach. However, stations that have expanded their SCPC network beyond scores of channels find it necessary to test the channels in a more automatic manner. Noninterfering, continuous monitoring of in-service channels is preferable, such as monitoring of overhead or framing information. Although this technique is somewhat slow to detect failure (error rate accumulation of low rate overhead channels) it is easier to implement than other methods being evaluated, such as "eye pattern" monitoring.

Credits

The work described in this paper represents some of the collective work of the entire technical staff of DCC. The authors acknowledge the contributions of many at DCC in the development of the various systems described herein. These developments have resulted from company sponsored investments.

References

1. O.G. Gabbard, "An Overview of Satellite Multiple Access Techniques," Digital Communications Corp., Gaithersburg, Md. Jan. 1978.
2. A.M. Werth, "Trends in Digital Communication via Satellite," Microwave Systems News, April-May 1974.
3. S.B. Salamoff, "SCPC Is Efficient Satellite Technique," Communications News, February 1978.

Table 1. Typical Monthly Cost Per Channel-End for Digital Data and Voice Earth Stations

NUMBER OF VOICE CHANNELS	13M E.S. FDM-FM 120-1200 VC. (64 kb/s PCM) (FULL TRANSP.)	13M E.S. TDM-PSK 120-1200 VC (FULL TRANSP.)	13M E.S. TDMA-PSK 120-1200 VC (SHARED TRANSP.)	10M E.S. TDMA/PSK 24-240 VC (SHARED TRANSP.)	7M E.S. TDMA/PSK 24-240 VC (SHARED TRANSP.)
24				870/170	800/170
48				450/135	412/135
120	280/350	246/350	246/108	200/108	186/108
240	178/174	142/174	142/87	117/87	110/87
480	130/87	90/87	90/87		
1200	87/35	58/35	58/35		
NUMBER OF 64 kb/s DATA CHANNELS					
60	317/195	67/38			

LEGEND: 280/350:
Earth Station $280/mo/channel end +
Space segment $350/mo/channel

ASSUMPTIONS:
1. Transponder Lease: $500K/year projected (Projection for 1985)
2. Monthly Total Operating Cost: 3.33 percent of capital investment
3. Costs Estimated Installed (Turnkey)
4. Redundant Electronics Configuration

Table 2. Current Terrestrial Tariffs (Costs in Dollars per Month)

TRANSMISSION	DISTANCE (Miles)	MONTHLY CHARGE
Voice	10	132
	30	189
	100	290
	300	422
56 kb/s Data	10	1482
	30	1846
	100	3120
	300	6420

SOURCE: ATT Tariffs for Interstate Transmission

Table 3. Equipment Availability

	SCPC (64 kb/s)	TDMA (60 Mb/s)
MTBF of Redundant Common Equipment	480,000 hours	178,000 hours
MTBF of Channel Port	190,000 hours per voice channel	49,000 hours per T1 port
MTTR	0.4 hours	0.28 hours (manned site)
Common Equipment Availability	99.99992 percent	99.9998 percent
Voice Channel Availability	99.9997 percent	99.9998 percent
Common Equipment Maintenance Rate	50,000 hours	2,000 hours
Maintenance Rate Per Voice Channel	180,000 hours*	640,000 hours **

LEGEND: MTBF: Mean-Time-Between-Failures
MTTR: Mean-Time-To-Repair

* Fully loaded terminal (64 voice channels)

**Fully loaded terminal (28 T1 ports x 24 voice channels per port) excluding D3 channel bank. Including channel bank reduces this figure to 450,000 hours per voice channel.

4. L.S. Golding, "Single Channel Per Carrier Transmission For Satellite Communications," IEEE NTC Conference Record, 1975.
5. O.G. Gabbard and Pradman Kaul, "Time-Division Multiple Access," Proceedings of EASCON 1974, pp. 197-184.
6. O.G. Gabbard and Pradman Kaul, "A Cost Effective TDMA System For Domestic Applications," Third International Conference on Digital Satellite Communications, November 1975, pp. 1-6.
7. O.G. Gabbard, Pradman Kaul, A. Walker, J. Hangen, and Pradeep Kaul, "The Common TDMA Terminal Equipment For The TELESAT TDMA System," Proceedings of the International Conference on Communications, San Francisco, 1975, pp. 44-6 to 44-10.
8. S. Mittal, E. R. Cacciamani, Jr., and J. Hangen, "Use Of TDMA In A Domestic Satellite Communications System," Proceedings of EASCON 1979, pp. 69-71.
9. J. Hangen and P. Gaske, "Dynamic Traffic Reconfiguration For Time Division Multiple Access (TDMA) Systems," NTC Conference Record, 1979.
10. R.B. McClure, J. Husted, F. Giorgio, "Maritime Satellite Communications Terminal Implementation," Digital Communications Conference, Kyoto, Japan, 1975.
11. S.B. Salamoff, D. Roos and J. Steinhorn, "DYNAC: A Low-Cost Data/Voice Communications Network," Telecommunications, August 1979.
12. Pradman Kaul and D. Muzumdar, "A Flexible Low Cost Interface Between TDMA Common Equipment and Multiple Terrestrial Extensions," International Communications Conference, Conference Record, 1977.
13. A. Werth, "Recent Developments In DAMA Systems," IEEE NTC Conference Record, 1976.
14. J. Husted, "Low Cost Satellite Data Transmission Networks Using Demand Assigned TDMA," Digital Communications Conference, Montreal, 1978.
15. L.C. Palmer, "Economic Trends In Data Transmission By Satellite," Proceedings of the Data Communications Symposium, Snowbird, Utah, September 27-29, 1977.

80-0492

SCANNING SPOT BEAM SATELLITE FOR DOMESTIC SERVICE

Y. S. Yeh
Bell Telephone Laboratories
Holmdel, N. J. 07733

Abstract

This paper reports the progress and experimental efforts toward the realization of a high-capacity, scanning-spot-beam satellite for domestic service. An experimental 12 GHz phased array transponder was constructed which achieves rapid beam switching and the cophasing of all the array elements toward widely-spaced receiving stations. We summarize the status of the experiment, and review the previously published work on this system concept. In addition, we describe in detail the operation of the cophasing system that establishes element phase values for each earch station.

I. INTRODUCTION

Satellite service to a large area such as continental USA suffers a basic constraint in that the antenna gain on board the satellite is limited to about 30 dB. To achieve higher EIRP, spot beams with perhaps 20 dB higher antenna gains can be placed at densely-populated areas. However, due to the narrow beamwidth of the high-gain antenna, it is extremely difficult even with multiple spot beams to provide complete coverage to all the potential users.

A scanning spot beam[1,2] concept had been proposed which noted that, in the TDMA mode of an area coverage satellite, only two earth stations use the satellite transponder at the same time. Therefore, an area coverage antenna can be replaced by a pair (up-link and down-link) of rapidly-scanning, high-gain antenna beams. These beams concentrate the radiation patterns only on the two earth stations for the duration of the data burst according to the TDMA slot assignments among the earth stations. By replacing the area coverage antenna with spot beams, we may obtain 20 dB higher antenna gains and, further, open up frequency reuse possibilities. These two advantages combined can result in reliable high-capacity domestic service.

This paper reports the progress and experimental efforts toward the realization of the scanning beam system. The technology advances which lead to a 12 GHz experimental scanning array demonstration are reported in Section II. The cophasing technique and its performance are reported in Section III. In the last section, the evolution of the simple scanning beam system into larger capacity systems is discussed by means of a review of previously published work.

II. SIMPLE SCANNING BEAM SYSTEM

A pair of scanning spot beams,[1,2] one for the up-link and one for the down-link, is capable of supporting 600 Mbs 4-PSK modulation if the full 500 MHz bandwidth is used. Using 32 Kbs per voice circuit as a guideline, the system has a capacity of 9000 two-way voice circuits. Shown in Fig. 1 is the time sequence of the parking of the up-link and down-link beams. We note that the up-link is parked at station K and the information bursts coming out of station K are distributed by the down-link beams to stations 1, 2, and 3 in time sequence. After the traffic from station K is exhausted, the up-link beam moves to another station and repeats the down-link distribution sequence. Eventually all stations in the network would be scanned, and the process repeated.

Figure 2 is a block diagram which gives an overview of a scanning spot beam satellite. We see on the lefthand side that a 14 GHz signal is incident upon a phased array antenna and arrives at the 14 GHz preamplifiers. One preamplifier is required for each element of the array, and this establishes the up-link noise figure. A reasonable noise temperature of these amplifiers might be about 300°K, which can be realized using state-of-the-art GaAs FET amplifiers.

Following the preamplifiers are phase shifters which serve to point the up-link antenna beam toward the earch station which is transmitting at any given moment in time. The properties required of these phase shifters are that they be capable of changing state very rapidly, that they consume very little power, and that their insertion loss be relatively low. Following the phase shifters, the signals are added together coherently.

On the down-link side, the 12 GHz signal is first split into 100 or so components, one for each antenna element. These identical signals now pass through down-link phase shifters very similar to the up-link phase shifters, where a proper phase is added to the signals so that a spot beam is sent directly toward a particular receiving area. Before travelling to the antenna elements, each signal is amplified to a common output power level which would be of the order of 1/2 watt or less. A desirable property of these amplifiers would be equal power output levels and high efficiency.

In order to demonstrate the salient feature of the scanning beam system, research efforts were focused on the crucial components and functions. We shall report in the next few paragraphs on recent advances in some of these areas and on their incorporation into an experimental scanning beam array.

The array antenna would need an aperture diameter of 12.3 feet and the individual array elements would be bulky and widely dispersed. A novel antenna design[3] (Fig. 3) uses optical imaging techniques to reduce the size of the array by a factor of 7. Through careful alignment of the axes of the parabolic reflectors, polarization purity is maintained which allows dual polarization operation. Theoretical and experimental results[4]

Copyright © American Institute of Aeronautics and
Astronautics, Inc., 1980. All rights reserved.

have indicated that, with careful choice of the tapering length of the feed horns, the array can scan its intended service region of ±3.5° without encountering blind spots.

A compact 4-bit pin diode phase shifter/driver module[5,6] was built using microstrip technology. The phase shifter has a low insertion loss, 1.6 dB ±0.2 over the 11.7-12.2 GHz band. It is capable of handling up to 800 mW of RF power. Individual bits can switch phase states in 1 nsec, while the worst switching time for the entire phase shifter is under 8 nsec. The dc power consumption of the driver, when switching occurs at a 1-MHz rate, is only 36 mW in the worst case. The low switching time and dc power consumption represent substantial improvements over previously-available phase shifter/driver modules.

To account for thermal variations, component aging and the satellite station keeping and pointing errors, the satellite phase array needs periodic updating of the phase values. This permits proper focusing of the transmitting and receiving beams. The phasing information is derived two elements at a time. The phase shifter of one element is periodically stepped in staircase fashion to change the output frequency by +400 KHz, and the phase shifter of the other element is stepped in the opposite direction to change the output frequency by -400 KHz. These frequency offsets tag the radiation of the two elements and a special phasing receiver uses matched filter techniques to measure the phase difference between them. Signal-to-noise considerations indicate that this beam focusing technique will provide reliable phase information even under fading conditions which make the communication channel inoperable. The technique and its limitations will be described in Section III.

A microprocessor is needed to control the scanning beam array. Its primary functions are (1) to divide the TDMA frame period (25 msec. in the demonstration system) into a sequence of time slots, tagging each slot with a specific beam position and dwell time; (2) to retrieve, in each dwell period, the array element phase values from the phase memory; and (3) to feed this information to the array phase shifters. These functions must be performed with adequate speed and low power consumption.

Since the beams change position at intervals of microseconds (minimum dwell time is ~2.5 μsec.), low-power MOS memories can be used for most functions. Low-power TTL logic is used to provide the high-speed switching of the phase shifters. A microprocessor controller[7] was developed which is capable of memorizing 256 possible beam locations and dwell times together with 100×256 phase shifter settings. The total power consumption of the controller is about 25 watts.

An experiment [8] using a 16-element linear phased array and incorporating most of the above features is depicted in Fig. 4. Under software supervision by the controller, the beam is alternately scanned between the two receivers. A TV signal, derived from a video tape recorder, is modulated, up-converted, and transmitted by the array. The signal, alternating between the two receivers, is detected and displayed on the respective TV monitors. Measured beam switching time is demonstrated in Fig. 5. As can be seen, the rise and fall times of the RF signal during a beam switch are well under 10 nsec. Measured times for various orientations of the array relative to the receivers were 5 to 7 nsec.

The next stage of the planned demonstration is the construction of full transmitting and receiving arrays with 600 Mbs 4ϕ-PSK modulation. Considerable progress has been made toward the buffering of the high-speed data burst at the earth stations so that the interfacing with the terrestrial links can be done at a much slower speed.[9] A novel frame synchronization detection scheme which is capable of working at 300 megabauds has been reported.[10] The signalling and ranging functions are done using in-band dedicated time slots, as reported in Reference 11.

III. COPHASING RECEIVER FOR SCANNING SPOT BEAMS

The cophasing of an N-element array is accomplished by using a digital phase shifter with each element which is periodically stepped up or down in phase (to approximate positive or negative frequency shifts). This is done at a high rate by the central controller. One element of the array is designated a reference element to which all other elements are compared. During comparison periods, the reference element carrier is offset up in frequency while the test element is simultaneously equally offset down in frequency. This process is periodically repeated, element-by-element, until all array elements have been compared to the reference element. The cophasing receiver, through the use of matched filters, compares the RF phase difference generated by each comparison to that of a stable local oscillator. The resulting data are used to cophase the array. This section deals primarily with cophasing of the downlink, although cophasing of the uplink is done in a similar manner and is described briefly.

During the cophasing time period, the satellite broadcasts only CW signals, i.e., baseband modulation is removed. The framing structure is shown in Fig. 6. The cophasing receiver utilizes the first half of the subframe (125 μsec) to measure the phase difference between elements No. 1 and No. 2 and the second half (125 μsec) for elements No. 1 and No. 3.

During half of the first cophasing subframe period, the transmitter (satellite) offsets the frequency of element No. 1 by $-P_0$ and that of No. 2 by $+P_0$. The resultant burst (125 μs duration) reaches the ground station having the form

$$y_{in} = \cos(\omega_c t - 2\pi t + \theta_1) + \cos(\omega_c t + 2\pi P_0 t + \theta_2) + E\cos(\omega_c t + \psi) + n \qquad (1)$$

where ω_c is the carrier frequency, in rps;
P_0 is the offset frequency (0.4 MHz)
θ_K is the phase of element K
$E\cos(\omega_c t + \psi)$ is the contribution of the remaining (N-2) elements; and
n is the front end noise with one-sided spectral density N_0. (This signal

magnitude per element is normalized to unity, with no loss in generality.)

The ground station applies this burst to two narrowband filters centered at $\omega_c + 2\pi P_0$ and $\omega_c - 2\pi P_0$. These filters have a dual purpose: they must effectively block the carrier term $E \cos(\omega_c t+\psi)$, necessitating steep skirt characteristics, and also have a sufficiently large bandwidth relative to 8 kHz that the 125 μsec phasing pulses pass through undistorted. The filters used in this receiver are five cavity helical resonator type Butterworth response bandpass filters each having a total 3 dB bandwidth of 0.2 MHz and centered at 70 ±0.4 MHz, respectively. The outputs of the two filters are:

$$y_1 = \cos(\omega_c t - 2\pi P_0 t + \theta_1) + n_1' \tag{2}$$

$$y_2 = \cos(\omega_c t + P_0 t + \theta_2) + n_2' \tag{3}$$

where n_1' and n_2' are narrowband Gaussian noises, each with power $\doteq N_0 \times (0.2 \text{ MHz})$.

These outputs are now mixed and the lower sideband product is:

$$z_1 = \frac{1}{2}\cos(4\pi P_0 t + \theta_2 - \theta_1) + n_c'' \cos 4\pi P_0 t + n_s'' \sin 4\pi P_0 t \tag{4}$$

where n_c'' and n_s'' are baseband Gaussian noises, eacn with power $\frac{1}{2} N_0 \times (0.2 \text{ MHz})$. The noise times noise product term is neglated to a first approximation.

The phase of z_1 is detected by matched filters. Referring to Figure 7, a stable oscillator of frequency $2P_0$ is split to provide in-phase and quadrature-phase demodulation of z_1. Each mixer output is integrated for 125 μsec and sampled to provide an x and y output where $\tan^{-1} \frac{y}{x}$ is the relative phase between z_1 and the reference local oscillator. The following is the estimated phase angle:

$$\hat{\theta}_2 = \tan^{-1} \frac{\int_0^T z_1 \sin(4\pi P_0 t + \alpha_{LO})dt}{\int_0^T z_1 \cos(4\pi P_0 t + \alpha_{LO})dt} \tag{5}$$

where α_{LO} is the relative phase of the local oscillator. If α_{LO} were equal to $\theta_2 - \theta_1$, it is easy to show, using Eqs. (4) and (5), that θ_2 would be

$$\hat{\theta}_2 = \tan^{-1}\left\{\frac{2\int_0^T n_s''dt}{T + 2\int_0^T n_c''dt}\right\}$$

Since phase measurement errors should be independent of α_{LO}, for an arbitrary α_{LO} we have

$$\hat{\theta}_2 = \theta_2 - \theta_1 - \alpha_{LO} + \tan^{-1}\left\{\frac{2\int_0^T n_s''dt}{T + 2\int_0^T n_c''dt}\right\}$$

$$\cong \theta_2 - \theta_1 - \alpha_{LO} + X_s \tag{6}$$

where $X_s \cong \frac{2}{T}\int_0^T n_s''dt$ is a zero-mean Gaussian variable with variance

$$\langle X_S^2 \rangle = \frac{2N_0}{T} . \tag{7}$$

The next cophasing period (half subframe later) yields

$$\hat{\theta}_3 = \theta_3 - \theta_1 - \alpha_{LO}' + X_s' \tag{8}$$

where X_s' is uncorrelated with X_s and has the same variance, and the estimated phase difference is (neglecting of LO phase difference which will be discussed later),

$$\hat{\theta}_3 - \hat{\theta}_2 = \theta_3 - \theta_2 + \varepsilon \tag{9}$$

where

$$\varepsilon = X_s' - X_s \tag{10}$$

If ε is small, the differential phase between element No. 2 and element No. 3 can be accurately measured. After N cophasing periods, all the differential phases between the elements and element No. 2 will be known, including element No. 1, which is compared to the last element in the sequence. The receiver (ground station) can send this focusing information to the satellite transmitting array via the telemetry link.

Proper operation of the matched filter detector necessitates that a stable local oscillator be used for the source at frequency $2P_0$. Since the measurements $\hat{\theta}_2$ and $\hat{\theta}_3$ are performed within a 250 μsec interval, the phase error $(\alpha_{LO}' - \alpha_{LO})$, caused by the drifting between the LO and the satellite clock must be small. If a 2 degree drift is allowed, the stability of the local oscillator must be

$$\delta = \frac{1}{720 P_0 T} = \frac{1}{720 \times 0.4 \times 10^{-6} \times 125 \times 10^{-6}}$$

$$= 2.78 \times 10^{-5} \tag{11}$$

This value represents the minimum frequency stability required between the local oscillators on the ground and on the satellite. The crystal-controlled LO in this receiver has a short-term stability of $\pm 5 \times 10^{-8}$/day and a long-term stability of $\pm 2 \times 10^{-6}$/year, thereby exceeding the required stability criterion.

This section primarily concerns the downlink cophasing, but, as a digression, it is interesting to note the simpler timing format of the uplink. Referring to Figure 6B, the uplink cophasing timing sequence is shown. In every subframe, element No. 1 is compared with one other element ($\theta_1-\theta_2, \theta_1-\theta_3, \ldots\ldots, \theta_1-\theta_N$) for the entire subframe period (250 μs). Since the clock is local and can be infinitely stable relative to itself, one subtraction process is saved, and a 6-dB lower noise power is obtained than with the downlink cophasing format.

The required integration time (T) depends on the array CNR, the number of elements, and the allowable variance in the estimated phase. Referring to Equation (1), the RF carrier-to-noise ratio at the ground receiver during the communication mode is

$$\rho_{RF} = \frac{N^2}{2BN_0} \qquad (12)$$

where B is the channel bandwidth; and N is the number of array elements.

Combining Equations (7), (10), and (12), the variance of the phase error is

$$\langle\varepsilon^2\rangle = \frac{2N^2}{\rho_{RF}BT} \qquad (13)$$

For the experimental model, N = 16, B = 500 MHz, and T = 125 μsec. During fading which renders $\rho_{RF} = 1$ (0 dB), the phase output will still have a standard deviation of 5 degrees and this is sufficient to cophase the scanning beam array. In the final system design, given the parameters and the requirements of the scanning array, the integration time T can be decided upon using Equation (13).

IV. EXTENSIONS TO HIGHER CAPACITY SYSTEM

The extension of a pair of scanning beams to larger capacity systems has been reported[11,12,13] where a pair of scanning spot beams is supplemented by several fixed spot beams as shown in Fig. 8. Here the fixed spot beams and the scanning beam would have to be interconnected by a satellite TDMA switch. From the TDMA switch point of view, the scanning spot beam is no different from a fixed spot beam. Thus, the problem is reduced to that of the TDMA connection of a large number of spot beams.

A satellite TDMA switch is required to interconnect the beams on a time division basis to satisfy the total communication needs among all the earth stations in each beam. Furthermore, these stations are by no means uniform in their interbeam traffic requirements. The actual interbeam traffic may range from a few voice circuits for a small earth station to hundreds of voice circuits for a high-volume earth station. Occasionally, high data rate service, e.g., video conferencing service, must be available to even the smallest earth stations to maintain the flexibility of the system. To accommodate these diverse requirements and yet maintain a porper balance between burst efficiency and earth station high-speed buffer size is of utmost importance in system planning.

In Reference 11 the aggregated interbeam traffic, disregarding the fine details of the individual needs of the many earth stations in each beam, was examined. A satellite TDMA switch interconnects all the beams with the connecting time proportional to the aggregated interbeam traffic. These connections are set-up for long-term traffic variations, hourly or longer. Next, a frame format and burst organization were proposed which can satisfy the needs of the earth stations in each spot beam. Here we satisfy the fine details of the interbeam traffic. The approach maintains high burst efficiency even for the smallest earth stations. Integral to the system is built-in demand assignment which allows local channel assignment upon request. Also, high data-rate channels are available on demand and require very little extra effort on the part of the participating earth stations to accommodate these special situations.

Another important aspect of any TDMA system is the signaling hierarchy and the means to achieve system-wide synchronization of the TDMA bursts. The problem becomes complicated when we enter the switched spot-beam era because of the inability of the individual earth stations to monitor their own transmissions. With so many earth stations in the system, it is highly desirable to have a fast, inexpensive means to achieve system-wide synchronization. An organization which allows one master station to serve as the nerve center for the entire system has been described.[10,11] It establishes dedicated two-way signaling links to all the earth stations. Each earth station can hit its TDMA switching window in the cold-start mode using only a moderately stable local clock. Following this, a closed-loop feedback technique is used to "fine tune" transmission so that guard times become minimal.

The combination of a pair of scanning beams and a multiple number of spot beams still suffers the drawback that traffic in the spot beam regions may not be equal. It therefore suffers in traffic efficiency. To correct this inefficiency, a further development[14] is to break the CONUS into several regions, each with its own scanning beam. The regions are drawn in strips, where the populations in each strip are approximately equal. In a sample design, the CONUS is broken into seven NW-SE strips. Since each strip covers only one-seventh of the conus the individual radiating element of the phased array has about 38 dB gain. To obtain the same 50 dB gain as the CONUS coverage scanning spot beam, the total number of elements required for the strip-scanned system is only slightly larger than for the CONUS scanning spot beam.

ACKNOWLEDGEMENT

The author wishes to thank his colleagues at Bell Laboratories for the permission to report on their work. In most cases the individual contributions are cited in the reference list.

REFERENCES

1. D. O. Reudink and Y. S. Yeh, "A scanning spot-beam satellite system," BSTJ, pp. 1549-1560, October 1977.

2. D. O. Reudink and Y. S. Yeh, "A rapid scan area coverage communication satellite," 7th AIAA Conference, San Diego, April 1978.

3. C. Drogone and M. J. Gans, "Imaging reflector arrangement to form a scanning beam using a small array," BSTJ, vol. 58, No. 2, February 1979, pp. 501-515.

4. M. J. Gans and N. Amitay, "Design of arrays of oversized aperture tapered waveguide horn elements," 1979 International Symposium on Antennas and Propagation, pp. 356-359, vol. 1, Seattle, Washington.

5. B. Glance, "A fast low-loss microstrip P N phase shifter," IEEE Trans. MTT, Vol. MTT-27, No. 1, pp. 14-16, January 1979.

6. B. Glance and N. Amitay, "A fast switching, low loss, low drive, 12 GHz PIN phase shifter," IEEE MTT/s International Microwave Symposium, Orlando, Florida, 1979.

7. W. L. Aranguren, R. E. Langseth and C. B. Woodworth, "Sequence design for scanning beam satellites," BSTJ, November 1979.

8. N. Amitay and A. J. Rustako, Jr., "12 GHz scanning spot beam phased array for satellite communication," Ninth European Microwave Conference Proceedings, September 1979, London, England.

9. A. S. Acampora and R. G. Langseth, "Baseband processing in a high-speed burst modem for a satellite-switched TDMA system," 4th International Conference on Digital Satellite Communication, Montreal, Canada, October 1978, pp. 131-138.

10. A. S. Acampora and R. E. Langseth, "A 300 megaband frame synchronizer and interface design for variable capacity TDMA ground terminals," CC 1979, Boston, Mass., pp. 6.2.1-6.2.10.

11. Y. S. Yeh and D. O. Reudink, "The organization and synchronization of a switched spot-beam system," 4th International Conference on Digital Satellite Communication, Montreal, Canada, October 1978, pp. 191-196.

12. D. O. Reudink, A. S. Acampora and Y. S. Yeh, "Methods for achieving high-capacity universal service satellites," NTC, 1978.

13. D. O. Reudink, Y. S. Yeh, and A. S. Acampora, "A phased array for a 12/14 GHz TDMA transponder," EASCON, 1978.

14. A. S. Acampora, C. Dragone, D. O. Reudink, "A satellite system with limited-scan spot beams," IEEE Trans. on Communication Theory, October 1979.

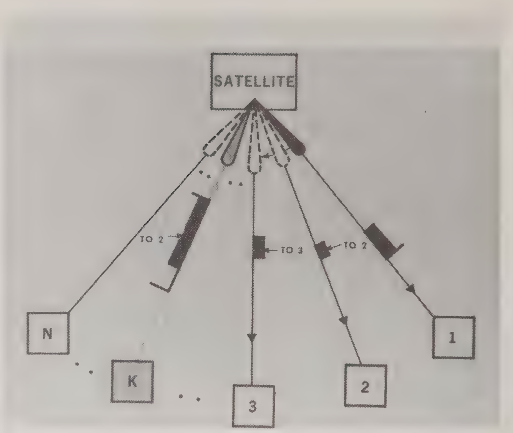
SATELLITE
TO 2
TO 3
TO 2
N
K
3
2
1

Fig. 1 Scanning Satellite with TDMA

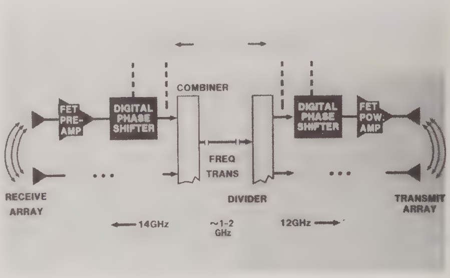
COMBINER
FET PRE-AMP
DIGITAL PHASE SHIFTER
FREQ TRANS
DIGITAL PHASE SHIFTER
FET POW. AMP
RECEIVE ARRAY
DIVIDER
TRANSMIT ARRAY
14GHz
~1-2 GHz
12GHz

Fig. 2 Block Diagram of a Scanning Spot Beam Satellite

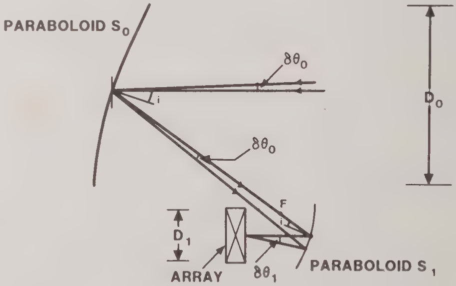
PARABOLOID S_0
$\delta\theta_0$
i
D_0
$\delta\theta_0$
F
i
D_1
ARRAY
$\delta\theta_1$
PARABOLOID S_1

Fig. 3 Compact Array Design

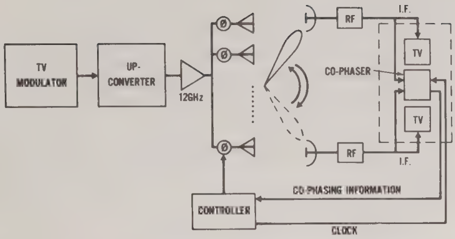
TV MODULATOR
UP-CONVERTER
12GHz
RF
I.F.
TV
CO-PHASER
TV
RF
I.F.
CO-PHASING INFORMATION
CONTROLLER
CLOCK

Fig. 4 Scanning Array Demonstration

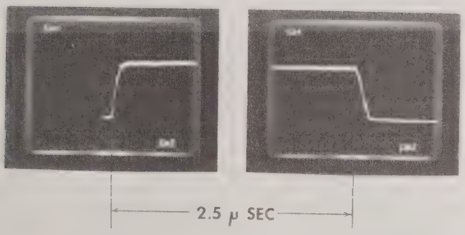

a) RISE TIME

b) FALL TIME

Fig. 5 Array Beam Switching

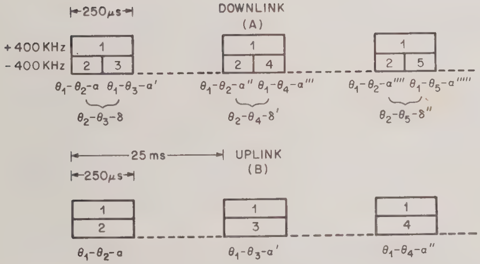
250µs
DOWNLINK
(A)
+400 KHz
-400 KHz
1
2
3
1
2
4
1
2
5
θ1-θ2-α θ1-θ3-α'
θ2-θ3-δ
θ1-θ2-α'' θ1-θ4-α'''
θ2-θ4-δ'
θ1-θ2-α'''' θ1-θ5-α'''''
θ2-θ5-δ''
25 ms
250µs
UPLINK
(B)
1
2
1
3
1
4
θ1-θ2-α
θ1-θ3-α'
θ1-θ4-α''

Fig. 6 Cophasing FORMAT

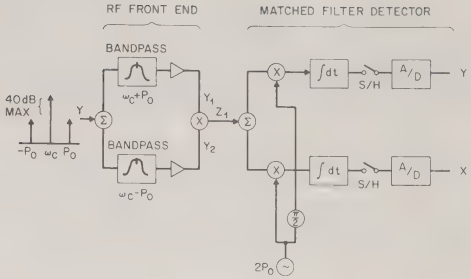
RF FRONT END
MATCHED FILTER DETECTOR
BANDPASS
40dB MAX
Y
-P0 ωc P0
ωc+P0
BANDPASS
ωc-P0
Y1
Y2
Z1
∫dt
S/H
A/D
Y
∫dt
S/H
A/D
X
π/2
2P0

Fig. 7 Cophasing Receiver

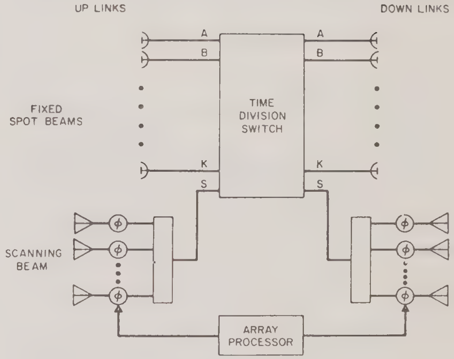
UP LINKS
DOWN LINKS
A
B
A
B
FIXED SPOT BEAMS
TIME DIVISION SWITCH
K
S
K
S
SCANNING BEAM
ARRAY PROCESSOR

Fig. 8 Combined Scanning and Fixed Beam Satellite

80-0493

THE NATO DIGITAL SATELLITE COMMUNICATIONS SYSTEM

M. Celebiler*, J. Munns*, E. Turner**

Abstract

The paper describes the design specification and the implementation of the baseband portion of the NATO digital satellite communications system.

The technical specifications and the factors on which they were based are discussed. Those factors were technical and operational requirements, cost effectiveness and implementation time. The design and performance characteristics of the equipment designed and manufactured to meet these specifications are presented.

I. Background

The existing NATO SATCOM II system has been operational for seven years and consists of 12 static ground terminals (SGT), two control centres and three geosynchronous X band satellites. The system utilises 18 frequency modulated multi-destination carriers and provides some 150 voice and 100 low speed telegraph circuits by the use of frequency division multiplex equipment.

The principle characteristics of the existing SGTs are:

Bandwidth: 50 MHz
Figure of merit for the receive sub-system: 35dB/°K
Effective isotropic radiated power: +125dBm
Carrier to noise density for test tone to noise ratio of 30dB in top channel: 68dBHz

The design phase of the NATO III system has recently been completed and the equipment is now being manufactured. The new system will be completed in mid-1983 and will consist of the 12 existing static SGTs modified to SATCOM III standards, nine new static SGTs, two new transportable SGTs and two control centres. The new system will utilise over 200 single-destination QPSK carriers and will provide some 500 voice, 400 low speed telegraph and 200 medium speed data circuits by the use of time division multiplex equipment.

The principle characteristics of the modified and new static SGTs will be:

Bandwidth: 200 MHz
Figure of merit for the receive sub-system (G/T): 35dB/°K
Effective isotropic radiated power: +125dBW
Carrier to noise density for test tone to quantisation noise ratio of 30dB in a CVSD channel: 41dBHz

II. Baseband Design

General Description

The requirement to implement a digital system and thus completely replace the current analogue baseband equipment in the existing SGTs provided an opportunity to design the baseband without restrictions of compatibility with existing equipment. It was thus possible to design this sub-system to meet the requirements of the NATO Integrated Communications System (NICS) using new concepts and technology. This in turn provided an efficient utilisation of resources.

The baseband sub-system was designed to provide the following:

a. Digital communication channels for use as trunks in a switched network

b. A capability to modify the trunk size according to traffic requirements

c. An engineering service network with automatic switching and connections to the terrestrial network

d. Facilities for centralised control of the system

The broad design goals listed above could surely be met by a variety of systems. The system designed was therefore further refined to satisfy various technical and operational requirements. Effort was also spent to keep cost, implementation time and equipment complexity as low as possible. The system which resulted from these considerations has the following characteristics:

Mode of access to the transponder:	(FDMA) Frequency Division Multiple Access
Type of modulation:	(QPSK) Quarternary Phase Shift Keying
Type of Multiplexing:	(TDM) Time Division Multiplexing
Type of Analogue-to-Digital and Digital-to-Analogue (A/D-D/A) Conversion:	(CVSD) Continuously Variable Slope Delta and PCM; single voice channel per codec
Engineering Service Channels:	CVSD, either through a sub-multiplexer or as single channel per carrier
Control Facilities:	By using Control Monitor and Display (CM&D) consoles located at each satellite ground terminal (SGT) and connected to control centres

These characteristics together with the design goal (b) above led to the equipment specifications. Some important features of the equipment specifications are given below:

---

* NATO Integrated Communications System Management Agency, Brussels, Belgium
**Ford Aerospace & Communications Corporation, Palo Alto, Ca. USA

Copyright © American Institute of Aeronautics and Astronautics, Inc., 1980. All rights reserved.

Equipment Specifications

Description of the Baseband Sub-system

A simplified block diagram of the baseband sub-system is shown in Figure 1. The A/D-D/A converters are in the form of single codec per channel and are placed in a container separate from the multiplexers. This container can accomodate both CVSD and PCM codecs placed on single cards. The sub-multiplexer (sub-TDM) is used for multiplexing the engineering service channel, medium and low rate data and telegraph channels. The Time Division Multiplexer (TDM) is a synchronous multiplexer. Its output data rate is dependent on the number and type of codecs used over the link. The modem uses offset quaternary PSK and contains a two rate convolutional encoder Viterbi decoder unit. The service channel associated with the modem is for use in link alignments. It is an analogue voice channel transmitted using frequency modulation (FM). The modem is a multi-rate modem. It can operate at any rate within the limits of 100 kbit/s to 10 mbit/s. The status and control wires carry the status information to the CM and D console and the control commands from the CM and D console.

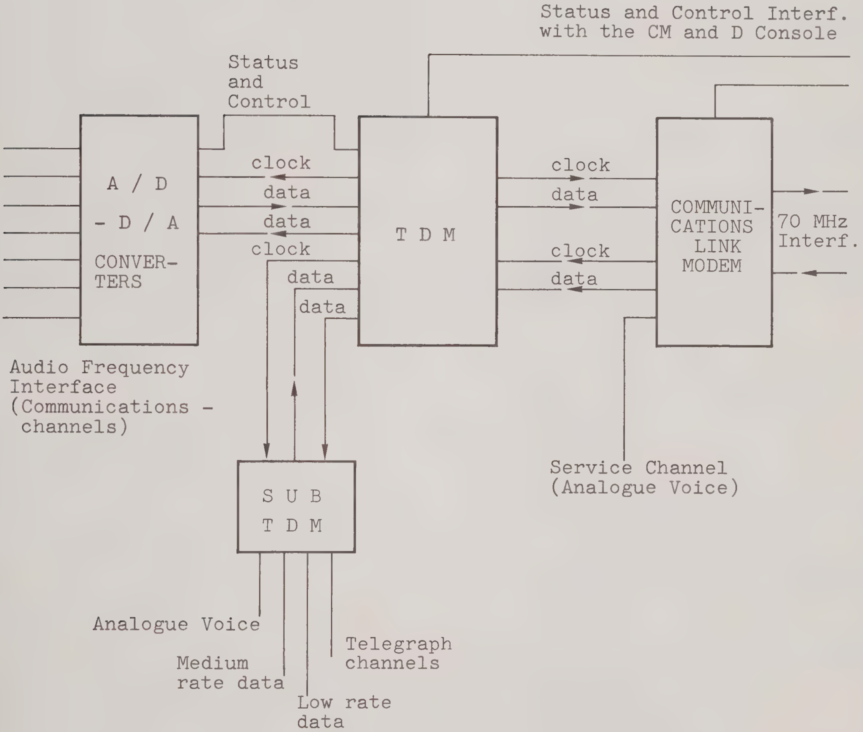
Status and Control Interf. with the CM and D Console
Status and Control
A / D - D / A CONVER-TERS
clock
data
data
clock
data
data
T D M
clock
data
clock
data
COMMUNI-CATIONS LINK MODEM
70 MHz Interf.
Audio Frequency Interface (Communications - channels)
Service Channel (Analogue Voice)
S U B T D M
Analogue Voice
Medium rate data
Low rate data
Telegraph channels

Figure 1. THE BASEBAND SUBSYSTEM

The A/D-D/A Converters

There are at present basically two A/D-D/A conversion techniques for telephony which offer digital transmission with trunk quality. The reference for this quality is the quality of the voice channel obtained by using analogue transmission techniques and which meets the relevant CCITT recommendations. These digital techniques are the Pulse Code Modulation (PCM) and the Delta Modulation (DM). The basic difference between them is that PCM is more of a channel coding technique while the DM is more of a source coding technique. The basic difference from the implementation point of view is that there are well established standards for PCM while there is very little standardisation for DM.

The standard transmission rate for PCM is 64 kbit/s per voice channel. A widely used rate for DM is 32 kbit/s. This difference in transmission rates implies a similar difference in the bandwidths required and makes the DM an attractive alternative to PCM. However, since there are no universal standards for DM the saving in the bandwidth can only be accomplished if a DM codec could be built to operate at 32 kbit/s and offer a quality similar to that offered by PCM at 64 kbit/s.

As mentioned above the DM is a source codec and consequently the transmission quality it offers is dependent on the type of source signal. A telephone channel basically carries speech signals, but it also carries signalling and supervisory tones and line modem signals. The transmission quality for speech can best be determined by subjective assessment. But subjective evaluation methods may cause a number of problems and are best to be avoided in contractual specifications. The signal to noise ratio on the other hand is a quantity which can easily be measured and offers a measure of quality, especially since there exists standard measurement techniques and recommended levels for PCM these may also be applied to DM. The signal to noise ratio does not fully characterise the transmission performance for the signalling and supervisory tones because the DM introduces non-linearities in the signal path. This performance has to be insured by specifying saturation levels for single tones and intermodulation product levels by two tones.

The above considerations are summarised in the following specifications for a DM codec operating at 32 kbit/s:

Signal-to-noise ratio (quantisation noise):	minimum 24dB for an 805 Hz test tone at all input levels between 0 and 40dB below nominal
Saturation Characteristic:	The level of a 2500Hz tone at the output is required to exceed the nominal test tone level when its level at the input is 20dB above the nominal test tone level.
Intermodulation product levels:	The levels of intermodulation products caused by simultaneous application of two tones each at the test tone level and having frequencies chosen from the set (2n + 1) x 100 Hz, $4 \leq n \leq 9$, are required to be at least 22dB below the test tone level.

As will be explained in the implementation part of this paper the above specifications can be met by at least one equipment. The signal to noise ratio can even be better than 24dB.

The Sub-TDM

The DM codecs discussed above provide trunks for telephone traffic. But there is also a need for interstation communication channels for housekeeping purposes. The engineering service channel provides such a facility. This channel does not have to meet the requirements of trunk channels. The use of one of the DM channels would result in a waste of capacity. On the other hand the use of a signal processor totally different from the DM would increase the complexity and consequently the cost of the TDM. A solution to this problem is the use of a sub-TDM which has a multiplexed output format identical to the DM 32 kbit/s digital signal. With this solution the sub-TDM can be built to multiplex digitised speech, data and telegraph signals which are required for housekeeping and other purposes.

The speech signal processor to be used in connection with the sub-TDM can be designed to operate optimally at a rate lower than the aggregate rate of 32 kbit/s. However this means additional cost and complexity. A more acceptable approach is to use the same DM equipment but operate it at 16 kbit/s. The set of specifications summarised below are in accordance with the above considerations.

Multiplexed data rate:	32 kbit/s
Voice Communications:	Analogue interface; digitised by the DM codec specified above but operating at 16 kbit/s
Channels other than voice:	4 telegraph, 1 600 bit/s data, 1 1200 bit/s data, 1 3600 bit/s data
Type of operation:	Either through the TDM or through a 32 kbit/s PSK modem

The last requirement above is due to the fact that if a TDM has all ports filled it would be more economical to set up a 32 kbit/s link with a low rate modem rather than to use another TDM and the high rate modem.

The TDM

The role of the TDM's equipment appears to be fairly simple: it has to multiplex a number of 32 kbit/s synchronous signals. There are, however, some other requirements, because the DM channel described above may not, as already mentioned, fulfil all the requirements that can be met by use of a PCM channel. Furthermore, there is a requirement to modify the output rate of the multiplexer according to the number of its ports in use. The DM PCM issue is resolved by designing the TDM to accept from the same ports a 32 kbit/s or a 64 kbit/s synchronous data stream. The TDM must also take care of the PCM word synchronisation. This issue is resolved by requiring the TDM to have an aggregate bit rate no more than the sum of the rates at its ports plus an overhead.

The characteristics given below summarise the basic requirements for the TDM:

Channel interfaces:	Synchronous 32 kbit/s data and 64 kbit/s PCM signals with only one present at any time
Aggregate interface:	Serial data at a rate not exceeding the sum of the rates at its ports plus 8.5% overhead
Control of active ports:	Both locally and remotely

The Communications Link Modem

The modem is an important part of the link because it determines the efficiency of the power and bandwidth utilisation. Its specification requires a number of choices such as the types of modulation, detection and filtering. These choices together with the transponder characteristics determine the power and bandwidth requirements. Numerous methods, analytical, numerical or based on simulation have been developed to predict these requirements under given sets of circumstances. Nevertheless, it is still very difficult to make those choices which are optimal for a given set of circumstances. For this reason modems are usually designed to operate over a simplified channel model such as the Additive White Gaussian Noise (AWGN) channel with band limiting. Their performances over other channels are established by simulation or computation. Modem specifications therefore usually state performance over the AWGN channel.

The modulation techniques either used or considered for use in satellite communications are Phase Shift Keying (PSK) and Minimum Shift Keying (MSK). Each one of these two modulation techniques has advantages over the other depending on the transmission medium through which they operate. For example, the effect of noisy reference on the bit error rate for a given signal to noise (White Gaussian Noise) ratio is less in MSK compared with offset QPSK, the latter being better than QPSK[4]. According to the literature (5 and 6) MSK where signal is moderately band limited peforms better through a limiting transmission medium while QPSK performs better when the signal is more severely band limited.

In FDMA operation the effect of intermodulation products caused by the transponder non-linearities is more important than the effect of the non-linearities on each carrier. An intermodulation product can be considered as an interfering signal. In FDMA therefore a modulation technique which is more robust against interference is preferable.

These considerations and the requirement to conserve power and bandwidth led to the following characteristics for the Communications Link Modem:

Type of Modulation:	Offset QPSK
Type of Detection:	Coherent with ambiguity resolution by use of differential encoding
Data rate:	Any rate from 100 kbit/s to 10 mbit/s
Spectral occupancy:	1 bit per Hz with 0.2dB degradation in performance in the presence of two adjacent carriers, one on each side, modulated at the same rate, but having 6dB higher carrier powers
Implementation Loss:	2dB for an error rate of 1 in 10^7 or higher
Rate Change Command:	Both local and remote
Error Correction:	Convolutional encoding with Viterbi decoding; coding rates are 1/2 and 3/4

The spectral occupancy specification given above is not very strict for a modem operating at a single rate. It is however more difficult to achieve a modem operating over a wide range of rates. Effort was spent to specify a limit which conserved satellite bandwidth but remained achievable with existing technology.

III. Baseband Implementation

The A/D-D/A Converters

General Description

The A/D-D/A converters are housed in the Channel Bank, which consists of: a tray assembly, a power supply module, a number of PCM and CVSD channel unit modules, and a Sub-TDM address select module. Up to 31 full duplex audio channels can be accommodated by the Channel Bank. Either PCM or CVSD plug-in modules are inserted into slots matching the channels that are to be used on that link. These modules are interchangeable and can be used in any combination from a minimum of 3 to a maximum of 31 channels. In addition, an address select module can be used to assign one of the 31 channels to the Sub-TDM data.

The channel unit modules contain self test circuitry which sends alarm signals to the multiplexer and provides front panel indication when a fault is detected. The Sub-TDM address select module is used to save a position in the multiplexers data stream for the data from the Sub-TDM.

Functional Description

The PCM channel units operate at 64 kbit/s and the CVSD channel units operate at 32 kbit/s. The clocks for both transmit and receive are provided to the Channel Bank from the Main multiplexer.

The multiplexer determines which type of module is in each slot by using an address and a status bus. Each of the 32 slots has a unique binary address between 0 and 31 inclusive. The multiplexer sequentially addresses the slots in the Channel Bank. When the address on the address bus matches the slot address the module puts out three status bits that indicate its module type and whether it is properly functioning.

Performance Characteristics

The PCM Channel Unit uses the 8 bit, 15 segment M = 255 companding law. This unit is in accordance with the CCITT Recommendations G.711 and G.712. In particular the measured values of the signal to quantisation noise ratio are given in Table 1.

Table 1: PCM Channel Unit Signal to Noise Ratio

Input Level (dBm0)	Signal to Noise Ratio (dB)	
	Measured	Specified
-3	34.1	26.3
-6	39.1	33.9
-10	39.1	33.9
-20	38.2	33.9
-27	36.8	33.9
-34	34.8	32.2
-40	31.9	27.6
-50	24.5	17.6
-55	20.0	12.6

The CVSD Channel Unit uses a digitally controlled compander. The control is based on the values of the signal to quantisation noise ratio (SNR). These values show that with this unit a SNR of 30dB is achievable over a range of 40dB input level. In fact, as can be seen by comparing tables 1 and 2, this unit would meet the SNR specification for PCM. The unit also meets the requirement for intermodulation product levels for any two tones chosen from the set 2(n+1)x100Hz for 4 n 8.

Table 2: CVSD Channel Unit Signal to Noise Ratio

Input Level (dBm0)	Signal to Noise Ratio (dB)	
	Measured	Specified
9	29.5	-
6	34.8	-
0	34.8	24
-10	34.5	24
-20	33.5	24
-30	33.0	24
-40	26.5	24

The Sub TDM Equipment

General Description

The Sub-TDM accepts multiple input signals including data from a CVSD codec which is used to convert an analog speech signal to a 16 kbit/s digital signal. This CVSD codec is identical to those employed in the Channel Bank but operated at 16 kbit/s. The Sub-TDM then combines the converted analog signal and the other digital signals into a 32 kbit/s serial digital stream which is then supplied to the main TDM for further multiplexing. If additional service channels are required in the network the Sub-TDM can operate directly with a Service Link modem rather than via a TDM and Link Modem.

Functional Description

The multiplex and demultiplex functions are performed on a single printed circuit board. The interface to the CVSD codec is handled as if it were a separate 16 kbit/s data channel.

Each input is clocked into a buffer where it is then reclocked out into a frame buffer in a sequence established by a microprocessor frame controller. The frame buffer is clocked out at the 32 kbit/s transmit data rate.

The Sub-TDM Demultiplexer receives data and clock from the Main TDM or the Service Link Modem and demultiplexes the signal.

The Sub-TDM also accommodates four asynchronous telegraph channels operating at either 50 or 75 bauds. These telegraph channels are oversampled at a rate of approximately 900 Hz. When received, the telegraph channels are decoded using a majority vote logic that improves the bit error rate performance. All other data channels are handled on a one bit for bit basis.

The Time Division Multiplexer

General Description

The TDM can accommodate from one to thirty-one parallel signals of either 32 kbit/s or 64 kbit/s data rate. These two rates are employed by the voice conversion equipment for converting voice telephone signals to digital data signals. In addition, the TDM accommodates a 32 kbit/s channel from the Sub-TDM. The number of channels to be handled by the multiplexer, is selectable and the output signal data rate is changed to maintain a high transmission efficiency for any number of selected channels.

Functional Description

The TDM is comprised of Input Storage, Output Storage, and Central Processing Unit (CPU) printed circuit boards. The Input Storage Board has a 16 bit buffer for each of the 31 Channel Bank channels. An additional buffer is used for the Sub-TDM input. The MUX Format Control sequentially clocks data out of the active channel buffers in 8 bit blocks at the data rate of the output digital stream. The MUX Format Control input is provided from the CPU Board which includes a microprocessor which determines the format of the multiplexed data stream from the channel address and status data received from the Channel Bank. The format, which includes frame synchronisation words, is changed according to the number of active channels to maintain a greater than ninety percent over-all data rate efficiency. Table 3 shows the frame structure for the TDM. The CPU also controls a programmable clock synthesiser and clock synchroniser which are used to generate the transmit clock. The clock synchroniser is used when an external clock source is required. The clock synthesiser is used when an internal transmit clock source is required.

In the receive direction, both clock and data are accepted from the modem. Sync detection logic establishes frame synchronisation and the CPU provides an input to the DEMUX Format Control which clocks data into the Output Storage buffers in reverse to the way it was clocked out of the Input Storage buffers.

Whenever a channel configuration is to be changed, the Channel Bank is equipped with the desired combination of CVSD and PCM channel units and the Sub-TDM Address Module is inserted into the proper channel slot. The front panel Channel Configuration Selector is then momentarily manually switched to the RESET position. The TDM CPU will then change format to the new Channel Bank configuration.

The TDM can also operate in a Remote Control Mode wherein the channel configuration can be changed remotely. In this mode, the channel status is reported from the TDM to the Control Computer via a data reporting network which is also utilised to receive commands from the control computer to change the channel configuration.

Table 3: The TDM Frame Structure

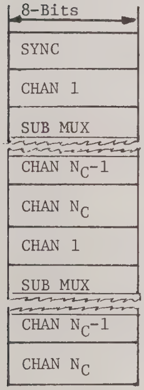

N_C = Number of Channels Selected 32 kHz Equivalent	N_R = Number Access Per Channel Per Frame	Bit Rate in kHz
4	4	136
5	4	168
6	2	192
7	2	240
8	2	272
9	2	304
10	2	336
11	2	368
12	1	416
13	1	448
.	.	.
.	.	.
.	.	.
.	.	.
60	1	1952
61	1	1984

Frame size in Bits = $8\ N_C\ N_R + 8$.

Bit rate = $32(N_C + \frac{1}{N_R})$ K b/s

The Communications Link Modem

Functional Description

The Communications Link Modem is required to operate over a wide range of data rates. In addition it is required that a high bandwidth efficiency be achieved.

A very complex trade-off between bandwidth efficiency, detection efficiency and ease of implementation was made in establishing the basic design approach for the Link Modem.

A combination of bandpass filtering and baseband pre-distortion filtering was selected as the optimum design to meet these requirements. To achieve this two approaches were considered. In the first approach, the input data bit is pre-distorted into a time varying signal, with an ideal shape of sin t/t. This signal is then used to phase modulate the carrier which results in a rectangular spectrum with no bandpass filtering required. Since the pre-distortion is performed at the digital baseband, it can be made to be all rate. Unfortunately, as it is with all idealised solutions, when it comes to implementing them, finite limitations are incurred. Practical implementation of the pre-distorted signal requires truncation of the sin t/t waveshape. This results in some residual sideband energy which must be removed by either a fixed low pass or bandpass filter, thus reducing the operating data rate range of the modulator. Other limitations incurred are high sensitivity to clock jitter, complexity of circuitry, and speed limitations of semiconductor devices.

The second approach is to use a cosine roll-off spectrum. The impulse response of the composite filter consisting of the pre-distortion and the receive matched filters is given by:

$$h(t) = \frac{\sin \pi t/Ts}{\pi t/Ts} \quad \frac{\cos \alpha \pi t/Ts}{1-4\alpha^2 t^2/T^2 s}$$

where $0.5 \leq \alpha \leq 1$. and Ts = symbol duration.

An analysis of the performance of the modem with these two types of filtering resulted in the data given in Table 3. Based on these data the cosine roll-off spectrum with d = 0.5 was chosen. The shaping is equally distributed between the transmit transversal and the receive transversal filters. That is each filter has the complitude characters tic HIC(f)1 where H(f) is the inverse transform of h(f).

Table 3: Modem Error Budget Comparison

	Implementation Loss in dB	
	Square Spectrum Eb/No = 10dB	Cosine roll-off spectrum Eb/No = 10dB
Carrier Phase Noise	0.05	0.05
Intersymbol Interference	0.95	0.3
Detection Mismatch	0.5	0
Allowable Hardware Degradation	0.4	1.55
Total Allowable Degradation	2.0	2.0

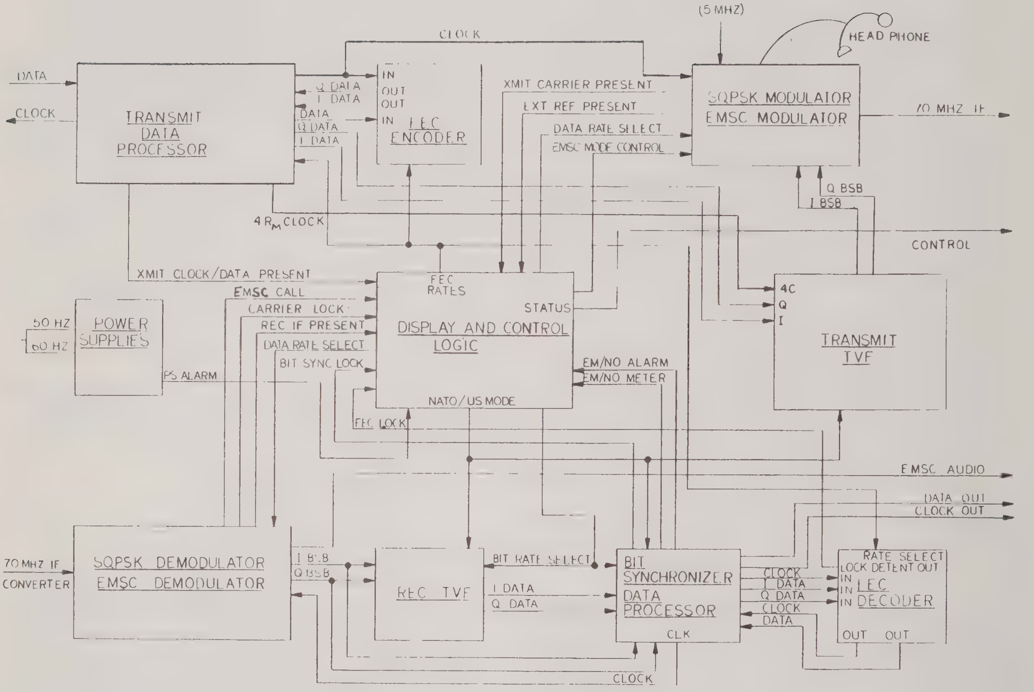
(5 MHZ)
HEAD PHONE
CLOCK
DATA
CLOCK
TRANSMIT DATA PROCESSOR
Q DATA
I DATA
DATA
Q DATA
I DATA
IN
OUT
OUT
IN
FEC ENCODER
XMIT CARRIER PRESENT
EXT REF PRESENT
DATA RATE SELECT
EMSC MODE CONTROL
SQPSK MODULATOR
EMSC MODULATOR
70 MHZ IF
Q BSB
I BSB
4 R_M CLOCK
CONTROL
XMIT CLOCK/DATA PRESENT
EMSC CALL
CARRIER LOCK
REC IF PRESENT
DATA RATE SELECT
BIT SYNC LOCK
FEC RATES
STATUS
DISPLAY AND CONTROL LOGIC
EM/NO ALARM
EM/NO METER
NATO/US MODE
FEC LOCK
50 HZ
60 HZ
POWER SUPPLIES
PS ALARM
4C
Q
I
TRANSMIT TVF
EMSC AUDIO
DATA OUT
CLOCK OUT
70 MHZ IF CONVERTER
SQPSK DEMODULATOR
EMSC DEMODULATOR
I BSB
Q BSB
REC TVF
BIT RATE SELECT
I DATA
Q DATA
BIT SYNCHRONIZER
DATA PROCESSOR
CLK
CLOCK
I DATA
Q DATA
CLOCK
DATA
RATE SELECT
LOCK DETENT OUT
IN
IN
IN
FEC DECODER
OUT
OUT
CLOCK

FIGURE 2: COMMUNICATIONS MODEM FUNCTIONAL BLOCK DIAGRAM

Figure 2 is a functional block diagram of the Traffic Modem. Data from the TDM is fed to the Transmit Data Processor (TDP) which divides the data stream into two channels for the in-phase and quadrature channels which are fed to the Forward Error Correction (FEC) Encoder. Convolutional encoding and Viterbi decoding is used by the FEC to reduce the link error rate. Either Rate 1/2 or Rate 3/4 operation may be selected for the FEC.

The FEC Encoder output is routed through the TDP to the Transmit Tranversal Filter (TVF) which provides the baseband wave shaping required for the a = .5 cosine rolloff characteristic. The TVF converts each data pulse into a shaped pulse consisting of approximately sinusoidal lobes covering ±3 data pulse periods; portions of the shaped waveform due to successive data pulses overlap. The TVF is implemented using a shift register that stores a number of data bits corresponding to the expanded duration of an individual data bit. The contents of the register are used to address a read-only memory that generates a sequential set of digital words that are coded to represent sequential samples of the desired waveform. A D/A converter translates these digital words into an analog waveform for driving the QPSK Modulator.

The Emergency Service Channel (EMSC) analog voice input frequency modulates a sub-carrier that is offset from the QPSK carrier. These two signals are combined in the Modulator Module to form the composite transmit signal which is bandpass filtered to further reduce sideband energy.

The received signal is demodulated using a rather standard times four carrier recovery loop and a bit synchroniser employing a numerically controlled oscillator that is programmed from the Display and Control Logic. The demodulated output signal is processed by a Receive TVF that operates as a matched filter detector to the signal generated by the modulator. The Receive TVF output is processed by the Receive Data Processor (RDP) which generates the "soft decision" input required by the FEC Decoder. The RDP also processes the soft decision data bits to determine the E_m/No of the received signal which is displayed on the modem front panel meter and is also reported to the Control Computer. The modem, when operated in the REMOTE Mode, accepts data rate commands from the Control computer. The status and control signals available to the computer from the modem and the Main TDM provide for the control of data rate and power thus resulting in a network that is adaptable to the varying requirements due to weather conditions and changing traffic loads.

IV. Conclusions

This paper presented the specification and implementation of the digital baseband sub-system of the NATO III Satellite Communications System. The salient characteristics of the system discussed are summarised below:

- Variable data rate capability on a link-by-link basis
- High spectrum efficiency for all rates achieved by digital filtering equipment
- High efficiency software controlled variable rate Time Division Multiplexing for voice traffic
- Plug-in PCM and CVSD modules capable of operation in mixed configuration with the variable rate multiplexer
- Use of CVSD operating at 32 kbit/s for trunk circuits

V. Acknowledgement

The authors of this paper thank the Communications Division of the SHAPE Technical Centre, the SATCOM Project Staff at NICSMA and the Design Staff at FACC for their work which enabled this paper to be written.

References

1. The International Telegraph and Telephone Consultative Committee (CCITT), sixth plenary Assembly, Orange Book Vol. III-1, International Telecommunication Union, 1976.

2. H. G. Suyderhoud et al., "Subjective Assessment of delta modulation in terms of equivalent noise at 16, 24, 32 and 40 kbit/s" Fourth International Conference on Digital Satellite Communications, 23-25 October, 1978.

3. The International Telegraph and Telephone Consultative Committee (CCITT), sixth plenary Assembly, Orange book Vol. III-2 International Telecommunication Union, 1976.

4. Robert Matyas, "Effect of Noisy references on coherent detection of FFSK signals", JEEE transactions on Communications, Vol. COM-26, No. 6, June 1978.

5. S. A. Gronemeyer and A. L. McBride, "MSK and offset QPSK modulation", JEEE Transactions on Communications, Vol. COM-24, No. 8 August 1976.

6. D. F. Harwood et al., "MSK and Offset QPSK through band limited satellite channels" Fourth International Conference on Digital Satellite Communications, 23-25 October 1978.

7. M. I. Celebiler and G. M. Coupe "The effects of filtering, interference and thermal noise in transmission by M-ary PSK carriers", SHAPE Technical Centre Technical Memorandum, STC TM-511, May 1976.

80-0494

AN ADVANCED MIXED USER DOMESTIC SATELLITE SYSTEM ARCHITECTURE*

Herbert G. Raymond
Senior Systems Engineer
Systems Engineering Laboratory
Electronic Systems Division
TRW Defense and Space Systems Group
One Space Park
Redondo Beach, CA 90278

W. Morris Holmes, Jr.
Advance System Engineering Director
for Communication Systems
Space Systems Division
TRW Defense and Space Systems Group
One Space Park
Redondo Beach, CA 90278

Abstract

This paper reports the results of a study performed for NASA LeRC that investigated an advanced TDMA system that permits communications among a mixed class of users. The transmission rate for each terminal is proportional to its information needs. With such a technique, both the efficiency of TDMA operation and the operational terminal flexibility of FDMA can be simultaneously achieved. By combining such a multiple rate architecture with several other key satellite technologies, i.e., a multiple narrow-beam antenna, satellite switching and routing, and on-board regeneration; a cost-effective system can be synthesized that satisfies both the increasing needs of small low-cost ground terminals and the demands of large sophisticated trunking stations.

The operational system concept is described in detail in the NASA study final report (Reference 1).

Introduction

TRW has recently concluded a study of a 30/20 GHz domestic satellite system architecture for the 1990 to 2000 time frame. This architecture mixes various types of users in a single integrated system. Mixed users in this context are defined to include the entire range of communication customers, from large trunking terminals with data rates approaching gigabits to the smallest user whose terminal supports one or more digital voice circuits and is located at the user's location. This terminal is known as a customer premises service (CPS) terminal.

The mixed user TDMA/FDMA architecture described here allows users to select TDMA burst data rates that minimize their costs and still permit efficient use of the available spectrum. The system architecture proposed to accomplish these goals employs a very sophisticated satellite payload. This payload exploits advanced processing techniques to accommodate a hybrid TDMA/FDMA format and provides a degree of interconnectivity unavailable in current or planned domestic satellite systems. The rationale for this approach of concentrating the system complexity in the spacecraft is primarily economic. The ground rules of the NASA study required that the satellite architecture be capable of servicing a very large number of CPS customers. In order to minimize system cost and provide cost-effective communications, a large, high-capacity system must be employed where reasonable economics of scale are available to all users. Furthermore, in a system with several thousand terrestrial terminals, satellite capability must be maximized even at the expense of more costly satellites, so that terminal unit cost can be minimized. This effort to transfer complexity from the user terminal to the satellite has been only partially successful, since the CPS terminal in the proposed architecture is still more complex than desired. Further refinement of the mixed-user techniques developed in our study is needed to provide additional reductions in terminal costs.

An artist's conception for the type of satellite required by the mixed user architecture is shown in Figure 1. It is a large, high-power, synchronous - orbit, three-axis stabilized satellite employing complex multiple-beam parabolic antennas. It also possesses a high-speed baseband processor to permit not only regeneration of the incoming signal but also demultiplexing, and routing to facilitate a high degree of network interconnectivity.

User Traffic Model

The postulated 20/30 GHz mixed user system accommodates a total traffic demand of 10 Gbps. This requirement was generated from data resulting from traffic demand studies by ITT and Western Union (Reference 2). Eight Gbps of the system traffic is generated by users located in 18 high traffic density regions and covered by fixed antenna beams as shown in Figure 2. The other 2 Gbps of system traffic is generated by users outside these areas. Coverage for these users is provided through multiple scanning beams which scan the rest of the area within the forty-eight contiguous states. Of the 10 Gbps total data flow in the fully loaded system, about 8 Gbps is trunking data and 2 Gbps is CPS traffic. The split between high density and low density regions and between trunking and CPS traffic is not independent, since a large portion of the CPS traffic originates within the high density regions.

To accommodate this situation the traffic has been divided in two classes: SSTDMA-switched data and demodulated/processed/remodulated data. When the data is divided in this way, the allocation between classes is 7 Gbps SSTDMA-switched and 3 Gbps processed. The 7 Gbps consists only of data flowing between the large trunking terminals located in the high density areas. The 3 Gbps consists of all CPS traffic (including cross traffic between the CPS and trunking users) and all trunking data from terminals outside the high density areas, i.e., the so-called "thin-route" stations.

System Architecture

The mixed user architecture has been formulated to accommodate two widely disparate user communities in a single integrated satellite system. This

---

*This paper reports work carried out under Contract NAS3-21933 sponsored by NASA Lewis Research Center.

Released to AIAA to publish in all forms.

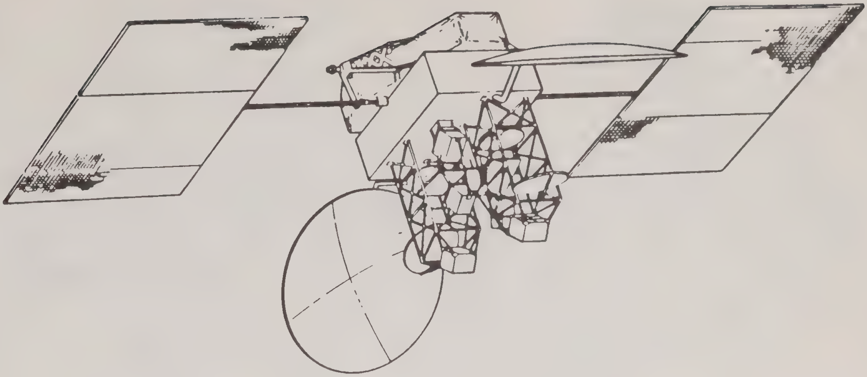

Figure 1. Satellite Design

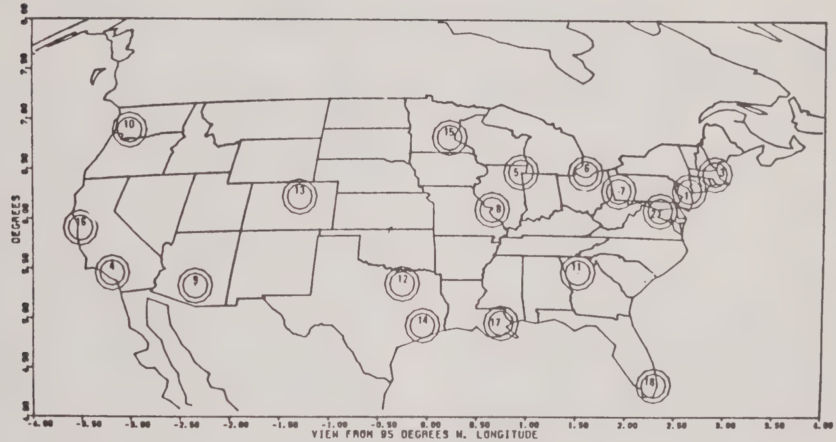

Figure 2. High Density Coverage

provides trunking economies-of-scale to the direct user, but more importantly, permits a high degree of interconnectivity. This can be illustrated by considering the network topologies used to satisfy each user class.

Traditionally the trunking users satellite requirements are met by using a highly interconnected topology. In Figure 3 the interconnection diagram for the net-connected trunking users shows the most extreme case of this topology; a fully-connected network where every node is connected to all other nodes. The SSTDMA trunking subsystem employed in this architecture provides interconnectivity among all pairs of trunking users for some fraction of the total TDMA frame. But in a cost-effective system the CPS users cannot afford the terminal complexity required to communicate in such a network. Small users require the assitance of a central switching node to handle interconnection problems for them. The classical topology for this class of users is the star network also shown in Figure 3. Here each node is connected to a single central node and all communications among users flow through that node. Hardware located at that node may provide services, e.g. routing, to all users in the network.

In a satellite communication system handling voice (telephone) traffic, such a node must be located on board the satellite to avoid introducing multiple transmission delays in the signal path. For traffic types where circuit delays are less important, a central node could be located at a terrestrial terminal which would then connect to the satellite by communication links.

Complete interconnectivity among direct users through the central node is only one advantage

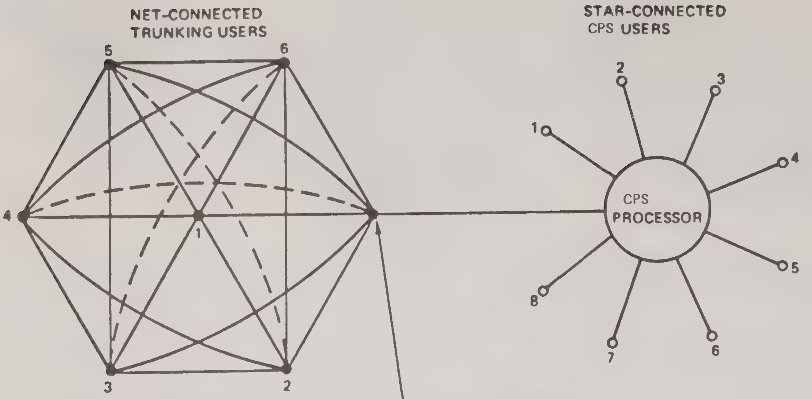

- 6 TRUNKING USERS SHOWN. EACH LINK IS 2-WAY THROUGH SATELLITE TRUNKING BMA AND SSTDMA SWITCH

PSEUDO-TRUNK USER
ON-BOARD SATELLITE
SYSTEM INTERCONNECTION

- 8 CPS USERS SHOWN. EACH LINK IS 2-WAY. SOME THROUGH TRUNKING MBA SSTDMA SWITCH TO CPS PROCESSOR. SOME THROUGH CPS TRANSMIT AND RECEIVE MBA's

Figure 3. System Network Concept

offered by the proposed satellite system. Additionally the mixer user architecture permits interconnectivity between trunking and CPS users as shown schematically in Figure 3. Satellite interconnection as represented by the psuedo-node of the fully-connected network, allows the mixed user architecture to offer a number of network advantages not available (or difficult to implement) in two separate satellite-based systems. First, it provides CPS users access to the trunking network and its community of users on a single-loop basis. Second, it permits the common carriers operating the trunking network to off-load a significant portion of their business traffic directly into the CPS networks, thereby providing additional network capacity to the trunking community. This approach also permits the minimization of trunking "tails" by providing economical access for thin-route trunking stations to the satellite trunking network through the use of smaller less expensive terminals similar to the CPS terminals.

The key to this mixed user topology is a Satellite-Switched Time Division Multiple Access (SSTDMA) technique with varying user burst rates. In such a SSTDMA system all users share a common time reference and interconnectivity is achieved by switching sequentially among various user pairs. Since each transmitter is assigned a specific segment (or slots) of the TDMA frame that is independent of other users, there is no need for adjacent slots to operate at the same burst rate. Theoretically, each user pair that communicates within each time slot is free to transmit at a different burst rate. (In a practical system a limited number of burst rates would be employed.) Because of the capability of SSTDMA to accommodate different burst rates, individual user terminals can match their burst rates to their information needs in a manner analogous to FDMA operation. The small user with limited information needs is not constrained to operate at the burst rate required by the largest users in the system, as required in conventional TDMA systems.

With multiple beam antennas, a large number of users can simultaneously access the satellite using a number of different burst rates. Moreover, since the lower burst rates require less bandwidth than the higher burst rates, time slots may be shared using FDMA techniques. An illustration of this process is given in Figure 4. The timeline shown in this figure assumes six beams (each centered on a single large trunking station in six different cities) which are used simultaneously for both uplink and downlink communications. The Chicago trunking station in this illustration is sequentially connected to the New York, Los Angeles and Atlanta stations for a specified (unequal) time period. Moreover, while Chicago is transmitting to New York, Los Angeles can be transmitting data to San Francisco, and Atlanta can be transmitting data to Cleveland.

Trunking users make the most efficient use of this bandwidth during their appropriate time slots by transmitting at the maximum data rate that this bandwidth can support. Note that after Chicago had been connected to all the trunking stations, there remains some time left within the TDMA frame. This time can be used by smaller, lower-rate users as shown in the figure. In the example there are two burst rates for these CPS terminals, 125 Mbps and a lower rate compatible with a 31.25 MHz bandwidth. Thus the 500 MHz channel can be subdivided into four 125 MHz bands with one of the 125 MHz band further divided into four 31.25 MHz bands. Thus, seven CPS users can simultaneously access the satellite (at differing burst rates) in the same bandwidth used by a single trunking user. Moreover, the time remaining in the TDMA frame can be subdivided to permit several CPS users to access the satellite in each of these subbands. The flexibility of such an approach is readily apparent. The low burst rates available to small CPS users reduce EIRP and G/T requirements. This results in significantly lower terminal costs for these users and make this mixed user architecture very attractive.

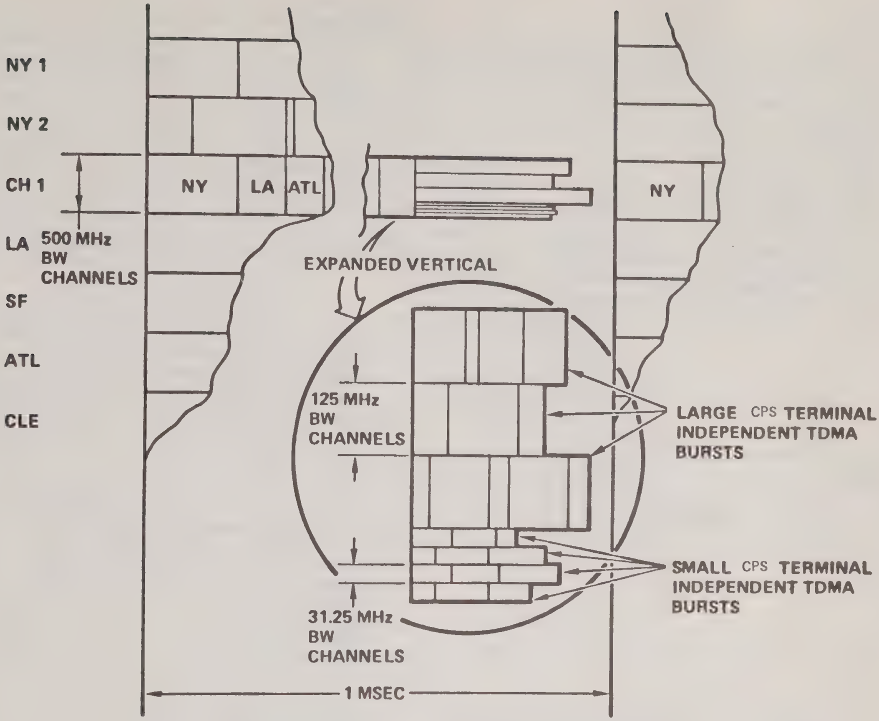

Figure 4. SSTDMA Frame Timeline, Fixed Beams

The satellite communication subsystem architecture needed to realize this operational approach and to provide the previously discussed network interconnectivity is shown in Figure 5. The system employs two types of satellite antennas to service the combined trunking and CPS user community. A fixed multiple beam antenna (MBA) provides coverage to the 18 largest population centers. All users within these coverage areas, both trunking and CPS, access the satellite through these beams. Both transmit and receive functions can be accommodated by a single antenna. The remainder of the country is covered by scanning beam antennas which covers their service areas in a programmed sequential manner. Both CPS and trunking users can communicate with the satellite through these scanning beams.

Lower-rate signals accessing the satellite through the receive scanning beam antenna are demodulated by on-board demodulators regardless of whether they are from CPS or trunking users. Demodulated bit streams are demultiplexed, buffered and routed to the appropriate transmitter by the onboard processor. Signals destined for large trunking users are combined into a composite trunking channel and routed through the SSTDMA switch to the appropriate fixed beam. Similarly a small portion of the signals from large trunking users are demodulated, buffered, and input to the processor for routing to CPS and small trunking users.

Users in the fixed beams follow a different processing technique in the satellite. Incoming signals from the fixed beam MBA are segregated into two classes by the SSTDMA switch. Signals being routed between high-rate trunking users are completely routed by the SSTDMA switch. High rate trunking signals intended for CPS users or small trunking users, as well as signals from the CPS users are routed to the on-board processor via demodulators. This occurs even for those CPS users wishing access to the trunking network, since a data rate conversion is required.

Link Characteristics

The trunking system channel burst rate, or peak data rate during TDMA bursts, has been set at 500 Mbps. It is important to note that in a TDMA system, the channel burst rate does not need to have any particular relationship to standard terrestrial trunking data rates, since all interfacing occurs through burst buffers which change data rate. The 500 Mbps rate was selected on the basis of technology projections and a reasonable match to the largest trunking channel requirements.

The Metropolitan New York area is an exception to this comment, since it requires trunking data rates in excess of the 500 Mbps burst rate. Providing adequate capacity to this very high traffic-density area can be accomplished by using two or

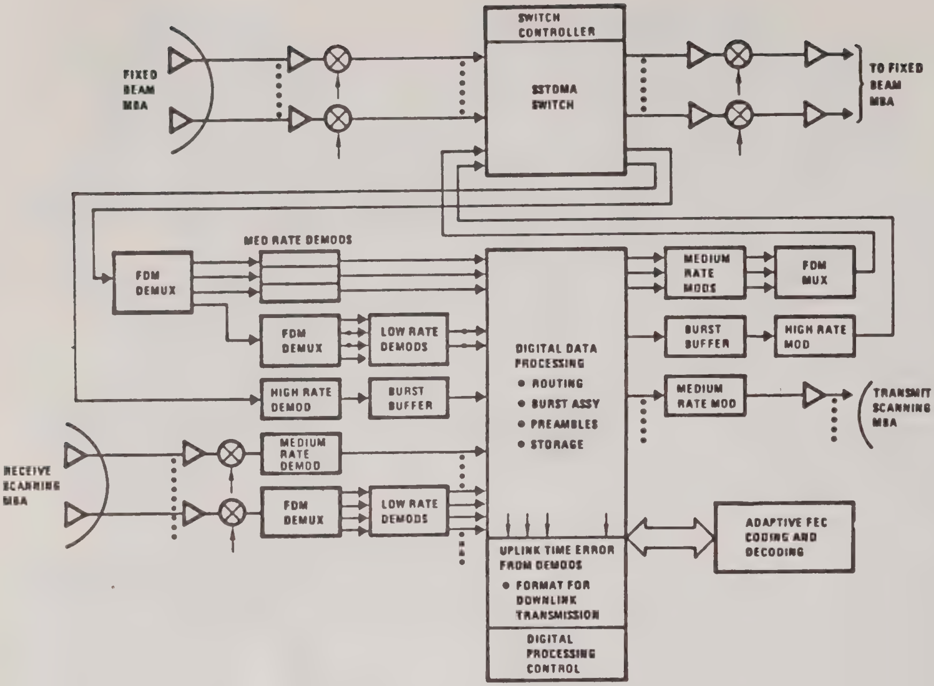
SWITCH CONTROLLER
FIXED BEAM MBA
SSTDMA SWITCH
TO FIXED BEAM MBA
MED RATE DEMODS
FDM DEMUX
MEDIUM RATE MODS
FDM MUX
FDM DEMUX
LOW RATE DEMODS
BURST BUFFER
HIGH RATE MOD
DIGITAL DATA PROCESSING
• ROUTING
• BURST ASSY
• PREAMBLES
• STORAGE
HIGH RATE DEMOD
BURST BUFFER
MEDIUM RATE MOD
TRANSMIT SCANNING MBA
MEDIUM RATE DEMOD
RECEIVE SCANNING MBA
FDM DEMUX
LOW RATE DEMODS
ADAPTIVE FEC CODING AND DECODING
UPLINK TIME ERROR FROM DEMODS
• FORMAT FOR DOWNLINK TRANSMISSION
DIGITAL PROCESSING CONTROL

Figure 5. Satellite Communication Subsystem Block Diagram

more independent links. Increasing the channel burst rate to match this single area would not be a cost-effective solution, since this would result in increased receiver costs and reduced performance margins for all trunking stations.

In a reversal of most satellite link design, the CPS uplink is the limiting factor in overall CPS system operation, since the uplink rain margin to achieve the required 0.999 availability is significantly greater than the downlink margin. Thus, CPS uplink channel burst rates must be minimized to reduce the terminal EIRP requirement. Because the terminal transmitters are peak power-limited, any reduction in uplink burst rate provides a proportional reduction in the required transmitter power. Uplink burst rate reduction at the price of increased satellite receiver complexity appears to be a valid trade-off approach.

To implement this trade, multi-beam receive arrays (which seem to be simpler than high-efficiency multiple-beam transmit arrays) have been employed on the satellite. Using FET-element receivers, the number of simultaneous receive beams is limited only by the amount of beam-forming hardware in the satellite.

A compromise between satellite complexity and user terminal requirements is needed. With a large number of uplink beams and a high degree of satellite complexity, the optimum solution for minimum CPS terminal cost appears to be to provide variable data rate transmission for each terminal, with multiple terminals in a given antenna beam accessing the satellite in a FDMA format. This approach minimizes the EIRP requirement and/or maximizes the rain margin for each terminal.

A detailed design of the satellite receiving system complexity with the terminal costs as a parameter is required to minimize the overall system cost. Such a trade study was not conducted as part of this effort, because of funding limitations and because the conclusions would be heavily dependent on 1990 state-of-the-art technology which is difficult to predict at this time. The approach utilized in the study was to select a "reasonable" set of design parameters.

Because the minimum data rates within each low density region was found by the traffic model to be less than 125 Mbps, this rate was selected as the upper bound for the CPS uplink channel burst rate. Lower burst rates were provided to reduce EIRP requirements for the many users with information needs less than 1 Mbps. However, these rates should be some submultiple of the basic rate with very low rates avoided since they may make the satellite too complex.

The baseline uplink design in this study settled on two CPS channel burst rates, 125 and 25 Mbps. The number of burst rates and their exact rates, however, need to be reevaluated for the operational system. The design trade-off determining uplink data rate flexibility by balancing terminal EIRP impact against satellite complexity is a major, critical design trade, and as such should be constantly reevaluated as technology advances.

One of the prime features of a satellite payload employing baseband processing techniques is that the CPS downlink channel burst rate selection can be made independently of the uplink selection due to the capability of the on-board processor to change burst rates. This is central to the utility of the proposed approach since the factors affecting uplink and downlink channel burst rate selection are very different.

The desire to use high-efficiency TWTA transmitters rather than solid-state amplifiers drives the system design towards a smaller number of higher burst-rate, simultaneous, downlink antenna beams. Also, FDM operation which is very attractive for uplinks, is not an efficient use of a single TWTA, because of intermodulation losses. The FDM advantage of the CPS uplink consists of allowing many CPS terminal transmitters to operate simultaneously. Because the number of transmitters available on-board the satellite is limited, there is no similar advantage on the downlink.

By using microwave LSI techniques with batch fabrication, the cost effect of high downlink burst rates on CPS terminals should be small for burst rates as high as several hundred, perhaps even five hundred, megabits per second. Minimizing the CPS terminal G/T requirement is a much better criteria for downlink design than minimizing burst rate. The baseline CPS downlink burst rate selected was 250 Mbps. This rate also is critically effected by technology development and must be reviewed at the time the operational system is developed. For a more detailed description of the on-board processing subsystem and the CPS terminal characteristics the reader is referred to Reference 3.

Conclusions

A domestic satellite system architecture that can efficiently and economically accommodate a wide variety of disparate user classes has been developed and a baseline system configuration identified. This approach provides the flexibility of TDMA operation with the cost attractiveness of FDMA systems. The architecture is still embryonic and requires additional study both to identify detail design requirements and to evaluate its cost-effectiveness for the various user classes. Its promise is so great, however, that not only should the study efforts be continued but a technology program to demonstrate selected key technologies, e.g. the baseband processor, scanning beam antenna, and on-board modems should be initiated.

References

1. NASA CR-159687, Final Report, "30/20 GHz Mixed User Architecture Development Study," TRW Inc., Prepared for NASA Lewis Research Center under contract NAS-3-21933.
2. Unpublished Presentation Charts, Western Union and ITT Study Results, NASA/LeRC, June 1979.
3. W. Morris Holmes, Jr., "Multigigabit Satellite On-Board Digital Processing," this conference, session on Advanced Satellite Communication Systems.

80-0498

PUBLIC SERVICE SATELLITE APPLICATION AFTER WARC-79

Dr. Peter McManamon
Associate Director
Institute for Telecommunication Sciences
National Telecommunications and Information Administration
Boulder, Colorado

Abstract

International frequency allocations and regulations have been reviewed and revised at the 1979 General World Administrative Radio Conference (WARC). Those changes which concern U.S. public service satellite communication applications are reviewed. The 1979 WARC results will have favorable impact on possible U.S. applications including thin-route, small earth terminal systems.

Introduction

Applications of satellite telecommunications for public services have shown dramatic recent growth. Some principal examples are the Public Broadcasting System television distribution network of CPB, the venture of National Public Radio into satellite networks, the emerging Community Service Network (CSN), the National Satellite Network of the Public Service Satellite Consortium (PSSC), and the new forum provided by the Cable Satellite Public Affairs Network (C-SPAN) of the National Cable Satellite Corp.[1] Millions of CATV network subscribers benefit from satellite program distribution.

Service applications cover a wide range. Television broadcast of activities on the floor of the House of Representatives is provided by C-SPAN. The National Telecommunications and Information Administration plans to fund wholesaler organizations to operate and manage communication systems with distributed video service for public service users and a Federal teleconferencing/training system of one-way distribution of video.

Public service communities are beginning to realize some of the economic benefits of satellite networks. In the applications served by one-way video distribution networks, satellite communications offers cost benefits over terrestrial network services.[2]

To the present time, operational domestic public services provided by satellite have been in the domestic satellite common carrier frequency allocations known as the 4/6 GHz bands. These allocations of 3.7-4.2 GHz (downlink) and 5.925-6.425 GHz (uplink) are utilized by the U.S. domestic Fixed Satellite Services (FSS) of WESTAR, SATCOM and COMSTAR.

Many organizations tested the technological and service potential of satellite communications through the use of NASA applications satellites in the ATS series and the U.S.-Canada CTS satellite. ATS-6 provided experiments in the 2.5-2.690 GHz downlink allocation. The CTS satellite utilized the down/up allocations of 11.7-12.2 GHz and 14.0-14.5 GHz. These pilot programs served many purposes including contributing to a better understanding of the various relationships between service applications, technology, spectrum-orbit policies and spectrum allocations.

Future public service applications will expand beyond the 4/6 GHz systems, particularly in today's competitive growth environment for satellite transponder use. Expansion to higher frequency allocations will permit the introduction of new technology and services.

Public Service Interests Before WARC-79

The public service community was an interested party in the preparations for the World Administrative Radio Conference for Broadcasting Satellites (WARC-BS) in 1977. That conference introduced the policy of orbit arc segmentation to the BSS and FSS allocations at 11.7-12.2 GHz in ITU Region 2 (North and South Americas). Also, the concept of orbit and channel planning was implemented in the 11.7-12.5 GHz allocation of Region 1 (Europe, Africa, and USSR) and the 11.7-12.2 GHz allocation of Region 3 (Asia and Oceania). Planning of the 11.7-12.2 GHz allocation and orbit for the Region 2 BSS was delayed to a future conference to be devoted to this purpose in 1983.

In the preparations for the 1979 General WARC, the substantial growth of operating and planned satellite systems by U.S. domestic satellite common carriers created considerable need for additional spectrum for the FSS. The needs were shared by the public service sector. As noted earlier, the 4/6 GHz bands provide all of these services now.

INTELSAT growth led to similar needs for spectrum expansion of FSS international services. In Region 2, other administrations identified plans for the BSS and other services. Most parties, including the public service sector, noted the need for added spectrum for both the FSS and BSS. These needs were addressed during the Federal Communication Commission (FCC) preparations and Notices of Inquiry. The Eighth Notice of Inquiry[3] and an analysis of related questions[4] brought many of these issues and needs together. The U.S. position for the 1979 WARC[5] was published in late 1978. A subsequent sharing study outlines the difficulties inherent in the process of satisfying demands for new spectrum allocations.[6]

1979 WARC Results for Public Service Users

The 1979 WARC Final Acts[7] must be consulted for definitive information since many new footnotes have been added. Hence, the allocation tables cannot be consulted without reviewing the applicable footnotes.

Downlinks

No change in allocation was made at 620-790 MHz.

In the 2500-2690 MHz pre-WARC (1979) allocation, an FSS downlink was added at 2535-2690 MHz in ITU Region 2. In the 2500-2690 MHz band, the power flux density limits for satellite transmissions in the BSS were not changed and the power flux density

This paper is declared a work of the U.S. Government and therefore is in the public domain.

limits of the FSS were changed to equal those for the BSS in this band. These changes are beneficial for the public service sector since many existing and planned services are FSS as opposed to BSS. Use of this band for satellite services will require development of sharing criteria and considerable coordination in the United States especially with the Instructional Television Fixed Service.

In Region 2, the BSS allocation was moved from 11.7-12.2 GHz to the 12.1-12.7 GHz band with 12.1-12.3 GHz shared with the FSS until the 1983 Regional Administrative Radio Conference (RARC). The FSS (downlink) allocation was extended to cover 11.7-12.3 GHz until the 1983 RARC. The arc segmentation plan of the 1977 WARC-BS was eliminated.

In addition, the lower band of 11.7-12.1 GHz may also be used for BSS transmissions as long as the satellite equivalent isotropically radiated power (e.i.r.p.) does not exceed 53 dBW per television channel and interference is no greater than FSS assignments. Also, the 12.3-12.7 GHz band can be used for the FSS subject to the condition that such FSS transmissions do not cause greater interference than BSS transmissions. The band 12.1-12.3 GHz will be divided at the 1983 RARC into two sub-bands. The lower sub-band will be allocated to the FSS. The upper sub-band will be allocated to the BSS, broadcasting, mobile (except aeronautical mobile) and fixed services, all services being on a primary basis.

The 11.7-12.7 GHz band now provides much greater capacity and flexibility to meet the needs in the FSS and BSS. Under suitable sharing criteria, the concept of hybrid satellites can be implemented, if appropriate.[8]

The allocation of the 22.5-23.0 GHz band to the BSS in Region 3 was extended to Region 2.

Uplinks

Prior to the 1979 WARC, the need for additional uplink allocations for both the FSS and BSS was considerable. Additional FSS (uplink) allocations were made for Region 2 in the bands of 4.5-4.8 GHz, 6.425-7.075 GHz, 12.75-13.25 GHz, 17.3-18.1 GHz and 27-27.5 GHz. The uplink FSS band of 17.3-18.1 GHz will be planned at the 1983 RARC in conjunction with the BSS downlink planning of the fx-12.7 GHz band where fx is to be selected from the range 12.1-12.3 GHz at that conference.

While sharing criteria for uplink FSS use will be important to achieve full utilization of these allocations, the expanded spectrum capacity creates new opportunities for thin-route satellite systems.

References

1. Hill, D.A. (1979), Public Service Satellite Programming: Coming of Age, Satellite Communications, May.
2. McManamon, P., P. Wells, and J. Payne (1979), Public Service Satellite Video Network Costs, EASCON Conference Proceedings, Vol. 3, pp. 536-542, Washington, DC, October.
3. FCC (Federal Communications Commission) (1978), Eighth Notice of Inquiry, in the matter of an inquiry relative to preparation for a General Administrative Radio Conference of the International Telecommunication Union to consider revision of the international Radio Regulations, Docket No. 20271, released May 5, 1978. (The full text was not published in the Federal Register. See the short notice, Federal Register, 43, p. 18748, May 2, 1978.)
4. Akima, H., P.M. McManamon, and P.I. Wells (1978), Fixed-Satellite and Broadcasting-Satellite Service Considerations for 1979 GWARC Planning, NTIA Special Publication 78-2, October.
5. FCC (1978), Report and Order, Docket No. 20271 (see Reference 3 above), released December 28, 1978. (The full text was not published in the Federal Register. See the short notice, Federal Register, 44, pp. 2683-2685, January 12, 1979.)
6. Akima, H. (1980), Sharing of the Band 12.2-12.7 GHz Between the Broadcasting-Satellite and Fixed Services, private communication.
7. ITU (International Telecommunication Union) (1979), Final Acts of the World Administrative Radio Conference, ITU, Geneva, Switzerland.
8. McManamon, P.M. (1979), A Hybrid Satellite for Pacific Nations Using Small Earth Stations, Pacific Telecommunications Conference Proceedings, pp. 4B-24/4B-33, Honolulu, Hawaii, January.

80-0499

SATELLITE BROADCASTING AFTER WARC-79

Robert R. Bowen*
Department of Communications,
Ottawa, Ontario
Canada

Abstract

At the 1979 WARC six frequency bands were allocated for broadcasting by satellite: the 700 MHz band, the 2.5 GHz band, the 12 GHz band, the 23 GHz band, the 41 GHz band, and the 84 GHz band. The different bands are regulated in different ways: some are subject to agreement of neighbouring administrations, some are subject to power flux density constraints, some have specific uplinks associated with them. In the near term the 12 GHz band seems the most desirable for broadcasting satellite application, with perhaps the 2.5 GHz band as alternate choice.

Satellite Broadcasting After WARC-79

1. Introduction

The 1979 WARC allocated, or reallocated, a total of six bands to broadcasting by satellite: the 700 MHz band, the 2500 MHz band, the 12 GHz band, the 23 GHz band, the 41 GHz band, and the 85 GHz band. None of these are entirely new bands, although some are shifted in centre frequency, changed in bandwidth, or are allocated differently in different Regions. Two other significant developments are, first, that in two cases, the 2.5 GHz band and the 12 GHz band, spectrum is shared between the fixed-satellite and broadcasting-satellite services, and second, that in the case of the 12 GHz and 41 GHz bands specific fixed-satellite uplink bands are to be used as feeder links. A third factor is that only in the case of the two lowest bands are there power flux density (p.f.d.) constraints applied to satellite transmissions.

Each of these bands is considered in turn, leaving the 12 GHz band till last because the regulations governing its use are by far the most complex.

2. Specific Broadcasting-Satellite Bands and Their Use

2.1 The 700 MHz Band:

This band, a maximum of 170 MHz wide from 620 to 790 MHz, can be used on a subject-to-agreement basis for frequency-modulated signals, providing that the p.f.d. is no greater than -129 dBW/m^2 per television signal. It may be noted that if an 800 KHz wide spectrum-spreading signal format is used, this power constraint is the same as that for low elevation angles in the 2.5 and 4 GHz bands.

This band is used by the Stationar-T system of the USSR. No changes in the allocation were made at the 79 WARC. However, given the increasing use of the band for terrestrial TV broadcasting, and also by fixed and mobile systems in some locations, it is not seen as an attractive band for satellite-broadcasting, when compared with the 2.5 GHz and 12 GHz bands.

2.2 The 2.5 GHz Band:

There were no changes made at the 79 WARC to the use of the 2.5-2.69 GHz band by broadcasting-satellites. The p.f.d. limits remain the same, at levels very similar to those imposed on the fixed-satellites at 4 GHz. Again, as with the 4 GHz fixed-satellite band, the most attractive uplink is at 6 GHz. The major constraint of this band is its narrow width and, therefore, capacity, although the INSAT satellite system of India uses this band, and it is planned that the ARABSAT satellite will also use the band.

The major change at the WARC was not in the broadcasting-satellite service, but rather in the fixed-satellite service in the same band. Before the WARC, there were two 35 MHz bands for fixed service in the overall band, one uplink and one downlink, on a world-wide basis. In Region 2 only, the fixed-satellite downlink band was extended over the full 190 MHz with the same p.f.d. constraints as those for the broadcasting satellites. These regulations will allow such services as tele-health and tele-education, that were and are being developed in the ATS, HERMES, and ANIK-B programs, to be implemented at 2.5 GHz, without debate as to whether the use is in the fixed-satellite or broadcasting-satellite service. This situation also exists in the new regulations at 12 GHz, as is indicated below.

2.3 The 23 GHz Band:

Before the 79-WARC, the band 22.5-23.0 GHz was allocated to the broadcasting-satellite service in Region 3 only. At the WARC this allocation was extended to also include Region 2. No p.f.d. limitations were imposed on this service, but use is on a subject-to-agreement basis. A new fixed-satellite uplink for Regions 2 and 3 was allocated from 27.0 GHz to 27.5 GHz, but no constraints are imposed on the use of this uplink band.

The band is not as attractive as the 12 GHz band, primarily because of the much larger rain attenuation at

---

*Chief, Spectrum/Orbit Planning,
Space Programs Branch,
Department of Communications

This paper is declared a work of the Canadian Government and therefore is in the public domain

the higher frequencies, and because components are not yet available at low cost at these frequencies. Moreover, it is not expected that an individual user would have a terminal at both 12 GHz and 23 GHz, and so it is not likely to be developed for direct-to-home use in the near future. It might, however, have application for delivery of high-definition television signals, either for individual or community use.

2.4 The 41 GHz and 84 GHz Bands:

Each of these frequency bands has a bandwidth of 2 GHz, without any p.f.d. constraints. The intended uplink for the broadcasting-satellite systems in the 41 GHz band is at 47.2 to 49.2 GHz (by footnote 3814B), but there is no specific uplink associated with the 84 GHz downlink. The only advantage in using these bands is the wide bandwidth available. The disadvantages are the unavailability of subsystems and the large propagation losses that would be encountered in rain and even due to water vapour. It is not expected that these bands will have widespread operational use in this century.

2.5 The 12 GHz Band:

There were significant changes in the allocation of space services in the 12 GHz band and/or associated uplinks in all three Regions.

In Region 1

There were no changes in the downlink allocation of 11.7-12.5 GHz at the 79 WARC. Rather, the allocation changes were to provide sufficient uplink bandwidth in the 10 to 20 GHz portion of the spectrum. There is now a significant excess of uplink spectrum, primarily to meet the diverse requirements of different administrations. In addition to the 12.75-13.25 GHz band and the 14.0-14.5 GHz band, thought of as uplinks for the 10.7-11.7 GHz fixed-satellite band, there are three bands dedicated for use as broadcasting-satellite feeder links: 10.7-11.7 GHz, 14.5-14.8 GHz, and 17.3-18.1 GHz, a total of 2100 MHz uplink bandwidth for 800 MHz downlink bandwidth. Given this amount of excess spectrum, it is not evident how the feeder links to 12 GHz broadcasting-satellites will be planned for Regions 1 and 3 in 1984.

In Region 2

Quite significant changes were made to the 12 GHz allocations in Region 2. Moreover, the changes are not yet complete, but are expected to be completed at the 1983 Regional Conference. In addition to three allocated bands between 11.7 GHz and 12.7 GHz there are nine footnotes referring to the use of the band in the region, and five Resolutions, made part of the regulations through a linking footnote. A complex package, which can perhaps best be understood by thinking of it as those aspects which affect Region 2 only, and those which affect the sharing between Region 2 and the other two regions.

Let us concentrate on Region 2 per se first. The lower band, from 11.7 GHz to somewhere between 12.1 GHz and 12.3 GHz, is to be used primarily in the fixed-satellite service, but can also be used for satellite broadcasting as long as the broadcasting-satellite has a boresight EIRP not more than 53 dBW. The higher band, from somewhere between 12.1 GHz and 12.3 GHz to 12.7 GHz, is to be used primarily for satellite broadcasting. This band will be planned in 1983, in much the same way as planning was done at the 1977 WARC, but not necessarily with the same technical parameters. Moreover, channels allotted to a given administration in that plan can be used also in the fixed-satellite service. The actual division point between the upper and lower band will be determined in 1983.

These new allocations allow implementation of satellites such as ANIK-B, ANIK-C, and the SBS satellite in the lower band, and broadcasting-satellites in the upper band. They also allow for dual-purpose satellites to be used in either the lower or upper bands, with the higher-power satellites presumably in the upper band. The ability to use such dual-purpose single-band satellites is important for the initial development of a satellite network, for use by developing countries, and for the provision of a variety of services such as telephony, television-delivery, tele-health, and tele-education to a remote community or location at minimum cost. As previously mentioned, this multi-purpose capability is also possible in the 2.5 GHz band.

With respect to consideration of potential inter-Regional interference effects, Resolutions CI, CJ, CK, and CL reflect a major effort at the 1979 WARC to extend the 77 WARC Final Acts into the new bands and to account for situations not envisaged in 1977. Detailed analyses of a number of interference situations will have to be made, and inter-Regional agreements made as part of the 1983 RARC planning process. These analyses include the sharing between fixed-satellite and broadcasting-satellite systems serving different regions, and also the permissible levels of interference between satellite systems and terrestrial fixed systems. However, given the technical characteristics of the systems involved, and their locations, no serious problems are foreseen.

It should be noted that the prime uplink band for satellites in the upper band in Region 2 will be the 17.3 to 18.1 GHz band, with the 14.0-14.5 GHz band used for satellites using the lower downlink band. The upper band will be planned in 1983 as part of the BSS planning process.

In Region 3

Before the '79 WARC, the 11.7-12.2 GHz band was allocated to BSS in Region 3, and planned at the 77 WARC. At the '79 WARC it was decided that the 14.5-14.8 GHz band and the 17.3-18.1 GHz band would be used as uplinks to the planned systems. The major reasons for requesting the 14.5-14.8 GHz band as well as that at 18 GHz were that rain attenuation is greater at the higher band, and that equipment was not available at the higher band.

New downlink allocations were made for Region 3 use above 12.2 GHz, for both fixed-satellite and broadcasting-satellite use. Specifically, broadcasting-satellites can be operated in Region 3 on condition that the p.f.d. per television program does not exceed -111 dBW/m^2, i.e. that the satellite EIRP does not exceed about 55 dBW. Based on Canadian experience in its HERMES and ANIK-B programs, this is not a serious constraint, even for the implementation of a direct-to-home broadcast system.

3. Summary

There are a total of six distinct frequency bands available for satellite broadcasing, if one considers the various allocations at 12 GHz as a single band. Of these six it is expected that the three at higher frequencies, certainly the two at 41 GHz and 84 GHz, will not be used in the short term for direct-to-home transmission, because the technology is not developed at the higher frequencies and because of the higher inherent propagation losses at these frequencies. Further, the 700 MHz and 2.5 GHz bands have limited usefulness because of the narrow bandwidth available and because of the severe p.f.d. constraints imposed by the WARC. Thus the 12 GHz band is clearly the most suitable for direct-to-home television delivery in the foreseeable future. It is expected that the 1980's will see the development of several such systems in Region 2, particularly after the 1983 Regional Conference. There is already a set of field trials underway in Canada for one such system, using the ANIK-B and possibly ANIK-C satellites, in the 11-7-12.2 GHz band.

80-0501

FLIGHT PERFORMANCE OF THE LES-8/9 THREE-AXIS ATTITUDE CONTROL SYSTEM*

Dr. Franklin W. Floyd**
Carl H. Much+
Dr. Norval P. Smith+
Joseph R. Vernau+
John P. Woods+

Massachusetts Institute of Technology, Lincoln Laboratory
Lexington, Massachusetts 02173

Abstract

The Lincoln Experimental Satellites 8 and 9 were developed for the US Air Force and Navy by MIT Lincoln Laboratory and have been operating successfully in synchronous orbit since March, 1976. This paper is the first report in the open literature on the three-axis stabilization systems of these satellites. We briefly review the system design and describe its flight performance and some of the lessons learned during four years of flight experience. We emphasize material that we hope will benefit other satellite programs. The topics include: use of an experimental gyro, platform jitter, fuel consumption, ball-bearing life and finally, a review of the brief list of problems encountered in orbit.

I. Introduction

The Lincoln Experimental Satellites 8 and 9 were launched into geosynchronous, ecliptic orbits, aboard a Titan III-C on 15 March 1976. Since then they have successfully demonstrated several new techniques in strategic space communications(1,2) with emphasis on survivable, anti-jam links between mobile terminals (see Fig. 1). LES-8 and -9 communicate by crosslinks from satellite to satellite as well as with earth terminals. Table 1 summarizes the principal features of these satellites. The general arrangement of LES-9 is illustrated in Figure 2. LES-8 is essentially identical.

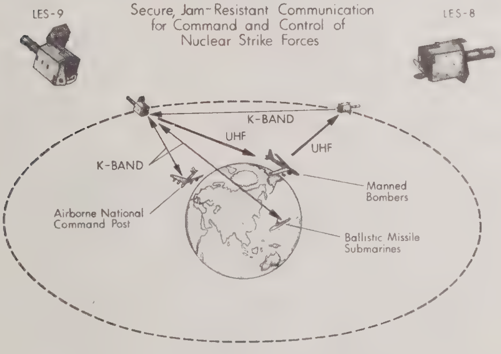
LES-9
Secure, Jam-Resistant Communication for Command and Control of Nuclear Strike Forces
LES-8
K-BAND
UHF
UHF
K-BAND
Manned Bombers
Airborne National Command Post
Ballistic Missile Submarines

Fig. 1 The LES-8/9 mission.

Although LES-8 and -9 are military R&D satellites with rather non-typical requirements, some of their unique features may be applicable to other military or commercial missions. Therefore, the purpose of this paper is to describe the attitude control systems of these satellites and review the flight experience of the past four years. We have attempted to emphasize those aspects of LES-8/9 design and performance that may apply to other missions.

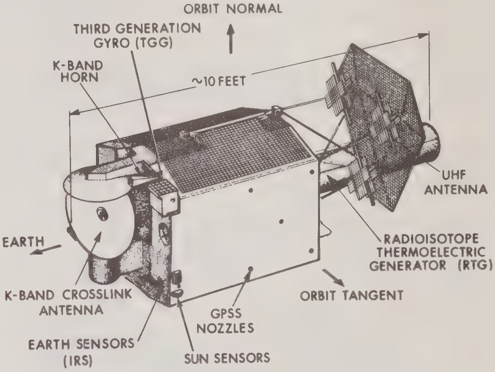
ORBIT NORMAL
THIRD GENERATION GYRO (TGG)
K-BAND HORN
~10 FEET
UHF ANTENNA
RADIOISOTOPE THERMOELECTRIC GENERATOR (RTG)
EARTH
ORBIT TANGENT
K-BAND CROSSLINK ANTENNA
GPSS NOZZLES
EARTH SENSORS (IRS)
SUN SENSORS

Fig. 2 LES-9 general arrangement.

Table 1 LES-8/9 Spacecraft Characteristics

3-axis stabilized, earth oriented
~1000 lbs each
300 W - RTG powered
Synchronous, ecliptic orbit
K-band, UHF communications
Titan IIIC launch

---

* This work was sponsored by the Departments of the Air Force and Navy
**Leader, Space Technology Group
+ Staff Member

"The views and conclusions contained in this document are those of the contractor and should not be interpreted as necessarily representing the official policies, either expressed or implied, of the United States Government."

Copyright © American Institute of Aeronautics and Astronautics, Inc., 1980. All rights reserved.

II. System Description

LES-8 and -9 have essentially identical attitude control systems which we will refer to here as "the" LES-8/9 system. The LES-8/9 control concept is based on the gimbaled momentum bias principle, which (to our knowledge) was first suggested in 1964 by A. C. Barker as a method for stabilizing satellites(3). Its principal advantage is that it achieves 3-axis stabilization with only two sensors (pitch and roll). It does not require a yaw axis sensor, which is the one most difficult to realize on an earth-oriented satellite. A block diagram of the LES-8/9 momentum-bias stabilization system is presented in Figure 3. Table 2 lists some of its distinguishing characteristics along with a weight and power statement. In the next few paragraphs we will give a brief, non-analytical description of the system. More detailed descriptions and control system analyses are available in references 4 through 8. The gas propulsion subsystem (GPSS) has been described in reference 9 and will be mentioned here only in its relation to the attitude control system.

Table 2 LES-8/9 attitude control system characteristics.

Pointing accuracy		
pitch and roll:	±0.1°	
yaw:	±0.6°	
Gimbaled momentum wheel (GMW)		
wheel angular momentum:	7.9 ft-lb-sec (1160 rpm)	
nominal speed range:	990-1330 rpm	
gimbal motion:	±1° (nom.), ±13° (max.)	
Attitude sensors		
IRS:	infrared earth horizon sensor	
TGG:	Third Generation Gyro (pitch only)	
X-Link:	cross-link antenna	
VERS:	visible earth horizon sensor	
SAZ:	sun azimuth sensor (pitch only)	
Gas propulsion subsystem (GPSS)		
propellant:	ammonia	
specific impulse:	100 sec	
total impulse:	7500 lb-sec	
thrusters (10):	0.01 lbf, pulsed	
nominal torque:	10^{-4} ft-lb	
nominal thrust:	88×10^{-6} to 2×10^{-3} lbf	
Weight and Power Summary		
GMW + drive circuits	51 lb	4.3 W
TGG	18 lb	20 W
IRS	20 lb	11 W
VERS, SAZ	14 lb	5.0 W
control electronics	10 lb	7.4 W
Total	113 lb	47.7 W

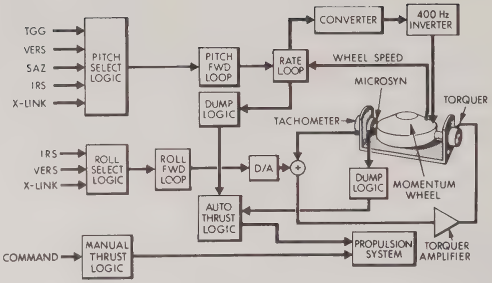

Fig. 3 LES-8/9 attitude control system block diagram.

Ground Operation

Before proceeding with the description, it will be helpful to digress momentarily to the subject of ground supervision of the attitude control system. LES-8 and -9 are managed from the LES Operations Center (LESOC) at Lincoln Laboratory(2). Figure 4 shows one of several display panels used by ground operators in monitoring and supervising the on-board control systems. The panel is inscribed with a rather detailed block diagram of the control system. Real-time telemetry data are processed and converted to engineering units in a microprocessor behind the panel and are presented on LED displays on the block diagram. A switch position is represented as closed by a lighted LED. This type of data presentation helps the operators comprehend overall system status at a glance and has proved invaluable as an operating aid. There are similar panels for other sub-systems. Telemetry is also processed and displayed in other, more detailed formats by separate real-time computers in LESOC and is also recorded on tape. Most of the performance curves presented in the following sections were recovered from post-processed telemetry tapes.

Figure 4 is introduced at this point because it contains a more detailed system block diagram, which will aid in the following discussion.

Gimbaled Momentum Wheel (GMW)

The GMW (see Fig. 5) is the heart of the LES-8/9 system. It contains a variable speed momentum wheel made by the Bendix Corporation. The wheel's spin axis points nominally along the orbit normal vector (satellite pitch axis). The wheel is driven by a 2-phase, 32-pole induction motor operating at 442 Hz. A magnetic tachometer produces eight pulses per revolution for speed sensing.

The wheel rides in a single-axis gimbal which can rotate up to ±13° around the satellite roll axis (orbit tangent vector). In normal operation the gimbal moves no more than ±1°. The gimbal is mounted on flexural pivot bearings and is activated by a permanent magnet, direct drive, DC torque motor. A microsyn angle

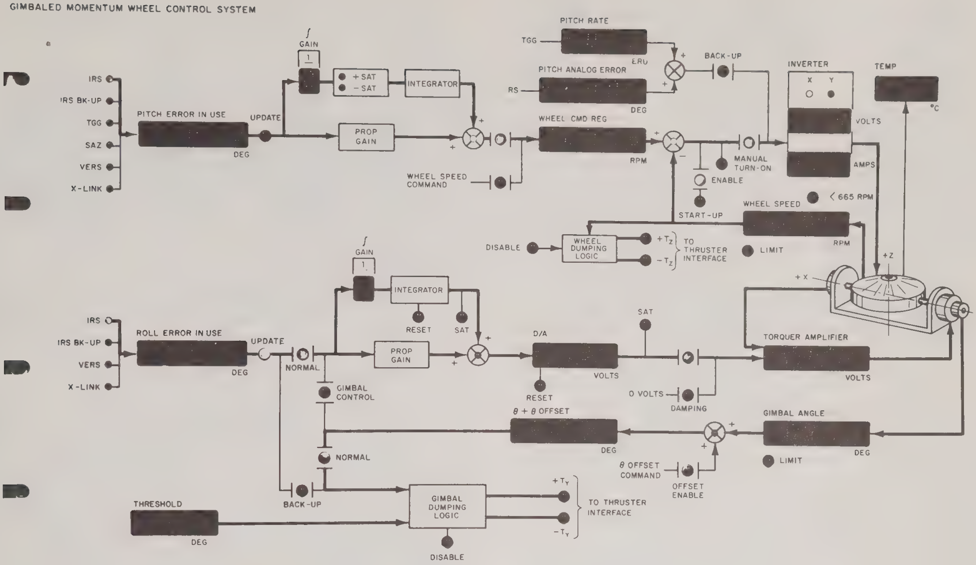
GIMBALED MOMENTUM WHEEL CONTROL SYSTEM
IRS
IRS BK-UP
TGG
SAZ
VERS
X-LINK
PITCH ERROR IN USE
DEG
UPDATE
∫ GAIN
1
+SAT
−SAT
INTEGRATOR
PROP GAIN
WHEEL SPEED COMMAND
PITCH RATE
TGG
ERU
PITCH ANALOG ERROR
RS
DEG
BACK-UP
WHEEL CMD REG
RPM
MANUAL TURN-ON
ENABLE
START-UP
INVERTER
X Y
VOLTS
AMPS
TEMP
°C
WHEEL SPEED
< 665 RPM
RPM
LIMIT
DISABLE
WHEEL DUMPING LOGIC
$+T_Z$
$-T_Z$
TO THRUSTER INTERFACE
+Z
+X
IRS
IRS BK-UP
VERS
X-LINK
ROLL ERROR IN USE
DEG
UPDATE
NORMAL
∫ GAIN
1
INTEGRATOR
RESET
SAT
PROP GAIN
D/A
VOLTS
RESET
SAT
0 VOLTS
DAMPING
TORQUER AMPLIFIER
VOLTS
GIMBAL CONTROL
θ + θ OFFSET
DEG
GIMBAL ANGLE
DEG
LIMIT
NORMAL
θ OFFSET COMMAND
OFFSET ENABLE
BACK-UP
GIMBAL DUMPING LOGIC
DISABLE
$+T_Y$
$-T_Y$
TO THRUSTER INTERFACE
THRESHOLD
DEG

Fig. 4 Attitude control system telemetry display panel for ground operations.

transducer and a permanent magnet tachometer provide gimbal angle and angle-rate readouts. Electrical power and signals cross the gimbal axis on an extremely low-torque wire crossover. The GMW was designed and assembled at Lincoln Laboratory.

In Figures 3 and 4 we see the GMW embedded in the LES-8/9 attitude control system, which consists of essentially separate and decoupled pitch and roll control systems. The GMW is employed as a reaction wheel by the pitch system and as a control moment gyro by the roll system. It also serves as an active nutation damper. The control loops are implemented with TTL digital logic.

Pitch Control

The pitch control system has three, nested feedback loops. The innermost one is the rate loop (see Fig. 3) which regulates the speed of the momentum wheel according to a 16-bit wheel speed command, which is input either by ground command (see Fig. 4) or by the pitch forward loop. Each revolution the speed is sampled to a resolution of 0.04 rpm. The motor drive is turned on or off according to whether the speed is above or below the commanded value. The motor driver consists of an 85V DC-DC converter followed by a 442 Hz, 2-phase inverter with the "on-off" control. The driver circuits are fully redundant. The average power measured at the inverter input is approximately 3 W at 1160 rpm. The rate loop regulates speed to better than 0.1 rpm under normal conditions.

At the intermediate level is the pitch forward loop, which provides the wheel speed command to the rate loop. The speed command is derived from the pitch-error-in-use signal (see Fig. 4) which is the output of the selected pitch sensor. (There are several sensors available, as will be discussed.) The function of the pitch forward loop is, of course, to null the error signal, thereby stabilizing the satellite about its pitch axis. The forward loop derives the speed command by low-pass filtering the error signal in a proportional-plus-integral compensation network. The forward loop is nonlinear in that the integrator input is clipped at ±0.35° (see Fig. 4). This allows for rapid recovery from large errors combined with high quiescent pointing accuracy. These characteristics will be discussed again in the sections on performance.

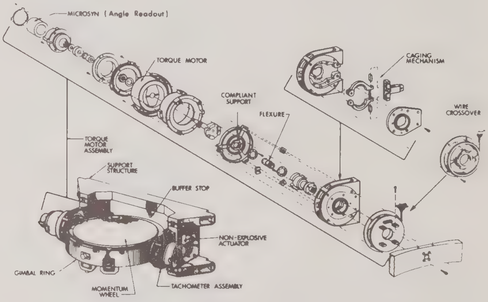
MICROSYN (Angle Readout)
TORQUE MOTOR
CAGING MECHANISM
COMPLIANT SUPPORT
FLEXURE
WIRE CROSSOVER
TORQUE MOTOR ASSEMBLY
SUPPORT STRUCTURE
BUFFER STOP
NON-EXPLOSIVE ACTUATOR
GIMBAL RING
MOMENTUM WHEEL
TACHOMETER ASSEMBLY

Fig. 5 Gimbaled momentum wheel (GMW) mechanical assembly.

The outermost pitch control loop includes the wheel dump logic and the GPSS. Through the action of the pitch forward and rate loops, a disturbance torque acting on the satellite's pitch axis results in a wheel acceleration or deceleration.

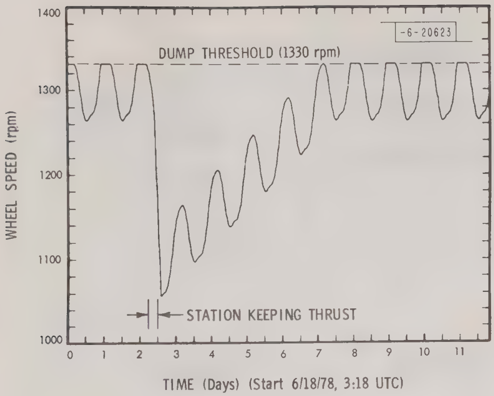

Fig. 6 12-day record of LES-8 momentum wheel speed.

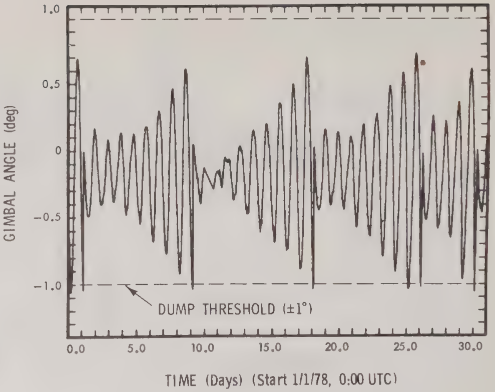

Fig. 7 30-day record of LES-8 gimbal angle.

The speed will eventually exceed the desired limits of 990 and 1330 rpm. When it reaches the upper threshold (for example) the wheel dumping logic activates the gas propulsion subsystem (GPSS). By pulsing an appropriate pair of thrusters, the GPSS creates a small impulse of pitch torque which decreases the wheel speed by about 0.4 rpm. This continues as long as the disturbance torque tries to increase the speed. The result is illustrated by Figure 6, a 12-day record of LES-8 wheel speed in orbit. Starting on day 2 the speed has a constant acceleration as well as a daily cycle. It reaches the 1330 rpm threshold on day 8 and the effect of wheel dumping is clearly evident thereafter. Incidentally, the large wheel speed change on day 2 resulted from a routine station-keeping operation. The station-keeping thrusters are slightly misaligned with the satellite's center of mass. In this case the resulting disturbance torque was such as to cause a decrease in the wheel speed.

Roll Control

Like pitch, the roll control system contains three nested loops. The innermost one is the damping loop, which is a direct, analog feedback path from the gimbal tachometer to the torque motor (see Figs. 3 and 4). This causes the GMW to be a very efficient, active nutation damper for the satellite. Next is the roll forward loop, whose function is similar to the pitch forward loop. It nulls the roll-error-in-use signal, thereby stabilizing the satellite about its roll axis. It is a digital low-pass filter (proportional-plus-integral lag compensation) whose output is D/A-converted and analog-combined with the tachometer output. Through the control action of the roll forward loop, disturbance torques along either roll or yaw axes cause the gimbal angle to precess in an oscillatory fashion at the orbital frequency (one cycle per day). This precessional motion is not to be confused with nutational gimbal motion, which has a period of a few minutes. Nutational motion is not normally encountered when the roll forward loop is operating.

The outermost roll loop is the gimbal dump logic which keeps the gimbal precessional motion within desired bounds. The dump threshold is selected by command. (It has typically been 1° in orbit.) When the gimbal angle reaches 1° in either direction, the gimbal dump logic activates the GPSS, which creates a yaw control torque that drives the gimbal back to the 0° position. We see this in Figure 7, which is a typical 30-day record of the LES-8 gimbal angle. The amplitude envelope of the precessional motion increases linearly until every 8 to 10 days it reaches the 1° threshold and is zeroed.

Yaw Control

It is through the gimbal dump logic that the satellite yaw axis is stabilized without need of a yaw sensor. Yaw error is not measured, but if it were it would look very much like Figure 7 except shifted by six hours in time. By limiting the gimbal precessional motion to a maximum amplitude of ±1°, we have also limited the yaw rotation of the satellite to ±1°. The yaw error is therefore not tightly controlled in this type of system, but its amplitude is limited to an acceptable value.

Sensors

As Figures 3 and 4 show, several sensors are available for pitch and roll control. The choice is made via a ground command to the sensor selection logic. This unit can also subtract commanded pitch and roll offset angles from the selected sensor outputs to allow for offset pointing the satellite. The selection logic's outputs are the pitch and roll error-in-use signals mentioned previously.

IRS

The infrared sensors are the primary attitude control sensors, and their performance is described in some detail in the following section. Manufactured by TRW Inc., each IRS has a 14 to 26 micron infrared bolometer with a 0.6° field-of-view (FOV). The FOV is mechanically scanned at a 4 Hz rate across the earth (see Fig. 8) and both horizon crossings are detected as changes in infrared radiance. An incremental

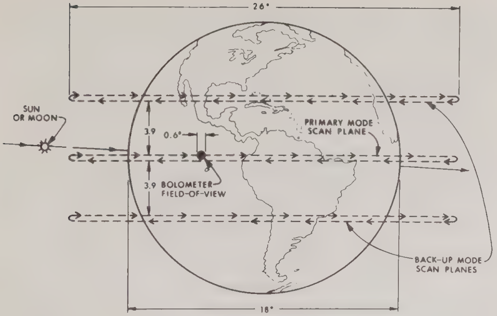

Fig. 8 Pitch IRS scan planes showing typical sun or moon encounter.

angular resolver measures the angle between the sensor's boresight and each horizon. The pitch error is the angle from boresight to the midpoint between horizons. This is equal to one half the difference in the boresight-to-horizon angles.

Figure 8 shows two back-up scan planes as well as the primary plane (shown on the equator). For the purpose of redundancy, the back-up mode allows the pitch sensor to measure roll as well as pitch (and vice versa). This is done by measuring the arc length between horizon crossings of either the upper or lower scan plane and determining if it is greater or less than the value it should have at zero roll error. Alternatively, the sensor can switch scan planes periodically and compare the arc lengths of the upper and lower planes. This is a somewhat more accurate mode. The backup mode logic is external to the IRS electronics and was added by Lincoln Laboratory. The primary scan plane can be commanded to one of the backup positions even though the sensor is not operating in the backup mode. This feature will be mentioned again.

TGG

The Third Generation Gyro is a single-degree-of-freedom, rate integrating, gas bearing gyro developed by the C.S. Draper Laboratory for the U.S. Air Force. It was flown on LES-8/9 as a technology demonstration to accredit this class of instrument as a long-lived, low-drift, survivable attitude sensor. Its in-orbit performance has been analyzed and reported by CSDL.(10,11) In this paper we will describe the operational aspects of using this gyro as a pitch attitude sensor and also discuss some measurements of platform stability made with the TGG.

X-Link

This acronym refers to the independently steerable antenna for the EHF satellite-to-satellite cross link.(12) The use of this antenna as a sensor for closed-loop attitude control of the satellite and also for three-axis attitude determination is described below.

The remaining two sensors are the VERS, a visible-light horizon sensor which backs up the IRS, and the SAZ, a 360° field-of-view sun sensor with 0.01° resolution, which allows sun-referenced pointing in pitch. These have seldom been used for attitude control and are not discussed further in this paper.

Redundant Control Loops

Aside from the IRS backup mode and the redundant wheel drive electronics, Figure 4 reveals two other fall-back control loops. The analog pitch backup loop, at the top of the diagram, stabilizes the satellite's pitch axis with direct, analog signals from either the IRS, the TGG or both. It bypasses the selection logic, forward loop and rate loop and inputs directly to the on-off switch of the wheel drive inverter.

The roll backup mode bypasses the roll forward and damping loops. It inputs the roll-error-in-use signal directly to the gimbal dump logic. In this mode the roll error is zeroed by GPSS thrusters whenever its amplitude reaches the threshold setting (typically 1°).

This completes our description of the LES-8/9 system. We will now proceed with a discussion of its operating characteristics and flight performance.

III. Operating with the IRS

As previously mentioned, there are several sensors available for both pitch and roll control, however, the infrared sensor (IRS) is the nominal choice. The LES-8/9 system was originally designed and optimized for that sensor, therefore it serves as a natural starting point for a discussion of system performance. We will describe the measured transient response and quiescent pointing accuracy of the IRS mode and how sun or moon interference is dealt with. LES-9 has spent most of its operational life in the IRS mode, whereas LES-8 typically uses the TGG for pitch control and the IRS for roll.

Transient Response

The ±10° angular offset capability of the IRS allows a convenient means of measuring transient response in orbit. This was done by first commanding offsets of +5° and -5° to the pitch and roll systems, allowing the satellite to stabilize at that point, and then commanding 0° offsets in quick succession to pitch and roll. Figure 9 shows the resulting transient error-in-use signals. We see that the satellite settles to within ±0.1°

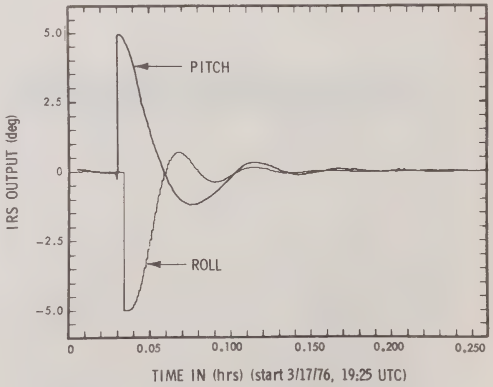

Fig. 9 LES-9 IRS mode transient response.

of earth center in about 7 minutes. In the IRS mode, the control system least-significant bit (LSB) represents 0.011° in angle. The IRS updates its pitch output every 0.5 sec and its roll output every 4 sec. The 4 sec sampling effect is clearly evident in the roll response (See Fig. 9). The telemetry update rate was 0.64 sec during this measurement. Figure 9 agrees very closely with computer simulation results and with pre-launch measurements made with the flight hardware mounted on a three-axis air bearing table. In a similar manner we checked the in-orbit transient response characteristics using all of the other possible sensor inputs and compared them with predictions and pre-launch results.

Quiescent Accuracy

Two important characteristics of any autonomously stabilized satellite are: its pointing accuracy under quiescent conditions, and how much ground supervision or 'babysitting' it requires. An indication of these for the LES-8/9 system is given by Figures 10a and b, which are records of the LES-9 IRS pitch and roll outputs for the year of 1978. This year was chosen because it is representative of routine communications satellite activity. The two previous years were marked by high levels of attitude control activity in support of the LES-8/9 test and evaluation program.(13) The data in Figure 10 were measured directly at the sensor outputs and are quantized to 0.0055° (compared to the 0.011° control system quantization). Figure 10 was prepared by sampling recorded telemetry data approximately every 30 minutes. Note that the pointing errors are nominally within ±0.011° (the control system LSB). An indication of the low level of ground supervision required is the fact that only three events during the year caused the pitch error to exceed ±0.1° and only one the roll. The roll event (labelled "test command" on Fig. 10b) was a mode change commanded from the ground in relation to testing another on-board subsystem. The 0.05° spikes in the roll sensor output result from automatic gimbal dumps. The three pitch events include IRS encounters with the sun and the moon. These events are discussed below. The third event was a station-keeping operation which, as previously mentioned, causes a higher than normal pitch disturbance torque.

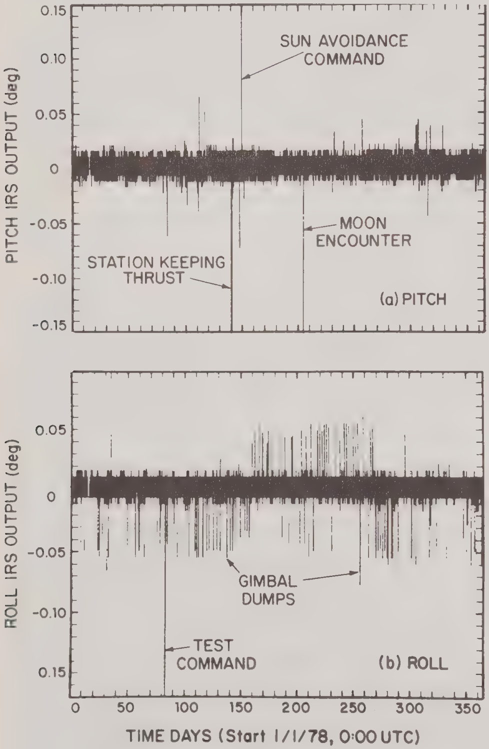

Fig. 10 LES-9 IRS mode quiescent performance.

Sun and Moon Encounters

The LES-8 and -9 orbit planes are within a few degrees of the ecliptic plane. Consequently, sensor encounters with the sun or moon are much more frequent than in equatorial orbit. Sun encounters are of more concern because the IR bolometer will be blinded for several minutes if it sweeps across the solar disc. This could cause loss of earth orientation (no permanent damage should result). A moon encounter, on the other hand, can only induce a pointing error for a short time.

The geometry of a typical sun or moon encounter is illustrated by Figure 8. Unless avoided, sun encounters with the pitch IRS will occur daily for periods of several weeks twice a year. Encounters are avoided by deflecting the bolometer scan plane so as to keep the sun 3° or more away from it. The IRS has an automatic avoidance feature to accomplish this. It uses a visible light sensor to detect the sun's proximity. We have elected not to depend on automatic avoidance, but rather to command the pitch IRS scan plane to one of the backup positions (see Fig. 8) prior to the expected interval of encounters. This is done twice a year, and it is left in the backup position for the duration of the encounter period. Switching scan planes does not normally cause a transient. The pitch transient in Figure 10a labeled "sun avoidance command" was caused by an operator error while commanding the plane change.

Since the moon's orbit is inclined 5° with respect to the ecliptic, moon encounters are much more rare and isolated events than sun encounters. Autonomous detection and avoidance of the moon would be difficult because both its visible and IR radiances are comparable to the earth's. Moon encounters are predicted by computer and could be avoided in the same way as sun encounters, but since their effects are minimal, we choose to ignore them.

Figure 11 shows the pitch IRS radiance signal when the moon is near the limb of the earth in the scan plane of the bolometer. The moon's effect is to alter the apparent location of the earth's horizon on one side thereby inducing an error of half that amount in the IRS output (pitch error-in-use). The pitch control system then rotates the satellite so as to null the erroneous output, and the result is a pitch pointing error. Figures 12a and b show the IRS output and the related satellite motion during a LES-8 moon encounter. The two transients, separated by one hour, occur when the moon goes behind the earth and then emerges on the other side. The actual platform motion cannot be determined from the IRS output, however in this case it was measured directly by using the TGG as a pitch position sensor. We see that the pointing error reached +1° for a short time and then was -0.6° for a period of about 15 min.

There is another interesting aspect of control system performance--platform jitter, the small angle, high frequency motion that results from sensor noise, quantization effects, etc. These motions were too small to be observed with the IRS, therefore they are addressed in the next section on the TGG.

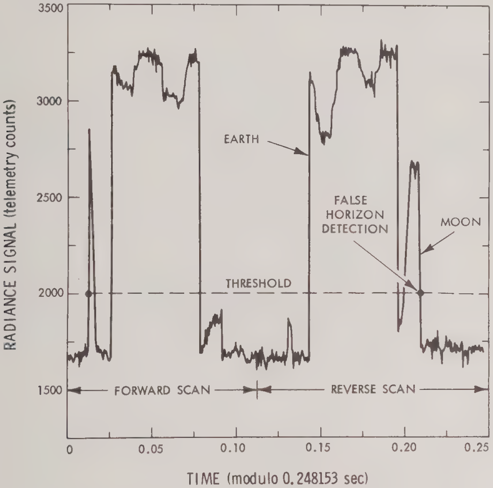

Fig. 11 IRS radiance signal during a moon encounter.

IV. Operating with the TGG

The Third Generation Gyro (TGG) was developed in response to the need for a sensor that could maintain a satellite's nominal orientation for days to weeks after loss of optical sensors. Such a sensor must be low drift (if it is inertial), reliable, long-lived, and require low power. The TGG design approaches long life and low power through the use of helium-filled gas bearings for the spin motor. The low-drift characteristics result from careful attention to thermomechanical stability and by use of sophisticated thermal controls.(10)

To demonstrate this technology, LES-8 and -9 each carry a single TGG, which can be used to control the pitch axis in conjunction with IRS roll control (a second gyro would be used in an operational system). The LES-8 TGG has operated continuously since launch and has controlled pitch for most of that time. The LES-9 TGG has operated for a total of only 280 days.

The C. S. Draper Laboratory has reported the results of the LES-8 TGG experiment from the point of view of gyro performance.(11) We will comment on it from the control system engineer's point of view. Being basically an inertial angle-rate sensor, a gyro has two main sources of error when used as an angle sensor. The first is rate error in the gyro itself (drift rate), and the second comes from the failure to compensate precisely for satellite motion in inertial space. These effects cause the gyro, and hence the satellite it controls, gradually to drift away from the desired pointing direction. From the control system point of view, the practicality of a gyro sensor depends on (among other things) how often this drift must be corrected by ground command (i.e., the update rate). Many of today's gyros would require updates at least daily to hold satellite orientation to within ±1°. An indication of our typical experience with the TGG is given by Figure 13. It shows the LES-8 pitch pointing error as sensed by the IRS while the TGG was in control of pitch. Notice that the error was held to within about ±0.25° for 90 days with only a single gyro update. The daily oscillation of ±0.2° results from the slight orbit ellipticity, which was not compensated for. The long-term motion is a combination of gyro drift and satellite orbital drift. LES-8 was not perfectly stationary at the time. Our experience with the TGG has therefore left us with a very positive opinion of its capability as an attitude sensor.

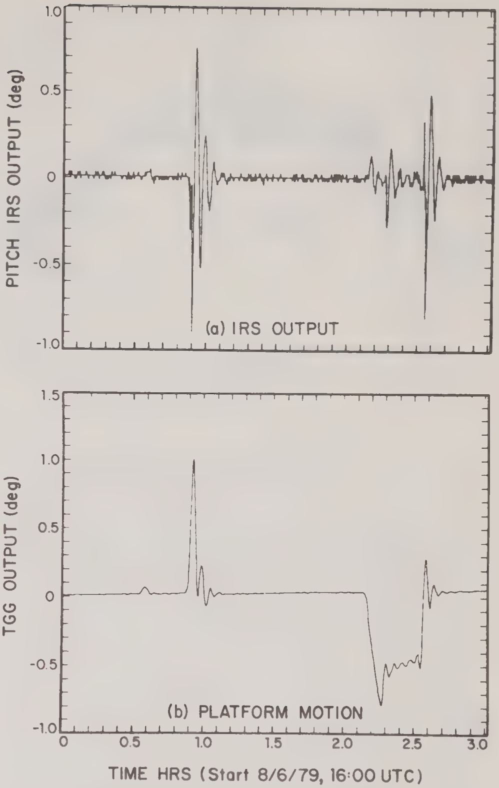

Fig. 12 Effect of Moon encounter on (a) IRS output and (b) platform motion for LES-8.

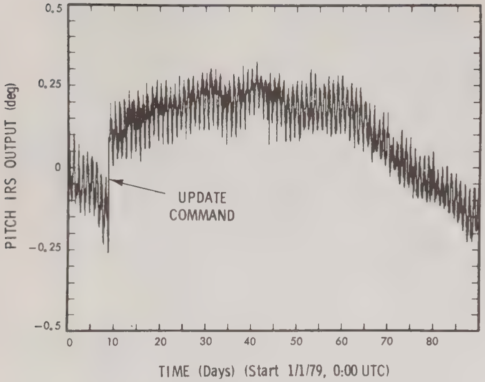

Fig. 13 90-day record of LES-8 pitch error (sensed by the IRS) with the TGG in control

In addition to its primary purpose, the TGG has made possible some interesting observations of control system performance. An example is the moon encounter data (Sec. III). The TGG angular resolution (0.35 arc sec) together with the high telemetry sampling rate (0.64 sec) allows direct observation of small angle platform jitter.

In the IRS mode the principal sources of jitter are: sensor noise, the "on-off" wheel speed regulator, and pulsed operation of GPSS thrusters during momentum dumping. Figure 14a shows a typical one hour sample of IRS noise and 14b is the corresponding platform motion, or jitter, as sensed by the TGG. There are two components of jitter. The higher frequency component, with a peak-to-peak amplitude of 0.005°, is associated with the wheel speed regulator. The lower frequency component reflects control system limit cycling between quantization levels. For comparison, Figure 15 shows a similar measurement made during a wheel dump. The thrusters are pulsing approximately every 80 to 100 sec in this example, consequently the platform jitter is much greater than before (0.034° peak-to-peak).

The TGG has much higher resolution and lower noise than the IRS, therefore we would expect much greater platform stability when it is in control. This is confirmed by Figure 16, a 24-hour plot of TGG output while it is controlling pitch. Of course this output does not represent absolute pointing accuracy. It represents platform motion relative to the gyro's inertial reference axis. We see a daily, cyclic error of ±0.005° which is caused by the same cyclic solar torque that produces the daily cycle in wheel speed (see Fig. 6). In the TGG mode the pitch control system LSB represents an angle of 0.00154° (5.54 arc sec). The quantization effect is clearly evident in Figure 16. The peak-to-peak noise between quantization jumps is 0.001° (3.6 arc sec), again related to the wheel speed regulator. The effect of thruster operation is clearly evident. In conclusion, the TGG, like other gyros, has the characteristic of good short-term stability at the expense of longer-term errors of the type illustrated in Figure 13.

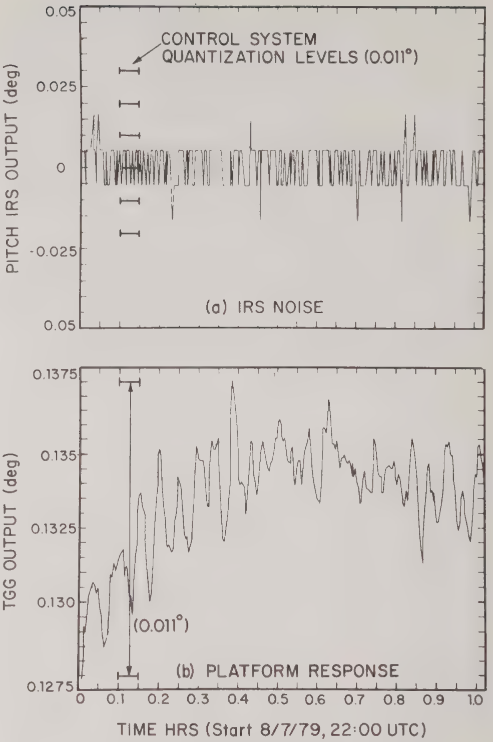

Fig. 14 LES-8 IRS mode platform jitter as measured by (a) IRS and (b) TGG.

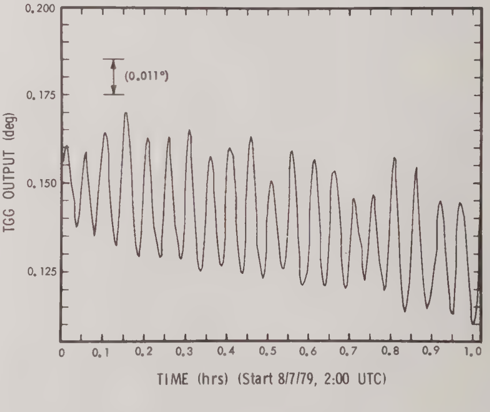

Fig. 15 LES-8 IRS mode platform jitter with thrusters on (wheel dump).

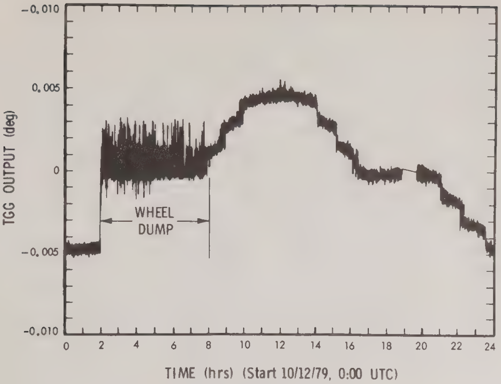

Fig. 16 LES-8 TGG mode jitter (24 hrs).

V. The X-Link Mode

The K-band crosslink antenna,(12) or X-link (see Fig. 2), is independently steerable and has a half-power beamwidth of 1.2° at 38 GHz. It has an autotracking capability which keeps its electrical boresight fixed on the line-of-sight (LOS) to the distant source, which may be an earth station or the other satellite. Angular resolvers measure the azimuth (AZ) and elevation (EL) of the LOS in satellite-fixed coordinates. If we know the direction of the LOS in inertial space, then AZ and EL are measures of satellite orientation. The X-link can therefore serve as an attitude sensor. We have employed it as such in two ways: yaw error determination and closed-loop attitude control.

Figure 17 illustrates both methods in a single example. In the configuration shown, LES-9 is in the IRS control mode with a crosslink established to LES-8, which is 90° westward in longitude. The X-link is serving as the LES-8 autonomous attitude control sensor. This is accomplished by selecting "X-link" for both the pitch and roll inputs (see Fig. 4). This inputs AZ to the pitch system and EL to the roll. In this example the pitch axis is offset 45° (by command) to keep LES-8 nominally earth-oriented. Alternatively, LES-8 can be rotated with respect to the earth by commanding changes in the pitch offset. An incidental, but interesting feature illustrated by Figure 17 is that the crosslink carrys the LES-8 command and telemetry channels, which are routed to the ground via LES-9. In this configuration LES-8 is therefore independent of direct earth control, either through attitude sensors or RF links.

As shown in Figure 17, the LES-9 X-link, in conjunction with the IRS, provides two lines-of-sight separated by a large angle (45°). Both satellite orbits are known, therefore the X-link LOS direction is known. This is sufficient information to establish the three-axis orientation of LES-9. We have used this mode for determination of the yaw pointing error in situations where full knowledge of the satellite's attitude was desired.

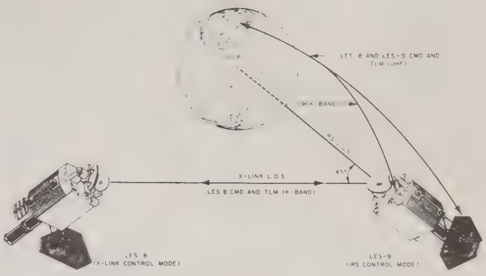

Fig. 17 Use of X-link antenna for attitude control (LES-8 and yaw error determination (LES-9).

VI. Momentum Wheel Life

The momentum wheels are obviously critical components of the LES-8/9 system, therefore since early in the program we have put considerable thought and effort into monitoring the state of their health. Probably the most sensitive indicator of a wheel's health is the drag torque. This is comprised of bearing friction torque and windage torque. It therefore reflects the status both of the ball bearings and the hermetic seal. (The wheel housing is pressurized to 7 psia with helium.) On the ground the wheels were monitored by making detailed torque vs. speed measurements with a special test instrument. This sampled the speed every revolution while the wheel was coasting down unpowered. The drag torque was calculated using the known rotor moment of inertia. Figure 18 is a typical test result. Both the shape of the curve and the noise level are significant and comprise a signature of that particular wheel.

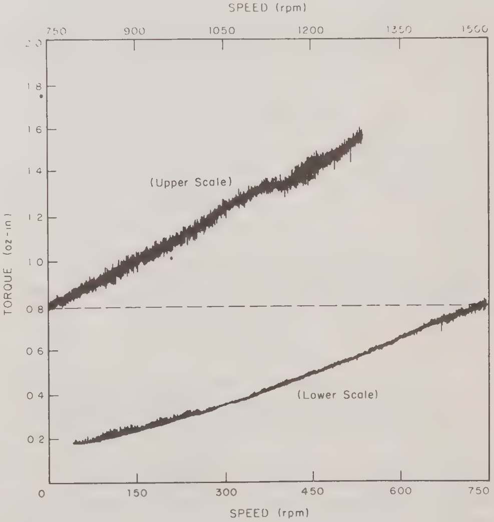

Fig. 18 Pre-launch measurement of drag torque vs. speed (LES-8).

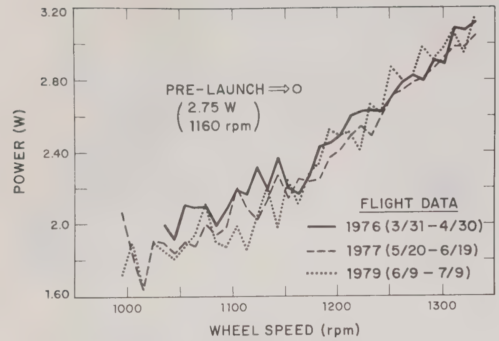

Fig. 19 In-orbit measurements of LES-8 wheel power vs. speed.

The signature is sensitive to wheel orientation (relative to vertical), external pressure and temperature. These tests were repeated at several critical points of the satellite assembly and test program during the three years before launch. No significant changes in the signatures occured as long as test conditions were identical.

In orbit we have continued monitoring the wheels, but on the basis of drive power rather than drag torque. This is almost an equivalent technique because the two are related as follows (as long as acceleration is negligible).

$$\eta \cdot P_{av} = \omega \cdot T_{drag} \qquad (1)$$

where ω is the radian speed, P_{av} the average electrical power and η the electromechanical conversion efficiency. P_{av} is available from telemetered voltage and current inputs to the wheel drive inverter. These data are very noisy due to the "on-off" speed regulator and much averaging is required. About one month of low-rate telemetry data is processed to produce a power vs. speed curve. The LES-8 test results are shown in Figure 19. From the first in-orbit measurement, we were interested to find that the wheel drive power had decreased by 22 percent between ground and space. It has remained absolutely stable since then (last measured 7-79). The initial decrease in power is attributed to the smaller bearing load in the zero gravity environment. This is supported by our pre-launch measurements in which drag torque often changed 20 percent or more between the horizontal and vertical wheel orientations. The fact that no in-orbit trends are evident in the power vs. speed measurements makes us hopeful of long lives for these wheels.

VII. Fuel Consumption

The average rates of ammonia consumption for attitude control and station keeping can be determined quite accurately on LES-8/9. There is no convenient way to implement a fuel gauge on the GPSS as, for example, the pressure of a hydrazine blow-down system. Therefore, we must monitor fuel usage closely to know how much remains. This is done with the aid of an on-board register that counts the milliseconds of "thruster on" time for all 10 thrusters starting at launch. Since one ultimate limit of a satellite's useful life is to run out of propellant for attitude control, we found it interesting to compare measured fuel consumption rates with our original predictions. This comparison is shown in Table 3 for the LES-8 satellite. We see that LES-8 is using propellant for stabilization at about one-third the predicted rate. The original prediction allowed for an average pitch torque of 10^{-5} ft-lb and a gimbal dump rate of one per day. By comparison, the in-orbit numbers are: 3.2×10^{-6} ft-lbs and 0.29 dumps per day. These results are based on analysis of one year's flight data (1978). The LES-8 propellant remaining at the end of 1979 was 6600 lb-sec, which allows for several more decades of life. A similar situation prevails on LES-9. It is unlikely, therefore that either will pass away for lack of fuel.

Table 3
LES-8 Fuel Consumption Rates for Attitude Control

Function	rate, lb-sec per year	
	predicted	measured
Wheel dump	300	87.1
Gimbal dump	32	15.3
Total	332	102.4

VIII. A Possible Static Discharge Effect

The phenomenon of static discharge in surface materials has caused electronics interference in some other synchronous orbit spacecraft.(14,15) This possibility was recognized early in the LES-8/9 program, and considerable effort went into material selection, grounding practices, etc. to avoid the problem. The results have been quite successful with one possible exception. There is an isolated problem in the LES-9 TGG electronics that is suggestive of a static discharge mechanism.

LES-8 and -9 each have a total of several hundred low-power TTL storage registers. One such register is the TGG command rate register, which stores the rate compensation data commanded from the ground. As mentioned in Section IV, this is updated infrequently (weeks-to-months). On LES-9 the command rate register occasionally flips a bit -- not always the same one. (The LES-8 TGG is not affected). When this happens the TGG drifts away from its inertial reference point. Careful screening of telemetry data has revealed no plausible explanations such as power line transients or command activity in other subsystems.

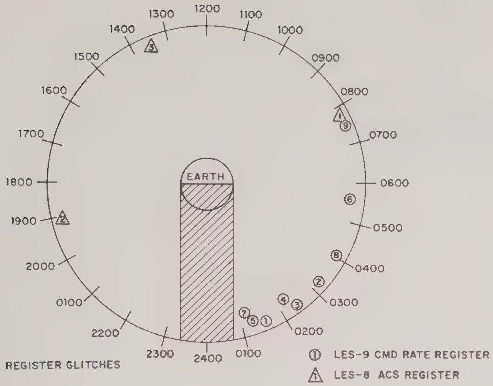

Fig. 20 Local time of occurrence of register glitches.

The most probable time for a static discharge to occur is just after the satellite emerges from eclipse, which is a daily event for LES-8 and -9. The occurrence times of the LES-9 register glitches were therefore plotted in satellite local time (see Fig. 20) and we see that they are indeed clustered in the hours after eclipse. Another piece of evidence is that the glitch frequency decreased drastically with time. Events 1, 2, and 3 occurred on three successive days immediately after launch. Events 4 through 7 were spread over the next month. Six weeks after launch the TGG was turned off. It was restarted 18 months later for a period of 8 months. Only two glitches (8 and 9) occurred during this time. (Since then the TGG has been off to make more power available for the communications payload.) These data hint, but do not prove, that static discharge is the explanation for the register glitches. Correlation with temperature for example, would cause a clustering of events similar to Figure 20.

IX. Other Problems

Over the past four years in orbit the LES-8 and -9 stabilization systems have proved themselves to be highly effective and dependable. However, few things are perfect and this paper would not be completely credible without mention of the problems that we have encountered since launch.

Three times since launch registers in the LES-8 attitude control system have glitched in a manner reminisent of the LES-9 TGG register. The differences are that each glitch was in a different register and that the glitches were not correlated with local time (see Fig. 20). Two of these events caused a temporary loss of earth-lock. These glitches are as yet unexplained.

For the first ten days after launch the LES-9 roll IRS stopped scanning for a period of 1 to 3 hours each day. This problem was definitely temperature-correlated. It was bypassed by using the IRS back-up mode until the problem cleared up by itself. The sensor has worked flawlessly since then. The probable cause (suggested by ground tests on the spare unit) was a contamination particle in the scan mechanism. The vendor was in no way implicated as Lincoln had accepted the sensors several years previously.

In August, 1979 the LES-8 gimbal torquer amplifier tripped an overcurrent relay. Apparently shorted, it was bypassed by the roll back-up mode (see Fig. 4).

X. Conclusions

With these few exceptions the LES-8/9 attitude control systems have served admirably for a combined total of almost eight orbit-years. We have been very satisfied with the momentum bias technique. It lends an inherent stability to the satellite that makes loss of earth-lock an unlikely event, even through operator error. If it does lose lock, the satellite simply rotates slowly in pitch and recovery is easy.

The reliability of these systems (and of LES-8/9 in general) we attribute to the rigorous testing philosophy that guided the LES-8/9 development effort. Every test anomaly that aroused the suspicion of the responsible engineer was tracked down and corrected regardless of whether or not it "met spec". This practice uncovered both defective parts and design errors that could have plagued us later in orbit. Although tedious and expensive, this kind of test effort is nonetheless cheaper than a failure in orbit. From our perspective, the best measure of success we can apply to these systems is that, once in orbit, they have demanded very little personal attention on our part.

Acknowledgements

It would be impossible to acknowledge individually the efforts of all who contributed to the success of LES-8/9 and thereby to this paper. Special mention is due C. Sullivan, who designed the GMW and H. Hoover and the LESOC crew for LES-8/9 operations. We thank E. Swenson, M. Coley, and R. Pelletier for the data processing, and Dr. W. Ward, who now oversees the LES-8/9 activity, for his helpful comments.

References

1. "The Lincoln Experimental Satellites LES-8 and -9," F. W. Sarles, Jr., L. W. Bowles, L. P. Farnsworth, P. Waldron, EASCON-77, Arlington, VA, 1977 Sept. 26-28, Conf. Rec. p. 21-1A through 21-1U.

2. "Developing, Testing, and Operating Lincoln Experimental Satellites 8 and 9 (LES-8/9)," W. W. Ward, MIT Lincoln Laboratory Technical Note TN 1979-3, 16 January 1979, DDC No. AD-A069095.

3. "Momentum Bias Attitude Control for a Synchronous Communications Satellite," A. C. Barker, Aerospace Corporation Report, TDR-269 (454 D-70-1), May 1964.

4. "Three-Axis Attitude Control of a Synchronous Communications Satellite," J.U. Beusch, F. W. Floyd, C. H. Much, V. J. Sferrino, and N. P. Smith, "Progress in Astronautics and Aeronautics," Vol. 25, MIT Press 1971, pp. 97-111.

5. "Satellite Attitude Control with a Gimballed Reaction Wheel Digital Control System," C. H. Much and N. P. Smith, Automatica, Vol. 8, pp 9-21 Pergamon Press, 1972.

6. "LES-8/9 Attitude Control System Numerical Simulation," C. H. Much, N. P. Smith, F. W. Floyd, E. Swenson, MIT Lincoln Laboratory Technical Note, TN 1971-10, 5 Feb. 1971, DDC No. AD-726096.

7. "Attitude Control Dynamics for LES-8/9," N. P. Smith, R. W. Brockett, MIT Lincoln Laboratory Technical Note, TN 1973-27, 27 July 1973, DDC No. AD-765548.

8. "Stable Equilibria of Satellites Containing a Momentum Wheel in a Controlled Gimbal," J. U. Beusch, N. P. Smith, J. Spacecraft and Rockets, p. 736, July 1971.

9. "The Cold-Ammonia Propulsion System for the Lincoln Experimental Satellites LES-8 and -9," C. K. Murch, F. W. Floyd, Jr., 1976 JANNAF Propulsion Meeting, Atlanta, GA, 1976 Dec. 07-09, Vol. 3, pp 491-512.

10. "Third Generation Gyro System Final Report," L. J. Freier et al., C. S. Draper Laboratory, Inc., Report R-843, February 1975.

11. "In-Orbit Performance of the LES-8/9 Third Generation Gyro (TGG) System," R. A. Harris, The C. S. Draper Laboratory, Report R-1112, September 1977.

12. "Satellite-to-Satellite Data Transfer and Control," D. M. Snider and D. B. Coomber, AIAA Paper No. 78-596, 7th Communications-Satellite-Systems Conf., San Diego, CA (24-27 April 1978), Conf. Proc. pp 457-470.

13. "LES-8/9 Communications-System Test Results," L. D. Collins, et al., AIAA Paper No. 78-599, 7th Communications-Satellite-Systems Conf., San Diego, CA (24-27 April 1978), Conf. Proc. pp 471-478.

14. "Proceedings of the Spacecraft Charging Technology Conference," C. P. Pike, R. R. Lovell, Ed., AFGL-TR-77-0051, NASA TMX-73537 1977 Feb. 24. (This Conference was held at the USAF Academy, CO, 1976 October 27-29).

15. "Spacecraft Charging by Magnetospheric Plasmas," A. Rosen, Ed., Vol. 47 of "Progress in Astronautics and Aeronautics," AIAA (New York) and MIT Press (Cambridge, MA), 1976.

80-0503

THE THERMAL CONTROL SYSTEM OF THE GERMAN DIRECT TRANSMITTING COMMUNICATION SATELLITE TV-SAT

Dr. Helmut Kreeb   Walter Schwarzott

DORNIER SYSTEM GMBH
Postfach 13 60
7990 Friedrichshafen 1
Federal Republic of German

Abstract:

The German TV-SAT belongs to the new generation of direct transmitting communication satellites, which consumes some kilowatts of electrical power and therefore produces severe thermal problems concerning heat rejection and temperature stabilisation. Heat pipe technology must be introduced to overcome the thermal difficulties. The main heat dissipators on the payload module are the travelling wave tubes (TWT), the electrical power converters (EPC) and the output-multiplexer (OMUX) which is located on the earth panel. Three TWT's and three EPC's are placed at the north panel, two TWT's and two EPC's are placed on the south panel of the A3 satellite version which is under detailed development since July 79. In the worst case, all TWT's and EPC's are active at one panel and no dissipation is produced on the opposite panel. This requirement demands for a thermal connection between both panels which is performed by means of heat pipes which connect the north with the south panel via the OMUX. The OMUX heat dissipation therefore can be transferred either to the north- or the south panel whichever is colder; also a heat flux from the hotter to the colder panel can take place. Beside this, the temperature of the OMUX can be held within the required small range without any other thermal control mechanism. For the satellite bus, the service module and the propulsion module, a conventional passive thermal control system assisted by heaters is foreseen. The highlights in this area are the thermal design of the batteries and the shunts which both need separate individually designed radiators for heat rejection.

Keywords: Thermal Control, Communication Satellite Systems, Temperature Stabilisation, Heat Pipes.

1. INTRODUCTION

The TV-SAT A3 spacecraft is the first satellite designed for an operational direct TV broadcasting service within Germany. The main design requirements concerning weight and dimensions are dictated by the Ariane launcher. The spacecraft is foreseen for 3 simultaneously operating channels with a lifetime of 5 years of operation. The design is carried out according to the following system requirements:

- Construction:	Modular design with . communication module . service module . propulsion module
- Stabilisation:	3 axes by electrical engines system RITA-1 and by chemical propellant system
- Mass limitation:	1760 kg
- Communication frequency bands:	18,3 ÷ 18,7 GHz (uplink) 11,7 ÷ 12,1 GHz (downlink)
- EIRP:	65,5 DBW
- Repeater:	5 Channels with 260 W TWTA's (3 Channels simultaneously active)
- Electrical power input	3990 W BOL, equinox 2990 W EOL, solstice
- Thermal dissipation:	2500 W (average)
- Required eclipse power:	270 W

By cost and schedule reasons only 3 spacecraft models will be manufactured:

- STM (Structure Thermal Model)
- ETM (Engineering Test Model)
- PFM (Protoflight Model).

The master time schedule is oriented on a launch date in March 1983, therefore the manufacture of the STM and ETM will start in the early 1980. The design activities had been mainly done in the period July-December 1979. The basic subsystem design is carried out in view of the requirements for the later operational satellites:

Copyright © American Institute of Aeronautics and Astronautics, Inc., 1980. All rights reserved.

10 years for the bus subsystems, consisting of 5 years standby plus 5 years operation with the repeater. For this lifetime the reliability and redundancy is aimed to be better than 0.8. A total view of the satellite is given in Fig. 1. The TV-SAT modular design divides the S/C into the payload module, the service module and the propulsion module shown in Fig. 1 where also the main thermal design features are indicated.

2. THERMAL DESIGN DESCRIPTION

At it is shown in Fig. 1 the waste heat rejection from the satellite is done by north and south radiators only for the payload as for the service module. The remaining surfaces of the satellite are covered by superinsulation. Diurnal variations of the electrical dissipation which are caused by different operating modes during sunlight are compensated by an auxiliary heater system.

Fig. 1: Total view of TV-SAT A3

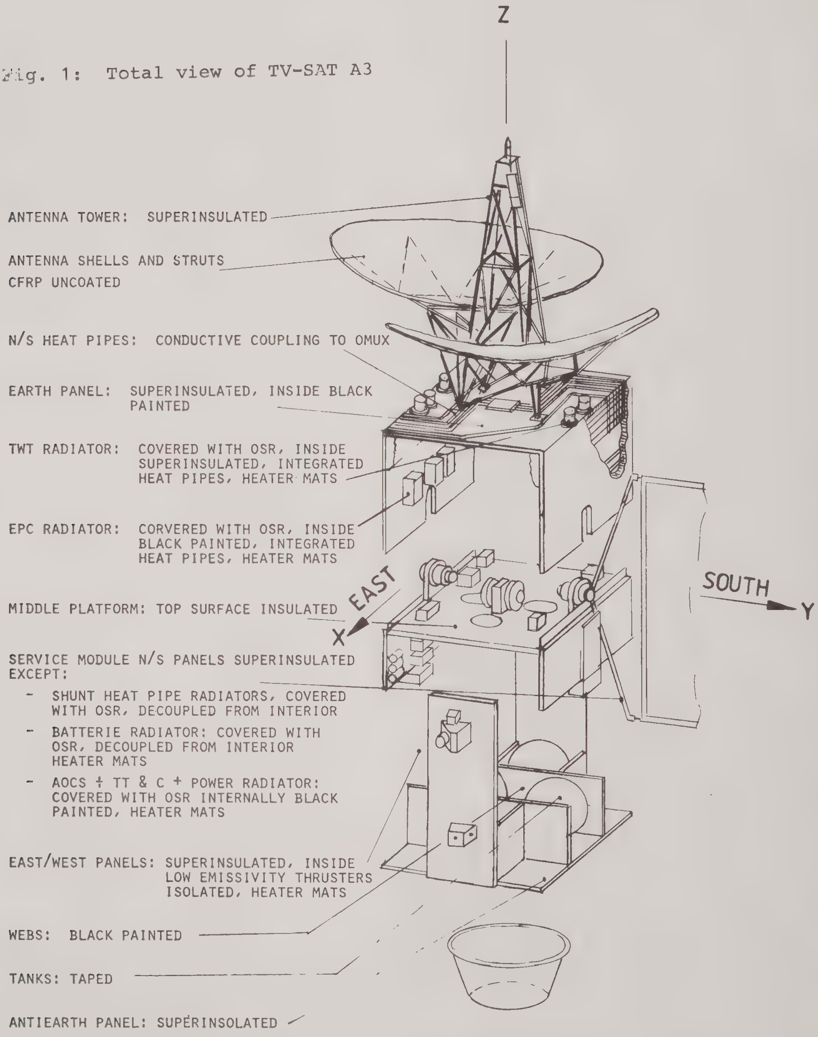

ANTENNA TOWER: SUPERINSULATED

ANTENNA SHELLS AND STRUTS
CFRP UNCOATED

N/S HEAT PIPES: CONDUCTIVE COUPLING TO OMUX

EARTH PANEL: SUPERINSULATED, INSIDE BLACK PAINTED

TWT RADIATOR: COVERED WITH OSR, INSIDE SUPERINSULATED, INTEGRATED HEAT PIPES, HEATER MATS

EPC RADIATOR: CORVERED WITH OSR, INSIDE BLACK PAINTED, INTEGRATED HEAT PIPES, HEATER MATS

MIDDLE PLATFORM: TOP SURFACE INSULATED

SERVICE MODULE N/S PANELS SUPERINSULATED EXCEPT:

- SHUNT HEAT PIPE RADIATORS, COVERED WITH OSR, DECOUPLED FROM INTERIOR
- BATTERIE RADIATOR: COVERED WITH OSR, DECOUPLED FROM INTERIOR HEATER MATS
- AOCS ÷ TT & C + POWER RADIATOR: COVERED WITH OSR INTERNALLY BLACK PAINTED, HEATER MATS

EAST/WEST PANELS: SUPERINSULATED, INSIDE LOW EMISSIVITY THRUSTERS ISOLATED, HEATER MATS

WEBS: BLACK PAINTED

TANKS: TAPED

ANTIEARTH PANEL: SUPERINSOLATED

2.1 Payload Module

The basic problems of the payload module thermal design are to reject ernormous heat dissipations especially at the north panel (that means to guarantee the upper temperature limits for the satellite hot case), to stabilize the temperature of components which are sensitive to thermal deflections and to thermally decouple components with different operating temperature levels. Tab. 1 gives an overview on the thermal data of the most important payload components.

The high dissipation of the payload, mainly caused by TWT's EPC's and the OMUX requires a high specific heat rejection because of the limited radiation surface on the north and south panels. The total dissipation energy has to be radiated via these two panels.

	Max. Dissipation W Component	Total	Allowed Acceptance Temperature Limits (Guaranteed Temperatures) °C Max.	Min
Payload Module:				
TWT				
Collector	258	774	355	TBD
Body	108	324	70	0
EPC	103	309	45	- 10
OMUX	38	114	80	50
Isolator	13	39	65	- 5
Wave Guides	11.8	35.4	105	- 5
Service Module:				
Battery	(during eclipse)	65		
	for charging periods	5	10	- 5
Shunt	163	326	65	- 45

Tab. 1: Dissipation and Temperature Limits for the Main S/C Components

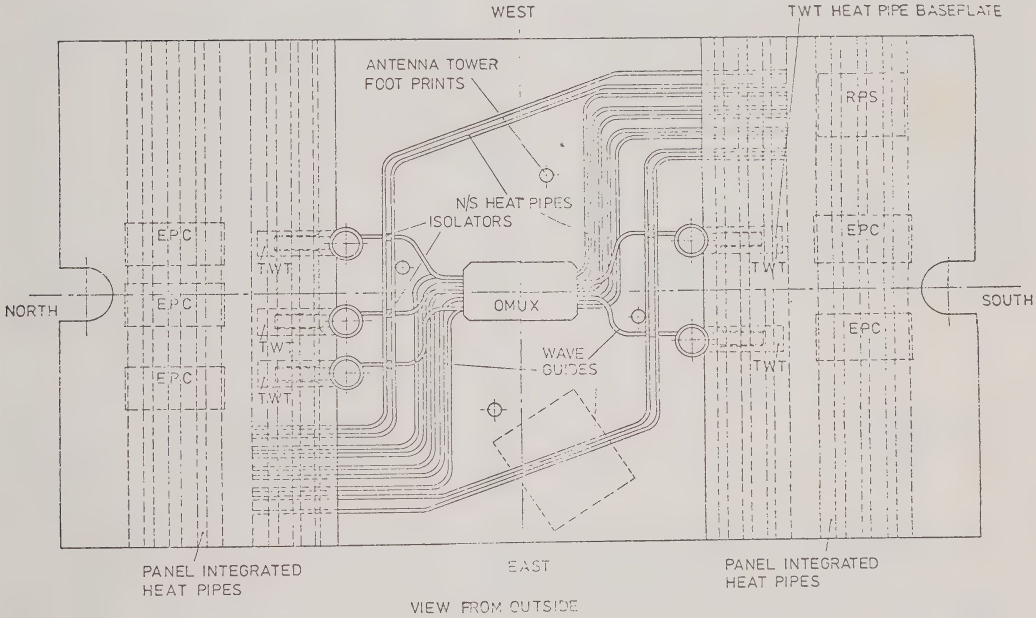
WEST
TWT HEAT PIPE BASEPLATE
ANTENNA TOWER FOOT PRINTS
RPS
N/S HEAT PIPES
ISOLATORS
EPC
TWT
EPC
TWT
OMUX
NORTH
SOUTH
EPC
TWT
EPC
TWT
WAVE GUIDES
TWT
PANEL INTEGRATED HEAT PIPES
EAST
PANEL INTEGRATED HEAT PIPES
VIEW FROM OUTSIDE

Fig. 2: Payload Module Inboard Profile

Cooling of Travelling Wave Tubes

As shown on Fig. 2; three TWT's and three EPC's are located on the north panel, two TWT's and two EPC's are located on the south panel; the Omux is fixed on the earth panel below the feeder tower and is thermally decoupled from the feeder tower and the S/C interior.

The maximum number of operating channels is three. During normal operation, two channels are operating at north panel and one at south panel. In case of a channel failure, it is possible that three channels on the north panel and one at south panel. In case of a channel failure, it is possible that three channels on the north panel are active, so that the hot case can be defined for 3 active TWT's (and EPC's) and the sun on the north panel.

Fig. 3 shows the energy balance of a TWT and the heat flux profile versus the length of a TWT baseplate under the boundary conditions of the proposed radiator design. Approximately 30% of the total TWT dissipation is rejected by the self-radiating collector. The remainder has to be withdrawn from the TWT body baseplate while about 80% of the heat dissipation of the TWT body must be conducted to the radiator in the upper quarter of the baseplate at the collector's side. Consequently in that area there exists a high local heat flux density which has to be distributed to the radiator. This a done by an additional baseplate for each TWT, an extruded Aluminum profile including four grooved heat pipe profiles. This heat pipe baseplate distributes the heat flux nearly homogeneously to the eight radiator heat pipes which are integrated in the TWT radiator panel in east west direction.

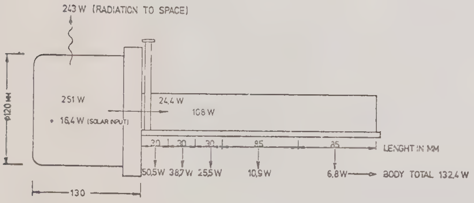
243 W (RADIATION TO SPACE)
ϕ120 MM
251 W
+ 16,4 W (SOLAR INPUT)
24,4 W
108 W
30
30
30
85
85
LENGHT IN MM
50,5 W
38,7 W
25,5 W
10,9 W
6,8 W
BODY TOTAL 132,4 W
130

FIGURE:3: DISSIPATION PROFILE OF A TRAVELING WAVE TUBE

Fig. 4 gives view of the thermal coupling of the TWT's to the radiator and shows also the cross section of the heat pipe baseplate.

The higher operating temperature of the TWT's requires thermal decoupling from medium temperature components as the EPC's and several electronic boxes mounted on the inner side of the earth panel. Thermal decoupling between diametrically opposed TWT and EPC sections is achieved by superinsulating the TWT's and the TWT-radiator rear side.

The distance between TWT's and EPC's on one panel is designed such that the hot TWT radiator section is not affecting the EPC radiator.

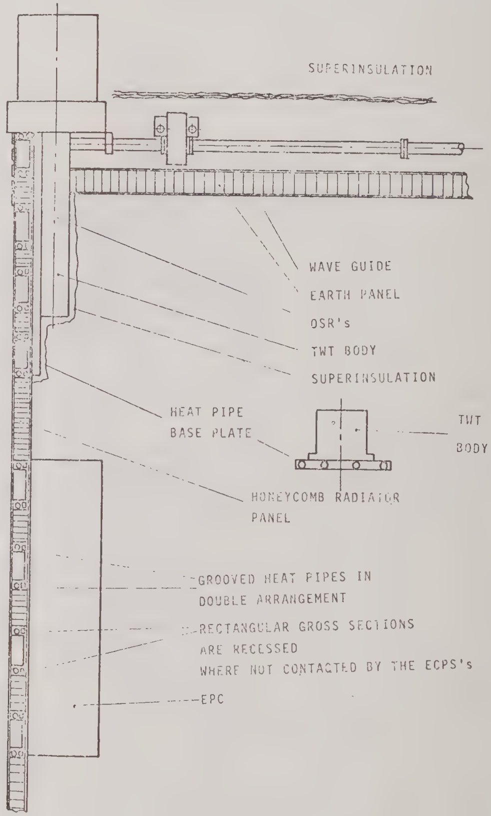
SUPERINSULATION
WAVE GUIDE
EARTH PANEL
OSR's
TWT BODY
SUPERINSULATION
HEAT PIPE BASE PLATE
TWT BODY
HONEYCOMB RADIATOR PANEL
GROOVED HEAT PIPES IN DOUBLE ARRANGEMENT
RECTANGULAR GROSS SECTIONS ARE RECESSED WHERE NOT CONTACTED BY THE ECPS's
EPC

Fig. 4: Cross section of payload Module showing the integrated Heat Pipes

Cooling of the Electric Power Converters

Because of the limited radiation area and the different upper temperature limits of the TWT's and EPC's, the north and south panels are each thermally devided in a TWT-radiator and an EPC-radiator.

The EPC boxes are screwed against the heat profiles which are integrated in the radiator panel as it is shown in Fig. 2 and Fig. 4. Most of the heat dissipation of a EPC has to be conducted from a stripe shaped area of 65 mm width and the length of the whole box which is 350 mm. A special heat pipe profile has been designed to meet the requirements for high joint conductance values with limited number of screw fixations. A smaller part of the dissipation is radiated by the EPC-box surfaces to the opposite EPC panel thus minimizing the thermal heater power on the south panel in the case of 3 operating channels at the north panel.

Cooling of the Components at the outer Earth Panel

The OMUX and other components located outside the earth panel as high power isolators and waveguides are not allowed to transmit significant heat into the satellite via the earth panel in order not to exceed upper temperature limits. A raditive coupling of these components to space would create too high temperature fluctuations by solar incidence. The heat rejection of these components therefore will be carried out via heat pipes which are connected with both, the north and south panel, so, the heat flux from the OMUX to either the north or the south panel is possible. In total there are 9 north-south heat pipes, 5 of them are coupled to the Omux the others are to cool the waveguides and isolators. With this thermal design, shown in Fig. 2 and 5 the following major advantages are established: the heat pipes enable heat rejection of earth panel components and their temperature stabilization. The heat rejection capability of the north and south panel components (TWT's) is improved.

As illustrated in Fig.5 the heat dissipation of the OMUX waveguide and isolators is conducted via the heat pipes either to the north- or the south-panel or partially to both radiators according to the actual temperature levels of the two TWT-radiators which are determined by the operating TWT's and the solar input. Beside the energy removal, the requirement of the temperature stabilisation for the OMUX can be reached by passive means with this heat pipe system. Additionally, the radiator areas possess an optimal efficiency, especially because a heat flux from the north- to the south-radiator and reverse via the OMUX is possible.

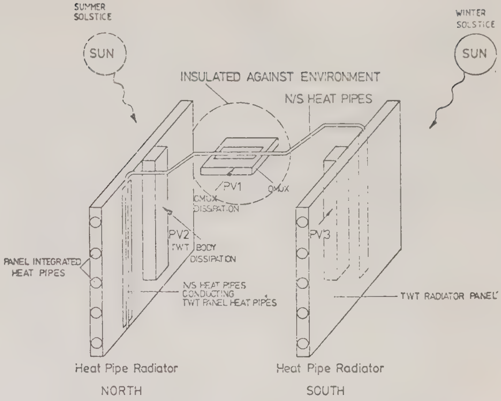

FIGURE 5: PRINCIPLE OF THERMAL CONNECTIONS OF NORTH AND SOUTH RADIATORS

All heat pipes applied in this satellite are Aluminum extruded types. For weight reasons parts of the material are locally milled off at those places where no heat transfer to or from the heat pipe is required. Fig. 6 shows an example of a weight optimized heat pipe. This heat pipe is located under the EPC's in the N/S panels taking into account the pinhole image of the EPC's.

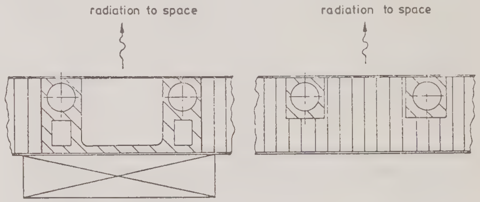

Fig.6a

Fig. 6b

Heat Pipes imbedded in honeycomb panel

section below componets

radiator section without components
(Profile partially milled off)

Figure6: Weight optimized Heat Pipe Profile

Distribution of Heat Fluxes in the Payload Module

Fig. 7 gives an impression on the heat flux distribution in the payload module for a typical operational case.

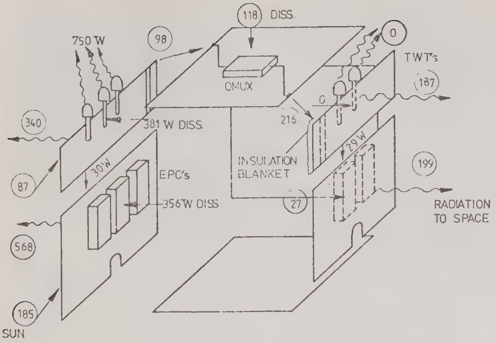

FIGURE 7: TYPICAL HEAT FLUX DISTRIBUTION IN THE PLAYLOAD MODUL (HOT CASE) FLUXES IN WATTS

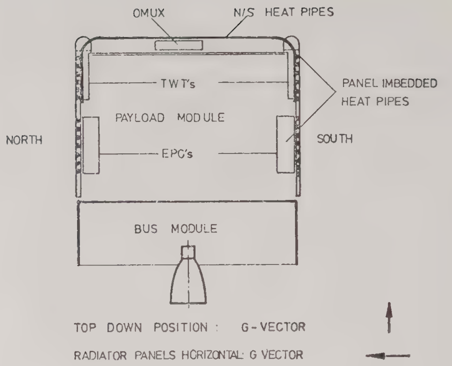

FIGURE 8: THERMAL GROUND TEST POSITIONS OF THE SATELLITE

Thermal Testing

Because of the heat pipes, special attention must be given for all ground tests of this payload module. A zero-g-environment can be simulated for heat pipes on ground only by an arrangement of the heat pipes in a horizontal position. This is impossible with the bent heat pipes. So, a testing position must be found where the heat pipes are either horizontally arranged or in a gravity assisted arrangement where this position gives a verification of the temperature distribution but not of the heat pipe performance. This performance must be verified by a separate test serie with horizontal position before integration into the satellite.

Two test arrangements of the satellite on system level are possible regarding the above mentioned test philosophy: (See Fig. 8)

1) Earth panel horizontally positioned below the S/C (top down)

2) North- and south panel horizontal; earth panel vertical.

Position 1 will be the preferred test position; the dissipation energy of the OMUX leads to a gravity assisted test mode for the heat pipes.

The heat pipe shunt radiator however is only testable in position 2. For all subsystem and system tests performed in position 1 the shunt radiator will be replaced by a uniformly heated radiator dummy.

2.2 Service Module

This module contains the attitude and orbit control system (AOCS), the Telemetry, Telecommand and Control (TT&C) the Double Gimballed Momentum Wheel (DGMW), the Bearing and Power Transfer Assembly (BAPTA), the Power Supply and Power Conditioning electronics. Fig. 9 shows the inboard profile of the Service Module.

One shunt and all power supply components are located on the north panels. The other shunt, the AOCS and TT&C electronics are located on the south panel. The BAPTA electronics, the DGMW and Gyro electronics and the Central Unit are located on top of the middle bus platform.

The lay-out is done in a conservative manner: The west and east panels are insulated. A total available N/S panel area of about 2.7 m^2 each provides some radiator growth potential considering a total maximum heat dissipation of about 500 W in the components of the service module. In order to utilize the full temperature range of the shunts of up to 65°C, which is in excess of the other service module equipment, the two shunts' temperature control is provided by means of two separate radiators of equal size, one facing towards north, the other facing towards south. The distribution of the heat from the dissipating shunt elements to the total shunt radiator area is done by parallel heat pipes which are integrated in the honey comb of each separate shunt radiator. Both radiators are conductively decoupled from the adjacent structure and radiative decoupled from the Spacecraft structure.

The battery operating temperature range from -5° C to 10° C is less than that of all other service module equipment. However a relatively simple thermal design is foreseen: The two battery units are conductively coupled to the inner face sheet of the service module north panel. The battery radiator is preferably located at the north panel, this panel being subjected to insolation only during summer, where the insolation intensity is less than during winter, so that the radiator area can be kept smaller than a south panel located battery radiator. A heater system guarantees the low temperature limits of the battery.

The hydrazine thrusters and the RITA-1 system must be thermally insulated to minimize the required heating power. The RITA-1 electronic boxes located outside the east and west panels are thermally controlled by adequate surface coatings and a guard heater system which guarantees the allowed minimum temperatures.

2.3 Propulsion Module

During firing the apogee boost engine reaches approximately up to 800° C. A radiation shield is applied to prevent degradation of the antiearth panel superinsulation.

The propulsion module MLI of approximately 8.8 m^2 total area is of aluminized Kapton, it may reach at the antiearth panel temperatures up to about 200°C, which is acceptable for the Kapton MLI. Thus the thermal control of the UPS is a conventional one it uses multilayer insulation blankets and a guard heater system to prevent freezing of propellant.

2.4 Antenna System Thermal Control

The thermal control for the antenna system, the mechanical built up of which is shown on Fig. 1, has mainly to deal with the thermal deflection requirements due to the required antenna pointing accuracy. The antenna design proposed for all components as antenna dishes, antenna supporting framework and feeder tower uses the carbon fibre technology. Thus reasonable temperature gradients and fluctuations can be allowed without exceeding the maximum allowed distortions. By this reason antenna dishes and support frames will remain without any thermal cover. A detailed thermal analysis together with deflection calculations and verification by tests with guarantee the required geometrical stability. The feeder tower however will be wrapped into multilayer superinsulation in order to decrease the temperature fluctuations. A special thermal problem in this area is caused by the high dissipative waveguide which connect's the OMUX with the feeder system. It is proposed to have this waveguide outside the insulation of the tower, properly covered with OSR's for heat rejection to space.

Conclusion

The major items of the TV-SAT thermal control system has been presented. The development activities up to now indicate the practicability and reliability of the design principles. In spite of the extremely high required heat rejection capability and the necessity of extensive heat pipe application the design is of limited complexity by using only fixed conductance heat pipes. The thermal design principle offers the possibility of extension from the 3-channel version of the preoperational satellite A3 to the operational A5 version with 5 simultaneously operating channels.

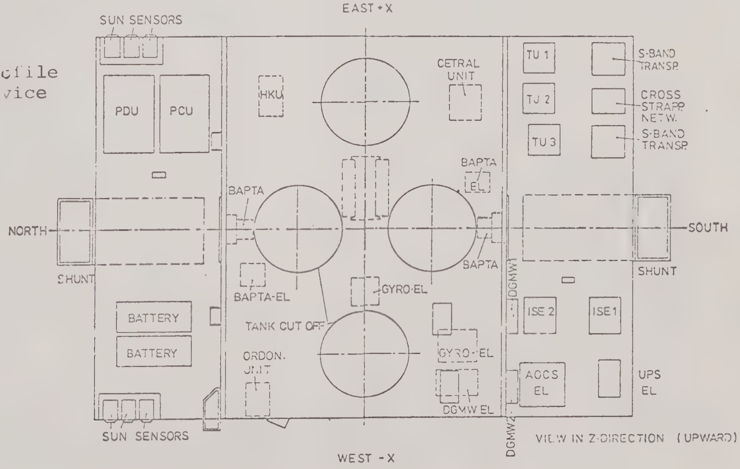

Fig. 9: Inboard Profile of the Service Module

80-0504

WIDEBODY BUS EXTENDS SHUTTLE ECONOMY TO SYNCHRONOUS ORBIT

Thomas C. Eakins   Garrett W. Durling
Hughes Aircraft Company
El Segundo, California

INTRODUCTION

Communications satellites using the Space Shuttle in the 1980s will have a significant economic advantage over alternate approaches to providing many communications services. The high reliability, low launch cost, and large payload capability of the Space Shuttle will be used by satellite systems to compete for new communications services and to meet the economic challenge presented by such emerging systems as fiber optics and microwave cables. The benefit of Shuttle economy is presently limited to the low earth orbit phase of a spacecraft launch; but, this limitation will be removed as spacecraft buses are developed to extend Shuttle economics to subsequent phases of a synchronous orbit mission. A spacecraft bus capable of doing just this is now being built by Hughes Aircraft Company. This bus, the Widebody Bus shown in Figure 1, is being used on two of Hughes' ongoing contracted programs. One of these, the LEASAT spacecraft, is described in this paper.

Comparison to other buses of similar capability currently scheduled for Space Shuttle launch shows that the Widebody Bus will reduce synchronous orbit launch costs by as much as 13 million dollars. Reduced launch cost is only one of the economic benefits of using the Widebody Bus.

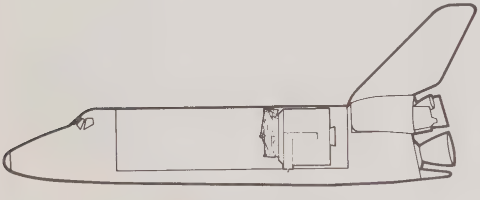

WIDEBODY BUS IN SHUTTLE

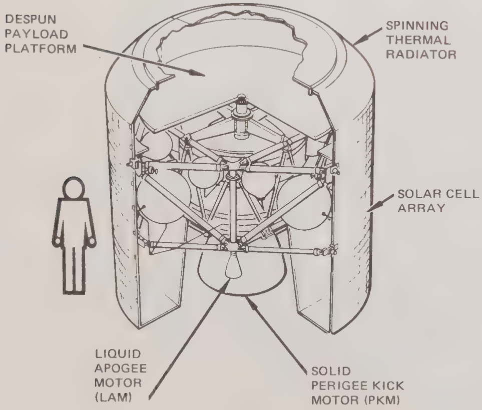
DESPUN PAYLOAD PLATFORM
SPINNING THERMAL RADIATOR
SOLAR CELL ARRAY
LIQUID APOGEE MOTOR (LAM)
SOLID PERIGEE KICK MOTOR (PKM)

Fig. 1 Widebody bus.

Optimization of the spacecraft design exploits the Space Shuttle capability to launch large heavy payloads. Efficient use of the Shuttle's large payload capability frees the system planner from the traditional constraints of weight and volume limits imposed by expendable launch vehicles. This latter feature makes the economies of scale realizable, which may well be a deciding factor in selecting satellites for communications missions in the 1980s.

The economies of scale will dramatically reduce system cost for both small and large capacity carriers. For example, more transponders with frequency reuse via multiple spot beams will be available for large capacity carriers. Small carriers will be able to incorporate more redundancy in their spacecraft to achieve the longer life necessary to amortize their investment over a considerably greater satellite life span than currently available.

BACKGROUND

The spacecraft bus Hughes has designed for the large communications payloads of the 1980s was conceived to take maximum advantage of the Space Shuttle's physical launch capability and lower launch cost. Key features which make the Widebody Bus Shuttle-optimized are its integral propulsion and simple cradle system which minimize both length and perigee stage cost. This configuration allows the use of a single cylindrical widebody spinning solar cell array, 4.27 meters in diameter, capable of supporting a 2 kW satellite load without array deployment. This capacity is notable since power levels projected for most communication satellites in the 1980s are below 2 kW. The dual spin configuration used by the Widebody Bus has been extensively flight-proven in well over 100 in-orbit satellite years on spacecraft launched with expendable boosters.

The Widebody Bus was developed on the Hughes funded Syncom IV program that began in 1976. Launch was slated for an early Shuttle development flight. Under that program satellite development was carried through the design phase and partway into hardware construction. In September 1978, the United States Navy awarded Hughes a contract for UHF satellite communication services under the LEASAT program. The LEASAT spacecraft design is a continuation of the Syncom IV Widebody Bus development. Shuttle launches of LEASAT have been requested to start in February 1982, to permit service to begin by April 1982.

Described below are the application and design of the Widebody Bus being used for the LEASAT program. Following the LEASAT description is a discussion of the capability of the bus to accomodate other payloads and guidelines for determining launch costs for these other missions.

Copyright © American Institute of Aeronautics and Astronautics, Inc., 1980. All rights reserved.

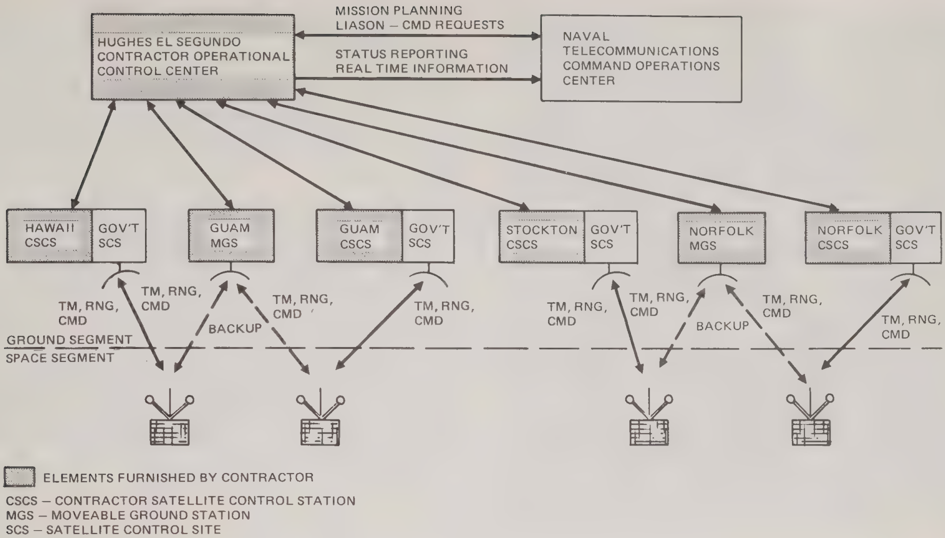
MISSION PLANNING
LIASON – CMD REQUESTS
STATUS REPORTING
REAL TIME INFORMATION
HUGHES EL SEGUNDO CONTRACTOR OPERATIONAL CONTROL CENTER
NAVAL TELECOMMUNICATIONS COMMAND OPERATIONS CENTER
HAWAII CSCS
GOV'T SCS
GUAM MGS
GUAM CSCS
GOV'T SCS
STOCKTON CSCS
GOV'T SCS
NORFOLK MGS
NORFOLK CSCS
GOV'T SCS
TM, RNG, CMD
TM, RNG, CMD
BACKUP
TM, RNG, CMD
TM, RNG, CMD
TM, RNG, CMD
TM, RNG, CMD
BACKUP
TM, RNG, CMD
TM, RNG, CMD
GROUND SEGMENT
SPACE SEGMENT
ELEMENTS FURNISHED BY CONTRACTOR
CSCS – CONTRACTOR SATELLITE CONTROL STATION
MGS – MOVEABLE GROUND STATION
SCS – SATELLITE CONTROL SITE

Fig. 2 LEASAT system elements.

LEASAT, A CURRENT EXAMPLE OF WIDEBODY BUS APPLICATION

The LEASAT system will provide worldwide communication for the Department of Defense beginning in 1982. Service will be provided on a leased basis by Hughes Communication Services, Inc. (HCSI). System elements provided by HCSI include four geosynchronous orbit satellites and associated telemetry, tracking, and command (TT&C) facilities. The four satellites will be located over the continental United States, Atlantic Ocean, Pacific Ocean, and Indian Ocean, as shown in Figure 2. Four fixed ground stations, or primary satellite control sites, will be located in Hawaii, Norfolk, Guam, and Stockton, California. Two movable ground stations are also included, to be used for transfer orbit support and as backup to the SCSs. Centralized satellite control facilities will be located at the HCSI operational control center.

The LEASAT communication payload provides service in the UHF (240-400 MHz) and SHF (7250-7300 MHz and 7975-8025 MHz) frequency bands. Characteristics of the 12 UHF repeaters are shown in Table 1, together with the fleet broadcast channel which employs an SHF uplink and UHF downlink.

Table 1 LEASAT communication channel characteristics

Channel Type	Quantity	Bandwidth, kHz	EIRP*, dBW	G/T*, dBi/K
Relay	6	25	26	-18
Wideband	1	500	28	-18
Narrowband	5	5	16.5	-18
Fleet Broadcast	1	Onboard Processing	26	-20

*Specified minimum values over coverage area for full service period.

LEASAT Spacecraft Description

The LEASAT bus shown in Figure 3 is designed specifically for Shuttle launch, resulting in an arrangement distinctly different from transition designs. Its most notable feature is the relatively short axial length when installed in the Shuttle. This feature is made possible by the characteristic 4.27 meter diameter Widebody Bus envelope which permits installation of the perigee propulsion stage centrally within the spacecraft enclosure, as shown in Figure 4, rather than as an axial extension of the spacecraft. The compact axial length of the spacecraft requires a length fraction of Shuttle capability closely matched to the required mass fraction of Shuttle capability. Since Shuttle launch fees are based on the fraction of the 18.3 meter bay length used, or the fraction of the 29,550 kg liftoff rating used, whichever is greater, the LEASAT system efficiently uses the Shuttle resources and benefits from the resulting reduced launch cost.

The mission sequence shown in Figure 5 from Shuttle ejection to acquisition of geosynchronous orbit is shaped to optimize performance of the integral perigee stage and the associated propulsion systems carried in the LEASAT design. The major perigee boost is provided with the jettisonable solid perigee stage or perigee kick motor (PKM). This motor provides a nearly impulsive velocity increment at the 260 km altitude of the Shuttle orbit, placing the spacecraft in an elliptical subtransfer orbit with an apogee altitude of some 6450 km. Following jettison of the burned-out PKM and its adapter, a bipropellant liquid apogee motor (LAM) is fired at perigee of the subsynchronous transfer orbit, resulting in a cumulative perigee velocity increment of 2440 m/sec and raising the elliptical transfer orbit apogee to geosynchronous altitude. The LAM is then fired at apogee to introduce another 1830 m/sec velocity increment and place the spacecraft in geosynchronous orbit. In order to make final corrections in the orbit geometry, and to control drift to the final desired longitude, a monopropellant reaction control subsystem (RCS) is used. The RCS is subsequently used for on-station operations, including inclination and longitude position control, spin speed control, and maintenance of spin axis attitude normal to the orbit plane.

The above mission sequence represents a nominal case. However, the combined propulsion systems carried onboard offer an inherent flexibility to accommodate variations in payload mass or propulsion stage performance requirements. In particular, LAM augmentation at perigee can be varied, RCS propellant can be used to contribute to apogee ΔV, and maneuvers using axial thrusters (e. g., transfer orbit reorientation, north-south stationkeeping, and attitude control) can be shared between LAM and RCS to optimize propellant usage. For mass or performance changes identified a priori, liquid propellant loading change may be considered.

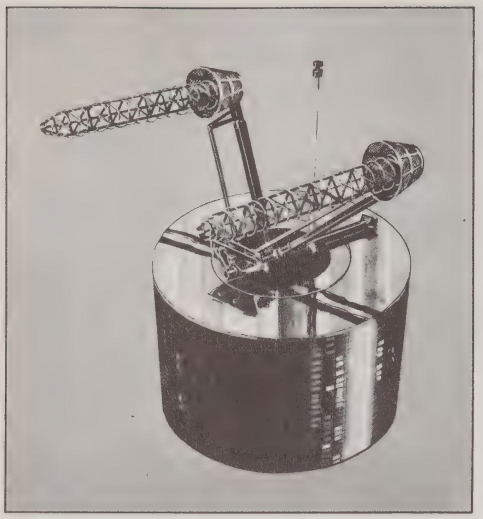

Fig. 3 LEASAT overall configuration.

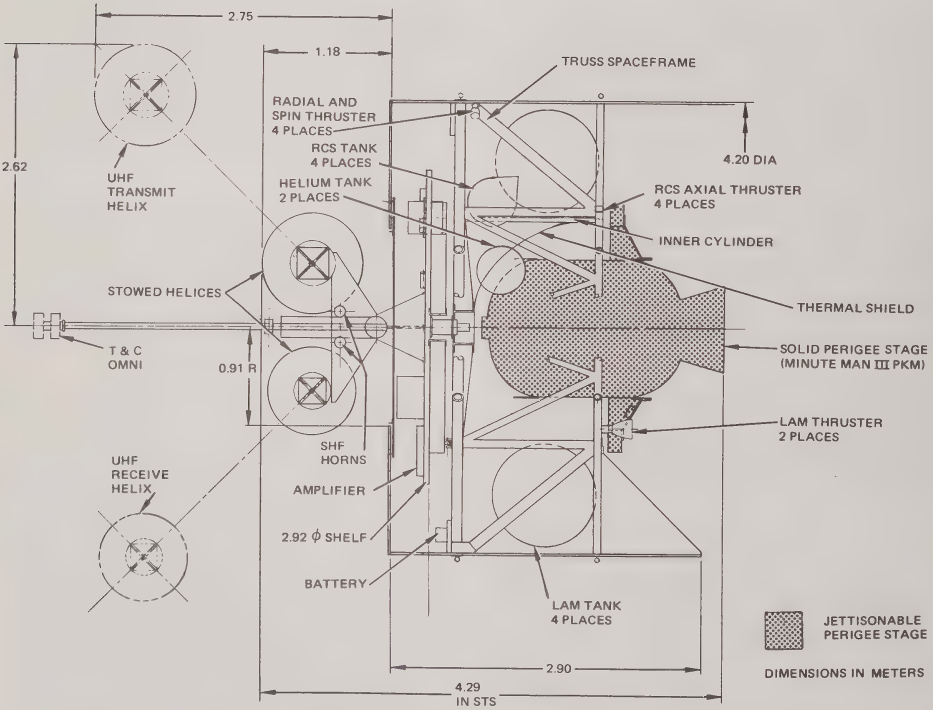
2.75
1.18
TRUSS SPACEFRAME
RADIAL AND SPIN THRUSTER 4 PLACES
RCS TANK 4 PLACES
HELIUM TANK 2 PLACES
4.20 DIA
2.62
UHF TRANSMIT HELIX
RCS AXIAL THRUSTER 4 PLACES
INNER CYLINDER
STOWED HELICES
THERMAL SHIELD
T & C OMNI
0.91 R
SOLID PERIGEE STAGE (MINUTE MAN III PKM)
LAM THRUSTER 2 PLACES
SHF HORNS
UHF RECEIVE HELIX
AMPLIFIER
2.92 ϕ SHELF
BATTERY
LAM TANK 4 PLACES
▨ JETTISONABLE PERIGEE STAGE
DIMENSIONS IN METERS
2.90
4.29 IN STS

Fig. 4 LEASAT general arrangement.

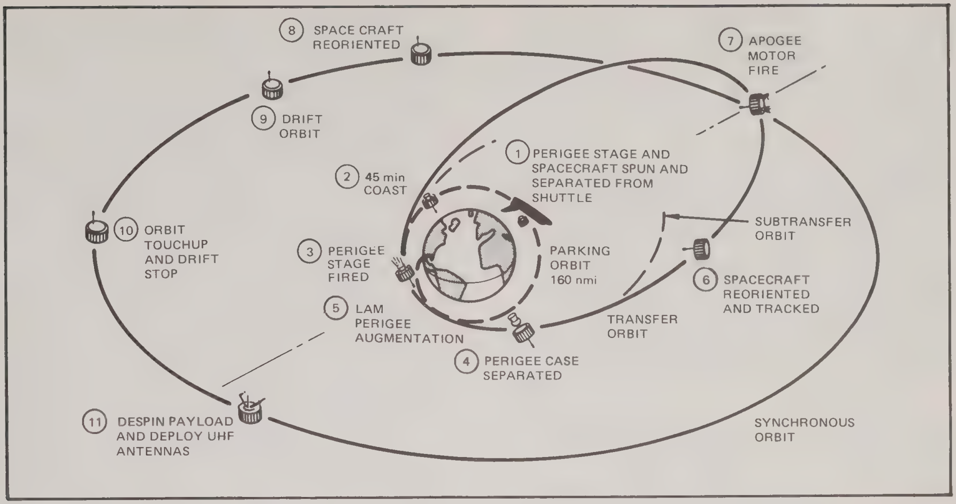
8 SPACE CRAFT REORIENTED
7 APOGEE MOTOR FIRE
9 DRIFT ORBIT
1 PERIGEE STAGE AND SPACECRAFT SPUN AND SEPARATED FROM SHUTTLE
2 45 min COAST
10 ORBIT TOUCHUP AND DRIFT STOP
SUBTRANSFER ORBIT
3 PERIGEE STAGE FIRED
PARKING ORBIT 160 nmi
6 SPACECRAFT REORIENTED AND TRACKED
5 LAM PERIGEE AUGMENTATION
TRANSFER ORBIT
4 PERIGEE CASE SEPARATED
11 DESPIN PAYLOAD AND DEPLOY UHF ANTENNAS
SYNCHRONOUS ORBIT

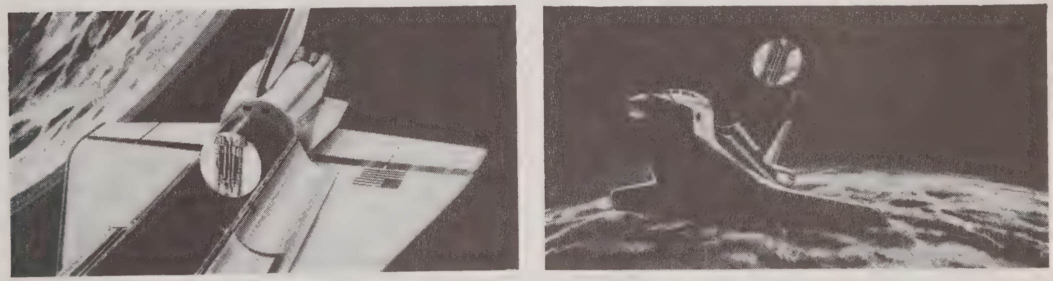

IN SHUTTLE BAY

EJECTION AND SPINUP

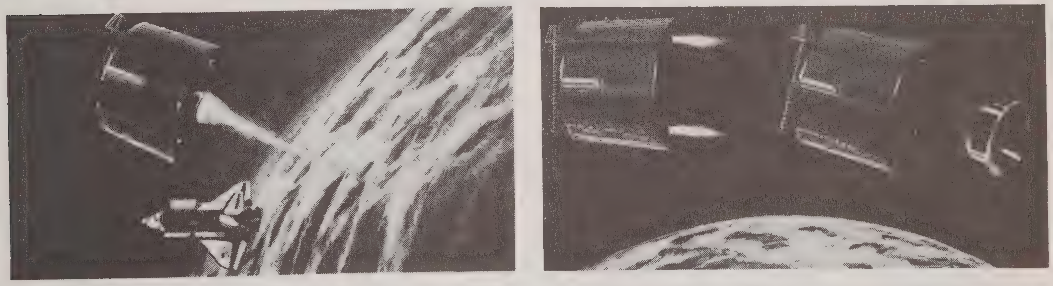

PERIGEE MOTOR FIRING

PERIGEE MOTOR CASE EJECTION AND APOGEE MOTOR FIRING

Fig. 5 LEASAT mission sequence.

LEASAT Detailed Design

Key performance characteristics of the spacecraft are summarized in Table 2. The spacecraft supports a communication payload weight of 204 kg. With expendables, including the jettisonable perigee stage, the total separated weight from the Shuttle is 6898 kg. A subsystem weight summary is shown in Table 3. The power summary in Table 4 shows a payload power requirement of approximately 0.7 kW. The total spacecraft requirement is approximately 1.1 kW, which is supported throughout sun and eclipse with a power source sizing of 1.2 kW. The spacecraft provides an earth oriented platform maintaining UHF antenna RF boresight pointing to earth center within 0.5 degree which is appropriate for the gain profiles of the earth coverage antennas employed. This allocation is dominated by alignment and thermal excursion allowances for the large deployed UHF helices. Balance of the passive thermal control characteristics of the spacecraft provides equipment deck bulk temperatures near room temperature. Sufficient reserve radiation surface area exists to adjust the equipment temperature as required.

The general arrangement of the LEASAT spacecraft is shown in Figure 4. Surrounding the PKM are the bipropellant LAM tanks. From the PKM and LAM elements, which represent the majority of the spacecraft liftoff mass, loads are transferred through a graphite composite tubular truss structure to pickup points at the spacecraft periphery where they are carried through the cradle to the Shuttle attachment points. Besides serving as a load transfer element, the cradle carries spacecraft holddown and release mechanisms and interface electronics.

Table 2 LEASAT spacecraft bus performance characteristics

Design life	10 years (5 required)
Weight, kg	Payload: 204 Bus: 985 Total at liftoff: 6898
Power watts (sun and eclipse, 5 years)	Payload: 732 Bus: 361 Total source availability: 1180
Orbit position requirement	±1° longitude ±3° latitude
Antenna alignment, thermal excursion, and pointing control (4 m UHF earth coverage helices)	±0.5° (2 week attitude correction interval, ground controlled)
Equipment thermal control	29°C maximum bulk temperature

Table 3 LEASAT weight summary

Subsystem	Weight, kg
Communications	204
T&C	75
Attitude control	25
Reaction control (dry)	16
Liquid apogee motor (dry)	127
Power and distribution	309
Thermal control	65
Structure	368
Dry hardware	1189
Minimum margin	45
Expendables (perigee, apogee, on-orbit)	5350
PKM/adapter	314
Weight at Shuttle separation	6898

Table 4 LEASAT power summary, watts

Communications	732
T&C	61
Attitude control	34
Thermal control	55
Power and distribution	69
Battery charge/heaters	142
Required	1093
Minimum source sizing	1180 (5 years)
Minimum margin	87 (5 years)

All communications equipment is carried on a shelf forward of the truss spaceframe. During launch, the shelf is structurally locked to the truss. On-orbit following lock release, the shelf is despun and earth pointed by means of the bearing and power transfer assembly (BAPTA) and despin control subsystem. Power and spacecraft T&C signals are carried across the BAPTA on sliprings. All RF connections from the shelf to the SHF horns, T&C omnis, and UHF helix antennas are via coax or waveguide with no rotating RF interfaces. UHF helices are deployed in a simple planar motion by means of spring/damper actuators and composite construction parallel-bar support tubes. The deployable T&C antenna mast is controlled through a single-pivot motion by spring/damper actuator.

Two LAM 225 N axial thrusters are located at the aft end of the spacecraft. Six 22 N RCS thrusters are used, two providing axial thrust, and four providing lateral thrust. Lateral thrusters provide spinup and spindown control and are the primary means of providing east-west longitude control and repositioning on orbit. Axial RCS thrusters provide spin axis attitude and orbit inclination control.

An annular shelf is located at the outboard extremity of the spun truss spaceframe for spacecraft subsystem equipment mounting. Carried here are batteries and power regulation electronics, attitude control units, spun T&C, and driver units for pyrotechnic and propulsion valve operation.

A solar cell array installed on a composite sandwich substrate forms the outer spacecraft enclosure.

Primary heat rejection from the communications electronics is by means of radiation from the spinning forward barrier. The barrier external surface provides solar rejection by means of a low solar absorptance, high infrared emissivity finish. Internally, the barrier surface finish is varied to provide the degree of coupling desired for optimal thermal balance. Spun equipment dissipations are accommodated by coupling to the solar panel and forward barrier. The aft enclosure and PKM cavity are insulated.

LEASAT/Shuttle Integration

Shuttle integration requirements have influenced the spacecraft structural, thermal, and electrical design. These requirements have stemmed not only from the need for physical interface compatibility between spacecraft and launch vehicle but also from the Shuttle safety standards. The more prominent features of the spacecraft design resulting from the unique Shuttle integration requirements are noted below.

In contrast to the usual thrust-tube type structural interface between spacecraft and commercial expendable boosters, the Shuttle structural interface consists of multiple discrete attachments along longerons and keel. The LEASAT integrated spacecraft/cradle structural arrangement was developed to accommodate the discrete load path geometry and the restrictions on load type, orientation, and magnitude at the discrete sites.

The Shuttle safety requirements have influenced the LEASAT bus design in several ways. The spacecraft postejection sequencer (PES), which provides on-board timing and control for operations including spinup and PKM arming/fire, incorporates internal triple series redundancy to meet the Shuttle 3-failure level protection against critical events such as inadvertent propulsion firing. External interlocks that include umbilical disconnects and separation switches are also employed. Other interlocks utilize g switches which sense spacecraft spinup.

Series redundant valves and valve actuation switches are used in the liquid propulsion subsystems to preclude leakage or firing in the Shuttle. The PKM safe and arm devices are left in the safe position for 45 minutes after the spacecraft has been ejected from the Shuttle. As an additional precaution, batteries are not connected to the spacecraft loads while the spacecraft is in the Shuttle, the PES (which initiates PKM firing) is unpowered, and no power is on the spacecraft while the Shuttle doors are closed preventing sun illumination of the solar panel.

WIDEBODY BUS FLEXIBILITY IN ACCOMMODATING PAYLOADS

The LEASAT system described above is one example of Widebody Bus application. The Widebody Bus, however, is capable of efficiently accommodating a wide range of payloads. A large payload power capability can be achieved through simple body mounted solar arrays providing 2 kW of power without requiring extendable or oriented panels. The payload equipment platform can accept large payloads since it can be increased to a diameter of 4 meters with mounting surface provided on both sides. The 4.27 meter diameter spinning thermal radiator can provide ample radiator surface capable of dissipating at least 2 kW. Fixed antenna reflectors up to 4.6 meters in diameter can be accommodated.

Extremely accurate antenna pointing can be achieved with the Widebody Bus, partly owing to the large spin inertia of the spacecraft which provides a very stiff base for antenna mounting and control. A payload platform pointing accuracy of ±0.1 degree is provided. Antenna pointing accuracy of ±0.03 degree can be achieved using RF beacon tracking with the despin motor providing east-west pointing and an antenna pointing mechanism providing north-south control. This antenna pointing capability will soon be demonstrated on a smaller dual spin spacecraft.

Payload weight capability far in excess of LEASAT can be obtained by increasing propellant loading of the propulsion subsystem. Selection of PKM solid propellant loading establishes payload capability (in the absence of LAM perigee augmentation), with propellant tank sizes for the LAM and on-orbit monopropellant hydrazine systems selected to match PKM capability. A wide range of qualified tanks already exists for these liquid systems, and the cost of qualifying other sizes, if required, is relatively small.

WIDEBODY ECONOMICS

The economy of the Widebody Bus is derived from a fundamental approach similar in important ways to the Shuttle itself. Table 5 lists factors which make the Shuttle a low cost launching system for low orbit and draws parallels to similar features on the Widebody Bus which have the effect of extending this economy to synchronous orbit. These additional economies enhance the basic Shuttle launch cost saving accrued through the compact length of the Widebody Bus. A consolidation of these savings is reflected in the estimated launch costs shown in Figure 6.

Using that cost relationship, the economy of the Widebody Bus approach will be shown through several examples. These examples are summarized in Table 6. First, the Intelsat V communications package will be used as a common reference payload. The launch cost using the Widebody Bus for this payload would be about 13 million dollars less than the Intelsat V spacecraft launch cost using the SSUS-A perigee stage on the Space Shuttle. Or, as a second example, if the Intelsat V spacecraft were modified by completely collapsing the antenna tower to reduce launch costs, currently dominated by length, the Widebody advantage would still be some 3 million dollars per launch. This comparison to the Intelsat V and SSUS-A bus system is based on 1984 prices and includes perigee stage costs.

Table 5 Economic concepts parallel shuttle approach

Concepts Leading to Lower Launch Cost	Economic Parallels	
	Space Shuttle	Widebody Bus
Launch system reused	Orbiter reused	Cradle reused
Expendables minimized	Liquid propellant tank is only expendable	Solid propellant case is only expendable
Subsystems reused in all mission phases	Orbiter systems used throughout mission	Spacecraft subsystems used in both transfer and final orbit
Large payload capability permitting economy of scale	Cargo capability of 29,545 kg	Large communications payloads accomodated (e.g., 680 kg, 2kW, and 4.3 m diameter antenna)

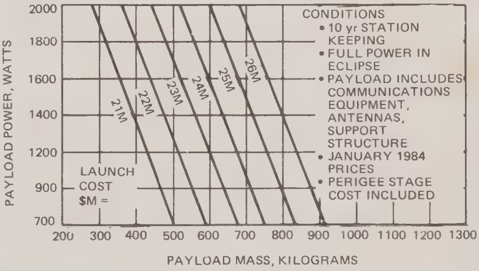

Fig. 6 Launch cost.

Table 6 Launch cost comparison

Example	Comparison	Major Cost Discriminators	Launch Cost Difference
1	Widebody bus/ Intelsat V payload	1/4 cargo bay, integral perigee motor	Widebody bus less by $13 M
	SSUS-A/Intelsat V spacecraft	1/2 cargo bay, separate perigee stage	
2	Widebody bus/ Intelsat V payload	Integral perigee motor	Widebody bus less by $3 M
	SSUS-A/shortened Intelsat V spacecraft	Separate perigee stage	
3	Widebody bus/ 2273 kg payload	45% of shuttle capacity, integral propulsion	Widebody bus less by $20 M
	IUS/2273 kg payload	70% of shuttle capacity, separate propulsion systems	
4	Widebody bus/dual Intelsat V payload	1/3 cargo bay, integral perigee motor	Widebody bus less by $8 M
	SSUS-A/single Intelsat V spacecraft	1/2 cargo bay, separate perigee stage	

As a third example, when compared to the IUS rather than the SSUS-A, the Widebody Bus would save at least 20 million dollars per launch. This comparison includes the perigee and apogee stage costs for the Widebody and is based on the reference 2273 kg synchronous orbit payload capability of the IUS. An allowance was made for the extra structure and propulsion system (i. e., nonpayload) weight carried into synchronous orbit by the Widebody Bus, and the comparison uses 1984 prices.

As a fourth example, an appreciation for the economy of scale can be gained by comparing the launch cost of an Intelsat V class payload on the Widebody Bus to the launch cost of a payload having twice the weight and power carried on the Widebody. This doubling of payload weight and power is well within the generic capability of the Widebody Bus and increases the launch cost by only 5 million dollars, which is still less than the Intelsat V/SSUS-A launch cost. Hence, on one hand, an Intelsat V class payload could be launched on the Widebody Bus at a savings or, alternatively, the same launch investment could be used to launch more than double the payload.

CONCLUSIONS

The potential of the Shuttle launched Widebody Bus to economically carry payloads to synchronous orbit has been illustrated. Such economy is required if communications satellites are to compete effectively with microwave and fiber optic cables. The Widebody Bus will make a significant contribution toward ensuring that economic trades favor communication satellite systems in the 1980s.

THE GEO-SPAS PLATFORM —
A THIRD GENERATION COMMUNICATION SATELLITE CONCEPT

80-0505

D.E. Koelle and W. Kleinau
MBB Space Division, Ottobrunn/Germany

Abstract

The first chapter of the paper deals with the definition of the third generation of communication spacecraft being characterized by mass values beyond 2 000 kg and power level above 3 kW. The first generation in this context are spinners and dual-spin spacecraft with body mounted rigid solar arrays, and the second generation the 3 axis-stabilized conventional satellites with deployable solar arrays.

The third generation platform-type satellites will be different in configuration by having a structure backbone with externally mounted decentralized equipment. The paper describes a practical approach for a first geosync communication platform which fulfils three major requirements:

- large payload mounting area (for multiple antennae)
- large radiation areas for heat dissipation, and
- minimum launch cost.

The conceptual approach is making use of MBB's SPAS concept (Shuttle PAllet Satellite) with a CFC truss structure directly mounted into the cargo bay as a bridging structure. This does not require special rigs or cradles for transportation by the Shuttle. Deployment of the spacecraft will be performed by the STS-Remote Manipulator System, using the standard grapple fixture on the platform.

The second basic feature is the integrated unified propulsion system, making a special perigee kickstage obsolete. The platform incorporates a multitank propellant assembly which performs the perigee impulse, the apogee impulse, orbit corrections and attitude control. The GEO-SPAS modular structure and the subsystems are outlined including their integration and (decentralized) thermal control.

The final chapter describes the economic advantages of the new platform concept. The Shuttle launch cost are minimized as well as the propulsion system cost, resulting in about half the cost compared to a conventional solution.

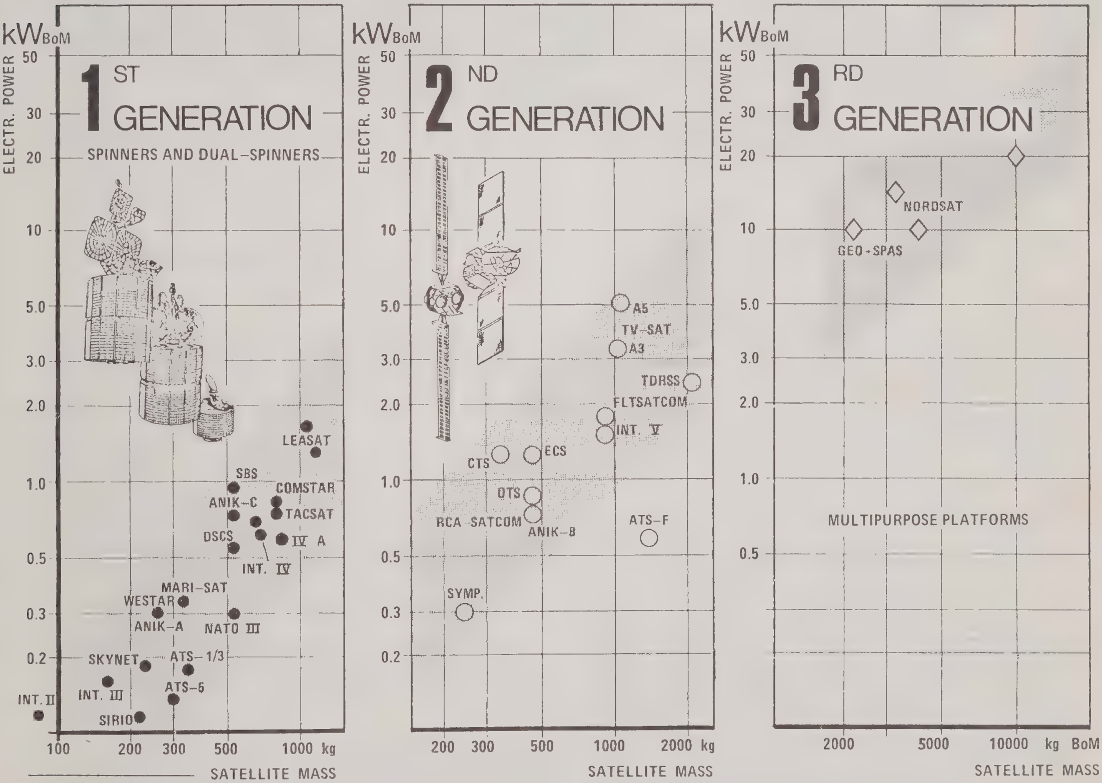

Fig. 1: Definition of Communication Satellite Generations

---

* Mgr., Adv. Systems and Technology Development
** Senior System Engineer

Copyright © American Institute of Aeronautics and Astronautics, Inc., 1980. All rights reserved.

I. Communication Satellites Concept Evolution

The capacity and capabilities of communication satellites will continue to be growing in the future, as it has been the case in the past 20 years. In Fig. 1 it has been tried to visualize the growing capabilities by the definition of satellite "generations". In this context the initial series of spinners and dual-spinners historically form the "first generation". The second generation consists of the generally more powerful Earth-oriented spacecraft with sun-tracking solar arrays. A "third generation" would be the future "multipurpose platforms" - subject of this paper. They can be characterized by having a mass of more than 2 000 kg and a power level above 3 kW (up to 20 kW and more). For such geosync platforms the launch operations are not yet defined. The Space Shuttle itself is limited to low Earth orbits and the auxiliary transfer stages required like IUS (or later the OTV) allow only the design of conventional (box-shaped) spacecraft with some 4 m maximum diameter, occupying a great deal of the cargo bay length.

The next generation of satellite platforms need some new technical ideas, new in the sense of implementation. Of course one could imagine sophisticated vehicles dedicated for orbital assembly with electrically powered transfer, etc. For the beginning, however, this may be too ambiguous, expensive and - unnecessary. The Shuttle provides the possibility of launching complete platforms with severatons initial mass if the SPAS concept with an integrated propulsion system is being applied.

II. The GEO-SPAS Concept

In 1977 MBB has conceived the "Shuttle Pallet Satellite" (SPAS) concept, a new type of spacecraft dedicated to Shuttle launches. It applies a flat truss structure bridging the cargo bay and uses modular (building-block) elements. The principle and its application also for geosync platforms was mentioned first in Ref. 1 (1978). In this paper the project is discussed in more detail.

The GEO-SPAS platform is characterized by its integrated unified propulsion system. This provides all propulsive functions after the platform has left the Shuttle cargo bay by assistance of the Shuttle manipulator, eliminating the need for a special (expensive) kick stage. The platform transfers itself from LEO to geosynchronous orbit (GEO). Depending on the initial platform mass and the engine thrust level the transfer to geosync orbit will comprise more than two propulsive maneuvers, i.e. two or more intermediate transfer orbits will be used.

The propulsion system is completely integrated, thus requiring no own structure and electronics. This is one of the reasons for the outstanding cost effectiveness of the new platform concept.

Instead of optimizing propulsion system performance by applying staged propulsion for LEO → GEO transfer, it has rather been tried to minimize cost. This can only be achieved by a reduced number of systems (i.e. elimination of a separate perigee injection system) instead of reducing the amount of propellants.

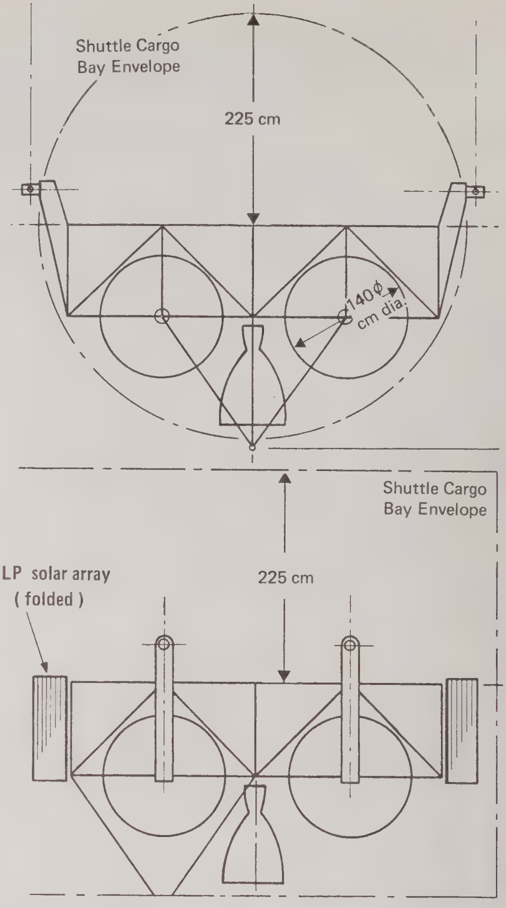

Fig. 2: GEO SPAS Conceptual Design and Geometry

Fig. 2 shows the GEO-SPAS concept with its bridging structure configuration and dimensions. The CFC truss structure is mounted directly to the Shuttle cargo bay by two sill fitting plus a keel support. This means that no special cradle mechanism is required for spacecraft support and release.

The platform size can be adapted to the payload requirements: either to the payload mass or antenna farm geometry, whatever is more demanding. Fig. 3 shows the full scope of the Modular Building-Block (MBB-) concept: with the same elements a family of spacecraft platforms can be realized, from a small one (Delta-satellite class communication payload) to a large 32 m^2 platform (GEO-SPAS IV) with 500 to 1 000 kg communication payload capability.

Platform size and mass are optimized with respect to the Shuttle charging policy, i.e. both mass and length of the cargo bay are fully utilized, resulting in the minimum feasible launch cost.

The platform concept provides a large Earth-pointing area thus allowing for a family of antennas. These antenna systems can be installed rigidly, thus avoiding complex deployment mechanisms. The platform/

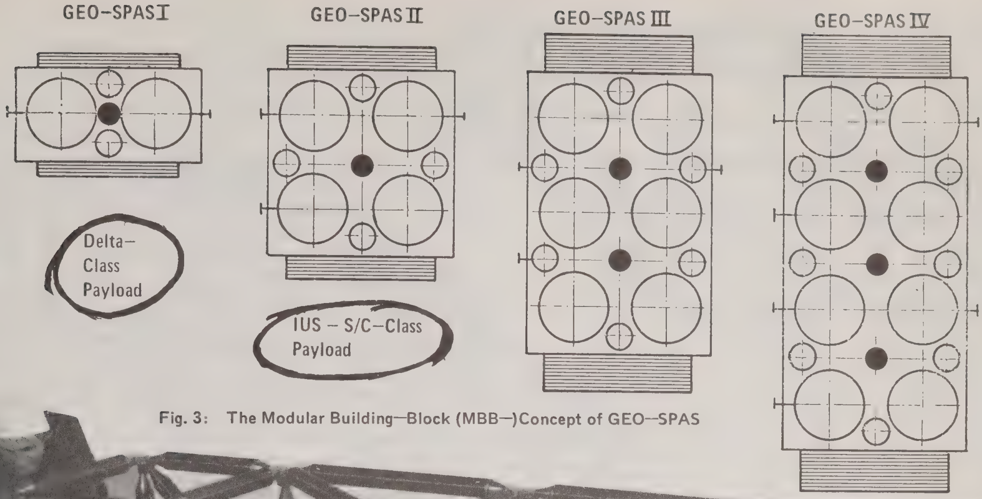

Fig. 3: The Modular Building-Block (MBB-)Concept of GEO-SPAS

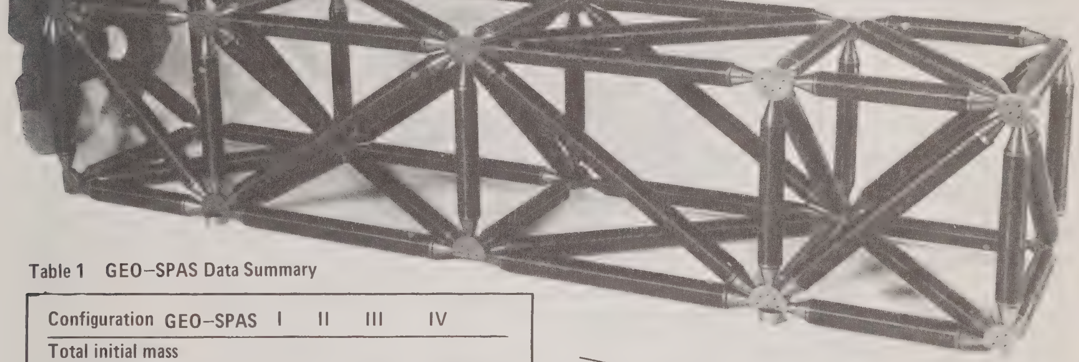

Table 1 GEO-SPAS Data Summary

Configuration GEO-SPAS	I	II	III	IV	
Total initial mass M_0 (Launch)	4.6	9.0	13.5	18.0	Mg
Propellant mass for GEO transfer	3.5	6.8	10.2	13.6	Mg
Spacecraft mass BoM (M_1)	1.1	2.2	3.3	4.4	Mg
Platform area	8	16	24	32	m^2
Length of basic platform	2.1	4.1	6.1	8.1	m
Length available according to Shuttle charging policy	2.6	5.2	8.0	10.5	m
Basic platform mass	760	1300	1870	2430	kg
Payload equipment, thermal control, eclipse battery, Solar array	210	660	1100	1510	kg
Bipropellants for attitude-/orbit control Ion thruster system and Mercury prop.	130	240	330	400	kg
Shuttle Launch Cost (1980)	7	13	20	26	Mio. $

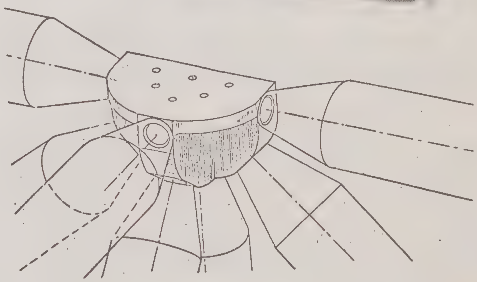

Fig. 4: Truss Structure with CFC Tubes and Ti-Interconnections

cargo bay geometry allows for 2.2 m free space between platform and the top of the cargo bay for the repeaters and antenna assembly. This could consist of a single large deployable antenna or a farm of different antennas.

Main data of the various GEO-SPAS platform sizes as well as the launch cost are summarized in Table 1 with a new philosophy for the mass and payload capability (being discussed in chapter 4).

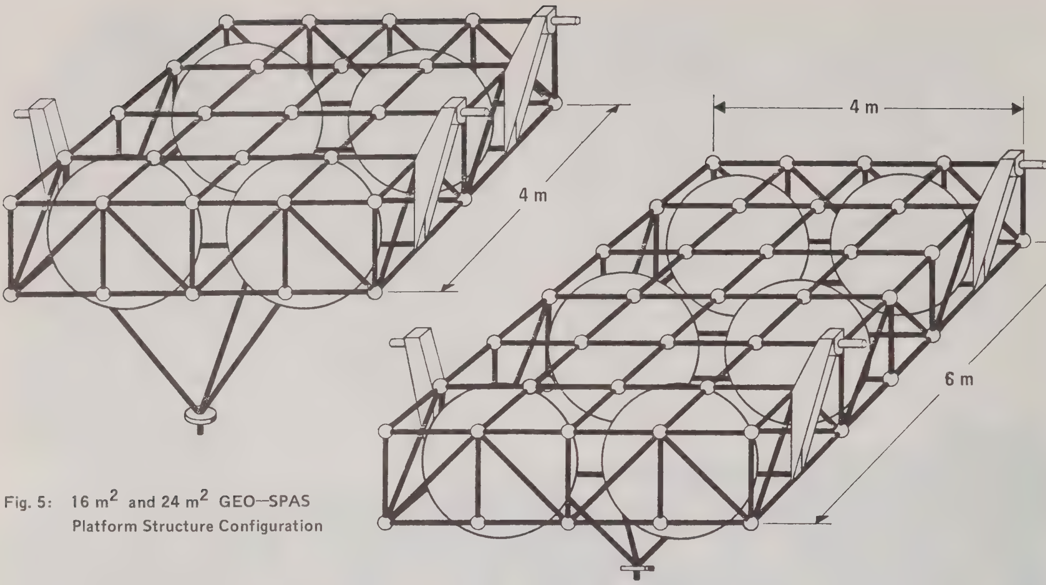

Fig. 5: 16 m^2 and 24 m^2 GEO–SPAS Platform Structure Configuration

III. GEO-SPAS Platform Design

The overall design is characterized by the flat modular truss structure with a span of 4.1 m, determined by the Shuttle cargo bay width. Fig. 4a shows the first element built and tested (flight hardware). The truss structure uses CFRP-tubes of high stiffness and low mass interconnected by titanium node elements (Fig. 4b). The total mass of the basic structure for a 4 x 4 m platform is 520 kg, for a 4 x 8 m structure about 780 kg. Fig. 5 shows the structure configuration for the 16 m^2 and the 24 m^2 GEO-SPAS platforms with mounting and support provisions.

The spherical propellant tanks are integrated into the structure. With a diameter of 1.4 m a pair of two tanks can carry a load of 3 600 kg MMH and N_2O_4.

The main engine thrust level is optimum in the 5 to 10 kN range, however, no engine is existing yet in this size. Therefore, a new engine has been conceived with 5 kN thrust level, based on the comprehensive bipropellant engine experience of MBB (Astris, Symphonie, Galileo). The engine has a specific impulse of more than 310 sec and a mass of 20 kg. Probably also a modified Shuttle attitude control engine would be applicable.

The main engine(s) requires an electrically driven (slow) gimbal system for thrust vector alignments while attitude and orbit control is performed by rigidly installed small 10 N thruster clusters. The latter are already being used on the NASA GALILEO spacecraft.

The other platform subsystems are housed within equipment boxes mounted externally of the primary SPAS-Structure. Each box has its own subharness and thermal control (passive plus heaters). The design approach of the subsystems, in particular of the power supply and data systems is modular, to cope with various payload requirements. The 3-axis stabilization system employs a redundant momentum wheel system controlled by a central modular digital electronics based on Earth-IR and Sun-sensor informations. The pointing accuracy of about 0.2^0 can be improved if required by applying an RF-sensor integrated into the payload antenna feeder system.

An example of GEO-SPAS II for a NORDSAT-TV-SAT application is shown in Fig. 6. This spacecraft carries two transmit antennas for the eastern and western service areas, a common receive antenna and, in addition, a repeater comprising 8 x 450 W - TWTAs and 8 x 250 TWTAs, whereby 8 x 450 W- and 5 x 250 W-channels could be operated simultaneously.

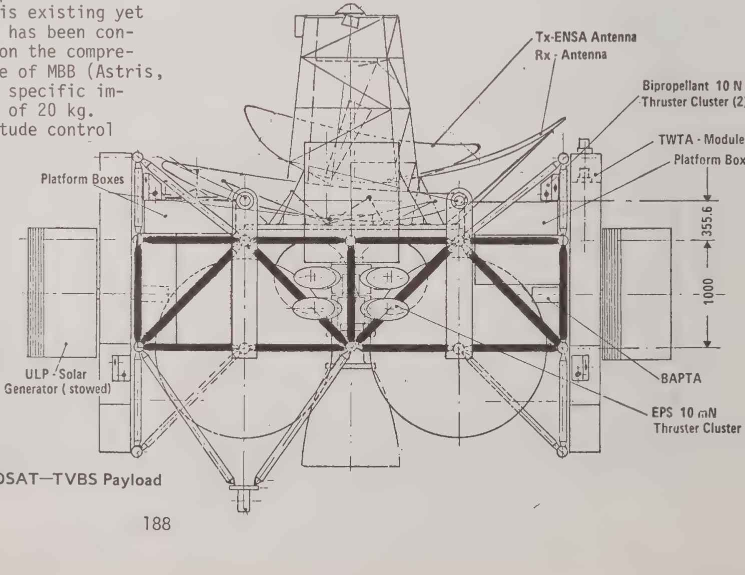
Tx-ENSA Antenna
Rx - Antenna
Bipropellant 10 N Thruster Cluster (2
TWTA - Module
Platform Box
Platform Boxes
355.6
1000
ULP - Solar Generator (stowed)
BAPTA
EPS 10 mN Thruster Cluster

Fig. 6: GEO–SPAS Design Example for NORDSAT–TVBS Payload

IV. GEO-SPAS Capabilities and Performance

The GEO-SPAS systems are conceived as "basic platforms" as identified in Table 2, including structure, propulsion system, attitude control, subsystem, TM/TC and data handling. The basic platform mass excludes the payload with its thermal control and power supply (both solar array and eclipse batteries). In addition, the option is left open whether ion thrusters for orbit control are chosen (RITA-2 system) or chemical propellants only. The choice is a trade-off between payload (+ payload-associated) mass, and orbital lifetime.

For 7 years lifetime chemical propellants may be sufficient, for 8 to 15 years orbital operations ion thrusters allow for essentially higher payload. Table 2 illustrates the philosophy for a 350 kg/5 kW payload: 7 years are feasible for bipropellants only while 15 years can be achieved using ion thrusters (RITA-2) for E/W and N/S-stationkeeping.

Fig. 7 shows the payload power requirement vs. communication payload mass. Two branches can be identified: the high-power branch of direct TVBS and the "low-power" branch of global and regional telecommunications. Some platforms may have mixed payloads with power requirements over the full range indicated in Fig. 7 for GEO-SPAS II and III.

The overall performance analysis (Table 2) has been conceived a bit different from standard procedures: starting from the available mass beyond the basic platform (900 kg for GEO-SPAS II) the payload mass and the required power supply mass are deducted, the rest being the mass for orbit control. Fig. 8 shows the mass of the ULP solar array vs. power for conventional solar cells and advanced 50 μ thin cells.

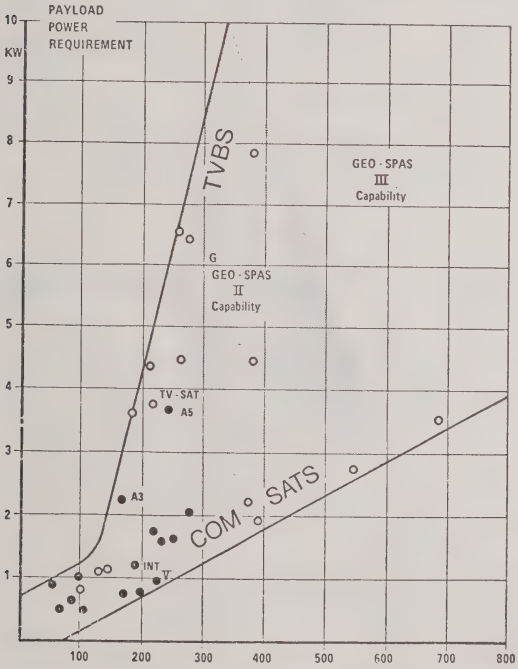

Fig. 7: Payload Power vs. Payload Mass and GEO—SPAS II and III Performance Range

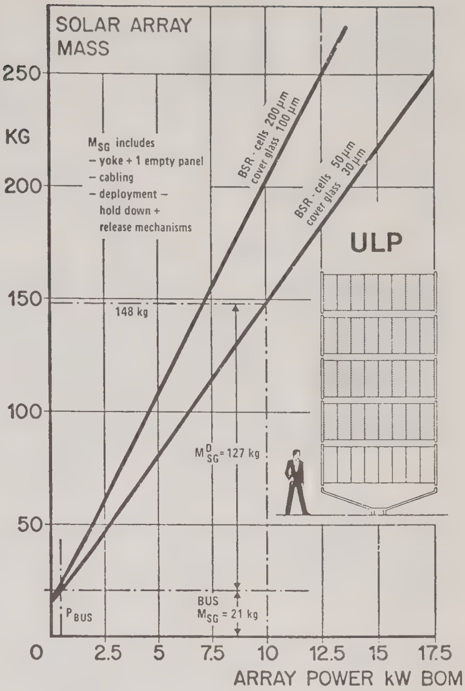

Fig. 8: ULP Solar Array Mass vs. Power (BoM)

Table 2 GEO—SPAS Performance / Lifetime Philosophy

Configuration GEO—SPAS	I	II	III	IV	
Total Mass M_{GEO} (BoM)	1100	2200	3300	4400	kg
Basic Platform Mass	760	1300	1870	2430	kg
available for payload and support equipment, orbit control	340	900	1430	1970	kg
– payload mass (repeater, antennas and thermal control)		– 350 kg (PL) + 100 kg (PL—TC)			
– solar array		– 130 kg (Fig. 8) 1)			
– eclipse battery mass		– 80 kg (Fig. 9) 2)			
Rest available for orbit control over n years		340 kg			
		7 years with chem. propellants only (Fig. 10)	or	≈15 years with ion thrusters incl. 2 year chem. capability (Fig. 11)	

1) e.g. 10 kW BOM, EQ for 50 µ BSR cells

2) e.g. 1400 Wh required stored energy (DoD 60 %)

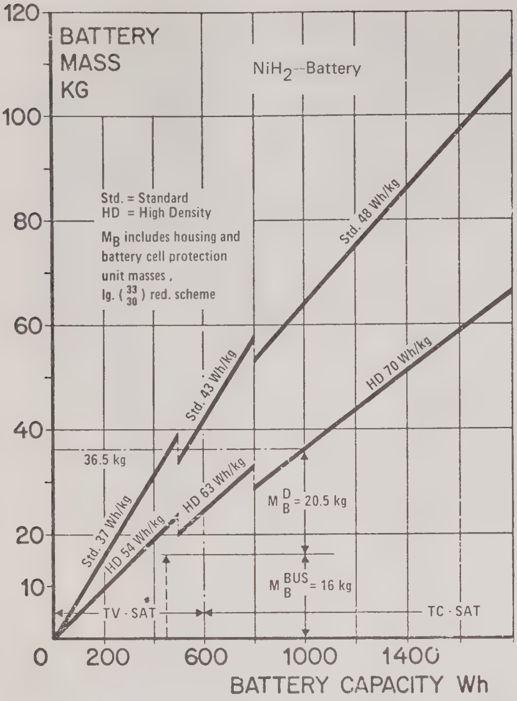

* no TV - operation during eclipse

Fig. 9: Battery System Mass vs. Capacity (Payload Eclipse Battery)

Since the latter have a lower degradation in orbit the gain is even greater. Fig. 9 shows the mass for Nickel-Hydrogen batteries vs. capacity required. Direct TV-broadcasting satellites need much lower battery capacity than telecom-satellites because no eclipse operation is required.

After substraction of the payload mass (incl. thermal control) and the solar array and battery mass from the basic platform mass the rest is available for orbit control over a certain period of years.

With assistance of Figs. 10 and 11 the required propellant mass vs. years in orbit can be determined. The solar array size has an influence on the E/W control maneuver propellants; the range is indicated. In Fig. 11 the total system mass is shown for a hybrid system, i.e. electric propulsion in addition to a 2 year bipropellant operation. The reference point in both figures shows the mass saving of 250 kg for a 12 year orbit design lifetime (GEO-SPAS II), respectively a lifetime extension from 5 to 12 years in case of a limited RCS mass.

V. GEO-SPAS Cost Advantages

The GEO-SPAS design is Shuttle-dedicated and optimized in accordance with the NASA charging policy. In other words, both volume and mass capacity of the Shuttle are utilized to the maximum possible extent.

This means that the Shuttle launch cost charge for GEO-SPAS II is only about 13 Mio. $ (1980), derived from the occupied length of 5.5 m or the mass of 9 000 kg. This is based on a 32.4 Mio. $ total dedicated Shuttle flight price (1980).

For the same payload or an initial spacecraft mass of 2 200 kg in GEO the charge for a conventional satellite plus the IUS vehicle required is about 30 Mio. $ (1980), based on the total initial mass of 21 000 kg. This means that in this case practically a full Shuttle flight has to be paid for, although some 8 m length of the cargo bay are not utilized.

However, this is only one aspect of the GEO-SPAS efficiency. The second major cost advantage is the fact that no additional propulsion stage and no special support equipment (ASE) is required.

The Integrated Unified Propulsion System (IUPS) is certainly more expensive than a conventional spacecraft RCS equipment, however, far less expensive than a separate stage. No dedicated structure, electronics, attitude control, guidance and power supply are required. The relevant systems of the spacecraft are utilized instead.

Fig. 12 summarizes the cost comparison with some rough cost figures (estimates).

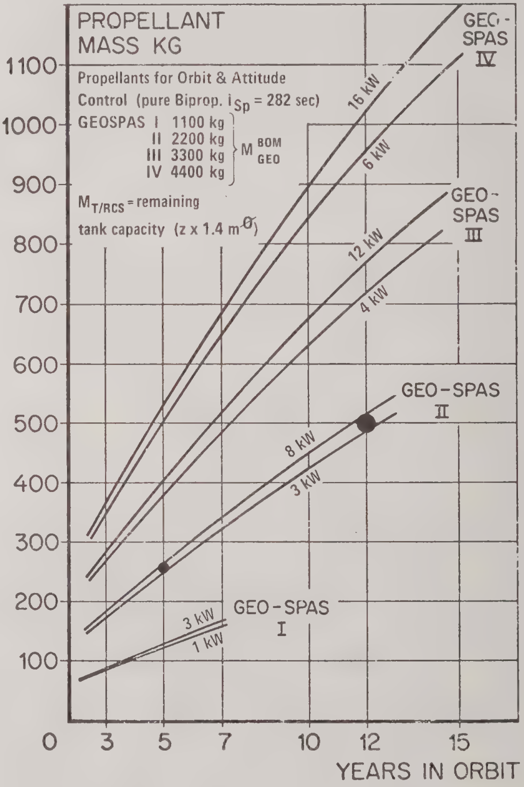

Fig. 10: Propellants Required for Orbit and Attitude Control vs. Lifetime, with Array Size as Parameter

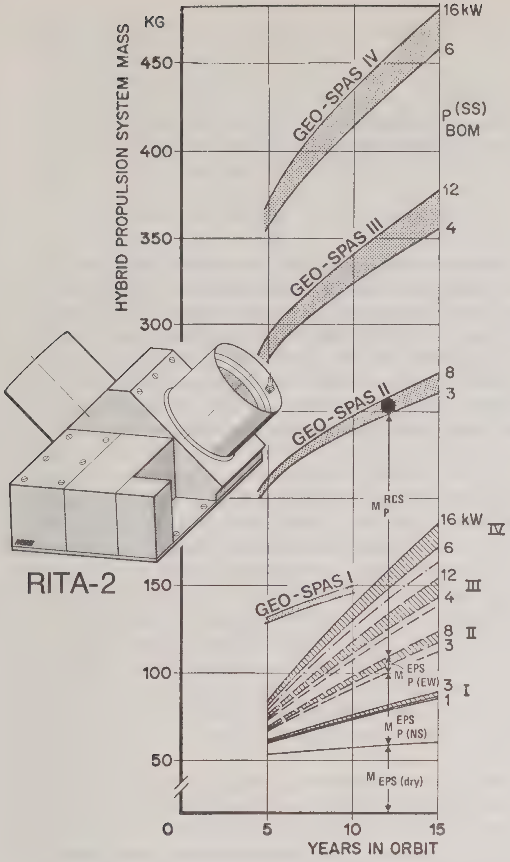

Fig. 11: Mass of the Hybrid System vs. Time (Electrical Thrusters and Mercury required for Orbit Control plus Chemical Propellants for Attitude Control and 2 Years Orbit Control

The third major cost advantage of GEO-SPAS is the modular structure design. The principle applied for construction and mounting eases the load analysis and fabrication effort considerably. It also does not require to start the whole effort again and again for each new spacecraft.

As a conclusion it can be stated that the approach described in this paper represents the most economic solution for the next generation of communication satellites.

VI. Development Aspects

GEO-SPAS represents a new concept and a new orbit transfer philosophy, however, does not require new technology. Except the structure which is under development presently, the subsystems envisaged are all existing hardware. The structure will be flown on the FSLP (First Spacelab Mission) and with SPAS-01 in early 1982. In line with the overall cost efficiency philosophy consequently applied for launch cost and spacecraft design the subsystems are selected from existing and qualified hardware with minimum adaptation.

The unified propulsion system, by example, is under development for the GALILEO Jupiter Orbiter and the German TV-SAT. Due to this fact the development model philosophy can be limited on system level to an engineering test model and the protoflight unit.

The new platform concept can be realized within the next years and could be operationally used in the second part of the decade.

References:

1 D. DAVIDTS and D.E. KOELLE: The Shuttle-dedicated Pallet Satellite (SPAS) and its Applications, 1978 AAS Goddard Memorial Symposium, Washington, D.C., March 1978.

2 D.E. KOELLE: Economic Considerations for Geosync and LEO Spacecraft Design, 30th International Astronautical Congress, Munich, Sept. 1979 - Paper 79-A-07.

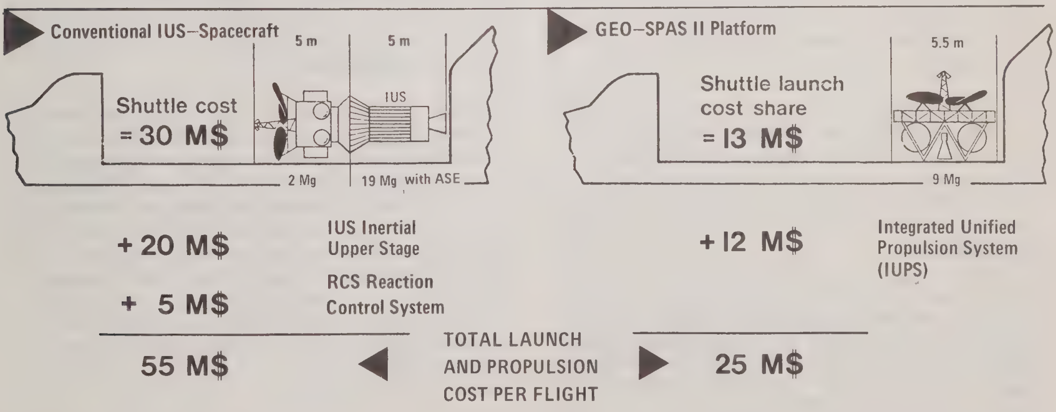
Conventional IUS–Spacecraft
5 m
5 m
Shuttle cost
= 30 M$
IUS
2 Mg
19 Mg with ASE
+ 20 M$
IUS Inertial Upper Stage
+ 5 M$
RCS Reaction Control System
55 M$
GEO–SPAS II Platform
5.5 m
Shuttle launch cost share
= 13 M$
9 Mg
+ 12 M$
Integrated Unified Propulsion System (IUPS)
TOTAL LAUNCH AND PROPULSION COST PER FLIGHT
25 M$

Fig. 12: Shuttle Launch Cost Comparison for Conventional (IUS–) Launched Spacecraft and GEO–SPAS II

80-0506

DEVELOPING THE CONCEPT OF A GEOSTATIONARY PLATFORM*

By

W. T. Carey, NASA Marshall Space Flight Center
R. M. Bowman & G. R. Stone, General Dynamics Convair Division

Abstract

Market demand forecasts for telecommunication services show the demand far exceeding planned on-orbit capacity in the 1985-1995 time frame. Orbital slots and available frequency spectrum are rapidly disappearing. A geostationary platform concept with a proliferation of low-cost earth stations offers an optimum solution with lower user costs, new services, and increased capacities. Candidate platform concepts, servicing, life and OTV options are considered, using a Life Cycle Costing model to select the minimum cost concept meeting program criteria. Transportation costs have proven to be the pacing factor in selecting the final platform concepts.

Introduction

During the last five years several papers[1] have discussed the development of large orbital antenna farms (OAF) or geostationary platforms. As conceived, these would be large structures either constructed (assembled, fabricated or deployed) in low earth orbit (LEO) and transferred to geostationary earth orbit (GEO) or perhaps even constructed at GEO. The platform would provide basic housekeeping functions for a wide variety of communications payloads with various types and sizes of antennas. Inherent to these space systems is the ability to interconnect several different payloads to provide a truly versatile capability (e.g., domestic or international telephone service could be interconnected with a maritime payload). Because of the power and mass available these platforms could also accommodate other uses including meteorology, earth observations, and a wide range of scientific explorations. They would be capable of servicing to update payloads and to do necessary repairs.

It has been well recognized that very large space platforms might not be feasible until sometime in the 1990s, since they would require multiple shuttle launches and development of advanced technologies. However, these large platforms represent an ultimate goal, and it is quite probable that they will evolve from small systems.

Fundamentally, a platform is a space system providing basic housekeeping support to a variety of payloads (i.e., communications, meteorology, etc.) and providing connectivity and isolation between them as required. They offer the distinct advantages of: 1) economies of scale which come from the shared support, and 2) the new and improved services which flow directly from the interconnectivity.

Based on the above definition, satellites like MARISAT, FLTSATCOM, INTELSAT V and TDRSS could be considered initial steps toward platforms, since they provide basic housekeeping and some interconnectivity to different payloads. These are not of the size or complexity envisioned by the early authors, but can certainly be considered as the beginnings of an evolutionary growth. Systems like INTELSAT V and TDRSS demonstrate the advantages of economy of scale and connectivity of large satellites. As the STS becomes available and fully utilized, these systems may evolve into large, permanent space facilities.

Initially, the platforms may be single shuttle launched systems fully utilizing the cargo bay and perhaps offering 1000 kilograms of payload and several kilowatts of primary power with reliability comparable to or better than today's satellites. The recently proposed satellite cluster concept[2] may also be a step in this evolution, albeit only providing the connectivity without the economy of scale. From these first single-shuttle launched platforms, the development would be toward facilities in the late 1990s or post 2000 period that could be serviced by manned or unmanned vehicles. Payloads could be varied or upgraded and the platform would be essentially permanent.

While the main purpose of these platforms would be improved communications capability throughout the world, the platforms would also provide support for other uses mentioned earlier. In terms of both communications and other payloads it is likely that several users and probably organizations will be involved in each platform. This raises difficult institutional questions that must be resolved before the full benefit of these platforms can be made available. These will not be addressed here but there are indications[3] that the institutional questions will soon be coming under discussion.

---

*This paper is based in part upon work performed under NASA Marshall Space Flight Center Contract NAS8-33527, in part upon work performed under the sponsorship of General Dynamics Convair Division at San Diego, and in part upon work performed at COMSAT Laboratories under the sponsorship of the Communications Satellite Corporation.

This paper is declared a work of the U.S.
Government and therefore is in the public domain.

Market Demand

There are a great many potential payload applications for platforms in geostationary orbit, including communications, meteorology, earth observation, and a wide range of scientific exploration. Of prime importance are the communications applications.

Many expect the '80s to be the Decade of Telecommunications. Certainly there are ample indications to support that expectation. As Morgan has shown, Figure 1, costs of telecommunications services have actually come down as costs for everything else have gone up[4]. More and more, communications and transportation are coming to be viewed as alternatives. Entertainment, shopping, household management, banking, business meetings — all can be conducted from one's living room using modern full spectrum communications (voice, data, video). The attractiveness of this becomes clearer if one considers the cost history of petroleum fuels, Figure 2, on which transportation depends.

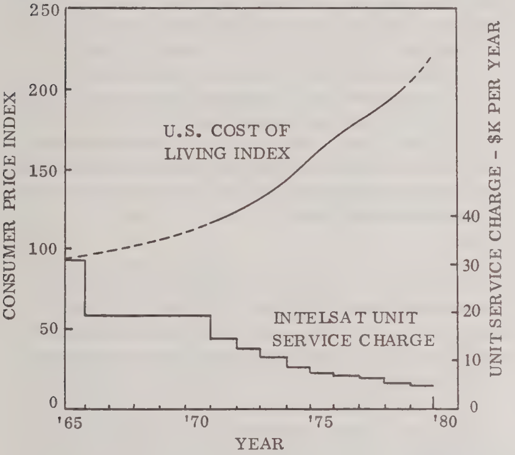

Fig. 1. Cost of living vs communication costs.

Even if these signs are completely ignored, however, and a conservative, linear extrapolation of the market is projected,a shortage of satellite capacity is indicated in the next few years, Figure 3. 4-6 GHz slots for 50-state coverage are gone, and the less desireable 48-state slots are rapidly disappearing. Projections for 11-14 GHz saturation are out of date almost before they are printed. Even though we understand that as a result of GWARC 79, some additional 4-6 GHz and 11-14 GHz spectrum has been made available, this action only serves to delay by a year or so the inevitable saturation. The fact is that the currently accepted approach to satellite communications is no longer viable and cannot be applied to the newer, high frequencies like 30-20 GHz as the technology for these frequencies becomes available. The trend must be reversed to make more efficient use of prime slots, new frequencies, and the more desireable existing frequencies.

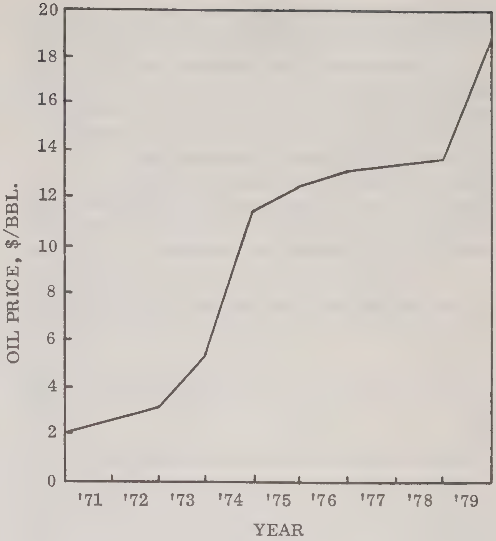

Fig. 2. Rising cost of crude oil.

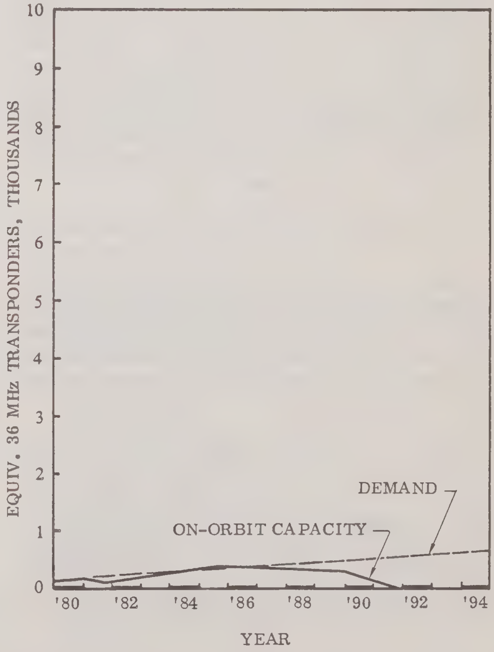

Fig. 3. On-orbit capacity vs. demand (conservative).

New Services and Capabilities

The bandwidth-efficient platform approach to the telecommunications market is required even if ultra-conservative demand projections are used which ignore newly available services. If new services such as video-conferencing mature, however, (as has TV satellite-to cable distribution), the demand will look more like Figure 4. Such new services will emphasize the requirement for an approach with the inherent advantage of the geostationary platform.

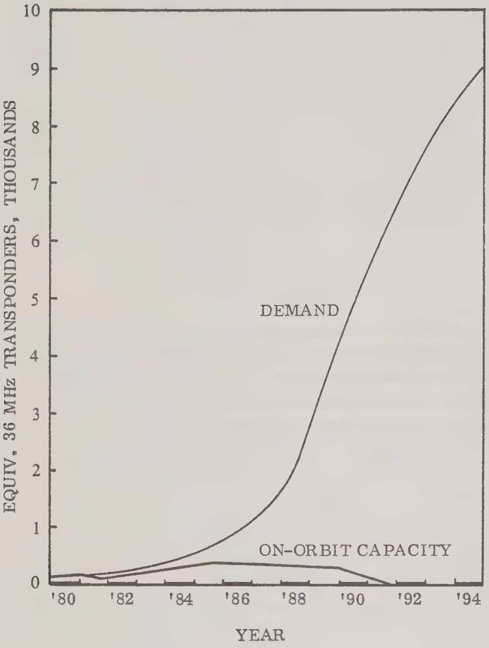

Fig. 4. On-orbit capacity vs. demand (realistic).

Many new services, or existing services with little implementation, will burgeon only when customer rates are lowered and these services become affordable to the majority of potential users. Customer rates can be lowered only by reducing the total systems cost of providing these services.

The cost of providing customer services is made up of space segment costs and ground segment costs. Today, the bulk of the systems cost lies in the ground segment, which includes the earth stations, user terminals, and the interconnects - a network of switchboards, landlines, and microwave links which connect the earth stations to the users, and which comprises about 97% of the ground segment costs.

Total systems costs can be drastically reduced by increasing the number of earth stations (thus reducing the interconnect lengths), reaching a minimum when every building has its own earth station connecting directly to user terminals at desks throughout the building. This "Direct-to-User" (DTU) or "Customer Premise Service" (CPS) capability, as it is now called, would provide voice, date, and video transmissions directly from small rooftop antennas to the satellite and down to the proper rooftop antenna at the call's destination.

To implement this concept, low-cost earth stations with non-tracking antennas and simplified electronics are projected, requiring large, complex geostationary (platform) facilities. When one considers a ratio of perhaps 10,000 earth stations to one platform, the economics become obvious for exploiting the capabilities of a large geostationary satellite or platform.

At least two studies in addition to this one have shown that what is commonly called a platform has a significant economic advantage over conventional satellites. Both Stamminger[5] and Castleman[6], in quite different analyses, showed that space segment costs could be reduced 50 to 70% by a platform approach. They both started with a particular platform concept for use in the comparison. Castleman's platform was serviced twice a year, Stamminger's not at all. Castleman's platform also supported non-communications payloads. Stamminger's did not. There are many other differences, but both agreed on the economies to be gained with platforms.

Implementation of the "minimized total cost" concept with geostationary platforms and low-cost ground stations will provide the low customer service costs needed to conceive and encourage growth of the myriad new and embryonic services needed in the near future, Table 1.

Table 1. Near-term communication needs.

Aeronautical communications
Bush voice
Cable TV
Data
Data collection
Direct TV broadcast
Trunk telephone
Earth exploration
Educational TV
Electronic funds transfer
Electronic mail
Electronic office
Telelibrary
International

Land mobile
Low orbit relay
Navigation
Network TV
Maritime
Paging
Personal communication
Private lines
Public Safety
Remote printing
Search and rescue
Teleconferencing
Telehealth
Time & frequency standards
Weather

Concept Requirements

From a technical standpoint, the capacity and utility of the CPS networks will depend on their ability to connect with a large number of other users, and into the public telephone trunking system when necessary. These factors determine the technical requirements which must be imposed on the space segment, or geostationary platform, Table 2.

Table 2. On-orbit communication technology requirements in the near future.

- Large multi-beam antennas
- Frequency reuse
- High power
- Accurate stationkeeping
- Accurate pointing
- Optimum use of all available frequencies
- On-orbit switching (beams and frequencies)

These basic requirements in turn impose design requirements on both the platform communications and housekeeping systems, details which evolve as the concept is developed.

From a program standpoint, candidate platform concepts must first be developed which satisfy three basic screening criteria: feasibility, reliability, and Shuttle compatibility. Once these are satisfied, selection of an optimum candidate concept can then be made on the basis of trade studies to minimize Life Cycle Costs and to provide a fundable program plan.

Developing the Concepts

To develop a feasible, reliable, fundable, operationally economical and STS-compatible platform concept, a staggering number of interrelated variables are encountered, producing a multi-dimensional matrix for trade-off and ultimate concept selection. Though hundreds of specific concepts representing points on this matrix have been compared during our trade studies, the total number of possible point designs is essentially limitless. Therefore, to obtain positive results, a brute force approach must be abandoned in favor of a more rational attack on the problem. The variables which could be uncoupled from the others were therefore identified to gauge sensitivity to changes in the variables, singly and in combinations.

The major, fundamental variables currently being considered are shown in Table 3. The first four provide a simplified trade study matrix. Eighteen viable OTV candidates compatible with the Geostationary Platform mission have been selected for analysis. Each is being considered using four platform operational modes - 8 or 16 year life (serviced or non-serviced) to provide a total of 72 OTV/platform-mode candidates. Payloads were then allocated to these 72 options, based on OTV performance capability, and payload weight and power. For each option, the number of platform modules required to satisfy the traffic model is being determined, varying from one to 168.

Table 3. Major variables in platform concept analysis.

- Size and number of platform modules
- Platform life
- Servicing schedules
- Transfer vehicle (LEO to GEO) availability and performance
- Construction (deployment, fabrication, assembly) options
- Modular growth options
- GEO configuration - integrated structure or constelation

The interrelationship of the variables is complex. The economics of servicing, for instance, are influenced by platform size, which in turn is driven by available transfer vehicle options and affected by design and deployment schemes. Servicing frequency is also directly affected by transfer vehicles available to perform that function, by the assumed life of subsystems and components, and by the comparative reliabilities obtainable by redundancy, servicing, and combinations thereof.

The most important selection criterion in the trade studies is the total Life Cycle Cost, made up of many elements which can, of course, be grouped in many different ways. Three major cost groups have been considered - platform, payload, and transportation, Table 4. To facilitate analysis, a costing program has been developed at General Dynamics and is now in use.

Table 4. Cost breakdown
(Total Program Life-cycle Costs)

- Platform Costs
  - Platform Research & Development
  - Platform Production
  - Platform Integration
  - Spare subsystems and components for servicing
  - Servicer use charges
- Payload Costs
  - Payload Research & Development
  - Payload Production
  - Payload Integration
  - Spare payloads and components for servicing
- Transportation Costs
  - Delivery Transportation to LEO (Shuttle)
  - Delivery Transportation LEO to GEO (Transfer Vehicles)
  - Servicing Transportation to LEO (Shuttles)
  - Servicing Transportation LEO to GEO (Transfer Vehicles)

The program considers payload and platform costs and weight, transportation unit and total costs for Shuttle and OTV, and operational costs such as assembly or construction time, mating time, and loiter time.

Preliminary results indicate that the sum of all the costs in the platform and payload groups will be about the same over most of the matrix and is fairly insensitive to most of the variables, Figure 5. Transportation costs seem to be another matter, however. The total transportation cost for a platform at a single orbital position varies among concepts by as much as an order of magnitude.

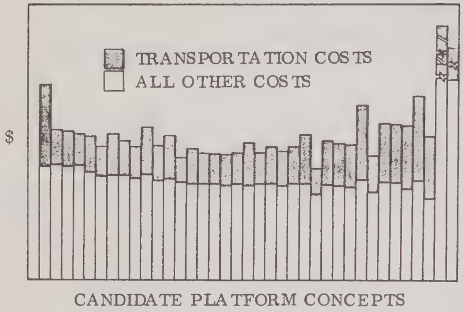

Fig. 5. Preliminary cost trends.

With these preliminary trends, the lowest cost options, then, will likely be those with the lowest transportation costs. Specifically, the concept which minimizes the number of shuttle flights required for all purposes over the life of the platform appears to be the most economical concept overall.

Minimizing the number of shuttle flights can be accomplished by:

(1) reducing the total mass in orbit by multiple-use antennas, shared subsystems, and simple lightweight structures.
(2) maximizing Orbiter payload density
(3) reducing servicing flights to the minimum feasible number.

Concept Selection

The specific platform concept to evolve from these guidelines will depend heavily on the available transfer vehicles. As the time frame for platforms approaches, a new generation of Orbital Transfer Vehicles will be needed which are capable of handling large modules or entire platforms. These OTVs may well be specifically designed to the requirements of the Geostationary Platform. Even then, however, year-to-year affordability may dictate a platform made up of moderate-sized modules launched every year or two. This allows funding to be spread over a longer period, while building up platform capacity along with the growth in the market. Preliminary indications are that the total cost of such a scheme is very close to the cost of putting up everything at once.

Another aspect of platforms to be included in our studies is a detailed tradeoff comparing the alternatives of docking modules at GEO versus flying in formation. It appears at this point that the cost of developing, demonstrating, and incorporating docking will more than pay for itself in the savings obtained through shared subsystems and the elimination of equipment for precise relative orbit maintenance and microwave links.

A typical concept developed early in the study is shown in Figure 6. The six-arm configuration lends itself well to the buildup of a large platform by the docking of such modules.

Attitude control and propulsion are the most critical platform subsystems. The more missions on a platform, the more important it is that these subsystems not fail. A multiple number of sensors, momentum devices, and thrusters will be required. Even with much redundancy, preliminary studies indicate that the reliability of some individual components will have to be raised above the present state of the art. The electrical power subsystem will need to be on a multiple bus system and some isolation will be needed to prevent service interruptions from short circuits. Required reliability can be achieved with present components and suitable redundancy, with the exception of batteries where 16-year life has not been demonstrated. Assuming technology developments such as those discussed above, platform service availability required by users can be achieved.

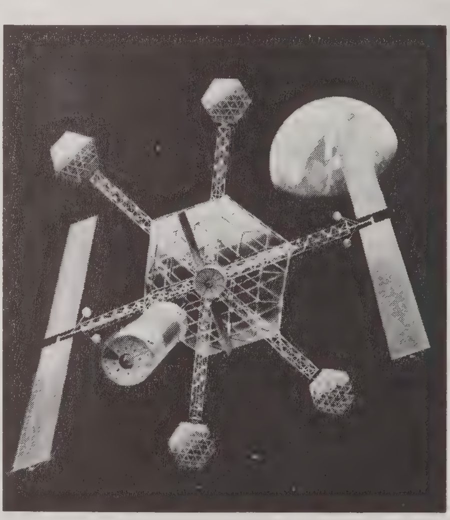

Figure 6. Geostationary platform concept.

Conclusions

We are in the middle of an initial Concepts Definition Study and much work remains to be done. What we have learned so far, however, convinces us that the Geostationary Platform is a sound, practical, economical approach to providing expanding communications services within the limitations imposed by the available frequency spectrum and orbital arc.

To take maximum advantage of the orbital slots and frequencies allocated by the International Telecommunications Union and the FCC, there is a need to exploit existing technologies to the fullest and move into the feasible technologies of the near future. Such technologies must include both telecommunications and space system advances. With such advances, we can look forward to decreased costs and availability of many new services in commerce, communications, finance, public service, science applications, transportation, and the home.

Acknowledgement

The authors would like to extend their thanks to the Geostationary Platform Concepts Definition Study team members at NASA/MSFC, General Dynamics/Convair, and COMSAT Labs for their contributions to the study and input to this paper.

References

1. Edelson, B. I. and Morgan, W. L., "Orbital Antenna Farms," Astronautics and Aeronautics, September 1977, pp. 20-29.

   Morgan, W. L., "Multi-Mission Space Stations; the Case for Developing Orbiting Antenna Farms," Satellite Communications, April 1978, pp. 32-39.

   Fordyce, S. W., and Jaffe, L., "Future Communications Concepts; Switchboard in the Sky," Satellite Communications, Feb. and Mar., 1978.

2. Visher, Paul S., "Satellite Clusters," Satellite Communications, Sept. 1979, pp. 22-27.

3. Smith, Delbert D., "Viewpoint: A Communications Flow," Satellite Communications, December 1979, pg. 6.

4. Morgan, W. L., and Esch, F. H., "Orbital Antenna Farm Power System Challenges," 14th IECEC Conference, August 1979, pp. 1207-1212.

5. Stamminger, R., "Large Communications Platforms Vs. Smaller Satellites," Future Systems Inc. Report No. 221, NASA Contract NASW-3212, February 1979.

6. Castleman, M. W., "Geostationary Platform Cost Comparison Analysis," George C. Marshall Space Flight Center, November 1978.

80-0507

LONGITUDE-REUSE PLAN DOUBLES COMMUNICATION SATELLITE CAPACITY OF GEOSTATIONARY ARC

Donald v. Z. Wadsworth*
Hughes Aircraft Company
El Segundo, California

Abstract

Communication satellites placed in the geostationary orbital arc must be separated by at least 3° to 4° in longitude to avoid mutual interference. The demand for C and Ku band longitude slots will soon exceed the capacity of the arc. Relief can be provided by the Longitude-Reuse Plan which permits doubling or tripling the number of satellites while meeting mutual interference constraints. Three or four satellites in slightly inclined orbits occupy the same orbital arc longitude slot, replacing or augmenting an existing geostationary satellite. By handing over the communications links at times of close approach, these satellites are used to create two full time "virtual" communications satellites, one remaining north of the equatorial plane and the other south.

Introduction

For communications links at C band frequencies (5.925 to 6.425 GHz uplink and 3.7 to 4.2 GHz downlink), geostationary satellites must have a minimum orbital spacing of approximately 4° of longitude to avoid mutual interference from earth station antenna sidelobes (Figure 1). All of the C band longitude slots for North American coverage (between 75° and 136° longitude) are occupied by or allocated to the COMSTAR, WESTAR, SATCOM, and Anik domestic satellites. Consequently, additional satellites covering this region are being designed to operate at Ku band and include SBS, Advanced WESTAR, "BELLSTAR", Anik B, Anik C1, and Anik C2. The Anik B, Advanced WESTAR, and BELLSTAR satellites will operate at both Ku and C band. Ku band commonly refers to the uplink band, 14 to 14.5 GHz, and the downlink band, 11.7 to 12.2 GHz.

A concern of long range planners is that within the next decade the demand for satellite communications may exceed the C and Ku band capacity of the geostationary arc, despite improvements in frequency-reuse, bandwidth efficiency, digital speech interpolation, etc. One solution under active consideration is the development of satellites operating in the higher frequency Ka band at 17.7 to 30 GHz, permitting closer orbital spacing of satellites and utilizing the large 2500 MHz bandwidth allocation. This may be attractive for point-to-point trunking using multibeam satellites. Unfortunately, the higher frequency carriers are subject to strong attenuation by rain, requiring expensive diversity sites and/or power boosting to mitigate deep rain fades. One possibility is to cluster C, Ku, and Ka band satellites within a few tenths of a mile of each other and crosslink them by a switching satellite.[1]

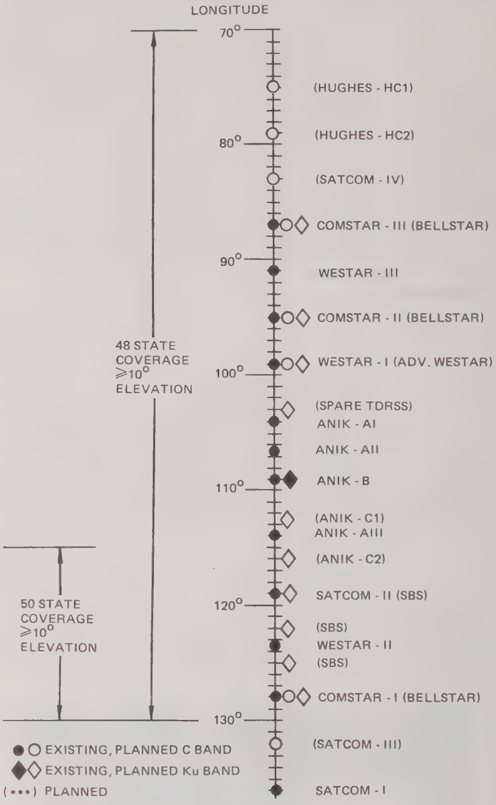
LONGITUDE
70°
(HUGHES - HC1)
80°
(HUGHES - HC2)
(SATCOM - IV)
COMSTAR - III (BELLSTAR)
90°
WESTAR - III
COMSTAR - II (BELLSTAR)
48 STATE COVERAGE ≥10° ELEVATION
100°
WESTAR - I (ADV. WESTAR)
(SPARE TDRSS)
ANIK - AI
ANIK - AII
110°
ANIK - B
(ANIK - C1)
ANIK - AIII
(ANIK - C2)
50 STATE COVERAGE ≥10° ELEVATION
120°
SATCOM - II (SBS)
(SBS)
WESTAR - II
(SBS)
COMSTAR - I (BELLSTAR)
130°
(SATCOM - III)
SATCOM - I
●○ EXISTING, PLANNED C BAND
◆◇ EXISTING, PLANNED Ku BAND
(•••) PLANNED

Fig. 1 Satellite spacing in geostationary arc.

Another solution is provided by the Longitude-Reuse Plan described herein. This permits doubling or even tripling the C band or Ku band capacity of the geostationary arc. The basic idea is to replace or augment a single geostationary satellite by the equivalent of two or three full time communications satellites located at essentially the same longitude but separated in latitude (declination) to avoid interference. The minimum latitude separation angle would be the same as the minimum longitude spacing required to avoid interference.

---

*Senior Scientist, Member AIAA

Copyright © American Institute of Aeronautics and Astronautics, Inc., 1980. All rights reserved.

The separation would be maintained by employing either three or four satellites in low inclination orbits and handing over the communications links between satellites at appropriate instants. This is illustrated in the nonrotating, geocentric coordinate frame of Figure 2 for the configuration IA case of four satellites placed in orbits with the ascending nodes spaced 90° apart (in terms of right ascension angle) in the equatorial plane. In the illustration, the satellites are phased to be at the same right ascension at 0 hours when satellites No. 1 and No. 4 are on. At 3 hours, satellites No. 1 and No. 4 turn off and hand over their communications links to satellites No. 2 and No. 3 which are turned on. Handovers occur at the points marked SW in the figure. In effect, two full time "virtual" communications satellites have been created, one remaining north of the equatorial plane and the other south. Each virtual satellite is quasi-stationary in that, to the earth station observer, it describes a small daily cyclic motion about a fixed point in the sky.

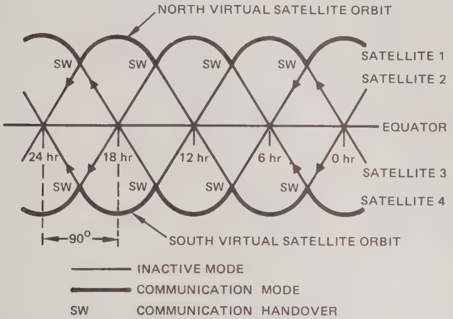

Fig. 2 Configuration IA orbits in nonrotating geocentric reference frame.

The virtual satellites could be used to double or triple the number of satellite circuits interconnecting a set of earth stations, in which case each earth antenna would have two or three separate beams. Alternatively, each virtual satellite could be associated with a different set of single-beam earth station antennas which could be located in the same or different countries.

The switching at the time of handover of the communications links could be made "hitless" if the inactive satellite synchronizes its clock to that of the active satellite (or to a ground master clock) shortly before the switch. The number of handovers per day per virtual satellite varies from two to four, depending on the configuration.

The remote possibility of collision between satellites traveling north and south at the equatorial plane crossing could be avoided either by employing slightly elliptic orbits or by slightly offsetting the lines of the nodes and the times of nodal passage.

The idea of using inclined orbits to obtain efficient spacing of synchronous satellites is not new. Rowe and Penzias[2] have thoroughly analyzed the possibilities when there is no handover of communications links between satellites. Their results are not of practical interest for the C or Ku bands, even for the most favorable three satellite configuration, since inclination angles of about 20° or 23° are required to ensure the minimum separations for noninterference. System costs would be prohibitive to accommodate the correspondingly large elevation and azimuth angle swings.

The more interesting possibilities when handover of communications links is permitted are embraced in the Longitude-Reuse Plan of this paper. The basic idea was originally proposed in 1966 by Dr. Samual G. Lutz of Hughes Aircraft Company in an unpublished memorandum. The various configurations and the operational requirements are analyzed in the following sections. Solar outage, earth-station and spacecraft antenna pointing, antenna noise temperature, gravitational perturbations, and a comparative cost analysis are included.

Satellite Orbit Configurations

In addition to the four-satellite configuration illustrated in Figure 2 (configuration IA), there are several others of interest for longitude-reuse. The relative merits are most easily analyzed in terms of the orbital motion as seen from a geostationary (geocentric, earth-fixed) coordinate frame. To an observer at an earth station, the satellites corresponding to a particular longitude slot appear to follow each other on an elongated figure eight path, completing a full cycle each day. The shape of the figure eight depends on the longitude and latitude of the observer relative to the satellites. For the purposes of this section, the analysis can be simplified by assuming the earth station to be at the equator on the same meridian as the satellites at the times of nodal passage The results will apply qualitatively to other geometries.

The salient points of the various configurations are summarized in Table 1, where the orbit inclinations were calculated to satisfy a minimum C band separation of 4° in longitude and latitude (declination) between active satellites. Configurations involving five, six, or more satellites were not analyzed since these require greater orbital inclinations which are unattractive from the antenna cost standpoint.

Configurations Which Double Orbital Arc Capacity

In Figure 3 the positions of the four satellites of configuration IA are shown in earth-fixed (geostationary) coordinates at intervals of 3 hours. The orbital motion has a 24-hour period in terms of sidereal hours (23 hours 56 minutes, 4.09 seconds in ordinary mean solar time). The circular satellite orbits are inclined at angle i with the right ascensions of the ascending nodes spaced 90° apart. If the upper loop of the figure eight is considered to be in the northern hemisphere, then orbital dynamics and the sense of the earth's rotation dictate that the satellite trace this loop in the counterclockwise sense as seen from the earth. This will be demonstrated later.

The satellites which are in the inactive mode are indicated by the open circles and those which are in the active communications mode by the solid circles. The points at which the communications links are switched from one satellite to another are denoted by the SW label and the dashed

Table 1 Features of longitude-reuse configurations

Design requirements				Implementation (for C band satellites)					
Augments existing geostationary satellite	Avoids solar transit outage	Self-sparing	Handover slew angle, deg	Configuration type	Satellite duty cycle, %	Orbit inclination angle, deg	Longitude motion of virtual satellites, deg	Latitude motion of virtual satellites, deg: South	Latitude motion of virtual satellites, deg: North
No	Yes	Yes	0	IB	50	4	0.14	-4 to 0	0 to 4
No	No	No	0.054	II	67	2.67	0.062	-2.67 to -1.33	1.33 to 2.67
No	No	No	0.07	IA	50	2.83	0.07	-2.83 to -2	2 to 2.83
No	No	No	0.14	IC	67	4	0.14	-4 to 0	0 to 4
No	No	No	0.093	IC*	67	4	0.19	-4 to 0	0 to 4
No	Yes	Yes	0.14	IA	50	4	0.14	-4 to -2.83	2.83 to 4
No	Yes (Slews 4°)	No	0.16	II	67	4.62	0.19	-4.62 to -2.31	2.31 to 4.62
Yes	No	No	0.28	IA	50	5.66	0.28	-5.66 to -4	4 to 5.66
No	Yes (Slews 4°)	No	0.28	III	67	5.66	0.28	-5.66 to 0	0 to 5.66
Yes	No	No	0.48	II	67	8	0.56	-8 to -4	4 to 8

*Staggered orbit version.

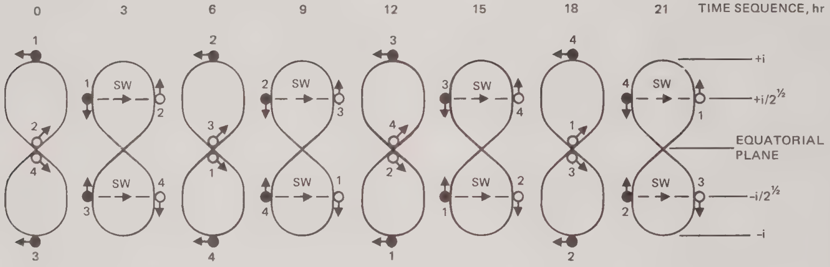

a) CONFIGURATION IA

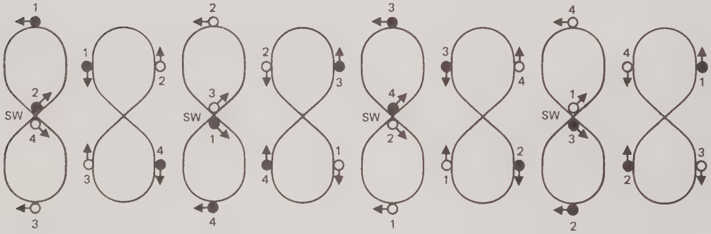

b) CONFIGURATION IB

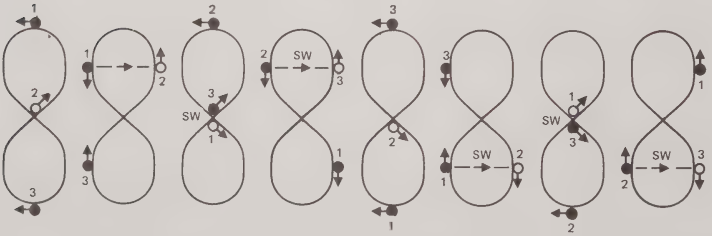

● COMMUNICATION MODE
○ INACTIVE MODE
SW COMMUNICATION HANDOVER

c) CONFIGURATION IC

Fig. 3 Configuration I satellite orbits in geostationary reference frame.

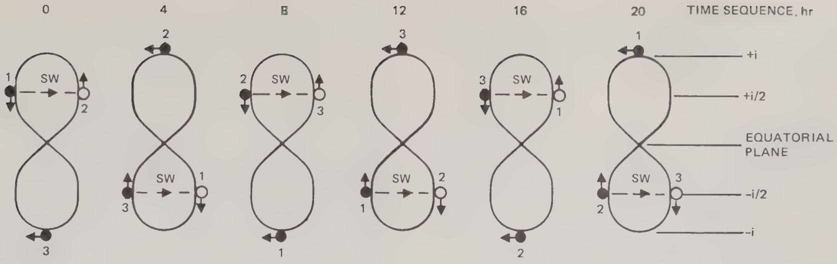

Fig. 4 Configuration II satellite orbits.

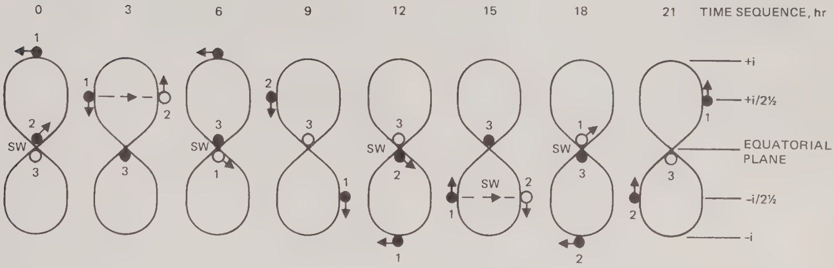

Fig. 5 Configuration III satellite orbits.

lines. The north virtual communications satellite moves in a closed orbit between $i/2^{1/2}$ and +i of latitude, while the south virtual satellite moves between $-i/2^{1/2}$ and -i. Configuration IB differs from IA only in its switching pattern. Configuration IC of Figure 3 is a variant obtained by omitting one satellite.

When three satellites are deployed with ascending nodes spaced 120° apart in the equatorial plane, the motion illustrated in Figure 4 results (configuration II).

The satellites of configurations IC and II have a 67 percent communications duty cycle while those of configurations IA and IB have only 50 percent duty cycles. Configurations IA and II permit the smallest latitude (declination) motions of the virtual satellites, consistent with the mutual interference requirements. This minimizes antenna pointing angle requirements. Configuration IB avoids antenna slewing during handover of the communications links since this occurs only at the equatorial crossing when the satellites have the same longitude. Combinations of the IA and IB switching patterns are also possible.

Configuration III, illustrated in Figure 5, requires two satellites in inclined orbits and one geostationary satellite. It is less attractive than the previous configurations because it requires a larger antenna elevation angle motion to avoid mutual interference.

Configurations Which Triple Orbital Arc Capacity

If it is preferable to retain an existing geostationary satellite, the capacity of the associated longitude slot can be increased by superimposing the three or four satellites of configurations IA or II. This results in three full time communications satellites per orbital arc slot, trebling the orbital capacity.

Spare Satellites

When there is no geostationary satellite in the orbital slot, configurations IA and IB have the advantage of being self-sparing -- failure of any one satellite merely causes the configuration to degenerate into configuration IC without the need for restationing. Of course if the minimum 4° latitude (declination) separation between virtual satellites is to be maintained after the failure, then the configuration IA or IB satellites would require orbital inclinations of 4°. At the time of failure, the earth station antennas would be slewed to one of the inactive satellites and the communication links handed over.

Orbit Mechanics

The figure eight motion of the satellites seen from the origin of a geocentric, earth-fixed reference frame can be analyzed with the aid of Figure 6. The direction of the "first point of Aries" can be considered a fixed point among the stars, neglecting the slow precession of the equinoxes. The angle $\Upsilon P_0 P_1 = \Omega$ measured in the equatorial plane is the right ascension of the ascending node of the satellite orbit which has an inclination angle i.

For simplicity of illustration, it is assumed that the earth station is on the same meridian as the satellite at the time of the ascending nodal passage. Other geometries can be handled by a coordinate rotation. The orbital motion can be analyzed in terms of the satellite declination δ and geographic longitude L (measured westward in the positive sense) relative to the earth station.

During the time the earth station rotates through the angle $P_1 P_0 P_2 = f$, the geosynchronous satellite travels through the same angle f in its orbital plane. Due to the inclination, the satellite's meridian falls behind by the angle L. When f = 90°, both the earth station and the satellite reach the same meridian. By symmetry, it is apparent that between f = 90° and 180° the satellite's meridian will lead the earth station meridian and L will be negative. Similar reasoning shows that, as the satellite enters the southern hemisphere, L will be again positive for f between 180° and 270° and negative for f between 270° and 360°, resulting in an apparent figure eight motion where the upper loop is traced in the clockwise sense as seen from the earth.

From spherical trigonometry it can be shown that

$$\sin\delta = \sin i \sin f$$

$$\tan L = \frac{\sin^2(i/2)\sin 2f}{1 - 2\sin^2(i/2)\sin^2 f}$$

For small inclinations useful approximate formulas are

$$\delta \approx i \sin f \text{ and } L \approx (i^2/4)\sin 2f.$$

From symmetry, for satellites which are phased 90° apart in terms of f and Ω, the points of closest approach (excluding the equatorial crossing) are at f = 45°, 135°, 225°, and 315°. Then, denoting the magnitudes at handover by the subscript h,

$$\delta_h \approx i/2^{1/2} \text{ and } L_h \approx i^2/4$$

where the handover slew angle, $2L_h$, is also the maximum width of the figure eight. For satellites phased 120° apart in terms of f and Ω, the points of closest approach (excluding f = 0) correspond to f = 30°, 150°, and 270°. Then at handover,

$$\delta_h \approx i/2 \text{ and } L_h \approx i^2 3^{1/2}/8$$

where the handover slew angle, $2L_h$, is 86.6 percent of the maximum width of the figure eight. The height of the figure eight is 2i, so the height-to-width ratio is 4/i for both 90° and 120° phasing. The slope of the figure eight orbit at f = 0 (equatorial crossing) is readily found to be $d\delta/dL = 2/i$.

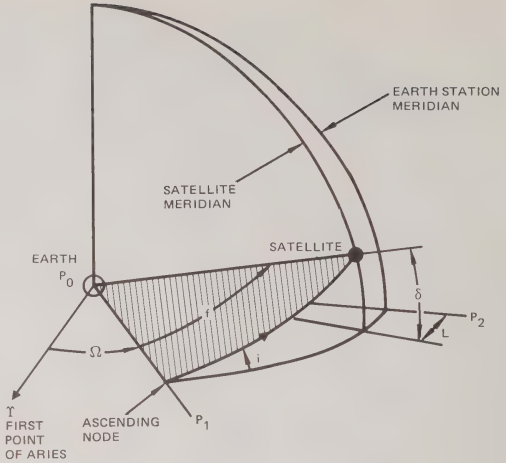

Fig. 6 Satellite orbit geometry.

Staggered Configuration

In the case of configuration IC, if the orbits were staggered in longitude, orbit 1 translated by $2L_h/3$ to the west and orbit 3 translated by the same amount to the east, the earth station antennas would need only slew (2/3) $2L_h$ at the handover points. Of course, the overall longitudinal motion of the virtual satellites in a day would be (5/3) $2L_h$.

Solar Outage Avoidance

At intervals of 6 months the sun will move into the main lobe of the earth station's receive antenna, in line with the communications satellite. Because the sun acts as an intense RF noise source, at these times there will be a communications outage. The length of the outage is readily calculated, assuming that the sun's noise disc subtends an angle of about 0.5° at the earth station and that the apparent longitudinal motion of the sun is about 0.25° per minute.[3] If the sun's track is phased so that the center of the solar disk passes behind the satellite, the outage will last (between 3 dB points)

$$(\Theta + 0.5°)/0.25° \text{ minutes}$$

where Θ is the halfpower beamwidth of the earth station antenna.

For an earth station at the subsatellite point on the equator, the outages would occur at the times of the vernal and autumnal equinoxes. At northern latitudes, the outages occur earlier and later, respectively. From spherical trigonometry, it can be seen that on successive days the track of the sun, as it crosses the satellite orbits, moves up in latitude by an amount

$$\frac{(360°)\ (1\ \text{day})}{365.25\ \text{days}} \sin(23.5°) \approx 0.393°.$$

Also, the tracks are inclined at about 23.5°, the inclination of the ecliptic to the equatorial plane. The outages may occur on several successive days, depending on the antenna beamwidth.

Common practice is to accept the solar outages as part of the downtime budget or to offload traffic onto terrestrial long-haul facilities. Alternatively, a procedure suggested by Lundgren[4] can be used to avoid outages. A variation of this procedure can be applied to the configurations of the Longitude-Reuse Plan, except when an existing geostationary satellite is retained at the center of the figure eight orbits. As an example, consider configuration IA and assume the satellites have been phased so that at the time of solar transit they are in their extreme positions, 0 hours in Figure 3. Outages can be avoided on the days in which the sun transits satellite No. 3 at 0 hours by modifying the switching pattern: instead of the No. 2/No. 3 switch at 21 hours, No. 2 remains on until it passes No. 4 at 0 hours, at which time No. 2 hands over the links to No. 4 and the original pattern is resumed by 3 hours. An analogous modification can be performed on the days in which the sun transits satellite No. 1 at 0 hours. Evidently i must be at least 4° to satisfy the C band minimum separation requirement at all times. Similar modifications to the switching pattern can be made to avoid outages in the case of configuration IB.

Solar transit outages also can be avoided for configurations II (transits planned at 2 hours, 6 hours, 10 hours, etc.), IC (transits planned at 0 hours or 12 hours), or III (transits planned at 9 hours or 21 hours) providing that $i \geq 4°/(3^{1/2}/2)$, 4°, or $4°/(2^{1/2}/2)$, respectively, to satisfy the C band separation requirement. In these cases, while the earth station antenna beam is slewed between satellites, there will be a short communications fade.

Whichever configuration is selected, it is necessary that the satellites be phased to have maximum mutual separation at the time of solar transit. This can be planned at the time of launch, noting that the orbital period on the figure eight is 23 hours 56 minutes 4.1 seconds. If the configuration I satellites are phased to lie on the vertical symmetry axis of the figure eight at the time of the vernal equinox, they will automatically be on this axis (with positions reversed) at the autumnal equinox 6 months later without expenditure of propellant, since (365.25/2 days) x (235.9 seconds/day) = (23 hours 56 minutes 4.1 seconds)/2 where 235.9 seconds is the difference between the sidereal and mean solar days. The configuration II satellites have the desired maximum separation when one satellite crosses the equatorial plane and the others are at declinations ± sin i cos 30°.

Earth Station and Satellite Antenna Pointing

For narrow beam designs, the earth station antennas or the feedhorns would be programmed to follow the motion of the virtual satellites. A microprocessor or cams could be used to control the elevation and azimuth angle drive motors. No tracking would be required since the cyclic motion could be preprogrammed. For the wider beamwidths of 0.5° to 1°, little or no steering would be required. Whenever the communications links are handed over from one satellite to another the controller would slew the antenna beam in azimuth. A fade might be avoided during slewing by temporarily increasing uplink gain.

The satellite antenna could be pointed by means of an earth sensor or a two-axis, monopulse beacon tracking system such as used by current geostationary satellites (Anik, WESTAR, Palapa). The center of the antenna beam footprint (the boresight aimpoint) would remain essentially stationary on the earth's surface.

Effect of Virtual Satellite Orbit on Gain and Signal-to-Noise Ratios

Although the antenna boresight is aimed at a fixed point on the earth's surface, the orbital motion of the virtual satellite will cause the 3 dB contour of the antenna footprint to shrink and expand during each orbital period. For earth stations in the same hemisphere as the virtual satellite, an increase ΔG in satellite antenna gain, compared to that of a geostationary satellite is required to offset the footprint shrinkage. Elementary analysis shows that

$$\Delta G \simeq -0.15i\,(\sin\delta_b/\sin\psi_o)$$
$$\cdot\,\tan(\psi_o \mp 1.7\Theta/\cos\psi_o),$$

in decibels, where the inclination i is in degrees, δ_b is the geocentric latitude of the boresight aimpoint, Θ is the 3 dB beamwidth, and ψ_o is the earth-central angle between the boresight aimpoint and the position of an equivalent geostationary satellite. For a typical CONUS coverage beam with $\Theta = 3°$ and $\psi_o = 40°$, the gain penalty for the i = 4° northern virtual satellite is less than 0.6 dB.

If the earth station and virtual satellite are in opposite hemispheres, then the increase in sky noise temperature is bounded by

$$\Delta T \simeq T_T\,\alpha h\,(\csc(E-i) - \csc E)$$

where T_T is the effective tropospheric temperature (290°K), α the clear sky absorption coefficient (0.00067/km at C band), h the equivalent atmospheric thickness (15 km), and E the antenna elevation angle. For the worst case with an earth station at 60° latitude, E = 22° and i = 4°, $\Delta T \simeq 1.7$°K. For a high performance earth station with a system noise temperature of 60°K, a 1.7°K increase corresponds to a $4.34\,(\Delta T/60) \simeq 0.1$ dB increase in received noise power. The corresponding increase in signal attenuation is just $4.34\,(\Delta T/T_T) \simeq 0.02$ dB. The above formulation can be derived from Reference 3.

The combined effect of the above factors is a worst case (i = 4°) reduction in the uplink and downlink signal-to-noise ratios of 0.6 dB.

Gravitational Perturbations and Stationkeeping

As in the case of geostationary satellite orbits, stationkeeping jets are required to offset lunar-solar perturbations, the equatorial ellipticity perturbation, and the effect of solar radiation pressure. In addition, for an inclined geosynchronous orbit, there is a nonperiodic effect of the earth's oblateness (equatorial bulge) perturbation which causes a westward regression of the nodes. For small inclination angles, the angular regression per orbital period is given by the well known formula:

$$\Delta\Omega = -2\pi J(R_e/R_s)^2 \text{ radians} \simeq 0.013°$$

where J is the coefficient of the second harmonic of the earth's gravitational potential (1.623×10^{-3}) and $R_e/R_s \simeq 6.61$ is the ratio of the mean equatorial radius to the radial distance of the synchronous orbit.

Due to the regression of the nodes, the time for a satellite to complete a figure eight orbit (i.e., between subsequent nodal passages) is less than its synchronous orbital period, T. Noting that T is the same as a sidereal day, simple geometry gives the difference as $T(\Delta\Omega \cos i)/2 \simeq 3.1$ seconds for small inclinations. This has operational significance in connection with avoidance of solar outages. If the satellites are phased initially to be on the vertical axis of the figure eight at the time of solar transits during equinox, then they will be out of phase by an amount $(366)(3.1) \approx 0.32$ hour a year later. For a typical 7-year lifetime design the phase offset reaches 2.2 hours, which is unacceptable if solar transits are to be avoided by switching between satellites as previously described. By initially biasing the satellites relative to the figure eight axis, the maximum phase offset during solar transits can be reduced to ±1.1 hours over the 7 years, which is acceptable. Consequently, no additional stationkeeping propellant is required to offset the oblateness perturbation.

A bonus of using inclined orbits is that the apogee boost for injection into synchronous orbits is less than that for equatorial plane orbits. This saving could be converted into additional payload, offsetting the extra electronics required for link handovers - about 7i kg for an Atlas-Centaur boost vehicle where i is in degrees.

Summary and Cost Comparison

The price to be paid for doubling or tripling the capacity of the geostationary arc under the Longitude-Reuse Plan includes: 1) earth station antenna beams must be steered on a daily cycle, 2) communications links must be switched between adjacent satellites several times per day, and 3) three or four identical satellites are required (67 or 50 percent duty cycles to obtain two full time (virtual) communications satellites. On the other hand, the stationkeeping propellant budget is the same as for a geostationary satellite, and the degradation in uplink and downlink signal-to-noise ratios is negligible, less than 0.6 dB for the worst case.

For the sake of cost comparison, suppose a buyer has the option of selecting a communications system with two geostationary satellites and one on-orbit spare or the longitude-reuse configuration IB with four satellites. Both options provide the same communications capacity and nearly the same reliability. If p is the probability of a single satellite failure, the probability of system failure (failure of at least two satellites) is approximately $3p^2$ for the geostationary system and $6p^2$ for the longitude-reuse system.

The installed cost for adding beam steering to an earth station antenna, including two-axis precision motor drives, controllers with digital readout, and a programmable step control unit, varies from \$27,000 (4.5 meter antenna) to \$45,000 (12 meter antenna). The corresponding fixed-antenna earth station costs vary from \$150,000 to over \$1,000,000. The average incremental cost for beam steering will be taken as 15 percent. The cost for adding the beam switching electronics onboard the satellite is less than one percent of the satellite cost and will be neglected.

Making the reasonable assumptions that the basic satellite cost is \$50,000,000 on-orbit and that the earth station and satellite investment costs for the entire system are equal, the following first order cost comparison can be made:

	Geostationary System	Equivalent Longitude-Reuse System
Satellite Investment	\$150,000,000	\$200,000,000
Earth Station Investment	150,000,000	172,500,000
Total	\$300,000,000	\$372,500,000

References

1. P. S. Visher, "Satellite Clusters," Satellite Communications, September 1979, pp. 22-27.

2. H. E. Rowe and A. A. Penzias, "Efficient Spacing of Synchronous Communication Satellites," BSTJ, Vol. 47, December 1968, pp. 2379-2433.

3. D. C. Hogg, "Ground Station Antennas for Space Communications," Advances in Microwaves, New York, Academic Press, 1968, pp. 1-66.

4. C. W. Lundgren, "A Satellite System for Avoiding Serial Sun-Transit Outages and Eclipses," BSTJ, Vol. 49, October 1970, pp. 1943-1972.

80-0508

EUROPEAN MULTIPURPOSE TELECOMMUNICATION SATELLITE :

DEVELOPMENT PLANS

B. L. Herdan
Programme Manager,
European Space Agency
Noordwijk, The Netherlands.

Abstract

To prepare for the next generation of communication satellites, the European Space Agency has investigated the relevant market which can be foreseen and its main characteristics. The background to the decision to proceed with the definition phase of a large multipurpose satellite design concept is explained and key design tradeoff results are presented. Main features of the large platform design are described and examples given of its considerable capability to accommodate a range of future payload types. The communications payload selected for the first demonstration flight is outlined and the paper concludes with details of programme implementation planning.

1. Introduction

During the last few years, satellites have been steadily supplementing or replacing more traditional means of communication as well as facilitating the introduction of new types of service and often modifying the basic system economics. With such a rapid development of the utilisation of satellite-based communications techniques, it is particularly difficult to predict their future evolution with accuracy. The divergence in views between different authorities which may be detected in the literature tends to confirm this. On the other hand, communication satellites are no longer a novelty, and no government agency or commercial organisation would be prepared to finance new developments without a sound demonstration of their future prospects. With this in mind, and recognising that on a worldwide basis the pace of development of new communications satellite systems and technologies will in all probability be maintained, the European Space Agency (ESA) has recently undertaken an investigation of future market prospects and trends for communications satellite systems. Based on the results of this investigation, a new development programme has been formulated which will prepare the European space industry to meet the demands of the future market as well as stimulate certain communications market sectors. This development programme is focused on the concept of a large multipurpose satellite designed to meet a range of predicted future requirements, and currently denoted by the abbreviation "L-SAT".

By means of introduction, it is opportune to summarise the current European communication satellite situation. Following the launch of a series of experimental/preoperational satellites in the 1974-78 period (Symphonie 1 and 2, SIRIO, OTS Europe is now constructing a series of eleven medium size operational satellites of the so-called "Delta class" to support the Eutelsat ECS, Inmarsat global maritime, and French Telecom 1 systems. The European Space Agency has for some time been promoting a follow-on programme to develop the first of the next generation of larger satellites whose eventual need had been generally anticipated. To prepare this development, ESA has already executed detailed studies of the so-called "heavy satellite" (also known as H-SAT) which consisted of an Ariane single launch class platform associated with a payload mainly devoted to direct-to-home television broadcasting. In the area of technology, ESA has begun an accelerated programme of supporting research and development work directly relevant to future telecommunications satellite needs under the title "Advanced System and Technology Programme". On account of the complex - and almost entirely non technical - issues surrounding the question of direct-to-home satellite broadcasting, the H-SAT development programme could not proceed as planned. Instead, it was decided at the beginning of 1979 that ESA should conduct a more general and extensive survey of the future market for large telecommunications satellites, at the same time extending the work already performed in the H-SAT context as concerns the space segment characteristics, with a view to preparing for the development of a truly multipurpose large satellite concept.

This paper provides in Section 2 a brief summary of the results of the ESA market survey and explains in Section 3 the reasons which lie behind the decision of ESA Member States to proceed with the definition phase of a large multipurpose satellite with certain payload capacity characteristics. Key aspects of the top-level satellite design tradeoffs are presented and the platform design solution is outlined together with some examples of derivative configurations in Section 4 and 5 respectively. The payload to be associated with the first flight model is discussed in Section 6 and finally Section 7 looks ahead to the development phase implementation planning.

2. Investigations Of The Future Telecommunication Satellite Market

Scope And Methodology

Investigations of the future global telecommunication satellite market have been regularly undertaken by various organisations and recent publications underline the general consensus that a dramatic growth can be foreseen in the use of satellites for various communication and broadcasting applications over the next decade or so. The recently undertaken ESA market survey differs somewhat from the majority of recent surveys of predominately US origin. The objective of the survey was to consider

Copyright © American Institute of Aeronautics and Astronautics, Inc., 1980. All rights reserved.

the future possible market for satellites of European origin, and in particular to establish the proportion of this potential market which would lead to requirements for a larger class of satellite to quantify the characteristics of this class. Thus from the outset, it was decided to exclude from the survey those markets apparently not open to European industry : the US, Japanese and USSR/ Eastern Bloc domestic markets. The military satellite market was not specifically considered.

In the execution of the survey, use was made of previous market surveys and extensive literature on specific future missions and market sectors, knowledge already available within ESA through contacts with user organisations and governments, the results of specific visits made during the last two years to different parts of the world, and consultancy support. It is beyond the scope of this paper to give more than a general impression of the market survey work, it being preferable to concentrate here on the conclusions and how they support the ESA large satellite programme and its technical objectives. The following thus provides only a brief summary of the identified main market sectors, and then leads into the conclusions of the work.

Summary Of Main Market Sectors

European Fixed Services

The EUTELSAT ECS system will provide telephony and TV relay between all European countries, employing the 11/14 GHz band. These services will be supported from 1982 onwards by the ECS satellites now under construction. However traffic predictions show that this space segment capacity will become saturated possibly before 1987 depending on the precise policy adopted concerning proportion and type of traffic routed via satellite and decisions on the introduction of new services. The next generation space segment for this system will require greater capacity, growth from nine to up to twenty four channels per satellite being foreseen. Such a space segment provides a clear market for a developed large European platform.

In addition to the essentially regional EUTELSAT ECS services, it is envisaged that certain European countries may develop their own national satellite-based systems for trunk services between major cities. Quantitative studies have been performed which show that this will be economically justified where, for example, intercity distances are (relatively) large, where the existing network is not already highly developed, or where rapid growth is desired. As examples, it can be mentioned that, within Europe, Italy is already studying the possible installation of such a system for telecommunications between major cities and studies have been performed in Norway with positive results. Use of the 20/30 GHz bands is envisaged for the Italian case and detailed analyses based on traffic predictions have shown that a large satellite will be needed to support the envisaged service.

It is predicted that a market will develop in Europe for satellite systems to support a range of new services including :-

- text transmission
- telecopying (facsimile),
- data transmission, data store interrogation, computer-to-computer high-speed links, data transfer (including data from remote sensing satellites)
- audioteleconference,
- videoteleconference,
- teleforum and distribution of TV programmes.

The provision of these services on an economic basis over the whole of Europe and directly between small low cost terminals on the premises of private organisations (industrial, commercial, governmental) may be achieved either by a dedicated space segment or in association with the Eutelsat regional trunk service space segment. In technical terms the main "driver" in this class of service could ultimately be the videoconference application which will need considerable bandwidth once a convenient service is established. Use of the 12.5 - 12.75 GHz band for downlinks can be envisaged in the near future (as in the French TELECOM 1 system) but larger satellites operating in the 20/30 GHz bands will be needed as demand grows and bandwidth limitations arise.

It can be anticipated that some or all of the above categories of European fixed services will be supported by a space segment employing larger satellites with multiple payloads. Indeed such a policy could prove the key to stimulating market growth due to resultant space segment economies. The rate of growth of demand for specialised services to small terminals via satellite will to a large extent dictate evolution here.

European Broadcast Services

In a comparatively developed region such as Europe, with extensive existing TV coverage, the advantages of direct to home broadcasting may be summarised as :

- increase in the number of channels available, both in terms of adding new channels or improving exchange of existing ones between countries.
- possibility of economically attaining almost 100% population coverage.

The 1977 WARC allocated to each European country a number of channels with specified frequencies(in the 11.7 - 12.5 GHz band), polarisations, and orbital locations Transmission of sufficiently high power per channel is permitted for the population of any individual country to receive programmes either directly or through community receive systems. At the present time, France and Germany are preparing for the development of preoperational national direct broadcast systems, Luxembourg is studying a system of its own, and the Nordic countries are considering the development of a regional system for programme exchange and direct broadcast. It should be noted, however, that various factors could delay the introduction of truly operational services until at least 1985. These factors include basic questions of possible new standards to be adopted, the situation on legal rights, commercial and political implications of overspill, and the content of new TV programmes. Both national and multinational systems (sharing a single platform) can be envisaged leading to a range of demands on the large satellite platform needed to support them.

Intelsat Global Trunk Services

Forecasts show a continuing rapid growth in traffic to be carried by the Intelsat global trunk system. The Intelsat V system now being deployed is already expected to saturate in the Atlantic and Indian Ocean areas around end 1984. At the time of writing, the Intelsat organisation is considering various options for dealing with this situation, through deployment of an interim satellite system followed by the new generation Intelsat VI system, the interim system consisting of more Intelsat V models with or without improvements, or a series of smaller satellites with certain specific functions. Various options are also being considered for Intelsat VI, and information on the latest situation here will be provided in another paper from the Intelsat organisation at this Conference. In any case there is little doubt that the trend will be towards a larger satellite type.

Global Transponder Leasing

Over the last few years, Intelsat has been supporting a steadily growing demand for the lease of transponders to support domestic services at national or regional level. In mid 1979, 16 transponders were being leased to a total of 15 countries and it was estimated by Intelsat that at least 26 transponders could be in service for this application by 1982. Market surveys show a mushrooming growth in this market such that in 15 to 20 years hundreds of equivalent transponders will be needed for domestic telephony and television services, some supported by dedicated national or regional satellites and others by transponder leasing. Up to now, Intelsat has supported this kind of service on a pre-emptible basis using spare capacity in the inter-continental system. However as the domestic system demand grows, and as the Intelsat global system expands and becomes more complex, this becomes increasingly difficult, and the establishment of a space segment specifically tailored to meet the needs of the domestic transponder lease market may be necessary. This presents another potential market for Europe and developments are awaited with interest. Consideration has also been given by ESA to a space segment generating higher levels of EIRP than those likely to be provided in the Intelsat context and employing reconfigurable multibeam antennas.

Global Mobile Services

There is clear evidence of growing market potential for satellite-based services to mobiles at sea, in the air, and on land. However the cost of deploying such systems is quite high and will only become economically justified where traffic is sufficiently high, this in turn being decided by the user terminals becoming sufficiently cheap to acquire and operate.

In the maritime domain, Inmarsat is preparing for a service to relatively large vessels which need to be equipped with good quality terminals and which demand a fairly high standard of service. The market is well defined, is growing slowly and will continue to do so, possibly stimulated by the promotion of new services concerned with data transmission. A successor to the likely Intelsat V/MCS plus MARECS global system will be needed in due course, and some increase in capacity is predicted with implications for the space segment. A second class of maritime service concerns small ship communications where relatively inexpensive terminals would be needed and lower quality of service could be accepted. This implies a space segment which operates with the ship terminals able to receive and transmit at lower power levels than terminals of the current INMARSAT standard. The market could grow rapidly as soon as terminal costs and tariffs are brought down to a sufficiently low level.

As concerns a future aeronautical satellite-based system, studies are continuing on an international basis in the aftermath of Aerosat and there is good evidence to support the existence of a future market both for voice communications over ocean and remote land areas and - more especially - for data communications. The latter application could be of particular interest for the automatic relay of meteorological data from air to ground to optimise flight paths and hence save fuel, as well as for automatic relay of aircraft position to ground and retransmission of positions of all nearby aircraft from ground to air for cockpit display.

Use of a satellite system for land mobile communications offers interesting new perspectives for services which cannot be provided by other means. These are mainly relevant to less developed regions and include extension of the public telephone network to isolated, underdeveloped and desert areas, provision of a safety/distress service for land vehicles in remote areas, emergency communications for areas suffering natural disasters, and provision of paging facilities. Just as in the case of the small ship market, inexpensive terminals and low tariffs will be needed, the trend of the market is difficult to quantify, but it automatically leads to the necessity of providing high flux-density satellites in order to minimise the terminal cost. Another type of land mobile market already exists in developed regions where, for example, car mobile phones are generally available. Market surveys have shown that rapid growth of this market can be expected, but for the European case at any rate it seems probable that this demand will be met by terrestrial rather than space-based systems.

In summary, a slow growth can be predicted in all the satellite mobile communications market sectors. It seems probable that the trend will be towards the combination of services with payloads sharing a common platform in each region. Analyses of the technical implications of this conclusion show that a need is demonstrated for large satellites to support such combined requirements.

Non-European Regional And Domestic Services

The likely demand for satellite services which could be of relevance to exports by the European space industry in this sector has been investigated. The countries and regions which have been covered in some detail are :

- Arab League
- Australia
- Brazil
- Canada
- China
- Colombia
- India
- Indonesia
- Iran
- Nigeria
- South America
- Sub Saharan Africa

The types of service which are or will be provided by satellite in these countries and regions include :

- fixed service trunk services (telephony and TV relay) between larger stations (4/6 GHz band and sometimes also 11/14 GHz band);
- thin route trunk services (telephony) between smaller low cost stations;
- TV broadcast services of the community reception type (2.5 GHz or 12 GHz downlinks);
- TV broadcast services of the direct type (12 GHz downlinks), only relevant to the most developed countries;
- TV transmission services of the local reception and redistribution type (4/6 GHz);
- UHF sound radio broadcast to simple portable receivers (1.4 - 1.5 GHz).

Certain countries or regions can be expected to deploy their own operational systems and maintain them in future. Aside from Canada, Indonesia and India who already have systems in construction or operation, the most promising future candidates appear to be Australia, the Arab League, China and possibly Brazil. For many developing countries the likelihood is that several of the above services will be combined and provided in a given country or region by a single system. Since each service needs only a modest capacity space segment, this leads to the conclusion that the most economic solution would be the deployment of satellites to serve large areas with flexible regional/national zonal coverage and a mix of general purpose transponders available for leasing. This is especially true for South America and Africa. Apart from leasing through Intelsat, another solution here could involve international aid organisations.

Market Survey Conclusions

The market survey work which has been outlined above has led to a series of conclusions concerning two major points :

- the magnitude of the market and the scope for its penetration by European industry.
- the main characteristics of the future satellite types which will be needed and - in particular - their sizes in payload mass/power and antenna terms

Concerning the magnitude of the market considered in the survey, it has been concluded that the total number of satellites which will be needed in the 1983-94 time period to fulfil the requirements of the six main market sectors defined above is in the region of 150. Europe can expect to sell in these market sectors either where they are a protected European domain - which may be the case for some but not all European national/regional systems, or where Europe has some political advantage, or where European industry gains a competitive advantage on technical and/or cost grounds. On the latter score, Europe is naturally at a disadvantage when compared with the US both for historical reasons, because of the small European domestic market, and - recently - because of the falling value of the dollar. However Europe now has developed space-proven hardware to offer, and an increasing domestic production base which will help to improve cost effectiveness. Moreover, there are firm plans to continue development of technologies and hardware to keep European industry abreast of requirements. The message that European industry must be well placed to compete on expanding world markets with off-the-shelf hardware has been understood by a number of European governments who are consequently ready to continue funding relevant development activities. The ESA large satellite programme described later in this paper is a concrete demonstration of this readiness.

Based on these various considerations it has been calculated that, out of the total theoretically available market, Europe could reasonably expect to capture sales of between 35 and 60 satellites including equivalent subsystem and platform sales. For reasons which will be explained below, it was further calculated that the majority of such satellites (around 85%) would be of the larger class. These estimations are, despite the optimism expressed above, in fact based on the probably realistic hypothesis that even in the future, Europe will rarely be able equal US prices in an open competition.

The next section deals with the second series of conclusions which have been drawn from the market survey and associated technical studies.

3. The Case For Large Multipurpose Telecommunication Satellites

As concerns the characteristics and size of satellites which will be required to meet identified market requirements, it has been found that the medium size, so-called "Delta-class", satellite will be insufficient for most future applications and that larger satellites will be needed. This is in each case due to one or more of the following factors :

a) increase in capacity requirements for satellites dedicated to a single type of service.
b) increasing demands on satellite design sophistication to find ways around the shortage of spectrum as service demands grow.
c) introduction of new types of satellite-based service operating with small ground terminals and hence putting more demands on the space segement.
d) use of a single satellite to support several payloads dedicated to different service types over the same coverage area, leading to space segment economies.
e) use of a single satellite with a general purpose-type payload for several types of service, again for economic reasons.

For example, large satellites will be needed for European fixed services both because of increasing capacity demand, (factor a)), the introduction of small terminal services as well as trunk services (factors c) and d)) and possibly because of factor b) as spectrum and orbit location begin to present problems. The growth in size of Intelsat satellites which has already taken place is due primarily to factor a) but also reflects to some extent b), d) in the case of the addition of the maritime package on Intelsat V, and e) with particular reference to transponder leasing. Such growth may well continue. In the direct broadcast field, factor c) predominates in the trend towards large satellites in view of the high transmit flux levels needed to work into home receivers. In the mobile field, introduction of an integrated maritime/aeronautical/land mobile service can be foreseen leading to requirements for large satellites primarily on account of factors c) and d) and - to a lesser extent - a). For the non European regional and domestic case, each national/regional system can normally be satisfied for the time being by smaller satellites - although this may change before long - but the type of flexible regional system covering parts of a whole continent as mentioned earlier leads to larger satellites on account of factors a), c) and e).

To establish how large is "large", and whether it is sensible to talk about one class, albeit a flexible one, of multipurpose large satellite able to support a high proportion of the foreseen missions without being grossly oversized for some or too constraining for others, a detailed analysis has been made of a range of future typical mission requirements. A sample of ten specific missions was selected from those fields covered by the market survey and an in-depth assessment made of the corresponding typical satellite communications payload characteristics and consequent demands which each would impose on the platform. A calculation of specific typical payload parameters and demands and an estimation of the range of likely variations about this data was made for each case. The result of this exercise has been the generation of sufficient information to be able to display in graphical form a plot of payload mass versus payload power demand for the various typical cases considered and hence to derive the envelope of desirable payload-carrying capacity for a single truly multipurpose class of large platform. This plot is shown in Figure 1.

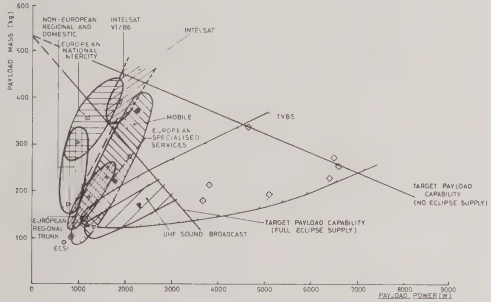

FIG. 1 Payload Requirements And Target Capabilities

The mass of payload hardware and the payload power demand have been calculated for each example mission as noted above, as well as for quantified variations in each mission whenever possible, and in the plot of mass against payload power this enabled zones to be designated for each category of mission identified in the market survey. As an example, the TV direct broadcast (TVBS) zone contains specific points for a number of reference missions including regional/national systems for the Nordic countries, Italy, the UK, Luxembourg, Canada, France and Germany. Variations about each point are based on varying numbers of channels per country within realistic limits. The curve shows the envelope of all calculated cases: it is open-ended since more ambitious systems are under consideration. Each of the zones is based on calculations performed in a similar manner. The other data generated by this part of the work have been the characteristics of the various antenna farms for each typical future mission. From the platform design and launcher capability and launch cost viewpoint, this is also both important in itself and relevant to the feasability of a multipurpose common platform. The results of this work have been used as explained later for the more accurate layout evaluations necessary to establish feasibility and launcher capability.

Based on the series of future payload requirements identified above, we can now consider the questions posed earlier in this section and characterise payload-derived requirements on a large multipurpose platform. It has been found possible to derive two curves which envelope practically all foreseen required payload mass/power combinations. These curves have already been superimposed on the plot of Figure 1, the upper curve corresponding to the case where no payload eclipse operation is needed (typical for direct broadcast) and the lower curve corresponding to the case where 100% eclipse operation is needed (typical for other types of service). The conclusions of this parametric exercise are that a platform sized to support an effective payload mass of 530 kg or so will be able to support almost all foreseen missions with some well defined possible exceptions which might, however, eventually be constrained to match the capability of the platform/launcher combination for reasons of economy or launch choice flexibility. Payload mass is defined here to include all effective contributors including repeater and antenna hardware, the proportion of solar array, battery and power conditioning electronics which are relevant to payload, and all other payload-specific elements. The figure of 530 kgs is derived as the intercept on the payload mass axis of Figure 1 corresponding to the zero power case.

In addition to mass, communications payloads tend to be demanding in terms of thermal control requirements. Again, each of the ten typical payload was analysed from this viewpoint and it was established that the basic configuration must provide not less than 9m^2 of radiating area with a clear view to cold space. The actual area would be tailored to meet individual payload requirements. In terms of level of power generation, the platform design must be conceived to permit the generation of from one to seven kilowatts of sunlight power and from zero to two kilowatts of eclipse power at e.o.l. Finally, the technical studies have highlighted the severe requirements on flexibility of antenna accommodation which must be met. For the range of missions considered it was concluded that from one to six principal antennas would have to be accommodated, these of widely varying sizes (up to around 10m diameter with the majority around 1-3 metres), of various types (single feed, multifeed, frontfed, Cassegrain etc) and with differing mechanical constructions which could involve reflectors being rigid and fixed to the body, hinged, deployable or unfurlable.

In conclusion, our work has demonstrated that larger satellites than those currently available or under development will eventually be normal for most applications, and that the demand exists for a single large multipurpose platform which would have capabilities enveloping the majority of requirements foreseen for the next ten years or so without being oversized for too many cases. Some tailoring of platform design to missions relatively far from the basic capability target line should be envisaged, eventually in line with matching to launch systems more or less performant than the cases considered for the basic design optimisation process.

4. Satellite Design Optimisation : The Main Decisions

In this section, four main topics are treated. These concern respectively the question of launch vehicle choice and compatibility, the choice between spin and three-axis stabilisation in synchronous orbit, the series of system level tradeoffs currently in progress, and the main design guidelines to be imposed on subsystem designers in line with overall programme objectives.

Launch Vehicle Choice And Compatibility

An essential element in the definition of the large platform characteristics has been an evaluation and tradeoff between candidate launching systems with emphasis on the relation between satellite geometry, launcher compatibility, and launch cost. The majority of identified mission requirements being well beyond the capabilities of the Delta or Space Shuttle (STS)/PAM D launch combination, attention was focused on the potential for launch by Ariane (as single launch payload) or the equivalent more performant US system, STS. While it might seem natural for a European programme to baseline the Ariane launcher, it was also considered expedient to investigate the feasibility and cost of launch by STS in order to evaluate future cost competitivity in the global market of ARIANE-launched satellites versus US systems optimised for STS. Moreover, it was in any case considered essential that a multi-purpose European platform be designed to be STS-compatible so as to permit sale in those non-European market cases where STS might be the specified launcher, and preferable for the platform to be so conceived for the system to be cost-optimised for all launch configurations.

As concerns the launch by Ariane, the analysis of the total satellite mass compatible with the above identified payload requirements and with a launch from the Ariane French Guiana launch site leads to the conclusion that the maximum lift off mass would normally be around 2300 Kgs, corresponding to about 1380 Kgs mass on station at beginning of life with an optimised apogee motor. This is compatible with the capabilities of the improved Ariane 3 version now in development whose performance is currently estimated at 2350 Kgs and which will enter service in 1983. The Ariane shroud diameter of 3 metres is, of course, an important constraint to be taken into account in optimisation of the satellite configuration to ensure that all required antenna farms can be accommodated. In effect, and when compared to the STS situation, this constraint means (in some special cases) more antenna deployments or hinging of reflectors - but would only produce an infeasible solution in the rare situation where a rigid reflector antenna is essential whose minimum dimension exceeds 3 metres.

As concerns accommodation on STS, the situation is more complex, The level of performance required to match that of the Ariane 3 puts the satellite in the class where there is a gap in the available inventory of American perigee stages able to inject the satellite from the STS low earth orbit into a synchronous transfer orbit. The MDAC PAM-A stage can only inject 2000 Kgs into transfer orbit (roughly equivalent to 1090 Kgs on station b.o.l.) while the Boeing IUS stage is too performant and costly, being able to inject 2300 Kgs into final synchronous orbit. The following solutions exist :

- use of the PAM A stage/motor with "top up" by a liquid motor to provide the full impulse, also possibly used for the apogee burn.
- use of an improved more performant solid motor for the perigee stage, either in a modified PAM A configuration or integrated into the satellite.
- use of a new all liquid stage to perform the complete perigee burn in steps

A comparative analysis of these solutions has been performed taking account of both technical factors and of the perigee stage plus STS launch cost for each solution. At the same time, the associated satellite geometrical alternatives have been assessed for two main types of configuration :

- those with a relatively small cross-section longer body, which are compatible with launch by Ariane without change in geometry, and which involve the perigee stage being mounted externally as a separate module.
- those with a large cross-section shorter body, not compatible with launch by Ariane, and with the perigee stage in some cases integrated inside the main body.

It is beyond the scope of this paper to detail all the configuration studies or to give the full results of the associated technical and financial analyses. The conclusions of the work are, however, of fundamental importance. It was found that for this class of satellite it would indeed be possible so to design the platform geometry as to permit a unique basic configuration to be launched on either ARIANE or STS, and that such an ARIANE optimised platform (i.e. thin body configuration) would be equivalent or only very slightly more expensive to launch by STS than one carrying the same payload but configured with a "short fat body" solely optimised for launch by STS, the details depending on the precise antenna configuration involved.

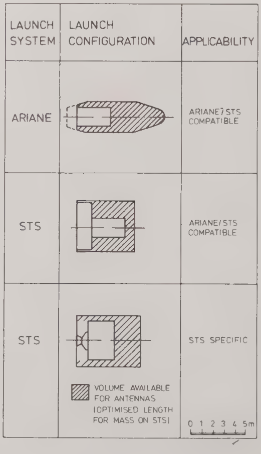

FIG. 2 Comparison Of Launch Geometries

The alternatives are shown pictorially and to scale on Figure 2 where the volumes occupied by the satellite options and the associated volumes available for antennas are presented. For STS-launched configurations the volume available for antennas is derived from the length in STS equivalent to the total satellite/perigee stage mass so as to achieve the minimum launch cost for the class of satellite concerned. This shows that for the cases of an Ariane 3 compatible satellite and its STS specific equivalent, the overall masses and hence optimum lengths for STS launch are very similar. In fact the main difference between the two approaches is in their antenna accommodation capability. For the STS specific configuration, antenna mounting space is mainly situated on what, for three-axis stabilized configurations, is the earth pointing satellite face, while for the Ariane compatible configuration antennas can also be mounted from the sides of the satellite, this being in fact more desirable for large antennas. This latter position can provide advantages for many missions since the satellite body itself can then be used as the antenna feed tower for front-fed antennas, thus avoiding long waveguide runs and extra mass for the feed tower. This is particularly attractive at high frequencies. It is assumed for this assessment that the STS/Ariane compatible configuration when flown on STS, would employ a liquid perigee stage, this having been judged the optimum out of the options studied. This stage consists of a bipropellant motor and its propellant tanks arranged into a configuration occupying a minimum length in the STS bay. Preliminary designs show that such a perigee stage would have a dry mass of about 830 Kg and would occupy 1.2 m of the STS bay.

In conclusion, it has been decided to adopt the approach of developing an Ariane/STS compatible solution for this programme while noting that - to maintain STS compatibility - the development of an improved performance perigee stage is now essential.

Choice Of Stabilisation Method : Spin or Three Axis

As explained earlier the large platform is to be suitable for missions extending over a wide payload power and mass requirement range. At the lower levels (below 2 Kw) a spin-stabilized satellite may be attractive because of its relatively simple attitude control and thermal design, hence potentially lower recurring cost. However, power generation capability of a spinning satellite is limited by the area available for mounting solar cells. This restriction will limit the power capability of an Ariane compatible spin stabilised satellite to around 1.0 to 1.5 KW, and for a satellite designed to occupy the full diameter of the STS bay to around 1.5 to 2.0 KW. The use of deployable array sections or "skirt" leads to an increase in these limiting values, but missions requiring payload powers much greater than 2 KW will be impractical with a spinning satellite.

To encompass the power range from one to seven kW implied by the range of large platform missions, only a three-axis stabilised satellite is therefore considered suitable. In addition to the power generation arguments developed above, a three-axis stabilised satellite has other advantages. Firstly, the availablility of unobstructed North and South facing surfaces permits efficient thermal control of higher power missions which would present major difficulties for a spinner. Secondly, freed from the need implied by spin stabilisation to provide the large surface area for solar cell mounting, the body of a three axis satellite can be made smaller, and hence lighter, its size now being determined only by thermal control, apogee motor and equipment mounting requirements. Thirdly, only approximately one third of the number of solar cells are needed compared with a spinner saving at least half a million dollars in cell costs for every kilowatt of installed power.

In conclusion, a number of factors have dictated the choice of three axis stabilisation for this programme in order to ensure optimum performance and compatibility with the needs of the full range of future foreseen mission requirements. This choice is also well matched to the existing European competence and background in three axis satellite design and hardware.

System Level Trade Offs

Within the framework of the basic decision on STS/Ariane configuration compatibility derived above, several major system decisions are still to be made and detailed trade-offs and studies are planned.

There is a strong interest in the use of liquid apogee boost motors (ABM's) to take advantage of their improved performance over solid propellant motors, as well as better configurational flexibility. However the presence of large quantities of liquids in the satellite might, some argue, lead to stability problems. Associated with this choice is the question of the stabilisation mode to be used in transfer orbit. When a solid ABM is employed, a spinning transfer orbit is almost mandatory. If a liquid motor is selected a three axis stabilised approach becomes a possibility and will also alleviate the potential stability problems due to the presence of large quantities of liquids. These points are still under study.

A further major impact on the basic layout of the satellite will arise from the final decision on the configuration of the solar arrays. The choice is between a conventional "I" - form satellite with two array wings oriented North/South, and an "H" - form satellite with four array wings oriented East/West. This latter configuration, although introducing more deployment mechanisms and possibly restricting the volume available for antennas, may simplify the problems of maintaining accurate attitude control during N/S station keeping for very large solar arrays and reduces the deployed length of each wing.

For a satellite platform which is intended to be used throughout the 1980's a careful examination and selection of the appropriate technology level will be necessary to ensure that on one hand problems are not caused to early missions by the use of too advanced concepts and on the other hand that a too conservative approach does not lead to a rapidly outdated or obsolescent design. The approach being adopted here is to ensure that interfaces are such that foreseen improvements in technologies can be introduced on later missions without the need for major redesigns if the technologies concerned are "too late" for the first flight. Examples of this could be the replacement of nickel cadmium by metal-hydrogen batteries and the introduction of ion motors for station keeping. A particular study is being made of the systematic application of microprocessors in the satellite design.

Main Design Guidelines For Subsystems

The prime objective of the development of the large platform is to ensure the availability of a bus that can be reused for a wide range of future commercial communications satellite missions. To ensure a successful commercial product, the driving features of the large platform must be maximum performance and reliability at minimum cost. All design studies and trade-offs are being assessed against the achievement of these goals. In particular, subsystem solutions are being selected which are directly applicable, or can easily be modified - for example by modularity - to the widest range of future payloads. The unique requirements of the first flight service demonstration mission described later in this paper will not be permitted to direct the platform design to special solutions which do not have wide applicability. A careful Value Engineering assessment is being made of proposed design solutions. Factors in each trade-off are systematically translated into impacts on reliability, mass, and recurring cost for each proposed solution, with system - level evaluations being made of the achieved performance or reliability improvement versus cost and payload capability increment for each option. A total satellite recurring cost target is being established and apportioned to subsystem level considering the predicted global competitive situation.

5. Platform Design Solution

Based on the series of objectives, requirements and constraints identified above, and taking into account the results of system-level optimisation tasks which have just been described, a multipurpose large platform design solution is currently emerging and becoming progressively refined. Figures 3 and 4 show respectively the basic satellite concept in its launch configuration (Ariane case) and in its in-orbit operational configuration. These figures in fact show the platform equipped with the first flight service demonstration payload which will be described in the next section.

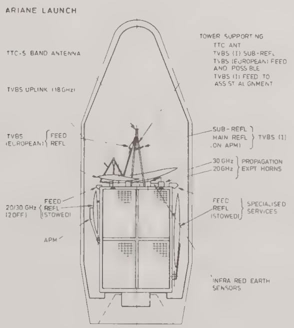

FIG. 3 L-SAT - Launch Configuration

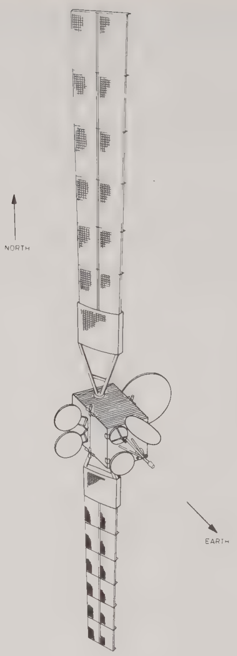

FIG. 4 L-SAT In Orbit Configuration

Optimisation of the platform geometry, in particular in view of the launcher compatibility and antenna accommodation requirements, has led to the choice of a box-like body structure with dimensions of 1.75 x 2 x 3 metres approx. including the payload module structure. The North and South panels are used on-station as the main radiating surfaces, while in launch configuration these panels are covered by the stowed solar array. Payload antennas can be mounted either on the earth facing panel or deployed from the East and West walls as shown for example in Figures 3 and 4. The satellite body is used as the antenna tower for larger antennas, only smaller antennas or a single large antenna being mounted on the earth facing platform. Where the body is used as the tower, feeds or subreflectors are mounted from the top platform and main reflectors are pivoted from the service module East/West faces. This solution eases multiple large antenna accommodation, reduces waveguide losses, and facilitates cost optimum launch by STS as explained earlier. To permit parallel design, assembly and test activities, the satellite separates into three modules, comprising service module, propulsion module and payload module. As its name implies, the service module contains the majority of equipment associated with the service functions of attitude control, power supply and data handling, the exceptions being the earth sensor used for on-station platform attitude control and the TTC S-band antenna. The propulsion module consists of the apogee motor and the reaction control system used for attitude manoeuvres and momentum wheel off-loading, while the payload module is used to support the communications repeaters and antennas. The modular concept is illustrated by Figure 5.

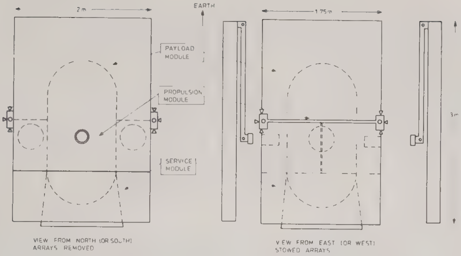
2m
EARTH
1.75m
PAYLOAD MODULE
PROPULSION MODULE
SERVICE MODULE
3m
VIEW FROM NORTH (OR SOUTH) ARRAYS REMOVED
VIEW FROM EAST (OR WEST) STOWED ARRAYS

FIG. 5 General Modular Design Concept

Since L-SAT is effectively the start of a second generation of European communication satellites following on from OTS, ECS and MARECS, the opportunity has been taken of critically re-evaluating the basic configuration and technology of all the service subsystems while respecting the guidelines given in the last section. The type of solar array, for example, has been assessed and the conclusion reached that for the range of high power missions foreseen, the classical rigid fold-out array concept must be abandoned in favour of a flexible or hybrid array. This in turn has drawn more attention to the interaction between the array and the attitude control system which could result in the need for more sophisticated control techniques than previously used, at least in Europe.

Considerable work has been done on a zero momentum attitude control system and this is another example where in-depth cost and technical analysis is being performed to determine whether it should replace the currently baselined momemtum bias system. This step, however, will only be taken where the arguments are convincing, no innovation being considered merely for the sake of it. Similarly, the wide variety of payloads envisaged has forced a re-appraisal of main bus regulation concepts and a trade-off between regulated, unregulated, and AC bus configurations is being performed to establish the optimum system from cost, performance, reliability and risk points of view. This trade-off will pay particular attention to the increasing demand for eclipse operation and the resultant impact on battery capability, hence leading to important decisions on battery technology type as mentioned earlier.

Another key area of importance is the choice of reaction control system. The ABM options have already been discussed in Section 4, but such a trade-off must also consider the overall propulsion requirements and in this context it is clear that a combined bipropellant RCS and ABM approach has many advantages. Nevertheless, these advantages are being rigidly weighed against the known disadvantages, and the remaining questions of controlling an unstable satellite configuration in the presence of high masses of mobile propellants, are being analysed before reaching a final decision.

In the area of thermal control, it seems clear that the envisaged range of highly dissipative payloads and the marked differences between sunlight and eclipse operation of some payloads will necessitate the application of more sophisticated thermal control concepts and the introduction of heat pipes appears to be the obvious solution. Whether these be of the constant conductance or variable conductance type remains to be analysed.

The detailed design of the platform will continue to evolve over the next months. In parallel with this evolution and the definition of the payload which will be carried on the first flight, a continuous check is being kept of the compatibility of the platform design with a series of defined future mission requirements, emphasis being put on mass/power compatibility and accommodation of antennas which is verified through the preparation of layout drawings.

6. Payloads For The First Flight Model

In reaching their decision to proceed with the definition phase of the L-SAT programme, the ESA Member States concluded that it should comprise on the one hand the development of a multipurpose platform as described already, and on the other hand the development of a multi-element payload to be accommodated for the first flight of the platform and used for demonstration of new payload technologies and several new types of service.

It was decided that the selection of the payload elements should be based on the strength of market predictions for each mission type, the interest in demonstrating certain new services, the benefit of in-orbit demonstration and qualification of the relevant payload technologies, and the willingness of participating Member States government and/or user authorities to finance both payloads and corresponding minimum necessary ground segments. The attractive features and objectives of such an approach are

- to demonstrate in a concrete fashion the multi-purpose nature of the platform and its ability to support a demanding payload
- to produce a satellite which would prefigure future foreseen operational satellites of a multi-mission nature, the market survey having shown that multi-mission satellties will be common in future
- to provide facilities to promote new markets for satellite telecommunication services,
- to provide a well-publicised demonstration of European capabilities, particularly in the payload domain and in a wide range of frequency bands.

In order to arrive at a suitable demonstration payload combination which is compatible with the series of objectives given above, ESA has taken contact with a wide range of users including government authorities, PTT administrations, scientific and technical organisations, governmental and commercial broadcast authorities, and European organisations such as the EEC and the EBU. These contacts have been employed to investigate the degree of interest and financial support for various possible missions and payloads. As a result, a shortlist of payloads has been derived and industrial studies engaged to define each of them and the payload combination.

The series of payloads which it is currently envisaged to support consists of:

- a two channel 12 GHz television direct broadcast payload with one channel providing preoperational services for one European country and the other steerable to support experiments and demonstration in time sharing mode over the whole European region.
- a payload for pilot European specialised or business services in the 12.5 - 12.75 GHz downlink band for operation with small terminals located at private or local premises.
- a payload for experiments and demonstration in the 20/30 GHz band as relevant to its future utilisation for specialised services such as videoconferencing, and supporting scientific and technical objectives of relevance to a range of other future applications.
- a payload to support experimental measurements of propagation effects in the 20/30 GHz bands.

The varied nature of this payload and the ambitious technical features are a concrete demonstration of the multimission features of the platform and the forward-looking nature of the European programme of satellite communications system and payload hardware development. The detailed definition of each payload and of its utilisation is a current high priority task. First assessments of the compatibility of the payload combination with the platform show that there is absolutely no problem in terms of mass and power as evidenced by the power and mass budgets of Tables 1 & 2. As for antenna accommodation, the eight antennas implied by the payload combination utilise most of the available space as illustrated by Figure 6.

	At Main Bus	At Array
Payload		
Specialised Services	135 W	
Broadcast	2046 W (sunlight only)	
20/30 GHz Transponder	345 W	
20/30 GHz Propagation	60 W	
TOTAL	2586 W	2741 W
Service Functions		287 W
TOTAL		3028 W

Table 1 : L-Sat Power Budget (First Flight Payload)

	Kg
Repeater (four payload elements incl.harness)	199
Antenna (four payload elements)	120
Platform Dry Mass (Incl. payload-dependent services)	682
Total dry mass	1001
Margin (10% dry mass)	100
TOTAL dry mass with margin	1101
RCS fuel	227
ABM fuel (Ariane 3 launch option)	912
Balance mass	15
Margin for additional payload	45
Lift off mass	2300

Table 2 : L-SAT Mass Budget (First Flight Payload)

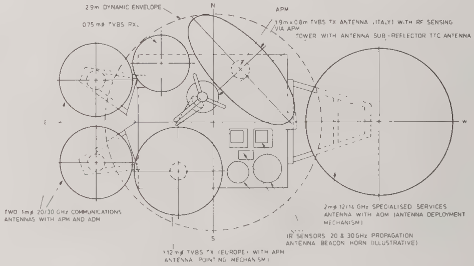
2.9m DYNAMIC ENVELOPE
0.75 mø TVBS RX
N
APM
1.9m x 0.8m TVBS TX ANTENNA (ITALY) WITH RF SENSING VIA APM
TOWER WITH ANTENNA SUB-REFLECTOR TTC ANTENNA
E
W
S
TWO 1mø 20/30 GHz COMMUNICATIONS ANTENNAS WITH APM AND ADM
2mø 12/14 GHz SPECIALISED SERVICES ANTENNA WITH ADM (ANTENNA DEPLOYMENT MECHANISM)
IR SENSORS 20 & 30GHz PROPAGATION ANTENNA BEACON HORN (ILLUSTRATIVE)
1.12mø TVBS TX (EUROPE) WITH APM (ANTENNA POINTING MECHANISM)

FIG. 6 Layout Of Antennas For L-SAT First Payload

7. Implementation Planning

In July 1979, a number of the ESA Member States decided to authorise the start of the definition phase of the L-SAT programme. In November, following a brief competitive period, British Aerospace was selected as Prime Contractor and the definition phase Prime Contract was awarded early in December. The definition phase, which encompasses system, platform and payload activities, will run until the end of 1980 and the total budget approved for all types of activity during this phase - including a fair proportion of critical hardware development and advanced parts procurement - is about $17 million. Towards the end of the definition phase when the subcontractors have been selected and a fixed price proposal for the development phase has been submitted to ESA, authorisation will be sought from Member States for full programme go ahead. At this point it is anticipated that the countries participating in the programme will consist of some or all of the following : United Kingdom, Italy, The Netherlands, Belgium, Switzerland, Denmark, Spain, Austria and Canada. Each will contribute to the programme in proportion to work won in competition by its own industries, the total programme cost being estimated at $200-250 million including the satellite development, procurement of a flight model and flight spare, one launch, post-launch operations, ground segment, and ESA technical and management costs.

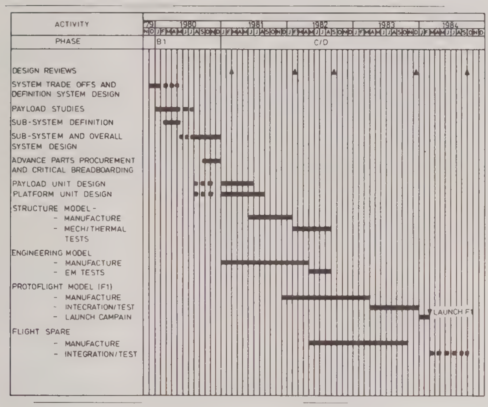

FIG. 7. L-SAT Implementation Schedule

Figure 7 shows an outline of the current implementation schedule and also illustrates the basic model philosophy which is to be adopted. The definitive schedule will not be finalised until later in 1980 when subsystem design choices have been detailed and the precise payload configuration defined and elaborated. However, if all goes well, we are looking forward to achieving a launch in the first quarter of 1984, by which time it is also anticipated that derivative designs should already be in production.

Acknowledgements

Contributions to the genesis of the Large Satellite Programme have been made by colleagues at ESA too numerous to mention and these contributions are widely reflected in this paper. Assistance in the preparation of the paper itself by Messrs. J. B. Atkinson, A. Dickinson and R. Steels is gratefully acknowledged.

THE EFFECTS OF GEOGRAPHY ON DOMESTIC FIXED AND BROADCASTING SATELLITE SYSTEMS IN ITU REGION 2*

Peter H. Sawitz
Principal Scientist
ORI, Inc.
Silver Spring, Maryland

ABSTRACT

Geographical features, such as latitude, size, shape, terrain, and climate of a service area, can have significant effects on the extent of the orbital arc from which useful service can be provided and on the possibilities of frequency reuse, which is the single most important factor determining the efficiency of spectrum-orbit utilization. This paper discusses the effects of geography on service arcs and on the various techniques used to achieve frequency reuse and applies the results to the domestic fixed and broadcasting satellite systems of ITU Region 2.

1. Introduction

The International Telecommunications Union (ITU) divides the surface of the earth into three Regions. Region 1 essentially contains Europe, Africa, all of the USSR, and Mongolia. Region 3 comprises the rest of Asia and Australasia. Region 2 essentially contains the Western Hemisphere and Greenland. Region 2 is of special interest for at least three reasons. There are at this time more satellites in orbit providing domestic services in the fixed-satellite service (FSS) in Region 2 than in the other two Regions combined. Until very recently, only in Region 2 did the FSS have an allocation in the 11.7 to 12.2 GHz frequency band, sharing this band with the broadcasting-satellite service (BSS). And last not least, Region 2 includes the USA.

Both the FSS and the BSS are using, or plan to use, the geostationary orbit for reasons that are well known. More than sixty satellites already have been launched into this orbit, most of them to operate in the FSS (point-to-point) both for international and for domestic services. The 1977 World Administrative Radio Conference for Broadcasting Satellites (77 WARC-BS) adopted a plan for the BSS which calls for 26 broadcasting satellites to serve ITU Regions 1 and 3. Even now, there is considerable crowding at certain locations for satellites in the FSS operating in the 4 and 6 GHz frequency bands, and it is becoming increasingly difficult to find suitable orbit positions for new systems operating in these bands.

One proposed solution to this problem is to make detailed usage plans, assigning to each country or group of countries orbital positions and frequencies to be used at each position. It is alleged that this assures equitable distribution of the available scarce resource. However, such a plan may result in inefficient spectrum-orbit utilization because, being based of necessity on the technology prevailing at the time of its adoption, it cannot make use of subsequent advances, and because some potential users may not use their assignments for many years, having neither immediate requirements nor the necessary economic resources.

A detailed plan, made for the entire world or for a part thereof, naturally takes into consideration all the geographic features of the area served. However, a more flexible approach can take these features into consideration also, though in a more general way. This becomes important, for example, in making estimates of the capacity of the spectrum-orbit resource, and in making comparisons between rigid plans and other approaches.

In the past, the effects of geographic features have often been neglected in general analyses, and as a result some misleading conclusions were drawn. For example, a study by Reinhart(1) on spectrum-orbit sharing between the FSS and the BSS, which expounds all the important principles of sharing between these two services and became the basis for United States policy for many years, stops short of considering the effects of the specific geographic features of the areas to which the principles were applied. This paper discusses these features in detail and assesses their effects and importance.

2. Background

The 77 WARC-BS adopted a plan for the BSS in Regions 1 and 3. It also called for a Regional Administrative Radio Conference in 1983 for the purpose of planning the BSS in Region 2. The recently concluded General World Administrative Radio Conference of 1979 adopted a resolution to hold a special conference in the near future on planning the space services in all frequency bands allocated to them. Thus, the broad problems of how best to plan the BSS and FSS so as to meet the legitimate requirements of all nations are constantly being reexamined and will be the topics of two future international conferences. The information presented in this paper is meant to be a contribution to the solution of

---

*This work was supported, in part, by the Goddard Space Flight Center of the National Aeronautics and Space Administration (NASA) under Contract No. NAS5-24393.

Copyright ©, 1980 by ORI.

Released to AIAA to publish in all forms.

these planning problems.

3. Spectrum-Orbit Utilization

Both the frequency spectrum and the geostationary orbit are limited natural resources. The limitations of the frequency spectrum arise from mutual interference. It is less obvious, but true nevertheless, that the limitations of the geostationary orbit arise from the same source. Thousands of satellites could be placed in that orbit without danger of physical interference. But when they operate in the same frequency band, considerations of radio interference require satellite separations that vary from a degree or less to as much as twenty degrees or more, depending on the system characteristics. Therefore, the two resources are usually grouped together. The general topic of providing the maximum amount of useful services from the geostationary orbit within a given frequency band is referred to as spectrum-orbit utilization.

While the capacity of the spectrum-orbit resource, whatever is used as its measure, is not infinite, one cannot assign a definite number to it unless both the technical characteristics of all systems involved and their operational modes are completely specified. In fact, the capacity has steadily increased in recent years as technology has advanced, and there are ample reasons to believe that this trend will continue. It is for this reason that it is so important to factor all available information, including the geographical features of the intended service areas, into the planning process. Then a flexible approach can be used that allows the identified requirements to be met at each epoch without foreclosing the utilization of technological advances in the future to meet new and expanding requirements of all nations.

4. Frequency Reuse

The key to efficient spectrum-orbit utilization is frequency reuse. If each frequency, or band of frequencies, were used only once, the capacity of the spectrum-orbit resource would simply be the total number of communication channels that can fit into the available bandwidth. The number of satellites would be irrelevant, as would be their positions and the distribution of service areas. There would be no interference, except perhaps between adjacent channels.

Frequency reuse is possible primarily through three techniques: orthogonal polarization, earth-station antenna discrimination, and satellite antenna discrimination. Geographic features have some effects on all three; but the one affected most is the satellite antenna discrimination. All three will be discussed below.

5. Service Arcs

The service arc of an area is defined as that portion of the geostationary arc from which useful service can be provided to all points in that area. The emphasis here is on "useful". The service arc is not identical with the visible arc. Visibility, i. e. the existence of an unobstructed line-of-sight path, is a necessary but not a sufficient condition for useful service. Other conditions that must be satisfied are elevation angles that exceed certain minimum values and, for some services, eclipse protection.

Elevation angles are important because many service impairments, such as natural and man-made noise and attenuation due to rain, increase with decreasing elevation angles. The minimum elevation angle required for satisfactory service is a strong function of the rain statistics of an area, particularly at frequencies above about 10 GHz. Thus, the geographical feature of climate has a significant effect on the service arc of an area. Service areas with high average rain rates require higher elevation angles and therefore have smaller service arcs. Systems in the FSS usually require minimum elevation angles of ten to fifteen degrees, except in areas with very high rain rates. Systems in the BSS may require minimum elevation angles of twenty to as high as forty degrees. Of course, such high elevation angles are not always possible at high latitudes. Then more elaborate (and more expensive) receiving systems will be required, or a lower quality of service must be accepted.

As an example of the rapid increase of attenuation with decreasing elevation angle, Figure 1 shows the attenuation due to rain as a function of elevation angle at 12 GHz(2). Figure 2 shows the rain zones of the world as defined by the ITU in the Radio Regulations. It is interesting to note that most of the areas with high rain rates lie at low latitudes.

Most satellites in geostationary orbit are powered by solar cells. Twice a year, for periods of about 44 days centered on each of the equinoxes, they pass through the shadow of the earth every night. This eclipse lasts only a few minutes at the beginning and end of the eclipse period, but increases to a maximum of 72 minutes on the equinoxes themselves. During these times, the satellite is without solar power and therefore inoperative unless it carries enough batteries. For high-powered satellites, such as are usually assumed for direct-to-the-home broadcasting, this could be an excessive burden. The eclipse is centered on midnight local time at the subsatellite point. By "eclipse protection" is meant a satellite position sufficiently west of the service area so that the eclipse will not occur during the time considered essential for providing services. For direct-to-the-home broadcasting, eclipse protection is usually interpreted to mean that the eclipse should occur no earlier than one a. m. in the time zone of the service area. While the eclipse is not a geographical feature, it does impose serious restrictions on the service area if protection is required, decreasing it to less than half of what it would be otherwise. It thus combines with the geographical features in affecting spectrum-orbit utilization.

Figures 3 and 4 show the service arcs of some likely service areas in North, South, and Central America for elevation angles of 10 degrees and, whenever possible, also for 20 and 40 degrees without regard to eclipse protection.

6. Effect of Latitude

For a single receiver located at a given point and for an assumed minimum elevation angle, the length of the service arc is a function of latitude only. Figure 5 shows the length of service arc for such a point as a function of latitude for elevation angles of zero, ten, twenty, thirty, and forty degrees. For an area that is narrow in latitude, so that all of its points are approximately at the same latitude, this length will be decreased by the difference in longitude between its easternmost and westernmost points. The curves of Figure 5 clearly show how the service arc decreases with latitude, slowly at first, and then with increasing rapidity at higher latitudes. They also show the severe restrictions on elevation angles at the higher latitudes.

7. Effects of Size and Shape

The service arc of an extended area of irregular shape is determined by the latitudes and longitudes of the two points on the boundary of the area at which the elevation angle first falls below the given minimum value as the satellite moves east or west, as the case may be. These points frequently are not obvious by inspection and must be determined by trial and error or by graphical means. In general, the larger the service area, the smaller its service arc other things remaining equal. For example, the service arc of Brazil, a very large country, is about 83 degrees at 20 degrees elevation angle, while that of the much smaller Paraguay, which is at about the same latitude, is about 108 degrees.

As far as shape is concerned, a long narrow area has a smaller service arc than a roughly circular one of the same size. However, for long areas that are not roughly parallel to a line of latitude, the most extreme latitude is usually more important than its length.

8. Orthogonal Polarization

The discrimination obtainable between two crosspolarized beams depends on two geographical features: the climate (which determines the rain statistics) and the relative locations of the areas served by the beams. Depolarization caused by rain is an important effect with both linear and circular polarization. The variation of the received polarization angle with latitude and longitude, which may or may not significant depending on the antenna characteristics, is present only with linear polarization. Both these effects are discussed in detail in a report by the Consultative Committee on International Radio (CCIR)$^{(3)}$.

9. Earth-Station Antenna Discrimination

The effect of geography on the earth-station antenna discrimination is a minor one. It comes about because of the variation of the ratio of topocentric to geocentric angle with latitude and relative longitude. This ratio varies from a maximum of 1.18 at locations near the subsatellite point and for geocentric angles less than about 15 degrees to a minimum of 0.99 at locations near the edges of the field of view of the satellite or for geocentric angles near 90 degrees. At locations in the United States and for geocentric angles that are not too big, the value of 1.1 is a good approximation. While the variations are small, they may be significant because, in some regions of the antenna patterns, the discrimination varies rapidly with off-axis angle.

10. Satellite Antenna Discrimination

Of the three techniques that make frequency reuse possible, the satellite antenna discrimination is the one most dependent on geographical factors, namely the separation of service areas.

The discrimination obtainable from the satellite antenna depends on its gain pattern. In the absence of specific information about the actual antennas, the CCIR, the technical arm of the ITU, recommends two reference patterns, one for the FSS and one for the BSS. These two patterns are shown in Figure 6. It is seen that the sidelobe envelope of the BSS pattern lies ten decibels below that of the FSS pattern, except at very large off-axis angles. The reason for this is not some fundamental difference between BSS and FSS satellites, but rather the different times of adoption. The FSS pattern was adopted in 1974 and has not been changed since then. The BSS pattern was adopted in 1977 and reflects the advances in technology in the intervening years. Because of that, the BSS pattern has been used in all computations made here. The results will change when shaped beams and sidelobe reduction techniques now under intensive investigation are incorporated into future systems.

According to the BSS reference pattern, the maximum discrimination obtainable is the on-axis gain. This can be as high as 49 dB for a very small beam about 0.6 degrees wide between 3-dB points, or as low as 32 dB for a large beam of about 3.5-degree width. A value of 35 dB is frequently used for the required single-entry protection ratio, corresponding to a total protection ratio, considering the combined interference from all other satellite systems, of about 31 dB. The value of 35 dB is reached, if at all, at a point about five beamwidths away from beam center. Hence, frequency reuse from the same satellite, or from colocated satellites, is possible provided that the satellite beams are no wider than about three degrees and that the separation between areas using the same frequencies is at least five beamwidths. Such service areas cannot easily be found within the United States, or even within the combined areas of the United States and Canada, under reasonable assumptions. But such areas do exist in the combined areas of North, Central, and South America. (These results apply strictly only to homogeneous systems, but they are valid approximately in non-homogeneous systems also as long as the non-homogeneities are not too great.)

However, substantial values of discrimination from the satellite antenna are available at points with much smaller separations. The antenna pattern used has a plateau that gives a discrimination of 30 dB at points that are between 1.6 and 3.2 beamwidths away from beam center. Thus, very little additional discrimination is required to make frequency reuse possible. This additional discrimination can be obtained from the earth-station antenna when the two areas are served by two different satellites. The separation required between the two satellites depends on the additional discrimination required.

To show this in more detail, the separation angles required between pairs of satellites of four different systems have been computed for coincident service areas and for service areas separated by 1.6 beamwidths. To compute these angles, it was assumed that the relevant parameters of the four systems are those listed in Table 1; that the frequency is 12 GHz; that the BSS earth-station receiving antennas have the characteristics adopted by the 77 WARC-BS for Region 2; that the FSS earth-station receiving antennas follow the CCIR reference sidelobe pattern (gain = 32 - 25 log θ, where the gain is in decibels and the off-axis angle θ is in degrees); that this last reference pattern is valid for angles smaller than one degree, contrary to the CCIR recommendations; that the required protection ratio is 35 dB for the BSS and 32 dB for the FSS; that the BSS reference pattern of Figure 6 is valid for the FSS as well as the BSS; and that the ratio of topocentric to geocentric angle is 1.1 in all cases. Furthermore, 0.2 degrees were added to all separation angles to acoount for a station-keeping tolerance of 0.1 degrees for satellites, and possible differences in center frequencies and bandwidths used by the various systems were ignored, i. e., it was assumed that all interfering power from one (and only one) system was received by the other. For a service-area separation of 1.6 beamwidths, the discrimination was taken to be 27 dB, the difference between the 30-dB discrimination from the satellite antenna and the 3-dB gain reduction of a receiver at the edge of its service area. The resulting separation angles are listed in Table 2. It is seen that the effect of area separation is dramatic.

For adjacent service areas, the beam coverages usually overlap. In that case, the satellite antenna discrimination may be negative at some points. For then it is possible for a receiver that is located at or near the edge of its own service area to be on a higher gain contour of the interfering beam than of its own. Then the values of the required satellite separation angles may be substantially larger than those listed in Table 2 for coincident service areas.

Table 1. Typical System Parameters.

	System	Antenna diameter m	Satellite EIRP dBw
1	BSS, indiv. recep.	1.0	64
2	BSS, commu. recep.	1.8	56
3	FSS, high capacity	7.0	52
4	FSS, low capacity	4.5	46

Table 2. Satellite Spacing Required (Degrees).

Interfering Systems	Separation of Service Areas	
	Coincident	1.6 Beamwidths
1 and 1	19.0	1.8
1 and 2	18.3	1.7
1 and 3	6.4	0.7
1 and 4	14.0	1.3
2 and 2	8.9	0.9
2 and 3	6.2	0.7
2 and 4	6.8	0.8
3 and 3	2.0	0.4
3 and 4	4.8	0.6
4 and 4	2.8	0.4

11. Features of Region 2

The two outstanding geographical features of ITU Region 2, from the viewpoint of spectrum-orbit utilization, are its isolation from the other two Regions and its natural subdivision into three subregions.

The three ITU Regions are shown on a world map in Figure 7. It may be seen that the boundaries of Region 2, both on the east and on the west, are entirely over water. And, with the exception of Iceland and eastern Siberia, there are no significant inhabited land masses outside the boundaries and close to them. Furthermore, both the eastern and the western boundaries run in a generally north-south direction. These features greatly reduce the interaction between services in Region 2 and services in Regions 1 and 3. With the satellite-antenna gain patterns used here, a separation of 1.6 beamwidths (where a discrimination of 30 dB is reached) seems to be a reasonable criterion for "strong" interactions. With that definition, only three areas in Region 2 can have strong interactions with areas in Regions 1 or 3: Alaska and eastern Siberia, Greenland and Iceland, and eastern Brazil and western Africa.

Also, there is comparatively little overlap of the service arcs of Region 2 and those of Regions 1 and 3. On the east, the arc from about zero to forty degrees west longitude is useful for many countries both in South America and in Africa and Europe. In fact, this potential conflict was explicitly recognized by the 77 WARC-BS and resulted in some special provisions of its Final Acts. On the west, the overlap between the service arcs of Alaska and those of eastern Siberia, New Zealand, and some parts of Australasia do not appear to be significant. Thus, as may be seen from Figures 3 and 4, in most of the arc useful to Region 2, satellites can be placed with almost complete disregard of the interactions with the satellites serving Regions 1 and 3. No similar features exist to isolate Regions 1 and 3 from each other. In fact, from the point of view of spectrum-orbit utilization, they must be considered as a single region.

Figure 8 shows a possible coverage pattern for Region 2 in which the medium-size and the large countries are covered by single beams and the smaller countries are grouped together (without regard to political alliances) and covered by regional beams. The obvious subdivision into three subregions is evident. It is the same as that recognized by common nomenclature: South America, Central America, and North America. Greenland, which is part of Region 2, is not formally part of North America, but geographically it is an appendage thereof. The relative independence of North and South America is based on the geographical fact that no service area in either one of these two subregions is less than 1.6 beamwidths away from any beam center in the other. On the other hand, the service areas of Central America have "strong" interactions with either North or South America or both. But these service areas are comparatively small and lie at low latitudes, so that their service arcs include portions that are useful to the countries of North and South America only marginally or not at all.

Figure 9 shows another coverage pattern for Region 2 in which no two countries are covered by the same beam and the larger countries are covered by many beams. The conclusions arrived at above will hold a fortiori for the smaller beams of this case.

Another feature of the division into subregions is the geographical fact that most of South America lies entirely to the east of most of North and Central America. While the east-west separation between South America and the rest of Region 2 is not as pronounced as the north-south separation, it does lead to the existence of a portion of the orbital arc (east of about 40 degrees west longitude, the very same portion that is also useful to some countries in Region 1) that is useful to South America, but not to North America. However, considerations of eclipse protection will make the eastern portions of their service arcs less attractive to the countries of South America. All this is made less important by the fact that all countries of South America, because of their size or latitude, have comparatively large service arcs.

12. Consequences

One of the consequences of these features is that Region 2 on the one hand and Regions 1 and 3 on the other can use different approaches to planning if they so desire, as in fact they have done at the 77 WARC-BS for the BSS at 12 GHz. Another consequence is that planning services both in the FSS and the BSS for North and South America can proceed relatively independently. But planning for Central America must be coordinated closely with both North and South America, and vice versa.

As was pointed out before, the same satellite (or colocated satellites) can provide services at the same frequencies to areas that are separated by about five beamwidths or more. Figure 7 shows that no two service areas in Region 2 are separated by angles as big as that with the large beams used in that example. With the smaller beams assumed in Figure 9, there are two South American service areas (southern Chile and southern Argentina) that are sepseparated sufficiently from all of the US and Canada to allow colocated satellites. Some Canadian service areas and Alaska could be paired with many more South American ones for colocation of satellites. But it is unlikely that there will be satellites providing services exclusively to these northernmost regions without also having beams covering more southern areas. On the other hand, practically all of the South American service areas are separated sufficiently from the US and Canada to allow satellite spacings of 1.5 degrees or less. Considering the satellite spacings of 6 degrees adopted by the 77 WARC-BS for the broadcasting satellites of Regions 1 and 3, and recalling the spacings listed in Table 2, which give very small values only for the unrealistic cases of exclusive use of very large earth-station antennas, satellite spacings of less than four degrees are not likely to be useful in any subregion. Thus, even though colocation of satellites will be possible only in exceptional cases, the satellites serving North and South America can generally be interspersed without compromising the freedom of planning for either subregion.

It must be emphasized that the specific results given are based on the antenna patterns adopted by the 77 WARC-BS. The use of shaped beams and sidelobe reduction techniques would increase the relative independence of subregions and extend the applicability of the results to many portions of Central America.

13. References

1. "Orbit-Spectrum Sharing between the Fixed-Satellite and Broadcasting-Satellite Services with Applications to 12 GHz Domestic Systems" by Edward E. Reinhart. R-1463-NASA, May 1974, The Rand Corporation, Santa Monica, California 90406.

2. ITU, Broadcasting Satellite Conference, Final Acts, Geneva 1977.

3. "Factors to be Considered in the Choice of Polarization for Planning the Broadcasting-Satellite Service", CCIR Report 814, Geneva 1978.

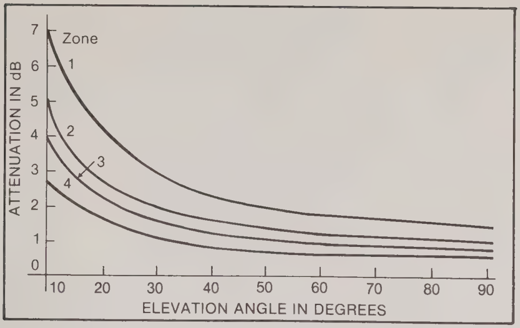

Figure 1. Predicted Attenuation Exceeded for not More than 1% of the Worst Month at 12 GHz.

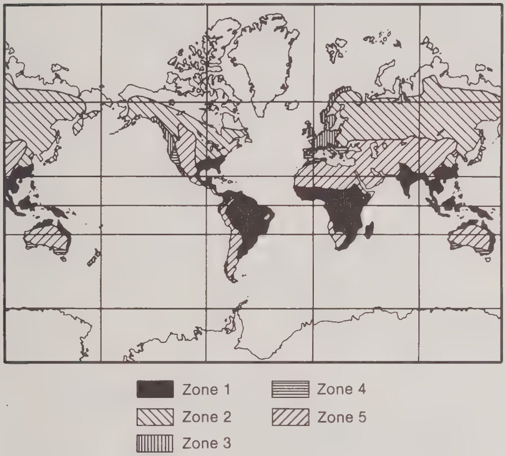
Zone 1
Zone 2
Zone 3
Zone 4
Zone 5

Figure 2. Rain-Climatic Zones of the World.

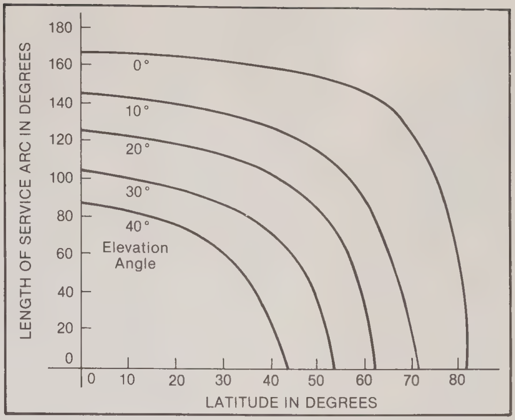

Figure 5. Service Arc of Single Receiver.

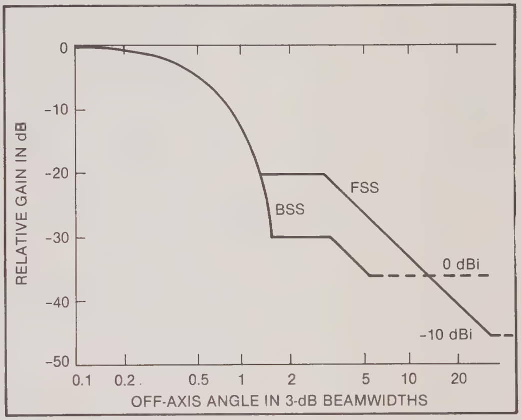

Figure 6. CCIR Antenna Patterns.

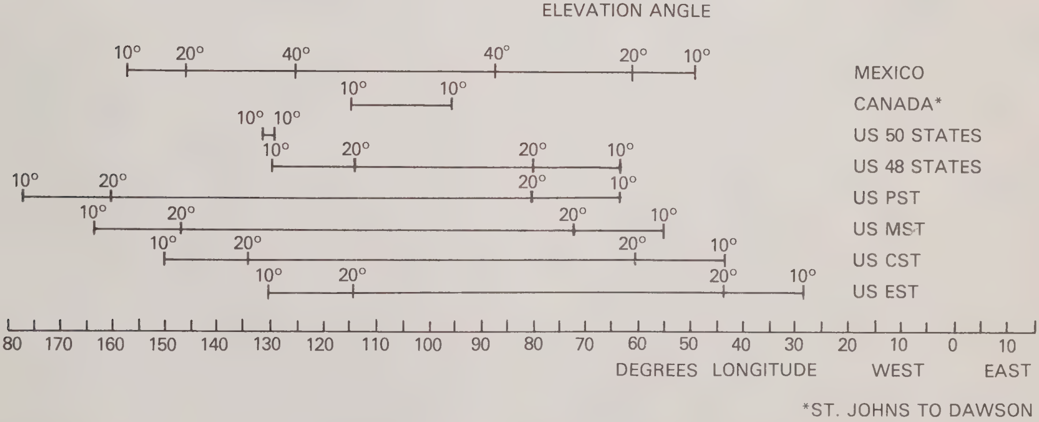

Figure 3. Service Arcs for North America.

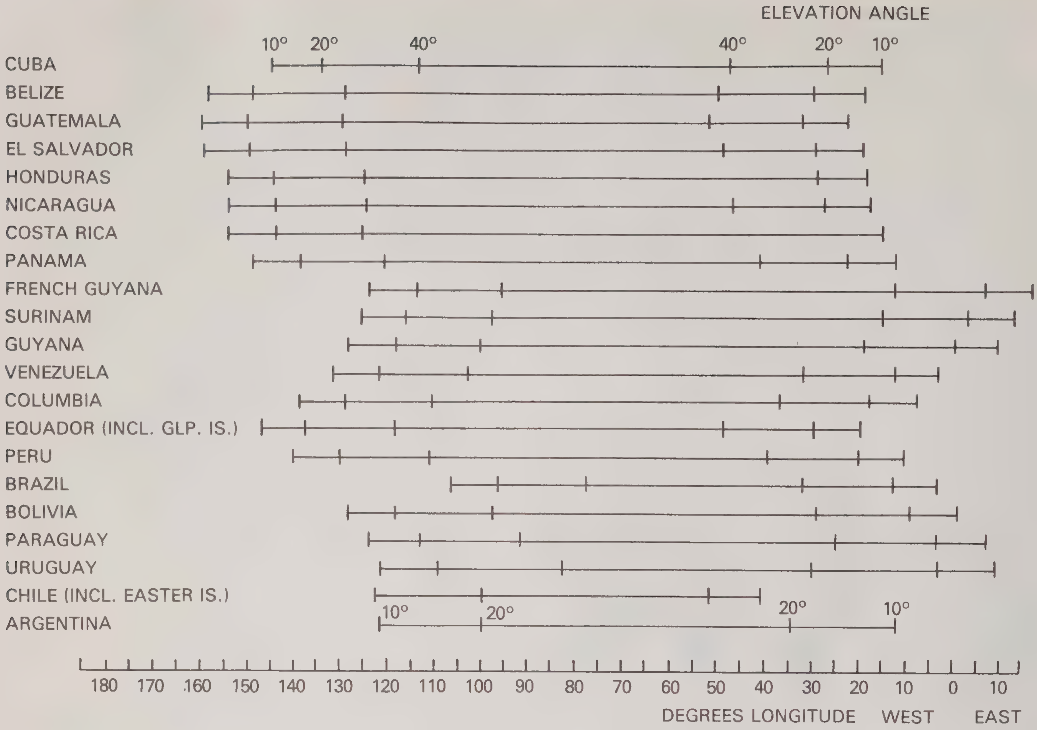

Figure 4. Service Arcs for South and Central America.

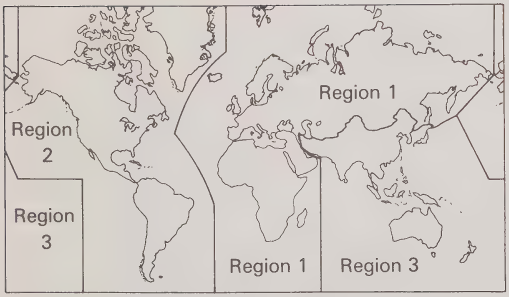
Region 1
Region 2
Region 3
Region 1
Region 3

Figure 7. ITU Regions of the World.

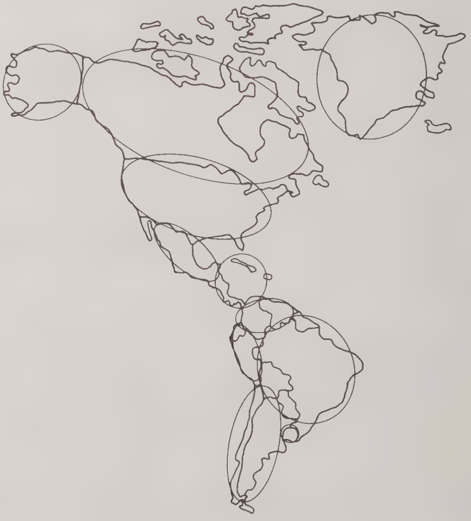

Figure 8. Large-Beam Coverage of Region 2.

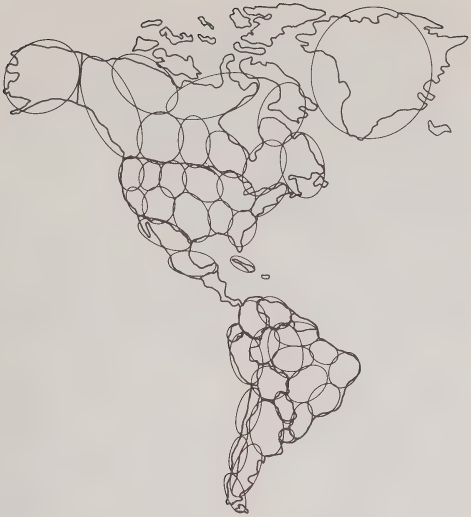

Figure 9. Small-BeamCoverage of Region 2.

80-0510

IN-ORBIT MEASUREMENTS OF OTS PAYLOAD PERFORMANCE

C.D. Hughes
Head of Earth Segment and In-orbit Testing
and
R.A. Gough
Principal In-orbit Test Engineer
Communications Satellite Department, European Space Agency,
Noordwijk, The Netherlands.

Abstract

An extensive programme of tests and demonstrations have been carried out using the European Orbital Test Satellite (OTS) which has been in operation for nearly two years. The paper describes and gives results of the radio frequency measurements of the OTS payload made by ESA from the ground, which form part of the overall test programme. The results agree well with pre-launch measurements and show good operation of the spacecraft hardware. The techniques employed for measurement are discussed and conclusions drawn concerning methods to be employed for future missions.

1. Introduction

On May 11th 1978 the European Space Agency's Orbital Test Satellite (OTS) was launched from Cape Kennedy. The satellite was placed in geostationary orbit by the Agency's operations control centre in Germany on May 16th. As its name implies the OTS is a test satellite. It was built to verify the spacecraft technology and communications system design needed for ECS, (European Communication Satellite [1]),the operational satellite system for Europe in the eighties

The test programme for OTS is a comprehensive plan which covers basic measurements of in-orbit hardware performance, radio frequency measurements of the payload, transmission tests using high speed digital signals and television test signals, propagation tests and pre-operational traffic.

This paper describes the radio frequency measurements of the satellite payload which were undertaken by ESA and gives detailed information on the results obtained, the problems encountered and the techniques used to overcome them.

Before dealing with the tests themselves it is necessary to gain an understanding of the satellite payload and the earth station network employed by ESA for the measurements. These will now be described in outline.

2. The OTS Payload

A simplified block diagram of the satellite payload is shown in figure 1. The OTS payload is divided into two major functional areas. Module A which has four channels, two of 40 MHz bandwidth and two of 120 MHz bandwidth, and module B which has two channels each having a nominal bandwidth of 10 MHz. All channels are arranged in frequency re-use pairs, the up path signals being in the 14 GHz frequency band and the down path signals being in the 11 GHz frequency band. The module A channels employ orthogonal linear polarisations and the module B channels employ orthogonal circular polarisations. The module A signals are received on redundant dual linear polarised antennas having a wide elliptical "Eurobeam A" coverage. The transmit antennas of module A provide a "Eurobeam A" coverage for the 40 MHz channels and a "spot beam" coverage for the 120 MHz channels. There are two antennas in module B of the payload, one transmit and one receive, each of which handles both senses of circular polarisation and has "Eurobeam B" coverage. The coverage of the antennas is shown in Figure 2.

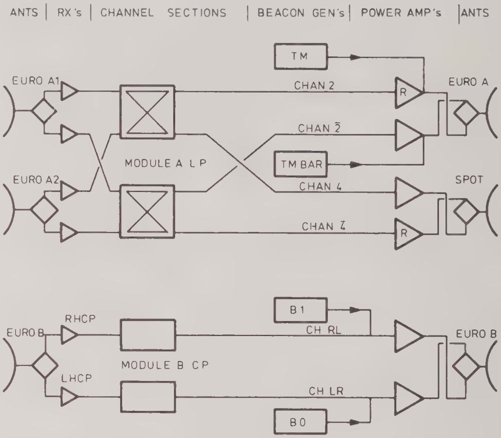

R=FULLY REDUNDENT RL=RHCP TO LHCP AND VICE VERSA
$\bar{2}$=OPPOSITE POLARISATION OF CHAN 2 ETC

FIG1 SIMPLIFIED BLOCK DIAGRAM OF OTS PAYLOAD

In addition to the repeaters described above OTS radiates two on board generated beacon signals. A linearly polarised beacon (TM) is associated with the output section of the 40 MHz channels. The module B radiates a circularly polarised beacon signal (Bo). Both beacons have back-up units which can radiate on the opposite sense of polarisation. These are called $\overline{TM}$ and B1 respectively. Figure 3 shows the frequency plan of the OTS with channels and beacon signals in their correct relative position. A more detailed description of the OTS payload is given by Wearmouth [2].

Copyright © American Institute of Aeronautics and Astronautics, Inc., 1980. All rights reserved.

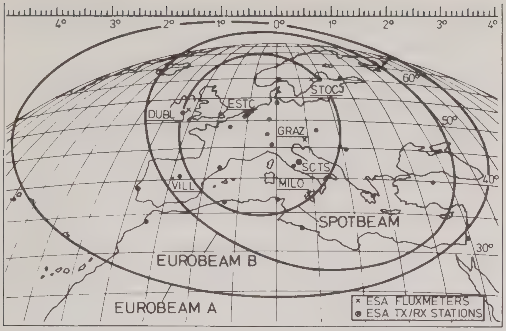

FIG 2 NOMINAL 4dB COVERAGE OF OTS ANTENNAS

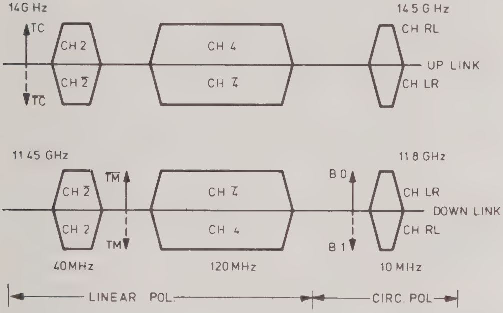

FIG 3 FREQUENCY PLAN OF OTS

3. The Earth Station Network

The OTS earth station network is quite extensive ^{3}. The outline description here is limited to ESA facilities used for the tests described. ESA's principal measurement station has been the Satellite Control and Test Station (SCTS) jointly procured by ESA and Telespazio and located at Fucino, 200 km's from Rome. SCTS can access all elements of the Satellite payload. It was designed to carry out payload tests, a wide range of communications tests, and propagation measurements. The station has two antennas with associated equipment, the larger being linearly polarised and having a G/T of 39 dB/K with three 2 KW transmitters and the smaller being circularly polarised and having a G/T of 24 dB/K with two TWT transmitters of 140 Watts and 15 Watts respectively. Both the antennas are dual polarised in receive and transmit directions.

In view of its key role within the measurement programme the gain of the 17m SCTS antenna was measured as accurately as possible before the launch of OTS using radio star techniques. The conventional "star ratio" technique could not be employed due to the comparatively low excess noise available. A radiometer technique using a Dicke switch was therefore adopted. Using this technique ^{4} the antenna gain was measured using a number of sources in different parts of the coverage to an estimated accuracy of ± 0.3 dB at a number of frequencies in the frequency band 11.45 to 11.7 GHz. The results obtained were very close to those measured using a calibration source on a mountain at 20 km's distance from the station which gave good confidence in the results. Based on these preliminary measurements it was possible later on to measure the flux arriving at the earths surface from OTS and to transmit known eirp's to the satellite.

The SCTS contains an extensive measurement and data logging system which can be connected to the intermediate and radio frequency interfaces of the station in both the transmit and receive directions. This measurement set was constructed from standard test equipment together with a number of specially built facilities. The measurement set provided the means to carry out the various payload tests described hereafter and in its routine configuration automatically measured and stored long term satellite data on magnetic tape, (e.g. beacon frequency/amplitude, crosspolar ratio etc..)

Due to its geographical position the SCTS could only make measurements close to the centre of the OTS coverage zone. To supplement the measurements possible from SCTS, four receive-only flux measurement earth stations (flux meters) were installed around the 4 dB contour of the OTS spot beam coverage. The stations were located at Stockholm (Sweden), Dublin (Ireland), Villafranca (Spain) and Milo (Sicily). The target accuracy of flux measurement using these stations was ± 0.4 dB absolute. Considerable care was taken to accurately calibrate the antennas, and pilot comparison techniques were used in the receivers to refer all measurements to known standards. However, although the long term stability was very good, an absolute accuracy of better than ± 0.8 dB was never obtained. This problem was solved by using the satellite pitch and roll biases to point the spot beam directly at each station in turn and to thereby refer all measurements to the SCTS antenna calibrations.

A small transmit/receive earth staion was installed at ESTEC (The Netherlands) which was used as a general purpose test instrument. The station can measure flux and crosspolar discrimination in any of the OTS channels. It can also radiate signals of accurately known e.i.r.p. towards the satellite on orthogonal polarisations for measurement of up-path cross polar discrimination. A radiometer was installed adjacent to each of the stations in the ESA network to enable the effects of atmospheric attenuation to be measured and calibrated out. Figure 2 shows the location of the ESA earth stations.

4. The Payload Tests

This section covers the payload activation tests, measurements of satellite G/T, input power flux density for saturation (IPFD), satellite saturated eirp, Amplitude/frequency response of repeaters, Group delay/frequency response of repeaters, Gain stability of repeaters, Antenna tests and other payload tests.

4.1 Payload Activation and Initial Test Sequences

The SCTS locked onto the satellite's telemetry beacon whilst OTS was still in drift orbit and it was then possible to transfer tracking, telemetry and telecommand (TTC) from the VHF network to the SCTS at SHF. The TTC functions were then checked and found fully operational.

When the satellite was at a position of 2° E (8° from its station of 10° E) the payload switch-on procedure was started. The procedure was aimed at exercising all elements of the payload including redundant units and making outline performance measurements at each stage of the operation. A total of fifteen configurations were examined during the switch-on sequence, the final configuration being the nominal configuration with all six repeaters plus the beacon signals on. The procedure was executed in ten hours, this time being necessary to allow sufficient telemetry and RF performance data to be obtained for each configuration.

The results of the outline performance measurements showed no significant deviations from the expected results for any of the payload elements with the exception of the levels and frequencies of the two beacon signals, B0 and B1. They were initially 300 KHz high in frequency and 4 dB low in level but reached nominal level and frequency within two hours. It later became clear that this was due to outgassing of the beacon generators.

As an additional part of the initial test sequences the behaviour of the payload was examined with all repeaters fully loaded with representative communications signals. During this "full load" test a number of measurements were made to find the satellite's degree of tolerance in potentially sensitive areas. In particular measurements were made to find the effect of spectrum spreading of the digitally modulated communications carriers on the telecommand and telemetry system of the satellite. Many combinations of signals were applied which simulated the most unfavourable conditions the satellite would meet during its life. In general the satellite was found to be very tolerant to anything the communications earth stations were likely to produce. The only anomaly found was that one of the TWT amplifers switched itself off if rapid overload transients were applied from the ground. This was later traced to an over-sensitive protection circuit in that particular repeater (Channel 4). The problem was obviated in the later testing phases by taking care in the application of signals to Channel 4 from the earth stations.

4.2 Satellite G/T Measurements

A simplified block diagram of the measurement configuration is shown in figure 4. The measurement procedure was as follows :-

a) The repeater section of the satellite was switched off. Power meter 2 then read power proportional to the earth station noise temperature.

b) The satellite repeater section was switched on and the increase in noise power measured by Power meter 2 (ΔP_1) was noted.

c) A continuous wave carrier was then radiated from the earth station through the satellite over a range of known eirp steps. For each step the increase, ΔP_2, in the power meter 2 reading with respect to ΔP_1 was noted.

$$\text{when } \Delta P_2 = \Delta P_1 \; ; \qquad P_{in} = KT_{ss}B \tag{1}$$

where K is Boltzmann constant, T_{ss} is the satellite system noise temperature and B is the equivalent noise bandwidth of the earth station receive filter.

The satellite receive antenna gain, G, can be expressed as :

$$G = \frac{P_{IN}}{P_e} \tag{2}$$

where P_e is the effective power incident upon the antenna.

Combining equations (1) and (2) yields

$$\frac{G}{T_{SS}} = \frac{KB}{P_e} \tag{3}$$

where P_e is the earth station eirp minus the free space path loss and the atmospheric attenuation at the uplink frequency.

The earth station eirp was determined from the readings of power meter 1 and an accurate knowledge of the earth station antenna gain and associated losses. The filter noise bandwidth, B, was accurately measured. The atmospheric attenuation was measured by a radiometer station co-located and pointed in the same direction as the earth station. The atmospheric loss was typically 0.3 dB in clear weather.

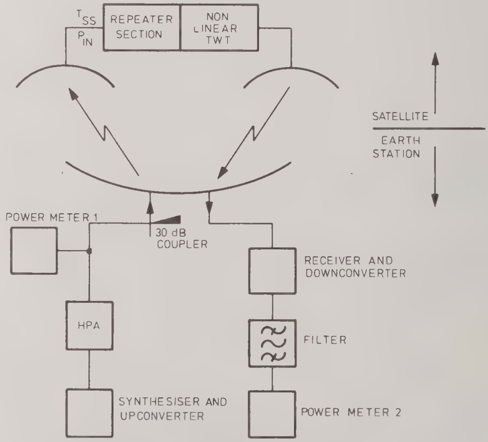

FIG 4 SIMPLIFIED ARRANGEMENT FOR SATELLITE G/T

The following should be noted concerning the measurement technique :

- Absolute measurement of received power is unnecessary. From an error point of view, only relative errors contribute.
- A knowledge of the satellite repeater gain is unnecessary. It is sufficient that the gain does not change during the measurements.
- The accuracy of the measurement is mainly determined by the uncertainty in knowing the earth station eirp which is used to calculate P_e in equation 3.
- For accurate results the satellite noise power, ΔP_1 should be significantly greater (6 dB, say) than the earth station noise. This implies that the repeater be operated at high gain, but care must be taken that the gain is not so high that the TWT operating point enters its nonlinear region.
- The earth station eirp required must be produced with a high carrier-to-noise ratio, hence the use of a coupler and dummy load (effectively a 30 dB attenuator in Fig. 4) with a consequently high value of HPA output power.

The uncertainties in the in-orbit results were calculated as ± 0.6 dB RSS, the largest component being the SCTS eirp. The uncertainty of the pre-launch results is a little higher (± 0.7 dB, RSS,) since the antennas and receivers were measured separately and a calculated value for "earth noise" added. The values of G/T_{SS} obtained are those in the direction of SCTS. There is a small correction (<0.4 dB) to obtain beam-centre values using the off-axis gain loss to SCTS of the satellite receive antennas determined from the measured pre-launch antenna patterns. The results are shown in table 1. As will be seen the results were rather close to the predictions and all are substantially better than specification.

4.3 Input Power Flux Density for Saturation (IPFD)

During Satellite eirp and IPFD measurements it is essential to be able to hold the satellite TWT's exactly at saturation for long periods. In order to ensure that this was achieved for each repeater under test, a technique termed Automatic Satellite Saturation Control (ASSC) was used. This technique is an improvement on earlier methods [5] which only permit measurement rather than maintenance of the saturation point.

The ASSC equipment (developed at ESTEC) was used extensively during the payload testing. The technique operates using an amplitude modulation on the uplink carrier (163 Hz sinusoid with a modulation index < 2%). The downlink modulation is coherently detected and the resulting signal used to control a PIN diode attenuator in the earth station transmit chain. When the satellite repeater chain is at saturation the amplitude modulation is removed from the signal by the re-entrant characteristics of the Satellite TWT, and the output of the coherent detector is zero. Any changes of gain in the up-path elements (earth station Tx chain, antennas, propagation path, satellite repeater) are compensated by this overall earth station-satellite-earth station feedback loop. The results of tests and analysis indicate that saturation is automatically maintained to within ± 0.1 dB in terms of TWT input power. The time constant of the system is of the order of 2 seconds to take account of the 250 mS round trip signal delay. Since the amplitude modulation on the signal is the controlling factor, the system is insensitive to signal level variations on the downlink and to any frequency modulation, such as energy dispersal, which may be applied to the transmitted signal.

The input power flux density for saturation is calculated from the recorded SCTS eirp with the ASSC system in operation taking into account the known free space path loss and the atmospheric attenuation measured by the co-located Radiometer.

Typical IPFD results for the linearly polarised channels are shown in Table 2. The RSS error associated with the in-orbit measurements has been calculated at ± 0.6 dB. The pre-launch values shown are based on separate measurements of antennas and repeater chains, the calculated uncertainty being ± 0.4 dB.

The diurnal stability of IPFD was measured in orbit to be better than ± 0.5 dB for all linearly polarised channels, which was the same as measured during pre-launch thermal vacuum tests. The specification is ± 1.5 dB. The OTS channels RL and LR have no well defined saturation point since the upconverters have been designed to limit just prior to TWT saturation. Thus IPFD is not meaningful for these two repeaters.

Table 1 Satellite G/T (Beam Centre, Midday)

				Measurements (dB/K)				
Satellite				Feb 78	Sept 78		Nov 79	
Ant.	Pol.[b]	Chan.	Spec.	Pre-launch	In-orbit	Δ[a]	In-orbit	Δ[a]
Euro A(1)	H	2	-3	+1.0	+1.4	+0.4	+0.7	-0.3
Euro A(1)	V	2	-3	0	-0.5	-0.5	Not Measured	
Euro A(1)	H	4	-3	+1.1	+1.5	+0.4	+1.4	+0.3
Euro A(1)	V	4	-3	+0.3	-0.3	-0.6	0.0	-0.3
Euro A(2)	H	2	-3	+1.2	+1.1	-0.1	Not Measured	
Euro A(2)	V	2	-3	+0.6	-0.2	-0.8	Not Measured	
Euro A(2)	H	4	-3	+0.9	+1.1	+0.2	+1.4	+0.5
Euro A(2)	V	4	-3	+0.5	-0.5	-1.0	-0.6	-1.1
Euro B	RHCP	RL	-3	+2.6	+3.2	+0.6	Not Measured	
Euro B	LHCP	LR	-3	+2.8	+3.1	+0.3	Not Measured	

(a) Δ refers to pre-launch measurements

(b) H = Horizontal V = Vertical

Table 2 Satellite IPFD (Near Beam Centre, Midday)

Satellite			IPFD(dBWm^{-2})	In-orbit Δ from Pre-launch (dB)			
Ant/RX	Pol.	Chan.	Pre-launch	BOL (b)	Sept 78	May 79	Nov 79
Euro A(1)	H	2M(a)	-80.5	+1.3	+0.9	+0.2	-0.1
Euro A(1)	H	2R	-81.4	+1.4	+1.0	+0.2	+0.1
Euro A(2)	H	2M	-81.3	NM(c)	NM	NM	+1.2
Euro A(2)	H	2R	-81.4	+0.4	+0.4	+0.45	+0.5
Euro A(1)	V	$\bar{2}$	-80.5	+1.4	TWT Failed		
Euro A(1)	H	4	-81.5	+0.2	+0.1	+1.0	+1.7
Euro A(2)	H	4	-81.5	NM	-0.1	+1.3	+2.1
Euro A(1)	V	$\bar{4}$M	-79.5	+0.1	-0.2	+1.2	+1.3
Euro A(1)	V	$\bar{4}$R	-79.3	+0.1	+0.0	+0.6	+1.1
Euro A(2)	V	$\bar{4}$M	-79.5	NM	+0.3	+2.2	+2.4
Euro A(2)	V	$\bar{4}$R	-78.9	NM	NM	NM	+1.4

(a) M = Main TWT, R = Redundant TWT. (b) BOL = Beginning of Life (c) NM = Not Measured.

4.4 Saturated EIRP

The saturated e.i.r.p. of OTS was derived from measurements of received flux at the SCTS and the various fluxmeter stations. The measurements were made over 24 hour periods and continuously recorded together with atmospheric attenuation as measured by the co-located radiometers. The necessary corrections for atmospheric effects (in the range 0.2 to 2.0 dB) and free space path loss were made off-line after the measurement sessions. The ASSC system described in 4.3 was an essential element in these measurements since it maintained the repeaters at saturation in the presence of uplink fading and repeater gain variations. The technique employed for flux measurement involved the use of an accurate and stable pilot signal injected into a calibrated coupler immediately behind the earth station antenna feed against which all received signals were compared. Careful calibration of the earth station antenna gain and associated waveguide losses together with continuous monitoring of the pilot signal level were typical of the precautions taken to achieve sufficient accuracy. As part of this exercise it was discovered that the earth station antennas were themselves subject to gain variations with temperature and these effects also had to be calibrated out. The measurement accuracies achieved were calculated as ± 0.6 dB R.S.S. which compares with ± 0.45 dB for the pre-launch measurements.

Table 3 shows some results of e.i.r.p. measurements made at SCTS during the first 18 months of OTS operation.

At beginning of life the in-orbit measured values were at least 3 dB better than the specified minima and, as can be seen from the table, were in close agreement in every channel with the pre-launch measurements. The TWT amplifier in channel $\bar{2}$ failed about two months after launch. The reasons for the failure are now well understood and corrective action has been taken to prevent a failure of this type in future missions. However, for OTS, this particular channel remains unusable since it has no tube redundancy. Channels 2, 4 and $\bar{4}$ have produced a virtually constant eirp over the 18 month period within the limits of measurement accuracy. The circularly polarised channels RL and LR have shown an eirp degradation since August 1978 of 2 dB and 1.2 dB respectively which, whilst still within specification, is not considered nominal.

Measurements made at all fluxmeter stations confirm the overall situation shown in table 3.

The diurnal variation of eirp has two components; the repeater power output variation and the antenna and satellite attitude effects (e.g beam swing, gain change etc). The repeater output variation was confirmed to be less than 0.1 dB in all channels both from telemetry data and from 24 hour near beam centre eirp measurements. The maximum diurnal variation in the channel 4 and $\bar{4}$ eirp's at the fluxmeter stations was 0.5 dB which corresponds with an East-West beam swing of the spot beam of less than 0.1 degrees (the specified value was 0.2 degrees). The channel 2 (Eurobeam A) swing was also less than 0.1 degrees. The channel RL and LR (Eurobeam B) diurnal variations were higher than expected. These were later confirmed by the in-orbit antenna measurement to be due to about 0.3 degrees swing North-East during the night, coupled with a mean depointing of about 0.5 degrees.

Table 3 Satellite e.i.r.p. (At SCTS, Midday)

Satellite			eirp (dBW)	In-orbit Δ from Pre-launch (dB)				
Chan.	Pol.	Tube[a]	Pre-launch	BOL[b]	Aug 78	Nov 78	May 79	Nov 79
2	V	M	39.1	+0.6	+0.7	NM	(Not Measured)	
2	V	R	39.4	+0.5	+0.7	+0.4	+0.5	+0.7
$\bar{2}$	H	NR	40.3	-0.1	TWTA Failed			
4	V	NR	47.0	+0.2	+0.1	0	+0.5	+0.3
$\bar{4}$	H	M	46.3	+0.2	+0.1	+0.4	+0.8	+0.5
$\bar{4}$	H	R	46.3	NM	+0.2	+0.2	NM	NM
RL	LHCP	NR	42.7	+0.3	+0.3	-1.2	-2.0	-2.0
LR	RHCP	NR	42.6	+0.2	-1.1	-0.8	-1.6	-1.2

(a) M = MainTube R = Redundant Tube NR = No Redundancy (b) BOL = Beginning of life.

4.5 Amplitude/Frequency Response of Repeaters

The method used is based on a conventional swept frequency response technique using a spectrum analyser and associated tracking generator. The main difference between using this method in a laboratory and using it for a satellite in-orbit is that the frequency tracking of the spectrum analyser/tracking generator combination must be offset to take account of the round trip delay of the signal, otherwise an inordinately long time would be needed for a single sweep. Figure 5 shows the arrangement of equipment for the test.

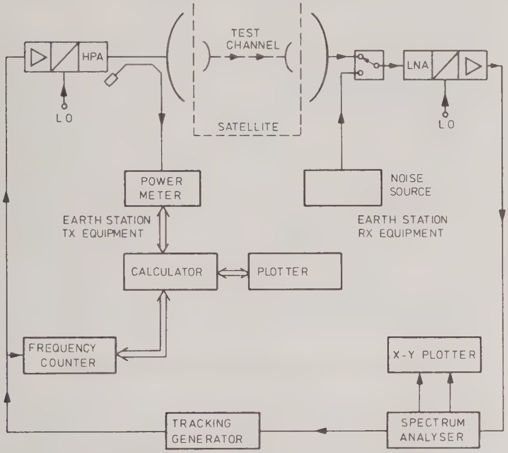

FIG 5 TEST ARRANGEMENT FOR AMPLITUDE / FREQENCY RESPONSE

The calculator, power meter and plotter are only used to determine the frequency response of the SCTS transmit chain, which is a fully automatic procedure controlled by the calculator. The noise diode shown is used to determine the frequency response of the SCTS Receive chain.

The amplitude-frequency response measured via the satellite is not that of the repeater under test alone. The frequency responses of the SCTS transmit and receive chains are also contained in the resulting amplitude-frequency plots, and these must be removed. The earth station transmit chain response is effectively compressed by the repeater under test depending on the satellite tube working point, and to compensate for this effect it was necessary to measure the frequency response of the SCTS transmit and receive chains separately. The receive chain frequency response was directly subtracted from that measured via the satellite. Before subtracting the transmit chain response it was first modified (compressed) according to the operating point of the satellite repeater TWT.

Typical results are shown for in-band responses in Figures 6 and 7, together with the pre-launch test results. The in-orbit and pre-launch results differ slightly for the following reasons :

- The repeaters were tuned slightly low in frequency before launch to compensate for the upward frequency offset in space due to the difference between air and vacuum in the filters.
- The pre-launch results are measured via directional couplers at the input and output of the satellite antenna subsystem. The responses of these couplers have not been removed from the pre-launch results.
- Although the back-to-back frequency response of the test equipment used for the pre-launch measurements was measured, it has not been subtracted from the pre-launch curves shown in Figs. 6 and 7. All amplitude/frequency responses of the repeaters were well within the specification masks.

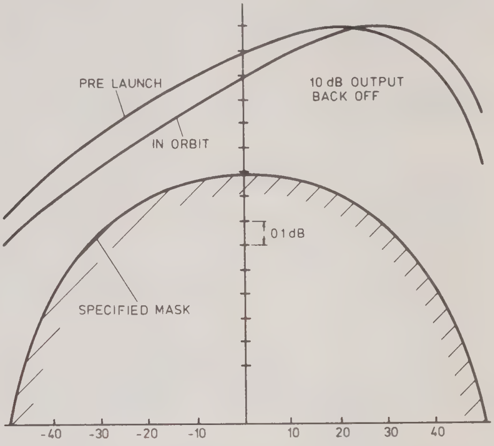

FIG.6 TYPICAL AMPLITUDE / FREQUENCY RESPONSE (CHAN.4)

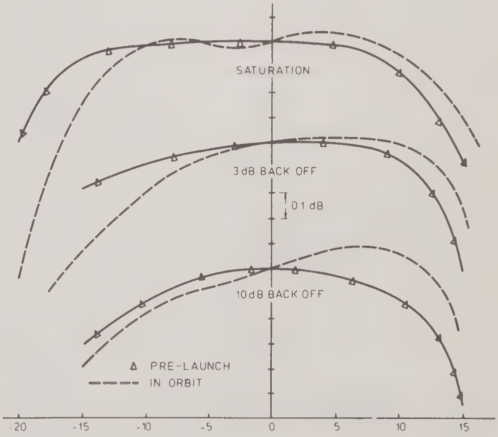

FIG 7 TYPICAL AMPLITUDE / FREQUENCY RESPONSE (CHAN $\overline{2}$)

4.6 Group Delay/Frequency Response of Repeaters

The test method which was used is based on a conventional laboratory technique. If a carrier at frequency f_c is AM modulated by a signal of frequency fm and the composite signal is passed through a device, then the sidebands at frequencies (f_c-f_m) and (f_c+f_m) will experience different phase shifts according to the phase-frequency characteristics of the device. In the time domain this is seen as a phase shift, $\emptyset$, of the envelope of the signal. The phase shift of the envelope can be measured by demodulating the signal from the output of the device and comparing the phase of the resulting sinusoid with the phase of the modulating signal using a vector voltmeter. If the carrier frequency, f_c, is swept over the bandwidth of the device under test then the vector voltmeter display is proportional to the group delay/frequency response of the device. The test arrangement is illustrated in figure 8.

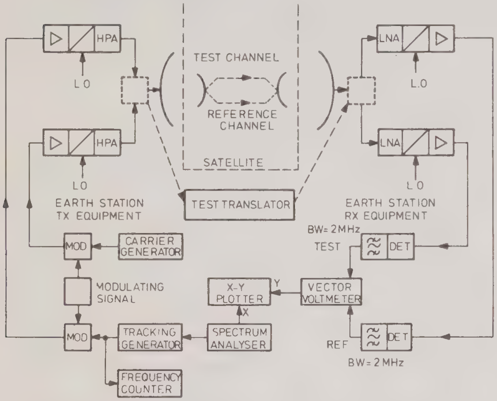

FIG 8 TEST ARRANGEMENT FOR GROUP DELAY / FREQUENCY RESPONSE

In order to elliminate the effects of satellite path length variations an unswept reference channel was established through the satellite on the opposite polarisation. The vector voltmeter therefore compares the phase of the modulation on the unswept reference channel with that on the frequency swept test channel. No frequency offset is required to elimate the effects of loop-round delay because both the reference and the test signals pass through the same path. The effects of the earth station equipment were removed by making an in-station loop measurement using the test translator (which had a very flat group delay response) immediately prior to each satellite loop measurement and subtracting the results.

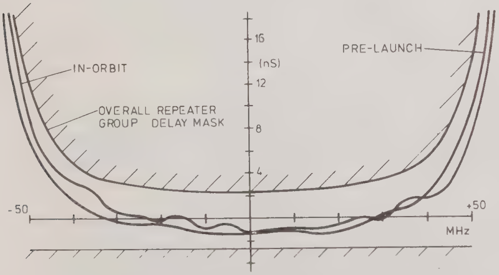

FIG 9 GROUP DELAY / FREQUENCY RESPONSE (CHANNEL 4, 10 dB BACK OFF)

In Figure 9, typical in-orbit results obtained for channel 4 are plotted together with the corresponding pre-launch results inside the specified mask. The frequency offset is due to the pre-launch measurements being made in air, as opposed to vacuum. Figure 10 shows the excellent group delay stability of channel 2 over a 24 hour period which included an eclipse. The full results for all channels are shown by Gough [6]. All of the group delay measurements made showed very good agreement with the pre-launch results and were well within the specified masks.

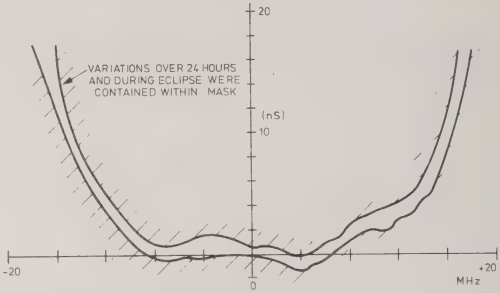

FIG 10 GROUP DELAY / FREQUENCY RESPONSE (CHAN 2)

4.7 Gain and Gain Stability of Repeaters

This test was aimed at checking the linear gains of the OTS repeaters (not including antennas) and the gain stability. It was decided that any attempt to extract the repeater gain directly from measurements of transmitted and received powers would not yield accurate results. Two parameters of the repeaters themselves were therefore used as effective references for the measurement. These were :

- The noise temperature (T_{SS}) at the repeater input, which was known to be relatively stable with time and temperature.
- The saturated power output (P_{SAT}) of each satellite TWT, which could be accurately determined from telemetry data.

The equipment arrangement is as shown for the G/T test (figure 4). The procedure was as follows:

(a) The power produced at the earth station receiver output (power meter 2) by the earth station system noise when the satellite repeater was switched off was measured.

(b) The increase in power (ΔP_1) at the receiver output (power meter 2) which occured when the repeater was switched on was then measured.

(c) The increase in power (ΔP_2) at the earth station receiver output (power meter 2) with respect to (a) when a carrier was transmitted through the repeater to just saturate the satellite TWT was then measured. The ASSC system was employed for this measurement to ensure accurate saturation .

$$\frac{\Delta P_2}{\Delta P_1} = \frac{P_{SAT}}{A\ K\ T_{SS}\ B} \qquad (4)$$

$$A = \frac{P_{SAT}\,\Delta P_1}{K\,T_{SS}\,B\,\Delta P_2} \qquad (5)$$

where A is the linear gain of the repeater, K is Boltzmann's constant, and B is the bandwidth of the measurement system. This relationship applies provided the measurements are all made through the same known filter bandwidth. This was arranged by making the filter shown in figure 5 relatively narrow compared to all other band limiting elements in the system and carefully measuring its noise bandwidth.

The test was carried out over 24 hour periods on all channels to obtain the absolute gain for each channel and the diurnal variation. The test was also conducted during eclipse and the gain variations measured as a result of the eclipse were consistant with the day/night variation measured in the diurnal tests. In general the results measured for absolute gain were within 0.5 dB of the expected values. However, there was one inconsistancy on channel 2 of the satellite which yielded a result 2 dB higher than expected. This is not yet understood.

The total gain variation of the repeaters was less than 0.5 dB diurnally and during eclipse. The specified value for the satellite was ± 1.5 dB.

4.8 Antenna Tests

Extensive measurements were made of the OTS antenna performances in orbit as part of the test programme. The objectives were to characterise the antennas in terms of gain, polarisation purity, relative polarisation alignment and pointing accuracy over the widest possible sector of the coverage. The results were then used to confirm the performance of the antenna subsystem predicted from pre-launch measurements of the individual antennas.

The measurements were made in both hot (nightime) and cold (daytime) conditions to assess the effects of the 190 degree centigrade diurnal temperature change which occurs in orbit.

In addition to making measurements at nominal satellite attitude, the attitude was varied under ground control over ± 2 degrees in pitch and roll whilst making time-referenced measurements of the signals received at widely separated earth stations in Western Europe. The ASSC system described in section 4.3 was essential for these tests to continuously hold the repeaters at saturation. The large quantity of data collected was later processed off-line together with the telemetered satellite pointing information to synthesise the desired contour plots.

To simplify and shorten the presentation of the results only the worst figures measured from each class of test are shown below. The detailed techniques and complete results are given by Brain [7,8].

OTS Receive Antennas (3 antennas, 2 ports per antenna).

Gains

Margin with respect to Specification: At least 1dB.
Maximum difference between pre-launch and in-orbit measurement : 0.9 dB
Maximum change between hot and cold conditions : 0.5 dB

Pointing

Specification : 0.2 deg.
Measured maximum depointing : 0.2 deg.
Measured maximum swing (day/night): 0.09 deg.

Beamshape

As predicted and within specification.

Crosspolar Isolation

Worst value within 3 dB coverage : 26 dB
(for Eurobeam B receive)

OTS Transmit Antennas (3 antennas, 2 ports per antenna).

Gains

Margin with respect to Specification

Eurobeam A : At least 1.8 dB
Eurobeam B : At least 0.2 dB
Spotbeam : At least 0.1 dB

Maximum difference between pre-launch and in-orbit measurements : 1.3 dB

Pointing

Specification : 0.2 deg.
Maximum measured depointing
Eurobeam A : 0.1 deg.
Eurobeam B : 0.5 deg.
Spotbeam : 0.2 deg.

Maximum measured swing (day/night)
Eurobeam A : 0.1 deg.
Eurobeam B : 0.3 deg.
Spotbeam : 0.1 deg.

Beamshape

As predicted and within specification.

Crosspolar Isolation

Greater than 30 dB within the 3 dB coverage.

All measured in-orbit performances were nominal except those for the Eurobeam B transmit antenna which showed lower than expected gain (-1.3 dB during antenna tests), greater than expected depointing (0.5 deg. South) and greater than expected beam swing (0.3 deg.). This evidence, coupled with the degrading e.i.r.p. from both ports of this antenna (See Table 3) and the results of subsequent special investigative tests has led to the conclusion that this particular antenna was mechanically damaged, possibly during satellite launch. However, given the available system margins there is no immediate impact on the mission requirements of the circularly polarised section of the satellite.

Figures 11 and 12 show co- and cross-polar isolation contours, respectively, for the spotbeam antenna synthesised from measurements made at one of the earth stations during the antenna tests, and are typical of the results obtained [7,8].

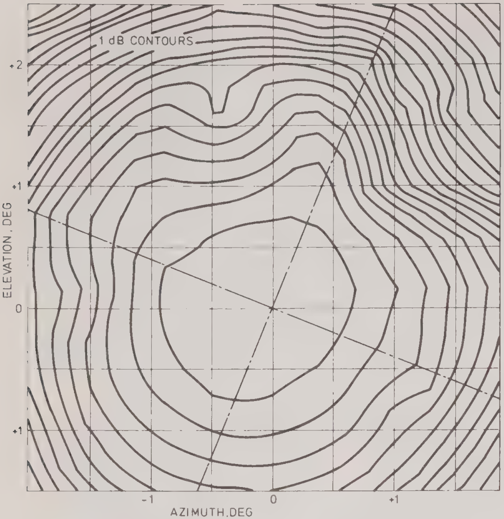

FIG 11 SPOT BEAM CO-POLAR PLOT TAKEN FROM ESTEC STATION

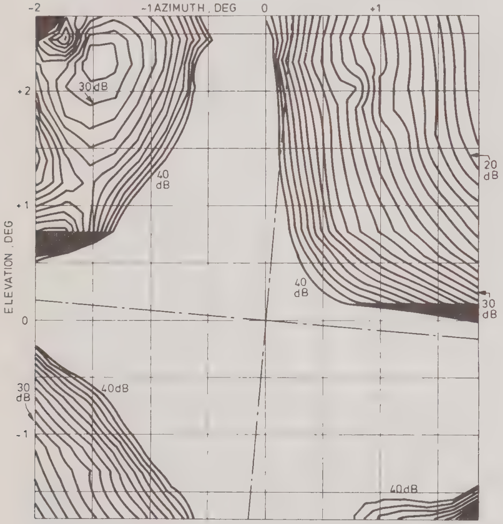

FIG.12 SPOTBEAM X POLAR PLOT TAKEN FROM ESTEC STATION

4.9 Other Payload Tests

There have been a large number of other in-orbit payload measurements made with OTS. These include: Beacon frequency and amplitude stability, checking of the on board gain adjustment ranges, checking for spurious outputs, measurement of translation frequency stability etc [6]. All these measurements have shown performances substantially within the satellite specifications and in close agreement with the pre-launch results.

Many of these measurements are recorded continuously by the ESA earth stations for later analysis. In particular, much of these data are currently being analysed to produce propagation statistics at 11 and 14 GHz for the European Area.

5. Conclusions

A number of useful lessons and techniques have been identified which can be applied to the in-orbit testing of the future ECS satellites as they are brought into service.
The most notable among these are :-

a) The OTS measurements have shown that it is very difficult to make reliable measurements of absolute flux from the satellite at widely spaced points on the earth's surface. This difficulty was overcome in the OTS measurements by swinging the satellite attitude to each measuring station in turn and referring all calibrations to a large antenna which could be accurately checked with radio stars. This would not be desirable in an operational system since it takes time and also implies a certain risk to the satellite. Future flux measuring stations would therefore be made smaller and readily transportable enabling a central calibration of all stations against a good reference before dispersing them.

b) It was possible to carry out very extensive in orbit antenna measurements with OTS because it was a test satellite. This is not recommended for operational satellites due to the different nature of the ground facilities and the time required. However, limited measurements at critical points in the coverage should be made.

c) It is very important to measure the satellite parameters before launch in a manner which can be directly related to in-orbit measurements so that a direct comparison can be made at the most critical and sensitive points.

d) The ASSC technique for maintaining the satellite tubes at saturation during in-orbit tests has proved very valuable and many of the tests could not have been done with reasonable accuracy without it.

e) For an operational system it is important to have the satellites in service as soon as possible. The in-orbit tests for ECS will also form part of the satellite acceptance from the manufacturer and subsequent handover to the users. The testing will be concentrated into a much shorter time period and will have more serious contractual significance than was the case with the test satellite. The basic test techniques which have been described will be retained but the procedures will be streamlined and further automated. In particular for OTS much of the test data was analysed off-line from the raw measurements. In the case of ECS, on-the-spot immediate analysis of the results and comparison with preflight data will be maximised.

The measurements made have shown very satisfactory performance of all payload elements of the OTS with the exception of one TWT amplifier which failed a few months after launch and one of the antennas which appears to have suffered mechanical damage.

The tests conducted cover the most important aspects of payload performance in orbit and show that basic OTS technology is suitable for inclusion in the operational ECS satellites which will follow.

Acknowledgement

The authors would like to acknowledge the work of Mr. C. Moens who devised and developed the ASSC system described in this paper and also Mr.D..Brain who devised and executed the antenna tests.

References

1 Bartholome, P.J.,

"European Communications Satellite System"
6th AIAA Conf. on Communications Satellite Systems, April, 1976.

2 Wearmouth, C., McLaurin, D.E.,

"Development of the OTS Satellite"
6th AIAA Conf. on Communications Satellite Systems, April, 1976.

3 Collette, R., Ashford, E.W., Hughes, C.D.,

"OTS's First Year in Orbit"
ESA bulletin No. 19, August, 1979.

4 Hughes, C.D., Baars, J.W.M.,

"Antenna Measurement Techniques at 11 GHz"
IEE Conf. on Satellite Communication Systems Technology, April, 1975.

5 Standing, A.

"A Null Technique for Accurately Determining the Drive Level Required to Saturate a TWT."
Comsat Technical Review, Vol.4, No.2, Fall 1974. P.493.

6 Gough, R.A.,

"Group Delay Measurement"
ESA Report on in-orbit measurements with OTS, Vol. 1, Dec. 1979.

7 Brain, D.J.

"Antenna Patterns"
ESA Report on in-orbit measurements with OTS, Vol.2, Dec. 1979.

8 Brain, D.J.,

"In-orbit Antenna Pattern Measurements on the European Orbital Test Satellite"
IEE Conference on Antennas and Propagation, Nov. 78.

80-0513

OVERVIEW OF DIGITAL SATELLITE COMMUNICATION NETWORKS

Pradman Kaul*
Digital Communications Corporation

ABSTRACT

Commercial satellite communications as we know it today started with the launch of Early Bird (Intelsat 1) in 1965. Most of the satellite networks in the 60's used analog techniques. The early 70's saw the introduction of digital techniques into satellite networks. By the end of the 70's, there has been tremendous increase in the number of implemented and planned digital networks.

This paper presents an overview of a cross section of these networks. It starts off by discussing the first commercial digital network, SPADE, and follows that by describing other networks that are operational or in the process of being implemented today. A number of common carriers both domestically and abroad have put in digital networks in the past few years. These include SBS, American Satellite, Western Union's Advanced Westar System, Telesat Canada, Intelsat, the European domestic system and the French Telecom 1 System. In each case, a brief description of the network is given along with the kind of service offered. Characteristics of the satellite and transmission techniques used are also discussed.

Introduction

Commercial satellite communications, as we know it today, started with Early Bird (Intelsat 1) in 1965. There are now about 40 synchronous communication satellites in orbit with another 50 in various planning and/or implementation stages. Almost all the networks initially used analog techniques for transmission and multiple access. The most common technique used was Frequency Modulation/ Frequency Division Multiple Access (FM/FDMA).

The early 70's saw the beginning of the introduction of digital techniques in satellite networks. The first major digital network was the SPADE system which was implemented by INTELSAT. SPADE is a fully demand assigned single channel per carrier system that is now operational in over 30 countries in the Atlantic Ocean Region.

The last few years have seen a significant increase in the number of digital networks that have been implemented all over the world. In addition, most of the new domestic and international satellite networks are planning on using digital techniques.

The two major multiple access techniques used by all the present digital satellite networks are Single Channel Per Carrier (SCPC)/Frequency Division Multiple Access (FDMA) and Time Division Multiple Access (TDMA).

SCPC/FDMA[1] is a technique where multiple carriers access a transponder at different frequencies. In addition, each carrier contains only one voice or data channel. For example, an analog voice channel could be digitized using Pulse Code Modulation (PCM) or Delta Modulation techniques; the digital stream becomes the input to a Phase Shift Key (PSK) modulator. The IF output of the modulator is the modulated carrier that is transmitted over the satellite. The carrier frequency can be pre-assigned in which case no other carrier could use that particular frequency. An example of such a pre-assigned SCPC/FDMA system is the Telesat Canada thin route network. The carrier frequency can also be assigned on demand. This permits more efficient usage of the transponder but also makes the ground station equipment more expensive. SPADE is an example of this kind of demand assigned SCPC/FDMA system.

TDMA[2] is an effective method of significantly increasing satellite channel capacity and improving satellite system flexibility. As a result, there is increasing worldwide interest in using this technique in newer networks. TDMA is a technique whereby a multiplicity of satellite earth stations share a common transponder by transmitting bursts of carrier signals which arrive at and pass through the transponder in a sequential, non-overlapping mode. Figure 1 shows a pictorial representation of TDMA operation. One earth station acts as reference and transmits periodic bursts without closed loop control. The other stations in the network use closed loop synchronization through the satellite to place burst transmissions within their assigned time slots. A pre-assigned TDMA system has its burst slots fixed for each access. An example of such a system is the Telesat TDMA network. If the burst slots are assigned on demand, the TDMA network becomes like the SBS system. There are low bit rate TDMA networks that use open loop synchronization such as the Marisat system. The power-bandwidth efficiency of TDMA offers attractive increases in current satellite transmission capacities and overall network flexibility.

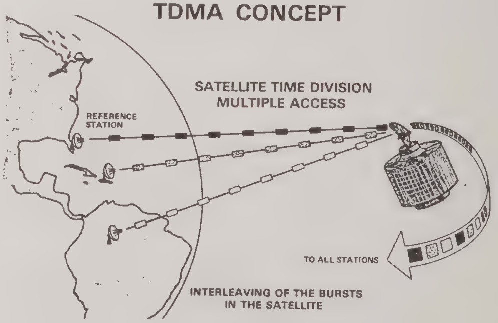
TDMA CONCEPT
SATELLITE TIME DIVISION MULTIPLE ACCESS
REFERENCE STATION
TO ALL STATIONS
INTERLEAVING OF THE BURSTS IN THE SATELLITE

Figure 1.

---

*Group Vice President, Digital Communications Corporation, Gaithersburg, Md.

Copyright © American Institute of Aeronautics and Astronautics, Inc., 1980. All rights reserved.

This paper describes some major digital networks that use the above techniques that have been implemented or are in the process of being implemented. These include the following networks:

- SPADE
- Telesat Thin Route
- Telesat TDMA
- Intelsat TDMA
- SBS
- Advanced Westar SS/TDMA
- American Satellite TDMA
- Eutelsat
- Telecom

SCPC Networks

The SPADE system [1] was the first digital satellite system and also the first system to use demand assignment multiple access (DAMA) capability in satellite communications. Demand assignment serves as a traffic concentrator. It allocates channels on demand to a location that has traffic at that particular instant. This permits each channel to carry more traffic than it could on a pre-assigned basis.

A typical SPADE installation consists of a terrestrial interface unit, voice channel unit, a demand assigned signalling and switching (DASS) unit and an intermediate frequency (IF) subsystem. The system operates with a single voice channel assigned to each RF carrier frequency. PCM is used for digitizing the voice (7 bits per sample) and the carrier modulation scheme used in four phase coherent PSK. System coordination is maintained through a protected common signalling channel employing TDMA. When a call request is received from a local transit center, the DASS unit automatically selects a frequency pair from the pool of available channels and alerts the destination station to the incoming call and frequency channel assignment. This message is transmitted over the CSC channel and all stations receive this message. The DASS units in all stations update a channel table listing the frequencies that are available for calls. When a call is completed, a control signal from the CT allows the DASS unit to return that circuit to the frequency pool for reassignment. The SPADE system has been designed to operate with a variety of signalling and switching systems; the primary one being used is the CCITT no. 5 signalling system.

SPADE has been operational in the INTELSAT system for over 7 years now and is now being used in more than 40 countries. INTELSAT also allows countries to use pre-assigned single channel per carrier (SCPC). This equipment is identical to the SPADE equipment except that its frequency allocation is fixed and therefore, it does not need the DASS unit. The SPADE system is the most complex SCPC network in operation today. It has been extremely successful in commercial use and consequently gave a lot of impetus to the use of digital techniques in satellite communications.

Telesat Canada has been a pioneer in introducing digital techniques into their satellite networks. Their first major digital system was a thin route SCPC system using delta modulation for digitizing the voice signal and PSK for modulating the carrier. Figure 2 shows a pictorial representation of this network. The carriers are on preassigned frequencies and up to sixteen telephone circuits can be carried from a remote location via the main earth station (Allan Park) to the Canadian telephone system. Voice activiation is used on most carriers to increase the system capacity and the equipment is capable of being upgraded to a fully demand assigned system. One of the novel features of this network is the capability to transmit four TTY channels at rates up to 110 baud or a 2400 bps channel simultaneously with the voice service. The earth stations themselves have 4.5 meter antennas and a G/T of 21.7 dB/°K. This SCPC system because of its preassigned operation is more simple than SPADE. In addition, SPADE is a mesh network that allows full interconnectivity between all sites. The Telesat network is a star network, because all remote sites communicate only with the Central site and vice versa.

In the United States there are a number of small private data networks which also use SCPC/FDMA techniques. These handle data generally at bit rates from 56 Kbps to 3 Mbps on a single carrier. American Satellite, Western Union, RCA and ATT have a number of these in operation.

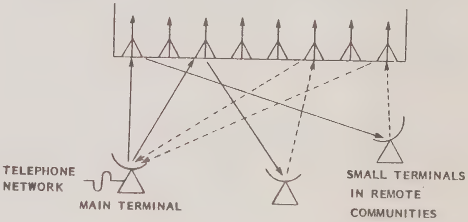

Figure 2.

TDMA Networks

In 1975, Telesat went operational with the first high speed TDMA system in the world [4.5]. This was a two access TDMA system having a capacity of 800 voice channels and carried a part of the traffic from the CANTAT II Trans-Atlantic cable system serving Canada and the U.K. The baseband input to the system was a special 400 channel mastergroup. A PCM codec was used to directly encode this mastergroup. The average noise per voice channel is less than 1200 pico watts. The key features of this system are listed below:

- Transmission rate of 61.248 Mbps
- 250 microsecond frame length
- Use of Rate 3/4 forward acting error coding at 61 Mbps in one link to make up for lower G/T station
- Fully automatic time slot acquisition
- Fully redundant equipment with automatic switchover

This system has been operational for approximately four years and has achieved an availability of better than 99.98% during this period.

Recently, Telesat has announced their 90 Mbps digital service over the Anik C satellite.[6] This is an all digital satellite system that uses the 14/12 GHz bands and frequency re-use by orthrogonal polarization. The Anik C satellites will be placed into service in 1981 and are designed to provide high capacity message and television distribution for the Trans Canada Telephone system.

Each satellite has 16 transponders and a transponder can handle either a 90 Mbps digital stream or 2 FM/FDMA video signals. The principal features of the earth station are listed below:

Antenna Diameter:	8 meters
G/T	35.0 dB/°K
Receiver Front End	Uncooled paramp ($T_A=130^\circ K$)
HPA	1KW Klystrom
Cross polarization Isolation	34.0 dB
Tracking Type:	Step Track

The earth stations achieve a G/T of 35 dB/°K by combining a high efficiency 8 meter antenna with two 100°K low noise amplifiers in a redundant configuration mounted at the feed.

Three system performance objectives have been set. They are:

1.	BER:	10^{-4} for 99.95% of the time 10^{-7} for 99% of the time
2.	Timing Jitter:	3.2 nsec
3.	Short Interruptions:	Max: 4 per day Avg. 2 per day per month

The baseband interface has been chosen to be the DS-3 level and the modulation scheme used is QPSK. This will be the first major TDM network to go operational.

American Satellite Corporation will also use TDMA terminals in their General Services Digital Transmission Network.[7] This will be the first business oriented wideband TDMA network to go into commercial operation, in the United States. Three earth stations located in New York, Los Angeles, and San Francisco have been equipped with the TDMA terminals and operational service will commence in early 1980. The baseband chain will utilize optimized bandwidth voice processors and digital multiplexers. A block diagram of the system configuration is shown in Figure 3. The Central Office contains the voice digitizing equipment, mux, and one half of a digital radio link. This link operates at 78 Mbps in the 6 or 11 GHz band. At the earth station, the demultiplexed T-1's form the input to the TDMA terminal which operates at a bit rate of 64 Mbps. This corresponds to a traffic handling capacity of up to 39 T-1's. The equipment can also operate over multiple transponders. A picture of the TDMA terminal equipment is shown in Figure 4. ASC's TDMA system is fairly typical of the type of wideband TDMA that will be used in domestic satellite networks. It uses preassigned burst positions and has standard T-1 interfaces on the baseband side. This allows easy interfacing with entrance links such as digital radios. In addition, it permits the placement of the source encoding device in a remote location such as a Central office. The equipment also has extensive maintenance capability, including microprocessor controlled automatic diagnostic facilities, printers, on-line BER monitoring, etc.

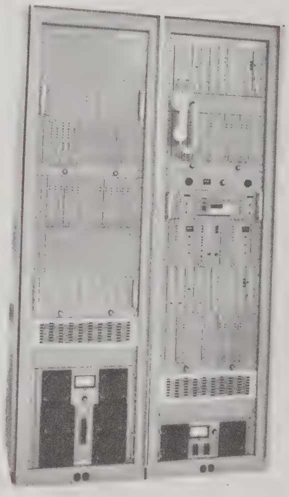

Figure 4.

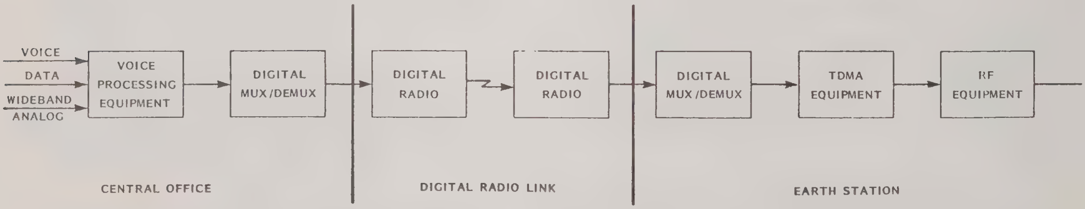

Figure 3.

SBS

In late 1975, Satellite Business Systems (SBS) announced its plans for a domestic communications Satellite system. SBS is a partnership sponsored by COMSAT, IBM and the Aetna Casualty and Surety Company. Its filing with the FCC asked for approval to provide private-line networks.

Figure 5 shows a block diagram of the SBS system.[8] The main feature of the SBS concept is to provide earth stations at the customer premise in order to have minimum dependance on costly local distribution. The other prominent features are:

- Fully integrated Voice, Data and Video services.
- Use of TDMA as the multiple access technique.
- 5 and 7 meter antennas.
- Use of Demand Assignment to allocate satellite capacity where needed.
- Voice activity compression (VAC) to provide a reduction in channel capacity requirement.
- Unattended operation of earth stations.

The earth stations will have direct interface capability to co-located terminals, PBX's and other equipment. Remote locations would have to be connected via terrestrial local distribution means. The principal components of the SBS earth stations are:

- RF terminal which consists of the 14/12 GHz Up and Down Converters, High Power Amplifier, Low Noise Amplifier and antenna.
- TDMA Burst Modem which interfaces with the RF terminal at 70 MHz IF and performs the modulation and demodulation function. The modulation technique used is 4 phase QPSK.
- Sattellite Communications Controller (SCC) which is an integral hardware/software device comprised of processors, storage units and control programs. It performs the voice digitization and activity compression, demand assignment and the other TDMA functions.
- Monitor and Command loop which enables a central station to determine the status of a remote station.

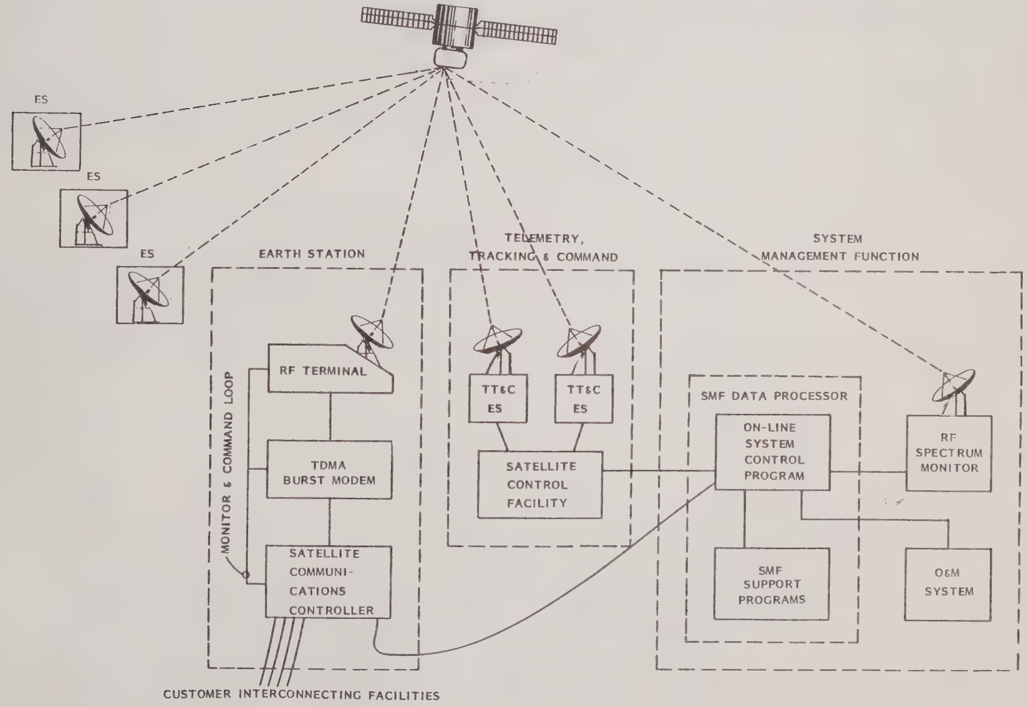
ES
ES
ES
EARTH STATION
TELEMETRY, TRACKING & COMMAND
SYSTEM MANAGEMENT FUNCTION
RF TERMINAL
TDMA BURST MODEM
MONITOR & COMMAND LOOP
SATELLITE COMMUNICATIONS CONTROLLER
TT&C ES
TT&C ES
SATELLITE CONTROL FACILITY
SMF DATA PROCESSOR
ON-LINE SYSTEM CONTROL PROGRAM
RF SPECTRUM MONITOR
SMF SUPPORT PROGRAMS
O&M SYSTEM
CUSTOMER INTERCONNECTING FACILITIES

Figure 5.

As mentioned earlier, the SBS system is designed for private networks of business and government organizations. A large company may have 20 earth stations. It would be assigned satellite capacity on demand. This concept allows a number of networks or stations to share the same satellite or transponder capacity thus enabling the satellite to be a central concentrator and achieve the trunk usage normally associated with high traffic intensity earth stations or nodes.

The RF channel performance objectives of the SBS system are listed below:

Maximum Bit Error Rate (BER)	Availability
1×10^{-6}	95%
1×10^{-4}	99.5%
1×10^{-2}	99.8%

An option is available to add forward error correction coding to individual ports to improve the BER to 1×10^{-7} for 99.5% availability.

The TDMA burst rate will be either 43 or 48 Mbps. Since there are 10 transponders on the satellite, this will give a worst case capacity of the satellite as 430 Mbps or 12,000 equivalent voice circuits. The communications subsystem in the satellite will include the ten transponders. The channel spacing is nominally 49 MHz with a usable bandwidth of 43 MHz. The output TWTA will have an output power capability of 23 watts. The launch vehicle used will be a Delta 3910. The first launch is expected to occur in the fall of 1980 with the system going into operation in early 1981.

The SBS concept uses some of the most advanced TDMA and satellite technology. It will be one of the first networks with large scale use of customer premise earth stations. In addition, it will also be the first network to use demand assigned TDMA along with sophisticated voice processing techniques. SBS plans to initially install about 200 earth stations in the U.S. Its progress will be closely watched by the other common carriers and if successful, will surely inspire others to use TDMA.

Advanced WESTAR SS/TDMA

Western Union's Advanced Westar satellites offer the potential to be the most advanced digital satellite nework in the world. The Advanced Westar satellite is equipped with both C-Band and K-Band transponders [9]. The C-Band payload consists of 12 conventional 36 MHz bandwidth transponders. The K-Band payload consists of a 4 x 4 satellite switch with a total transmission capacity of 250 Mbps in each beam or 1000 Mbps for the whole payload. It operates exclusively in a Satellite Switched/Time Division Multiple Access (SS/TDMA) mode and carries digital traffic only. The satellite switch permits interconnection of all channels on a sequential basis. A block diagram of the payload is shown in Figure 6. The beams are grouped into four satellite channels. The antenna beams for the New York spot and the Miami spot are coupled at RF before the receiver and after the transmitter. The four satellite channels actually consist of four independent receiver and transmitter combinations. The switch matrix connects the output of each receiver to the input of each transmitter sequentially.

SS/TDMA is one of the most effective techniques for maintaining interconnectivity among earth stations when a satellite and multiple spot

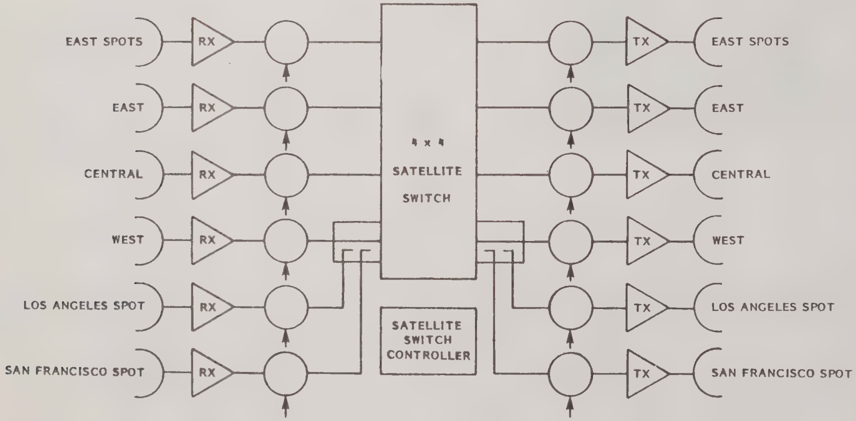

Figure 6.

beams is used. Western Union has described one possible network configuration [9]. The network would consist of large, medium and small capacity earth stations with full inter-station connectivity. There would be 6 large stations, 20 medium stations and 80 small stations. Table 1 shows the results of calculations for this mix of stations for voice traffic only. It is based upon 8-bit PCM per voice channel. Other traffic service such as data or video could be substituted for the voice traffic.

The performance ojbectives for this network are shown below:

	EARTH STATION CAPACITY		
	Large	Medium	Small
Average Availability (One Way)	99.98%	99.9%	99.9%
BER (Voice)	10^{-4}	10^{-4}	10^{-4}

The large capacity stations would use either a 7 meter or a 13 meter antenna depending on the location. The medium capacity stations would use a 7 meter antenna and the small stations would use a 5 meter antenna. The size of the HPA's would vary from 400 watts to 3K watts.

The major feature of this network is that it provides full one hop interconnectivity between all stations and the cost of the station can be made directly proportional to its traffic handling capacity requirements.

The Advanced Westar system will be the first operational network to use any form of onboard processing. As spacecraft and launch technology progresses, more processing will be done onboard the satellite. This will lead to more sophisticated digital networks.

International TDMA Networks

Intelsat has recently completed a TDMA field trial. The TDMA system operated at 60 Mbps and used Digital Speech Interpolation (DSI) to achieve a 2 to 1 reduction in channel capacity required for voice. Five countries participated in these field trials. Intelsat is now in the process of defining their operational TDMA system. It will operate over the Intelsat V satellite at a bit rate of 120 Mbps and will also use DSI. Its main application will be to handle the large trunked traffic between Intelsat earth stations. This network is expected to be operational in 1983.

Europe has been looking at digital networks exclusively for their domestic satellite network. The OTS satellite was used for TDMA experiments at 120 and 180 Mbps. A new European agency called EUTELSAT is writing a technical specification for an operational 120 Mbps TDMA system. The thrust seems to be to make the EUTELSAT and Intelsat TDMA specifications compatible with each other. This would obviously result in lower cost equipment.

In the meantime, France has announced plans for a large domestic TDMA network called "TELECOM 1". The main application of this network are:

1. Business communications in France using the 14/12 GHz band and TDMA.
2. Video transmission to French territories in the same frequency band.
3. Telephone traffic between France and their overseas territories using the 6/4 GHz band.

The first application is for an SBS type system using customer premise earth stations with 3 meter antennas and TDMA. Other characteristics are listed below:

° Bit Rate:	24.576 Mbps
° Frame Length:	24 Milliseconds
° Modulation:	2 phase differential PSK
° Channel Bandwidth	36 MHz
° HPA:	150 Watts
° LNA:	FET type with 400°K noise temperature
° Antenna:	About 3 meters

Representative AW Satellite Traffic Handling Capacity Model

		PER STATION CAPACITIES			TOTAL CAPACITIES BY STATIONS TYPE		
STATION TYPE	NO. OF STATIONS	MBPS	NO. OF T-1s		MBPS	NO. OF T-1s	NO. OF ONE-WAY VOICE CIRCUITS
LARGE CAPACITY	6	54,040	35	840	324	210	5,040
MEDIUM CAPACITY	20	10,808	7	168	216	140	3,360
SMALL CAPACITY	80	1,544	1	24	124	80	1,920
TOTAL NUMBER OF STATIONS:	106				664	430 T-1s	10,320 VFs

Table 1.

This system is expected to go operational in the 1983-84 time frame and, if successful, could expand to other European countries.

MARISAT

The Marisat system was put into operation by COMSAT General to provide voice and data communications to ships on the high seas. The main objectives of this network are [10].

- Full duplex voice, data and teleprinter services.
- Interconnection with existing networks
- Safety and distress services.
- Operation with multiple shore stations

The system uses SCPC/FDMA, TDM and TDMA techniques to meet the above objectives. In addition, it also uses a demand assignment technique to allocate channel capacity. The network is configured as ships at sea communicating in a star network. The network control is centralized at the shore station and great care has been taken to keep the ship terminals simple and inexpensive. The voice service is provided using SCPC. Teleprinter and signalling information from the shore station to the ship are transmitted on a separate carrier using TDM. The return data traffic from the ships to the shore uses TDMA. The TDMA system operates at low bit rates and consequently uses an open-loop synchronization technique. The shore stations operate in C-band frequency while the ship terminals operate in the L-band frequency. A block diagram of the complete system is shown in Figure 7. Each shore station transmits at least one TDM carrier. Every one of these carriers has a paired TDMA signal in the ship to shore direction which provides full-duplex teleprinter operation. Each active ship terminal transmits a single burst per frame.

At the U.S. shore stations, the terrestrial trunks are equipped for CCITT no. 5 signalling. Calls are operator assisted to obtain reliable billing data for shore originated calls and to permit person-to-person calls from mobile terminals. After a through connection has been established, the shore station is transparent except for clearing signals initiated from either side.

The Marisat System has been in successful commercial operation for more than four years. It has been a significant advance in providing high quality, reliable maritime communcations.

Conclusion

This paper has presented a brief overview of the major digital satellite networks that are in commercial operation today. In addition, description of some networks that are in various planning stages have also been presented.

Most new networks are using digital techniques. This trend has accelerated due to the rapid introduction of digital switches. The use of integrated digital networks is clearly the path that will be increasingly followed in the decade ahead.

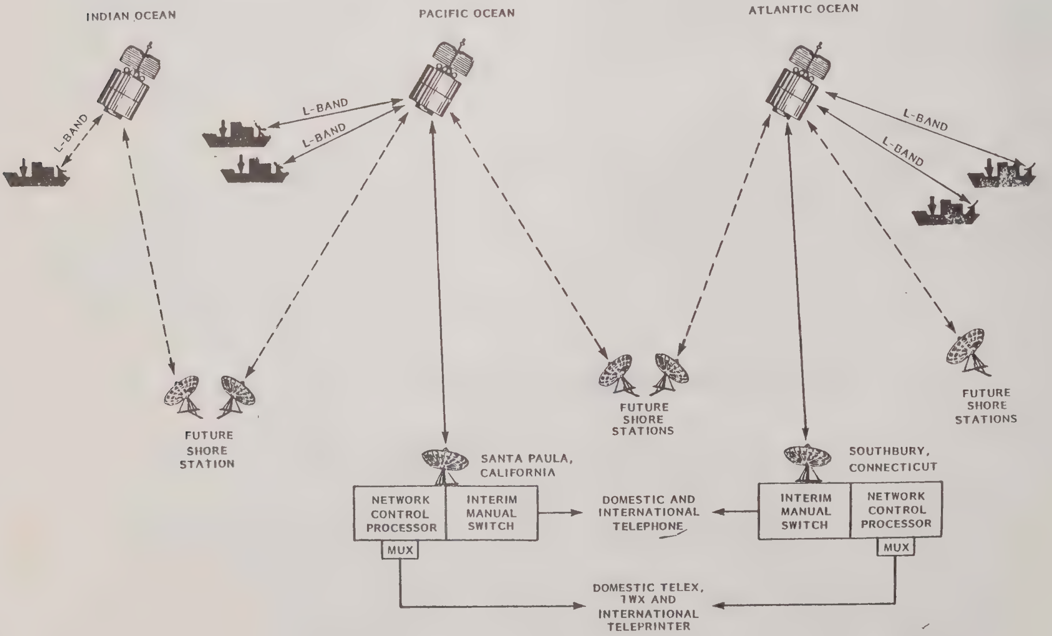
INDIAN OCEAN
PACIFIC OCEAN
ATLANTIC OCEAN
L-BAND
L-BAND
L-BAND
L-BAND
L-BAND
FUTURE SHORE STATION
FUTURE SHORE STATIONS
FUTURE SHORE STATIONS
SANTA PAULA, CALIFORNIA
SOUTHBURY, CONNECTICUT
NETWORK CONTROL PROCESSOR
INTERIM MANUAL SWITCH
MUX
DOMESTIC AND INTERNATIONAL TELEPHONE
INTERIM MANUAL SWITCH
NETWORK CONTROL PROCESSOR
MUX
DOMESTIC TELEX, TWX AND INTERNATIONAL TELEPRINTER

Figure 7.

References

1. "SPADE System Progress and Application", B. Edelson and A. M. Werth, COMSAT Technical Review, Volume 2, No. 1 Spring 1972.

2. "Time Division Multiple Access," O. G. Gabbard and Pradman Kaul, EASCON - 74 Proceedings, Washington

3. "Telesat Canada, A Technical Description", Document No. TC-79-001, September 1979.

4. "The Telesat TDMA System", R. K - Kwan, ICC -75, San Francisco.

5. "The Common TDMA Terminal Equipment for the Telesat TDMA System", Pradman Kaul et al, ICC-75 San Francisco.

6. "The Anik C 90 Mb/s Digital Service", F. H. Smart, 4th Int'l Conference on Digital Satellite Communciations, 1978, Montreal, Canada.

7. "Use of TDMA in a Domestic Satellite Communications System", S. Mittal, E. R. Cacciamani, Jr., J. Hangen, EASCON 1979.

8. "The SBS Digital Communications Satellite System" J. D. Barnia and F. R. Zitzmann, EASCON 77 Proceedings.

9. "Advanced Westar SS/TDMA System", J. Ramasastry et al, AIAA Proceedings, 1978.

10. "MARISAT - A Maritime Satellite Communications System", D. W. Lipke et al, COMSAT Technical Review, Vol 7, No. 2, Fall 1977.

80-0515

AT&T/GSAT DOMESTIC SATELLITE OPERATIONAL NETWORK

R. F. Latter*
AT&T Company - Long Lines Department
Bedminster, New Jersey

Abstract

This paper discusses operational experience with the AT&T/GSAT Satellite System which has been in operation since May of 1976.

The system is described, and its integration into the AT&T long distance network explained. System availability compared to design criteria is compared and the work done to improve customer acceptance of satellite circuits in the domestic network is explained.

1. The AT&T/GSAT Domestic Satellite System

The system consists of three satellites in orbit at 87, 95 and 128° West Longitude. They are identical 24 transponder spin stabilized units, built by Hughes Aircraft Company and leased to us by Comsat General. There are eight major earth stations - four provided by AT&T, three by GSAT, and one by All America Cables and Radio, Inc., an IT&T subsidiary for Puerto Rico service. These are equipped with antennas approximately 100 feet in diameter manufactured by different suppliers, but having similar electrical characteristics. Smaller antennas are also used at various other locations for government services and experimental work.

The satellites use orthogonal polarization and the large earth stations employ automatic polarization tracking. Thus the system uses the 4/6 GHz band twice. Each satellite provides 24 transponders with nominal bandwidths of 34 GHz.

2. Growing Importance of Satellite Facilities in the Domestic Long Distance Network

The major use of the AT&T/GSAT Satellite System has been to supplement the facilities of the nationwide long distance network. This network as it existed before satellites is shown in Figure 1. About two-thirds of these facilities are microwave radio operating in the 4 and 6 GHz common carrier bands, and the remaining third are coaxial cable, all engineered to fit our customers requirements for Long Distance telephone Message and Private Line Services.

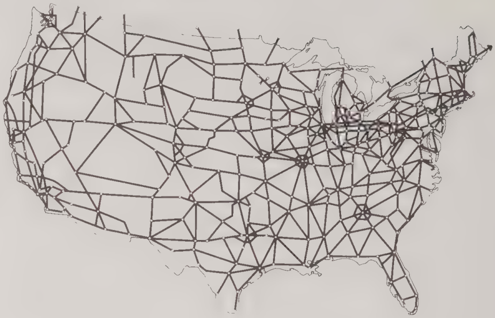

Fig. 1 Major Bell System Communications Highways

You can see that unlike Canada or Alaska, telephone and network broadband services such as TV are available essentially everywhere in the lower 48 states, so the system was initially designed to supplement these facilities rather than to add new paths of connectivity. As such, it was designed to be capable of the same reliability and transmission performance in the eyes (or ears) of our customers as existing terrestrial facilities. Our major efforts have been directed toward how to enhance the network using satellite facilities.

Figure 2 shows the current connectivity of the satellite system. These paths were selected primarily to use the satellite facilities where they are the most economical on a network basis. Satellite facilities are economic between widely separated metropolitan areas which are within reasonable distances of earth stations. The number of message circuits assigned to satellite facilities is increasing rapidly, jumping from about 3,700 in January of 1979 to approximately 13,000 at the end of the year.

---

*Engineering Director, Transmission Planning. Member AIAA. Copyright ©, 1980

Released to AIAA to publish in all forms.

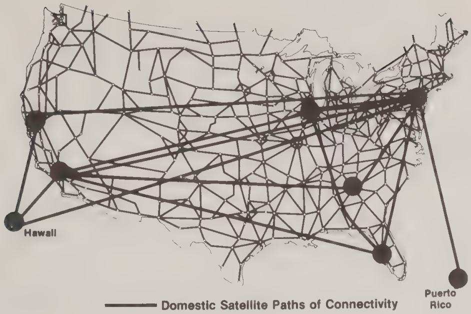

Fig. 2 Major Bell System Communications Highways (Including Satellite Facilities)

3. Reliability Results

One of the satellite system's design criteria was to achieve the 99.98 percent reliability of the terrestrial microwave and coaxial cable transmission systems in the network.

We designed the system to meet this objective by careful component selection and testing, and with automatic substitution of major components if required, as well as the use of a protection satellite tracked by a separate antenna at each earth station. So far, the results have been good as Table 1 indicates. Except possibly for a portion of 1979 when very severe microwave fading reduced the availability of some of our microwave connecting links between the earth stations and the junction offices, the system has met its design standards.

Table 1

COMSTAR SYSTEM AVAILABILITY

1976	
MUS* Availability	99.980%
E.S.** Availability	N.A.
1977	
MUS Availability	99.991%
E.S. Availability	99.994%
1978	
MUS Availability	99.995%
E.S. Availability	99.997%
1979	
MUS Availability	99.914%
E.S. Availability	99.997%

*MUS - Message Unit Satellite
**E.S. - Satellite Earth Station

4. Satellite User Reaction Tests

In my judgment, the work done to improve the long distance telephone customer perception of transmission over satellite facilities is a very important success story which will contribute greatly to the use of satellite facilities. This work has progressed to the point that these customers cannot distinguish between terrestrial and satellite facilities. Furthermore, the equipment used is economic, and it is no longer necessary to use a mixture of terrestrial and satellite facilities for opposite directions of transmission, thereby increasing the number of satellite facilities that can be used in the nationwide long distance network.

In literally thousands of interviews, telephone customers have been asked how they rated a call just completed over various types of facilities including satellites. Figure 3 shows that using standard echo suppressor techniques, over three times as many people (26 versus 8 percent) rate a call unacceptable over satellites as compared to terrestrial facilities.

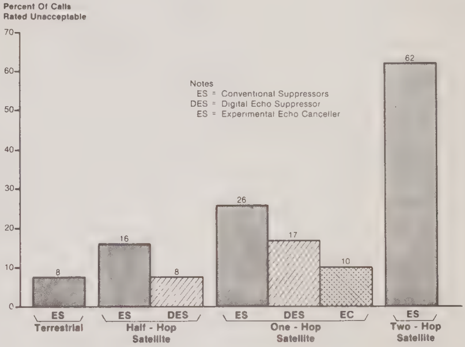

Fig. 3 Domestic Satellite User Reaction Test Results

However, some time ago as the chart also illustrates, we were able to show that by the use of an echo canceller* this difference is essentially eliminated. The only problem was that the models used in these tests used conventional TTL logic and cost upwards of $20,000 each.

*Patented by Bell Telephone Laboratories in 1970.

5. The Echo Canceller Principle

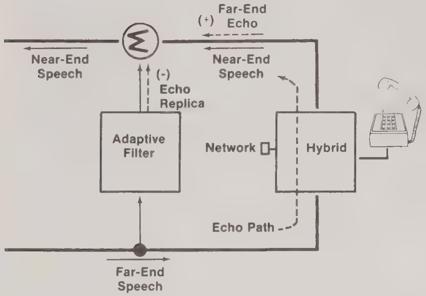

Fig. 4 Echo Canceller Principle

Figure 4 shows the principle of the echo canceller. It does not block or suppress transmission in one direction to eliminate echo as do conventional echo suppressors, but rather generates an artificial echo similar to, but 180° out of phase from the real echo, thus cancelling it out. Since the circuit functions normally in each direction, speech from either talker is not interrupted during double talking, thus eliminating a major cause of difficulty. It has been apparent for some time from four wire tests that the major problem in single hop satellite circuits was not the delay in the circuit, but rather the speech mutilation that the echo suppressors caused (chopping and clipping) under certain conditions.

6. Echo Canceller Cost Reduction

Using electron beam techniques, Bell Labs has been able to fabricate a VSLI chip that contained the essential elements of a canceller at a small fraction of the cost of the original TTL model. It contains some 35,000 transistors and replaces seven circuit boards.

The chip, with minor modifications, is used in three types of cancellers which are or soon will be employed in the Bell network. Those designed for circuits terminating on the two major domestic switching systems are plug-in to minimize expensive installation costs.

By contrast, plug-in units can be installed as part of normal circuit order work. One unit plugs into the echo suppressor mounting used with our 4A switching systems and converts it to a canceller. Similarly, the other is used with our 4E digital switchers and CCIS signaling, and plugs into the LT connector. The remaining canceller is a stand alone unit for overseas use where the tail circuits may be very long. This requires an adaptive filter network capable of accommodating an echo delayed about twice as long as the design needed for domestic use, and it must work with several signaling systems.

7. Multihop Satellite Connections

While the echo canceller has been used successfully to make satellite circuits the equivalent of terrestrial circuits for single hop connections, another important question is "Are satellite circuits equipped with echo cancellers sufficiently equivalent to terrestrial circuits so that all restrictions on tandem satellite circuits can be dropped?"

A clue to the answer to this question comes from the White Plains-London and Hawaii-Wayne, Pennsylvania tests. Figure 5, "Percent Calls Unacceptable versus Round Trip Delay" shows that the percent unacceptable for tandem satellite circuits equipped either with suppressors or echo cancellers is much higher than for tandem terrestrial circuits, although the echo canceller equipped circuits are better. An additional question, "What characteristics of satellite circuits equipped with cancellers makes two in tandem worse than tandem terrestrial circuits?" is suggested.

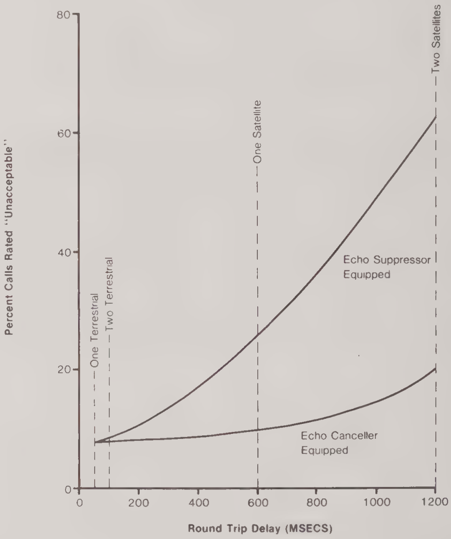

Fig. 5 Percent Calls Unacceptable vs. Round Trip Delay

Let's look at why people said they rated a call unfavorably for an answer. Figure 6 shows that the percent who said "Delay" increases very rapidly beyond one hop. The other reasons given did not correlate with an increase in circuit round-trip delay. Thus this factor, which is relatively insignificant up to one hop, appears to be the reason.

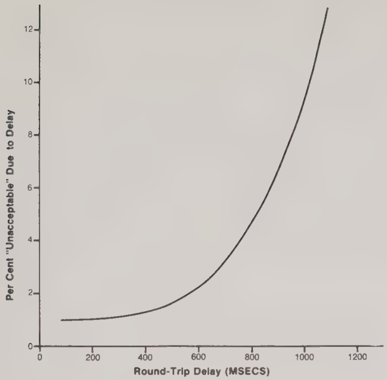

Fig. 6 Percent Calls Rated
Unacceptable Due To Delay
vs.
Round Trip Delay

For the time being it appears that we should continue to restrict tandem satellite connections.

8. Conclusion

I have briefly described the AT&T/GSAT Domestic Satellite System, how we are using it to supplement the facilities in the MTS network, and some of the results we have obtained. The work we have done to improve the transmission quality of satellite circuits has been particularly interesting and the results gratifying.

80-0516

NETWORK ORGANIZATION AND OPERATION OF THE WESTERN UNION DIGITAL EXCHANGE SYSTEM (DES)

J. Baer, Member Sr. Technical Staff
F. R. Hanvey, Jr., Assistant Vice President
G. Parowski, Consultant Engineer
Western Union Telegraph Company
Upper Saddle River, N.J.

Abstract

The Western Union Digital Exchange System (DES) is one of the largest commercial circuit-switched record communication networks. Its hierarchic architecture is based on very highly distributed microprocessor application, under centralized control. DES provides TWX and TELEX service nationwide. In operation since mid-1978, it will serve up to 100,000 TWX and TELEX terminals, located in some 1,600 cities, in 1982. Inter-city trunking is largely based on Western Union owned microwave, satellite, and T-1 cable facilities. This paper focuses on the influence of the chosen architecture on flexibility, maintainability, availability and serviceability.

Introduction

In 1976, the confluence of Western Union business needs and prior technological advances in areas of microelectronics and terrestrial and satellite communications created a unique opportunity for innovation in nationwide circuit-switching systems. The result is the Western Union Digital Exchange System (DES).

The Western Union DES currently is operational and undergoing staged cutovers. DES provides service to USA TWX and some Telex, and is architectured to be capable of supporting other data terminals for automatic, circuit-switched, conversational communications or data access/egress over terrestrial and satellite communications facilities. The circuit-switching and efficient data-multiplexing functions of DES are performed by an extremely distributed processing system utilizing programmable microprocessor equipment interconnected by a synchronous hybrid (terrestrial/satellite) communications facility complex. This paper discusses some of the background for this nationwide USA network and then the network organization and operation of the Western Union DES.

Background

The TWX service was acquired by Western Union from AT&T in 1971, at which time it had approximately 40,000 subscriber terminals. TWX is a uniquely North American Service, available only in the USA and Canada. It began in the 1930's as a public, switched teleprinter service requiring manual operator intervention for each call set-up, and was converted to automatic dial-up operation in the 1960's. TWX evolved, in both the USA and Canada, as a telephone company offering and, in view of the well-developed telephone networks of the countries, it was designed to use the common facilities of these networks. As such, and significantly, the TWX service as acquired by Western Union is based on analog signalling and transmission facilities. TWX uses 8-bit ASCII-code, asynchronous transmission at a rate of 110 Baud, and permits operation at 100 words-per-minute.

Telex is a world-wide, public, switched teleprinter service, many of the key technical and operating characteristics of which have been standardized by the CCITT. Telex was started as an automatic, dial-up service in Great Britain in 1932 and became an international service in Europe with the addition of the Netherlands in 1936 and Germany in 1937. Western Union introduced Telex into the USA in 1958. Since 1960, the U.S. Telex Network has been interconnected with the rest of the world. Telex, having evolved from basic D.C. telegraph techniques, is based on binary digital signalling and transmission. Telex uses 5-bit so-called "Baudot" code, asynchronous transmission at a rate of 50 Baud, and permits operation at 66.67 words per minute.

Evidently, past precedents and evolution have produced certain disparities between the TWX and Telex systems. When one realizes that the acquisition of TWX by Western Union from AT&T eliminated any rationale for keeping TWX dependent upon its host telephone network, the stage was set for a network evolution toward one integrated TWX/Telex exchange system. The necessity to transfer TWX to Western Union facilities at some point (now scheduled to be completed in 1981), along with the need for cost-effective support of Telex growth, coalesced with the newly available technology of 1976 to define the DES development project. Although DES is an integrated TWX/Telex network, it does not currently provide for conversational interchange between the two services. This feature is just one of the many possible add-on features which might be provided by additional investment on such a programmable, distributed-processing network, if market desires so dictate. (A store and forward interchange between the two is already provided via Western Union's INFOMASTER® System.)

DES Overview

Before describing how the network got to be as it is (geographically, topologically, etc.), it would be well to examine a top level overview of DES. One way of doing so would be to examine the nodal hierarchy involved, going from the lowest traffic intensity (third level) node to the highest.

The network is hierarchical, with an "outer layer" of some 1600 cities, an "inner layer" of about 200 cities, and four major switching sites (see Figure 1). The inner and outer locations provide various levels of data concentration and multiplexing. DES uses a selected mix of satellite and terrestrial transmission facilities. The concentration and multiplexing devices used in DES are programmable, microprocessor-based units which provide for both local and remote diagnostics as well as down-line loading.

The production of the hardware nodal elements, such as digital data multiplexers, data concentrators, and programmable front-end processors

Copyright © American Institute of Aeronautics and Astronautics, Inc., 1980. All rights reserved.

commenced by late 1977. Actual TWX transfer from telephone switching centers began, as scheduled, on July 15, 1978, with completion of the last phase scheduled for 1981. The Digital Exchange System capitalizes on many concepts which in 1976 were technologically advanced; e.g., distributed network architecture, time-division switching technology, integrated switching/multiplexing and reliance on digital, programmable, intelligent network elements, at every point in the hierarchical structure of the system. By 1981, DES will have combined concentrator/multiplexer units in nearly 1600 cities. Many of the larger cities will have multiple locations for deployment of additional concentration equipment in the business districts.

Reference to Figure 1 shows the three distinct levels of DES concentration and multiplexing, and the nodal equipment commonly found at each level. The lowest (third) level is the subscriber access level which exists in 1600 cities throughout the contiguous United States. Each of the 1600 third-level cities has at least one integral TWX concentrator/multiplexer equipped with a built-in data modem (TWX-V). In a subset of these cities, where a Telex population exists that can advantageously be served by DES, a programmable Telex concentrator/multiplexer (SIM-200) is in place. An additional feature is the capability of the SIM-200 to accept the already time-division multiplexed TWX-V output trunk and combine it with the SIM-200's multiplexed stream. The result of this is that, in general, only one 2400 b/s line is necessary to interconnect a DES third-level city with a second-level city in the hierarchy.

Approximately two hundred of the 1600 third-level cities also function as second-level cities. The primary function of the second level is to combine multiplexed streams directed to it from the third-level cities, so that a minimum number of 9600 b/s inter-city lines are required between the second-level and the primary switching centers located at the four first-level cities in the U.S. Basically, the second-level multiplexers further combine the already multiplexed signal-streams from the third-level, and have the capability to improve circuit utilization efficiency by eliminating unassigned time-slots emanating from lower level cities.

Switching Centers

The four primary switching centers constitute the highest level of the DES hierarchy. In these centers the circuit switching function is accomplished for the DES. The switching function is performed in the programmable front-ends (PFE), controlled by a medium size Univac 418 computer. The PFEs interface with the multiplexed data lines emanating from the second-level cities, and perform time-slot switching on a character basis, using a high-speed, time-division computer-bus

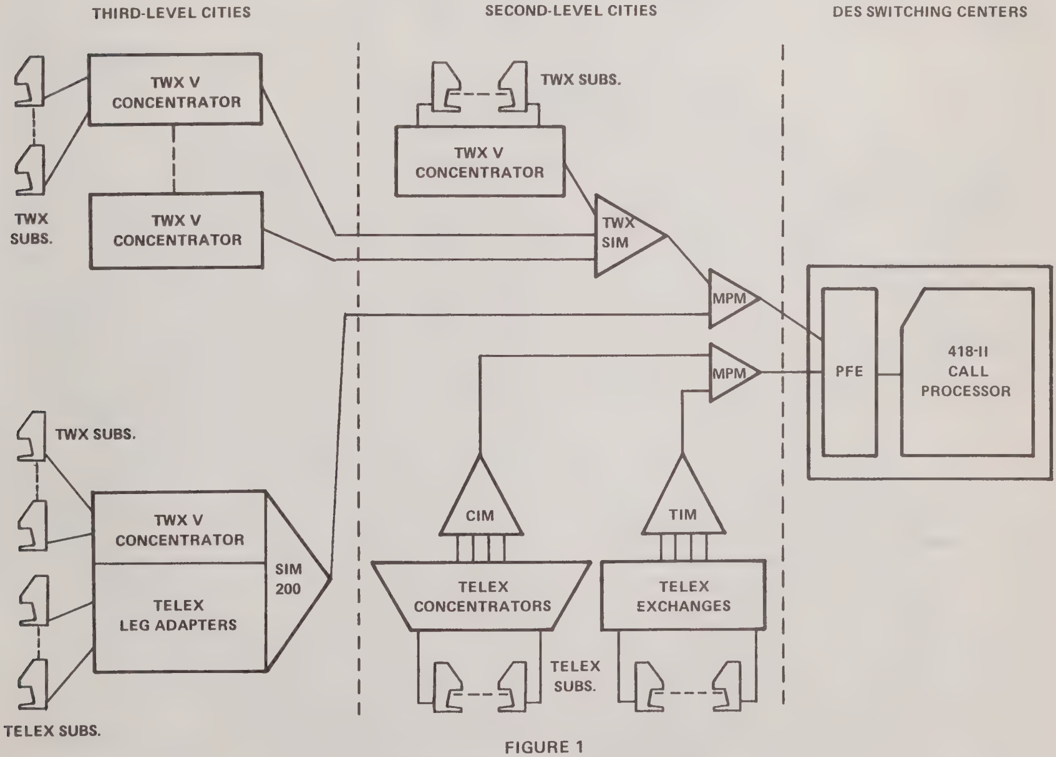

FIGURE 1
DIGITAL EXCHANGE SYSTEM OVERVIEW

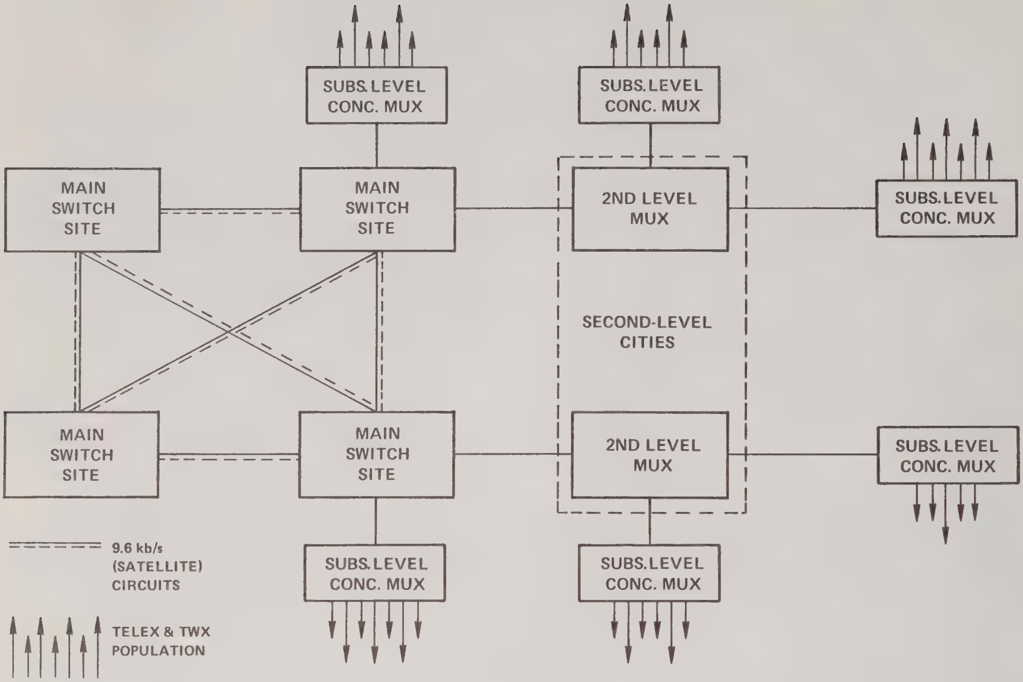

FIGURE 2
DES SWITCHING CENTER/NETWORK INTERCONNECTION

technique. The DES switching centers are fully interconnected (see Figure 2), using high-speed data-links generally routed via the WESTAR satellite. These four switching centers interface with other systems, including InfoMaster®, International Record Carriers, Canadian TWX, AT&T TWX Primary Offices (until 1981), and the existing Western Union Telex Exchange system. Interfaces to other networks are facilitated through programmable conversion and multiplexing equipment, so that the only interfaces at the PFE ports are time-division-multiplexed data streams. Thus, a single type of interface at the PFE is realized.

Network Topology

A valid question to raise upon examining the DES network is how one could come to a distributed processing architecture involving something like 1600 city locations, where prior circuit switching hierarchies had tended to be considerably more compact. The answer to this question is provided by the now ubiquitous microprocessor, its economics and the ease with which it can move between the previously somewhat disparate disciplines of transmission and switching. If one examines the communications-channel cost factors for a typical hierarchical network serving 100,000 terminals, it will be seen that there is a communications-channel cost to bring each of the terminals to the closest nodal point of the hierarchy and then a second communications-channel cost to go from this closest node to the second level and so on. If the network hierarchy is a meaningful one, it will generally be true that the communications-channel cost increments to serve each successive stage of the hierarchy are less than those for the preceding stage. In fact, for a well designed hierarchical network, the dominant (more than 50%) communications channel-costs may well be those from the terminals to the first nodal point of the network. Since these channel costs tend to be critically dependent upon distance, it is highly desirable that they be minimized by placing "smart" network nodal equipment as close to the input terminal as possible. For the network designer, this communications-channel cost minimization has to be traded-off with the capital investment required to equip a great many nodes with "smart" equipment. In the past, this trade-off has tended toward larger switching equipments located in a few cities, supported by independent communications-channel equipment placed primarily for path-segment efficiency. The use of cost-effective microprocessors in the nodal equipment - whether said equipment be a concentrator, a multiplexer, or a switching element - frees the network designer from prior constraints and allows for a network design containing many more nodal elements than would have otherwise ensued. A theoretical design analysis done on the DES network resulted in an optimization point (minimum total equivalent costs) at around 2000 cities. The selected 1600-city network represents a compromise between cost minimization theory and the practical aspects of installing and maintaining an integrated network of such a magnitude. (See Figure 3.)

Network Nodal Elements Commonality

The full DES network is made up of a small number of fundamental equipment building-blocks. Although a wide variety of somewhat different functions is accomplished in the nodal elements, a surprising amount of hardware commonality exists between the various units. This hardware similarity was deliberate for purposes of maintenance and spares provisioning.

The evolution of microprocessors had, by 1975, reached a point which permitted the design of a family of microprocessor-based modules for the various multiplexing and concentration functions required in DES. All but one of these modules allow down-line loading and both local and remote diagnostics. The family divides into two major groups. (Refer again to Figure 1.) The first group interfaces with TWX terminals and trunks, which use analog signalling, and the modules of this group (TWX-V and its variants) contain analog-to-digital (A/D) convertors. They multiplex and concentrate TWX traffic and feed it to modules of the second group.

The second group interfaces either with the digital side of TWX-V modules or with Telex terminals and trunks. It is therefore, completely digital. The modules of this group (SIM-200, SIM, CIM, TIM) perform multiplexing and, in certain categories, concentration functions at the subscriber or line level.

Both the line and trunk interfaces of the TWX-V group of modules are asynchronous. The second group of modules has asynchronous line, and synchronous trunk, interfaces. Additionally, there are multiport multiplexers (MPMs) in DES for the purpose of higher order trunk multiplexing. These are derivatives of the second group of modules. The basic characteristics of the different modules in each group are summarized in Tables 1 and 2.

The magnitude of the system can be gauged from the fact that, by 1981, it is expected that DES will comprise some 2,700 modules of Group 1, about 2,000 modules of Group 2 and approximately 500 MPMs.

Module Application

The TWX-V type modules interface TWX subscribers, AT&T TWX switch trunks and TWX lines from the International Record Carriers (IRCs) with DES. All of these units provide analog-to-digital conversion

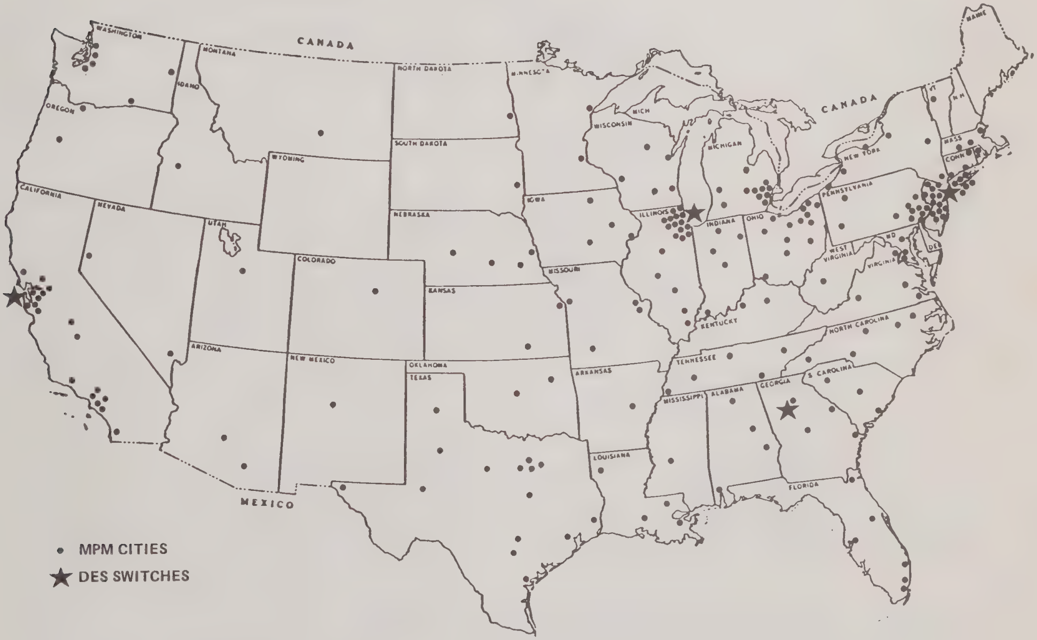
CANADA
CANADA
MEXICO
WASHINGTON
OREGON
CALIFORNIA
NEVADA
IDAHO
MONTANA
WYOMING
UTAH
ARIZONA
COLORADO
NEW MEXICO
NORTH DAKOTA
SOUTH DAKOTA
NEBRASKA
KANSAS
OKLAHOMA
TEXAS
MINNESOTA
IOWA
MISSOURI
ARKANSAS
LOUISIANA
WISCONSIN
MICH
MICHIGAN
ILLINOIS
INDIANA
OHIO
KENTUCKY
TENNESSEE
MISSISSIPPI
ALABAMA
GEORGIA
FLORIDA
S CAROLINA
NORTH CAROLINA
VIRGINIA
WEST VIRGINIA
PENNSYLVANIA
NEW YORK
MD
DEL
CONN
MASS
NH
VT
MAINE
● MPM CITIES
★ DES SWITCHES

FIGURE 3
DES SYSTEM MAP

Table 1 DES TWX-V Analog-To-Digital Multiplexers/Concentrators

		OUTPUT TRUNK		
TWX-V TYPE	INPUT (110 BAUD ASYNCH)	INTERFACE	TO	FUNCTION
A	8 TWX SUBS.TERMINALS	1200 b/s ASYNCH.	SIM	A/D, MUX
B	24/48 TWX SUBS.TERMINALS	1200 b/s ASYNCH.	SIM	A/D, MUX, CONC.
C	8 EA. AT&T TWX TRUNKS	1200 b/s ASYNCH.	TIM	A/D, MUX
D	8 EA. IRC TWX LINES	1200 b/s ASYNCH.	SIM	A/D, MUX

(NOTE: IRC = INTERNATIONAL RECORD CARRIER)

so that compatibility is achieved between the traditional analog approach of the past with the newer digital technology of DES. TWX-V units accommodate eight to forty-eight lines or trunks, and on the DES side appear as one medium-speed, time-division-multiplexed trunk. An internal concentrator function, at the third level in the network, is performed in the 24- and 48-line TWX-Vs designated for subscriber-line terminations. The space-division concentrator function is accomplished using an array of interconnected 4x4 matrices of silicon-controlled-rectifiers. A built-in, medium-speed modem board is provided for those TWX-Vs that are remote from the next order of multiplexing. TWX-Vs are all microprocessor-controlled, using the Motorola 6800 microprocessor.

The access device for Telex subscriber terminals and trunks is the Telex Subscriber Interface Module (SIM). These units have functions parallel to the TWX-V units and can terminate 50 Telex lines. Their architecture differs from TWX-V because of the nature of Telex signals, which makes analog-to-digital conversion unnecessary. The Telex SIM is a programmable unit and provides time-division concentration and multiplexing. An optional feature of the Telex SIM is to equip one of the input line-board positions with a medium-speed, asynchronous board to terminate the trunk side of a TWX-V and accomplish dual multiplexing. A Telex SIM so configured

Table 2 DES Digital Multiplexers

	INPUT LINES					OUTPUT TRUNKS		
	(ASYNCHRONOUS)				(SYNC.)	(SYNCHRONOUS)		
TYPE:	TELEX SUBS. LOOPS (50 BAUD)	TELEX CONCENTRATOR TRUNKS (50 BAUD)	TELEX EXCHANGE TRUNKS (50 BAUD)	TWX-V TRUNKS (1200 b/s)	SIM-200 TRUNKS (2400 b/s)	TO MPM OR PLI (2400 b/s)	TO MPM OR PLI (4800 b/s)	TO PLI (9600 b/s)
TELEX SIM	50					X		
TELEX CIM		50				X		
TELEX TIM			50			X		
TWX SIM				6			X	
TWX TIM				6			X	
SIM-200	44			1		X		
MPM					4			X

NOTE:
CIM = CONCENTRATOR INTERFACE MODULE
MPM = MULTIPLE PORT MULTIPLEXER
PLI = PROGRAMMABLE LINE INTERFACE (PART OF DES SWITCH)
SIM = SUBSCRIBER INTERFACE MODULE
SIM-200 = SUBSCRIBER/CONCENTRATOR MODULE
TIM = TRUNK INTERFACE MODULE

is designated a SIM-200. The major components of a SIM-200 include line cards, scanner, PROM, RAM, Motorola 6800 microprocessor and a control panel.

The major components of the other network units used in DES are quite similar to the Telex SIM and SIM-200. The differences are primarily in the software and firmware utilized. In the other applications, multiplexing and interface compatibility are the primary functions. The Telex Trunk Interface Module (TIM) is used to interface with Western Union Telex exchanges. The device translates the CCITT "B" signalling into the internal signalling protocol of the DES. It accepts fifty 50-Baud Telex trunks and time-division multiplexes them into one 2400 b/s trunk towards the DES switching center. The Telex Concentrator Interface Module (CIM) is identical to the Telex SIM except that it is programmed to handle different variations of CCITT "B" signalling that are a characteristic of the older types of subscriber-line concentrator. An integral, synchronous modem can be a part of the SIM package.

TWX SIM is the designation given to the network element that performs a second order of multiplexing for TWX-V multiplexed character-streams. The TWX SIM has the capability to accept six TWX-V data streams and multiplex them into a single, synchronous 4800 b/s data stream. In essence, the TWX SIM is the same as a SIM-200 that is equipped with only medium-speed, asynchronous line-boards.

TWX TIM is the network element that multiplexes the TWX-Vs that provide the A/D conversion for trunks terminating on the AT&T and Bell Canada switching centers. The network elements interfacing AT&T trunks will no longer be in service for that purpose by mid-1981, when TWX transfer onto DES is completed. Physically, the TWX TIM is identical to the TWX SIM.

Another major network element is the Multiport Multiplexer (MPM) which has some commonality with the previous network elements. Its function is to multiplex four synchronous lines of multiplexed data streams and combine them into one 9600 b/s data line destined to a DES switching center. This device may be scheduled, if desirable, to be upgraded with minor retrofitting to handle six, rather than four, subchannels. The MPM assembly permits the inclusion of an integral 9600 b/s modem.

DES Switch Operation

At each of the DES switching centers, circuit switching is performed in several programmable front-ends (PFEs), on a time-division, byte transfer basis. The PFE switching process is initiated at the beginning of a call by the computer-controller which acts as the Call Processor. Each PFE consists of 64 Programmable Line Interfaces (PLIs), and each PLI has two ports which, singly or in combination, can terminate 9600 b/s serial, synchronous data-streams from the network elements, or from colocated or remote PFEs at the other three sites. The major componentry of a PLI consists of an M6800 microprocessor, 2 kbit PROM, 16 kbit RAM and dual interfaces to two internal 24-bit wide data and control buses. A pair of control microprocessors is used to supervise and control the individual PLI microprocessors.

The interaction of the PFE and the call processor is, briefly, as follows: A subscriber network element forwards origination and destination terminal addressing information through the various multiplexing levels to the PFE. The PFE passes this call-routing information in packet form to the Call Processor. The Call Processor, based on the information passed to it, informs the originating PFE where the called address is located. The PFE then sets up a time-division path to a PFE on the route to the destination terminal. During the course of a connection, the Call Processor does not play an active role. It comes into play again at the end of each call, when the PFE informs the Call processor that the Call has been terminated. It can be seen that the Call Processor, being relieved of the actual data transfer, can direct its attention to matters such as call-setup, call-completion, and logging for billing and post-diagnostic purposes.

Network Flexibility

All network elements, with the exception of the MPM, use RAM for program and data storage. This allows for the alteration of control characteristics and line configurations from the central switching center, by down-line loading from the Call Processor under automatic or manual control. In turn, this removes the need to dispatch field personnel to perform configuration and programming changes at remote concentrator/multiplexers. It should be noted that each of the remote units also has 1-2 kbits of PROM for bootstrapping and simple diagnostics. The combination of PROM and operational RAM memory has proven in the field to provide the desired flexibility and operability. For example, a line port on a TWX-V unit can accommodate either rotary dial, dual tone multi-frequency (DTMF) or keyboard addressing. Another example is the ability to interface easily with a variety of Telex exchanges which differ in call-supervision and call-addressing protocols, both in type and time duration. As previously described, the same generic multiplexer/concentrator is used for seven applications (TWX SIM, TLX SIM, SIM-200, TLX CIM, TLX TIM, TWX TIM, MPM), which greatly simplifies production and logistics. This universality also minimizes the effort required to change a unit's function from one use to another. In many cases, all that may need to be done is to connect the unit's line and trunk ports, and after down-line loading the unit becomes operational. At most, some line boards may need to be added or changed.

Many of the network elements in the DES are not for the exclusive use of one service, i.e. Telex or TWX. Instead, SIM-200, MPM, and PLI units are simultaneously used for both TWX and Telex connections. In fact, DES has the capability to handle the gamut of asynchronous data terminals since it is a programmable, software-based system.

Enhancements to TWX and Telex service on DES are in the planning stage. One of these will permit conversational, real-time interchange between the dissimilar Telex and TWX terminals. The DES can provide this interconnectibility by performing speed, code, and control-signal conversion. This differs from the current interchange service provided on Western Union's Infomaster®

which is a message-switched service, on a store-and-forward basis. More definitive call-progress signals may also be offered, so that subscribers will receive printed service signals defining the reason for failure to complete a call.

Serviceability and Reliability

Built into the DES is the capability to isolate and diagnose faults and line conditions. This is a prime necessity due to the distributed nature of the system. Diagnostic tools exist throughout the DES for both remote and local testing. Remote testing is exercised from four central system service positions, one in each DES center. For example, loopbacks can be effectuated from the central site at any remote unit, in any place in the hierarchical levels of the network. These loopbacks can be actuated so that the turn-around occurs either at the trunk or at the terminal side of multiplexers/concentrators, as desired. Another capability provided is that of the TWX-V concentrators to keep tally of all-trunks-busy conditions and periodically forward this information to the call processor for traffic analysis and grade-of-service monitoring. Off-line testing of connectivity, components, signals, and line-balance at the TWX-V can be initiated remotely. Furthermore, at TWX-V and SIM/CIM/TIM/MPM equipments extensive local diagnostic tests can be performed to localize faults down to the card level. It should be noted that down-line loading can also be used to clear software faults as well as to provide new system/service programming updates. The philosophy has been to centralize trouble reporting, clearing, and monitoring. This approach has proven effective in improving the efficiency of operational and maintenance activities.

The design of the DES network achieves high overall long-term system availability. The switching center design criterion was to attain 99.9% availability in terms of (non-planned) system down-time due to hardware failures. This was accomplished by providing redundant systems and subsystems within the PFEs and Call Processors. For example, the PFE is designed with redundant subsystems and an automatic switchover capability if one of the subsystems should fail. Moreover, the PFE monitors the Call Processor and provides automatic switchover in the event of a CPU or peripheral subsystem failure. The network elements are all microprocessor-based systems that have MTBFs, for their common segments, in excess of 15,000 hours. Per-line MTBFs are in excess of 5,000 hours for the various input-line types that are accommodated by the multiplexers and concentrators. Therefore, the typical Telex and TWX subscriber can expect the chain of equipment serving him to be in the operational state better than 99% of the time. Through the present, operability of the DES has approached the reliability and MTBF objectives.

Satellite Transmission Considerations

As an important part of its efforts toward better services, Western Union has consistently developed and implemented its own long-haul transmission facilities. In 1947 it established the first commercial line-of-sight microwave communications system, and completed its transcontinental microwave system in 1962. In 1974, it put into operation the first U.S. domestic communication-satellite system, which presently comprises 3 satellites, 7 transmit-receive earth stations, and numerous receive-only stations. The ownership and availability of both terrestrial and satellite networks, coast-to-coast, allows Western Union to make optimal choices of transmission facilities for its various services.

The system design considerations for DES included the requirement to use either terrestrial or satellite transmission facilities in any part of the network. Accordingly, it is necessary to minimize call-setup delays which might be induced by tandem satellite links. In traditional, hierarchic switching systems, selection codes are not forwarded to and between switches until the distant switch has acknowledged its readiness to accept the incoming selection code. The usual sequence is the following:

- Originating equipment seizes distant switch port,
- Distant switch transmits "proceed-to-send" signal to originating equipment,
- Originating equipment transmits selection code.

Thus, with multiple tandem switching, each link in the hierarchy involves a 1 1/2 round-trip transmission-delay in setting up a call. For each satellite link in the chain, this is approximately 1 second.

While DES is a hierarchical network, it involves switching only at the highest level; the other levels being functionally confined to multiplexing and concentration. Links between terminals and multiplexers/concentrators, those among multiplexers/concentrators and those between multiplexers/concentrators and switches, do not require the above interactions; and the transmission delay on these links is that of a single "hop" - i.e. about 270 ms for each satellite link.

Only the inter-switch links of DES involve the 1 1/2 round-trip delay in setting up calls. As a result, call-setup delays are minimized and do not generally differ significantly from those experienced in traditional networks.

Further, and finally, it should be noted that the DES network design only goes part of the way in the development of a distributed processing system which maximally exploits the broadcast nature of satellite transmission. Revised software and mildly enhanced nodal elements should fit well into the (as yet) emerging small earth station TDMA technologies.

80-0517

THE DIGITAL NETWORK OF AMERICAN SATELLITE CORPORATION

Townsend D. Breeden*
Edmund J. Habib

American Satellite Corporation

Introduction

American Satellite Corporation (ASC) will be the first of the nation's domestic satellite carriers to offer its commercial services via a digital network. Planning of the network conversion from Frequency Division Multiple Access (FDMA) to Time Division Multiple Access (TDMA) began in 1975 and was completed in 1978. The latter year also marked the beginning of hardware procurements that were used to convert the first three earth stations to digital operation. The conversion of the Los Angeles, San Francisco and New York earth stations was completed in the Fall of 1979 with installation of the central óffice equipment occuring in the Winter of 1980. Operational TDMA commercial service is scheduled to commence in mid-1980. This paper is intended to report on conversion and operational experiences.

Table 1
Service Arrangements

- Automatic Private Lines
- Outside Extensions
- Tie Lines
  - Manual
  - Automatic
  - Dial Repeating
- Foreign Exchange Circuits
- Common Control Switching Arrangements (CCSA)
  - Trunk Circuits
  - Access Lines
- Alternate Voice-Data (AVD)
  - 2400 BPS
  - 4800 BPS
- Simultaneous Voice-Data (SVD)
  - Low Speed TTY
- Medium Speed Data
  - 2400/4800/9600 BPS
  - Conditioned Private Lines
- High Speed Data
  - 50 Kbps-1.544 Mbps

Background

American Satellite Corporation, which was originated in 1972, initiated operations in 1974 with the types of services listed in Table 1. These service arrangements were offered to sectors of the United States serviced by earth stations and nearby central offices located in the metropolitan areas of New York, Dallas and Los Angeles. In the following years, the earth station at San Francisco was added as well as many dedicated systems employing their own earth stations. Today ASC operates a US domestic network as shown in Figure 1 and conducts business throughout the network as summarized in Figure 2. The four earth station locations identified above continue to support the general services of ASC

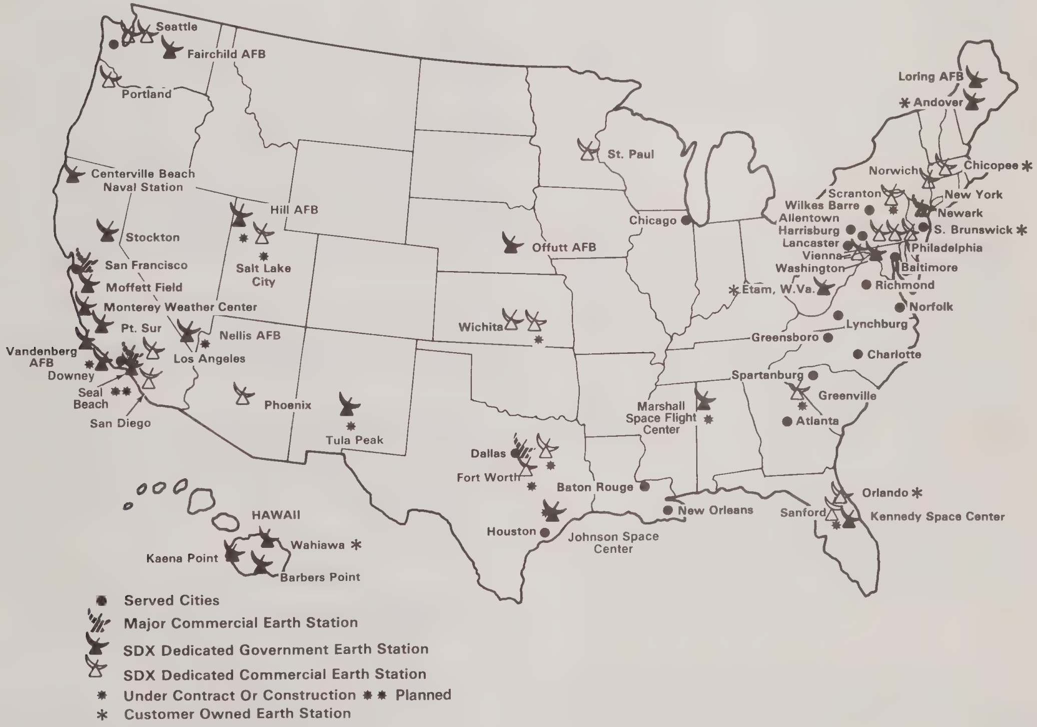
Seattle
Fairchild AFB
Portland
Centerville Beach Naval Station
Hill AFB
Stockton
San Francisco
Salt Lake City
Moffett Field
Monterey Weather Center
Pt. Sur
Nellis AFB
Vandenberg AFB
Los Angeles
Downey
Seal Beach
San Diego
Phoenix
Tula Peak
St. Paul
Chicago
Offutt AFB
Wichita
Dallas
Fort Worth
Baton Rouge
New Orleans
Houston
Johnson Space Center
Marshall Space Flight Center
HAWAII
Wahiawa
Kaena Point
Barbers Point
Loring AFB
Andover
Chicopee
Norwich
New York
Scranton
Wilkes Barre
Newark
Allentown
Harrisburg
S. Brunswick
Lancaster
Philadelphia
Vienna
Washington
Baltimore
Etam, W.Va.
Richmond
Norfolk
Lynchburg
Greensboro
Charlotte
Spartanburg
Greenville
Atlanta
Orlando
Sanford
Kennedy Space Center
Served Cities
Major Commercial Earth Station
SDX Dedicated Government Earth Station
SDX Dedicated Commercial Earth Station
Under Contract Or Construction
Planned
Customer Owned Earth Station

Fig. 1 Satellite Communications Network

"Copyright ©, 1980 by American Satellite Corp.

* Associate Fellow, AIAA.

Released to AIAA to publish in all forms.

shown in Figure 2 and, in that role, perform as a four node major path subnetwork. Since its implementation, the four stations, which are referred to as the General Services earth stations, have operated with the WESTAR space segment* in a Frequency Division Multiple Access (FDMA) mode.

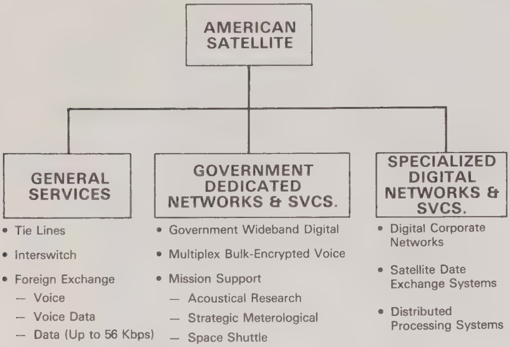
AMERICAN SATELLITE
GENERAL SERVICES
GOVERNMENT DEDICATED NETWORKS & SVCS.
SPECIALIZED DIGITAL NETWORKS & SVCS.
• Tie Lines
• Interswitch
• Foreign Exchange
— Voice
— Voice Data
— Data (Up to 56 Kbps)
— Audio
• Government Wideband Digital
• Multiplex Bulk-Encrypted Voice
• Mission Support
— Acoustical Research
— Strategic Meterological
— Space Shuttle
• Digital Corporate Networks
• Satellite Date Exchange Systems
• Distributed Processing Systems

Fig. 2 Family Tree of Business

Analyses indicated that improved service quality and utilization of the space segment could be realized through conversion to a Time Division Multiple Access (TDMA) technique. Further analyses indicated that the savings in space segment would more than offset the capital expenses required to convert to TDMA. For these two reasons, the planned conversion was initiated for three General Services earth stations in 1978 and the Dallas earth station in 1979. Access to the four earth stations from other locations was continued in the form of FDMA to limit the cost impact to smaller stations in the network.

Network and Service Considerations

A satellite network offering end-to-end communications services consists of four basic elements: the central office, the terrestrial interconnect, the earth station, and the satellite. For high capacity systems such as a General Services earth station it is necessary to site the station in a location where several satellite transponders of bandwidth can be cleared.** The siting process locates the earth station in an area characterized by low density microwave interference paths. Such a location is usually outside a major metropolitan area remote from potential customer locations. Therefore, the communications facility must be extended toward the metropolitan core area to access the customer. This process extends the high capacity capability of the earth station through the terrestrial interconnect path to a downtown central office to which local loop distribution can be made to each individual customer. Because the terrestrial interconnect must also be of high capacity it is usually in the form of a broadband microwave facility. The general discussion above describes all of the ASC General Service earth station implementations. A specific earth station-to-central office path for the Los Angeles area is shown in Figure 3. Because the earth stations were designed for FDM/FDMA the terrestrial microwave was configured in an FDM heirarchy. Converting to a digital network allows the designer a basic choice between: (1) digitizing in the central office and converting the total system to a digital transmission system or (2) maintaining the analog terrestrial network and providing the digital conversion in the earth station. To take full advantage of higher quality service, ASC selected alternative (1), and converted all three of the terrestrial elements comprising the transmission system. This selection results in a purely digital general services network extending from central office to central office in the four cities.

System Description

The central office-to-earth station digital transmission system is shown in basic form in Figure 4. The central office accepts various inputs including analog voice, data and wideband analog and develops a standard digital heirarchy.

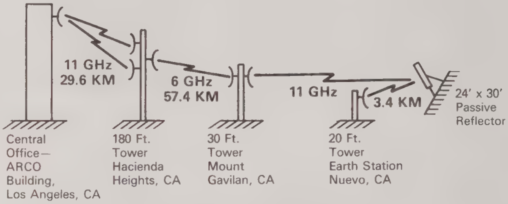
11 GHz
29.6 KM
6 GHz
57.4 KM
11 GHz
3.4 KM
24' x 30' Passive Reflector
Central Office— ARCO Building, Los Angeles, CA
180 Ft. Tower Hacienda Heights, CA
30 Ft. Tower Mount Gavilan, CA
20 Ft. Tower Earth Station Nuevo, CA

Fig. 3 Los Angeles Central Office—
Earth Station Transmission Path

The digital multiplexing heirarchy is based upon a fundamental transmission rate of 1.544 Mbps, or a T1 carrier rate. All basic service offerings—whether voice or data—are developed at lower bit rates and multiplexed together to form a T1 data stream. In this manner the system accepts direct data channels of 1.2, 2.4, 4.8, 9.6, 56 Kbps and higher rates as well as conventional analog voice/data which is digitized to 32 Kbps. Up to sixteen T1 data streams are combined in the digital multiplexer of the microwave equipment to form a 25.72 Mbps data stream. Three such data streams are combined with clock and overhead to form a composite 78 Mbps for 8-phase PSK modulation of the 6 GHz and 11 GHz microwave frequencies. The data streams are demultiplexed back to T1 streams at the terminal ends located at the central offices and the earth stations.

At the earth station the TDMA equipment accepts continuous rate T1 streams and outputs the same in bursts of 64 Mbps at 750 microsecond intervals. At the rate of 64 Mbps the satellite transponder is able to accommodate a maximum of 38-T1 data streams.

The earth station-satellite link parameters have been designed to support an uncoded bit error rate (BER) of 10^{-6}. Rate 7/8 rate coding is available which provides a BER improvement of better than 3 orders of magnitude on channels selected for high quality service. As the coding is applied on a selected T1 port basis, the overall transmission efficiency is retained at a high level approximating 90 percent.

System Implementation

Conversion of the transmission system required new equipment in the Central office, Microwave Interconnect and Earth Station.

Central Office (CO)

The major equipment elements are shown in Figure 5 and consists of (1) the voice/data (V/D) channel banks, (2) digital mux-demux, (3) the centralized clock system, and (4) the crossconnect and test facilities. Two types of channel banks are utilized. These are standard DS-1 commercial PCM channel and NIC (nearly Instantaneous Companding) providing digitization at 32 Kbps per channel. A centralized clock system has been implemented through the use of protected clock sources with frequency stabilities of one part in 10^{-10} per day. The clocks are locked to one of two input Bell DDS timing sources at each CO to ensure network synchronization.

---

* In 1979, American Satellite Corporation reached an agreement in principle with respect to partial ownership in the WESTAR System. In previous years ASC leased WESTAR transponders from Western Union.

** A single satellite transponder is nominally 36 MHz wide; therefore, a high capacity earth station must be cleared for at least 100 MHz of transmission bandwidth.

Microwave Interconnect

The existing analog microwave interconnect routes were overbuilt with high capacity 6 and 11 GHz digital radio channels. Each terminal includes its own mux-demux as well as the modems and radios as shown diagrametrically in Figure 6. The terminal interfaces with the Central office and Earth Station at the Tl level. Each system can accept up to 48 Tl data streams and combine them into a 8-phase PSK 78 Mbps data stream modulated onto the appropriate carrier. Space and polarization diversity schemes are employed with ''hitless' switching to achieve a design goal availability objective of 0.99994 or greater for a BER performance level of 1×10^{-6}.

Earth Stations. The earth station equipment includes the TDMA subsystem and standard transmit and receive chains consisting of Up/Down Converters, High Power Amplifiers, Low Noise Amplifiers, and the Equipment Shelter and Antenna. The input to the earth station is the multiple Tl data streams provided by the microwave digital radio. The output of the earth station is a C-band carrier frequency burst of 750 microseconds duration containing a TDMA frame format as shown in Figure 7.

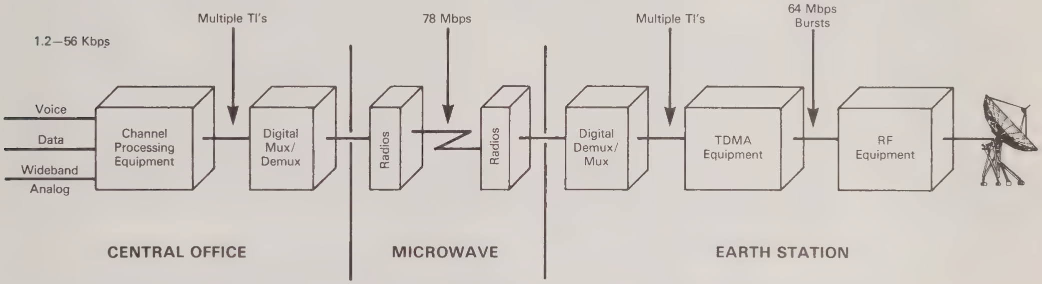
1.2—56 Kbps
Multiple Tl's
78 Mbps
Multiple Tl's
64 Mbps
Bursts
Voice
Data
Wideband
Analog
Channel
Processing
Equipment
Digital
Mux/
Demux
Radios
Radios
Digital
Demux/
Mux
TDMA
Equipment
RF
Equipment
CENTRAL OFFICE
MICROWAVE
EARTH STATION

Fig. 4 Terrestrial Digital Transmission System

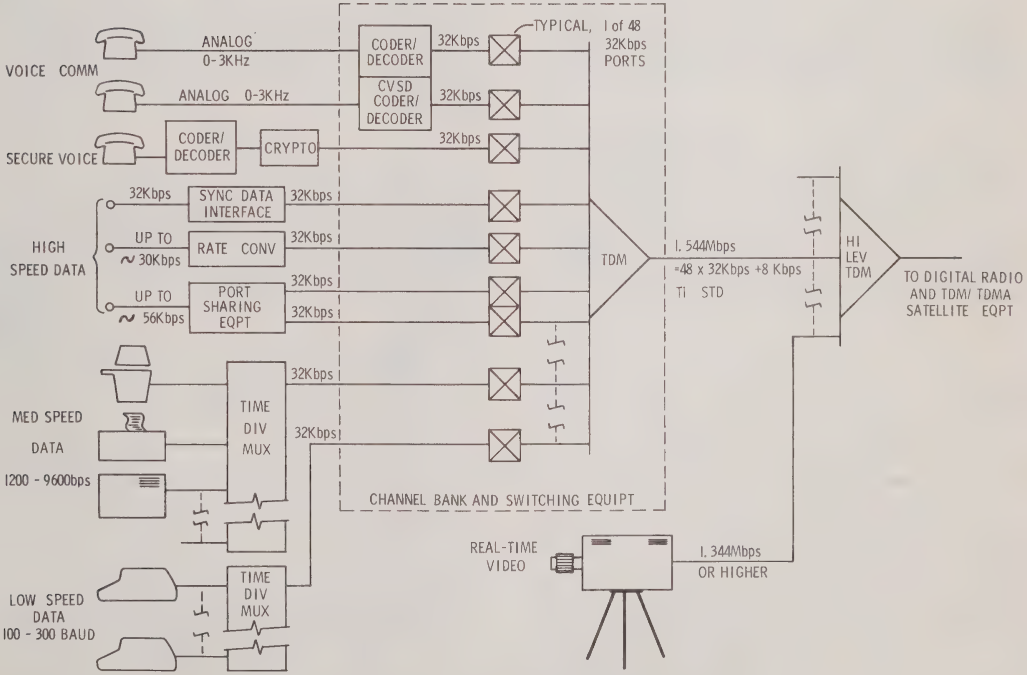
VOICE COMM
ANALOG
0-3KHz
ANALOG 0-3KHz
SECURE VOICE
CODER/
DECODER
CRYPTO
CODER/
DECODER
CVSD
CODER/
DECODER
32Kbps
TYPICAL, 1 of 48
32Kbps
PORTS
HIGH
SPEED DATA
32Kbps
SYNC DATA
INTERFACE
UP TO
~ 30Kbps
RATE CONV
UP TO
~ 56Kbps
PORT
SHARING
EQPT
TDM
1. 544Mbps
=48 x 32Kbps +8 Kbps
Tl STD
HI
LEV
TDM
TO DIGITAL RADIO
AND TDM/ TDMA
SATELLITE EQPT
MED SPEED
DATA
1200 - 9600bps
TIME
DIV
MUX
LOW SPEED
DATA
100 - 300 BAUD
CHANNEL BANK AND SWITCHING EQUIPT
REAL-TIME
VIDEO
1. 344Mbps
OR HIGHER

Fig. 5 Digital System Architecture

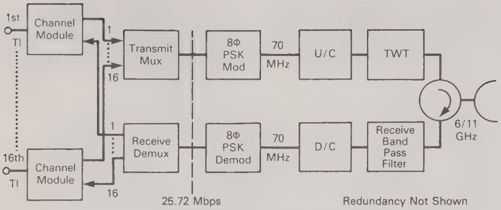
1st
Tl
Channel Module
1
16
Transmit Mux
8Φ PSK Mod
70 MHz
U/C
TWT
6/11 GHz
1
16
Receive Demux
8Φ PSK Demod
70 MHz
D/C
Receive Band Pass Filter
16th
Tl
Channel Module
25.72 Mbps
Redundancy Not Shown

Fig. 6 Terrestrial Digital Radio

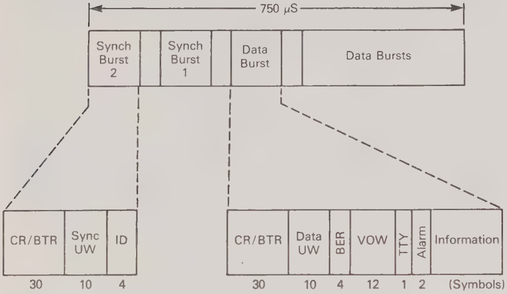
750 μS
Synch Burst 2
Synch Burst 1
Data Burst
Data Bursts
CR/BTR
Sync UW
ID
30
10
4
CR/BTR
Data UW
BER
VOW
TTY
Alarm
Information
30
10
4
12
1
2
(Symbols)

Fig. 7 TDMA Frame Format

TDMA Subsystem Implementation

The purpose of the TDMA subsystem is to provide the earth station transistion from the Tl data streams of the Terrestrial digital radio to a Phase Shift Keyed-Time Division Multiple Access (PSK-/TDMA) signal at the 70 MHz interface of the Up/Down Converters.

The TDMA subsystem can be separated into three basic sections as shown in Figure 8. The first section, consisting of the Mux/Demux equipment, includes the Time Interface Modules (TIMS) which contain individual Tl channel cards and compression/decompression buffers. Timing signals are received from the Mux/Demux to ensure that the proper Tl port transmits its compressed signal at the proper time interval indicated as a data burst within the frame format illustrated in Figure 8.

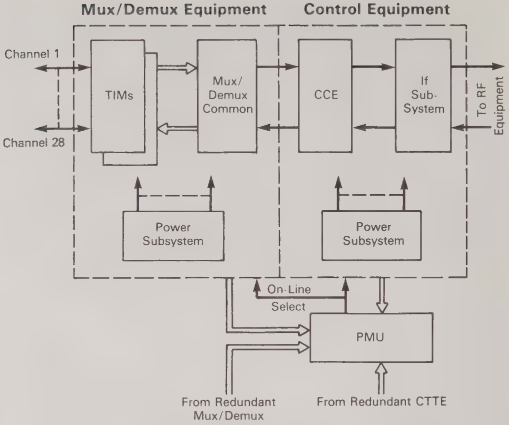
Mux/Demux Equipment
Control Equipment
Channel 1
Channel 28
TIMs
Mux/ Demux Common
CCE
If Sub-System
To RF Equipment
Power Subsystem
Power Subsystem
On-Line Select
PMU
From Redundant Mux/Demux
From Redundant CTTE

Fig. 8 TDMA Subsystem Block Diagram

The Mux/Demux equipment is controlled by the second section, the Common Control TDMA Equipment (CTE). The CTE performs the control frame formatting and QPSK modulation/demodulation functions.

The CTE and Mux/Demux equipment are monitored by the third section, the Performance Monitoring Unit (PMU). The PMU, which is based upon an 8085 microprocessor design, performs continuous monitoring of all on-line TDMA subsystem elements and provides routine loopback tests at periodic intervals to ensure proper operation. Redundancy switching and diagnostics are also provided by the PMU.

The TDMA subsystem of the earth station is configured to permit the distribution of individual Tl data streams to at least twelve accessing TDMA earth stations with up to 24 data bursts per frame. Additional operational flexibility provides for a minimum of 15 accesses from the same earth station at separate times within a single frame.

Conclusions

It is the intention of American Satellite Corporation to offer an improved service while achieving more efficient use of the satellite transponder. As a first step toward implementing this policy, the conversion of the ASC system to a digital network has been initiated. Experience to data indicates that the TDMA and microwave portions of the system are exceeding the objectives of an overall system bit error rate (BER) of 10^{-6}.

80-0518

NETWORK AND CONTROL FOR TACTICAL SATELLITE COMMUNICATIONS SYSTEM*

Randolph W. Bricker, Jr.**
J. Plumer Leiphart**
Booz, Allen & Hamilton Inc.
Bethesda, Maryland

Abstract

A conceptual system which provides immediate access (no control delay) for all users of a tactical satellite communication system is presented. The proposed distributed system will allow each user to transmit without delay by providing communication control at each earth terminal receiver. Each receiver will accept low data rate messages from all transmissions through a satellite and will sort them according to address, priority and further routing requests. The system will require no elaborate central control system, will transfer signals from one satellite coverage area to another, and will permit conferencing among its users.

I. Introduction

Consider the scenario of 50 to 300 globally distributed mobile earth platforms (surface ships, submarines and large aircraft) and major shore installations, (depicted in Fig. 1) which are to communicate essential, low data rate, secure information through communication packages located on satellites in a variety of orbits. Among a number of issues to be considered by the network architect is the type of system control (central or distributed) that would provide the best connectivity as well as the maximum acceptable time for a message, once formulated for transmission, to be sent and received by the intended party.

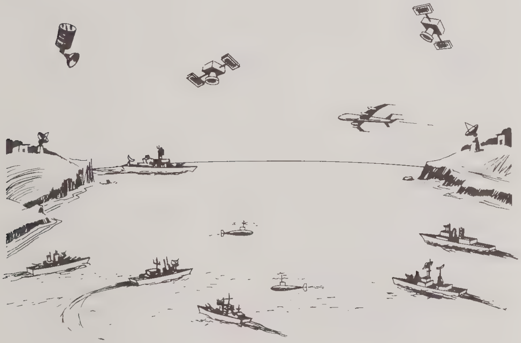

Fig. 1 Globally distributed mobile platforms and numerous satellites in a variety of orbits.

A centralized network with a node to assume the communication access function is practical in many cases. However, for a system having communication packages dispersed on satellites in a variety of orbits and with the majority of earth terminals in motion and scattered over the globe, a complex centralized system centered at a satellite or earth-terminal node may be inappropriate. Over a period of time, satellites accessible to users in a region would move to other global regions while others would orbit into the area. Such satellite movement might require excessive burdens on a system centered at the satellite. Central control earth stations could be vulnerable in a hostile scenario and if eliminated the total network could be rendered useless. Since, for this application, minimum control (e.g., maximum flexibility) is the best control, a distributed system is generally more appropriate.

The system architect must design the network to achieve an acceptable system response time. This time is defined as the maximum time required for delivery of an acceptable percentage of message traffic before perishable time is exceeded. (Perishability time is the time after which the receipt of a message is no longer of operational significance or is of such limited value as to render the message useless.) During critical operations or under crisis conditions perishability time for certain critical messages can be extremely short. During less stressful times, the message delivery time constraints can probably be relaxed. However, the system must be designed to perform satisfactorily during all levels of stress primarily because the system will undoubtedly be needed most when the threat level to the system is highest.

In recognition of the potential value of distributed network control with immediate access, a tactical satellite communications system has been conceptualized that provides these features through communication control at every (earth terminal) receiver (CCAR). CCAR is explained in three sections: a general

---

*This work was performed for the Special Communications Branch of the Naval Research Laboratory under Contract No. N00014-75-C-0041

**Member AIAA

Copyright © American Institute of Aeronautics and Astronautics, Inc., 1980. All rights reserved.

description of the system addressing the basic functions of the transmitters, satellites and receivers; the overall system considerations of efficiency, satellite handover, message routing and conferencing; and an example of a single satellite system.

II. CCAR System

A distributed CCAR system can provide for the unrestricted transmission from many (50 to 300) worldwide terminals with messages addressed to any or all terminals in the global satellite network. A segment of that network is shown in Fig. 2. At the earth terminal transmitter, each user can transmit low data rate messages (75 bps for data and 2400 bps for voice) without delay for establishing communication circuits. Large users would be allowed more than one access for both data and voice. After the message has been formulated, the user would provide the correct address, priority and further routing request (if necessary) to the message header, and would transmit the message immediately without network authorization.

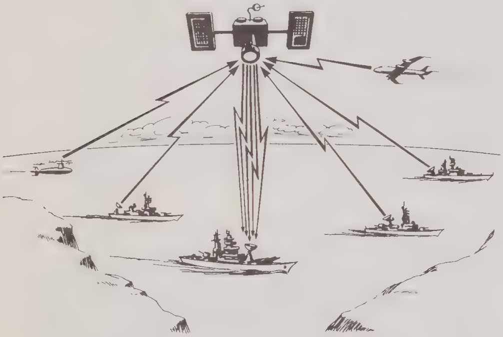

Fig. 2 Unrestricted transmission - multichannel simultaneous reception.

At the satellite, the messages are received through earth coverage antennas and channelized with a channel dedicated to each user. The term channel refers to a non-interfering communications link. Although a non-processing relay satellite would permit the objectives of the CCAR system to be realized (i.e., immediate access), on-board satellite processing is expected to be available on future military satellites for antijam enhancement and that processor can be used to format the downlink transmission. The satellite transmits the messages to all users through an earth coverage antenna.

At the earth terminal receiver, those messages with the receiver's address are promptly processed, sorted by both priority and further routing requests and acknowledged automatically. In force at all times but particularly useful during peak data traffic reception, the preassigned priority determines whether the message at the receiver is transferred directly to a teletype or vocoder or stored for later transferral when higher priority messages subside. For major tactical terminals which can expect a large volume of traffic, CCAR has a large number of parallel output lines to teletypes, facsimile receivers, voice terminals, computer inputs, and relays for further routing so that little or no time is spent in storage.

III. System Considerations

The general description of the CCAR system leads to a number of system considerations. These include transmission anarchy, system efficiency, satellite handover, message routing and conferencing.

At first glance, unrestricted transmission by every user in an uncontrolled manner to potentially every receiver might seem to be anarchy. However, this proposed system can operate without confusion due to advancing satellite technologies and present day microprocessor capabilities. As technology advances, the channel capacity of processors is expected to increase. Four channel satellite processors have been built, and a 100-channel processor is being developed.[1] Applications of inexpensive microprocessors using simple algorithms to make decisions are a reality today. For example, microprocessors are to be a part of the NAVSTAR GPS receiver design where they will receive sample data from six satellites in view, process the data and direct the receiver to lock on to the three satellites that provide the most accurate positioning.

The price for immediate access in the CCAR system is system inefficiency, particularly in bandwidth usage, numbers of satellite channels and expense of earth terminals. Since the system must accommodate the maximum uplink and downlink transmissions (i.e., when all users are communicating), anything less than total capacity operation is wasteful of bandwidth resources. A dedicated satellite channel per user requires a large capacity processor. Even with advanced technology, the cost and weight of such hardware is expected to be relatively high. To lower total system costs, it is desirable to tradeoff satellite complexity for terminal simplicity when considering a large number of terminals. The CCAR terminal, because it performs message control, is more expensive than simpler terminals. These inefficiencies may be too great for some requirements, but in a tactical environment where communications for the command and control of a limited number of mobile forces is extremely timely and where immediate access is highly desirable, such inefficiencies may have to be tolerated.

Since the scenario calls for communication packages on satellites in various orbits, a satellite designated for use in a particular theater may periodically go out of view and a new satellite would be designated. The handover operation in the CCAR system allows communication to be resumed among the users in a given region as soon as the users repoint their antennas to the newly designated satellite. The distributed control system, at the receiver, does not require the reestablishment of a network control as needed by a central control system, and with the automatic acknowledgment feature the CCAR users are quickly informed that their messages are received and that the new satellite network has been established.

Messages may be transferred from one satellite coverage area to another by message routing. Terminals wanting to communicate with each other, but not located within the same coverage area of a single satellite, may use an intervening terminal as a relay point by entering the appropriate header information. This routing is completed in real time if the relay earth terminal has two antennas; otherwise a delay will be incurred as the single relay antenna is redirected from one satellite to another and the stored message is retransmitted. Algorithms, which allow the transmitted terminal to optimally select satellites that are most likely being used by the intended receiver, are being investigated[2] and are not addressed here.

Conferencing may be established with the CCAR system by multiply addressing the message or by addressing it to a user type or group. As a proposed protocol, the terminal initiating the conference would be the designated conference leader and, after receiving the responses to his initial statement which may have been received simultaneously but sorted, stored, and retrieved by the receivers' microprocessors as appropriate, may make another statement, thus eliminating a chaotic situation.

IV. System Illustration

As an example of a single satellite system, Fig. 3 shows a representative CCAR system, which is intentionally reduced to a channel capacity of seven for discussion purposes. Although inconsistent with CCAR but out of practical consideration to today's limited satellite capacity, time division multiple access (TDMA) for some users is proposed. As the system grows with increased processor capability, TDMA will be eliminated so that the transmitter may use totally frequency division multiple access (FDMA) or code division multiple access (CDMA) for continuous transmission.

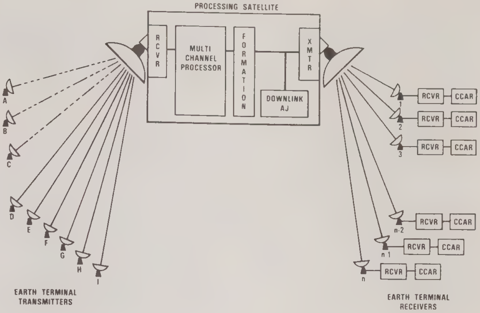

Fig. 3 Tactical satellite communication system using CCAR

Of the nine transmitters in the figure, six have unrestricted access to the system using FDMA or CDMA. The remaining three transmitters use preassigned time blocks (TDMA), the length of which is determined by the requirements of the intended system. Even when the time block control is required the only time delay is at the transmitter and no time is wasted bringing the receiver on-line.

At the satellite, the uplink signals are received, processed and retransmitted. The received signals are channelized by the appropriate uplink format (either FDMA, TDMA, or CDMA) and processed by the seven channel on-board processor. Because the satellite processor already exists for protection against jammers, a portion of that processor can be used for downlink signal formation. Although shown as earth coverage antennas, the satellite up- and downlink antennas may provide greater received (G/T) and radiated (EIRP) capabilities by hopping antenna beams of greater gain. This will permit more modest earth terminals but cause additional delay to the desired immediate access objective.

The satellite processor output can provide a number of signal formations for transmissions with one final format to be received and processed by all CCAR users. These downlink signal candidate formations are highly dependent on specific program requirements as well as cost and technology considerations. Several downlink possibilities are briefly presented.

A TDMA downlink would provide the least complicated receiver design. In a TDMA downlink system, the receiver would require fewer independent parallel down conversions since one TDMA channel could service several users. As a result, the cost of the receiver would be less than the cost of receivers with alternative downlink designs. A TDMA downlink can be designed to be compatible with a TDMA uplink but to accommodate the FDMA/CDMA uplink, a small delay of several bit periods at the satellite is required.

FDMA and CDMA are downlink access candidates that would provide immediate access, but for a multichannel output (50 to 300) the hardware impact to both the satellite and receivers is substantial. For a CDMA downlink, a combination of time and frequency hopping spread over a wide bandwidth with hopping patterns unique to each receiver could provide essentially immediate access to the receivers. As long as the downlink data rate accommodates the total uplink data rate (75 and 2400 bps per access) in real time, little storage on the satellite is required and almost negligible delay occurs.

There are many ways to configure the CCAR receiver, but the final configuration will depend on total system requirements and cost considerations. One conceptual design for a CCAR terminal is shown in Fig. 4. At the receiver the organized data stream is demultiplexed, the multichannel output is placed in temporary storage, and simultaneously the received messages are acknowledged, all automatically. To provide instantaneous (other than propagation time) and simultaneous reception of the signals, simple digital hardware (microprocessors) using simple algorithms can efficiently sort through this information.

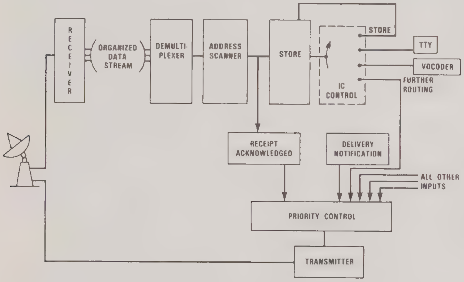

Fig. 4 CCAR terminal functional block diagram.

The time in storage depends on the priority of the message and number of output circuits. At major terminals, CCAR will have a large number of parallel output lines so that little or no time is spent in storage, while at minor terminals where message traffic is considerably less only a few output lines would be necessary. When the message is transferred from storage to output lines, a second acknowledgment, called a delivery notification message, is sent back to the user who transmitted the message. The acknowledgment, delivery notification, and all other inputs to the transmitter are prioritized for transmission by the transmitter.

V. Summary

In keeping with the large number of alternative SATCOM system configurations being studied to provide essential military communications links with tolerable vulnerability, the consideration of a scheme that allows any surviving user of a system to use any surviving satellite with the compatible communications package has significant benefits. If, in addition, it provides the user with a better responsiveness when all assets are in place, even better. The days when anyone with a receiver and transmitter could communicate with anyone else who could "come up on" the same frequency may be gone, but as we move toward the other extreme of communication specialization, dependence on four parties (sender, receiver, satellite and control) may be too high a price to pay for maximum satellite throughput. CCAR may just be the simple alternative.

Acknowledgement

The authors thank H. Clark Stroupe and James R. Conrad for their encouragement and helpful suggestions.

References

1. D. M. Boronson, et al.: "A Surface Acoustic Wave Demodulator for MFSK Signals," 1979 Conference Record. Washington, D.C., National Telecommunications Conference, November 1979. P. 33.6. (IEEE Catalog Number 79CH1514-9).

2. R. S. Orr and M. Meen, "Connectivity in Multisatellite Networks," 1979 Conference Record. Washington, D.C., National Telecommunications Conference, November 1979. p. 11.2. (IEEE Catalog Number 79CH1514-9).

80-0519

19 AND 28 GHZ PROPAGATION CONSIDERATIONS AFFECTING SATELLITE COMMUNICATIONS SYSTEM DESIGN

H. W. Arnold, D. C. Cox, H. H. Hoffman and R. P. Leck
Bell Laboratories
Crawford Hill Laboratory
Holmdel, New Jersey 07733

Abstract

Attenuation, dispersion and depolarization of 19 and 28 GHz signals from a COMSTAR satellite are measured at Bell Laboratories, Crawford Hill, New Jersey. Cumulative distributions of attenuation for one year are presented. No evidence has been found of variable amplitude or phase dispersion due to multipath or resonances in the propagation medium. The linear polarization orientation that minimizes depolarization is usually within a few degrees of vertical or horizontal at the earth terminal. Depolarization for fixed vertically and horizontally polarized signals is very low, usually below -35 dB.

Introduction

Earth-space propagation phenomena have a large effect on the design of satellite communications systems above 10 GHz. Perhaps the three most important of these are attenuation, dispersion, and depolarization. Attenuation over the free space spreading loss is due largely to rain.[1] Dispersion is a potential limitation to the use of high bit rate digital signals in the wide bandwidths available around 20 and 30 GHz. Depolarization due to rain and ice crystals[1,2] is a source of crosstalk in dual polarization systems. This paper presents results from measurements of these propagation phenomena at Bell Laboratories, Crawford Hill, New Jersey, using 19 and 28 GHz beacons on the COMSTAR satellites.[3-5] Other results from this experimental program are in References 6 through 10.

The Experiment

Parameters of the experiment are summarized in Table I and described in detail in References 3 through 5. Rain attenuation[8] is measured by comparing received signal levels in clear air with received levels during attenuating propagation events.

Phase and amplitude dispersion[10] over a 528 MHz bandwidth is measured using the 28 GHz carrier and coherent sidebands. An indication of dispersion over a 9.5 GHz bandwidth results from the measurements on the 19 and 28 GHz carriers.

The polarization switching of the 19 GHz beacon signal allows measurement of the amplitudes and relative phases of the two received signal components copolarized with the transmitted signals and of the two signal components crosspolarized to the transmitted signals. The diurnal variation of the clear air residual crosspolarized signals is repeatable and, since amplitudes and phases are measured, the residuals can be removed from depolarization events by vector subtraction. The complete set of transmission parameters determined from the 19 GHz measurements is used to calculate depolarization* for signals with polarizations different from those transmitted by the COMSTAR satellite.[7,9] The calculations involve decomposing the desired different incident polarizations into components aligned with the measured polarizations, determining the medium effects on the components from the measured amplitudes and phases, and recombining the components back into the desired incident polarizations. The only assumption required for these calculations is that the propagation medium is linear so that superposition is applicable.

The calculated transmission parameters are equivalent to those that would result if the polarizations of the satellite transmitter and earth receiver were rotated in synchronism to any desired incident angle. Statistics relating attenuation and depolarization are accumulated from the direct measurements at 21 degrees incident polarization and from calculations for other incident polarizations.

The data reported here were recorded on digital magnetic tape and span the year May 18, 1977 to May 18, 1978. The overall

---

*Depolarization in dB is defined as

$$20 \log_{10} \frac{E_x}{E_c}$$

, where E_x is the amplitude of the E field component of the received signal that is crosspolarized (orthogonal) to the E field of the transmitted signal and E_c is the amplitude of the E field component of the received signal that is copolarized (aligned) with the transmitted signal.

Copyright © American Institute of Aeronautics and Astronautics, Inc., 1980. All rights reserved.

data base is nearly complete on the digital tape or backup chart recordings; only three propagation events have data missing after lightning-induced failure of the antenna tracking electronics or because of failure of primary ac power toward the end of the three storms. These parts of three events spanning < 15 minutes at > 10 dB and < 13 minutes at > 20 dB are not a significant part of the overall data base since the times are smaller than the year-to-year variation**

Attenuation

Attenuation produced by rain is sometimes severe on earth-space paths at 19 and 28 GHz. A typical attenuating propagation event resulting from the passage of a thunderstorm through the COMSTAR-Crawford Hill path is illustrated by the chart recordings in Fig. 1. The polarizations 21 degrees from vertical and horizontal are indicated as V and H on this figure. Time in GMT runs from right to left with 10-minute and 1-minute intervals marked by the square timing waveforms. The top trace is the 28 GHz copolarized signal attenuation. The middle and bottom traces are the 19 GHz copolarized signal attenuations. Strong rain attenuation is evident between 11:00 and 11:20, between 11:30 and 12:00 GMT, and between 13:00 and 13:20.

CRAWFORD HILL, N.J. 8-12-78

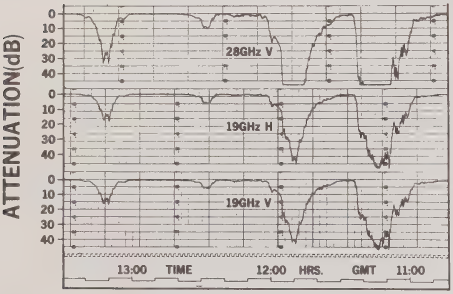

Figure 1: Typical rain attenuation event

One-year cumulative distributions of attenuation at 19 and 28 GHz are shown in Fig. 2. These distributions indicate the total time during the year that a given attenuation level was exceeded. On the right-hand ordinate, the times are converted to a percentage of the total 1-year period. If the attenuation axis is interpreted as the fading margin of a radio link, then these curves yield the link outage time (or percentage) caused by rain attenuation.

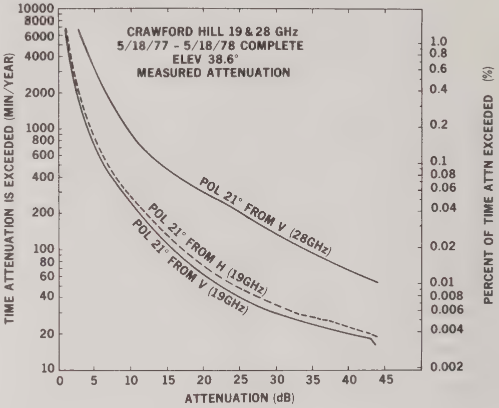

Figure 2: One-year attenuation distributions

As an example, at 19 GHz with transmitted polarization 21 degrees from vertical, measured attenuation exceeded 20 dB for 62 minutes of the year (0.012 percent). For the orthogonal polarization, 21 degrees from horizontal, 20 dB attenuation was exceeded for 72 minutes (0.014 percent). This increase is due to the predominantly horizontal orientation of the major axes of the raindrops, as is discussed later. At 28 Ghz with polarization 21 degrees from vertical, the attenuation exceeded 20 dB for 310 minutes (0.06 percent).

The relation between measured 19 and 28 GHz attenuations may be examined in several ways. The so-called statistical relation is a set of paired 19 and 28 GHz attenuations that are exceeded for equal amounts of time. Points obtained from the attenuation distributions in Fig. 2 are plotted in Fig. 3 as a series of open circles.

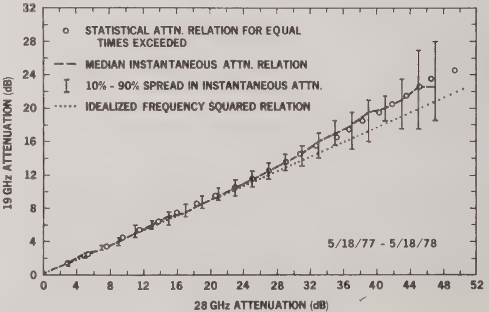

Figure 3: Two-frequency attenuation relations

** The missing data is estimated by considering (1) the data records up to the time of failure, (2) similar events, and (3) the same events recorded on a companion experiment[11] not experiencing a failure.

The instantaneous attenuation relation may be determined from simultaneous data recordings of attenuation determined at the two frequencies. This instantaneous relation is also shown in Fig. 3. The dashed curve indicates the median 19 GHz attenuation observed for values of 28 GHz attenuation. The bars in the figure indicate the span between the 10 percent and 90 percent points in the distribution of 19 GHz attenuations observed for the 28 GHz attenuation values. The statistical relation and the median instantaneous relation are essentially identical.

The dotted line on Fig. 3 is the line for $A_2 = (f_2/f_1)^2 A_1 = 2.25A_1$, where A_1 is the attenuation in dB at frequency f_1 = 19.04 GHz and A_2 is the attenuation in dB at frequency f_2 = 28.56 GHz. The relationships between the measured attenuations depart from this frequency squared relation, particularly at high attenuation. The observed A_2/A_1 ratio is 2.1 up to $A_1 = 20$ dB and is lower for higher attenuations. These results agree qualitatively with theoretical results relating attenuation and rain rate.[1]

Dispersion

A gross indication of amplitude dispersion is obtained from the results in Fig. 3. The small spread in the instantaneous attenuation relationship indicates that dispersive mechanisms such as multipath propagation or resonances in the medium are absent and that attenuation is dominated by the bulk absorption characteristics of rain.

Phase measurements were also made between three tones (carrier and sidebands) spaced over a 528 MHz bandwidth at 28 GHz, and between 28 and 19 GHz carriers. A sample of measurements during a thunderstorm is shown in Fig. 4. The four middle traces show the attenuations of each of the three tones at 28 GHz and a carrier at 19 GHz. The two upper traces indicate the phase measured between the three 28 GHz tones. The rapid fluctuations are attributable to the low signal-to-noise ratio due to attenuation at 28 GHz. Phase dispersion is less than 4 degrees over the 264 MHz tone spacing.

The lower trace indicates the phase between 19 and 28 GHz carriers. This measurement is contaminated by satellite motion, but indicates phase dispersion on the order of 60 degrees at 30 dB attenuation over the 9.5 GHz tone separation. This wideband result is consistent with the narrower bandwidth observation.

These results are typical of all observations. Statistics accumulated from many events indicate that phase dispersion across a 528 MHz band at 28 GHz is below 5 degrees for attenuations less than 45 dB. This minimal dispersion can be attributed to the stable bulk phase shifting properties of rain.

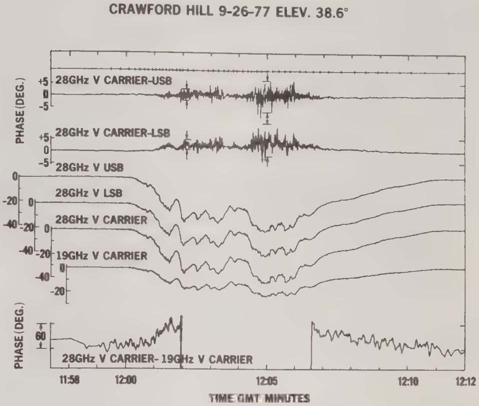

Figure 4: Phase variations during typical rain attenuation event

Depolarization

Crosstalk from medium-induced depolarization may be a significant problem for satellite communication systems employing dual-polarization frequency reuse. Since system outages occur when specific attenuation OR depolarization levels are exceeded, the experimental data were summed to indicate the amount of time and percentage of time in the year that a given pair of attenuation OR depolarization levels was exceeded. These results are shown in Figures 5 and 6 for 19 and 28 GHz incident polarizations oriented 21 degrees from vertical. Attenuation is plotted on the abscissa and time on the ordinate with depolarization as a parameter. The bottom curves in Figures 5 and 6 are for the lowest depolarization level that was never exceeded. The bottom curves are, then, the cumulative distributions of attenuation presented earlier.

To illustrate the use of these curves, consider the 19 GHz results shown in Fig. 5. The bottom curve indicates that attenuation exceeded 20 dB for 62 minutes of the year. A dual-polarization link capable of operating with 20 dB attenuation and -15 dB depolarization would experience 65 minutes outage, a small increase over that due to attenuation alone. A system tolerant of only -20 dB depolarization, however, would experience 100 minutes outage, almost twice the outage time from attenuation considerations alone. Thus, depolarization is clearly a problem to be considered seriously.

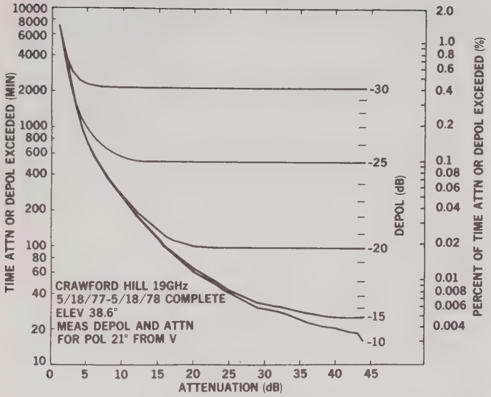

Figure 5: 19 GHz attenuation-depolarization distribution.

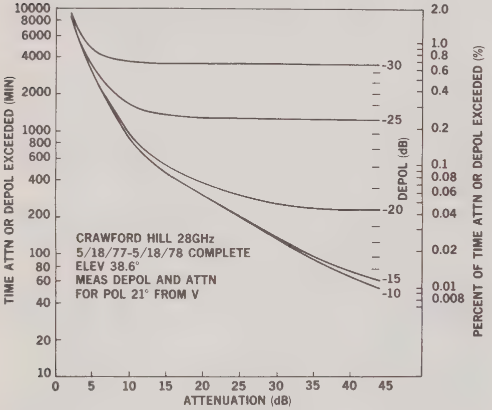

Figure 6: 28 GHz attenuation-depolarization distribution.

As described earlier, depolarization at 19 GHz may be calculated for any incident polarization. This technique was used to examine every data sample in the one-year digital data base to determine those incident linear polarizations yielding instantaneously minimum depolarization. These depolarization minima occur when the incident polarization is aligned with the average symmetry axes of the raindrops or ice crystals along the path. Figure 7 illustrates the relation between the angle of the depolarization minimum and the copolarized signal attenuation. The middle curve indicates the median angle for each attenuation value. Eighty percent of the data fell between the upper and lower curves. These results show that incident polarizations producing minimum depolarization are clustered around the local vertical and horizontal, as seen at the earth terminal. For 19 GHz attenuations exceeding 15 dB, when rain is the dominant source of depolarization, the optimum incident polarizations were within 3 degrees of local vertical and horizontal more than 80 percent of the time. At lower attenuations, when ice depolarization becomes dominant, the spread around local vertical and horizontal increased to nearly ±10 degrees.

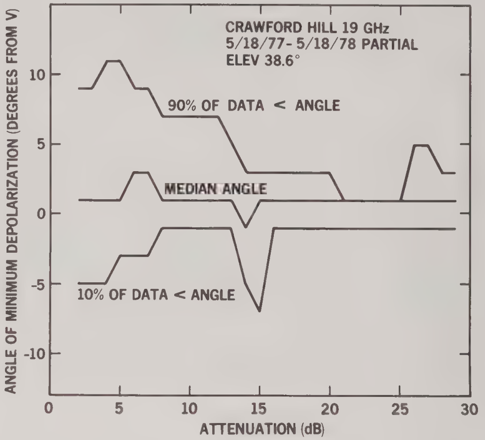

Figure 7: Angle of minimum depolarization as function of rain attenuation

The greater angular spread of the average symmetry axis at low attenuations is further evident in Fig. 8. This figure illustrates the observed angular distribution of the more-nearly-vertical angle of minimum depolarization for several ranges of copolarized attenuation. The three curves illustrate, for each attenuation range, the total time during the year that the angle was within each 2-degree bin. The upper curve shows the angular distribution for copolarized attenuation less than 1.5 dB. Here all significant depolarization is produced by ice, since depolarization from rain is below -40 dB. These ice-dominated data are excluded from Fig. 8. The two lower curves indicate the angular distributions for copolarized attenuations of 6 to 10 dB and 10 to 30 dB. The decreased spread at higher attenuations is quite evident. The occasional significant deviation from vertical of the average symmetry axis of ice crystals is also evident in the tails of the distribution for attenuations less than 1.5 dB.

Statistics were accumulated relating attenuation and depolarization at 19 GHz for the optimum incident polarizations described above and for several fixed linear polarizations. The median relations between attenuation and depolarization are shown in Fig. 9 for these incident polarizations. The upper curve indicates the depolarization observed at an incident polarization 45 degrees from vertical.

Results for circular polarization were essentially identical.[7] The next two curves show the actual measured data at incident polarizations 21 degrees from horizontal and vertical. Going downward, the solid and dotted curve pair indicates the depolarization for fixed vertical and horizontal incident polarizations. The solid and dashed curve pair which starts at the lowest depolarization levels illustrates the depolarization seen at the instantaneously-optimized linear polarizations discussed earlier.

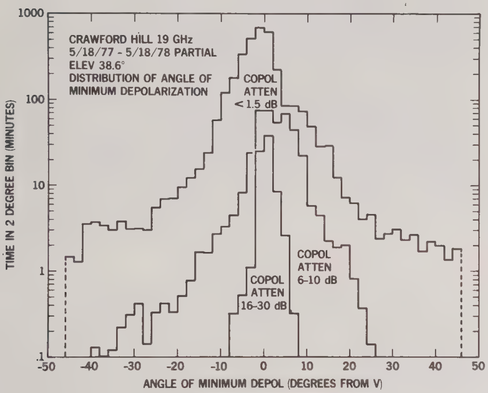

Figure 8: Angular distribution of depolarization minimum

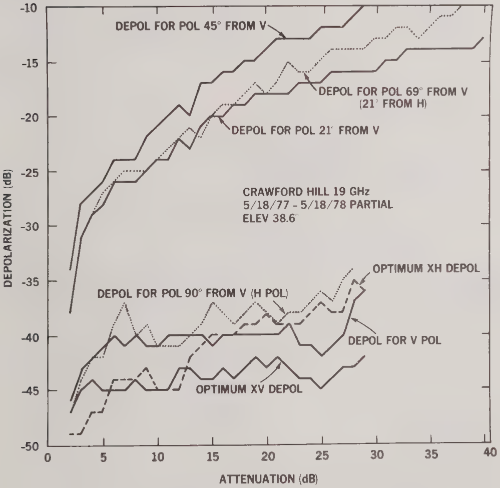

Figure 9: Attenuation-depolarization relations for several incident polarizations

The variation in depolarization with incident polarization angle is quite evident in Fig. 9. Instantaneous linear polarization optimization has clearly reduced depolarization, often lowering it below -40 dB to the limits of measurement precision. More interesting, perhaps, is the low depolarization (below -35 dB) observed at fixed vertical and horizontal incident polarizations. These results are consistent with the previous observations of the narrow angular distribution of the average symmetry axes of ice and rain. Linear polarization incident at 45 degrees to vertical or circular polarization, however, result in maximum depolarization; e.g., at 20 dB attenuation the median depolarization was -13 dB. These results show the need for careful choice of incident polarizations to all earth terminals.

Conclusions

Rain attenuation poses significant obstacles to reliable earth-space link performance at 19 and 28 GHz. For the COMSTAR-Crawford Hill path, a 20 dB attenuation margin would be needed to achieve 0.06 percent outage at 28 GHz. Spatial diversity is clearly needed to achieve reliable link performance.

Phase and amplitude dispersion measurements indicate an absence of dispersive mechanisms other than the frequency dependent bulk absorption and phase shifting properties of rain. Thus, dispersion should not significantly affect the design of wideband satellite links.

Depolarization can produce significant cross-talk on dual-polarization links. Outage time may be doubled on a link with 20 dB attenuation margin if it can tolerate simultaneously only -20 dB depolarization. This depolarization is maximized for incident polarizations oriented 45 degrees to local horizontal at the earth terminal and for circular polarization. Use of vertical and horizontal incident polarizations reduces depolarization significantly, usually to below -35 dB. Spot-beam satellite antennas can permit such polarization optimization for all RF links simultaneously.

REFERENCES

1. D. C. Hogg and T. S. Chu, "The Role of Rain in Satellite Communications," Proc. IEEE, 63, September 1975, pp. 1308-1331.

2. D. C. Cox, H. W. Arnold and H. H. Hoffman, "Depolarization of 19 and 28 GHz Earth-Space Signals by Ice Particles," Radio Science, 13, May through June 1978, pp. 511-517.

3. D. C. Cox, "An Overview of the Bell Laboratories 19 and 28 GHz COMSTAR Beacon Propagation Experiments," BSTJ, 57, May through June 1978, pp. 1231-1255.

4. T. S. Chu, R. W. Wilson, R. W. England, D. A. Gray and W. E. Legg, "The Crawford Hill 7-meter Millimeter Wave Antenna," BSTJ, 57, May through June 1978, pp. 1257-1288.

5. H. W. Arnold, D. C. Cox, H. H. Hoffman, R. H. Brandt, R. P. Leck and M. F. Wazowicz, "The 19 and 28 GHz Receiving Electronics for the Crawford Hill COMSTAR Beacon Propagation Experiment," BSTJ, 57, May through June 1978, pp. 1289-1329.

6. H. W. Arnold and D. C. Cox, "Some Results from 19 and 28 GHz COMSTAR Beacon Propagation Experiments," Proceedings of the Seventh AIAA Communications Satellite System Conference, San Diego, California, April 27, 1978.

7. H. W. Arnold, D. C. Cox, H. H. Hoffman and R. P. Leck, "Characteristics of Rain and Ice Depolarization for a 19 and 28 GHz Propagation Path from a COMSTAR Satellite," IEEE International Conference on Communications (ICC '79), Boston, Massachusetts, June 10, 1979 to June 14, 1979, and to be published in IEEE Trans. Antennas and Propagation.

8. H. W. Arnold, D. C. Cox, H. H. Hoffman and R. P. Leck, "Rain Attenuation Statistics from a 19 and 28 GHz COMSTAR Beacon Propagation Experiment: One Year Cumulative Distributions and Relationships Between the Two Frequencies," IEEE Trans. on Communications, COM-27, Nov. 1979, pp. 1725-1728.

9. H. W. Arnold and D. C. Cox, "Dependence of Depolarization on Incident Polarization for 19 GHz Satellite Signals," BSTJ, 57, November 1978, pp. 3267-3276.

10. D. C. Cox, H. W. Arnold and R. P. Leck, "Phase and Amplitude Dispersion for Earth-Space Propagation in the 20 to 30 GHz Frequency Range," Submitted to IEEE Trans. on Antennas and Propagation.

11. H. W. Arnold, D. C. Cox and D. A. Gray, "The 19 GHz Receiving System for an Interim COMSTAR Beacon Propagation Experiment at Crawford Hill," BSTJ, 57, May through June 1978, pp. 1331-1339.

TABLE I

Parameters of this Experiment

COMSTAR Satellite Beacon - 95 Degrees W Longitude		
Frequencies	19.04 GHz	28.56 GHz
Polarization	Switched between two orthogonal linear	Linear (aligned with one 19 GHz)
Modulation	1 kHz Polarization Switching	264.4 MHz Phase (coherent with carrier)
Crawford Hill Receiving Facility - 40.39 Degrees N Latitude, 74.19 Degrees W Longitude		
Altitude	115 Meters	
Climate	Continental Maritime	
Antenna	7-Meter Parabola	
Polarization	Dual Linear	Dual Linear
Beamwidth	0.15 Degrees	0.1 Degrees
Path Azimuth	210.5 Degrees	
Path Elevation	38.6 Degrees	
Path Polarizations	Rotated 21 Degrees from Vertical and Horizontal	Rotated 21 Degrees from Vertical
Receiver Channels	Two Copol Two Xpol	One Copol Carrier Two Copol Sidebands One Xpol Carrier
Received S/N in Clear Air		
Copol Carrier Channels	>60 dB	>60 dB
Copol Sideband Channels	-	>53 dB
Xpol Carrier Channels	>70 dB	>70 dB
Residual Received Xpol due to Beacon and Receiving Antennas (over entire -3 dB beamwidth)	<-35 dB	<-35 dB

80-0520

RAIN ATTENUATION OVER EARTH-SATELLITE PATHS: A SEASONAL, OCEANIC MODEL

Nathaniel E. Feldman,*
Howland H. Bailey,** and
Ralph E. Huschke†
Science Applications, Inc.
Los Angeles, CA 90067

Abstract

This analysis of precipitation-attenuation over earth-satellite paths for ocean and coastal terminals extends a model proposed by R.K. Crane. Refinements to correct for local measured total rainfall and frequency of occurrence are proposed. The authors convert Crane's model to a seasonal one and extend it up to the 6 to 36 percent of the time region. Four maps of the world's oceans show the nine precipitation-rate regions by season. Four world maps of mean freezing height adequately present these seasonal inputs to the model. A method for estimating the outage duration distribution is proposed and used to estimate the median and mean daily outage durations and the average number of outages per day.

Introduction

This paper summarizes a study(1) of rain attenuation for ocean and coastal terminals performed for the Naval Electronics Systems Command. Starting with the best of the existing precipitation models (2,3), one proposed by R.K. Crane, we utilized readily available meteorological data (4-9) to refine his model further.

We do not now have and will never have enough real data e.g. at least 10 to 15 years of satellite beacon measurement data are required to estimate the infrequent, extreme events, at each geographic location at each frequency and for every elevation angle of interest. Thus we have no choice but to model the rain attenuation as a function of these parameters. However, more experimental data will ensure better models.

If we could specify the rain rate R over each element of the earth-to-satellite path and properly characterize the rain (by drop size distribution, shape of drops, canting angle due to wind, the temperature of the water drops) at every instant, theory permits us to calculate rather accurately the resultant attenuation A as a function of frequency. Using the formula $A = aR^b$ for each element of the path (10), one could in principal calculate the overall path attenuation. This approach can best be described as an exact solution to a theoretical problem. Even over short terrestrial paths, it has proven prohibitively costly and complex to evaluate all the necessary parameters, thus some surrogates must be used. The model recently developed by R.K. Crane(2,3) uses surrogates to provide world-wide estimates for earth-satellite paths. Models such as the one in Reference 11 give excellent results for a specific location e.g. Washington, D.C., but cannot easily be extended world-wide because the inputs are not readily available. Thus we started our study using Crane's rain-rate model.

"Rain gauges," despite the nomenclature, measure total precipitation, liquid and frozen. For snowfall, the precipitation amount is the liquid water equivalent of the snow. One measures it either by melting or weighing the snow. Precipitation amounts for snow are generally less reliable than for rain. Crane's model uses one-minute surface point precipitation-rate distributions, R_p. Although Crane refers to his model as a rain-rate model, we prefer to call it a precipitation-rate model.

Definition of the Nine Precipitation-rate Regions

Some modifications of Crane's climate types (denoted by the prime symbol in the following list) and of the precipitation-rate distributions assumed typical of those climate types proved necessary. The basic guidelines used for delineating the nine ocean precipitation rate regions were as follows:

A', Polar Ice Cap - The Arctic Basin portion of Crane's type A (Polar Tundra) climate; over ice-covered oceans and significantly poleward of the paths of most major extra-tropical cyclones; insignificant precipitation amount and very low frequency. Differs from Crane's type A in that it excludes the summertime precipitation regime found over continental tundra.

B', Polar Maritime - The maritime portions of Crane's type B (Polar Taiga) climate; the transition zone between the ice-cap and temperate maritime climates, located along the sea-ice fringe. Average precipitation about 1 mm/day; high frequencies of light, nonconvective precipitation is possible. Frequencies of high precipitation rates should be much less than indicated by Crane's distribution for type B, because the latter distribution includes a convective component found over continents much more frequently than over the polar oceans.

F, Subtropical Arid - Primarily the westward extensions of the subtropical continental deserts; poleward boundaries can be highly variable from year-to-year (e.g., off the California and Chile coasts); average precipitation about 1 mm/day or less and frequency about 0.1 or less, varying from convective at low latitudes to partially stratiform at higher latitudes.

This analysis was performed for NAVELEX, Advanced SATCOM Systems, Code PME-106-15 under contract N00039-79-C-0136. Technical monitor was Michael A. Plunkett. To order the final report from the Defense Documentation Center, request AD-A075390.

*Chief Scientist, Systems Research Operation; Associate Fellow AIAA.

**SAI Consultant

†SAI Consultant

Copyright © American Institute of Aeronautics and Astronautics, Inc., 1980. All rights reserved.

C, Temperate Maritime - The major portions of the oceans, generally poleward and westward of the subtropical highs (F-type regions) and excluding the primary paths of extra-tropical storms; average daily precipitation ranges from 1 mm to 4 mm, and frequency from about 0.1 to greater than 0.5; stratiform precipitation predominates in poleward portions, convective in equatorward portions.

C' Maritime Cyclonic - A new precipitation rate region introduced to account for the high precipitation amounts (average greater than 3.5 mm/day) and high frequencies (0.25 to greater than 0.5) associated with the most frequent oceanic paths of extratropical cyclones. We assume it has a precipitation-rate frequency distribution midway between types C and G (i.e., near type D) at the high precipitation-rate end of the distribution, and approaching types B and C at the low precipitation-rate end.

D', Temperate Continental - Minor eastward extensions from the major continents into offshore waters; a mixture of stratiform and convective precipitation averaging 1.5 to 3.5 mm/day at frequencies of about 0.1 to 0.2.

G, Tropical Moderate - Includes essentially all of the tropical oceans except those portions that (seasonally) experience intense and frequent convective precipitation; precipitation amounts vary widely (perhaps too widely) from more than 1 mm/day to less than 6 mm/day at frequencies of less than 0.1 to about 0.3; precipitation is essentially all convective.

E, Subtropical Wet - A minor summertime region near the southeast coasts of North America and Asia, characterized by convective rainfall generally less intense than that found in type H (Tropical Wet); average precipitation amounts about 3.5 to 6 mm/day with frequency of about 0.1.

H, Tropical Wet - The most intensely convective portions of the intertropical convergence zone; the ocean regions of heaviest rainfall, enhanced (and perhaps the data are biased by) local land effects in the East Indies and Central America; precipitation averages greater than 5 mm/day with frequencies of about 0.1 to 0.4.

The preceding narrative description is summarized in Fig. 1 which illustrates the oceanic climate-type boundaries in terms of precipitation amounts and frequencies. This way of depicting the climate types serves two purposes:

1. It clearly reveals the range of precipitation characteristics included within each region. For example, large ranges of precipitation amount and frequency are covered by types C and G, which also cover major portions of the oceans, and there is a substantial overlap between them.
2. Figure 1 provides a check for logical consistency in mapping the climate regions geographically. In addition to the obvious rule that polar climate types should not be adjacent to tropical and subtropical types, no two climate regions should touch that do not touch or overlap in Figure 1.

Crane's one-minute surface precipitation-rate distributions cover the range from 1 to 250 mm/hr. The short duration, infrequent but severe precipitation events around 250 mm/hr were of little interest in this Navy application. The commonplace events around 1 mm/hr and below were of primary interest. To extend Crane's distributions, we first assume that 0.1 mm/hr approximates the rate of the lightest liquid precipitation recorded in weather records, and correspondingly use 0.05 mm/hr for snowfall. It follows that the frequency at which these values are equaled or exceeded is approximated by the maximum frequency of occurrence observed at any given location. Characteristic, subjectively-weighted values of overall precipitation frequency are estimated for all climate types from the guidelines used in delineating the ocean precipitation-rate regions. The estimated characteristic values for precipitation frequency and average daily precipitation are given in Table 1.

Table 1. REGIONAL CHARACTERISTIC VALUES OF PRECIPITATION FREQUENCY AND AVERAGE DAILY PRECIPITATION

Region	Characteristic Values	
	Precipitation Frequency	Average Precip. (mm/day)
A'	0.10	0.5
B'	0.25	1.0
C	0.30	2.5
C'	0.35	4.5
D	0.15	2.25
E	0.10	4.25
F	0.08	0.75
G	0.20	3.25
H	0.20	6.5

The set of the oceanic precipitation-rate distributions, including the new tentatively proposed ones, appears in Figure 2. Values above 100 mm/hr are unchanged from Crane's values. A logarithmic ordinate is used in Figure 2 in order to better reveal the shape of the curves at low precipitation-rates. The remarkable achievement of Crane's process is that the distributions for geographically adjacent climatic regions bound the expected variations (both point-to-point and year-to-year) in the precipitation-rate distribution for each region. Table 2 presents numerical values to facilitate computer calculations.

Table 2. CUMULATIVE PRECIPITATION-RATE DISTRIBUTIONS FOR A PROPOSED OCEANIC CLIMATE MODEL (SEE FIGURE 2).

P, Percent of Year	Value of Precipitation Rate (mm/hr) that is Exceeded P Percent of the Time								
	A'	B'	C	C'	D	E	F	G	H
0 001	7.5	15.0	80	102	102	168	66	129	251
0.002	7.1	13.7	62	86	86	144	51	109	220
0.005	6.4	11.2	40	64	64	117	33	83	178
0.01	5.6	9.1	28	48	48	96	22.5	67	147
0.02	4.6	7.1	19	35	35	77	15.0	51	115
0.05	3.4	4.8	11	22	22	52	8.5	33	77
0.1	2.5	3.4	7.3	15	15	35	5.3	22	51
0.2	1.75	2.4	4.8	9.8	9.8	20.5	3.3	14	30
0.5	1.05	1.5	2.7	5.2	5.2	8.7	1.7	7.0	13.5
1.0	0.68	1.0	1.75	3.1	3.1	4.1	1.0	4.0	6.6
2.0	0.40	0.64	1.10	1.8	1.8	1.8	0.56	2.2	3.0
5.0	0.145	0.31	0.56	0.77	0.70	0.49	0.21	0.78	0.88
10.0	0.05	0.16	0.33	0.38	0.24	0.10	0.00	0.30	0.31
20.0	0.00	0.07	0.16	0.19	0.00	0.00	0.00	0.10	0.10

It is possible to make a rough check on the consistency of the precipitation-rate distributions (Figure 2) with the precipitation criteria (Figure 1) by comparing the integral under the distributions with the typical annual precipitation amounts in the precipitation-rate regions. The integration cannot be precise because (a) there is no analytic formulation for these empirical curves, and (b) the great range of the variables precludes plotting them on linear graph paper and using conventional planimetric techniques. However, we approximate this process using straightforward numerical integration by multiplying the value of the differential probability for a given precipitation rate interval by the midpoint precipitation rate, and then summing these products over all intervals. We have done this, assuming all precipitation at rates less than 0.1 mm/hr (or 0.05 in the polar regions) vanishingly small, i.e., this assumes that lower rates contribute nothing to the integral we calculate.

The final results are shown in Table 3, where the integral under the curves of Figure 2 is compared with the total precipitation obtained by multiplying the right-hand column in Table 1 by 365. The two approaches are consistent to 30 percent or better in all cases.

Table 3. COMPARISON OF INTEGRATED PRECIPITATION RATE WITH CHARACTERISTIC ANNUAL PRECIPITATION FOR EACH CLIMATIC REGION

Climatic Region	Integral of Precipitation-Rate Distribution[a] (mm)	Characteristic Annual Precipitation[b] (mm)
A'	200	200
B'	500	375
C	850	900
C'	1400	1650
D	1050	825
E	1600	1550
F	350	275
G	1500	1200
H	2300	2375

[a] Rounded to nearest 50 mm.

[b] Rounded to nearest 25 mm. This is an estimate of the weighted average for each region.

Description of the Proposed Oceanic Model

The first step in this extension of Crane's model was the definition of the nine climatological regions, i.e., nine regions characterized by distinct one-minute surface precipitation-rate distributions. Then we carried out the piecemeal allocation of the entire oceanic surface of the earth to one of these nine regions. Four maps delineate the region boundaries, Figures 3-6.

Three independent analyses of ocean precipitation and cloudiness were used to generate the climate region maps over the oceans: (1) a global, monthly analysis of precipitation amounts(4), (2) a global, monthly analysis of precipitation frequency(5), and (3) a monthly analysis of average cloud amount over the Pacific Basin(6). Precipitation amount is not generally measured on ships at sea. The available data(4) probably represent the 1930s through the mid-1940s. The precipitation frequency analysis(5) used all available data from the early 1940s through the early 1960s. The frequencies are defined as the fraction of all "present weather" observations reporting precipitation. The cloud amount analysis(6) comes from meteorological satellite data over the Pacific Basin, 1965-1973. It is the least uncertain and most objective of the three analyses; however, it is only an indirect and crude indication of precipitation amount and frequency. These comments illustrate the inherent difficulties in describing precipitation over the oceans.

Comparison of Figures 3-6 shows some significant seasonal variations in ocean climate:

- o Most major climatic features shift five to ten degrees in latitude toward the summer pole.
- o The subtropical arid areas tend to expand in the summer hemisphere and contract in the winter hemisphere.
- o "Wetness," in general, but especially in the subtropics and tropics, varies considerably from season to season.

To look in more detail at seasonal variations, we selected thirteen specific locations of possible Navy communications interest. We selected them with an eye to representing the complete spectrum of precipitation-rate regions, and we estimated monthly and seasonal values of precipitation parameters using available sources. Seasonal (three-month) precipitation amounts were extracted from the Möller maps(4), monthly precipitation frequencies were extracted from the Crutcher and Davis maps(6), and estimates of monthly and annual "thunderstorm days" were extracted from maps and tables published by the World Meteorological Organization(7). All are tabulated in Table 4; and the locations are mapped in Figure 7.

In Table 4, we underlined precipitation amount for locations exhibiting a seasonal variation of precipitation (mm) of 2:1 or more. The seasonal variations revealed in Table 4 are most striking in the moist tropics (locations 7, 8 and 13, with location 5 an exception) and, to a smaller extent, in the temperate region storm belts (locations 1, 2, 9 and 11) and the arid subtropical regions (locations 3 and 6). As a general rule, the three parameters vary consistently, the major exception being location 9 (Sea of Japan), where the highest frequencies of precipitation appear to coincide with the smallest amounts.

So far we have only discussed surface point rain rates. However, for the purpose of calculating earth-to-satellite path attenuation, the spatial distribution of rain rate over the propagation path represents the more relevant quantity. This involves the spatial correlation function for rain rate, which itself is a function of rain rate. For example, very high rain rates are known to have relatively short correlation distances and vice versa. In Crane's model, the correction for spatial correlation is not made directly on precipitation rate, but rather as a precipitation rate-dependent correction to the total attenuation. This correction is of the form

$\gamma(D)R_p^{-\delta(D)}$ where R_p is the one-minute

Table 4. MONTHLY AND SEASONAL PRECIPITATION DATA FOR SELECTED OCEAN LOCATIONS

Location	Parameter	Dec	Jan	Feb	Mar	Apr	May	Jun	Jul	Aug	Sep	Oct	Nov
1. Mid Atlantic 40N 40N	Precipitation (mm)	←	300	→	←	250	→	←	175	→	←	200	→
	Precipitation Freq.	.21	.26	.25	.23	.20	.18	.14	.12	.11	.15	.18	.20
	Thunderstorm Days	2	1	2	2	1	0	1	1	2	1	1	1
2. North Atlantic 65N 0	Precipitation (mm)	←	$\underline{200}$	→	←	100	→	←	$\underline{100}$	→	←	$\underline{200}$	→
	Precipitation Freq.	.36	.40	.38	.35	.30	.20	.20	.20	.30	.30	.31	.33
	Thunderstorm Days	0	0	0	0	0	0	0	1	0	0	1	0
3. Mediterranean 35N 20S	Precipitation (mm)	←	$\underline{150}$	→	←	50	→	←	$\underline{20}$	→	←	75	→
	Precipitation Freq.	.10	.10	<.10	<.10	<.10	<.10	<.10	<.10	<.10	<.10	.09	.09
	Thunderstorm Days	3	4	3	2	2	2	2	1	2	2	3	4
4. Persian Gulf 15N 60S	Precipitation (mm)	←	25	→	←	20	→	←	25	→	←	25	→
	Precipitation Freq.	<.10	<.10	<.10	<.10	<.10	<.10	.08	.08	<.10	<.10	<.10	<.10
	Thunderstorm Days	0	0	0	0	0	0	0	1	1	1	0	0
5. Indian Ocean 0N 75E	Precipitation (mm)	←	450	→	←	400	→	←	400	→	←	525	→
	Precipitation Freq.	.10	.10	.11	<.10	.09	.12	.12	.12	.12	.11	.09	.08
	Thunderstorm Days	1	1	2	1	2	2	1	1	1	1	1	2
6. W. Australia 20S 115E	Precipitation (mm)	←	$\underline{75}$	→	←	50	→	←	50	→	←	$\underline{20}$	→
	Precipitation Freq.	<.10	.08	<.10	<.10	<.10	<.10	<.10	<.10	<.10	<.10	<.10	<.10
	Thunderstorm Days	2	3	3	2	1	0	0	0	0	0	0	1
7. East Indies 5S 120E	Precipitation (mm)	←	$\underline{600}$	→	←	500	→	←	200	→	←	$\underline{150}$	→
	Precipitation Freq.	<.10	.12	.10	<.10	.10	.10	<.10	<.10	<.10	<.10	<.10	<.10
	Thunderstorm Days	5	8	4	4	5	2	1	1	1	2	3	5
8. Philippines 15N 120E	Precipitation (mm)	←	$\underline{200}$	→	←	300	→	←	$\underline{400}$	→	←	$\underline{200}$	→
	Precipitation Freq.	.11	.08	.09	.08	.08	.08	.09	.11	.11	.10	.11	.09
	Thunderstorm Days	1	1	1	2	2	6	5	4	5	4	3	2
9. Sea of Japan 40N 135E	Precipitation (mm)	←	$\underline{100}$	→	←	$\underline{300}$	→	←	200	→	←	180	→
	Precipitation Freq	.40	.44	.35	.20	.19	.20	.21	.19	.17	.17	.20	.23
	Thunderstorm Days	0	0	0	0	0	1	1	2	2	1	1	0
10. Bering Sea 60N 175W	Precipitation (mm)	←	100	→	←	75	→	←	100	→	←	100	→
	Precipitation Freq.	.38	.25	.33	.31	.31	.30	.25	.31	.31	.30	.35	.35
	Thunderstorm Days	0	0	0	0	0	0	0	0	0	0	0	0
11. NE Pacific 45N 125W	Precipitation (mm)	←	$\underline{400}$	→	←	200	→	←	$\underline{150}$	→	←	$\underline{400}$	→
	Precipitation Freq.	.17	.20	.17	.15	.13	.12	.10	.10	.04	.10	.17	.17
	Thunderstorm Days	0	0	0	0	0	1	1	1	1	0	0	0
12. Hawaii 20N 155W	Precipitation (mm)	←	125	→	←	80	→	←	75	→	←	100	→
	Precipitation Freq.	.09	.08	.10	.08	<.10	<.10	<.10	.10	.10	<.10	<.10	.09
	Thunderstorm Days	1	1	1	0	0	0	0	0	0	0	0	0
13. Panama 10N 80W	Precipitation (mm)	←	$\underline{200}$	→	←	400	→	←	$\underline{600}$	→	←	$\underline{600}$	→
	Precipitation Freq.	.10	.10	.10	.10	.10	.10	.17	.20	.20	.18	.15	.10
	Thunderstorm Days	3	4	4	2	4	6	12	10	11	9	6	4

NOTE: Underlined values indicate $\geq$2:1 seasonal variation

surface point rain rate for a given exceedance probability (P) and γ and δ are empirical functions of D. D is the surface projection of the appropriate portion of the propagation path.

Crane's model makes two additional assumptions to facilitate specific path attenuation calculations. The first is that, for the frequencies of current interest (i.e., $f < 50$ GHz), only liquid water need be considered; ice crystals and snow flakes can be neglected. It follows from this assumption that, if the mean freezing height ($\overline{FH}$) can be estimated or modeled, the path length for propagation at an elevation angle θ above the horizontal is simply $L = (\overline{FH})/\sin\theta$ and $D = (\overline{FH})/\tan\theta$. The second assumption is that the "specific attenuation" in dB/km due to rain can be fitted by an expression of the form αR_p^{β} where α and β are empirical functions of the carrier frequency. Tables of α and β, based on applying logarithmic regression to Mie scattering calculations, have been given by Olsen et al(10) for five published drop-size distributions and for three different rain temperatures. We used the Laws and Parsons (LP) drop-size distributions which are the most widely tested and the most widely used. Olsen gives two regressions, LP_L and LP_H, for "low" and "high" rain rates, and he suggests that LP_L be used for $R_p < 40$ mm/hr and LP_H be used for $R_p > 40$ mm/hr. Following Olsen's recommendations, we use the LP_L and LP_H values for α and β. Graphical interpolations between Olsen's published data were used to determine values at the frequencies specified for this study. Olsen presented equations (see his equations 25 and 26) which were intended as convenient approximations for computer computations, but they give rise to errors as Olsen showed in his Fig. 5. Therefore, we interpolated to determine more accurate values. Table 5 lists the values used for α and β, interpolated where necessary. A temperature excursion for region E tested both 0° and 20°C; it indicated that the magnitude of the temperature effect was small. Thus we used 0°C values generally with a few exceptions. The exceptions are the tropics (regions G and H) and the lowest latitudes of region C (within 30° of the equator) where we used 20°C values.

Finally, the attenuation in dB as a function of the exceedance probability P (the cumulative probability of being exceeded) expressed as percent of a year, is given by:

$$A(P) = L(\Lambda,\theta)\ \alpha(f,R_p)\ \gamma(D)\ R_p(P)^{[\beta(f,R_p)-\delta(D)]} \quad (1)$$

We calculate

$$\gamma(D) = 1 + (D^*/4.5) - 0.23(D^*/4.5)^2 + 0.0215(D^*/4.5)^3$$

and

$$\delta(D) = (D^*/21.5) - 0.98(D^*/21.5)^2 + 0.446(D^*/21.5)^3,$$

where

$D^* = D$ for $D \leq 22.5$ km

$= 22.5$ for $D > 22.5$ km.

We read $R_p(P)$ from Figure 2 or Table 2, noting whether $R_p < 40$ mm/hr or $R_p > 40$ mm/hr.
We calculate A(P) in dB using the appropriate values for α and β from the two choices available (LP_L or LP_H).
Then, we list or plot A versus P*,
where $P^* = P$ for $D \leq 22.5$ km
$= (D/22.5)\overline{P}$ for $D > 22.5$ km,
where P is the tabulated value of percent of the year corresponding to the value of R_p used in calculating A.

Table 5. TABULATION[a] OF α, β FOR USE IN αR_p^{β}

Frequency (GHz)	$\alpha(LP_L)$	$\alpha(LP_H)$	$\beta(LP_L)$	$\beta(LP_H)$
Temperature = 0°C				
1.0	6.41×10^{-5}	5.26×10^{-5}	0.891	0.947
7.5	5.49×10^{-3}	4.28×10^{-3}	1.1850	1.2585
8.2	6.95×10^{-3}	5.84×10^{-3}	1.1870	1.2396
21	7.05×10^{-2}	8.21×10^{-2}	1.1141	1.0728
40	0.313	0.467	0.981	0.864
41	0.330	0.490	0.973	0.857
43	0.365	0.534	0.958	0.845
44	0.382	0.555	0.951	0.840
45	0.400	0.575	0.943	0.835
Temperature = 20°C				
1.0	3.84×10^{-5}	3.17×10^{-5}	0.889	0.945
7.5	3.52×10^{-3}	2.77×10^{-3}	1.2941	1.3644
8.2	4.72×10^{-3}	4.29×10^{-3}	1.2998	1.3322
21	7.68×10^{-2}	9.66×10^{-2}	1.1016	1.0367
40	0.312	0.452	0.972	0.864
41	0.329	0.473	0.965	0.858
43	0.363	0.515	0.951	0.846
44	0.380	0.535	0.944	0.841
45	0.397	0.555	0.936	0.836

[a] Based on Olsen et.al., reference 6; interpolated where necessary. LP refers to the Laws and Parsons drop-size distributions. The subscripts L and H refer to low and high rain rates; the transition is at about 40 mm/hr.

Along with the maps for the oceanic precipitation-rate regions a correspondingly detailed set of seasonal mean freezing height approximations must be used to calculate attenuation. Crutcher and Meserve(9) prepared seasonal maps of freezing heights worldwide. Figures 8-11 are simply redrawn versions of their charts with an estimate of the 4.5 km freezing height added.

Application of Proposed Oceanic Model to 13 Selected Locations

A FORTRAN IV program was established for carrying out the indicated computations on an IBM 360/91 computer. In all cases, the attenuation at 1 GHz is less than 1 dB, and was ignored. The effect of freezing height is seen to be major because freezing height directly determines the amount of rain that the signal must pass through on any given path. In all cases, we show a single smooth curve joining the LP_L and LP_H curves, and do not bother to show the small step at 40 mm/hr.

The precipitation-rate climate model of the ocean areas was used to calculate earth-satellite path attenuation for the thirteen locations plotted in Figure 7 and defined by latitude and longitude in Table 4. By comparing Figure 7 with Figures 3-6, the precipitation-rate region assignments by season can be read directly for each of the 13 locations; the corresponding mean seasonal freezing height can be read or interpolated from Figures 8-11. One further refinement has been included. By taking the total seasonal precipitation for each location listed in Table 4, dividing by 90 to convert it to a daily average, and forming the ratio of this number to the characteristic precipitation (mm/day) assumed for each of the nine standard ocean precipitation-rate types listed in Table 1, a correction factor k is generated. This k factor is applied to each of the precipitation rates given in Figure 2 or Table 2 before inserting them into the formula for attenuation.

Five graphs have been selected to illustrate particular features. The mid-Atlantic, Figure 12, represents a case where the seasonal extremes (best and worst seasons) are not significantly different. Note also that the best season (Jun-Aug for the 21 GHz curve) at 0.001 percent of time can become the worst season at 5 percent of the time. In the Philippines, Figure 13, one of the highest attenuation areas, the seasonal difference is large at 0.001 percent of the time but small at 10 percent of the time. In many instances the effect of freezing height dominates; consequently, the best and worst attenuations do not coincide with one's intuitive notions about "good" and "bad" weather. The Sea of Japan, Figure 14, constitutes an extreme case where the "best" season is winter, with zero attenuation because the mean freezing height is on the surface; but of course the weather can be miserable. At 44 GHz, Hawaii, Figure 15, clearly shows the rapid falloff of attenuation from Sep to Nov which is characteristic of a subtropical-arid region. Figure 16 shows the dependence on elevation angle, and emphasizes the need for numerous satellites at geostationary or low inclination orbits to assure high elevation angles for terminals in the high rainfall tropical areas such as Panama, the Indian Ocean, the East Indies and the Philippines.

Outage Duration Statistics

To evaluate the impact of a given cumulative outage time on communications requires knowledge of the outage duration statistics. The system design alternatives are radically different depending on whether typical outage durations are microseconds, seconds, minutes or hours.

We will consider one location in detail: #8, the Philippines in summer. At this location, Figure 13 gives the percent of time that various levels of attenuation in dB are exceeded. We can interpret such numbers as the percent of the time that outages will occur given the amount of precipitation margin (assuming that all system margin allowance is consumed). These values are listed in Table 6. The time percentages were converted to hours per season simply by multiplying by 2192 (one-fourth of the number of hours in a year, which is 8766). We use the time percentages to enter the appropriate precipitation-rate distribution curve of Figure 2 to obtain the nominal precipitation rate for that climate type. This in turn can be converted to the precipitation rate at the specified location by multiplying the abscissa by the correction factor k' and the ordinate by k/k'. Precipitation rate, mean freezing height and path length are also given in Table 6 in order to assist the reader in visualizing the conditions.

Table 6. EXCEEDANCE TIMES FOR VARIOUS MARGIN LEVELS: LOC. #8, PHILIPPINES, JAN-AUG, RAIN TYPE H

Point-season precipitation frequency = 0.11
Mid-region precipitation frequency = 0.20
Precipitation frequency ratio, k' = 0.55

(a) Elevation angle $\theta = 10°$, $\overline{FH} = 4.9$ km, L = 28.2 km

44 GHz			Link Margin (dB)	21 GHz		
Percent of time	Hrs. per Season	Rain Rate (mm/hr)		Percent of Time	Hrs. per Season	Rain Rate (mm/hr)
15.0	330	0.04	5	2.4	53	1.2
7.8	170	0.19	10	1.07	23	3.5
4.8	105	0.41	15	0.60	13	6.4
3.3	73	0.73	20	0.40	8.7	10.0
2.4	53	1.17	25	0.27	6.0	14.0
1.8	40	1.75	30	0.19	4.2	19.0

(b) Elevation angle $\theta = 30°$, $\overline{FH} = 4.9$ km, L = 9.8 km

44 GHz			Link Margin (dB)	21 GHz		
Percent of time	Hrs. per Season	Rain Rate (mm/hr)		Percent of Time	Hrs. per Season	Rain Rate (mm/hr)
2.2	47.0	1.5	5	0.58	12.7	6.5
1.15	25.0	3.0	10	0.25	5.4	16.0
0.75	16.0	5.0	15	0.15	3.3	25.0
0.54	11.9	7.2	20	0.11	2.3	34.0
0.41	9.0	9.9	25	0.08	1.8	42.0
0.32	7.0	12.8	30	0.065	1.4	50.0

An outage of a communications link can be related to the occurrence of a precipitation rate of a particular magnitude, given a particular freezing height. In the present model, freezing height is assumed constant over a three-month season at any given location. Therefore, the minimum precipitation rate associated with an outage is that rate that is equalled or exceeded with the same frequency as the expected occurrence frequency of the outage. If the frequency distributions of precipitation-rate exceedance durations were known, then we could assume their corresponding attenuation exceedance duration distributions to be the same.

Only one precipitation-rate duration frequency distribution was found in the literature(12); an exhaustive survey might discover more. Those precipitation-rate duration statistics come from an analysis of 10 years of data recorded by a precipitation gauge at McGill University, Montreal. A plot of the data from Reference 12 shows that the distribution of durations is very nearly lognormal. We therefore drew a straight-line lognormal approximation through the points. According to Lin (Reference 13), all the fade duration frequency distributions that he calculated were nearly lognormal; they were found to be parallel to the Montreal precipitation-rate duration frequency distribution. An inferred relationship among these meager data (see ref.1) was used to generate the curves of Figure 17.

Figure 17 can be used with the data in Table 6 to estimate outage duration probabilities for specific conditions. This has been done at 44 GHz, and the results appear as probability density functions in Figure 18. Table 7 presents the same information in still another form, in terms of the median and mean outage durations and the average number of outages per day during the rainy season.

Conclusions

Because it makes no sense to use a world-average precipitation rate when a captain knows where his ship is, we retained Crane's division of the earth's surface into precipitation-rate regions. Since the captain knows what month it is, it makes no sense to lump the rainy and dry seasons together. We have separated them. Thus the attenuations are a function of latitude, longitude and season of the year. We accounted for local variation from point to point within a climate region by adjusting parameters to match known data at the selected locations. The one-minute surface point precipitation-rate distributions have been extended down to 0.1 or 0.05 mm/hr, which are values that approximate the smallest rates of observed precipitation. The extension of the surface point precipitation rates to the minimum observable amount extends the model from 2 percent to as much as 35 percent of the time.

The refined oceanic precipitation model developed in this study provides estimates of the slant path attenuation through the atmosphere over a wider range of frequency of occurrence and precipi-

Table 7. MEAN OUTAGE DURATION AND AVERAGE NUMBER OF OUTAGES PER DAY FOR LOC. #8, PHILIPPINES, JUN-AUG, RAIN TYPE H

ELEVATION ANGLE (Deg.)	LINK MARGIN (44 GHz) (dB)	R_M (mm/hr)	P (%)	MEDIAN OUTAGE DURATION* d(min)	MEAN OUTAGE DURATION* d(min)	CUMULATIVE DAILY OUTAGE* (min)	AVG. NUMBER OF OUTAGES* PER DAY
10	5	0.04	15.0	95.2	232.1	216.0	0.9
10	10	0.19	7.8	29.6	72.2	112.3	1.6
10	15	0.41	4.8	16.6	41.2	69.1	1.7
30	5	1.5	2.2	6.3	15.3	31.7	2.1
30	10	3.0	1.15	3.7	9.1	16.56	1.8
30	15	5.0	0.75	2.6	6.2	10.8	1.7

* Rounded off to one decimal place

tation rates than has appeared in the literature. At one end of the scale, we cover extreme events which are infrequent and short-lived, i.e., which occur only 0.001 percent of the season which corresponds to a total of 1.3 minutes per season. At the other end of the scale, we cover commonplace events, i.e., light drizzles or snow which occur about 6 to 36 percent of the season. (These percentages correspond to a total of 130 to 790 hours per season and spread uniformly throughout the season, would occur 1.4 to 9 hours per day).

For the worst season of the year at each location, the table which follows summarizes the attenuations at 44 GHz and 20° elevation angle. In the table, the four highest attenuation values for each cumulative outage level are marked with an asterisk. Note the dramatic change in precipitation margin depending on whether one requires 99.9 percent availability, or only 99 or 90 percent. Table 9 indicates the range of the four highest attenuation values and their design implications.

For the worst season of the year at each location, the table which follows summarizes the attenuations at 44 GHz and 20° elevation angle. The correction for total amount of precipitation is already included in the figures from which this data was taken.

TABLE 8. PRECIPITATION MARGIN REQUIREMENTS FOR THIRTEEN SELECTED LOCATIONS (dB)

	Availability (percent):	99.9	99.0	90.0
Location	Cumulative Outage ("):	0.1	1.0	10.0
# 1 Mid-Atlantic		32	13	4.4
# 2 North Atlantic		13	4.1	1.1
# 3 Mediterranean		25	8.7	1.3
# 4 Persian Gulf		19	7.3	1.4
# 5 Indian Ocean		108*	40*	8.6*
# 6 W. Australia		34	13	2.2
# 7 East Indies		127*	40*	6.9*
# 8 Philippines		100*	31*	5.0*
# 9 Sea of Japan		60	22	4.6
#10 Bering Sea		12	4.8	1.3
#11 N.E. Pacific		43	15	3.5
#12 Hawaii		41	15	3.5
#13 Panama		130*	41*	6.6*

Table 9. HIGHEST PRECIPITATION MARGIN REQUIREMENTS AND THEIR DESIGN IMPLICATIONS (44 GHz, 20° elevation, worst season)

Cumulative Outage (percent)	0.1	1	10
Precipitation Margin, dB	100 to 130	30 to 40	5 to 9
Design Implications	Probably technically and economically infeasible unless there are exceptional circumstances, e.g., if greatly restricted coverage area were acceptable.	Large satellite investment required but technically feasible.	Readily achievable with current technology for a modest incremental cost.

From the above estimates, one concludes that reasonable downlink precipitation margins i.e., 10 to 15 dB will provide availabilities over 90 percent. That such high availability could be achieved at 44 GHz and 20° elevation angle with only 10 to 15 dB margin for precipitation was an unexpected conclusion. While this conclusion remains tentative because of the quick-response nature of this study, such a conclusion makes it particularly important to further refine the model.

Rather than terminate the study with these estimates of cumulative outage, we chose to go one step further and examine the outage durations which make up the cumulative outage. We computed the probability density function for the outage durations. As an example, consider the rainiest season in a high rain rate area like the Philippines. With 10 dB margin at 44 GHz and 10° elevation the average outage lasts 72 minutes, but a 15 dB margin reduces the average outage to 41 minutes. With 10 dB margin at 30° elevation, however, the average outage lasts only 9 minutes. A 15 dB margin now reduces the average outage to 6 minutes. Furthermore, there would be an average of less than two such outages per day. We consider this analysis of outage durations a fitting conclusion to any discussion of slant path attenuation due to precipitation.

References

1. Feldman, Nathaniel E., "Rain Attenuation Over Earth-Satellite Paths," Science Applications, Inc., SAI-171-80-573-LA, May 1979, AD-A075390.
2. Crane, R. K., "A Global Model for Rain Attenuation Prediction," Eastcon Conference Proceedings, 1978.
3. Crane, R. K., "Rain Attenuation Prediction," Draft Submission to the CCIR Special Preparatory Meeting in Geneva, 1978, Document F5/003, April 25, 1978.
4. Möller, F., "Viertelsjahrskarten des Niederschlags fur die ganze Erde," Petermanns Geographische Mitteilungen, Justus Perthes, Gotha, 1951, pp. 1-7.
5. Crutcher, H. L. and O. M. Davis, U. S. Navy Marine Climate Atlas of the World, Volume VIII, The World, NAVAIR 50-1C-54, Naval Weather Service Command, March 1969.
6. Sadler, J. C., L. Oda and B. J. Kilonsky, Pacific Ocean Cloudiness from Satellite Observations, UHMET 76-01, Dept. of Meterology, Univ. of Hawaii, October 1976.
7. World Meteorological Organization, World Distribution of Thunderstorm Days; Part 2: Tables of Marine Data and World Maps, Secretariate of the WMO, Geneva, 1956.
8. United States Air Force, Handbook of Geophyics, Revised Edition, The Macmillan Co., New York, 1960.
9. Crutcher, H. L. and J. J. Meserve, Selected Level Heights, Temperatures and Dew Points for the Northern Hemisphere, NAVAIR 50-1C-52, Naval Weather Service Command, January 1970.
10. Olsen, R. L., et. al., "The aR^b Relation in the Calculation of Rain Attenuation," IEEE Transactions On Antennas and Propagation, Vol. AP-26, No. 2, March 1978, pp. 318-329.

11. Mundie, L. G. and N. E. Feldman, The Feasibility of Employing Frequencies Between 20 and 300 GHz for Earth-Satellite Communications Links, The Rand Corporation, R-2275-DCA, May 1978.
12. Drufuca, G. and I. Zawadzki, "Statistics of Raingage Data," J. Appl. Meteorol., Vol. 14, No. 8, Dec. 1975, pp. 1419-1429.
13. Lin, S. H., "Statistical Behavior of Rain Attenuation," The Bell System Technical Journal, Vol. 52, No. 4, April 1973, pp. 557-581.

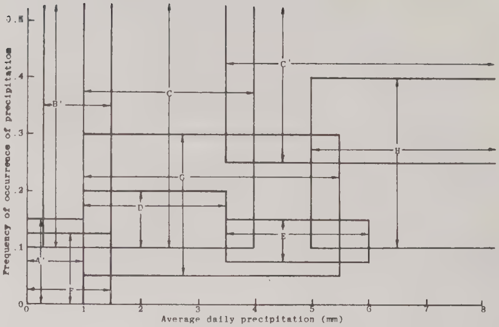

Fig. 1. Bounds for the oceanic precipitation-rate regions

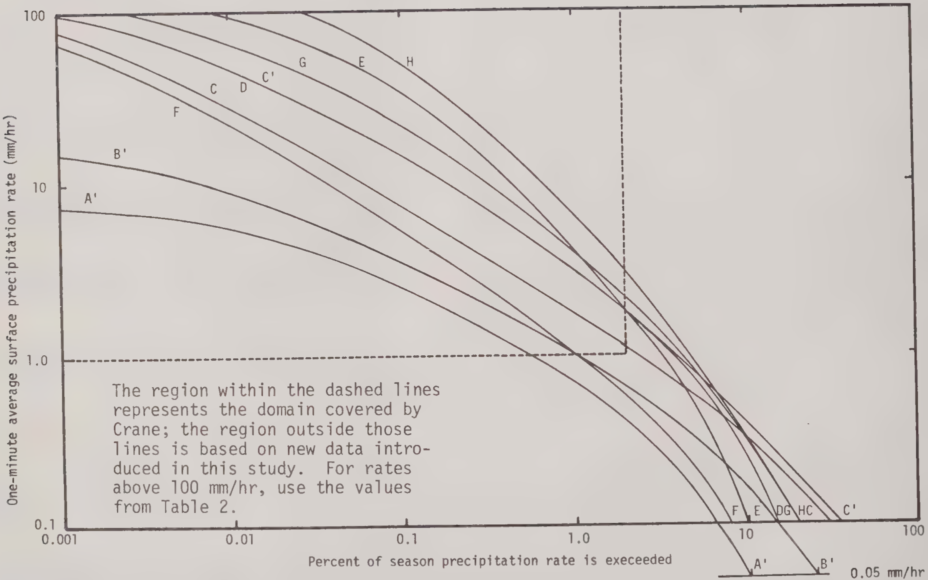

The region within the dashed lines represents the domain covered by Crane; the region outside those lines is based on new data introduced in this study. For rates above 100 mm/hr, use the values from Table 2.

Figure 2. Cumulative distribution of one-minute average surface precipitation rates for nine climatic regions -- proposed oceanic model

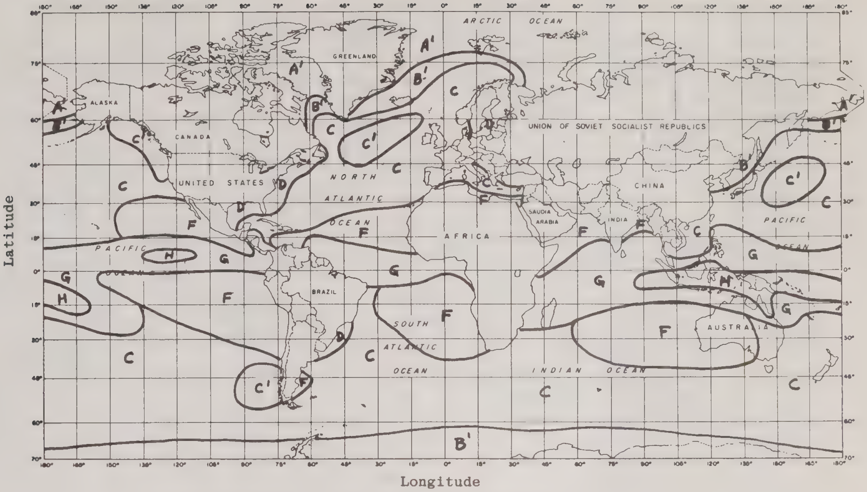
Latitude
Longitude
ARCTIC OCEAN
GREENLAND
ALASKA
CANADA
UNITED STATES
NORTH ATLANTIC OCEAN
UNION OF SOVIET SOCIALIST REPUBLICS
CHINA
INDIA
SAUDIA ARABIA
AFRICA
BRAZIL
SOUTH ATLANTIC OCEAN
INDIAN OCEAN
AUSTRALIA
PACIFIC OCEAN
A'
B'
C
C'
D
F
G
H

Fig. 3. Oceanic climate regions for December through February

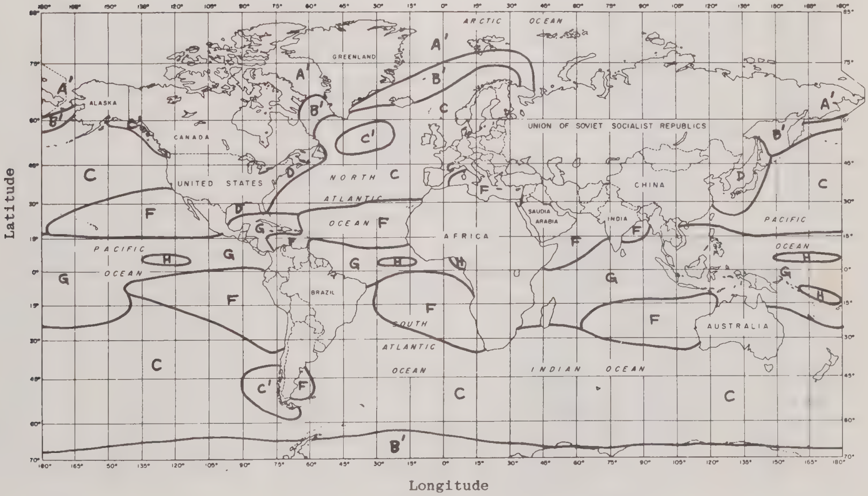
Latitude
Longitude
ARCTIC OCEAN
GREENLAND
ALASKA
CANADA
UNITED STATES
NORTH ATLANTIC OCEAN
UNION OF SOVIET SOCIALIST REPUBLICS
CHINA
INDIA
SAUDIA ARABIA
AFRICA
BRAZIL
SOUTH ATLANTIC OCEAN
INDIAN OCEAN
AUSTRALIA
PACIFIC OCEAN
A'
B'
C
C'
D
F
G
H

Fig. 4. Oceanic climate regions for March through May

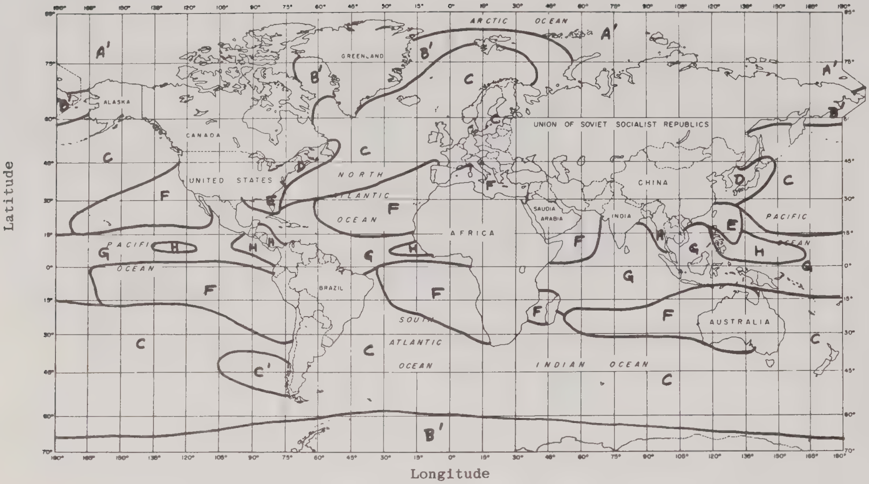
Latitude
Longitude
ARCTIC OCEAN
GREENLAND
ALASKA
CANADA
UNITED STATES
UNION OF SOVIET SOCIALIST REPUBLICS
CHINA
INDIA
SAUDIA ARABIA
AFRICA
BRAZIL
AUSTRALIA
NORTH ATLANTIC OCEAN
SOUTH ATLANTIC OCEAN
PACIFIC OCEAN
INDIAN OCEAN
A'
B'
C
C'
D
E
F
G
H

Fig. 5. Oceanic climate regions for June through August

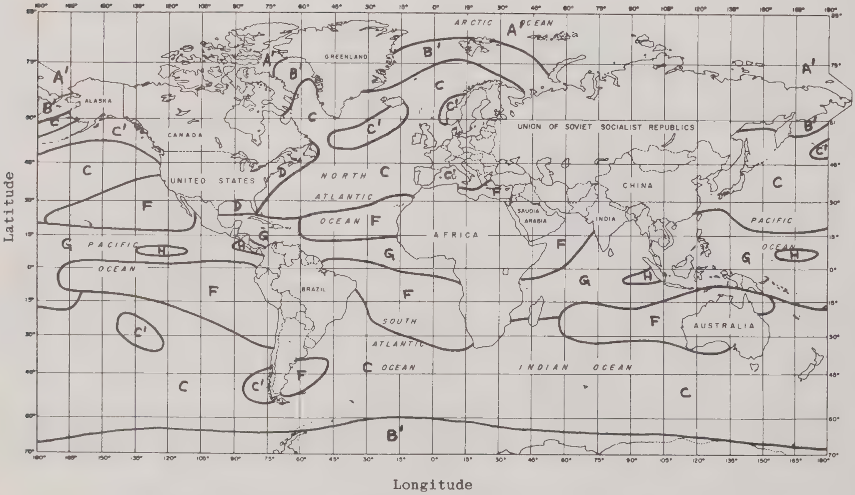
Latitude
Longitude
ARCTIC OCEAN
GREENLAND
ALASKA
CANADA
UNITED STATES
UNION OF SOVIET SOCIALIST REPUBLICS
CHINA
INDIA
SAUDIA ARABIA
AFRICA
BRAZIL
AUSTRALIA
NORTH ATLANTIC OCEAN
SOUTH ATLANTIC OCEAN
PACIFIC OCEAN
INDIAN OCEAN
A'
B'
C
C'
D
F
G
H

Fig. 6. Oceanic climate regions for September through November

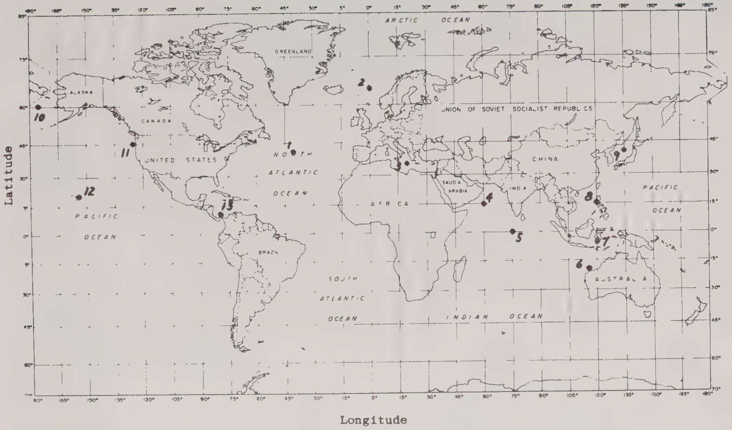
ARCTIC OCEAN
GREENLAND
ALASKA
CANADA
UNITED STATES
UNION OF SOVIET SOCIALIST REPUBLICS
CHINA
INDIA
SAUDI ARABIA
AFRICA
BRAZIL
AUSTRALIA
NORTH ATLANTIC OCEAN
SOUTH ATLANTIC OCEAN
INDIAN OCEAN
PACIFIC OCEAN
1
2
3
4
5
6
7
8
9
10
11
12
13
Latitude
Longitude

Fig. 7. Locations of the 13 points examined

From Ref. 12

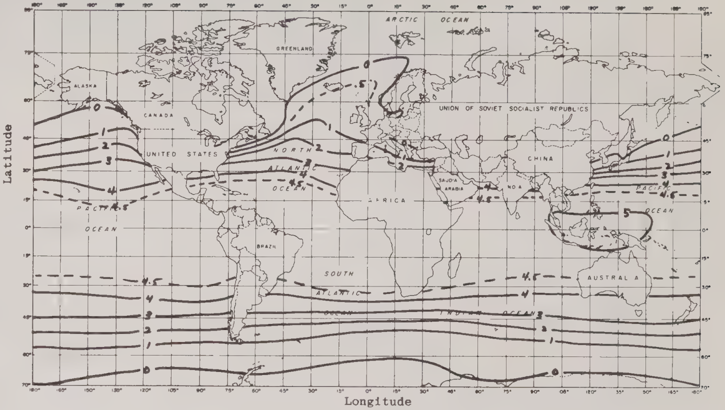
ARCTIC OCEAN
GREENLAND
ALASKA
CANADA
UNITED STATES
UNION OF SOVIET SOCIALIST REPUBLICS
CHINA
INDIA
SAUDI ARABIA
AFRICA
BRAZIL
AUSTRALIA
NORTH ATLANTIC OCEAN
SOUTH ATLANTIC OCEAN
INDIAN OCEAN
PACIFIC OCEAN
0
.5
1
2
3
4
4.5
5
Latitude
Longitude

Fig. 8. Average freezing height (km) for December through February

From Ref. 12

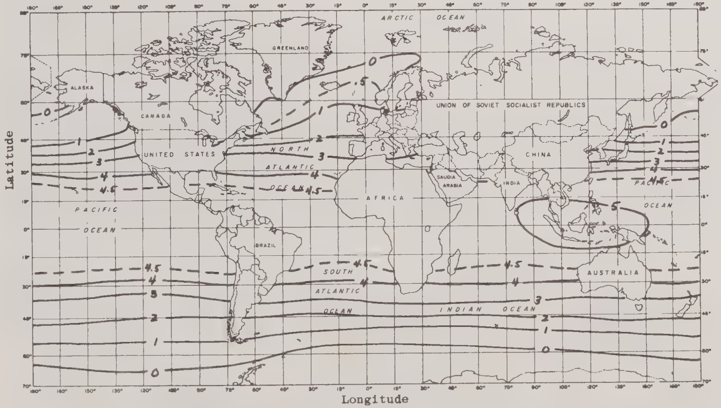
ARCTIC OCEAN
GREENLAND
ALASKA
CANADA
UNITED STATES
UNION OF SOVIET SOCIALIST REPUBLICS
CHINA
INDIA
SAUDI ARABIA
AFRICA
BRAZIL
AUSTRALIA
NORTH ATLANTIC OCEAN
SOUTH ATLANTIC OCEAN
INDIAN OCEAN
PACIFIC OCEAN
0
.5
1
2
3
4
4.5
5
Latitude
Longitude

Fig. 9. Average freezing height (km) for March through May

From Ref. 12

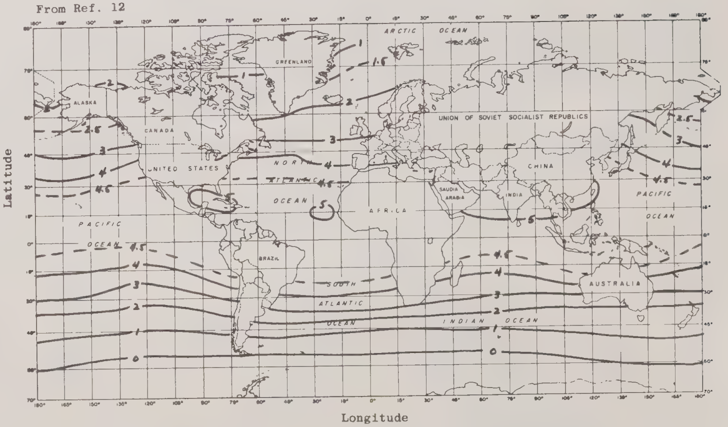
ARCTIC OCEAN
GREENLAND
ALASKA
CANADA
UNITED STATES
UNION OF SOVIET SOCIALIST REPUBLICS
CHINA
INDIA
SAUDI ARABIA
AFRICA
BRAZIL
AUSTRALIA
NORTH ATLANTIC OCEAN
SOUTH ATLANTIC OCEAN
INDIAN OCEAN
PACIFIC OCEAN
0
1
1.5
2
2.5
3
4
4.5
5
Latitude
Longitude

Fig. 10. Average freezing height (km) for June through August

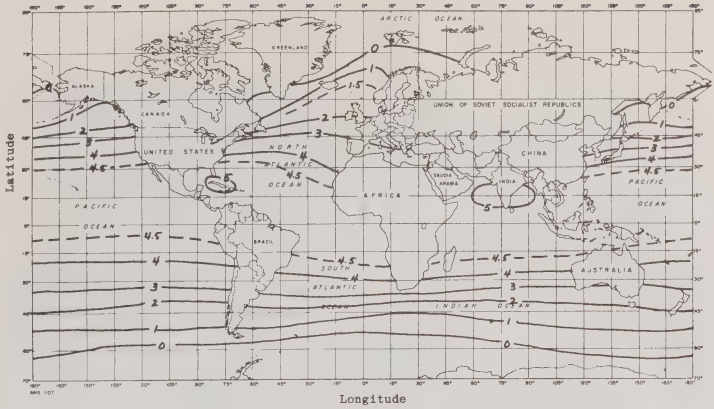

Latitude
Longitude
ARCTIC OCEAN
GREENLAND
ALASKA
CANADA
UNITED STATES
UNION OF SOVIET SOCIALIST REPUBLICS
CHINA
INDIA
SAUDIA ARABIA
AFRICA
BRAZIL
AUSTRALIA
NORTH ATLANTIC OCEAN
SOUTH ATLANTIC OCEAN
INDIAN OCEAN
PACIFIC OCEAN
0
1
1.5
2
3
4
4.5
5

From Ref. 12

Fig. 11. Average freezing height (km) for September through November

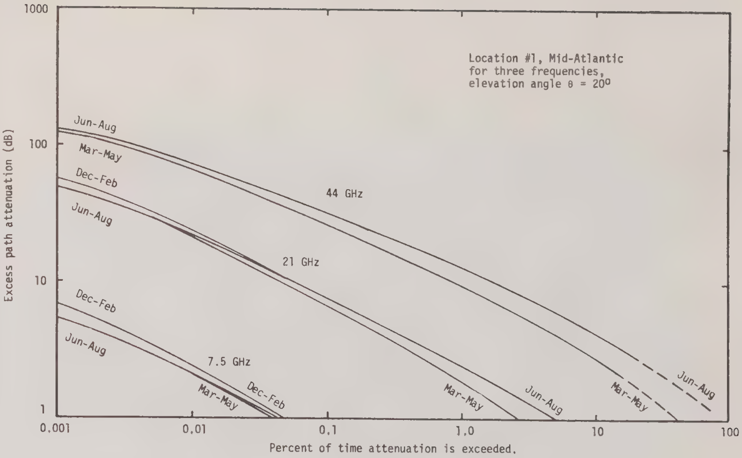

Figure 12. Seasonal max. and min. attenuation exceedance probabilities for Mid-Atlantic

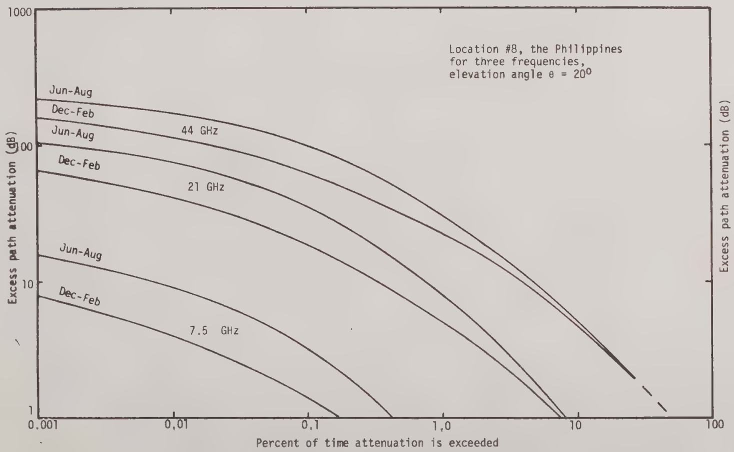

Figure 13. Seasonal max. and min. attenuation exceedance probabilities for the Philippines

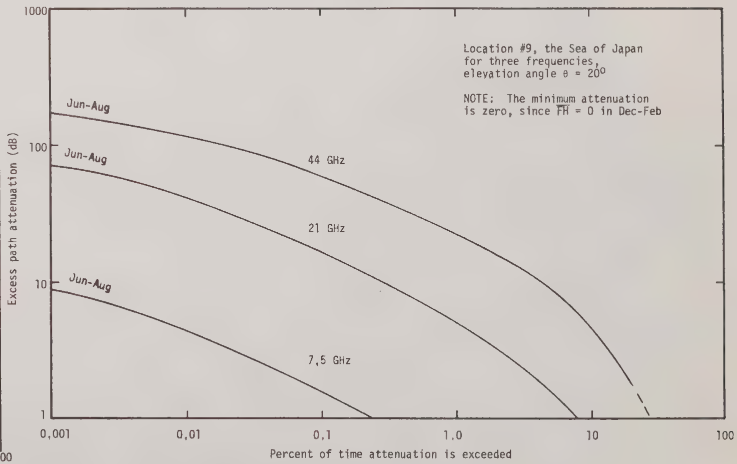

Figure 14. Seasonal max. and min. attenuation exceedance probabilities for the Sea of Japan

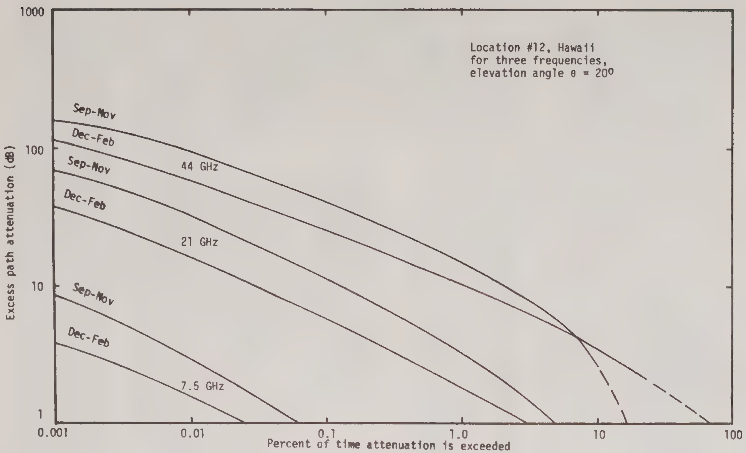

Figure 15, Seasonal max. and min. attenuation exceedance probabilities for Hawaii

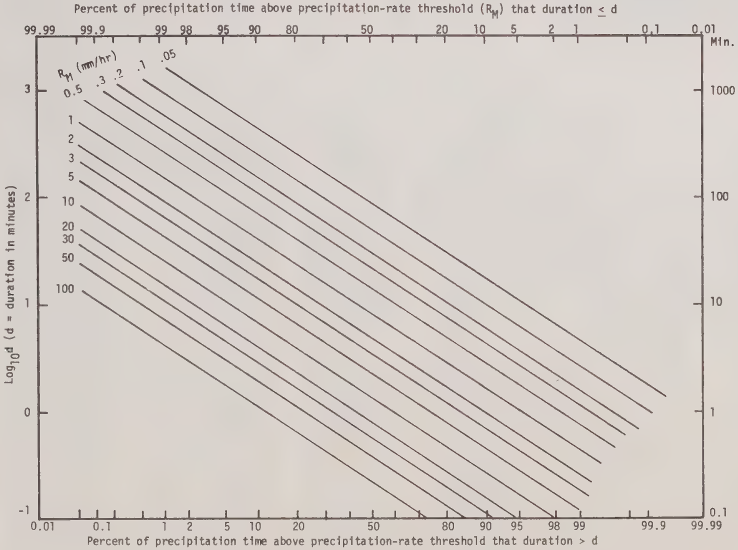

Figure 17. Cumulative precipitation-rate duration distributions for various precipitation-rate thresholds

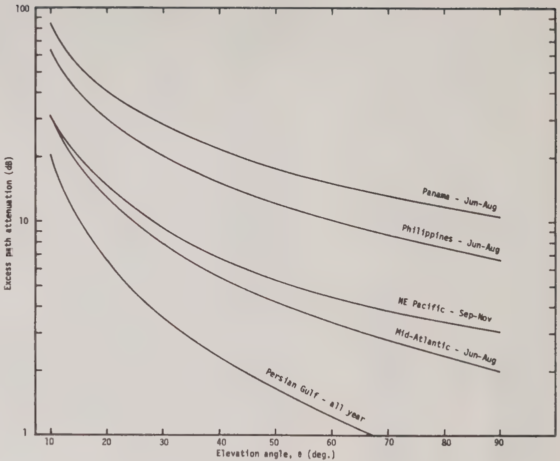

Figure 16. Attenuation vs elevation angle at 1% exceedance level for f = 44 GHz

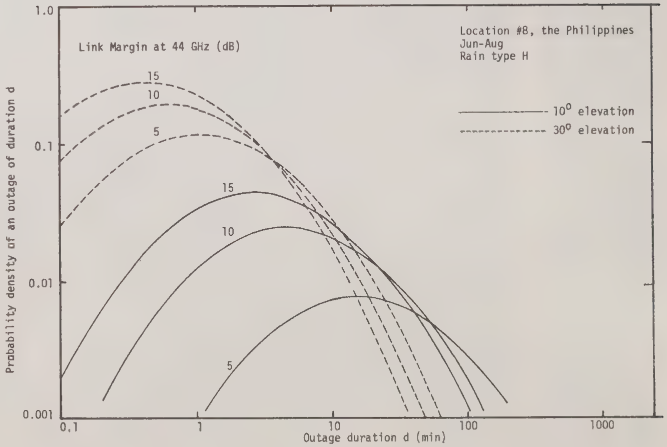

Figure 18. Outage duration probability density function for the Philippines, Jun-Aug

80-0521

A NEW ADAPTIVE CONTROL SYSTEM FOR COMPENSATING CROSS-POLARIZATION-COUPLINGS ON THE UP AND/OR DOWN PATH IN FREQUENCY REUSE SATELLITE COMMUNICATION SYSTEMS

H. Makino Y. Orino S. Orui
Kogakuin University

H. Fuketa T. Inoue
Yokosuka Electrical Communication Laboratory, N.T.T.

Abstract

A new system for compensating cross-polarization-couplings is proposed. This system enables individual compensation without using a beacon signal on each radio channel included in a TDMA satellite link. The principle is a cancellation of the cross coupled components by supplying the compensation signal adaptively. A Farady rotator is used for discrimination of amplitude and polarity of the compensation signal. Modified orthogonal modulations are applied to the compensation signal for independent controllings of amplitude and phase. Guard time slots between signal bursts radiated from earth stations are used in order to get information for compensation. This also enables uplink compensation at each earth station. Experimental results have shown that the XPD of about 40 dB can be obtained when the XPD without compensation is 15 dB. Some considerations on the proposed system are described.

1. Introduction

In a frequency reuse system utilizing the orthogonal polarization, various orthogonality restoring systems, cross compensation systems, and hybrid systems have been proposed by many authors in order to compensate for the cross coupling between the two polarizations (1)~(6). However, they are compensation systems in which all radio channels included in the link are commonly compensated by equipments for compensation controlled by information obtained from a beacon signal allocated in the link. For this reason, they can be called "common compensation system".

On the other hand, a compensation system in which the compensation can be performed individually in each radio channel without using a beacon signal has not been proposed yet. This system can be called "individual compensation system".

In order that the common compensation systems are effective, the overall frequency dependence of the cross-polarization-couplings on the transmission path including antennas, feed systems, and the propagation path should be compositely uniform both in amplitude and phase over the whole bandwidth of the radio link.

In the quasi-millimeter-wave bands such as 20 or 30 GHz, it is too optimistic to assume that the frequency dependence of the cross-polarization-coupling due to various causes is compositely uniform over the whole bandwidth of about 2.5GHz. In these frequency bands, the frequency dependence of the cross-polarization-coupling due to oblate and canted rain drops is not negligible (7)~(10). It also has not been guaranteed that the frequency dependences of the cross coupling on antennas and feeders are uniform.

In the common compensation system, therefore, even if a perfect compensation is performed for a beacon signal, compensations for radio channels using frequencies different from the beacon signal becomes imperfect. In other words, it can be said that the compensation approaches perfect as the bandwidth under compensation is made narrow.

In the individual control system, on the contrary, approximately perfect compensations can be expected for each radio channel because the bandwidth of the signal under compensation is quite narrow as compared with in the common compensation system. In the individual compensation system, however, information necessary for compensation must be obtained from each radio channel itself since a beacon signal is not used as an information source.

In any system for compensating cross-polarization coupling, compensation should be performed independently for the up and downlink. On an uplink, moreover, signal bursts radiated from several earth stations get to the satellite via different propagation paths. Each signal burst, therefore, suffers different cross-polarization-coupling. The solution to this problem is that pre-compensation is performed on each signal burst before transmission.

The frequency reuse system proposed here, which is a kind of cross compensation system, makes possible individual compensation without using a beacon signal and also provides the compensation for each signal burst on the uplink of a TDMA communication satellite system.

2. Concepts of the proposed compensation system

In a cross compensation system, the following requirements should be satisfied for every signal spectrum under compensation.

1) The amplitude of the signal for compensation can be made zero when the orthogonality between two polarized signals is complete because the cross-polarization-coupling does not exist in this condition.
2) The polarity (or sign) of the signal for compensation can be reversed on both sides of the zero amplitude point, because the polarity of the coupled component is reversed on both sides of the orthogonal condition as shown in Fig. 1. This does

Copyright © American Institute of Aeronautics and Astronautics, Inc., 1980. All rights reserved.

not mean a phase shift of 180 degrees but means the inversion of the polarity.

3) The amplitude of the signal for compensation can be controlled as equal to that of the coupled component.

4) The phase difference between the coupled component and the signal for compensation can be controlled as equal to 180 degrees.

5) The above controllings can be accomplished adaptively according to the changing of coupled components.

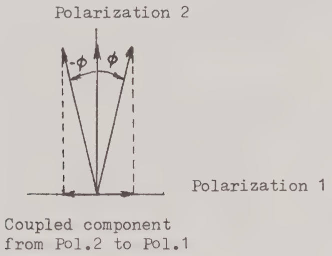
Polarization 2
-ϕ
ϕ
Polarization 1
Coupled component
from Pol.2 to Pol.1

Fig.1 Polarity inversion of coupled component

Fig. 2 shows a schematic block diagram of the proposed cross compensation system applied to the downlink. The system proposed here can meet the above requirements. Only the compensation for the signal in polarization 1 will be explained here because the circuits are identical for signals with polarization 1 and 2 as shown in Fig. 2.

In Fig. 2, signals received by an antenna are converted from circular to linear polarization by the circular/linear polarizer (CLP) and separated in polarization by the ortho-mode transducer (OMT1) and amplified by the low noise amplifier (LNA) and branched to several radio channels by the branching filters (BRFs). Although cross coupling compensations are performed for every channel pair having the same frequency in the frequency reuse system, only one pair of communication channels is shown in Fig. 2.

The rotatable waveguide (RWG) following the BRF, as shown in Fig. 3(a), is an waveguide having circular cross sections at both ends and a rectangular cross section at the middle part and this is rotatable around the waveguide axis by supporting both ends with rotary joints (not shown in the figure). In the RWG, the mode of electric field is TE11 at the input port, TE10 at the rectangular part, and TE11 again at the output port.

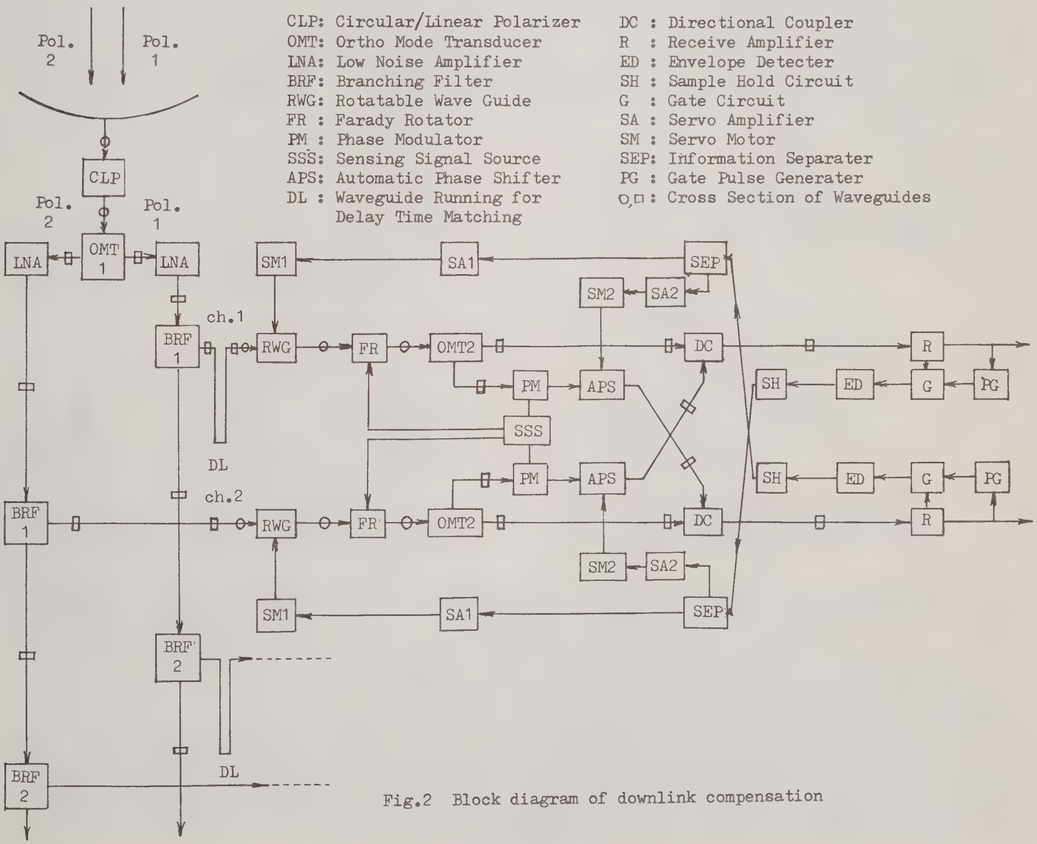
CLP: Circular/Linear Polarizer
OMT: Ortho Mode Transducer
LNA: Low Noise Amplifier
BRF: Branching Filter
RWG: Rotatable Wave Guide
FR : Farady Rotator
PM : Phase Modulator
SSS: Sensing Signal Source
APS: Automatic Phase Shifter
DL : Waveguide Running for Delay Time Matching
DC : Directional Coupler
R : Receive Amplifier
ED : Envelope Detecter
SH : Sample Hold Circuit
G : Gate Circuit
SA : Servo Amplifier
SM : Servo Motor
SEP: Information Separater
PG : Gate Pulse Generater
○,□ : Cross Section of Waveguides
Pol. 2
Pol. 1
CLP
Pol. 2
Pol. 1
LNA
OMT 1
LNA
SM1
SA1
SEP
SM2
SA2
ch.1
BRF 1
RWG
FR
OMT2
DC
R
PM
APS
SH
ED
G
PG
SSS
DL
SH
ED
G
PG
ch.2
PM
APS
BRF 1
RWG
FR
OMT2
DC
R
SM2
SA2
SM1
SA1
SEP
BRF 2
DL
BRF 2

Fig.2 Block diagram of downlink compensation

As shown in Fig. 3(b), when the rectangular part of this element is tilted by the angle of θ from the horizontal plane and the input field vector E is in the vertical direction, the output veator becomes Ecosθ and the component of Esinθ is cut off by the rectangular part. The FR will be explained later.

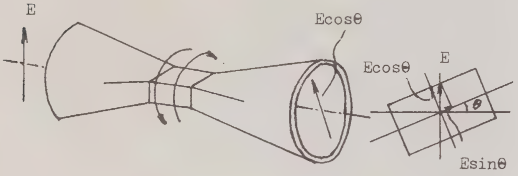

(a) (b)

Fig. 3 Rotatable Waveguide (RWG)

The OMT2 following the FR, as shown in Fig. 4(a) and (b), has two output ports A and B. When the signal Ecosθ from RWG is input to the OMT2, Ecosθ sinθ appears at port A and Ecosθ at port B. The output at port B is the main signal in polarization 2. The output at port A is a part of the main signal in polarization 2 and used for cancelling the cross coupled component to the main signal in polarization 1. It is obvious that the requirement 1), 2), and 3) described at the beginning can be satisfied by the use of the RWG and the OMT2. In order to meet the requirement 4), the variable phase shifter (APS) is inserted into the circuit of the compensation signal. Thus, the signal for compensation can be obtained.

In an actual case, however, the amplitude, the polarity, and the phase of the coupled component are changing in time, so the compensation signal should be controlled adaptively. For this purpose, it is necessary to discriminate always the result of compensation.

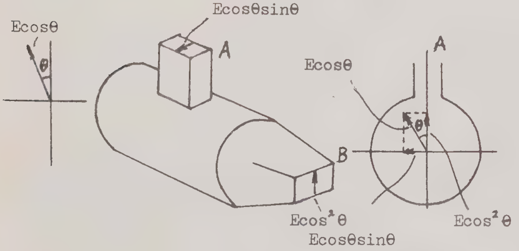

(a) (b)

Fig. 4 Ortho-mode transducer (OMT2)

In discriminating the amplitude and the polarity, the Farady Rotator (FR) shown in Fig. 5(a), inserted between the RWG and the OMT2, plays an important role. In a Farady Rotator, when an alternating magnetic field is applied along the axis of circular waveguide, the tilt angle of polarization plane changes periodically around the original position with the same frequency as that of alternating magnetic field as shown in Fig. 5(c). This technique can be called "Polarization Sensing".

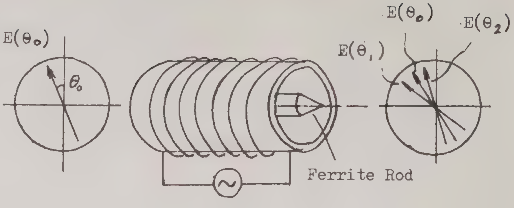

(b) (a) (c)

Fig.5 Farady Rotator (FR)

At the OMT2 following the FR, the output signal at port A is the projection of the input vector on the horizontal plane as shown in Fig. 6(a), (b), and (c). In any case, the amplitude modulation is generated on the output signal at port A. For this reason , the polarization sensing can be also called "Amplitude Sensing". The frequency of the AM envelope is the same as that of the alternating magnetic field but there is a phase inversion of the AM envelope between state (a) and (b). At the state (c) where the average tilt angle is zero, the frequency of the AM envelope is doubled. The AM envelope is detected by the envelope detecter (ED) after branched from the receive amplifier (R). Thus, the output signal of the ED indicates the tilting states of the polarization plane in the OMT2. The tilt angle of RWG can be adjusted by a two-phase servo motor(SM1) which is driven by the output of servo amplifier (SA1) which amplifies the output signals of the ED.

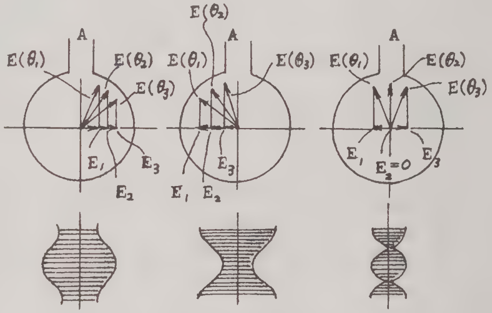

(a) (b) (c)

Fig.6 Output signal from the OMT2

When a cross-polarization-coupling does not exist, the servo-motor torque is generated in the direction so that the polarization plane in the OMT2 becomes state (c) from the initial state (a) or (b) and becomes zero at the state (c) and the RWG stops at that state.

When cross-polarization-coupling exists, it is required that the output signal from port A is able to cancel the coupled component at the directional coupler (DC). In other words, at the DC, the compensation signal should have equal amplitude and anti-phase against the cross coupled component.

The phase adjustment can be done by the automatic phase shifter (APS) as described later. Under the anti-phase condition, the servo loop for amplitude control works so that the RWG stops when the coupled component has been just cancelled.

For controlling the phase angle of compensation signal, the APS can be adjusted by a two-phase servo motor (SM2). In order to decide the direction of rotation of the servo-motor, the phase modulator (PM) is inserted to the circuit so that the compensation signal can be phase-modulated by a low frequency signal. Fig. 7(a), (b), and (c) show vector diagrams of the coupled component and the phase-modulated compensation signal. The phase modulation can also be called "Phase Sensing".

An amplitude modulation is generated on the resultant vector in any case and the frequency of the AM envelope is the same as that of phase modulation but there is a phase inversion of the AM envelope between state (a) and (b). In state (c), where average phase angle is 180 degrees, the frequency of the AM envelope is doubled. The AM envelope is detected by the ED and amplified by the servo amplifier(SA2) and drives a servo-motor (SM2). Thus the phase difference between two signals can be held at 180 degrees.

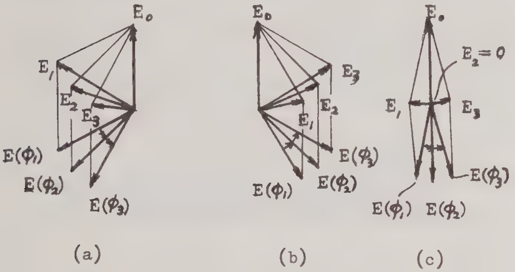

(a) (b) (c)

Fig. 7 Effects of phase modulation

3. Independent controls of amplitude and phase

As described in the previous section, sensing the polarization and the phase generates two amplitude modulations on the compensated signal and they are detected by the same detector. Therefore, it is necessary to avoid a cross talk between amplitude sensing and phase sensing in order to control the amplitude and the phase of the compensation signal independently. Three methods are considered for this purpose.

a) Frequency division modulation
b) Time division modulation
c) Orthogonal modulation

As a result of experiments, it has been found that method c) modified slightly gives the most successful result.

In method c), modulation signals used for the polarization sensing and the phase sensing have the same frequency and a phase difference of 90 degrees. A sensing frequency of 65 Hz has been used in the experiment. In this method, the cross talk between both sensings can be avoided as long as the phase difference of 90 degrees is kept. However, there is a difficulty in the long term stability of the phase difference. Waveforms having a zero-volt pedestal as shown in Fig. 8 are very effective in avoiding the cross talk due to drift of the phase angle.

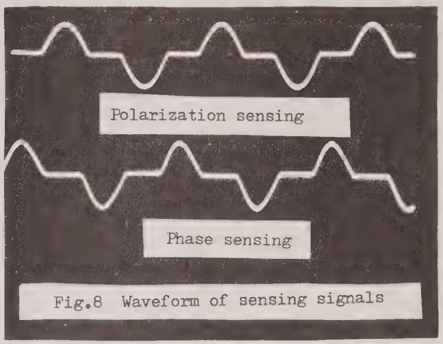

Fig.8 Waveform of sensing signals

The signal from the ED has a waveform in which two waveforms shown in Fig. 8 are synthesized in various amplitudes and polarities. In order to control the RWG and the APS independently, information on amplitude and phase must be separated from the synthesized waveform. By gating the peak voltages of the signal at the information separater (SEP) in Fig. 2, two bipolar pulse trains shown in Fig. 9 are obtained and there is not any cross talk between them. Each servo-motor is driven by the signal derived respectively from these pulse trains. Thus the RWG and APS can be controlled independently.

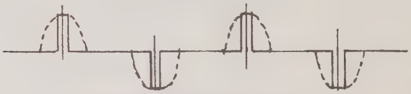

For amplitude control

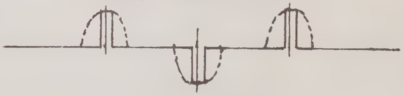

For phase control

Fig.9 Bipolar pulse trains

4. Use of guard time slots to get information for compensation

In the cross polarization compensation system without using a beacon signal, information necessary for compensation must be obtained from each communication signal itself.

In a TDMA satellite communication system, as shown in Fig. 10(a), guard time slots τ_A, τ_B, τ_C, τ_D which have pre-determined time duration intervene between signal bursts S_A, S_B, S_C, S_D radiated from earth stations A, B, C, and D, respectively.

These guard time slots can be used in order to get information on the cross-polarization-couplings with the least disturbance since signal energy does not exist in these time slots. In the proposed system, in two communication channels 1 and 2 having the same frequency in the orthogonal polarization, as shown in Fig. 10(b), an appropriate time difference τ_0 is set up between signal bursts in the channel 1 and 2 radiated from each earth station so that guard time slots of both channels do not coincide in time. Thus, as shown in Fig. 10(b), the cross coupled components from signal bursts of channel 2 appear in each guard time slot τ_{A1}, τ_{B1}, τ_{C1}, τ_{D1} in channel 1. In the same way, the cross coupled component from signal bursts of channel 1 appear in each guard time slot τ_{A2}, τ_{B2}, τ_{C2}, τ_{D2} in channel 2. These signal burst trains are received and amplified by the receive amplifier (R), and the output of the receive amplifier is branched and gated by a gate circuit (G) which opens only for the guard time period. The gating pulse can be obtained by the envelope detection of the burst train. Thus, cross coupled components can be obtained as a form of PAM carrier signal as shown in Fig. 11.

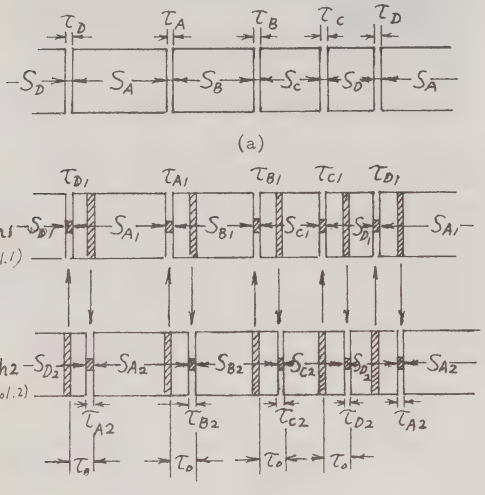

(a)

(b)

Fig.10 Signal bursts radiated from earth stations

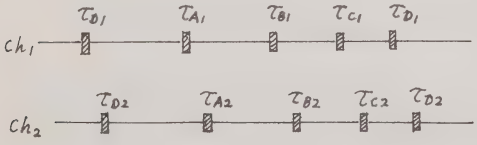

Fig. 11 Gated cross coupled components

In this case it is desired that each cross coupled component appearing in each time slot is not modulated in order to make it easy to discriminate the information on amplitude and phase. For this purpose, a c.w. signal is inserted for the time period of the channel 2 (or 1) interfaced in time to the guard time slot of the channel 1 (or 2) as shown by the hatched part of signal bursts in Fig. 10(b). It is necessary, moreover, that time durations of signal bursts in each pair are made equal to each other in order to keep equal the interface condition in each pair of signal bursts.

5. Restoring of the sensing waveform

In order to discriminate the results of compensation, the cross coupled components generated in the guard time slots are gated out from the receive amplifier and detected by the ED. The signal from the ED has a waveform of PAM as illustrated in Fig. 12(a) and its envelope is needed for controlling the servo loop. The sample hold circuit is very useful to derive the envelope waveform efficiently from the PAM signal. The output waveform of the sample hold circuit is illustrated in Fig. 12(b). This waveform can be smoothed easily by passing it through a proper low pass filter. Thus, the waveform needed for compensation can be obtained as illustrated in Fig.12(c).

Although the output signal from the sample hold circuit contains information on both amplitude and phase, these information can be separated and the RWG and the APS can be controlled independently as described in section 3.

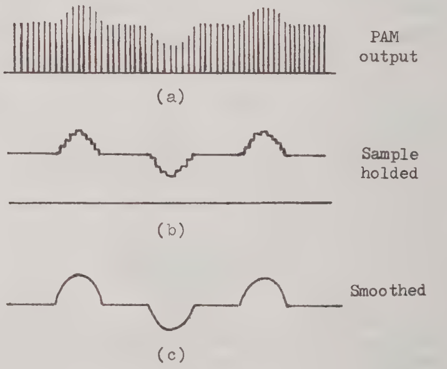

(a)

(b)

(c)

Fig. 12 Restoring the waveform by sample holding

6. Compensation for the uplink

A schematic block diagram for uplink compensation is shown in Fig. 13(a) and (b). On an uplink, as shown in Fig. 13(c), signal bursts radiated from several earth stations get to the satellite via different propagation paths. Each signal burst suffers different cross-polarization-coupling from each other. Pre-compensations, therefore, must be performed for each signal burst at each earth station.

MOD: Modulator
DEM: Demodulator
DMPX: Demultiplexer
HPA: High Power Amplifier
Other symbols are same as in Fig. 2.

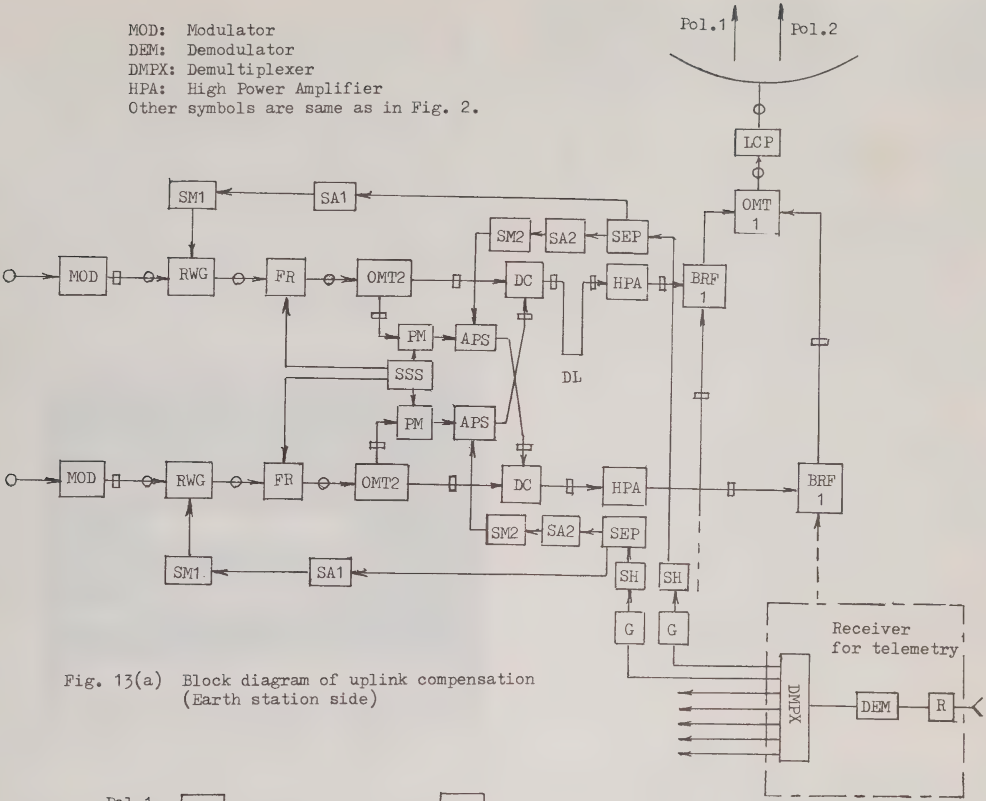
Pol.1
Pol.2
LCP
OMT 1
SM1
SA1
SM2
SA2
SEP
MOD
RWG
FR
OMT2
DC
HPA
BRF 1
PM
APS
SSS
DL
SH
G
Receiver for telemetry
DMPX
DEM
R

Fig. 13(a) Block diagram of uplink compensation (Earth station side)

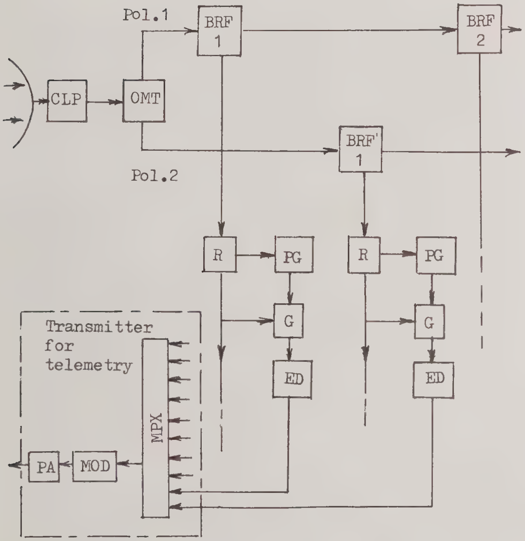
Pol.1
Pol.2
CLP
OMT
BRF 1
BRF 2
BRF' 1
R
PG
G
ED
Transmitter for telemetry
MPX
MOD
PA

Fig. 13(b) Block diagram of uplink compensation (Satellite side)

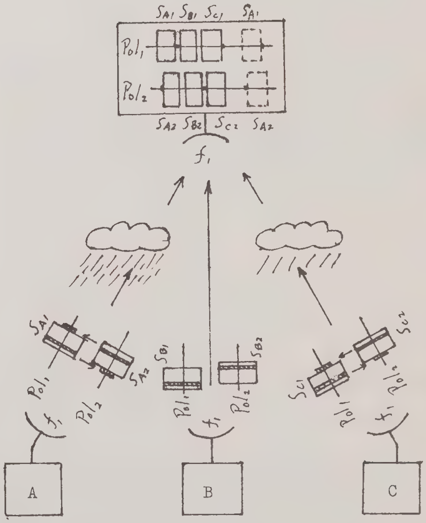
S_{A1} S_{B1} S_{C1} S_{A1}
Pol$_1$
Pol$_2$
S_{A2} S_{B2} S_{C2} S_{A2}
f_1
S_{A1}
S_{A2}
S_{B1}
S_{B2}
S_{C1}
S_{C2}
Pol$_1$
Pol$_2$
A
B
C

Fig. 13(c) Concept of the uplink compensation

This means that each earth station radiates the signals which have been cross-coupled intentionally in the earth station and the cross coupled components are just cancelled by rain drops on the propagation path when signals have reached to the satellite.

The result of compensation appears in the guard time slots as a envelope of the PAM signal on the satellite. The pulse trains obtained by envelope detection on the satellite are sent back to the earth station through the telemetry link by multiplex modulation as shown in Fig. 13(b). At each earth station, only the pulse train corresponding to the signal burst radiated by that station is selected from the pulse train sent back, and, the RWG and the APS in the earth station are controlled in the same way as the downlink compensation as shown in Fig. 13(a). Thus, the cross-polarization-coupling on an up-path can be compensated for each signal burst at each earth station.

An inherent problem in uplink compensation is the delay time due to the propagation velocity of a radio wave. The delay time of about 0.24 seconds is included in the servo loop of uplink compensation for the distance of 36000 Km between the earth and the satellite. Therefore the servo loop may not respond when the changing velocity of cross polarization coupling is so rapid. In the propagation data obtained so far, however, the changing velocity of cross-polarization-coupling due to rainfall is quite slow and it seems that the servo loop is able to have an adequately rapid response against the chaging of cross-polarization-coupling.

7. Experimental results

Experiments have been done at a frequency of 9.5 GHz in the laboratory. The reason this frequency has been used is simply due to measuring equipment and waveguide elements on hand.

Fig. 14 and 15 show the current sensitivities of the Farady rotator and the phase modulator used in the experiments, respectively.

Fig.16 shows the received PAM pulse and its envelope waveform obtained by sample holding.

Fig.17 shows improvements of the XPD (cross polarization discrimination) by the proposed system. It is shown in Fig.17 that the improvement of the XPD depends almost upon the amount of sensing.

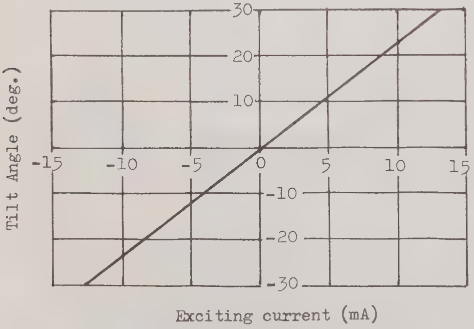

Fig. 14 Sensitivity of the Farady Rotator

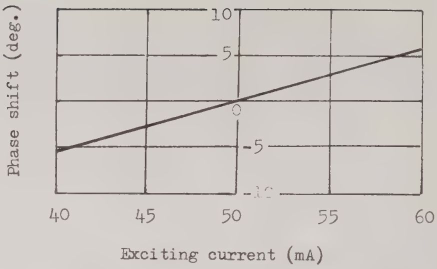

Fig. 15 Sensitivity of the phase modulator

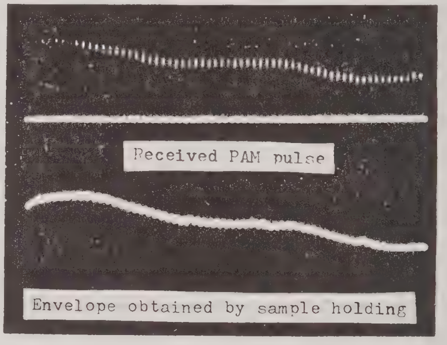

Fig.16 Received PAM pulse and its envelope

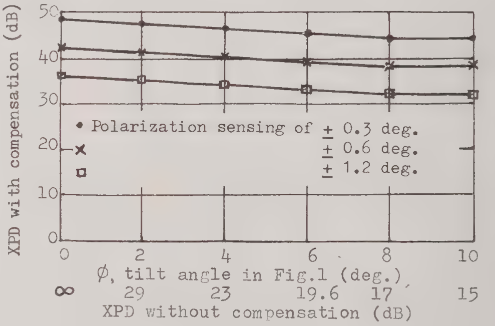

Fig. 17 Improvements of the XPD

8. Considerations on the proposed system

8.1 Analysis of the compensation bandwidth

The configuration of transmission system including the cross compensation is shown in Fig. 18. In the figure, $S_1(jw)$ and $S_2(jw)$ are signals radiated from the sending end in the polarization 1 and 2, respectively. Transmission properties are represented by $x_{11}(jw)$ and $X_{22}(jw)$, and cross couplings between the polarization 1 and 2 by $x_{21}(jw)$ and $x_{12}(jw)$, and $S_1'(jw)$ and $S_2'(jw)$ are signals received after separation in each polarization by the OMT. The block consisting of B_1, B_2, C_1, C_2, $K_{12}(jw)$, and $K_{21}(jw)$ is the cross compensation circuit, and $S_1''(jw)$ and $S_2''(jw)$ are output signals after cross compensation.

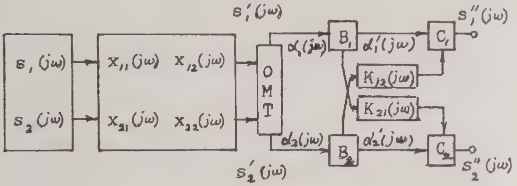

$$X_{mn}(j\omega) = X_{mn}(\omega)\, e^{-j\gamma_{mn}(\omega)}$$
$$\alpha_m(j\omega) = \alpha_m(\omega)\, e^{-j\theta_m(\omega)}$$
$$K_{mn}(j\omega) = K_{mn}(\omega)\, e^{-j\phi_{mn}(\omega)} \quad \text{where } m,n = 1,2$$

Fig. 18 Transmission system including cross compensation

$S_1''(jw)$ is given by the following equation.

$$\begin{aligned} S_1''(jw) = {} & S_1(jw)\, x_{11}(jw)\left\{\alpha_1(jw)\alpha_1'(jw) + \alpha_2(jw)\, K_{12}(jw)\, \frac{x_{21}(jw)}{x_{11}(jw)}\right\} \\ & + S_2(jw)\, x_{22}(jw)\left\{\alpha_1(jw)\alpha_1'(jw)\, \frac{x_{12}(jw)}{x_{22}(jw)} + \alpha_2(jw)\, K_{12}(jw)\right\} \end{aligned} \qquad (1)$$

In eq. (1), the first term gives the desired signal in polarization 1 and the second term gives the cross coupled component from the polarization 2.

The cross compensation means that the second term of eq. (1) is made zero. Therefore, $K_{12}(jw)$ should satisfy the following conditions.

$$\left.\begin{aligned} &\text{For amplitude:} \quad K_{12}(w) = -A(w)X_{12}(w) \\ &\text{where} \\ &\qquad A(w) = \frac{\alpha_1(w)\alpha_1'(w)}{\alpha_2'(w)} \\ &\qquad X_{12}(w) = \frac{\chi_{12}(w)}{\chi_{22}(w)} \end{aligned}\right\} \qquad (2)$$

$$\left.\begin{aligned} &\text{For phase:} \quad \phi_{12}(w) = \theta(w) + \Gamma_{12}(w) \\ &\text{where} \\ &\qquad \theta(w) = \theta_1(w) + \theta_1'(w) - \theta_2(w) \\ &\qquad \Gamma_{12}(w) = r_{12}(w) - r_{22}(w) \end{aligned}\right\} \qquad (3)$$

Compensation for every signal spectrum in the transmission band can be shown by the vector diagram in Fig. 19, where $a(w)$ is the amplitude of the cross coupled component, $b(w)$ is the amplitude of the compensation signal, $\psi(w)$ is the phase angle between $a(w)$ and $b(w)$, and $c(w)$ is the amplitude of the residual cross coupled component.

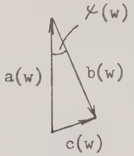

Fig. 19 Vector diagram of compensation

In Fig. 19, $c^2(w)$, the power spectrum of the residual component, is given by

$$c^2(w) = a^2(w) + b^2(w) - 2a(w)b(w)\cos\psi(w) \qquad (4)$$

When $\alpha_1(w)$, $\alpha_1'(w)$, $\alpha_2(w)$, and $\alpha_2'(w)$ in Fig. 18 can be regarded as unity, eq. (4) can be written as

$$X^2(w) = X_{12}^2(w) + K_{12}^2(w) - 2X_{12}(w)K_{12}(w)\cos\psi(w) \qquad (5)$$

The XPD, the cross polarization discrimination, is defined as the ratio between the total power of cross coupled components in the band and the total power of desired signal in the band. That is,

$$\mathrm{XPD} = \frac{\int_{-\delta}^{\delta} c^2(w)\, dw}{\int_{-\delta}^{\delta} S_1''^2(w)\, dw} \qquad (6)$$

where 2δ is the bandwidth.

By using a proper approximation, the XPD is given as follows.

$$\mathrm{XPD} = \frac{1}{2\delta}\int_{-\delta}^{\delta} X^2(w)\, dw \qquad (7)$$

From eq. (5), conditions that the XPD becomes zero (i.e. $-\infty$dB) for arbitrary w in the band are

$$\left.\begin{aligned} &K_{12}(w) = X_{12}(w) \\ &\psi(w) = \phi_{12}(w) - \{\theta(w) + \Gamma_{12}(w)\} = 0 \end{aligned}\right\} \qquad (8)$$

It is generally impossible to satisfy the above condition because frequency dependences of $X_{12}(w)$ and $\Gamma_{12}(w)$ are not uniform and changing in time. Assumming that the XPD without compensation is 15 dB and a perfect compensation has been done at the center frequency of the band, numerical results are illustrated in Fig. 20(a) and (b).

Fig. 20(a) shows the improvement of XPD for the bandwidth δ when both $K_{/2}(w)$ and $X_{/2}(w)$ are uniform and $\psi(w)$ is linearly inclined within the band.

Fig. 20(b) shows the improvement of XPD for the bandwidth δ when both $K_{/2}(w)$ and $\psi(w)$ are uniform and $X_{/2}(w)$ is linearly inclined within the band.

It is shown in these figures that the improvement of XPD is degraded as the bandwidth becomes wide and as the inclination of transmission characteristics in the band increases.

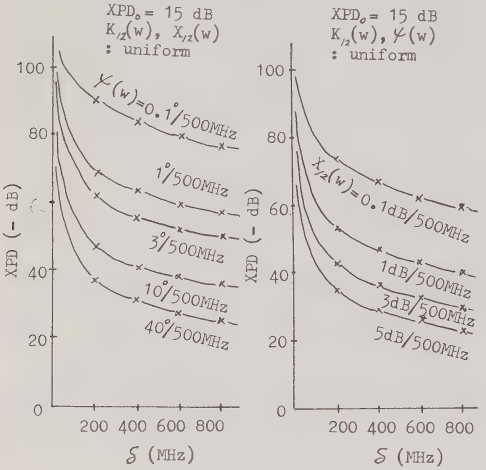

(a) (b)

Fig. 20 Relation between the bandwidth and the improved XPD

8.2 Attenuation of the main signal due to the RWG

Fig. 21 shows the relation between the tilt angle θ of the RWG and the attenuation of the main signal at port B of the OMT2. The main signal being cut off completely when θ is 90 degrees, it is necessary to place a mechanical stopper in the RWG so that the RWG can not tilt beyond a pre-determined angle. This angle can be determined from the worst XPD predicted.

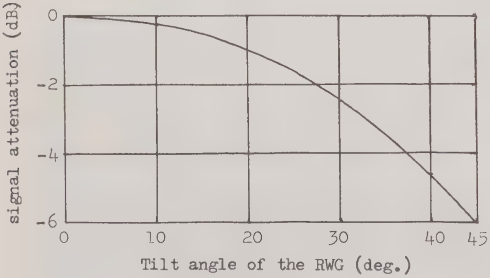

Fig. 21 Relation between tilt angle and signal attenuation

8.3 Considerations on a sensing method

In an adaptive control system without using a sensing method, the error voltage is obtained in a form of positive or negative d.c. voltage. A servo loop works in the direction so that the error voltage becomes small and stops when the error voltage has just become zero. The error voltage can be generally obtained as the output voltage of the coherent detection in the intermediate frequency circuit, and there is no matter when the output voltage is generated only by a control error.

In an actual case, however, the output voltage of the coherent detecter contains false error voltages which are generated by various causes such as a drift of the signal frequency, changing of the circuit constants due to temperature and aging, changing of the signal voltage etc.. Since it is impossible to distinguish the difference between the true error voltage and the false error voltages, the servo loop works so as to make the output voltage of the detecter zero. Thus the servo loop generates a control error.

On the contrary, in an adaptive control system using a sensing technique, the error voltage is obtained in the form of an a.c. voltage and the servo loop works in the direction which is decided by the polarity of the error voltage and stops when the frequency of the error voltage has been just doubled. In a sensing method, therefore, a simple envelope detecter can be used instead of a coherent detecter and any d.c. components does not affect the performance of the servo loop.

On the other hand, as an inherent property of sensing method, the residual cross coupled component always exists. In the sensing method, a positive and negative control error generates alternatively around the complete compensation in the doubled sensing frequency. This means that the average energy of the residual coupled component is not zero. Therefore the limitation of compensation depends almost upon the sensing level. For this reason, the sensing level should be as low as possible.

8.4 Problems of power loss and noise temperature

In a common compensation system, compensation equipments must be equipped between the antenna and the OMT. For an uplink compensation, this construction increases the loss of transmitted power and a heat-safe ability is also needed for compensation equipments. For an downlink compensation, the loss of received power due to compensation equipments increases a noise temperature. These problems become severe as the frequency becomes high.

In an individual compensation system, on the contrary, compensation equipments can be equipped preceeding the HPA for uplink compensation. Therefore the circuit loss is not a critical problem and a heat-safe ability is not needed for compensation equipments. For downlink compensation, equipments can be equipped behind the LNA and therefore increasing of the noise temperature is negligible. That is, an individual compensation system has much more merits than a common compensation system in the power loss and noise temperature.

8.5 Ability for fail-safe

In a common compensation system, there is a danger that the XPDs of all radio channels included in the link are much more degraded than without compensation when some failure has occurred in the control circuit. In other words, the ability for fail-safe is poor in a common compensation system.

In an individual compensation system, on the other hand, a shutter (e.g. a flap attenuator) can be inserted to each circuit for supplying the compensation signal, though not shown in Fig. 2 and Fig. 13(a). This shutter is closed manually or automatically when some failure has occurred in each control circuit. Thus the XPD keeps the value without compensation and does not affect the other channels at all. That is, the ability for fail-safe is rich in the cross compensation system.

9. Conclusion

A new adaptive control system for compensating the cross-polarization-couplings has been presented. Features of the proposed system are summarized as follows.

(1) An approximately perfect compensation can be obtained since compensations are performed for each radio channel which has relatively narrow bandwidth.

(2) Compensations for each up-path in an uplink can be individually performed by the use of guard time slots in order to get information required for compensations.

(3) The long term stability and reliability of adaptive compensation can be realized by applying the sensing technique to control the amplitude and the phase of the compensation signal.

(4) The cross talk between information of amplitude and phase generated by sensings can be avoided by using concept of the orthogonal modulation.

(5) The power loss in the uplink compensation and the noise temperature in the downlink compensation are not increased in the proposed system, as any equipment for compensation is not inserted between the antenna and the OMT.

(6) The fail-safe ability can be obtained by inserting a shutter to the circuit for supplying the compensation signal.

Although the proposed system has not been applied to an actual satellite link and further investigations are still needed, experiments in the laboratory have revealed satisfactory performances in the fundamental actions.

In further investigations, it is desired to stabilyze the loop gain by adding the AGC function to the servo loop. As the inherent problem on an uplink compensation, the long delay problem should be solved relating to the changing velocity of the cross-polarization-coupling on an actual satellite link.

References

(1) T.S. Chu, "Restoring the orthogonality of two polarizations in radio communication systems, I and II," Bell Syst. Tech. J., vol.50, pp3063-3069, Nov. 1971 and vol.52, pp. 319-327, Mar. 1973.

(2) D. F. Difonzo et al, "Adaptive polarization control for satellite frequency reuse system", COMSAT Technical Review, Vol. 6, No. 2, Dec. 1976.

(3) H. Kannowade, "An Automatic Control System for Compensating Cross Polarization Coupling in Frequency-Reuse Communication Systems", IEEE Trans. on Comm., Vol. 24, No. 9, Sept, 1976.

(4) S.K. Barton, "Methods of Adaptive Cancellation for Dual Polarization Satellite Systems", The Marconi Review, Vol. XXXIX No. 200, First Quarter 1976.

(5) R.E. Kreutel, "The orthogonalization of polarized fields in dual-polarized radio transmission systems", COMSAT Tech. Rev., vol.3, pp. 375-386, No.2, Fall 1973.

(6) L.S. Lee, "A Polarization Control System for Satellite Communications with Multiple Uplinks," IEEE Trans. on Comm., Vol. Com-26, No.8, August 1978.

(7) J.A. Morrison et al, "Perturbation Calculations of Rain induced Differential Attenuation and Differential Phase Shift at Microwave Frequencies", B.S. T.J. 52, No. 10, Dec. 1973.

(8) J.A. Morrison er al, "Rain-Induced Differential attenuation and Differential Phase Shift at Microwave Frequencies," B.S.T.J. Vol. 52, No.4, April, 1973.

(9) T. Oguchi, "Scattering properties of Pruppacher and-Pitter form raindrops and cross polarization due to rain: Calculations at 11, 13, 19.3, and 34.8 GHz", Radio Science, Vol. 12, No. 1, p-p 41-51, Feb-Jan 1977.

(10) T.Oguchi and Y.Hosoya, "Differential Attenuation and Differential Phase Shift of Radio Waves due to rain, Calculations at Microwaves and Millimeter Wave Regions", Journal Recherches Atmospheriques, Vol. III, Nos. 1-2, 1974.

80-0522

MICROWAVE FILTERS AND MULTIPLEXING NETWORKS FOR COMMUNICATIONS SATELLITES IN THE 1980s

C.M. Kudsia
K.R. Ainsworth
M.V. O'Donovan
Com Dev Ltd.
Cambridge, Ontario, Canada

Abstract

This paper describes recent and proposed developments in the performance and realization of microwave filters and multiplexers for the next generation of communications satellites. It includes tradeoffs for materials selection, realization of generalized transfer characteristics, performance comparison between externally equalized networks and self-equalized linear phase filters, amplitude and phase tracking between similar units in a spacecraft, contiguous versus non-contiguous multiplexers, and considerations of high power and passive intermodulation in synchronous orbit. There is a generous sprinkling of hard data at frequencies from 300 MHz to 20 GHz to support and highlight the practical tradeoffs.

Finally, there is discussion on emerging technologies that could result in advancing the state-of-the-art of microwave multiplexers for space application.

Introduction

Microwave filters and multiplexers continue to demand attention because of the payoff in terms of communications performance which results from even minor improvements in areas such as unloaded Q, function optimization techniques or hardware realization. Progress over the last decade has been impressive, as evidenced by use of significantly different and improved multiplexers on each successive generation of spacecraft. The status of filters currently used in operational satellite systems or scheduled to be launched in the near future are summarized in Table 1.

This paper describes the various tradeoffs involved in the selection of filters and multiplexers applicable to the present and next generation of satellites. Developments currently underway to effect further improvements for satellites of the 1980s are highlighted.

TABLE 1 MICROWAVE FILTERS & MULTIPLEXERS IN COMMUNICATIONS SATELLITES: STATE-OF-THE-ART

	FREQUENCY BAND	CONFIGURATION	PROGRAM	MULTIPLEXER SUPPLIER
Output Multiplexing Networks	4 GHz	4-Pole dual-mode elliptic function TE_{111} filters in INVAR on curved manifold	INTELSAT IV-A	Hughes Aircraft Co. (HAC)
		GFRP* 6-Pole dual-mode quazi-elliptic TE_{111} filters combined contiguously on a straight manifold	INTELSAT V	Ford Aerospace & Communications Corp. (FACC)
		6-Pole dual-mode quazi-elliptic TE_{111} filters in INVAR on curved manifold	ANIK-D PALAPA-B	COM DEV LTD. COM DEV LTD.
	11/12 GHz	4-Pole dual-mode elliptic function TE_{103} filters in INVAR	ANIK-B INTELSAT V	COM DEV LTD. COM DEV LTD.
		6-Pole dual-mode quazi-elliptic TE_{113} filters in INVAR	ANIK-C	COM DEV LTD.
		6-Pole Canonical dual-mode elliptic function TE_{113} filters in INVAR	SBS	HAC
Input Channelizing Filters	4 GHz	8-Pole dual-mode quazi-elliptic TE_{111} filters in INVAR	INTELSAT IV-A	HAC
		8-Pole dual-mode quazi-elliptic TE_{111} filters in GFRP*	INTELSAT V ANIK-D	FACC Spar Aerospace Ltd.
		6-Pole Canonical dual-mode elliptic function TE_{111} filters in INVAR	PALAPA-B	COM DEV LTD.
	11/12 GHz	8-Pole dual-mode quazi-elliptic TE_{113} filters in INVAR in cascade with 2-pole dual-mode allpass TE_{113} equalizer	ANIK-C	COM DEV LTD.
		6-Pole Canonical dual-mode elliptic function TE_{113} filters in INVAR in cascade with 4-pole dual-mode allpass TE_{113} equalizer.	SBS	HAC

* Graphite Fiber Reinforced Plastic.

Copyright © American Institute of Aeronautics and Astronautics, Inc., 1980. All rights reserved.

Material Selection Tradeoffs

The choice of materials to realize microwave filters and multiplexers is primarily determined by the frequency of operation and the filter bandwidth. In rare instances, where there is a specification for passive intermodulation, the chosen material must be non-ferrous and is typically aluminum. To highlight material selection tradeoffs, it is necessary to consider the equivalent linear frequency drift (ELFD), as described in Appendix 1, over the desired temperature range. In addition, some allowance must be made for the manufacturing and alignment tolerances. The allowance provided for these tolerances will increase as operating frequency is increased. In Table 2 they are taken into account in the 'TOTAL ELFD' column.

The mechanical properties of the materials in conjunction with the manufacturing techniques primarily determine the minimum wall thickness necessary to fabricate the filters and multiplexers. Table 2 provides the material selection tradeoffs and lists the key assumptions. Based on this table, the following conclusions are drawn:

- There is marginal difference in weights for filters composed of aluminum, magnesium or graphite fiber reinforced plastic (GFRP). Magnesium and GFRP are difficult materials to work with and can be very costly. Thus, for applications where frequency drift associated with aluminum can be tolerated, its use provides the most cost effective approach.
- For wideband filters (>5% BW) irrespective of the frequency of operation, or narrow-band filters below 1 GHz, aluminum can be used with all its advantages.
- For narrow-band filters (up to 2% BW) at 2 GHz and up, use of Invar or GFRP is invariably required to keep the equivalent linear frequency drift a small fraction of the design bandwidth. Here, the tradeoff is between the higher cost, slightly inferior performance but lower weight of the GFRP units relative to those fabricated in Invar. At 8 GHz and above, the balance tilts decisively in favour of Invar. There are three reasons for this. Firstly, the weight differential between Invar and GFRP units above 8 GHz is quite small in the absolute sense. Secondly, the mechanical tolerances of half-a-mil or less required above 8 GHz are difficult to achieve in GFRP. Finally, the effect of long term "creep", while acceptable at 4 GHz [1], could lead to the use of additional cavities at higher frequencies to ensure performance integrity. This would eliminate the weight advantage which is the raison d'être for the use of GFRP. It is expected that, with the space shuttle, the lower cost of launch will further bias the choice towards Invar.

TABLE 2 MATERIAL SELECTION TRADEOFFS FOR MICROWAVE FILTER NETWORKS

Operating temperature range 0°C to 50°C

Allowance for misalignment & manufacturing tolerances in TOTAL ELFD = ±.25 MHz at 4 GHz; ±.5 MHz at 12 GHz; ±.75 MHz at 20 GHz

MATERIAL	COEFFICIENT OF THERMAL EXPANSION (α) RAW MATERIAL ppm/°C	EFFECTIVE 'α' FOR A FINISHED FILTER * ppm/°C	SPECIFIC GRAVITY	NORMALIZED** WEIGHT OF A FINISHED RF FILTER	TOTAL ELFD IN MHz CENTER FREQUENCY IN GHz					
					.3	1	2	4	12	20
Magnesium	29.8	35	1.74	1	.5	1.15	2	3.8	11	18.3
Aluminum	22.4	25	2.7	1.2	.45	.9	1.5	2.8	8	13.3
Stainless Steel	5.3	6	7.9	1.45	.3	.4	.55	.85	2.3	3.8
Invar	1.6	2 to 2.5	8.05	1.5	.27	.3	.4	.5	1.2	2
GFRP***	1.5	2 to 3.0	1.35	1.1	.27	.3	.4	.55	1.4	2.25

* Coefficient of thermal expansion in a finished filter is always greater than that of the raw material. This discrepancy is due to manufacturing processes, non-ideal shapes of resonant cavities, and use of tuning elements in the finished filter.

** This is based on using 20 mil average thickness for Invar and steel units, 40 to 45 mil average thickness for Al & Mg, and 50 mil thickness for GFRP. Other hardware like screws, bushings, plating etc., is the same for all units.

*** GRFP temperature data does not take into account long term "creep" effects which will result in a slightly larger allowance for ELFD. At 4 GHz, available data [1] indicates an ELFD of .365 MHz due to long term "creep" over a 10 year life span.

Realization & Structure Tradeoffs

At microwave frequencies, the practical range of impedances that can be realized in a given structure is typically 40 to 1. This is a severe constraint in realizing microwave filters and has resulted in a large variety of structures to suit the operating frequency band and the required bandwidths. In addition, the achievable unloaded Q in a given realization is a key consideration as it determines the size of the structure. For waveguide networks [2, 3], an additional degree of freedom exists since either single-mode or orthogonal dual-mode structures can be used. For low loss filters requiring moderate to high Qs, the typical realizations are in waveguide, coaxial and interdigital structures. Table 3 and Figures 1 to 3 describe the various tradeoffs and achievable unloaded Qs for these realizations.

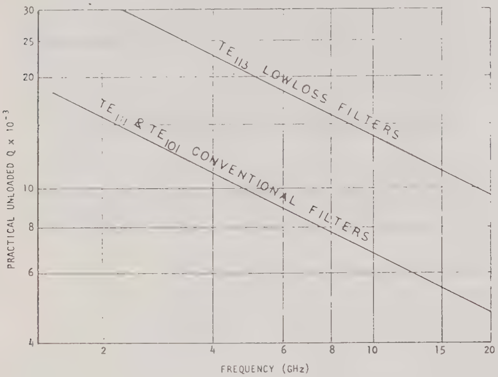

FIGURE 1 PRACTICAL UNLOADED Q OF WAVEGUIDE FILTERS AS A FUNCTION OF FREQUENCY

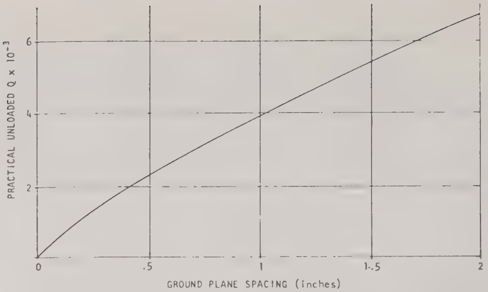

FIGURE 2 PRACTICAL UNLOADED Q OF INTER-DIGITAL FILTERS FOR NARROW BANDWIDTH

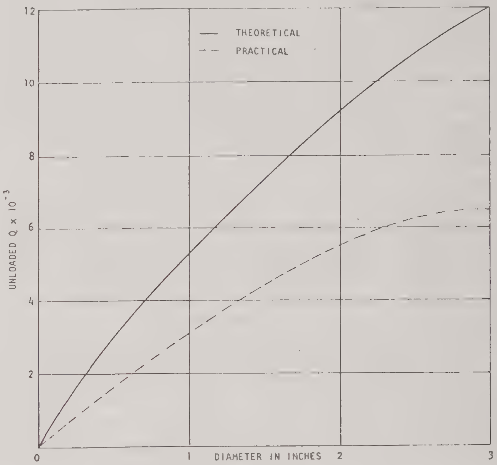

FIGURE 3 UNLOADED Q OF COAXIAL FILTER AT 1.5 GHz

TABLE 3 FILTER REALIZATION & STRUCTURE TRADEOFFS

FILTER STRUCTURE	PREFERRED OPERATING FREQUENCY BAND (GHz)	PRACTICAL UNLOADED Q	AVAILABLE BANDWIDTH	SALIENT CHARACTERISTICS
Standard Waveguide	2 - 90	See Fig. 1	<10%	Simplest but bulky structure. Single-mode operation. Poor isolation response beyond 1.5 x f_o. Restricted to all-pole response functions.
Circular/Square Waveguide	2 - 90	See Fig. 1	<10%	Simple construction & permits dual-mode operation. No restriction on response functions under dual-mode operation. Poor isolation beyond 1.5 x f_o. Greater incidence of spurious.
Evanescent Mode Structure	.2 - 12	Typically half of standard WG structure	<15%	Simple construction but sensitive to temperature. Superior wideband isolation characteristics. Provides a practical Q vs size tradeoff.
Inter-Digital (ID) Structure	.1 - 14	See Fig. 2	<70%	Simple construction but bulky to realize high Qs. No restriction on bandwidth. Superior wideband isolation characteristics.
Coax Cavity Structure	.1 - 8	See Fig. 3	<5%	High Q structure but bandwidth limitations. Construction can be difficult depending upon requirements of response functions and weight.
Dielectric Loaded Resonator Filters	.1 - 4	Typically half of ID structure	<25% in ID structure	Compact structure but lower Qs. Sensitive to temperature. Requires superior dielectric materials. Construction can be difficult.

As can be seen, there is an enormous range of Q that is possible and, therefore, proper evaluation of this parameter is an important design consideration. As an approximate guide, the unloaded Q varies as the ratio of volume to surface, i.e., the bigger the volume, the higher the available Q. Other considerations are that of realizable bandwidth and spurious passbands which are different for different realizations.

There is no restriction in realizing any response functions with any of these structures. However, a dual-mode waveguide configuration is the simplest structure for the realization of generalized transfer characteristics with dominant or higher-order TE_{10n} or TE_{11n} propagation modes.

Dual-Mode Canonical Realization

The present generation of communication satellites use dual-mode, longitudinal (in-line) RF filters for separating and combining channels in the spacecraft. This is the simplest dual-mode realization with input and output ports located in the first and last physical cavities as shown in Figure 4(a). This realization restricts the number of available couplings and hence the response shape.

A canonical realization will permit the maximum permissible number of couplings in a dual-mode configuration. This implies the realization of virtually any response shape. It will be a prime design candidate for satellite multiplexers in the next decade.

COMSAT [4] described the symmetrical canonical structure shown in Figure 4(b). An asymmetrical dual-mode canonical structure based on work at Siemens [5] is shown in Figure 4(c).

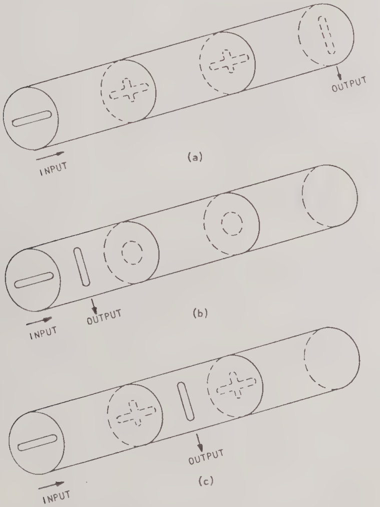

FIGURE 4 DUAL-MODE FILTER REALIZATIONS IN CIRCULAR WAVEGUIDE
(a) LONGITUDINAL IN-LINE STRUCTURE,
(b) SYMMETRICAL CANONICAL STRUCTURE, AND
(c) ASYMMETRICAL CANONICAL STRUCTURE

Both types are capable of realizing the generalized response characteristics. For the symmetrical structure, the couplings required between the physical cavities are equal for the two orthogonal modes. This simplifies the fabrication and assembly of the irises. However, it requires that the input and output ports be located in the same physical cavity. This results in interaction between the input and output and makes the structure sensitive to both the fabrication and alignment tolerances necessary for optimum performance. On the other hand, the asymmetrical realization requires coupling irises which permit the input and output ports to be located in separate physical cavities. This design will require extra effort in the fabrication of irises; also their assembly must ensure orthogonality of the two modes. The location of input and output ports in separate cavities significantly simplifies the alignment of the filter. At this time, one would be hard pressed to declare a preference between these two realizations.

The realization of a completely generalized transfer characteristic in a dual-mode configuration represents an important advance in the state-of-the-art. It provides the communications system designer with a menu of attractive tradeoffs, hitherto unavailable, to assist in optimizing the communications capacity of the RF channel.

Linear Phase Versus Externally Equalized Dual-Mode Filters

There is continuing controversy between external equalization and self-compensating linear phase networks whenever linearization of phase or group delay is required. It is the authors' experience that most of these comparisons are based on qualitative measures and, depending on the spokesman, one or the other network may be argued to be superior. To crystallize this comparison, filter responses for both cases were computed with respect to the specifications for input multiplex filters for the ANIK-C and SBS spacecraft. For the ANIK-C filters, a longitudinal dual-mode structure is chosen whereas for SBS filters, realization is in dual-mode canonical configuration. Tables 4 & 5 describe the respective tradeoffs for the two input multiplexers.

From these computed characteristics, the following conclusions are drawn:

- For typical satellite requirements, external equalization provides 5 to 10 dB higher isolation as compared to a linear phase structure. Alternatively, for the same isolation characteristics, external equalization provides better in-band group delay and gain slope response. The overall degree of the network is the same for both cases.

- External equalization results in a weight penalty because of the necessity of using coupling circulators. Space units must be very stable over the operating temperature range. For this reason, performance of group delay and amplitude variation and their slope stabilities tend to be better with linear phase structure.

TABLE 4 INPUT MULTIPLEXER FILTER TRADEOFFS FOR ANIK-C SATELLITE USING LONGITUDINAL DUAL-MODE TE_{113} FILTER & EQUALIZER

CRITICAL PERFORMANCE REQUIREMENTS*

Frequency Band : 11.7 to 12.2 GHz
Usable Channel Bandwidth : $f_o \pm 27$ MHz
Insertion Loss Variation : <1.2 dB over $f_o \pm 27$ MHz
Isolation : ⩾25 dB at $f_o \pm 36$ MHz
⩾45 dB at $f_o \pm 50$ MHz and beyond
Amplitude Slope : ⩽.01 dB/MHz over $f_o \pm 13$ MHz
Group Delay : ⩽2 ns at $f_o \pm 18$ MHz
⩽5 ns at $f_o \pm 21$ MHz
⩽1.5 ns ripple
Assumed equivalent linear frequency drift : ± 1 MHz
Assumed average Unloaded Q of Waveguide Cavities : 11,000

FILTER CONFIGURATION	ISOLATION AT ±36 (dB)	LOSS VARIATION OVER ±27 (dB)	GAIN-SLOPE OVER ±13 (dB/MHz)	GROUP DELAY (ns)		
				±18	±21	RIPPLE
10-pole linear phase filter with two pairs of real-axis zeros	15	.65	.006	1	3	.5
	20	.8	.007	1	4	1
	25	1.4	.013	1.8	5.5	1
10-pole linear phase filter with one pair of transmission zeros & one pair of real-axis zeros	20	.8	.011	3.5	8	0
	25	1	.016	7	11	0
	30	1.25	.016	7	12.5	0
8-pole filter with one pair of transmission zeros & 2-pole allpass equalizer	25	.75	.003	.7	3	.5

* These requirements are for the whole transponder prior to the TWTAs.

TABLE 5 INPUT MULTIPLEXER FILTER TRADEOFFS FOR SBS SATELLITE USING CANONICAL DUAL-MODE TE_{113} FILTER & EQUALIZER

CRITICAL PERFORMANCE REQUIREMENTS*

Frequency Band : 11.7 to 12.2 GHz
Usable Channel Bandwidth : $f_o \pm 21.5$ MHz
Insertion Loss Variation : <1.0 dB over $f_o \pm 21.5$ MHz
Isolation : ⩾15 dB at $f_o \pm 27.7$ MHz
⩾35 dB at $f_o \pm 31$ MHz and beyond
Amplitude Slope : ⩽.084 dB/MHz over $f_o \pm 15$ MHz
Group Delay : ⩽2 ns at $f_o \pm 15$ MHz
⩽5 ns at $f_o \pm 17$ MHz
⩽11 ns at $f_o \pm 19$ MHz
⩽27 ns at $f_o \pm 21.5$ MHz
⩽1.2 ns ripple
Assumed equivalent linear frequency Drift : ± 1 MHz
Assumed average Unloaded Q of Waveguide Cavities : 11,000

FILTER CONFIGURATION	ISOLATION (dB) AT		LOSS VARIATION OVER ± 21.5 (dB)	GAIN-SLOPE OVER ± 15 (dB/MHz)	GROUP DELAY (ns)				
	±27.7	±31			±15	±17	±19	±21.5	RIPPLE
8-pole filter with one pair of transmission zeros & two pairs of real-axis zeros	8.5	28	.65	.04	1	3.5	9	20	1
	10	30	.7	.04	1.2	4	9.5	25	1
	15	⩾35	1.1	.045	2.0	6.0	12.5	35	1
8-pole filter with two pairs of transmission zeros & one pair of real-axis zeros	15	⩾35	1.1	.055	6.5	10	17	40	0
	20	⩾35	1.2	.06	7	11	18.5	43	0
	25	⩾35	1.35	.065	7.5	12	20	48	0
6-pole elliptic function filter with two pairs of transmission zeros plus 2-pole allpass equalizer	15	⩾35	.9	.016	1	3.5	10	29	1.1

- Alignment of the channel is considerably simpler using external equalization. This is because the filter and allpass networks are completely independent of each other and their characteristics add algebraically. For the linear phase structure, one must monitor amplitude and group delay response simultaneously or go back and forth from amplitude to delay response during the alignment of the filter. This makes the network difficult to tune and sensitive to manufacturing tolerances.

On the whole, it is our contention that external equalization yields superior characteristics and is more cost-effective to implement. This statement is valid for typical satellite requirements but should not be extrapolated to imply universality. The optimality of a response function depends very strongly upon the specification requirements. It is to be noted that, in view of the design simplicity, the linear phase structure was analyzed with respect to real-axis zeros alone. The more general case, including the complex set of zeros, may provide a greater variety of tradeoffs but is unlikely to change the basic conclusions.

Typical measured data of a linear phase and externally equalized filters is shown in Figures 5 and 6.

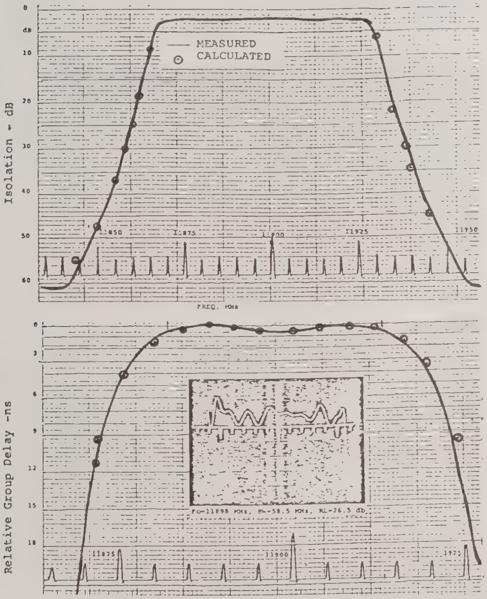

FIGURE 5 MEASURED VERSUS COMPUTED RESPONSE OF THE LINEAR PHASE FILTER
(a) AMPLITUDE RESPONSE AND
(b) GROUP DELAY RESPONSE

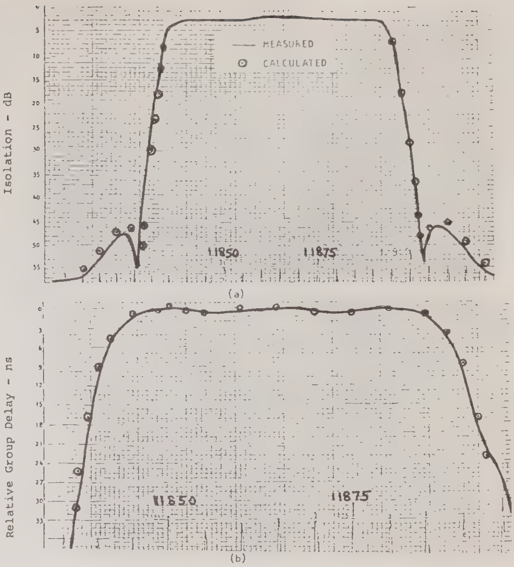

FIGURE 6 MEASURED VERSUS COMPUTED RESPONSE OF THE EXTERNALLY EQUALIZED FILTER
(a) AMPLITUDE RESPONSE AND
(b) GROUP DELAY RESPONSE

Multiplexing Networks for Satellites Employing Beam Reconfiguring and Switching

The Intelsat IV-A satellites use a T-switch in conjunction with circular waveguide directional filters to perform beam switching or reconfiguration [6]. A block diagram of such a network is shown in Figure 7. The directional property of the filters is used to discriminate the polarization of the signal coupled into the filters. Signals possessing right or left circular polarization will propagate in opposite directions through the output manifold and into two separate antenna feeds. Switching is obtained via the T-switch by launching right, left, or both right and left circularly polarized wave through a circular iris of the directional filter. The T-switch consists of a linear mode launcher and a rotatable polarizer. Right-hand, left-hand, or any mix of both polarizations can be achieved by properly orienting the polarizer with respect to the linear input mode. The polarizer orientation is controlled by a commandable stepping motor.

The drawback of this scheme is the necessity of using directional filters. The directional property is obtained by employing two orthogonal modes and hence the dual-mode filter configuration is excluded for such designs. This, in turn, also restricts the response functions to the all-pole variety like Chebyshev and Butterworth, requiring higher order networks to achieve a given isolation response. All this adds to the weight and volume of the mux as well as its design and alignment complexity. Furthermore, it is difficult to achieve greater than 1% bandwidth for directional filters.

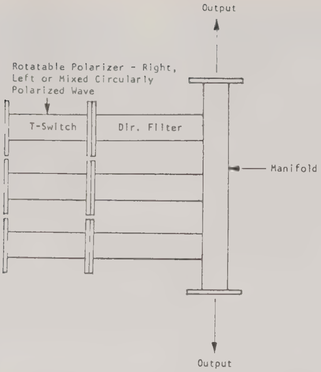
Output
Rotatable Polarizer - Right, Left or Mixed Circularly Polarized Wave
T-Switch
Dir. Filter
Manifold
Output

FIGURE 7(a): BEAM SWITCHING NETWORK USING T-SWITCHES AND MUXES USING CIRCULAR DIRECTIONAL FILTERS

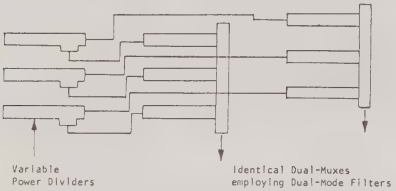

FIGURE 7(b): BEAM SWITCHING NETWORK USING VARIABLE POWER DIVIDERS (VPDs) AND IDENTICAL PAIR OF MULTIPLEXERS EMPLOYING DUAL-MODE GENERALIZED RESPONSE FILTER NETWORKS.

An alternative way of achieving the same switching arrangement is by employing two identical muxes whose input ports are connected to the two output ports of variable power dividers (VPDs) as shown in Figure 7. This scheme is used in the ANIK-C spacecraft. It is a potential candidate for a number of satellites to be launched in the 1980s. In this scheme, the functions of filtering and power division are independent and hence dual-mode filters with generalized response are used for the multiplexing networks. The VPD is very similar to a T-switch. It has a rotatable 180° polarizer with an orthomode transducer at the output. Rotation of the linear output provides the varying power at the two ports of the orthomode coupler.

In such a configuration, the phase and amplitude of a given channel in alternate paths must track for optimum performance. This puts a new requirement on spacecraft output muxes, and severely limits the allowable manufacturing and alignment tolerances. Filters corresponding to the same channel in each arm of a dual mux must exhibit nearly identical characteristics. In terms of mechanical tolerances, this implies tolerances of .0002" in cavity and iris dimensions at 12GHz and .0005" at 4 GHz. To compute the most probable phase and amplitude tracking in terms of realizable filter parameters, it is necessary to assume a definitive response shape to avoid the infinite number of possibilities that would otherwise exist. Figure 8 describes the bounds within which the phase tracking of a pair of 6-pole, quazi-elliptic, 0.5% BW filters can be held at 12 GHz. Measured results of amplitude and phase tracking for a flight quality dual-mux for the ANIK-C spacecraft are shown in Figure 9. A photograph of a complete flight configuration mux assembly is shown in Figure 10. The filters use TE_{113} as the mode of propagation.

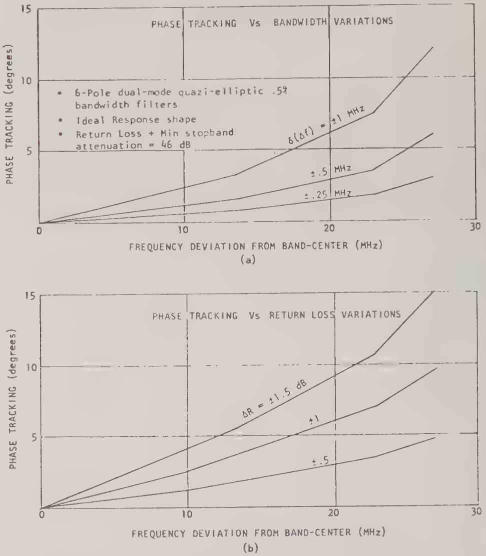

FIGURE 8 COMPUTED PHASE TRACKING FOR DUAL-OUTPUT MUXES, (a) AS A FUNCTION OF BANDWIDTH VARIATIONS, AND (b) AS A FUNCTION OF VARIATIONS IN RETURN LOSS

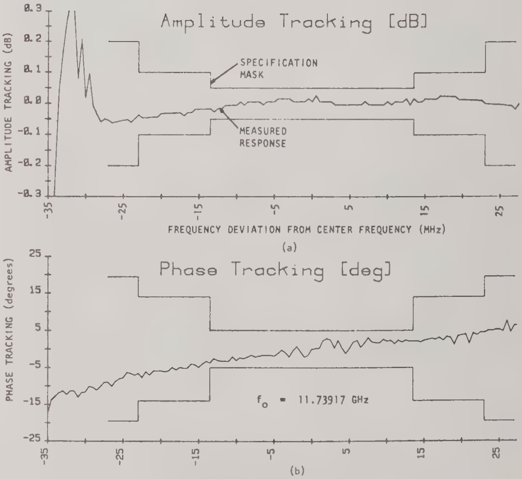

FIGURE 9 MEASURED DATA OF THE FLIGHT QUALITY ANIK-C OUTPUT DUAL-MUX, (a) AMPLITUDE TRACKING, AND (b) PHASE TRACKING

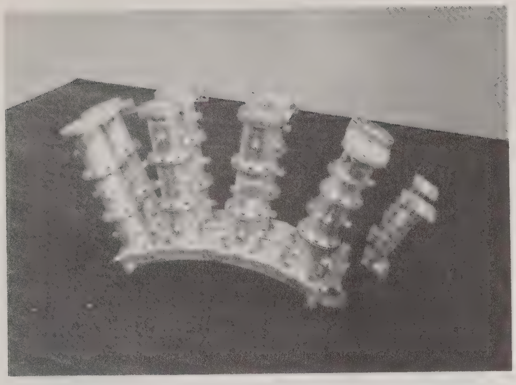

FIGURE 10 PHOTOGRAPH OF A FLIGHT QUALITY DUAL OUTPUT MULTIPLEXER ASSEMBLY AT 12 GHz FOR THE ANIK-C SATELLITE

Future systems are looking at beam optimization for varying traffic patterns and satellite positions. This requires multiplexing and beam forming networks as shown in Figure 11. Light weight and low loss variable power dividers (VPDs) and variable power combiners (VPCs) are essential to make such a system viable.

Figure 14 on page 12 shows a prototype 12 GHz beam reconfiguring network for use in a communications satellite. It employs waveguide VPDs which route the TWT outputs to a dual output mux assembly via flexible waveguides. The outputs of the muxes are channelled to separate feed horns in the Antenna Subsystem.

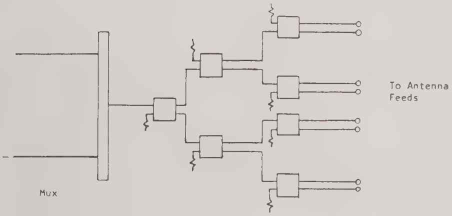

FIGURE 11 BEAM FORMING NETWORK

Multiplexers with Contiguous and Non-Contiguous Channels

As the number of RF channels to be combined in a multiplexer increases, so does the variance between ideal and achievable performance. As the frequency separation between channels is decreased, the channel interactions become a dominant factor and the performance deteriorates further. For these reasons, non-contiguous multiplexers are used almost exclusively for combining the transmitter outputs in satellite transponders. As of this date, the only exception is the Intelsat V series of satellites where 4 GHz contiguous multiplexers are used. Contiguous combining is achieved in most satellites through the use of additional antenna feed elements which enable the output powers of individual muxes to be merged in the near field of the antenna subsystem. Ten years ago this seemed a good tradeoff; the antenna subsystem bore the burden of increased weight, design complexity and some deterioration in performance, but no major technology advances were required, whereas no acceptable contiguous multiplexer hardware existed.

In the past five years, the demand for more RF satellite channels has been alleviated through the employment of frequency re-use via cross polarization which results in a factor of 2 increase in communications capacity but at the expense of an extremely complex and somewhat inefficient antenna design. The simplification and overall performance enhancement which would result if efficient contiguous multiplexing techniques were available, has spotlighted this area as an attractive technology target.

Two design techniques are currently under investigation. One approach is based on singly terminated lowpass filters being used as the prototype to derive the bandpass filters coupled onto the waveguide manifold. This design necessitates using dummy filters to imitate channels at the edges of the total multiplexer bandwidth. In addition, compensating elements are needed for other channels to achieve the level of performance required for typical satellite application. This results in increased weight and volume for the multiplexer. The practical feasibility of such a unit has been proven [7]. It has been used, with some modification, in the design of the five channel, Intelsat V, contiguous multiplexer [1].

An alternative design approach [8] utilizes the doubly terminated lowpass filter as the prototype for the individual channels. The multiplexer design then modifies the elements in each channel together with the separation between filters along the waveguide manifold (phase lengths) to realize the desired channel response in the multiplexed configuration. Such a multiplexer would look similar to the non-contiguous unit and preserve most of its advantages in terms of weight and volume.

R & D programs following both avenues are currently underway. The development of a practical, hardware proven synthesis technique for contiguous multiplexers will probably emerge in the next five years.

High Power Handling Considerations

For space application, handling of high power under vacuum environment is a major consideration in the design of filter networks. The limiting phenomenon is 'multipaction' which takes place under vacuum conditions only [9-12]. For RF voltages, the multipactor mechanism becomes effective when the mean free path is of the order of the physical spacing between conductors. Based on these considerations, one sees three possible ways to counteract multipactor breakdown:

- Pressurize and seal the unit with some inert gas,
- Use a low loss, low dielectric constant and lightweight material to fill the unit,
- Select appropriate dimensions to prevent multipactor for a given level of peak voltages.

There is little to be said about pressurization. It is completely effective but requires extreme care in sealing the unit to prevent leaks. Connectors would require a custom design incorporating a hermetic seal. This may pose special problems to achieve low passive intermodulation (PIM). Consequently, this method is costly and spacecraft customers and suppliers generally tend to be apprehensive about this approach.

Use of foam material as a filler tends to degrade the unloaded Q of the filter and adds weight. In addition, the design must incorporate ways to vent any outgassing of contaminants to prevent ionization breakdown.

Choice of appropriate dimensions implies bigger volume to handle higher powers. This also yields higher Qs but the penalty is that of increased weight and volume. Increase in weight is partially offset by the lower losses and hence lower power requirement and weight of the power subsystem.

For filter networks, Cohn [13] has shown that peak voltages developed vary as the square root of the percentage bandwidth. This puts additional constraint on the design of narrow-band filters if they are required to handle high powers. For wideband filters, calculations based on parallel-plane conductor theory are generally adequate. In any event, owing to the different geometrics involved as well as the different materials and processes, it is invariably necessary to perform high power tests in vacuum before a unit is acceptable for space application.

Figure 12 shows the photograph of a space qualified high power L-Band diplexer at 1.5 GHz for use in the Maritime Communications Package on the INTELSAT-V satellites. Owing to the high transmit-receive isolation requirement, the bandpass filters comprising the diplexer are of Chebyshev design, and use coaxial resonators to achieve low loss ($Q_o > 4500$) and high power handling capability in vacuum. In addition, coaxial lowpass filters are connected in cascade to provide isolation at third harmonic and beyond. Figure 13 shows the measured isolation response of this unit. Other measured results indicate:

(i) Efficiency of 65% for the coaxial-cavity resonators. Unloaded Q based on measured loss is in excess of 6,000. Cavity size is 2"x2"x2.25".

(ii) Power handling capability of greater than 200 watts in vacuum for the complete diplexer assembly including the lowpass filters.

(iii) Passive intermodulation power of less than -140 dBm in the receive band for two 70 watt carriers 4 MHz apart in the transmit band.

(iv) Weight for the complete assembly is less than 1.2 kg.

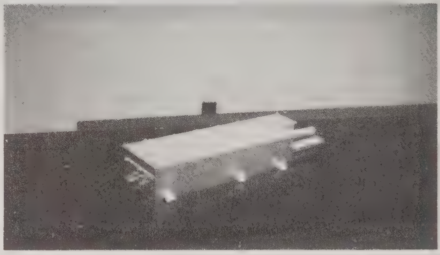

FIGURE 12 PHOTOGRAPH OF A SPACE QUALIFIED HIGH POWER L-BAND DIPLEXER ASSEMBLY AT 1.5 GHz

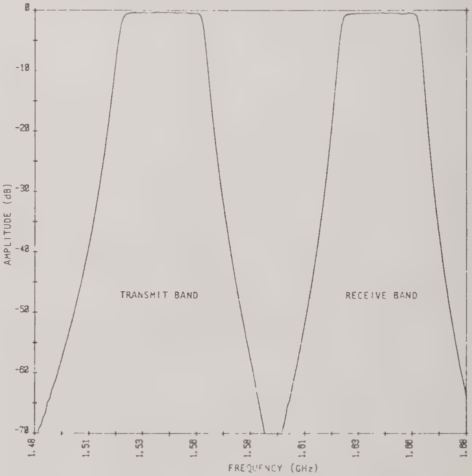

FIGURE 13 MEASURED ISOLATION RESPONSE OF THE SPACE QUALIFIED HIGH POWER LOW PIM L-BAND DIPLEXER ASSEMBLY

Passive Intermodulation (PIM) Considerations

It has been the experience of UHF spacecraft suppliers and those involved in military projects dealing with ground/ship based high power transmitters that intermodulation products are generated by passive components that involve some kind of contact, be it metal-to-metal or involving plastics like graphite fiber reinforced plastic (GFRP). Systems involving high gains (>120 dB), as in UHF transponders or the high isolation requirements of other ground based transmitters/receivers, are especially prone to this phenomenon. The level of any IM produced by the transmit portion in the receive band has to be at least 20 dB below the power of the received signal. This condition results in a carrier to passive IM requirement (C/I) of anywhere from 140 to 200 dB depending upon the system gain, frequency plan, transmit-receive configuration and the requirements of other stations in the overall system. Table 6 describes the state-of-the-art for low PIM components.

TABLE 6 STATE-OF-THE-ART: INTERMODULATION IN PASSIVE COMPONENTS

	PASSIVE IM - 3RD ORDER LEVEL FOR TWO +45 dBm CARRIERS	
COMPONENT	CONVENTIONAL UNITS (dBm)	STATE-OF-THE-ART UNITS (dBm)
Diplexer	-70	-135
Multiplexer	-60	-120
Hybrid	-60	-140
Circulators	-70	-115
Coaxial Connectors	-60 to 100	-155

N.B.: Intermodulation products in passive components do not follow the normal relationships with respect to changes in the fundamental powers, or as a function of the order of the IM products.

Based upon the PIM requirements, review of the available literature [14-17] on PIM (it is meagre) and experimentation with elementary units, the following steps are recommended to minimize PIM in passive components:

- Use of aluminum for fabricating the unit,
- Minimization or possible elimination of tuning screws,
- Wherever possible, use of soldering or brazing to join metals rather than pressure contact,
- Careful selection of input/output connectors or flanges as the case may be,
- Complete elimination of any and all ferrous materials like Invar, Ni, steel etc., from the multiplexer configuration,
- General 'magnetic sanitation'.

Testing PIM at levels of -150 dBm or below represents an elaborate and expensive piece of equipment. But testing is essential both as a design tool and to ensure that specification requirements are met. As said earlier, PIM is not well understood and, at the present time, quantitative prediction of PIM levels is not an acceptable criterion for equipment suppliers.

Present Trends and Future Innovations

A familiarity with the present state-of-the-art, coupled with some knowledge of related R & D programs currently underway, formed the basis of the predictions classified below in the category of present trends.

The listing of probable future innovations was undertaken with some trepidation and should be treated as educated guesses rather than presumptuous prophesies.

Extrapolation of Present Trends

Dual Mode Canonical Filters remove virtually all restrictions on the response function that can be realized. Such filters will become a dominant multiplexer element in the next 5 to 10 years.

No hardware proven theory exists for the design of multiplexers. R & D programs now underway in both Europe and North America will result in the establishment of synthesis techniques which will enable the realization of practical multiplexers without restrictions on either channel spacing or response shape.

A number of high power broadcast satellites will be launched in the next decade. The requirements of this type of system will place a premium on the realization of high unloaded Q structures. The basic simplicity and flexibility of the TE_{11n} filter make it the leading contender for low loss high power application.

Probable Future Innovations

Increasing use of very wideband digital traffic will necessitate the realization of channelizing filters equalized over virtually 100% of their passbands. Innovations involving filter structures incorporating both external and internal equalization will be necessary to meet these requirements.

Computer aided tuning of satellite multiplexers would result in substantial cost saving. Availability of low cost, powerful computers will provide impetus in achieving this objective.

Requirements for computer controlled "packet" communications will necessitate major technology innovations in multiplexers which will be required to accommodate instantaneous beam switching and beam forming functions. Technology advances in such areas as low loss microwave ferrites and diode switches could provide some of the building blocks for these multiplexers.

Acknowledgements

Much of the work described herein was funded as part of the Industrial Research Assistance Program of the National Research Council of Canada to whom the authors are indebted.

References

1. J.C. Redd, H.C. Hyams and D.E. Collins, "Use of Graphite-Epoxy Pseudo Elliptic Function Multiplexers for Intelsat V," Paper presented at the EASCON Conference, Washington, D.C., 1978.

2. C.M. Kudsia, S. Kallianteris, K. Ainsworth and M.V. O'Donovan, "Status of Filter and Multiplexer Technology in the 12 GHz Frequency Band for Space Application," Paper presented at the 7th AIAA Communications Satellite Systems Conference in San Diego, April 1978.

3. C.M. Kudsia and M.V. O'Donovan, "Microwave Filters for Communications Systems," Artech House Inc., 1974.

4. A. Atia and A. Williams, "Dual-Mode Canonical Waveguide Filters," International Microwave Symposium, San Diego, June 1977.

5. G. Pfitzenmaier, "An Exact Solution for a Six-Cavity Dual-Mode Elliptic Bandpass Filter," International Microwave Symposium, San Diego, June 1977.

6. J.L. Dicks and M.P. Brown Jr., "Intelsat IV-A Satellite Transmission Design," Paper presented at the AIAA 5th Communications Satellite Systems Conference, Los Angeles, Calif., April 1974.

7. M.H. Chen, F. Assal and C. Mahle, "A Contiguous Band Multiplexer," Comsat Technical Review, Fall 1976.

8. J.D. Rhodes and R. Levy, "A Generalized Multiplexer Theory and Design of Manifold Multiplexers," International Microwave Symposium, Ottawa, June 1978.

9. "The Study of Multipactor Breakdown in Space Electronic Systems," Hughes Aircraft Co., Culver City, Calif., NASA CR-448, July 1966.

10. E. Vance and J. Nanevicz, "Multipactor Discharge Experiments," Stanford Research Institute, AFCRL-68-0083, December 1967.

11. R. Woo, "Multipacting Breakdown in Coaxial Transmission Lines," Proc. IEEE, April 1968.

12. F. Kossel and K. Krebs, "Die Pendelvervielfachung von Sekundarelektronon (Multipactoreffeckt) also Zundbedingung von Hochfrequenzentladungen," Z. Physik 175, pp. 382-390 (1963).

13. S.B. Cohn, "Design Considerations for High-Power Microwave Filters," IRE Trans. on Microwave Theory & Techniques, Jan. 1959.

14. "An Update on Intermodulation Generation by RF Connector Hardware Containing Ferromagnetic Materials," E.C. Young, Naval Research Laboratory, Washington, D.C.

15. "Reduction of Transmitter Intermodulation Product Signals in Air Force Communications Systems," RADC-TR-72-312, Dec. 1972.

16. "H.T. MT Terminals Program Intermodulation Generation in Normally Passive Linear Components," Contract DAA B07-72-C-0207. WDL TR 5242, 24 August 1973.

17. "Non-linearities of Flange Connections in Transmission Lines Carrying High RF Power," E. Nuding, AEG Telefunken, Germany, Proc. 4th European Microwave Conference.

Appendix 1

Equivalent Linear Frequency Drift (ELFD)

For filter applications in microwave communications systems, the term equivalent linear frequency drift is employed to characterise the behaviour of filters under thermal cycling. This provides a measure of the temperature stability.

Prediction of a filter's response changes - especially with a large temperature excursion - is difficult and an exercise in approximation at best. This is due to filter complexity, geometry and structural strength of materials and joints, tuning screws and their interactions, etc. As the temperature varies, these factors change the internal geometry of the filter in an unpredictable manner. The electrical response not only shifts in frequency but changes in shape as well. This latter change makes the usual concept of frequency-shift, that tacitly assumes no shape change, quite meaningless.

Based on extensive experience in filters and overall communications systems, the following definition of ELFD was derived:

> "Equivalent Linear Frequency Drift is the total frequency excursion of the nominal center frequency of a filter over a specified temperature range as determined by a given set of passband, and out-of-band isolation constraints."

The governing passband and out-of-band criteria are selected as follows:

1) The filter characteristics as measured at ambient temperature are used to determine

   a) The relative group delay at a frequency $f_o \pm \Delta f_1$ and

   b) The isolation at a frequency $f_o \pm \Delta f_2$, where f_o is the normal center frequency.

   Δf_1 is a frequency band chosen such that $2\Delta f_1$ is less than the total passband bandwidth but approximately equal to the bandwidth which contains 99% of the signal energy.

   $2\Delta f_2$ is chosen as a stopband bandwidth at which the isolation provided by the filter can be measured accurately, e.g. 20 to 30 dB.

   Δf_2 is normally chosen to coincide with an adjacent channel isolation requirement which has significance from the viewpoint of overall communications system performance.

2) The measured filter characteristics at ambient temperature are used to input a computer program which simulates the filter's group delay and isolation characteristics with small incremental upward and downward shifts in nominal center frequency.

3) The group delay at $f_o \pm \Delta f_1$ and the isolation at $f_o \pm \Delta f_2$ as measured at the maximum specified operating temperatures are determined.

These measured values are compared with the simulated filter responses. The maximum simulated shift in center frequency which provides a group delay equal to or less than the measured value at $f_o \pm \Delta f_1$ and an isolation equal to or greater than the measured value $f_o \pm \Delta f_2$ is the "Equivalent Linear Frequency Drift" (ELFD) due to the specified temperature excursion above ambient. The ELFD due to the temperature excursion below ambient is determined in a similar manner.

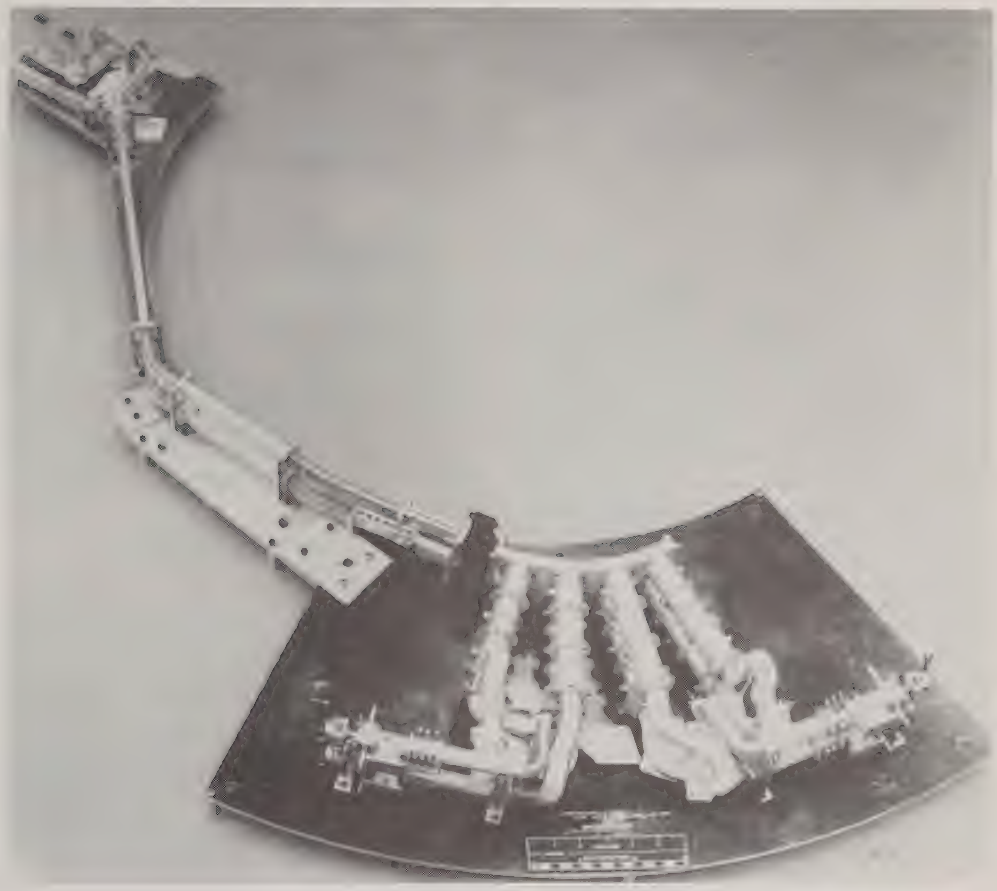

FIGURE 14 12 GHz SATELLITE BEAM RECONFIGURING NETWORK

80-0523

CROSSBAR SWITCHING REQUIREMENTS FOR FUTURE MULTIBEAM TDMA COMMUNICATIONS SATELLITES

Murray Hoffman
The MITRE Corporation
Bedford, Massachusetts 01730

Abstract

This paper summarizes a study of requirements for microwave switching in space based on a frequency translating multibeam satellite interconnecting the more than 70 U.S. metropolitan areas with populations over half a million. A 100 x 100 switch with a bandwidth of 2.5 GHz is assumed. The switch supports a TDMA system whose characteristics are described, as are the switch specifications derived therefrom. The study investigated switch architectures and developed a new and promising architectural form. Switching devices were evaluated, logic requirements were considered, and reliability was addressed. Conclusions and recommendations for steps needed to develop the switch are presented.

Introduction

Satellite communications systems of the future can be expected to extend today's technology and provide increased information transmission employing multiple high-gain beams to connect traffic generating and concentrating centers (TGCs) in a national network. Multifold frequency reuse will depend on beams sufficiently narrow to have the same center frequency in a bandwidth of 2.5 GHz. Transmitter power will be a few watts per beam using efficient solid state amplifiers. There will be a receiver for each uplink and a transmitter for each downlink using frequency translation to achieve low cost.

The greater metropolitan areas will be the TCGs of the future. Rand McNally maps of the United States[1] show 73 areas with populations greater than one-half million people. These fixed areas will concentrate traffic for the rest of the country. Movable beams will also be provided. With allowance for growth, a set of 100 uplink and downlink beams is considered.

Since an uplink beam is connected to one downlink beam at a time, but all centers need to communicate, time division multiple access (TDMA) techniques are called for. A microwave switch is required which supports such an environment. It must have a large number of input and output ports, 100 x 100, providing 10,000 cross point connections. The TDMA system requires a method of control for network traffic. This implies a network control station which accumulates traffic information, performs routing computations in real time, and controls the switch.

The satellite transponder is divided into uplink and downlink chains; the switch between them enables it to operate at some advantageous intermediate frequency. Technologies investigated suggest a frequency between 2 and 4 GHz. High-gain beams imply satellite operation at K-band or at millimeter wave frequencies. This will require translation to intermediate frequency (IF) at 3 GHz, switching, and translation to the downlink frequency.

The progress of a signal through the satellite illustrated in figure 1 is as follows:

1. Each TGC has an uplink and a downlink beam with 2.5 GHz bandwidth.
2. An uplink signal enters a receiver chain at the satellite, is demuxed, amplified, translated in frequency to IF, and further amplified.
3. The signals are switched to the appropriate downlink transmitter chains.
4. These chains amplify and translate the signals and multiplex them to the downlink beams thus completing the interconnection of separate TGCs.

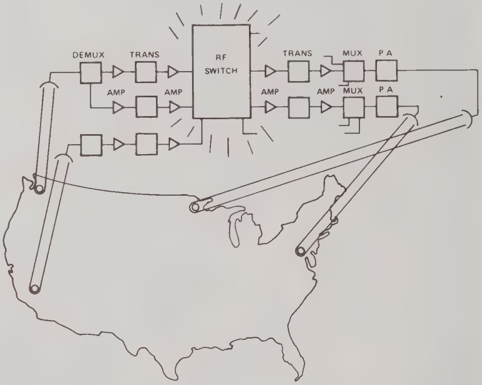

Fig. 1 Interconnection of fixed geographic regions

Frames and Slots in TDMA

The set of switch connections existing at a given time is called a switch state. The switch undergoes a succession of states during a period of time called a frame. When the frame is over, the switch repeats it periodically, supporting the satellite communications channels (through signal sampling via TDMA). The period is 125 microseconds long – a pulse code modulation (PCM) telephone standard. The frame, composed of TGC schedules as shown in figure 2, is based on work of Yeh and Reudink.[2] All schedules are executed simultaneously during the frame. The second, labeled B, might be for Boston, which is connected back to itself through the switch in the first slot of the frame for 5.5 microseconds. During this interval, Boston ground terminals perform loopback tests and traffic can move between terminals in the Boston area. In the second slot, Boston might be connected to Chicago for 12.5 microseconds; then it is switched for the third slot to Dallas for 15.3 microseconds.

This paper is declared a work of the U.S. Government and therefore is in the public domain.

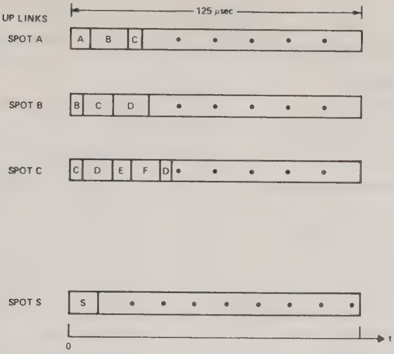

Fig. 2 TGC schedules

Slot durations are set by traffic demand and are changeable at the command of the computer in the control station. The traffic pattern changes slowly during the day and the statistics are well known so that the control station can keep up and formulate schedules in real time.

Based on the work of Yeh and Reudink,[2] a 2 microsecond slot can support 781 voice channels of 8-bit PCM, assuming 100 percent utilization of the slot in a 2.5 GHz bandwidth. In practice, synchronization and other headers about 100 bits long are needed, accounting for 12.5 percent of the 2 microsecond slot. Time must be provided for switching during which communication is not possible. If only 15 percent total can be spared for slot management, then 2.5 percent remains for switching time or 50 nanoseconds. This leaves 85 percent for communication. Since slot sizes are not equal, switches do not all throw at the same time. This aids in both minimizing the power required to run the switch, and matching connectivity to the traffic load.

Technologies and Media

A radio frequency (RF) switch is composed of transmission lines, switching devices, device drivers, and logic. Logic is not a problem because current practice is capable of meeting the requirements. A large number of drivers has been designed for phase shifters and simple switches so art is available: however, there is a problem in power consumption.

Figure 3 shows three forms of printed circuit microwave lines plus an optical medium. The earliest of these is stripline, which consists of a center conductor supported between two metallic ground planes by a dielectric. The second and perhaps most widely used is microstrip in which the dielectric above the center conductor and the upper ground plane are dispensed with. The field is mainly concentrated in the dielectric below the center conductor. Microstrip is preferred because of the accessibility of the center conductor and ease of connecting devices to it. In the future, a microstrip switch circuit might become monolithic as shown in the central sketch of the figure. The dielectric could then be composed of low loss intrinsic semiconductor material. Active devices, such as the diode shown or transistors, could be diffused or epitaxially grown where needed. The optical medium is driven by a laser transmitter. The material is lithium tantalate in which it is possible to form waveguides by application of a static electric field between two electrodes. The difference in index of refraction caused provides the guidance. The medium of space can serve a multiple beam phased array used as a switch. Analysis shows, however, that this interesting possibility requires an unacceptably large number of components at K-band or millimeter wave frequencies and would be too expensive and too heavy.

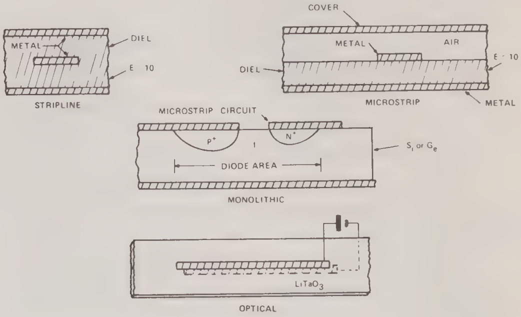

Fig. 3 Printed microwave and optical lines

Switch Architecture Principles

Switch architecture is significant because it determines specifications, affects modes of switch operation, helps set reliability levels, and determines size, weight, parts count, and ease of fabrication. Important principles can be seen in the prototype crossbar shown in figure 4. On the left side are TGC source receiver inputs. These inject traffic which flows horizontally to the right along transmission lines. In a similar way, columns are provided for switched outputs to transmit chains serving destination cities. The crossing of transmission lines implies that a crossbar switch has several layers.

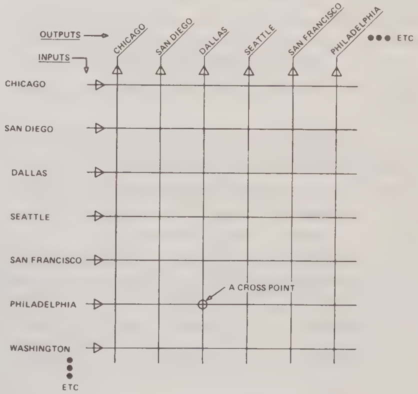

Fig. 4 Prototype crossbar

The intersection of an input and output transmission line is called a cross point. Devices are required for interconnecting input and output line at a cross point. Both an input signal and an output signal must be able to pass an unmade (open) cross point undisturbed.

For a network consisting of TGCs operating on a TDMA basis via a switch, the following requirements are implied:

1. Connection time slots are not equal.
2. Connectivity between two communicating TGCs may not be interrupted while other connections are made.
3. Any free input may be connected to any unoccupied output regardless of other conditions.

These requirements are characteristics of a "strictly nonblocking" switch appropriate for channels carrying large volumes of traffic.

If a signal is inserted into the switch of figure 4 by receiving a chain for Dallas destined for Chicago, a low loss switch at the Dallas-Chicago cross point is closed and this signal proceeds up the C transmission line to the C transmitting chain. All the other inputs to the switch, approximately 99 in number, also carry signals at the same power level not destined for C. Because isolation is not perfect, a small crosstalk signal from each line is coupled onto output line C. In this case, the intentionally coupled signal could be equalled by the sum of the crosstalk signals. The signal to crosstalk ratio, S/C, might be unacceptable.

Suppose the number of input ports is N. Then it can be shown that the isolation factor of a switch, A, is given in dB by

$$A = N(S/C) \qquad (1)$$

i.e., the isolation required of a cross point depends on the number of input ports as well as the required signal to crosstalk ratio. Using equation (1), the isolation required of a cross point for a 100 x 100 switch with a desired signal to crosstalk ratio of 20 dB is 40 dB, and for S/C of 40 dB it is 60 dB.

Signals should be injected into the switch at a reasonable level of one milliwatt. The total input signal power to the switch would be only 100 milliwatts. This level ensures that the signal to noise ratio through the satellite will hardly be affected by the insertion loss of the switch. With entering signal carrier to noise ratio, C/N, of 10 dB, and switch insertion loss of 60 dB, the emerging C/N level degrades to only 9.58 dB in a 2.5 GHz bandwidth.

It is highly desirable that output signal levels from the switch be approximately equal, independent of the path taken. This eases the dynamic range burden on the transmit chains and reduces the need for specialized power conditioning as a function of switch port output number. The switch transfer function should be compatible with satellite specifications. The switch should have minimum possible size, weight, power consumption, and cost consistent with performance. It would be desirable at times for the switch to provide a one to many broadcast capability.

Tentative specifications for the switch are listed in table 1.

Table 1 Tentative satellite TDMA switch specifications

Size (inputs, outputs)	100 x 100
Bandwidth	2.5 GHz
Switching Time	50 nanoseconds maximum
Mode of Operation	TDMA
Path Attenuation	50 dB maximum
Attenuation Variation	1.0 dB/2.5 GHz, 0.5/10 MHz maximum
Frame Duration	125 microseconds
Slot Duration	proportional to traffic
Slot Length	2 microseconds minimum
Slot Communications Efficiency	85 percent
Switching Occurrence	independent times
Accessibility	to any unused output
Interception of Estab. Comm.	none due to switching
Signal Flow, Open Crosspoint	signal pass unaffected
Input Power Level	1.0 milliwatts
Crosspoint Isolation	40 dB minimum
Group Delay Variation	1.0 ns/2.5 GHz maximum
One-to-Many Facility	provided
Redundancy	to overcome failure rate
Port-to-Port Output Variation	6 dB maximum
Environment Launch/Store	survive
Environment Space	operate duration of mission
Probability No Connect Failure	99.99 percent 7 years
Frame/Slot Schedule	reconfigurable

Architecture Realization

The cross point diagram of figure 4 shows that more than one layer is required because microwave transmission lines are seen crossing. If the switch could be realized with only two layers, it would have the most efficient form from a volume standpoint. Form is discussed assuming use of a solid state device such as a diode or transistor.

Fan-Out Architecture

Figure 5 shows how utilizing two tiers of switches permits one input to be connected to any one of 100 outputs. The arrangement is called a fan out. These can be used as elements of a 100 x 100 switch as shown in figure 6. 100 horizontal 1 x 100 fan outs are stacked vertically to provide 100 inputs and 10,000 outputs, the latter equal to the number of cross points in the switch. A single vertical fan can be used to sample one output from each horizontal layer and present at its one output a signal from any one of the 100 inputs. 100 horizontally stacked vertical fan outs thus provide 100 outputs, each connectable to any input.

A switch of this type is bulky and difficult to assemble. A failure in a first-tier switch will eliminate ten outputs for a given input. The advantage of the switch is that, except for transmission line and device losses, the entire signal appears at the selected output. Total attenuation is expected to be about 10 dB.

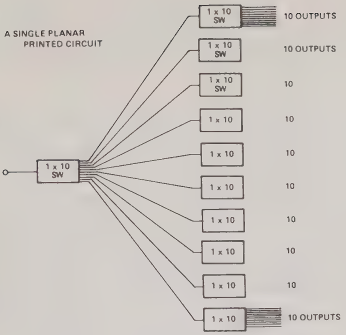

Fig. 5 Two tier fan-out

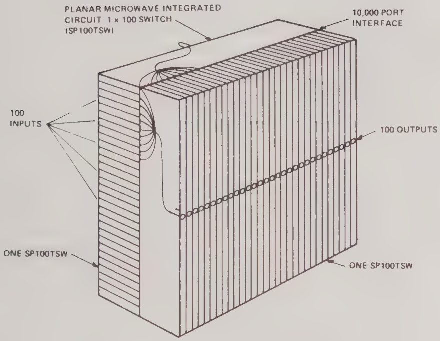

Fig. 6 Fan-out assemblage for 100 x 100 switch

Fan out can be achieved using symmetrical Wilkinson printed circuit couplers. In this case, the switching devices are located in the plane at which the horizontal and vertical fan outs join. This improves reliability but the signal is more highly attenuated. The switch is larger because a central section must be added for the switch devices and a high voltage standing wave ratio (VSWR) is generated at the input to the switch.

One vendor was willing to speculate about the properties of a switch fan out crossbar and extrapolated his rules of thumb for small switches to produce table 2.

Table 2 Extrapolated properties for 100 x 100 fan-out switch

Dimensions	50" high, 50" wide, 12" thick
Weight	1875 lb
Total Current	150 amperes
Average Drive Power	750 watts
Average Diode Current	15 milliamps
Power Division Drive/Diodes	0.80/0.20
Switching Speed	50 nanoseconds
Path Insertion Loss	10 dB
Isolation	60 dB
Bandwidth	2.5 GHz
Center Frequency	3.0 to 4.0 GHz
Recurring Cost	$500,000

Rearrangeable Architecture

A rearrangeable switching network composed of "beta" elements developed by Y. Ito, et al., of KDD in Japan[3] may be used as a crossbar. A beta element is the microwave equivalent of a double pole double throw switch. The network utilizes a changing series of crossing paths. The algorithm for adding one new connection requires rerouting for all the other previously connected ports and is extremely complicated. All slot lengths in a schedule have to be the same, which is unacceptable for TDMA. The rearrangeable switch has switch critical failure points at the input and also internally since rerouting algorithms begin to fail. For these reasons, rearrangeable architecture is unsuitable for the postulated TDMA system.

Cross Bar Architecture

Cross bar architecture is less dependent on layering than fanned architecture. As seen from figure 4, cross bar architecture can be accomplished in two layers if good feed throughs can be built to interconnect them. New switch architecture is described here which uses the feed through concept. The feed through is an infinitesimal antenna capable of launching a wave in the printed circuit board dielectric. This unguided wave is undesirable.

The total radiated power, W_t, from a feed through can be shown to be

$$W_t = 40\pi^2 I_m^2 / \lambda^2$$

where

$k = 2\pi/\lambda$

I_m = maximum current in feed through

λ = wavelength of the carrier frequency

S Suppose a 1 mW signal is transferred via a matched 0.010 inch long feed through. The formula just derived for total radiated power yields,

$$W_t = 1.0 \times 10^{-6}\ \mathrm{W}$$

This level is 30 dB below the specified input signal of 1 mW so that little power is lost, but it represents an isolation level which may not be high enough to meet the criterion of S/C + n in dB since the switching devices themselves will couple unwanted signals in the outgoing transmission lines. It will therefore be necessary to use shielded feed throughs. These are shown in figure 7. Two one ounce copper microstrip center conductors are connected via a metal pin in the center of a plated through hole. The added shielding needed is provided by the metal collars shown.

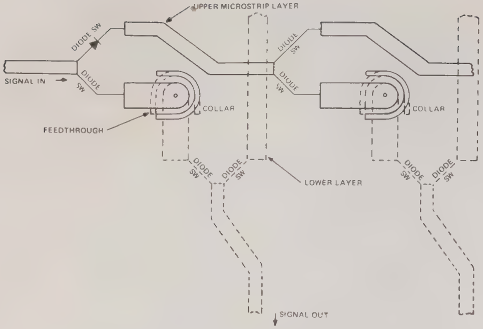

Fig. 7 Physical Cross Bar and Feed Throughs

Tandem Switch Cross Bar. Two cross points which indicate the construction of the cross bar switch are shown in figure 8. A horizontal signal input line is shown entering from the left in the upper layer (drawn with solid lines). The output transmission lines, shown dotted, conduct switched signals downward in the figure. The entering signal approaches a single pole double throw junction at the cross point. If the signal is not to be connected to the output line, the signal is connected to the upper microstrip line in the junction by forward biasing the diode shown. The signal then continues to the next cross point.

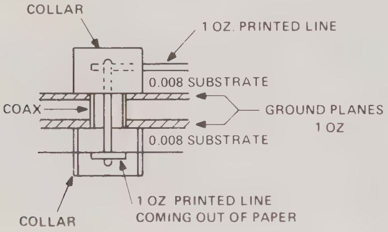

Fig. 8 Detail Microstrip Feedthrough

If the signal were routed downward, the upper diode would be back biased and the lower diode at the junction would be forward biased. This would direct the signal to the shorter alternative line in the upper layer which is connected to the first feed through. The signal would proceed to the transmission line in the lower layer which is shown dotted. Another switch would connect the lower layer line to the main part of the output line. A third switch would disconnect the preceding part of the output line in favor of the line from the feed through.

The particular cross bar shown in figure 8 has several disadvantages. The first is that four switches must operate in cooperation at every cross point. This requires 40,000 switches for a 100 x 100 cross bar. The second disadvantage is unreliability. Since a large number of switches must operate in tandem, the failure of any one of them destroys the path. A city would be totally disconnected from the other cities on that path. In addition, the insertion losses can be prohibitively high for paths where more than 50 cross points must be traversed. Thus, the tandem switch cross bar of figure 8 appears unsuitable. However the concept of cross bar architecture is feasible using feed throughs and is the subject of proprietary ongoing research by NASA.

Switching Devices

The four most prominent device classes are ferrites, optical switches, PIN diodes, and field effect transistors (FETs).

Ferrites

The ferrite three-port junction circulator is a compact device which has been extensively investigated for switching.[5,6] Broadband isolation of a single switch is only about 15 dB, however. An arrangement of three junctions minimum would be needed for a cross point, switch size would be large, and weight high. If each junction required one microjoule to switch, the drive power to the switches would be 6 kW. Switching times reported are half a microsecond, an order of magnitude greater than the required time. Ferrite switches require drivers. For these reasons ferrites are not promising for the TDMA switch.

Optical Switches

Research and development is being supported in optical switching for laser-powered fiber optics communications systems. The switches have the advantage of eliminating the need to leave the optical domain in order to switch and then transduce back. The opposite situation applies to a microwave satellite where the expense of transducing out of and back to microwaves must be borne.

The switch depends on small changes in index of refraction produced by several hundred volts in a crystal, i.e., lithium tantalate. Despite the small wavelength of light, switching cross points are large since reflections are consequently restricted to grazing incidence. Optical switching does not reduce switch size, requires electronic and optical transducing equipment, and does not appear practical for microwave switching.

PIN Diodes

PIN diodes are well-established microwave-switching devices first investigated by Spencer and Armistead.[7] Two comprehensive books on the subject, one by Garver,[8] the other by White,[9] are readily available. The switching capability of the PIN diode is based on two differing impedances when forward or back-biased with dc current. Biasing currents are a few milliamps and switching times are fast (from 100 to 10 ns) between impedances of 2 ohms and 1000 ohms.

A crossbar switch can be designed to meet the specifications using PIN diodes, but because the devices have one port, separation of biasing control and signals requires special circuitry and filtering. Separate drivers are required for PINs. Power consumption for control is expected to be about 500 watts. Layout problems may be severe to accommodate mounting, biasing, filtering, and heat dissipation. The PIN diode switch is the most mature electronic switching technology for microwaves but may be bulkier and require more power than newer switching devices.

MESFETs

A most promising device for use in a large microwave switch is the metal epitaxial semiconductor FET (MESFET) which has three epitaxially-grown electrodes lying on the surface of a semiconductor channel as illustrated in figure 9. The middle electrode or gate can encourage or hinder the electron flow through the channel from source to drain by means of an electric field. This back bias can rapidly clear the channel of carriers halting conduction. The MESFET is a three-terminal device capable of amplification and control. Microwave operation of the MESFET is described by Liechti.[10]

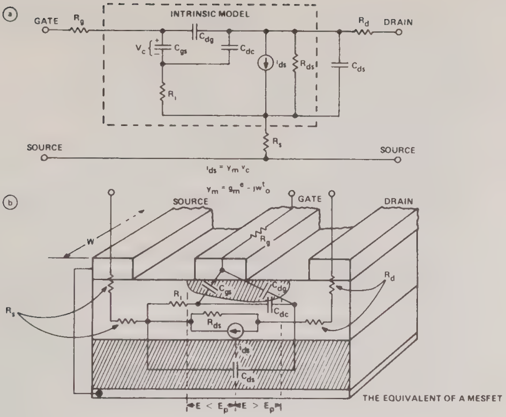

Fig. 9 MESFET principles

A fan-out switch configuration was constructed by Gaspari and Yee,[11] who connected FETs in series. They used a Plessy 2 micron gate device and achieved a broadband single-stage isolation of 15 dB from 3.5 to 5.5 GHz after tuning. A switching time of only 1 nanosecond was observed.

Goel and Volkstein[12] employed a dual-gate MESFET as an amplifier. One gate was used to inject the signal and the other to control switching. The amplifier exhibited a maximum gain of 20 dB, a gain flatness of 0.75 dB, and group delay of 0.3 nanosecond, over a 4 to 8 GHz band. By varying the gate 2 voltage from +1 to –2 volts, the gain can be changed over the entire band from +20 dB to –40 dB while maintaining gain flatness. When a 0.7 volt pulse with 200 picoseconds rise time and 1.5 nanoseconds duration was applied to gate 2, it changed the gain by 18 dB while causing less than 100 picoseconds increase in microwave signal rise and fall time.

The MESFET, which is now simple to make, is not yet optimized for switching, but already has the following advantages:

1. The FET is a multi-port device which makes biasing and filtering more convenient.
2. Drivers are not needed. Drive can be taken directly from control logic. Control power is low.
3. The FET provides a distinct speed advantage over the PIN.
4. Operation of an FET switch as an amplifier provides gain and reduces the possibility of shorting or opening a line when used with the coupler crossbar.

The FET is so promising that research effort should be expended to optimize it for switching.

Switch System Considerations

There are 10,000 solid-state cross points in the TDM switch. FET failure rates from MIL Handbook 217-B indicate that ten cross points are expected to fail during a seven-year postulated life. The switch must be so designed that:

1. Failed cross points can be located.
2. Cross point failures are isolated and non-catastrophic.
3. The switch can make the desired connection even if a cross point fails.

Requirement 3 is achieved by a wrap-around process illustrated in figure 10. One or more extra output and input lines are provided in the switch. In the event of a cross point failure, the input signal proceeds across to one of the extra output lines and is connected to it. The output line then wraps around the whole switch to an extra input line. This line is a complete row with connections to all output columns. The signal proceeds on the extra input line until switched to the output column for which it was intended, thus reaching its destination despite the cross point failure.

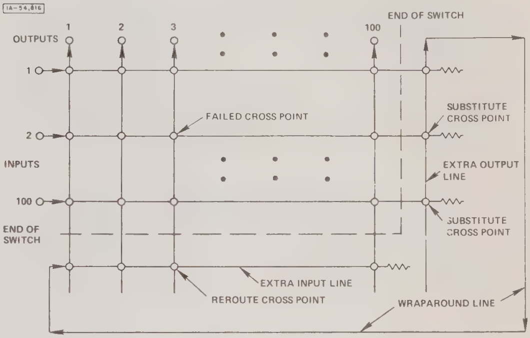

Fig. 10 Wrap-around scheme

The wrap-around system consists of an extra column containing 100 cross points, an extra row with 100 cross points, and a line which wraps around to connect them. This form of redundancy necessitates 200 extra cross points, but protects against a failure in any one of 10,000 switches. Since the probability of failure of any switch is 0.001 in seven years, the expectation of a failed switch in any group of 100 that are connected is 0.1: it appears that one wrap-around system will suffice. However, there must be an allowance for both a skew distribution of failures and for failures in the wrap-around lines. Two wrap-arounds bring the probability of no connection failure up to 99.99 percent.

Conclusions

1. A 100 x 100 microwave switch supporting a nationwide multibeam TDMA satellite will afford a significant increase in communication capacity. The switch can meet necessary performance and reliability requirements.
2. Coupler crossbar architecture should be used because it minimizes weight and volume, provides broadcast capability, and enhances reliability.
3. PIN diodes are mature and can be used, but require more power, separate drivers, more microwave circuitry, and are slower than FETs.

4. FETs should be optimized for switching. They are fast and can be directly driven by control logic. Reliability and signal-to-noise ratio are enhanced by their ability to amplify.
5. Neither ferrites nor optical switch devices are optimum for a microwave TDMA switch.

Sponsor

This work was performed for the Communications Dept., NASA Lewis Facility, Cleveland, Ohio under MITRE Contract 8680.

References

1. Rand McNally, "Map of Standard Metropolitan Statistical Areas 1978," New York: Rand McNally, 1978.
2. Y.S. Yeh and D.D. Reudink, "The Organization and Synchronization of a Switched Spot-Beam System," International Conference on Communication Systems Proceedings, 1978.
3. Y. Ito, et al., "SDMA On-Board Switching System Using Rearrangeable Multistage Network," Proceedings of IEEE International Conference on Satellite Communication System Technology, Apr. 1975.
4. C. Clos, "A Study of Non-Blocking Switching Networks," Bell System Technical Journal, Vol. 32, pp. 406-424, 1953.
5. Y.S. Wu and F.J. Rosenbaum, "Wide Band Operation of Microstrip Circulators," IEEE Transactions, Microwave Theory and Techniques, Oct. 1974.
6. J. Helszajn, et al., "Circulators Using Triangular Resonators," IEEE Transactions, Microwave Theory and Techniques, Feb. 1979.
7. M.A. Armistead, E.G. Spencer, and R.D. Hatcher, "Microwave Semiconductor Switch," Proceedings IRE, Vol. 44, Dec. 1956.
8. R.V. Garver, "Microwave Diode Control Devices," Dedham, MA: Artech House, Inc., 1976.
9. J.F. White, "Semiconductor Control," Dedham, MA: Artech House, Inc., 1977.
10. C.A. Liechti, "Microwave Field-Effect Transistors – 1976," IEEE Transactions, Microwave Theory and Techniques, June 1976.
11. R.A. Gaspari and H.H. Yee, "Microwave GaAs FET Switching," Proceedings IEEE, Symposium on Microwave Theory and Techniques, 1978.
12. J. Goel and H.G. Wolkstein, "A 4-8 GHz Dual Gate Amplifier," International Solid State Circuits Conference Proceedings, 1978.

80-0524

"Development Status of Low Noise Amplifiers"

Nippon Electric Co., Ltd.
Satellite Communications Development Dept.,
Microwave & Satellite Communications Div.

Mitsugi KAJIKAWA, Isao HAGA, Sachiro FUKUDA, Wakoto AKINAGA

Abstract

Low Noise Amplifiers for Satellite Communications were significantly advancing in recent year. This paper describes the current status of LNA development and applications at various frequency bands in regards to its noise temperature characteristics and design features. A 12 GHz FET LNA is described in some detail in particular since great strides are taking place in the 12 GHz frequency range. Finally an outlook for technical trends in the future such as in noise temperature improvement and applications is discussed.

1. Introduction

Low noise amplifiers (LNA) developed for satellite communications are used extensively in Intelsat and Domsat operation, including TVRO. (TV Receive Only earth terminals).

In Intelsat applications, the main development requirements for LNAs are performance improvement and cost reduction. Since the international traffic is expanding rapidly year by year, it is necessary to satisfy the increasing demand for communications by improved LNA performance. Consequently, untiring and continued efforts are directed toward broadening the bandwidth and reducing the noise temperature of the LNA. From as economical standpoint, the total system cost of satellite communications must be minimized to be competitive with submarine cable systems. An LNA noise temperature reduction is most effective in reducing the system cost because the diameter of the earth station antenna can be reduced by improving the noise temperature performance.

On the other hand, in Domsat applications emphasis is placed on LNA maintenance free characteristics as well as on low noise and wide band performance, since unattended operation is becoming more and more universally preferred in these systems, especially TVRO.

The LNA for satellite communications may be divided into two types - the paramp LNA and the FET LNA. These LNAs are used in several frequency ranges, including 4 GHz, 12 GHz and a millimeter wave band. While these LNAs possess unique features, they also have specific merits and demerits. This paper describes the current status of LNA development and applications at various frequency bands, in regards to noise temperature characteristic and design features. A 12 GHz FET LNA is described in some detail, since great strides are being made in the 12 GHz frequency band.

Finally, an outlook for technical trends in the future, such as noise temperature improvement and applications, is discussed.

2. 4 GHz LNA

2.1 General

The 4 GHz band is currently the most popular frequency range for satellite communications and is utilized for applications in both Intelsat and Domsat operations, including TVRO. In these areas, a wide variety of LNAs have been developed and applied. The paramp LNA and the FET LNA are divided into three types, namely, the cryogenically cooled type, the thermo-electrically cooled type and the uncooled type, depending on the individual cooling system.

The cryogenically cooled paramp LNA was used extensively in the infancy of satellite communications. Today, however, except for special applications this type is not nearly and widely used as before for several reasons, including maintenance difficulties.

The thermo-electrically cooled and uncooled paramp LNAs are used mainly for Intelsat and occasionally for the key station in Domsats. These LNAs feature almost as low noise temperature as do the cryogenically cooled paramp, thanks to improvement in the varactor and the increase in pump frequency.

The FET LNA is employed mainly for Domsats and especially for TVRO systems. Thermo-electrically cooled and uncooled versions are used almost universally in these fields. The cryogenically cooled type is used for special applications.

2.2 4 GHz Paramp LNA

Requirements on this LNA as used in satellite communications are widely diversified. Important considerations are noise temperature, bandwidth, size, weight and maintainability. With respect to noise temperature, several kinds of paramp LNAs have been developed, with noise temperature characteristics from 30K to 60K according to the requirements of the individual system.

Typical noise temperature curves and outside views of the 35K TE cooled, 45K TE cooled, 55K Uncooled paramp LNAs are shown

Copyright © American Institute of Aeronautics and Astronautics, Inc., 1980. All rights reserved.

in Fig. 1, Fig. 2, and Fig. 3, respectively.

These LNAs offer many features including:

- (a) Ultra low noise temperature
- (b) Solid-state Gunn oscillator
- (c) Highly reliable varactor
- (d) High reliability
- (e) Small size and lightweight
- (f) Simple installation
- (g) Easy transportation

The most outstanding features are the location of bias voltage and pump power controllers for frequency response alignment, airtightness of the housing, and the nitrogen pressurization system for long term operation.

Although the present paramp LNA has been significantly improved and is providing very stable operation, frequency response alignment has to be made at least once a year. Taking this into account, the bias voltage and pump power controllers are mounted in the control and monitor panel located away from the RF unit. The RF unit which contains the paramp is mounted at the location of the antenna feed. Consequently, frequency response alignment can be performed remotely from the location where the control and monitor panel is installed and it is therefore not required to climb the antenna hub where the RF unit is installed.

To prevent water vapour in the air from condensing and in order to offer long term reliability, the housing of the RF unit is made airtight in a vacuum jacket and so ruggedly built that it is capable of being evacuated for cleaning.

A nitrogen pressurization system is provided for the termo-electrically cooled LNA version to prevent water vapour condensation during long term operations. The pressurized nitrogen gas, which is contained in a tank, is continuously being supplied to the housing of the RF unit, and is regulated at moderate pressure regulator. As the housing internal pressure is always kept positive, the possibility of water vapour penetrating into the housing is prevented. This method is more reliable than utilizing dry air from a Dehydrator, since this air inherently contains water vapour and is liable to an ingress of water vapour due to degradation of the Dehydorator.

2.3 4 GHz FET LNA

The performance of the 4 GHz FET LNA is primarily attributed to the characteristics of the FET proper. Current noise temperature is less than 100K and 80K for the uncooled and thermo-electrically cooled versions, respectively

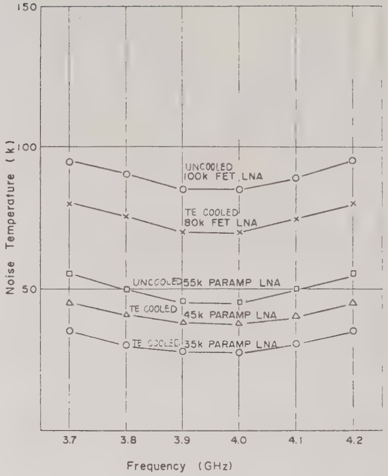

FIG. 1 TYPICAL NOISE TEMPERATURE OF 4 GHz LNA

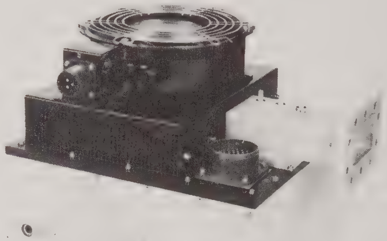

FIG. 2 4 GHz 35K TE COOLED PARAMP LNA

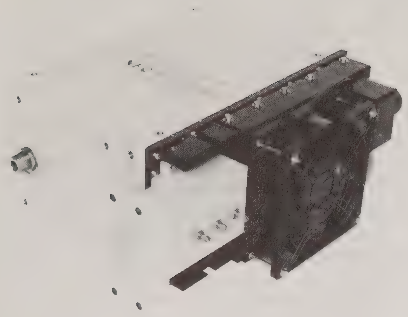

FIG. 3 4 GHz 55/45K PARAMP LNA

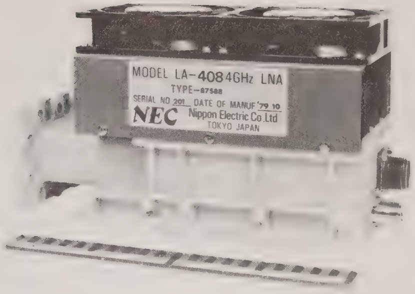
MODEL LA-408 4GHz LNA
TYPE-87588
SERIAL NO 201 DATE OF MANUF '79 10
NEC Nippon Electric Co.Ltd
TOKYO JAPAN

FIG. 4 4 GHz 80KTE COOLED FET LNA

as shown in Fig. 1. Figures 4 and 5 illustrate outside views of the 100K and 80K FET LNAs.

The 4 GHz FET LNA is maintenance free and has a higher reliability figure than the 4 GHz paramp LNA. In addition, the uncooled version may be installed where it is exposed to outside weather conditions such as rain, since its housing is made airtight by provision of O-rings at all sealed junctions. This is likewise the case for the thermo-electrically cooled version. The FET LNA is directly connected to the antenna feed without any additional support other than the input waveguide flange connection.

Considerably lower noise temperature than the lowest value of 80K would be available if the required receive frequency band were narrower than the traditional 500 MHz.

2.4 Future Trend

The 4 GHz LNA is showing a marked technological advance, and the development of an ultra low noise temperature below 30K for the paramp LNA and 70K for the FET LNA can be forecast for the near future.

In regard to the mechanical configuration, the era when the LNA occupied a quite large floor space in the earth station is now ending; in the future the LNA will take up only a small part of the antenna installation, since physically the LNA will be reduced to about half the size of what it is now.

Future LNAs must be able to withstand the rigors of severe outdoor environmental condition. This is partly because the LNA is directly connected to the feed and also partly because the protection enclosure for the LNA increasingly tends to be simplified.

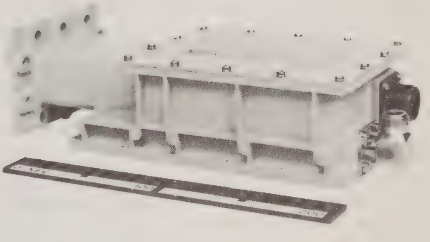

FIG. 5 4 GHz 100K FET LNA

3. 12 GHz LNA

3.1 General

The 12 GHz band has come to be utilized as a second generation satellite communications band and is used for Intelsat and Domsat operations in addition to the 4 GHz band.

Paramp LNAs are used mainly for Intelsat stations and FET LNAs for Domsats. Because, LNAs for intelsat stations are still demanded to decrease the noise temperature due to the antenna cost.

In the STD-C earth stations, down link performance is specified in G/T ratio.

From the standpoint of noise temperature comparison, the thermo-electrically cooled FET LNA has now nearly caught up with the uncooled paramp LNA. Considering the status of FET development, the pace at which the FET LNA is being improved and refined now almost exceeds that of the paramp LNA's.

A major problem caused by changing the frequency to a higher band, say, from 4 GHz

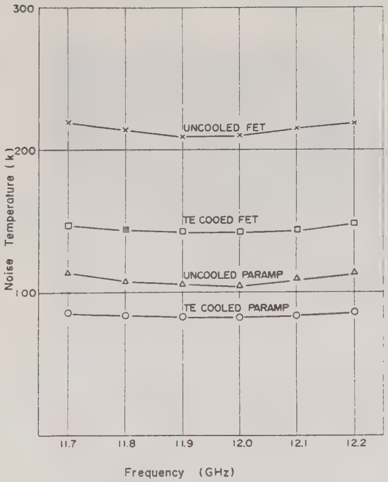

FIG. 6 TYPICAL NOISE TEMPERATURE OF 12 GHz LNA

to 12 GHz is the increase is the noise temperature contribution by connecting components such as waveguide switches and waveguide lines. As the frequency increases, the connecting elements introduce more loss and corresponding higher noise temperatures. Thus, the overall design configuration becomes extremely important. For example, the difference in noise temperature contribution between a WR-90 and a WR-75 type of waveguide is as large as 7 K/m.

3.2 12 GHz Paramp LNA

Typical noise temperatures and outside views are shown in Fig. 6 and Fig. 7, respectively. Figure 8 is a block diagram of this LNA. The outside view and blockdiagram shown illustrate a thermo-electrically cooled version.

This LNA satisfies the requirements for the Intelsat standard C earth station. The amplifier is highly reliable because it used a proven varactor and a direct Gunn oscillator as a pump source. The small and lightweight design results in easy installation. Frequency response alignment is performed remotely since the design concept is the same as for the 4 GHz LNA. No water vapour condensation is anticipated due to an airtight housing that acts like a vacuum jacket.

3.3 12 GHz FET LNA

Recent progress in FET technology, especially in the frequency range of 12 GHz, has been very rapid and dramatic. The 12 GHz LNA is so greatly advanced technically that it is now beginning to find growing applications for Domsat.

Typical performance of the NE13783 FET used in the amplifier is shown in Fig. 9. It is a super low noise FET specifically developed for the equipment as an FET of 2nd generation.

Fig. 10 shows a block diagram of the equipment. Each FET AMP unit, which consists of two FET chips, provides a total gain of about 15 dB. The unit is composed of two FET chips for the following reasons.

(1) If it consisted of one FET chip, additional isolators would be required between units, which in turn would cause noise temperature degradation due to the isolator loss. Overall cost would also be higher.

(2) If three FET chips were combined in one unit in tandem, superiority to some extent may be realized with respect to loss between stages and a corresponding reduction in the cost of materials. However, the alignment work would be so difficult that it is almost impossible to accomplish optimum performance.

The calculated noise temperature and the

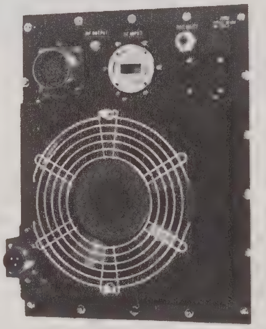

YCP-997

FIG. 7 12 GHz TE COOLED PARAMP LNA

estimated improvement introduced by thermo-electric cooling is shown in Fig. 11. The actual measured data for thermo-electric cooling is also shown in Fig. 11. The noise temperature reduction attained by thermo-electric cooling is non-uniform and depends on such factors as differences in input circuit alignment and in the performance of each FET chip.

The noise temperature budget is shown in Fig. 12. In the design, two points are of the utmost importance - one is the technique for incorporating the super low noise FET and the other, to reduce the loss of the input circuit. The most difficult point hitherto has been to develop a super low loss circulator with a loss lower than 0.1 dB per one path.

Typical noise temperatures and an outside view are shown in Fig. 6 and Fig. 13, respectively. This LNA is also enclosed in an air-tight housing of the same design as for other LNAs, and thus the water condensation problem is eliminated by replacing the inside air with dry nitrogen at the implant production process. Maintenance free operation and high reliability are other features as in the case of other FET LNAs.

3.4 Future Trend

As mentioned above, the noise temperature performance of the thermo-electrically cooled FET LNA is rapidly approaching that of the uncooled paramp LNA. This trend is expected to continue for the time being and ultimately catch up in the near future.

The further development of paramp LNAs will also proceed by improvements in the varactor diode, increase in pump frequency, reduction in losses of various components such as circulators, and Lowering of the cooling temperature of the thermo-electric cooler. A minimum noise temperature of 80K is expected. Only the thermo-electrically cooled version is expected to find applications.

The FET LNA will attain a noise temperature of lower than 130K in the near future as a result of continuous development efforts in shortening the gate length, improvement of input circuits and reduction of the cooling temperature.

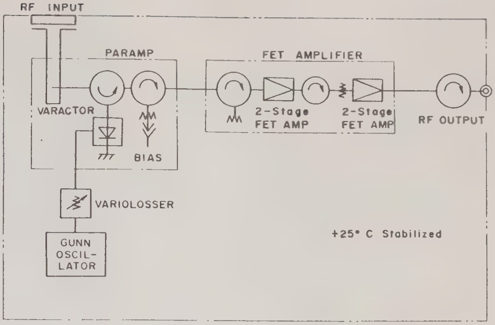

FIG. 8 LNA UNIT BLOCK DIAGRAM OF 12 GHz PARAMP LNA

ITEM	PERFORMANCE	UNIT
DRAIN CURRENT : IDss	100	mA
PINCH OFF VOLTAGE : Vp	-1	V
TRANSCONDUCTANCE : gm	25	m℧
MAXIMUM GATE VOLTAGE : BVgs	-12	V
MAX. OSCILATION FREQUENCY	80	GHz
MAX. AVAILABLE GAIN : MAG. (I=10mA, f=4GHz)	14	dB
NOISE FIGURE : NF (I=10mA, f=4GHz)	0.9	dB

FIG. 9 TYPICAL CHARACTERISTICS OF NE 13783

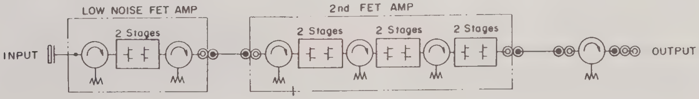

FIG. 10 BLOCKDIAGRAM OF 12 GHz FET LNA

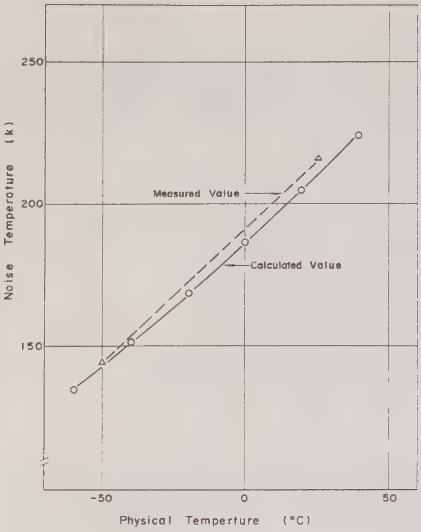

FIG. 11 NOISE TEMPERATURE VARIATION VS PHYSICAL TEMPERATURE OF 12 GHz FET AMP

CONFIGURATION	GAIN/LOSS (dB)	NOISE TEMPERATURE (K)	
		Each Stage	At LNA Unit Input
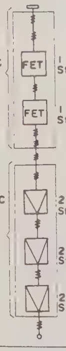	-0.15 -0.10 -0.25	0.05925 Ta	0.05925 Ta
-50°C Cooled FET 1 Stage	+8.3	Te	$\frac{1}{0.944}$ Te.
	-0.30	0.07152 Ta	0.07152 Ta
FET 1 Stage	+8.3	Te	$\frac{1}{5.96}$ Te
	-0.3 -0.1 -0.4	0.09648 Ta	$\frac{0.09648}{40.3}$ Ta
+20°C 2 Stages	-0.3 -0.1 -0.4	28.27	0.77
	+15.5	$\frac{1}{1.026} T'_{FET} = 256K$	7.64
2 Stages	-0.5	35.75	0.03
	+15.5	$\frac{1}{1.026} T'_{FET} = 427K$	0.40
2 Stages	-0.5	35.75	Neg
	+15.5	$\frac{1}{1.026} T'_{FET} = 427K$	0.04
	-0.7	51.25	Neg
Totel=T'LNA			1.227 Te+ 0.1332 Ta+885

FIG. 12 NOISE TEMPERATURE BUDGET OF LNA UNIT (AT THE CENTER FREQUENCY)

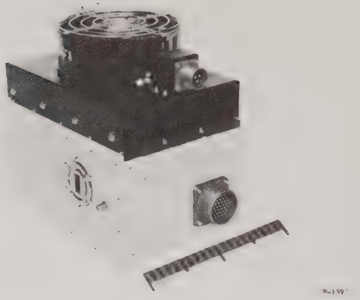

FIG. 13 12 GHz TE COOLED FET LNA

4. Millimeter Wave LNA (32 GHz LNA)

4.1 General

Since this frequency range will be utilized for future expansions in satellite communication traffic and since the band is capable of providing huge communication capacity, initial experimental approach as are proceeding in this band.

The atmospheric absorption and losses of various components in the band are extremely high, as compared to those in the lower bands. Thus, it is very important to carefully minimize the loss of various components such as waveguides and waveguide switches, which compose the receiving system.

A cryogenically colled LNA has been developed for one experiment. It consists of two stages of cryogenically cooled parametric amplifiers and two stages of uncooled FET amplifiers in tandem as shown in Fig. 14. The outside view of the Paramp Mount is shown in Fig. 15.

4.2 32 GHz Parametric Amplifier

The two stages of parametric amplifiers connected in cascade incorporate waveguide type cryogenically cooled circulators, GaAs Schottky carrier varactors (1SV 52) and a 80 GHz pump source. The noise temperature is shown in Fig. 16.

4.3 32 GHz FET Amplifier

An FET amplifier has been designed as a next stage for the parametric amplifier described above. It is a reflection type amplifier for increased gain per stage. The FET itself is the same NE388 enclosed in a 83 package as is used in other bands. The noise temperature and the gain of one stage of the FET amplifier are shown in Fig. 17.

4.4 Future Trend

The equipment described above is the first attempt in the field but it is expected to be fully applied to actual use, based on investigations of the field data observed so far.

It is expected that the equipment will be applied when the band is allocated for practical use. Furthermore, this equipment development is meaningful in response to the push for higher and higher frequencies. An important fact at such high frequencies as 32 GHz, is the confirmation of stable operation of the FET amplifier.

The FET amplifier is a very practical device by virtue of its easy application, although it is inferior to the parametric amplifier with respect to noise temperature performance.

Both the parametric amplifier and the FET amplifier technology if expected to advance under continuous development efforts.

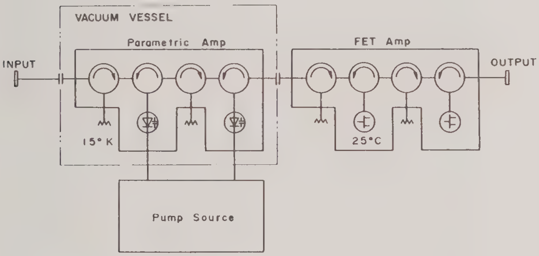

FIG. 14 BLOCKDIAGRAM OF 32 GHz LNA

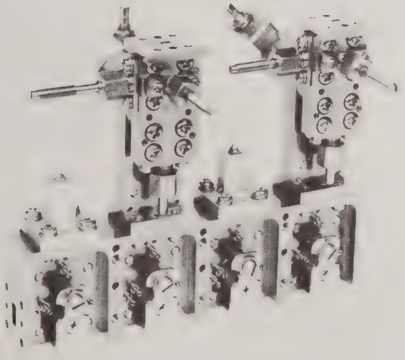

YCP-1367

FIG. 15 32 GHz LOW NOISE AMPLIFIER

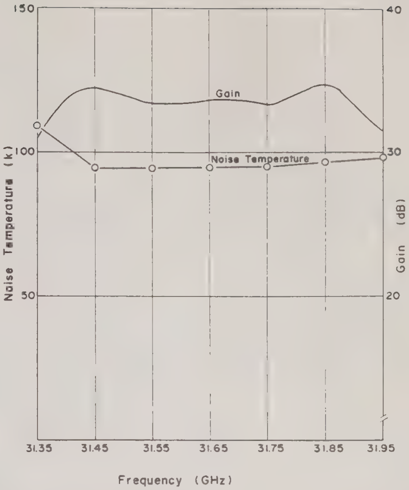

FIG. 16 TYPICAL NOISE TEMPERATURE OF 32 GHz LNA

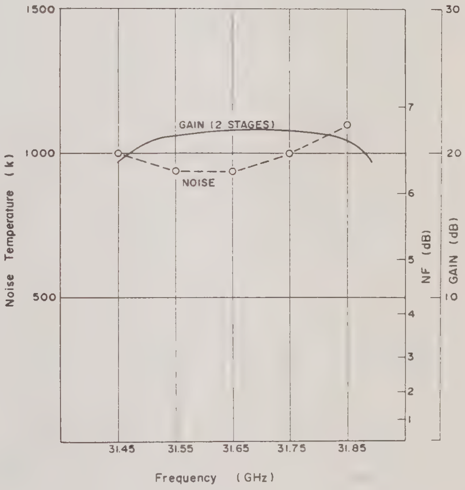

FIG. 17 TYPICAL NOISE TEMPERATURE OF 32 GHz FET AMP

5. Conclusion

LNAs offered today come in an increasingly wide variety of types. Thus, frequency range, noise temperature, etc. vary with individual type and cooling method employed.

The progress status of NEC's LNA development is shown in Fig. 18. In the 4 and 12 GHz bands, the FET LNA has almost caught up with the paramp LNA and is expected to proceed at the same development pace as at present in the future. Above the millimeter wave range, the paramp LNA has superior advantages over the FET LNA with respect to noise temperature.

In conclusion, parametric amplifiers with progress to higher and higher frequencies and will show lower and lower noise performance. In the case of the FET amplifier, it will continuously expand its application territory and will eventually occupy the existing area of the parametric amplifier.

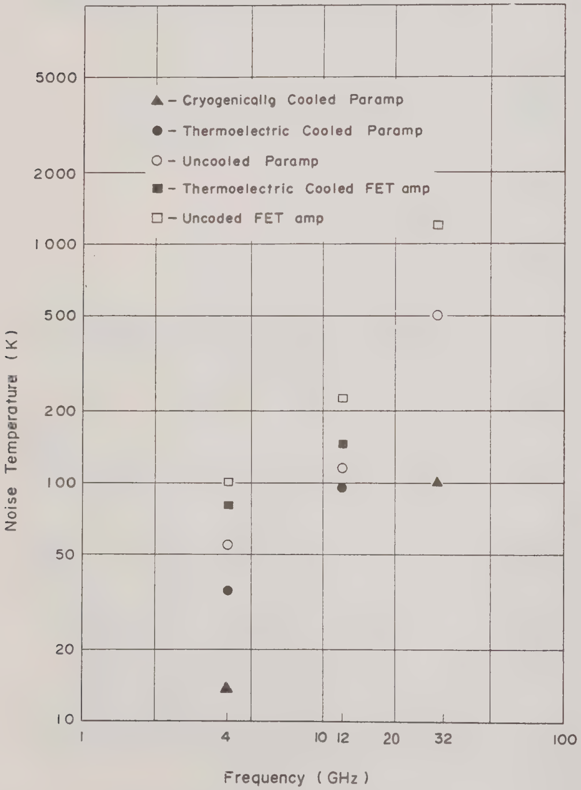

FIG. 18 DEVELOPMENT STATUS OF SATELLITE COMMUNICATIONS LNA

6. Acknowledgement

The authors wish to express their sincere thanks to Dr. N. Fugono, Dr. R. Hayashi and the staff concerned at the satellite communications division, Radio Research Laboratories, Ministry of Posts and Telecommunications, for useful discussions and encouragement. Thanks are also due to Dr. Y. Kaito, Mr. A. Saburi, Mr. K. Koyama and the staff concerned at the Satellite Communications Division and Semiconductors Division, NEC for their kind advice and cooperation.

80-0527

TDRSS MULTIPLE ACCESS
TELECOMMUNICATIONS SERVICE

R. Blyth*
Project Staff
System Engineering Operations
System Engineering and Integration Division
TRW, Defense and Space Systems Group
Redondo Beach, California

D. Haldeman
Member Technical Staff
System Engineering and Integration Division
TRW, Defense and Space Systems Group
Redondo Beach, California

Abstract

The paper discusses the Multiple Access (MA) service provided by the Tracking and Data Relay Satellite System (TDRSS), the theory of beamforming, the requirement for MA calibration and the calibration technique used. The thirty element adaptive antenna on the TDRSS is beamformed via ground station beam processing and inherently experiences time dependent phase and amplitude errors. A calibration technique for compensating these uncertainties and maintaining open-loop beam pointing by ground station signal processing has been developed and is described. Error budgets are shown for the MA service.

Introduction

The Tracking and Data Relay Satellite System (TDRSS) consists of two operational geostationary relay satellites approximately 130 degrees longitude apart and nominally located at 41 and 171 degrees west longitude and a ground station at White Sands, New Mexico. A third Tracking and Data Relay Satellite (TDRS) acts as an in-orbit spare for either of the operational satellites and can also be used as a third operational relay. A fourth satellite completes the system as shown in Fig. 1 and is used as an Advanced Westar satellite providing services to Western Union Telegraph Company. The third in-orbit TDRS can also act as a spare for the Advanced Westar since all four satellites are identical in configuration. Western Union Space Communications Inc. will own and operate the entire TDRSS system, leasing tracking and data relay services to NASA and commercial service to Western Union Telegraph Company. TDRSS is being built for Western Union Space Communication Inc. by TRW DSSG and Harris Corp. as principal subcontractors.

The ground station shown in Fig. 2 has three 18 meter K-band tracking antennas to support the two operational TDRS and the third shared spare TDRS. Each TDRS provides forward link service defined from the ground station through the TDRS to the user and return link service defined from the user through the TDRS to the ground station. By properly employing the satellite antennas shown in Fig. 3, the TDRS provides for Multiple-Access (MA) and Single-Access (SA) services. To support the SA service, each TDRS has two 4.9 meter deployable parabolic antennas operating at both S-band and K-band. Each SA antenna can simultaneously provide K-band forward and return service and S-band forward and return service to a tracked user satellite.

Multiple access (MA) telecommunication service is provided using a satellite mounted thirty element phased array antenna. The 30 element array is beam-formed at the ground terminal by phase and amplitude weighting. Ground station equipment is provided to form up to 20 independent beams from any of the satellite antenna arrays with each beam providing a forward multiple access MA service. Frequency division multiplexing on K-band is used to transmit the 30 antenna element signals from the satellite array to the ground. To correct for inherent phase and amplitude uncertainty build up over time between the thirty antenna element channels in the beam-forming process, a multiple access calibration technique was required and developed. Calibration maintains the necessary phase and amplitude stabilities for proper beamforming to assure the MA return link performance. Calibration is performed periodically to compensate for the time dependent instabilities. This calibration technique has been implemented using microcomputer-based firmware utilizing a gradient search algorithm to optimize the sum channel signal-to-noise ratio on the return MA telecommunication service. Satellite characteristics and system performance are given in Tables 1 and 2 repectively.

Multiple Access Service

The 30 element antenna array supports both MA forward and return service. Twelve of the antenna helical elements operate with 5.6 dBw saturated power amplifiers and diplexers to provide the required MA forward link Effective Isotropic Radiated Power (EIRP) to the user spacecraft. Only eight transmitters will be operational at any one time, while four remain on standby and can be switched into operation in case of failure. The eight elements forming the MA forward beam can be phased shifted by ground command to form a beam approximately 8 degrees wide and may be pointed anywhere within the required ±13° field of view coverage. Each TDRS can provide a single dedicated MA forward service at a maximum bit rate of 10 Kb/sec. The MA forward service is time-shared, operates at 2106.41 MHz, uses a signal bandwidth of 6 MHz and has a total EIRP at end-of-life of +34 dBw

---

*Member AIAA

Copyright © American Institute of Aeronautics and Astronautics, Inc., 1980. All rights reserved.

with left hand circular polarization. The return MA service operates at 2287.5 MHz with a signal bandwidth of 5 MHz and left hand circular polarization. Each antenna helical element gain is 13 dB or more over ±13.5 degrees field of view.

All MA users operate at the same return or forward link frequency and polarization and are discriminated by unique PN codes and antenna pointing. The return link data is modulo-2 added asynchronously to two PN codes which then biphase shift key modulate quadrature phases of the carrier. This provides two quadrature channels, I and Q, in a PN spread spectrum staggered quadraphase signal format for return link data rates of 0.1 to 50 Kb/s. The PN codes are either a long code (261,888 chips) or a short code (2047 chips). All data is rate one-half encoded using convolutional coding of constraint length 7 to provide forward error correction (FEC).

The MA forward link to the user spacecraft uses the same center frequency as the nominal TDRS S-band Single-access forward links and provides for a standardization in user transponder design. All forward links incorporate spread spectrum modulation techniques to satisfy the flux density restrictions imposed upon TDRSS forward link services by the Interdepartment Radio Advisory Committee. The MA forward carrier frequency transmitted by the TDRS will be compensated for doppler shift within a predictable tolerance to minimize the acquisition requirements of the user transponder. Compensation of the doppler effect is inhibited during coherent two-way measurements. The forward link signal is composed of separate but simultaneous command and range channels by using an I and Q channel modulation. The command channel includes a rapidly acquirable PN code and contains all command data. The range channel is acquired separately and contains a PN code which satisfies the range ambiguity requirement. The range and command channel codes are different but are both time-synchronized and coherent with the forward link carrier. MA forward link data is directly modulo-2 added to the command channel PN at the ground terminal. A user-unique PN code assignment for range and command channels is made. The TDRS does not process the forward range, command or user spacecraft data. The user spacecraft, tracked by the TDRS eight transmitting elements, receives the MA forward signal, locks to the command and range channel, processes the data, translates the received frequency by the ratio 240/221 and generates the PN coded return link back to the MA array on the TDRS which uses all thirty elements for tracking the MA return signal.

MA return link PN codes perform several functions. PN modulation spreads the user transmitter power to reduce flux-density at the earth's surface below specified limits. Assigning different PN codes to each user greatly reduces mutual interference. Many MA users can share the same frequency band using code division multiple access (CDMA), and narrow-band interference sources are also greatly rejected by the PN code tracking receiver.

Return link signals received at the 30 elements of the TDRS MA array are processed by the TDRS to produce a 30-channel frequency division multiplex (FDM) signal that is transmitted from the TDRS to the White Sands ground terminal via the K-band downlink in combination with other signals. The ground terminal separates out and demultiplexes the signal to recover the 30 separate antenna elements at an IF frequency of 160 MHz plus doppler shift. Each of the three 60 foot K-band ground antennas can provide a set of 30 antenna element channels at a time by using the two operational TDRS and the in-orbit spare.

Twenty weighter-and-combiner units, each having the capability to receive, weight and combine 30 input signals to form an MA return beam, are available at the ground terminal. Any of the twenty beamforming units can be assigned by ground control to accept any of the three TDRS inputs. A single TDRS can serve all 20 processors or likewise 3 TDRS can serve the 20 in any combination.

The output of the beamforming equipment consists of the MA user spread spectrum signal including noise and interference. This signal is doppler corrected using ground station estimates of doppler generated by user tracking software and translated to an intermediate frequency for PN correlation and demodulation in the MA ground receivers.

The demodulated user signal is time and level quantized by a soft-decision bit synchronizer. Data is extracted by a Viterbi-algorithm error-correction decoder and the data routed to the proper NASA communication interface by the baseband and IF configuration switch. The TDRS MA return link is shown in Fig. 4 and the ground processing MA return link block diagram is shown in Fig. 5.

Theory of Beamforming

Pointing of the 20 formed user beams is accomplished by computing complex weight values for each of the 30 element channel signals from the selected TDRS. Weight values are based principally on (1) predicted line-of-sight direction from the TDRS to the user satellite as known from ephemerides and (2) the antenna element coordinates as known from the array element geometry on the TDRS. Open-loop beamforming calculations are computed every 20 seconds for each user channel to compensate for user satellite motion relative to the TDRS.

Given the line-of-sight direction from the TDRS to the user satellite in terms of a unit pointing vector

$$\vec{\ell} = (\ell_X, \ell_Y, \ell_Z) \tag{1}$$

the RF phase of the received signal at the ith antenna element is

$$\theta_i = \frac{2\pi}{\lambda} \left[\ell_x X_i + \ell_y Y_i + \ell_z Z_i\right] \tag{2}$$

where X_i, Y_i and Z_i are the cartesian coordinates of the ith antenna element in the same coordinate system as the pointing vector, λ is the wavelength of the received signal and θ_i is the RF phase of the ith element channel signal relative to a hypothetical antenna located at the origin of the coordinate system. The receiver user satellite signal at the output of the 30 antenna element array can be denoted as a complex column vectory $\underline{\xi}$ whose ith entry, ξ_i, is the phase and amplitude of the signal at the output of the ith antenna element. $\underline{\xi}$ is called the signal correlation vector.

In order to establish how the weights are derived, a brief description of the antenna element noise processes is also required. Consider the ith antenna element channel with a bandlimited zero mean thermal noise process, N_i, and user signal ξ_i. The thermal noise power in the array of 30 elements can be expressed in terms of a thermal noise covariance matrix, ϕ_T, whose entry in the ith row and jth column is $E\,[N_i\, N_j{}^*]$. In practice, the thermal noise in different element channels is generated principally from noncoherent noise sources and internal channel mechanisms. Adjacent channel thermal noise processes are therefore uncorrelated and the noise covariance matrix reduces to a diagonal matrix whose ith entry along the diagonal is the thermal noise power in the ith element channel.

Using the above notation, the optimum theoretical complex weights for open-loop beamforming of a single user satellite is based on the theory presented in reference 2:

$$\underline{W} = \beta\, \phi_T^{-1}\, \underline{\xi} \tag{3}$$

where $\underline{W}$ is the vector of complex weights and β is an arbitrary constant.

The MA return system also has a requirement to form a single null upon request for any of the 20 user channels on the ground. Based on a designated earth fixed location, the theoretical complex weights are

$$\underline{W} = \beta\, \phi_N^{-1}\, \underline{\xi} \tag{4}$$

where

$$\phi_N = \phi_T + \alpha\, \underline{\rho}\, \underline{\rho}^{*T} \tag{5}$$

The complex vector $\underline{\rho}$ describes the location of the single null and is analogous to $\underline{\xi}$ for the user satellite. The real parameter, α, determines the degree of null depth required.[2]

Return Channel Calibration Requirement

Open-loop beamforming of the MA return channel requires knowing the relative phase and amplitude of the user satellite signal at the antennas on the TDRS. Equally important is knowledge of the phase and amplitude of the user satellite signal at the input to the beamforming equipment in the ground terminal. Since the MA return link introduces phase shifts and amplitude changes in each of the 30 element channels between the antennas on the TDRS and the beamforming equipment on the ground, open-loop beamforming requires a method for determining phase and amplitude offsets in the MA return link.

The principal cause of degradation in array performance is differential phase and amplitude errors which accumulate in the 30 element channels of the return link over time and a changing environment. Phase and amplitude coherence of the 30 element channels is therefore essential to optimal open-loop performance. All reference frequencies for up and down conversion are coherently related and derived from a pilot tone generated by a cesium frequency standard in the ground terminal, and transmitted to the spacecraft. In the spacecraft, the pilot tone is extracted from the forward processor and applied to a phase-locked demodulator in the master frequency generator. A 30-MHz frequency derived from the phase-locked demodulator provides the reference for synthesis of all TDRS oscillator frequencies. In addition to providing most of the local oscillators directly, the master frequency generator provides a reference frequency to a separate MA frequency generator, which generates the frequencies used to multiplex the 30 multiple access return channels. Nevertheless, slowly varying phase and amplitude drifts are inherent in the 30 element channels of the MA return link due to temperature cycling and aging on the TDRS and in the ground station processing equipment, spacecraft and ground frequency multiplexer phase drifts, and ionospheric phase dispersion in the K-band downlink. Consequently, a method of calibration is required to compensate for phase and amplitude offsets which occur between the antennas on the spacecraft and the beamforming equipment on the ground and to maintain open-loop pointing capability of the MA return link. Maintaining open-loop pointing of the return link is satisfied when the allocated degradations are met.

The concept of MA return calibration is depicted in Fig. 6. Phase and amplitude of the 30 element-channel signals at the input to the beamforming equipment, $\underline{\gamma}$, are measured during reception of a known MA return signal; phase and amplitude of the 30 element-channel signals at the antennas, $\underline{\xi}$, are known by geometry. Based on these two complex vectors, an estimate of the system's effect on phase and amplitude in each of the 30 element channels from the antennas on the TDRS to the beamforming equipment on the ground can be determined. That is, mathematically, the MA return link is modeled as a spatially independent diagonal matrix, $\underline{D}$, that transforms $\underline{\xi}$ at the antennas on the TDRS to $\underline{\gamma}$ at the input to the beamforming on the ground according to the rule.

$$\underline{\gamma} = D\, \underline{\xi} \tag{6}$$

Thus, during open-loop pointing of the MA return link, one can predict the phase and amplitude of a user satellite signal in each of the 30 element channels at the input of the beamforming equipment and the corresponding weights necessary to point the beam from knowledge of the system matrix and the signal correlation vector at the TDRS.

---

*Denotes complex conjugate

The MA return link is required to support a single user beam; the array gain in the direction of the user satellite has been allocated a maximum link budget degradation of 0.5 dB. In addition, the antenna may be required to support a single beam and a single out-of-beam earth fixed null at a null depth of 25 dB; the array gain in the direction of the user satellite for this case has been allocated a maximum link budget degradation of 0.8 dB. An analysis of the statistical properties of the signal-to-noise ratio of the 30 element MA array antenna[3] led to an overall system requirement of 10 equivalent degrees rms error for both phase and amplitude drifts in each of the 30 element channels.

The effective system rms error, σ_x, represents the maximum allowable rms phase and amplitude error per element channel in equivalent degrees that can be tolerated by the open-loop MA system. This requirement has been broken down into differential phase and amplitude error allocations between any two element channels for the ground station, weight quantization, weight errors, instrumentation error, ionospheric phase dispersion and the TDRS payload as outlined in Table 3. The resulting allocations for element channel-to-channel phase and amplitude errors for the ground station, weight quantization, and weight errors require the ground station to maintain these stability requirements for a period of at least 4 hours. Allocations for the TDRS payload must be maintained for a period of at least 18 minutes - with a design goal of 30 minutes.

Based on the degradation expected and their allocations, calibration of the MA return link to update an estimate of the system matrix, D, will be required every 18 minutes to 30 minutes in order to maintain open-loop MA system performance requirements.

Calibration Technique

Periodic calibration of the MA return link is accomplished on the ground by a closed-loop adaptive control algorithm that iteratively adjusts weight values to maximize signal-to-noise ratio of the combined user channel signal (or sum channel signal) at the output of the beamforming equipment. Estimates of the phase and amplitude of the 30 element-channel signals are then sent to the automatic data processing equipment where they are compared with the line-of-sight prediction to estimate the system matrix, D.

In the case of open-loop beamforming, it follows from (3) that for an arbitrary user satellite with a line-of-sight predicted correlation vector at the antennas on the TDRS, $\underline{\xi}$, and a system matrix, D, the optimum weights for the beamforming equipment on the ground will be

$$\begin{aligned} \underline{W} \text{ optimum} &= \beta \left[D\, D^{*T}\right]^{-1} \underline{\gamma} \\ &= \beta \left[D^{*}\right]^{-1} D^{-1} \underline{\gamma} \qquad (7) \end{aligned}$$

where $\underline{\gamma}$ is the signal correlation vector at the input to the beamforming equipment. Using equation (6), (7) reduces to

$$\underline{W} \text{ optimum} = \beta \left[D^{*}\right]^{-1} \underline{\xi} \qquad (8)$$

where β, a normalization constant, is used to minimize the effects of quantization. In the case of open-loop beamforming with a single null, it follows from (4) and (5) that

$$\begin{aligned} \underline{W} \text{ optimum} &= \beta \left[D\, \phi_N D^{*T}\right]^{-1} \underline{\gamma} \\ &= \beta \left[D^{*}\right]^{-1} \phi_N^{-1} \underline{\xi} \qquad (9) \\ &= \beta \left[D^{*}\right]^{-1} \underline{W}_T \end{aligned}$$

where $\underline{W}_T$ are the theoretical weights computed as if the beamforming equipment were located just after the antennas on the TDRS.

Regardless of the type of open-loop calculation required, phase shifts and amplitude changes in the 30 element channels from the antennas on the TDRS to the input of the beamforming equipment on the ground can be accounted for by the matrix

$$\beta \left[D^{*}\right]^{-1} \qquad (10)$$

The diagonal entries in (10) are stored in a weight correction table and implemented as described in (8) and (9). All subsequent open-loop pointing calculations of the MA return link utilize this weight correction table to optimize MA system performance.[4]

MA Calibration

The MA calibrator employs a gradient algorithm that assumes control of the beamforming equipment and searches for the optimum signal-to-noise ratio by means of small steps, or weight changes, in the direction of the estimated gradient. The 30 element channel signals at the input to the beamforming equipment as well as the sum channel signal at the output of the beamforming equipment are routed to the calibrator. Therein, the calibrator performs a narrow band correlation between each of the 30 element signals and the sum channel signal to derive an estimate of the element channel signal's phase and amplitude. This is called the signal loop estimate. A wideband correlation is also performed to derive a quadrature estimate of the noise power in the element channel. This is called the noise loop estimate. As shown in Fig. 7, these two estimates are used to determine a new set of weights which improve the signal-to-noise ratio in the sum channel at the output of the beamforming equipment.

The output of the 20 MA ground receivers and the 20 sum channel signals are applied to a receiver select switch under control of the microcomputer. The RF hardware selects which ground processing channel shall be calibrated, prefilters the element sample channel and the sum channel signals in a 6 MHz bandpass filter and performs automatic gain control to provide signals within the full dynamic range of the A/D's in the digital signal processor. The RF hardware also remodulates the digital PN from the ground receiver and mixes this signal with the sum and element sample channels. As a result of this mixing, the PN is effectively stripped from the signal carrier leaving only signal plus wide band noise energy. The digital signal processor is a high speed special purpose digital signal processor that performs bandpass filtering, AGC control and complex correlations using digital arithmetic. Digital signal processing is used to provide precise control of phase delays through this portion of the circuit. The microcomputer is a computer system centered around a microprocessor CPU and contains all parts of a classical computer system, i.e., CPU, memory and I/O. The firmware is the programming needed to control the MA calibrator plus execute the calibration algorithm.

Convergence of the calibration algorithm is detected in firmware by a separate algorithm that operates on the gradient error. Typical performance of the MA calibrator is shown in Fig. 8 and is based on computer simulations that include random errors, offsets and quantization errors to emulate actual hardware performance. Given sufficient signal-to-noise ratio to permit PN code lock in the demodulator, the MA calibrator can iteratively optimize the signal-to-noise ratio at the output of the beamforming equipment (sum channel) for any initial performance degradation. A large initial beam degradation with resulting convergence is shown in Fig. 9.

Calibration of an MA return link requires the use of any one of the 20 user channels and the reception of a specific calibration signal for a period of one minute with another minute for signal processing. The calibration signal is identified by its unique PN spread spectrum code. After convergence, the calibrator provides the estimate of the signal's correlation vector at the input to the beamforming equipment[3] to within a link budget degradation of 0.1 dB.

Periodic calibration of the MA service is under control of the ground data processing software. Scheduling of calibration for the MA return service includes:

a. Maintaining MA system equipment calibration status

b. Scheduling return path equipment chain

c. Performing equipment reservation conflict analysis

d. Setting up reserved equipment chain

e. Control of the calibration special signal source

f. Control of the calibration equipment

g. Processing of the calibration results and display and printout of calibration results

h. Termination of calibration process.

The calibration process is normally initiated automatically by the ground data processing software; however, the software also processes requests from the ground station operator control console.

Whenever the calibrator is not commanded to perform calibration, it is in a continuous self test mode. After the MA return service setup has been completed by the site software, the calibrator takes control of the selected weighter and combiner and the element sample switch, and commands them until the completion of the calibration process. Once the calibration process is completed, the calibrator notifies the site software of this fact and the software may then command the calibrator to transmit its beam optimization data, relinquish control of the element sample switch and weighter and combiner, and resume self test. Additionally, site software automatically notifies site operator control of a calibrator self-test failure or a calibration signal source failure.

Conclusion

Although the selection of open-loop beamforming for the 20 processed MA return channels results in a severe systems design requirement for phase and amplitude stability, the calibration process described can very nearly keep the beamforming optimum to insure MA user service. By developing ground station software to automatically monitor the calibration status of all MA return service equipment chains and to assign calibration as required to maintain the required phase and amplitude error budgets, the phase array beamforming through any of the on-orbit satellites can be kept within the design requirements. To accomplish this, special attention was required in (1) design of the payload MA processing equipment, (2) antenna element channel matching, (3) computer modeling and estimation of MA return channel instabilities and (4) design of ground processing equipment for phase, gain and dynamic range requirements. In addition, two other major objectives were met. One, the design and implementation of the calibrator equipment; and second, the development of a workable method to timeshare a calibrator over the 20 ground processing chains incorporating three ground antenna systems and three satellite antenna arrays with associated on-board MA processing.

REFERENCES

1. Steinberg, B. D., Principles of Aperture and Array System Design (Chapter 1), Wiley, 1976.

2. Applebaum, S.P., "Adaptive Arrays," IEEE Trans. On Antennas and Propagation, Vol. AP-24, No. 5, September 1976.

3. TDRSS-79-213.H-002, "MA Return Calibration - An Overview," TRW Interoffice Correspondence, TRW Defense and Space Group, Redondo Beach, California.

4. Weber, C., et al., "TDRSS Telecommunications MA Return Channel," Proceedings of the 1978 International Telemetering Conference.

5. Performance Design Specification Multiple Access Link Calibrator, EQ4-2085A, 17 January 1979.

Table 1. Satellite Characteristics

Size	17.42 m (57.2 ft) x 12.98 m (42.6 ft)
Weight	1088.63 kg on orbit (4400 lb)
Electrical Power	1700-watt end of life Ni-Cad batteries supply full power in eclipse
Attitude Control	3-axis stabilization
Steerable Antennas Pointing Accuracy	0.2 degree
Telecommunications Channels	2 S-band duplex 2 K-band duplex One 20-user S-band multiple access return One time-shared S-band multiple access forward
Service	Global telecommunications and tracking for up to 32 simultaneous user services Data rates of 100-bps to 300 Mbps
Antennas	6 (3 steerable)
Operational Orbit	Geosynchronous. 22.300 statute mile circular with 0.1 degree stationkeeping
Launch Vehicles	Space Shuttle/Inertial Upper Stage
Lifetime	10 years
Operational Use	Post 1980

Table 2. TDRS System Performance per TDR Satellite

Access	Multiple Access		S-Band Single Access		K-Band Single Access	
	Forward	Return	Forward	Return	Forward	Return
Number of Channels	1	20	2	2	2	2
Effective Radiated Power (dBW)	34	-	46.4	-	49.4	-
G/T (dB/°K)	-	-14.7	-	8.9	-	24.4
Maximum Data Rates (Mbps)	0.01	0.05	0.3	12	25	300
Channel Bandwidth (MHz)	10	5	20	10	50	225
Bit Error Rate	-	10^{-5}	-	10^{-5}	-	10^{-5}
Frequency Band Assigned (MHz) TDRSS/User	2103.1 to 2109.7	2284.5 to 2290.5	2020.4 to 2123.3	2200 to 2300	13747 to 13802	14887 to 15119

Table 3. MA Return Phase and Amplitude Error Budget

Contribution	Per Element			Element-to-Element		
	σ_{XY}	σ_X (phase)	σ_Y (amp)	$\Delta\sigma_{XY}$	$\Delta\sigma_X$ (phase)	$\Delta\sigma_Y$ (amp)
Ground Station RMS Phase Error	0.062	0.062 (3.6°)	-	0.088	0.088 (5.0°)	-
Ground Station RMS Amplitude Error	0.040	-	0.040 (0.3 dB)	0.057	-	0.057 (0.5 dB)
Quantization	0.026	0.018 (1.0°)	0.018 (0.2 dB)	0.037	0.026 (1.5°)	0.026 (0.2 dB)
Weight Inaccuracy	0.105	0.074 (4.2°)	0.074 (0.6 dB)	0.148	0.105 (6.0°)	0.105 (0.9 dB)
Instrumentation Error	0.037	0.022 (1.3°)	0.030 (0.3 dB)	0.052	0.031 (1.8°)	0.042 (0.4 dB)
Payload RMS Phase Error Ionospheric Phase Dispersion	0.143	0.143 (9.2°)	-	0.202	0.202 (11.6°)	- *
Payload RMS Amplitude Error	0.149	-	0.149 (1.2 dB)	0.211	-	0.211 (1.6 dB)*
Total RMS Error	0.247	0.175 (10°)	0.175 (1.4 dB)	0.349	0.247 (14.1°)	0.247 (1.9 dB)

*Payload element-to-element rms phase error 11.6°
Payload element-to-element rms amplitude error 1.6 dB

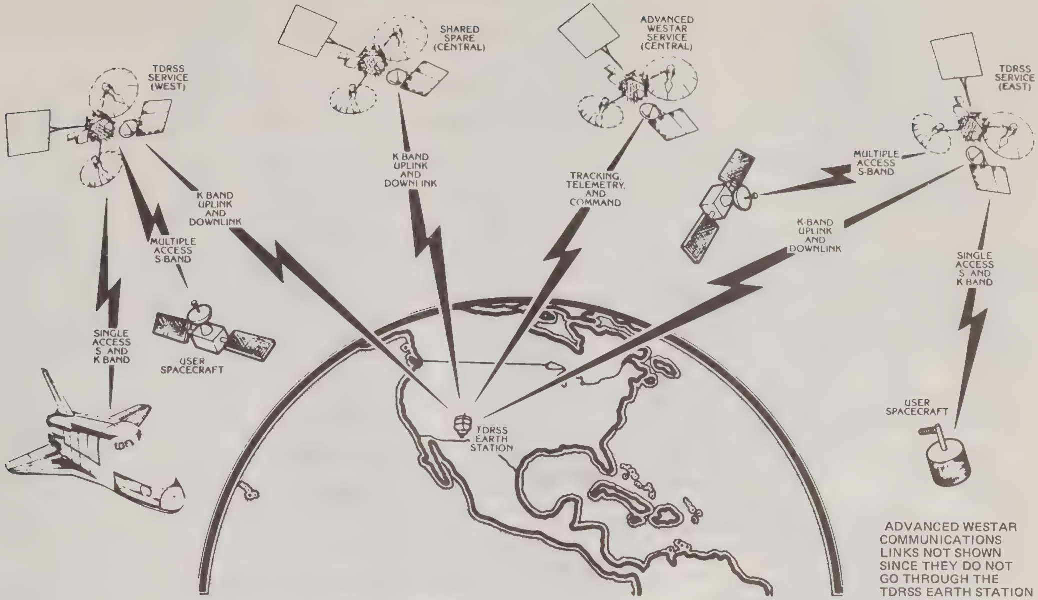
TDRSS SERVICE (WEST)
SHARED SPARE (CENTRAL)
ADVANCED WESTAR SERVICE (CENTRAL)
TDRSS SERVICE (EAST)
K BAND UPLINK AND DOWNLINK
MULTIPLE ACCESS S-BAND
K BAND UPLINK AND DOWNLINK
TRACKING, TELEMETRY, AND COMMAND
MULTIPLE ACCESS S-BAND
K-BAND UPLINK AND DOWNLINK
SINGLE ACCESS S AND K BAND
SINGLE ACCESS S AND K BAND
USER SPACECRAFT
TDRSS EARTH STATION
USER SPACECRAFT
ADVANCED WESTAR COMMUNICATIONS LINKS NOT SHOWN SINCE THEY DO NOT GO THROUGH THE TDRSS EARTH STATION

Fig. 1. Tracking and Data Relay Satellite System

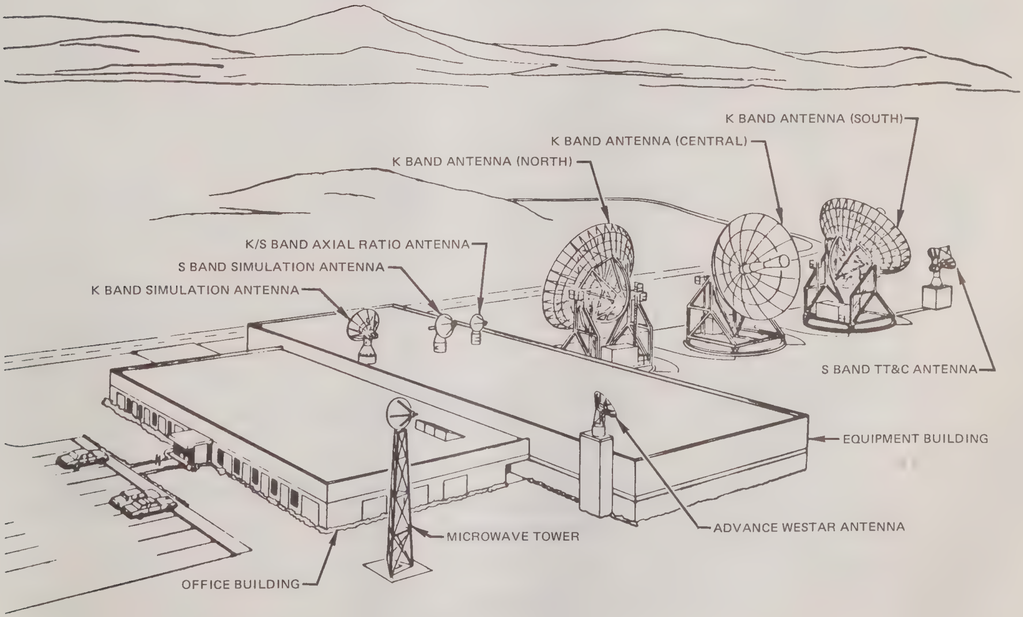
K BAND ANTENNA (SOUTH)
K BAND ANTENNA (CENTRAL)
K BAND ANTENNA (NORTH)
K/S BAND AXIAL RATIO ANTENNA
S BAND SIMULATION ANTENNA
K BAND SIMULATION ANTENNA
S BAND TT&C ANTENNA
EQUIPMENT BUILDING
ADVANCE WESTAR ANTENNA
MICROWAVE TOWER
OFFICE BUILDING

Fig. 2. TDRSS Ground Terminal White Sands, New Mexico

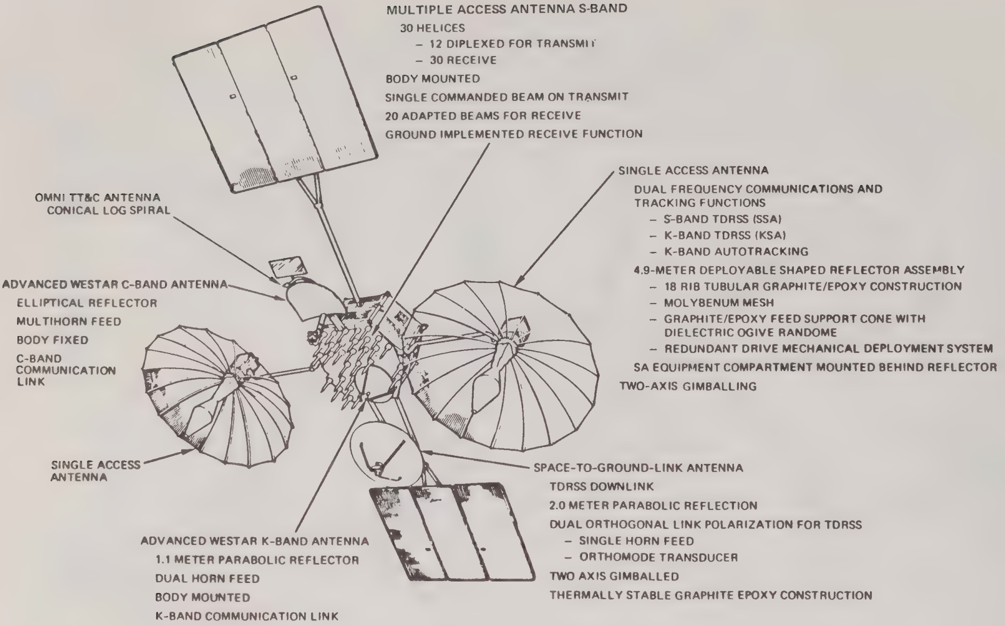
MULTIPLE ACCESS ANTENNA S-BAND
30 HELICES
– 12 DIPLEXED FOR TRANSMIT
– 30 RECEIVE
BODY MOUNTED
SINGLE COMMANDED BEAM ON TRANSMIT
20 ADAPTED BEAMS FOR RECEIVE
GROUND IMPLEMENTED RECEIVE FUNCTION
OMNI TT&C ANTENNA
CONICAL LOG SPIRAL
SINGLE ACCESS ANTENNA
DUAL FREQUENCY COMMUNICATIONS AND TRACKING FUNCTIONS
– S-BAND TDRSS (SSA)
– K-BAND TDRSS (KSA)
– K-BAND AUTOTRACKING
4.9-METER DEPLOYABLE SHAPED REFLECTOR ASSEMBLY
– 18 RIB TUBULAR GRAPHITE/EPOXY CONSTRUCTION
– MOLYBENUM MESH
– GRAPHITE/EPOXY FEED SUPPORT CONE WITH DIELECTRIC OGIVE RANDOME
– REDUNDANT DRIVE MECHANICAL DEPLOYMENT SYSTEM
SA EQUIPMENT COMPARTMENT MOUNTED BEHIND REFLECTOR
TWO-AXIS GIMBALLING
ADVANCED WESTAR C-BAND ANTENNA
ELLIPTICAL REFLECTOR
MULTIHORN FEED
BODY FIXED
C-BAND COMMUNICATION LINK
SINGLE ACCESS ANTENNA
SPACE-TO-GROUND-LINK ANTENNA
TDRSS DOWNLINK
2.0 METER PARABOLIC REFLECTION
DUAL ORTHOGONAL LINK POLARIZATION FOR TDRSS
– SINGLE HORN FEED
– ORTHOMODE TRANSDUCER
TWO AXIS GIMBALLED
THERMALLY STABLE GRAPHITE EPOXY CONSTRUCTION
ADVANCED WESTAR K-BAND ANTENNA
1.1 METER PARABOLIC REFLECTOR
DUAL HORN FEED
BODY MOUNTED
K-BAND COMMUNICATION LINK

Fig. 3. TDR Satellite Antenna Equipment

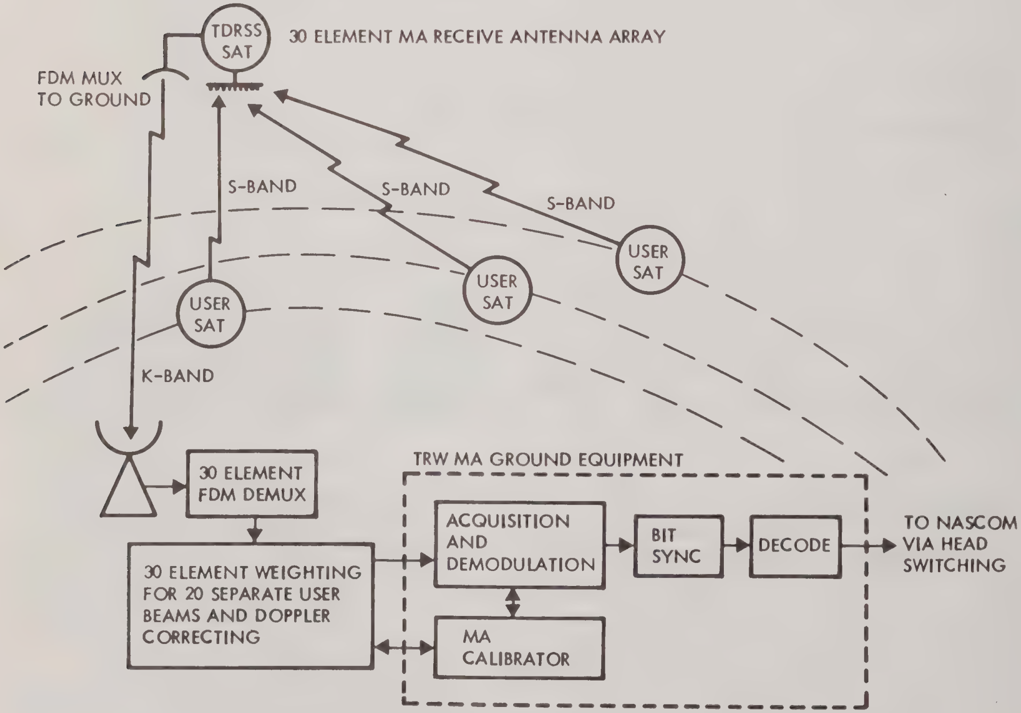
TDRSS SAT
30 ELEMENT MA RECEIVE ANTENNA ARRAY
FDM MUX TO GROUND
S-BAND
S-BAND
S-BAND
USER SAT
USER SAT
USER SAT
K-BAND
TRW MA GROUND EQUIPMENT
30 ELEMENT FDM DEMUX
30 ELEMENT WEIGHTING FOR 20 SEPARATE USER BEAMS AND DOPPLER CORRECTING
ACQUISITION AND DEMODULATION
BIT SYNC
DECODE
MA CALIBRATOR
TO NASCOM VIA HEAD SWITCHING

Fig. 4. TDRSS Multiple Access Return Link

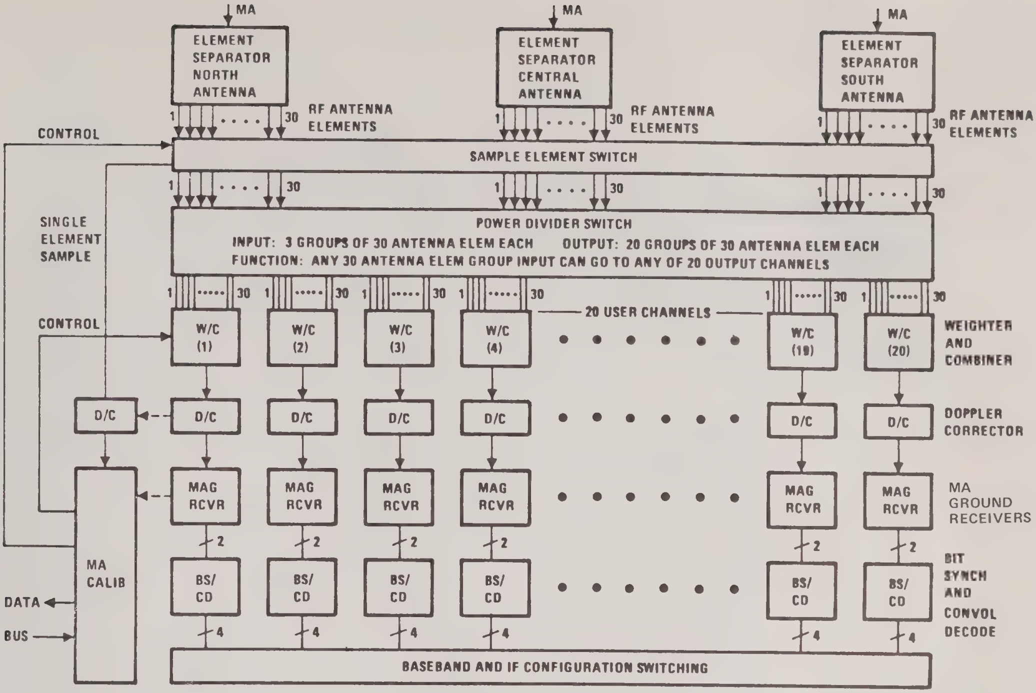
MA
ELEMENT SEPARATOR NORTH ANTENNA
ELEMENT SEPARATOR CENTRAL ANTENNA
ELEMENT SEPARATOR SOUTH ANTENNA
1
30
RF ANTENNA ELEMENTS
CONTROL
SAMPLE ELEMENT SWITCH
SINGLE ELEMENT SAMPLE
POWER DIVIDER SWITCH
INPUT: 3 GROUPS OF 30 ANTENNA ELEM EACH
OUTPUT: 20 GROUPS OF 30 ANTENNA ELEM EACH
FUNCTION: ANY 30 ANTENNA ELEM GROUP INPUT CAN GO TO ANY OF 20 OUTPUT CHANNELS
20 USER CHANNELS
W/C (1)
W/C (2)
W/C (3)
W/C (4)
W/C (19)
W/C (20)
WEIGHTER AND COMBINER
D/C
DOPPLER CORRECTOR
MAG RCVR
MA GROUND RECEIVERS
2
BS/ CD
BIT SYNCH AND CONVOL DECODE
4
MA CALIB
DATA
BUS
BASEBAND AND IF CONFIGURATION SWITCHING

Fig. 5. MA Return Block Diagram

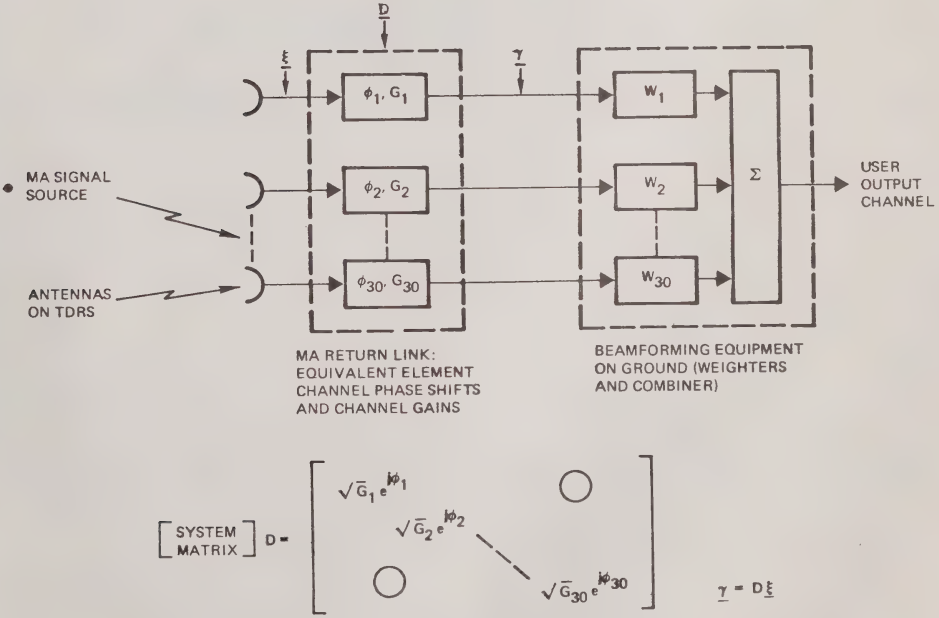
D
ξ
γ
ϕ_1, G_1
ϕ_2, G_2
ϕ_{30}, G_{30}
W_1
W_2
W_{30}
Σ
USER OUTPUT CHANNEL
MA SIGNAL SOURCE
ANTENNAS ON TDRS
MA RETURN LINK: EQUIVALENT ELEMENT CHANNEL PHASE SHIFTS AND CHANNEL GAINS
BEAMFORMING EQUIPMENT ON GROUND (WEIGHTERS AND COMBINER)
[SYSTEM MATRIX] D =
$\sqrt{G_1}e^{j\phi_1}$
$\sqrt{G_2}e^{j\phi_2}$
$\sqrt{G_{30}}e^{j\phi_{30}}$
0
0
$\gamma = D\xi$

Fig. 6. Concept of Calibration

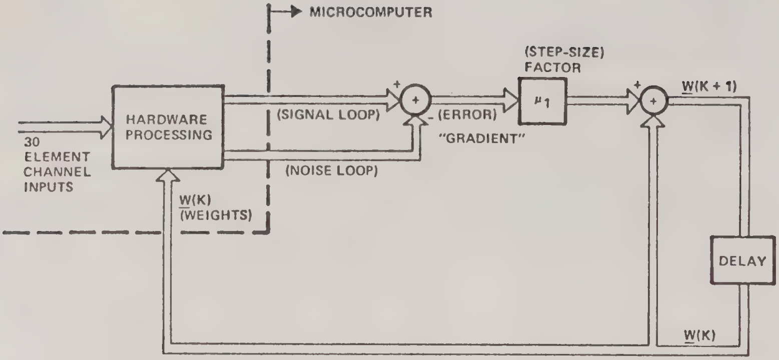
MICROCOMPUTER
(STEP-SIZE) FACTOR
μ_1
+
+
W(K + 1)
HARDWARE PROCESSING
(SIGNAL LOOP)
-
(ERROR)
"GRADIENT"
30 ELEMENT CHANNEL INPUTS
(NOISE LOOP)
W(K) (WEIGHTS)
DELAY
W(K)

Fig. 7. MA Calibration Algorithm Functional Concept

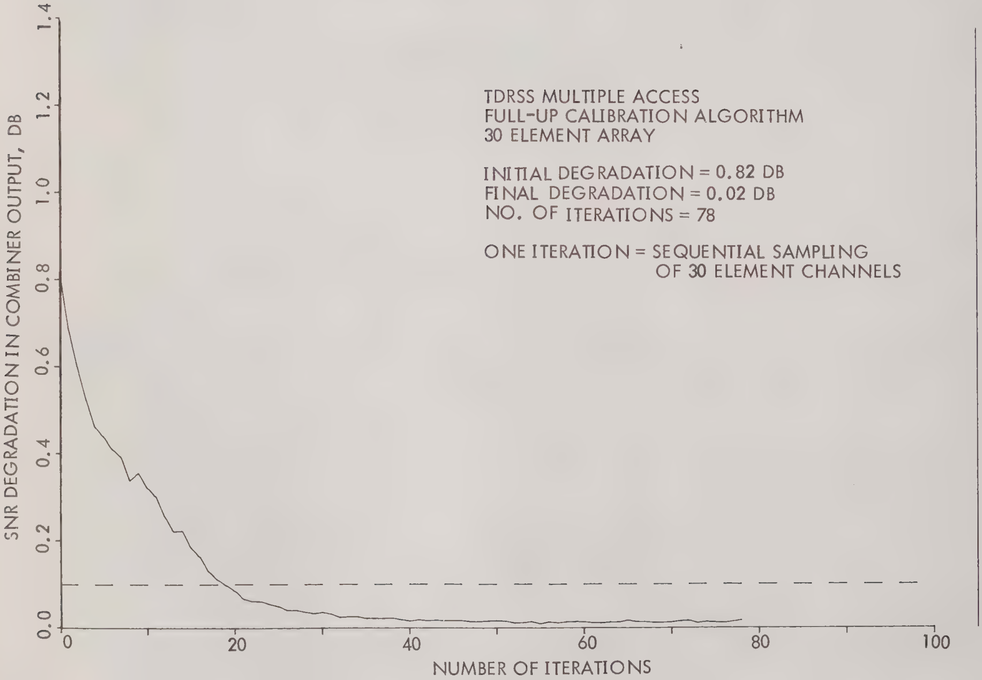

Fig. 8. Typical Convergence of MA Calibrator

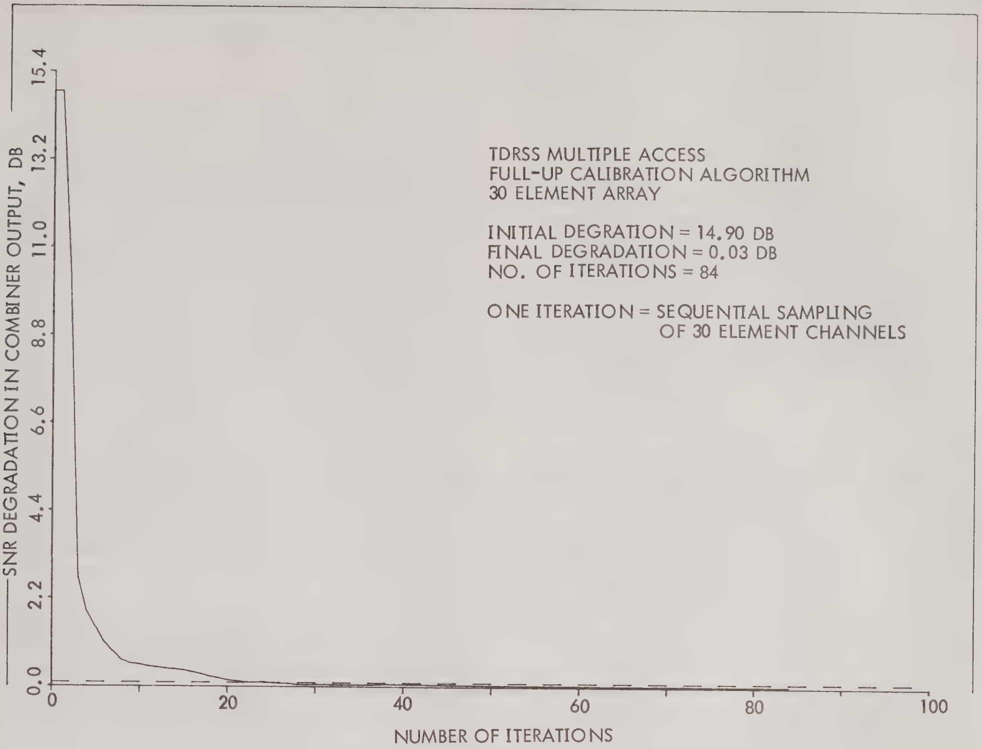

Fig. 9 Convergence of Calibrator with Large Initial Degradation

80-0528

LANDSAT D TELECOMMUNICATIONS PAYLOAD: EARTH IMAGING DATA VIA TDRS

H. B. Poza*
TRW Defense and Space Systems Group
One Space Park
Redondo Beach, California 90278

Abstract

This paper describes the telecommunications payload for the Landsat D spacecraft. The salient design features of the electronic equipment, as well as the performance requirements that such equipment must satisfy to fulfill GE and NASA communication functions, are presented. Operational characteristics associated with the process of relaying earth imaging information to the White Sands Ground station via the Tracking and Data Relay Satellite (TDRS) are also highlighted.

1. Introduction

The Landsat D spacecraft is designed to collect earth-imaging data and transmit it to domestic and foreign users for processing and evaluation. It will allow assessment of the capability of the Thematic Mapper (TM) to provide improved information for Earth Resources Management and provide a transition for both domestic and foreign users from the Multi-Spectral Scanner (MSS) data to the high resolution and data rate of the TM.

A single Landsat can survey nearly every area of our planet every 18 days. The view from one Landsat (through MSS or TM) can cover an area requiring more than a hundred aerial photos, and can reveal vast features that may be obscured in mosaics made from aerial photographs. Correspondingly, a complete photo-mosaic of the United States can be assembled using approximately 570 Landsat images, while nearly 30,000 aerial photos would be needed to cover the same area. Landsat photographic images are taken in the red and green bands of visible light and in near infrared bands. These images are converted to radio signals which are transmitted to Earth, where computers reconstruct them to produce black and white or colored pictures and bring out features of the observed terrain or vegetation. In this fashion, healthy vegetation may stand out in bright red while diseased or insect-infected plants may appear gray.

The telecommunications payload (Ku-, X-, and S-band equipment) provides the Landsat D spacecraft with the capability of transmitting TM and MSS instrument data to both TDRS and selected ground-based recipients. The image data collected is returned to the ground processing system via two paths. The first, and primary path, is via a Ku-band (15.003 GHz) link through the Tracking and Data Relay Satellite System (TDRSS). TM data is transmitted at 85 Mbps, with MSS data at 15 Mbps, and both are recorded on high density tape at the TDRSS receiving site at White Sands, New Mexico. The data is then relayed via a domestic communications satellite (DOMSAT). To effectively use the DOMSAT bandwidth, the TM data rate is reduced by one half to 42.5 Mbps, and the MSS rate is doubled to 30 Mbps. The data, at these rates, is recorded in the Landsat D data management system (DMS) located at the Goddard Space Flight Center (GSFC). A DOMSAT is also used to transmit processed MSS data from GSFC to the United States Department of the Interior's Earth Resources Observation System (EROS) data center at Sioux Falls, South Dakota. Figure 1 illustrates the Landsat D system and its major interfaces.

The second data path from the Landsat D satellite is direct links, at X-band (8.212 GHz) for TM and MSS data and at S-band (2.187 GHz) for MSS data, to GSFC. This data is recorded in the DMS at real-time rates: 85 Mbps for TM and 15 Mbps for MSS. The X- and S-band links are also used for direct readout of image data to foreign ground stations.

The Data Management System at GSFC satisfies the functions of data quality check, estimation of cloud cover, application of radiometric corrections, and generation of geometric correction coefficients. Selected images have the geometric corrections applied and are converted into products for users. All data is sent to Sioux Falls for further distribution to the general public.

2. Telecommunications Subsystem Description

The Landsat D communications subsystem consists of the components necessary to accept digital data signals from the MSS and TM sensors, modulate the selected data outputs onto the appropriate RF carriers, amplify the RF signals, and transmit each RF signal from its dedicated antenna to designated receiving terminals. It further provides the spacecraft with the capability of acquiring and tracking TDRSS forward link emissions at Ku-band.

The telecommunications payload is comprised of a wideband module, an RF compartment, and a gimbal drive assembly (see Figure 2). The wideband module attaches to the instrument module and provides mounting for the S-band shaped beam antennas and the X-band antenna. This module contains the X-band transmission link equipment, signal and power control electronics, gimbal drive electronics, the modulator portion of the Ku-band transmission link equipment, and the autotrack receiver (see Figure 3).

The RF compartment contains the Ku-/S-band antenna and the switching, diplexing, upconversion, and power amplification components (TWTAs), and the downconverter for the autotrack system (see Figure 4). The RF compartment and Ku-/S-band antenna are attached to the spacecraft articulated

---

[*] Assistant Program Manager, Landsat D Design and Development

Copyright © American Institute of Aeronautics and Astronautics, Inc., 1980. All rights reserved.

boom by means of the gimbal drive assembly, a two-axis rotary mechanism consisting of an elevation-over-azimuth mount (Figure 5). A simplified functional block diagram of the Landsat D telecommunications subsystem is shown in Figure 6.

Unbalanced quadriphase shift keying (UQPSK) modulation is utilized for transmission of TM and MSS data at both Ku- and X-bands.* For the Ku-band transmission link via TDRS, the UQPSK signal is properly upconverted and amplified by a 22-watt traveling wave-tube amplifier (TWTA; see Figure 7) prior to being transmitted via the Ku-/S-band antenna. The Ku-/S-band antenna (see Figure 8) is composed of a 70-inch diameter cassegrain reflector, a five-horn Ku-band tracking feed, a 12-inch dichroic subreflector (resonant at Ku-band, transparent at S-band), and a focal point S-band feed. This Ku-/S-band steerable antenna also receives the forward link signal from TDRS by way of its five-horn feed. The center horn is utilized for the primary transmit/receive function, while the four small monopulse horn feeds surrounding it provide the autotrack capability. The closed-loop monopulse tracking system accepts the autotrack signal and drives the gimbal motors to position the antenna in a direction which minimizes the angular error between the antenna boresight and the TDRS signal line-of-sight.

In addition to allowing transmission to and reception from TDRS at Ku-band, the Ku-/S-band antenna also contains an S-band feed which provides a high-gain antenna receive/transmit capability for S-band command reception and telemetry data transmission. Command/telemetry functions are performed onboard the spacecraft by the Communications and Data Handling (C&DH) module.

For the X-band direct-access downlink, modulated signals from the UQPSK modulators are upconverted and amplified by means of a 44-watt TWTA prior to transmission to GSFC or desired foreign users. The TWTA drives a 23-inch shaped-beam X-band antenna (Figure 9) which provides essentially constant EIRP over the illuminated surface of the earth.

The balance of this paper will concentrate primarily on the Ku-band links through TDRS utilized by Landsat D for transmission of its collected imaging data and reception of ground signals. These links constitute the Ku-band return and forward channels, respectively.

3. Ku-Band Forward Link

The TDRSS ground terminal at White Sands transmits a composite signal which contains, among others, the Landsat D K-band single access (KSA) signal. This composite signal is received at the TDRS by the 2.0-meter space/ground link (SGL) antenna (Figure 10). The TDRS K-band receiver (Figure 10) translates the uplink signal to an intermediate frequency, amplifies it, and sends it to the forward processor assembly. The forward processor assembly filters and demultiplexes this composite signal into the separate signals that were multiplexed at the ground terminal. The Landsat D KSA signal is sent at an intermediate frequency (IF) from the forward processor to the single-access antenna compartment where a KSA upconverter converts it to Ku-band. A 1.5-watt TWTA amplifies this signal for transmission to the Landsat D spacecraft via a 4.9-meter steerable antenna.**

The Ku-band forward link signal (3 megachips/sec PN spread spectrum) from the TDRS is received at the Landsat D spacecraft by the five-horn feed assembly of the 70-inch Ku-/S-band steerable antenna. Four small monopulse horn feeds, which surround the sum channel feed horn, and the autotrack comparator synthesize the azimuth and elevation difference signals. These signals are proportional to the angular error between the antenna boresight and the received TDRS signal line of sight. They are biphase modulated (A/T combiner; Figure 11), time multiplexed, and added to the reference sum channel received signal by means of a 10 dB coupler to generate the amplitude-modulated autotrack signal. As shown in the block diagram of Figure 12, the sum channel signal is fed to the downconverter via the diplexer/filter which provides receive band selection in addition to attenuation of the receiver image band and Ku-band TWTA broadband noise.

The composite single channel AM autotrack signal is downconverted and routed through the cable wrap assembly and down the boom to the autotrack receiver (Figure 13) located in the wideband module. Coax switches provide cross-strap redundancy between the downconverters and the autotrack receivers. The signal is amplified by an automatic gain-controlled IF amplifier prior to square-law detection to remove the amplitude modulation representing the normalized azimuth and elevation error signals. Separation of the azimuth and elevation error signals is accomplished by a demultiplexer contained within the autotrack receiver. The demultiplexing waveform which separates both these signals is identical to, and synchronized with, the multiplexing waveform. A low frequency filtered dc signal derived from the AGC control circuit provides signal strength indication. The two pointing error signals, together with the signal strength signal, are digitized by the Remote Interface Units (RIUs) and provided to the onboard computer via the spacecraft multiplex data bus. The signal strength signal is processed by the onboard computer to activate the autotrack mode and is also telemetered to the TDRSS ground station via the C&DH subsystem to verify that the TDRS-to-Landsat link has been established.

The autotrack receiver, antenna, gimbal drive assembly, and onboard computer form a closed loop monopulse tracking system. The azimuth and elevation error signals are processed by the onboard computer to generate appropriate command signals which, in turn, are fed back through the RIUs to the gimbal drive assembly. In response to these signals, the gimbal motors position the antenna in a direction which minimizes the angular error between the antenna boresight and the TDRS signal line-of-sight.

---

*The unbalanced nature of this modulation scheme results from using the in-phase (I) channel for transmission of TM data (85 Mbps), while the quadrature (Q) channel accommodates the MSS data (15 Mbps). A 4 to 1 power ratio in favor of the I-channel is maintained.

**Details of the TDRS forward link communications payload are contained in Reference (1).

In addition to the autotrack mode of operation, the steerable high gain antenna also operates in a program track mode. Position feedback to the onboard computer via the RIUs is provided by azimuth and elevation gimbal resolvers.

4. Ku-Band Return Link

The collected earth imaging data (TM and MSS) is first routed to the digital switching unit (Figure 14) in the wideband module where it is reclocked by means of associated clock signals prior to mode selection. Independent mode selection is provided for both X-band and Ku-band operation, activating one of fifteen data output combinations for the two links. Mode selection is implemented in a manner which precludes ground demodulator data dropouts and violations of power flux density limitations. The outputs from the digital switching unit, consisting of differentially encoded TM and MSS data on separate in-phase (I) and quadrature phase (Q) lines, are provided as inputs to unbalanced quadrature phase-shift keyed (UPQSK) modulators. The UQPSK modulators modulate the selected TM and MSS data onto S-band RF carrier references.

For the Ku-band transmission link via TDRS, the UQPSK modulated S-band signal is routed up the boom on redundant coaxial cables and through the cable wrap assembly to redundant Ku-band upconverters in the RF compartment (Figure 15). The upconverters, driven by frequency sources in the wideband module, translate the modulated S-band signal to the Ku-band. The upconverter output is amplified by one of two redundant 22-watt traveling wave-tube amplifiers (TWTA) prior to being transmitted via the diplexer/filter and Ku-/S-band antenna.

The lowpass filter portion of the diplexer/filter attenuates the TWTA second harmonic to a level compatible with radio astronomy power flux density constraints. A transmit bandpass filter, also part of the diplexer/filter, attenuates TWTA regenerated signal components and tube broadband noise to a level which is not only compliant with power flux density requirements, but is also below that required to degrade the autotrack system performance. The output from the diplexer/filter drives the 70-inch high-gain antenna.

The Landsat D K-band single access (KSA) return signal is received at the TDRS by the 4.9-meter antenna. This signal is isolated from the transmit signal by a diplexer, amplified by a parametric amplifier, downconverted to an intermediate frequency, and sent to the return processor assembly (Figure 16). The return processor assembly accepts the incoming Landsat D KSA signal and performs either of the following functions: 1) multiplexes this signal with other incoming S-band signals, the TDRS telemetry and the downlink pilot tone, prior to upconversion or 2) routes this signal to a separate (dedicated) K-band upconverter. Signal transmission to the White Sands ground station is accomplished in either case by means of a 27-watt TWTA and a 2.0-meter antenna. *

5. Performance Requirements and System Capabilities

The overall performance requirements for the Landsat D Ku-band telecommunications equipment return and foward links are contained in Tables 1 and 2, respectively. The expected flight performance for each of the link parameters, based on finalized breadboard/development model tests and detailed analyses performed as part of the Landsat D program, is also included. A more detailed evaluation of payload performance and presentation of test results is contained in Reference (2).

6. Conclusions

This paper has described the design features, operational characteristics, and performance requirements associated with the Landsat D telecommunications subsystem. The communications payload depicted herein is projected to meet or exceed all performance requirements. Moreover, it is expected to provide greater than 5 dB margins for both the Ku-band downlink through TDRS and the X-band direct access downlink for transmission of either TM or MSS data.

Breadboard testing of units has provided initial verification of the excellent performance expected of the Landsat D communications hardware. This data, combined with TDRS channel test data (3) and computer simulation results now available (4), support the claim that extremely high quality earth-imaging data will be collected throughout the 1980's via the Landsat D — TDRS information system.

References

(1) H. B. Poza, "TDRSS Telecommunications Payload: An Overview," IEEE Trans. on Aerospace and Electronic Systems, May 1979.

(2) "Landsat D Wideband Communications Subsystem Detailed Design Review," TRW, Report LD-79-1-1600, August 1979.

(3) "TDRSS Space Segment Critical Design Review," TRW, Report 29000-200-013, August 1978.

(4) H. B. Poza, H. L. Berger and D. M. Berstein, "A Wideband Link Simulation Model," Int. Journal of Computers and Electrical Eng.," July 1978.

---

* Details of the TDRS Ku-band return link communications payload are contained in Reference (1).

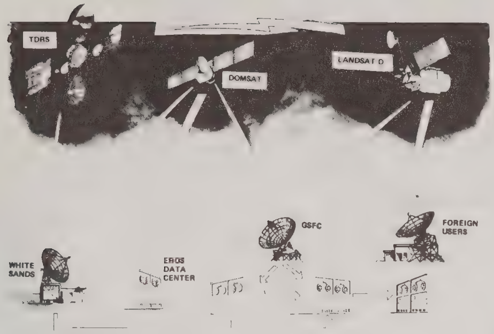
TDRS
DOMSAT
LANDSAT D
WHITE SANDS
EROS DATA CENTER
GSFC
FOREIGN USERS

Figure 1. Landsat D — TDRSS Information System

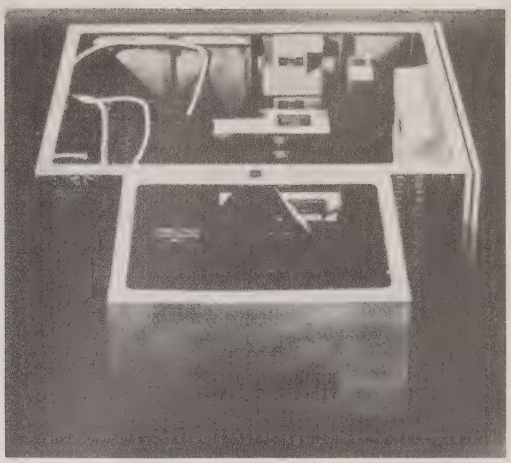

Figure 3. Wideband Module Mockup

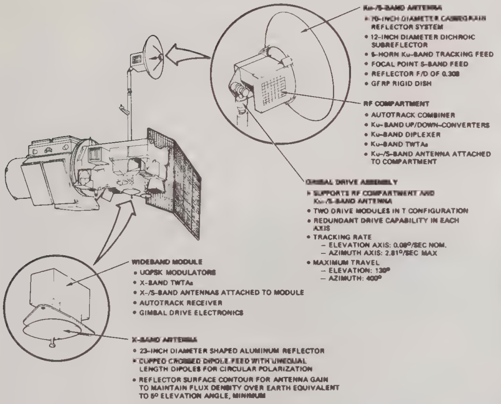
Ku-/S-BAND ANTENNA
• 70-INCH DIAMETER CASSEGRAIN REFLECTOR SYSTEM
• 12-INCH DIAMETER DICHROIC SUBREFLECTOR
• 5-HORN Ku-BAND TRACKING FEED
• FOCAL POINT S-BAND FEED
• REFLECTOR F/D OF 0.308
• GFRP RIGID DISH
RF COMPARTMENT
• AUTOTRACK COMBINER
• Ku-BAND UP/DOWN-CONVERTERS
• Ku-BAND DIPLEXER
• Ku-BAND TWTAs
• Ku-/S-BAND ANTENNA ATTACHED TO COMPARTMENT
GIMBAL DRIVE ASSEMBLY
• SUPPORTS RF COMPARTMENT AND Ku-/S-BAND ANTENNA
• TWO DRIVE MODULES IN T CONFIGURATION
• REDUNDANT DRIVE CAPABILITY IN EACH AXIS
• TRACKING RATE
– ELEVATION AXIS: 0.08°/SEC NOM.
– AZIMUTH AXIS: 2.81°/SEC MAX
• MAXIMUM TRAVEL
– ELEVATION: 130°
– AZIMUTH: 400°
WIDEBAND MODULE
• UQPSK MODULATORS
• X-BAND TWTAs
• X-/S-BAND ANTENNAS ATTACHED TO MODULE
• AUTOTRACK RECEIVER
• GIMBAL DRIVE ELECTRONICS
X-BAND ANTENNA
• 23-INCH DIAMETER SHAPED ALUMINUM REFLECTOR
• CUPPED CROSSED DIPOLE FEED WITH UNEQUAL LENGTH DIPOLES FOR CIRCULAR POLARIZATION
• REFLECTOR SURFACE CONTOUR FOR ANTENNA GAIN TO MAINTAIN FLUX DENSITY OVER EARTH EQUIVALENT TO 5° ELEVATION ANGLE, MINIMUM

Figure 2. Landsat D Flight Segment Configuration

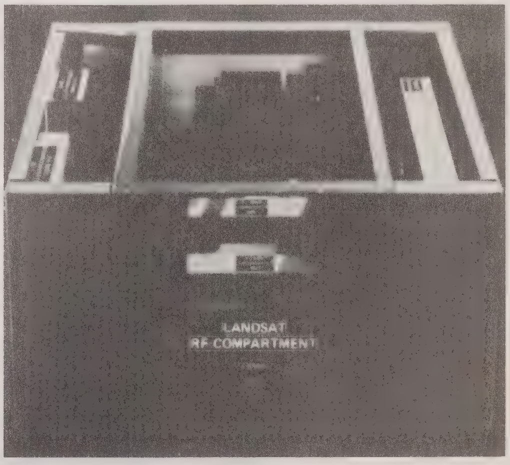
LANDSAT
RF COMPARTMENT

Figure 4. RF Compartment Mockup

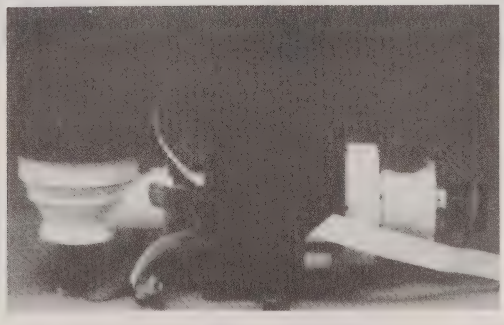

Figure 5. Gimbal Drive Assembly

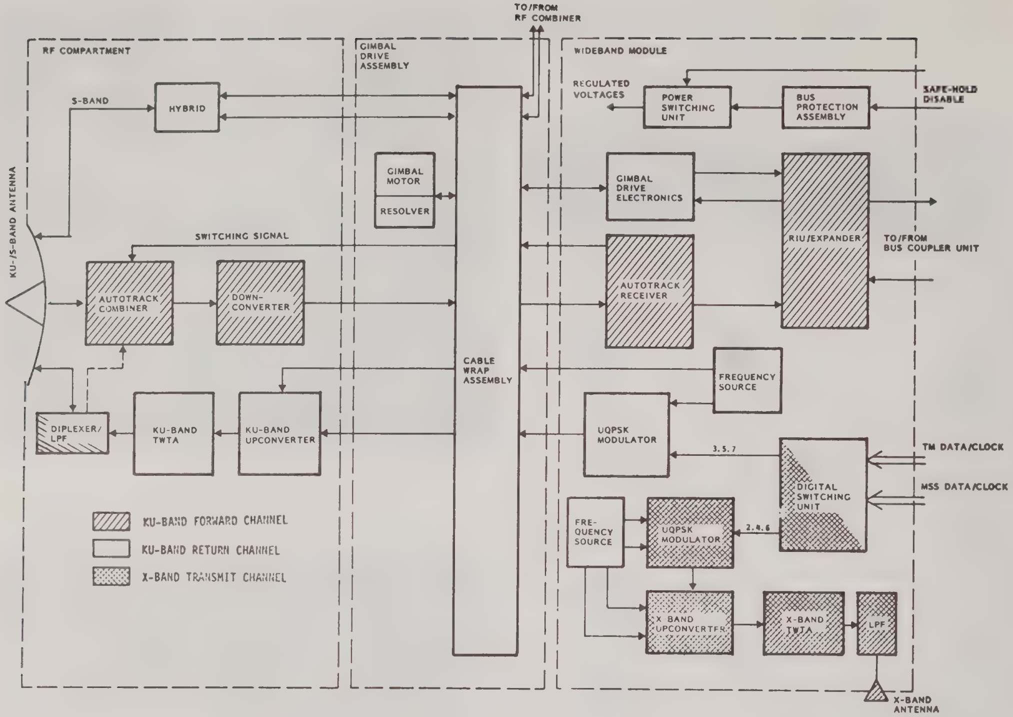
TO/FROM RF COMBINER
RF COMPARTMENT
GIMBAL DRIVE ASSEMBLY
WIDEBAND MODULE
S-BAND
HYBRID
REGULATED VOLTAGES
POWER SWITCHING UNIT
BUS PROTECTION ASSEMBLY
SAFE-HOLD DISABLE
KU-/S-BAND ANTENNA
GIMBAL MOTOR
RESOLVER
GIMBAL DRIVE ELECTRONICS
RIU/EXPANDER
TO/FROM BUS COUPLER UNIT
SWITCHING SIGNAL
AUTOTRACK COMBINER
DOWN-CONVERTER
AUTOTRACK RECEIVER
CABLE WRAP ASSEMBLY
FREQUENCY SOURCE
DIPLEXER/LPF
KU-BAND TWTA
KU-BAND UPCONVERTER
UQPSK MODULATOR
3, 5, 7
TM DATA/CLOCK
DIGITAL SWITCHING UNIT
MSS DATA/CLOCK
FRE-QUENCY SOURCE
UQPSK MODULATOR
2, 4, 6
X BAND UPCONVERTER
X-BAND TWTA
LPF
X-BAND ANTENNA
KU-BAND FORWARD CHANNEL
KU-BAND RETURN CHANNEL
X-BAND TRANSMIT CHANNEL

Figure 6. Landsat D Telecommunications Subsystem

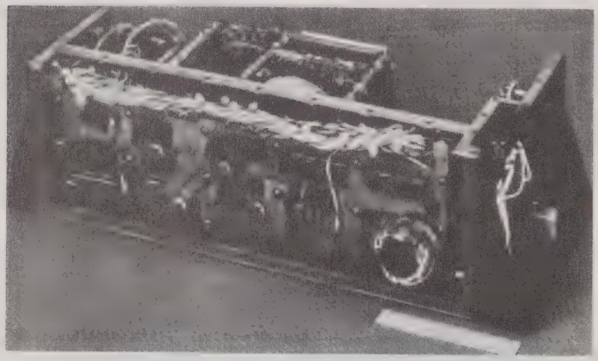

Figure 7. Ku-Band TWTA

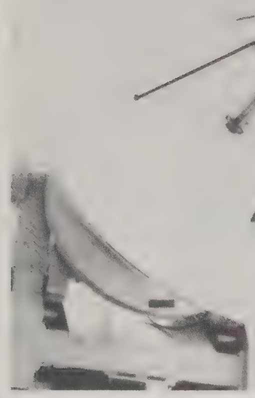

Figure 8. Ku-/S-Band Antenna Assembly

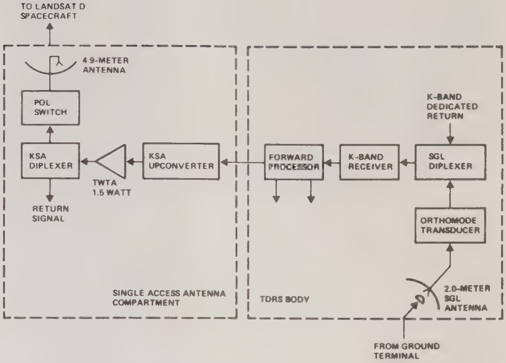
TO LANDSAT D SPACECRAFT
4.9-METER ANTENNA
POL SWITCH
KSA DIPLEXER
TWTA 1.5 WATT
KSA UPCONVERTER
RETURN SIGNAL
SINGLE ACCESS ANTENNA COMPARTMENT
FORWARD PROCESSOR
K-BAND RECEIVER
SGL DIPLEXER
K-BAND DEDICATED RETURN
ORTHOMODE TRANSDUCER
TDRS BODY
2.0-METER SGL ANTENNA
FROM GROUND TERMINAL

Figure 10. Forward Link Signal Flow Through TDRS

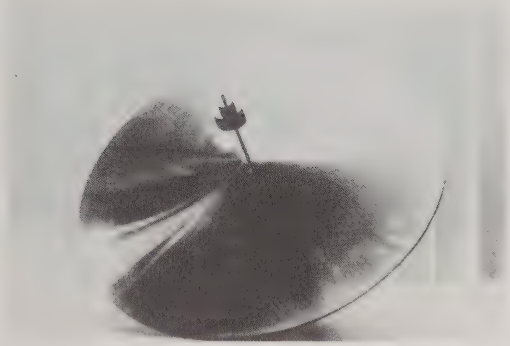

Figure 9. X-Band Shaped-Beam Antenna

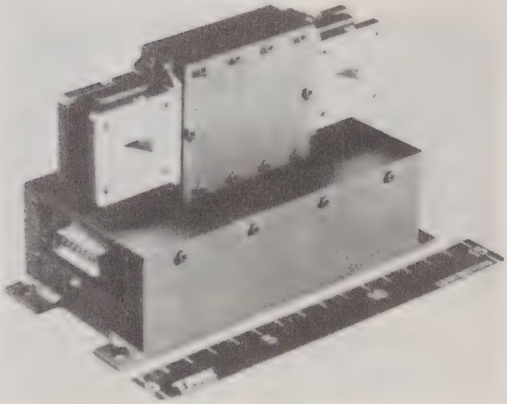

Figure 11. Autotrack Combiner

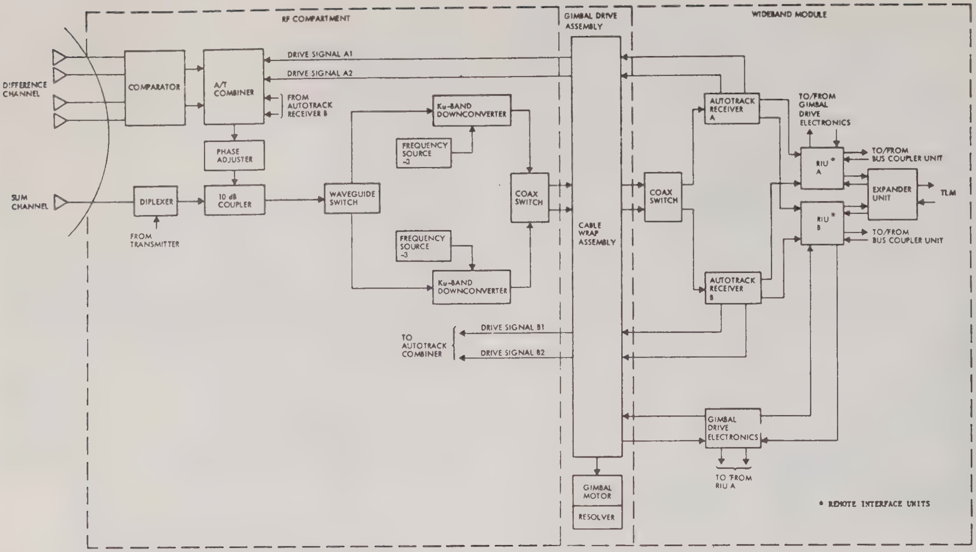
RF COMPARTMENT
GIMBAL DRIVE ASSEMBLY
WIDEBAND MODULE
DIFFERENCE CHANNEL
COMPARATOR
A/T COMBINER
DRIVE SIGNAL A1
DRIVE SIGNAL A2
FROM AUTOTRACK RECEIVER B
Ku-BAND DOWNCONVERTER
FREQUENCY SOURCE -3
PHASE ADJUSTER
SUM CHANNEL
DIPLEXER
10 dB COUPLER
WAVEGUIDE SWITCH
FROM TRANSMITTER
FREQUENCY SOURCE -3
Ku-BAND DOWNCONVERTER
COAX SWITCH
CABLE WRAP ASSEMBLY
COAX SWITCH
AUTOTRACK RECEIVER A
TO/FROM GIMBAL DRIVE ELECTRONICS
RIU * A
TO/FROM BUS COUPLER UNIT
EXPANDER UNIT
TLM
RIU * B
TO/FROM BUS COUPLER UNIT
AUTOTRACK RECEIVER B
TO AUTOTRACK COMBINER
DRIVE SIGNAL B1
DRIVE SIGNAL B2
GIMBAL DRIVE ELECTRONICS
TO FROM RIU A
GIMBAL MOTOR
RESOLVER
* REMOTE INTERFACE UNITS

Figure 12. Landsat D Ku-Band Autotrack System Block Diagram

Figure 13. Autotrack Receiver Development Model

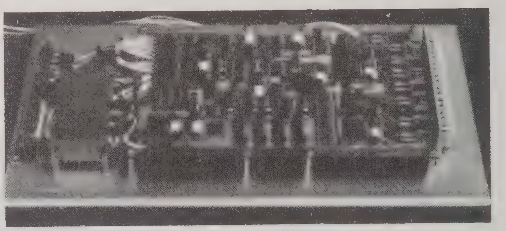

Figure 14. Digital Switching Unit Development Model

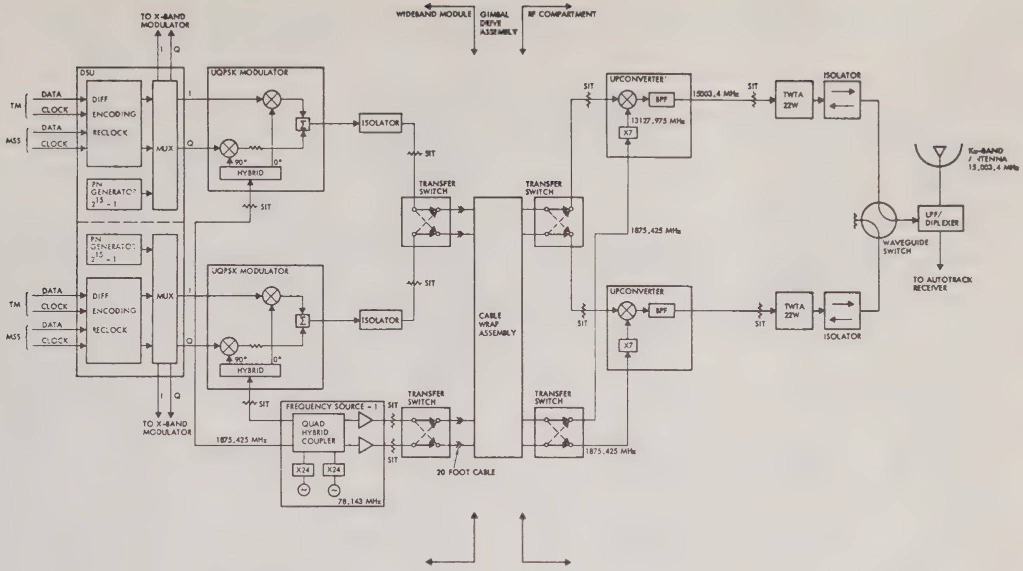
TO X-BAND MODULATOR
I
Q
WIDEBAND MODULE
GIMBAL DRIVE ASSEMBLY
RF COMPARTMENT
DSU
TM
DATA
CLOCK
MSS
DATA
CLOCK
DIFF ENCODING RECLOCK
PN GENERATOR $2^{15}-1$
MUX
UQPSK MODULATOR
90°
0°
HYBRID
Σ
ISOLATOR
SIT
TRANSFER SWITCH
CABLE WRAP ASSEMBLY
UPCONVERTER
BPF
X7
13127.975 MHz
15003.4 MHz
1875.425 MHz
TWTA 22W
ISOLATOR
Ku-BAND ANTENNA 15,003.4 MHz
LPF/DIPLEXER
WAVEGUIDE SWITCH
TO AUTOTRACK RECEIVER
FREQUENCY SOURCE - 1
QUAD HYBRID COUPLER
X24
78.143 MHz
20 FOOT CABLE

Figure 15. Landsat D Ku-Band Return Channel Block Diagram

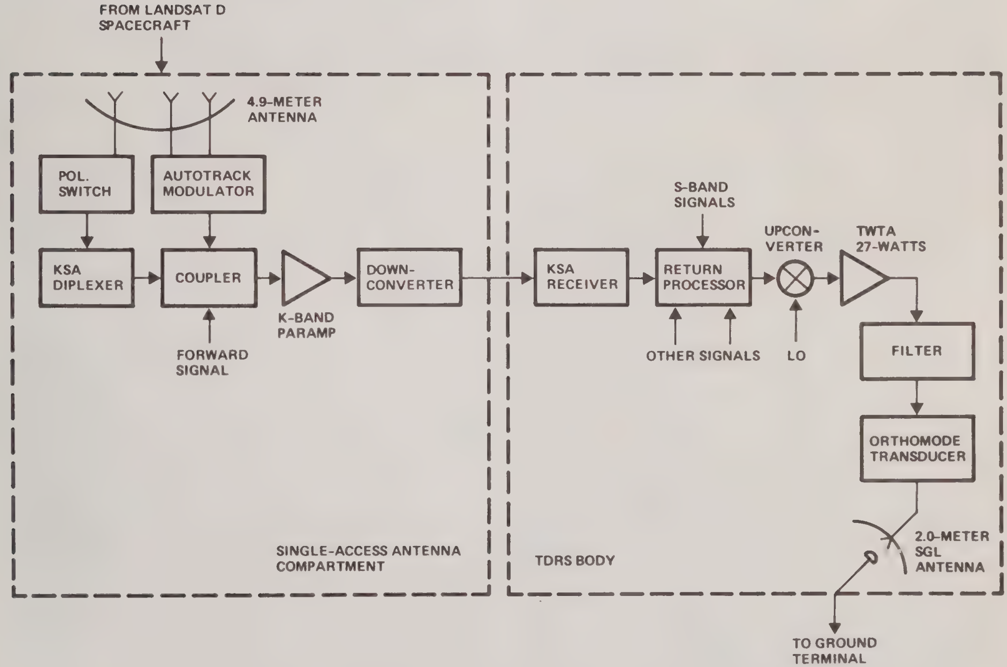
FROM LANDSAT D SPACECRAFT
4.9-METER ANTENNA
POL. SWITCH
AUTOTRACK MODULATOR
KSA DIPLEXER
COUPLER
FORWARD SIGNAL
K-BAND PARAMP
DOWN-CONVERTER
SINGLE-ACCESS ANTENNA COMPARTMENT
KSA RECEIVER
S-BAND SIGNALS
RETURN PROCESSOR
OTHER SIGNALS
UPCON-VERTER
LO
TWTA 27-WATTS
FILTER
ORTHOMODE TRANSDUCER
2.0-METER SGL ANTENNA
TDRS BODY
TO GROUND TERMINAL

Figure 16. Return Link Signal Flow Through TDRS

Table 1. Landsat D Ku-Band Return Channel Requirements vs Capabilities

PARAMETER	REQUIREMENT	ESTIMATED CAPABILITY
TRANSMIT FREQUENCY	15003.4 ±0.76 MHZ	15003.4 ±0.2 MHZ
POLARIZATION	RHCP	RHCP
ANTENNA GAIN	≥46.2 DBI	46.9 DBI
AXIAL RATIO	≤1.0 DB	<1.2 DB
LINK MARGIN (BER 10^{-6})	≥4.7 DB	TM 5.2 DB, MSS 6.9 DB
GAIN FLATNESS	≤±0.3 DB OVER 170 MHZ	±0.18 DB OVER 170 MHZ
PHASE LINEARITY	≤±3 DEG OVER 170 MHZ	±3.1 DEG OVER 170 MHZ
GAIN SLOPE	≤0.1 DB/MHZ	0.08 DB/MHZ
AM-TO-PM	≤12 DEG/DB	6.7 DEG/DB
INCIDENTAL AM	≤5%	<5%
SPURIOUS PM	≤2 DEG RMS	<2 DEG RMS
SPURIOUS OUTPUT		
• 170 MHZ	≤-30 DBC	<-35 DBC
• 170 TO 225 MHZ	≤-15 DBC	<-22 DBC
• 225 TO 450 MHZ	≤-25 DBC	<-31 DBC
• 450 MHZ	≤-30 DBC	<-35 DBC
PHASE NOISE		
• 1 TO 10 HZ	≤15 DEG RMS	<14.3 DEG RMS
• 10 TO 100 HZ	≤7.5 DEG RMS	<7.1 DEG RMS
• 0.1 TO 1 KHZ	≤2 DEG RMS	<2.0 DEG RMS
• 1 K TO 150 MHZ	≤2 DEG RMS	<2.0 DEG RMS
FREQUENCY STABILITY		
• 1 SEC AVE	$\pm 3 \times 10^{-9}$	$\pm 1 \times 10^{-9}$
• 5 HR AVE	$\pm 1 \times 10^{-7}$	$\pm 5 \times 10^{-8}$
• 48 HR AVE	$\pm 3 \times 10^{-7}$	$\pm 1 \times 10^{-7}$
• 3 YEAR	NONE	$\pm 4 \times 10^{-6}$
EIRP VARIATION	≤12 DB	3 DB
EIRP VARIATION RATE	≤10 DB/SEC	2 DB/SEC
MAX EIRP	≤60 DBW	58.6 DBW
MIN EIRP	≥30 DBW	>53.0 DBW
DATA TRANSITION INDUCED PM	≤6 DEG RMS	5.8 DEG RMS
PHASE IMBALANCE	≤±3 DEG	±1.5 DEG
GAIN IMBALANCE	≤±0.25 DB	±0.15 DB
DATA SYMMETRY	≤±3%	±2.5%
DATA TRANSITION TIME		
• I-CHANNEL	≤2.3 NSEC	2.0 NSEC
• Q-CHANNEL	≤3.3 NSEC	<2.0 NSEC

Table 2. Landsat D Ku-Band Forward (Autotrack) Channel Requirements vs Capabilities

PARAMETER	REQUIREMENT	ESTIMATED CAPABILITY
RECEIVE FREQUENCY	13.775 ±0.7 MHZ	13.775 ±0.7 MHZ
POLARIZATION	RHCP	RHCP
ANTENNA GAIN	≥44.7 DBI	45.5 DBI
AXIAL RATIO	≤1.0 DB	<1.2 DB
DYNAMIC RANGE	-163 TO -158 DBWI	-168 TO -153 DBWI
PULL-IN RANGE	≥0.4 DEG	0.45 DEG
POINTING ERROR (A/T MODE)	≤0.1 DEG	0.08 DEG
A/T SCALE FACTOR (MINIMUM)	≥0.087 V/V/DEG	0.11 V/V/DEG
A/T SCALE FACTOR VARIATION	≤12.0 DB	9.6 DB
Σ-CHANNEL TO MECHANICAL Z-AXIS ALIGNMENT	0.08 DEG (3σ TIME VARYING)	<0.08 DEG
A/T NULL TO Σ-CHANNEL ELECTRICAL ALIGNMENT	0.02 DEG (3σ TIME VARYING)	<0.02 DEG
MINIMUM SCALE FACTOR SIGNAL STRENGTH	≥1.0 DB/V	3.0 DB/V
A/T ERROR VOLTAGE SNR AT PULL-IN	≥35.0 DB WITHIN 1 HZ	40.0 DB WITHIN 1 HZ
CHANNEL GAIN STABILITY	≤±0.4 DB	±0.25 DB
RMS A/T NOISE JITTER AT BORESIGHT	≤0.002 DEG WITHIN 1 HZ	0.0015 DEG WITHIN 1 HZ
SIGNAL STRENGTH SNR	≥60 DB WITHIN 1 HZ	70 DB WITHIN 1 HZ

80-0529

TIROS-N - THE OPERATIONAL ENVIRONMENTAL SATELLITE OF THE 80'S

A. Schnapf
Manager, Satellite Program Support
RCA Astro-Electronics
P.O. Box 800
Princeton, New Jersey 08540

Abstract

TIROS-N, the 3rd-generation operational environmental satellite, was placed into orbit in October 1978. It is the first of eight satellites in this series that will provide service between 1978 and 1985. TIROS-N provides operational data products to the U.S. and many countries around the world through its multifrequency telecommunication and data handling and processing systems. The unique design of the spacecraft permits growth for future missions. Spacecraft 6, 7, and 8 in this series are being designed for additional payload. These Advanced TIROS-N spacecraft will carry a search-and-rescue system that will permit the spacecraft to pick up distress signals from downed aircraft or ships in distress, a Solar Backscatter UV Radiometer to measure the ozone about the planet, and an Earth Radiation Budget Experiment to measure the radiation input and loss to the planet. This paper briefly describes the TIROS-N and Advanced TIROS-N spacecraft and their operational products.

Introduction

The TIROS satellite was orbited 20 years ago on April 1, 1960 to initiate a continuing program of polar-orbiting satellites that are serving the needs of this country and the world at large. Figure 1 depicts the TIROS evolution.

TIROS-N, the first satellite of the third-generation operational environmental satellite series, was placed into orbit in October 1978. NOAA-6, the second satellite in this series, was launched in June 1979 to complement TIROS-N. These two satellites and six additional satellites in this series will provide service between 1978 and 1985. Satellites of the TIROS-N series are in sun-synchronous, near-polar orbits. Through their multifrequency telecommunications and data handling and processing systems, they provide operational data products to the U.S. and many countries around the world.

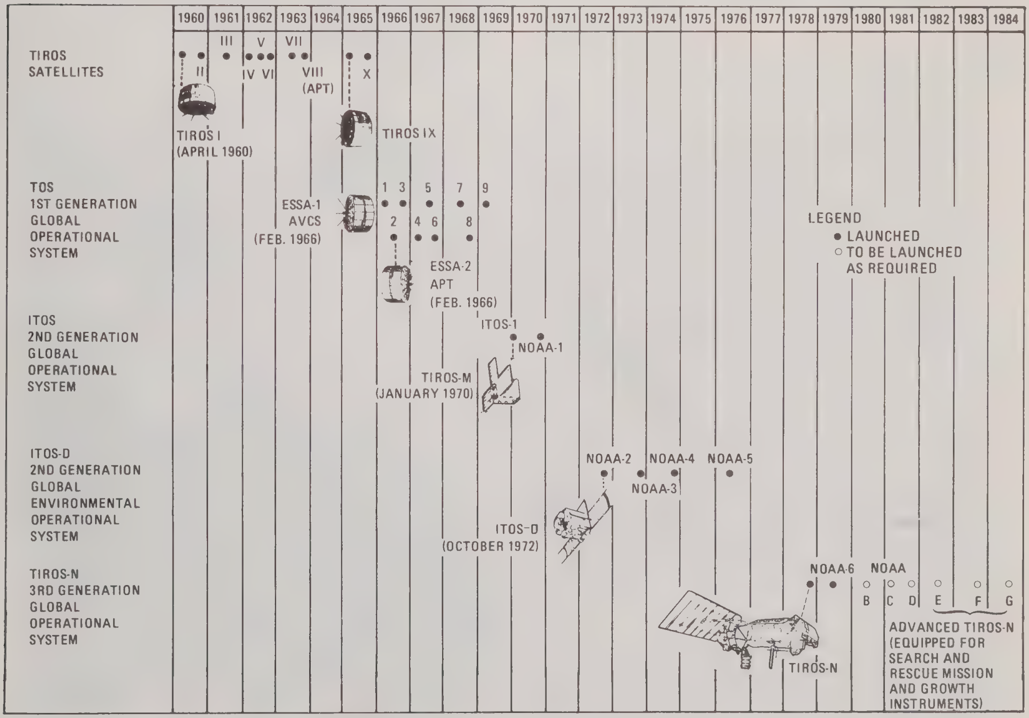

Figure 1. Evolution of TIROS/ITOS/NOAA Meteorological Satellites

Released to AIAA to publish in all forms.

In fulfilling the requirements of the National Oceanic and Atmospheric Administration (NOAA) and its commitment to provide worldwide data, the TIROS-N satellite system, shown in Figure 2, provides real-time direct readout data as well as globally-stored data for playback to the primary U.S. CDA (Command and Data Acquisition) stations. This data is used for meteorological prediction and warning, oceanographic and hydrologic service, and space environment monitoring and prediction.

Spacecraft of the TIROS-N series are equipped with instruments that provide data on temperature and humidity in the Earth's atmosphere, surface temperature, cloud cover, water-ice moisture boundaries, and the proton and electron flux in the vicinity of Earth. The spacecraft's data collection system permits the reception, processing, and transmission of data from fixed and floating platforms, buoys, and balloons throughout the planet.

The unique design of the TIROS-N spacecraft permits growth for future missions. Spacecraft 6, 7, and 8 in this series are undergoing design modifications to add three additional instruments to the payload. These advanced TIROS-N spacecraft will carry a search-and-rescue system that will permit the spacecraft to pick up distress signals from downed aircraft or ships in distress. The emergency signals will be relayed through a repeater system to the emergency rescue forces or will be processed to indicate the location of downed aircraft and then relayed. Additional payload will consist of a Solar Backscatter Ultraviolet Radiometer to measure the ozone about the planet and an Earth Radiation Budget Experiment to measure the radiation input and loss to the planet.

The National Environmental Satellite Service (NESS) of NOAA operates a network of polar satellites (TIROS-N series and geostationary satellites (GOES series) to acquire the data needed to generate the output products for which NOAA is responsible. The two satellite systems (polar and geostationary) are complementary, each uniquely qualified to meet its particular mission requirements. The TIROS-N series of satellites provides the global environmental data required by NOAA. The TIROS-N system also supports U.S. international programs by providing data for the Global Weather Experiment and the World Weather Watch. Additionally, the direct readout of data from TIROS-N throughout its orbital flight permits over 800 small ground stations in 120 countries around the world to receive satellite environmental data in real time.

The first TIROS-N satellite was funded by NASA; subsequent satellites in that series are funded by NOAA. The NASA Goddard Space Flight Center manages the program for designing and building these satellites.

Spacecraft Description

Instrument Payload

The primary environmental instruments carried by the TIROS-N/NOAA satellites are:

(1) The TIROS Operational Vertical Sounder (TOVS), a three-instrument group consisting of:
    (a) The High-Resolution Infrared Sounder (HIRS/2);
    (b) The Stratospheric Sounding Unit (SSU); and
    (c) The Microwave Sounding Unit (MSU).
    Data from the TOVS is available locally as a part of the HRPT (High-Resolution Picture Transmission) and the spacecraft beacon transmission.

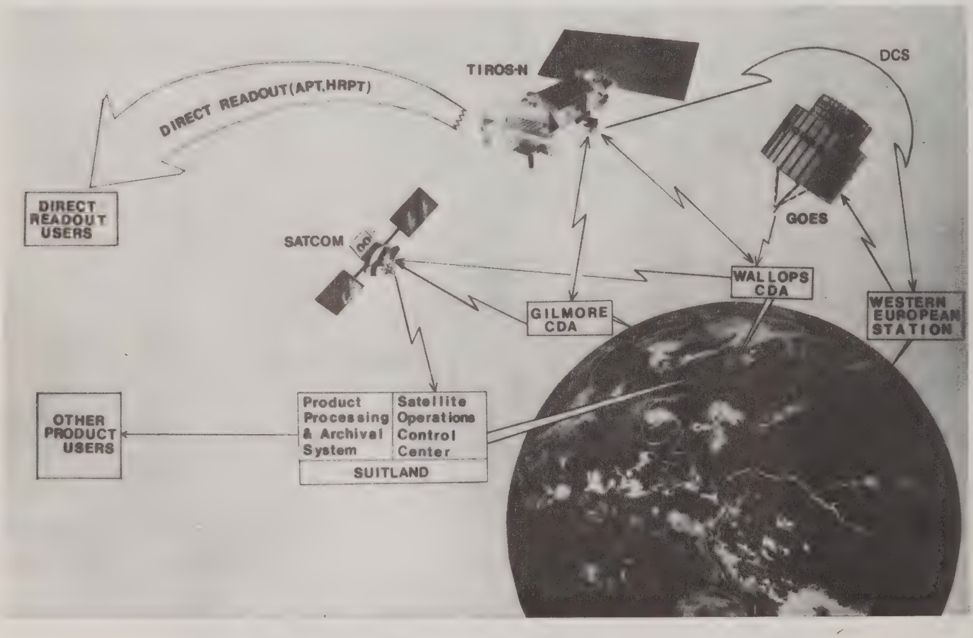

Figure 2. TIROS-N Operational System Network

(2) The Advanced Very High Resolution Radiometer (AVHRR);

(3) The Space Environment Monitor (SEM); and

(4) The Data Collection and Location System (DCS).

The High Resolution Infrared Radiation Sounder. The HIRS/2 is a 20-channel instrument that makes measurements primarily in the infrared region of the spectrum. The instrument provides data that permits calculation of (1) temperature profile from the surface to 10 mb; (2) water vapor content in three layers in the atmosphere; and (3) total ozone content. The design is based on the HIRS instrument flown on the Nimbus satellite.

The Stratospheric Sounding Unit. The SSU employs a selective absorption technique to make measurements in three channels. The spectral characteristics of each channel are determined by the pressure in a carbon dioxide gas cell in the optical path. The amount of carbon dioxide in the cells determines the height of the weighting function peaks in the atmosphere. This unit was built by the British Meteorological office in the U.K.

The Microwave Sounding Unit. The MSU is a 4-channel Dicke radiometer, which makes passive measurements in the 5.5-mm oxygen band. This instrument, unlike those making measurements in the infrared region, is little affected by clouds.

The Advanced Very High Resolution Radiometer. The AVHRR is a 4-channel (5 channels on later satellites of this series) scanning radiometer sensitive in the visible, near infrared, and infrared window regions. This instrument provides data for central processing, APT (Automatic Picture Transmission), and HRPT (High-Resolution Picture Transmission) outputs. HRPT data (all spectral regions) is transmitted at full resolution (1.1 km); APT (two selectable spectral regions) has reduced resolution (4 km).

The Space Environment Monitor. The SEM consists of three separate instruments and a data processing unit. The instruments are:

(1) The Total Energy Detector (TED) which measures a broad range of energetic particles from 0.3 keV to 20 keV in 11 bands.

(2) The Medium Energy Proton and Electron Detector (MEPED), which senses protons, electrons, and ions with energies from 30 keV to several tens of MeV.

(3) The High Energy Proton and Alpha Detector (HEPAD), which senses protons and alphas from a few hundred MeV up through relativistic particles above 840 MeV.

The data from the SEM instruments are included in the HRPT and beacon transmissions.

The Data Collection and Location System. The DCS is a random-access system that provides a means of obtaining environmental data such as temperature, pressure, altitude, etc. from fixed and/or free-floating terrestrial and atmospheric platforms. The environmental data messages sent by the platforms vary in length depending on the type of platform and its purpose. The data from each platform contain identification as well as environmental measurements. When necessary, location of the platforms may be computed by differential doppler techniques using data obtained from the measurement of platform carrier frequency as received on the satellite. When several measurements are received during a given contact with a platform, location can be determined. Accuracy of location depends upon the number of messages received from the platform. Position can be determined to within 3 to 5 km rms; velocity to within 0.5 to 1.5 m/sec rms. The onboard DCS instrument is designed to receive the incoming platform data, demodulate the incoming signal, and measure both the frequency and relataive time of occurrence of each transmission. Platform signals are received by the receiver search unit at 401.65 MHz. Since it is possible to acquire more than one simultaneous transmission, four processing channels, called Data Recovery Units (DRU), operate in parallel. After the doppler frequency is measured, the sensor data are formatted with other internally generated data, and the output is transferred to a buffer interface with the spacecraft data processor (TIP, for TIROS-N Information Processor).

Data from the DCS are included in the HRPT and beacon transmission. After the stored data is received at the central processing facility, the DCS information is decommutated and sent to the CNES, ARGOS processing center in Toulouse, France. Resulting outputs are sent to system users and are retained on magnetic tape for archival purposes.

The DCS is designed and built by the Centre National D'Etudes Spatiales (CNES) of France, who refer to it as the ARGOS Data Collection and Location System.

Spacecraft Bus

The TIROS-N spacecraft series are built and tested by RCA Corporation. They are an adaptation of the DMSP (Defense Meteorological Satellite Program) Block 5D spacecraft built by RCA Corporation for the Department of Defense and first launched in 1976. Each TIROS-N satellite is an integrated system deigned to provide for the control injection into a nominal 833- or 870-km (450 or 470 nautical mile) circular, near-polar, sun-synchronous orbit after separation from the Atlas-E/F launch vehicle. Figure 3 depicts key features of TIROS-N.

Structure. The spacecraft structure consists of four components: (1) the Reaction System Support Structure (RSS); (2) the Equipment Support Module (ESM); (3) the Instrument Mounting Platform (IMP); and (4) the Solar Array (SA). Instruments are located on both the IMP and the ESM. With the exception of the SEM, all instruments face the earth when the satellite is in mission orientation.

The satellite, including the injection motor assembly, is approximately 3.71 meters (12 ft. 2 in.) in length in the launch mode (21 ft. when the array is deployed) and 1.88 meters (6 ft. 2 in.) in diameter. Satellite liftoff weight is 1418 kg (3127 lb) and the in-orbit weight is 737 kg (1620 lb). Of this weight, approximately 230 kg (507 lb) is used for the payload.

Power System. Spacecraft power is provided by a direct energy transfer system whose primary source is an 11.6-meter^2 (125-sq. ft.) planar solar array; the secondary source is a pair of nickel-cadmium batteries. The solar array is made up of eight panels of solar cells, each 61.4 cm x 237.5 cm

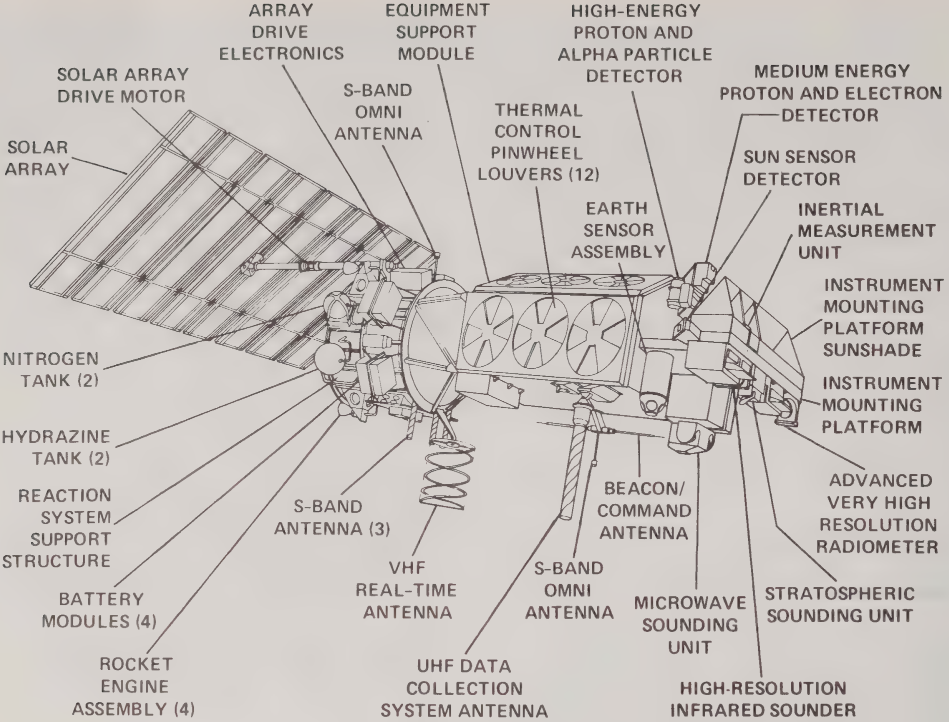
ARRAY DRIVE ELECTRONICS
EQUIPMENT SUPPORT MODULE
HIGH-ENERGY PROTON AND ALPHA PARTICLE DETECTOR
MEDIUM ENERGY PROTON AND ELECTRON DETECTOR
SOLAR ARRAY DRIVE MOTOR
S-BAND OMNI ANTENNA
THERMAL CONTROL PINWHEEL LOUVERS (12)
SUN SENSOR DETECTOR
SOLAR ARRAY
EARTH SENSOR ASSEMBLY
INERTIAL MEASUREMENT UNIT
INSTRUMENT MOUNTING PLATFORM SUNSHADE
NITROGEN TANK (2)
INSTRUMENT MOUNTING PLATFORM
HYDRAZINE TANK (2)
ADVANCED VERY HIGH RESOLUTION RADIOMETER
REACTION SYSTEM SUPPORT STRUCTURE
S-BAND ANTENNA (3)
BEACON/ COMMAND ANTENNA
VHF REAL-TIME ANTENNA
S-BAND OMNI ANTENNA
STRATOSPHERIC SOUNDING UNIT
BATTERY MODULES (4)
MICROWAVE SOUNDING UNIT
ROCKET ENGINE ASSEMBLY (4)
UHF DATA COLLECTION SYSTEM ANTENNA
HIGH-RESOLUTION INFRARED SOUNDER

Figure 3. TIROS-N Spacecraft

(24.2 x 93.5 in.). The array, which must be deployed from its launch stowed position, is canted at 36 degrees to the orbit normal. A solar array drive system causes the array to rotate once per orbit so that the array continuously faces the sun. Current supplied to the satellite through slip rings during daylight portions of the orbit is used to operate the satellite and to charge the two 26.5 ampere-hour nickel-cadmium batteries.

These batteries supply spacecraft power during dark portions of the orbiter and augment the array during daylight peak load conditions. Total orbit average load capacity for the system is about 420 watts at the end of 2 years in orbit at a worst-case sun angle.

Reaction Control Equipment (RCE). The TIROS-N satellite includes an integrated system for guidance and control of orbital injection following separation from the Atlas vehicle. The Reaction Control Equipment (RCE) provides ascent phase, attitude control (3-axis), and orbital velocity trim for final injection. The RCE is operational from Atlas separation to handover to the orbital control system.

Attitude Determination and Control (ADACS). The on-orbit Attitude Determination and Control Subsystem (ADACS) provides 3-axis pointing control for the satellite. The ADACS maintains system pointing by controlling torque in three mutually orthogonal reaction wheels (a fourth skewed wheel is available in the event of failure of one of these three). The torque is determined by analysis of spacecraft orientation in space. Inputs to these computations are acquired from the Earth Sensor Assembly (ESA) for pitch and roll, and an inertial reference with sun sensor updates for yaw. Figure 4 is a simplified block diagram of ADACS.

The ADACS controls spacecraft attitude to maintain orientation of the three axes to within ±0.2 degrees (3σ) of the local geographic reference. Information is also available to permit the yaw, pitch, and roll that existed at any particular time to be computed to within 0.1 degree by computer processing on the ground. Analysis has shown that except for short duration perturbations of up to 0.2 degree, the attitude is generally maintained to within approximately 0.12 degree.

The ADACS is a nominally zero momentum control system which includes:

(1) An Earth Sensor Assembly (ESA);
(2) A Sun Sensor Assembly (SSA);
(3) Four Reaction Wheel Assemblies (RWA's);
(4) Magnetic Control Coils; and
(5) Inertial Measurement Unit (IMU).

The ESA is a static infrared (15 m region) sensor designed to operate over the range of 740 to 926 km (400-500 n.mi.). Nominally, the earth is centered between four independent detectors which view a segment of the horizon in each of four quadrants. If the earth view were perfectly centered, the spacecraft roll and pitch error

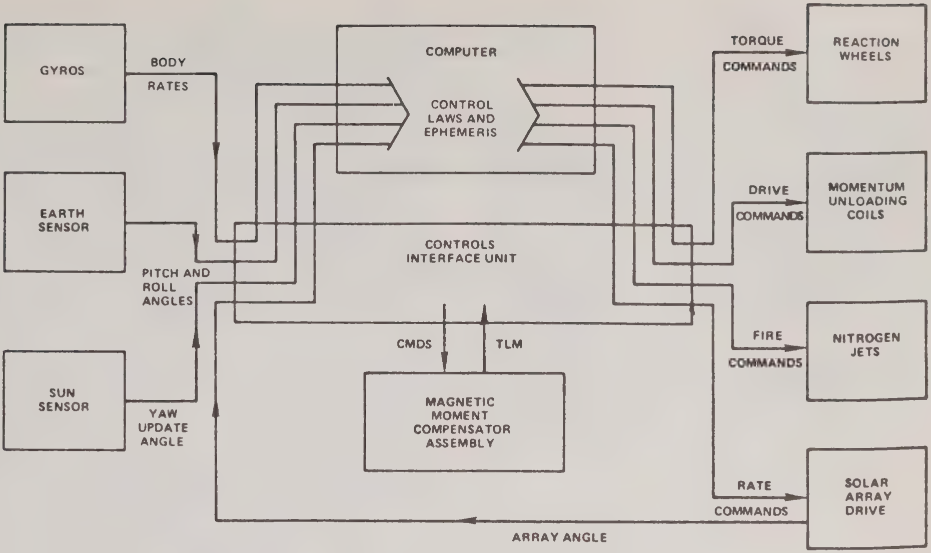

Figure 4. ADACS Block Diagram

would be zero. In practice, pitch and roll are determined from these readings, and the control system tries to keep the error as close to zero as possible.

The SSA is a single-axis digital sun sensor whose output is used to compute the satellite yaw attitude error. The calculated yaw error is used to update the spacecraft yaw attitude once per orbit. Attitude changes between this update and the following update are derived from the combined yaw, roll, and pitch gyro outputs.

The RWA's provide active attitude control by generating reaction torques about the three orthogonal spacecraft axes. Three of the RWA's are mounted orthogonally to produce torques about each of the three primary spacecraft axes; the fourth RWA is canted at an angle of approximately 54.7 degrees with respect to each of the three axes, so that a portion of its torque resolves into all three of the axes. This fourth RWA is normally idle unless one of the orthogonal RWA's fails.

Two magnetic torquing coils (a pitch coil and a roll-yaw coil) included in the ADACS provide a capability for unloading accumulated satellite momentum. Current flowing in these coils generates an electric field that interacts with the earth's magnetic field to remove momentum.

The ADACS also contains four gas-bearing, rate-integrating gyros. Like the RWA's, three gyros are orthogonal, while the fourth is canted to the spacecraft control axes. The gyros measure the attitude rates around each of the three axes for control-loop damping and for deriving yaw attitude between periodic sun-sensor determinations.

Thermal System. The thermal design of the satellite provides accurate temperature control of both the spacecraft structure and the instrument payload. Both active and passive elements are used for this purpose.

Data Handling System. The TIROS-N data handling subsystem, as shown in Figure 5, consists of the following primary components:

(1) The TIROS Information Processor (TIP);

(2) The Manipulated Information Rate Processor (MIRP); and

(3) Five Digital Tape Recorders (DTR's).

The TIP formats all low bit-rate instrument and telemetry data available for transmission from the satellite. It also controls the data outputs from these sources (instruments and satellite systems), and accepts command verification data. The TIP adds synchronization, identification, and time code before simultaneously transferring the data to the beacon transmitter, tape recorder interface (by command), and MIRP. Within the MIRP, the TIP data is combined within three output data formats (HRPT, Global Stored, and Limited Area Stored).

The MIRP processes data from the AVHRR to provide separate outputs for: (a) HRPT transmission in real time, (b) APT transmission in real time, (c) tape recorded Global Area Coverage (GAC) for central processing of reduced resolution data, and (d) tape recorded Local Area Coverage (LAC) for central processing of selected areas of high-resolution data. The MIRP, in addition to formatting, adds synchronization, identification, telemetry, time code, and (except for APT) the TIP output to the AVHRR. The high resolution AVHRR is reduced in resolution by averaging for both APT and GAC uses.

The five digital tape recorders, each with a single electronic module and dual tape transport, provide recorded data for subsequent transmission through the CDA to the central data processing facility. Each transport has an adequate tape capacity to record approximately 45×10^8 bits of data.

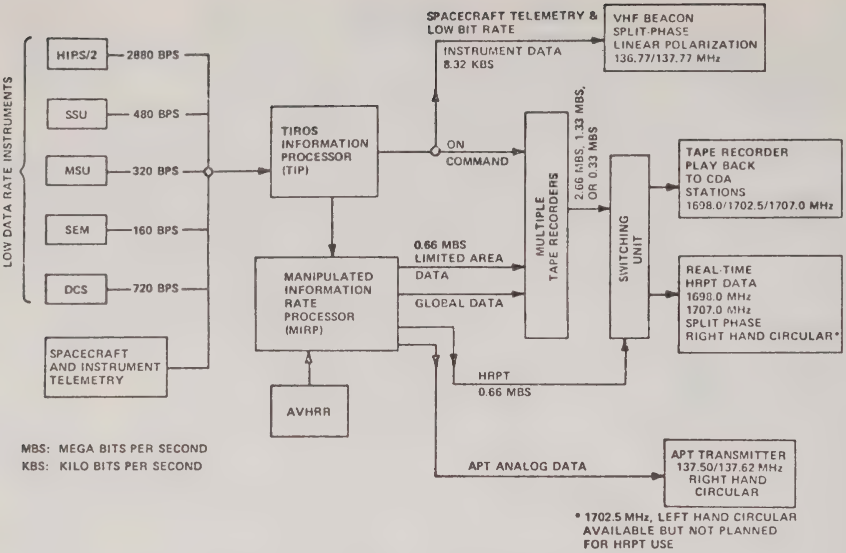
LOW DATA RATE INSTRUMENTS
HIRS/2
2880 BPS
SSU
480 BPS
MSU
320 BPS
SEM
160 BPS
DCS
720 BPS
SPACECRAFT AND INSTRUMENT TELEMETRY
TIROS INFORMATION PROCESSOR (TIP)
SPACECRAFT TELEMETRY & LOW BIT RATE
INSTRUMENT DATA 8.32 KBS
VHF BEACON SPLIT-PHASE LINEAR POLARIZATION 136.77/137.77 MHz
ON COMMAND
2.66 MBS, 1.33 MBS, OR 0.33 MBS
MULTIPLE TAPE RECORDERS
SWITCHING UNIT
TAPE RECORDER PLAY BACK TO CDA STATIONS 1698.0/1702.5/1707.0 MHz
REAL-TIME HRPT DATA 1698.0 MHz 1707.0 MHz SPLIT PHASE RIGHT HAND CIRCULAR*
0.66 MBS LIMITED AREA DATA
GLOBAL DATA
MANIPULATED INFORMATION RATE PROCESSOR (MIRP)
HRPT 0.66 MBS
AVHRR
APT ANALOG DATA
APT TRANSMITTER 137.50/137.62 MHz RIGHT HAND CIRCULAR
MBS: MEGA BITS PER SECOND
KBS: KILO BITS PER SECOND
* 1702.5 MHz, LEFT HAND CIRCULAR AVAILABLE BUT NOT PLANNED FOR HRPT USE

Figure 5. TIROS-N Data Flow Diagram

Command and Control. The command and control group provides the functions for decoding ground commands, storing commands for later execution, and issuing control signals. Redundant Crystal Oscillators (RXO) are used to provide a highly stable frequency source for all spacecraft clock-related functions.

The Controls Interface Unit (CIU) obtains data and control signals from the spacecraft computer, buffers them, and transmits them to other spacecraft components for action. It also contains all the circuitry necessary to generate the clocks and timing signals used by the satellite.

Two Central Processing Units (CPU's) regulate the final stages of injection into orbit by computing required thrust levels and issuing control commands to the Reaction Control Equipment. The CPU's also control operation of the satellite in orbit and issue commands to maintain spacecraft attitude within predetermined limits.

TABLE 1. COMMUNICATION LINK SUMMARY

Link	Carrier Frequency	Information Signal	Baseband Bandwidth	Modulation Modulation
Command*	148.56 MHz	Digital commands	1 kbps	Ternary FSK/AM
Beacon	137.77 MHz or 136.77 MHz	Low bit rate instrument data and spacecraft telemetry. All from TIP	8320 bps	Split-phase PSK
VHF Real-time - APT	137.50 MHz or 137.62 MHz	Medium resolution video	2 kHz	AM/FM
S-Band Real-time - HRPT	1698 or 1707**MHz	High resolution video data, and TIP data from MIRP	665.4 kbps	Split-phase PSK
S-Band playback to CDAs	1698, 1702.5 or 1707 MHz	High resolution video data from MIRP, medium resolution video data from MIRP	2.6616 Mbps	Randomized NRZ-PSK
Data collection*	401.65 MHz	Data from earth-based platforms and balloons	400 bps	Split phase PSK
S-Band TIP data playback	1698, 1702.5 or 1707 MHz	TIP data recovered from tape recorders	332.7 kbps	Split-phase PSK

*Uplink to the satellite.
**1702.5 may be used for HRPT in the event of failure of primary transmitters.

Communications System. The seven TIROS-N primary communications links are summarized in Table 1. Each of the three 5.25-watt output S-band transmitters is coupled to one of three quadriphase antennas. Normally, one of the transmitters is used continuously for transmission of HRPT data while the other two are used to play back tape recorders to one of the centralized data acquisition stations. All three transmitters may be used in parallel when required to retrieve data from the on-board recorders. Two of the S-band antennas are right-hand circularly polarized (1698 and 1707 MHz), while the third is left-hand circularly polarized (1702.5 MHz). During the ascent phase only, one of the S-band transmitters is connected to an S-band omnidirectional antenna to provide spacecraft telemetry.

Each of the two VHF APT transmitters has a 5-watt output and operates at a preselected frequency of either 137.50 or 137.62 MHz. One of the transmitters operates continuously. The transmitting frequency is chosen to preclude interference between signals emanating from two satellites in orbit at the same time. Either transmitter is coupled to the VHF real-time quadrifilar antenna via an RF switch. The signal is an amplitude-modulated 2.4-kHz subcarrier which frequency-modulates the carrier. The antenna, a four-element quadrifilar, provides a shaped pattern.

Launch and Orbit Constraints

The TIROS-N satellite series has been designed to operate in a sun-synchronous orbit at 833 + 90 km (450 + 50 n.mi.). The choice between nominal altitudes is made to keep the orbital periods of two operational satellites in similar orbits sufficiently different (1 minute) so that they do not both view the same point on the earth at the same time each day. Nominal orbital parameters are shown in Table 2 below:

TABLE 2. TIROS-N SPACECRAFT SERIES, ORBITER PARAMETERS

Parameter	833 km Orbit	870 km Orbit
Inclination	98.739 degrees	98.899 degrees
Nodal Period	101.58 minutes	102.37 minutes
Nodal Regression	25.50 degres/ orbit W	25.59 degrees/ orbit W
Nodal Precession	0.986 degree/ day E	0.986 degree/ day E
Orbits per day	14.18	14.07

Equator Crossing Time

The TIROS-N satellite series has been designed to operate with a southbound equator crossing between 0600 and 1000 Local Solar Time (LST), or a northbound equator crossing between 1400 and 1800 LST. The morning satellite is launched into a 07:30 LST descending orbit, while the afternoon satellite is LST ascending.

Orbit Injection

Satellites of the TIROS-N series are launched into sun-synchronous orbits. The first-stage booster is an Atlas E/F; second-stage propulsion is provided by a rocket motor integral with the satellite.

The guidance system of the Atlas vehicle controls the first stage of the spacecraft launch. The spacecraft system monitors the launch parameters and controls the flight after the spacecraft is separated from the Atlas vehicle. Body rates and accelerations are provided to the Central Processing Unit (CPU) by the Inertial Measurement Unit (IMU), which is made up of rate integrating gyros and accelerometers. The CPU uses a stored set of equations to determine the optimum flight profile which, after first stage separation, is maintained by the Reaction Control System (RCS). Hydrazine and nitrogen thrusters are used to provide spacecraft control during the apogee kick motor burn and to trim orbital velocity after spacecraft insertion into orbit. These thrusters are also used during the period when the solar array is deployed. Unused nitrogen gas is retained on the satellite for use in the event of unexpected momentum buildup during the lifetime of the satellite.

TIROS-N/NOAA Operational System Elements

The two primary NOAA Command and Data Acquisition (CDA) stations are located near Gilmore Creek, Alaska, and Wallops Island, Virginia. Programming and commanding of the satellite originates at the NESS Satellite Operations Control Center (SOCC) located in Suitland, Maryland. The commands, satellite telemetry and environmental data are relayed between the SOCC and CDA's via a commercial communications satellite, RCA's Satcom, in geostationary orbit at 119 degrees West longitude. This domestic satellite communications system, which includes the RCA "earth stations" at Suitland and Wallops, delivers the data to the SOCC at 1.33 megabits per second. The CDA's

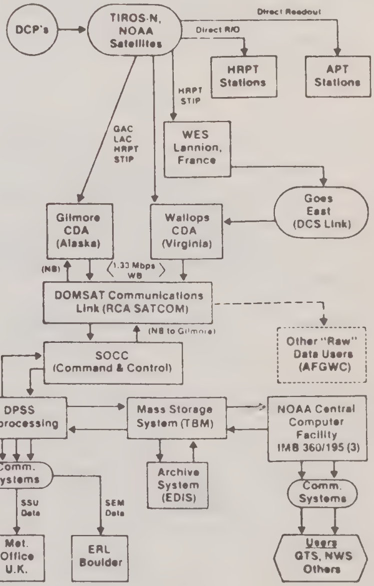
DCP's
TIROS-N, NOAA Satellites
Direct Readout
Direct R/O
HRPT Stations
APT Stations
HRPT STIP
GAC LAC HRPT STIP
WES Lannion, France
Goes East (DCS Link)
Gilmore CDA (Alaska)
Wallops CDA (Virginia)
(NB)
1.33 Mbps WB
DOMSAT Communications Link (RCA SATCOM)
(NB to Gilmore)
Other "Raw" Data Users (AFGWC)
SOCC (Command & Control)
DPSS Preprocessing
Mass Storage System (TBM)
NOAA Central Computer Facility IMB 360/195 (3)
Comm. Systems
Archive System (EDIS)
Comm. Systems
DCS Data
SSU Data
SEM Data
CNES France
Met. Office U.K.
ERL Boulder
Users
GTS, NWS Others

Figure 6. TIROS-N Operational System Data Flow Diagram

communicate with the TIROS-N satellite by means of the S-band links and read out the data stored on the satellite's digital tape recorders in addition to receiving direct data transmission during the satellite contact.

The TIROS-N Operational System data flow is illustrated in Figure 6. The TIROS-N Ground System consists of two major subsystems, the Data Acquisition and Control Subsystem (DACS) and the Data Processing and Services Subsystem (DPSS). The DACS includes components at the two NOAA CDA stations, at the Satellite Operations Control Center, at the Western European Station in Lannion, France, and at the Satellite Field Services Station in San Francisco. all the DPSS components are in the NOAA facility at Suitland, Maryland.

The DACS includes all components necessary to command and control the spacecraft, minitor its "health" via housekeeping telemetry, and to retrieve and transmit the spacecraft environmental data to the DPSS processing and data handling facility.

The DPSS subsystem ingests the raw satellite data, preprocesses and stores it along with appended auxiliary information such as earth location and quality control parameters. This subsystem consists of several unique segments of high speed computers, intermediate disk storage units, and a mass data storage system.

Future of the TIROS-N NOAA Satellite System

The TIROS-N type satellites have been designed with sufficient space, weight, and data-handling capability to allow additional instruments to be installed. New instruments currently planned for inclusion within this growth capability are:

(1) A Search and Rescue (SAR) system comprised of repeater and processor units;

(2) A Solar Backscatter Ultraviolet Radiometer (SBUV/2); and

(3) Two Earth Radiation Budget Experiment (ERBE) instruments (a scanner and a non-scanner version).

The new spacecraft configured with these instruments will be known as the Advanced TIROS-N (ATN) spaccraft. The ATN design will be incorporated into the last three spacecraft of the TIROS-N series: NOAA-E, -F, and -G. The SAR payload will be included on NOAA-E, -F, and -G, and the ERBE will be included on NOAA-F and -G. Figure 7 highlights the ATN configuration.

The ATN spacecraft bus will have a modified, elongated (approximately 20 inches longer than TIROS-N) design, including an additional set of pinwheel thermal control louvers. The planned launch weight of the ATN spacecraft, 1693 kg (3725 lb) including the apogee motor, is a 270 kg increase over the TIROS-N spacecraft. An increase in the Reaction Support System low-level thrust to 100 pounds is planned as a consequence of the greater spacecraft mass, but no additional propellant capacity is planned. The basic instrument payload, with the exception of the new instruments, will remain essentially the same as that flown on TIROS-N.

The Search and Rescue (SAR) experiment to be installed on ATN will enable detection and location of downed aircraft or marine vessels in distress on a timely basis and dramatically reduce casualty losses by alerting potential rescue teams and guiding them to disaster scenes. Figure 8 depicts the SAR system elements.

The SAR system will detect signals from aircraft Emergency Locator Transmitters (ELT's) and from Emergency Position Identification Radio Beacons (EPIRB's) on ships. Government regulations require that general aviation be equipped with ELT's. Over 170,000 ELT's have been installed on U.S. civil aircraft. Similarly, over 1700 U.S. vessels under mandatory regulations are equipped with EPIRB's. ELT's and EPIRB's transmit distress signals on 121.5 or 243 MHz automatically. A new

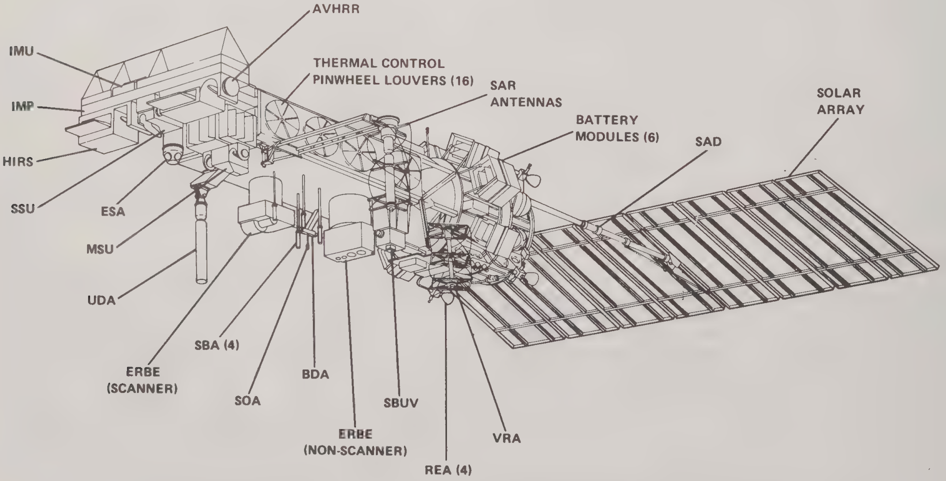

Figure 7. Advanced TIROS-N Spacecraft

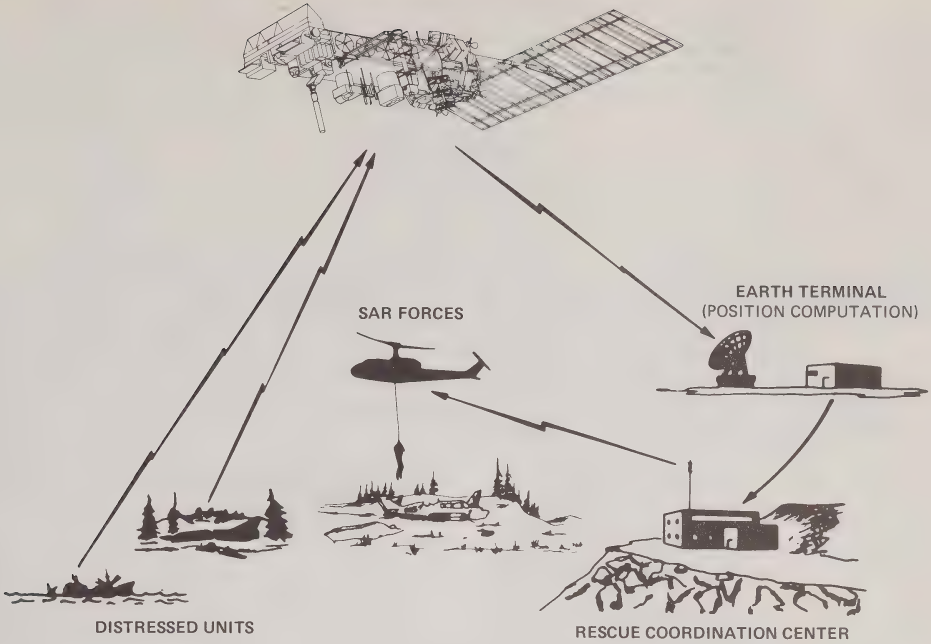

Figure 8. SAR Concept

and improved ELT operating on 406 MHz is to be introduced. It will have more power (5 watts), more stable crystals, and a user identification code.

The SAR experiment is a joint U.S. - Canadian project. Canada will furnish the communication repeaters for receiving distress signals at 121.5, 243, and 406 MHz and for real-time relay of the search-and-rescue data to the ground sites at 1543 MHz. In addition to the repeater mode of operation, the 406-MHz signal will be processd by the satellite's 406-MHz processor. It will detect the signals, measure the doppler frequency, and this doppler data together with the SAR message from the 406-MHz ELT or EPIRB will be transmitted in real time via the 1543-MHz downlink and will also be stored in the spacecraft tape recorders. The 406-MHz processor will be provided by CNES of France.

The 121.5-MHz and 243-MHz signals will be processed by one of the four local user terminals located at Scott Air Force Base, Illinois; San Francisco; Kodiak, Alaska; or at Ottawa, Canada. These stations will use 3-meter parabolic antennas, driven automatically by a mini-computer program, to track the ATN satellite. When the satellite is in view of both the distress transmitter and the ground terminal, the ELT or EPIRB signal will be detected and tracked. The doppler data extracted will then be used to calculate the position of the distress signal. A minimum of 4 minutes of contact time is needed to determine location by doppler. The relayed distress signals (121.5-MHz or 243-MHz) will be processed to determine positive location of the distressed vehicle; the 406-MHz signal will be transmitted in real time or stored. When processed, the 406-MHz signal will provide the location of the distress, identify the vehicle in distress, and display a message concerning the nature and time of the distress. Location accuracy of the 121.5-MHz and 243-MHz signals will be 10 to 20 km; that of the 406-MHz signal will be between 2 to 5 km. Figure 9 diagrams the SAR mission data flow.

The USSR, as well as other countries, has expressed interest in participating in the SAR experiment.

Benefits

Over the past 20 years the quantity, quality, and reliability of satellite coverage have improved greatly. Since 1966 the entire earth has been photographed at least once daily on a continuous basis. The photographs are not only used in real-time operations, but are also placed in archives from which they can be retrieved for use in research case studies. Satellite data is now being used by meteorologists and environmental scientists on a wide-spread basis in routine operations throughout the world, and is considered almost indispensable for analyses and short-range forecasts.

The satellite information has proven extremely useful in two broad types of situations. First, there are extensive areas of the earth from which conventional reports are sparse, namely: the oceanic regions of the northern and southern hemispheres, deserts, and the polar regions. Satellite information fills these voids by locating the large-scale features depicted by the cloud formations. These features include storm systems, fronts, upper level troughs and ridges, jet streams, fog, stratus, sea ice conditions, area of snow cover, and to some extent upper level wind directions and speeds. The satellite data is also used in conjunction

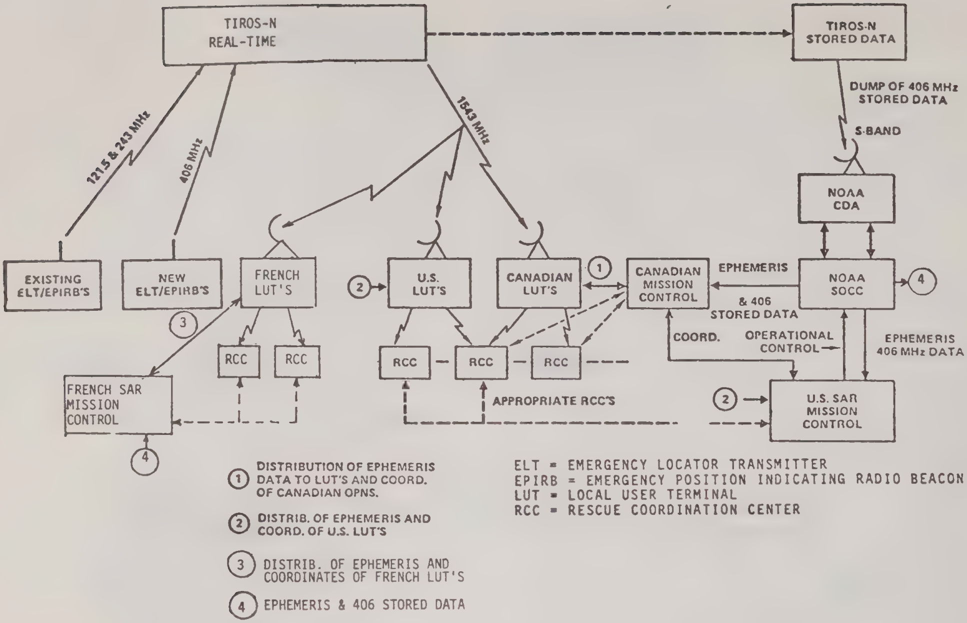
TIROS-N REAL-TIME
TIROS-N STORED DATA
DUMP OF 406 MHz STORED DATA
S-BAND
121.5 & 243 MHz
406 MHz
1543 MHz
NOAA CDA
EXISTING ELT/EPIRB'S
NEW ELT/EPIRB'S
FRENCH LUT'S
U.S. LUT'S
CANADIAN LUT'S
CANADIAN MISSION CONTROL
EPHEMERIS
& 406 STORED DATA
NOAA SOCC
COORD.
OPERATIONAL CONTROL
EPHEMERIS 406 MHz DATA
RCC
RCC
RCC
RCC
RCC
FRENCH SAR MISSION CONTROL
APPROPRIATE RCC'S
U.S. SAR MISSION CONTROL
① DISTRIBUTION OF EPHEMERIS DATA TO LUT'S AND COORD. OF CANADIAN OPNS.
② DISTRIB. OF EPHEMERIS AND COORD. OF U.S. LUT'S
③ DISTRIB. OF EPHEMERIS AND COORDINATES OF FRENCH LUT'S
④ EPHEMERIS & 406 STORED DATA
ELT = EMERGENCY LOCATOR TRANSMITTER
EPIRB = EMERGENCY POSITION INDICATING RADIO BEACON
LUT = LOCAL USER TERMINAL
RCC = RESCUE COORDINATION CENTER

Figure 9. SAR Mission

with other data to provide quantitative heights of constant pressure surfaces as inputs to conventional analyses.

The second type of situation to which satellite data is usefully applied is the location and tracking of hurricanes, typhoons, and tropical storms. Coastal and island stations with little or no adjacent conventional weather information can make maximum use of APT data and the processed stored data from facsimile circuits. The satellite data provides information on the presence and position of frontal patterns, storms, and general cloud cover.

The infrared data from the TIROS/NOAA satellites can be used to produce charts showing the sea-surface temperature over a larger area and with more frequency than is possible from any other source. This information is useful to shipping interests and the fishing industry, and is a vital input to meteorological forecasts. Satellite pictures display the extent and character of ice fields in the Arctic and Antarctic Seas, and on the Great Lakes, with a frequency and geographic coverage never before approached.

Worldwide atmospheric temperature soundings provided by the satellite result in more complete and accurate analyses for use in weather forecasts. Soundings by satellite provide coverage over oceans and remote areas not covered by conventional sounding instruments. Individual soundings from satellites aid in the interpretation of satellite picture data by providing correlation at specific geographical locations. The continual soundings enable the location of atmospheric temperature gradients for use in studying atmospheric phenomena.

The TIROS-ESSA-ITOS-NOAA family of satellites has fulfilled U.S. operational requirements by providing a reliable in-orbit system that transmits routine observations on a timely basis without interruption in service. Its evolutionary design has permitted a cost-effective approach in achieving program objectives and provided a gradual and effective improvement in service with existing worldwide receiving stations. With the advent of the Advanced TIROS-N, further improvements in observation and in the processing and dissemination of data will provide the polar-orbiting data required by the long-term goals of the National Operational System.

ACKNOWLEDGEMENT

For further details in this particular subject, reference is made to NOAA-TM-NESS-95 by A. Schwalb, and paper titled "The TIROS-N NOAA Operational Satellite System" presented by J. Hussey at the NOAA-A Scientific Colloquium, May 1979, Washington, DC.

80-0530

EMERGENCY RESPONSE COMMUNICATION SATELLITE SYSTEMS OF THE '80'S

Lois Clark McCoy *
National Association for Search and Rescue
(NASAR)
San Diego, California

ABSTRACT

An augmenting satellite communications system, permitting coordinated response, command and control of emergency operations, is possible for the eighties. Such a system will insure the ability to operate independently of local weather, geographic or conventional communications conditions. The lack of responsive emergency communications in remote areas (or areas of degraded communications), often causes unnecessary delays in providing relief to people in distress. In the adoption of new technology there are political, cultural, economic and social constraints to its early acceptance. A demonstration project of an integrated system for emergency response and public safety communications would stimulate the early adoption of such a system. The cost to the United States of public accidents is measured in the billions of dollars each year. The increase in effective and efficient emergency response, made possible by an augmenting satellite communications system, will decrease these expenditures.

INTO THE '80'S

In advance of the WARC '79 Conference, several reports appeared on the application of high technology and satellite communications for emergency humanitarian response, rescue and recovery.[1,2,3] A singular amount of smoke, fire and controversy surrounded the evaluation of these reports. Such reactions were surprising, in what is generally thought to be the un-emotional fields of electrical engineering and systems design. But it appears that, as frequently happens, the technological cart had come before the total systems-design horse and we can now perceive a common ommission in the technologic basis of these surveys.

The serious problems of social, economic, and political feasibility in implementing an improved emergency response communications system, either via satellite or by more conventional terrestrial augmentation have not been addressed. Each report seems to assume that the potential user will quickly accept the need for some improved system and come forth with the necessary endorsement and funding.

This appears to be an unrealistic assumption in view of the recently concluded ATS-6 experiment in Emergency Communications conducted by the National Association for Search and Rescue (NASAR) and the United States Air Force.[4]

There are very real political, cultural, economic and social constraints that come into play in implementing any improved program, especially one involving high technology.

As an example of economic constraints, rural and remote areas would benefit immediately from the proposed satellite emergency communications systems but they are the least able to provide financial support to the system.

Then there are the distinctions in the benefits to an emergency which creates undue demands and saturation of the normal existing systems, and the benefits to the situation where the emergency itself prevents existing systems from functioning.

There are true political constraints present under today's conditions. In principal, each community's emergency service provides for its own communications. When these systems prove inadequate in establishing the coordination required to deal with the emergency of the larger short-lived phenomena, interagency and political frictions may arise. When the proposed solution involves satellite high technology, entire new systems have to be designed for its employment. And society, especially in its bureaucratic form, resists such change.

Added to the multiple problems of ecomomics and politics, is the additional problem of the responsible bureaucracies having to cope with a new reality in the increased satellite communications capability.

The state-of-the-art satellite communication now provides to the bureacracies the ability to "command". Command means control. And the exercise of control implies the possiblity of either success or failure. What was formerly a tragic, but nevertheless unsolvable, emergency can now be acted upon. The former "Act of God" now becomes a solvable problem that demands rapid deployment of skilled emergency managers and capable, trained rescue personnel.

In a very real way, this new ability to make a difference in the emergency, can become a threatening thing. Today, a coordinating agency has no means for emergency communication to the scene of the emergency except a telephone line. Often that telephone system is inoperative due to the same emergency. The principal function of the bureacrat today is as an information channel; and as a concerned, and sometimes horrified, spectator. He is seldom the "on-scene commander" with command and control over life or death in that emergency.

---

* Administrator, National Association for Search and Rescue, Member AIAA

Copyright © American Institute of Aeronautics and Astronautics, Inc., 1980. All rights reserved.

Not so with satellite high technology. It will permit the saving of additional lives and surely large savings of dollars during the recovery process. However, is it any wonder that the bureacracies are not jumping over each other in the effort to assume this new operational challenge?

When emergencies strike, there is a very large "Hassle Factor". Roger Mattson, director of the Nuclear Regulatory Commission's division of systems safety, believes that the operators at 3 Mile Island were victims of the "hassle factor" peculiar to all emergencies. And the less accustomed to emergencies, the greater the probability that the hassle factor will accelerate Murphy's law. This may explain why law enforcement and military reactions to emergencies tend to be more professional and more successful than the reactions of civilian plant managers. After all, the U.S. Navy and Adm. Rickover have been operating nuclear reactors within the extremely confined areas of submarines and ships at sea for years. They have had their share of emergencies and of shut-downs, but not of "accidents".

By providing our bureacratic coordinators with high technology we now permit them to become participants, instead of spectators, in the hassle of an emergency. Is it any wonder that they may find our solution of satellite communications more threatening to them than the disaster itself--which probably does not threaten their personal or political safety at all?

The experiences of the National Association for Search and Rescue experimental program on ATS-6 indicate that there is a great deal of skepticism among responsible emergency agencies that, indeed, communications satellite technology can perform "as advertized" in emergency and disaster environments. Interestingly enough, this skepticism is equally offset by the general public who believe that, since the need is so obvious, emergency response resources are already equipped with augmented high technology satellite communications.

In an effort to make the emergency end user more aware of the increased communications capabilities now available due to technologic advances, the United States Air Force Rescue & Recovery Service and the Emergency Response Communications Program (ERCP) carried out 5 Regional ERCP Communications Symposia as well as 4 Regional State Search & Rescue Awareness conferences during 1978-79. Attending these 9[1] symposia were state and local law enforcement, civil defense, rural and remote health care, emergency medical services, disaster assessment and relief, drug enforcement, border patrol, communication officers and agency representatives.

It became obvious that a demonstration project, a "hands on" experiment, was necessary to bridge the cultural gap between conventional capabilities and the new era of space communications.

ATS-6 EXPERIMENT

To answer this need, the National Association for Search and Rescue was permitted a 2 month emergency response communication experiment at the end of the useful life of NASA's ATS-6 satellite.

NASA, pioneering in the introduction of Applications Technology Satellites[7](ATS) identified their objectives before launch as:

1. to demonstrate the feasibility of a 9.1 meter deployable parabolic antenna in synchronous orbit.
2. to provide a 3 axis stabilized spacecraft with 0.1 degree pointing capability in all 3 axes.
3. to provide an oriented stable spacecraft platform at synchronous altitude for advanced technological and scientific experiments.

All of these objectives were satisfactorily realized.

Additionally the test objective of the NASAR/ERCP experiment was to examine the effectiveness of space communications equipment during coordinated emergency response missions. This objective was also satisfactorily realized.

The NASAR experiment was the result of an 18 month effort by the Emergency Response Communication Program, a working group of the Interagency Committee on Search and Rescue consisting of representatives of DOD, NASA, FCC, USCG, NPS, DOC, and NASAR.

The ATS-6 experiment provided an Emergency Response Management System structured around an all terrain, selfcontained, mobile, satellite communications capability that was flyable anywhere via HC-130 or similar aircraft. Transceivers designed and built originally by General Electric Corporate Research and Development Center for another experiment on[6] ATS-6, were installed in two jeeps stationed at 303 ARRS(R) March AFB, California and at 305 ARRS(R) Selfridge ANGB Michigan.

The antenna on the mobil units was a Wheeler type also designed and built by GE. The coordinating Base Station was installed at Scott Air Force Base, Illinois. This base transceiver was actually a modified portable "briefcase" unit developed by NASA and Westinghouse technicians for other ATS-6 experiments. It was attached to a 3 meter roof mounted antenna on the headquarters building of the AFRCC at Scott. Additionally there were two more briefcase units that were made available on an 'as needed' basis by NASA for actual emergency distress operations. This equipment was kept on alert for deployment aboard HC-130 aircraft.

The Applications Technology Satellite Operation Center (ATSOC) at NASA Goddard Space Flight Center, Greenbelt Maryland and the Earth Station Laboratory operated by GE at Schnectady N.Y., controlled the priorities and operating hours available and the spacecraft pointing required.

NASA, GE and Westinghouse technicians supported the equipment installations and conducted the initial operator training. The bulk of the experiments were conducted by personnel of the Air Force Rescue and Recovery Service (ARRS). In addition personnel from the Lemoore Naval Air Station, the National Park Service (Yosemite), and the National Association for Search and Rescue provided assistance, equipment and personnel for the experiment.

The original test area was the eastern half of the United States. The initial experiments were so successful and the ATS-6 pointing and fan beam antennas proved so flexible that ATSOC and GE turnaround station expanded its assistance to cover the entire country and Howard AFB, Canal Zone, where different satellite antenna patterns were used.[7]

The jeeps and/or "briefcases" were used in 3 full scale experimental exercises and one acutal emergency response to Wichita Falls, TX after their tornado disaster April 11-14, 1979.

The three exercises were:[4]

1) 403 RWRW search and rescue exercise near Gulfport, Mississippi from March 24, 1979 to April 4, 1979.
2) Yosemite National Park, California for a search and rescue exercise involving the National Park Service, the State of California, Lemoore Naval Air Station, NASAR and the 303/305 ARRS(R), May 14-16, 1979.
3) Howard AFB, Canal Zone as a contingency for the possible evacuation of Americans from Nicaragua, June 18 to August 3,1979.

The effectiveness of this ATS-6, L Band system, originally designed for confirming a wide application of data for space and spaceflight, proved far superior to even the experimenters hopes. The space system was compared to conventional long-range high frequency (HF) communications by attempting to establish contact from the field to any coordinating center or alternate communications or logistic center. Conventional HF phone patches were possible in some cases but the satellite system was far superior.

The patches were characterized by normal HF noise and delays and were difficult to understand, especially during poor weather conditions. There were no satellite communications failures during the experiment. The satellite transmissions were always crisp and clear regardless of the weather, the geographical location of the equipment, and/or the level of expertise of the operator.

One of the most exciting events in the experiment was the excellent in-flight communications via satellite from the Lemoore NAS helicopter at Yosemite to Scott Air Force Base, Illinois. Contrary to some expectations there was no interference to the L band communications from the RF build-up of the helicopter roter blades. The 'brief case' transceiver was jury-rigged in the helicopter and the 18 inch Wheeler-type antenna was held out the side door of the helo. For the future the installation of a permanent antenna for the helicopters can be developed. There was only one minor repair problem involved during the time of the experiment and that was thought to be caused by transporting one of the briefcase units (without packaging) as air baggage to the Canal Zone. The repair was made on scene by personnel attached to the 303rd Air Force Reserve Unit. The only other problem was a recharging reversal on one of the battery packs, a case of "operator error" that never re-occurred. No injuries or property damage were incurred during the test as evidence that satellite communications systems in support of emergency communications has minimal safety risks.

The NASAR/ERCP emergency communications experiment was deemed a total technical success. But we felt some cultural resistance to the new technology.

WICHITA FALLS TORNADO

For example, let us discuss in greater detail the actual response to the Texas tornado. Just before 6 p.m. on April 10, 1979, a supercell storm over Wichita Falls, Texas collasped upon itself. The dome of thunderheads fell into a horseshoe crater and at the same moment a tornado formed at the base of the cloud. That tornado killed 60 people and caused the total destruction of homes throughout an area 3/4 to 1¼ miles wide and 8 miles long. It remained on the ground for 47 miles and destroyed all 7 power lines, each strung 5 miles apart to minimize the chance of just such a storm interrupting community services. The simultaneous destruction of the telephone lines effectively cut off the striken area of Wichita Falls and its tornado devasted neighbors from all outside aid.[8]

In the ensuing night-time hours, the established local public safety networks coordinated the emergency response: 60 bodies were recovered, 896 persons received emergency medical treatment, 3 hospitals in the area received all wounded and 30,000 people were known to be homeless. Only 6 persons were unaccounted for at daybreak.

By ten a.m. that morning USAF/NASAR experimental satellite communication moved in to assist the local government in its recovery operations. Until then only a single emergency telephone link had been re-established between the local telephone office and the telephone company's division office in Fort Worth. Now, Emergency communications via NASA's experimental ATS-6 satellite were established with the State Capitol in Austin and the emergency response agencies of State and federal government.

Wichita Falls was a community with a workable disaster plan, which had been exercised and practiced immediately before the tornado of April 10th. It's emergency services and public safety personnel knew what to do, where to report and how to respond. Nevertheless, recovery operations were slowed and fragmented in the initial recovery hours as the normal information channels remained inoperative because of the disaster.

But, even so, there was a reluctance to employ the new experimental satellite capability. The responsible persons in Austin had come to work in office attire, prepared to use a telephone at their own desk - not to sit in an emergency communications jeep parked in front of the steps of the State Capital and bristling with "funny" antennas.

Understandably, the public safety officers in Wichita Falls wanted to talk on their "own" radio frequencies to their "own" departmental people in the Capital. Since the power was out to the microwave repeaters, this was not possible. But they appeared reluctant to use a military jeep - even one equipped with satellite communications - as a facilitator. The impression was one of skepticism, and a hesitancy to use anything so new, in such difficult circumstances.

From these experiences the USAF/NASAR experimenters developed the following additions to the satellite transceivers in order to enhance their cultural acceptance:

1. A "telephone instrument", connecting via a long wire, the satellite transmitter in the jeep to the office of the responsible officer who could then talk via satellite from his desk.
2. Total phone patch capability via satellite from the satellite tranceivers in the field.
3. A matching device on the satellite transceiver that permitted any HF, VHF, or UHF frequency to be input onto the satellite frequency for broadcast to the receiving earth station.

There is a tremendous need for a land based emergency mobile/portable communications system. The emphasis is on mobility. The real beauty of the ATS-6 system was that it had the technical capability to go anywhere. The locations of these experiments ranged from sea level to 14,000 feet, with temperatures ranging from 120°F to 29°F. The 18 inch Wheeler type antenna gave the system total flexibility. The ATS-6 system was small, compact, and energy efficient.

Today, the lack of responsive communications in remote areas or areas of degraded communications often causes unnecessary delays in providing relief to people in distress. All agree that the loss of communications within the disaster area, and from the striken area to mutual outside aid, compounds the disaster, whatever its cause. Yet, in the matter of emergency communications we are still relying on out-moded, vulnerable wire systems while new satellite applications become available.

TODAY'S FRAGMENTATION

At present, emergency response on land in the United States is fragmented into a morass of independent entities. Each genuinely believes that it is an entity in its own right, rather than a part in an overall national umbrella of emergency response dedicated to the mutual protection of all the citizens in the United States; not just those few folks who pay taxes in their immediate local area.

Even under escalating emergency conditions, the cooperating agencies continue to view themselves as separate systems, merely "supporting" each other in the emergency. Therefore, since the perception of such a national system is lacking, the operational system for a coordinated emergency response to a nuclear accident, large earthquake, or major terrorist threat does not exist, in fact, in an operational form today. Of necessity, the emergency resource resorts to its' volunteer industry and ad hoc "synthetic" form of organization.[9]

There exist no figures documenting the size of the total emergency response need for the United States today. Nor does there exist figures documenting the vast, essentially volunteeer effort made for the relief of Public Accidents over the land areas of the United States.

However, consider:[10]

- Billions of dollars are spent by states and municipalities on emergency response and recovery every year.
- $500 million a year is spent on federal disaster aid to states where about 50 Presidentially declared disasters and emergencies occur.
- Two, three, or more sizeable hazardous materials accidents, explosions, and train derailments occur daily in the United States. Man-made emergencies represented two-thirds of the cases in 1978, in contrast to only one-fifth of the cases dealt with during the past 5 years.
- Fire accounts for $11-12 billion in losses annually.
- 35% of our United States population, and 39 states, are at major or minor earthquake risk.
- Between 1920 and 1973, tornadoes killed as many as 9,000 people, compared with 5,000 deaths from floods and 4,000 from hurricanes.
- Flash floods have recently emerged as the major killer among storm-weather hazards, largely because of urban development and recreational use of flood prone areas. Since 1968, the average annual U. S. death toll from flash floods has risen to about 200.

Add the numbers involved in these cataclysmic events to the 22,000 public accidents that happen annually off the highway. Add to that number, the ever increasing man-made disasters, poisonous material spills, oil-well blowouts, and railway hazardous material wrecks. And now, the emergency response field has burgeoned into a full scale industry supported by volunteers.

Using figures developed by James O. Page of the ACT Foundation, an ill or injured person (regardless of the cause of his distress) when recovered, contributes an average of $3,484 per year to the Federal Treasury during the remainder of his expected wage-earning years.[11] Even without a data base, simple actuarial figures permit us to see that saving useful working lives is an economically desirable outcome of effective, efficient life-saving emergency response.

Without waiting for the advances in knowledge that the Data Base will provide for the future, there are some steps to be taken immediately.

First we must recognize and agree that inefficient emergency response operations cost money and cost lives. The ad hoc "synthetic organization" for emergency response is costing the American people dearly. A volunteer industry, by its very nature, is unsuited to the increasing number of disaster responses that (at least in modern industrialized societies) are placed upon us at an increasing rate each day.

It is not very difficult to see what must be done. The Emergency Response Industry must have pre-established structure, with rules for interdependence, lists of resources, and known channels of effective communications. How to do it is a problem to be addressed at the highest federal level, as was the highway accidental death rate in the sixties.

This may prove to be the ideal time for such an effort. To have attempted to bring into being such a structured Emergency Response organization prior to the availability of an effective communications network, invulnerable to the disaster or emergency itself, may not have been possible.

DEMONSTRATION PROJECT

But with the eighties, emergency satellite communications will become an actuality. In "A Forecast of Public Service Satellite Communications"[12] a variety of public services were modeled. In the computer runs for public safety the adoption of Satellite Communications modeled as a virtual certainty by 1991. Additionally, its earlier adoption was stimulated by a demonstration project. To quote from their findings "Penetration of one percent of the public safety market occurred in 1982 in nearly half the runs, and occurred by 1991 in virtually all the runs. Thus we forecast that early adoption of satellite communications by public safety agencies is likely."

It would appear from the criteria developed through the NASAR/ERCP investigation into Emergency Response needs,[1] that such a demonstration project is the first order of business to bring about restructure in the industry.

With the final spectrum determinations from the World Administrative Radio Conference (WARC),[13] it is possible to go forward with the appropriate licensing and technology as needed.

Then, with continued experience from the demonstration project and with the basic effort for a national data base being pushed ahead, these two necessary foundation blocks can come together in the eighties. This will permit the establishment of organizational structure within the previous "ad hoc" emergency response system.

CONCLUSIONS

The following recommendations are made for consideration in establishing the technologic system structure in the Emergency Response Industry:

1. Systems analysis of the functional requirement for emergency communication: Who needs to communicate with whom, when, where, on what subjects and under what constraints.

2. Systems level requirements can now be addressed upon completion of the previous task. Once we know who has to talk to whom and why; we can determine how often they have to talk.

3. Social organization analysis: Organizational needs, with the distiction of operational needs vs. informational and evaluative needs. Since each emergency service provides its own telecommunications planning, the present "system" is a mixture of reluctance to become an actor in the emergency operations "hassle," versus the status of having one's "own" satellite (even if only to be a spectator in the evaluation of the emergency drama).

4. Comparative analysis of systems and mixes of systems must be undertaken to determine which needs identified in steps 1,2, and 3 can be served adequately and economically by terrestrial systems and what indentifiable needs can be served only through the high technology of satellite communication?

5. And finally, we can arrive at that part of the task that is the most fun: The conceptual design of the emergency communications technologic system itself.

Underlying all these tasks is the question: - How much will it cost and how can we arrange the various components of needs and systems so that we can afford the whole?

Once we know the systems needs, costs can be manipulated. Do we need de-code/re-code capability or could that be handled on the ground? What degree of compatibility do we need? Would common FM/SCPC suffice? To increase performance, digital modulation could supply increased noise immunity and each channel could be demodulated and remodulated. Could we perform the switching in the sky with our present size of switch matrix and be commercially viable in the near term?

Obviously, the more of the operation that can be performed in the sky, the cheaper the ground equipment will be. However that means higher technology for the satellite and higher annual cost for operation time on the satellite. If ground-based system control appears feasible and sufficient, then the cost trade-offs between various mixes of ground and space segments can be analyzed. The most successful match of design, cost, and needs can then be achieved.

"Cost" is where we usually start all discussions about new technology. And then we talk only about the cost of the new technology itself. We never talk about what the lack of that technology is presently costing the economy.

The fact that, in 1977 alone, public accidents "cost" the United States 5.4 BILLION dollars or the fact that all accidental deaths (not including injuries) in 1977 "cost" 62 BILLION dollars, are figures with which we, as technical people, are not familiar. Even a small decrease in accidental and catastrophic death brought about by increased command and control through improved communications, would save money. SIXTY TWO BILLION a year buys a lot of satellite technology. The Fairchild/Hiller assessment of operational costs for one satellite system for a 10 year life cycle was $500 Million (or between 40 and 54 million a year).

Let's hope that the appealing self-delusion of Crisis Management can be brought under control without the disastrous results of another Galveston hurricane -- or another San Francisco earthquake, or even another 3 Mile Island. As "logical" beings we should be able, with the above information, to progress to logical satellite technology application for humanitarian response.

REFERENCES:

1. Emergency Response Communications Program, Interagency Committee for Search and Rescue, Washington D.C., November 1979
2. Joseph N. Sivo, Satellite Communications for Disaster Relief Operations, NASA Lewis Research, Cleveland, Ohio, September 1979
3. Quick Reaction Communications, American Satellite Corporation, Germantown, Maryland, June 1979
4. Operational Test and Evaluation, Directorate of Operational Requirements, DCS/Plans, HQ Military Airlift Command, Scott AFB, Illinois, October 1979
5. Report of the Special Inquiry Group, Mitchell Rogovin, Nuclear Regulatory Commission, October 1979
6. Communications Satellite Experiments and Studies Applicable to Mobile Telephone Services, R. Anderson and R. Milton, General Electric Co. and J. Brown, NASA Goddard Space Flight Center, November 1979
7. ATS-6 Users Guide, Goddard Space Flight Center, Greenbelt, Maryland, June 1977
8. Henry Lansford, Mystery of Electrical Storm, "Smithsonian," Washington, D.C., August 1979
9. Organizations In Action, James D. Thompson, McGraw Hill, 1967
10. State Comprehensive Emergency Management, Hilary Whittaker, National Governor's Conference, Washington, D.C., July 1979.
11. James O. Page, J.D., EMS Action, Basking Ridge, New Jersey, 1979
12. Martino, Lenz and Chen, A Forecast of Public Service Satellite Communications, "Satellite Communications," July 1979.
13. Glen O. Robinson, Preparing for WARC-79, "Satellite Communications," September 1979

80-0531 THE EARTH STATION FOR TV-RELAY FROM THE ANTARCTIC CONTINENT

M. Takahashi and S. Mizuarai
Japan Broadcasting Corporation (NHK). Tokyo, Japan
E. Miyata
Kokusai Denshin Denwa Co., Ltd. (KDD). Tokyo, Japan
K. Tsunoda
Nippon Electric Co., Ltd. (NEC). Yokohama, Japan

Abstract

This paper describes the configuration, transportation, installation and operation of an INTELSAT Standard-B type transportable earth station which was used at the Antarctic Continent for TV-relay. The antenna diameter was 10 meters and the RF communication equipment, including the 3-kW HPAs, was housed in specially designed small shelters. The whole station was transported in the cabin of a medium size helicopter from the Japanese icebreaker "Fuji" to the Antarctic base, and was installed in a short period by a limited number of engineers, together with technically inexperienced personnel, under severe climatic conditions. The project was performed successfully.

1. Introduction

Live TV broadcast, for the first time in the world, covered activities of the Japanese Antarctic Research and Expedition team, from Antarctica to Japan and was successfully made in January 1979. Communications by an extremely compact earth station via an INTELSAT IV-A satellite above the Indian Ocean was established. The earth station used was specifically designed for this purpose and met INTELSAT Standard-B specifications. The station was designed aiming at durability against the severe Antarctic climatic conditions, light weight and transportability by a medium-sized helicopter of the type Sikorsky S-61A. An air transportable earth station(1),(2) designed by NEC (Nippon Electric Co., Ltd.) for a single DC-8 class aircraft was modified for this purpose.

The station was installed at Japan's Antarctic "Syowa Base", and the satellite communication link was established with the Yamaguchi earth station operated by KDD (Japan's international communications carrier). The live color TV broadcasts were carried throughout Japan by NHK (Japan Broadcasting Corporation).

2. System Configuration

Fig. 1 and 2 show external views of the 10 meter antenna with radio equipment shelters at the Syowa Base.

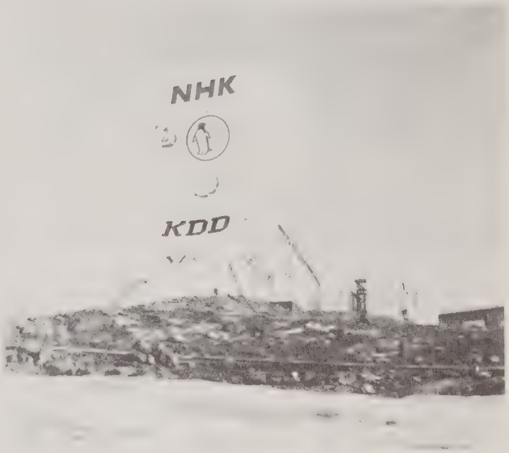

Fig. 1 Front view of the station at the Syowa Base in Antarctica

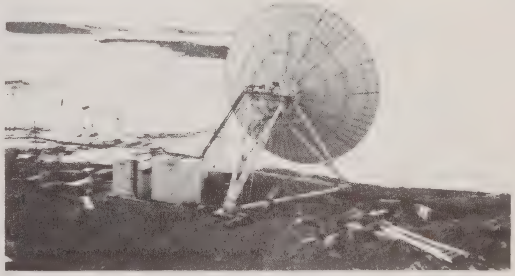

Fig. 2 Back view of the station at the Syowa Base in Antarctica

Copyright © American Institute of Aeronautics and Astronautics, Inc., 1980. All rights reserved.

Design parameters of the earth station installed at the Syowa Base during the summer season are summerized in Table 1. Fig. 3 shows a simplified station block diagram.

The high power amplifier (HPA) for TV video transmissions employed a 3-kW aircooled klystron, and another HPA klystron was used for TV sound and PCM/PSK-SCPC voice communications. No redundant HPA was available for TV transmissions. However, a spare high voltage power supply and parts for all main units of the HPA were provided.

Redundant up-and down converters were provided for TV video and SCPC signal paths. The TV sound equipment was not redundant, but could be replaced by an SCPC shannel if necessary.

TV video reception seemed critical in the Yamaguchi to Syowa Base direction as shown in Table 2 (Link Budget), so the TV receive chain was used for monitoring purposes only.

The main performance of the earth station is shown in Table 3.

Table 1 Design parameters of the earth station

Performance	INTELSAT standard-B specifications
Transmission capacity	TV 1 ch, SCPC including ESC, 3 chs
Antenna diameter	10 meters
LNA noise temperature	42 K (parametric amp.)
HPA output power	3-kW (klystron)
Wind-resistivity	27 m/s (operation possible) 45 m/s (stow position)
Ambient temperature	0 ±10°C
Power requirement	50 kVA, 3-phase, 50/60 Hz
Transportation	Icebreaker and medium size helicopter

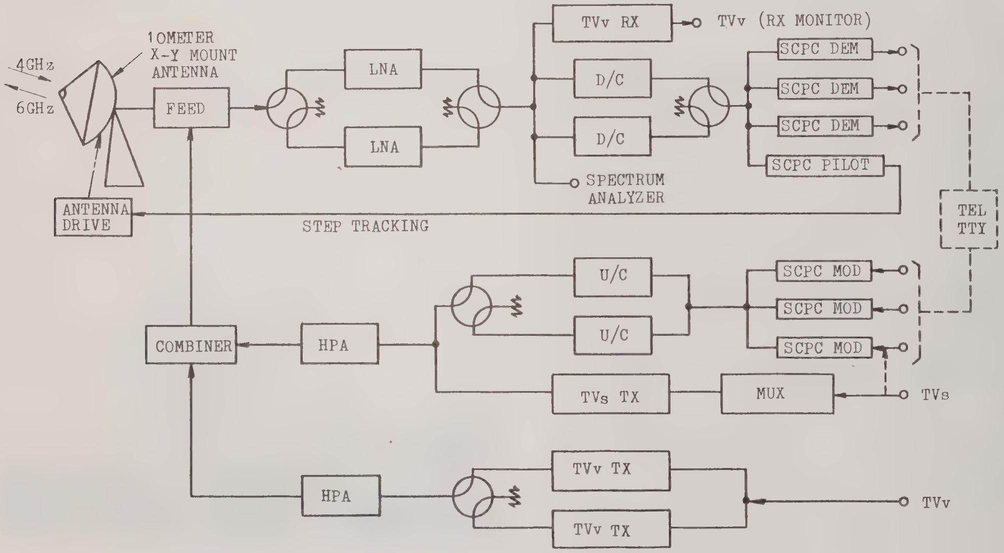
4GHz
6GHz
10METER
X-Y MOUNT
ANTENNA
FEED
ANTENNA
DRIVE
LNA
LNA
TVv RX
TVv (RX MONITOR)
D/C
D/C
SPECTRUM
ANALYZER
SCPC DEM
SCPC DEM
SCPC DEM
SCPC PILOT
STEP TRACKING
TEL
TTY
U/C
U/C
SCPC MOD
SCPC MOD
SCPC MOD
COMBINER
HPA
TVs TX
MUX
TVs
HPA
TVv TX
TVv TX
TVv

Fig. 3 Block diagram of the standard-B earth station installed at the Syowa Base in Antarctica.

Table 2 Link budget

Transmit Carrier / Parameter		Syowa Base → KDD Yamaguchi			Yamaguchi → Syowa	
		TV VIDEO (Half Transponder)	TV SOUND (2.5 MHz)	PCM/PSK -SCPC	TV VIDEO (Half Transponder)	PCM/PSK -SCPC
1. UP LINK $(C/T)_U$	dBW/K	-133.2	-144.5	-156.9	-131.2	-151.4
1) E/S e.i.r.p.	dBW	85.0	73.7	61.3	87.1	66.9
2) Path Loss (6GHz)	dB	-200.6	-200.6	-200.6	-200.7	-200.7
3) Sat G/T	dB/K	-17.6	-17.6	-17.6	-17.6	-17.6
2. SAT. IM $(C/T)_I$	dBW/K	–	-147.2	-164.5	–	-159.0
1) Sat e.i.r.p.	dBW	–	5.4	–	–	–
2) Sat e.i.r.p. Saturation	dBW	–	22.0	–	–	–
3) $(Cs/Nc)_{100kHz}$	dB	–	48.0	–	–	–
3. DOWN LINK $(C/T)_D$	dBW/K	-140.1	-150.7	-163.1	-147.0	-166.5
1) Sat e.i.r.p.	dBW	16.0	5.4	-7.0	18.0	-1.5
2) Path Loss (4GHz)	dB	-196.8	-196.8	-196.8	-196.7	-196.7
3) E/S G/T	dB/K	40.7	40.7	40.7	31.7	31.7
4. OPERATION $(C/T)_T$	dBW/K	-140.9	-153.0	-167.3	-147.1	-167.3
(C/N)	dB	15.7	12.7	15.5	9 5	15.5
(S/N)	dB	47.3	50.8	–	41 1	–
(B.E.R)		–	–	$>1\times10^{-6}$	–	$>1\times10^{-6}$
5. (C/T) THRESHOLD	dBW/K	-147.0	-158.4	-169.3	-148.2	-169.3
(S/N)	dB	41.0	43.0	–	40.3	–
(B.E.R)		–	–	1×10^{-4}	–	1×10^{-4}
6. THRESHOLD MARGIN	dB	6.1	5.4	2 0	1.1	2.0

Table 3 Main performance of the earth station (measured values in the factory)

G/T (10° EL)	32.9 dB/K at 4.0 GHz
Max. EIRP	87.3 dBW at 6.125 GHz
ANT gain	51.4 dB at 4.0 GHz
	54.4 dB at 6.125 GHz

3. Equipment Summary

3.1 Antenna

A limited steerable X-Y mount antenna with step-track equipment was designed specifically for this project. The aperture diameter of the shaped Cassegrain antenna was 10 meters and its main reflector consisted of stretch-formed aluminum alloy panels for a quasi-parabolic surface. The main reflector was divided into 24 panels, and the back-up structure such as center-hub and antenna legs were specifically designed to be contained in the S-61A helicopter cabin.

A pilot signal in the SCPC band from the satellite was used for step tracking of the antenna.

3.2 Low Noise Amplifiers (LNA) (3)

A redundant low noise amplifier was provided at the antenna center-hub, at the back of the main reflector. The nominal noise temperature was 45k in the 4 GHz band at an ambient temperature range of 0 °C to 45 °C. Because of the lower ambient temperature (0 °C ±10 °C) at the Syowa Base during midsummer, the noise temperature was expected to be 3 degrees less, since the temperature of the thermo-electric cooler was reduced from -20 °C to -40 °C for the parametric amplifier. Fig. 4 shows the noise temperature of the LNA for a temperature of -40 °C of the cooler.

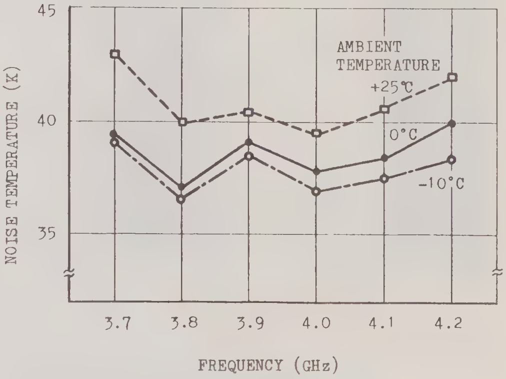

Fig. 4 Measured noise temperature of the 4 GHz LNA

3.3 Equipment Shelters

Particularly small and specially designed shelters were used for the electronic equipment. Requirements for the shelters were as follows:

(i) Compact design to meet transportation constraints,

(ii) Necessity of space for maintenance and operation,

(iii) Simple cabling between shelters,

(iv) Light in weight (less than 2,000 kg including equipment) due to helicopter capacity constraints.

Table 4 Equipment Shelters

Name	Equipment to be contained	Size in meter during transportation	Size in meter during operation	Weight in Kg during transportation
		(D x W x H)	(D x W x H)	
HPA-1 SHELTER	HPA for TV video	1.0 x 1.0 x 2.1	1.9 x 1.0 x 2.1	640
HPA-2 SHELTER	HPA for TV sound and SCPC	1.0 x 1.0 x 2.1	1.9 x 1.0 x 2.1	640
GCE SHELTER	Up and down converters	0.8 x 1.2 x 2.4	2.6 x 1.2 x 2.4	634
CONT SHELTER	Ant tracking unit and Station cont/mon unit	0.9 x 1.2 x 2.1	1.8 x 1.2 x 2.1	770

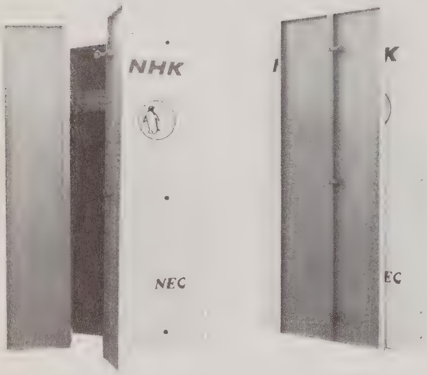

Fig. 5 External view of the equipment shelter
Left: opened for equipment access
Right: closed for transportation

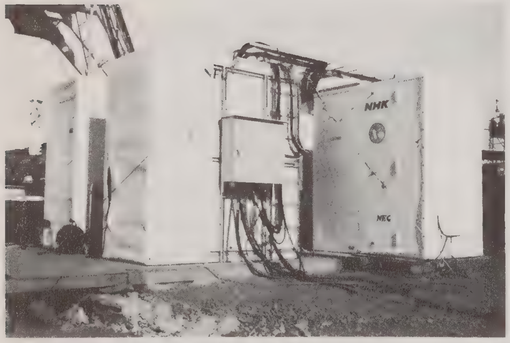

Fig. 6 Installed shelters at the Syowa Base

As a result of investigations, the parameters of the shelters were decided as indicated in Table 4. A total of four shelters were provided. Each shelter had a sliding door, and maintenance space was approximately 1 meter x 1 meter. Fig. 5 and 6 show the external views of a shelter.

4. Transportation

All equipment, including odds and ends, was packaged in wooden crates. The crates were specially designed for easy assembling and disassembling, and were strong enough to withstand rolling of more than ±40° at the 40 to 60° south latitudes, and they furthermore were light enough for air-transportation.

Although the weight of the earth station itself was only about 16 tons, the total gross weight of all crates was about 26 tons as listed in Table 5. The total number of crates was 94. Miscellaneous items included cement, paint, tents, etc.

The crates were transported from Tokyo on board the icebreaker "Fuji" (7760 tons displacement), which carried Japan's 20th Antarctic Research and Expedition team and appropriate supplies. From the "Fuji", iced up 100 km away from the Syowa Base, the crates were delivered to the base by two S-61A helicopters, each with a cabin size of approximately 1. 8(W) x 6. 3(L) x 1. 65(H) meters. Although the weight limit for the helicopter transportation was 2, 000 kg, most crates were kept to below 500 kg for ease of handling. Furthermore, the size of the crates were limited as shown in Fig. 7. A total of 22 flights were made by the two helicopters to carry the 94 crates from the "Fuji" to the Syowa Base. Fig. 8 shows external views of the S-61A helicopter and a scene of unloading an antenna panel from the helicopter.

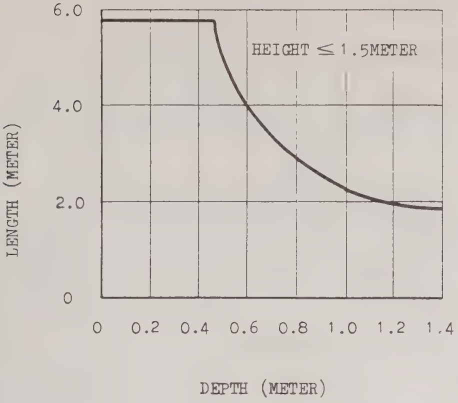

Fig. 7 Limit of crate which can be contained in the S-61A helicopter cabin.

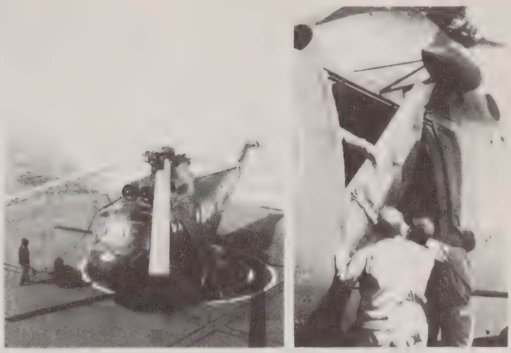

Fig. 8 S-61A helicopter and scene of unloading an antenna panel

Table 5 Packing list

	Item	Number of Crates	Net Weight (kg)	Gross Weight (kg)	Crates Volume (m^3)
1	Antenna	37	8,849	12,324	62.02
2	Equipment Shelters	4	2,684	3,384	13.24
3	Klystrons including a spare	3	165	306	1.35
4	Other Communication Equipment	19	2,459	3,312	11.89
5	Measuring Equipment	10	526	885	5.38
6	Installation Materials	11	2,377	2,913	10.10
7	Tools	1	300	366	1.43
8	Spare Parts	3	440	562	1.38
9	Miscellaneous	6	1,860	2,064	6.08
Total		94	19,660	26,116	112.87

NOTE: Item 4 includes the equipment to be installed in the shelters (Item 2).

5. Installation

The Syowa Base is located at a rocky slope, and the earth station site was selected at the east part of the Base where the terrain was rather flat (Fig. 9). The elevation angle to the satellite was approximately 10.7 degrees.

The construction of the earth station took place in the severe Antarctic weather. Though it was mid-summer, frozen snow on the antenna often interrupted the work. The installation team totalled four persons, comprising one NHK, one KDD and two NEC engineers. In addition, members of the scientific wintering team and the ship's crew-members participated. Two installation teams worked from 0800 to 1700 and from 1700 to 2400 hours. Each team comprised 9 persons. Outdoor installation was continued round-the-clock, since the sun never set. The main problems encountered during the antenna installation were lack of time, slow progress due to low temperatures and corresponding need for thick clothings, and unfamiliarity of working in elevated places for most of the personnel. Only one of the NEC engineers had some previous experience in erection of antennas and only a light-duty 5 tons mobile crane was available.

The installation of the antenna and equipment took five days and was completed on January 10, 1979. The TV studio equipment together with the SCPC terminal and supervise/monitoring equipment, was housed in an already existing shelter about 30 meters away from the antenna. Engine generated power was already available at the Showa Base.

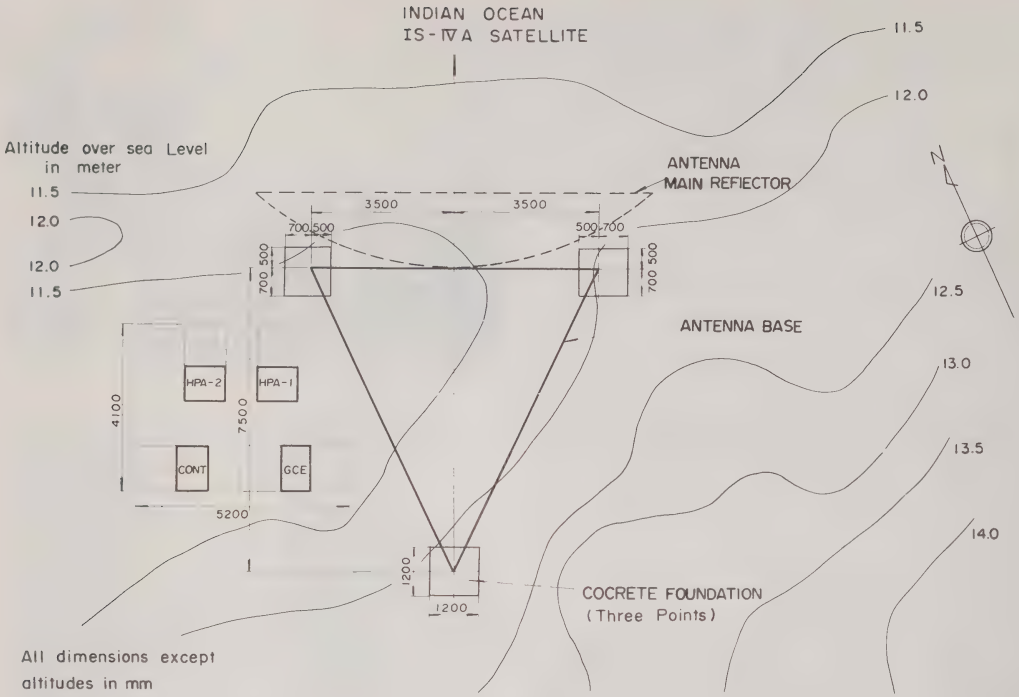
INDIAN OCEAN
IS-ⅣA SATELLITE
11.5
12.0
Altitude over sea Level in meter
11.5
12.0
12.0
11.5
ANTENNA MAIN REFIECTOR
3500
3500
700
500
500
700
700
500
700
500
N
ANTENNA BASE
12.5
13.0
13.5
14.0
HPA-2
HPA-1
4100
7500
CONT
GCE
5200
1200
1200
COCRETE FOUNDATION (Three Points)
All dimensions except altitudes in mm

Fig. 9 Layout of antenna site of the Syowa Base

6. On-site testing

Adjustments of the earth station, including antenna surface accuracy, was started on Jan. 11, 1979. On the night of Jan. 14 adjustments of the receiving chains were finished, and the satellite beacon carrier was acquired on the first try, by pre-setting the antenna direction. That was a rare success since several hours are normally necessary to lock on to the satellite.

Alignment of the reflector surface and subreflector position was made by using the INTELSAT IV-A beacon signal, and the electronic equipment was adjusted and tested at the same period.

The initial coordination circuit from the Syowa Base to KDD Yamaguchi was short wave to "Fuji", and MARISAT from "Fuji" to Yamaguchi.

Mandatory INTELSAT Standard-B verification tests were completed by January 19, and line-up tests with the KDD Yamaguchi earth station were finished on January 22.

Applicable link parameters are listed in Table 2, and the result of TV video signal quality is shown in Table 6.

Table 6 Result of TV video quality tests

	Syowa Base → IS-IV A → KDD Yamaguchi	Syowa Base → IS-IV A → Syowa Base
S/N	49 dB	41.3 dB
DG	< 5 %	-
DP	2°	-

NOTE:

Syowa Base Earth Station: STD-B, EL=10.7°

KDD Yamaguchi Earth Station: STD-A, EL= 9°

7. Operation

The three SCPC channels were used for order wire communications between the two earth stations, coordination between the Syowa Base and the NHK Tokyo studio, and as an audio back-up channel.

The historical live TV relay from the Antarctica was broadcast, for the first time in the world, throughout Japan in the early morning of January 28, 1979. It brought a new era in telecasting technique, and continued intermittently until February 3.

There was no interruption of the communications during the period by any causes. The maximum measured instantaneous wind speed was 21 m/s, and the maximum and minimum temperature of the atmosphere was +9.1 °C and -8.2 °C, respectively. Approximately 3 dB receiving level degradation was measured due to snow and ice on the antenna surface. The ice was removed by hot jet water.

Table 7 Schedule

Month, Day	Description	Note
Nov. 25 (1978)	Departure from Tokyo, Japan by icebreaker "Fuji"	
Jan. 5 (1979)	Airtransportation of crates. Total weight of the crates was 29.5 tons including 3.5 tons of broadcating equipment.	22 flights of helicopter, 100 km away
Jan. 6 Jan. 10	Installation of the earth station, including 10 meter diameter antenna	180 man-days for 5 days
Jan. 11 Jan. 17	Adjustment of the earth station including antenna surface accuracy	117 man-days
Jan. 19 Jan. 22	Verification of INTELSAT and SSOG tests	
Jan. 22	Start of operation of the earth station	
Jan. 28 Feb. 3	Live TV boradcast from Antarctica to Japan	
Feb. 3 Feb. 6	Disassembly and airtransportation	24 flights of helicopter, 80km away. 66 man-days
Apr. 20	Arrival in Tokyo, Japan by icebreaker "Fuji".	

8. Schedule

The implementation schedule of this project is summerized in Table 7. The icebreaker "Fuji" was 100 km away from the Syowa Base on Dec. 29, 1978. Unfortunately, air transportation of equipment was delayed until Jan. 5, 1979 due to bad weather. From then on, however, the schedule proceeded smoothly without major problems. The project was also fortunate in the sense that no injuries or sickness were encountered.

9. Conclusion

It has been verified that all earth station equipment of an INTELSAT Standard-B type can be transported by a midium-size helicopter, and that the antenna can be erected in five days by a team where only one person has previous experience. The climatic conditions under which the station was installed and operating was rather severe. Furthermore, the earth station equipment has made a 30,000 km round trip without any degradation.

The successful outcome of the Antarctic challenge, including helicopter transportation, coupled with the fact that all the equipment of a Standard-B type earth station easily fits into a cargo plane of the type DC-8/ Boeing 707 at one time, has proved that reliable voice and TV communications can be established efficiently and quickly from practically anywhere in the world.

Acknowledgement

Numerous people have contributed in one way or another to this project.

However, special thanks are due to members of the Japanese Antarctic Research and Expedition team, and crew members of the icebreaker "Fuji", for the transportation and installation of the earth station.

The authors also wish to extend an appreciation to the many staff members at the NHK, KDD and NEC, who participated in this project, for their advice and cooperation.

REFERENCES

(1) S. Soma, K. Yoda and K. Tsunoda, "A Transportable Earth Station in 4/6 GHz Band", Tech. Group on Commun. System, Inst. Electr. and Commun. Engrs. of Japan, Paper CS74-173, Feb., 1975.

(2) S. Soma, K. Yoda, and K. Tsunoda, "A Transportable Earth Station", Paper for Radio Research Board Symposium on Satellite Communications for Australia May, 1974.

(3) M. Kajikawa, H. Hayashi and H. Shioya, "Low Noise Parametric Amplifiers", Paper for Radio Research Board Symposium on Satellite Communications for Australia May, 1974.

80-0532

DESIGN AND PERFORMANCE OF 30/20 GHZ BAND EARTH STATIONS FOR DOMESTIC SATELLITE COMMUNICATION SYSTEM

Hiroaki FUKETA Minoru KURAMOTO Takeo INOUE and Haruhiko KATO

Yokosuka Electrical Communication Laboratory,
Nippon Telegraph and Telephone Public Corporation
1-2356, Take, Yokosuka-shi, Kanagawa-ken, 238-03 JAPAN

Abstract

High performance hardwares for K-band (30/20 GHz) earth stations, e.g. 300 watts output power and 200 MHz bandwidth 30 GHz high power amplifiers, 80 K noise temperature and 2.5 GHz bandwidth low noise amplifiers, etc., have been newly developed. Two K-band earth stations were constructed for experiments using Medium Capacity Communications Satellite for Experimental Purpose "CS". Presented here are K-band fixed earth station design methods, basic sub-systems performance, and experimental results using CS.

Introduction

A medium capacity domestic satellite communications system has been under development by Nippon Telegraph and Telephone Public Corporation (NTT). One of the main missions of this system is to provide circuit relief after failure of terrestrial transmission systems. This is accomplished by using K-band fixed earth stations installed on roof top of telephone offices which correspond to regional centers in the overall Japanese telephony hierarchy.

Selection of the K-band was made after taking into considerations; that (1) radio interferences between terrestrial radio relay systems and satellite communication systems are slight, and that (2) a wide bandwidths of 3.5 GHz are alloted for satellite communications. In the K-band, radio wave attenuation due to rainfall is so severe that it is important to raise margins of the EIRP and G/T of the earth station.

Yokosuka Electrical Communication Laboratory of NTT (YECL) has been conducting researches on K-band earth station equipments since 1967. In 1972, a water-cooled 26 GHz high power amplifier(1) and 18 GHz band low noise amplifier(2) cooled by liquid helium were developed. An experimental K-band earth station(3) was constructed in 1972 by integrating the above mentioned technologies. This earth station is the first K-band earth station for communications purposes in the world. Since 1972, improvement of earth station hardware performance, e.g. output power, noise temperature, gain flatness, group delay, VSWR, weight, size and reliability, has been continuing. To evaluate the total system performance through "CS"(4) lounched in 1977, NTT constructed two new experimental earth stations using the technologies established by the above mentioned research since 1967.

This paper describes the novel design considerations and main characteristics of the newly developed K-band fixed earth stations, including the main communication sub-systems, which obtained satisfactory results.

NTT Medium Capacity Domestic Satellite Communications System Outline

Nippon Telegraph and Telephone Public Corporation plans to put the medium capacity domestic satellite communications system into commercial use in 1983. In this system, two spin stabilized-satellites, i.e. prime and orbital redundant satellites, simular to "CS", will be used. Each satellite with a shaped beam antenna, will have six K-band and two C-band transponders. The system outline is shown in Table 1. The K-band fixed earth stations are used for two missions, i.e. "Communication between fixed earth stations", and "communication between small transportable earth stations and a fixed earth station (type A)". Both communication systems are to provide network relief after failure of transmission lines due to natural disasters, e.g. earthquakes, storms.

Table 1 NTT Medium Capacity Domestic Satellite Communications System Outline

	Communication between Fixed Earth Stations	Communication between Remote Island & Mainland Earth Stations	Communication between Small Transportable Earth Station & a Fixed Earth Station		
			(type A)	(type B)	(type C)
Frequency	30/20 GHz	6/4 GHz	30/20 GHz	6/4 GHz	6/4 GHz
Transmission mode	TDMA	TDMA	FM	FM	FM
Transmitting capacity	1920 two-way TP	192 two-way TP 2 color TV	132 two-way TP	60 two-way TP	1 color TV
Transponder number	4	1	1	1	
Earth Station	Small Earth Station with 11.5 m antenna	Small Earth Station with 10m antenna	Vehicle mounted transportable 2.7 m antenna	Vehicle mounted transportable 3 m antenna	Vehicle mounted transportable 3 m antenna

Copyright © American Institute of Aeronautics and Astronautics, Inc., 1980. All rights reserved.

The TDMA-60M [5] system was adopted for communication between fixed earth stations. This system can transmit 960 one-way voice channels per transponder. In the communication between small transportable earth stations and a fixed earth station, the K-band fixed earth station is used as a base station. A small transportable earth station is composed of an antenna system and two containers which can be easily transported by truck or helicopter.

Experimental K-band Fixed Earth Stations Configurations

Two experimental fixed earth stations were constructed for CS experimental use. One is constructed in YECL which is located about 60 km south of Tokyo i.e. the Yokosuka Earth Station. Another was installed in a NTT telephone office in Sendai about 300 km north of Tokyo, i.e. the Sendai Earth Station. The fundamental configurations of the two earth stations are the same as commercial earth stations. An example of the Sendai earth station configuration is shown in Fig.1.

The RF transmitting system is composed of transmitting frequency converters, 30 GHz high power amplifiers (HPA), and a transmitting channel multiplexer. The IF signals are transmitted to transmitting frequency converter through low loss coaxial cable.

The RF receiving system is composed of two low noise amplifiers (LNA) i.e. prime and stand-by amplifiers, and receiving frequency converters. Receiving signals (six channels) are commonly amplified by an LNA. Each amplified signal frequency is converted to IF(1.7 GHz) and transmitted to the TDMA equipment and FM MODEMs etc. through IF switching equipment and the coaxial cable.

The antenna tracking system is composed of a tracking receiver and an antenna controler.

The photographs of experimental K-band fixed earth stations are shown in Fig.2.

Fundamental Design Considerations

Design Objectives of the K-band Fixed Earth Stations

The following items are considered;

(1) stations should be as simple as possible so as to facilitate installation in telephone offices,

(2) stations should be of high mechanical strength so as to withstand earthquakes, storms etc.,.

(3) systems availability should be larger than 99.5 % in communications between every earth station including earth station equipment availability. System availability is limited by rain attenuation, ground segment and space segment availability. Availability objectives for rain attenuation was set at 99.6 %. Thus, earth station EIRP and G/T had to be larger than 91 dBW and 44 dB/K, respectively. Design objectives of K-band fixed earth stations are shown in Table 2.

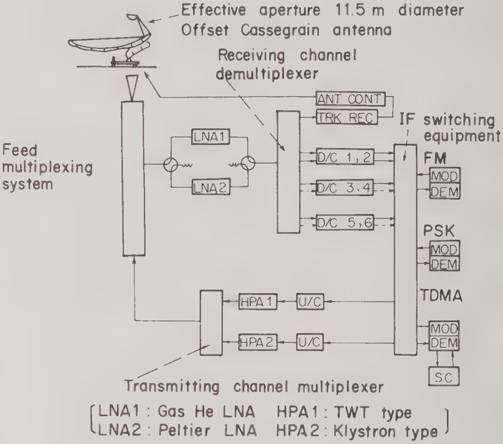
Effective aperture 11.5 m diameter
Offset Cassegrain antenna
Receiving channel demultiplexer
ANT CONT
TRK REC
IF switching equipment
Feed multiplexing system
LNA1
LNA2
D/C 1,2
D/C 3.4
D/C 5,6
FM
MOD
DEM
PSK
MOD
DEM
TDMA
HPA1
U/C
HPA2
U/C
MOD
DEM
SC
Transmitting channel multiplexer
LNA1 : Gas He LNA HPA1 : TWT type
LNA2 : Peltier LNA HPA2 : Klystron type

Fig. 1 Experimental K-band Fixed Earth Station Configuration (Sendai Earth Station).

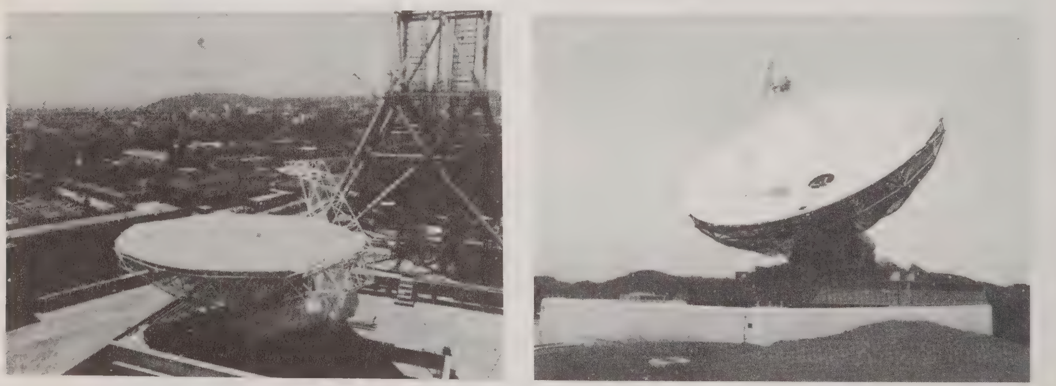

(a) Sendai Earth Station

(b) Yokosuka Earth Station

Fig 2. Photographs of Experimental Fixed Earth Stations.

Antenna Sub-system Design

The K-band earth station antenna has many remarkable features distinguishing it from conventional earth station antennas for C-band international satellite communication systems. Communication system requirements for an earth station antenna are as follows:

(1) Gain : In K-band, a radio wave suffers rain attenuation. Therefore, antenna gain is required to be as high as possible. Antenna gain objectives were 69 dB and 66 dB, in 30 GHz and 20 GHz band, respectively.

(2) Bandwidth : Both the 20 and 30 GHz band have a 3.5 GHz bandwidth. This is seven times as wide as that of the C-band communication system.

(3) Sidelobe levels : In Japan, satellite down path and terrestrial radio relay frequency commonly use the 20 GHz band. To avoid interferences between systems, low sidelobe directivity is required over a wide angle range.

(4) Installation on a building : The earth station antenna is installed on the roof top of telephone office building. Therefore, the antenna structure should be light, compact, wind resistant, and amenable to various installation requirements.

(5) Mechanical requirements : High mechanical accuracy for mounting main reflector panels and for reflector axis alignment is required in K-band. This requirement is also necessary to ensure electrical performance without use of a collimation tower, which can not be constructed in large cities.

(6) Tracking accuracy : A precise satellite tracking system is required due to the sharp beamwidth.

For earth station antennas satisfying the above mentioned requirements, the following two types of antennas have been developed :

(1) Axisymmetrical Cassegrain antenna (6)
(2) Offset Casegrain antenna (7)

Table 2 Design Objectives of Experimental K-band Fixed Earth Station.

Simulteneous transmitting RF channel numbers	2 channels (feasible to access all channels of CS)
Simulteneous receiving RF channel numbers	6 channels(Yokosuka Earth Station) 4 channels(Sendai Earth Station) (feasible to receive all signals from CS)
EIRP	above 91 dBw
G/T	above 44 dB/K
Antenna gain	above 69 dB (30 GHz band) above 66 dB (20 GHz band)
Bandwidth	200 MHz/CH

The axisymmetrical Cassegrain antenna was installed at the Yokosuka Earth Station. The offset Cassegrain antenna was installed at the Sendai Earth Station.

The vernier auto-track system (VAT) was adopted to antenna tracking because of high tracking accuracy and low transmission loss. A phase locked narrow bandwidth beacon receiver (5 kHz bandwidth) has been developed to keep the rainfall attenuation margin above 40 dB. Antenna tracking sub-system performances are shown in Table 3.

RF Sub-systems

[1] Arrangements

To obtain the higher EIRP and G/T, it is necessary to reduce waveguide loss between HPA and LNA and the antenna feeding system. Several possible HPAs arrangements, (a) tandem arrengement, (b) radial arrangement and (c) back-to-back arrangement, are shown in Fig. 3. In (c), HPAs can be more closly connected than with the other two arrangements. Cosequently, the back-to-back arrangement was adopted. The HPAs and LNAs are directly connected to the feeding system as shown in Fig. 4.

Table 3 Antenna Tracking Sub-system Performances.

Item	Performances	
	Offset Cassegrain Antenna	Axisymmetrical Cassegrain Antenna
Tracking method	VAT	VAT
Antenna mount method	Az-El	X-Y
Antenna driving method	limited steerable driving by two jack-screws	same as left
Tracking accuracy	0.01 °rms & less (average wind velocity 25 m/s & less)	0.01 °rms & less (average wind velocity 20 m/s & less)
Tracking receiver receiving frequency	19.45 GHz ± 2 MHz	same as left
Threshold level	-132 dBm(LNA input)	same as left
Consumed power	3.3 kVA & less	5 kVA & less

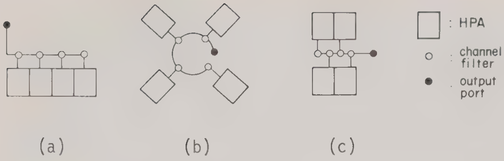

(a) : Tandem arrangement
(b) : Radial arrangement
(c) : Back-to-back arrangement

Fig. 3 High Power Amplifier Arrangements.

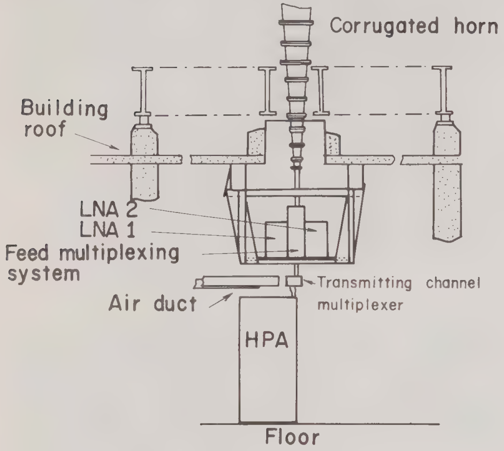

Fig. 4 RF Equipment Arrangement of Experimental K-band Fixed Earth Station.

[2] High Power Amplifier Design

Three hundred watts output power transmitters were necessary to achieve a 91.0 dBW EIRP. Two types of high power amplifiers were developed, i.e. TWT and klystron types. Researches on HPAs were put emphasis on realizing high effective output power, a wide bandwidth, simplification, and high stability performance.

(a) HPA output circuit

To reduce waveguide loss, rational methods of arc detection, i.e. arc detector position and numbers, reduction of high power circulator loss, etc. were investigated. Before designing an RF output circuit, experiments on arc discharge in a waveguide were carried out for tube protection circuit design. Through the these experiments, arc photo-detector numbers and optimum position were determined. The arc which is produced in the antenna feeding system can be detected by monitoring reflected RF power at HPA output port. Therefore, the tube protection circuit could be simplified and output circuit loss was reduced by 1.5 dB, compared with the water cooled HPA(1) developed in 1972. A simplified RF circuit block diagram and circuit loss are shown in Fig. 5. Output RF circuit loss is about 1.0 dB.

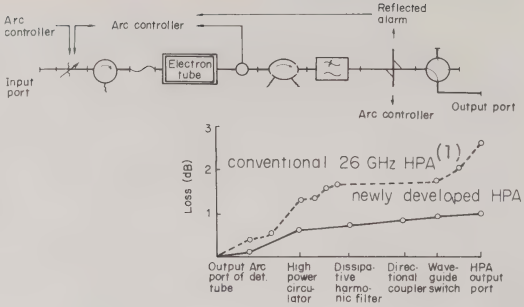

Fig. 5 High Power Amplifier RF circuit and Measured Loss Value.

(b) forced air cooling

The most effective air cooling system for realizing a simplified and compact HPA was sought. A 750 watts blower was selected under the conditions that collector temperature was to be maintained below 160°C. Moreover, to suppress noise below 65 phone 1 meter apart from the HPA, hermetical sealing for air cooling system was employed.

(c) TWT HPA configuration

The RF circuit of TWT(8) is the coupled cavity type with three sections severed by carbonized bereyllia. High gain and stable characteristics are accomplished. Beam focusing is done by solenoide type electro-magnet.

The TWT HPA is composed of an amplifier and a power supply bay. In the amplifier bay, a TWT, a blower, low loss RF circuit and a low voltage power supplies are mounted and in the power supply bay, high voltage power supplies (collector and body voltage) are mounted. To realize a simplified and compact HPA, simple power supply configurations were sought. Body voltage is given by DC/DC converter. The DC/DC converter chopping frequency was raised to 10 kHz and input voltage, i.e. three phase 200 volts, is stabillized by SCR. In this power supply, the high voltage supply was shielded with teflon and resin order to the utilization efficiency. As a result, small-sized power supply could be accomplished. Amplifer frequency of TWT HPA can be electronically shifted over 3.5 GHz by changing the body voltage. The whole CS frequency range can be covered by one kind of TWT.

(d) Klystron HPA configuration

Six-cavity klystron has been newly developed Beam focusing is done by parmanent magnet. The resonant frequency of each cavity is controlable by adjusting the short plunger in the cavity. This mechanism offers rapid and precise changes in channel selection over 1.5 GHz by using the microproccessor control, Therefore, the whole CS frequency range, i.e. 2.5 GHz can be covered by two kind of klystrons. Automatic power control, which responcse to high spped level changing as the burst signal used in TDMA system, was adopted.

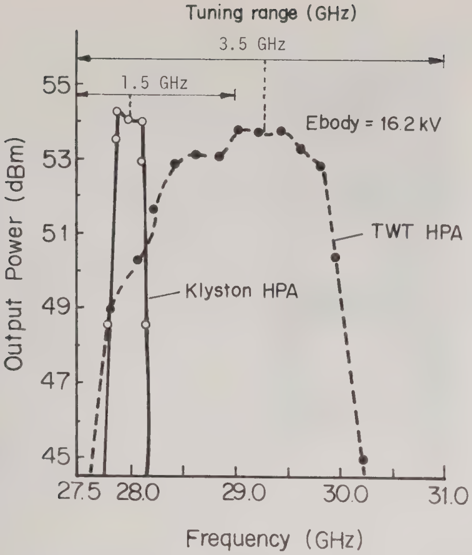

Fig. 6 Typical HPA Frequency Responces.

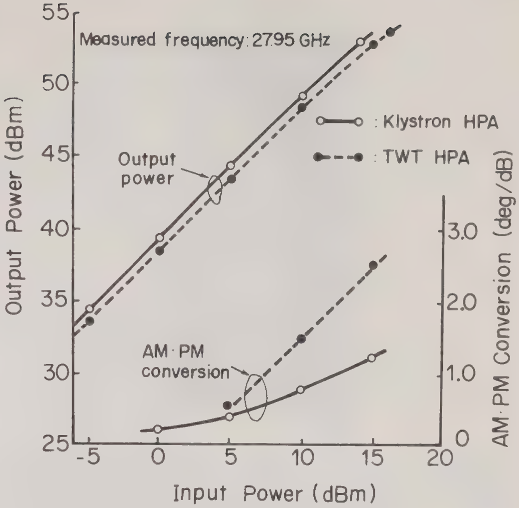

Fig. 7 Typical HPA Characteristics.

Table 4 HPA Performance Summary.

	Design objectives		Measured results	
	TWT HPA	Klystron HPA	TWT HPA	Klystron HPA
1 dB bandwidth	200 MHz		200 MHz	200 MHz
Center frequency tuning range			3.5 GHz	1.5 GHz
Output power	200W/200MHz	200W/200MHz 300W/150MHz	200W/200MHz	200W/200MHz 300W/150MHz
Harmonics level	-45 dB & less		-60 dB	-70 dB
AM/PM conversion coefficient	5 °/dB & less		4 °/dB max	2.2 °/dB max
Noise figure	32 dB & less	47 dB & less	28.5 dB	44.3 dB
Cooling method	Forced air cooling		same as left	
Consumed power			8.2 KW	6.4 KW

Measured power frequency responces of TWT and klystron HPAs are shown in Fig. 6. Output power and AM/PM conversion characteristics are shown in Fig. 7. Communication band-width are more than 200 MHz for both HPAs. A summary of the HPA electrical performances is given in Table 4. Photographs of TWT and klystron HPAs are shown in Fig. 8 and Fig. 9.

[3] Low noise amplifier (LNA) designs

Low noise temperature (100 K), wide bandwidth (2.5 GHz for CS), wide linearlity range, and easy maintenance are required for LNA. Two LNA types have been developed. One is a gas helium cooled parametric amplifier. The other is a Peltier effect cooled parametric amplifier. In this experimental earth station, the gas helium cooled parametric amplifier is employed as the prime LNA and the Peltier effect cooled parametric amplifier as the stand-by LNA. In the helium gas cooling system, maintenance is required about once a year. The Peltier effect cooled parametric amplifier was adopted as a stand-by LNA because maintenance is very easy.

The receiving G/T, when using the stand-by LNA, decreases by 1.5 dB during rainy periods with a 10 dB down-path loss. However, it is felt that the overall periods over which stand-by LNAs are used is very short in comparison with prime LNAs and that such periods seldom coincide with periods of heavy rainfall. Therefore, total system availability degradation is negligible.

The parametric amplifier was designed considering the following points ;

(a) low noise operation
(b) wideband operation
(c) realization of small-sized equipment and high reliable performance.

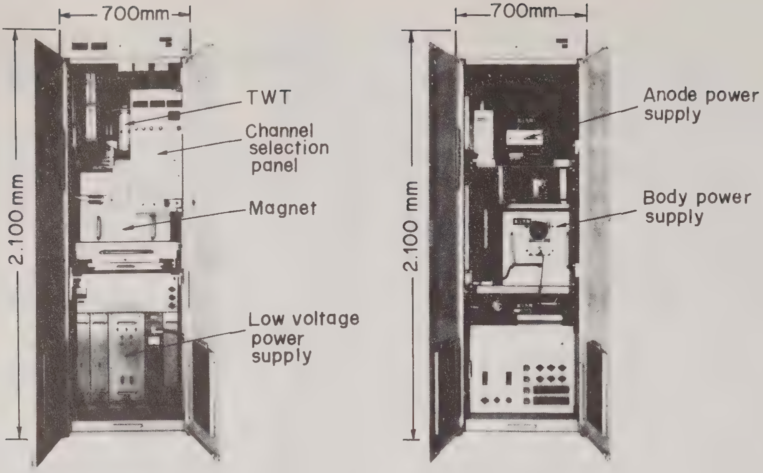

Amplifier section (including low voltage power supply)

High voltage power supplysection

Fig. 8 TWT High Power Amplifier.

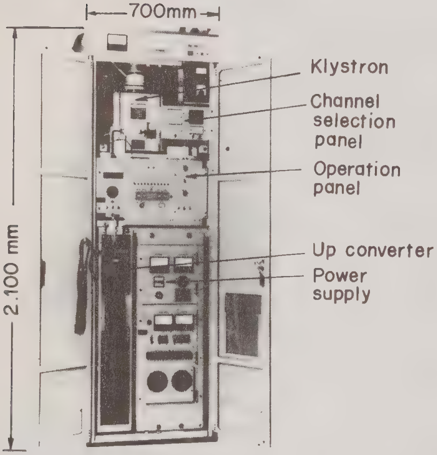

Fig. 9 Klystron High Power Amplifier.

(a) low noise operation : Optimum diode parameters and packaging methods were investigated to obtain low noise performances. Parametric amplifier noise temperature is given by Eq. 1. The higher dynamic Q, the lower T_{e0} becomes. High dynamic Q GaAs Schottky barrier varactor diode in a minidot package were newly developed. Dynamic Q of the varactor is about 4 at 20 GHz. Thus, optimum pumping frequency is 80 GHz from Eq. 1 :

$$\frac{T_{e0}}{T_s} = (1-1/G)\ \frac{Q^2(f_1/f_2)^2+1}{Q^2(f_1/f_2)-1} \qquad (1)$$

where,

T_{e0} : noise temperature,

T_s : junction temperature,

Q : dynamic Q at fl,

f_1 : input signal frequency,

f_2 : idler frequency,

G : gain.

The parallel resonant frequency of the minidot type package used in this amplifier, is about 57.6 GHz. By using this frequency as the idler frequency, pumping frequency is about 76.5 GHz. This is nearly equal to optimum pumping frequency giving the lowest noise temperature. Furthermore, the parametric amplifiers are cooled by helium gas or Peltier effect devices.

(b) wideband operation : Two methods were tried to realize the wideband characteristics. One is employment of double tuned characteristics using new half wave length resonant type input signal circuit between the input port and varactor mount. By this method, a one-stage parametric amplifier[9] with a 2 GHz bandwidth was developed. Another method is to spread the bandwidth by connecting two or more of the above wideband parametric amplifiers in cascade. Noise characteristics depend almost entirely upon the first and second stage amplifier noise characteristics. The higher the frequency, the higher noise temperature becomes. Therefore, the second stage center frequency was set to the lowest frequency to get the inverse characteristic to the first stage. Consequently, the frequency response of both noise temperature and gain become almost flat.

(c) Realization of small sized equipment and high reliable performance : GaAs MES FET amplifiers were used as post amplifiers to accomplish a reduction of amplifier stages. Pumping source is composed of high reliable solid-state circuit. The LNA configuration is shown in Fig.10. The prime LNA consists of two stage parametric amplifiers and four stage GaAs FET amplifiers. The parametric amplifiers and the former two stage FET amplifiers were cooled to about 20 K by adiabatic expansion of helium gas. The stand-by LNA is the same configuration as the prime LNA except that the parametric amplifiers are cooled to about -50°C by Peltier effect devices. The FET amplifiers operate at room temperature. The pumping power source of both the prime and stand-by amplifiers are composed of 80 GHz IMPATT diode oscillator stabillized by a high Q cavity and IMPATT injection locked amplifiers.

Amplitude frequency responces of the helium cooled and Peltier effect cooled LNAs are shown in Fig. 11. Performance characteristics of the LNAs are outlined in Table 5. These characteristics satisfied design objectives. A photograph of the LNA is shown in Fig. 12.

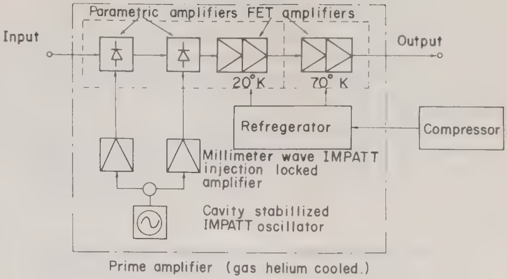
Parametric amplifiers
FET amplifiers
Input
Output
20°K
70° K
Refregerator
Compressor
Millimeter wave IMPATT injection locked amplifier
Cavity stabillized IMPATT oscillator
Prime amplifier (gas helium cooled.)

Fig. 10 Low Noise Amplifier Configuration.

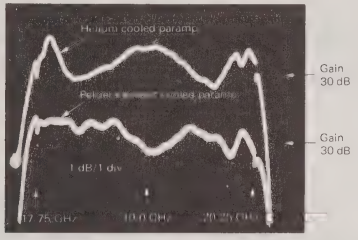

Upper : Gas Helium Cooled LNA
Lower : Peltier Effect Colled LNA

Fig.11 Frequency Responces of LNAs.

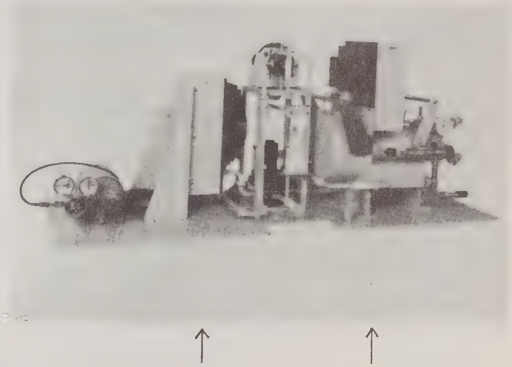

Petier Effect Cooled LNA

Gas Helium Cooled LNA

Fig. 12 Low Noise Amplifier.

Table 5 Low Noise Amplifier Main Characteristics.

	Design objectives	Measured results
Bandwidth	2.5 GHz(17.75-20.25 GHz)	2.5 GHz(17.75-20.25 GHz)
Noise temperature	100 K & less (Gas helium cooled.)	80 K & less (Gas helium cooled.)
	270 K & less (Peltier effect cooled.)	220 K & less (Peltier effect cooled.)
Gain	30 dB & more	33 dB & more
Gain deviation	±1 dB & less	±1 dB & less
Group delay deviation	±1 ns & less	±1 ns & less
Input & output VSWR	1.2 & less	1.2 & less

[4] Other communication sub-systems

(a) transmitting frequency converters

This equipment is used to convert IF to 30 GHz band frequency signal which has high power enough to drive HPA. Amplitude and delay equallizers for the transponder are used in IF stages. Three stage IMPATT stable amplifiers are used in the final stage.

(b) receiving frequency converters

This equipment is used to convert the 20 GHz receiving signal to IF signals. Signal peak detected automatic gain control suitable for TDMA signals are used.

EIRP and G/T Measured Results of Experimental K-band Fixed Earth Stations

Performances of the experimental K-band fixed earth stations were measured. Measured EIRP, G/T and circuit loss of the Sendai Earth Station F3/f3 channel is shown in Table 6. Obtained results satisfied the design objectives shown in Table 2.

Table 6 EIRP and G/T Measured Results of Sendai Earth Station(F3/f3 channel).

	Transmitting system (28.55GHz)	Receiving system (18.75GHz)
Antenna gain(dB)	69.2	65.9
Feed multiplexing sytem loss (dB)	0.29	0.54
Channel multi-& demultiplexer loss (dB)	1.26	1.85
Output power(dBW)	24.8	
System noise temperature (K)		125
EIRP (dBW)	92.5	
G/T (dB/K)		44.4

Experimental Results through "CS"

[1] C/N_0 characteristics

Carrier power to noise power density : C/N_0 through "CS" were measured using the Sendai and Yokosuka earth stations. Measured C/N_0 and calculated C/N_0 are shown in Table 7. Differences between measured and calculated C/N_0 values were less than 1 dB.

Required C/N_0 of TDMA-60M system is 86.7 dB Hz (BER:1×10^{-4} with error correction). Therefore, margins of the up and down path, taking C/N_0 degradation due to spin into account are 17.0 dB and 12.3 dB, respectively (including the inreasing the sky noise temperature). These margins correspond to unavailability of 0.1 % and 0.05 % in Sendai, respectively.

[2] Transmission characteristics

Frequency responces through CS using the Yokosuka earth station is shown in Fig. 13 under condition that an equalizer is used. deviation of amplitude and group delay are 1 dB and 2.4 ns in the $f_0 \pm$ 70 MHz range, respectively.

Bit error rate performance through "CS" using the Sendai Earth Station and the Yokosuka Earth Station is shown in Fig. 14. The C/N degradation at an average bit error rate of 10^{-4} is about 2 dB from theoritical value, and about 1 dB from TDMA IF loop back measured results.

Conclusion

Newly developed K-band fixed earth stations and their RF sub-systems were described with satisfactory measured performances and feasibilities of 30/20 GHz satellite communication systems were proved. The developed earth stations are the first ones in the world for communication purposes.

It is felt that the newly developed technologies in this paper contribute to the growth of 30/20 GHz band satellite communication systems in the world.

Table 7 Comparisons of Measured C/N_0 with Calculated C/N_0.

dB·Hz

		F1/f1	F3/f3	F4/f4	F5/f5
Sendai→Sendai	Measured	101.6	101.5	102.2	101.8
	Calculated	101.3	102.2	101.8	102.4
Yokosuka →Yokosuka	Measured	99.6	100.1	99.9	100.2
	Calculated	100.2	101.0	100.6	100.5
Sendai→Yokosuka	Measured	99.5	100.1	100.5	100.9
	Calculated	100.3	101.1	100.7	101.2
Yokosuka →Sendai	Measured	100.2	101.3	101.4	101.2
	Calculated	101.2	102.0	101.6	101.6

Output power : 100 W, fine day
Sendai : Gas helium LNA   Yokosuka : Peltier LNA

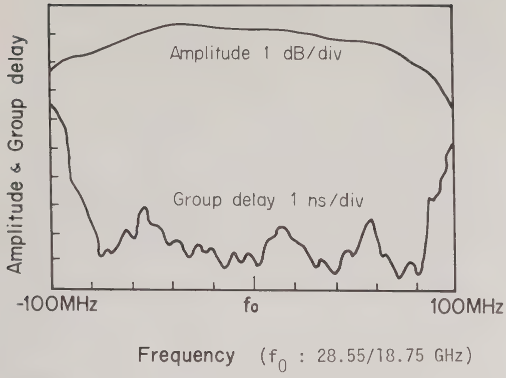

Fig. 13 Frequency Responce through CS (Earth Station : Yokosuka)

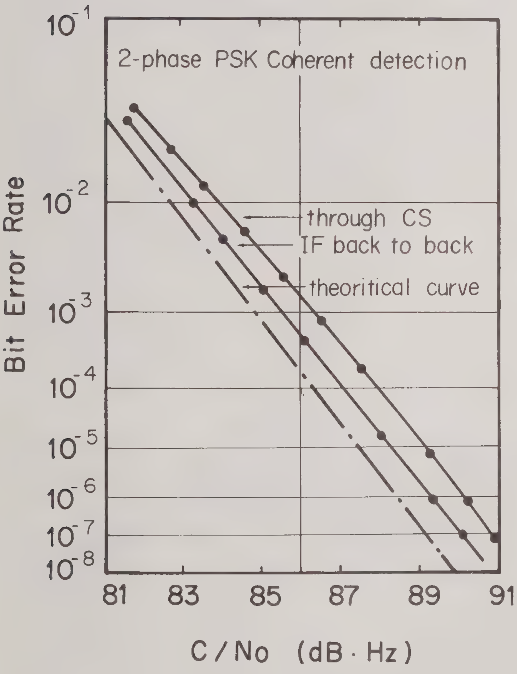

Clock frequency : 64.136 MHz

Fig. 14 Bit Error Performances versus C/N$_0$.

Acknowledgements

The authors would like to express their gratitude to Dr. Kazuhiro MIYAUCHI, Director of Integrated Transmission Division of ECL, NTT, and Masayoshi MUROTANI, Director of Kagoshima Telecommunication Division, NTT, for continuous guidance in development of the K-band fixed earth stations. Sincere appreciation is also extended to Makoto NAKAMURA and Masatake KAJI of ECL, NTT.

References

(1) M.Kudo and H.Hirata: "Transmitter for Experi mental Earth Station", Review of ECL, Vol. 22, Nos. 5-6, p. 487, 1974.

(2) T.Okajima and M.Kudo: "Cryogenically Cooled Low Noise Amplifier Equipment for Experimental Earth Station", Review of ECL, Vol. 22, Nos. 5-6, p. 502, 1974.

(3) Y.Mori, S.Morimoto and H.Fuketa: "Experimental Earth Station Outline", Review of ECL, Vol. 22, Nos. 5-6, 1974.

(4) T. Ishida, K.Tsukamoto, M.Hirai and H.Okamoto: "Program of Medium-Capacity Communication Satellite for Experimental Purpose", AIAA/CASI, 6th commun. Sat. Sys. Conf. AIAA paper no 76-244, 1976.

(5) K.Miyauchi, H.Fuketa and Y.Watanabe: "Digital Techniques for Domestic Satellita Communication Systems of Japan", AIAA/CASI, 7th Commun. Sat. Sys, Conf. AIAA paper no 78-601, 1978.

(6) T.Takano, E.Ogawa, M.Shinji and N.Ishida: "20,30 GHz Band Cassegrain Earth Station Antenna for the Japanese Domestic Satellite Communication System", IEEE Trans. COM. Vol. 27, No. 11, p. 1728-1731, Nov. 1979.

(7) E.Ogawa, T.Takano, M.Shinji and Ishida: "An Offset Cassegrain Antenna for the Satellite Communication System Earth Station", 1978 Int'l Symp. on Antenna and Propagation, Japan, B-2-3. (Aug. 1978).

(8) T.Okamoto and T.Igo: "SHF High Power TWT's for Earth Stations", IEDM 76, pp. 389-392, 1976.

(9) S.Egami: "In-Line Signal Circuit for Broad-Band Parametric Amplifiers", IEEE Trans. MTT, Vol. 23, No. 3, p. 282, March 1975.

80-0536

HIGHLY MOBILE GROUND STATION FOR THE OTS EXPERIMENTAL PROGRAM

H. Fröhlich, G. Bommas

DORNIER SYSTEM GMBH
Friedrichshafen, Germany

Introduction

The European Communication Satellites ECS and the precursor OTS serve as a complement to the European terrestrial telecommunication network. The system operates in the 11/14 GHz band and permits use of small ground stations by high transponder gain.

The paper describes the layout of a highly mobile ground station which will be used in a High Bit-Rate, Computer-to-Computer Data Transmission Experiment (STELLA) linking high energy physics laboratories within Europe.

Objectives of the STELLA Experiment

In the least decade there has been a trend in the design of computing systems using the general concept of Distributed Data Processing. This has resulted in a growth of studies and experiments on data networks and a development of new computer architectures and data base systems. All of this is aimed at use of data processing systems which are spread over large geographical areas and have a large numbers of users.

Much of this work originated in the USA, but recently in Europe CEPT (European Conference of Postal and Telecommunications Administrations) and also the CCITT have been working on future services.

Though the terrestrial telecommunication networks in Europe are well developed, the efficiency of computer links suffers from a mismatch between speed and quality achieved in modern computer systems and the corresponding characteristics of switched and dedicated data circuits. The introduction of advanced techniques will improve digital transmission, however, the service offered to computer communications users will still remain substantially below the requirements for an efficient data transfer between medium and high speed computers.

The high speed computer-to-computer communications applications using satellite links could be regarded as a complement to services provided by terrestrial data communication networks and will link computers via transmission lines operating at similar data rates and with similar error rates to the internal computer lines.

The high speed computer-to-computer link would be mainly used to exchange large quantities of data between computer data storage media and to enable remote operation of computer centres. The following tasks are anticipated:

- File transfer
- Computer load-sharing
- Computer resource sharing
- Computer redundancy on standby systems.

To support these activities the Commission of European Communities (CEC) encouraged the European data processing industry to work on standardization, transportable languages, etc. which are very relevant to the needs of distributed data processing systems. A weak point in the efforts to establish a common policy in this field has been the poor information on user requirements for technical facilities such as data transmission services.

Copyright © American Institute of Aeronautics and Astronautics, Inc., 1980. All rights reserved.

Overall system description

The STELLA experiments have been proposed as a contribution towards progress in this field. Their starting point was a search by the Commission of the European Communities (CEC) for projects to promote its second program on the development of Data Processing in Europe. Following contacts with ESA (European Space Agency) and CERN (European Organisation for Nuclear Research), the CEC in 1975 made a proposal to its Council for the support of a set of experiments involving ESA's OTS and several national laboratories led by CERN who work in the field of High Energy Physics.

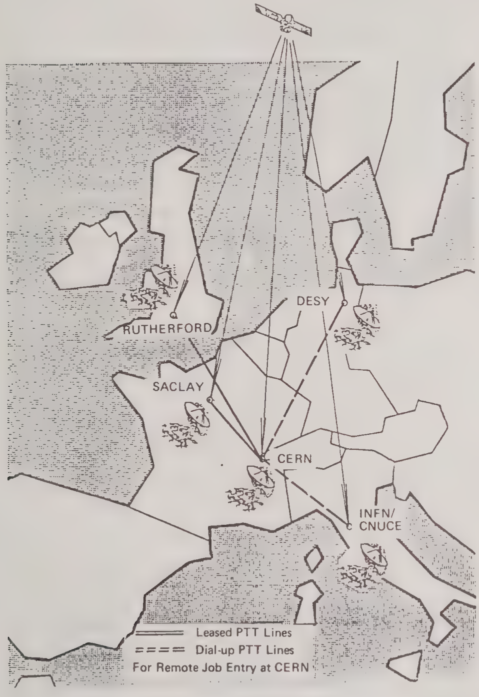
DESY
RUTHERFORD
SACLAY
CERN
INFN/
CNUCE
Leased PTT Lines
Dial-up PTT Lines
For Remote Job Entry at CERN

Fig. 1: **Geographical layout of Stella Experiment**

Figure 1 presents the geographical layout and the main interconnections. The main components of the system are:

- the large data processing centres associated with four national laboratories:
  - DESY in Germany
  - INFN in Italy
  - RUTHERFORD in United Kingdom
  - SACLAY in France
- the main source of data, High Energy Physics Experiments, being run by groups of research physicists mostly associated with the national laboratories, is located at CERN in Switzerland
- the satellite data links running at 0.5 Mbps or 1 Mbps between earth stations connected to the Link Driving Computers (LDC) at CERN and in the other laboratories, which can transmit and receive data, and pass it to the large computers for processing.

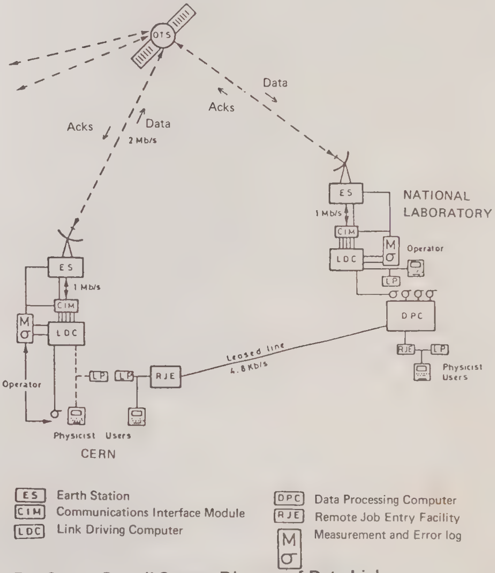
OTS
Data
Acks
Acks
Data
2 Mb/s
NATIONAL
LABORATORY
ES
1 Mb/s
CIM
LDC
M
σ
Operator
LP
DPC
RJE
LP
Physicist
Users
Leased line
4.8 Kb/s
ES
1 Mb/s
CIM
M
σ
LDC
Operator
LP
LP
RJE
Physicist Users
CERN
ES Earth Station
CIM Communications Interface Module
LDC Link Driving Computer
DPC Data Processing Computer
RJE Remote Job Entry Facility
M σ Measurement and Error log

Fig. 2: **Overall System Diagram of Data Link**

Figure 2 shows the overall system diagram of this data link.

The design of this experimental system will cover the following principal areas of study:

- measurement on the technical performance of components whose behaviour is not already well known

- analysis of how this system is used by the physicists as an extension or improvement to their normal methods of data processing, and of what a corresponding public service would be worth to them later on.

The topic in the first of these areas of study is the performance of the satellite links themselves.

The design goal for the links in distributed computer systems is that they are effectively transparent and do not introduce problems which are not present if all the equipment were at the same location. This implies that they should work at the normal data rate of the equipment they connect, and should not introduce errors or a significant system overhead.

For communication between parts of computers, including fast mass memories, the normal speeds today are in the region of 1 to 10 Mbps. In addition, connections must be effectively error free, that is, must be associated with powerful error correction and recovery procedures. The design goal of one undetected error per year implies a bit error rate (BER) of about 10^{-13} on an active 1 Mbps link. This can only be achieved by a mixture of efficient error recovery and high quality circuits. On a satellite link it takes about one second to detect and clear an error, because of propagation time, so that with a BER of 10^{-6} a 1 Mbps link would be in a recovery state most of the time. For this reason as a design target a BER of 10^{-8} to 10^{-9} under normal link operation conditions is appropriate, giving some marging for link degradation.

To achieve the required low BER forward error correcting coding will be used, with half-rate convolutional encoding and Viterbi decoding. The effective maximum data rate will be 1.024 Mbps with the possibility of running at one half of that speed.

The data will be transmitted in blocks containing nominally 4 Kilobytes, and lasting about 35 ms. Other sizes will be possible. These blocks will be separated by an approximately equal time interval in which the receiving stations can return acknowledgement signals or other short messages.

Each block of data is sent via standard HDLC frame format, with cyclic redundancy checking which will allow the receiving station to detect any remaining error with a high level of certainty.

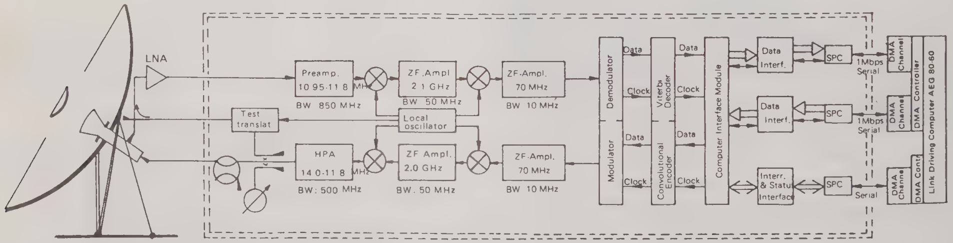
LNA
Preamp.
10.95-11.8 MHz
BW 850 MHz
ZF Ampl.
2.1 GHz
BW 50 MHz
ZF-Ampl.
70 MHz
BW 10 MHz
Test translat.
Local oscillator
HPA
14.0-11.8 MHz
BW: 500 MHz
ZF Ampl.
2.0 GHz
BW. 50 MHz
ZF-Ampl.
70 MHz
BW 10 MHz
Demodulator
Modulator
Data
Clock
Viterbi Decoder
Convolutional Encoder
Computer Interface Module
Data Interf.
SPC
1Mbps Serial
Interr. & Status Interface
Serial
DMA Channel
DMA Controller
DMA Cont.
Link Driving Computer AEG 80-60

Fig. 3: Block Diagram of OTS-Station for DESY

Station Block Diagram

The block diagram of the DESY-earth station is presented in Figure 3. The Link Driving Computer (LDC) is a medium sized dedicated machine (AEG 80-60). Besides acting as source or receiver of data, which will be stored on magnetic tape at either end, the LDC will perform, call set-up and closure, acknowledgements, and error recovery. It will also log all status and error information needed for the performance measurement part of the STELLA experiment.

The data connection between the LDC and the encoder/decoder of the earth station is performed via a Communications Interface Module (CIM) specially developed by CERN/DESY. The CIM will handle the HDLC line protocol and will indicate any transmission errors to the LDC. The CIM and the LDC are connected by three serial data lines, two operating in full duplex at 1 Mbps are used for data transfer, the other one in half-duplex is used for signalling.

Also in front of the CIM the station has full duplex capability, but the satellite repeater will work in half-duplex, i.e. only one station can transmit at any time.

The data to be trasmitted will be encoded before the modulator by a half-rate convolutional encoder and the received signal will be decoded at the output of the modulator before being sent to the CIM. The coder/decoder unit will be mounted close to the modem, since a quantizing modem will be used, which requires several high speed connections to the decoder.

The modulation technique used is binary phase shift keying (20-PSK) with coherent demodulation in the receiver. Special features of the modem are the burst gate control of the modulator and the fast acquisition facility of the demodulator.

The transmitter subsystem uses conventional IF-ampliers (70 MHz, 2 GHz) and up-converters and a high power TWTA (200W). An automatic level control is provided.

The receiver subsystem uses a FET preamplifier with a 4 dB noise figure. It is followed by conventional down-converter and IF-amplifier (2 GHz, 70 MHz).

Though the station in principle will work only with module B of OTS, it can be operated in the whole ECS/OTS frequency bands: 10.95 GHz to 11.20 GHz and 11.45 Ghz to 11.80 GHz and 14.00 GHz to 14.50 GHz.

Expected results and possible applications

The slow development of data communication facilities in Europe is one of the most important limiting factors in the establishment of a coherent European data processing industry. The results which should come out of the STELLA experiments will be relevant in this context and will cover:

- The performance of the satellite link, particularly in the area of what error rates are actually achievable under a range of operational and environmental conditions
- The performance of the control software in a variety of different Link Driving Computers
- The use of a flexible microprocessor controlled high speed interface (CIM) easily adaptable to a wide range of computers
- Possible ways how high speed data links could be used to improve the efffectiveness of using geographically dispersed data processing systems.

Mechanical Layout of the OTS-Station for DESY

The mechanical layout of this ground station is based on the requirement that it can be installed close to the computers and that the whole equipment is integrated in a transportable shelter. For convenience of transportation and installation a highly mobile design was selected.

The mobility of a ground station is mainly determined by the construction principle of the antenna.

Antenna dishes for ground stations usually consist of adjustable or non-adjustable reflector sections which, in all cases, are mated to very stiff supporting structures in order to maintain the antennas contour under the various environmental conditions and elevation angles.

Aluminum alloys are the most commonly used material for reflector construction. However, with the trend to higher frequencies in satellite communications, the requirements on the contour and alignment accuracy become more and more stringent. This is valid especially for segmented, nonadjustable reflectors, which are of particular interest for mobile ground stations. High mobility on the other hand requires a light weight construction, which in addition, has to provide high mechanical and thermal stability against wind and temperature loads.

To overcome these conflicting problems new materials and corresponding manufacturing techniques have to be applied. Segmented glassfiber epoxy sandwich antenna dishes with an aluminum honeycomb core fulfill all these requirements. The RF-reflectivity of the Glas-Fibre-Reinforced-Plastic (GFRP) after coating with a conductive layer (flame spraying) equals that of aluminum.

Figures 4 to 7 show the antennas and illustrate two production steps.

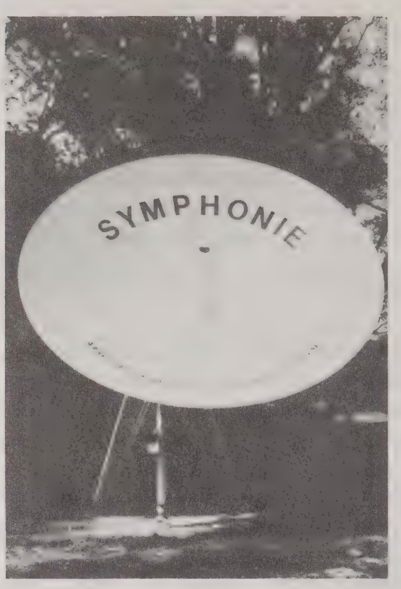

Fig. 4: 4,5 m Fibreglas Antenna

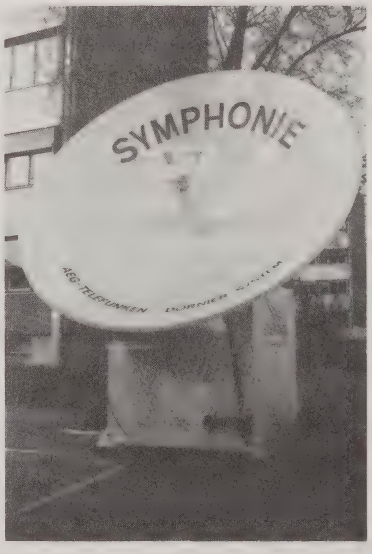

Fig. 5: 3,3 m Antenna mounted on equipment shelter

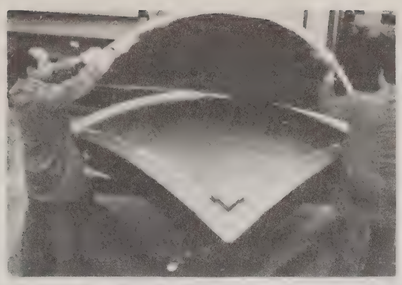

Fig. 6: Production of a segment (3,3 m)

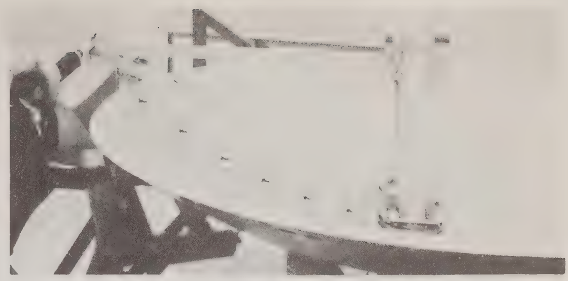

Fig. 7: Measurement of suface accuracy

For the feed system the compact Cassegrain principle is applied. Feed horn and subreflector form one unit which is easily mounted via a central flange and requires no further alignment. This feed system is shown in Figure 8.

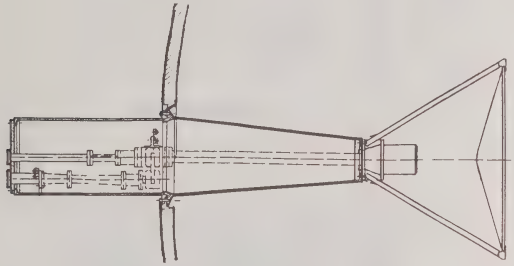

Fig. 8: Sketch of the Compact Cassegrain Feedsystem

Highly accurate tooling, fabrication methods, and contour measurement devices have been developed and are applied under strict quality control supervision to assure the best and most reproduceable quality of manufacture.

To prove strength and stability of the antenna wind tunnel tests with wind speeds up to 190 km/h have been performed.

The main mechanical features of the antennas are:

- diameter 3.3 m and 4.5 m
- self-supporting antenna dish
- lowest weight to stiffness ratio:
  weight of 3.3 m dish: 95 kp
  weight of 4.5 m dish: 230 kp
- 4 segment stressed GFPR-sandwich reflector
- high surface accuracy suits 11/14 GHz requirements: 0.25 mm rms max. deviation from ideal contour
- excellent reflectivity

The high contour accuracy of the antenna together with a state of the art feed system resuls in extraordinary electrical performance data especially with respect to radiation pattern and polarisation decoupling.
Figures 9 and 10 and Table 1 illustrate these data.

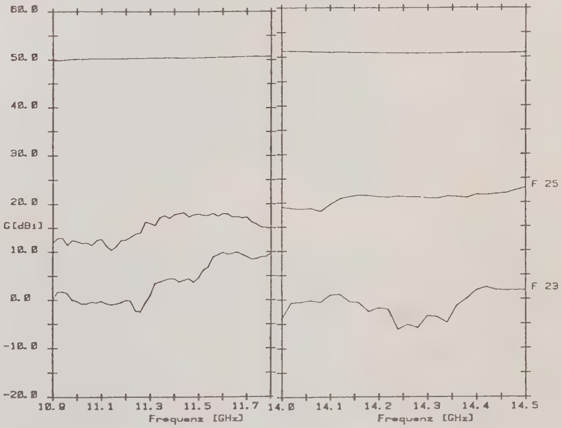

Fig. 9: Polarisation decoupling of 3,3 m antenna
F23: at center beam
F25: 0,35° from antenna axis

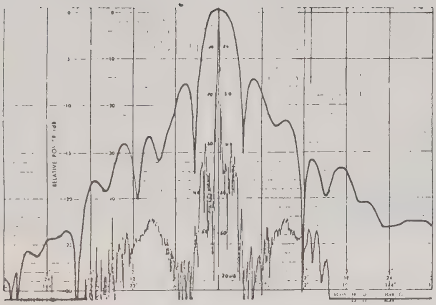

Fig. 10: Radiation pattern of 3,3 m antenna over + 5⁰ and over + 180⁰ in azimuth

Table 1: TECHNICAL DATA OF GFRP ANTENNAS

	3.3 m	4.5 m
Diameter	3.3 m	4.5 m
Weight	ca. 90 kg	ca. 190 kg
Receive frequency band	10.95 GHz to 11.80 GHz	
Gain at 11.45 GHz	50.5 ± 0.2 dB	52.6 ± 0.2 dB
Half power beamwidth	0.51⁰	0.37⁰
Noise temp. at 30⁰ elevation	33 K	26 k
Transmit frequency band	14.00 GHz to 14.50 GHz	
Gain at 14.25 GHz	50.9 ± 0.2 dB	53.8 ± 0.2 dB
Half power beamwidth	0.41⁰	0.30⁰
Polarization	circular and linear (selectable), frequency reuse feedsystem available	
Ellipticity ratio in 0.15⁰ beamwidth	30 dB	30 dB

Container

The container is on one hand a shelter of the equipment during operation forming part of the pedestal for the 3.3 m dish. On the other hand the container stores during transportation everything needed for operation including the antenna stowed inside. The container fulfills commercial aircraft transportation requirements (IATA Contour No. 5, e.g. for Boeing 707).

Rail and road transportation, even on small trucks is possible. Easy handling of the fully equipped container is guaranteed by fork guides and shackles for crane or helicopter. The container, an aluminum PU-foam sandwich construction, has excellent thermal insulation properties and can be equipped with RF-sealing.

The equipment is integrated in shock absorbing cabinets and remains in an operating configuration during transportation (Figures 11 and 12).

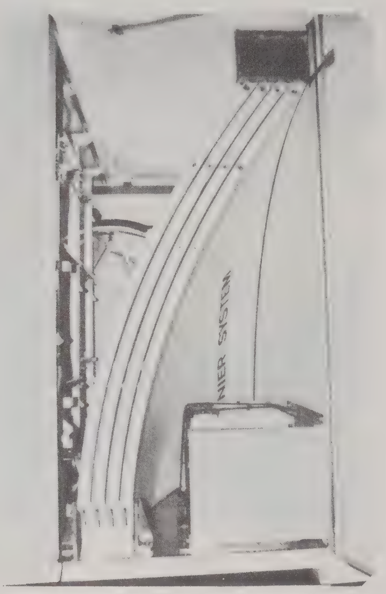

Fig. 11: Container with 3,3 m antenna stowed inside

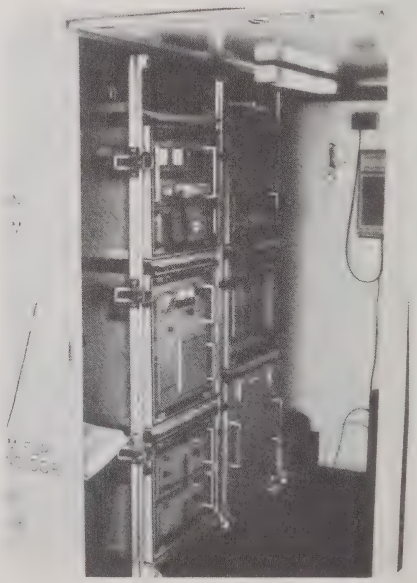

Fig. 12: Equipment installation

On site the station can easily be put into operation. About half a day and three man are necessary to set up the antenna and to put the electrical system into commission.

Summary

High-Speed computer-to-computer data communication links using satellites require small ground stations which can be located close to computer centers. The presented design of a small and highly mobile station fulfills these requirements. This station can be easily installed and is connected to the computer by a simple serial interface. The operation of the station is fully automatic. For control and monitoring of the RF-/IF-subsystems a microprocessor based controller connected to a CRT display in the computer room is used.

80-0537

PACKET COMMUNICATIONS IN SATELLITES WITH MULTIPLE-BEAM ANTENNAS AND SIGNAL PROCESSING*

by

R. Davies**, F. Chethik, M. Penick

Ford Aerospace & Communications Corporation
Palo Alto, California

Abstract

A communication satellite with a multiple-beam antenna and onboard signal processing is considered for use in a "message-switched" data relay system. The signal processor may incorporate demodulation, routing, storage, and remodulation of the data. A system user model is established and key functional elements for the signal processing are identified. With the throughput and delay requirements as the controlled variables, the hardware complexity, operational discipline, occupied bandwidth, and overall user end-to-end cost are estimated for a) random-access packet switching; and b) reservation-access packet switching. Other aspects of this network (eg, the adaptability to channel switched traffic requirements) are examined. For the given requirements and constraints, the reservation system appears to be the most attractive protocol.

Introduction

The expected growth of data communications requirements will generate increased demand for efficient, cost-effective communication techniques. Many of these requirements are characterized by data occurring in short bursts with low duty cycles. The data packet communication concept dedicates a data circuit to an individual user only when his data packet is actually (or about to be) transmitted. Communication circuit utilization by these techniques greatly surpasses that obtained with conventional dial-up or dedicated leased circuit facilities.

Candidates for packet communications techniques include remote computing services, electronic mail, facsimile transmission, and travel reservation services. Because of these potential applications, considerable development of and experiments with packet communications techniques, utilizing INTELSAT IV-A by DARPA[1], have demonstrated the feasibility of such systems.

DeRosa and Ozarow[2] analyized a slotted ALOHA system applied to a communication satellite with a multiple uplink and single downlink. It was shown that use of processing in the satellite increased the throughput. Eaves[3] extended these results to the multiple downlink case, showing further increase in throughput.

Narrow, multiple-beam satellite antennas (MBA), particularly at K_u-or K_A-band frequencies, prevent a transmitting earth station from monitoring the success of its own transmissions through the satellite. A switching matrix must accompany the MBA to interconnect each receive beam to a specific transmit beam, usually in time sequence. The flexibility of the MBA satellite, given a non-uniform time varying traffic distribution, can be enhanced by demodulation, collision detection routing, storage, and retransmission of the individual packets on board the satellite[4].

A study, including MBA techniques and demodulation, was performed for NASA/Lewis Research Center in 1978-1979 to investigate processing satellite concepts for packet communications. Several types of packet systems were considered. In this paper, the random-access (ALOHA) and reservation-access systems are described and compared. It was found that: a) use of onboard satellite processing led to significant cost reduction in a random-access system (compared to use of a conventional frequency translation satellite repeater); and b) the reservation system, with or without satellite processing, is more cost effective than the random-access system.

System Concept

A baseline network concept was formulated to serve as a framework for performance and cost trades. This system, illustrated in Figure 1, consists of a single satellite at synchronous altitude, illuminating the continental United States with 25 contiguous beams, each about 1 degree in beamwidth. The satellite is sized to provide a total RF power of 250 watts, or 10 watts per beam. The ground segment consists of up to 100,000 earth terminals, 2.5 to 4.5 meters in diameter. The 18/30 GHz (K_a) band was postulated in this study, though the basic concepts are also applicable to other frequency bands.

The Random-Access System

The processing, random-access satellite system shown in Figure 2, demodulates and extracts the address from the uplink bursts. Detecting and discarding packets that collide in the uplink, together with buffering, allow a downlink rate approximately equal to the throughput rate.

The uplink message structure shown in Figure 3 includes a start pattern and a downlink zone address word. The satellite demodulator and processor detects the start and stop sequences. Collision of uplink packets (of same size) is detected by a failure to correctly detect the stop sequence anticipated to occur at a fixed interval after the detected start sequence. After demodulation, the packet is stored in buffer memory until correct reception is validated by the "START/STOP" matched filter as shown in Figure 4. The downlink zone address allows the packet to be transferred to the appropriate downlink buffer. All uplink data

---

*This work was supported by the NASA Lewis Research Center, under Contract NAS3-21364.
**Member AIAA

Copyright © American Institute of Aeronautics and Astronautics, Inc., 1980. All rights reserved.

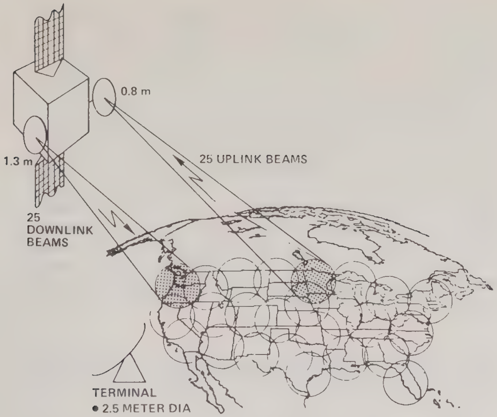
0.8 m
1.3 m
25 UPLINK BEAMS
25
DOWNLINK
BEAMS
TERMINAL
● 2.5 METER DIA

SPACECRAFT
- 250 W TOTAL RF
- DEMODULATION
- STORE AND FORWARD

SYSTEM CAPACITY
FULL CONUS COVERAGE
1,000–100,000 TERMINALS

18/30 GHz BAND ASSUMED
- ADVANCED CONCEPTS
- APPLICABLE TO C-, Ku-BAND ALSO

Figure 1. Baseline System

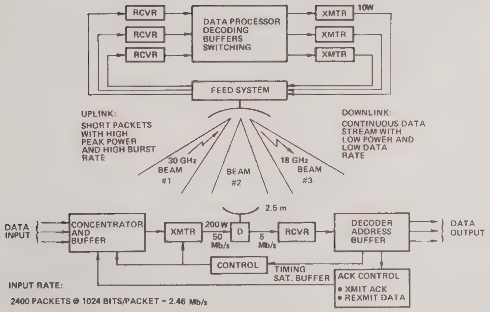
RCVR
RCVR
RCVR
DATA PROCESSOR
DECODING
BUFFERS
SWITCHING
XMTR
XMTR
XMTR
10W
FEED SYSTEM
UPLINK:
SHORT PACKETS
WITH HIGH
PEAK POWER
AND HIGH BURST
RATE
DOWNLINK:
CONTINUOUS DATA
STREAM WITH
LOW POWER AND
LOW DATA
RATE
30 GHz
BEAM
#1
BEAM
#2
18 GHz
BEAM
#3
2.5 m
DATA
INPUT
CONCENTRATOR
AND
BUFFER
XMTR
200 W
50
Mb/s
D
5
Mb/s
RCVR
DECODER
ADDRESS
BUFFER
DATA
OUTPUT
CONTROL
TIMING
SAT. BUFFER
ACK CONTROL
● XMIT ACK
● REXMIT DATA
INPUT RATE:
2400 PACKETS @ 1024 BITS/PACKET = 2.46 Mb/s

Figure 2. Random Access System

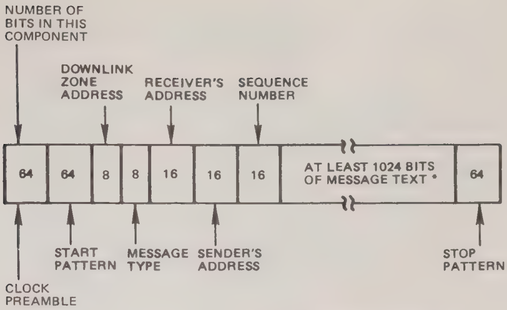
NUMBER OF
BITS IN THIS
COMPONENT
DOWNLINK
ZONE
ADDRESS
RECEIVER'S
ADDRESS
SEQUENCE
NUMBER
64
64
8
8
16
16
16
AT LEAST 1024 BITS
OF MESSAGE TEXT *
64
START
PATTERN
MESSAGE
TYPE
SENDER'S
ADDRESS
STOP
PATTERN
CLOCK
PREAMBLE

TOTAL OVERHEAD = 256 BITS

$$\text{PACKET EFFICIENCY} < \frac{1024}{1280} = 0.8$$

*STANDARD FOR ALL MESSAGE PACKETS. THIS COMPONENT ABSENT FOR ACKNOWLEDGEMENTS.

Figure 3. Format for Uplink Data Packets for Random Access System

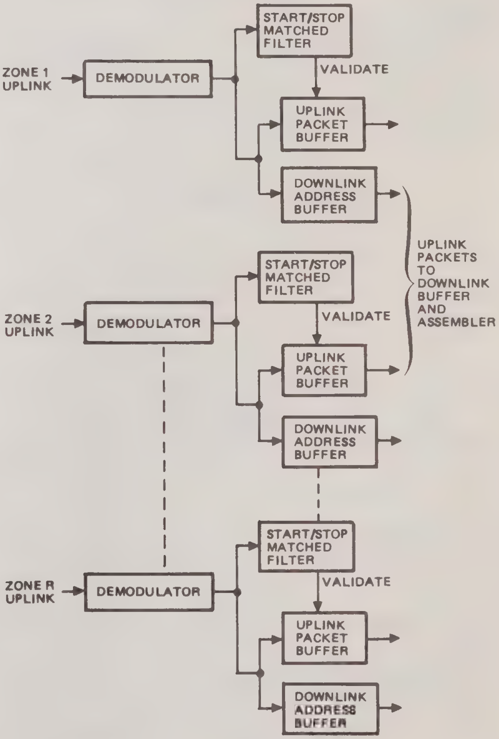
ZONE 1
UPLINK
DEMODULATOR
START/STOP
MATCHED
FILTER
VALIDATE
UPLINK
PACKET
BUFFER
DOWNLINK
ADDRESS
BUFFER
ZONE 2
UPLINK
DEMODULATOR
START/STOP
MATCHED
FILTER
VALIDATE
UPLINK
PACKET
BUFFER
DOWNLINK
ADDRESS
BUFFER
UPLINK
PACKETS
TO
DOWNLINK
BUFFER
AND
ASSEMBLER
ZONE R
UPLINK
DEMODULATOR
START/STOP
MATCHED
FILTER
VALIDATE
UPLINK
PACKET
BUFFER
DOWNLINK
ADDRESS
BUFFER

Figure 4. Uplink Satellite Processor for Random Access System

packets are made the same length to simplify the collision detection circuitry and buffer storage logic.

The downlink satellite processor block diagram shown in Figure 5 provides buffers, each with a capacity of 64, 1024-bit words. This is sufficient to store at least 50 1024-bit data packets plus overhead data contained in the packets and in the downlink frame. The downlink frame as shown in Figure 6 describes a frame duration of 1/75 second, and a downlink transmission rate of approximately 5 Mb/s. Two alternating buffers are used for each downlink: one is being loaded by incoming data, while the other is being read out to the downlink transmitter.

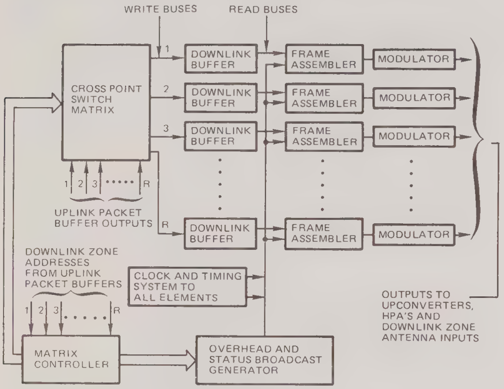
WRITE BUSES
READ BUSES
CROSS POINT SWITCH MATRIX
1
2
3
R
DOWNLINK BUFFER
DOWNLINK BUFFER
DOWNLINK BUFFER
DOWNLINK BUFFER
FRAME ASSEMBLER
FRAME ASSEMBLER
FRAME ASSEMBLER
FRAME ASSEMBLER
MODULATOR
MODULATOR
MODULATOR
MODULATOR
1 2 3 ..... R
UPLINK PACKET BUFFER OUTPUTS
DOWNLINK ZONE ADDRESSES FROM UPLINK PACKET BUFFERS
1 2 3 ..... R
CLOCK AND TIMING SYSTEM TO ALL ELEMENTS
OUTPUTS TO UPCONVERTERS, HPA'S AND DOWNLINK ZONE ANTENNA INPUTS
MATRIX CONTROLLER
OVERHEAD AND STATUS BROADCAST GENERATOR

Figure 5. Downlink Satellite Processor for Random Access System

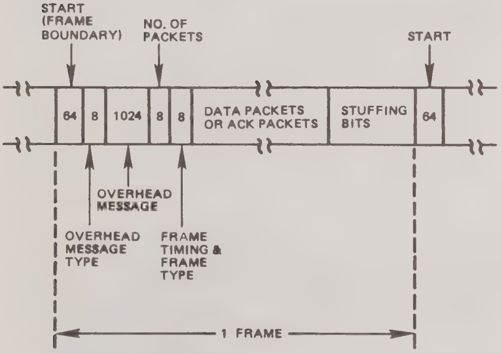
START (FRAME BOUNDARY)
NO. OF PACKETS
START
64
8
1024
8
8
DATA PACKETS OR ACK PACKETS
STUFFING BITS
64
OVERHEAD MESSAGE
OVERHEAD MESSAGE TYPE
FRAME TIMING & FRAME TYPE
1 FRAME

FRAME RATE = 75/SECOND
DATA RATE = 75 x 65, 536 = 4.9152 Mb/s

Figure 6. Format of Random Access System Downlink Frame

Each successfully received packet must be acknowledged by the addressee transmitting an ACK message back to the sender. The format shown in Figure 3 is used, except the ACK packet length is only 256 bits. The system must thus accommodate two packet lengths, a message packet (MSG) and an acknowledgement packet (ACK). A simple and convenient means of segregating these functions is to allow, say, 0.1 seconds for acknowledgements and 0.4 seconds for message text packets within a 0.5 second basic frame interval, as shown in Figure 7. System timing can be maintained easily and inexpensively to the few millisecond accuracy required using satellite beacon timing and open-loop range predictions. The segregation is required to avoid undetected MSG/ACK collisions.

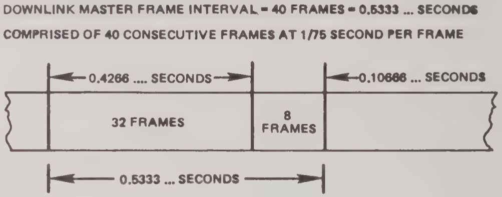
DOWNLINK MASTER FRAME INTERVAL = 40 FRAMES = 0.5333 ... SECONDS
COMPRISED OF 40 CONSECUTIVE FRAMES AT 1/75 SECOND PER FRAME
0.4266 .... SECONDS
0.10666 ... SECONDS
32 FRAMES
8 FRAMES
0.5333 ... SECONDS

UPLINK ACCESS FRAMING CONSISTS OF:
0.4 SECONDS — MESSAGE TEXT PACKETS
0.1 SECONDS — ACKNOWLEDGEMENT PACKETS
TIMING (AT SATELLITE) COINCIDENT WITH DOWNLINK MASTER FRAMING ARRANGEMENT

Figure 7. Uplink Access Framing and Downlink Timing

Using the system parameters described above, the average message delay is about 1 second if both the data packet and the ACK packets are successfully received. (Message delay is defined as the time interval between the first transmission of the data packet and successful reception of the corresponding ACK message at the sender terminal.) If an ACK message is not received by the end of the third frame following the initial transmission, the data packet is retransmitted.

Assuming no packets are lost in the satellite due to buffer overflow, or by poor downlink performance, the increase in average message delay caused by packet collisions in the uplink can be calculated simply. The results, shown in Figure 8, take into account the loss of ACK packets as well as data packets due to collisions. At low throughput rates, the probability of collision is small, and the average delay approaches 1 second. Increasing the throughput rate increases the collision rate (hence, the average number of packet transmissions) as well as increasing the average delay. For the baseline system, an input data rate of 2400 packets per second was assumed. During the message text interval, this rate is increased by a factor of 1.25 to allow time for the ACK message transmission. Each message text packet contains 1280 bits and the throughput rate is 3.84 Mb/s. The required uplink burst rate of 50 Mb/s leads to a throughput ratio of 0.0768 and an average delay of 1.68 seconds.

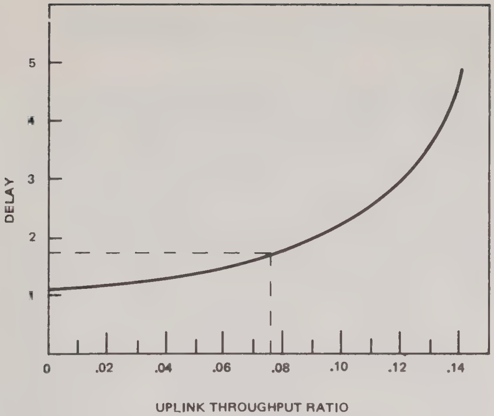

$$\text{UPLINK THROUGHPUT RATIO} = \frac{\text{THROUGHPUT RATE}}{\text{BURST RATE}}$$

$$= \frac{5 \times 10^6 \times 0.768}{50 \times 10^6} = 0.0768$$

DELAY = 1.68 s

Figure 8. Throughput vs Delay - Random Access System with Acknowledgement Loss with no Buffer Overflow

If a downlink buffer fills before the end of a downlink data frame, overflow may occur, and those lost packets must be retransmitted in subsequent frames. Downlink buffer size affects probability of overflow and average message delay. Table 1 shows the results of a computer simulation obtained for the baseline system in which the downlink buffer size is allowed to vary from 10 to 50 packets. A 50-packet buffer reduces the buffer overflow probability to 0.01 and has negligible impact on message delay.

Table 1. Effect of Buffer Capacity on Packet Survivability

Baseline Random Access System 2400 Packets/Beam

Buffer Capacity (Packets)	Prob Packet Survives Uplink	Prob Packet Reaches Downlink*	Prob Ack Survives Uplink	Avg Number Transmission Per Packet	Average Delay (Sec)
10	0.786	0.906	0.875	1.607	1.91
20	0.795	0.960	0.869	1.510	1.77
50	0.800	0.990	0.868	1.454	1.68

*Equals 1 — Prob Buffer Overflow

Note: Prob Ack Packet Reaches Downlink = 1.000
(No Buffer Overflow with Ack Packets)

If the input packet rate is increased, both the probability of buffer overflow and average message delay will increase as shown in Figure 9. The dotted line refers to the baseline input rate of 3000 packets per second during the 0.4 second data transmission period. At this input rate, 76.8% of the 5 Mb/s downlink capacity is utilized. Increasing the input packet rate to 90% of downlink capacity increases message delay by only 28%, even though the probability of buffer overflow will lead to significant increases in delay and eventual instability. These relationships augur a maximum downlink load of 70 to 90 percent. Any increases in downlink capacity which reduce downlink load below 70% affords virtually no improvement in throughput performance.

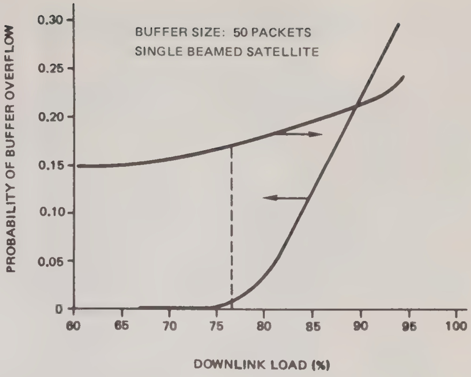

Figure 9. Probability of Buffer Overflow vs Downlink Load

A common buffer shared by all downlinks allows storage capacity to be allocated according to traffic loading on individual downlinks. While this technique adds complexity to the processor logic, the probability of buffer overflow during high traffic peaks could be substantially reduced since it is unlikely that all downlinks would receive peak traffic simultaneously.

The Reservation-Access System

In the example reservation-access system concept shown in Figure 10, the up- and downlink capacities are 5 Mb/s. The reservation-satellite system has a set of channels used for reserving capacity on the communications processor. These channels are intra-zone connected only (ie, each channel loops back on the downlink to the same zone from which the uplink originated), enabling all nodes in a zone to monitor uplink activity and thus identify available accesses. The reservation channel operates on a contention basis in which each user monitors the satellite retransmission of his random-access reservation message to determine if a collision thereupon has taken place.

The "reservation channel" can either be time-division multiplexed with the communication channel on a common frequency, or be provided as a separate time-continuous-frequency offset channel. Reduced timing accuracy requirements favor the frequency offset approach, even though an additional up-down converter and modem is required at each earth terminal channel. The reservation channel requires a small fraction (~1/10) of the communications channel capacity requirements and thus its bandwidth and EIRP requirements do not impact greatly upon the satellite power and weight.

The proposed method of slot capture and data packet transmission is shown in Figure 11. The basic access slot is 260.4 µs, or 1280 bit packets, and the reservation slot is the same duration. The reservation "marker" packet is 128 bits long, requiring a transmission rate of 500 kilobits per second.

It should be noted that the "markers" precede their corresponding packets by one basic (~0.5 second) frame. The number of markers successfully transmitted is required to be one less than the number of data packets. Thus, maximum efficiency of the communications channel can be obtained since an empty reservation slot must be observed before it can be accessed (on a contention basis). Thus, the last communications channel data packet of a message is sent without a corresponding marker to allow recognition of the available slot as soon as possible; otherwise, the communication slot would be unnecessarily idle each time a message was completed.

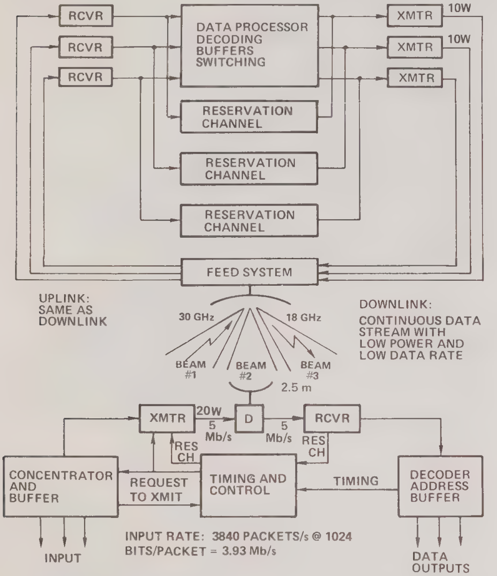
RCVR
RCVR
RCVR
DATA PROCESSOR
DECODING
BUFFERS
SWITCHING
XMTR
XMTR
XMTR
10W
10W
RESERVATION CHANNEL
RESERVATION CHANNEL
RESERVATION CHANNEL
FEED SYSTEM
UPLINK: SAME AS DOWNLINK
30 GHz
18 GHz
DOWNLINK: CONTINUOUS DATA STREAM WITH LOW POWER AND LOW DATA RATE
BEAM #1
BEAM #2
BEAM #3
2.5 m
XMTR
20W
5 Mb/s
D
5 Mb/s
RCVR
RES CH
RES CH
CONCENTRATOR AND BUFFER
REQUEST TO XMIT
TIMING AND CONTROL
TIMING
DECODER ADDRESS BUFFER
INPUT
INPUT RATE: 3840 PACKETS/s @ 1024 BITS/PACKET = 3.93 Mb/s
DATA OUTPUTS

Figure 10. Reservation Access System

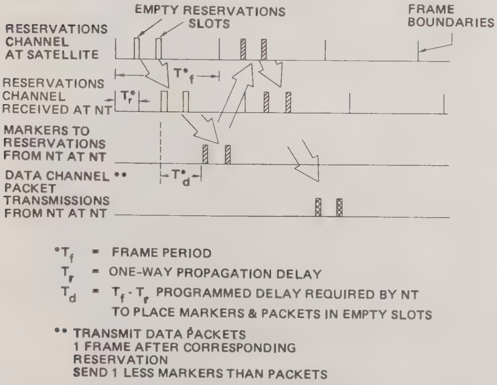
EMPTY RESERVATIONS SLOTS
FRAME BOUNDARIES
RESERVATIONS CHANNEL AT SATELLITE
RESERVATIONS CHANNEL RECEIVED AT NT
T*f
Tr*
MARKERS TO RESERVATIONS FROM NT AT NT
DATA CHANNEL ** PACKET TRANSMISSIONS FROM NT AT NT
T*d
*Tf = FRAME PERIOD
Tr = ONE-WAY PROPAGATION DELAY
Td = Tf - Tr PROGRAMMED DELAY REQUIRED BY NT TO PLACE MARKERS & PACKETS IN EMPTY SLOTS
** TRANSMIT DATA PACKETS 1 FRAME AFTER CORRESPONDING RESERVATION
SEND 1 LESS MARKERS THAN PACKETS

Figure 11. Sequence of Slot Capture in Reservation ALOHA

Figure 12 and 13 show block diagrams of the satellite payloads contrasting the translation and processing configurations. The impact of signal processing on system performance and cost was found to be small, reducing the required earth station EIRP, G/T, and cost by only a small amount. The key component in both of these systems is the switching matrix. The relative size, weight, power consumption, and reliability of the microwave versus baseband switch may decide if onboard signal processing is worthwhile for a reservation system.

The processing satellite shown in Figure 13 does not employ address decoding. Uplink packets are routed by the switching matrix which is programmed by ground control, based on average traffic demand. Individual users access the satellite only when the switch provides the satellite beam interconnect necessary to complete the circuit. Incorporation of address decoding and routing in the satellite would provide more flexibility in adapting to changing traffic load distributions, and would also provide a broadcast capability (ie, one uplink to multiple downlink beams), but with increased complexity.

Performance Cost Comparison

Performance-cost trades were performed, using, as the baseline, a 2.5 m diameter earth terminal antenna and the 25-beam, 10 watt-per-beam satellite described in the previous sections. The baseline system parameters are listed in Table 2.

Table 3 lists the key parameters and cost estimates for the space segment of the system. The annual space segment cost was obtained by taking the total 10 year cost and dividing by 10 years to obtain $27 M per year. A more precise determination would require the preparation of a detailed schedule and financing plan. It is conjectured that the results would not differ greatly from the simplified derivation.

Figure 14 shows the unit earth terminal costs for the two systems, with and without redundancy. A 2.5 meter diameter with step track pointing was assumed. The figure shows that HPA costs dominate the random-access earth terminal, especially if redundancy is used. This is a direct result of the high burst rates, and consequently the high transmit powers required in the random-access system. The reservation-access system requires additional equipment for implementing the reservation channel,

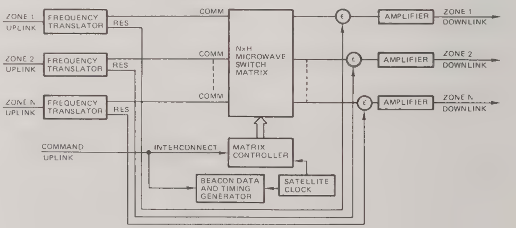
ZONE 1 UPLINK
FREQUENCY TRANSLATOR
RES
COMM
ZONE 2 UPLINK
FREQUENCY TRANSLATOR
RES
COMM
ZONE N UPLINK
FREQUENCY TRANSLATOR
RES
COMM
NxH MICROWAVE SWITCH MATRIX
AMPLIFIER
ZONE 1 DOWNLINK
AMPLIFIER
ZONE 2 DOWNLINK
AMPLIFIER
ZONE N DOWNLINK
COMMAND UPLINK
INTERCONNECT
MATRIX CONTROLLER
BEACON DATA AND TIMING GENERATOR
SATELLITE CLOCK

Figure 12. Reservation Access Satellite Using Frequency Translation

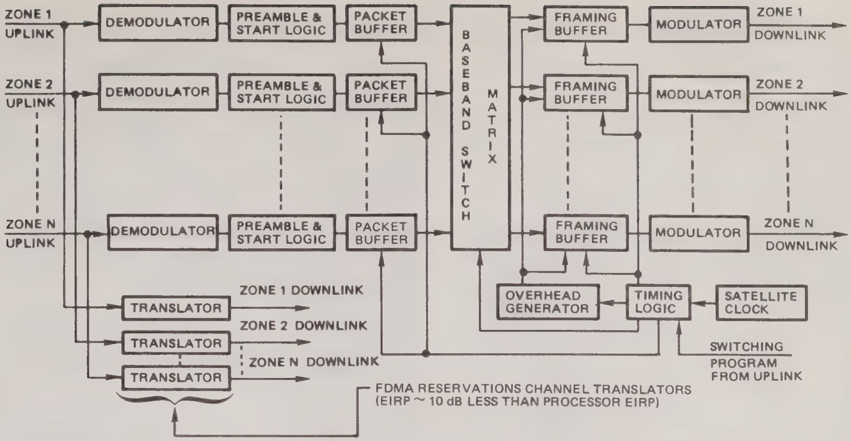
ZONE 1 UPLINK
DEMODULATOR
PREAMBLE & START LOGIC
PACKET BUFFER
ZONE 2 UPLINK
DEMODULATOR
PREAMBLE & START LOGIC
PACKET BUFFER
ZONE N UPLINK
DEMODULATOR
PREAMBLE & START LOGIC
PACKET BUFFER
BASEBAND SWITCH MATRIX
FRAMING BUFFER
MODULATOR
ZONE 1 DOWNLINK
FRAMING BUFFER
MODULATOR
ZONE 2 DOWNLINK
FRAMING BUFFER
MODULATOR
ZONE N DOWNLINK
OVERHEAD GENERATOR
TIMING LOGIC
SATELLITE CLOCK
SWITCHING PROGRAM FROM UPLINK
TRANSLATOR
ZONE 1 DOWNLINK
TRANSLATOR
ZONE 2 DOWNLINK
TRANSLATOR
ZONE N DOWNLINK
FDMA RESERVATIONS CHANNEL TRANSLATORS
(EIRP ~ 10 dB LESS THAN PROCESSOR EIRP)

Figure 13. Reservation Access Satellite Using Onboard Processing

Table 2. Baseline System Parameters

Frequency: Uplink:	30 GHz
Downlink:	18 GHz
Terminal Diameter:	2.5 m
Elevation Angle:	20°
Step Track Accuracy:	0.1°
Antenna Efficiency:	60%
Antenna Gain:	51.2 dB @ 18 GHz 55.7 dB @ 30 GHz
Terminal Line Loss:	
Transmit:	-1.5 dB
Receive:	-1.0 dB
Data Rate:	
Uplink:	
Random:	50 Mb/s
Reservation:	5 Mb/s
Downlink:	5 Mb/s
Satellite Antenna (Transmit and Receive):	
Number Beams:	25
Half Power Beamwidth:	0.91°
Minimum Gain (EOC):	40.6 dB
Pointing Error:	0.1°
Satellite Line Loss:	
Transmit:	-2.0 dB
Receive:	-1.5 dB
Satellite Receiver System Temperature:	1800°K
Satellite Transmit Power:	10 W
Rain Margin:	
Uplink:	7 dB
Downlink:	3 dB
Minimum E/N_o:	12.9 dB
Redundancy in Earth Terminals:	None

Table 3. Space Segment Cost

(1978 $)	
3 Spacecraft Program – 2 Production Plus Refurbished Prototypes	
3 Shuttle Launches	
Ten-Year Operation in Orbit	
Spacecraft:	
Total RF Power:	250 W
Primary Power (EOL):	1500 W
In-Orbit Weight:	1000 kg
STS Launch Weight:	7600 kg
S/C Length:	6.55 m
R&D Prototype Development:	76.1 M
Prototype Refurbishment and Launch:	29.4 M
Two Flight Units Plus Two Launches:	100.3 M
TT&C Hardware and 10-Year O&M:	36.9 M
Profit and On-Orbit Incentives:	33.0 M
Total Space Segment (10 Years)	275.7 M

control, and timing functions. It is estimated that the added fixed equipment costs of the reservation system is less than the added HPA cost of the random-access system.

Figure 15 shows the cost dependence on earth terminal antenna diameter. While the 2.5 meter baseline antenna is about optimum for the reservation system, a 4.5 meter diameter antenna would be more cost effective for the random-access system. The increased antenna diameter decreases the HPA power requirement leading to reduced total terminal costs.

The costs shown in Figure 14 and 15 are estimated for a single terminal operating at K_A-Band. In large-quantity production, these costs are expected to decrease by 50% or more. A learning curve function was included in deriving the system costs described in the next paragraph.

The cost per kilopacket for a 10,000, 2.5 m terminal network and a traffic load of 135 megapackets/terminal/year is shown in Table 4. This traffic

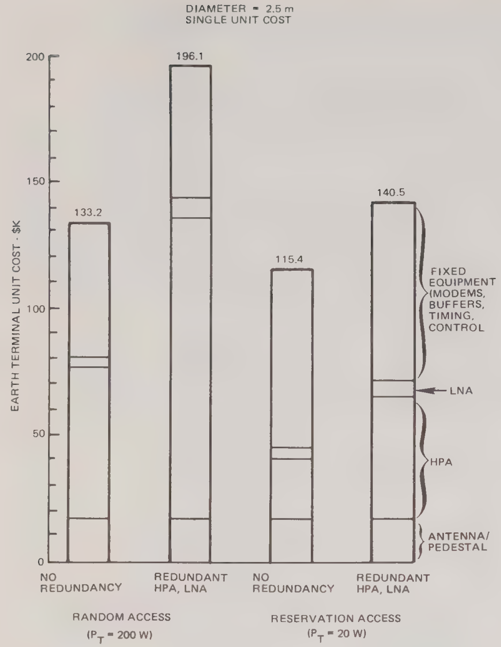

Figure 14. Earth Terminal Costs

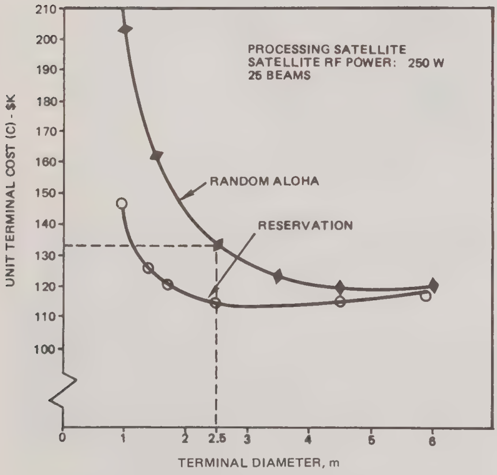

Figure 15. Terminal Cost vs Diameter

Table 4. Cost per Kilopacket

Baseline System
Satellite System Costs Only

10,000 Terminals — 135 Megapackets/Terminal/Year

	Cost Per Kilopacket — $	
Configuration	**Repeater**	**Processor**
Random	0.47	0.24
Reservation	0.22	0.21

Existing Terrestrial Service (TELENET):
$0.50/KILOPACKET

*Average Satellite Throughput Rate = 43.75 Mb/s

OR: 1.75 Mb/s Per Beam
OR: 4.375 kb/s Per Terminal

load is equivalent to an average transmission rate of 4.27 (1024 bit) packets per second per terminal or an average data throughput rate of 4.4 kb/s. The cost per kilopacket of a reservation-access system is less than that of the random-access system, and the cost of using a satellite with onboard processing is more economical than a system with a frequency translation repeater. (The random-access system with repeater is especially costly because the downlink must also support a high burst rate which necessitates the use of a high-cost LNA in the earth terminals.)

The transmission cost is inversely proportional to the average traffic per user, as shown in Figure 16. High traffic throughput for each earth terminal is required for a cost-competitive system. User concentration at each terminal and perhaps mixed-mode (packet and stream traffic) services can increase terminal utilization and may reduce costs to be competitive with existing terrestrial rates of about $0.50 per packet.

The effect of several users sharing one terminal was investigated and the results are shown in Table 5. A 100,000 user network was assumed, with each user generating 13.48 megapackets per year. If each user has its own earth terminal, the transmission cost is $1.74 per kilopacket; too high to be competitive. Reducing the number of terminals to 10,000, where each terminal services (on the average) ten users, the transmission cost reduces to $0.38 per kilopacket. This estimate includes digital tail circuit costs of $2,300 per year (20 miles @ $0.40/mi/mo, plus $180/mo for terminal equipment). Further concentration of traffic to 100 users per terminal provides greater economies. Cost competitiveness requires that user traffic be concentrated at the nodal terminals.

Suppose future technology growth reduces the unit cost of the terminal to $30,000 ($15,000 in large quantities), then the cost per kilopacket for a single user-per-terminal, 100,000 terminal network would be around $0.45.

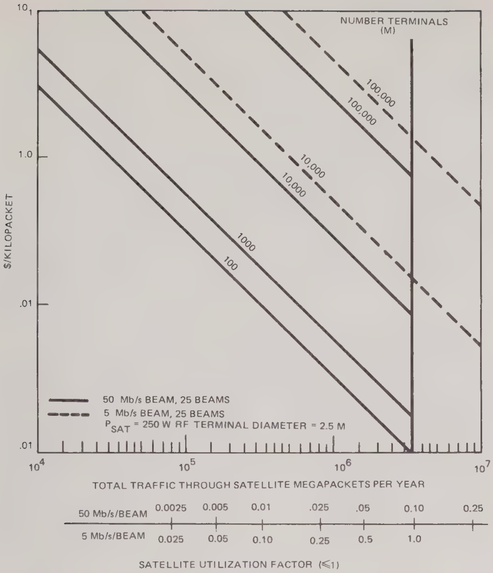

Figure 16. Effect of Total Traffic Throughput on Cost — Full-CONUS Coverage, Reservation System

Table 5. Nodal Terminal vs Dedicated-User Terminal

Assume: Baseline Reservation System With Processing Satellite
100,000 Users

13.48 Megapackets Per Year Per User

(Equivalent To 1 Packet Every 2.34 Sec or 437.5 b/s Average Data Rate)

Number Earth Terminals	**1000**	**10,000**	**100,000**
Number Users Per ET	100	10	1
Satellite System Cost $ / Kilopacket	0.041	0.21	1.74
Tail Circuit Cost * $ / Kilopacket	0.17	0.17	–
Total — $ / Kilopacket	0.21	0.38	1.74

* Estimated 20-Mile Leased Data Service @ $2300 / Yr. Between Each User And ET

Study Results

The general results of the study are given in Table 6 and summarized as follows:

a. The random-access system benefits strongly from use of processing in the satellite to reduce downlink costs. Timing and control requirements are minimal, but significant buffering is required at the earth terminal. Overall satellite throughput efficiency is limited by the requirement for a separate acknowledgement channel and by the size of the downlink buffers. The random-access system is limited to transmission of bursty (packetized) data only since it cannot accommodate stream traffic. The uplink also makes inefficient use of the RF spectrum.

b. The reservation system, on the other hand, appears most promising for a system containing a large number of user terminals. The use of onboard processing is beneficial though a simpler frequency translation repeater satellite is also cost effective. The reservation system could be adapted to accommodate stream traffic and is generally more conservative of RF spectrum.

The results demonstrate that the reservation system is the preferred implementation within the known constraints and assumptions.

Table 6. Conclusions

- Random Access Strongly Benefits From Processing Satellite
  - Reduced Downlink Costs
  - Minimum Timing, Control Requirements
  - Limited to Bursty Data for Effective Use
  - Inefficient Use of Spectrum
- Reservation System Most Promising
  - Distributed Control; Relatively Simple
  - Reduced Complexity in Satellite Due to Lower Received Data Rates
  - Satellite Processing Benefits Still Significant, Though Less Than Random ALOHA
  - Can Accommodate Stream Traffic

References

1. I. M. Jacobs, R. Binder, E. V. Hoversten, "General Purpose Packet Satellite Networks" Proceedings of the IEEE, Vol. 66, No. 11, pg. 1448-1467; November 1978.

2. J. K. DeRosa and T. H. Ozarow "Packet Switching in a Processing Satellite," Proceedings IEEE, Vol. 66, pp 100-102; January 1978.

3. R. E. Eaves, "ALOHA/TDM Systems with Multiple Downlink Capacity," IEEE Transaction on Communications, Vol. COM-27, pp 537-541; March 1979

4. R. S. Davies, "Use of a Processing Satellite for Digital Data Transmission Between Low-Cost Earth Terminals". Seventh AIAA Communications Satellite Systems Conference; 23-27 April 1978.

80-0538

A TWO-LEVEL MULTIPLE ACCESS SCHEME FOR A PACKET SATELLITE SYSTEM OF MANY TERMINALS

S. L. Kota B. E. White
The MITRE Corporation
Bedford, MA 01730

Abstract

A two-level packet satellite network architecture is proposed to provide efficient communications for a large number of terminals. At the first level, disjoint subnets of relatively few prioritized users employ a mini-slotted alternating priorities (MSAP) protocol. At the second level a TDMA or FDMA uplink and a TDM or FDM downlink organization is assumed with the satellite regenerating and reformating the data appropriately. The system throughput-delay performance is analyzed and compared with single-level TDMA, polling, and Slotted ALOHA protocols with the number of subnets and number of terminals per subnet as the principal parameters. Realistic examples with 100 terminals show that the two-level scheme possesses superior delay performance over these single-level methods for wide ranges of throughput.

I. Introduction

An increasing demand for satellite communications services to mobile terminals in both military and commercial environments dictate the need for efficient multiple access schemes for sharing expensive communication satellite resources. A number of multiple access protocols based on packet broadcast concepts have been proposed and investigated for mobile-satellite communications(1). In this kind of packet satellite system, many low duty factor terminals can transmit essentially independently and asynchronously under a distributed control philosophy with superior end-to-end packet delay but at relatively low channel efficiency. Demand assignment techniques offer higher throughput for busier nets under centralized control but delay is generally increased and the survivability and/or reliability of the critical control node may be a problem. In addition, the complexity of such methods may not lead directly to lower cost terminal designs. This paper is concerned with a network organization that will retain the main features of packet broadcasting, distributed--or at least subcentralized--control, and attractive end-to-end packet delay, while gaining the opportunity for significantly higher throughput with large numbers of terminals.

Among the random access schemes of greatest interest, Slotted ALOHA is unstable and can achieve a maximum throughput of only 37%. Capetanakis's schemes hold great promise due to their stability and adaptability but the maximum channel efficiency of the simpler methods is still less than 50%(2). Capture ALOHA can approach 100% efficiency in certain processing satellite models(3) but the associated packet delays may be intolerably long in certain scenarios(4).

Carrier sense multiple access (CSMA) protocols can be very channel efficient if propagation delays are short compared to packet lengths and the number of users is small(5). Polling can achieve high throughput levels with moderate delay but has the disadvantages of central control. Fixed assignment schemes such as frequency or time division multiple access (FDMA or TDMA) can certainly achieve high efficiency but only with high duty factor terminals.

All of the techniques mentioned thus far have a single-level architecture, i.e., terminals are completely connected by a single relay node as in a star net. A hierarchical structure would allow this network to be decomposed into subnets of fewer terminals which may permit the application of more efficient protocols. This is possible with CSMA protocols if each subnet contains terminals within line-of-sight of each other, and if a single designated platform within each subnet serves as an interface relay with the satellite. A two-level multiple access model of this nature is defined and analyzed in section 2. Performance comparisons between this two-level architecture and three single-level schemes are given in section 3 with examples. Section 4 contains conclusions and suggestions for extending this work.

II. Two-Level Multiple Access Model

Figure 1 depicts a two-level multiple access network consisting of a regenerating satellite and M subnets. Each subnet of N terminals interacts with the satellite indirectly through a single designated platform in the subnet called a local access controller (LAC). The terminal-LAC links and the LAC-satellite links constitute the first and second levels of the network hierarchy, respectively.

A CSMA-type protocol called mini-slotted alternating priorities (MSAP) to be explained shortly is employed at the first level in each subnet. At the second level a TDMA uplink and a time division multiplexed (TDM) downlink is arbitrarily assumed for definiteness. Alternatively, an FDMA uplink and frequency division multiplexed (FDM) downlink, or FDMA/TDM, or TDMA/FDM could have been assumed. Derviations of similar results for these other three combinations are straightforward and will not be included in this paper. These fixed assignment multiplexing schemes were selected for initial second-level consideration since they are easy to analyze. Naturally, they imply differences in implementation complexity in the LAC-satellite links.

Protocol Description

A generic uplink frame structure is shown in figure 2. In the MSAP protocol each user in a given subnet senses whether that level-1 subnet channel is busy. It is assumed that this channel belongs to any (kth) subnet user that is currently transmitting concatenated packets until his transmit buffer is empty. In that event all subnet users

Copyright © American Institute of Aeronautics and Astronautics, Inc., 1980. All rights reserved.

will sense that the channel is idle within a mini-slot of duration τ, equal to the maximum one-way propagation delay within a subnet. The next (k + 1-st) user in a predetermined but programmable priority sequence will immediately take control of the channel if he has a ready packet by transmitting his first packet. This transmission will arrive at the subnet LAC within the next mini-slot interval, and the process continues. If user k+1 has no packets to transmit, another mini-slot is required before the following (k + 2-th) user in the priority sequence is guaranteed an opportunity for transmission, etc. Any packet received by an LAC from a terminal in its subnet is retransmitted in that subnet's allocated slot of the TDMA frame over the level-2 satellite channel.

In the TDMA/TDM configuration selected for analysis, the satellite does nothing more than demodulate and remodulate packets, i.e., there is no on-board buffering or switching. Thus, except for adding a processing delay equal to one TDM(A) slot duration, the satellite acts as the usual "bent pipe" in this instance. The subnet LACs will listen to the TDM downlink broadcast and receive, buffer, and rebroadcast transmissions destined for their local area terminals according to packet header information.

In this paper it is assumed that packets need to be retransmitted only if there are packet collisions. For the two-level protocol just defined there is no possibility of packet collisions anywhere in the system.

Throughput Analysis

For the time being, assume that the one-way propagation delays within a subnet are negligible, i.e., let $\tau = 0$ for now.

Each terminal independently generates packets of duration T at an average rate λ packets/sec according to a Poisson process. The expected number of packets generated per terminal in a T sec packet interval, or the average terminal traffic load, is

$$g = \lambda T. \tag{1}$$

Since there can be no packet collisions, the average terminal throughput s or carried load, i.e., the expected number of successfully transmitted packets per packet interval, is simply g for $Ng \leq 1$, where N is the number of terminals in a subnet. For larger traffic loads, packets are lost to transmitter buffer overflow, i.e.,

$$s = \begin{cases} g, & g \leq 1/N \\ 1/N, & \text{otherwise.} \end{cases} \tag{2}$$

Similarly, let G_1 be the average subnet traffic load, or the expected aggregate number of packets generated per packet interval in a subnet of N terminals. Since there are no packet retransmissions, the average subnet load is due to new packets only, i.e.,

$$G_1 = Ng = N\lambda T. \tag{3}$$

Then S_1, the average subnet throughput, or the expected aggregate number of successful packets transmitted in a subnet per packet interval is

$$S_1 = Ns = \begin{cases} G_1, & G_1 \leq 1 \\ 1, & \text{otherwise} \end{cases} = \begin{cases} Ng, & g \leq 1/N \\ 1, & \text{otherwise.} \end{cases} \tag{4}$$

Finally, let G be the average network load, or the expected total number of packets generated per packet interval in the entire network. Since there are M subnets,

$$G = MG_1 = MNg. \tag{5}$$

Because of the higher burst rate by factor of M at level 2, the average total network throughput, S, from the M subnets, or the expected total number of successful packets transmitted per packet interval in the network, is

$$S = MS_1 = \begin{cases} MNg, & g \leq 1/N \\ M, & \text{otherwise.} \end{cases} \tag{6}$$

Actually, since the maximum one-way propagation delay τ within a subnet is positive, the average network throughput is only $\alpha S < S$, where the factor $1 - \alpha \ll 1$ characterizes the relative overhead, or the expected number of mini-slots of duration τ per packet interval due to idle users, i.e., terminals with no packets to transmit when there is the opportunity. There is no attempt to compute α in this paper. It is simply assumed that $\alpha = 1$, so far as average throughput is concerned.

Delay Analysis

The expected end-to-end packet delay D is the average time between the source terminal generation of a packet and the correct reception of that packet at the intended sink terminal normalized by T. A few assumptions and definitions are listed before estimating D for the proposed two-level scheme.

The time for a terminal to detect the presence of a carrier from another terminal in the same subnet is taken as zero. The maximum one-way propagation delay τ within each subnet is small compared to a packet length T, i.e., $a = \tau/T \ll 1$; normally, this ratio will be between 0.001 and 0.1. Let b be the ratio of the maximum round-trip propagation delay δ between the satellite and an LAC (or terminal), and the packet length T, i.e., let $b = \delta/T$.

In various polling-type schemes, the time between the end of transmission of one terminal and the beginning of the next terminal's opportunity for transmission is called the change-over time. If r is the change-over time in mini-slots of duration τ, r = 1 for the MSAP protocol(5).

Uplink Level 1: According to a previously derived delay formula for polling, which can be specialized to the MSAP protocol, the expected delay D_1 at the first level is given by(5)

$$\begin{aligned} D_1 &= 1 + \frac{S_1}{2(1-S_1)} + \frac{a}{2}\left(1-\frac{S_1}{N}\right)\left(1 + \frac{Nr}{1-S_1}\right) \\ &= 1 + \frac{Ng}{2(1-Ng)} + \frac{a}{2}(1-g)\left(1 + \frac{N}{1-Ng}\right), \quad g \leq 1/N \end{aligned} \tag{7}$$

by (4) and since r = 1 for the MSAP protocol. The first term of (7) corresponds to packet transmission time; the remaining terms represent queueing delay, except for the term a/2 which results from an average worst-case inter-terminal propagation delay.

Uplink Level 2: Delay at the second level results from buffering at the LAC's and transmissions at a TDMA burst rate M times larger than at level 1. The expected delay D_2 at level 2 is

$$D_2 = \frac{1}{M}\left(1 + \frac{M}{2}\left(\frac{S_1}{1-S_1} + 1\right)\right) \qquad (8)$$

$$= \frac{1}{M} + \frac{1}{2(1-Ng)}, \quad g \leq 1/N$$

again using (4). The first term in the first expression for D_2 corresponds to the regenerative processing (retransmission by the LAC) delay, and the second term accounts for the queueing delay, modeled as an M/D/1 queueing system(6). The third term results from assuming that terminal packets may arrive at a LAC at any time during a TDMA slot because of differences in propagation delay within the subnet; this term is present only if the differences in propagation delay can exceed the duration of the TDMA/TDM slots but this is usually the case.

Regenerating Satellite: The normalized delay D_3 for the satellite is simply

$$D_3 = \frac{1}{M} + \frac{\delta}{T} = \frac{1}{M} + b \qquad (9)$$

the sum of the satellite processing (demodulation/remodulation) delay at the higher burst rate and the round-trip delay between the satellite and an LAC.

Downlink Level 2: The downlink traffic to each LAC is assumed to follow a Poisson process with an aggregate generation rate of Nλ packets/sec for tractability. The validity of this assumption could be tested by system simulations in a future investigation. The queueing delay is obtained by considering the usual M/D/1 queue with Poisson arrivals and constant service time. Then since the expected throughputs at each LAC are the same in both directions, the normalized delay D_4 at level 2 on the downlink is the same as the uplink delay D_2, except for the retransmission delay 1/M, i.e.,

$$D_4 = \frac{1}{2(1-Ng)}, \quad g \leq 1/N. \qquad (10)$$

Downlink Level 1: For downlink transmission from a LAC to a terminal, the normalized delay D_5 includes just the packet transmission time plus the mean propagation delay within the subnet

$$D_5 = 1 + a/2. \qquad (11)$$

Note that these terms also appeared in D_1.

Hence, the expected end-to-end packet delay D is given by

$$D = \sum_{i=1}^{5} D_i$$

$$= 2 + \frac{2}{M} + b + a\left(1-\frac{g}{2}\right) + \frac{2 + (1-a)Ng + aN}{2(1-Ng)}, \qquad (12)$$

$$g \leq 1/N$$

from (7) - (11).

III. Performance Comparisons

The end-to-end expected packet delay for the two-level architecture is compared with the delays for single-level TDMA, polling, and Slotted ALOHA in this section. For the sake of fair comparisons, the satellite channel capacity of M message packets per T sec is maintained the same for all schemes discussed. Also, the total number L = MN of terminals in the network is held constant, and the aggregate packet generation rate is the same, i.e., the total expected traffic load, or the average number of packets per T sec interval, is $G = MNg = Lg$, cf. (5).

TDMA

In this single-level scheme all terminals access the satellite directly, i.e., the LACs are removed, and the terminal burst rate increases by a factor of M.* A unique slot of duration T/M sec is reserved for each terminal according to some fixed periodic sequence of period L. Thus, there are L slots in the frame of duration NT sec, and a given terminal must burst a packet to the satellite, if there is one ready to transmit, only in one of the assigned slots for that terminal. The total expected throughput, i.e., average number of packets per T/M sec slot, is now S_1, cf. (4), repeated here for convenience,

$$S_1 = \begin{cases} Ng, & g \leq 1/N \\ 1, & \text{otherwise} \end{cases} . \quad \text{(TDMA)} \qquad (13)$$

However, there is still no possibility of packet collision.

The average uplink packet delay in TDMA slots divided by the number of TDMA slots in a T sec interval is

$$D_{12} = \frac{1}{M}\left(1 + \frac{L}{2}\left(\frac{S_1}{1-S_1} + 1\right)\right) \qquad \text{(TDMA)} \qquad (14)$$

$$= \frac{1}{M} + \frac{N}{2(1-Ng)}, \quad g \leq 1/N$$

from (13). The first term in the first expression for D_{12} is due to packet transmission, and the second term results from the standard M/D/1 queueing formula(6). The third term reflects the generation of packets at the terminal transmitter at random instants with respect to the beginning of a slot in the same way that propagation delay differences entered into (8) and (10).

The satellite processing plus round-trip delay in T sec intervals is

$$D_3 = \frac{1}{M} + b \quad \text{(TDMA)} \qquad (15)$$

the same as (9).

The downlink delay D_{45} is zero because the processing delay due to receiver demodulation of 1/M is already counted as a transmission delay in (14) in the implicit double-buffer approach to demodulation/remodulation:

$$D_{45} = 0. \quad \text{(TDMA)} \qquad (16)$$

---

*This generally implies more complex terminals.

The total TDMA delay is therefore

$$\begin{aligned} D &= D_{12} + D_3 + D_{45} \qquad \text{(TDMA)} \\ &= b + \frac{2}{M} + \frac{N}{2(1-Ng)}, \quad g \leq 1/N. \end{aligned} \tag{17}$$

Polling

In roll-call polling, a central controller sends a polling packet to each terminal in turn. When a terminal is polled, it transmits all its packets before indicating an empty buffer condition. Then the next terminal in sequence will be polled. The burst rate is again M times that of the terminals in the MSAP protocol of the two-level architecture, so that the satellite channel capacity remains the same.

For definiteness, an earth-based central access controller is postulated. Then the polling or change-over time overhead required to query one terminal, this time in mini-slots of duration δ, is

$$r = \frac{2\delta + 2\beta T/M}{\delta} = 2(1 + \frac{\beta}{bM}) \quad \text{(Polling)} \tag{18}$$

where $\beta < 1$ is the polling packet length normalized by the message packet length, and b is the worst-case normalized round-trip delay between the earth and the satellite. If the controller were in the satellite, the polling overhead would be r/2. In the case of the earth controller, (18) follows because there is a regeneration processing delay in both the satellite and the terminal due to the polling packet. There is no such delay in the return direction because it is assumed that the central controller can sense whether the polled terminal has a packet to transmit after just the propagation delay.

The expected packet delay, normalized by T, for polling is now given by$^{(5)}$

$$\begin{aligned} D &= \frac{1}{M}(1 + \frac{S_1}{2(1-S_1)} + \frac{bM}{2}(1-\frac{S_1}{L})(1 + \frac{Lr}{1-S_1})) \quad \text{(Polling)} \\ &= \frac{1}{M}(1 + \frac{b(M-g)}{2} + \frac{N(2bM(M-g)(1+\frac{\beta}{bM})+g)}{2(1-Ng)}), \\ &\qquad g \leq 1/N \end{aligned} \tag{19}$$

using (18) and taking $S_1 = Ng$, $g \leq 1/N$, for Polling, as in (13), which again ignores the loss of throughput due to polling overhead.

Slotted ALOHA

In Slotted ALOHA, terminals with packets to transmit do so at random except for aligning the beginning of a packet with an uplink slot of the same duration. Again, the terminal burst rate is M times larger than in the two-level structure to maintain the same satellite channel capacity.

If q is the probability that a single packet transmission is successful, and if G_1 is the expected value of the aggregate contending packet traffic (number of new and retransmitted packets per slot of duration T/M sec), then the expected throughput, i.e., the average number of packets per T/M sec slot, is given by$^{(6)}$

$$S_1 = G_1 q = G_1 \exp(-G_1) \quad \text{(Slotted ALOHA).} \tag{20}$$

In addition to a regenerating satellite it is assumed that a packet broadcast means for acknowledging successful uplink transmission is employed. That is, the transmitting terminal is able to determine whether one of his packets was involved in a collision by monitoring the downlink. The round-trip processing and propagation delay between the terminal and the satellite is

$$r = 2 + bM \text{ (slots of duration T/M).} \qquad \text{(Slotted ALOHA)} \tag{21}$$

If each terminal retransmits an unsuccessful packet in one of K consecutive slots selected at random immediately following the round-trip delay for that packet, then the expected packet delay normalized by T is

$$\begin{aligned} D &= \left(1 + \sum_{i=0}^{\infty} \left[R + (R + \frac{K-1}{2})i\right] q(1-q)^i\right)/M \qquad (22a) \\ &= \left(1 + R + (R + \frac{K-1}{2})(\frac{1-q}{q})\right)/M \quad \text{(Slotted ALOHA)} \end{aligned}$$

where

$$\begin{aligned} R &= r + 1 - \{bM\} \\ &= 3 + [bM] \end{aligned} \tag{22b}$$

with {.} and [.] denoting the fractional and integral part of ., respectively. The 1 - {bM} of (22b) arises from having to wait until the next slot time to retransmit an unsuccessful packet.

Examples

For illustrative purposes, consider a system with N = 10 terminals per subnet, M = 10 subnets, a packet length of 1000 bits and a data transmission rate of 1 kbps. If the maximum distance between terminals within a subnet is about 200 miles, the relative propagation constant is approximately a = 0.001. For a geostationary altitude satellite the round-trip propagation delay δ is about 0.25 sec, which implies b = 0.25, since packets are 1 sec long. This also implies that R = 5 for Slotted ALOHA, from (22b); K = 6 is assumed to approximate the maintenance of Poisson arrivals in Slotted ALOHA. A polling packet of 100 bits is assumed for single-level polling, so $\beta = 0.1$.

The expected packet delay, normalized to T sec slots, vs. throughput curves are shown in figure 3 for the two-level architecture of (12), and the single-level schemes of (17), (19) and (22). The proposed MSAP/TDMA system achieves shorter delays than pure TDMA and polling, and the same total throughput of $S = MS_1$ packets/T sec. In the desirable segment of the performance curve below $S_1 = 37\%$ on a T/M sec slot basis, single-level Slotted ALOHA achieves shorter delays than MSAP/TDMA, which is not surprising. But note that MSAP/TDMA can achieve much higher throughput values than this random access scheme.

IV. Conclusion

A two-level network architecture for a packet satellite system is proposed to provide efficient communication for a large number of terminals. The introduction of a second level of hierarchy allows much increased throughput while maintaining the ability to handle many users. The delay-throughput performance of the proposed two-level scheme is better than single-level Slotted ALOHA, polling, and TDMA.

Extensions of this work would include more complex on-board processing/buffering/storage models and their processing and queueing delay impacts on the end-to-end delay performance. The validity of the assumption of the Poisson downlink traffic could be tested by system simulations. Straightforwardly defined alternative configurations, e.g., two-level ALOHA, and MSAP at the first level and FDMA at the second level with a TDM downlink could also be analyzed. The reader is invited to compute the delay-throughput performance for such examples to obtain additional data on this proposed two-level access method.

References

1. Jacobs, I.M., Binder, R., and Hoversten, E.V., "General Purpose Packet Satellite Networks," Proc. IEEE, Vol. 66, November 1978, 1448-1467.

2. Capetanakis, J.I., "The Multiple Access Broadcast Channel: Protocol and Capacity Considerations," Ph.D. Dissertation, Cambridge, MA: M.I.T., August 1977.

3. DeRosa, J.K., Osarow, L.H., and Weiner, L.N., "Efficient Packet Satellite Communications," IEEE Trans. Commun., Vol. COM-27, October 1979, 1416-1422.

4. White, B.E., Wilson, Q.C., and Kota, S.L., "Satellite Communications System Netting Concepts for Mobile Terminals," NTC 78 Conference Record, Birmingham, AL, 3-6 December 1978, 28.2.1-28.2.5.

5. Kleinrock, L., and Scholl, M., "Packet Switching in Radio Channels: New Conflict-Free Multiple Access Schemes for a Small Number of Data Users," ICC 77 Conference Record, New York, 12-15 June 1977, 22.1-105 - 22.1-111.

6. Kleinrock, L., Queueing Systems, Volume I: Theory, New York: Wiley, 1975, Volume II: Computer Applications, New York: Wiley, 1976.

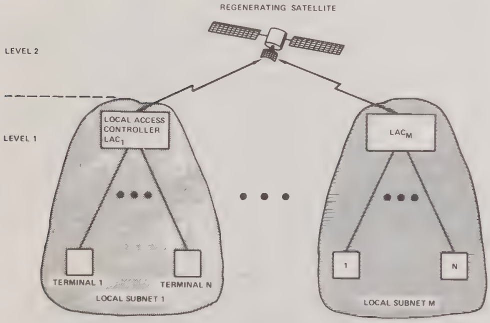
REGENERATING SATELLITE
LEVEL 2
LEVEL 1
LOCAL ACCESS CONTROLLER LAC1
LACM
TERMINAL 1
TERMINAL N
LOCAL SUBNET 1
1
N
LOCAL SUBNET M

Figure 1. A TWO-LEVEL MULTIPLE ACCESS MODEL

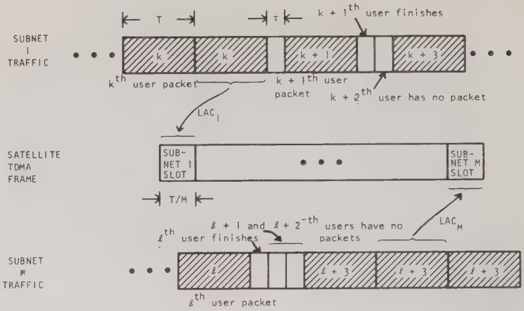
T
τ
k + 1th user finishes
SUBNET 1 TRAFFIC
k
k
k + 1
k + 3
kth user packet
k + 1th user packet
k + 2th user has no packet
LAC1
SATELLITE TDMA FRAME
SUB-NET 1 SLOT
SUB-NET M SLOT
T/M
ℓ + 1 and ℓ + 2-th users have no packets
ℓth user finishes
LACM
SUBNET M TRAFFIC
ℓ
ℓ + 3
ℓ + 3
ℓ + 3
ℓth user packet

Figure 2. Generic Uplink Frame Structure

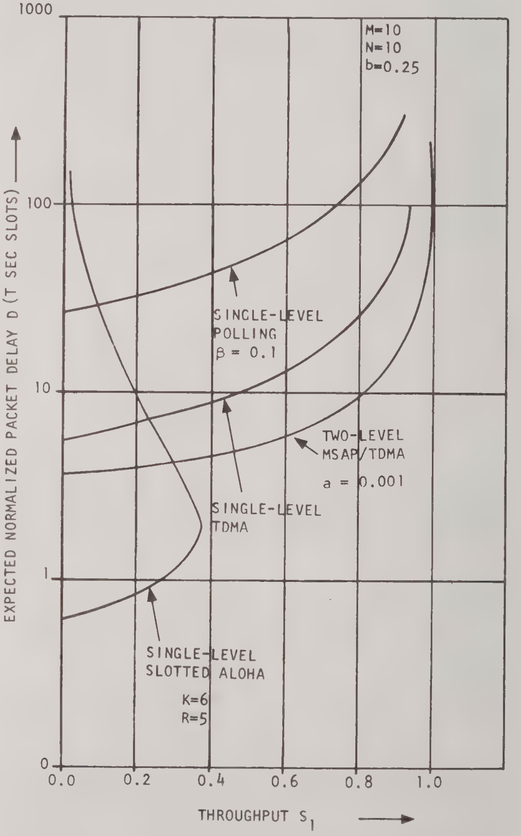

Figure 3. Delay-Throughput Performance

80-0540

DIGITAL PHASE MODULATION METHODS GIVING A BAND-LIMITED SPECTRUM FOR SATELLITE COMMUNICATIONS

D. Muilwijk, J. Noordanus

Philips' Telecommunicatie Industrie B.V.

P.O. Box 18, 1270 AA Huizen, The Netherlands

SUMMARY

This paper highlights a new class of digital phase modulation methods which are designed to obtain very low out-of-band radiation of a hard-limiting radio transmitter without the use of output filtering.

After enumerating the main requirements of a digital modulation method for satellite communication in a multiple FDMA mode, usable in small and simple ground terminals, known digital modulation methods such as QPSK and MSK are scrutinized regarding these requirements.

It appears that there is a need for spectrum control to reduce the out-of-band radiation to a lower level. A general outline of the measures necessary to achieve this is given, and these are illustrated by two practical examples, TFM and COR-PSK (4-5), which were invented at the Philips Research and Advanced Development laboratories.

Calculations and measurements of the output spectra indicate a monotonic decreasing sideband level at a rate of about 80 dB per f_{bit} frequency change.
The phase trajectories are compared with those of some known digital phase modulation methods. Good phase control is essential for exact spectrum control, therefore new types of phase modulators which perform this function are described.

Finally, the obtainable channel separation with TFM is indicated and some details of the receiver circuitry application in small ground terminals are discussed.

INTRODUCTION

Digital modulation is becoming very important in satellite communication systems. Up to now, however, most digitally modulated radio signals need a linear power amplifier to preserve the signal characteristics and to maintain a narrow-band limited spectrum.

For large ground stations where high power levels are involved, as well as for smaller (mobile) earth terminals with only one or two communication channels, non-linear amplification without output filtering is much more economical. It is also very practical to organize a system consisting of small independent earth terminals as a frequency-division multiple access (FDMA) system with a high frequency-packaging density to obtain spectrum economy.[1]

The resemblance with land mobile radio techniques is striking, therefore new digital transmitting methods evolved for land mobile radio applications are of interest to satellite communication.

REQUIREMENTS

The main requirements for a digital modulation method for FDMA satellite communication are :

1. Low out-of-band radiation.
2. Constant amplitude.
3. High noise resistance.
4. High co-channel resistance.
5. Optimum relative bit speed.
6. Hardware feasibility.
7. Stability.

Copyright © American Institute of Aeronautics and Astronautics, Inc., 1980. All rights reserved.

re 1. Low out-of-band radiation

In terms of spectrum efficiency, it goes without saying that individual transmissions must be confined to a definite frequency band so that neighbouring transmissions can go on without mutual interference, raising in this way the number of usable channels to a maximum. This means a high adjacent channel selectivity for the transmitter and receiver of the terminal.

In practice the problem is not so much situated at the receiver, which can indeed have a high dynamic selectivity, but at the transmitter, in the form of unwanted radiation outside the channel bandwidth. Thus, the transmitter must be constructed in such a way that very low out-of-band radiation emerges. This adjacent channel radiation should be measured with the dynamic level variations in mind. This means that, with a 5 dB variation caused by transmitter power and propagation changes, a level of about 25 dB below transmitter output power is wanted.

A new digital modulation method has to fulfill this first requirement, but the transmitter power amplifier should preserve the spectrum quality of the output signal.

re 2. Constant amplitude

If the modulation is only in the phase of the carrier, such as in FM, hard limiting cannot affect this information and the signal can pass high-efficiency power amplifiers and limiters in receivers. A known digital modulation method with constant envelope is MSK or FFSK.[2]

Prefiltered or endfiltered QPSK (4-PSK) digital modulation methods do not have a constant envelope.

re 3. High noise resistance

In satellite communications, optimum sensitivity is needed to reduce antenna diameter and transmitter power on the ground and in space. It is this fact which makes digital transmission, with its inherent high noise resistance, so important.

If we now consider different digital phase modulation methods, it is known that two- or four-phase level modulation methods have the highest interference resistance, caused by a maximum distance existing between the signal vectors in the signal space diagram.

Therefore, 4-phase (QPSK) modulation giving the lowest frequency use, with the signal vectors spaced at an angle of $\pi/2$ radians, is optimum in this respect.

If more than 4 phase levels are used the noise resistance is reduced.

re 4. High co-channel resistance

This is important in satellite communication systems which apply frequency reuse for better frequency economy. Spillover from other satellite beams on the same frequency is less harmful if the co-channel resistance is high, and so the frequency economy of the system can be upgraded.

Digital modulation normally offers a better safeguard against co-channel effects than analogue methods. For the same reason as given in re 3 this leads to the choice of a 4-phase modulation method.

re 5. Optimum relative bit speed

Another important requirement for a modulation method is the relative bit speed which can be obtained. The number of bits per second per unit of bandwidth (bit/s Hz) determines the channel spacing needed at a given bit rate.

For example, if digital voice has to be transmitted, a DCDM (Digitally Controlled Delta Modulation) coder is needed with a bit rate of 32 kbit/s to obtain good telephone quality. The choice of the modulation method and the voice coding method thus fix the minimum frequency distance which can be employed. It is possible to raise the relative bit speed by multilevel modulation at the cost of transmitting power and hardware complexity. However, this becomes particularly objectionable in satellite communication.

It will be clear that new, more effective source encoding methods will affect the traffic capacity to a large extent.

re 6. Hardware feasibility

A further requirement for the implementation of a modulation method is that it be practically feasible within reasonable costs.

It will be stressed in the following that new types of modulation require innovations in the modulator and demodulator design. The resulting performance depends fully on these RF modems.

Greater complexity of the hardware can only be accepted if drastic microminiaturization is possible. Fortunately this is easily accomplished with digital circuitry.

re 7. Stability

Phase modulators which fulfill the abovementioned requirements must be constructed to maintain the desired phase deviations in a reproducible and accurate manner.

The application of digital control circuitry will facilitate this.

USEFULNESS OF EXISTING DIGITAL MODULATION METHODS

Based on the foregoing discussion, four-phase constant amplitude modulation will presumably fulfill requirements 2), 3), 4), 6) and 7) and deliver a moderate relative bit speed for requirement 5).

The known constant-amplitude phase-modulation methods, such as hard-switched QPSK and phase-shaped QPSK [3], Minimum-Shift Keying (MSK or FFSK), baseband-filtered MSK [4], AQPSK, SQPSK or OQPSK and SFSK [5], deliver an output spectrum that does not fall off sharply and sometimes rises again at a greater distance from the carrier (see fig. 1).

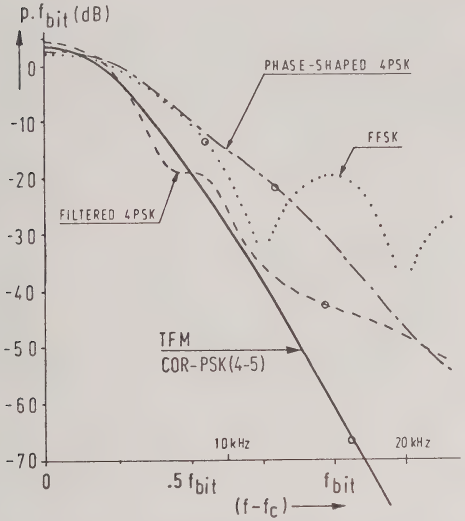

FIG. 1 SPECTRA OF QPSK, FFSK, TFM AND COR-PSK (4-5)

Only the output-filtered QPSK gives good spectrum roll-off down to -40 dB, but this modulation does not fulfill requirement 2 (constant envelope).

It appears that what is needed is an improvement in spectrum control. Efforts in baseband shaping and windowing over one or two bits, reflected in the large number of different PSK modulation methods mentioned above, are limited by the restraints of hardware feasibility (6) and stability (7).

An example of such precise gaussian shaping of MSK (G-SM-MSK) is given in [6]. However, this sharp filtering raises the intersymbol interference.

In the Philips Research and Advanced Development Laboratories methods for direct radio spectrum control were studied, which resulted in the following philosophy.

METHODS FOR SPECTRUM CONTROL : GENERAL OUTLINE

Intuitively it is easy to understand that the sharp changes and bends in the phase trajectories of the modulated signal are responsible for the out-of-band radiation. It has been long known that phase discontinuities were disastrous in this respect, and continuous phase modulations such as FFSK were introduced for this reason.

Following this line of thought, solutions could be presented by applying the rules given below.

1) Rigid control of the transmitter output phase in absolute phase change ($\frac{2\pi}{n}$ radian) and phase trajectory per bit.
2) Establishment of more digital phase-change levels (k) in the transmitted signal than in the input signal.
3) Use of this additional degree of freedom to establish the most suitable overall phase trajectory to obtain spectrum compactness, taking into account the past phase history.
4) This choice of the phase trajectory is further influenced by the practical feasibility of carrier and clock regeneration in the receiver. This means that the phase path has to dwell long enough around the $\frac{2\pi}{n}$-separated phase positions.

Two examples of application of these rules are TFM and COR-PSK (4-5). TFM uses a 2-level input signal and a 5-level ($0, \pm\frac{\pi}{4}, \pm\frac{\pi}{2}$ radian) output signal. COR-PSK (4-5), a member of the Correlative-PSK family, utilizes 4 input levels and 5 transmit levels ($0, \pm\frac{1}{2}\pi, \pm\pi$).

Tamed Frequency Modulation (TFM)

A short explanation of the principle of TFM can best be given starting from Minimum Shift Keying (MSK).

In MSK, a binary "one" is transmitted by changing the carrier phase through $\pi/2$ upwards in a linear way, and a "zero" by the same change downwards (fig. 2b, dotted line). This is, in fact, a special four-phase method because all $\pi/2$-multiples are used. In MSK we find discontinuities in the derivative of the phase, which cause a lot of out-of-band radiation.

In TFM [7] the phase changes are smoothed considerably with respect to MSK without loss of information (fig. 2b, solid line). Each data symbol is spread out over three symbol intervals. This process can be described as correlative coding (or partial response coding) followed by proper filtering. It is described in detail in [8]. The phase changes per input symbol remain multiples of $\pi/2$, but this variation is now reached over several bit intervals instead of one. Excepting delays, the phase change begins one bit interval before the input signal changes and stops one interval later.

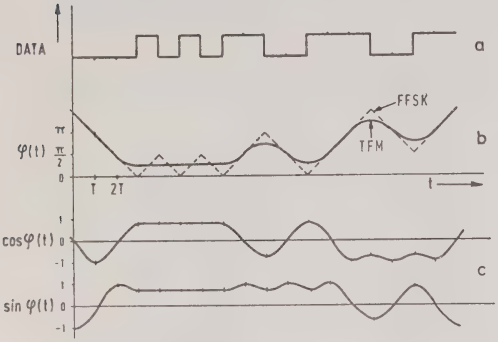

FIG. 2 TFM PHASE TRAJECTORIES

The smoothing of the phase goes so far that data reversals (0 1 0 1 0 1 ...), normally giving rise to a repetitive signal with a frequency at half the bit rate, now result in a constant phase signal.

From the sketches in fig. 2c of cos ϕ and sin ϕ (the orthogonal signals obtained after coherent detection) we can see that the highest frequency of importance occurring in these components is ¼f_b (f_b = bit rate). This also means that in the receiver higher frequencies can be filtered out.

A considerable improvement in the spectrum has been reached with this method as demonstrated by the graph of the power density as a function of frequency for TFM in fig. 1. It shows a steep and continuous decrease for TFM.

At bit rate distance from the carrier the spectrum density is already 60 dB down with respect to total power. The spectrum decrease at bit rate distance is at least one order of magnitude better than for the other methods.

An adjacent channel interference ratio of -25 dB is reached at a channel distance of 0.75 f_{bit}.

A further account of the obtainable channel spacing with TFM is given in the paragraph about channel separation with TFM.

Considering the theoretical BER-versus-C/N_o curve in reference [8], (fig. 13 of that paper), calculations show only 1 dB degradation with respect to unfiltered PSK.

Another calculation published in the appendix of [9] gives the same result.

A simple explanation to demonstrate that the BER behaviour is comparable with that of MSK is the following : Fig. 2b and c show that the output of a coherent demodulator (giving cos ϕ and sin ϕ at the sampling moments) can have values of $\pm\sin\frac{\pi}{4} = \pm 0,7$ in addition to the value ±1. This means a loss of 3 dB. However the demodulator filter bandwidth can be made roughly ¼f_{bit} in the case of TFM, as compared to the ½f_{bit} value normally used with MSK, and this compensates for the loss of 3 dB.

Evaluation of laboratory models in ref. [9] revealed that the theoretical curves of the TFM spectrum can be approximated in practice to within 1,5 dB (see fig. 3 curve 1).

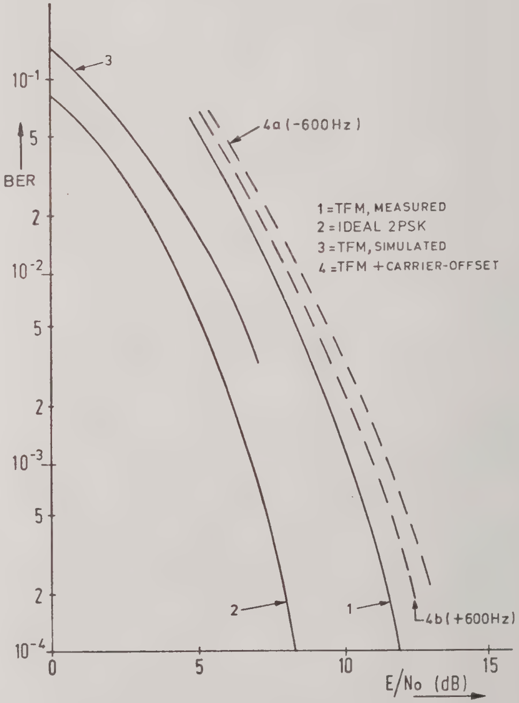

FIG. 3 BIT ERROR RATE (BER) VERSUS SIGNAL TO NOISE RATIO E/N_o ($f_{carrier}$ = 11 MHz, bit rate 16 kbit/s)

Correlative PSK (COR-PSK)

As a result of the research on TFM, a new family of constant amplitude modulation methods was invented recently at the P.T.I. Advanced Development Radio Department [10]. These modulation methods also have spectrum conserving properties.

Compared with TFM, COR-PSK is also applicable to more than two level input signals. In general, with an n-level input signal, the phase changes will be an integral multiple of $2\pi/n$ radians, but in order to have additional freedom in spectrum shaping, the number of phase-change levels of the transmitter is k, k being larger than n (k and n are integers).

Furthermore the next phase step can be defined on the basis of more than two foregoing phase changes, using an algorithm that minimizes spectrum width.

As illustration we will consider the simple case of a four-level input signal (n=4) and 5 levels of discrete phase changes (k=5) in the transmission path. These five levels are 0, $+\pi/2$, $-\pi/2$, $+\pi$ and $-\pi$.

The difference between normal QPSK and COR-PSK is that in the former method each input level uniquely corresponds to a fixed phase change of 0, $\pi/2$, $-\pi/2$ and π (or $-\pi$), but in the latter a deliberate choice is made between $+\pi$ or $-\pi$ phase change to obtain the smoothest phase trajectory.

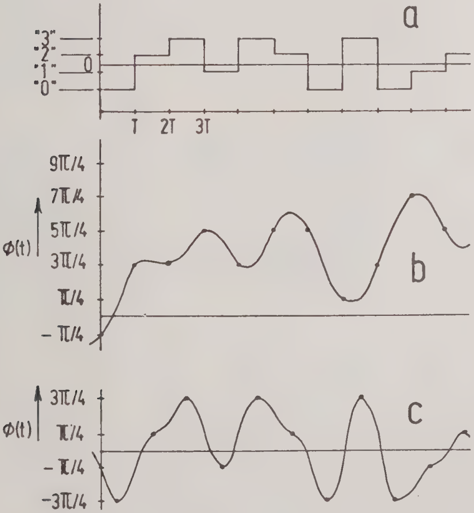

FIG. 4 COR-PSK and QPSK PHASE TRAJECTORIES

In fig. 4 line a, the four-level input signal with a speed of $\frac{1}{T}$ baud is depicted (levels "0", "1", "2" and "3"), where

"1" corresponds with $\Delta\phi = -\pi/2$

"2" with $\Delta\phi=0$

"3" with $\Delta\phi=+\pi/2$

If the signal is "0", a choice is made between $\Delta\phi=-\pi$ or $+\pi$, depending on the foregoing phase changes (fig. 4b). The phase changes for QPSK (fig. 4c) are more irregular and larger, giving rise to the prediction of lower out-of-band radiation for COR-PSK (4-5).

Calculations of the spectrum confirm this prediction (see fig. 1). There is little or no difference compared to the TFM curve. The same applies to the BER behaviour. (See ref. [11]).

COMPARISON OF PHASE TRAJECTORIES OF QPSK, TFM AND COR-PSK (4-5)

In fig. 5 a comparison of the phase trajectories of the above systems is made in the vector space with the same digital input signal.

For clarity of presentation some amplitude modulation is shown.

Fig. 5a shows constant amplitude QPSK, fig. 5b, the trajectories of TFM and fig. 5c, the vector path for COR-PSK (4-5).

Note also that in fig. 5b and 5c there are, $\frac{\pi}{2}$ radians apart, points where the phase remains constant or is reversed. These locations in the vector diagram are important to recover the reference phase in the receiver.

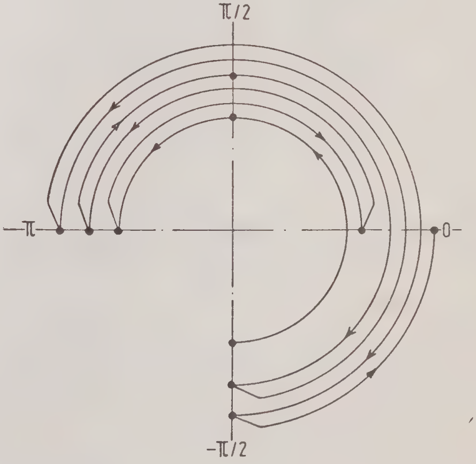

FIG. 5a VECTOR TRAJECTORIES FOR QPSK

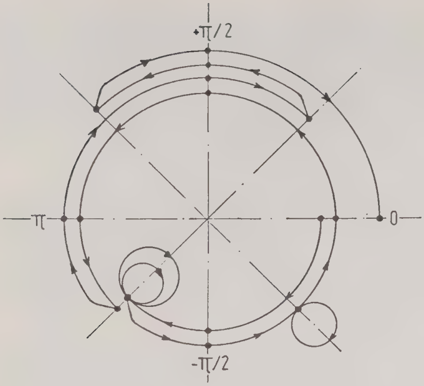

FIG. 5b VECTOR TRAJECTORIES FOR TFM

PHASE MODULATORS

As stated above, good spectrum control means exact control of the phase trajectory of the RF output signal.

From the descriptions of TFM and COR-PSK an additional requirement for the phase modulators emerges, that is, that the phase must be manipulated continuously over a very broad range, amply exceeding 2π radians. This excludes the use of classical phase modulators with their limited phase switching range. The required phase synthesis can be obtained with a voltage controlled oscillator, but direct digital phase synthesis can also be used.

The first solution is indicated in the block diagram of fig. 6. There is a double control loop to stabilize not only the centre frequency of the VCO, but also the frequency deviation Δf. The block marked "detector" measures the output phase of the VCO at suitable sample times and delivers correction signals to change centre frequency and frequency deviation, to guarantee that the output phase traverses the right phase points.

After differential encoding of the input data, Nyquist III prefiltering is performed before the signal enters the frequency modulation circuits.

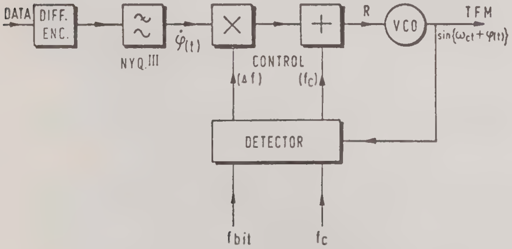

FIG. 6 TFM MODULATOR DOUBLE LOOP

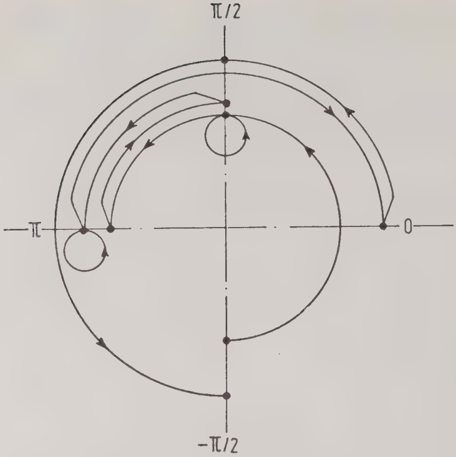

FIG. 5c VECTOR TRAJECTORIES FOR COR-PSK (4-5)

A second solution is given in fig. 7.

A digital phase synthesizer can be made by using a quadrature signal generator driven by input voltages which represent the cosine and the sine of the required output phase.

Via a suitable algorithm, the digital input signal addresses cosine and sine tables stored in a ROM. After digital-to-analog conversion and filtering, the required driving signals are obtained. In this way each wanted phase trajectory can be synthesized, and remains under full digital control.

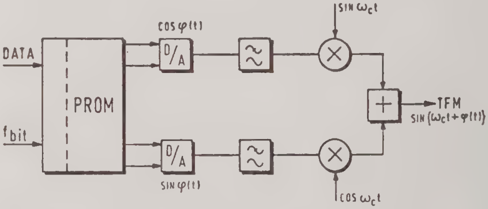

FIG. 7 TFM MODULATOR (QUADRATURE) DIGITAL

RECEIVER CIRCUITRY

A block diagram of a receiver for TFM is given in fig. 8 and 9.

After passing an IF filter, which is needed for the receiver selectivity, the signal is demodulated orthogonally. The IF filter does not influence the signal shaping, which is performed by the post-detection filters. Fig. 8 also shows a

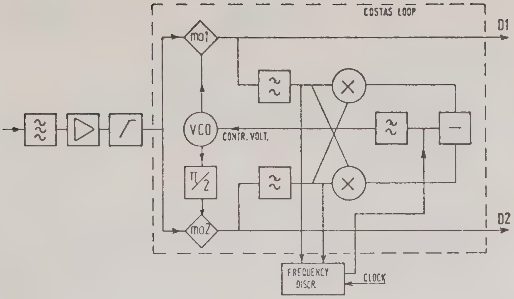

FIG. 8 DEMODULATOR AND CARRIER REGENERATOR

Costas carrier regenerator, with a frequency discriminator circuit to enlarge the catching range under low S/N conditions. From the zero crossings of both demodulated and filtered signals the clock frequency is recovered (see fig. 9), which drives the decision circuits after the post-detection filters. In this way the digital output signals are obtained.

CHANNEL SEPARATION WITH TFM

To get an insight about the allowable channel spacing, results of some computer simulations will be given. These simulations are of a preliminary nature because no optimalization of receiver and satellite filters is included, and only one interferer is considered.

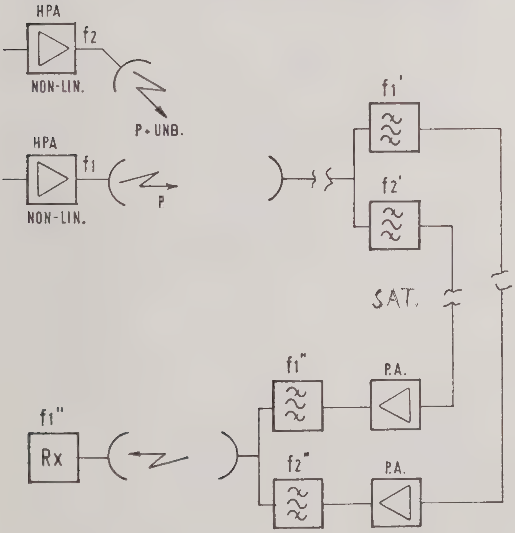

FIG. 10 MODEL OF SATELLITE LINK FOR INTERFERENCE CALCULATION

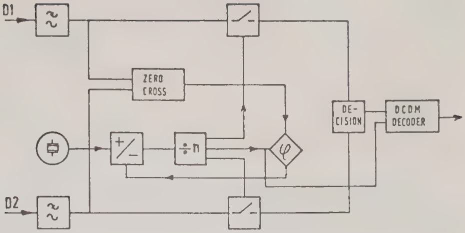

FIG. 9 DECISION CIRCUITS AND CLOCK REGENERATOR

A block diagram of a satellite link is given in fig. 10. Two nonlinear power amplifiers with zero back-off emit the neighbouring frequencies f_1 and f_2, which traverse the satellite transponders.

In fig. 11 the degradation in the channel with frequency f_1, caused by f_2, is depicted. Curve 1 and 2 apply when the satellite amplifier is linear, but for curve 2 the interferer f_2 is 6 dB stronger than f_1. This is typical for use in the S.C.P.C. mode. In these cases the satellite is a more or less linear medium without filters affecting the narrow channels centered at f_1 and f_2.

Curve 3 applies to the broadband TDMA application, where nonlinear power amplification in the satellite transponder is used.

The channels are then filtered before and after the nonlinear amplifiers with sharp ideal filters having a bandwidth equal to the channel spacing.

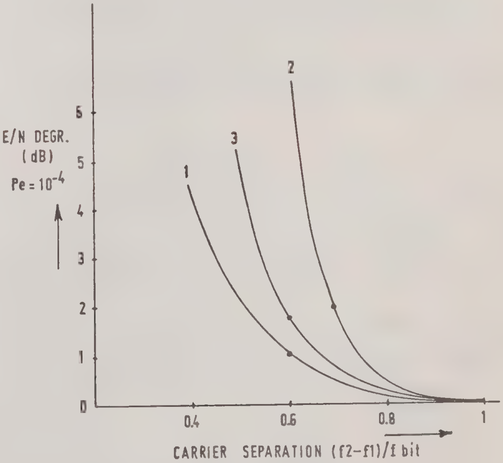

FIG. 11 TFM : DEGRADATION CAUSED BY ADJACENT CHANNEL INTERFERENCE

The figure shows that if the level differences between the emissions are small, a relative carrier separation $\Delta f/f_{bit}$ of only 0,6 to 0,65 is sufficient (with not more than 1 dB degradation).

This frequency spacing compares favourably with other modulation schemes.

Furthermore a benefit of about 6 dB is gained in the ground transmitter terminals, as no back-off is needed there.

APPLICATION IN SMALL SATELLITE GROUND TERMINALS

An example of a block diagram of a two-channel transmitter with hard-limiting output amplifiers is given in fig. 12.

After TFM modulation of the digital input streams at a suitable intermediate frequency, for example 11 MHz, the signals are upconverted to a band around 70 MHz by means of a frequency synthesizer which defines the transmitter channel.

The next upconversion translates the signals to the GHz range, for example 6 GHz, whereafter nonlinear amplification is performed.

Harmonic filters and isolators following the amplifiers deliver their signals to a hybrid (3 dB) coupler. In this way the intermodulation problem of multi-channel transmitters is solved. However, the use of this technique is limited to a low number of transmitters by the increasing loss in the hybrid couplers.

If more channels have to be created solutions could be found in using multiple antennas or feeds.

Another method is to multiplex the digital input streams to a higher bit rate and then perform TFM modulation.

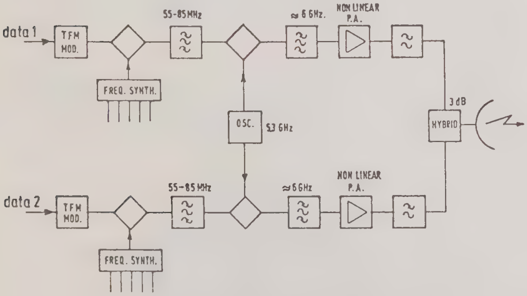

FIG. 12 TRANSMITTER EARTH TERMINAL
TWO CHANNEL

REFERENCES

1. "Efficient Digital Satellite Communications", CCIR Report 767. Recommendations and reports of the CCIR 1978, XIV Plenary Assembly, Kyoto, Volume VIII Mobile Services, pp. 486-487.
2. Subbarayan Pasupathy. "Minimum Shift Keying : A Spectrally Efficient Modulation", IEEE Communications Magazine, Vol. 17, No. 4, July 1979 pp. 14-22.
3. L.J. Greenstein. "Spectra of PSK-signals with Overlapping Baseband Pulses", IEEE Transactions on Communications, Vol. COM-25, No. 5, May 1977 (concise paper), pp. 523-530.
4. F. Amoroso, "Pulse and Spectrum Manipulation in the Minimum (Frequency) Shift Keying (MSK) Format", IEEE Transactions on Communications, Vol. COM-24, No. 3, March 1976. (Correspondence), pp. 381-384.
5. T.S. Seay. "Bandwidth Efficient Phase Modulation Techniques". Paper presented at the International URSI Meeting, Helsinki, Finland, 31 July - 8 August 1978.
6. K. Hirade and K. Murota. "A study of Modulation for Digital Mobile Telephony". Conference record of the 29th Vehicular Technology Conference, Arlington Heights, March 27-30, 1979.
7. F. de Jager, C.B. Dekker, D. Muilwijk. Dutch patent application 7709917, dated 9 Sept. 1977.
8. F. de Jager and C.B. Dekker. "Tamed Frequency Modulation. A Novel Method to Achieve Spectrum Economy in Digital Transmission", IEEE Transactions on Communications, Vol. COM-26, No. 5, May 1978, pp. 534-542.
9. D. Muilwijk. "Tamed Frequency Modulation - a bandwidth-saving digital modulation method, suited for mobile radio", Philips Telecommunication Review, Vol. 37, No. 1, March 1979, pp. 35-49.
10. D. Muilwijk, F. de Jager, C.B. Dekker. Dutch patent application 7901865, dated 8 March 1979.
11. D. Muilwijk. "Correlative Phase Shift Keying - a bandwidth and power efficient constant envelope modulation". Paper to be presented at ICC '80, June 1980, Seattle.

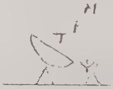

80-0541

A NEW APPROACH TO THE ENCODING OF MULTIPLE DATA SETS

Michael Hankamer*
Texas A&I University
Kingsville, Texas 78363

Abstract

A new approach to encoding multiple data sets is suggested. The method is applicable to both block and convolutional code designs, provided only that a maximum likelihood decoding algorithm is used. Several examples are given to illustrate the power and limitations of this method.

Nomenclature

(n,k)	block code parameters; n is the number of symbols output from the encoder per k digit message block.
(K,b,n)	convolutional code parameters; b is the number of input digits and n is the number of output symbols per shift of the K length shift register.
MPX	multiplexer
DMPX	demultiplexer

Introduction

Consider two simplified models of a time-shared, multi-user communication channel, as one might see in a communication satellite application. In Figure 1(a), the channel is operated uncoded at some prescribed bit-error-rate. Any user requiring better data quality has the option to precode his data prior to using the channel in order to improve his error rate beyond that guaranteed by the channel. In Figure 1(b), the channel is itself coded in order to meet its guaranteed error rate. Again, users wishing to improve on the channel quality have the option of precoding.

One might think that for a fixed total decoding complexity (e.g., channel code plus precode), the method of Figure 1(b) would be superior. Experience has taught us that this is not so, for two reasons. First, the user decoder in Figure 1(b) no longer has access to channel quality information** that it had in Figure 1(a); with less information, the user decoder makes less reliable decisions.† Second, the channel decoder tends to organize its errors into bursts which are harder than random errors for the user decoder to correct.

Yet the pressure is to adopt a communication satellite link of the second form. Higher data rates, more channels and relatively limited spacecraft power all imply channel coding. At the same time, the increasing number of users mandate that at least some will require user coding for improved performance. In this paper, we show that the best of both worlds is achievable -- the transmitter structure of Figure 1(b) can be decoded by a receiver structure similar to that of Figure 1(a).

The Composite Code

In this section we take advantage of an obvious but often overlooked fact: the concatenation of two (or more) codes is also a code. A code can be thought of as a 1-1 mapping from a set of data sequences into another set of code sequences. For example, let $C_1: D \rightarrow S$ and $C_2: S \rightarrow T$ be 1-1 mappings of D into S and S into T respectively. Since C_1 and C_2 are 1-1, their composition (concatenation) $C_2 \circ C_1$ is a 1-1 mapping of D into T -- it is a code. There is a restriction implied in this construction of the composite. Only a maximum likelihood decoding algorithm can be used to decode the composite, since there is no reason to believe that the composition preserves any algebraic properties associated with C_1 and C_2.

It is now evident that even though the received sequence was generated by a pair of encoders, it can be decoded by a single decoder -- provided only that the decoder uses a maximum likelihood algorithm. Each composite decoder now has full access to the channel state information; moreover, there is no "burstiness" due to a channel decoder. A typical structure is given in Figure 2 (note the similarily of the transmitter with that of Figure 1(b) and the receiver with that of Figure 1(a)).

Code Performance

In general, the asymptotic performance of concatenated codes is not easily established. However there are two cases worthy of comment. First, consider the concatenation of two block codes: an (n_1,k_1) precode with an (n_2,k_2) channel code. The concatenation so formed is at most an (n_1n_2,k_1k_2) block code. Assuming a memoryless channel and maximum likelihood decoding, a well known asymptotic bound for code performance is given by

$$P_E < e^{-n_1 n_2 E_B(R)}$$

where $E_B(R)$ is the block coding exponent and R is the code rate expressed in nats per channel transmission[4].

---

*Assistant Professor, Electrical Engineering Member AIAA

**This is the difference between hard and soft quantization at the decoder. The generally accepted loss factor is about 2 dB[1].

†Some channel state information has been passed between the decoders. Forney[2] devised the generalized minimum distance decoding rule for concatenated block codes and Hankamer[3] devised a similar procedure for concatenated convolutional codes.

Copyright © American Institute of Aeronautics and Astronautics, Inc., 1980. All rights reserved.

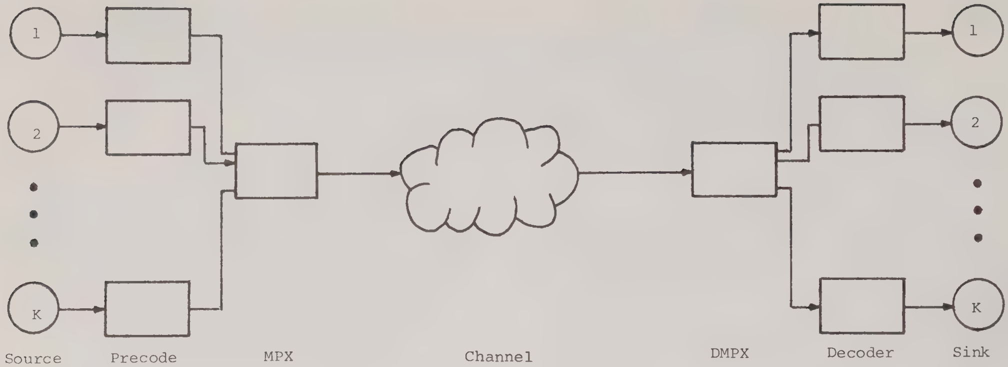
1
2
K
Source
Precode
MPX
Channel
DMPX
Decoder
Sink
1
2
K

a) uncoded channel system.

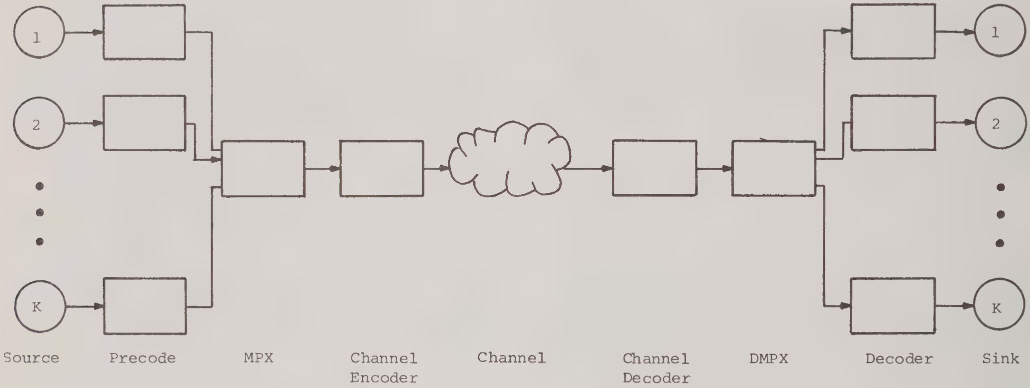
1
2
K
Source
Precode
MPX
Channel Encoder
Channel
Channel Decoder
DMPX
Decoder
Sink
1
2
K

b) coded channel system

Figure 1 Typical communication channels.

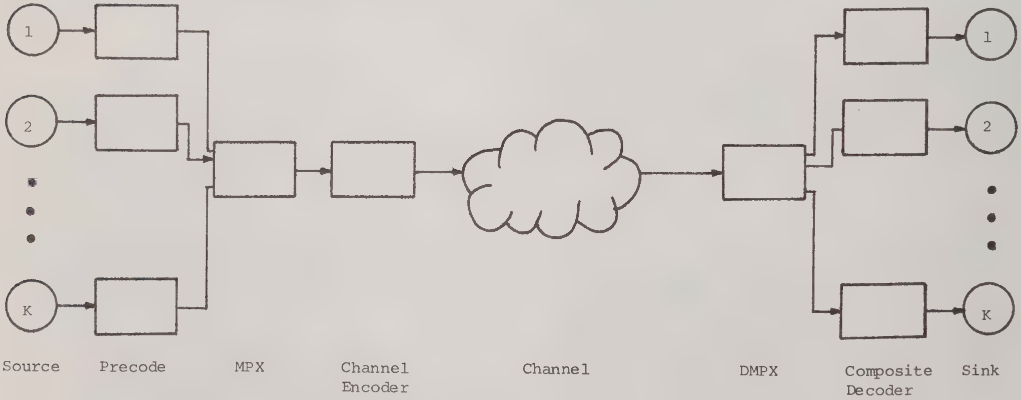
1
2
K
Source
Precode
MPX
Channel Encoder
Channel
DMPX
Composite Decoder
Sink
1
2
K

Figure 2 A new communication system.

In a similar fashion, it can be shown that concatenating a (K_1, b_1, n_1) convolutional precode with a (K_2, b_2, n_2) channel code produces a $\left(K_1 + \left\lceil \frac{b_1}{n_1}(K_2 - 1) \right\rceil, b_1 b_2, n_1 n_2\right)$ composite. The appropriate asymptotic result for the class of linear, time-varying convolutional codes is given by[5]

$$P_E < \frac{\exp[-n_1 n_2 K_c E_c(r)]}{1 - \exp[-n_1 n_2 r (E_c(r) - \rho)]}$$

where K_c is the constraint length of the composite, r is the code rate in nats per channel transmission, $E_c(r)$ is the convolutional coding exponent, and ρ is a parameter used to maximize $E_c(r)$.

It must be pointed out that both asymptotic bounds are averages over the entire class of codes; that is, there is at least one member of the class for which the bound holds true. Since the composite codes constitute only a subclass, it does not necessarily follow that there is at least one member of the subclass that meets the bound. Yet the asymptotic bounds have in the past been a good guide to code performance; it follows that there is some reason to believe that the class of composite codes will perform adequately.

Examples with Convolutional Codes

We choose to consider as examples only concatenations of convolutional codes. There are two reasons. First, convolutional codes are well known to be more powerful than block codes for fixed decoding complexity. Second, and more germane to this paper, is that the two most powerful decoding algorithms for convolutional codes are maximum likelihood algorithms.

Consider first a four user, channel coded system. The channel code is a (3,1,2) code -- the simplest non-trivial convolutional code. User 1 does not precode; user 2 uses the (3,1,2) code as a precode; user 3, a (5,1,2) precode; and user 4, a (7,1,2) precode. The receiver structure is as given in Figure 2. User 1 uses a (3,1,2) decoder; user 2 has a decoder matched to the (4,1,4) composite code, user 3 has a decoder matched to the (6,1,4) composite; and user 4 has a decoder matched to the (8,1,4) composite code. Performance, assuming a Viterbi decoding algorithm for each user, is given in Figure 3. For constrast, we give in Figure 4 the performance for the same transmitter structure using the two-stage receiver structure of Figure 1(b). The difference is striking.

Two more examples are given which illustrate both the breadth and limitations of this approach. Consider a 3-user system. The channel code is a (3,1,2) code, as before. User 1 uses the channel directly; user 2 precodes with a (3,1,2) code; and user 3 precodes with a (4,1,4) code (a concatenation of two (3,1,2) codes). A possible transmitter structure is given in Figure 5. After transmission through the channel, users 1, 2, and 3 utilize (3,1,2), (4,1,4) and (5,1,8) Viterbi decoders, respectively. The performance is given in Figure 6. Again, note the striking difference in relative

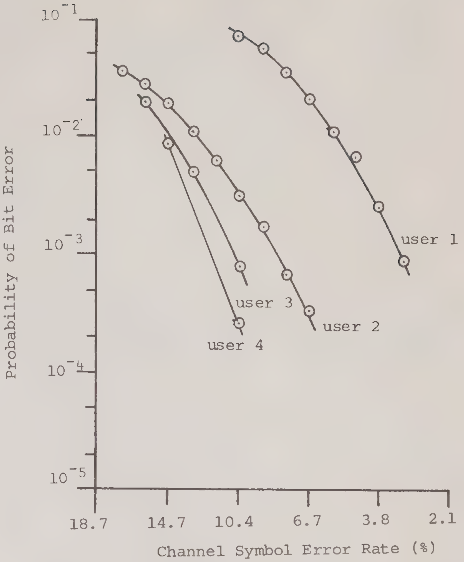

Figure 3 Composite code performance

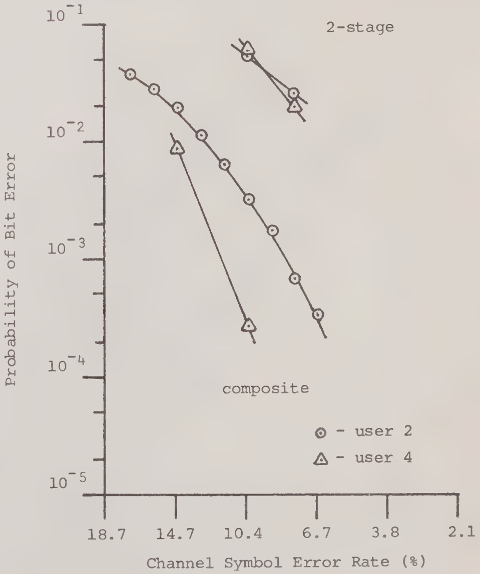

Figure 4 A comparison of two-stage decoding versus the composite code for the system of Figure 3.

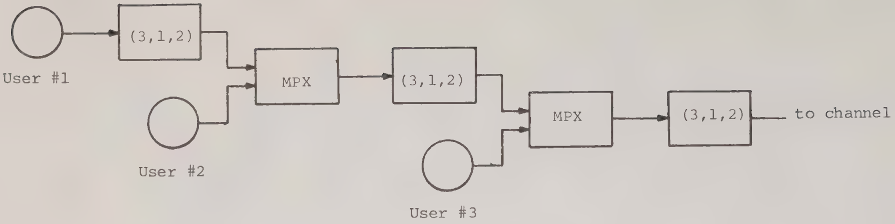

Figure 5 A possibe 3-user communication channel.

performance among the users. For a nominal channel error rate 5.6%, user 1 sees an error rate of about 1%, user 2 sees an error rate of about 0.02% and user 3 sees virtually no errors.

In our final example, we consider the effects of reversing the channel code and the precode. Recall that the (8,1,4) code of Figure 3 resulted from a (7,1,2) precode and a (3,1,2) channel code. Reversing the two codes yields a (6,1,4) composite whose performance is given in Figure 7. The (6,1,4) code again has very good performance relative to the two-stage decoding also shown in Figure 7. From Figure 3, one may note that performance is approximately equal to that of the (6,1,4) composite code formed by the (5,1,2) precode and (3,1,2) channel code; but somewhat disturbing is the "flattening" of the performance curve at low error rates. This tendency of performance to degrade will be discussed in the next section.

Summary of Results

The hybrid method outlined in this paper clearly works. Performance improvement over a direct two-stage decoding is dramatic. In a multi-user environment, relative performance can be easily and independently controlled by choice of the precodes.

As to general structure, it appears that the best form should be to use a relatively weak high rate code for the channel code with lower rate more powerful codes for the precode. The reasons are two. First, one desires, for maximum efficiency, to have the channel code just powerful enough to meet the quality requirement for the least sensitive user ... implying a relatively weak channel code. Second, and more importantly, the concatenation involving a long precode and a short channel code seems to produce a more powerful composite. As evidence consider the two (6,1,4)

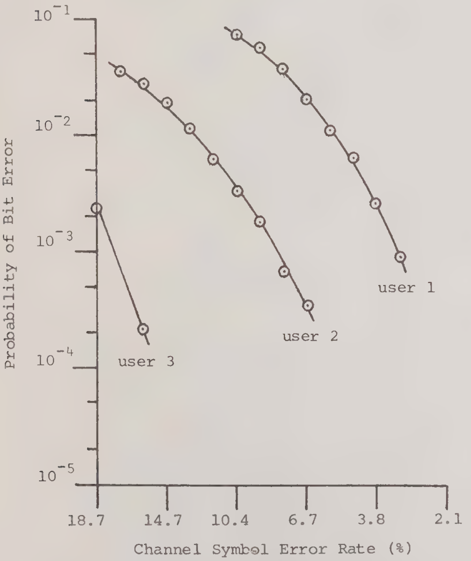

Figure 6 Composite code performance for the transmitter structure of Figure 5.

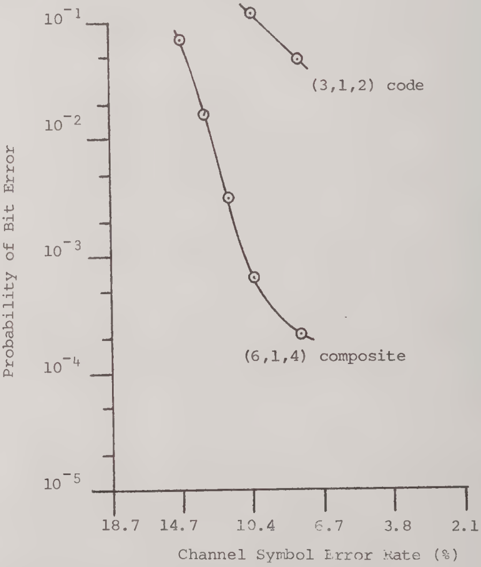

Figure 7 Composite Code Performance for a system with a short precode.

composite codes introduced in this paper. Both showed approximately equal performance, except that the code formed from the (3,1,2) precode showed a definite flattening of the performance curve at an error rate of about 10^{-4}. The flattening is caused by the increasing likelihood of an extremely long error; that is, the (6,1,4) code has at least one long error that encodes into a channel symbol sequence that is "close" to the true channel symbol sequence.

This flattening tendency has been observed in the (4,1,4) composite code as well, although not as severely as is seen in the (6,1,4) composite. It has not been observed in any concatenation involving a precode with a constraint length longer than that of the channel code. Why this is more likely when the precode has a shorter constraint length is not yet clear.

Further Research

While this method looks very promising, it is also clear that it needs further study. Two points in particular need more consideration. First is the performance of this method with non-binary codes. There appears to be no theoretical objection, but as yet is has not been tried. Second, and perhaps the more important question, involves code design. The composite codes utilized in this paper were found by concatenating two known codes. More realistically one is given a channel code and a performance requirement. How does one go about choosing a precode such that the composite meets the performance requirement?

References

[1] Viterbi, A.J. and J.K. Omura, Principles of Digital Communication and Coding, (McGraw-Hill, 1979).
[2] Forney, G.D., Jr., Concatenated Codes (MIT Press, 1966).
[3] Hankamer, M., Concatenated Convolutional Codes: Applications to Deep-Space Telecommunication. Doctoral dissertation, New Mexico State University (January 1978).
[4] Gallager, R.G., "A Simple Derivation of the Coding Theorem and Some Applications", IEEE Trans. Inform. Theory, IT-11 #1 (Jan. 1965).
[5] Forney, G.D., "Convolutional Codes II: Maximum Likelihood Decoding", Information and Control, Vol. 25 (1974).

80-0542

MULTI-SPECTRAL DATA COMPRESSION USING HYBRID CLUSTER CODING

BY

Johnetta R. MacCalla *
AVW Electronic Systems, Inc.
125 North Ash Avenue
Inglewood, California 90301

Ming U. Chang
System Analysis Laboratory
Space and Communication Group
Hughes Aircraft Company
Los Angeles, California 90009

Abstract

An adaptive technique achieving data compression of multi-spectral images through the use of clusters is studied. The algorithm consists of a modified multi-dimensional (multi-spectral) extension of a mode-seeking estimator due to Koontz et al. [1] followed by weighted minimum distance classifier. This estimator is applied to 16 x 16 blocks of Landsat (Earth Resource Satellite) multi-spectral scanner (MSS) data across the four spectral bands to select the number and relative positions of the modes of the data. These modes are used in the minimum distance classifier to assign the remaining points (pixels) of the block to their respective cluster centers. A map of the cluster assignment and the centroids of the clusters become the actual transmitted data. Excellent performance is demonstrated in terms of percent distortion of original and reconstructed data blocks.

I. Introduction

The engineering literature in the past decade documents numerous techniques which have been developed for compression of 2 and 3-dimensional images, based on transforms of linear prediction. In particular, techniques such as DPCM, Linear Transform methods and combinations of these techniques combined with variable length coding have been considered. These coding methods utilize the spatial redundancy within an image field to achieve efficient quantization and coding and are most suitable to applications concerned with subjective image quality. However, increasingly within the last several years, data compression is being applied to aid in the storage and transmission of high resolution data in which the primary use will be automatic computer controlled data extraction. In this case, the concern becomes the preservation of radiometric accuracy and classification efficiency. To meet this need, Hilbert (2) developed a joint feature extraction/data compression technique for removal of redundant data in image approximation and computer classification applications. The Hilbert cluster compression (HCC) algorithm achieves data compression through the use of clustering to extract multi-dimensional primitives from subsets of spatially contiguous measurements in the image data and then applies entropy encoding to the feature map. However, the major drawbacks in the HCC Algorithm are 1) the lack of optimal selection of the initial features to be extracted (called cluster centers by Hilbert) and 2), the inability of the clustering algorithm by its use of 'local means' to preserve 'isolated points'. The result of these two factors are severe smoothing and excessive degradation.

In this paper we present an adaptive technique of data compression which consists of a modified multi-dimensional extension of a mode-seeking estimator due to Koontz et al. [1], followed by a weighted minimum distance classifier. This algorithm achieves the same objectives as the Hilbert Clustering Algorithm without the smoothing or degradation. This estimator is applied iteratively to 16 x 16 blocks of Landsat multi-spectral data to select the number and relative positions of the modes of the data. These modes are used in the minimum distance classifier to assign the remaining points (pixels) of the block to their respective clusters. A map of the cluster assignment and centroids of the clusters become the transmitted or stored data.

The following section will describe the general details of the hybrid cluster algorithm. Section III describes and gives a general explanation of the mode-seeking algorithm as completely specified in terms of a single scalar control variable whose value is a function of the mean and variance of that particular block of data. In Section IV, we define the adaptive selection of the threshold control value and provide a graphical representation of the control equation. Section V discusses the computational aspects of the algorithm and presents results comparing adaptive hybrid cluster coding to various hybrid transform coding techniques and to the cluster/compression algorithm by Hilbert.

---

* Formerly at the System Analysis Laboratory, Hughes Aircraft

Copyright © American Institute of Aeronautics and Astronautics, Inc., 1980. All rights reserved.

II. The Data Compression Algorithm

The hybrid cluster compression scheme can be thought to be divided into the following major components:

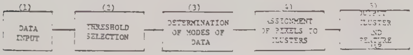
(1)
DATA INPUT
(2)
THRESHOLD SELECTION
(3)
DETERMINATION OF MODES OF DATA
(4)
ASSIGNMENT OF PIXELS TO CLUSTERS
(5)
OUTPUT CLUSTER AND FEATURE MAP

FIGURE 1.

Since the hybrid clustering compression scheme is designed to compress multi-dimensional images, we shall use MSS data format to discuss the implementation of blocks (2), (3) and (4).

MSS has a total of four bands with sixteen detectors in each band. Therefore, the hybrid cluster compression algorithm as applied to the MSS data successively compresses 16 x 16 blocks of 4-dimensional data, which means that there are 256, 4-dimensional data points that must be manipulated and assigned, for each block. As each block of data is input, the statistics of that block of data is determined, and from these statistics, a threshold is selected to be used as an input into the mode estimator. The mode estimator, using a non-iterative procedure then selects the number and location of the modes and isolation points based on this threshold. If the number of modes fails to satisfy the convergence criteria of the algorithm, a new threshold is selected and the mode estimation algorithm is reinitiated. Iteration between the mode estimator and threshold selector insure that both the optimal number and location of cluster centers have been selected for the desired compression ration. Finally, all 256 pixels are assigned to the nearest cluster center.

The output of the algorithm is in two parts: 1) the cluster definition, entitled local cluster features, defining the mean and variance of each of these clusters; and 2) an array of numbers entitled local feature map, giving an assignment for each 4-dimensional pixel to the cluster to which it belongs. An example of this can be seen in figure (2). These outputs are then coded and transmitted in some prearranged order.

The following is a flow diagram of the clustering compression algorithm.

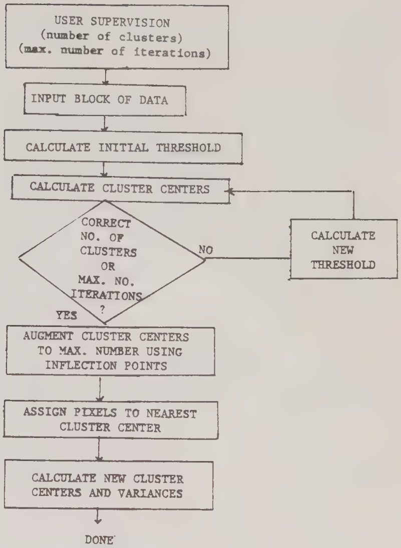
USER SUPERVISION
(number of clusters)
(max. number of iterations)
INPUT BLOCK OF DATA
CALCULATE INITIAL THRESHOLD
CALCULATE CLUSTER CENTERS
CORRECT NO. OF CLUSTERS OR MAX. NO. ITERATIONS ?
NO
CALCULATE NEW THRESHOLD
YES
AUGMENT CLUSTER CENTERS TO MAX. NUMBER USING INFLECTION POINTS
ASSIGN PIXELS TO NEAREST CLUSTER CENTER
CALCULATE NEW CLUSTER CENTERS AND VARIANCES
DONE

In the next section, we shall describe in detail the mode estimation algorithm, developed from graph-theoretic concepts, and relate this to gradient optimization techniques.

III. The Mode Estimation Algorithm

The mode selection algorithm is a multi-dimensional extension of an algorithm developed by Koontz et al. [1] that estimates the modes of a block of data. The modes are determined by means of a non-parametric density estimation algorithm that determines the modes through the construction of density neighborhoods. In the algorithm, each point x_l in the block of data has a density neighborhood assigned to it, of diameter θ, that represents the number of points in the block whose spectral signature are within the Euclidean distance of θ from x_l. If there are no points in the θ neighborhood of x_l then x_l is unique and is said to be an isolated point. The gradient of the density neighborhood is then calculated and the algorithm travels along the path of the maximum gradient of N_θ. By these means, the points selected as modes are those points which have the maximum θ neighborhood densities and those points which are isolated points.

The details of the mode selection algorithm are as follows:

1. Input 16 x 16 block of pixels
2. Find $D(x_l, x_j)$, the distance between pixels x_l and x_j for every x_l and x_j in the block.
3. Calculate for every x_l, $N(x_l, \theta)$, which is the number of points whose distance from x_l is less than θ.
4. For every x_l calculate the maximum G_{x_l} where

$$G_{x_l} = \frac{N(x_j)-N(x_l)}{D(x_j, x_l)}$$

5. If G_{x_l} maximum is less than 0, then call x_l a mode.

   If G_{x_l} maximum equals 0, keep x_l because it may be a mode.

   If $N(x_l, \theta)$ equals 0, then call x_l a mode since it is an isolated point.

The mode estimation algorithm as stated above will give, for a given value of θ, a certain number and position of cluster centers (modes) and a certain number of inflection points. However, the number of modes selected for a given θ, is dependent on the mean and variance of that block of data. Therefore, in order to attain a predetermined compression ration, θ must be calculated as a function of the statistics of the block of data to be compressed. In the next section, we shall explain the relationship between θ and the data statistics and describe the threshold selection algorithm.

IV. The Threshold Selection Algorithm

The threshold control θ, determines, based on its value, the number of clusters (η) selected in a given block of data B. However, for a given value of θ, the number of clusters determined in each block will vary as a function of the mean and variance of the pixel values in that block. Therefore in order to obtain, on the average, a fixed number (η) of clusters in each block, it is necessary to develop an estimate of the value of θ needed to obtain η clusters in block B.

An estimator for θ was determined through the use of 100 blocks of 4-dimensional Landsat D data. The mean and variance, value of the control θ needed, and the resultant number of clusters obtained was calculated for each block. Since our interest was in the value of θ required to obtain clusters, the control parameter θ was adjusted until the resulting number of clusters was between $\eta-4$ and $\eta+6$. The resluts of this simulation for η equal 16, are presented in figure 3. From these results, it can be seen, that there is a piecewise continuous relationship between the value of θ and the variance of the block, given that the number of clusters selected remains approximately constant.

The Threshold Selection Algorithm was determined as follows:

First, the equation required to calculate θ became a function of the three regions the block of data fell into. The first region is represented by a fairly homogeneous block of data with low pixel values. The middle region, in which the average pixel was in the mid range of values, had some inhomogeneity. The high region, in which the average pixel was in the high range of values, had widely differing pixel values and several bright spots within the block.

The Threshold Selection Algorithm is as follows:

1. Input 16 x 16 block of pixels B, where η is the desired number of clusters.
2. Find variance of B. {Var(B)}
3. If Var (B)<7.5

   $\theta = (\mathrm{Var}(B) - 4.5)\,\eta/73.7$

   If $7.5 \leq \mathrm{Var}(B) \leq 19.4$

   $\theta = (\mathrm{Var}(B) - 2.2)\,\eta/28.8$

   If Var(B)>19.4

   $\theta = (\mathrm{Var}(B) - 11.9)\,\eta/46.4$

The value of the variance in each block determines the region and therefore, the θ parameter value is calcualted. Once this value for θ is obtained, the mode estimation algorithm is performed to determine if it is within the required number of clusters. If not, θ is updated as a function of the error, and the mode estimation algorithm is once again performed.

It was found, for the classes examined, that the iteration between the mode estimator and threshold selector converges within 3 iterations. Once the control value θ has been selected, and the cluster centers determined, final assignment and mapping of the pixels are performed.

V. Results

The hybrid clustering algorithm was performed on several frames of MSS data. This simulation was compared to the compression of the same data using the hybrid transform techniques and the Hilbert clustering algorithm. The results are given in figures 4 and 5. From Figure 5, we can see that hybrid cluster compression consistently outperforms the Hilbert cluster compression by an increasing factor. This factor, we feel, represents the additional amount of degradation occurring in Hilbert cluster compression from non-optimal placement of cluster centers and the inability of the algorithm to select isolated points as clusters. In general, the hybrid cluster compression algorithm provides the minimum amount of degradation over all of the other techniques.

It is apparent from the method of compression that hybrid cluster coding can be easily extended to imagery with η spectral bands. Additional research is needed, however, to streamline the algorithm so that it can be implemented in real-time applications.

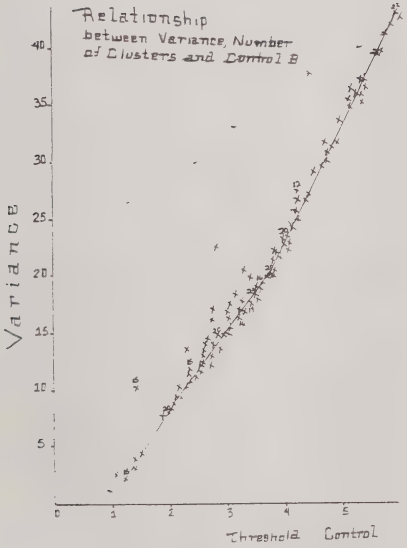

FIGURE 3

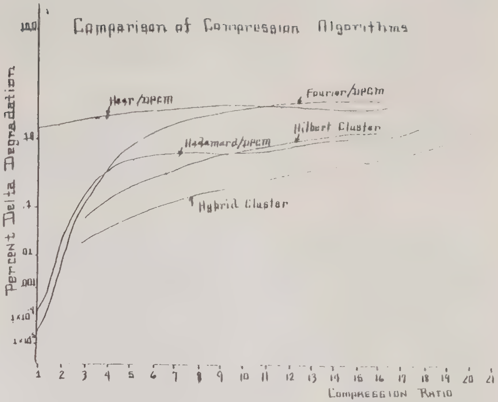

FIGURE 4

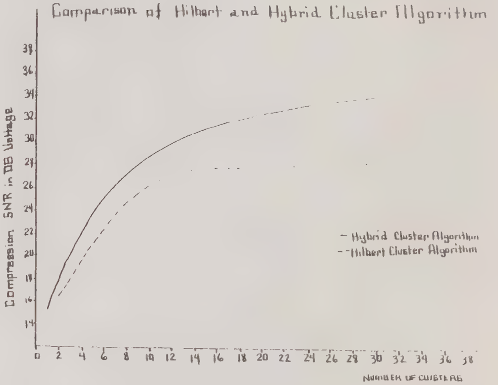

FIGURE 5

---

1. W. Koontz, P. Narendra and K. Fukunaga, "A Graphic-Theoretic Approach to Non-parametric Cluster Analysis," IEEE Trans Computer, vol. C-25, pp. 936-944, Sept., 1976.

2. E. Hilbert, "Cluster Compression Algorithm, A Joint Cluster/Data Compression Concept", JPL Publication, pp. 77-43, December, 1977.

3. C. T. Zahn, "Graph-Theoretical Methods for Detecting and Describing Gestalt Clusters", IEEE Trans. Comput., vol, C-20, pp. 68-86, 1971.

4. K. Fukunaga and L. Hostetler, "The Estimation of the Gradient of a Density Function with Applications in Pattern Recognition", IEEE Trans. Inform. Theory, vol, IT-21, pp. 32-40, 1975.

80-0543

IS THERE A SPACE PLATFORM IN INTELSAT'S FUTURE?

FACING THE INSTITUTIONAL CHALLENGES OF THE 1980'S AND 1990'S

Joseph N. Pelton
INTELSAT
Washington, D.C.

INTELSAT, the 102-member international organization that provides 60 percent of the world's overseas international telecommunications services, has been called the world's most successful international venture. Rapid traffic growth, reliability records of greater than 99.9 percent, and significant reductions in the cost of service, have all tended to make such compliments credible. In the opinion of some, at least, the technical requirements and discipline of space technology have finally served to create a well-disciplined international organization that works.

At times, however, INTELSAT would seem to be threatened by its own success. Any successful and appealing service or product quickly draws a crowd of customers -- and of imitators. Once INTELSAT had shown the world that satellite communications was more than a novelty, and once success, both technically and financially, was clear, the great satellite proliferation syndrome began to emerge. Over the last 15 years, INTELSAT has demonstrated that satellite communications made sense in virtually any application. It was INTELSAT that, in 1965, demonstrated that satellites could provide ocean-to-ocean telephone service; then, two years later, came multidestination television distribution. In subsequent years, communications to and from ships, and for high-speed data relay, demand access telephone service, domestic telephone and television distribution and many other services, were added to INTELSAT offerings. Countries, regional organizations, commercial enterprises and other international organizations began to say if INTELSAT is doing so well perhaps we should also directly pursue the benefits of this exciting new technology.

In the euphoria of the late 60's and early 70's, the bubble expanded rapidly. Domestic systems, maritime systems, aeronautical systems, military systems, experimental and scientific projects and regional systems were all announced with enthusiasm. Any suggestion that there could be congestion of the available radio frequencies in geosynchronous orbit was not taken very seriously. After all, there was quite limited ability in the launch vehicle field and the small satellites were power limited, not frequency limited. Within INTELSAT, international traffic grew, membership grew and demand for domestic service grew. Service demands on the INTELSAT global satellite network suddenly mushroomed in the mid-1970's.

By the time the 1970's drew to a close satellite communications had begun to experience the aftereffects of an orgy of success:

- Of 70 satellite systems in service or in planning, virtually all are or will be frequency limited, not power limited.
- Concepts to reuse frequencies twice, four times, even seven or eight times or more, were being demanded of satellite engineers.
- The 1979 World Administrative Radio Conference very predictably was characterized by a mad scramble for frequencies, new approaches to orbital assignments, and relaxed standards.
- More than 15 domestic satellite systems had become operational on the INTELSAT network.

Perhaps the most troubling aspect of the late 1970's, at least in terms of global satellite communications, was the initial emergence of regional satellite systems. Two regional satellite systems (the European Communications Satellite System ((ECS)) and the Indonesian PALAPA-B Network for Southeast Asia regional traffic) had been technically and economically coordinated under the provisions of Article XIV(d) of the INTELSAT Agreement. (The INTELSAT Assembly of Parties, in April 1979, determined these two regional systems, as planned, would be technically compatible and would not create "significant economic harm" to INTELSAT.) Many representatives at the INTELSAT Assembly of Parties, held in Manila in April 1979, however, were looking ahead to the time when other satellite systems, such as the ARABSAT System, would be coordinated. These representatives expressed doubts as to what the increase in separate satellite systems portended for effective and low-cost international communications on the INTELSAT System.

The question that presents itself as the 1980's begin is simply this: Is there any way for all countries, all commercial enterprises, and all international and academic institutions to continue to exploit rapidly and effectively the technical

Released to AIAA to publish in all forms.

advances being made in satellite communications without eventually creating a global telecommunications anarchy in outer space? In short, are we building a Tower of Babel without even a fire escape?

The question is easier to formulate than answer. Only time will provide the definitive response. Yet, there is one approach to this difficult issue that holds enoumous promise. INTELSAT certainly will in the 1980's give increasing attention to this possible solution. This "possible solution" is sometimes known as the space platform, sometimes the Orbital Antenna Farm (the OAF), and, to a few optimists like me, INTELSAT VII. It should be emphasized that other concepts may, in the long run, prove to be the best solution. Certainly the concept of a cluster of satellites around a central switching satellite service may have considerable merit. Under the space platform approach you, in effect, have to launch the orchestra (i.e., the telecommunications and other subsystems); the conductor (i.e., the network switching and control); and the stage (i.e., the platform). But in the second approach, you might be able to provide your celestial concert without the need of a stage.

But assuming for our purposes the space platform proves to be the best answer, then what? First of all, the advantages of a space platform, at least conceptually, are severalfold.

A. The platform would be large enough to support one or more large antenna reflectors that could be utilized by many "feeds" or multiple-phase arrays. This would allow frequency reuse as many as hundreds of times. Five to seven such platforms could perhaps meet all global needs if institutional problems could be solved.

B. The platform would allow efficiencies of scale and avoid needless duplication that many small satellites would involve. This approach would mean the consolidation and optimization of power systems, stabilization mechanisms, thermal control, etc. Excess power not needed in off-peak hours could even possibly be beamed back to earth to run a small city.

C. The platform could be structured to accommodate the individual packages of a wide diversity of users that could be designed, built and operated "independently," even though platform accommodations would be leased in common. Most significantly, the individual users could flexibly interconnect their packages by cables hooked to switches. The platform could, in a sense, be viewed as a community cable TV system and switching network in the sky. Such a platform could of course be maintained and retrofitted by service crews as needed. New packages could be "plugged in" and old packages "unplugged" as needed. It would have the potential for providing meteorological and earth resource services, hundreds of thousands of international telephone and data channels, and millions of domestic telephone and data channels.

Translating conceptual advantages into practical gains is not, however, an easy task. Sometimes it seems easier to derail a good idea than a bad one. Three of the more difficult problems to be anticipated are the following:

1. Overkill: A space platform for communications and other applications, such as earth resources, meteorology, navigation, etc., need not be large or extravagant. It particularly need not be a manned space station nor involve massive new launcher development. A serious misstep that could be made by a national space agency, for instance, is proposing a full-scale demonstration project for the early-to-mid eighties, when a technical demonstration project at one-tenth the cost would do very well as a first step.

2. Space Platform Proliferation: If there is a race to build space platforms on a nationalistic or regional basis, i.e., a jumble of Japanese, Soviet, U.S., French or European Space Agency platforms, it would accomplish little except to push up the stakes in the satellite proliferation game. Rather than solving anything, the old problem would be restated, but with much higher stakes. Clearly, institutional arrangements for international cooperation must be found -- and found soon -- if this and the following problems are to be solved in a timely way.

3. Lack of Effective Institutional Arrangements: Unless effective international procedures and appropriate operational structures are created for the design, construction and use of space platforms, the promise of the technology will mean little. Commercial enterprises and other non-governmental organizations will want to be able to have a meaningful say in the use of the space platform -- otherwise they will go their own way. Socialist nations may balk at participating in strictly commercial operations. Operating telecommunications agencies will demand first and foremost reliable and low-cost service. They will care little about whether space platforms provide the service. To the ultimate user, advanced technology is something to be tolerated as long as it does not get in the way of the service objective.

An effective organizational solution for the use of the space platform that meets everyone's concerns is thus the biggest problem of all. In this regard, the results of a recent Delphi survey that I personally conducted among some eighty experts in aerospace and telecommunications is instructive. Virtually unanimous agreement was reached among these experts that space platforms would not be deployed, owned or operated by a specialized agency of the United Nations. Opinion was almost equally divided among four possible approaches that they felt could occur: (a) private enterprise; (b) government projects; (c) multilateral government projects; and (d) INTELSAT or a like technical international agency.

The problems are frequently easy to see, but devising the right solution is the hard part. Writing a "successful scenario" leading to a network for Global Applications Space Platforms (GASP) in the mid- to late-1990's is not so easily done if one honestly faces up to the political and technical obstacles to be overcome. But let us try.

First of all, during the 1980's, national technical problems, as well as international cooperative projects, must show positive results. In particular, European, Japanese, Soviet and U.S. technical studies and demonstrations must proceed in the following areas: (a) intersatellite links (ISL); (b) on-board processing and signal regeneration; (c) space platform structure and materials research, including structural beam-forming machines; (d) high-resolution imaging devices for meteorological, earth resource and other applications optimized for geosynchronous operation; (e) optimized systems designs to achieve switched interconnection of subsystem packages, maximum redundancy and reliability, flexibility for expansion and maintenance, effective use of multipurpose antenna reflectors, and the lowest weight and cost, consistent with reliability.

International organizations like INTELSAT, as well as research institutions and commercial organizations, should supplement these national efforts. INTELSAT will most likely make its most useful contributions with regard to the intersatellite link, on-board signal reprocessing and multi-phase array antenna farms, since all of these technologies may well be included in our INTELSAT VI planning.

The question of an appropriate launch vehicle for a space platform will, of course, be of dominant concern in the 1980's. Chief among these questions will be the performance of the Space Transportation System (or Shuttle) and the availability of a high-thrust perigee motor to relay large payloads from low orbit to geosynchronous orbit. Currently, the candidates range from the Inertial Upper Stage (IUS), Payload Assist Module (PAM) and the Centaur, to newer technologies, such as electrothermal thrusters that could gradually boost large masses out to the desired orbit over a number of months. Whatever the answer found, one conclusion should be inescapable. The scope of technical demonstrations, as well as the subsequent operational GASP platforms, should be modest. In particular, they should range in size from 3,000 to 8,000 kilograms and thus be consistent with the launch capability of no more than two U.S. or Soviet Shuttle missions. Nothing would serve to kill the GASP network faster than runaway costs. At least, for INTELSAT to take the space platform approach seriously, ways must be found to reduce projected costs significantly.

The third essential ingredient in the GASP recipe for the 1980's is the beginning of a common international understanding on institutional arrangements for the future. Sometimes institutional arrangements can be developed swiftly. In 1959 and 1960 Presidents Eisenhower and Kennedy called for global use of communications satellites; by 1962 the U.S. Comsat Act had been passed despite a Senate Filibuster; by 1964 INTELSAT had come into existence; and, by 1965, international service was initiated.

That success story will be repeated only if tremendous levels of international cooperation can be achieved. Potential customers of GASP must identify possible areas of common interests, as well as areas of conflicting competing requirements. Critical issues must be examined, including: financial arrangements; responsibilities for operation and maintenance; opportunities for retrofit; subsystem switching and interconnection; ownership; leasing arrangements; liability and insurance; shared versus exclusive use; decision making mechanisms; and a variety of technical, economic, political and legal tradeoffs. Key questions recently raised by Hughes Aircraft Company related to the near-term economic viability of space platforms must be examined and resolved. While the "right" institutional arrangements are not now clear, several principles are worth noting:

A. A successful GASP network will need to draw on the financial, technical and political resources of large aerospace, electronics and communications corporations, governments and international organizations.

B. The GASP, although likely multipurpose in function, will be dominated by telecommunications requirements in terms of services provided, potential sources of revenue and on-board hardware. Other applications will either be smaller (e.g., meteorological, earth resource, navigation, etc.), or too big or sophisticated to be compatible with the GASP concept (e.g., energy, space manufacturing, etc.).

C. The success of INTELSAT in marrying high technology, efficient international management and international cooperation cannot be easily ignored.

The possibilities for institutional arrangements that might evolve with regard to space platforms are large; but, of these, one approach seems particularly plausible and true to life. Perhaps this approach could best be presented in terms of a three-act play.

In the first act (covering the 1980's), serious technical demonstrations of the various aspects of a working platform would have been shown by several countries and the operation of such multiple purpose space platforms simulated on the ground. These would be followed by one or two full-scale projects in the early 1990's that would serve as operational prototypes.

In the second act, INTELSAT would be designated "Interim Manager" to take over operation of one or more space platforms that had been deployed by the U.S. or Europe, or maybe by a joint team from the U.S. and Japan. INTELSAT would pay a fixed amount for the platforms and contract internationally for other operational/prototype platforms to be built. The scope of the work would be large enough that awards to European, Canadian, Japanese, Soviet and U.S. industry, either as prime contractors or subcontractors, could be anticipated. After tests and evaluations had been completed on the subsystems and the network switching control, customers could begin leasing capacity on the platform through designated entities that each government would specify. Such customers could include private corporations or government agencies. International organizations, such an INMARSAT or ICAO, could lease capacity directly. All tactical military communications would, of necessity, remain forbidden on such GASP networks, as is the case with INTELSAT today.

In the third act, covering the mid- to late-1990's, there would be a smooth evolution toward permanent operational and institutional arrangements. Formal international agreements would have to be signed and new space hardware to augment or replace the initial operational prototypes would have to be built and launched.

During the second and third acts, INTELSAT would transition its services from the INTELSAT VI to the new GASP Network.

There are, of course, alternative endings to our play. Under one approach, the U.S. may decide to deploy a "bicycle" rather than a "unicycle" platform. The "bicycle" would be designed so that half of the platform would meet U.S. domestic needs and the second half could be sold or leased on a long-term basis to INTELSAT for its own use or for sublease to various customers. Europe, the Soviet Union or Japan might also devise bicycle or even tricycle solutions, wherein INTELSAT would have responsibility for only a part of the platform.

Certainly by the 1990's we will know if the play is a madcap comedy, an international tragedy, or a thrilling drama with a heroic and rewarding conclusion at the end. The title of the play might either be "The Last GASP" or "The First GASP." Let us hope it is The First GASP.

80-0544

A PROJECTION OF THE DEVELOPMENT OF HIGH CAPACITY COMMUNICATIONS SATELLITES IN THE 1980s

R. J. Rusch and C. Louis Cuccia
Ford Aerospace & Communications Corporation
Western Development Laboratories
Palo Alto, California

Abstract

The need for higher capacity communications satellites in the 1980s and 1990s will require new approaches to satellite design and space segment configuration. Design decisions are complicated by uncertainties in the availability of expendable launch vehicles and the space transport system. Other issues which need to be fully understood include projections of demand for satellite systems and the acceptability of more efficient signaling methods.

Several alternative design concepts have been advanced over the past several years. They include:

1. Numerous small special purpose satellites.
2. Very large satellites to be launched only by the STS.
3. Several smaller satellites connected by inter-satellite links.
4. Clusters of satellites which are interconnected and are collocated within the beam of an earth terminal.
5. Large space platforms.

This paper introduces a new approach (number 6) for providing high satellite capacity. It distributes the satellite payload between several spacecraft without requiring satellite interlinks, master control satellites, or large space structures. The advantages of this approach are explained and compared with the features of other advanced design approaches.

INTRODUCTION

The trend toward large multifunction satellites, of which Intelsat V and INSAT are excellent examples, has now begun to mature with critical considerations being given to maximizing satellite capacity and to minimizing cost. Spacecraft structures must be compatible with the weight and size limitations of both the shuttle and expendable launch vehicles such as the Atlas-Centaur, Thor-Delta or Ariane launch vehicles.

It now appears that delays in the shuttle program will extend the transition away from expendable launch vehicles for some time. Until a regular shuttle launch schedule is established, it will not be prudent to design spacecraft which can only be launched on the shuttle.

The era of extremely large and yet economically launched spacecraft has been pushed several years into the future. Consequently, new steps in the evolution of spacecraft must be considered. Various technologies are now available for increasing the capacity of satellites that are compatible with present expendable launch vehicles, including an increase of available dc power by use of more efficient solar cells and solar arrays. Such improvements would also be appropriate if the spacecraft were launched by the STS.

Several approaches, including use of intersatellite links and the satellite cluster concept, have been proposed to meet this requirement. This paper introduces a new concept, in which the total satellite payload is split among a plurality of satellites located at essentially the same position in the orbital arc. This distributed payload satellite system, as seen from the Earth, will appear as a single satellite to an earth terminal. It has the advantage of providing the capacity of a giant space platform of the shuttle era in today's era of expendable launch vehicles of specific types and capabilities, without need for satellite interlinks or master controller satellites. Each constituent element of the distributed set can be designed for minimum shuttle launch cost, as well as compatibility with expendable launch vehicles.

From this expanded base, then, the transition into a second era of shuttle usage may follow, where the advantages of EVA (extra vehicular activity) can be utilized and the multifunction satellite can grow into a large platform system such as an orbiting antenna "farm" housing a multitude of payloads and antenna systems.

The advantages and disadvantages of each alternate configuration will be presented in subsequent sections.

THE GROWING DEMAND FOR SATELLITE CAPACITY

Satellite communications was born less than two decades ago. Today, 60% of the world's international telephone communications is handled by communication satellites, and many domestic satellite systems now used in the United States, Japan, Indonesia, Canada, the USSR, and Europe are pioneering new uses for satellites - including cable TV, TV distribution, radio and telephone broadcast for space, transmission of newsprint and electronic mail, data communications including the interconnecting of remote computers, and public service communications.

Already the geostationary arc is filling up with C-band communications. The recent WARC-79 activity in Geneva, Switzerland was evidence of worldwide interest and demand for additional frequency bands for satellite communications and expansion of the allocated bands at 6 and 4 GHz.

Copyright ©, 1980 by Roger J. Rusch

Released to AIAA to publish in all forms.

Figure 1 shows the history of capacity growth in Intelsat satellite communications,[1] and the following table, provided by W. Pritchard,[2] lists typical growth rates which can be projected for various satellite systems. These projections show that the 1980s will be the era of significant growth in the use of the communications satellite. The dramatic expansion in demand for capacity in satellite systems has required innovative system technology. Thus far, capacity growth has been satisfied by expanding satellite power and bandwidth.

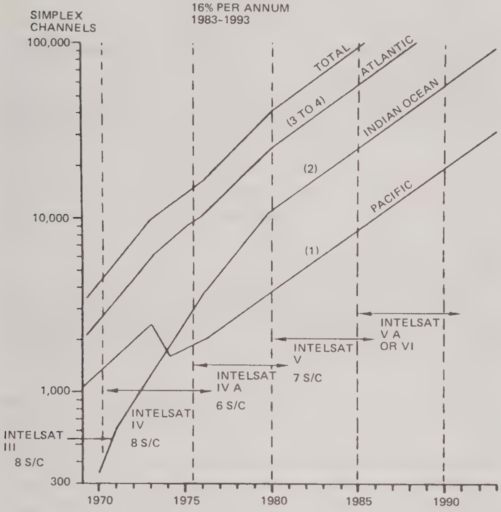

Figure 1. Intelsat Traffic History

Typical Growth Rates

World's Gross National Product	4%/year
GNP Emerging Nations	5%
World's Telephones (since 1950)	8%
Intelsat Traffic (last 2 years)	23%
Intelsat Traffic (last 7 years)	24%
Intelsat Traffic - 12 years	50%
U.S. Domestic Systems	20
Typical Regional Systems	10 to 20

Extra satellite bandwidth has been obtained through frequency reuse by beam isolation and polarization. New frequency bands have also been utilized to extend bandwidth.

The Canadian (Anik), Western Union, and Indonesian (Palapa) systems have all been expanded from 12 to 24 transponders by polarization reuse. The Canadian system has also used the newer frequency assignment at 14/12 GHz.

The following table lists the communication capacity in voice channels of present communication satellites in both international and domestic use.

Program	Procurement Date	Bandwidth	EIRP
Intelsat IV	1968	432 MHz	22 dBW global 33 dBW spot
Intelsat IVA	1973	720	22 dBW global, 26 dBW hemi
Intelsat V	1976	2136	23.5 dBW global, 29 dB Hemi/zone 41 to 44 dBW spot
Symphonie	1970	180	30 dBW
RCA Satcom	1973	816	33 dBW CONUS
COMSTAR	1973	816	33 dBW CONUS
Anik A/Westar A/Palapa A	1971 to 1974	432	33 dBW
Japan CS	1974	1600	29.5 dBW (C-band) to 37 dBW (K-band)
SBS/ANIK C	1978	430	40 dBW (area) 44 to 48dBw (spot)
Anik D/Palapa B/Westar B	1979	816	33 dBW to 35 dBw

Capacities of up to 14,400 voice channels have been achieved for satellite networks such as Comstar; Intelsat V capacity is 12,000 voice channels plus two TV channels. A significant constraint on the Intelsat network is the need to accommodate multiple accesses by a large number of earth terminals. Because of multiple accesses, the voice channel capacity of the Intelsat V is not as efficient as Comstar. On a comparable operating basis, ie single carrier per transponder, Intelsat V could carry more than 2.5 times as much traffic as the Comstar network. An additional need for flexible accommodation of unpredictable and sporadic growth rates in different regions is also recognized.

Intelsat satellites have grown in mass from Intelsat I, with only 39 kilograms at beginning of life (BOL) in orbit mass, to Intelsat V with 967 kg BOL. Intelsat V[3] is the largest satellite which can be launched on the presently available Atlas Centaur or Ariane launch vehicles. It has set many new design standards with its capability for interconnecting many regions on earth through use of an advanced antenna farm system, mounted on a 3-axis stabilized platform. Beginning with flight model 5, Intelsat V will also have a maritime capability to replace the present Marisat satellites.

Another example of satellite growth is INSAT. This satellite design includes not only a 12-channel C-band transponder, but a 2.54 GHz TV broadcast system, a 400 MHz data collection system, and a meteorology radiometer with provisions for transmitting the radiometer data to earth. These satellites illustrate the sophistication and adaptability to multiple-function operation for increased and maximized capacity which is now being demanded of modern communications satellites.

It may be that we have begun to see the limit to types of satellite capacity expansion which are cost effective. In the near future Intelsat will begin to introduce digital communications on an operational basis. The Intelsat methods of using TDMA with DSI can expand satellite capacity by five-fold without further changes in satellite design.

INCREASED SATELLITE CAPACITY DUE TO NEW TECHNOLOGIES

There are two approaches to increasing satellite capacity. The first is to increase launch vehicle in-orbit mass capability, and the other, given a maximum launch vehicle capability, is recourse to a variety of technologies that are described below.

Lightweight Materials

The use of new materials includes the transition from aluminum structures to graphite composite and Kevlar composite structures, as shown in the following table. This has led to significant savings in structure weight, which then allows use of more sophisticated frequency reuse satellite antennas and transponder bandwidth. The Intelsat V spacecraft makes extensive use of graphite materials in spacecraft structures and RF components. The estimated mass savings for Intelsat V is 100 kg when compared to more conventional spacecraft materials.

Technical Evolution of Satellite Materials

Skynet I	Aluminum structures
NATO II	Aluminum structures
SMS	Fiberglass and honeycomb sandwich structures
Viking	Fiberglass and honeycomb sandwich structures
NATO III	Graphite composite antennas
Voyager	Graphite composite antennas
CS, ETS II, ECS	Graphite composite antennas
ECS	Graphite composite and Kevlar composite primary structures
Intelsat V	Extensive use of graphite in structures and RF components
Future	Low cost graphite materials Lower cost composite manufacturing Graphite and graphite/beryllium Primary structures

Sun Oriented Solar Arrays

Similarly, oriented solar arrays (Figure 2) save substantial amounts of mass which can be used for communications. Whereas cylindrical arrays produce about 7 watts per kilogram, a sun oriented array can produce 20 to 40 watts per kilogram. The mass savings on Intelsat V by using sun oriented arrays was more than 125 kg.

As time goes on, more efficient cells are being developed that will further reduce the mass required to produce electrical power. As power becomes relatively cheaper and more available, more power can be used in concert with a thermal design to improve performance of communications equipment and lengthen battery life.

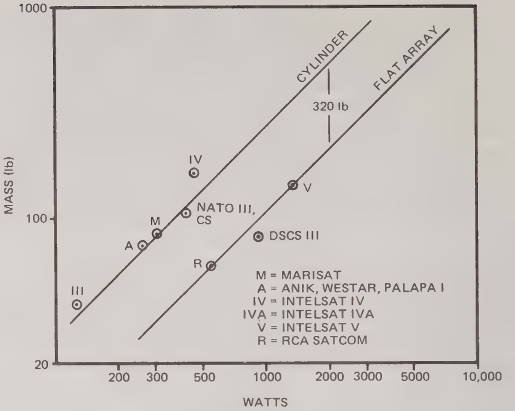

Figure 2. Mass of Solar Array (Including Substrate)

High Performance Antennas

One of the most powerful tools for added capability is sophisticated antenna design. Since antenna gain is a determining factor in EIRP and G/T, a high antenna efficiency can permit lower power output amplifiers. Consequently, additional mass and power can be available for payload. Some improvements remain to be made in high efficiency feed horns which reduce spillover loss and low loss antenna networks.

Solid State Power Amplifiers (SSPA)

Solid state amplifiers, such as FET amplifiers, can be used as subtitutes for TWTAs to not only reduce size and weight, but also to increase linearity and reduce AM-to-PM conversion. This reduces the degradation in link margin due to intermodulation and crosstalk.

Perhaps one of the most compelling advantages of SSPAs is the prospect of greatly extended life. There is no inherent life-limiting element for solid state devices, as there is for cathodes in traveling wave tubes. Considerable in-orbit experience indicates that the 4 GHz traveling wave tubes have mean times to failure of about 50,000 hours. Failures appear due to degradation in both the TWT and the associated high voltage power supply. Ford Aerospace & Communications Corporation laboratories have tested SSPAs at elevated temperatures for more than a year with no indication of performance degradation.

Bipropellant Propulsion

Until recently most spacecraft propulsion subsystems employed monopropellant hydrazine for stationkeeping, and solid racket motors for apogee boost. These systems only provided specific impulse (ISP) of 220 seconds to 290 seconds respectively. Over the past few years, high performance hydrazine thrusters have been developed which provide up to 300 sec Isp. These electrically heated hydrazine thrusters provide low thrust levels, and therefore can be used for frequent stationkeeping maneuvers, but cannot be used for apogee injection.

A more attractive approach is the use of bipropellant storable propellants such as nitrogen textroxide/monomethyl hydrazine. This system can provide 310 sec Isp for both apogee boost and stationkeeping. The additional advantage of bipropellants is their ability to restart the apogee motor. Very little fuel is needed for dispension errors since apogee injecton can be a two step process which efficiently matches the desired velocity vector. The net savings of an integrated bipropellant propulsion system ranges from 35 kg to 60 kg depending on spacecraft mass and mission duration.

Experimental data also shows that the bipopellant thruster pulses are crisply defined; the slow buildup and decay characteristics of monopropellant hydrazine are not matched by bipropellants. The precisely defined profile can yield short duration impulse bits and variable pulse widths which are perfectly matched to attitude control requirements.

THE INCREASE IN LAUNCH VEHICLE CAPABILITY IN THE 1980s

Satellite design for the 1980s depends upon many unknowns in launch vehicle capability which must be resolved.

The slippage in the NASA Space Transportation System (STS), which uses the shuttle orbiter, has raised the possibility that the first likely available date for a new commercial communications satellite may not occur until mid-1985. This makes it mandatory that the availability and capability of present U.S. launch vehicles in the Atlas-Centaur class be reevaluated. Also, the European Ariane launch vehicle must be considered as a very favored launch vehicle well into the 1980s, if the improvements from 1700 kg to 2350 kg capability from Ariane 1 to Ariane 3 are realized[4].

Figure 3 shows the potential increase in capability for the principal candidates for launching large satellites. It shows that Ariane 3 is the only vehicle capable of launching an in-orbit spacecraft mass above 5000 pounds (2350 kg), and that production of the Atlas-Centaur must be continued after Intelsat V Flight Model 5, if U.S. launch vehicle service is to be competitive with European launch vehicle service until the later 1980s.

ALTERNATE SATELLITE SYSTEM CONFIGURATIONS

A number of possible configurations for the space segment of satellite networks can be considered. The following paragraphs summarize the features of the basic types under consideration for systems designed in the 1980s, and the strengths and limitations of each one. Comparison will ultimately be based on assessment of cost, satisfaction of technical/operational requirements, and in some instances, political considerations.

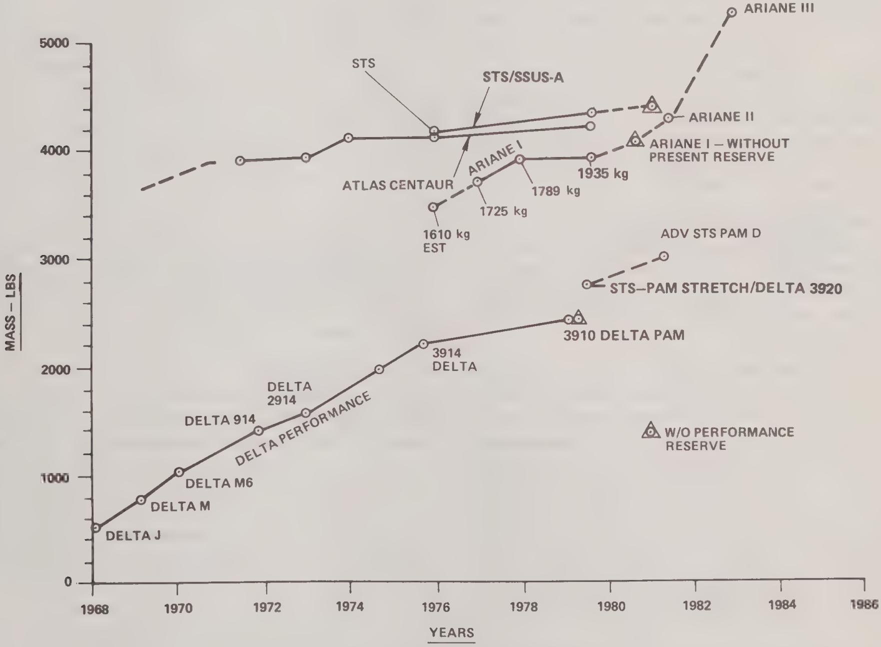

Figure 3. Increase in Launch Vehicle Capability

Smaller Special Purpose Satellites

Smaller special purpose satellites can be tailored to the requirements of a particular mission, without compromise or accommodation to the requirements of other missions. Small satellites can be launched for less cost on small expendable launch vehicles, or can qualify for lower rates on the STS. Operationally they present no special demands for careful deployment planning.

It is important, however, to view smaller satellites from a total system cost. Superficially it might appear that because these satellites are smaller and have lower launch cost that the total system cost is less. Studies have shown that to satisfy total demand more satellites are required. The total system cost is higher because small satellites carry a large overhead for housekeeping functions. These functions are shared by more communications hardware or other missions on a higher capacity or multifunction spacecraft. In some instances many more earth terminals may be required to access the numerous small satellites. Orbital space is used less efficiently, and frequency coordination is more complex with a large number of small satellites.

Large Multipurpose Satellites

Large multipurpose satellites have a substantial economy of scale when the ratio of payload to housekeeping functions is considered. Since they can be used in several applications on an interchangeable basis, development costs of a common design can be amortized over a larger number of spacecraft. Large size may permit higher levels of performance from large aperture antennas or greater amounts of electrical power.

However, if such satellites are so large that they can only be launched by the STS, there is a risk of launch delays until the STS becomes fully operational. If these satellites are greatly overdesigned for a certain class of missions, then the cost benefit may not be realized. Deployment and operational strategies may also need to be revised if a single mission capability fails on a particular spacecraft.

Satellites Connected by Intersatellite Links

If all satellites of a series are of identical design but must serve more than one region or mission, then the satellite must be designed for the highest demand region. Consequently, the common satellite may be vastly overdesigned or inefficiently designed for another region.

The use of satellites that are connected by intersatellite links may be an appropriate solution to the problem of overdesign to accommodate a particular mission or region. The use of intersatellite links allows traffic from a set of earth terminals to be split between two satellites. In the case of Intelsat, users from within a community of common interest would access one satellite, and users from another community would access a separate satellite. Communication between the limited number of users that require contact between the two communities would be via an intersatellite link which connects two satellites. In this way, an individual satellite can be about half as large as a single satellite filling the role.

Total cost assessment must consider that substantial mass and complexity is added to each satellite for the interlink. Furthermore, two launches are required to place the full capability in orbit. Cost per circuit is probably higher than for the larger satellite since the ratio of payload to housekeeping is lower.

Constellation (or Cluster) of Satellites

The cluster concept[5] is an extension of the satellite interlink approach (Figure 4). It has the advantage of flexibility in that if an individual satellite fails, it can be easily replaced without major problem. This flexibility probably comes at a significant cost, since there is no reduction in the cost of housekeeping functions. Since the beam of a typical satellite earth terminal is 0.1°, it covers a region about 50 miles in diameter at synchronous altitude. Stationkeeping is used to maintain the satellites within about 25 to 50 miles of the orbital arc. Several satellites would be positioned no more than a few miles apart. Their relative distances would be maintained during altitude control and stationkeeping maneuvers.

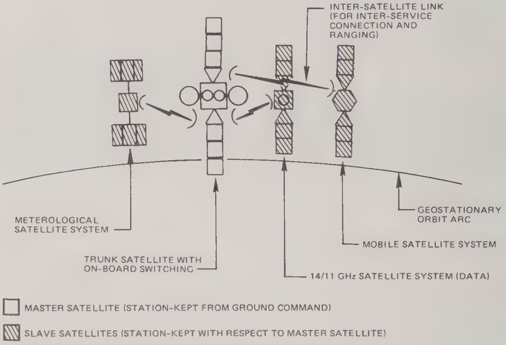
INTER-SATELLITE LINK (FOR INTER-SERVICE CONNECTION AND RANGING)
METEROLOGICAL SATELLITE SYSTEM
TRUNK SATELLITE WITH ON-BOARD SWITCHING
14/11 GHz SATELLITE SYSTEM (DATA)
MOBILE SATELLITE SYSTEM
GEOSTATIONARY ORBIT ARC
☐ MASTER SATELLITE (STATION-KEPT FROM GROUND COMMAND)
▨ SLAVE SATELLITES (STATION-KEPT WITH RESPECT TO MASTER SATELLITE)

Figure 4. Satellite Cluster

Considerable mission analysis must be performed to assess the means for performing stationkeeping simultaneously on 6 to 12 satellites. Even a small movement of one satellite relative to the others could cause the slave satellites to lose contact with the master switching satellite.

The Space Platform

The space platform is an elegant extension of the large multipurpose satellite[6]. It should have large cost benefits due to the high ratio of payload to housekeeping. From a technical point of view, the platform requires assembly of a large structure in space which can only be contemplated when the STS is fully operational. Once this structure is transported to synchonous orbit, enormous amounts of energy are required to physically access the platform. Methods must be developed for replacing a payload module which has failed.

The major problem with the space platform may be political. For such a system to be efficient, there must be multiple users and multiple payloads. The political problems associated with resolving all the special interests for such a large multimission vehicle could be insurmountable.

Distributed Payload Satellites

In the summer of 1979 satellite designers[7] made a breakthrough in the architecture of satellite networks. They suggested that intersatellite links are not necessary! They noted that several satellites of a smaller size could be situated within the beam of several earth terminals. Each would perform part of the mission and the functional division could be performed on the basis of frequency division (or conceivably time division). Figure 5 shows how an Intelsat VI concept[8] could be divided between two smaller satellites. Each satellite would have the same housekeeping functions; only certain aspects of the payload would be separate. Basically, the TDMA channels 1-2 and 3-4 would be installed on one spacecraft (A) and the FDMA channels 5-6, 7-8, 9-10, and 11-12, as well as global channels, would be on another spacecraft (B). The deployment strategy would be enormously flexibile. For the Indian Ocean or Pacific Ocean, perhaps only the B type spacecraft would be used until TDMA is introduced.

Stationkeeping would not be difficult since each spacecraft could easily be kept within the beam of earth terminals. Spacecraft cost would be somewhat higher than for a single large satellite, but this cost may be balanced by the deployment flexibility advantages. The distributed payload configuration also accommodates some mission failures.

The distributed payload network is ideally suited to the STS transition era. This approach provides a means for establishing a large payload capability, which can be launched on either the STS or an expendable vehicle such as Ariane. There is no practical limit to the number of satellites which could operate together in such an arrangement. It is therefore possible to assemble extremely large payloads as long as they can be partitioned. One interesting idea would be expansion of the current series of Intelsat V satellites by the supplement of a collocated satellite which employs the newly approved WARC-79 frequency bands.

Another attractive aspect of the approach is that such oversized payloads could be based on existing developed buses and developed technology.

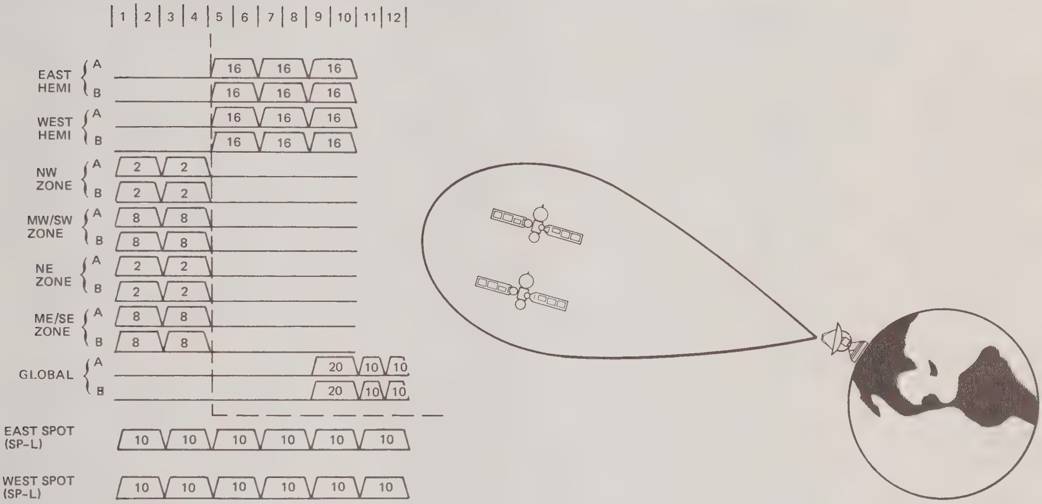
1 2 3 4 5 6 7 8 9 10 11 12
EAST HEMI A 16 16 16
EAST HEMI B 16 16 16
WEST HEMI A 16 16 16
WEST HEMI B 16 16 16
NW ZONE A 2 2
NW ZONE B 2 2
MW/SW ZONE A 8 8
MW/SW ZONE B 8 8
NE ZONE A 2 2
NE ZONE B 2 2
ME/SE ZONE A 8 8
ME/SE ZONE B 8 8
GLOBAL A 20 10 10
GLOBAL B 20 10 10
EAST SPOT (SP-L) 10 10 10 10 10 10
WEST SPOT (SP-L) 10 10 10 10 10 10

Figure 5. Distributed Payload Satellites

CONCLUSION

There are no sweeping issues which can clearly establish which space segment configuration is best for all satellite networks. The decisions will only be made after comprehensive design studies and cost tradeoffs. The outcome of these studies will depend to a large degree on the capability of launch vehicles available over the next decade[9].

At this stage in the evaluation, the near-term availability of the STS is uncertain, but the need for large capacity payloads is clear. We believe that for those payloads which can be partitioned, the distributed payload concept offers the best way to meet the needs of large satellite networks without the political and technical problems of the space platform or the slave/master and interlink complexities of a satellite constellation.

REFERENCES

1. J. L. Dicks, "Design Options for Future Communications Satellites," Proc. of Intl. Telemetering Conf., 1972, p. 880, Los Angeles, Ca.

2. W. Pritchard, "Economics of Satellite Communications Systems," XXX Congress 1AF, Munich FR6, Sept 17-22, 1979.

3. R. J. Rusch, J. T. Johnson, Dr. W. Baer, "Intelsat V Spacecraft Design Summary," 7th A1AA Committee Satellite Systems Conference, San Diego, Ca., April 24-27, 2978.

4. P. Marx, "Ariane Improvements," XXX Congress 1AF Munich, FR6, Sept 17-22, 1979.

5. P. Visher, "Satellite Clusters," Satellite Communications, September 1979.

6. W. Morgan, "Large Geostationary Communications Platform," XXX Congress 1AF, Munich FR6, September 17-22, 1979.

7. Bruce Burkart, Private Communication, July 1979.

8. O. Schmeller, "Future Intelsat Satellites," XXX Congress 1AF, Munich FR6, Sept 17-22, 1979.

9. C. L. Cuccia, "The Technology of Large Multi Function Communication Satellites in the Post Intelsat V Era," XX1X Congress, 1AF, Dubrovnik, Yugoslavia, October 1-8.

80-0546

THE PRESENT STATUS AND FUTURE DEVELOPMENT OF THE INTELSAT LEASED SYSTEM

T. Michael Kelley
Communications Engineering Department
International Telecommunication Satellite Organization
Washington, D.C.

Abstract

The first section of the paper addresses the current status of the 16 nations who lease spare INTELSAT transponders for domestic communications. Each domestic system is categorized by its choice of antenna coverage and by the amount of bandwidth leased. The widely varied communications services provided by INTELSAT leases are described, along with the earth station configuration chosen by the leasing nation to provide these services.

The second section addresses INTELSAT's recent reassessment of its role as a supplier of domestic satellite service. The central issues in the debates over INTELSAT's pricing philosophy and over the provision of fully guaranteed vs. pre-emptible service will be discussed. Some preliminary design concepts for new lease satellites are also addressed.

PRESENT STATUS OF THE INTELSAT LEASED SYSTEM

Consistent with the provisions of its formal Operating Agreement, the International Tele-Communications Satellite Organization (INTELSAT) began the practice of leasing satellite transponder capacity to its member nations for public domestic communications in 1974. At present, 16 of INTELSAT's 102 members lease capacity from INTELSAT. The units of bandwidth leased by these countries fill 16 36 MHz transponders, or nearly the equivalent of one and one-half INTELSAT IV satellites. In recent years INTELSAT has realized 5 to 10 percent of its total revenue from payments for lease service.

Table 1 shows the leases that are currently active or approved in principle within the INTELSAT System. Formal inquiries suggesting proposed domestic system have been received from at least 10 more nations. Figure 1 shows the growth of the INTELSAT leased system since the Algerian lease of early 1975.

Satellite capacity is leased in units of full transponders (36 MHz), half transponders (18 MHz), or one-quarter transponders (9 MHz), and is provided by INTELSAT on a pre-emptible or non-pre-emptible basis. In the event of a satellite or transponder failure, or, in the event of changes in the operational configuration of the operating satellites and their frequency plans, non-pre-emptible leases are restored to service with the same priority as international service. Pre-emptible service is restored using the remaining satellite resources but users are charged a lower rate for this type of lease. These services are currently available on INTELSAT IV global beam and spot beam transponders, and on INTELSAT IVA global beam, hemispheric beam and spot beam transponders. The normal leasing period for pre-emptible capacity is five years, but "short term" leases are available for periods as small as three months.

The satellite transponder resources allocated to the lessee are bandwidth and e.i.r.p., the satellite receiver resources allocated are operating flux density and G/T. The lessee must also adhere to several constraints which prevent his transmissions from causing harmful levels of interference into international INTELSAT traffic or into other leases. The precise definitions of the lease resources and constraints are discussed in detail in another paper by this author (see Conference Record of ICC78, Toronto, Canada, "Domestic Satellite Communications Using Leased INTELSAT Transponder", Vol. 1, pp. 2.3.1 - 2.3.5). The charges for INTELSAT leases, as of 1 January 1980, are given in Table 2.

TABLE 1
INTELSAT LEASED SYSTEMS
(As of 31 December, 1979)

	Country	Leased Capacity And Antenna Beam	Reason for Lease
		ACTIVE	
1	SPAIN	Half Transponder Global	Geographic Separation (Island-to-Mainland)
2	ALGERIA	One Transponder Global	Climate & Terrain
3	NORWAY	Half Transponder Global	Geographic Separation (Oil Platforms-to-Mainland)
4	MALAYSIA	One Transponder Global	Geographic Separation (Island-to-Island)
5	NIGERIA	Three Transponders Global	Climate & Terrain
6	FRANCE	Three Quarters of a Transponder Global	Geographic Separation (Island-to-Mainland)
7	CHILE	Quarter Transponder Global	Climate & Terrain
8	SUDAN	One Transponder Global	Climate & Terrain
9	COLOMBIA	Quarter Transponder Global	Climate & Terrain and Geographic Separation (Island-to-Mainland)
10	BRAZIL	Three and One Half Transponders - Hemi	Climate & Terrain
11	PERU	Quarter Transponder Global	Climate & Terrain
12	INDIA	Quarter Transponder Global	Climate & Terrain and Geographic Separation (Island-to-Mainland)
13	SAUDI ARABIA	Two and One Quarter Transponders - Global	Climate & Terrain
14	OMAN	One Transponder Global	Climate & Terrain
15	ZAIRE	One Transponder Global	Climate & Terrain
16	AUSTRALIA	Half Transponder Global	Climate & Terrain
		APPROVED IN PRINCIPLE	
	AUSTRALIA	Two Transponders Hemi	Climate & Terrain
	ARGENTINA	One and One Half Transponders Global	Climate & Terrain
	DENMARK (Greenland)	Quarter Transponder Global	Climate & Terrain
	EGYPT	Quarter Transponder Global	Geographic Separation (Embassy-to-Embassy)

The views expressed in this paper are the author's and not necessarily those of INTELSAT.

Copyright © American Institute of Aeronautics and Astronautics, Inc., 1980. All rights reserved.

TABLE 2

YEARLY CHARGES FOR INTELSAT LONG-TERM LEASE CAPACITY

(Effective 1 January 1980)

Size of Lease	GLOBAL BEAM * Non Pre-Emptible	 *** Pre-Emptible	HEMISPHERIC BEAM ** Non Pre-Emptible	 Pre-Emptible
Quarter Transponder (9 MHz)	$ 453,600	$ 250,000	$ 544,320	$300,000
Half Transponder (18 MHz)	$ 907,200	$ 500,000	$1,088,640	$600,000
Full Transponder (36 MHz)	$1,814,400	$1,000,000	$2,177,280	$1,200,000

(Values are in US $)

* This rate is pegged to the charge for 360 voice grade channels. This is the assumed average capacity of a global beam transponder when utilized in the international system.

** The rate for hemispheric beam transponders is 1.2 times the rate for global beam transponders. The rate for spot beam transponders is 2.0 times the rate for global beam transponders.

*** The possibility of a new charge for pre-emptible service will be studied during 1980.

NOTE: Short term pre-emptible leases are also available for domestic service. The allotment period begins at three months, and they may be extended on a month-to-month basis for up to one year. The charge for the first three months is $450,000 and $120,000 per month thereafter. Pro rata reductions will apply to half or quarter transponders. Service is available at increased charges for spot beam and hemispheric beam transponders.

FIGURE 1

GROWTH OF INTELSAT LEASED SYSTEMS

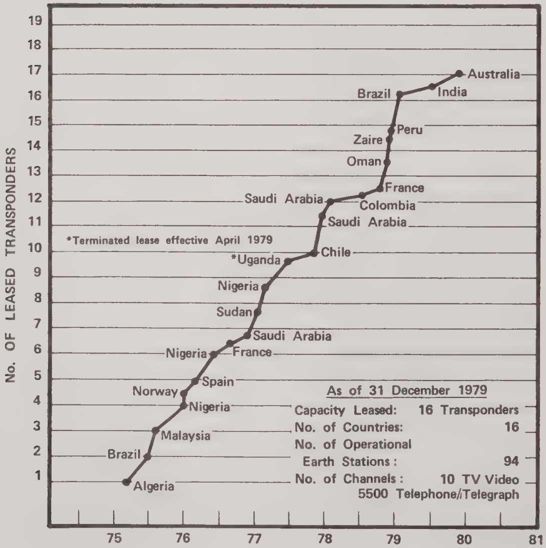

Table 3 shows the communications services required by each leasing nation, and the system of earth stations selected by the lessee in order to satisfy them. In many cases, the use of an INTELSAT lease has afforded a nation its first opportunity to provide its citizens living in remote areas with highly reliable, multi-destination communications. Most lease earth stations are also equipped with TV transmission and reception capability, either through the leased transponder or on an "occasional-use" basis on INTELSAT global system satellites. The ability to transmit and receive TV contributes greatly to the political unity of these nations, as well as providing news, educational, medical and sports programming to areas which have had few opportunities to participate in national cultural activities.

TABLE 3

COMMUNICATIONS SERVICES PROVIDED BY INTELSAT LEASES

COUNTRY	CAPACITY LEASED	TRAFFIC & MODULATION	NO. OF CHANNELS	NO. OF EARTH STATIONS	EARTH STATION SIZE & G/T(dB/K)
Algeria	Full Transponder (36 MHz)	TV Video - FM TV Audio - Wideband FM Telephone & Telegraph - SCPC/CFM	1 1 200 vox	15	11m / 31.7
Malaysia	Full Transponder (36 MHz)	TV Video - FM TV Audio - FDM/FM Telephone & Telegraph - FDM/FM	1 1 144	2	13m / 33.4
Norway	Half Transponder (18 MHz)	Telephone - SCPC/PSK @ 32 kb/s (Delta Modulation) Telegraph & Data - SCPC/PSK @ 32 kb/s	275	2 4	13m / 33.0 8m / 27.8
Nigeria	Three Full Transponders (36 MHz each)	TV Video - FM TV Audio & Radio - Wideband FM Telephone & Telegraph - SCPC/CFM	1 1 200 vox each	6 (Lease 1) 6 (Lease 2) 7 (Lease 3)	11m / 31.7 11m / 31.7 11m / 31.7
Spain	Half Transponder (18 MHz)	TV Video - FM	1	1 1	26m / 40.7 30m / 40.7
France	Three Quarters of a Transponder (27 MHz)	Telephone - 2.048 Mbit/sec 4ϕ - PCM/PSK	240	1 1	16.5m / 32.2 14m / 31.7
Saudi Arabia	Quarter Transponder (9 MHz)	Telephone & Telegraph - SCPC/CFM	15 No vox	2 2	11m / 31.7 6m / 24.5
Sudan	Full Transponder (36 MHz)	TV Video - FM TV Audio & Radio - Wideband FM Telephone & Telegraph - SCPC/CFM	1 2 200 vox	14	11m / 31.7
Australia	Half Transponder (18 MHz)	TV Video - FM	1	2	30m / 40.7
Chile	Quarter Transponder (9 MHz)	Telephone & Telegraph - FDM/FM	144	1 1	30m / 40.7 11.8m / 31.7
Oman	Full Transponder (36 MHz)	TV Video - FM TV Audio & Radio - Wideband FM Telephone & Telegraph - SCPC/CFM	1 2 200 vox	1 5	11.8m / 31.7 11.0m / 31.7
Saudi Arabia	Two Full Transponders (36 MHz each)	1st Lease TV Video - FM 2nd Lease Telephone & Telegraph - SCPC/CFM TV Audio & Radio - Wideband FM	1 734 vox 3	14	11m / 31.7
Colombia	Quarter Transponder (9 MHz)	Telephone & Telegraph - SCPC/CFM TV Audio & Radio - Wideband FM	186 vox 2	3	13m / 34.0
Brazil	Three & One-half Transponders (126 MHz)	TV Video & Audio - FM plus subcarrier Telephone & Telegraph - FDM/FM Telephone & Telegraph - SCPC/CFM	1 1740 480 vox	1 13	15m / 35.0 10m / 31.0
Zaire	Full Transponder (36 MHz)	TV Video - FM TV Audio & Radio - Wideband FM Telephone & Telegraph - SCPC/CFM	1 5 200 vox	13	14.5m / 33.4
Peru	Quarter Transponder (9 MHz)	Telephone & Telegraph - SCPC/CFM TV Audio - Wideband FM	192 vox 1	4	13.0m / 32.8
India	Quarter Transponder (9 MHz)	Telephone & Telegraph - SCPC/CFM	186 vox	2 5	11m / 31.7 7.5m / 25.7

FUTURE DEVELOPMENT OF THE INTELSAT LEASED SYSTEM

PAST OPERATIONAL PHILOSOPHY

Although the concept of providing satellite capacity to be leased for domestic communications was permitted in the INTELSAT Operating Agreement of 1973, a demand for this service did not evolve until 1974-75. At that time, several operational policies pertaining to the provision of domestic service in the INTELSAT system (whose primary objective is the provision of international service) were adopted.

First, most leasing nations took advantage of the proven high reliability of all operational INTELSAT satellites by leasing transponder capacity on a pre-emptible basis. By taking the small risk of pre-emption, the lessee would then pay substantially less than if he leased the non-preemptible or "fully spared" capacity of the international system. Secondly, most leases were assigned to fully operational spare satellites, or to ageing satellites whose operating capacity was not adequate for international service. Spare satellites could then provide communication services during their 7 year lifetime, and older satellites could contribute until they were retired. Thirdly, INTELSAT would not invest in new space segment resources in order to provide leased transponder capacity. All satellite procurement, launch and orbital allocations would be tailored to the international system, with the leased system to be incorporated within the international framework on a "first-come, first-served" basis.

NEW SUPPLY/DEMAND AND NEW SUPPLIERS

In the recent past, two unpredictable factors have arisen that have caused INTELSAT to re-assess its operational philosophy toward the leased network, as it looks toward the 1980's. These are: steadily increasing demand for INTELSAT leased services, and, the availability of domestic/regional services from other suppliers.

Most importantly, INTELSAT has concluded that unless it provides additional space segment by early 1983, pre-emptions in leased service are likely to occur solely due to a lack of available spare transponders. This conclusion was based on a conservative estimate of 26 transponders needed to serve domestic leases in early 1983. In contrast, all past pre-emptions have been the result of routine operational changes and have been measured in seconds or minutes. No lessee has ever been pre-emptied for days or weeks because transponder capacity was not available. The lack of capacity will be caused by:

1) The rapid increase in demand for international service, which requires the full resources of all the new INTELSAT V satellite series and,

2) The fact that most INTELSAT IVA satellites will be reaching the end of their service lifetime.

With regard to other suppliers of domestic/regional services, the past year has seen the ARABSAT consortium of 21 Middle East nations actively planning to pool their resources and launch their own regional/domestic system. Also, the second generation of the Indonesian Palapa Domestic Satellite System is being designed to include domestic service to other nations in South East Asia. In addition, several Western European nations are also actively planning a domestic/regional satellite system (ECS), and other systems for Japan, India and the Nordic countries are certain to appear in coming years.

All of these systems could be operating in the same timeframe that INTELSAT predicts its lessees will face increased chances of pre-emption. After enjoying a near monopoly on the supply of transponders for domestic leases, INTELSAT will then be sharing this role with several of its own member nations.

INTELSAT has been cautiously weighing its policy options toward the supply of future leased services for almost two years. Potential economic, technical and operational problems that could arise from the proliferation of regional and domestic systems had to be balanced against the best interests of the INTELSAT membership as a whole. It was imperative that the prime objective of INTELSAT, "to provide, on a commercial basis, the space segment required for international public telecommunications services of high quality and reliability" should not be impaired. Amid lengthy debate among its member nations, INTELSAT moved toward the adoption of a different approach toward its leased services in the 1980's.

A NEW PHILOSOPHY

In September of 1979, INTELSAT concluded that it was appropriate to assume, for planning purposes, that domestic leased services were to be treated on a "planned basis". This means that INTELSAT will incorporate the projected needs of the domestic service into its traffic data bases, into its projected procurement plans for future satellites, as well as consider technical issues relating to provision of leased service when considering the design of future satellites. By inference, it also means that INTELSAT could more formally consider the procurement of optimally-designed spacecraft for domestic/regional applications.

The possible recognition of domestic services on a "planned basis" gives the INTELSAT planners a new problem to consider: How much capital expenditure will be needed in the future to support the domestic systems? The early philosophy made it unnecessary for INTELSAT to consider investment in increased space or ground segment resources in order to support the domestic systems. Now, there could be future decisions requiring new expenditures that will have to be considered by INTELSAT's governing bodies.

Another important effect of the "planned basis" approach involves a reassessment of INTELSAT's charging philosophy. It may be desirable for the current price differential between pre-emptible and non-preemptible service to yield to a single price for fully guaranteed service for all lessees. Because so many nations are increasing their reliance on satellite communications, and because this level of service is offered by other suppliers, INTELSAT is considering this new pricing philosophy.

However, the proper price to charge is complicated by three other factors:

1) The price being charged by other suppliers

2) The contribution to costs that the leases are expected to provide, and

3) The desire for a smooth transition from the present pricing system to a new one.

The selection of a price that is economically sound for both the lessee and the other INTELSAT members (who have all contributed to the design, construction, and launch of the satellite, in proportion to their investment share), will indeed be a difficult task.

NEW SATELLITE CONCEPTS[1]

We have seen that the number of INTELSAT V spacecraft committed for the support of the international network will not be adequate to simultaneously support the projected demand for leased services after 1982. This led INTELSAT toward consideration of a new philosophy regarding the leased system, which for the first time could require the commitment of capital funds to build and launch more satellites than had been planned previously to satisfy the demands of international users alone. INTELSAT is currently assessing the number and type of atellites needed to meet projected demands for leased services, in the post-1982 era. The three satellite/scheduling options under considerations as of January 1980 are discussed below.

ADDITIONAL INTELSAT V SATELLITES

The first option is to procure two additional INTELSAT V satellites, one positioned in the Atlantic Ocean Region and one positioned in the Indian Ocean Region. (It is not anticipated that any additional satellites beyond those needed for international service will be needed for leased domestic service in the Pacific Ocean Region.) It is an appealing option because it is contractually the simplest to implement. A new satellite design is unnecessary as INTELSAT will exercise its procurement options in the present INTELSAT V contract. If a leased satellite fails, direct point-over to spare INTELSAT V satellites easily restores services. And since all current and anticipated transmission parameters in the domestic systems are designed for the resources of 36 MHz 22 dBW global or 26 dBW hemispheric transponders, two such leases are accommodated in the 29 dBW/72 MHz INTELSAT V hemispheric beam transponders.

There are several disadvantages as well. The INTELSAT V satellite has several 29 dBW/72 MHz "zone" beam transponders as well as two 14/11 GHz steerable spot beam transponders (East and West) for which there seems to be little demand. This represents a great deal of in-orbit satellite capacity that may go unused. However, if further demand develops, and the zone beam transponders are needed to support leases, many lease antennas will require retrofitting to maintain polarization purity from co-frequency hemispheric beam transmissions. In addition, though the hemi and zone transponders have adequate power per bandwidth to support currently requested domestic satellite communications needs, the emerging requirement for TV distribution networks using earth station sizes from 3M to 6M can not be satisfied efficiently in most cases.

In spite of these disadvantages INTELSAT may decide that using additional INTELSAT V satellites may be the most attractive short term means of satisfying the needs of its leasing member nations. In addition to its ease in implementation, it would give INTELSAT more time to assess the potential demand for TV distribution and other specialized telecommunications services that may be requested in the mid-80's, as well as more time to design a specialized satellite that could meet those needs best.

THE ADVANCED/SWITCHABLE INTELSAT V (INTELSAT VA/S)

The second spacecraft concept being considered by INTELSAT seeks to avoid some of the disadvantages of using an unmodified INTELSAT V.

First, some hemi and global transponders with relatively low power/bandwidth are sacrificed for high power/bandwidth transponders. One new beam, the so-called 'split-hemi", would have 32 dBW/80 MHz and another, the "movable spot", would have 34 dBW/40 MHz. Each would prove adequate for TV distribution networks or thin-route telephony networks where very small earth station sizes are a necessity. Secondly, this satellite design would provide greater overall capacity than an INTELSAT V satellite, because INTELSAT anticipates that these more desirable transponder parameters would stimulate latent demand for satellite services.

Such an excellent match between transponder supply and customer demand will not be without its price.

In order for service restoration of such a satellite, other spare INTELSAT V's will have to be similarly modified to serve as spares. The satellites will then be "switchable" between the international mode and the high capacity domestic mode. The complexity and flexibility built into such a system will tax existing technology and could conceivably add additional risk to the planned deployment of such satellites by the end of 1984. In addition, the modifications can only be made at the expense of added weight, which adds another element of risk with regard to launch vehicle availability and mass-saving techniques.

The INTELSAT VA/S satellite would be an ideal satellite for providing leased services to INTELSAT customers, but its costs and risks are somewhat higher than for other alternatives. INTELSAT is currently working on a performance specification for such a satellite, and is initiating negotiations with

---

[1] For a more detailed description of the satellite concepts under consideration, see paper No.80-0511 by R. Granger, "INTELSAT Alternatives for providing Domestic Services during the 1980's".

FACC, the INTELSAT V contractor, for a fixed-price proposal for this spacecraft.

DELTA-CLASS, ALL 6/4 GHZ, "HYBRID" SPACECRAFT (HYBRID-D)

The third alternative that INTELSAT is exploring, is the deployment of a satellite which is not only tailored specifically to supply domestic services but also can serve international users under particular loading conditions.

Although design of the Hybrid-D spacecraft is in its preliminary stages, the fundamental design principles rely on existing 6/4 GHz technology, as well as on the proven frequency reuse techniques of spatial beam isolation and cross polarization. Similarly, it is essential that the satellite mass be compatible with either of the known launch vehicles of the post 1983 era, namely, the Thor-Delta 3920, Ariane, and the Space Shuttle. Unlike the INTELSAT V, the beam-switching matrix of the Hybrid-D will handle service "imbalances", caused by the unequal distribution of the number and type of channels required by leases in the east and west. Indeed, since the hybrid satellite is envisioned to retain only two types of transponders (24 dBW/40 MHz "global" beams and 34 dBW/80 MHz and 31 dBW/40 MHz "spot" beams) it may prove desirable to locate the spacecraft directly over North/South America and Europe/Africa, rather than over the Atlantic and Indian Oceans. (It is also anticipated that the Hybrid-D could serve as the Pacific Ocean Region Primary and Spare, as well as satisfying the domestic service needs of that area).

Using existing technology and known launch vehicle capability, the Hybrid-D concept carries less risk than the INTELSAT VA/S concept, and is also less expensive. However, the satellite would have to be purchased under a competitive procurement process and could not be available by late 1982, which is the timeframe when INTELSAT predicted an increased probability of preemption, due to a lack of available transponders.

INTELSAT will be preparing a SOW and RFP for an INTELSAT-funded design competition in the 1st Quarter of 1980, which could lead to the selection of a contractor and satellite design by the end of 1980.

CONCLUSION

Pricing philosophy, guaranteed versus pre-emptible service, and the selection of dedicated spacecraft for lease services will continue to be debated through 1980. INTELSAT's decision regarding the three spacecraft options: INTELSAT V, INTELSAT VA/S, and Hybrid-D or a combination thereof, will need to be made no later than the end of 1980 or early 1981. The resolution of other questions will continue to evolve. Further debate is also expected on INTELSAT's position regarding the proliferation of regional/domestic services when they are not provided on INTELSAT satellites. The outcome of these debates is anxiously awaited by INTELSAT Signatories who are presently using or intend to use satellite communications to satisfy their domestic and regional communications needs. Similarly, potential suppliers of domestic/regional satellite services are equally anxious to hear the verdict. And spacecraft and earth station manufacturers the world over, are primed to enter the competition for supplying the necessary equipment.

But INTELSAT is wisely moving at a pace that fits the complexity of the problem. Whatever the outcome, the leasing of transponder capacity for domestic/regional communications on INTELSAT satellites will play an increasingly significant role in the engineering design and operational planning of the INTELSAT systems in the 1980's.

80-0547 EVOLUTION OF FIXED SERVICE COMMUNICATION SATELLITE SYSTEMS IN THE 1980'S

Giuliano BERRETTA
Future Telecom Missions Manager
Directorate of Planning and Future Programmes
European Space Agency
Paris, France

ABSTRACT

Current communication satellites are based on system concepts defined at the beginning of the 1970's. The existing system concepts will be further exploited during the first part of the 1980's with gradual innovations being introduced as necessary, due mainly to technological progress. A new generation of space communications will be needed at the end of the 1980's. Considering the development time required for a new generation, countries with an advanced space industry are faced with an imperative need to take decisions in the next few years. In the present paper, an analysis of the reasons that will encourage the introduction of a new generation of satellite systems is made, the evolution of satellite systems is outlined, and a specific representative example is described. The paper is based on the potential market of European interest. The problems of large multimission platforms are also discussed, concluding that a rapid evolution towards large space structures is doubtful.

1. Introduction

Looking back to the two decades of satellite communication history, we can see that the first service developed was the intercontinental point to point communication service. The reasons for this early development stemmed from the unique features of a satellite system for communication : the possibility and the cost of the connection is independent of the distance of the points to be connected and of interposed natural obstacles.

Intercontinental communications via satellite are nowadays well established with the Intelsat evolutionary system, and the use of satellite communications is extending to regional and national systems. A region in this context would be a large country like the USA or India, or a group of countries with a common telecommunications policy such as Western Europe. Moreover, application and services in the industrial and business field are candidates for new space communication systems, particularly in the developed countries.

To evaluate this potential market, a great number of surveys have been performed in the last years, but they were either sectorial or oriented to Intelsat and American domestic systems. In this context, ESA has recently carried out a comprehensive survey with the objective to establish the future possible market for satellites of European origin in the next 15 years. A consultant company (A.D. Little) has also been asked to make an independent market study.

Moreover, these studies show a potential market for services other than intercontinental communications, but system and technology innovations have to be introduced to ensure the development of this potential market for space communication systems.

In the next chapters it will be shown that system and technology innovations capable of ensuring positive development of satellite communications in new areas are potentially already known. It is however necessary to make investments in system studies, technology developments and in experimental systems. This type of investment cannot be expected to be undertaken by private enterprises which can operate only with a limited risk. National and International agencies will have to contribute with studies and experimental systems.

2. Conditions for a Positive Evolution

Regional, and especially national, services are the fields providing the most interesting potential market owing to the highest traffic concentration. However, there are a number of factors of economic and environmental nature that could limit the future expansion of satellite communication.

(a) The competition of alternative terrestrial transmission systems in developed countries will be very strong, in particular with the introduction and the rapid progress of optic fibers utilization.

(b) The distance between traffic centres that should be connected via satellite is reduced with, consequently, a lower number of kilometers by which to divide the cost per circuit.

(c) The number of ground stations will be large and their cost, added to the cost of terrestrial connections to the traffic centres, will become an important factor in the economy of the overall system.

(d) It will be very difficult to control the interference environment after the proliferation of ground stations (particularly if the stations are equipped with relatively small antennas).

(e) There is a limit of growth due to the saturation of orbital arc.

All these points are especially critical with respect to satellite communication developments in rich countries where ground telecommunication networks exist already. In less developed countries or even in rich countries with large but sparsely populated territories, it is easier to demonstrate that the satellite is still the most viable means of communication. For instance, the competition of optic fibers is strong where it is easy to install them (as along a motorway) and where there is electric power available for the repeaters' associated equipment.

Concerning the interference environment, it is also evident that it is less stringent in terms of terrestrial coordination areas in countries where radio links have a limited use and in terms of orbital interference where the geostationary orbit is less crowded. In less developed countries there are also problems, but of another type : financial, educational, infrastructure. Concerning the last point

Copyright © American Institute of Aeronautics and Astronautics, Inc., 1980. All rights reserved.

in particular, it is necessary to design the system around the existing infrastructure or in consideration of its development at moderate cost. Moreover, the system has to be designed to take account of a gradual growth of the need and, consequently, of the traffic.

However, the above drawbacks could be removed and the satellite system could be an economical alternative to ground systems and thus convey a considerable part of traffic :

A. If it can avail itself of small and cheap ground stations placed on the sites of communication centres, thus avoiding costly supplementary ground connections

B. If it is designed as an integrated part of the global network

C. If the interference environment can be controlled in order to make the best utilisation of the limited available spectrum of frequencies and orbital arc.

A. In order to avail itself of small and cheap ground stations the satellite system must be designed in such a way as to :

(i) concentrate the irradiated power on the communication centres, but still in the limits of flux density established by ITU regulations ;

(ii) reduce drastically the power requirement from the ground stations ;

(iii) simplify the terminals' functions.

B. The integration with the ground network will be obtained by :

(i) simplification of the interfaces between satellite and ground system ;

(ii) optimised organisation of function assignment and traffic distribution between satellite and ground system.

When good integration with a ground network is obtained, a communication systems satellite with many ground stations (typically in a national service via satellite at 20/30 GHz) should not be evaluated and costed in isolation from the ground network, thus increasing the global flexibility and economy. In particular, the satellite could provide at least the following to the advantage of the ground networks :

- service of overflow traffic so as to allow the terrestrial network to be dimensioned for average and not for peak traffic ;
- back-up function available anywhere in the coverage area, so as to relieve the terrestrial network from stringent redundancy requirements ;
- connection between distant points, so as to avoid loading intermediate traffic centres with transit traffic.

C. The problem of interference between satellite systems has been solved so far by increasing the discrimination, and thus the dimension, of the ground antenna and spacing the satellites in orbit. If a reduction of dimension of ground antennas is foreseen in order to reduce the cost of ground stations and place them on the sites of the communication centres, the discrimination could still be obtained with an increase of the satellite antenna dimension. This is so provided that careful frequency coordination on the ground between the ground station of the different satellite systems is foressen. In conditions of reduced dimensions of ground antennas, a requirement is also that different satellite systems in the same frequency band and with a coverage area in common are as much as possible homogeneous with on-board receiver antenna gain, unless the least sensitive satellites can be spaced away in geosynchronous orbit from the others.

The narrow spot beam concept with low side lobes will only solve the problem of frequency reuse and interference between satellite systems but, generally speaking, not the problem of interference with fixed services surrounding the ground stations. Strict coordination and/or the use of 20/30 GHz frequency band will be necessary, particularly because the number of ground stations will increase and should be located on the sites of the traffic centres, where ground networks also converge.

3. System and Technology Consequences

The three points analysed in the previous paragraph are strongly inter-dependent in generating system and technology consequences.

From all the above considerations, a spot beam concept should be envisaged. The ideal case would be to have very narrow beams. This implies large multibeam antennas with low side lobes, but enormous pointing problems. The use of higher frequencies, 20/30 GHz, will help to reduce the dimensions of the beams keeping the same physical size of antennas on-board, but problems in antenna technology and pointing will remain.

The concept of many spot beams will introduce access problems and will make FH (frequency hopping) techniques impracticable. SSTDMA (satellite switched TDMA) will be preferred to FH-TDMA used in present systems for several reasons :

(a) reduced satellite weight : a diode matrix is much lighter than a filter matrix, particularly considering that the number of filters will increase by the square of the number of spot beams ;

(b) easier traffic rearrangements : switching matrixes can be made reprogrammeable ;

(c) simpler earth station design due to single frequency operations.

Another step towards improvement is the use of on-board regeneration. SSTDMA with regeneration of the digital signal on-board implies development of on-board demodulators and modulators, and new system techniques. It presents several advantages, however, with respect to RF SSTDMA, particularly for communication systems, where it is very important to reduce ground station costs.

The following advantages can be identified :

- simplification of the digital equipment in the stations, and of system management, as a consequence of signal processing in the satellite ;

- reduction of the RF power requirements for both the uplinks and downlinks in some cases ;
- reduction and simplification of satellite hardware in the perspective of next satellite generation digital technology evolution.

Moreover, the use of regenerative repeaters opens up new systems possibilities such as :

- modulation conversion between uplink and downlink including analog to digital conversion ;
- encoding or decoding on the satellite to compensate for power limitation of either link with some bandwidth penalty ;
- bit rate conversion in order to serve users with different capacities, equivalent to an increased flexibility of the satellite system.

Integration with the ground network will be economically viable if :

- Direct digital interface is provided between terrestrial and satellite links, thus avoiding the proliferation of interface units presently necessary (TIM's TDM interface unit with COMSAT terminology). This implies that the terrestrial traffic is all digital, in line with present clear trends ;
- A signalling method for telephony is adopted in the network which is compatible with the delay of the satellite link ;
- By use of on-board signal processing (which implies on-board regeneration) the satellite is allowed to take over not only switching functions - as planned for SSTDMA system - but also some ground traffic routing functions ;
- Means are provided to avoid double satellite hops when connecting two satellite systems. This can be achieved, either by integrating international and national systems on the same platform, or by using inter-satellite links, or simply by using terrestrial routes for the national segment of international calls.

4. Satellite System Evolution In The Next Decade

The evolution of missions will depend on the telecommunication system and technology evolution outlined in the previous chapter. In the following, no distinction is made between voice and data missions.

Regional and national missions will be operated in the frequency bands 4/6 GHz, 11/14 GHz and 20/30 GHz. The last two bands will be used particularly in Europe. For the export market, 4/6 GHz will be largely used. At least in the next decade, Intelsat system will only use 4/6 GHz band and 11/14 GHz band.

The spot beam concept will be widely used, and consequently SSTDMA, in the next decade. On-board regeneration will probably not appear in the Intelsat system for some time due to compatibility problems with FDMA systems. Regional and national missions will make use of on-board regeneration, and later of sophisticated signal processing on-board for improved routing control flexibility and channel matching efficiency. Progressively, the space segment will take over many of the functions of the ground network. This evolution could be very rapid : already in this decade on-board regeneration will be implemented and before the year 2000 we could already have a sort of "Switchboard in the sky". The complexity of its functions will depend on the size of platforms and on the envisaged combination of missions.

In the next decade, network resource control will also be done by satellite processing. This will be important at 20/30 GHz band where deep fadings impose today large link budget margins with a consequent increase of statistical interference and power demand.

The diameter of antennas will increase not so much in order to augment the EIRP because there is in any case a power flux limitation to respect on the ground according to ITU regulations, but for a better frequency utilisation. In 4/6 GHz band, antennas up to 30 meters could be foreseen ; in 11/14 GHz band, dimensions of up to 15 meters are envisaged and 7 meters in 20/30 GHz band. These figures will pose enormous pointing stability problems. We think that to be more realistic they should be reduced to 20, 7 and 4 meters respectively for systems in the next two decades. For 20/30 GHz band, where a rigid reflector is the most suitable solution, about 4 meters diameter could be the best compromise to make the antenna compatible with the Shuttle size.

The increased size and complexity of antenna systems, and the transfer of functions from the ground network to the space segment, due to mission evolution, will require the support of large platforms. Owing to heavy development investment, it is expected that a proliferation of large platform types will be limited and that, as today the launchers cannot be sized to missions, in the future the platforms will not be sized to the missions. Standardisation will be necessary, particularly at European level, and will be linked to the types of available launchers.

In order to define the size of the platform to support the majority of the missions of European interest in the next decade, payload requirements have been quantified in terms of their demands on the platform design. Having obtained the parameters for specific examples, an assessment has then been made of the possible variations in these parameters due to uncertainties, satellite system evolution, redundancy system, and life time. This has been done in order to provide predictions of the requirements ranges.

The results of the exercise are shown in Fig.1.

5. Service Analysis Example

5.1 General

In order to clarify the concept of the previous chapters, a service example is analysed. The chosen example is a European national intercity mission, as it is the most demanding in terms of satellite performances to cope with high traffic requirements and relatively short connections if compared to a regional or intercontinental system.

Derivation of payload information for a typical case has been based on the Italian national mission, studies of which are ongoing at present.

The European Space Agency, in the frame of the Advanced System and Technology Programme, has carried out several studies on advanced communication systems ; in particular, a study contract on the chosen service example has been awarded to Telespazio (Italy).

The complete study should last 3 years. It started in 1978 and, at this stage, the most important parameters of the system based on 20/30 GHz frequency band utilisation have been defined. Hardware contracts for the antenna, repeater system and on-board regeneration have also been awarded to several European companies. Technology developments are also sponsored by national organisations in the frequency band of 20/30 GHz.

A notable reason in taking Italy as a study example came also from the Italian interest in developing a national satellite telecommunication system in this frequency band.

An Italian domestic telecommunications system via satellite should be implemented in the not-too-distant future and integrated in the existing ground network to satisfy effectively the requirements of telephony traffic as well as potential new special services traffic. The major goal in the system design is the introduction of improved satellite communications facilities at national level without increasing the global network cost beyond that applicable to a solely terrestrial transmission system using coaxial cables, radio relays and optical fibres.

It is foreseen that an operational mission (described in the next chapters) will be economically justified in the early 1990's, preceded by a pre-operational mission in the mid-1980's.

5.2 Traffic prediction

The Italian network has several hierarchical levels, namely compartments, districts and sectors. There are twenty compartments, which are fully mesh-linked and form the long distance network. Part of this traffic should be routed via satellite. The traffic routed via satellite must be large enough to achieve major economies of scale in the space segment common equipment and system operational costs, and should be related to intercity links which are as long as possible.

An initial hypothesis has been made that one-sixth of the traffic pertaining to links shorter than 500 km and one-third of the traffic pertaining to links longer than 500 km would be sent via satellite.

Using the existing forecast for the global traffic in the 1990's, the traffic that would be sent through satellite in Italy in the year 2000 has been evaluated. On the basis of this foreseen satellite traffic and distribution among compartments, a system has been designed. In subsequent interactions, modifications have been made to the distribution to optimise the system economically.

Finally, it has been calculated that a total number of about 80,000 circuits would be sent through satellites in Italy in the year 2000. A distribution of the traffic is given in Table 1. This is not the optimised final distribution, but is a good approximation.

This traffic forecast is only related to telephone type circuits. The use of the satellite system, which will use digital techniques, for other type of services, such as video teleconferencing, distribution of TV programmes, and high speed data transmission, could significantly increase the required system capacity or at least allow a much better utilisation of the satellite capacity.

Some of these services, i.e. data transmission, high speed facsimile, videophone, teleconferencing, should receive a vigorous stimulus by the progressive digitalisation of the terrestrial network and perhaps by the introduction of a high quality digital transmission medium such as the satellite system.

It is assumed that, on the digital satellite system, only the circuits which are in digital form at the output of the compartment centres will be routed.

It is difficult to estimate what degree of digitalisation the Italian network will reach in the 1990-2000 decade but it seems reasonable to assume that, once the introduction of a digital satellite system is planned, the digitalisation process could accelerate also in the switching part of the network.

Compartmental Centre Traffic (in telephone channels)	Total Traffic (year 2000)
Milano	23.900
Torino	11.650
Venezia	9.800
Bologna	11.000
Roma	12.900
Napoli	10.050
Verona	6.950
Genova	6.900
Firenze	5.950
Pisa	5.200
Bari	8.700
Catanzaro	8.300
Ancona	4.450
Pescara	3.750
Perugia	2.350
Cagliari	4.150
Potenza	4.850
Catania	5.850
Palermo	4.100
Bolzano	1.750
Total	154.950

TABLE 1 - Traffic forecast for the domestic satellite network at the end of the spacecraft lifetime (10 years)

5.3 Technical concept

The satellite concept is based on the exploitation of the 20/30 GHz bands where a 2.500 MHz bandwidth is available for this application. The system would operate with a ground station in each of the twenty compartment centres of the existing Italian telephony network, or in thirteen of them according to two different options. In the second option, seven compartment centres will be connected to ground stations located in other compartment centres via terrestrial routing. The satellite would provide one very narrow spot beam for each of these stations.

In Fig. 2, the case of coverage with one spot per compartment centre is indicated. It is very difficult to implement the discrimination required between the beams in this solution ; for this reason the second option with a lower number of spot beams is preferred (Fig. 3).

The ground stations would be situated close to the transit centre to avoid terrestrial connections. The antenna diameter of the ground stations will be 3 metres. The satellite design would support satellite-switched TDMA access techniques and the use of regenerative repeaters with base-band switching. On-board, regeneration offers the advantage of creating CW transmission on the down links, and also on the up links in the case of a one spot/station system ; this feature allows the implementation of very simple TDMA terminals, with relatively low production cost. For this reason, solutions with more than one station per beam have been considered less attractive.

The objective will be to meet CCIR quality criteria without space diversity, but this will be difficult at all earth stations unless very high link margins are adopted reaching 15 dB and 30 dB at 20 GHz and at 30 GHz respectively.

Economic trade-offs will provide elements for the decision on the number of space diversity stations or larger dish antennas in some unfavourable locations.

An important element in the design of the system is the choice of the optimum bit rate. The number of repeaters on board and the filling factor of the system depend on the choice of the bit rate. A high bit rate reduces the number of required repeaters with some penalties on the link budget. The use of more bit rates in the system allows both an increase of the filling factor and a decrease of the number of repeater on board, but the on-board bit rate conversion is required.

A good compromise seems the choice of a single 360 M/bit speed for the whole system. In this case, with 13 spots obtained with two multi-beam antennas of 4 metres serving 13 ground stations, it is possible to fulfil the mission with 17 repeaters and a filling factor of 74.9 %.

However, many other possibilities have been examined. For instance, with two speeds 120 Mbits/s and 240 Mbit/s, 28 repeaters are required and a filling factor of 91 % can be obtained.

In order to accept the use of space circuits for national connections, two technical problems must also be solved in the ground segment :

- echo degradation shall be avoided : this can be obtained using echo cancellation devices ;
- signalling system must be easily adaptable to satellite routing : this seems possible in Italy, for connections at compartment level, at the date of implementation of the system.

The signalling system which will be used on the Italian domestic satellite system in the years 1990-2000 will mainly be a national version of the CCITT No 7, which is already designed for use on satellite systems (CCITT No 7 can only be used on digital networks).

5.4 General validity of the example

The structure of the network in most large European countries is similar to that in Italy.

Concerning traffic in other large European countries, the number of trunk circuits is in general higher than in Italy and for the traffic growth the situation is very similar to the Italian case. The tendency to saturation, i.e. the situation where the traffic increase is very small (a few % in year 2000), is still more evident in other large European countries than in Italy.

Digitalisation of the long distance network is taking place in all the large European countries to a differing degree, but it seems reasonable to assume that a domestic satellite network for the years 1990-2000 will have to be integrated with largely digitalised networks.

In conclusion, the approach followed in the design of the Italian domestic system should be applicable to a large extent to other large European countries. Moreover, the approach should be also applicable to a future regional European system once the present types of systems will be saturated, but this will happen in the more distant future.

6. Use of Large Platforms

In the previous chapters, the evolution of satellite systems has been examined. This evolution will imply the use of large platforms to sustain more demanding missions in terms of power and weight.

The increasing dimension of the satellite antennas will necessitate, in particular, use of large platforms. The use of higher frequencies like 20/30 GHz and the increasing bandwidth assignment will, however, smooth the process of increasing platform dimensions.

Concerning multi-mission systems, large platforms present some interesting features. On large platforms, the following items could be in common to multiple communication functions : the complex antenna system, supporting structure, primary power supply, attitude control, station keeping, thermal conditioning, command and telemetry, on-board computer and programming functions, signal processors. Considering in particular the antenna system, a common antenna could perform roles in several missions and each mission could also use a number of other antennas mounted on the large platform.

However, we would like to underline some points that could make this concept less attractive than it seems at first sight, particularly when non-homogeneous missions are carried on the same platform :

1. Different requirements of the missions vis-à-vis platform performances
2. Different required life time of missions and different replenishment policy
3. Difficulties in decision process in the case of failure of one mission while the others still operate satisfactorily
4. Non-optimised orbit position for all the mis-

sions

5. Difficulties in decision process in case of emergency manoeuvres of the platform

6. Failure of one mission which affects the performances of the others

7. Use of orbit-frequency resources not optimised

8. Institutional difficulties on missions which often depend on different users.

On the customer's side, the requirement for systems optimised to his needs will tend to the direction of national missions, with large capacity and interconnections to the other systems. These interconnections can be accomplished on the same large space station or via intersatellite links.

The use of intersatellite links will create a system presenting the following advantages with respect to the large common station :

1. Less vulnerable
2. More easily expandable
3. More easily adaptable to technological innovations
4. Presenting less institutional and organisational problems
5. Less prone to monopoly of communications
6. More tailored to the real needs of communication developments
7. Permitting more gradual investments.

Some of the drawbacks of large multi-mission space stations will disappear once the sophisticated operations of docking and orbit replacement have been economically solved.

Conclusions

In the next decades, satellite communications will play an important role in areas other than intercontinental communications, provided that system and technology development removes the drawbacks that will make competition with terrestrial means difficult and will limit space system growth due to orbit congestion.

A new generation of space communications will be needed at the end of the 1980's. In view of the development time for a new generation, countries with an advanced Space industry are faced with an imperative need to take decisions within the next few years.

The national and international space agencies that can operate with long term plans on public budgets will be called in to prepare for the next generation with system studies, technology investments and implementation of experimental or preoperational systems. In general, exploitation of follow-on operational systems will be left to other commercial organisations or private ventures.

The point-to-point communication systems, apart from the normal evolution of intercontinental connections due to traffic increase, will then develop in two directions : (a) implementation of domestic services via satellites and (b) global satellite systems, the latter interconnecting regional or domestic systems and strongly integrated with ground networks. Through this process, economy and flexibility will be increased and interfaces reduced.

Rapid evolution in the next decade towards large multi-mission space stations still remains doubtful.

References

1. Outlook for satellite communication at 20/30 GHz - G. Berretta ESA Journal 1979 - Volume 3

2. Utilisation of the 20/30 GHz spectrum part for high capacity national communications - S. Tirro - International Conference : Space Telecommunications and Radio Broadcasting - Toulouse, 5-9 March 1979

3. Perspectives d'évolution des systèmes de Télécommunications par satellite - A.M. Hiéronimus, G. Berretta, M. Guionnet - International Conference : Space Telecommunications and Radio Broadcasting - Toulouse, 5-9 March 1979

4. Communication satellite evolution during the 1980's - L. Templeton, C.L. Cuccia - International Conference : Space Telecommunications and Radio Broadcasting - Toulouse, 5-9 March 1979

5. World Environment and satellite communication 1978-2003 - A revision of opportunities - Future System Incorporated, May 1978

6. Technology development programme for communication satellite payloads in ESA - G. Mica - AIAA, 1980

Acknowledgement

The author would like to thank Mr S. Tirro, of Telespazio, Rome, for the fruitful discussions they had together which proved of enormous help in writing this paper.

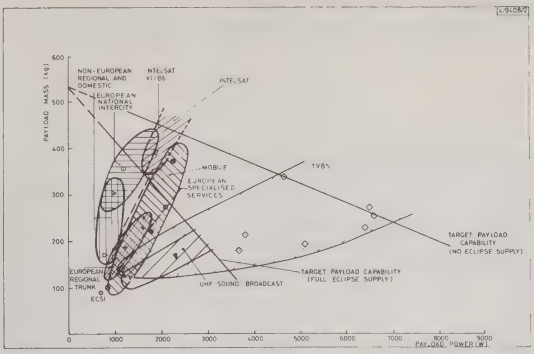

Fig. 1 - Required payload capability (Target payload capability refers to the limits of Ariane III launcher

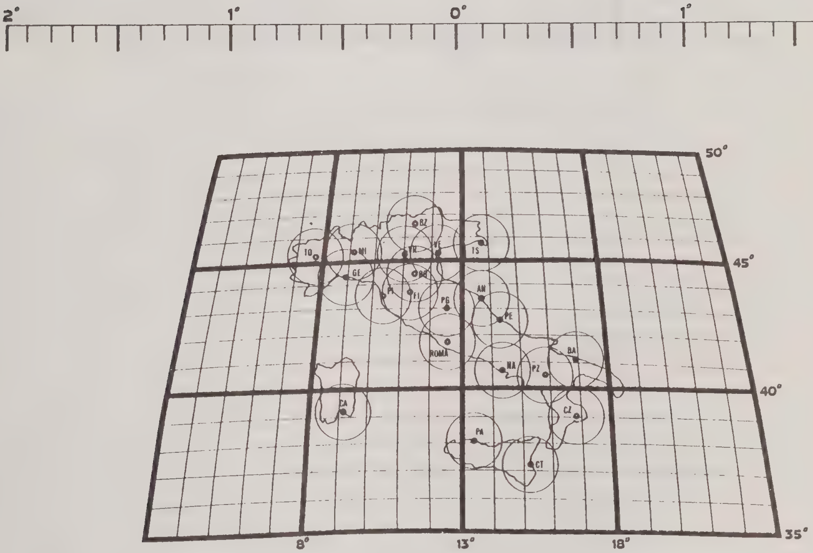
2°
1°
0°
1°
2°
50°
45°
40°
35°
8°
13°
18°
TO
MI
BZ
VR
VE
TS
GE
BO
PI
FI
PG
AN
PE
ROMA
NA
PZ
BA
CA
CZ
PA
CT

Fig. 2 - Coverage of Italian compartments with one spot per compartment centre

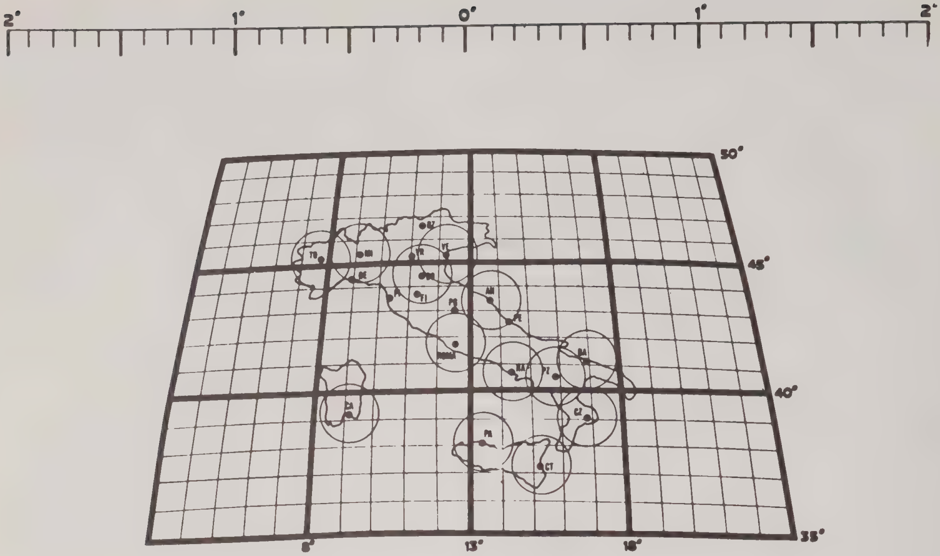
2°
1°
0°
1°
2°
50°
45°
40°
35°
8°
13°
18°
TO
MI
BZ
VR
VE
GE
BO
PI
TI
PG
AN
PE
ROMA
NA
PZ
BA
CA
CZ
PA
CT

Fig. 3 - Coverage plan with 13 spot beams

80-0548

SATELLITE COMMUNICATION TECHNOLOGY CHALLENGES FOR THE '80s

D.K. Sachdev*
International Telecommunications Satellite Organization
Washington, D.C.

Abstract

This is a survey paper aimed at highlighting some of the major technological developments in the satellite communication field during the 80's. Principal areas covered include Intersatellite Links, Digital networks, on-board processing, Reconfigurable Multiple Beam Antennas and significant aspects of transponder and spacecraft technologies. The range of ongoing as well as planned technology development programs in this field is too vast to be adequately covered in a single paper. Accordingly, the presentation has been limited to those programs which hold the promise of significantly increasing the spectrum utilization efficiency, capacity and flexibility of next generation satellite systems. Throughout the paper the emphasis is on the potential capabilities rather than on any specific or planned systems. Major part of the data and results presented are based on work being performed under INTELSAT sponsorship in a large number of organizations worldwide.

1.0 Introduction

With a modest beginning in the early 60's, satellite technology has matured enough to be accepted on a worldwide basis as one of the major media for the communication networks. Communication satellites have rapidly grown in size and complexity during the 70's and have proven their worth through steadily decreasing unit circuit cost as well as exceptional reliability. However satellite technology development is nowhere near saturation, and significant advances which could provide further reduction in cost as well as introduction of several new types of services are to be expected.

This paper presents salient aspects of the major technological challenges ahead in this field. While to a substantial extent, international communication has been used as a basis, most of the areas identified are relevant to domestic and regional satellite applications as well. The emphasis throughout is on individual technologies, rather than on specific system or network growth except for situations where these aspects are germane to the development of the technologies themselves.

The first few generations of communication satellites had - as seen from today's vantage point, - rather modest power and size and required comparatively large earth terminal antennas, high power amplifiers and cryogenically cooled low noise amplifiers. As the traffic increased, the necessary system growth was, by and large, accommodated by a corresponding growth in the launch vehicle size. To a certain extent, this trend has continued during the early 70's, influenced no doubt, to a degree, by already acquired assets in the ground segment. Commencing with INTELSAT IVA and maturing in the forthcoming INTELSAT V era, there has been significantly greater emphasis on technologies aimed at increasing the utilization efficiency of present and future launch vehicles and RF bandwidth.(1) (2) (3). The post INTELSAT V spacecraft are expected to see even further progress in this direction.(4)

The overall system aspects influencing the choice of technologies during the 80's are: the need to provide increased system capacity through more efficient utilization of available bandwidth, introduction of new frequency bands, optimum utilization of newer launch vehicles, longer spacecraft life through progressive elimination of limited life devices & subsystems, and flexibility to meet and adapt to a variety of space segment requirements.

In a field encompassing a large number of multidisciplinary efforts, several factors act as motivating or driving forces for the concurrent development of the diverse technologies involved. This indeed is true for the satellite communication technology in the 80's. Nevertheless a good starting point to introduce some of the technologies could be the impact of progressively increasing reuse of the available frequency bands.

To begin with, the very first communication satellite itself represented a frequency reuse application, since the 6/4 GHz bands were simultaneously utilized by terrestrial and space systems. Once the total 500 MHz band had been utilized in the INTELSAT IV class spacecraft,the reuse of this bandwidth in the space segment itself assumed importance. Arising out of these efforts, INTELSAT IVA achieved a modest spatial reuse. The INTELSAT V spacecraft will have a combination of both spatial and polarization reuse as well as the introduction of a new 14/11 GHz band. The next generation of spacecraft currently being planned are expected to have extensive reuse (up to 8 to 20 times depending on application) of some or all the frequency bands available today for satellite communication. Success in achieving such a high degree of frequency reuse is dependent on several system and payload technologies as well as on the ability of the spacecraft bus and other support subsystems and launch vehicles to efficiently accommodate the increased capability. The system and payload technologies are related to sophisticated multiple beam antennas, adaptability of the satellite configuration to benefit from the resultant flexibility and new modulation methods. While the increased circuit or communication capacity could be exploited by simply increasing the number of transponders, the weight and power requirements of several tens of transponders on a single bus dictates not only substantial progress in transponder technology itself but also concurrent development of newer or improved techniques of power generation, power storage, and reliability engineering.

---

*Manager (R&D), INTELSAT
Member AIAA

Copyright © American Institute of Aeronautics and Astronautics, Inc., 1980. All rights reserved.

Multiple reuse of frequency bands through a large number of physically separate beams requires an appreciable level of interconnectivity on-board the spacecraft. SS-TDMA and other digital technologies provide the necessary tools for providing this interconnectivity between different beams from a single satellite. From the overall global network point of view, all satellites - whether domestic, regional or international - are integrated with one or more telecommunication networks. Such networks achieve maximum flexibility when all the nodes are capable of being interconnected, generally, in a hierarchial fasion. Both from the point of view of providing network flexibility as well as mitigating the effects of propagation time delays in certain situations, direct links between satellites (Intersatellite or cross links) are emerging as one of the important tools for the 80's. Beginning with a point-to-point role, the ISL's, combined with baseband processing, are expected to ultimately unfold, the efficient and flexible role of "switchboards in the sky" for geostationary satellites in the global communication networks.

This paper highlights some of the principal facets of the technologies enumerated above.

2.0 Intersatellite Links

The effectiveness of any communication network is a function of the interconnectivity between its traffic nodes. This aspect has been the cornerstone of practically all domestic and international terrestial networks. For landmasses separated by vast stretches of water or undeveloped territories, the first step towards global interconnectivity has been provided by geostationary communication satellites. However, so far, satellites have been utilized only as 4-wire transmission path between several pairs of earth stations. At least two advances are required for enabling the growing population of satellites to play the role of truly efficient nodes in the global communication networks; the first is the capability of intercommunication between satellites and the second the provision of on-board satellite processing.

In principle, a link between geostationary satellites should be the simplest and almost ideal one through an ideal propagation medium, and at least in the foreseeable future with minimum interference constraints. ISL's have already been demonstrated experimentally (8). However, before such links are applied to public telecommunications, a number of new technologies need to be perfected, along with a better understanding of their role in global satellite based networks.

The starting point is choice of the frequencies. To some extent this is related to the type and volume of information rate over ISL's. Optical links are attractive for a space-to-space link (5) (6). However, the technology development of optical ISL's would possibly receive greater impetus once the traffic requirements increase further. In the near future, practically all the development work is concentrated on 500 MHz to 1 GHz bandwidths in the 23 to 60 GHz range (7).

The first experimental satellite-to-satellite link was part of the LES 8/9 system (8). It employed solid state ISL Transponders at 36-38 GHz for up to 100Kb/sec. data transfer between two satellites up to 40,000 km apart. This experiment proved several new technologies principally in the area of mm wave transmitters, antenna acquisition, etc. The forthcoming Advanced Westar/TDRSS system (9) will also have a Ka-band Intersatellite data link capability.

The global INTELSAT network can derive substantial benefits from Intersatellite links in view of its widely dispersed earth stations and multiple satellites in the same ocean region. It is expected therefore that the ISL technology will get established on a world wide basis though the INTELSAT network with the exciting possibility, sometime in the future, for interconnection of more than one satellite network through ISL's.

In a global network, ISL's could be provided either between two adjacent satellites in the same region or between individual satellites in adjacent regions. The intra-regional satellites provide the principal advantage of eliminating the need for multiple antennas at individual ground stations. Such links would continue to be of importance since multiple satellite operation provides the necessary operational reliability.The development of intra-regional ISL's, incidentally, would also provide the necessary technology for interconnection of two different networks in the same region, but that is a question which encompasses issues beyond pure technology development. Inter-regional ISL's on the other hand, would interconnect satellites from 40° to 120° apart and could be useful in the interchange of certain types of traffic. Such ISL's could still encounter the difficulties associated with excess time delay and would require much higher values of EIRP and G/T per channel than for intra-regional ISL's.

ISL's would operate at frequencies above 20GHz, where the flight-proven communication hardware still requires considerable development work and available RF power levels are limited. On the other hand, bandwidth constraints are less severe than at lower frequencies. These factors have led to a detailed examination of the optimum modulation and bandwidth - expansion techniques for such links (7). As a baseline, the up and down links of the two satellites forming an ISL have been assumed to utilize global beam transponders, following the current channellized 40 MHz transponder concept. Each of these transponders would have multiple FM-FDMA and SPADE carriers. The current development work is aimed at the need to transmit traffic over the ISL's for three adjacent 40 MHz transponders. Among the several possible modulation techniques examined are direct heterodyne, FM remodulation, FM Demodulation/Remodulation, PCM encoding, etc. The direct heterodyne approach is the simplest but the least efficient, since it suffers from the disadvantage of a back-off requirement of the power amplifier for multiple carrier transmission and does not trade the available bandwidth for power. The FM remodulation approach converts the multiple carriers in three transponders (typically 15 FDMA/FM carriers and over 300 SPADE circuits) into a single wide-deviation carrier occupying nearly 1 GHz bandwidth, and has approximately 10 to 15 dB advantage over the heterodyne approach. It has the added flexibility of providing a trade-off of capacity versus spacecraft separation distance. The FM Demodulation /Remodulation approach envisions complete demodulation to the SSB channels or digital baseband levels. On the overall transmission level, this approach retains all the advantages of FM remodulation and in addition, provides flexibility with regard to transponder assignments and permits substantial channel rearrangements within the spacecraft. However, the relevant spacecraft complexity would possibly be justified only when baseband processing reaches the stage of being introduced in the satellite systems as a whole. Fig. 1 shows the comparison of various modulation techniques.

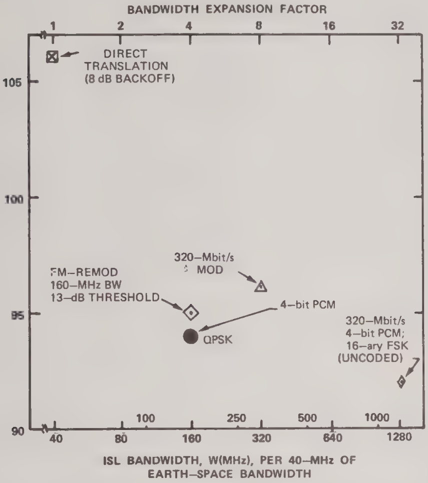

FIGURE 1. COMPARISON OF THEORETICAL REQUIRED $(C/N_0)_{SAT}$ AND BANDWIDTH

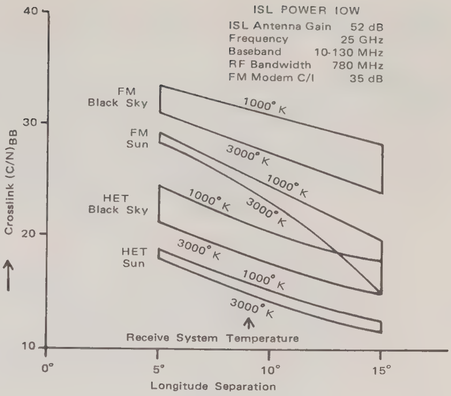

FIGURE 3. ISL BASEBAND C/N AGAINST SATELLITE SPACINGS

Taking into account the relative merits of various modulation techniques, the FM remodulation technique appears the most promising, at least for the first generation ISLs which it is expected would precede the on-board processing era in satellite communication. A simplified block schematic of such a transponder ISL is shown in Fig. 2 along with the principal electrical parameters. Fig. 3 shows the comparison of heterodyne and remodulation techniques for three typical spacings of satellites. Several conclusions are apparent. The heterodyne technique has limitations above 5° spacing, whereas remodulation technique provides excellent capability up to 15°. Further, during sun conjunction (of the order of 15 minutes in each eclipse season) unacceptable performance degradation will occur for spacings above 15°.

The ISL's with the above characteristics require several new technologies to be developed and space qualified. For the transmitter, 10 W TWT's are currently being developed at 23 to 32 GHz. Acquisition capabilities of the ISL antenna are also being developed. The most crucial components are the wideband modulator required to FM modulate a 23 or 32 GHz carrier with a multiple carrier baseband signal extending from 10 to 130 MHz and the corresponding demodulator. Fig. 4 shows the block schematic of the Modem currently

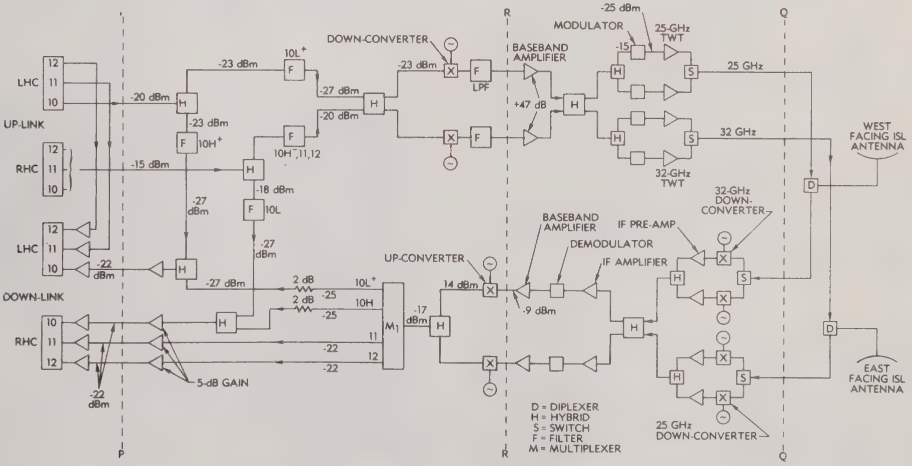
P
R
Q
LHC
12
11
10
UP-LINK
RHC
DOWN-LINK
-20 dBm
-23 dBm
-15 dBm
-27 dBm
-18 dBm
-22 dBm
10L+
10H+
10H-,11,12
10L
DOWN-CONVERTER
-23 dBm
-27 dBm
-20 dBm
LPF
BASEBAND AMPLIFIER
+47 dB
MODULATOR
-25 dBm
-15
25-GHz TWT
25 GHz
32 GHz
32-GHz TWT
WEST FACING ISL ANTENNA
32-GHz DOWN-CONVERTER
IF PRE-AMP
DEMODULATOR
IF AMPLIFIER
UP-CONVERTER
14 dBm
-9 dBm
-17 dBm
M1
2 dB
-25
10L+
10H
11
12
-22
5-dB GAIN
EAST FACING ISL ANTENNA
25 GHz DOWN-CONVERTER
D = DIPLEXER
H = HYBRID
S = SWITCH
F = FILTER
M = MULTIPLEXER

FIGURE 2. TYPICAL ISL TRANSPONDER

under development along with the principal technical objectives.

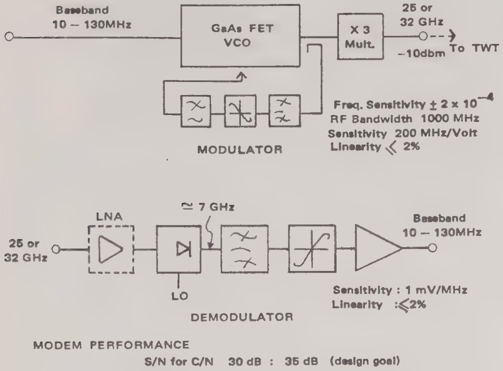

FIGURE 4. ISL MODEM

The role of ISL's in future networks is presently under detailed evaluation concurrently with the above technology development efforts. In principle, the ISL subsystems now under development could also be used for modest length inter-regional requirements but with lesser capacities. Further, with the rapid introduction of digital technology on satellite networks, it is reasonable to expect that dedicated digital ISL's would ultimately be more suitable and would be compatible with the SS/TDMA networks of individual multiple-beam, satellites. Additional development work to accommodate the path delay and its variations would then become necessary. As highlighted in the following paragraph, SS-TDMA could logically lead to on-board processing. At that stage, for ISL's the demodulation/remodulation approach would obviously be the choice. However, it is assessed that this transition would not call for any major technological development which would be exclusive to ISL's.

3.0 Digital Satellite Communication

The rapid advances in digital techniques are making a significant impact on practically all segments of communication technology as a whole. In the satellite communication field, the applications of digital technology fall in two categories; those which are common to the communication industry as a whole and the others which are unique to communication satellites. Examples in the first category would be the introduction of PCM Multiplex equipment, with or without DSI, digital rearward microwave links, etc. Applications unique to satellites are principally related to the multiple access capability.

Multiple zone coverage requires within the spacecraft flexible and efficient means of interconnection between the various zones. Without demodulation on-board, the FM-FDMA operation requires N^2 filters for providing full interconnectivity between N zones (10). Even with a modest number of zones, the weight of these filter-networks becomes unacceptable. Further, unless a very large number of zones are employed, it is still necessary to share a typical 40 MHz transponder among a number of carriers, leading to reduction in capacity due to back-off requirements.

The above limitation in FM-FDMA approach, coupled with advances in digital communication technology have led to the development of TDMA and SS-TDMA system concepts. By utilizing a single high speed time-shared carrier in one broad-band transponder, TDMA achieves higher capacity compared to FDMA, principally due to its ability to operate near saturation. The interconnectivity between zones is now provided through switching in the time-domain - the SS-TDMA System (11).

The technology for TDMA as well as SS-TDMA has been under development for nearly a decade, and it is expected that during 80's a number of operational systems would get introduced (9)(12-14). In the INTELSAT system, a 60/120 Mbits TDMA and SS-TDMA system has gone through several stages of development cycles and field trials. It is envisioned that the first step would be introduction of TDMA among a small group of users principally to relieve saturation of spacecraft capacity and to attain experience with digital systems in an operational environment. The next generation spacecraft (IS-VI series) which would heavily depend on multiple beam antennas are expected to have an operational SS-TDMA system.(4)

Apart from obvious technical differences, FM-FDMA and SS-TDMA systems are suited to different environments. Thus, FM-FDMA systems favor smaller number of access per transponder to minimize the back-off requirements and interconnectivity is provided fairly efficiently so long as global beam operation is acceptable. With multiple reuse of frequency bands through independent zones, the SS-TDMA system has definite advantages in terms of capacity, weight as well as flexibility with regard to interconnectivity. Further, in general, TDMA and SS-TDMA systems favor as large a transponder bandwidth as possible consistent with the technology requirements in both the space and ground segments.

FM-FDMA and SS-TDMA systems discussed so far have assumed no demodulation on-board the spacecraft and interconnection has been assumed to be at a common intermediate frequency in both cases. However, the growing complexity of networks as well as better performance achievable in all-digital systems through regeneration has motivated recent efforts towards system studies as well as hardware development for on-board demodulation/modulation as well as on-board processing of traffic. Seen from an overall global communication network, this represents a logical step towards the satellites assuming a role more akin to that of a 4-wire Tandem Switch in ground communication networks. This also provides the flexibility of matching the size of each carrier to its traffic as against the requirement in TDMA, where the ground transmitter has to deliver a power which is related to the overall system capacity and is not proportional to the local outgoing traffic. Further, the size and complexity of SS-TDMA matrix at microwave frequencies increases very rapidly with number of spot beams involved. Use of demodulation & regeneration on the other hand permits achieving the switching function through inexpensive integrated circuits, even for a large number of beams.

There are several stages - each with its own benefits as well as technological challenges - through which fully flexible on-board processing capability would perhaps be realized. A common denominator in all the approaches is that on-board regeneration leads to better overall performance since this essentially prevents the cumulation of degradation of up and down link performance (16, 17).

Fig. 5 shows an SS-TDMA system with a Microwave Switch Matrix (MSM) at RF frequency. Several versions of this configuration are in various stages of realization (12-15). Such a system would be characterized by efficient interconnection of multiple zones at the IF frequency. All the users utilize the same transmission rate (typically 60 to 250 Mbits/sec) irrespective of the traffic on each link. Such a configuration has the merits of a modest degree of complexity on-board the spacecraft but suffer from the disadvantage of requiring burst, as against CW, transmissions to and from each station and that too at the highest bit rate in the system. Fig. 6 shows a photograph of the MSM alongwith its Distributed Control Unit Fig. 7 shows the progressive steps involved in achieving total on-board baseband processing capability. The IF MSM is now replaced by a Baseband Switch Matrix (BSM) which could be realized with high speed digital integrated circuits and would be amenable to a substantial degree of flexibility which could be exploited even by simple ground commands. Of course, this degree of flexibility would be a function of the baseband hierarchical level at which the actual switching is carried out.

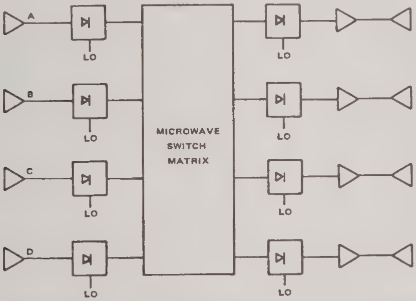

FIGURE 5. SS-TDMA BLOCK SCHEMATIC

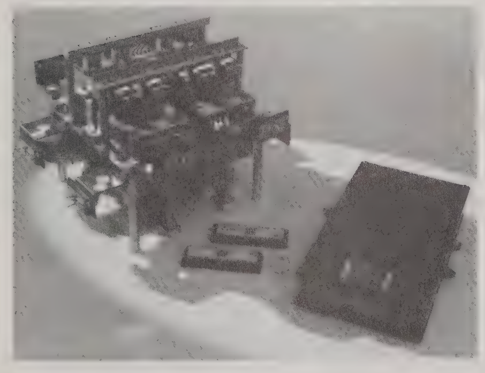

FIGURE 6. MICROWAVE SWITCH MATRIX AND DISTRIBUTED CONTROL UNIT

One implicit advantage of the introduction of BSM is that each downlink carrier could now a CW carrier and thus could carry all the traffic for a given earth station. In an analogous way, each demodulator could be interfaced to a single earth station. This leads us back to the concept where each earth station could be associated with a pair of frequencies (and filters) on-board the spacecraft. Each station would now radiate digital traffic on one carrier whose size would be matched to its traffic. At the satellite, after demodulation and rearrangement of the bits, all the traffic for any particular station would be sent down on one carrier which would be uniquely associated with that station. The above arrangement provides substantial routing flexibility and the earth station equipment no longer need to have the capability to radiate at the highest aggregate bit rate. On the other hand, each station can now have equipment tailored to its own traffic requirements as for FDMA. Such an approach is particularly attractive when the number of stations in a typical zone is not too large.

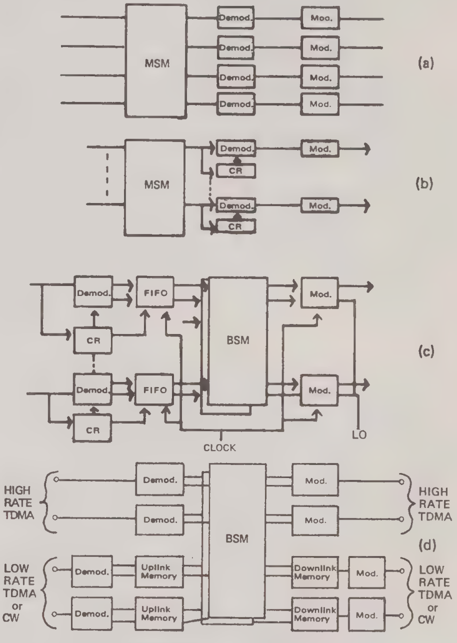

FIGURE 7. ALTERNATIVES FOR ON-BOARD PROCESSING

(a) MICROWAVE SWITCH MATRIX WITH ON-BOARD REGENERATION.
(b) (a) WITH CARRIER RECOVERY.
(c) BASEBAND SWITCH MATRIX WITH ALL CW DOWNLINK CARRIERS.
(d) HYBRID SYSTEM.

Fig. 7(c) shows such a system where all the traffic is demodulated, stored and sent down as CW carriers. In a practical situation, with a mix of high speed and low speed traffic, the arrangement shwon in Fig. 7(d) is possibly more suitable. High-speed TDMA traffic is demodulated, switched at baseband and remodulated for transmission to the destination without storage. Low-speed TDMA traffic or non-burst CW traffic is demodulated and stored in up-link memories to await insertion in one or more of the high rate down link TDMA bursts.

A discussion on digital satellite communication would be incomplete without at least a reference to the rapid strides in the exploitation of the properties of the signal source itself to reduce the required channel capacity or Source Coding. DSI, already receiving serious attention alongwith TDMA, can give at least two-fold enhancement of capacity. However, nearly instantaneous coding (NIC) and ADPCM hold a promise of providing substantial increases (up to 4 to 6 times when combined with DSI) in overall system cpapcity. Of course, these techniques are by no means unique for satellite communication.

4.0 Antenna Technology

The satellite antenna technology began with a single beam covering the whole or major part of the visible position of the earth and radiating all the available frequencies only once. The next step was concentration of the energy over the regions of traffic. With the increasing demands placed on the available frequency bands, consideration was given to resuse of the frequency bands (18). A measure of the increasing reuse is the equivalent bandwidth being derived from the 500 MHz bands in the 6/4 satellite bands.

							(planned)	
INTELSAT S/C	I	II	III	IV	IVA	V	VA	VI
Eqv. BW(MHz)	25	126	460	432	720	1480	1600	2560

The above progress has been achieved through advances in practically all subsystems which are put together to form a modern communication satellite antenna subsystem. While the bandwidth utilization efficiency has been steadily increased, the satellite antennas have utilized little or no reconfigurability in space. Thus, INTELSAT V antenna has the capability at present to realize certain marginal adjustments in the footprints by on/off switching of a number of feed elements. Reconfigurability in space could be desirable from several points of view; a flexible spacecraft design for all locations in the geostationary orbit; capability to handle either international or domestic/regional traffic, and in the case of receive antennas, the ability to suppress interference from an unwarranted radiation. The extent of reconfigurability would vary with applications, traffic patterns, etc. and is also to a large extent influenced by the progress in beam forming technology, maximum size of antenna reflectors permitted (19).

The complexity of a reconfigurable antenna depends on the demands which future satellites would place with regard to the size and proximity of the shaped beams, the extent of frequency reuse and the range of reconfigurable patterns. The first factor decides the size of the component beam which, in turn, dictates a certain minimum size of the reflector. The reconfigurability requirements lay down the number of layers of variable power dividers and phase shifters and the complexity of the associated electronics for providing control through ground command. Considerable amount of development work addressing one or more aspects of the Multiple Beam Reconfigurable Antennas (MBRA) has taken place in the past decade. Some of the major results of work being carried out by INTELSAT through its R&D Programs are summarized below: (20)(21).

The MBRA technology could provide switching capability for up to seven identically polarized beams, or in all 14 beams if dual polarization is utilized in each beam. The near term technology will provide the reduction of interbeam guard spacings below 3^{o} for a region at the edge of earth and about 2.7^{o} for regions corresponding to slightly smaller scan angles like North America and Western Europe. In principle, it should be possible to assign 24 independent transponders for each of the seven beams providing a maximum theoretical transponder capability of 168 in 500 MHz bandwidth, using both polarizations. Concurrent with MBRA technology, substantial development work is also underway towards increasing the percentage bandwidth in anticipation of new WARC allocations. Figure 8 shows a simplified practical version of a broadband system. The worst case polarization isolation in a ±6.5% frequency band would be better than 30dB. Typical polarization isolation against the nearest (adjacent) shaped beam will be at least 40 dB This increase in polarization isolation is achieved through newly developed multimode horns with an approximately 1.8 aperture diameter/wave length ratio (Fig. 9). In order to confirm the primary and secondary pattern performance of a fullscale MBRA, a representative 140" offset reflector with a 16 feed horn cluster is also being constructed. Fig. 10 shows a photograph of the tool for the reflector.

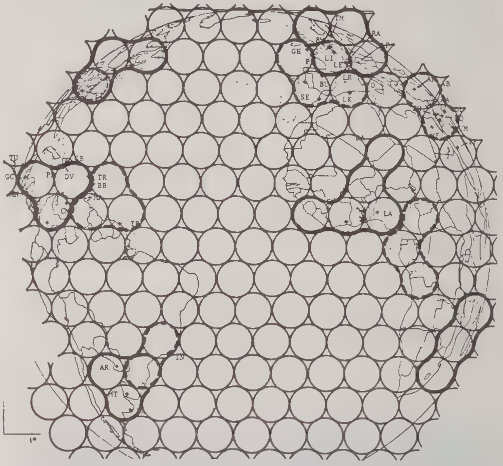

FIGURE 8. TRAFFIC MATCHED, NEARLY CONTIGUOUS ATLANTIC-INDIAN OCEAN COVERAGE BEAM PLAN

4.1 "Active" Antennas

So far, reconfigurability has been assumed to be achieved after the transponder multiplexers which has the advantage of introducing minimum changes in the payload configuration of current satellites adopting channellized transponders. However, this calls for fairly heavy beam-forming networks with minimum loss and the capability to handle fairly large amounts of power. This approach could also have limitations from the point of view of dynamically switching a given transponder to more than one beam. These and other system considerations have lead to substantial

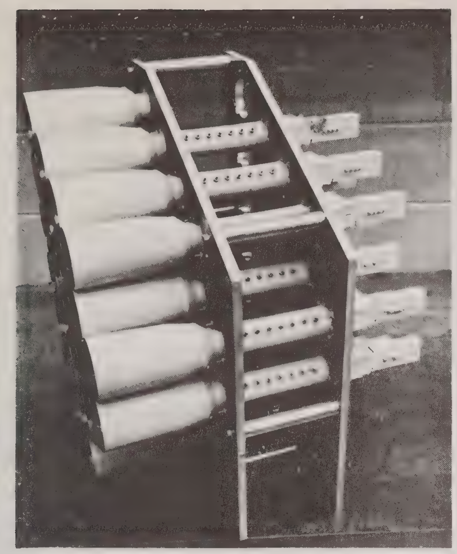

FIGURE 9. MULTI-MODE HORN

amount of effort towards developing "active" or phase array antennas for communications satellite applications.

Under the "active" antenna concept, the beamforming and reconfigurability is carried out at a lower power level and thus permits the use of miniaturizing techniques such as MIC's leading to substantial weight savings (22). This approach has the added advantage of control at much higher speeds - a fundamental requirement of the "scanning spot" beam satellites under consideration for contiguous coverage areas typical of highly developed domestic networks. (23).

Other areas of investigations in the antennas field which are expected to make significant impact on the performance of satellies being developed during the 80's are efforts towards increased minimum coverage gain for global antennas; improvements in software and the design tools; progress in materials and mechanical features of the next generation antennas (24).

FIGURE 10. TOOL FOR MBRA REFLECTOR

5.0 Transponder Technology

Concurrent with the development of newer system concepts and their associated hardware, there have been substantial efforts, industrywise, towards improving the performance, weight and reliability of the transponders. One notable example, now reaching a level of maturity is graphite epoxy lightweight filters and contiguous band filters. In the near future, it is anticipated that a significant impact would be made by the rapidly growing GaAs FET technology. These devices are challenging practically every available "slot" in the transponder, ranging from low noise front end amplifiers, switching matrices both at IF and baseband, high power amplifiers, etc. (25).

For the output stages, travelling-wave tubes have been the mainstay of communication transponders right from the beginning of satellite communication. Current TWT's provide efficiencies up to 40% and life have operational potential exceeding 7 years or more. Over 200 TWT's are currently under operation in space, mainly at C-band.

TWT's, notwithstanding their excellent record, have a finite life and substantial amount of work has been underway for nearly a decade to evolve their solid state replacements. While Impatt diodes have an edge at freqencies above 20 GHz, the real impact at bands of immediate interest is being made by the GaAs FET amplifiers (25-28). When replaced one-for-one, FETA's compared to TWTA's, are expected to provide comparable efficiencies, better IM products, smaller volume and, of course, simpler power supplies.

In the longer perspective, several approaches to the optimum utilization of solid state power stages are under various stages of development. Thus, solid-state amplifiers, unlike TWT's, can be optimized for IM and efficiency at a range of output power levels. Several approaches to linearization of the amplifiers, some of them common with TWT's, are currently receiving serious attention. These include push pull operation, predistortion (29) feed-forward. The possibility of substantial distortion reduction through negative feedback at microwave frequencies is a technological challenge motivating development of monolitic amplifiers with extremely small forward propagation delays. Concurrent with the development of "conventional" solid state power amplifiers is the substantial activity related to the active antenna field referred to in Para. 4 above. The latter would receive substantial impetus if wideband low distortion medium power (0.5 to 1 Watt) amplifier modules become a reality in the near future.

6.0 Spacecraft Technology

Principal aspects of the spacecraft technology which would be briefly considered here are the advances in power generation & storage techniques, impact of launch capabilities on spacecraft design and attitude and orbit control subsystem requirements.

6.1 Power Generation Technology

Commercial communications satellites to date have employed solar cells for primary power generation. Increases in spacecraft size, and the consequently higher total power demand, now dictate that the cells be mounted on deployable arrays, no matter whether the satellite be spin or body-stabilized. In the second category, the present total power demand (1 kw for INTELSAT V) can be met by the use of two deployed wings, each sub-divided into several rigid panels.

The structure of rigid panels consists in most cases of honeycomb cores covered with sheets of fiber reinforced polyimide foils. The stiffness of rigid panels prevents excessive vibration during launch and gives a stable configuration in orbit. However, the high weight of the panel structure will limit use of such panels to satellites not requiring more than 1,5 kW. Specific powers attainable are typically 20 W kg^{-1} and only considerable improvements in solar cell performance can extend this to 25 W kg^{-1}.

Alternative lightweight arrays have been under investigation for several years, and their further development is critical for the spacecraft of the '80s. They can be categorized as either semi-rigid or flexible. Semi-rigid arrays are based on a thin substrate foil mounted in a rigid frame. Representatives of this type are the GSR and ULP manufactured by SN/AS and MBB/AEG respectively, with a proven attainment of 30 W kg^{-1}. As before, the use of a more weight efficient solar cell would increase this figure of merit - possibly to 50 W kg^{-1}. Work on fully flexible arrays has already demonstrated that _ 100 W kg^{-1} is feasible for systems requiring 5 kw. Conceptual designs here include retractable roll-out and fold-out types.

It will already be clear that a second key development in this area will be the evolution of ever more weight efficient solar cells. This target becomes steadily more critical as the weight of the array substrate, support etc. is itself reduced. Two major development will merge during the early 80's. Thin substrate-thin coverslide (50 microns each typically) cells which have already been demonstrated to be fully compatible with several of the advanced arrays, will doubtless begin to incorporate the many efficiency optimization features now included and proven for standard, thicker substrate devices (textured front surface fields etc.). This will usefully supplement the presently rather low efficiencies obtained from 50 micron cells, whilst retaining the better radiation hardness typical of these devices. While the major part of this effort will involve cells fabricated from silicon, there will also be attention given to alternative materials. Gallium arsenide cells for example, offer a better maximum efficiency, a reduced temperature coefficient of efficiency and considerably better performance in a radiation environment than conventional silicon units. The use of compound semiconductor devices with concentrating array may also become attractive.

6.2 Power Storage Technology

The provision of power enabling full operational capability during the eclipse seasons has normally been achieved through the use of batteries. The sealed nickel-cadmium (Ni-Cd) battery has been used in all INTELSAT spacecraft to date. Currently (on INTELSAT V) the requirements made at the Ni-Cd units include: a minimum of 1000 charge/discharge cycles, during seven years, from a battery of 30-35 Ah capacity, the discharge rate being no greater than $^{C}/2$. Given the results of detailed investigations on Ni-Cd cells, these requirements appear feasible, providing that the depth-of-discharge is itself limited (to approximately 50%) and strict temperature control of the battery is maintained. The information obtained from recent analyses of performance degradation in Ni-Cd cells does not however lend support to the notion that any sizeable further step in operational capability can be obtained from Ni-Cd units. Doubtless efforts will continue to improve their overall reliability and stability; hinging on both optimization of the cell components as well as on improved routines for operational management through the early '80s. Particular attention will have to be paid to the chemical stability of the separator and the microstructural properties of the negative (Cd) electrode. Hydrolysis of nylon separator material leads to loss of overcharge protection in Ni-Cd cells, and cadmium migration from the negative plate to a loss of overall capacity. Operationally there is much current emphasis on reconditioning (30).

Partly in response to the difficulties which are encountered with Ni-Cd units, INTELSAT has sponsored the development of nickel-hydrogen (Ni-H$_2$) batteries. Successive R&D program, spanning six years, have been concerned with cell and battery design, and component development. It was appreciated very quickly that the Ni-H$_2$ system has several internal advantages compared to Ni-Cd cells, including in-built overcharge protection, a good overdischarge capability and an easily optimized energy density (31). The INTELSAT sponsored work - performed by COMSAT Labs. and several commerical battery manufacturers and consultants - has been paralled by efforts made at Hughes Aircraft Co. with the support of the U.S. Air Force. The production technologies and cell designs evolved by each are rather different, at the cell component as well as configuration level.

It is now clearly apparent that the Ni-H$_2$ battery will be able to provide a major increase in performance (relative to Ni-Cd) aboard communication satellites. Excellent performance, over 3000 cycles from 50 Ah cells at 75-80% depth-of-discharge, can be predicted from laboratory results (32). This will be available at a useable energy density at 35-40 Wh Kg^{-1}. By comparison, Ni-Cd batteries can offer only 15-20 Wh Kg^{-1}. The good performance and resistance to degradation of the Ni-H$_2$ battery has been fully confirmed by flight experience to date. A 35 Ah battery supplied by INTELSAT has provided power for the NTS-2 spacecraft for five eclipse seasons C and one short lunar eclipse) since its launch in June 1977 (33). Data from this battery, and another of the same design being run under psuedo-geostationary orbital conditions at Comsat Labs. is given in Table 1 below.

The performance of both batteries has been strictly according to demand. Current consideration is being given to the incorporation of 30 Ah Ni-H$_2$ batteries on the later flight models of the INTELSAT V spacecraft series, and involves the technology developments and

TABLE 1 End of discharge voltage performance for two Ni-H_2 spacecraft batteries.

	NTS-2 Battery	COMSAT Battery
Season 1	1.173V (DOD (max.) 60%	1.212V * 60%) +
Season 2	1.156V (DOD (max) 60%	1.170V 60%) +
Season 3	1.218V (DOD (max) 43%	1.142V 60%)
Season 4	1.254V (DOD (max) 30%	1.170 60%) **
Season 5	1.243 (DOD (max) 25%	1.183 60%)

* The COMSAT battery had completed 4 12-hr. (NTS-2) orbit eclipse seasons prior to the start of this test sequence.

+ Daily charge/discharge cycling undertaken between seasons 1-2 and 2-3; assessment of electric propulsion power demand compatibility.

** Zero volt reconditioning undertaken between seasons 4-5.

operational data outlined here. The ultimate cell performance capabilities and fabrication technology are not yet fully optimized however. Further developmental work will be continued, in order to meet the more demanding requirements of future generations of spacecraft. Topics likely to be addressed are; better thermal control of the cell stack; further optimization of component performance (in particular the positive (Ni) electrode and the separator); and the full development of 50-60 Ah cells.

6.3 Launch Vehicles

Satellite system planners, particularly those who have been associated with successive generations of spacecraft, find the present launch environment quite on enigma. On one side, we possibly have more choices than ever before and are at the beginning of the era of "cheap space freighter service" . On the other hand, the plethora of uncertainties which presently characterise the various programs are of such a magnitude that satellite system designers are finding it extremely difficult to commit to any particular bus approach for the coming decade. However, there is every reason to be optimistic about the inherent strength of the aerospace community to lift the clouds and soon provide the promised family of launch vehicles and systems.

The principal candidate launchers for the future generations of INTELSAT spacecraft, are the U.S. STS (Shuttle) and the French ARIANE. With its 1700 kg initial geosynchronous transfer orbit payload capability, ARIANE, whose launch and ascent sequence is similar to that of existing launchers (Delta, Atlas-Centaur), can meet the requirements of future spacecraft. A substantial difference is introduced by the shuttle, for launch and ascent sequence as well as payload weight and volume constraints. The Shuttle can place a payload with a cylindrical envelop of 4.5m diameter and 18m length and with weight of 27000 kg in low earth orbit. This leaves ample room (and therefore many options) to the choice of a stage vehicle for transferring the spacecraft from the Shuttle orbit to its geosynchronous orbit station. (33)

Options presently being considered include; traditional satellite design, integral with an apogee kick motor (AKM) and separate perigee stage; transfer (perigee/apogee) stage with separate satellite, and integral satellite/transfer stage. Within each one of these configuration, alternative trade-offs are available with the choice of solid or liquid propulsion systems. While the IUS could be a candidate for the second option, but alternative simpler, more cost-effective approaches are being investigated.

While the choice of solid motors for the transfer vehicle leads to the classical Hohmann (elliptical) transfer, intriguing new problems arise with the choice of liquid propellants and motors of lesser thrust. As the burn time required for the delivery of a given perigee and apogee total impulse varies inversely proportional to the corresponding available thrust, the impulse approximation and therefore a Hohmann transfer approach can still be implemented with liquid motors provided that the perigee/apogee burns (at constant attitude) are broken into a number of pulses which progressively raise the respective apogee/perigee. This is particularly true for the perigee burn where the true anomaly varies much more rapidly than at apogee. A drawback of the multi-pulse approach is the resulting extended time of the spacecraft in transfer orbit with its impact on spacecraft power and thermal system requirements. Another drawback is that, because the time-related practical limitation on the number of pulses, eafficiency degradation in each burn with respect to the impulsive approximation must be tolerated.

The alternative of low-thrust, continuous burn at non-constant attitude (perhaps along the gravity turn) is a way of expediting the transfer and maximizing the efficiency of the stage, but requires a guidance package. These approaches are actively being considered and are part of current INTELSAT R&D activities.

6.4 The Attitude and Orbit Control Subsystems

In the area of attitude and orbit control, advances continue to be made both at subsystem and component levels. From the earlier spin-stabilized configurations, the Attitude Control Subsystem (ACS) of the INTELSAT series has evolved into the bias momentum body stabilized configuration of INTELSAT V and other spacecraft.

To satisfy the requirements of high reliability over a life span of 7 - 10 years, multiwheel configurations have been studied, and a skewed, four-wheel ACS engineering model has been produced and tested on an air bearing facility (34). To meet higher pointing accuracy requirements, an integrated 3-axis attitude sensing system engineering model has also been developed and tested on an air bearing table. (35). The system uses one or two rate integrating gyros, updated by earth and sun sensors, and Kalmann filtering for an accurate estimate of the attitude errors. In the near future, multisensor arrangements (optical as well as inertial) with integrated microprocessing will be evaluated, for a reliable, fault-detective, accurate sensor system.

The rapid size increase in appendages such as solar arrays and antennas is motivating substantial work in the area of flexible spacecraft control. The constant demand for increasing spacecraft power will require larger solar arrays. This fact, coupled with improvements in the structural materials and in the power/weight ratio of advanced solar generators will result in structural flexibilities for which the lowest modal frequencies may no longer be immune from ACS interaction and self-excitation. Similar considerations apply to larger antennas and their support structures. In the expectation of potentially dangerous ACS-flexible spacecraft interactions, techniques are being studied for the design of improved control configurations employing distributed sensing and perhaps multiple actuators and judicious on board processing (36).

At the component level, significant advancement has been achieved in the area of high-speed momentum wheels. The elimination of mechanical friction by means of magnetic suspension and the development of high strength rotors fabricated with beryllium or composite materials has made possible the implementation of reliable, light weight momentum wheels with speed up to 40000 rpm. Two different magnetic bearing concepts have been developed, one radially passive and axially active, the other fully active (Fig. 11).

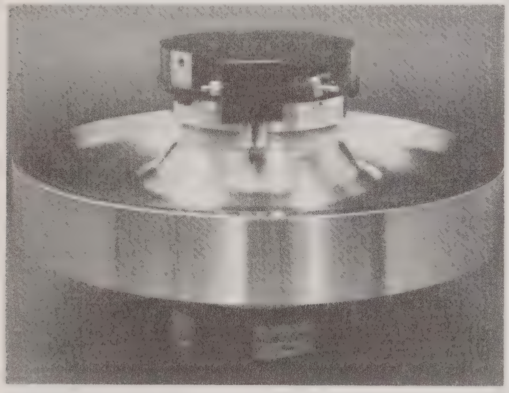

FIGURE 11. MOMENTUM WHEEL

Advanced work in the area of spacecraft control will address the possible application of high speed momentum wheels both for energy storage (electro-mechanical battery) and for attitude control. A wheel energy storage system is presently being investigated under contract. The contract will address both the power management aspects and the ACS/dynamics interaction of such a system, and will produce an engineering model of a component wheel capable of storing up to 0.5 KWh with a target energy density of 35 Wh/kg.

Orbit control requirements for longer spacecraft life will be alleviated by higher efficiency thrusters such as improved electro-thermal hydrazine thrusters (ETT) or electric propulsion. Both types of thrusters have been the object of extensive experimental work, although problems associated with the thermal control and the clogging of low thrust ETT's need further investigation. Improvement of the ETT's specific impulse by approximately 50% over that of catalytic thrusters will permit a saving of approximately 30% of the propellant weight, which for a spacecraft of 2000 kg and 10 year of life , means a saving of approximately 125 kg. Much larger savings will be possible using electric thrusters for which the specific impulse is about an order of magnitude larger. Studies are also being conducted for the assessment of the usage of bipropellant systems, possibly both for orbit attainment and control.

6.5 Space Platforms (37-39)

The expected availability during the 80's of economical launch of significantly large payloads by STS has motivated several studies towards large space platforms. While the definition of what is"large" is obviously a variable with time, the term "platform" has come to connote a geostationary structure with multiple ownership (or users) and with a capability of progressive addition and/or replacement of parts of the payloads.

From purely technological point of view, such platforms are attractive if they lead to reduction in the cost of, say, unit transponder and, preferably, also increase the efficiency of the utilization of the orbital arc. While applying the first criterion, considerable caution needs to be exercised towards comparing costs at comparable points of time and equivalent technological maturity for the two options. Under the criterion of orbital arc efficiency, the comparison is between a large multi-frequency platform against a cluster of colocated satellites (40). The platform concepts obviously suffer from the lack of flexibility of individual satellites but could end up being more efficient frequency-wise, if efficient interconnectivity is provided between a number of users. Obviously, the trade-offs would evolve in the next few years and would be in turn heavily influenced by the evolution of STS and the associated propulsion systems required to reach the geostationary orbit.

7.0 Conclusions

Satellite communication, in less than two decades, has more than matched the exacting technical as well as reliability challenges from the global communication world. Such a success record could lead one to relegate the satellite technology to a "stable" category and concentrate instead on reaping the benefits of the longterm and massive investments in technology by ordering "more of the same". However, as this brief survey has attempted to project, the technology is far from stable and the coming decade should see still bigger advances, though none of them will seem to be as spectacular as the SYNCOM which realized Arthur Clarke's dream.

One notable advance could be the Intersatellite Links. The technology development programs are well underway and should provide the building blocks in less than 5 years. Whether at the end of that period, ISL's would be in commercial use is a complex function of the traffic growth, investments in ground segments and the launch environment.

Surprisingly, a very high degree of success in launch vehicles could push ISL's a bit further away by improving the viability of space platforms! One aspect of ISL's which does require a serious look is their capability to interconnect different networks (40). This important role justifies development of international standards for the principal ISL parameters.

There is probably no longer any uncertainty about digital technology ultimately becoming the technology for the whole communication world. In the satellite communication world, at least in the author's view, it is already "overdue". Since a major change in the space segment technology occurs only at widely spaced intervals synchronised with the procurement of next generation spacecraft, the next major generation due in mid-80's is positively the last opportunity to go digital in a big way if we do not want to lose a major portion of the market to competitive media. In specific areas, TDMA and SS-TDMA technology are ready for system applications and could be followed closely on their heels by baseband processing.

If there is one subsystem which is going through revolutionary (and visible!) changes in the space segment, it is the spacecraft antenna subsystem. The technology has come a long way from the stage when a spacecraft antenna was a simple interface with space. Today's and more so tomorrow's satellites are complex farms of antennas and feeds and account for a very large fraction of satellite mass, volume and investment (24). And this is even before we have reached the stage of exploiting to any reasonable degree, the significant benefits from reconfigurability and the whole new field of active antennas!

In the transponder technology, possibly the most significant change in the near term should be the replacement of the TWTA's by solid state FET amplifiers. In fact the transponders of the next generation could well be all FET affairs.(25). The next step could possibly be greater utilization of monolithic technology in various parts of the transponder. The resultant benefits, in terms of lower mass, better reliability and higher linearity could be significant.

The payloads of future satellite generations will be far more complex not only in terms of transponders but also due to introduction of RF/IF dynamic switching as well as storage and processing of baseband. This significant increase in the parts count, if not adequately planned for, could lead to reduction in the reliability below acceptable limits. It is interesting to recall that the parts count in every successive INTELSAT spacecraft has increased by a factor of three (41). With the added complexity, this multiplier factor could be even higher for the next generation. In order to still meet the exacting reliability requirements, some of the measures under consideration include; significantly higher level of integration; development of monolithic low power analog subsystems such as microwave receivers, and reduction of control hardware through distributed processing techniques, micro processors.

The spacecraft technology encompasses a wide range of disciplines, some of which have been touched upon in Para. 6.0. While advances in solar power generation and storage will provide the necessary capability to match the future requirements, the one big challenge is the adjustment to the rapidly evolving launch capabilities, not excluding their current uncertainties.

Finally, the diverse developments in practically all aspects of spacecraft design definitely promise an exciting period of technological developments across the board, not counting the sleepless nights many program managers will go through grappling simultaneously with so many new techniques!

8.0 Acknowledgement

The work reported here emanates largely from the efforts of a worldwide community of engineers and scientists associated in one way or another with successive INTELSAT R&D Programs. I wish to particularly acknowledge the contributions of my colleagues at INTELSAT as well as several engineers and scientists at COMSAT Labs.

References

(1) Bargellini, P.L. and Edelson, B.I. "Progress and Trends in Commercial Satellite Communications - Survey" Proc. International Astronautical Congress, 1976
(2) Davis,R.C. et. al. "Future Trends in Communication Satellite System" Acta Astronautica Vol. 5, No. 3-4, March-April 1978
(3) Podraczky, E. & Morgan, W.L. "Technology Trends in the INTELSAT System" National Electronics Conference Vol. 28 pp. 202-205, Oct. 73
(4) Granger, R.L. & N.K.M. Chitre, "Post-INTELSAT V Systems Planning" WESCON, San Francisco Sept. 79
(5) Barry, T.D. et. al. "10000 Mbits Intersatellite Laser Comm. System Technology" IEEE Trans. Communication, April 1976 pp. 470-478
(6) Ross, M. et. al. "Multi Gigabit Laser Communications for Satellite Cross Links" Fourth Int'l Conference on Digital Satellite Communications Montreal, Oct. 78
(7) Welti, G.R. "Intersatellite Link for Multiple Access Telephone" EASCON '78
(8) Soleman, F.J. et.al. "The Ka-Band Systems of the Lincoln Experimental Satellites LES-8 and LES-9" AIAA 7th Comm. Sat. Systems Conference April '78
(9) Holmes W.G., "The Tracking & Data Relay Sat. System" ibid.
(10) Gardner "A System Comparison of SS-TDMA and FM-FDMA for Multi-beam Satellites" 2nd IC DSC, France Nov. 72
(11) Dill et.al. "Application of SS-TDMA in a Channellized Satellite" ICC 76
(12) Assal, F., Rozec, X. "Fast. Fully Redundant 4 GHz, 8x8 Microwave Switch Matrix for Communication Satellites" Ninth European Microwave Conference, Sept. 79
(13) Deal, J. "A Satellite Switched/Time-Division Multiple Access Acquisition and Synchronization Unit for INTELSAT Application".
(14) Campanella, S.J. et.al. "The INTELSAT TDMA Field Trial" COMSAT Technical Review, Fall 1979, Volume 9, No. 2
(15) Ramasashtry J. et.al. "Western Union's Satellite-Switched TDMA Advanced Westar System" 7th AIAA Sat. System Conference April 78
(16) Campanella, S.J., Assal, F., Berman, A. "On-Board Regenerative Repeaters" ICC '77

(17) Fiocica, F. "Use of Regenerative Repeaters in Digital Communication Satellites" 7th AIAA Sat. System Conference April 78

(18) Kreutel, R.W., et.al. "Antenna Technology for Frequency Reuse Satellite Communications": Proc. IEEE Vol. 65, No. 3, Mar. 77

(19) Foldes, P. et.al. "Multiple Beam Satellite Antennas" 7th AIAA Sat. Systems Conference April 78

(20) Foldes, P. and Berkowitz, M. "Reconfigurable Multibeam Antennas for Satellite Communication" ITU World Telecom Forum Sept. 79

(21) Foldes, P. "Control Aspects of Multibeam or Multielement Spacecraft Antennas" International Telemetry Conference, Nov.79

(22) Difonzo, E., et.al. "A Multiple Shaped Beam Reconfigurable Sat. Antenna" IEEE AP-5 Symposium June 1979

(23) Reudink, D.O., Yeh, U.S. "Rapid Scan Area-Coverage Comm. Satellite" AIAA 7th Comm. Sat. Conf. April '78

(24) English, W.J. "Improving Future Communications Satellite Antenna Designs" 8th AIAA Comm. Satellite Systems Conf. April 1980

(25) Cuccia C.L. & Ho. P. "The Impact of the FET on the Satellite Transponder - A Technology Prospective" 7TH AIAA April 78

(26) Ho, P.T. et.al. "Solid State Amplifiers in Communication Satellites" ibid.

(27) Cuccia C.L. et. al. "TWTA vs. FETA in Comm. Satellite Transponders" INTELCOM 79

(28) Drago, F., et. al. "C-Band FET Power Amplifier for TWTA Replacement" 1AF 79 (Munich) Sept. 79

(29) Markle, R.E. "The ARGA Single Sideband Long-hand Radio System" ICC June 77

(30) Proc. Goddard Space Flight Center Battery Workshops 1977, 1978

(31) Patterson, R.E., Luft, W., Dunlop, J.D. "Development of Spacecraft Power Systems Using NiH_2 Battery Cells" 6th AIAA Comm. Sat. Systems Conference, 1976

(32) Dunlop, J.D. and Stockel, J. F., COMSAT Tech. Review Vol. 7, P. 639 (1977)

(33) Spencer, T.M., Glickman, R., Porcelli, G. "Changing Inclination for Shuttle Payloads" Journal of Guidance and Control, Aug. 79

(34) Ramos A. "Air Bearing Testing of a Skewed Reaction Wheel System for Attitude Control" COMSAT Tech. Review Vol. 9 No. 1 1979

(35) Anstett P, Govin B, "Study of an Integrated Attitude Sensing System "8th IFAC Symposium on Attitude Control in Space, Oxford, England" July 1979

(36) Harris, R.S. Todman, D.C. "Three Axis Control of Flexible Spacecraft with Large Solar Array" ESA Symposium on Dynamic and Control of Nou. Rigid Space Vehicles, Frascati, Italy, May 79

(37) Edelson B.I. and Morgan, W. "Orbital Antenna Farms" Astro Aero (1977)

(38) Staminger R. & Fordyce, S. "The Use of Geostationary Platform for Future U.S. Domestic Satellite Communications" ICC '79

(39) Pelton, J.N. 'Is There a Space Platform in INTELSAT's Future? Facing the Institutional Challenges of the 1980's and 1990's" 8th AIAA April 1980

(40) Visher, P.S. "Satellite Clusters" Satellite Communications Sept. 79

(41) Strauss, R. & Owens, J.R. "Design Factors Affecting Communications Satellite Lifetime" 1AF XXVIII Congress Oct. 77

80-0549

OPERATIONAL EXPERIENCE WITH ANIK A

P. N. Wadham*
Telesat Canada
Ottawa, Canada

Abstract

After more than seven years in orbit, the first two Anik A 6/4 GHz communications satellites continue to be operational. They have provided good communications capability. The spacecraft bus has proven to be reliable and simple to operate with a minimum of problems. All subsystems generally continue to operate to specification, including the telemetry, command, power, antenna despin and reaction control subsystems. Fuel usage has been well within expectations. Maneuvres have been uncomplicated requiring a minimum of operations manpower. Stationkeeping and attitude control are held consistently to tight limits. However, wear-out mechanisms have marred the performance of the payload and of the batteries. Many of the output TWT's have suffered degradations in gain, and the batteries have lost more than half their original capacity. A third satellite, in orbit for five years, is also showing similar gain degradations but, due to a different storage regime, its batteries are showing excellent performance. A backup communications receiver of the first satellite has failed. Apart from the TWT problems, the overall picture has been one of success, with excellent availability and customer satisfaction.

Introduction

On November 9, 1972, the Western World's first domestic communications satellite, Anik A, was launched from Cape Canaveral aboard a Delta vehicle, to be followed by a second on April 20, 1973. The beginning of life performance was discussed in a paper presented to the AIAA in April 1974.[1] Now that a further six years have passed, the first two spacecraft have been in orbit longer than their seven year design life. A third satellite of the same Hughes HS333 design[2] has been added and even that is now five years old.

Operationally, this class of small spinning satellite has been as simple to operate as one could conceive. The 12 channel satellites have provided good 6/4 GHz communications capability and performance during their operational life and all have aged gracefully. Although this paper addresses the more interesting degradations in certain components, the basic design has been highly successful. It is unfortunate that rising launch costs have tended to make the limited capacity of small satellites such as these commercially uncompetitive, the trend being towards larger, more complex busses with a higher capacity.

This paper provides an overview of the performance of the bus and payload as the satellites approach their end of life.

Bus Performance

Telemetry and Command

The telemetry and command systems have performed reliably with no catastrophic failures. No problems have been encountered with the execution of commands, and there has been no significant change in the command carrier threshold level, except when caused by the F-2 "notch", discussed below.

On December 9, 1975, there was a partial failure of the #1 telemetry encoder of the F-2 satellite, in that one of the commutator input gates appeared to have shorted. The encoder is still operable, but encoder #2 has been in use since the event. It is possible that the failure was induced by a discharge to the wiring harness, caused by spacecraft charging phenomena. However, it should be noted that on the day in question the magnetosphere was extremely quiet.

Another phenomenon, thought to be related to spacecraft charging effects, has been the spontaneous switching of encoder modes, with no obvious cause. Each of the three satellites has suffered at least one such event. These have had no long-term operational impact, and have only occurred when the magnetosphere was relatively quiet. The events are summarized in Table 1.

TABLE 1
Spurious Encoder Mode Switchovers

Date	Time (GMT)	Satellite/ Encoder	From	To
15 July 1974	03:38	F2/2	Sensor	PAM
28 July 1974	21:38	F2/1	PAM	Ranging
		F2/2	Sensor	PAM
24 July 1977	01:58	F3/1	PAM	Sensor
4 Oct 1978	19:15	F1/2	Sensor	Ranging

The accuracy of the PAM telemetry system has been excellent, far surpassing its specified end-of-life limits of ±5%. The estimated accuracy remains generally better than ±1%, based on comparisons between satellites and in particular from the telemetered bus voltage, which has read consistently between 30.0 and 30.6 volts on all three satellites. This also indicates stable regulation of the bus. The only suspect channel, apart from those affected by the failure noted above, is one battery temperature sensor on F-3, which reads lower than the expected value by about 5^{0}F.

In the earlier paper[1] it was noted that there were irregular 'bumps' in the sensor analog pulse train, in the vicinity of the sun sensor pulse. These were then thought to be due to sun

---

*Supervisor, Satellite Engineering

Copyright © American Institute of Aeronautics and Astronautics, Inc., 1980. All rights reserved.

reflections in the earth sensor telescope barrel. It has since been ascertained that these are caused by the cyclic charging and discharging of the ungrounded barrel as the sensor goes from shadow into sunlight and back into shadow during each revolution of the satellite. The transient in barrel potential capacitively couples into the sensitive earth sensor electronics to produce a transient in the output. The validity of this theory was demonstrated on F-3, on which the barrel was grounded through a resistor, eliminating the transients. The F-1 and F-3 sensor trains are shown by comparison in Figure 1. The Master Index Pulse (MIP) is used to indicate the angular position of the antenna relative to the Earth.

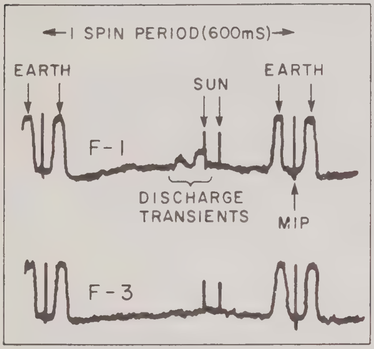

Figure 1: Sensor Pulse Trains

Antenna Tracking System

The antenna tracking system, or despin system employs a monopulse-type of RF sensor in the antenna receive pattern, which locks onto an uplink pilot signal. Loss of the pilot will cause loss of antenna lock or spin-up.

During the lifetime of the Anik A satellites, the system has provided satisfactory performance apart from some losses of lock on the F-2 satellite. One of these may have been associated with the "notch" phenomenon, referred to below, when the "notch" was coincident with the pilot frequency. From November 1, 1979 onwards, an intermittent fault in the despin control loop of the satellite resulted in a number of antenna spin-ups and this was corrected by switching to the redundant control electronics unit. When spin-ups have occurred, they have had no impact on the life or reliability of the satellite.

Telesat's confidence in this type of RF tracking system is demonstrated by their acceptance of similar systems on their future generation Anik C and D spacecrafts, currently being manufactured by Hughes Aircraft and by SPAR Aerospace respectively.

The performance of the bearings in the Motor Bearing Assembly has been excellent and over the lifetime of the satellites the motor current has tended to decrease significantly indicating a reduction in friction levels.

Reaction Control System

The reaction control system, comprising two separate fuel systems, each supplying an axial and a canted thruster in the aft (south) end of the satellite, generally has performed well and predictably, with a more than adequate fuel allocation. Fuel expenditures were within expectations. The fuel loading was sufficient to provide for 8½ years operation of F-1, 9 years on F-2 and 9¼ years on F-3, partly due to very low launch vehicle dispersions.

The only significant anomaly observed was with one canted jet on the F-1 satellite, normally used in a pulse mode for E-W stationkeeping. On one occasion in 1978, almost 2 years after its previous usage, it underperformed by about 50% relative to its initial calibration, whereas a 17% underperformance had been anticipated. The poor performance was thought to be due to a leakage of about 1 cc of fuel from the thruster valve, which is of a dual seat design. It was postulated that the fuel may have leaked from the space between the two seats during the dormant period.

The above theory was confirmed by an experiment, in which the pulsed operation of the jet in question was preceded, by about one hour, by a short one-spin continuous burn. The pulsed maneuvre performance was within the expected limits, demonstrating that the space between the valve seats had been filled with fuel during the earlier burn.

Because of the generally good performance, a stationkeeping limit of ±0.1% was easily achieved, and Telesat normally maintains its traffic carrying satellites to within ±0.05°, in both inclination and longitude.[3] Satellite attitude is controlled to within 0.15° of orbit normal. No nutation has been observed due to maneuvres, nor any effect on antenna pointing.

Thermal Control

In common with most dual-spin spacecraft, thermal management of Anik A has been quite straightforward with no active controls. TWTA's are the prime source of heat during sun eclipse. It has been found possible to survive with only four TWTA's on during these periods, provided there were eight TWTA's on prior to and following the eclipse.

The batteries generally remained above 35°F during eclipse, except for one on F-3. In this case, the transducer is suspected of reading low, as it is inconsistent with the other temperatures. The F-3 batteries in trickle charge storage sit at about 70°F. In general, the electronics shelf and despin motor assembly operate in a fairly benign thermal environment in the region of 60-70°F except for a cold wave after eclipse, when temperatures dip to the 35-40°F region.

Power System

The power system, apart from the batteries, has performed well and without failure, with adequate output from the solar array to power eleven of the twelve TWTA's. As of October 1979, the normalized array output of F-1 was determined to be greater than 290 watts, compared with a predicted value of 285 watts and a beginning of life value of 320 watts, at the 30V bus voltage. F-3 has shown performance similar to that of F-1 and F-2. The bus limiters have excellent long-term stability, maintaining the bus voltage at 30.3V ± 0.3V on all three satellites.

The battery charging system has been adequate. The simple approach of using additional array strings has operated well. On the F-3 satellite, the value of the series resistance used for slow charge was increased by 50% to provide a trickle charge rate of C/36 of nameplate rating (or C/45 of actual).

Battery Performance

The Anik A satellite uses two 28-cell battery packs, each with a nameplate rating of 7 AH. The measured capacity is about 9 AH. The nominal discharge current is 3.65A per battery, resulting in a maximum depth of discharge of about 47% of actual capacity.

Apart from the time-related degradation effects, the battery systems have performed reliably and without catastrophic failure. The end of discharge voltages for the first ten eclipse seasons are shown in Figure 2. Beyond that the loads on F-1 and F-2 were reduced. The F-3 performance has been excellent, but the F-1 and F-2 batteries suffered from an early decision to store them in an open circuit mode.

Before F-3 was launched, results from Telesat's battery test facility indicated that cells from the F-1 and F-2 lots operated under simulated in-orbit conditions were showing excessive cadmium migration and other problems. Attempts to recondition the flight batteries to 1.0 volt/cell using the single reconditioning resistor were quite successful in improving battery voltages in eclipse as indicated in Figure 2, but tended to be marred by indications of cell reversals. This has resulted in very poor reconditioning and consequent low battery voltages on F-1 and F-2.

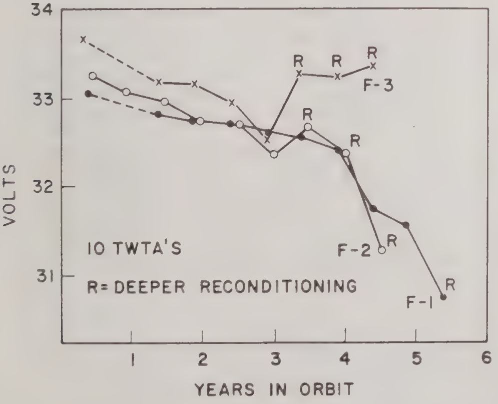

Figure 2: End of Discharge Voltages

By the Fall of 1979, it was necessary to reduce the F-2 spacecraft load in eclipse to one half by turning off TWTA's. Even so, one cell went into reversal for about three minutes at the end of one discharge as shown in Figure 3(a), although this was not consistent. In fact, on most subsequent days, the cell did not reverse as indicated in Figure 3(b). This may have been in part due to a longer recharging period, increasing the charge return from about 214% to more than 240%.

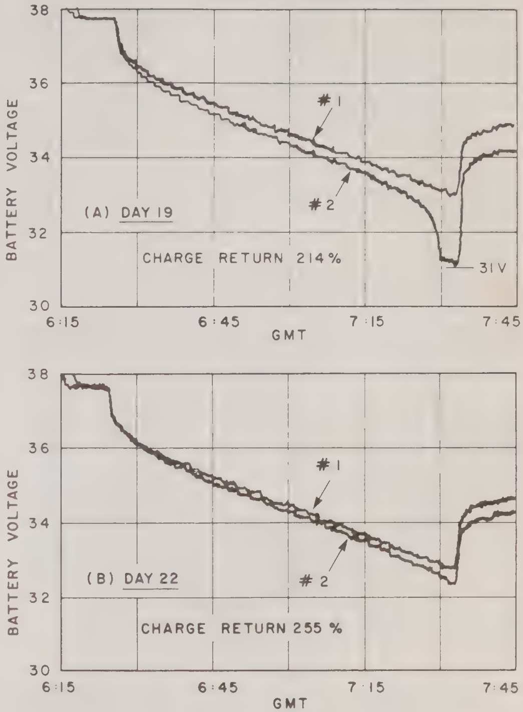

Figure 3: F-2 Battery Performance, Fall 1979

On the F-1 and F-2 batteries generally, there has been a tendency late in life for the voltage on charge to limit at a reduced voltage rather than to peak, suggesting a charge return problem.

F-1 has behaved much better in eclipse than F-2, despite the indications early in life that a cell on the #1 battery had developed an internal partial short. This short disappeared for long periods of time, and throughout the fourteenth season the F-1 batteries remained able to support 8 out of 12 channels.

The F-3 batteries have been stored in a trickle-charged mode. They were also reconditioned to 1.0 volt/cell commencing prior to the seventh eclipse season and this has had the effect of improving their voltage performance even further. It is reasonably certain that the performance will be more than adequate to support the number of useful TWTA's remaining to the end of life of the satellite. Table 2 shows the performance of all batteries as of the middle of the Fall 1979 eclipse season.

TABLE 2
Battery Performance in Eclipse, Fall 1979, Day 24

Serial	Season #	# of TWTA's	Batt. #	EOC Volts	EOC Temp.	Chg. Rtn. %	EOD Volts	EOD Temp.	DOD* %
F-1	14	8	1	40.1	70	184	30.8	37	44.9
			2	39.4	69	170	31.0	40	44.6
F-2	13	4	1	38.6	77	260	32.5	37	28.1
			2	38.4	75	250	32.2	37	28.5
F-3	9	10	1	40.1	68	115	33.1	52	56.5
			2	40.9	60	112	33.3	41	56.1

*Depth-of-discharge, referred to nameplate rating (7 AH).
EOC = End-of-charge. EOD = End-of-discharge. Temps. in ^{o}F

NOTE: Normal charge return on F-3 is about 105%. Prior to eclipse 24, batteries were "peaked up" for 15 minutes. No change in EOD voltages was observed.

Transponder Performance

Receivers

The F-2 and F-3 receivers, which employ tunnel diode amplifiers (TDA's) before and after the mixer, and a driver TWTA output stage, have operated well with stable gain. Their performance has been found to be generally consistent with that anticipated from pre-launch data.

The F-1 receivers suffered a number of temporary outages in the form of moderate to severe gain degradations. Both receivers suffered similar effects, although Receiver #1 showed a much greater attenuation, of the order of 25 dB, compared with about 10 dB for Receiver #2. Figure 4 shows the timing of these fades relative to satellite local midnight, and it will be seen that they mostly fall in the midnight-to-dawn period. The events often occurred during periods of high magnetospheric activity, but this was not always the case. Ultimately, Receiver #1 acquired an irreversible gain loss of about 26 dB.

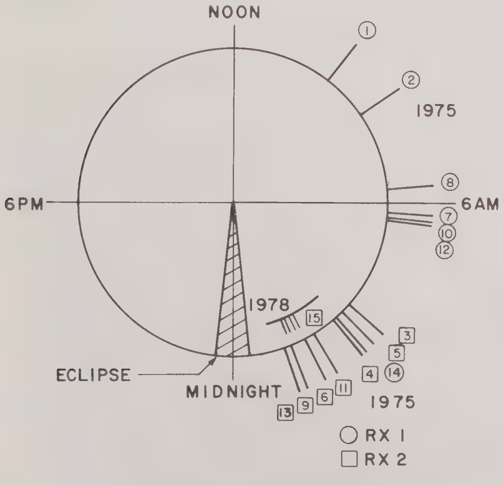

Figure 4: F-1 Receiver Fades vs Satellite Local Time

The spontaneous fades did not occur at the point of minimum receiver temperature resulting from the eclipse, but some time later during thermal recovery. Hence although the effects may have been thermally induced, there does not appear to be a very direct relationship. An experiment in October 1976 showed that fades in Receiver #1 could be induced by lowering the receiver temperature. A direct reason for the fades was never discovered, although many theories were generated, including, of course, those of spacecraft charging phenomena. However, the magnetospheric activity may have been a misleading coincidence.

The F-2 Notch

Early in life, the F-2 satellite was found to have an attenuation notch in its communications passband, some 3-4 dB deep and about 40 MHz wide. The centre frequency was variable, depending on the traffic loading. It was determined to be caused by spring fingers used in the rotary coupler which were not making the correct electrical contact. The problem was circumvented on F-3 by a change in design and has not been apparent on F-1. At times when it coincided with the despin pilot frequency, it tended to create interference problems. Otherwise, it has been more of a nuisance than a real operational hazard.

Performance of TWTA's

The Anik A series employs Hughes' travelling wave tube amplifiers (TWTA's) type 276HA. Over the first four years, these tubes showed stable gain and EIRP, based on frequent measurements. Saturating flux density (SFD) is measured on a regular basis, usually five measurements a week on each unused channel. EIRP is measured about once a month. As a result, Telesat probably has collected more data on individual TWTA in-orbit RF performance than any other user, over many years commencing in the Fall of 1973. It has been found possible to obtain a repeatability in SFD, channel to channel and day to day of the order of ±0.25 dB or better, although occasionally there have been systematic drifts of 1 dB or more especially under adverse weather conditions.

When F-1 was withdrawn from prime service, in November 1975, Channel 3 was found to be low in gain by some 3 dB. Later, early in 1976, Channel 7 of F-2 began to show signs of a declining gain, dropping by about 6 dB by the end of the year. Channels 11 of both F-1 and F-2 showed gain reductions by early 1977, but the coincidence was treated with some skepticism and the measurement system was suspected. However, a measurement of Channel 11 of F-3 confirmed the accuracy of the system. As time progressed, a number of other channels began to show signs of degradation, and by the end of 1977, a total of ten channels had degraded in gain, including Channel 6 of F-3. By October 1979, fifteen channels had failed.

For convenience, an SFD of -77 dBW/m^2 was defined as the failure point, being some 5-6 dB below the beginning-of-life value. Some typical plots of SFD versus time are shown in Figure 5 and the operating time to failure is presented in histogram of Figure 6.

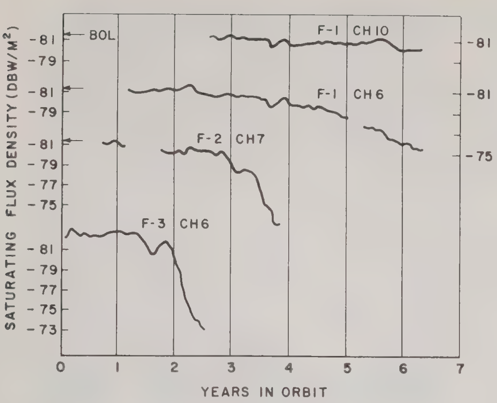

Figure 5: Gain vs. Time (Typical)

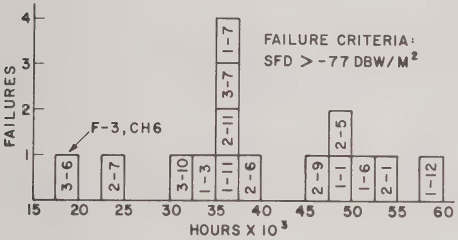

Figure 6: Histogram of Time-to-Failure of TWTA's

Although intense investigations had not, at the time of writing, revealed the precise cause of the foreshortened life of the TWTA's, the wear-out mechanism quite clearly corresponds to a loss of cathode emission. A "cold" turn-on test, in which the filament and high voltage supplies are applied to the TWTA simultaneously, showed the gain and bus current characteristics of Figure 7. This is typical of a TWTA with a cathode having low emission, being in a temperature-limited condition rather than being space-charge limited.

Another indicator of low cathode emission is the "hot" turn-on characteristic, where the high voltage is applied some 4-5 minutes after filament turn-on, allowing time for the cathode to reach its maximum temperature. On a new tube the gain and the bus current immediately reach a stable value. On degraded tubes, the gain and the bus current both show initial high values which degrade after a period of a few minutes. The reason for this behaviour is postulated as being due to a cooling of the cathode as electrons are drawn off. The bus current drawn by a failed TWTA is typically only 60% of that for a good tube.

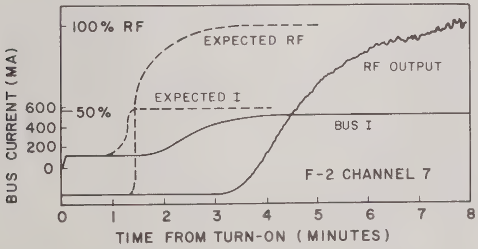

Figure 7: TWTA "Cold" Turn-on

On F-2, it became necessary to turn off a number of TWTA's in the eclipse seasons of 1979 on a daily basis, to reduce battery loading. The result was to cause Channels 7 and 9 to fail totally, and to cause some moderately good channels to degrade severely in gain.

Service Availability

Over the life of these satellites, service availability has been excellent. After 1973, the frequency of antenna spin-ups, due to earth station problems, became so low as to be almost a non-problem. The only time when a satellite failure caused a loss of service was during the F-1 receiver fades. The service availability is summarized in Table 3.

TABLE 3
Service Availability - Heavy Route System

Year	Satellite Outages*	Earth Station Outages	Availability %
1973	106.5 min	78.5 min	99.964
1974	0	3.1 min	99.999
1975	139.0 min	20.7 min	99.970
1976	15.8 min	0	99.997
1977	20.0 min	3.7 min	99.995
1978	0	72.4 min	99.986

*Includes earth-station induced spin-ups.

Acknowledgements

The author wishes to express his thanks to the many whose kind help and advise have often guided him and made this paper possible. In particular, he would like to thank Derek Thorpe of Telesat, Fred Weber and Jim Dunlop of COMSAT and Bob Eiermann of Hughes, not to forget Earl Martin and his crew who have maintained constant and alert vigil over the satellites.

References

(1) P.N. Wadham. Operational Experience with the Canadian Domestic Satellites, AIAA Fifth Communications Satellite Systems Conference, April 1974, paper no. 74-453.

(2) L. Harrison et al, Canadian Domestic Satellite (Telesat), a General Description, IEEE International Conference on Communications, June 14, 1971.

(3) F. Kes et al, Performance of the Telesat Real-Time State Estimator, AIAA Eighth Communications Satellite Systems Conference, April 1980, paper no. 80-573.

80-0551

FACSIMILE TRANSMISSION UTILIZING TDMA SATELLITE SERVICE

William L. Dunn, Glen C. Jenkins

Dow Jones & Company, Inc.
The Wall Street Journal
P.O. Box 300
Princeton, New Jersey 08540

Abstract

In 1961, Dow Jones began printing The Wall Street Journal using high speed facsimile scanners and recorders. High cost of transporting our papers to the customer was the motivating force. In 1965 data compression techniques were applied to facsimile scanning and recording, reducing bandwidth requirements and lowering communications cost. Microwave circuit cost was mileage sensitive and long distances restricted our expansion and prompted our investigation of satellite technology.

Laboratory and on-line tests with COMSAT in 1973 demonstrated the viability of satellite transmission of compressed facsimile data. Two earth stations were constructed for our private use in 1975, replacing terrestrial circuits between our two east coast plants.

Designs are now complete for a network utilizing TDMA techniques which will demand assign voice/data information. By 1983, seventeen locations are expected to be interconnected through satellite and TDMA equipped earth stations.

Text

Dow Jones' motivations in using high speed data transmission channels and associated terminal hardware are twofold: better service to our subscribers and improved economics.

Historically, we have had to use technology prior to its general acceptance to achieve these two goals; in early 1962 we initiated a new concept in the United States in newspaper publication using high quality facsimile between a central and a remote printing plant. On the west coast, a new receiving plant was built at Riverside, California, 400 miles south of an existing plant in San Francisco. Our purpose was to provide improved service to our subscribers in southern California and parts of Arizona. The only umbilical between the two plants was a 3 MHz (megahertz) microwave communications channel. At each end was a Westrex high speed facsimile scanner or recorder. Full pages were scanned at San Francisco and the resultant analog data was transmitted to Riverside for recording on photographic film.

The communications channel was a video circuit leased from Pacific Telephone & Telegraph costing $180,000 annually. Although expensive, it was more economical than operating a full composition plant such as San Francisco.

For this concept to be economically expanded into other geographical areas needing improved delivery service, we had to reduce our communications costs. In 1965 we began investigating redundancy removal techniques, or more commonly called data compression. Our goal was to transmit a full page in 3.5 minutes on a 48 KHz (kilohertz) circuit. This would require a data reduction of about 20:1.

We initiated a study to determine if such data reduction was feasible. The study was positive and we funded the design and development of the prototype hardware. The hardware, built by Rapicom, Inc., formerly Dacom, Inc., in Sunnyvale, California, never achieved the study results, but was still very good -- a data reduction on an average of 13:1 resulting in a page transmission time of about 7 minutes. We had production hardware built and began using it in 1975. That hardware is still in operation in our east coast plants. Similar equipment is being used by other newspapers, both in the United States and other countries.

However, to achieve our desired throughput of 3.5 minutes per page, which was our original goal, required two 48 KHz channels. Though less costly than microwave, the two circuits, over a long distance, were expensive. For example, a 1200 mile circuit consisting of two 48 KHz channels between Chicopee, Massachusetts, our east coast transmission plant, and Orlando, Florida, a remote printing plant, cost $264,000, annually. We continued exploring further alternatives.

In 1973, we investigated digital transmission via satellite. Jointly, COMSAT and Dow Jones conducted a test at the COMSAT lab in Maryland transmitting and receiving digital data at a 50 Kb (kilobit) rate. The data was transmitted from our data compression fax system to a COMSAT digital communications (DICOM) terminal which relayed it to an Intelsat IV satellite over the Atlantic Ocean. The signal was received successfully on the fax recording equipment.

Next, Dow Jones and COMSAT jointly established two actual operating stations with an experimental license from the FCC (Federal Communications Commission). We installed 4.5 meter antennae at our Chicopee transmission site and our South Brunswick receive site near Princeton, New Jersey, a distance of about 200 miles. On July 26, 1974, we began a three month test transmitting through the COMSAT DICOM terminal at Chicopee directly to Intelsat IV and receiving at South Brunswick -- a satellite link of about 45,000 miles -- a terrestrial distance of 200 miles. The primary purposes of the extended test were to determine system reliability, operational requirements, and economic feasibility. Figure 1 shows the 4.5 meter dish used during the test.

Copyright, 1980 by William L. Dunn and Glen C. Jenkins

Released to AIAA to publish in all forms.

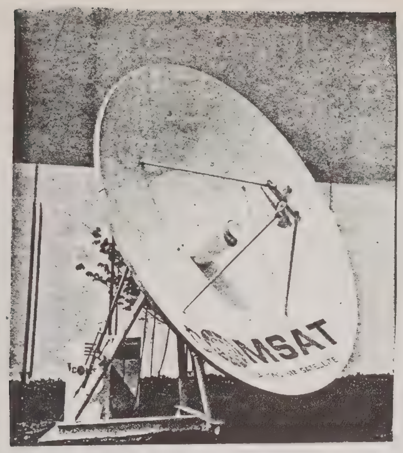

FIGURE 1 4.5 Meter Test Antenna

These tests proved to our satisfaction that we could transmit and receive "door-to-door" without terrestrial interconnections and could count on extremely reliable and essentially error free transmission.

Reliability was very important, but equally important was the necessity to have virtually no errors in transmission since the compressed data was highly coded.

The facsimile equipment compression was designed to check for errors and retransmit blocks of data if an error occurred. On terrestrial circuits, this correction routine occurs often. Our plan was to transmit from one station to many stations in a broadcast manner. We felt the transmitting station would have difficulty controlling the reply channels of more than one receiving station, particularly if we were to increase our transmit data rate.

Our newspaper page contains about 270,000,000 (2.7×10^8) bits of information. The compressor digests this amount and transmits an average of 21,000,000 (2.1×10^7) bits. One retransmission in fifty pages was acceptable, however a system error rate of 1×10^{-9} or one error in one billion would be required. During our tests, we experienced fewer errors -- 1×10^{-10} or one error in ten billion.

In May, 1975, we contracted American Satellite Corporation to build a transmit only and receive only earth station which would transmit from Chicopee, Massachusetts to a new printing plant being built in Orlando, Florida. The two earth stations began operation five months later in September, 1975.

Our transmission data rate was 150 Kb/s and used a rate 3/4 forward error correction scheme. We split the channels into two 75 Kb/s data streams using multiplexer/demultiplexer equipment designed by Digital Communications Corporation (DCC). Operationally, we can transmit and receive either from two fax terminals simultaneously at 75 Kb/s or one fax terminal at 150 Kb/s. Two systems operating at 75 Kb/s provide better page throughput than one operating at 150 Kb/s, due mainly to the speed limitations of the rotating facsimile drum.

After a few months of successful operations, American Satellite Corporation manufactured and installed another receive only earth station at our South Brunswick printing plant. This earth station became operational in February, 1977. Both the South Brunswick and Orlando earth stations record the facsimile data simultaneously after operational synchronization over a voice circuit. Figure 2 illustrates the three station network and terrestrial distance between locations.

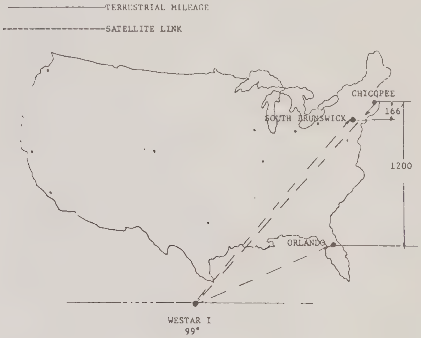

FIGURE 2 East Coast Network

With continuing experience in owning and operating earth stations, it became apparent that it was necessary for Dow Jones personnel to develop a broader experience than that gained by simply dealing with an outside vendor responsible for design and integration of the system. In 1977, Dow Jones personnel assumed this responsibility for the four earth stations currently in operation in the western United States. These stations link The Wall Street Journal printing plants at Palo Alto, California, the transmission point, to the receive stations in Riverside, California; Seattle, Washington; and Denver, Colorado. A typical receive station is shown in Figure 3; the west coast network is depicted in Figure 4.

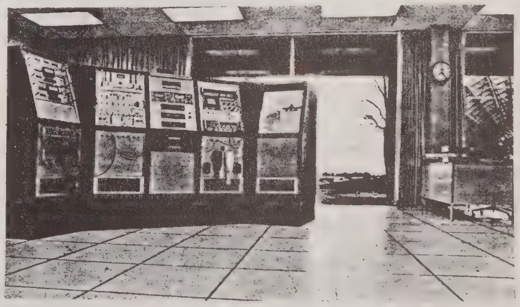

FIGURE 3 Typical Receive Station

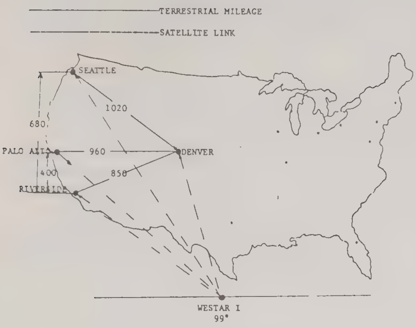

FIGURE 4   West Coast Network

While the earth stations were very similar to those being designed for the east coast, the operation is different. Our transmission data rate in this network is 600 Kb/s split into two 300 Kb channels; again, using a rate 3/4 forward error correction scheme. The higher bit rate was necessary because we were using a new facsimile compression system. We had determined with the relatively inexpensive cost of bandwidth associated with the satellite usage, the value of compression was not as great as ten years ago when we began using the Dacom equipment. We therefore asked Digital Communications Corporation to assist us in a co-development which resulted in a relatively inexpensive and simpler compression system. Although the new equipment was only about one-third as efficient as the Dacom equipment, its cost was much less. The incremental cost of the additional bandwidth required could not justify the investment in the more expensive data compression equipment. In addition, the new equipment was more compatible with a new facsimile system we are developing and will shortly be using.

We previously mentioned that the drum rotation speed of current facsimile systems was a limiting factor. We began a development program in August, 1974 to replace the traditional rotating drum facsimile equipment with a flatbed scanner/recorder that would use a rotating mirror to image a plate which could be speedily processed for offset printing. This equipment processes data at a rate of about six million bits per second and will scan, transmit, and record a full page of The Wall Street Journal in as little as 45 seconds for a page having 600 lines per inch resolution to a minute fifteen seconds (1:15) for a page having one thousand lines per inch resolution.

This prototype system was demonstrated at the American Newspaper Publishers Association (ANPA) convention in Las Vegas in 1976. In this demonstration, a 4.5 meter temporary earth station was erected in front of the convention center and received page one of The Wall Street Journal directly from a transmission from our Chicopee plant. The transmission was reproduced directly onto a printing plate. This new equipment coupled with our new data compression system will allow Dow Jones to transmit and receive a newspaper page having 800 lines per inch resolution in one minute.

While our seven current earth stations basically support this new facsimile transmission scheme, we felt it was necessary to improve the design of our future earth stations. Although we have been using satellite technology for less than four years, we are designing and building third generation equipment for our printing plants located in the midwestern part of the United States. We are currently building new printing plants in Naperville, Illinois, outside of Chicago; Bowling Green, Ohio; and Sharon, Pennsylvania. These three plants and an existing one in Highland, Illinois are shown in Figure 5 and serve as our midwest network.

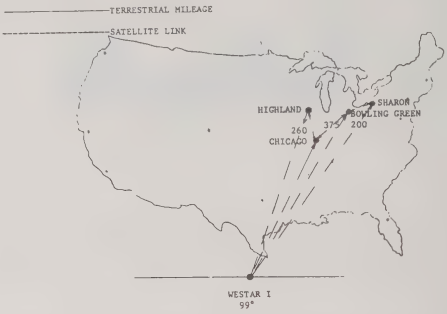

FIGURE 5   Midwest Network

Their earth stations will be the first of a kind to use a relatively inexpensive time division multiple access (TDMA) arrangement. They will be capable of handling not only our facsimile data, but all other data as well as voice transmission. They will be capable of full duplex operation with data rates up to 60 Mb/s. We are currently estimating our total internal communications requirements to total about 12 Mb/s. Simultaneous with the installation of our midwest network, which should begin operation shortly, we will begin converting our original stations which were based on single channel per carrier (SCPC) technology. In addition, we will be installing similar earth stations in other current Dow Jones printing plants as well as increasing the number of printing plants in the United States. According to our current planning schedule, by the end of 1983, we should have a complete operating TDMA network consisting of 17 earth stations at printing plant locations. While it seems like 1983 is a long way into the future, it is only three years-- the same amount of time we have been using the satellite for communication. Looking back to 1975, when we began, seems like yesterday.

80-0552

USERS - THE SECOND PHASE

Robert E. Button
President
TransCommunications Corporation
Greenwich, Connecticut

To the surprise of almost nobody the supply of communications capacity in domestic satellite systems had fallen considerably short of the demand even before the failure of Satcom III. It was possibly this situation which back in July 1979 led the FCC to lift the moratorium on the domestic satellite operations of ATT-GTE without the usual lengthy hearings and delays. However much this decision may have been deplored by the lawyers for the opposing sides, it must be regarded as a wise move, followed, as it was, by the opening of an FCC Docket on underutilization of these same facilities. As long as there is no monopoly on earth station ownership and satellite access, such as once existed in Telesat Canada and was broken, one can reasonably assume that the demand for space segment will be as infinite as the human need to communicate. The FCC climate seems to be encouraging this growth and other countries are taking interest in the resulting economic example it provides. A reasonable assumption, however, is that planners will now, as before, under-estimate the rate of growth and fail to provide the resources necessary to meet it. But at least we will know, as users, where we stand. As of this writing, one satellite carrier reported holding between 40 and 50 orders for full transponders beyond what was available, even taking into account their spacecraft which had not yet left the ground.

The failure of RCA Satcom III in December 1979 made the immediate shortage of video channels more acute. During the interval before a replacement can be placed in orbit, substitute service will be provided on other satellite systems, which in turn could have the effect of stimulating the emplacement of secondary receive-only earth stations for video service through Westar, Comstar, or even Telesat by users who now can access only one of the operational satellites. The proliferation of secondary dishes was sure to happen some day. The RCA satellite failure of December 1979 may have served thus to expedite the appearance of an alternate program source to that hitherto available primarily to the cable operators whose single earth station had the capability of receiving regularly only the programs carried on Satcom I.

Domestic satellite usage has undergone, so far, a two-phased development. The first phase of domestic commercial satellite expansion opened October 1, 1975. Sid Topol, of Scientific Atlanta, had moved hesitantly into the production of 10 meter receive-only stations, two of which were in place and operating with CATV systems in Vero Beach, Fla. and Jackson, Miss. on that memorable date. You are all familiar with the subsequent proliferation of receive-only earth stations at Cable TV systems. Teleprompter ordered twenty-four Scientific-Atlanta stations shortly after the October first demonstration. We all observed both the belated arrival of other manufacturers at the party, and the subsequent shrinkage in size as well as price of FCC-approved equipment as the demand for it expanded.

This period of growth was fueled mainly by the advantages which satellite distribution offered the cable television industry. Prior to October 1975, Home Box Office was a small northeastern microwave operation, losing money and beset by all the usual problems of terrestrial distribution. The instant success of the first HBO satellite venture, with its direct effect on subscriber revenue to the cable system, was one of the liveliest business events of that entire decade. For two years thereafter HBO had the field to itself, with two Satcom transponders in service and a hungry new management at RCA to deal with. There was considerable skepticism in some quarters at RCA over the potential viability of their satellite business at that time. Indeed, there were many rumors in the industry that RCA's satellite division would be going the same route as did its computer business. But cable operators came to the rescue, observing the immediate effects of HBO satellite programming on subscriber penetration. They signed up for earth stations in droves, first acquiring 10 meter dishes until the FCC authorized smaller sizes. In the process they created an entirely new market of accessible viewers. Program vendors then moved rapidly to take advantage of this opportunity. The result was a rapid shift from a buyers to a sellers market for space segment, and a sudden reversal of mood at RCA.

The market thus originally created by HBO and RCA attracted other program services offering both free and premium television to cable subscribers. The Christian Broadcasting Network came first, followed by two other religious broadcasters. Then occurred the phenomenon of Channel 17 Atlanta. Originally this had been planned for Westar, but Mr. Turner spun rapidly around to Satcom when he realized what RCA and HBO had achieved in creating an audience via satellite and CATV. Thereafter video program services, one after the other, bought up all the remaining space segment on Satcom F-1 toward which all the cable TV earth stations were aimed. Occasional use of space segment for special events and sports found its place on Westar.

In early 1978 Western Union staged a raid on RCA and almost succeeded in wooing away the HBO business. It was an all-or-nothing gamble for a national market built on the single-dish receiving stations at cable systems. With HBO would have gone all the other video services in order to stay with the only sizeable market that existed for satellite-carried programs. It was a near thing.

During these developments, the conventional broadcasters for the most part stood aside, except for some limited coast-to-coast feeds and occasional special and sports events. Broadcasters seem to have failed to understand the cable-satellite phenomenon either as an erosion of their market position or as a potential positive profit center for themselves. In those days, as now, they were long on cash and short on creativity, not realizing that you cannot always buy one with the other.

© 1980 R.E. Button

Released to AIAA to publish in all forms.

A few pioneers appeared like Ted Turner in Atlanta, Les Arries in Buffalo and Hal Protter at KPLR in St. Louis. Turner was quick to observe that a transponder on RCA Satcom I would give him a national audience for his broadcast signal and perhaps nationwide interest in his ball team. Les Arries built a complete common carrier-licensed transmit and receive earth station in Buffalo without really knowing what he was going to do with it, but pretty sure that it would be useful some day. It turned out to be a factor in the 1980 Winter Olympics, and in certain developing relationships with the Canadians. But in general the broadcasting people neglected satellites until 1977-78 when some of them read Arthur Clarke and began to realize that the entire industry was changing shape in the satellite era. They have only just started to equip themselves for the things to come. Their delay in doing so is all the more curious because of the family relationship between NBC and RCA, and the forthright challenge to the networks posed by HBO.

It was not until 1979 that RCA came up with its plan to offer earth stations to broadcasters. But by then many earth stations were in those hands already stimulated by such projects as Blairsat, and broadcasters had begun to enjoy the independence of networks that possession of an earth station gave them. As for operating an earth station as a profit center along common carrier lines, this concept was so far removed from the average broadcast station owner's mind or from the cable operators' as well, that very few such entities came into existence, of which, as mentioned, Buffalo and St. Louis were among the first examples. It may be assumed, of course, that both cable operator and broadcaster were reluctant to enter a regulated business arena unless the potential in terms of profit became more apparent. It is this profit potential that is now leading us into the second phase of domestic satellite development.

The cable satellite explosion started by HBO really began to attract program competitors in 1977. It took very little time for the buyers' market in space segment to reverse itself. The available transponders were bought up by broadcasters, by pay-cable vendors, by carriers of the super stations. The satellite carriers slowly came around to the realization that more space segment would be needed. Their timing was in the established leisurely tradition of communications industry planning. When RCA management finally realized what was taking place, authorization was quickly provided for flight models 3, 4, 5 and 6. The Hughes Aircraft Corporation, hitherto only making spacecraft on order, appeared on the consumer level in 1979 by announcing plans for a complete domestic satellite network of its own, to be on line in 1982. But a satellite on the drawing boards and one in orbit are separated by a considerable time, and suddenly it became apparent that not only were transponders sold out well into the future, but that technological and marketing factors had rendered obsolete the idea of selling a transponder anyway.

The first marketing effort mounted by RCA for its Satcom system had been directed at selling a facility, or the capacity of the satellite in transponder lots for video users.

When it later appeared that there were more video customers than transponders, the natural reaction was for the waiting customers to seek to share transponders that were not fully utilized. Another alternative was simply to purchase, if possible, somebody who had a transponder already. HBO itself, in 1979, then having six full transponders under contract, began to receive overtures from potential participants and purchasers, to no avail. Nor were HBO's engineers particularly interested in selling, on a regular or long-term basis, parts of their transponder time, or even sub-carriers for audio usage. The possibility of compressing two or more video channels into one transponder was known, and practiced, indeed, with the same general pattern developing in voice and data traffic. But a carrier practice was to sell a transponder as a "facility", not a "service", to the video users, and from 1979 on there were no more facilities as such to be had. Those who had "facilities" contracts for transponders were perfectly free to use all or part thereof, or to sell the unused portion for whatever the market would bear, none of which went back to the carrier. Under these terms a carrier often simply set up a retail business for someone else.

The shortfall in satellite video channel supply could have been alleviated by more timely construction and emplacement of new spacecraft, or possibly by packing more TV signals on each transponder. The former course of action fell victim to the chronic disease of the industry, underestimation of growth potential. The latter, while technically possible, involved considerable added expense both at uplink and receiving end. Its time will come. But current users are not eager to risk signal degradation, nor to share their transponders with possible future competitors.

The resulting squeeze on transponders may appear to have been the unforeseen result of a temporary and reversible business decision. Policy is changing, I am told. Users can now buy a service, or a percentage of a transponder, up to the total capacity, but it is the "service" rather that the "facility" concept that is now applied. Moreover this concept would apply to the non-video as well as the video forms of traffic. This may be a significant step in view of the current imbalance between supply and demand. However, its effect will be diminished by yet another policy question that impacts on the voice/data user who is also faced with a shortage of capacity, although not to the same extent as the video user. This is the question of the sale of space segment to other common carriers or users where one or both ends of a circuit do not happen to be owned or located in one of the backbone markets of the underlying satellite carriers themselves.

There is no regulation I know of which says that a carrier must sell pure space segment if requested. Nor is there one that says it cannot. As with most aspects of satellite communications, over-regulation comes first, and is followed by fits of de-regulation which leave many questions like this one unresolved or in abeyance pending an initiative taken by somebody who can afford a test case.

The principal satellite carriers have confined their earth station backbone to the major market areas of New York, Atlanta, Chicago, Dallas-Houston, San Francisco and Los Angeles. Even in these markets the earth stations in some cases have been established well out of the downtown area, for reasons not at all clear to outsiders. Chicago's main satellite port of entry, for example, is sixty miles north of the city. At one time there were carrier plans to build earth stations in many more markets, but the total backbone structure of RCA and Western Union seems permanently fixed at six. These are the heavy traffic routes and lend themselves most efficiently to FDM-FM transmission wherein the carrier offers end-to-end service and controls both ends. With the lifting of the moratorium on ATT/GTE, plans have been revealed to install common carrier earth stations in many more markets, in response to demand and economics. Additional stations may be owned by the major carriers, or they may be new business ventures created to serve markets not otherwise served, and may be created by cable operators, broadcasters or others. Totally unknown entities have filed for entry into this business, and diversified, conglomerate-type companies have added similar activities to their corporate inventories. Not to be overlooked is the obvious intent of Western Union to utilize commercially, if allowed by the FCC, the available capacity in any of the 160 PBS earth stations for message traffic where a reasonable profit potential might exist. This raises the question of indirect subsidization of rates to be charged Western Union customers, as PBS was built by legislated public funds.

The policy position of the Federal Government, since 1972, has been one of "open skies and open access". Of course, access is "open" if a message customer, remote from one of the six carrier gateways, chooses to take a service package that combines a terrestrial haul to the carrier's earth station and satellite links to the final destination. But there is no reason why another common carrier earth station at either end should not directly access the satellite system under proper technical controls, given the general policy under which satellites are regulated. Indeed, it is a fact that many of the best corporate prospects for private line satellite usage are in locations remote from the current six carrier backbone stations. For example, the second largest corporate headquarters concentration of the Fortune 500 is at present in Fairfield County, Connecticut which has no common carrier earth station at all, even though the second largest phone company (GTE) is located there and is itself in the satellite business. This is so obvious a lack that it is about to be remedied. There are many top-50 markets that have enough of a business base to make viable a common carrier earth station for in-and-out private line satellite service, but not all of the customers happen to want to connect with destinations within the six major earth station markets. What then occurs if a customer needs to interconnect two points neither of which is served directly by an earth station belonging to one of the major satellite carriers?

There are specialized common carriers in the field which are beginning to offer this type of service. Transponder Corporation of Denver, a Johns-Manville subsidiary, is an example. Denver was once intended as a carrier "backbone" station, but in the early doubtful days was eliminated. Today it is operating practically as an integrated but independent station on the RCA satellite network and is being equipped to work also with Westar and Comstar. Similar types of OCC ground stations are under construction in Detroit, Philadelphia, North Carolina, Boston and elsewhere.

If a satellite carrier chose to limit its service offering to space segment plus one or both ends of a circuit, the shortage of transponder capacity would become an artificial one based on considerations aside from actual availability of facilities. Such a posture would seem to contravene what is accepted as public policy. Under this mode of operation the proliferation of transmit/receive earth stations would come to a halt for lack of space segment. The open skies policy which has meant so much in terms of economic stimulus would be rendered ineffective.

It seems probable that competitive pressures would alter the sales policy of any carrier that took this position. But it also seems likely that if space segment is to be made available regardless of who owns either or both terrestrial termination points, and if the de-regulatory policy continues to favor unlimited proliferation of earth stations, the natural outcome would be to consume space segment at a greater rate than it can be provided. Earth stations and traffic routes will develop somewhat in the same manner as new airline routes appeared in the sixties, and new users will undoubtedly materialize from unlikely quarters. Those 10 meter dishes that were the principal sources of HBO and Showtime feeds in the seventies will be altered, wherever a private line user can be found, to handle other kinds of traffic than video entertainment reception. The hardware manufacturers know this and are planning for it. In fact it is to Sid Topol that I am indebted for the concept "The Second Phase" of domestic satellite development to describe this trend, and I hear that he is building extra facilities to meet the requirements of earth station owners who plan to upgrade their stations to meet the user demand.

Whether or not the space segment will ever provide enough capacity to accommodate all users is an unsettled question.

As of today we have Satcom, Westar, Comstar and soon, Hughes all in the field, in relatively unrestricted competition. There are even private industry groups who find economic and other justification for planning their own dedicated spacecraft. Independent broadcasters are installing their own stations at their broadcast points, some of them to be licensed common carriers. The use of space for corporate teleconference purposes has hardly begun, partly because few transponders or channels can be found to accommodate the necessary video requirements. And yet the communications industry generally regards teleconferencing as the next big explosion in satellite use. Where will the necessary space segment be found to accommodate all of these potential occasional-use customers?

As previously mentioned, bandwidth compression will perhaps double the capacity of existing transponders, and it must be assumed that the satellite carriers will re-assert the right to sell bandwidth rather than whole transponders in future space segment. They will thus be able to provide service to users who need only a fraction of the bandwidth and of the 24-hour daily schedule. This would accommodate some teleconference users perhaps in tandem with prime time entertainment vendors. The same would apply to off-hours computer traffic. But as of the time of writing, even this approach would not suffice to match the demand for satellite communications now on the books and visible on the business horizon.

The probable solution, one not readily at hand but feasible and in the planning stage, is the move to higher frequencies, such as 12-14 GHz, which would again double the capacity in space and relieve the earth segment of much of its difficulty with interference problems.

If the 12-14 GHz solution to a current space segment shortage proves effective, what indeed has been accomplished? The ability to locate transmitters in hitherto denied locations, characteristic of the 14 GHz band, will bring new users out of the woodwork in multitudes. Traffic routes will proliferate; earth stations will multiply and we will soon find ourselves back where we are now; faced with a shortage of facilities to accommodate the infinitely expanding need of people, computers, and businesses to communicate. It is my considered opinion that in this industry, the supply of space segment will never catch up with the demand, which if correct, should be good news to almost everybody. Faced with this kind of demand, and the capability of the industry for constantly greater if somewhat tardy leaps forward, I believe we are engaged in a non-cyclical, ever-expanding activity of interest and challenge to everyone but perhaps the Trappist Monks. And some day perhaps even they will order a few circuits for the distribution of silence, in prime time, if only to bring a little peace and quiet to the business of communications by satellite.

80-0553

A MEDIUM RATE INTEGRATED TDM/TDMA SATELLITE SYSTEM

S. N. Verma
Manager, Transmission Engineering
The Western Union Telegraph Company
One Lake Street, Upper Saddle River, N.J.

S. Salamoff
Manager, Multiple Access Equipment
Digital Communications Corporation
Gaithersburg, Md.

Abstract

Since the launch of domestic communications satellites in 1974, the United States communication network extensively uses C-band transponders for providing services to various locations in the CONUS, Hawaii, the Virgin Islands and Mexico. To meet the growing transponder capacity demands through satellites The Western Union Telegraph Company (WUTCO) launched Westar III in August 1979, and is planning to use all 3 Westar and Advanced Westar Satellites in the early 1980s. These satellite networks include earth stations with antenna dishes ranging from 15 meters to 4.5 meters for carrying messages, data, program material and video signals for broadcasting and point-to-point transmissions. The satellite systems are designed using Frequency Division Multiple Access (FDMA) and Time Division Multiple Access (TDMA) techniques for transmission of signals through transponders. The use of TDMA in accessing the transponders for multipoint transmissions provides substantial space segment cost savings and large system flexibility. WUTCO has developed a prototype communication network using low cost small earth stations (SES) employing Time Division Multiplexing (TDM) and Time Division Multiple Access (TDMA) transmission techniques for medium rate (up to 128 KBS) transmissions. The system is designed for carrying the low speed data signals between SES and large earth stations (LES). Each channel is designed to carry up to twelve 9600 baud lines using TDM from LES to SES and TDMA from SES to LES. The ground terminal equipment includes flexibility of system key features such as burst length and network configurations utilizing Field Programmable Logic Arrays (FPLA's). The frame formats are designed to allow for the inclusion of overhead signalling bits, which would permit automatic downline loading of the network information. This paper briefly describes the network configuration, the TDM/TDMA terminal and other system features. Further, the channel performance for different modes of operation are given. Finally, the system test results are shown. The extension of this system configuration for data transmission between SES locations is also described.

1.0 Introduction

Since 1974, Westar System (1-2) has been extensively used for carrying a wide range of channels for broadcasting and point-to-point transmissions. The channels carry analog and digital modulated signals employing Frequency Division Multiple Accessing (FDMA), Time Division Multiple Accessing (TDMA) and Single Channel Per Carrier (SCPC) techniques. Using 15 meter earth stations WUTCO developed and tested 62 MBPS TDM/TDMA through Westar transponders increasing the voice channel transponder capacity up to 1920 VF or three video channels. The system used Digital Speech Interpolation (DSI) and adaptive bit sharing techniques for VF channel and video compressions, respectively (3-4). Presently the WUTCO transmission network consists of Westar satellites, terrestrial microwave links and the local distribution facilities. The network provides services for transmission of video, message and data channels. The low rate data channels carry signals from 75 BPS to 9.6 KBPS for TELEX, TWX, Mailgram, Private Wire and on the Digital Exchange System (DES). The TELEX/TWX subscriber channels on DES are concentrated to 2.4 KBPS channels at concentrating cities (over 1500) throughout the United States for transmission to multiport multiplexer (MPM) cities (over 220) where these channels are further concentrated into channels up to 9.6 KBPS. These concentrated 9.6 KBPS channels from MPM are then combined with other 1.2 KBPS, 2.4 KBPS and 4.8 KBPS channels at four DES centers for transmission to other locations. The terrestrial microwave link presently connects MPM with DES centers. The four DES centers are interconnected through Westar Large Earth Stations (LES) located in the San Francisco, Chicago, New York and Atlanta areas. The switching center channels individual circuits for connection through their own hierarchical chain or through another DES switching center to complete the circuit routing, employing multiple satellite hops. The cost for these transmissions are reduced by using satellite links in place of terrestrial links between MPM and DES locations. To increase the system capability to reduce the transmission cost, a medium rate TDM/TDMA pilot system using Westar transponders is developed for transmission between MPM and DES locations using SES and LES ground terminals. In the following sections the description and operation of this pilot TDM/TDMA system is discussed. The channel performance for TDM/TDMA modes of transmission are considered and the system test results are shown. Further, the configuration for extending this system for single hop transmissions between MPM locations (with SES ground terminals) using DES center LES terminals for satellite selection and coordination, is also discussed.

2.0 System Configuration

The pilot TDM/TDMA system developed is described in Figure 1. The channels are transmitted through Westar transponders using LES (15 meter) ground terminals at DES centers and SES (5 meter) ground terminals at MPM sites. The pilot network consists of one LES location at the WUTCO Estille Fork earth station and four SES locations. Presently planned SES locations are Tampa, Orlando, Memphis and Charlotte, which may be changed depending upon WUTCO network requirements. The 1.2 KBPS to 9.6 KBPS signals can be transmitted between LES and SES ground terminals using nominal 262 KBPS channels through Westar

Copyright © American Institute of Aeronautics and Astronautics, Inc., 1980. All rights reserved.

transponders. These channels carry 128 KBPS information with half rate forward error correction coding for efficient space segment utilization. Large level carriers are required for transmissions from LES to SES while lower level carriers are required for transmissions from SES to LES. The typical channel performance and system transmission parameters are shown in Table 1. In following sections the LES and SES locations are referred to as central and remote locations respectively.

Table 1 Typical System Design Parameters

		LES → SES	SES → LES
UPLINK EIRP TO SATURATE	dBW	80.0	80.0
DOWNLINK SATURATED EIRP	dBW	34.0	34.0
UPLINK PATH LOSS	dB	200.0	200.0
DOWNLINK PATH LOSS	dB	196.5	196.5
SATELLITE G/T	dB/°K	-7.0	-7.0
EARTH STATION G/T	dB/°K	21.5	37.4
DOWNLINK EIRP PER CARRIER	dBW	14.0	4.0
UPLINK TERMAL	dB	21.8	11.8
DOWNLINK THERMAL C/N	dB	11.8	17.7
TOTAL INTERFERENCE C/I	dB	17.0	17.0
CHANNEL BER PERFORMANCE		10^{-5}	10^{-5}
SYSTEM C/N	dB	10.3	9.9
REQUIRED SYSTEM C/N	dB	9.8	9.8

Transmissions from the central site to the remote sites operate in a Time Division Multiplex (TDM) mode where one continuous carrier is broadcast to all remote sites. Field-Programmable Logic Arrays (FPLA's) to all sites contain preprogrammed timing information, which designates a certain portion of the TDM frame for use by that station.

Transmission from remote sites to the central site are obtained by using Time Division Multiple Access (TDMA) carrier. In TDMA operation, transmission from each remote site is synchronized to the incoming TDM frame, and occurs in a burst format, such that only one remote site is occupying the carrier bandwidth at any instant in time. The length of each burst is determined by the amount of information to be transmitted, and each remote terminal transmits one burst per TDMA frame. The system operates at 262.144 KBPS; the low transmission rate allows for an open loop synchronization scheme, which makes the hardware design less complex and cost effective without sacrificing the frame efficiency due to overhead requirements.

TDMA synchronization is achieved using the received TDM synchronization unique word (SUW). The transmission time of each remote site is delayed relative to the SUW reception. Each station is programmed for a different burst position such that no two sites transmit simultaneously. In this fashion, all remote site transmissions arrive at the satellite in a non-overlapping mode.

The central site TDM/TDMA controller is designed to be located in WUTCO Wire and Repeater rooms and communicates to the remote sites where the data channels from 1.2 KBPS to 9.6 KBS are terminated for transmission after proper concentrations. The satellite link RF subsystems upconverter and downconverter with their power supply are designed to be located next to the ground terminal antenna in an enclosure. The enclosure is air conditioned and connected to the TDM/TDMA subsystem through IF cables.

3.0 Central Site System

The central site digital hardware is configured for TDM Transmit/TDMA Receive operations. The system configuration is described in Figure 1. The system consists of uplink, downlink and the central TDM/TDMA controller. The TDM/TDMA controller is described in detail in Figure 2. The channel port contains WULL interface circuitry including compression/expansion buffers. The channel ports are capable of handling channel rates at 1.2 KBPS, 2.4 KBPS, 4.8 KBPS or 9.6 KBPS. The MUX/DEMUX provides all transmit and receive enable command (data gates) to the channel ports using information programmed into the FPLA's. The transmit data output of each channel port is sent to the high speed data bus; each channel port contains tri-state output buffers so that only one port occupies the bus when its respective data gate is active. The high speed data and MUX commands are timed to the high speed clock (131.072 kHz) which is locked using a phase-locked loop (PLL) to an incoming 9600 Hz reference clock.

The high speed serial data bus passes to the transmit controller, which generates the master frame timing, TDM (in the central case) unique word, and performs rate 1/2 encoding, scrambling, and differential encoding of the high speed data. Two parallel streams (P and Q), each at the symbol rate (131.072 kHz), are sent to the 4 Phase PSK Modulator.

The incoming (receive) IF Spectrum contains the TDM carriers being transmitted from the remote sites, as well as a 70.00 MHz pilot signal which is used for the AFC/AGC function. The 4 Phase PSK demodulator sees the frequency and gain corrected IF Spectrum, and is tuned to the desired TDMA IF carrier by a crystal L.O. in the REF OSC module. The carrier is demodulated and the hard-limited recovered data is sent to the Bit-Timing Recovery (BTR) circuitry, where the receive clock is extracted and the data retimed. Two parallel streams (P and Q) pass to the receive controller where differential decoding, descrambling, and rate 1/2 decoding take place. In addition, the unique word is detected which tells the start of each receive TDMA burst. The unique word is sought during a period of time known as the "aperture", which is timed to the transmit TDM frame. A priori knowledge of satellite delays and burst position allows the receive controller to determine which TDMA burst is from which remote site, without the need for different words.

The detection of the unique word (UWD) determines the start of burst and generates the timing "tick" for the DEMUX, which provides data gates and timing to the channel port receive sides, similar to that of the transmit (MUX) side. A serial high speed data bus is sent to all channel ports; selective enabling (via FPLA programming) allows the data to be routed to its proper port.

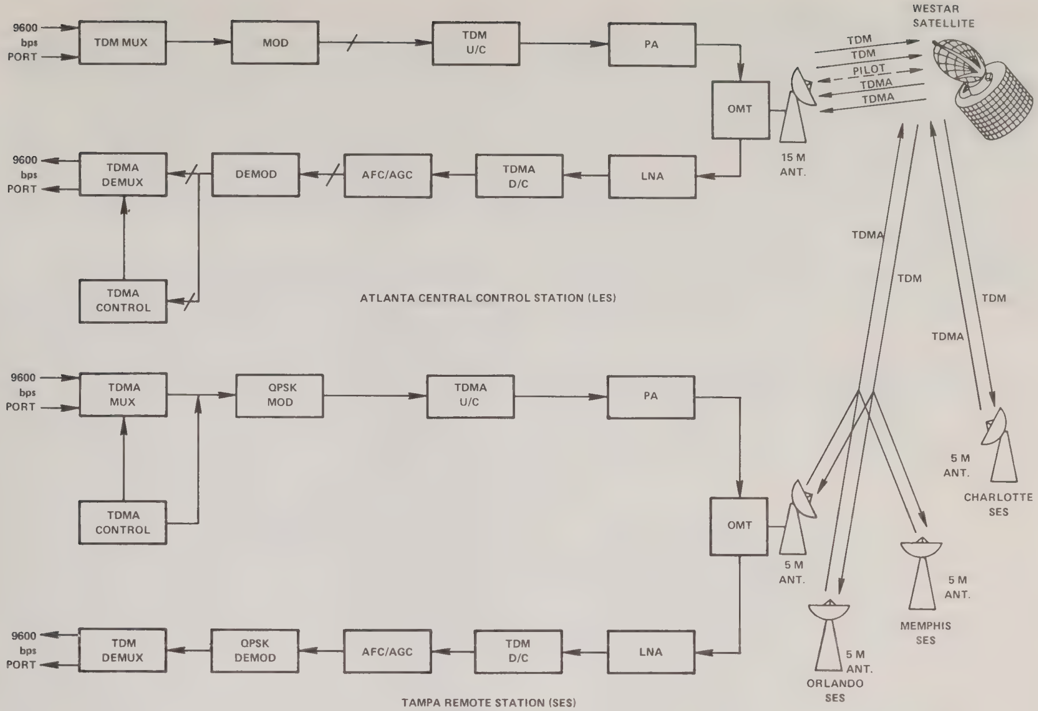
9600 bps PORT
TDM MUX
MOD
TDM U/C
PA
WESTAR SATELLITE
TDM
TDM
PILOT
TDMA
TDMA
OMT
15 M ANT.
9600 bps PORT
TDMA DEMUX
DEMOD
AFC/AGC
TDMA D/C
LNA
TDMA CONTROL
ATLANTA CENTRAL CONTROL STATION (LES)
TDMA
TDM
TDM
TDMA
9600 bps PORT
TDMA MUX
QPSK MOD
TDMA U/C
PA
TDMA CONTROL
OMT
5 M ANT.
5 M ANT.
CHARLOTTE SES
5 M ANT.
MEMPHIS SES
5 M ANT.
ORLANDO SES
9600 bps PORT
TDM DEMUX
QPSK DEMOD
AFC/AGC
TDM D/C
LNA
TAMPA REMOTE STATION (SES)

FIGURE 1

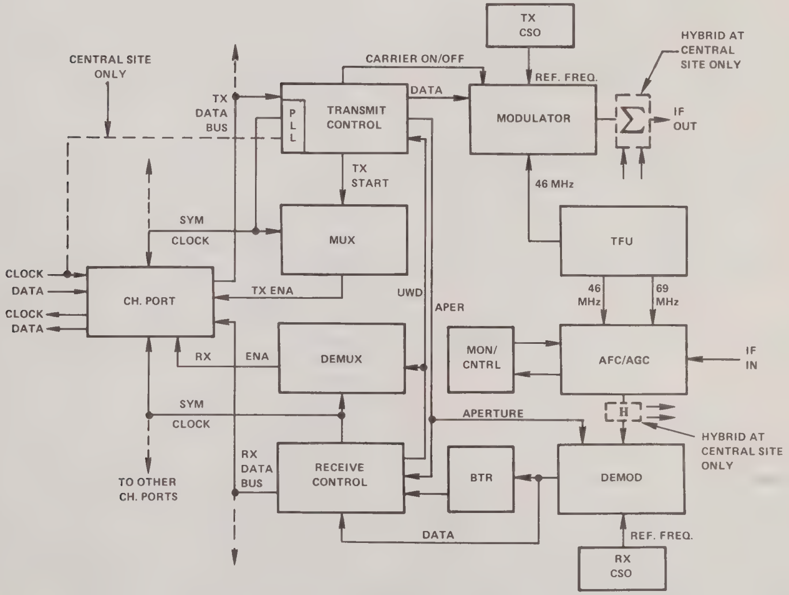
TX CSO
HYBRID AT CENTRAL SITE ONLY
CENTRAL SITE ONLY
CARRIER ON/OFF
REF. FREQ.
TX DATA BUS
P L L
TRANSMIT CONTROL
DATA
MODULATOR
IF OUT
TX START
46 MHz
SYM
CLOCK
MUX
TFU
CLOCK
DATA
CLOCK
DATA
CH. PORT
TX ENA
UWD
APER
46 MHz
69 MHz
RX
ENA
DEMUX
MON/ CNTRL
AFC/AGC
IF IN
SYM
CLOCK
APERTURE
H
HYBRID AT CENTRAL SITE ONLY
TO OTHER CH. PORTS
RX DATA BUS
RECEIVE CONTROL
BTR
DEMOD
DATA
REF. FREQ.
RX CSO

FIGURE 2
TDM/TDMA SUBSYSTEM BLOCK DIAGRAM

The modem for the TDM/TDMA controller employs 4 phase PSK modulation with differential coding to resolve phase ambiguity. The differential encoder/decoder uses a 16-bit shift register in the feedback path which effectively separates dual bit errors (inherent in any differential coding scheme) by 16 bits, which is outside the constraint length of the Rate 1/2 decoder (k=14); hence, both errors can be detected and corrected.

Reference frequencies for the modem subsystem are provided by the Timing and Frequency Unit (TFU) and Channel Select Oscillator (CSO). The TFU provides the high stability reference for the modulator and AFC/AGC modules; the CSO provides for a crystal - selectable transmit IF output and demodulator first L.O.

The AFC/AGC module operates on a 70 MHz pilot (transmitted from the Central Site) and is used to provide for frequency (±40 kHz) and gain (±7 dB) offsets in the satellite and downlink. The Monitor/Control module contains sample and hold and timing circuitry which is part of the AFC/AGC function.

4.0 Remote Site Subsystem

The remote site is configured for TDMA transmit and TDM receive operations. The system block diagram is shown in Figure 1. The system consists of a 5 meter antenna earth station with G/T of 21.5 dB/^{O}K for transmitting and receiving signals. The remote site TDM/TDMA controller is similar to central site, central controller, but is reconfigured for TDMA transmit and TDM receive operation using jumper straps on the modules and backplane wiring changes. The block diagram of the remote controller is shown in Figure 2. Operation is similar to that of the central controller, with the following exceptions:

- All internal timing at the remote site is generated from the recovered symbol clock (BTR clock). This ensures that all remote site transmission occurs synchronous with the Central Station Clock.

- The TDMA transmission is gated on by a delay timed from the recognition of the TDM unique word. (The frame counter used to time this delay is the same counter used at the master site to program the frame length.)

- The modulator output is in burst format (TDMA) rather than continuous, and is gated ON/OFF by the transmit controller.

The receive TDM data stream is fed to the Receive Controller, which performs the following functions:

A) Aperture Generation

B) Unique Word Detection

C) Descrambling

D) Rate 1/2 Decoding and Error Correction

In TDM, an aperture is generated so as to create a "window" for unique word detection. Assuming the data is a random sequence, the probability that the unique word will occur during the data is high; therefore, the Unique Word Detection (UWD) must be apertured. Initially, the aperture is wide open, and is closed upon the first UWD. At this point a frame counter is reset, and 250 ms (32768 symbols) are counted before opening the aperture once again. If the UW appears, the terminal stays synchronized; if it does not appear (i.e. the first detection was false) the aperture will open once again and the process repeats. The epsilon (number of errors allowed in the unique word) is set at 0 when the aperture is wide; when synchronized epsilon = 4.

The received high speed data stream is descrambled prior to being Rate 1/2 decoded. The data was scrambled with a 4096 bit PN sequence prior to transmission to ensure uniform energy spreading. The decoded data stream is fed to all channel port modules, while the UWD resets the DEMUX to provide receive timing gates.

UWD also serves to enable the transmit controller frame counter, whose function (at the remote sites) is to delay the transmit burst time relative to UWD. The frame counter is manually set via binary switches, however, could as well be down-line loaded via an overhead signalling channel. When the frame counter times out, the TX START resets the MUX, and the modem preample (CR/BTR/UW) is generated. Also, the Rate 1/2 encoder and scrambler are reset, so that the complementary circuits at the Central (TDMA) receive site can be synchronized to TDMA UWD.

Data is gated from the channel ports onto a tri-state data bus under control of the MUX. The transmit data (two symbol streams) is fed to the TDMA modulator, which is gated on for the duration of the burst length.

Each remote site recovers the symbol clock from the incoming TDM data stream. A phase-locked loop (PLL) locks to this frequency and generates all low speed clocks for both transmit and receive sides. In this manner, the network is synchronized to the master clock. At the master site, provision is allowed for locking the PLL to an external 9600 baud DDS clock.

5.0 Frame Formats

Figure 3 describes the frame formats for TDM and TDMA operations. The TDM frame is identified by a 10 symbol unique word. Provisions have been made to accommodate an overhead signalling channel (proposed at 256 symbols) which would allow for down-line loading of a new system network plan under dynamic assignment. Data blocks follow the SUW (or end of overhead block). Each data block consists of the time-compressed data from each of the n ($\leq$ 12) data ports at the central site. Depending upon the port rate (1.2 to 9.6 KBPS), each data block contains:

$$\text{Rate}_{\text{(port)}} \text{ X Rate}_{\text{(frame)}} = \text{Bits/Data Block}$$

For example, with the 250 ms frame rate, a 9600 BPS channel would have 2400 bits in each data block. Channel ports are addressed sequentially (once per frame), and data blocks are "butted up" to each other. Spare bits (non-information) occupy any remaining bandwidth in the TDM direction that has not been assigned.

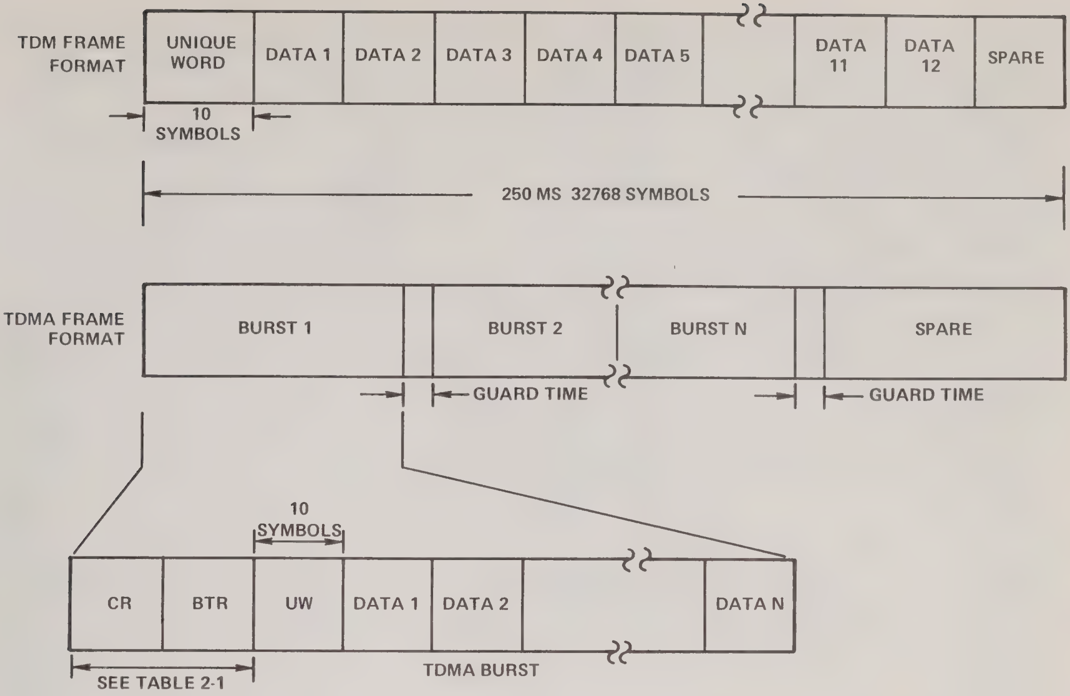

FIGURE 3

The TDMA frame is composed of several bursts; each burst originating from a different station. As with the TDM frame, up to 12 data blocks (or channels) can be handled by the TDMA frame; however each site transmitting a burst may have 1 through 12 blocks, as long as a total of not more than 12 is present in the frame. Each burst contains a Carrier Recovery (CR) and a Bit-Timing Recovery (BTR) sequence (known as the modem preamble) to allow for proper demodulator lock at the receiving (Central) site. The modem preamble is followed by the 10 symbol unique word, which in turn is followed by the first data block. When no remote site is transmitting, the burst is "blank". Data blocks in the TDMA frame are of the same lengths (rate dependent) as for the TDM frame. Each TDMA burst consists of a modem preamble (carrier recovery) and the Unique Word which identifies the start of data. The burst ends in a postamble of 14 symbol times, necessary to flush the parity bits from the Rate 1/2 Decoder.

A guard time of 300 microseconds separates the TDMA bursts. This value corresponds to the minimum requirement for an open loop synchronization scheme. Burst timing (referenced to UWD) may be offset slightly from one remote station to another, due to the satellite motion. (The path delay differentials can be computed first and included in the FPLA program, hence only the Doppler shift need be accounted for.) The 300 microseconds ensures that the bursts will not collide due to the satellite Doppler motion.

6.0 Pilot System Test

The equipment for central and remote sites has been extensively tested for performance and specifications. The central site equipment has been installed and sites are being prepared for installation of subsystems at remote sites. The system specifications and interface are summarized in Table 2. The TDM/TDMA subsystem operation and performance in plant was tested simulating the satellite links as shown in Figure 4. The tests performed using these test configurations are:

- E_b/N_o vs BER with and without coding
- Unique word miss vs E_b/N_o
- Variable length preamble
- Oscillator stability
- IF level stability
- Spurious and IM levels

The measured and predicted E_b/N_o vs BER performance of the channel are shown in Figure 5. The measured performance is found to be very close to the estimated values. The modem acquisition performance probability begins to dominate below 8 dB uncoded E_b/N_o. Various tests are planned for the pilot system after the installation. The results of these tests will be provided at a later date.

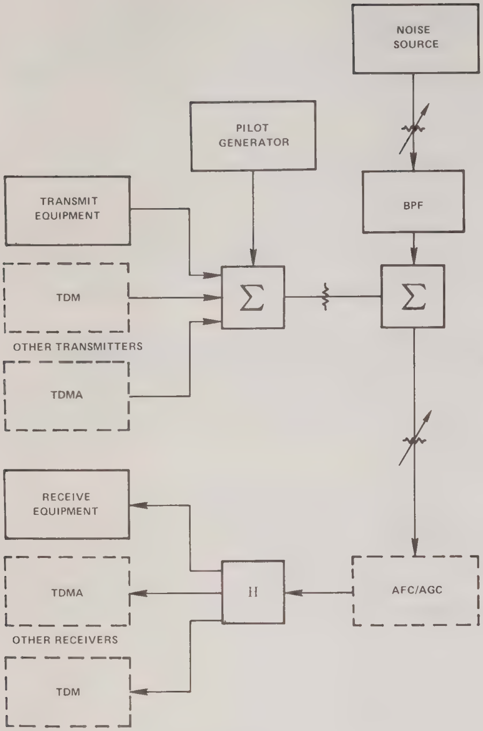
NOISE SOURCE
PILOT GENERATOR
TRANSMIT EQUIPMENT
BPF
TDM
Σ
Σ
OTHER TRANSMITTERS
TDMA
RECEIVE EQUIPMENT
TDMA
H
AFC/AGC
OTHER RECEIVERS
TDM

FIGURE 4

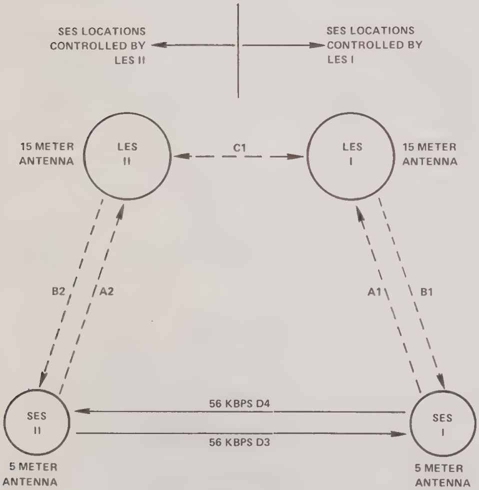
SES LOCATIONS CONTROLLED BY LES II
SES LOCATIONS CONTROLLED BY LES I
15 METER ANTENNA
LES II
C1
LES I
15 METER ANTENNA
B2
A2
A1
B1
SES II
56 KBPS D4
56 KBPS D3
SES I
5 METER ANTENNA
5 METER ANTENNA

FIGURE 5
SES TO SES TRANSMISSION CONFIGURATION

Table II System Specification Summary

MODULATOR		
	TYPE:	4 PHASE PSK, DIFFERENTIALLY ENCODED
	RATE:	131.072 ksps
	OPERATION:	TDM OR TDMA
	OUTPUT LEVEL:	- 20 ± 5 dBm
	OUTPUT IMPEDANCE:	50 OHMS
	LEVEL STABILITY:	± 1 dB (LONG TERM)
	OUTPUT FREQUENCY:	SELECTABLE FROM 52 TO 88 MHz
	SPURIOUS SIGNALS:	> 40 dB BELOW CARRIER LEVEL
DEMODULATOR		
	TYPE:	4 PHASE PSK, DIFFERENTIALLY ENCODED
	RATE:	131.072 ksps
	OPERATION:	TDM OR TDMA
	INPUT LEVEL:	- 39 ± 3 dBm
	AFC:	± 1 KHz
	AGC:	± 1.5 dB (TDMA)
		± 3 dB (TDM)
	INPUT SPECTRUM:	28 TO 64 MHz (INVERTED)
	BER PERFORMANCE:	
	BER	Eb/No (UNCODED)
	10^{-4}	10.8
	10^{-5}	12.4
	10^{-6}	14.1
	10^{-7}	15.8
AFC/AGC		
	PILOT FREQUENCY:	70.0000 MHz
	INPUT LEVEL:	- 31 dBm/PILOT
		- 34 dBm/CH.
	AFC RANGE:	± 40 KHz
	AGC RANGE:	± 7 dB
	INPUT SPECTRUM:	52 - 88 MHz
	OUTPUT SPECTRUM:	28 - 64 MHz (INVERTED)
	OUTPUT PILOT FREQUENCY:	45.9875 MHz
	OUTPUT LEVEL:	- 39 dBm/CHANNEL
	INPUT IMPEDANCE:	75 OHMS
	OUTPUT IMPEDANCE:	50 OHMS
DATA INTERFACES		
	INPUT/OUTPUT:	WESTERN UNION LOW LEVEL
	RATES (SYNCHRONOUS):	1200 BPS
		2400 BPS
		4800 BPS
		9600 BPS
	MAXIMUM NO. OF PORTS/SITE:	12
TDM/TDMA		
	FRAME RATE:	250 ms
	SYMBOL RATE:	131.072 ksps
	CODING:	RATE ½ HARD DECISION
	SCRAMBLING:	2^{12} MAXIMUM LENGTH
	PREAMBLE (TDMA ONLY):	2 ms MINIMUM

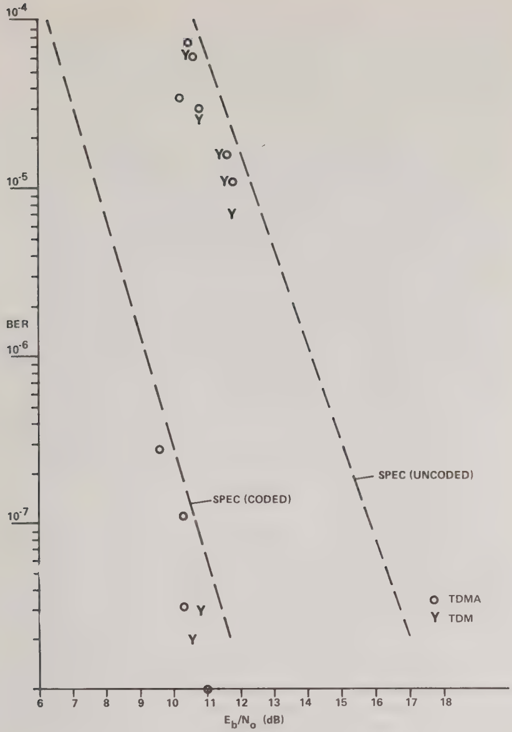

FIGURE 6

7.0 System Extension

With minor changes this pilot system configuration and hardware is also capable of providing the cost effective and simple transmissions up to 56 KBPS between MPM centers located at remote locations. The modified system can have the following main features:

- Single hop transmission of 56 KBPS data between two SES locations. This channel can be managed at the central station for use and billing.
- The flexibility of modular additional hardware for extending the system capability.
- Selection of satellite channel carriers for SES to SES transmissions from a pool of carriers.

The transmission in between SES locations is restricted up to 56 KBPS due to the limitations of 5 meter antennas used at SES locations. These SES locations can either be from one or many SES location groups, each controlled by separate central control stations. The concept of this network configuration and operation is described in Figure 6 The location SES 'I' is controlled by the LES 'I', while the SES 'II' location is controlled by the central station LES 'II'. The 56 KBPS channel requirement from SES 'I' to SES 'II' generates the request to the corresponding LES 'I' to search for a free carrier from the pool of carriers allocated for transmissions between SES 'I' and SES 'II'. The SES 'I' requests this service locally, the request message is forwarded to its LES 'I', a Common Signallying Channel (CSC) is activated such that the central station may set up the call, choose frequency assignments, and send assignment messages to the SES 'II' station. When the assignment message is received, the Remote controller activates the (56 KPBS) data modem, and the data service begins.

A similar sequency of events takes place upon termination of the data link. The SES stations can monitor modem ON/OFF for toll and tariff purposes, and forward this information to the LES stations at the end of the call. The use of various satellite carriers required and their operation is described in Table 3. The channels A_1, A_2, B_1, B_2 and C_1 are only used for selecting the carriers D_1 and D_2 from a pool of carriers for transmissions between SES 'I' and SES 'II' and are inactive after the contact. The transmissions A_1, A_2, B_1 and B_2 are obtained through the hardware and system described in Section 2. Hardware for channel C_1 can easily be added to the system equipment.

Table 3 SES to SES Channel Operation

SATELLITE CARRIER GROUP	SATELLITE CARRIER TYPE	SATELLITE CARRIER	TRANSMISSION	FUNCTION
A	262 KBPS	A1	SES I → LES I	USED FOR ESTABLISHING CARRIER ALLOCATION BETWEEN SES I & SES II
		A3	SES II → LES II	
B	262 KBPS	B1	LES I → SES I	
		B3	LES II → SES II	
C	2.4 KBPS	C1	MES I → MES II	COMMON SIGNALLING FOR SELECTING AND ASSIGNING D3 & D4
D	56 KBPS	D3	SES II → SES I	FOR 56 KBPS DATA TRANSMISSION
		D4	SES I → SES II	

References

1. J. W. R. Pope, S. N. Verma, and T. Rega "Small Earth Station: Modularity and Performance" National Telecommunications Conference, Birmingham, Alabama, Dec. 1978.

2. S. N. Verma "US Domestic Communications System Using Westar Satellites", World Telecommunications Conference, Geneva, October 1975.

3. S. N. Verma and D. Fraley "Sixty-two MBPS Transmissions Via Westar Satellites", National Telecommunication Conference, Birmingham, Alabama, December 1978.

4. S. N. Verma et al "A Microprocessor Controlled 961/48 Digital Interpolation Terminal" Fourth International Conference on Digital Satellite Communication, Montreal, Canada, 1978.

80-0554

IMPROVING FUTURE COMMUNICATIONS SATELLITE ANTENNA DESIGNS

William J. English
International Telecommunications Satellite Organization
Washington, D.C.

Introduction

Seven antenna design elements provide the key to improving future communications satellite antennas. Experience on recent satellite programs and new performance requirements expected for future antenna systems point to the need for focusing greater attention on these seven design elements and for ensuring their early interaction.

A review of the 15 year evolution of INTELSAT spacecraft antenna performance requirements sets the stage for a discussion of future trends in the design of communications satellite antennas. A consideration of the performance limitations of contemporary state-of-the-art antenna systems then leads into a discussion of the improvements required in seven key elements of an interactive antenna design process.

Summary of INTELSAT Spacecraft Antenna Performance Requirements

The 15 year evolution of communications satellite antenna performance requirements from INTELSAT I (Early Bird - 1965) to INTELSAT V (1980) has been remarkable . The communications antenna on Early Bird shown in Figure 1 weighed approximately 0.5 Kg. which represented 1% of the spacecraft end-of-life mass. Two communications beams (one transmit, one receive) at 4/6 GHz were generated from the single communications antenna structure. The communications antenna subsystem on INTELSAT V shown in Figure 2 weighs 68.8 Kg. which represents approximately 9% of the spacecraft end-of-life mass and 30% of the total communications subsystem mass. Eight communications antennas provide a total of 19 beams on flight numbers F-5 thru F-8 which incorporate 4 maritime communications subsystem (MCS) global coverage beams in addition to the 15 international fixed service beams. Frequency bands at 1.5, 1.6, 4, and 6 GHz are utilized for maritime services. Frequency bands at 4, 6, 11 and 14 GHz are utilized for the international fixed services. Table 1 summarizes the mechanical and electrical evolution in communications antenna performance requirements on the INTELSAT series of spacecraft from 1965 to 1980[1,2,3].

Future Trends in the Design of Communications Satellite Antennas

The mechanical and electrical complexity of communications satellite antennas has grown over the past two decades in order to meet ever more demanding performance requirements coupled with launch vehicle fairing diameter and volume constraints. The performance trends noted in Table 1, namely;

a. Multiple frequency bands
b. Greater effective bandwidths
c. Multiple coverage beams/antenna
d. Higher effective isotropically radiated powers (EIRP's)
e. Larger apertures
f. More radiating (feed) elements
g. Improved spacecraft pointing accuracies
h. Greater antenna subsystem mass
i. Extreme thermal environments
j. Improved sidelobe performance (30-40 dB.)
k. Improved polarization isolation performance (30-40 dB.)
l. Greater demands on efficiency (minimum gain x coverage area /41,253 square degrees)
m. Deployable antennas
n. Reconfigurable and steerable antennas

will continue in future communications satellite antenna designs.

INTELSAT, as well as others, have identified antennas as one of the key development technologies for future higher capacity satellites. As a result, development projects sponsored by INTELSAT are currently underway in the areas of reconfigurable beam antennas (beam coverage footprints adjustable in-orbit), broadband multiple beam antennas (40% relative bandwidths to permit utilization of new recently allocated frequency bands), variable power divider and phase shifters for spacecraft antennas, intersatellite link tracking antennas, active antennas (transmitters or receivers located at radiating elements) and optimized dual-polarization global coverage antennas. Several of these technologies are expected to be mature enough to warrant consideration during the planning of the INTELSAT VI spacecraft.

Shaped coverage beams, formed from many narrow component beams, imply large beam forming networks, feed arrays and reflector, lens or array aperture diameters[4,5,6]. Feed networks with 100-200 radiating elements are envisioned for the INTELSAT VI spacecraft presently expected to be operational in 1986.

Multiple beam frequency reuse utilizing both spatial and polarization isolation between beams has recently become a reality. Nevertheless, while the 27-30 dB beam isolations currently achieved in spacecraft and earth station antenna systems represents a tremendous advancement in technology over earlier designs, considerable frequency planning is still required in order to provide acceptable overall communications system carrier-to-interference (C/I) ratios. Spacecraft and earth station antenna systems achieving beam isolations in excess of 35 dB will be expected in future systems that seek to alleviate restrictions on carrier frequency assignments. Antenna systems providing beam polarization isolations in excess of 35 dB have already been demonstrated. Corrugated horns applicable to spacecraft use have realized 36 dB worst case polarization isolations over an 18 degree global coverage field-of-view and 500 MHz bandwidths at 4 and 6 GHz[7]. Two earth station antennas that will provide INTELSAT V

Copyright © American Institute of Aeronautics and Astronautics, Inc., 1980. All rights reserved.

pre-operational in-orbit test (IOT) facilities, one at Yamaguchi, Japan and one at Fucino, Italy, will also provide beam polarization isolations over their tracking beamwidths in excess of 35 dB.

Changes in future launch vehicle diameter and volume constraints, and the opportunity to possibly space-erect and test antenna subsystems at low transfer orbit altitudes, could dramatically redirect some of the current evolutionary trends in antenna development[8]. New requirements and considerations will also appear with the introduction of intersatellite link (ISL) antennas and active antennas on future communications spacecraft. The successful integration of several spacecraft antennas, each with stringent requirements related to multiple beam formation, low sidelobes, efficient coverage gain, dual-polarization isolation, reconfigurable and/or steerable beam coverages, lightweight and thermally stable (possibly deployable) structures, and stringent beam pointing accuracies requires a new perspective on the design approach to future communications satellite antennas.

Antenna Performance Limitations

The improvements in communications satellite antenna system technology over the past two decades have brought with them a new set of problems and the requirement to develop a new antenna design perspective. The complexity of today's multiple beam frequency reuse antenna and feed systems has introduced associated performance limitations, penalties and higher reliability risks. Redundant antenna systems typical of earlier spacecraft have disappeared except for critical telemetry and command antennas which provide control links for the satellites. Hence the communications antennas represent single point failure nodes. Multiple beam feeds have the advantage of compacting hardware to accomodate present launch vehicle mass, volume and diameter constraints and permitting multiple use of large reflectors, but they also result in reduced performance due to beam-forming network losses and aberration effects compared to providing the same beam coverages from a number of simple focused reflector systems. While recent designs have realized markedly improved sidelobe responses and hence improved beam efficiency to accomodate frequency reuse and beam coverage patterns tailored to particular sets of earth stations[9], the multiple beam-forming network losses and beam scanning aberration effects (resulting from feed element displacements relative to reflector focal points) have kept the efficiency parameter (measured as minimum gain x coverage area /41,253 square degrees) approximately constant as shown in Table 1.

Limitations on achieved sidelobe and polarization isolation performance can increasingly be attributed to "secondary effects" (i.e., to effects not specifically considered in the original antenna design and development process) rather than to hardware deficiencies. Consideration of "secondary effects" must therefore become an important part of improved antenna designs.

The classical method of engineering each antenna subsystem on a unit basis and subsequently assembling the antenna "farm" for spacecraft tests is yielding to an integrated approach that designs each antenna considering the full spacecraft configuration and environment and necessarily

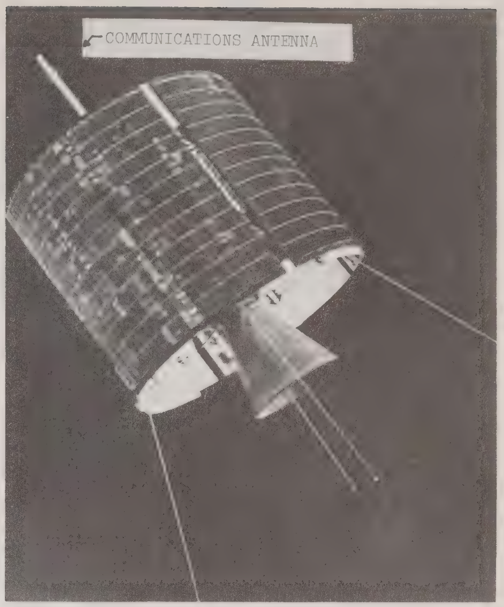

Figure 1. INTELSAT I (Early Bird)

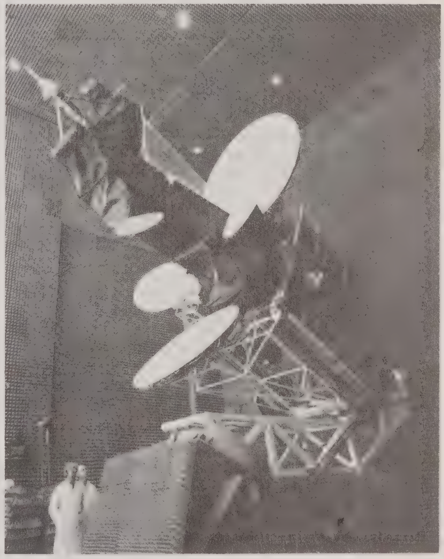

Figure 2. INTELSAT V Antenna Farm

includes many previously neglected "secondary effects" in the overall antenna design process. For example, realizing sidelobe responses at the 20-30 dB level over the past decade has been primarily related to achieving prescribed aperture illumination tapers while eliminating aperture blockage which could be done on a unit antenna basis. However, further performance improvements aimed at achieving sidelobe responses in the 30-40 dB range in the 1980's will require consideration of the total spacecraft configuration and environment in the antenna design process particularly with respect to electrical scattering effects.

Achieving improved antenna performance in the future will increasingly be a function of an early interaction between innovative structural, mechanical, and electrical design.

Seven design elements which require interactive and systematic attention in order to improve future communications satellite antennas are described in the following section. Experience on spacecraft programs to date has shown that an integrated interactive design approach will be necessary to realize the potentially significant performance improvements that future communications satellite antenna subsystems promise.

Improving Future Antenna Designs - Seven Key Elements

The continued development of innovative feed systems, beam forming networks, and reflector, array and lens configurations provides the basic foundation for future improved communications satellite antennas. In addition, however, seven practical elements that will require both interactive and early attention in the antenna design process are:

1. Analysis programs
2. Proximity interference
3. Spacecraft pointing accuracies
4. Interconnect and beam-forming network losses
5. Materials technology
6. Deployment and positioning mechanisms
7. Measurement technologies and facilities

These seven elements are now reviewed in light of recent advances and experience in the design of communications spacecraft antennas.

PARAMETER	INTELSAT I (65)	INTELSAT II (67)	INTELSAT III (68)	INTELSAT IV (71)	INTELSAT IVA (75)	INTELSAT V (80)
WEIGHT (kg.)	35	70	113	581	654	810
BANDWIDTH (MHz)	50	126	460	432	720(useable)	2137(useable)
FREQUENCY BANDS (GHz)	4,6	4,6	4,6	4,6	4,6	1.5, 1.6, 4, 6, 11, 14
G/T (dB/^{0}K)	(9dB N.F.)	(6dB N.F.)	(7dB N.F.)	-18.6	-18.6, -11.6	-18.6, -15, -11.6, -8.6 0, +3.3
EIRP (dBW)	9-10	15.5	22	22, 33.7	22, 26, 29	23.5, 29, 32.6, 41.1, 44.4
BEAMS	2	3	2	4	8(10FLT 2,3)	15(19 FLT 5-8)
ANTENNAS	1	1	1	6	5	7(8 FLT 5-8)
MAXIMUM DIMENSIONS(m)	0.4	0.6	0.9	1.27	1.34	2.44
WEIGHT (kg.) ANTENNAS	0.5 (1%S/C)	0.4 (0.6%S/C)	14.5 (12.9%S/C)	27 (5%S/C)	51 (8%S/C)	69 (9%S/C)
FEED HORNS	-	-	1	1	37 TRANSMIT 34 RECEIVE	88 TRANSMIT 90 RECEIVE
RECONFIGURABLE OR DEPLOYABLE	SPRING ERECTED	NONE	NONE	MECH. STEERABLE SPOTS	VIA SWITCHED FEES	2 STEERABLE SPOTS 4 DEPLOYMENTS 2 PITCH BIASABLE SWITCHED FEEDS
S/C POINTING	± 1.0^0	± 1.0^0	± 0.6^0	±0.35^0	±0.28^{0}N/S, ±0.20^{0}E/W	±0.15^{0}N/S, ±0.13^{0}E/W
THERMAL QUALIFICATION LEVELS (^{0}C)	21±7(Normal)	15.6±16.6 (Normal) -18 to -1 (eclipse)	-129/149	-198/+148 SPOT REFLECTORS	171/+117 REFLECTORS -65/+56 FEED ARRAYS -109/+94 APERTURE COVERS	-169/+89 REFLECTORS -109/+89 FEED ARRAYS -169/+204 APERTURE COVERS
MAXIMUM VSWR	-	-	1.2	1.2	1.15	1.15 SPOTS, GLOBALS 1.3 HEMI/ZONE
MAXIMUM POLARIZATION ELLIPTICITY (dB)	-	-	4.5	3	3(Specif.) 1(Typical)	0.75 HEMI/ZONE 0.40 GLOBALS 3.0 L-BAND ARRAY
SIDELOBE ISOLATION TO ADJACENT BEAM (dB)	-	-	-	-	27	27
MINIMUM GAIN x (COVERAGE AREA)/ 41,253 deg.^{2} = EFFICIENCY (TRANSMIT)	5.5dBi x (3920Deg^2) = .34	4.54Bi x (4310Deg^2) = .29	13.4dBi x (400Deg^2) = .21	16.4dBi x (289Deg^2) = .31 28.1dBi x (20.3Deg^2) = .32	16dBi x (324Deg^2) = .31 22dBi x (52Deg^2) = .20	21.82dBi(75.7Deg^2)= .28 25.47dBi(20.2Deg^2)= .17 37.4dBi(2.56Deg^2) = .34 17dBi(324Deg^2) = .39

Table 1. Evolution of Communications Antenna Performance Requirements and Characteristics on INTELSAT Satellites from 1965 to 1980.

1. Analysis programs

Computer analysis programs have revolutionized antenna design procedures over the past decade. Nevertheless a great deal of work remains to be done to further improve the capabilities of antenna design programs. For example, optimization of sidelobe responses (co-and cross-polarized) experimentally on antenna ranges is the most time consuming portion of the communications satellite multiple beam antenna design process at the present time. Six to twelve months of experimental optimization of the design following the establishment of the "computer solution" appears to be typical on recent programs. This problem is in fact a good measure of the need for modifications and improvements in computer program capabilities. Better correlation between computer predicted and initial measurement results must be established. The sidelobe prediction capabilities of computer analysis programs for antennas in the "farm" environment must receive major attention in the near future. The objective for mature large scale analysis programs must be to predict measured beam coverage gains to ± 0.30 dB and measured sidelobe and polarization isolation responses to ± 1.5 dB at the -35 dB level.

The incorporation of experimental feed horn data (amplitude and phase) and/or the development of better models for the complex radiation patterns of feed horns is a key factor required to improve the gain, sidelobe and cross-polarization isolation prediction capabilities of computer analysis programs. Also, the wide-angle radiation patterns of feed systems must be evaluated so that all illuminated spacecraft structures which could reflect or scatter energy are assessed.

At present, true optimization procedures for multiple beam communications spacecraft antenna design do not exist. The mathematical complexity of the non-linear optimization problem and the computer core size requirements are formidable. For multi-element feed/reflector systems, the conceptual procedure generally utilized today consists of generating a set of component beams, the beamwidth of which varies inversely as the reflector diameter to wavelength ratio, at fixed spatial positions and varying the individual component beam amplitudes and phases to achieve an "optimum" shaped beam gain and sidelobe isolation response which results from the complex summation of the component beams. While the resultant solution has been a good starting point for the initial experimental optimization of the antenna design, the lack of a true optimization procedure has led to the perplexing problem of judging when the experimental optimization on an antenna range should terminate, i.e , when the law of diminishing returns has set in. The development of closed-loop antenna design optimization procedures to meet the stringent coverage and isolation requirements of future communications spacecraft represents a challenging task.

Large scale computer programs should have the capability to accurately predict changes in antenna system performance parameters measured as a function of variation in the antenna range test distance. True far-field ranges have seldom been available for testing complete communications spacecraft antenna farms, particularly for system level tests on the fully integrated spacecraft configuration.

Simple computer programs illustrating conceptual ideas and effects also have their place. They often permit more insight into a particular problem and a reduction of computing time of an order of magnitude or more relative to the use of large scale programs.

Good engineering judgements and insights continue to constitute a major input to the innovative use of antenna computer analysis programs. From an infinity of design possibilities (i.e. mass, volume, diameter, feed array area and type, numbers of feeds, etc.) the antenna engineer, using his experience, intuition, and judgement, must select a few design candidates for extensive computer analysis and optimization. The analysis itself, primarily as a result of sidelobe prediction accuracy requirements for determining beam isolation, will increasingly incorporate many "secondary" effects which heretofore have been neglected.

2. Proximity interference

The electrical and mechanical aspects of interference and scattering contributions must be treated analytically early in the antenna design rather then only experimentally evaluated "after the fact" if 30-40 dB sidelobe and polarization isolation responses are to be achieved in-orbit. Near-and far-field scattering effects (including multiple scatterings) will have to be analytically evaluated as a function of antenna location. Feed system radiation patterns must be accurately predicted over a wide field of view to adequately model scattering from adjacent antennas and spacecraft structures. Scattering contributions will become major, dominant influences on the actual sidelobe and polarization isolation performance achieved in-orbit for future communications spacecraft antennas. An analytical consideration of proximity interference must therefore couple strongly into the mechanical and structural design aspects of the antenna subsystem, the antenna farm, and the overall spacecraft configuration. The INTELSAT V spacecraft incorporates rf. reflective screens, one of which is clearly visible in Figure 2., to deflect wide-angle feed array energy away from adjacent reflectors. Without the screens this spillover radiation illuminates the adjacent reflectors which results in a degradation of sidelobe responses.

3. Spacecraft pointing accuracies

Antenna performance specifications and design approaches in future communications satellites could in large measure be married to the spacecraft pointing accuracies achieved. For the near term, ± 0.10 degree spacecraft roll and pitch control are realistic objectives. Yaw axis control objectives, which have important implications for dual-linearly polarized systems, are generally several times those realized for roll and pitch. When antenna beam positions are fixed relative to the spacecraft, spacecraft pointing accuracies should be at least an order of magnitude smaller than the narrowest component beamwidths used. This would limit component or spot beamwidths to approximately one degree corresponding to a spot beam half-power beamwidth minimum gain of 41 dBi. Narrower beams, approximately 0.1 degree, could be quite attractive in the future, particularly in the context of satellite switched-time division multiple access (SS-TDMA) systems. It may then be feasible to utilize the spacecraft antennas themselves in either a mono-pulse or step-track mode of operation to assist the attitude control subsystem or individual antenna pointing control assemblies by actively tracking one or more ground based beacons. Thermal and structural considerations in large antenna farm configurations may eventually lead to independent tracking and pointing assemblies for each narrow beam spacecraft antenna.

A strong relationship will exist between the antenna system design and spacecraft pointing accuracies as antenna beamwidths (component or spot) shrink below one degree.

4. Interconnect and beam-forming network losses

As antennas have moved further away from the communications transponders on large spacecraft, interconnect losses have increased dramatically. Tower waveguide losses for the INTELSAT V 11/14 GHz antennas are 0.7 dB. Careful antenna location tradeoffs are necessary to minimize these interconnect losses. Multiple reconfigurable beam feed system losses have also increased along with performance demands. The INTELSAT V transmit hemi/zone beam-forming network has a loss of approximately 1.5 dB. Beam-forming network losses of 2-5 dB are expected in the future as performance demands become more stringent. A high degree of beam reconfigurability, for example, implies large beam-forming network losses. Increasingly in the future, active front-end receiver(s) or power transmitter(s) units will be physically located with the associated antenna subsystem to overcome the effects of either beam-forming network or interconnect losses on G/T and EIRP parameters. Careful assessment of rf shielding, feed location, temperature environments and materials technology will be necessary. Active antennas will increasingly be required to meet the most demanding of communications spacecraft antenna performance requirements.

Interconnect waveguide or cable losses have been reduced in some terrestrial and earth station applications by using beam waveguide configurations (essentially free space propagation in large over-moded waveguides) having much lower losses. Such systems may also find application on spacecraft employing many widely separated large antennas. Lightweight fiber optic connections may also replace conventional waveguide and cable runs.

5. Materials technology

Materials technology is becoming an increasingly important aspect of antenna design. Larger, more complex antennas and feed arrays have brought about the use of innovative materials and construction processes. Demand for lightweight, thermally stable materials such as graphite fiber reinforced plastic - GFRP (rf reflective) and Kevlar epoxy (rf transparent) will grow as surface accuracy and temperature environments become more stringent. The use of larger antenna structures will also couple solar reflectance and torque into materials technology considerations. Deployable reflectors, lens, or arrays with stringent mass, surface accuracy, and alignment constraints will place tremendous demands on materials. One of the greatest problem areas in recent spacecraft antenna designs has been mechanical construction techniques and materials. Spacecraft designs which thermally isolate antenna feeds and reflectors far from the main spacecraft body have led to large temperature excursions in antenna system components as Table 1 shows. Maintaining complex feed array amplitude and phase coefficient variations within acceptable limits (generally ± 0.3 dB, ± 15 degrees) has been a troublesome problem primarily as a result of the applied materials technology. The effects of different antenna locations, active and passive thermal control subsystems, and basic materials technology considerations will increasingly need attention early in the antenna design process.

6. Deployment and positioning mechanisms

Mechanical deployment and in-orbit repositioning of reflectors, subreflectors, and feed systems will be increasingly common in the communications satellite antenna designs of the future. The achievable alignments, surface accuracies, and thermal/solar interactions will be major determinants of final system level performance. Active beam repositioning will likely become necessary with the narrow beamwidths contemplated. RF (ground based beacon) sensing or localized spacecraft mechanical sensing is possible. As the number and overall size of antennas grow, it may well be necessary to independently control the pointing of several antenna subsystems. Deployment and positioning mechanisms are generally single point failure assemblies. Their design for operation in a 0 g environment is complicated by the task of finding suitable alignment and testing procedures in a 1 g environment.

Fig. 3 shows the INTELSAT V L-Band antenna array for the maritime communications subsystem (MCS) and illustrates just one small antenna subsystem that requires special deployment. A deployment arm is utilized to position the array in a location that minimizes scattering interactions with the adjacent reflector antennas while permitting a stowed configuration to accommodate launch vehicle fairing limitations (launch compatibility with Atlas-Centaur, Ariane and STS is maintained). In addition, an in-orbit pitch bias control of ± 2.00 degrees is provided by a positioning mechanism that rotates the deployment arm. The pitch bias is required to accomodate the optimization of INTELSAT V hemi/zone beam coverages for different orbital locations. Mechanical repositioning of simple shaped beams via either feed or reflector motion will continue to be an attractive alternative to reconfiguring beams electrically because of lower losses in many applications.

7. Measurement technologies and facilities

Automated, computer-controlled antenna ranges combined with swept frequency measurement of antenna parameters have enormously increased both the quantity and quality of data available. Nonetheless, limitations on amplitude, phase and polarization measurement accuracy due to test range and radome imperfections continue to be a major source of difficulty in developing improved spacecraft antennas. The limitations result in part from:

a. Range source antenna characteristics (particularly polarization isolation performance versus frequency and beamwidth).

b. Range geometries (specular reflections and total available distance between source and test antennas).

c. Radome materials (dielectric constant and thickness versus mechanical strength and lifetime requirements related to local weather conditions).

d. The necessity for an extended "quiet zone" test region when large antenna "farms" such as INTELSAT V are being evaluated.

e. Radome (multiple) reflections, particularly when testing sidelobe responses which require that the high gain main beam be variably pointed within the radome.

Multiple beam antennas with complex feed arrays utilizing feed element phase as a design parameter may also require range distances longer than the classical $2 D^2/\lambda$ criteria to simulate far-field antenna performance.

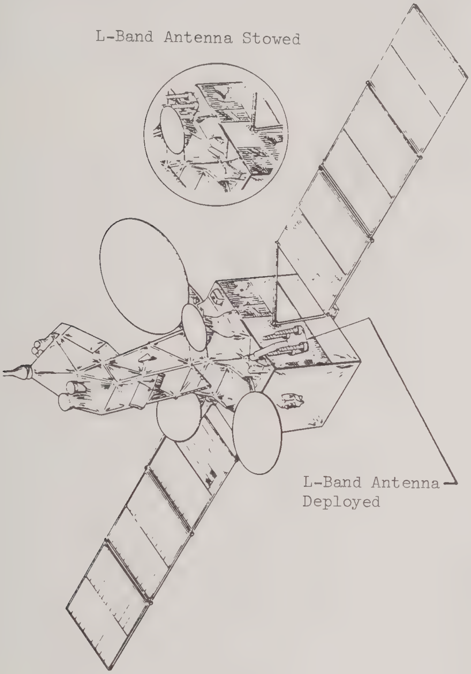

Figure 3. INTELSAT V L-Band Array Deployment Configuration

Near-field antenna test techniques which can substantially eliminate range and radome scattering problems have received considerable attention in recent years[10, 11]. These test techniques would considerably simplify the handling of the spacecraft (or antenna subsystem) during testing. The outdoor range and the necessity of transporting the spacecraft or antenna subsystem outside a high bay assembly area would be eliminated. Yet, such test methods have not been widely applied to communications satellite antenna designs. In the near-field techniques, the amplitude, phase, and polarization responses of the spacecraft antenna are measured over an extended surface area immediately in front of the antenna and these responses are computer transformed into the corresponding far-field patterns. The failure of near-field test techniques to accomodate communications satellite antenna swept frequency measurement requirements and a general lack of experience with such methods have been the primary reason they have not seen greater use to date. Near-field measurement techniques however will be used to a much larger extent in the communications satellite antenna designs of the future to eliminate dependence on the extensive outdoor ranges which would otherwise be required. They may also find interesting application as part of the spacecraft checkout facilities available on-board the space shuttle launcher.

Improvements in measurement technologies and facilities in general will be a key factor in achieving improved communications satellite antenna designs.

Conclusions

The remarkable evolution of communications spacecraft antenna performance parameters evidenced over the past two decades will continue throughout the 1980's. Spacecraft antenna performance will be a significant factor in realizing future higher capacity communications satellites. Recent antenna design problems and progress have brought about a new perspective. In addition to formulating innovative feed systems, beam forming networks, and reflector, lens, or array aperture configurations, future antenna system designs will have to become more systematic and interactive in seven key areas in order to realize stringent new performance requirements.

Mechanical design has become and will increasingly be a major determinant of ultimate in-orbit antenna performance. Optimization analysis and measurement of antenna subsystems must be performed taking account of the full antenna "farm" and spacecraft configuration. Indeed the configuration itself will become a major antenna subsystem design variable. Achieving 30-40 dB sidelobe and polarization isolation responses will require that early consideration be given to many design factors especially electrical scattering that heretofore have been considered "secondary" and hence neglected or evaluated "after the fact". Improved computer analysis programs and measurement technologies must be developed. Spacecraft attitude control and thermal subsystems will increasingly interact with the antenna design process. Intersatellite link antennas and active antennas will introduce a whole new breed of antenna performance requirements.

Finally, the antenna design engineer must continuously review and take full advantage of evolving communications spacecraft design possibilities. The complexity of many current antenna designs is in large measure a result of present launch vehicle packaging constraints. This complexity leads to fundamental performance and reliability limitations. Future antenna farm concepts utilizing space-erected, deployed or unfurlable antennas may be able to favorably trade complex antenna electrical designs for configurations with more but simpler antennas having overall improved electrical performance and reliability characteristics.

References

1. "Intelsat IV-A Transmission System Design," J. Dicks and M. Brown, Comsat Technical Review, Vol. 5, No. 1, Spring 1975, pp. 73-103.

2. "The Intelsat IV Spacecraft", E.T. Jilg, Editor, Comsat Technical Review, Vol 2, No. 2, Fall 1972, pp. 271-571.

3. "The Design of the Mechanically Despun Antenna For the Intelsat -III Communications Satellite", F. Donnelly, R. Graunas, and J. Killian, IEEE Trans. on Antennas and Propagation, Vol. AP-17, No. 4, July, 1969, pp. 407-415.

4. "Technology Considerations For the Use of Multiple Beam Antenna Systems in Communications Satellites", E.W. Matthews, C. L. Cuccia, M.D. Rubin, IEEE Trans. MTT, Vol. MTT-27, No. 12, December, 1979

5. "Reconfigurable Multi-beam Antennas For Satellite Communications," P. Foldes and M. Berkowitz, 3rd World Telecommunications Forum (ITU), Geneva, 24-26 Sept., 1979, pp 1561-15612.

6. "Control Aspects of Multi-beam or Multielement Spacecraft Antennas", P. Foldes, International Telemetering Conference (ITC-79), San Diego, 19-21 Nov. 1979.

7. "Design and Measurements of Satellite Antenna Systems For Frequency Reuse", R.W. Kreutel and W.J. English, Eascon-74 Conference Record, Washington, D.C., 1974, pp 513-518.

8. "The Orbital Antenna Farm Concept", W. L. Morgan and B. I. Edelson, Journal of the British Interplanetary Society, Vol 32, July 1979, pp. 243-254.

9. "Antenna Technology For Frequency Re-use Satellite Communications", R.W. Kreutel, D. DiFonzo, W. J. English, R. W. Gruner, Proc. IEEE, Vol. 65, No. 3, 1977, pp. 370-377.

10. "Determination of Far-Field Antenna Patterns From Near-Field Measurements," R. C. Johnson, H. A. Ecker, J. S. Hollis, Proc. of IEEE, Vol. 61, No. 12, December 1973, pp. 1668-1694.

11. "Basic Theory of Probe Compensated Near-Field Measurements", D.T. Paris, W. M. Leach, and E. B. Joy, IEEE Trans. on Antennas and Propagation , Vol. AP-26, No. 3, May 1978, pp. 373-379.

80-0555

SYSTEM TRADE OFF ON 20-30 GHZ MULTISPOT BEAM ANTENNA REQUIREMENTS FOR A DOMESTIC COMMUNICATION SATELLITE

*G. Manoni - G. Perrotta **
Selenia S.p.A.
Rome - Italy

Abstract

This paper is concerned with a system trade-off on 20-30 GHz multispot beam antenna requirements for an Italian communication satellite to be launched in the decade 1990-2000.

On board regeneration, SS-TDMA access method, frequency reuse and multibeam antenna are the main characteristics of the envisaged system.

In order to be able to reuse the frequency, meeting a required carrier to interference protection ratio under heavy propagation attenuation experienced at 20/30 GHz frequency band, a study of the constraints in the sidelobe and co-cross polarization level of the multiple spot beam antenna have been done and the constraints imposed on antenna configuration identified.

1. Background

A domestic satellite working at 20 and 30 GHz is presently being considered in Italy for serving the Intercity communication needs in the decade 1990-2000.

The operational system configuration studies under way (Ref. 1) are preparatory to the technology definition for both the satellite and the ground segment hardware.

An experimental phase will be defined before the end of 1980, aiming to achieve system concept validation, through in orbit tests of a satellite payload emboding key system features and carrying technological items by '84 ÷ '85, whereupon the final system development - with a technology uprating if required - will take place aiming at an operational satellite launch by 1989 ÷ 1990.

Some similarities in techniques and technologies between domestic needs and European Communication System Requirements exist (Ref. 2): accordingly part of these studies are conducted under European Space Agency (ESA) coordination. In the frame of the ESA's ASTP(*) the study of applications of the 20-30 GHz bands and overall system's architecture, and the design and development of advanced 20-30 GHz Repeaters and Multiple Spot Beams Antennas have been awarded to Italy.

2. System Outline

The Domestic Communication System aims to transmit via satellite a good portion of the trunking telephone traffic between the twenty Compartimental Centers of the Italian Telephone network; the traffic projections, by end of 1990, would imply an end of life satellite capacity of more than 150.000 telephone channels (Ref. 1).

The required RF bandwidth, assuming digital modulations and typical filling factors around 0.8, is about 3.8 GHz with DSI (Digital Speech Interpolation) and the double of this value without DSI. Clearly only the 20-30 GHz band may accomodate this capacity, and the 2500 MHz bandwidth there allocated would be re-used from 1.5 to 3 times.

Frequency re-use by polarization discrimination at 20 and 30 GHz is still controversial at this moment, and thus re-use will be exploited mainly by spatial discrimination. A multiple spot beam satellite antenna is used with high gain per spot beam, which is concurrent with the need for providing high satellite G/T and EIRP per channel considering that:

- almost all rain fades must be accounted for by large link margins in clear weather conditions
- cost reasons, and the operational requirement of putting the ground terminals directly at the Traffic Centre Premises, do suggest to avoid space diversity stations, except for climatically very unfavoured sites.

SS-TDMA with one transponder per channel per station on board the satellite is the baseline approach. This allows to use relatively simple continuous operation modems at the ground stations, with Continuous Frame Multi Destination (CFMD) carrier per each channel in the uplink; and a downlink which is a Continuous Frame Multiple Origin Single Destination carrier per station. Intra stations connectivity - that is origin to destination switching - is performed at baseband at the satellite as a consequence of the choice of SS-TDMA with continuous operation ground stations modems (Ref. 3, 4).

Baseband switching brings with it the need for on board demodulation of all input CFMD carriers and remodulation onto indipendent carriers of all the switched Multi Origin Single Destination frames.

At present the system bit rate, and thus repeater channel bandwidth, has been chosen as a compromise between the average per station traffic, system filling factor, and technology maturity. The bit rate is 360 Mbit/sec, for a satellite system interfacing with digitalized terrestrial network using, extensively, DSI. Should DSI not be implemented even higher bit rates might be considered.

A number of system trade offs oriented the satellite configuration to provide direct connectivity only for thirteen of the twenty Compartimental Centers, the other seven routing, via terrestrial radio links, their traffic to the closest Compartimental Center.

Thirteen satellite spot beams are thus envisaged (Fig.2.1) in a one station per spot scheme and while four stations have a traffic justifying two 360 Mbit/sec channels, all the remaining stations have only one 360 Mbit/sec channel, for a total of seventeen 360 Mbit/sec channels.

Table 2.2 gives the key system features and link parameters for the case under study (Ref. 5).

---

* System Engineer

** Head of System Engineer Group

(*) ASTP = Advanced Support Technology Program

Copyright © American Institute of Aeronautics and Astronautics, Inc., 1980. All rights reserved.

System parameters for 360 Mb/sec	Uplink Budget		Downlink Budget	
	Bit error rate 10^{-6}	Bit error rate 10^{-3}	Bit error rate 10^{-6}	Bit error rate 10^{-3}
Transmitter power (dBw)	15.5	28.5	12	12
Hardware losses (dB)	2	2	2.5	2.5
Transmitting antenna gain (dBi)	57.3	57.3	55	55
EIRP (dBw)	70.8	83.3	64.5	64.5
Free space attenuation (dB)	214	214	210.5	210.5
Atmosphere attenuation * (dB)	2	23	1	11
Receiving antenna gain (dBi)	59.5	59.5	54	54
Pointing losses and antenna aging (dB)	1.2	1.2	1.1	1.1
Noise temperature (dBK)	31	31	26	27.5
C/N 1 MHz (dB)	50.7	42.7	48.5	37
Bit rate (Mbit/sec) (dB)	25.6	25.6	25.6	25.6
Available E/No (dB)	25.1	17.1	22.9 **	11.4
Required E/No with interferences (dB)	16.7	12.7	16.2 **	10.3
Margin (dB)	8.4	4.4	6.7 **	1.1

TABLE 2.2 - LINK BUDGET KEY PARAMETERS FOR 360 MB/SEC

Note * : these values are related to a particular italian climatic zone which experiences rain attenuations in between the minimum and maximum values

Note ** : These values are relevant to the case of no down path power control.

3. Satellite Antenna Requirements and constraints

System performance factors: (table 3.1)

a) Ground segment

- System connectivity requires a large number of spot beams and small spot to spot distances, hence large antenna dimension;
- Low ground station's G/T and EIRP characteristics, set by cost considerations, demand very high satellite G/T and EIRP.
  Uppath Power Control (UPPC): under heavy uplink attenuation conditions, it may be required to adaptively vary the ground station transmitted EIRP to keep constant the carrier flux density at the satellite.
  UPPC affects the ground terminal design, and is therefore a major system decision.

b) Propagation factors

Link availability under severe rain attenuation conditions confirms importance of satellite antenna gain - as the prime requisite.
The different rain depolarization and attenuation characteristics, in circular or linear polarization, set a preference for linear polarizations, preferably with the plane of polarization coplanar with the local vertical (Ref. 6).

c) Transmission impairements

Cochannel Interference (CCI), and Adjacent Channel Interference (ACI) must be minimized.
Antenna sidelobe control and choice of polarization on contiguous spot beams are the main trade-offs areas, against antenna peak gain maximization and propagation factors.

d) Satellite and Launcher restraints

Mass, volume, and satellite configuration limit the size of the antenna reflector, and the launcher type sets constraints to the antenna configuration.
Re-use of the same reflector surface at the transmit and receive frequencies, is one approach which is in conflict with gain and interference optimization criteria before mentioned. It implies complex feed networks worsening the channel transmission characteristics.

e) Down path power control (DPPC)

To save DC power - all transponders could radiate normally at reduced power level, except those connected to beams aimed at the stations experiencing unfavourable propagation conditions. This may be achieved e.g., using a bi-level TWTA per channel.

f) Pointing accuracy

Satellite attitude errors require sophisticated antenna orientation and pointing control systems, and anyway limit the achievable EIRP and G/T due to residual pointing errors.

g) Costs

Satellite costs have a direct impact on the technology choices.
Materials and manufacturing techniques, will limit the size of the antenna.

In this range of frequencies and sizes, the updating of measurement techniques of both electrical and mechanical nature, is a major cost factor.
A good compromise between requirements and constraints was found, for the 20/30 GHz domestic system, in satellite antenna diameters between three and five meters as discussed in the following sections.

System performance Factors	Resulting Satellite Antenna Requirements
GROUND SEGMENT	
1. Connectivity	Large number of spot beams
2. Low Ground Station EIRP & G/T	High satellite G/T & EIRP: large antennas
3. Ground station transmitter UPPC (uppath power control)	Antenna sidelobe control
PROPAGATION	
Link availability	High satellite G/T & EIRP Linear polarization, preferably vertical throughout
TRANSMISSION IMPAIREMENTS	
CCI & ACI Control	Antenna Sidelobe control Orthogonal polarization on contiguous beams may help in controlling CCI & ACI

System Restraints	Resulting Satellite Antenna Constraints
LAUNCHER CONSTRAINTS	
Mass, Volume	Diameter of antennas: max gain (G/T, EIRP)
Geometry	Type of antennae, number of antennae, number of spot beams, achievable sidelobe control
SATELLITE CONSTRAINT	
DC power	Down path power control: antenna sidelobe control required,
Attitude control	Pointing losses: size of antenna, max gain per spot
COSTS	
Materials, Manufacturing & Measurement techniques	Diameter of antenna: max gain efficiency

TABLE 3.1 - SATELLITE ANTENNA REQUIREMENTS AND CONSTRAINTS

4. Antenna related system trade offs

4.1 Candidate System Configuration

A few antenna configurations were evaluated against the coverage requirements to compare their viability (fig. 4.1-2).
Coverage of the ground stations as in fig. 2-1 is considered, in the two limit cases of:

a- all twenty compartimental centers accessing the satellite;

b- only thirteen compartimental centers accessing the satellite.

A satellite stationed at 13° east is assumed.
Typical values of the angular distance - in satellite coordinates - between the considered compartimental centers are shown in table 4.1-1.
Fig. 4.1-3 shows for some antenna configurations, the range of antenna diameters that can be considered.
These antenna configurations are:

D_1: a single antenna dish concept, with one station per spot, one feed per spot, constrained by a minimum beam to beam spacing of 1.15 Bw: for D_1 the applicability bound is given by $Bw_{min} \cong \Theta_{i(min)}/1.15$;

D_2: two or more antennae concept with one station per spot, one feed per spot, constrained by a minimum beam to beam spacing of 1.15 Bw: for this configuration the lower bound is roughly given by $Bw \cong \Theta_{i(avg)}$ 1.15 for N=2 (N = number of antennae)

D_3: as D_1 with more than one station per spot. For three stations per spot an empirically found formula is: $Bw\ min \cong 1.2\ \Theta_{i(avg)}$

D_4: as D_2, with more than one station per spot. Figure 4.1-3 gives three points, from coverage exercises done for the italian case

D_5: a single antenna dish concept, with one station per spot, a feed cluster per spot allowing partial beam overlapping between the spots of the same antenna.

In principle D_5 can find application in the region of diameters below that of D_1; fig. 4.1-3 gives two possible points derived by coverage exercises for the italian case, one of which is shown in fig. 4.1-4.
Size constraints due to the requirement of a satellite compatibility with both ARIANE and Shuttle launches set at about five meters the upper bound of the antenna diameter, assuming rigid deployable antennas on board the satellite, thus excluding D_1.
Configurations D_3, D_4 are characterized by very low

gains in the directions of the stations, for a given antenna size, see table 4.1-5. Thus only configurations D_2 and D_5 were retained for further comparison.

4.2 Antenna efficiency considerations

A useful measure of the antenna efficiency is the ratio between the average spot beam gains G in the direction of the ground station(Sj) in the network, and the antenna aperture area A:

$$1)\ \eta_c = \frac{\sum_{j=1}^{K} G(Sj)}{K \cdot \frac{4\pi}{\lambda^2} A}$$ K is the number of stations

The net gain G (Sj) is given by:

$$2)\ G(S_j) = G_p \cdot \eta_{BS} \cdot \eta_{OFF} \cdot \eta_{PE} \cdot \eta_{SL} \cdot \eta_{INT} \cdot \eta_{TEC}$$

where:

G_p = peak gain of the beam, assuming optimum reflector illumination conditions;

η_{BS}= efficiency loss in a multispot beam antenna when the beam to beam spacing is lower than about two beamwidths;

η_{OFF}= efficiency loss due to the position of the j-th station inside the beam;

η_{PE}= efficiency loss due to antenna beams pointing losses including: satellite attitude errors, asymetric antenna deformations (aging and thermal) antenna spot beams mutual alignements;

η_{SL}= beam scanning loss;

η_{INT}=is the equivalent antenna efficiency loss due to interferences and is discussed in detail in para.4.3;

η_{TEC}=efficiency loss inherent to the technological implementation of the antenna

When comparing different configuration in a small range of diameters the factors $\eta_{PE} \cdot \eta_{SL} \cdot \eta_{TEC}$ are nearly independent of the size and the product $\eta_{BS} \cdot \eta_{OFF}$ is to be optimized. The influence of η_{INT} is considered at a later stage.
An example of such an optimization procedure is shown in fig. 4.2-1 for a D_2 configuration with N= two and a four meters diameter starting from the data of figg. 4.2-2 and 4.2-3.
A figure of merit, Q,is defined as follows:

$$Q = \frac{\sum_K \eta_{BS} \cdot \eta_{OFF}}{K \cdot \eta_{BS/}}$$ for a beam to beam spacing of 1.3 Bw

An optimum configuration results for a BBS = 1.3 Bw at 20 GHz and the beams configuration for Italy coverage is that shown in fig. 2.1.

4.3 Interference considerations

4.3.1 Co-Channel Interference (CCI)

In system re-using the frequency by spatial or polarization discrimination the co-channel is the most dangerous interference:fig.4.3-1 gives some theoretical and experimentally measured bounds for the E/No degradation due to co-channel interference.
For equal strength signals arriving at,or departing from the satellite on two spot beams, the CCI is only dependent on the sidelobe level of the beam j-th in the direction of the interfering station Si (fig. 4.3-2).
Since the E/No degradation is equivalent to a G/T degradation in the uplink and to satellite EIRP degradation for the down link, the E/No degradation can be directly interpreted as an equivalent antenna gain loss, hence the introduction of factor η_{INT} in the (2) of paragraph 4.2.
It should be pointed out that in our system there is only one interfering channel that contribute to the E/No degradation, being the available bandwidth re-used no more than one time.
A synthesis of our studies is presented in figg.4.3-3 to 4.3-6. The main conclusions are:

Uplink

1- Uppath power control at the transmitting ground stations cannot be avoided; a range of 20 dB of control is probably an upper limit due to errors in the evaluation of the additional rain attenuation (ref.7), and limits in earth station transmitter.

2- Frequency re-use by copolar beams is possible, over the territory of Italy, only in case of very narrow beamwidths. Fig. 4.3-3 shows for several C/CCI ratios the minimum beam to beam spacing in beamwidths, for differential rain attenuation at stations A,B of 20 and 30 dB maximum.
The antenna sidelobe level plays an important role in establishing frequency re-use by beam discrimination on the same polarization. Using the data of fig.4.3-1 and 4.3-3, for beam to beam separation between three and six beamwidths the sensitivity is about 0.1 ÷ 0.2 dB E/No improvement per dB of improvement in the antenna sidelobe level.

3- For orthogonally polarized beams frequency re-use is possible over shorter distances (fig. 4.3-4) or - conversely - obtain better CCI ratios for a given angular distance at which the frequency is re-used.

Downlink

1- Down path power control can be used. However:

2- re-using the frequency in copolar beams, the DPPC technique increases the CCI level or - conversely - requires a greater beam to beam spacing for the same level of CCI (fig. 4.3-5).
The worst CCI ratio does not depend on the amount of attenuation experienced at the site receiving the wanted channel.

3- Re-using the frequency in orthogonally polarized beams permits (fig. 4.3-6) to set the beams very close together.

Furthermore in this case the CCI ratio does not sensibly depend on the degree of down path power control. There is however some dependence from the attenuation experienced at the site receiving the wanted signal, due to the relationship between attenuation and depolarization (ref.8).

The above data, applied to the Italian case, permit to outline possible cases of frequency re-use:

a- beams with the same polarization throughout;

b- beams re-using the frequency only with orthogonal polarization

c- a mixed case

Fig. 4.3-7 shows the resulting trade-offs between channel performance degradation (Δ E/No) from CCI, and the use of different polarizations in beams re-using the frequency.

Case a-

All beams in the same polarization. Criteria for frequency reuse: $\Delta\theta$ (beam spacing) greater than 0.62° corresponding to a beam to beam separation greater than 2.6 Bw at 20 GHz, and greater than 3.6 Bw at 30 GHz (points A, A' in figg. 4.3-3 and 4.3-5).

Case b-

The beams, re-using the frequency, have orthogonal polarizations. Criteria for frequency re-use: $\Delta\theta$ greater than 0.62° (points C, C' in figg. 4.3-4, 4.3-6). The E/No degradation improves by about 1 dB with respect to case a-.

Case c-

Beams re-using the frequency in the same polarization only for distant stations.
Other beams, reusing the frequency, in orthogonal polarization.

Criteria for frequency re-use:

Copolar beams: $\Delta\theta$ greater than 0.93° corresponding to a beam to beam separation greater than 3.9 Bw at 20 GHz, greater than 5.2 Bw at 30 GHz (points B, B' in fig.4.3-3 and 4.3-5).

Crosspolarized beams: $\Delta\theta$ greater than 0.36° corresponding to a beam to beam separation greater than 1.5 Bw at 20 GHz, greater than 2 Bw at 30 GHz (points D, D' in fig. 4.3-4 and 4.3-6). The E/No degradation is about 0.4 dB worst than case b-.

4.3.2 Adjacent channel interference (ACI)

With R frequency reuses the average channel has R co-channel, and 2 + 2 R adjacent channel interferers entering the interfered channel via the spot beam sidelobes. In the case considered ($R \leq 1$) there will be in average four possible adjacent channels interferers, one or two of which might possibly contribute significantly to the system E/No degradation.
This is shown in fig. 4.3-8 for various C/ACI levels. The worst ACI occurs when both the ground station transmitter and satellite TWTA work at saturation, since spectrum spreading will dominate with typical spectra sidelobes at -18 dB over the adjacent channel (ref.9). Considering the propagation characteristics, uppath power control and down path power control limits per previous paragraph, a summary of the expected worst case C/ACI level, in the uplink and downlink, is given in figg. 4.3-9, 4.3-10.
The use of sjacent channels in copolar beams is allowed for beam to beam spacings greater than one beamwidth. For beams spaced below one beamwidth, orthogonal polarizations should be used.

	CASE A	CASE B	CASE B value CASE A "
a) minimum angular distance between the two closest compartimental centers: $\theta_{i(min)}$	0.075°	0.15°	2
b) average angular distance between adjacent compartimental centers: $\theta_{i(avg)}$	0.167°	0.239°	1.44
c) maximum angular distance between the two most distant compartimental centers: $\theta_{i(max)}$	1.3°	1.3°	1
d) average distance minimum distance	2.3	2.22	

TABLE 4.1-1 - TYPICAL VALUES OF THE ANGULAR DISTANCE BETWEEN THE COMPARTIMENTAL CENTERS OF TABLE 2.1
SEEN FROM SYNCHRONOUS ORBIT.
SUBSATELLITE POSITION: 13° EAST

CONFIGURATION	NUMBER OF ANTENNAS	SPOTS	NUMBER OF STATIONS	ANTENNA DIAMETER	20 GHZ AVERAGE GAIN LOSS DB	20 GHZ MAX GAIN LOSS DB	REMARKS
D_2	2 2 3	13 13 20	13 13 20	4 MT 4.5 MT 5.5 MT	Negligible " "	0.3 0.2 0.1	The average gain loss is defined by $\frac{\sum_i L_i}{N}$ where N is the number of stations and L is the gain loss with respect to the peak gain due to the position of the station inside the spot. The max gain loss is the difference between peak and station gain for the most unfavourable station position. All the values are taken from coverage exercises and should then be considered as typical for the configuration performance.
D_3	1 1 1 1	6 9 11 12	20 20 20 20	2.8 MT 4 MT 4.5 MT 5.5 MT	1.2 1.4 1	2.5 3 2.3 2.7	
D_4	2 2 2	8 12 18	20 20 20	2.8 MT 4 MT 5.5 MT	0.9 0.7 0.4	1.3 1.1 1.15	
D_5	1	13	13	4 MT	0.1	0.4	

TABLE 4.1-5 - PERFORMANCE COMPARISON FOR CONFIGURATION $D_2 \div D_5$ IN THE SIZE RANGE 2.8÷5.5 MT.

5. Antenna candidate Concepts

Table 5.1 presents initial antenna concepts which were evaluated and the main results of the preliminary analyses: the first two were retained for deeper studies, still in course.
For both approaches, that is:

a- single offset fed reflector and

b- offset Cassegrain reflector

two kinds of feeding arrangements are being evaluated:

- one feed per beam - corresponding to configuration D_2 of paragraph 4.1. Two antennas, one with seven and one with six beams, would provide the required coverage of fig. 2.1
- a cluster of feed horns per beam - attempting to approximate a coverage similar to that shown in fig. 4.1-4. However this feed arrangement, which aims to achieve overlapped beams, from the same reflector, by using orthogonal polarizations in some of the feeds of each cluster, is unsuitable if a system with only one polarization throughout is finally chosen.

At present the single offset fed reflector type antenna, being simpler while meeting all requirements, seems the likely candidate. The final choice will depend on the satellite configuration.

6. Conclusions

There is at present a strong system bias towards the use of vertical polarization for all beams at both the receive and transmit frequency bands, since the link advantage due to the propagation characteristics is much greater than the impairement loss due to the C/CCI increase (fig. 4.3-7).
This conclusion may well be particular of the system under study which:

a) re-uses the frequency no more than one time;

b) excludes stations operating in space diversity and accordingly accepts the uppath power control as an unavoidable consequence.

Thus under severe rain attenuation both links are thermal noise limited and not interference noise limited, the C/CCI and C/ACI contributing by about 1 dB to the total transmission impairement losses. The requirement for antenna gain maximization predominates, thus, on antenna sidelobe level control.
With rather conventional antenna designs acceptable antenna sidelobe levels, compatible with gain values which result optimum from a system viewpoint, can be achieved. Single offset fed reflector, illuminated by a set of individual primary sources working at both 20 and 30 GHz, providing 6-7 spot beams per antenna dish, is the simplest approach that meets the requirements.

References

1. S. Tirrò "Utilization of the 20-30 GHz spectrum part for high capacity national communications" Proceedings of the "International conference on space telecommunications and radio broadcasting: objective for the 80's " - Toulouse 5-9 March, '79
2. Lopriore, Maccol, Woode "ESA activities for millimeter wave space communications" AIAA 7th Communications Satellite Systems Conference
3. S. Tirrò "Point to point satellite systems at 20-30 GHz" Proceeding of symposium on "Advanced satellite communications systems using the 20 and 30 GHz bands" Genoa 1977
4. Fiorica, Stengel "On board regeneration in a satellite communications system operating at 20-30 GHz" Proceeding of symposium on "Advanced satellite communication systems using the 20 and 30 GHz bands" Genoa, 1977
5. Tirrò, Drioli " Possibilities offered by artificial satellites for national communications in a large euro-

pean country"
Proceedings of the 3rd World Telecommunication Forum" - Genoa, September 1979

6. Vilar "Choice of polarization for earth space links at 30 GHz"
Proceeding of symposium on advanced satellite communication systems using the 20-30 GHz bands"
Genoa, 1977

7. P.A. Watson "Propagation factors in the design of 20 and 30 GHz telecommunication satellite systems"
IEE Conference publication n. 169 (Nov. 1978) part 2, propagation pp. 130-134.

8. R.G. Howell and alt. "20 and 30 GHz cross polarization measurements using the ATS-6 satellite"
Proceeding of meeting held at ESTEC Noordwijk
ESA SP 131, October 1977

9. L. Lundquist and alt. "Transmission of 4 Ø PSK TDMA over satellite channel"
IEE Transactions on communications - vol. 22 - number 9 - September 1974.

Acknowledgment

The authors are grateful to Mr. Doro G. for his contribution in determining the antenna electrical performances relevant to the proposed solutions.

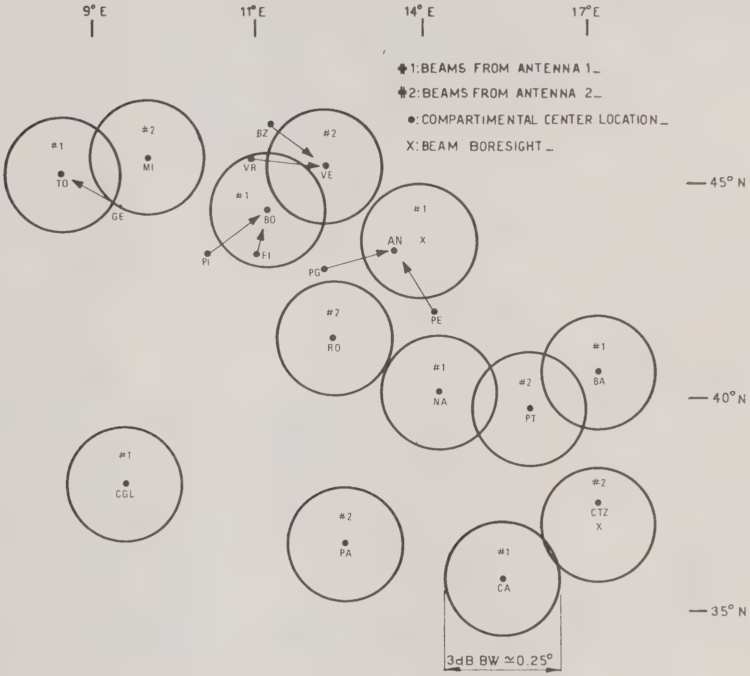
9° E
11° E
14° E
17° E
#1:BEAMS FROM ANTENNA 1_
#2:BEAMS FROM ANTENNA 2_
●:COMPARTIMENTAL CENTER LOCATION_
X:BEAM BORESIGHT_
45° N
40° N
35° N
#1
TO
#2
MI
GE
BZ
#2
VR
VE
#1
BO
PI
FI
#1
AN
X
PG
PE
#2
RO
#1
NA
#2
PT
#1
BA
#1
CGL
#2
PA
#2
CTZ
X
#1
CA
3dB BW ≃0.25°

FIG. 2.1 - ITALIAN COMMUNICATION SYSTEM COVERAGE AS SEEN FROM SATELLITE POSITIONED AT 13° EAST

ANTENNA CANDIDATE CONFIGURATIONS / PERFORMANCE PARAMETERS	A				B				C				D			
	SINGLE OFF-SET REFLECTOR 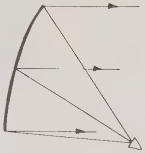				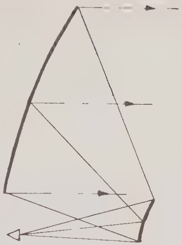 DOUBLE OFF-SET REFLECTOR				DOUBLE OFF-SET REFLECTOR WITH FREQUENCY SENSITIVE SUBREFLECTOR 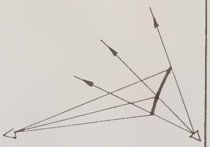				FULLY COMPENSATED DOUBLE OFF-SET REFLECTOR 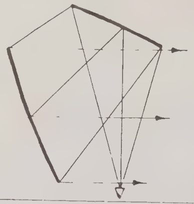			
A= WITHOUT FEED CLUSTER B= WITH FEED CLUSTER	A		B		A		B		A		B		A		B	
L = LOWER FREQ. BAND H= HIGHER FREQ. BAND	L	H	L	H	L	H	L	H	L	H	L	H	L	H	L	H
EFFICIENCY (NO BEAM DISPLACEMENT)	0.55	0.35	0.44	0.24	0.63	0.46	0.5	0.32	0.49	0.36	0.44	0.30	0.59	0.40	0.47	0.28
1ST SIDELOBE (DB) (NO SPACING DISPLACEMENT)	-26	<-30	-21	-25	-26	<-30	-21	-25	<-30	<-30	<-30	<-30	-26	<-30	<-21	<-25
CROSS POL. LEVEL (DB) (NO BEAM DISPLACEMENT)	<-18	<-26	<-20	<-26	<-20	<-30	<-20	<-30					-20	-30	-20	-30
SYSTEM DISADVANTAGES			ORTHOGONAL POLARIZATIONS ON OVERLAPPED BEAMS				ORTHOGONAL POLARIZATIONS ON OVERLAPPED BEAMS		QUITE LOW EFFICIENCY		ORTHOGONAL POLARIZATIONS ON OVERLAPPED BEAMS				ORTHOGONAL POLARIZATIONS ON OVERLAPPED BEAMS	
SYSTEM ADVANDANTAGES	EASY CONTROL OF INDIVIDUAL BEAM ANGULAR SETTING				SLIGHTLY BETTER EFFICIENCY				POSSIBLY BETTER CCI AND ACI LEVELS		POTENTIAL CONFIGURATION WITH ONLY ONE DISH INSTEAD OF TWO		APPARENTLY NONE			
MECHANICAL IMPLEMENTATION	SIMPLEST, 2 REFLECTORS NEEDED		MORE COMPLEX FEED NETWORK, MORE WEIGHT		MORE COMPLEX STRUCTURE, ALIGNEMENT PROBLEMS EXPECTED. MAY BE INTERFACES WITH SATELLITE CRITICAL		COMPLEX FEED NETWORK; MORE MASSIVE		TECHNOLOGY MOST CRITICAL, HIGHEST RISK FACTOR				TOO BULKY, SEVERE INTERFACE PROBLEMS WITH SATELLITE. STOWAGE PROBLEMS DURING LAUNCH PROHIBITIVE			

TABLE 5.1

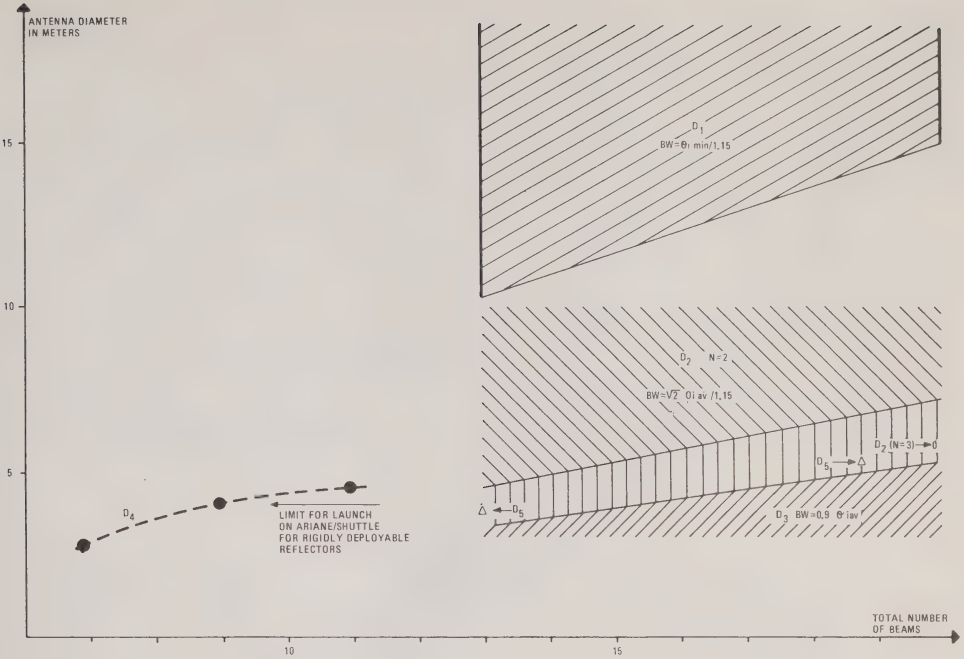

FIG. 4.1.3. - RANGE OF ANTENNA DIAMETERS

NAME	ANTENNA SCHEMATIC ARRANGEMENT	COVERAGE CHARACTERISTICS	RANGE OF ANTENNA DIAMTETER
D 1	ONLY 1 ANTENNA	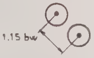 ONE STATION/SPOT ONE FEED/SPOT	ABOVE 10 mt
D 2	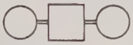 2 OR MORE ANTENNAE	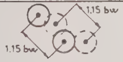 1.15 bw 1.15 bw ONE STATION SPOT ONE FEED/SPOT	FROM 4 mt. TO 10 mt.
D 3	ONLY 1 ANTENNA	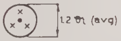 MORE THAN 1 STATION/SPOT ONE FEED/SPOT	FROM 3 mt. TO 5 mt
D 4	2 OR MORE ANTENNAE	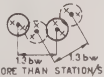 MORE THAN STATION/SPOT ONE FEED/SPOT	FROM 2.5 mt. TO 4.5 mt.
D 5	ONLY 1 ANTENNA	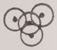 ONE STATION/SPOT A FEED CLUSTER/SPOT	FROM 4 mt TO 7 mt

FIG. 4.1.2. - EVALUATED ANTENNA CONFIGURATIONS

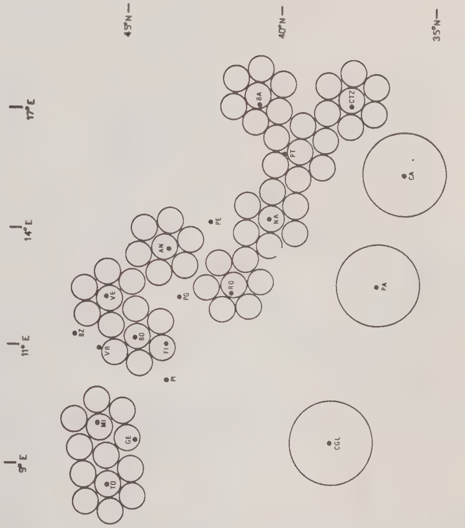
45°N
40°N
35°N
17°E
14°E
11°E
9°E
BA
CTZ
PT
CA
PE
NA
AN
RO
PG
PA
VE
BZ
BO
VR
FI
PI
MI
GE
TO
CGL

FIG. 4.1-4 - D_5 CONFIGURATION (ITALIAN) COVERAGE EXAMPLE AS SEEN FROM SATELLITE POSITIONED AT 13° E

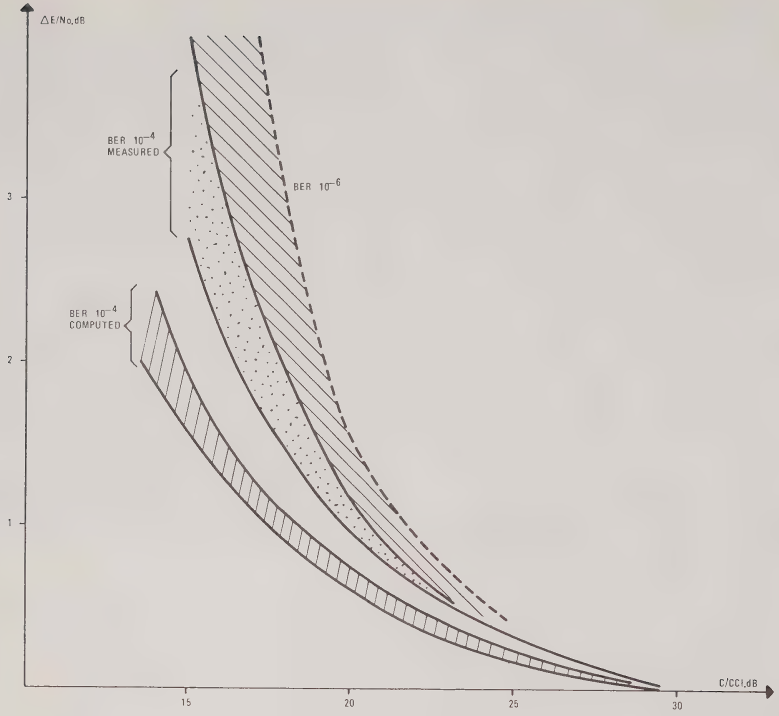

FIG. 4.3.1. - E/NO DEGRADATION VERSUS C/CCI INTERFERENCE LEVEL FOR VARIOUS BIT ERROR RATE.

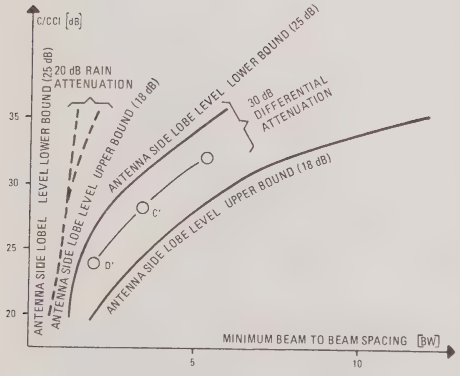

FIG. 4.3.4. - SYNTHESIS OF CARRIER TO CO-CHANNEL INTERFERENCE RATIO FOR UP-LINK CASE - SATELLITE CROSS POLAR BEAMS - 20 dB OF UP-PATH POWER CONTROL.

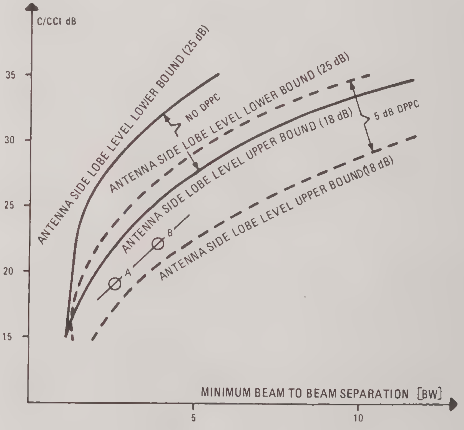

FIG. 4.3.5. - SYNTHESIS OF CARRIER TO CO-CHANNEL INTERFERENCE RATIO FOR DOWN-LINK CASE - SATELLITE CO-POLAR BEAMS - DOWN PATH POWER CONTROL AS INDICATE.

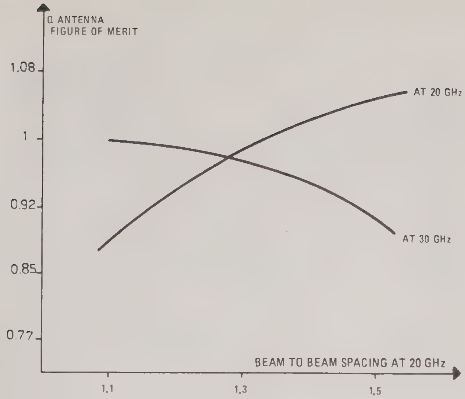

FIG. 4.2.1. - ANTENNA FIGURE OF MERIT. D_2 CONFIGURATION WITH TWO ANTENNAS OF 4 mt. DIAMETER.

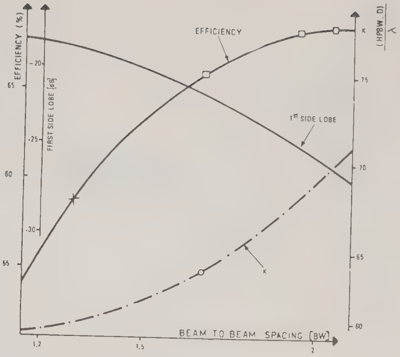

FIG. 4.2.2. - ANTENNA PERFORMANCE AT 18.95 GHz. OFF SET FED REFLECTOR ILLUMINATED BY A CONICAL HORN WHICH SUPPORTS THE TE_{11} MODE.

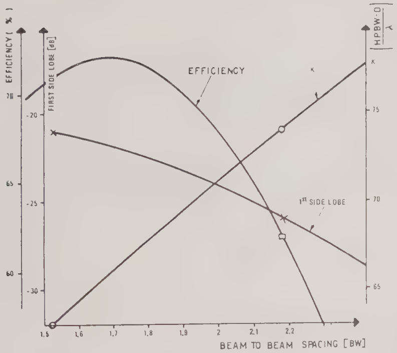

FIG. 4.2.3. - ANTENNA PERFORMANCE AT 28,75 GHz. OFF SET FED REFLECTOR ILLUMINATED BY A CONICAL HORN WHICH SUPPORTS THE $TE_{11} + TM_{11}$ MODE.

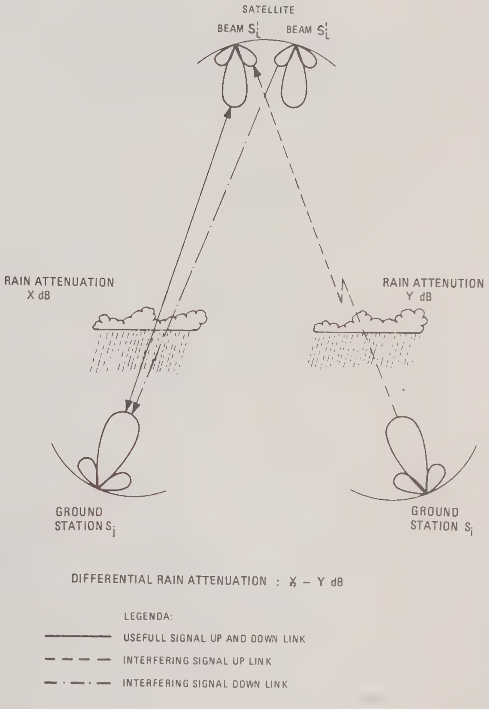
SATELLITE
BEAM S_i^j
BEAM S_i^i
RAIN ATTENUATION
X dB
RAIN ATTENUTION
Y dB
GROUND
STATION S_j
GROUND
STATION S_i
DIFFERENTIAL RAIN ATTENUATION : X − Y dB
LEGENDA:
USEFULL SIGNAL UP AND DOWN LINK
INTERFERING SIGNAL UP LINK
INTERFERING SIGNAL DOWN LINK

FIG. 4.3.2 - INTERFERENCE SCHEMATIC MODEL

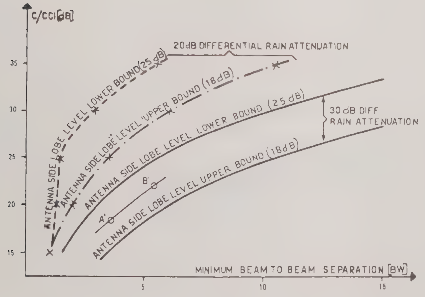

FIG. 4.3.3. - SYNTHESIS OF CARRIER TO CO-CHANNEL INTERFERENCE RATIO FOR UP-LINK CASE. SATELLITE COPOLAR BEAMS. 20 dB OF UP-PATH POWER CONTROL.

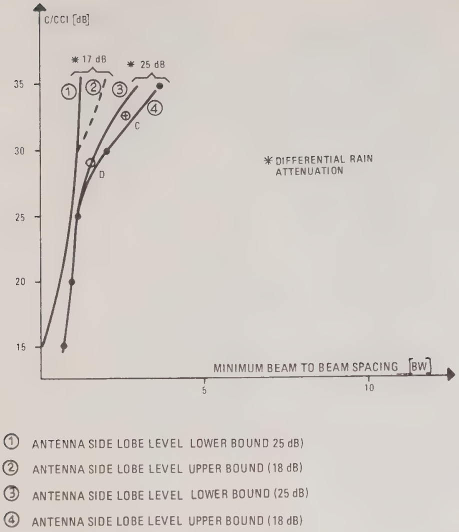

FIG. 4.3.6. - SYNTHESIS OF CARRIER TO CO-CHANNEL INTERFERENCE RATIO FOR DOWN-LINK CASE - SATELLITE CROSS POLAR BEAMS - VALID WITH AND WITHOUT DOWN-PATH POWER CONTROL.

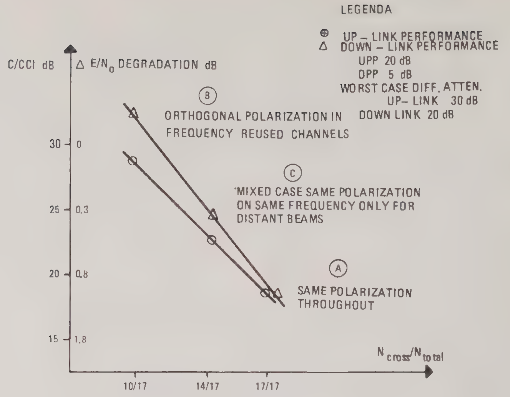

ANTENNA DIAMETER: 4 mt.
TOTAL NUMBER OF CHANNEL : 17
TOTAL NUMBER OF FREQUENCY RE-USED SLOT : 7

FIG. 4.3.7. - C/CCI AND E/NO DEGRADATION VERSUS THE RATIO OF NUMBER OF CROSS POLARIZED CHANNELS (N_{CROSS}) TO THE TOTAL CAHNNEL CHANNELS NUMBER (N_{TOTAL})

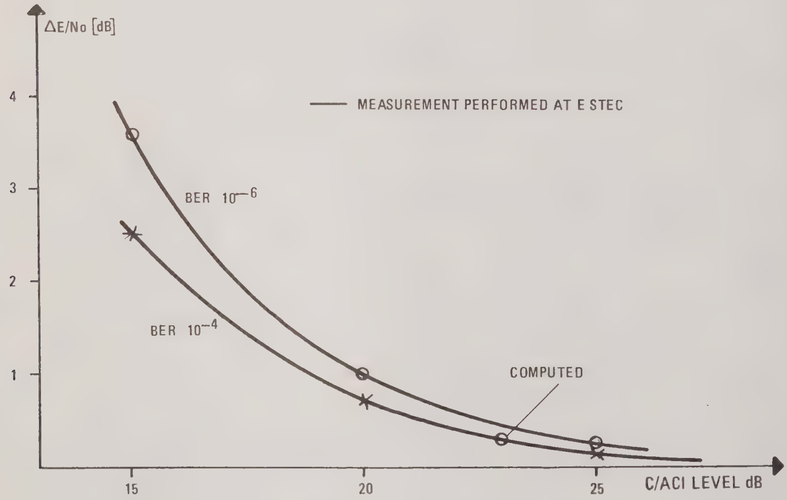

FIG. 4.3.8. - E/NO DEGRADATION VERSUS C/ACI INTERFERENCE LEVEL FOR VARIOUS B.E.R.

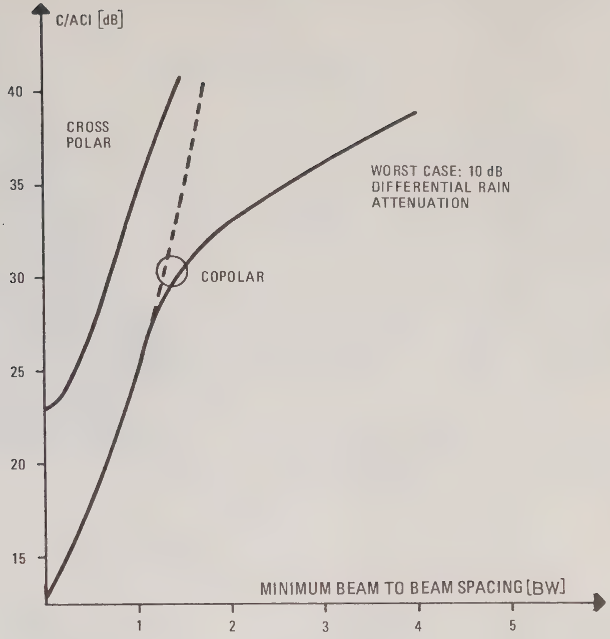

FIG. 4.3.9. - SYNTHESIS CARRIER TO ADJACENT CHANNEL INTERFERENCE RATIO FOR UP-LINK CASE - SATELLITE COPOLAR AND CROSS POLAR BEAMS - 20 dB OF UP-PATH POWER CONTROL.

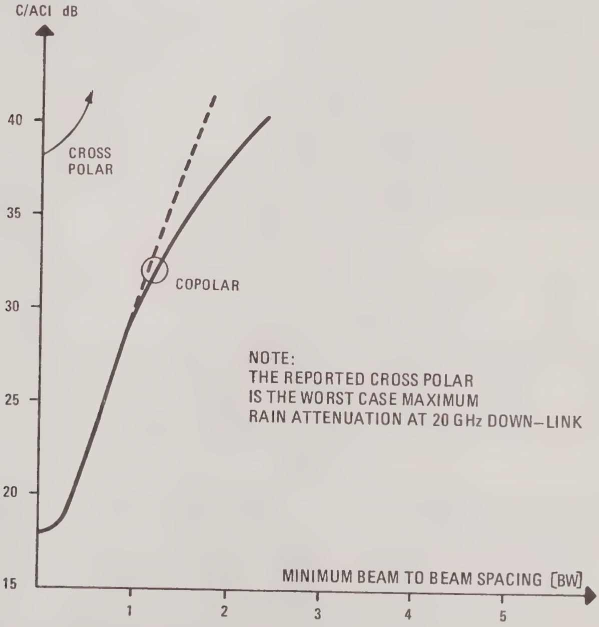

FIG. 4.3.10 - SYNTHESIS OF CARRIER TO ADJACENT CHANNEL INTERFERENCE RATIO FOR DOWN-LINK CASE - SATELLITE COPOLAR AND CROSS POLAR BEAMS - 5 dB OF DOWN-PATH POWER CONTROL.

80-0556

L-BAND PHASED ARRAY TRANSMITTER FOR COMMUNICATION SATELLITES

R. Coirault
European Space Agency
Noordwijk, The Netherlands

Abstract

An Electrical Demonstration Model of an L-Band phased array transmitter has been integrated and tested. It is fully representative of a communication satellite front end and can provide earth coverage with a cluster of 19 spot beams.

Tests in the laboratory, followed by a computer simulation, confirmed a total EIRP of 45 dBW and the spatial spreading of the intermodulation products. Outdoor tests on a far field range were in perfect agreement with the simulation results.

All the tests have been done with fully automatised test equipment. Large amount of data have been collected and processed, leading thus to a great confidence in the characterisation of the array.

Background

In order to cope with the ever increasing demand for worldwide communications, satellites represent still an attractive solution. However, the system engineer will have to face basic limitations in the natural resources available to him, especially the frequency spectrum and the DC power in the spacecraft. A more efficient utilisation of these resources will become mandatory and, consequently, satellite payload designs will have to evolve towards new concepts such as on board signal processing and generation of high gain spot beams.

As part of its Research and Development programme, the European Space Agency (ESA) is currently studying such advanced concepts (Ref. 1). In this context, the present article gives some of the preliminary results achieved in the development of a Phased Array Transmitter for direct radiation in the L-band.

Introduction

The ESA work in phased array techniques, particularly for communication satellites in L-band, has already been the subject of a presentation at the 7th AIAA Communications Satellite Systems Conference (Ref. 2).

Briefly one could recall the two essential motivations for this work:

a) The direct application to satellite systems for communication with mobile users, especially those equipped with modest terminal performances.

b) The flexibility of the concept which makes it possible to achieve high satellite EIRP without resorting to reflector deployment techniques.

The initial studies have been followed by the development of critical RF hardware (Ref. 2) and then by the integration/testing of a representative, full scale, Electrical Demonstration Model (EDM).

Design Constraints on the EDM

The EDM had to be as representative as possible of a satellite payload. This lead to the following design contraints.

i) Operating frequency in the L-band for communication with the maritime and aeronautical mobiles.

ii) Earth coverage from geostationary position.

iii) Mechanical, electrical, thermal characteristics compatible with the European Communication Satellite (ECS) bus.

iv) Critical RF units design as close as possible to flight standard (other units at commercial standard for cost effectiveness).

Furthermore it was also requested to implement automatic test procedure during integration and outdoor radiation measurements so that comprehensive and quick characterisation of the EDM performances be possible. The design parameters of these units have already been presented in Ref. 2. Measured data are indicated hereafter.

- *The Antenna Array* -

The array has an hexagonal outer shape. In order to match with the ECS bus, it consists of 18 radiating elements, all identical, positioned in a triangular lattice to give a structure of 11 λ.

The photograph of fig. 1 shows the array on the test range.

Each radiating element, of short backfire type, can generate left hand as well as right hand circularly polarised waves. Its outer diameter is 42 cm (2.2 λ). It can be operated both at transmit (1535-1560 MHz) and receive (1636-1661 MHz) frequencies. Excellent reproduction has been achieved during manufacturing at L.M. Ericsson.

The peak gain of each element is 15 dB and the gain at the edge of earth coverage is 14 dB. These data as well as other measured parameters have been processed by a calculator which simulated the complete array fed with perfect signals (i.e. without errors in amplitude and phase). The results have been plotted, see figure 2, and indicate that a minimum gain of 24 dB would be achieved from an 18 element system, capable of generating 19 spot beams towards the earth.

Released to AIAA to publish in all forms.

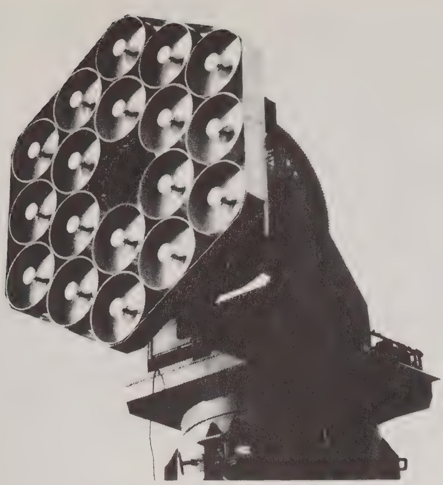

Figure 1: Array on the Test Range

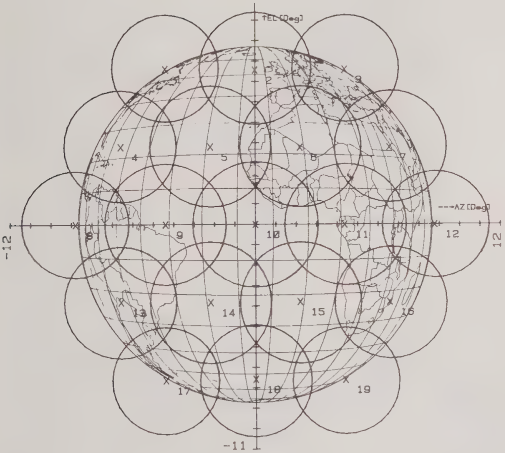

Figure 2: Array: 24 dB Gain Contours

- The Transistor Power Amplifiers - (TPA's)

The radiating elements of the array are fed by 18 linear TPA's manufactured by Mullard Ltd., they have the following performances:

- bandwidth (at 0.3 dB)	23 MHz
- gain	53 ± 0.2 dB
- phase tracking	< 5°
- output power	9W (rms)
- C/I (3 carriers)	> 23 dB
- efficiency	> 28%
- mass	< 600 g.

Typical input/output characteristics are shown in fig. 3.

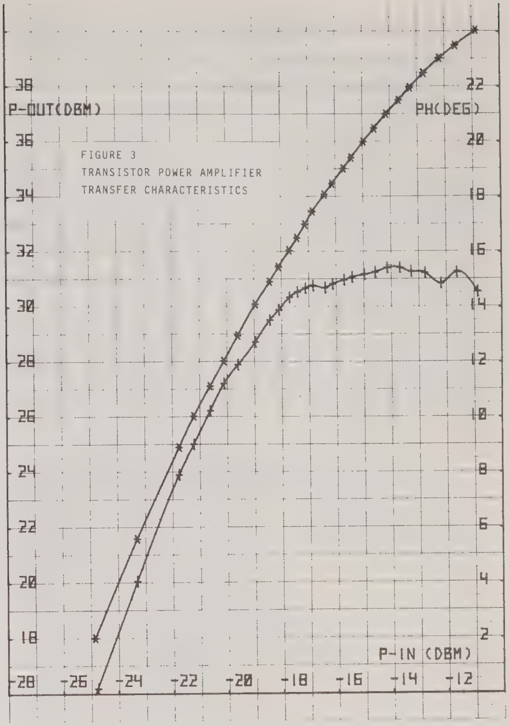

FIGURE 3
TRANSISTOR POWER AMPLIFIER
TRANSFER CHARACTERISTICS

The fact that Mullard have developed their own transistors for this applications has considerably helped in achieving these results.
The power transistor consists of 6 cells optimised for class AB Common Emitter operation. Each cell has an interdigital structure with an emitter pitch of 12 microns. The specified output power is achieved with two power transistors mounted in a balanced configuration.

A Commercial Power Conditioning Unit is associated to each TPA giving thus a rather compact assembly. However further improvement would be feasible in a flight model.

- The Up-Converters -

A set of 18 up-converters is associated with the TPA's. They translate the IF signals (30 MHz), delivered by the Beam Forming Matrix, to the operational frequency at L-band. Tough requirements on spurious signals and tracking led M.S.D.S., the manufacturer, to implement a novel design (Ref. 3) where the mixer is subharmonically pumped at 750 MHz.

Across the frequency band of 23 MHz, the gain spread between any two of the 18 up-converters is less than 0.5 dB rms and the phase tracking has been kept below 6° rms. These results have been achieved within the temperature range of -5°C to 50°C.
The 18 up-converters and the Local Oscillator distribution module weigh less than 2.7 Kg, the DC consumption is 7W.

- *The Beam Forming Matrix (BFM)* -

This unit, which operates at IF (30 MHz), is the heart of the EDM. It must generate, from each of its 19 beam inputs, the 18 element drive signals with the required phase/amplitude characteristics.

A resistive matrix concept (Ref. 4) has been selected for this application enabling thus significant advantage in mass, size, power consumption, reliability compared with other configurations employing phase frequency conversion.

Over the frequency range of 27.5 to 35 MHz and within the temperature limits of -5°C to +50°C, the average phase error is less than ± 2° and the mean gain spread is less than ± 0.35 dB. The variance of the error is, respectively, 2° for the phase and 0.1 dB for the gain. The weight of this unit, manufactured by MSDS, is 4.5 Kg and the DC consumption less than 20W.

The Electrical Demonstration Model

The main objective of the EDM was the assessment, with representative hardware, of the essential performances of a phased array transmitter at L-band.

The critical units, previously described, and other equipment necessary to operate the model have been mounted on a 1.6 x 1.2 platform. The block diagram of this assembly is shown fig. 4.

The two main phases of the test programme are described hereafter, with some emphasis put on the automatic test set up.

A. Integration Phase

The integration phase has taken place in a laboratory environment.

The elements, without radiating units, have been aligned first using the test set up shown on the block-diagram of fig. 5. The RF power at the antenna port being too high (~ 8W) for direct application to the Network Analyser (NA), the measurements have been done through the directional couplers. One element is permanently connected to the Reference Input of the NA. All the other elements (17) can be connected to the Test Input of the NA via a box of coaxial relays. A power dividing network inserted before the NA allows also power and spectrum monitoring of the signal.

The path from each directional coupler to the NA is carefully calibrated and the data are stored in the calculator. It is thus possible to refer the measurements done by the NA to the relevant antenna port.

With a single carrier at the input of the EDM the alignment is performed as follows:

1. One element is selected from the calculator keyboard.
2. The programme energizes the beam input 1. The amplitude and phase of the signal delivered by the NA is processed, as explained previously, so that they are referred to the antenna port of the selected element. The latter values are compared with the specification and an error is generated. All relevant information is then displayed and printed.
3. The sequence 2 above is then repeated for each of the 19 beam inputs.

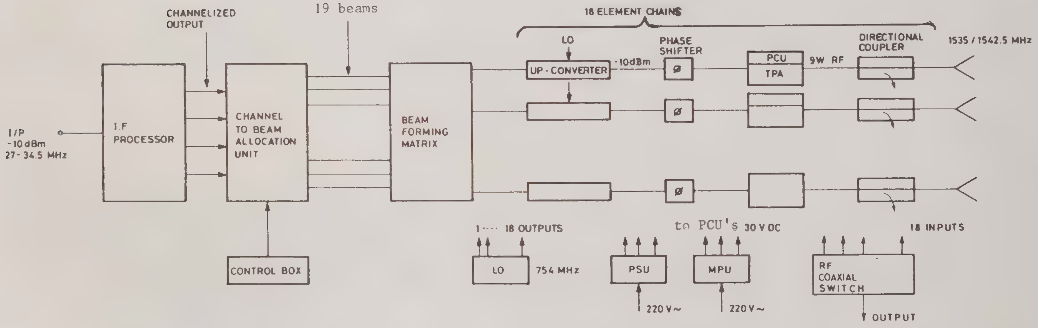
CHANNELIZED OUTPUT
19 beams
18 ELEMENT CHAINS
LO
PHASE SHIFTER
DIRECTIONAL COUPLER
1535 / 1542.5 MHz
UP - CONVERTER
-10dBm
φ
PCU
TPA
9W RF
I/P
-10 dBm
27-34.5 MHz
I.F PROCESSOR
CHANNEL TO BEAM ALLOCATION UNIT
BEAM FORMING MATRIX
1 .... 18 OUTPUTS
to PCU's 30 V DC
18 INPUTS
CONTROL BOX
LO
754 MHz
PSU
MPU
RF COAXIAL SWITCH
220 V~
220 V~
OUTPUT

TPA = TRANSISTOR POWER AMPLIFIER
LO = LOCAL OSCILLATOR
PCU = POWER CONDITIONER UNIT
MPU = MAIN POWER UNIT
PSU = POWER SUPPLY UNIT FOR LOW POWER DEVICES

Figure 4: EDM Block Diagram

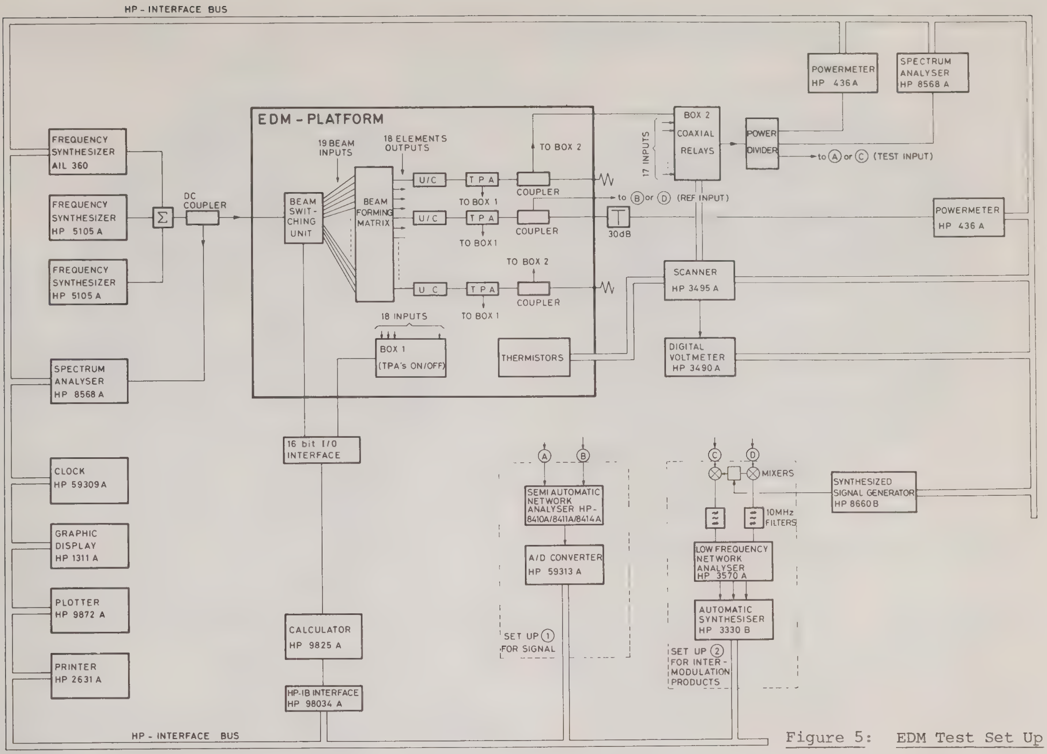
HP - INTERFACE BUS
POWERMETER HP 436 A
SPECTRUM ANALYSER HP 8568 A
EDM - PLATFORM
19 BEAM INPUTS
18 ELEMENTS OUTPUTS
TO BOX 2
BOX 2 COAXIAL RELAYS
17 INPUTS
POWER DIVIDER
to Ⓐ or Ⓒ (TEST INPUT)
FREQUENCY SYNTHESIZER AIL 360
FREQUENCY SYNTHESIZER HP 5105 A
FREQUENCY SYNTHESIZER HP 5105 A
Σ
DC COUPLER
BEAM SWIT-CHING UNIT
BEAM FORMING MATRIX
U/C
T P A
COUPLER
TO BOX 1
to Ⓑ or Ⓓ (REF INPUT)
30dB
POWERMETER HP 436 A
TO BOX 2
SCANNER HP 3495 A
18 INPUTS
BOX 1 (TPA's ON/OFF)
THERMISTORS
DIGITAL VOLTMETER HP 3490 A
SPECTRUM ANALYSER HP 8568 A
16 bit I/O INTERFACE
CLOCK HP 59309 A
GRAPHIC DISPLAY HP 1311 A
PLOTTER HP 9872 A
PRINTER HP 2631 A
CALCULATOR HP 9825 A
HP-IB INTERFACE HP 98034 A
Ⓐ Ⓑ
SEMI AUTOMATIC NETWORK ANALYSER HP-8410A/8411A/8414A
A/D CONVERTER HP 59313 A
SET UP ① FOR SIGNAL
Ⓒ Ⓓ
MIXERS
10MHz FILTERS
LOW FREQUENCY NETWORK ANALYSER HP 3570 A
AUTOMATIC SYNTHESISER HP 3330 B
SET UP ② FOR INTER-MODULATION PRODUCTS
SYNTHESIZED SIGNAL GENERATOR HP 8660 B

Figure 5: EDM Test Set Up

4. When all the beams have been energized, an average error is computed, as well as a standard deviation, for the phase and amplitude errors. These data are also printed.

5. The above sequence, from 1 to 4, is repeated for different frequencies in the bandwidth. In principle, and this has been verified in practice, the standard deviation is not much different from that measured on the BFM alone. The alignment consists then to offset, with phase shifter and attenuator pads, the average phase and amplitude errors.

6. Measurements as above, from 1 to 5, are repeated for each element, keeping always the same reference.

The sequence 1 to 5 took less than 45 minutes for each element. In this time more than 250 data have been collected and processed.

The photograph of fig. 6 shows the EDM, once integrated, and the test equipment in the ESTEC laboratories, in Noordwijk.

After the alignment of each element, the final results, i.e. the phase and amplitude of the signal at each of the 17 antenna port (compared to the references port) and corresponding to each of the 19 beams excitations, have been stored in a cassette. These data, combined with the pattern characteristics of the radiating units, have then been processed by a calculator which worked out the EIRP within the earth coverage. A typical example of plotted contours is shown in fig. 7.

Figure 6: EDM and Test Set Up

Correlation between phase/amplitude errors in the elements and EIRP performances is thus possible, although difficult to quantify. The elements have been aligned to ± 5° and ± 0.5 dB. The standard deviation of all the errors corresponding to all the beams/elements) is less than 5° for the phase and less than 0.3 dB for the amplitude.

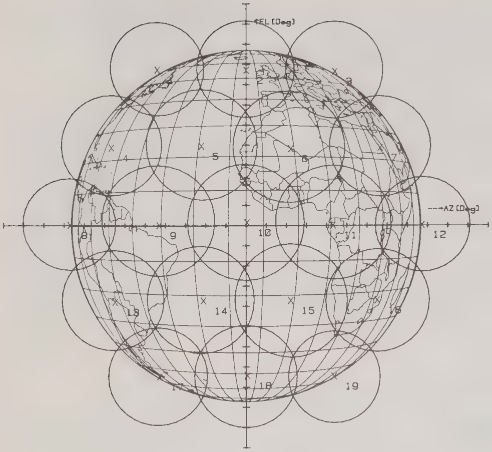

Figure 7: EDM Predicted 45 dBW EIRP Contours

EIRP PREDICTION

Plots are similar to the one shown fig. 7 but corresponding to various test conditions (frequency, temperature etc....), indicate that the minimum EIRP, within the earth coverage, is higher than 44.3 dBW for an average RF power of 20.5 dBW at the antenna ports. A perfect array (with 18 x 9W = 162W RF at the TPA's levels and 0.7 dB loss to the antenna port) would have given a minimum EIRP of 45 dBW. One can therefore conclude that a real array brings about a loss of 0.7 dB in EIRP compared with an ideal array.

INTERMODULATION PERFORMANCE

Operation with multicarriers has also been performed, with special attention paid to the intermodulation products (IMP). The test set up has been slightly modified since the NA could not discriminate between the various signals. The "set up 2" shown in the block diagramme of fig. 5 has therefore been implemented. Otherwise the measurement of the IMP signals has been done as described previously and the data processed similarly so as to give the EIRP of the IMP's.

Third and fifth order IMP have been considered and the plot of fig. 8 represents a configuration where three signal frequencies are radiated into different beams. As can be seen the IMP's are radiated in other beams the direction of which depends of which IMP is considered. These results are in perfect agreement with those predicted by a theoretical analysis of the phased arrays, that is to say that the array would improve the IM performances of the TPA by a factor of at least 10 dB leading to C/I, as seen by a ground terminal, of the order of 30 dB.

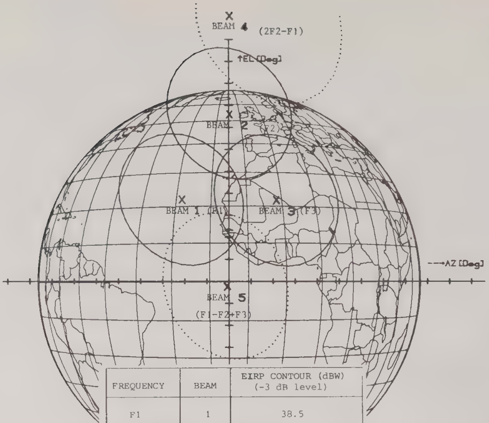

FREQUENCY	BEAM	EIRP CONTOUR (dBW) (-3 dB level)
F1	1	38.5
F2	2	38.2
F3	3	38.6
2F2-F1	4	11.7
F1-F2+F3	5	18.0

Figure 8: Signal and Intermodulation Beams

B. *Outdoor test phase*

The platform, previously integrated, has been assembled with the antenna array and mounted on an outdoor, far field, antenna test range at L.M. Ericsson in Sweden.

The turntable supporting the assembly can be elevated up to 33m above ground. On the receive site a 5.5m parabolic antenna is placed, with its associated equipment, on a pylon located at a distance of 1100m.

A telephone line is used to relay the data from the receiver to the control room. A desk calculator (HP 9845 A) is used to control the range (both on the transmit and receive sites) and to control/monitor the EDM as during the integration. The overall block diagram of the set up is shown in fig. 9

Signal EIRP pattern have been recorded, in two orthogonal plans for each of the 19 beams. It must be pointed out that, although the software took a long time to debug, the measurements have been done rather quickly in spite of the large amount of data involved. Intermodulation products EIRP pattern have also been recorded and, again, the calculator has been a powerful tool for this application.

Taking into account the inaccuracy inherent to the test range, the results obtained are in a very good agreement with the results that had been predicted in the integration phase. The beam peaks are within 0.10° (worst case 0.2°) of the expected value and the minimum coverage i.e. the beams cross over levels are about the same. The intermodulation beams are also in accordance with predictions.

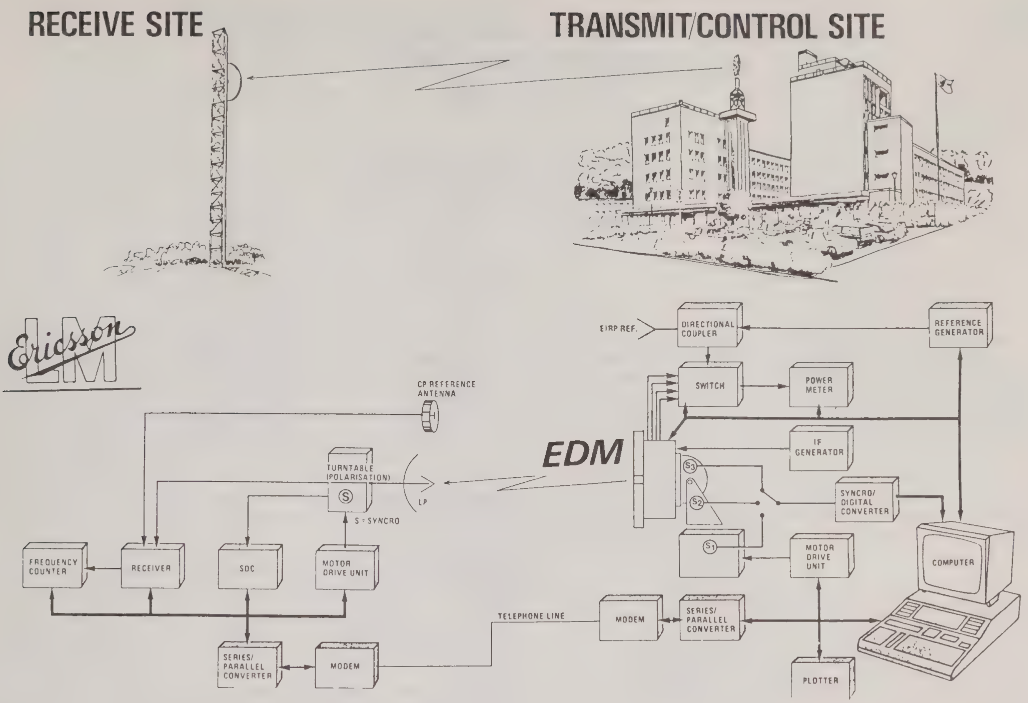
RECEIVE SITE
TRANSMIT/CONTROL SITE
Ericsson
LM
CP REFERENCE ANTENNA
TURNTABLE (POLARISATION)
S
S = SYNCRO
LP
EDM
EIRP REF.
DIRECTIONAL COUPLER
REFERENCE GENERATOR
SWITCH
POWER METER
IF GENERATOR
S3
S2
S1
SYNCRO/ DIGITAL CONVERTER
FREQUENCY COUNTER
RECEIVER
SDC
MOTOR DRIVE UNIT
MOTOR DRIVE UNIT
COMPUTER
TELEPHONE LINE
MODEM
SERIES/ PARALLEL CONVERTER
SERIES/ PARALLEL CONVERTER
MODEM
PLOTTER

Figure 9: Range Set up for EIRP Measurements

CONCLUSION

The main characteristics of a Phased Array Transmitter have been verified on a representative model at L-band. No special problem has been encountered during the manufacturing phase.

The automatisation of the test equipment, both in the laboratory and on the test range, made it possible to measure and process a large amount of data enabling thus a comprehensive characterisation of the phased array transmitter.

The results achieved confirm that phased array is a very powerful technique for direct radiation at L-band, without resorting to large deployable structures, to achieve high EIRP performances and flexibility in the apportionment of this EIRP in the various beams.
The EDM will be complemented with a receive section with 18 elements. The EDM will then be used as a test bed for more general system tests where various types of modems would be implemented.

ACKNOWLEDGEMENTS

The author would like to thank particularly Mr. W. Kriedte of ESTEC and Mr. A. Molker of L.M. Ericsson who have designed ans implemented the automatic test set up.

References

1. Technology development programme for communication satellite payload in ESA, by G. Mica - 8th AIAA communication satellites system conference, Orlando.

2. A multibeam array for communication with mobiles by J. Aasted and A. Roederer, 7th AIAA Communications Satellite Systems Conference. Proceeding, pages 400 - 406.

3. An 18 channel, phase matched. single conversion up converter from 30 MHz to L-band by A. Goacher, 8th European Microwave Conference (Paris) proceedings pages 146 - 149.

4. An Intermediate Frequency Beam Froming Network for a multibeam communication satellite antenna, by J. Carter, D. Ellis, D. Hindley, ICC 79, Boston.

80-0557

Ka-BAND, MULTIBEAM, CONTIGUOUS COVERAGE SATELLITE ANTENNA FOR THE USA

Peter Foldes*
General Electric Company, Space Division
Valley Forge Space Center
P. O. Box 8555
Philadelphia, Pa. 19101

1. Introduction

In recent years increasing attention was paid to the possibility of providing satellite communication coverage of the US by multibeam antennas. Because of the complexity of the problem in most cases a simplified antenna model was used from which some quantitative conclusions were drawn.

With the NASA decision to develop K_a-band multibeam satellite technology it became important to derive more accurate information about the capabilities and limitations of such a system.

It is assumed that spectrum convervation and optimum utilization of the Space Shuttle are major concerns. A given communication capability can be provided in decreasing allocation bandwidth as the antenna size and number of beams are increased. This approach, however, increases the complexity, cost and size of the communication payload and is eventually limited by the capability of the launch vehicle.

Under a NASA Lewis Research Center study contract, an accurate, vector field based computer program was employed to calculate the most important radiation characteristics of the required antenna. Eight different family of beam topologies were defined and analyzed. In these topologies the lower 48 states of the US were covered by a grid of circular footprints each with α "cell" diameter. The distribution of frequency bands and polarizations within the cells or component beams were different for the various plans. In order that the merits of the different plans could be compared the total communication capacity for standard weather conditions was kept constant at a nominal 250000 two-way voice channels for each plan. The up and downlink nominal minimum frequencies were 18 and 28 GHz respectively. The earth station antenna diameter was 2 m, the uplink transmit power 3.9 w/MHz, the peak transmit power available at the satellite PA output flange was 50 w, and earth station and satellite receiver noise temperatures were assumed to be 120°K and 712°K respectively.

It was assumed that the frequency allocation bandwidth for the down or uplink cannot exceed 2.5 GHz and it is desirable to limit it to much less. A further assumption was that unfurlable antennas with adequate accuracy and size cannot be expected for the application time period thus it is desirable to use solid surface, single section optics. This limits the aperture diameter of a single antenna to less than 4.5 m in order that it is Shuttle packagable.

Ideally the communication system must provide the designated capacity for a given geographical area in a traffic density match manner. In such a configuration the bandwidth is distributed optimally. Since user and traffic density varies within the overall coverage the available communication capacity must also vary. The resultant coverage is contiguous, but each cell within coverage shares the overall resources of the system according to its needs.1)

Such a traffic density matching results in less communication capability than a system in which the capability is maximized uniformly for the complete geographical area. The uniformly maximized communication capability is still a useful simple measure to compare various system concepts with each other. However, real life systems require traffic density matching, with a resulting lower capacity relative to the uniformly distributed capacity systems. Since improved matching in this sense reduces the system capacity the detailed design requires a compromise.

This compromise can be derived in two steps. First, the characteristics of basic antenna types can be established, which can provide the desired communication capacity and maximum reuse of the allocation bandwidth in a uniformly distributed manner. Second, necessary criterias can be established for modifying the basic systems into traffic density matched systems without any significant sacrifice in the utilization of spectrum.

It was found that for these conditions the most important characteristics representing system complexity are the following: satellite antenna diameter, number of feed horns, number of shaped beams (input terminals of the central onboard switch) average transmit power per shaped beam and average transmit power of the system.

The most important performance characteristics are the following: Total frequency band occupied by the communication system, bandwidth available within one shaped beam, bandwidth of a switched IF channel ("slot"), maximum bandwidth available within a "component beam", number of spectrum reuses, pattern slope at coverage contour and weather caused downtime.

Interestingly the most commonly used features of multibeam antennas, beam and polarization isolation did not appear directly as meaningful characteristics, however, their effect was included in the weather caused downtime.

---

*Manager of Antenna Engineering, Member AIAA

Table 1

Topology Characteristics of Studied Beam Plans

No.	Beam Plan	$\frac{\epsilon}{\alpha}$ Main Pol.	$\frac{\epsilon}{\alpha}$ Cross Pol.	Configuration	Number of Main Component Beams	Number of Auxiliary Component Beams in First Order Ring	Band Subdivision	Overlap
1	Triangular Layout Singlets, Single Pol.	1.232	NA	Singlet	1	6	3	No
2	East-West Overlapping Novets, Dual Pol., Pol. Reuse Strips	1.5	.5	Sextet or Novet	6 or 9	12 or 14	2	One Dimensional
3	East-West Overlapping Triplets, Dual Pol,, Pol. Reuse Strips	1.7	.5	Line Triplet	3	10	2	One Dimensional
4	Triangular Layout Septets, Single Pol.	2.145	NA	Septet	7	12	3	No
5	Overlapping Quadrupets, Dual Pol.	2.345	1.232	Rhombic Quadruplet	4	10	8	Yes
6	Triangular Layout Doublets, Dual Pol., Pol. Reuse Spots	2.145	.5	Doublet	2	8	3	No
7	Rhomboidal Layout Singlets, Single Pol.	2.5	NA	Singlet	1	6	9	No
8	Rhomboidal Layout Triplets, Dual Pol.	3.105	1.5	Triplet	3	9	4	No

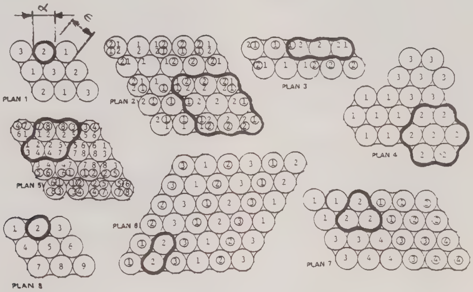

Detailed computer simulation of the achievable radiation characteristics with an offset fed paraboloid antenna with various beam topology plans was carried out. These calculations indicated that most of the commonly assumed beam topologies result either extreme complexity or poor performance for certain characteristics.

However, for the most favorable topology plan an acceptable compromise can be found between these conflicting requirements.

2. Three Central Issues

There are three central issues: 1) Selection of beam topology, 2) Determination of radiation characteristics, 3) Realization of antenna circuits.

The beam topology is concerned with the selection of the number of antenna beams, their spatial distribution, assignment of frequency-bands and polarizations to various users in the system. Generally the multibeam antenna produces n component beams from which N_B shaped beams are formed. The allocation bandwidth of the system, ΔF is divided into n_s channels with a bandwidth of $B = \Delta F/n_s$. A channel is assigned to each of the N_B shaped beams. Generally the B channel bandwidth is assigned to many shaped beams, thus the spectrum is reused. In order to provide adequate isolation between these beams they must be spatially separated or orthogonally polarized or both. Thus the contour of beam coverage footprints and their relative spatial distribution plays a major role in determining the achievable isolation between beams.

Virtually infinite topology plans can be visualized. Among these Table 1 exhibits eight examples. The examples are selected to represent various classes of topologies. Thus the results can be easily generalized and they cover most of the practically important configurations. The analyzed topology plans include shaped beams with single and multiple component beams, single vs. dual polarized systems and non-overlapping vs. overlapping shaped beams. Additionally the various plans allow a wide variation of the angular guard width between identical frequency band identically polarized shaped beams. The width of such a guard angle is the primary parameter in the control of achievable beam isolation.

Utilizing the basic topology plans examples can be worked out with different component beam numbers for a coverage area corresponding to the lower 48 states. Figure 1 shows some practically interesting cases.

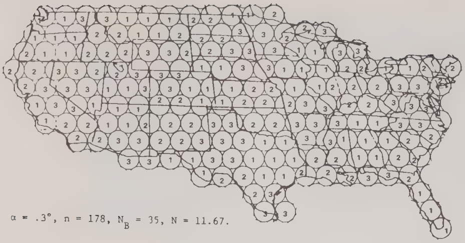

α = .3°, n = 178, N_B = 35, N = 11.67.

Figure 1.a. Beam Plan 4: triangular layout of septets, single polarization.

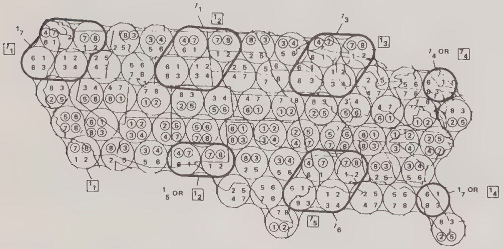

Figure 1.b. Serial No. designation of shaped beams for α = .5° Plan 5 and for modified Plan 5 (in brackets). Modification is for reduction of system complexity, resulting in N_B = 64 and N = 8. Channel 1.

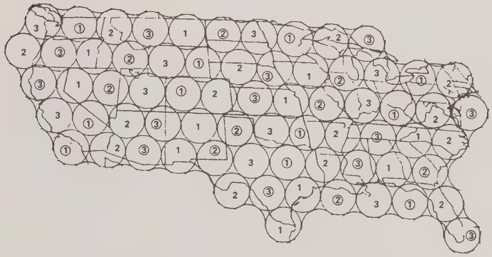

Figure 1.c. Beam Plan 6: triangular layout of doublets, dual polarization, polarization reuse spots.
α = .5°, n = 68, N_B = 45, N = 15.

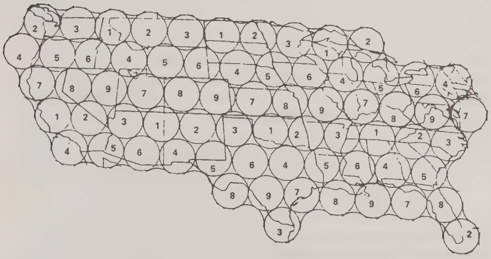

Figure 1.d. Beam Plan 7: rhomboidal layout of singlets, single polarization.
α = .50°, n = 68, N_B = 68, N = 7.55.

After the topology plans are established the radiation characteristics possible with these plans can be analyzed.

It is assumed for this analysis that the necessary component beams are realized by an offset fed paraboloid. The reflector is illuminated by a cluster of circular aperture horns. Such a system is realizable by a relatively well known optical configuration.

The same plans can be realized by other type of antennas, like lenses or phase arrays. While these configurations are physically different their radiation characteristics are not significantly different from the characteristics achievable by the much simpler offset fed paraboloid. Thus the selected optics does not represent a major restriction of generality.

The radiation analysis was performed by utilizing a rigorous vector field based computer program. Although this is an analytical approach, the assumed primary pattern of the radiating element was matched to experimental data. For this TE_{11} as well as higher order waveguide modes were assumed in the horn aperture as applicable for particular configurations.

The various topology plans required different degree of clustering of the component beams. Shaped beam patterns containing 1, 2, 3, 4 and 7 main component beams were computed for various α values and in the angular scanning range needed to cover the overall coverage area. Some cases were computed, for formation of shaped beams with additional, so-called "auxiliary" component beams. The auxiliary component beams are utilized for sidelobe level improvement.

After the topology plan of the antenna is selected and the corresponding aperture distribution is determined the last step of the design concerns with the realization of the aperture distribution. This is done by developing the architecture of the beamforming network.

3. Results

Figures 2-5 show the gain contours achievable with shaped beams using 1 (singlet), 2 (doublet), 4 (quadruplet) and 7 (septet) main component beams as needed for the topology plans presented on Figure 1. The examples give some idea about the effect of component beam numbers and the amount of scan on the shape and sidelobe distribution of the resultant beams.

The radiation characteristics are presented by main and for some cases by crosspolarized gain contour plots in an azimuth-elevation angle coordinate system. From these contour plots the sidelobe power from one shaped beam with the coverage contour of another shaped beam can be determined. The minimum level difference between the two is called adjacent beam isolation, I_{Badj}.

In a multi shaped beam system all the cochannel shaped beams, represent interferences within the coverage of a given beam. On the basis of the resultant interfering power the total beam isolation, I_B can be calculated.

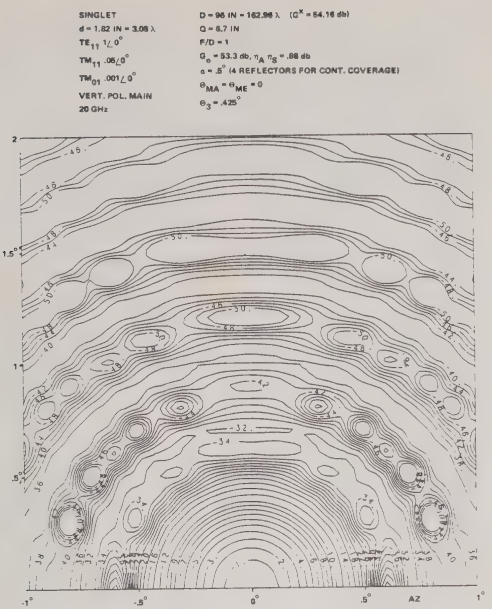

Figure 2.a. Gain contour plot of an unscanned, low sidelobe level singlet, achieved by a large diameter (d_λ = 3.08) multimode horn. Main polarization.

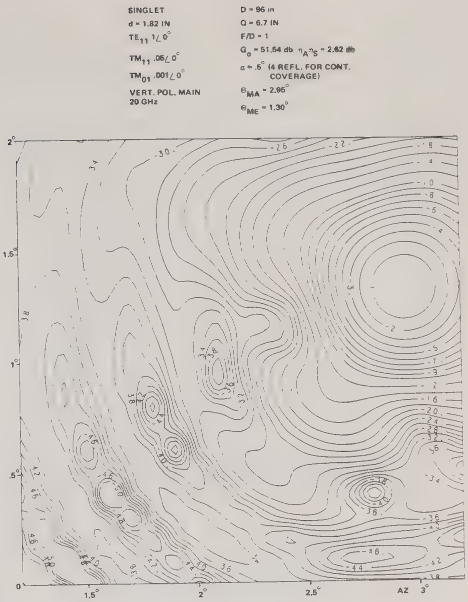

Figure 2.b. Gain contour plot of a scanned, low sidelobe level singlet, achieved by a large diameter (d_λ = 3.08) multimode horn. Main polarization.

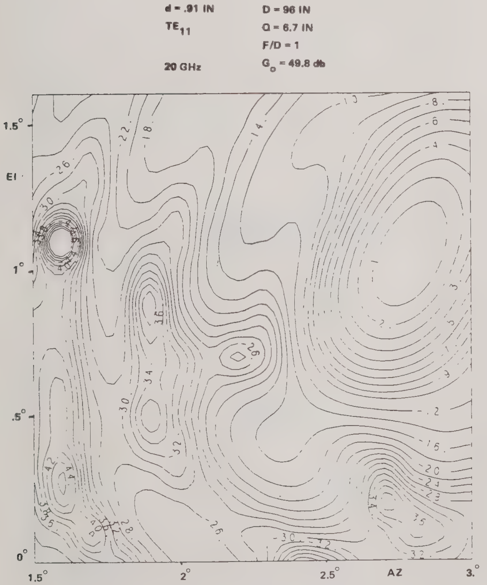

Figure 3. Gain contours of doublet beam. D_λ = 162.56, F/D = 1, d_λ = 1.54, α = .5. Θ_{MA} = 2.8°, Θ_{ME} = 1.05°, Vertical Pol. Main.

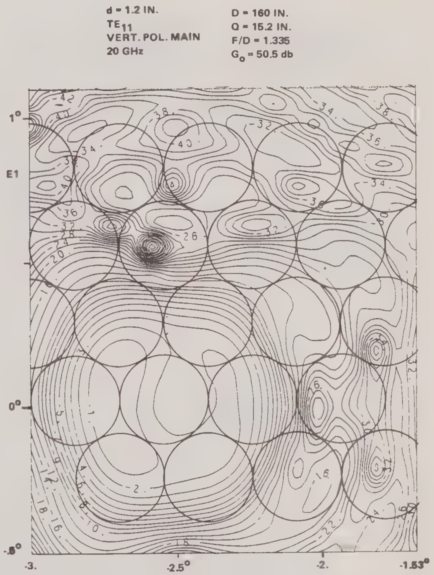

Figure 5. Gain contours of septet beam. D_λ = 270.93, F/D = 1.33, d_λ = 2.03, α = .3°. Θ_{MA} = 2.5°, Θ_{ME} = 0°, Vertical Pol. Main.

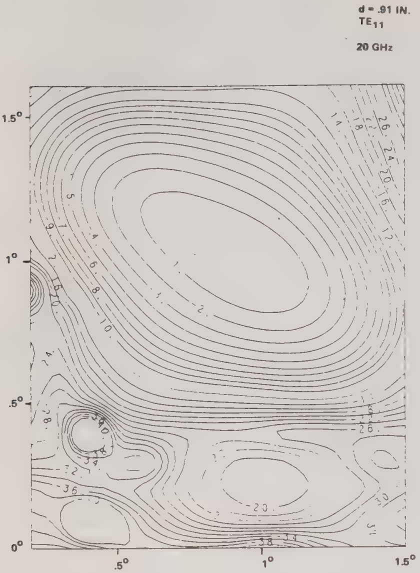

Figure 4.a. Gain contours of quadruplet beam. $D_\lambda = 162.56$, $F/D = 1$, $d_\lambda = 1.54$, $\alpha = .5°$. $\theta_{MA} = .95°$, $\theta_{ME} = 1°$, Vertical Pol. Main.

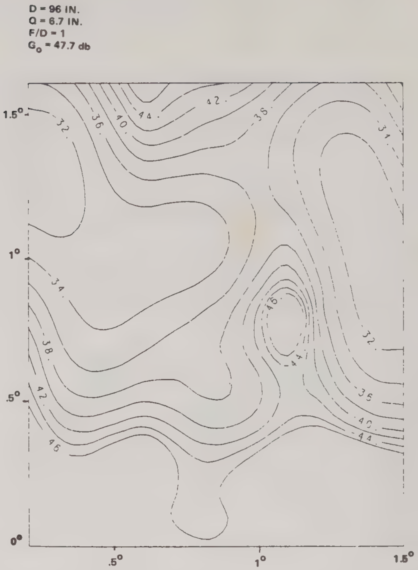

Figure 4.b. Gain contours of quadruplet beam, $D_\lambda = 162.56$, $F/D = 1$, $d_\lambda = 1.54$, $\alpha = .5°$. $\theta_{MA} = .95°$, $\theta_{ME} = 1°$, Horizontal Pol. Cross.

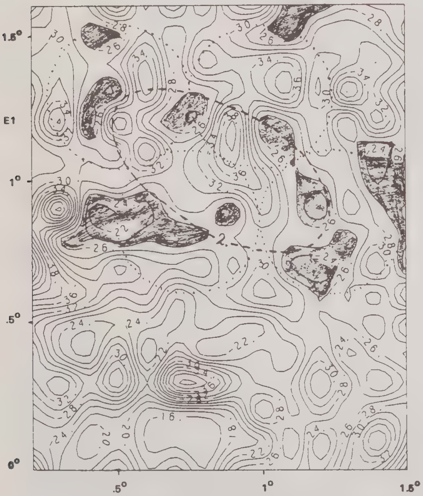

Figure 6.a. Contour plots of total interfering power for Plan 1, $\alpha = .5°$, vertical main polarization, $D_\lambda = 162.56$, $F/D = 1$, $d_\lambda = 1.54$. Plot shows interference in beam 1_2 from beams 1_1, 1_3, 1_4, 1_5, 1_6 and 1_7. Maximum EIRP of beams are equal, field are added in random phase.

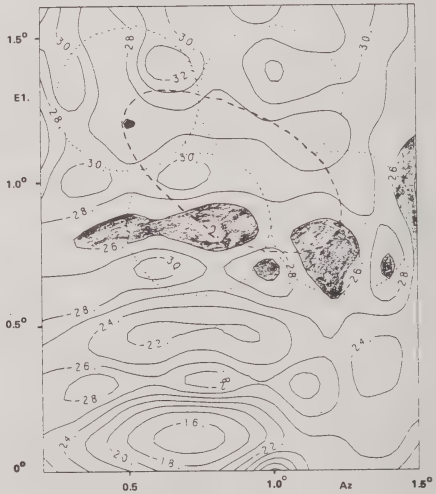

Figure 6.b. Contour plots of total interfering power for Plan 1, $\alpha = .5°$, vertical main polarization, $D_\lambda = 162.56$, $F/D = 1$, $d_\lambda = 1.54$. Plot shows interference in beam 1_2 from beams 1_1, 1_3, 1_4, 1_5, 1_6 and 1_7. Maximum EIRP of beams are equal, interference is added on power basis.

Figure 6 shows the results for such a calculation. The example corresponds to the beam plan given on Figure 1b and is for the vertically polarized channel 1 of this plan. According to Figure 1b there are a total of eight shaped beams in this plan which carry channel 1, four of these are full shaped beams (quadruplets), there is one doublet, and three singlets. The angular window shown on Figure 6 contains the Chicago beam (1_3). All the other beams represent interference into this beam.

It can be seen that the total interference level within the contour (-2 db level) of beam 1_3 is at -26 db level, thus I_B = 24 db. Figure 6a shows the resultant interference on the basis of adding the interfering fields with random phase, Figure 6b shows the interference on a power added basis. Although the fine structure of the gain contours are different the peak levels are about the same.

The data from the detailed radiation analysis was reduced into a series of charts, which can be used to design the discussed type of multibeam antennas. From these charts all important radiation characteristics for the various beam topology plans can be determined. These characteristics include sidelobe level as a function of scan angle; adjacent beam isolation as a function of the number of spectrum reuses, N; required cell size, contour gain, antenna diameter, and number of shaped beams versus number of spectrum reuses, N. Figures 7 to 19 exhibit these data.

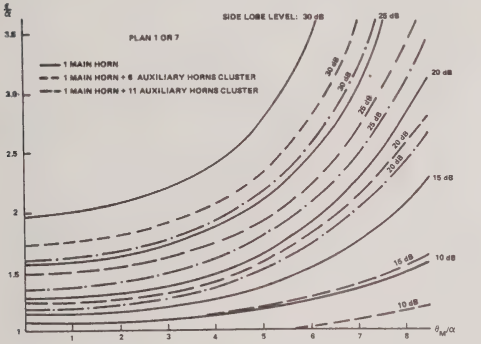

Figure 7.a. ε/α vs Θ_M/α for various sidelobe levels at or larger than ε/α angles from center of main beam. Beam shape: Singlet.

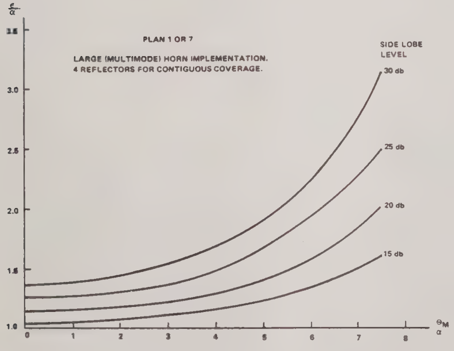

Figure 7.b. ε/α vs Θ_M/α for various sidelobe levels at or larger than ε/α angles from center of main beam. Beam shape: Singlet.

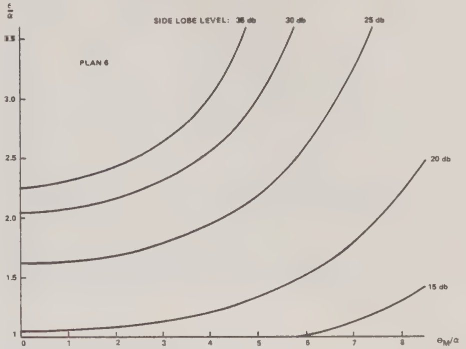

Figure 8. ε/α vs Θ_M/α for various sidelobe levels at or larger than ε/α angles from center of main beam. Beam shape: Doublet. (East/West.)

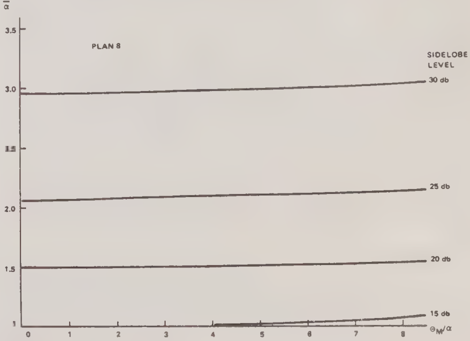

Figure 9. ε/α vs Θ_M/α for various sidelobe levels at or larger than ε/α angles from center of main beam. Beam shape: Triplet.

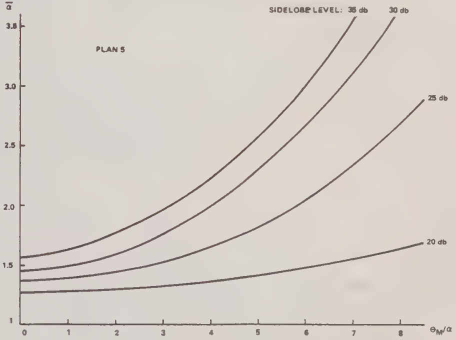

Figure 10. ε/α vs Θ_M/α for various sidelobe levels at or larger than ε/α angles from center of main beam. Beam shape: Quadruplet.

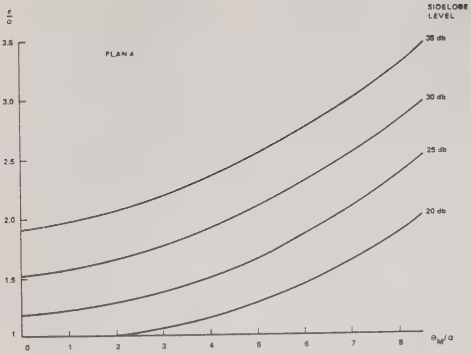

Figure 11. ε/α vs Θ_M α for various sidelobe levels at or larger than ε/α angles from center of main beam. Beam shape: Septet.

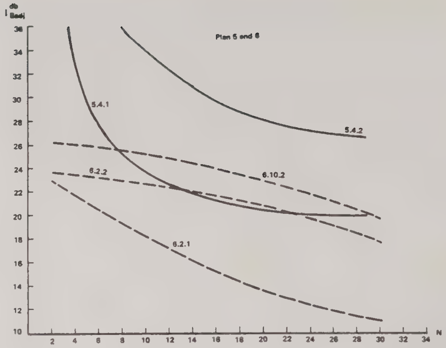

Figure 14. Adjacent beam isolation vs number of spectrum reuse. Plan 5 and 6.

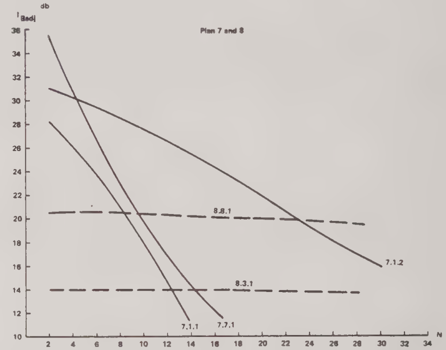

Figure 15. Adjacent beam isolation vs number of spectrum reuse.

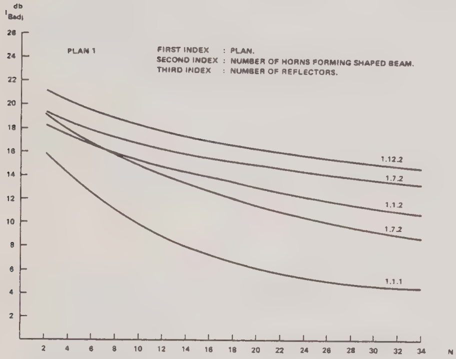

Figure 12. Adjacent beam isolation vs number of spectrum reuse. Plan 1.

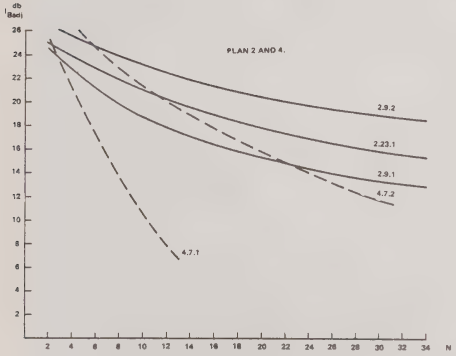

Figure 13. Adjacent beam isolation vs number of spectrum reuse. Plan 2 and 4.

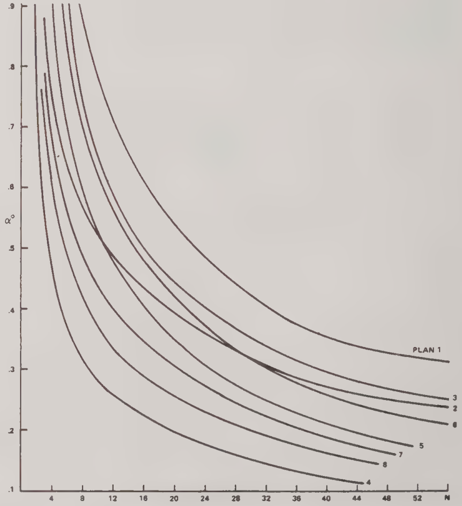

Figure 16. Component beam center to center separation vs number of spectrum reuse for various beam plans using one reflector.

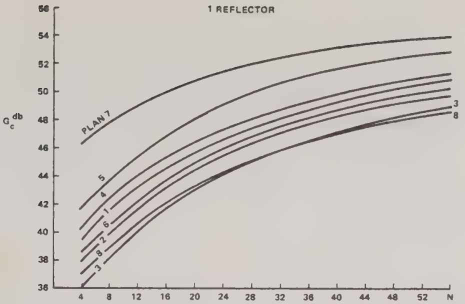

Figure 17. Contour gain vs. number of spectrum reuse for various beam plans using one reflector.

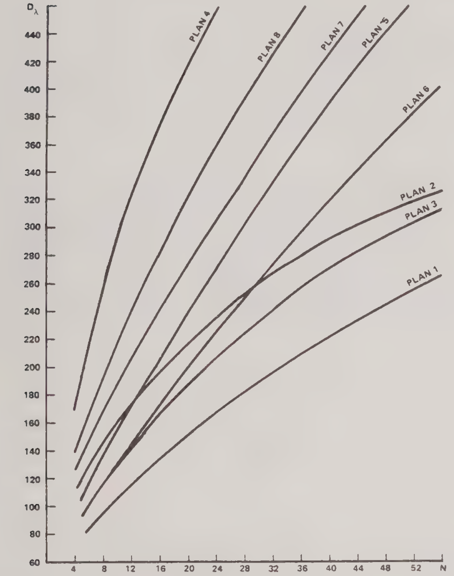

Figure 18. Antenna reflector diameter vs number of spectrum reuse for F/D = 1 for various beam plans.

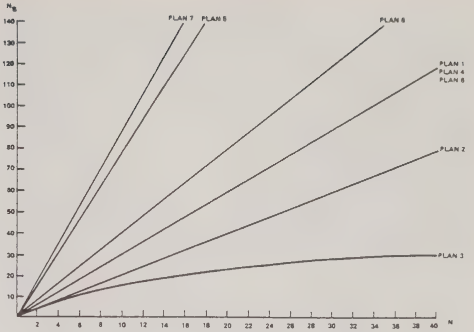

Figure 19. Number of beams vs spectrum reuse for various beam plans.

The application of the design curves can be illustrated by a practical example. In this example a total reused spectrum of approximately 16.3 GHz is selected. The dimensions and other characteristics of the antenna system are determined for seven different beam topology plans. The results are summarized in Table 2. For 16.3 GHz reused bandwidth many of the analyzed plans have some shortcomings in one or more characteristics. One of the topology plans, designated as No. 5, however, stands out as a reasonable practical compromise, without any untolerable characteristics.

Table 3 exhibits the most important electrical and mechanical characteristics with Plan No. 5 for $\alpha = .5°$.

The described Plan 5 realization employs four main component beams (quadruplets) and no auxiliary component beams. The shaped beams are mutually overlap each other. Because of the overlapping feature of this beam plan it can be easily modified into a traffic density matched system. Such an example is shown on Figure 20, exhibiting the percentages of allocation bandwidth available in each of the component beams with a modified Plan 5 type system.

Table 2

Summary of Characteristics for C_O = 16.384 GHz
Effective Communication System Bandwidth
(α_{atm} = -1.2 db, α_{ES} = -.5 db)

Plan	$\alpha°$	n	N_B	ΔF^{MHz}	B^{MHz}	F_B^{MHz}	N	$D_{20\ GHz}^{m}$	G_o^{db}	ΔG_c^{db}	$S_{.05°}^{db}$	α_{sat}^{db}	α_{Total}^{db}	G_{eff}^{db}	C/I^{db}
1	.75	32	32	1536	512	512	10.67	1.625	50.2	-4	1.2	-1.0	- 6.7	43.5	18.5
2	.30	178	44	744.7	372	372	22	4.063	48.6	-2 (EW)	1.8	-2.5	- 6.2	42.4	17.5
4	.30	178	32	1536	512	512	10.67	4.063	50.5	-8	7.1	-2.0	-11.7	38.8	21
5	.50	68	64	2048	256	1024	8	2.438	47.7	-2	1.0	-2.0	- 5.7	42.0	23
6	.50	68	45	1092.3	364	364	15	2.438	50.6	-7	3.5	-1.5	-10.2	40.8	24
7	.60	46	46	3205	356.2	356.2	5.11	2.032	52.1	-4	1.5	-1.0	- 6.7	45.4	22
8	.30	178	67	978	244.5	244.5	16.75	4.063	54.2	-12	10.7	-2.0	-15.7	38.5	20

Table 3

Characteristics Achievable by Plan 5 for $\alpha = .5°$

Beam cell diameter:	.5°
Antenna diameter for 18 GHz band:	2.44 m
Antenna diameter for 28 GHz band:	1.57 m
Number of component beams:	68
Number of shaped beams:	64
Average satellite PA output power:	9.97 w
Average total satellite output power:	638 w
System bandwidth (up or downlink)	2048 MHz
Bandwidth of a shaped beam:	256 MHz
Maximum bandwidth available in a component beam:	1024 MHz
Bandwidth of an IF channel (bandwidth handled by a switch port):	4 MHz
Effective spectrum reuse:	8
Carrier to interference ratio (standard weather):	23 db
Fading margin for full bandwidth downlink:	12.7 db
Fading margin for 1/4 bandwidth downlink:	18.7 db
Downtime for full bandwidth downlink (East Coast):	.045%
Downtime for 1/4 bandwidth downlink (East Coast):	.004%
Pattern slope at coverage contour:	1 db/.05°
Number of BFN components in 18 GHz antennas:	555
Weight of 18 GHz antenna:	Appr. 25 kg

The power distribution into the four component beams can also be adjusted from equal power to 75% into one component beam and 8.33% into the remaining three component beams. If a variable power divider2) is used for this power distribution, then a 9.5 db propagation fading in one cell can be reduced to 4.8 db apparent fading in all four cells of the quadruplet. In such a configuration the antenna can be used to reduce the required fading margin and thus peak transmit power of the system by 4.8 db.

If only main horns are utilized the above described antenna requires a relatively simple beamforming network, as it is exhibited on Figure 21. Each horn is excited by four transmitters and each transmitter feeds four horns. The circuit involves 4-way fixed or variable power dividers, a pair of diplexers or a quadruplexer at each feed. Half of the horns in the system are single the other half dual polarized.

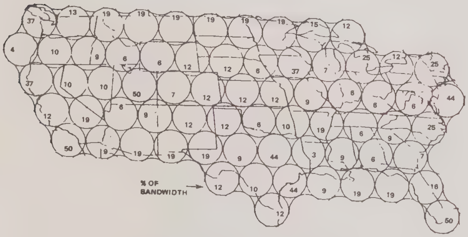

Figure 20. Example for contiguous beam plan providing traffic density matched bandwidth capability. Nonuniform channel distribution is obtained by modifying Plan 5.
Average bandwidth in 13 heavy traffic route cells: .382ΔF
Average bandwidth in 55 thin traffic route cells: .123ΔF

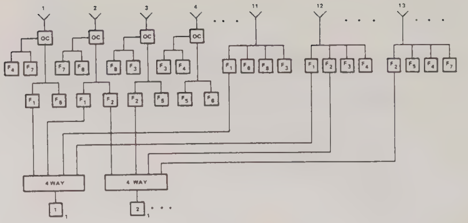

Figure 21. Antenna BFN for beam plan 5 without auxiliary horns.

4. Conclusions

1. The behavior of a multibeam antenna is determined by three major characteristics: beam topology, realizable radiation characteristics, realizable beamforming network architecture.

2. Eight canonic topology plans have been developed and analyzed. They are characterized by four features: a) angular separation between identical frequency cells, b) angular separation between orthogonally polarized identical frequency cells, c) number and configuration of cells forming coverage areas, d) crossover level between nonidentical frequency band cells.

3. In the most general case a topology plan can utilize subdivision of the allocation bandwidth into subbands (channels), orthogonal polarizations, shaped beams employing a number of main (coverage forming) and auxiliary (sidelobe controlling) component beams and some degree of overlap between shaped beams.

4. The generally defined topology plans are developed for the lower 48 states of the U.S. for 110° West synchronous satellite longitude. The topology plans cover the range of .25° to 1.5° cell size, and results in 251 to 10 component beams. These so-called basic plans provide uniform distribution of maximum available bandwidth in each shape beam. Generally the number of spectrum reuses, N increases with decreasing α, but vastly differs for the various topology plans.

5. The basic topology plans can be modified into plans with geographically nonuniformly distributed frequency band capability. These modified plans can "match" the distribution of traffic density. Starting from one of the more attractive topology plans (Plan 5, $\alpha = .5°$) two examples are presented. At the extreme out of the total available 68 component beams only 13 are utilized as main component beams, forming 12 shaped beams over the most important metropolitan areas of the U.S. This system results in N = 9 reuses of the spectrum and it is noncontiguous, because it has no communication capability outside the metropolitan areas.

The same antenna reflector can be used to produce a traffic matched system. An example shows that in this case all 68 potentially available component beams are utilized to form 87 shaped beams. This system reuses the spectrum $N = 11.73$ times but the share of spectrum of the metropolitan areas is smaller. In the first example the metropolitan areas have 9 spectrum units and the rest of the country has 6.76 spectrum units.

6. For increasing beam scan the beam isolation is limited by the increasingly distorted phase front in the optics and the resulting deterioration of sidelobes. This effect can be partly compensated by using an increasing number of auxiliary beams in the formation of a radiation with one main beam and low sidelobes. For such a situation the performance with an offset fed paraboloid optics is primarily characterized by the scan and not by the offset. It can be shown (not discussed in this paper) that for such a situation the radiation performance of the offset fed paraboloid and symmetrical fed lens are comparable, thus the reflector has the edge of simplicity.

7. For increased spectrum reuse decreasing cell size, α is necessary. This, however, increases the normalized scan angle, θ_M/α, which deteriorates the sidelobe level and achievable beam isolation. To counteract the effect of increased θ_M/α the number of horns in the shaped beam forming cluster must be increased or the coverage area must be divided among more reflectors or combination of these methods must be used.

8. When at least four main component beams form a shaped beam the topology plan can include beam overlap and reconfigurability. Reconfigurability can be used to adapt the antenna for fading reduction or traffic pattern changes. For such systems the beamforming network must include variable power dividers.

9. In a practical communication system nonuniform distribution of frequency band and EIRP can be employed simultaneously to build a system best adapted to traffic requirements. However, the flexibility in EIRP adjustment is limited since it effects the associated interference levels into all the other shaped beams.

5. Acknowledgement

The results in this paper were developed under a NASA Lewis Research Center Contract No. NAS3-21745. The author wishes to express its appreciation for this support and the useful comments of the many people who monitored this program. Additional acknowledgement is due to Dr. M. Afifi of GE who completed the computer simulation of the radiation characteristics.

References:

1) P. Foldes, M. Berkowitz, "Reconfigurable Multibeam Antennas for Satellite Communications," 3rd World Telecommunication Forum, Geneva, 23-26, September 1979.

2) P. Foldes, "Control Aspects of Multibeam or Multielement Spacecraft Antennas," International Telemetering Conference, San Diego, November 17-19, 1979.

80-0559

ANTENNAS ABOARD THE INSAT-1 COMMUNICATION SATELLITE

T. M. Smith, D. F. Ford, R. W. LeMassena, R. D. Bruno
Ford Aerospace & Communications Corporation
Western Development Laboratories
Palo Alto, California

ABSTRACT

The INSAT-1 communication satellite carries four antenna systems for various communication functions. A mathematical model has been formulated for each antenna to determine the expected performance. Engineering model hardware has been fabricated and tested to verify the electrical designs. In each case good correlation between the predicted and measured performance is demonstrated. Gain contour plots are presented to illustrate the coverage of the various Indian territories. The coverage demonstrated by the engineering model antennas achieves the communications system goals for the INSAT-1 spacecraft.

INTRODUCTION

The INSAT-1 spacecraft is a three-axis stabilized communication satellite carrying four antenna systems. The four antennas are: 1) C-band antenna for transmission and reception of 4/6 GHz band communications, 2) C/S band antenna for transmission of 4 GHz band and 2.5 GHz band communications, 3) UHF antenna for reception of 400 MHz band communications from various unmanned weather sites, and 4) TT&C antenna for telemetry, command, and ranging functions. Figure 1 shows the antenna placements on the INSAT-1 spacecraft.

The goal of the communication antennas is coverage of the Indian territories with varying emphasis on its constituents. The coverage is therefore broken into three regions: 1) primary coverage region is defined as the perimeter enclosing certain major cities of India, 2) secondary coverage region is defined as the mainland of India plus the Minicoy and Andaman Islands, and 3) tertiary coverage region includes the Laccadive and Nicobar Islands. These regions are illustrated in Figure 2.

The pointing uncertainty of the satellite is 0.2 degrees and the coverage regions in Figure 2 have been expanded to include pointing uncertainty. Antenna gain contour plots superimposed upon this map represent minimum gain levels in a coverage region for worst case pointing error. The goal of the TT&C antenna is to maximize coverage in the spherical volume about the spacecraft. In the following sections each antenna model is discussed. The predicted performance is compared to subsystem requirements. Engineering model measurements are also presented in this paper. In each case good correlation between predicted and measured performance is demonstrated.

ANTENNA DESIGN, PREDICTION VS PERFORMANCE REQUIREMENT, AND ENGINEERING MODEL ANTENNA MEASUREMENTS

C-Band Antenna

The C-band antenna transmits 4 GHz even numbered channels and receives 6 GHz communication channels. The dual frequency band operation is accomplished by use of a multi-element feed exciting a parabolic reflector. Each element of the feed array is driven by an orthogonal mode junction, with the 4 GHz transmit ports of the OMJs excited from the coaxial outputs of an air stripline power divider, and the 6 GHz receive ports combined in a waveguide power combiner.

A design tradeoff study was conducted to determine what combination of reflector size, feed size, and placement would result in optimum antenna gain in the coverage regions. The tradeoff study indicated that a 137 cm projected aperture offset fed parabola with a four element feed and each element driven with equal amplitude in phase excitation was capable of providing the desired gain in the coverage regions.

This design was adopted as the baseline C-band antenna design. Detailed gain contour plots were computed for three frequencies in the transmit band and four frequencies in the receive band. Figure 3 compares the C-band antenna requirement vs the predicted performance. The computed gain contour plots for the center frequencies of the transmit and receive bands are shown in Figures 4 and 5. The gain levels in the figures have been adjusted to account for the expected feed and reflector losses. These are 0.85 dB for the 4 GHz transmit band and 0.50 dB at the 6 GHz receive band. Figures 6 and 7 show the measured gain contour plots for the C-band antenna engineering model. The map of the Indian territory superimposed on the gain contour plots is that seen by a satellite positioned in the 74 degree East location of the synchronous equatorial orbit. Alternate locations from the 70 degree East to 110 degrees East positions have been evaluated and similar performance has been demonstrated.

Figure 8 compares the allocated and measured gain levels in each of the three coverage regions. It can be seen that the gain allocation is met nearly everywhere in the coverage regions. The areas where the measured gain falls below the system allocation represents much less than 1% of the total coverage.

Copyright © American Institute of Aeronautics and Astronautics, Inc., 1980. All rights reserved.

Spin linear patterns were measured to investigate the linearity of the field polarization of the engineering model antenna. The goal is 20 dB minimum axial ratio over the primary coverage region. This goal was achieved at all frequencies in the primary region. Figures 9 and 10 show principal plane patterns at the middle of the transmit and receive bands. Figure 11 tabulates the measured axial ratio at the beam peak, and the North, South, East and West extremes of the primary coverage region.

The flight reflectors for both the C-band and S/C band antenna are graphite epoxy construction. The C-band feed consists of electroform copper and nickel horns driven by chemically milled alum cast OMJs. The transmit band air stipline power divider is connected to the electroform copper coax to waveguide transitions at the transmit ports of the OMJs by coaxial cables. The receive band thin wall waveguide power divider mates directly to the receive ports of the OMJs. The C-band antenna flight feed will weigh 1.61 kg and the flight reflector will weigh 4.10 kg. This feed configuration satisfies the structural and light weight objectives of the C-band feed.

S/C Band Antenna

The combined S/C band antenna transmits two 50-watt TV signals at 2.5 GHz, plus the odd numbered communication channels at 4 GHz. The basic configuration is a deployable (hinged) 160 cm x 152 cm offset-fed reflector illuminated by a square cluster four element array of dual band square horns, driven in phase and equal amplitude.

At S-band, the copperplated graphite feed horns are excited by two orthogonal probes in square waveguide. Circular polarization is achieved by introducing a 90° phase shift between the probes. An air suspended stripline power division network is fastened to the rear of the feed cluster and coax cables interconnect the network with the probe.

A short length of TE_{10} guide introduced at the rear of each square horn causes C-band excitation. A four way air stripline power divider employing plug-in hook couplers (Intelsat V design) provides a low loss interconnect between the beam forming network and waveguide. Figure 12 pictures the S/C band antenna feed. The graphite epoxy construction of the feed horns is required for light weight and to ensure satisfactory operation in the thermal environment outside the spacecraft. In the case of the C-band feed, the power dividers and OMJs are located inside the spacecraft where the temperature variation is much less severe. The S/C-band flight feed weighs 1.50 kg and the flight reflector weighs 5.84 kg.

Computer modeling indicated that a 160 cm x 152 cm reflector is the minimum size capable of meeting the gain allocation while accommodating spacecraft mounting constraints. Figure 13 compares the required and predicted performance for the system described above. Figures 14 and 15 show predicted gain contour plots for the mid frequencies of the S- and C-bands. These predictions include the anticipated feed/reflector losses, -1.15 dB at S-band and -1.0 at C-band. Measured gains of the engineering model show good correlation with predicted values. Figures 16 and 17 show measured gain contours superimposed on the India coverage map, at the center of the S- and C- frequency bands. Figure 18 summarizes the required vs measured gain in each coverage region for two S-band frequencies and three C-band frequencies. The measured gain is satisfactory at all frequencies for each of the coverage regions. The polarization characteristic of the radiated field was measured at the five frequencies tested above. Polarization characteristics conform to that required at all frequencies.

Considerable attention has been given to the possibility of intermodulation products generated in the S/C antenna reaching the C-band antenna receive port. A test was devised that measured the radiated intermodulation product from the S/C feed structure. (See Figure 19.)

Levels below -100 dBm EIRP were noted at the 2nd order intermodulation product in the 6 GHz receive band. Additionally, isolation measurements were performed between full scale C- and S/C antennas that indicated maximum second order I.M. level coupled to the receive port of the C-band antenna is less than -170 dBm, well below the receiver noise threshold.

UHF Antenna

A UHF antenna is required on the earth facing surface of the spacecraft to receive unmanned weather station data. Due to the stowage of the solar array prior to deployment, it is desired that this antenna have an extremely low profile and mount directly to the earth face. A printed annular slot operated as a TE_{11} coaxial radiator was selected as the array element of the UHF four element array. A single element model was fabricated and tested, and four element array performance was projected from the single element results. Figure 20 compares the requirements and the predicted performance.

An engineering model was fabricated, using flight type construction that consists of two copper clad fiberglass epoxy ground planes, a glass epoxy board with an etched copper circuit, and a nomex honeycomb core holding the circuit board equidistant between the ground planes. The entire unit is bonded together at assembly and inserts are provided in the structure for attachment to the spacecrft earth-viewing panel. The entire assemby is 97 x 107 x 1.9 cm.

Circular polarization is provided by exciting each coaxial radiator with probes in space and time quadrature. Figure 21 shows the center circuit board that details the positions of the probes. In view of the narrow frequency band, the 90 degree phase shift is provided by a line that requires the probes be very well matched. Because of the reactive power divider and the 90 degree additional line length on one probe, a mismatch at the probes will translate directly into amplitude imbalance of the power division. This would degrade the element axial ratio.

The engineering model was tested in a 75 foot anechoic chamber with a known reflection level below -45 dB. The UHF antenna was mounted on a 158 x 152 cm metal panel to simulate the mounting on the spacecraft earth face. The measured radiation patterns demonstrated good correlation with the simple array superimposition indicating that mutual coupling had a negligible effect on the four-element array performance. Figure 22 shows this correlation for a principal plane pattern. The measured gain over the earth exceeds the +11 dBi requirement with 1 dB margin (as predicted), and the 1 dB measured axial easily conforms to the 3 dB specification. The engineering model measured performance correlates well with the prediction and satisfies the antenna system requirement.

TT&C Antenna

The TT&C coverage is provided by use of two element arrays of broad beam radiators located on the earth facing and anti-earth facing surfaces of the spacecraft. One array of opposing radiators operates at 4.031 and 4.039 GHz for transmission of telemetry signals, and the other two-element array of opposing radiators operates at 6.258 and 6.262 GHz for reception of command signals. In either case, the individual radiator is a square waveguide 0.64 wavelength on a side, with a septum polarizer located in the rear of the square waveguide. The septum polarizer[1] converts the linearly polarized fields in the rectangular waveguides formed by the bifurcated section of the square waveguide into circularly polarized fields in the common square guide. The two hook coupler inputs on either side of the septum provide LHCP and RHCP to be radiated from the waveguide. Since the ground polarization is linearly polarized, the orthogonal circular polarized inputs of each radiator satisfy the system redundancy requirement. Copolarized ports of the radiators on opposing faces of the spacecraft are summed through a hybrid, as shown in Figure 23.

The radiation characteristic of the two element array of broad beam radiators was modeled by a simple array program using the measured beam shapes of the radiators and the element separation. Since a more accurate assessment of coverage would involve a complex GTD (Geometric Theory of Diffreaction) analysis of the spacecraft, it was decided that measurements performed on a 1/5 scale model would be used as the basis for coverage estimates. Such a model was fabricated and tested in an anechoic chamber. Coverage was evaluated from a series of conical cut radiation patterns, for spacecraft configurations with no solar arrays present, transfer orbit solar arrays deployed, and synchronous orbit solar arrays deployed. Calculations were performed to evaluate percent coverage of the spherical volume for a number of minimum antenna gain criteria. Figures 24 and 25 show the percent coverage as a function of minimum antenna gain for the telemetry and command systems, respectively. As shown in the figures, the nomial minimum antenna gains for TT&C system threshold operation are -20 dBi for the telemetry link and -12.8 dBi for the command link. the corresponding coverage values are satisfactory to accomplish the goals of the TT&C system.

The flight hardware employs graphite epoxy waveguides with interior copper plating similar to those used as feed array elements on the Intelsat V program. The combined weight of the flight TT&C antenna system is 1.25 kg; 0.7 kg for the radiators and associated bracketry; 0.18 kg for hybrid couplers; and 0.37 kg for interconnecting coaxial cables.

CONCLUSION

In the preceding paragraphs, the antenna system design for the INSAT-1 spacecraft has been presented. Performance based on mathematical modeling of the antennas was computed. The predicted performance satisfied the communication system requirements and engineering model hardware was built to verify the electrical design. The engineering model antennas demonstrated good correlation with the predictions, thus satisfying the system requirement.

Both the engineering model and flight model reflectors are fabricated to a 0.030 inch rms surface tolerance specification to ensure close similarity to the perfect paraboloid used in the mathematical modeling. This is a necessary condition for good correlation between the predicted and measured performance.

The mechanical design of the four antenna systems realizes the program goal of light weight. The total communication antenna and TT&C antenna weight is 16.35 kg (5.71 kg C-band antenna, 7.34 kg S/C band antenna, 2.05 kg UHF antenna, and 1.25 kg TT&C antenna).

REFERENCES

1. M. H. Chen and G. N. Tsandoulas, “A Wideband Square-Waveguide Array Polarizer,” *IEEE Transactions on Antennas and Propagation,* May 1973.

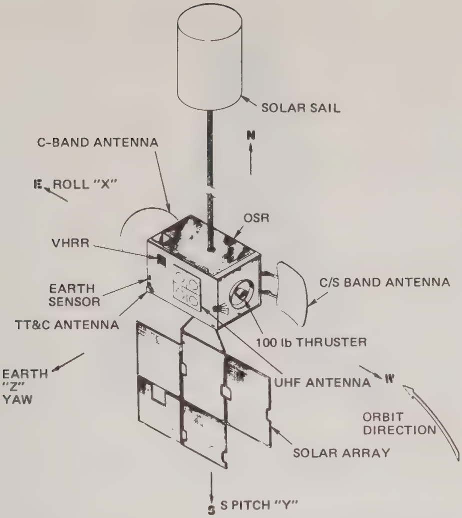
SOLAR SAIL
C-BAND ANTENNA
N
E ROLL "X"
OSR
VHRR
EARTH SENSOR
C/S BAND ANTENNA
TT&C ANTENNA
100 lb THRUSTER
EARTH "Z" YAW
UHF ANTENNA
W
ORBIT DIRECTION
SOLAR ARRAY
S PITCH "Y"

Figure 1. INSAT-1 Spacecraft Antenna Locations

Parameter	C-Band Transmit		C-Band Receive	
	Requirement	Capability	Requirement	Capability
Frequency	3710-4200 MHz	Same	5855-6425 MHz	Same
Polarization	Linear, roll/yaw plane	Same	Linear, yaw/pitch plane	Same
Axial Ratio (primary coverage)	>20 dB	Same	>20 dB	Same
Coverage Area	Indian Territory (primary, secondary and tertiary regions) including 0.2° pointing error			
Minimum Gain (dB)	Primary: 27.1 Secondary: 25.1 Tertiary: 22.1	27.7 25.4 23.2	Primary: 27.6 Secondary: 25.6 Tertiary: 22.6	28.1 26.1 24.8

Figure 3. C-Band Antenna Requirement vs Predicted Performance

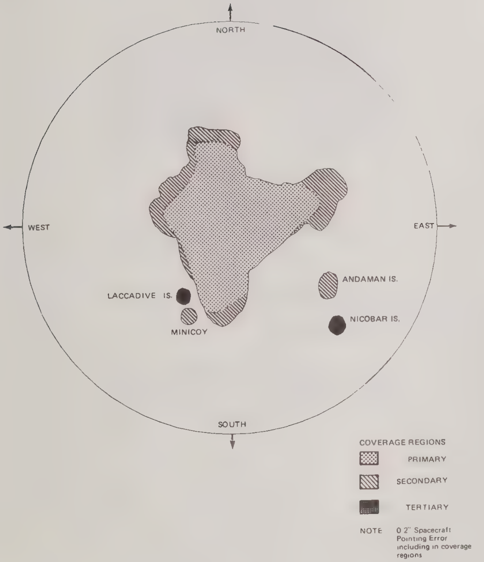
NORTH
WEST
EAST
SOUTH
LACCADIVE IS.
MINICOY
ANDAMAN IS.
NICOBAR IS.
COVERAGE REGIONS
PRIMARY
SECONDARY
TERTIARY
NOTE 0 2" Spacecraft Pointing Error including in coverage regions

Figure 2. India Coverage Regions

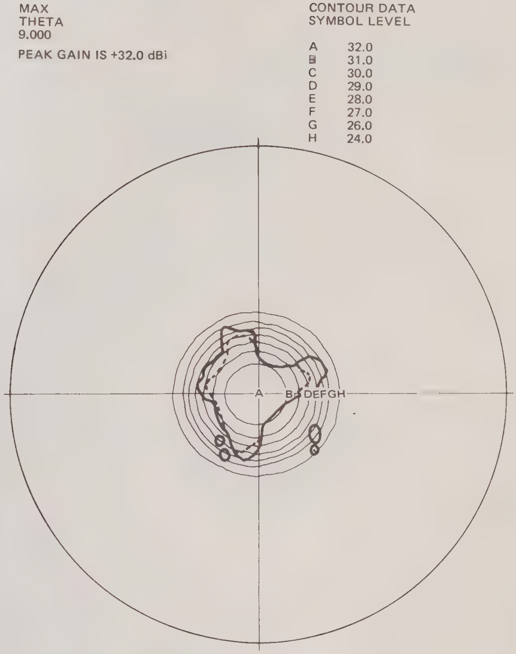

- INCLUDES FEED/REFL LOSSES
- INCLUDES 0.2 DEGREE POINTING ERROR
- 74 DEGREES EAST SATELLITE LOCATION

Figure 4. 3.97 GHz C-Band Antenna Predicted Gain Contour Plot

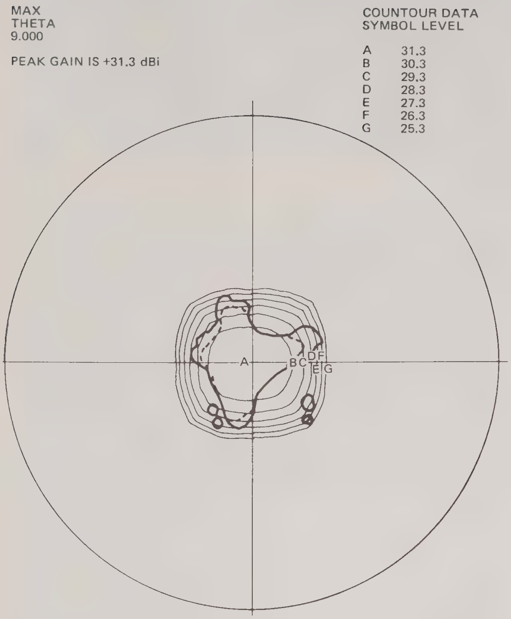

- INCLUDES FEED/REFL LOSSES
- INCLUDES 0.2 DEGREE POINTING ERROR
- 74 DEGREE EAST SATELLITE LOCATION

Figure 5. 6.195 GHz C-Band Antenna Predicted Gain Contour Plot

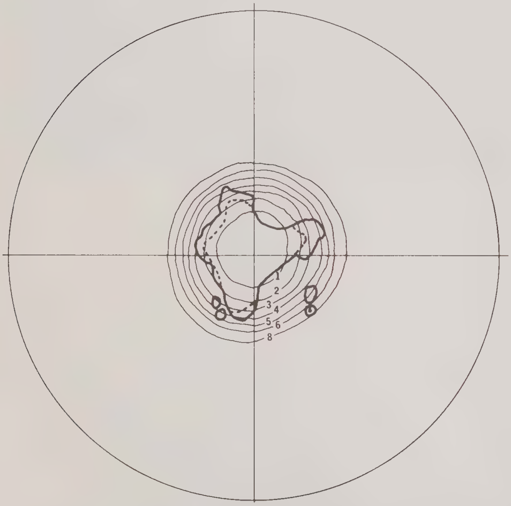

- Peak Gain is 32.0 dBi
- Includes Refl/Feed Losses
- Includes 0.2 Degree Pointing Uncertainty
- 74 Degrees East Satellite Location

Figure 6. 3.97 GHz C-Band Antenna Engineering Model Measured Gain Contour Plot

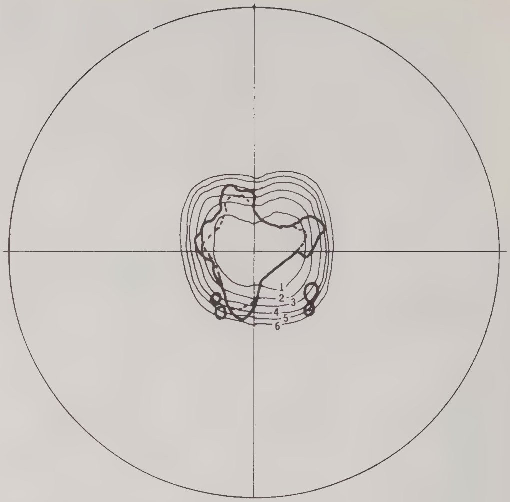

- Peak Gain is 31.5 dBi
- Includes Refl/Feed Losses
- Includes 0.2 Degree Pointing Uncertainty
- 74 Degrees East Satellite Location

Figure 7. 6.195 GHz C-Band Antenna Engineering Model Measured Gain Contour Plot

			Transmit			Receive			
Freq.	Required Gain Tx	Required Gain Rx	3.730	3.970	4.180	5.875	5.955	6.195	6.405
Peak Gain	–	–	32.0	32.0	32.1	32.0	31.7	31.5	31.1
Primary Gain	27.1	27.6	28.6	28.6	28.6	27.1	28.1	27.6	27.2
Secondary Gain	25.1	25.6	26.5	25.8	24.8	25.1	26.1	25.7	25.2
Tertiary Gain	22.1	22.6	25.2	24.0	23.1	25.7	26.7	25.5	25.1

- Includes 0.2 degree pointing uncertainty
- Includes feed/reflector
- 74 degree East satellite position

Figure 8. C-Band Antenna Allocated vs Measured Gain Levels in Three Coverage Regions

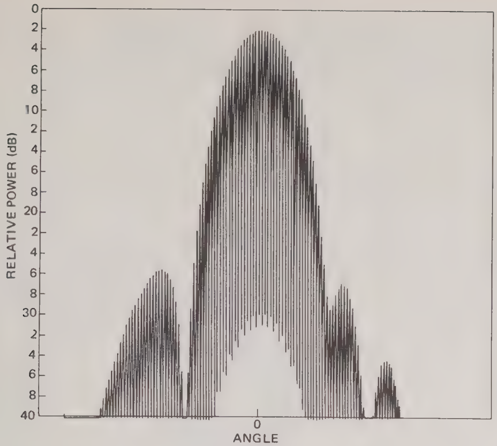

Figure 9. 3.97 GHz C-B and Antenna Engineering Model Spin Linear Pattern

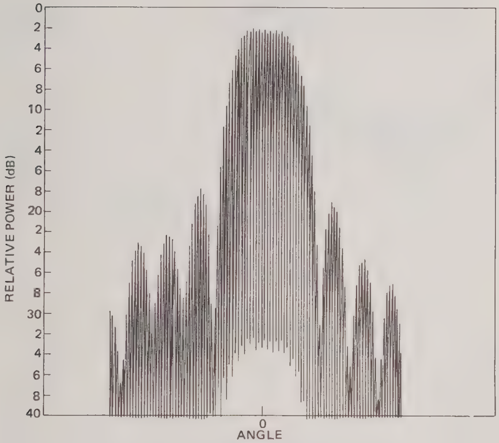

Figure 10. 6.195 GHz C-Band Antenna Engineering Model Spin Linear Pattern

Frequency	3.730	3.970	4.180	5.875	5.955	6.195	6.405
Beam Peak	26	29	34	32	30	31	28
North	24	26	25	26	27	29	25
South	26	24	26	31	31	29	30
East	26	28	33	33	31	30	28
West	27	30	34	32	30	30	29

Notes:
- 20 dB axial ratio is specification
- Values quoted for North, South, East, and West are extremes of primary coverage region in that direction (i.e., 1.50 degrees North, 1.75 degrees South, 2.1 degrees West, 1.55 degrees East).

Figure 11. C-Band Antenna Engineering Model Axial Ratio Characteristic

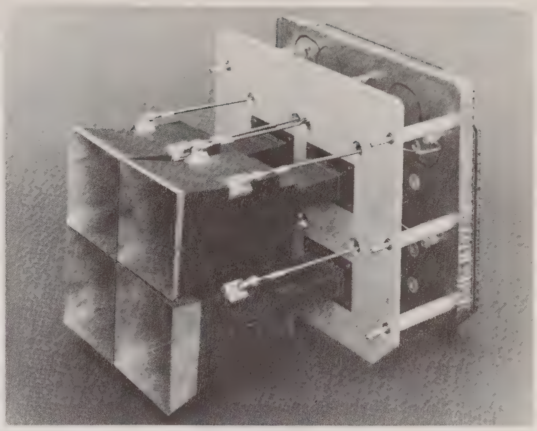

Figure 12. C/S-Band Antenna Feed

Parameter	C-Band Transmit		S-Band Transmit	
	Requirement	Capability	Requirement	Capability
Frequency	3710-4200 MHz	Same	2550-2640 MHz	Same
Polarization	Linear in roll/ yaw plane	Same	LHCP	Same
Axial ratio (primary coverage)	>20 dB	>20 dB	>3 dB	>3 dB
Coverage area	Indian Territory (primary, secondary and tertiary regions) including 0.2°			
Minimum gain (dB)	Primary: 27.1 Secondary: 25.1 Tertiary: 22.1	27.1 25.1 23.3	Primary: 27.0 Secondary: 25.0 Tertiary: 22.0	26.6* 24.7* 24.0

*These worst case gains occur over only a small fraction of the required coverage region.

Figure 13. C/S-Band Antenna Required vs Predicted Performance

MAX
THETA
9.000

PEAK GAIN IS +30.5 dBI

CONTOUR DATA

SYMBOL	LEVEL
A	30.5
B	29.5
C	28.5
D	27.5
E	26.5
F	25.5
G	24.5

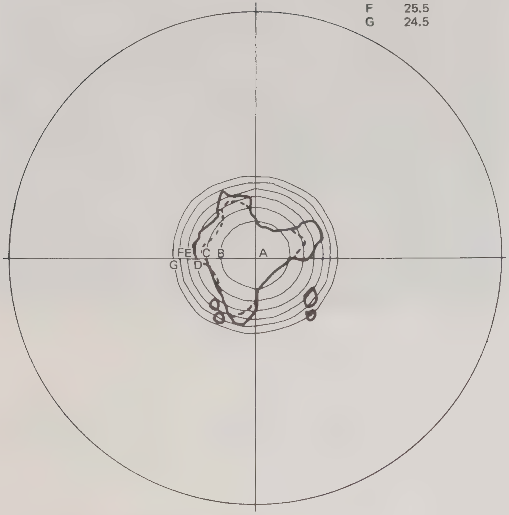

- INCLUDES FEED/REFL LOSSES
- INCLUDES 0.2 DEGREE POINTING ERROR
- 74 DEGREE EAST SATELLITE LOCATION

Figure 14. 2.615 GHz C/S-Band Antenna Predicted Gain Contour Plot

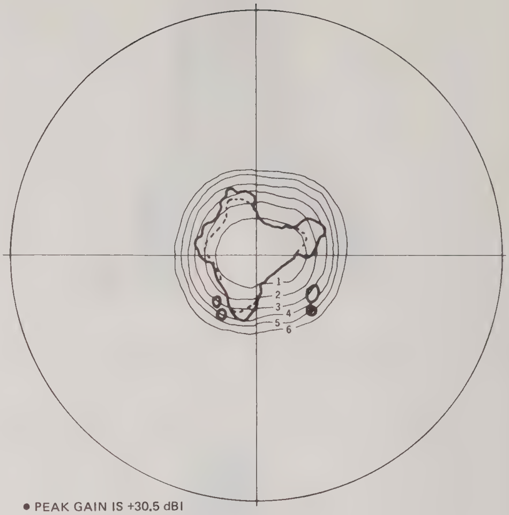

- PEAK GAIN IS +30.5 dBI
- INCLUDES 0.2 DEGREE POINTING ERROR
- INCLUDES REFL/FEED LOSSES
- 74 DEGREES EAST SATELLITE LOCATION

Figure 16. 2.615 GHz C/S-Band Antenna Engineering Model Measured Gain Contour Plot

MAX
THETA
9.000

PEAK GAIN IS +32.1 dBi

CONTOUR DATA

SYMBOL	LEVEL
A	32.1
B	31.1
C	30.1
D	29.1
E	28.1
F	27.1
G	26.1
H	24.1
I	22.1

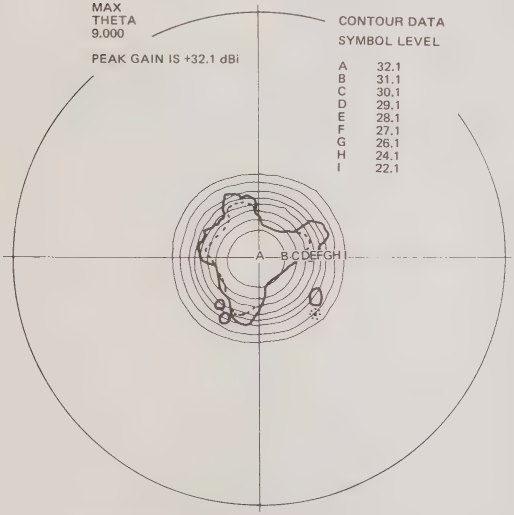

- INCLUDES FEED/REFL LOSSES
- INCLUDES 0.2 DEGREE POINTING ERROR
- 74 DEGREE EAST SATELLITE LOCATION

Figure 15. 3.970 GHz C/S-Band Antenna Predicted Gain Contour Plot

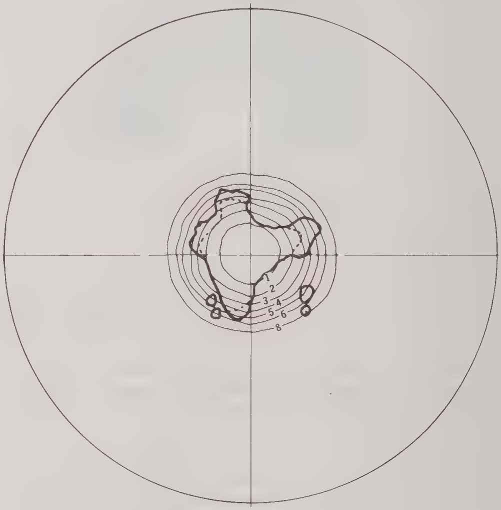

- PEAK GAIN IS +32.2 dBI
- INCLUDES 0.2 DEGREE POINTING ERROR
- INCLUDES REFL/FEED LOSSES
- 74 DEGREES EAST SATELLITE LOCATION

Figure 17. 3.970 GHz C/S-Band Antenna Engineering Model Measured Gain Contour Plot

Frequency	Required Gain		Measured Gain				
	S-Band	C-Band	S-Band		C-Band		
			2.575	2.615	3.730	3.970	4.180
Peak Gain	–	–	30.6	30.6	32.4	32.3	32.2
Primary Gain	27.0	27.1	26.9	27.3	27.7	27.7	27.6
Secondary Gain	25.0	25.1	25.1	25.6	24.9	25.3	25.3
Tertiary Gain	22.0	22.1	24.7	25.2	23.4	24.0	25.0

- Includes 0.2 degree pointing error
- Includes feed/reflector losses
- 74 degrees East satellite location

Figure 18. C/S-Band Antenna Engineering Model Measured Gain

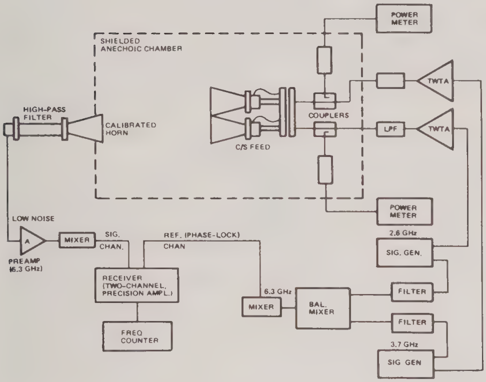
POWER METER
SHIELDED ANECHOIC CHAMBER
TWTA
HIGH-PASS FILTER
CALIBRATED HORN
COUPLERS
LPF
TWTA
C/S FEED
POWER METER
LOW NOISE
SIG. CHAN.
REF. (PHASE-LOCK) CHAN
2.6 GHz
MIXER
PREAMP (6.3 GHz)
SIG. GEN.
RECEIVER (TWO-CHANNEL, PRECISION AMPL.)
6.3 GHz
MIXER
BAL. MIXER
FILTER
FILTER
FREQ COUNTER
3.7 GHz
SIG GEN

Figure 19. C/S-Band Antenna Intermodulation Product Test Setup

Parameter	Requirement	Capability
Frequency	402.65-402.85 MHz	Same
Polarization	LHCP	LHCP
Axial ratio (earth disk)	<3 dB	<3 dB
Coverage region	Earth disk	Same
Minimum coverage gain (dBi)	11.0	11.5

Figure 20. UHF Antenna Required vs Predicted Performance Summary

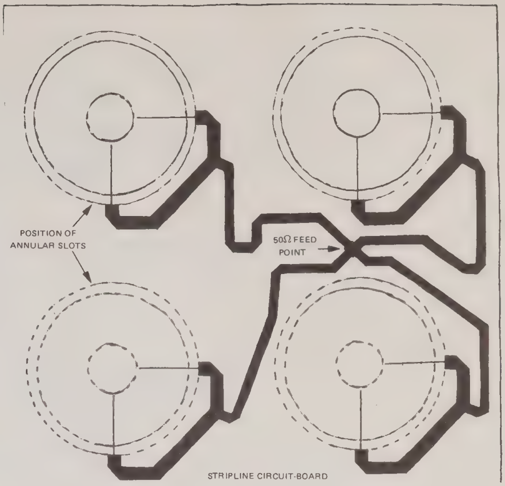
POSITION OF ANNULAR SLOTS
50Ω FEED POINT
STRIPLINE CIRCUIT-BOARD

Figure 21. UHF Antenna Engineering Model Feed Circuit

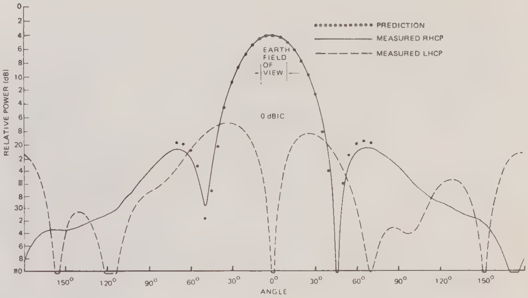

Figure 22. UHF Antenna Engineering Model Measured Principal Plane Pattern

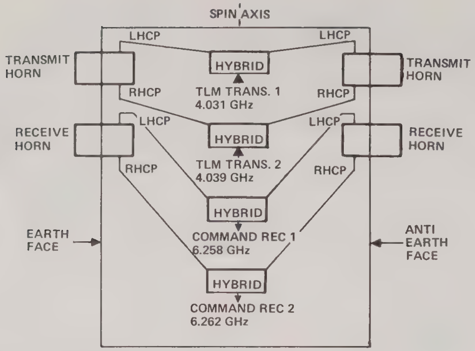
SPIN AXIS
LHCP
LHCP
TRANSMIT HORN
HYBRID
TRANSMIT HORN
RHCP
TLM TRANS. 1
4.031 GHz
RHCP
LHCP
LHCP
RECEIVE HORN
HYBRID
RECEIVE HORN
RHCP
TLM TRANS. 2
4.039 GHz
RHCP
HYBRID
EARTH FACE
COMMAND REC 1
6.258 GHz
ANTI EARTH FACE
HYBRID
COMMAND REC 2
6.262 GHz

- HIGHER POWER (4.5 WATTS) TRANSFER-ORBIT MODE
- SYNCHRONOUS-ORBIT TELEMETRY TRANSMITTERS ROUTED THROUGH COMM ANTENNA

Figure 23. TT&C Antenna System Block Diagram

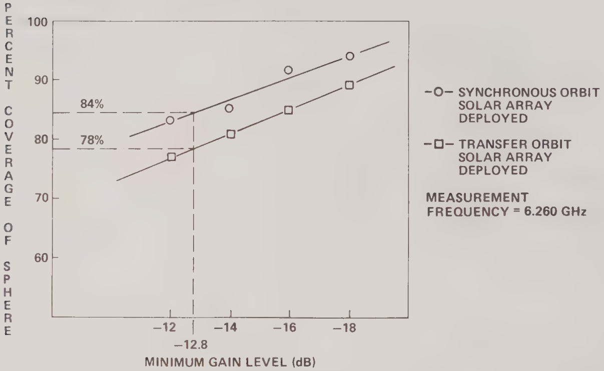

Figure 24. TT&C Antenna Engineering Model Measured Coverage - Command Link

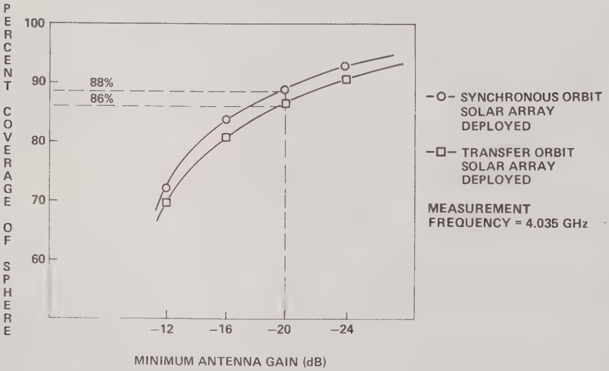

Figure 25. TT&C Antenna Engineering Model Measured Coverage - Telemetry Link

80-0561

EHF SYSTEMS FOR MOBILE USERS*

D. R. McElroy and R. E. Eaves
M.I.T. Lincoln Laboratory
Lexington, Massachusetts 02173

ABSTRACT

Use of the satellite communications frequency allocations in the EHF bands can overcome the present frequency congestion difficulties and provide the bandwidths required for increased capacity and interference resistance via spread-spectrum techniques. By using advanced spacecraft technologies such as uplink antenna discrimination, extensive on-board signal processing, and downlink beamhopping, a modest-size satellite can support considerable simultaneous capacity to large numbers of small, mobile user terminals. This paper reviews the advantages of EHF operation and the motivations for small terminals, describes spacecraft technologies which are needed to implement such systems, and indicates the space- and terminal-segment impacts of incorporating these technologies.

I. INTRODUCTION

Commercial as well as military satellite communications (MILSATCOM) systems strive to provide adequate capacity and/or interference protection to the users which they serve. However, with the growing importance of command and control communications as an effective force multipler, the potential MILSATCOM user community is increasing rapidly. Similar increased demands exist for commercial voice, data, and video services. These increases strain satellite communications systems in the following ways:

1) Presently-utilized frequency bands, i.e., UHF (225-to-400 MHz) and SHF (7-to-8 GHz) for MILSATCOM systems, are inadequate to support protected communications for all of the future users.
2) Frequency congestion considerations constrain expansion in the allocated SHF and lower-frequency bands.
3) For systems with many users, the terminal costs can become the dominant economic factor.

To mitigate these difficulties, several allocated EHF bands (e.g., 20.2-21.2 GHz* for downlinks, 30.0-31.0 GHz for uplinks, and several bands between 40.0 and 51.0 GHz for both links) are being investigated.[1] In addition to the wider bandwidths which are available for additional services, increased capacity, and interference resistant spread-spectrum modulation techniques, these higher frequencies offer the prospect of small, high-gain antennas and similarly reduced-size terminals which should be less expensive to procure and relatively easy to integrate into spacecraft payloads and mobile terminals. As EHF systems are developed, there is also an opportunity to select standard transmission formats and basic terminal configurations which can serve a variety of requirements for mobile, transportable, and fixed-site terminals. This paper reviews the advantages of EHF operation and the motivations for smaller terminals. It then describes the application and the associated impacts of utilizing advanced satellite communications technologies to provide future interference-resistant EHF systems which can serve many mobile users simultaneously.

II. MOTIVATIONS FOR EHF SATCOM SYSTEMS

Each of the above EHF bands offers the attractive potential of GHz wide channels with perhaps the greatest mobile-user uplink allocation prospects being in the 43-to-48 GHz band. In addition, this particular band is attractive because the higher frequencies offer larger EIRP from mobile terminals which are generally characterized by modest size antennas (<4 ft.) and transmitters (<1 kW). On the other hand, these advantages are somewhat mitigated by the increased weather-related (especially rain-induced) propagation degradations at the higher frequenices. Since the additional spacecraft EIRP required to overcome such degradations is often difficult to obtain, lower frequencies are generally preferred for downlinks. Hence, an EHF satellite communications system employing 44 GHz uplinks and 20 GHz downlinks seems to offer considerable potential for mobile user service.

The generic parts of a mobile SHF or EHF satellite communications terminal are shown in Fig. 1. Of these major subsystems, the input/output devices, the modem, and the lower power receiver/exciter circuits can be viewed as somewhat fixed overhead expenses** which are not significantly affected by

---

* This work was sponsored by the Department of the the Air Force, the Department of the Navy, the Department of the Army and the Defense Communications Agency.

The views and conclusions in this document are those of the contractor and should not be interpreted as necessarily representing the official policies, either expressed or implied, of the United States Government.

* Although the 20.2-to-21.2 GHz band is actually in the upper SHF portion of the frequency spectrum, this paper uses the term EHF to refer to all potential MILSATCOM frequencies in the 20-to-60 GHz range.

** Of course, these low-power subsystems may well vary with the processing capabilities which are included in the terminal (i.e., spread-spectrum, data rate).

Copyright © American Institute of Aeronautics and Astronautics, Inc., 1980. All rights reserved.

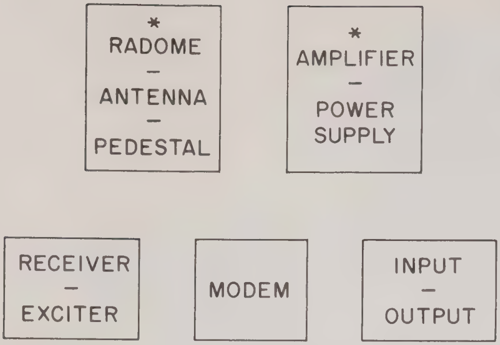

*LARGE WEIGHT/POWER/COST IMPACT

Fig. 1. SHF/EHF Terminal Subsystems.

the EIRP capabilities of the terminal or its frequency. However, investigations of terminals which have either been constructed or seriously studied reveal that there are usually substantial weight (and hence cost) differences between antenna subsystems employing 1-to-2 ft. antennas and those with 3-to-4 ft. antennas (Fig. 2). As indicated in Fig. 3, a similar observation about costs can be made between 10W and 1 kW power amplifiers. Therefore, it appears that the total cost of a microwave or millimeter-wave satellite communications system which serves a large number of mobile terminals can be strongly affected by limiting the required size of the individual user terminals.

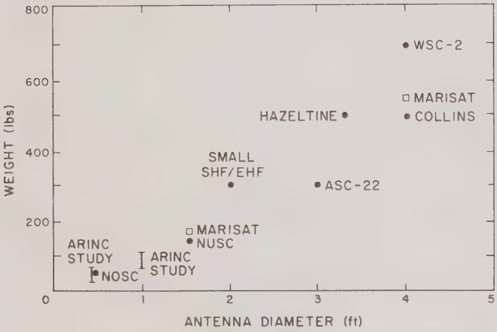

Fig. 2. Weight of Antenna, Pedestal, and Radome

III. APPROPRIATE SATCOM TECHNOLOGIES

Systems which employ conventional (transponder) communications satellites cannot provide the above desirable features. However, these attributes can be realized by exchanging increased spacecraft sophistication for reduced terminal size. As depicted in Fig. 4, one viable MILSATCOM approach involves the use of millimeter wavelengths, wideband frequency-hopping (spread-spectrum) signaling, and advanced spacecraft techniques such as uplink antenna discrimination, on-board signal demodulation/remodulation, and rapid beam-hopping of narrow downlink beams. Although incorporation of these concepts into a satellite system implies increased spacecraft complexity and size in a manner dependent on the number of simultaneous channels, N_c, and on the terminal parameters (characterized by a dish diameter, D_{ANT}, and an RF output power, P_{TX}), it will be shown in the next section that over a considerable range of the parameters the satellite subsystem increases are modest compared to the desired terminal size reductions. However, before presenting such tradeoffs, each of the advanced spacecraft techniques will be described and some useful scaling relationships presented.

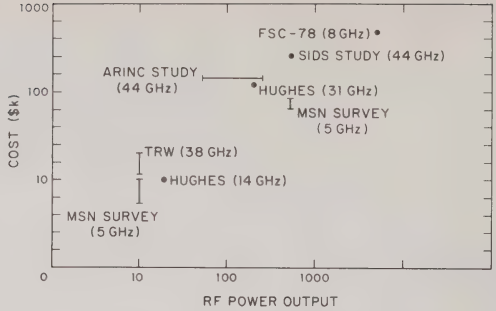

Fig. 3. Cost of Amplifier and Power Supply

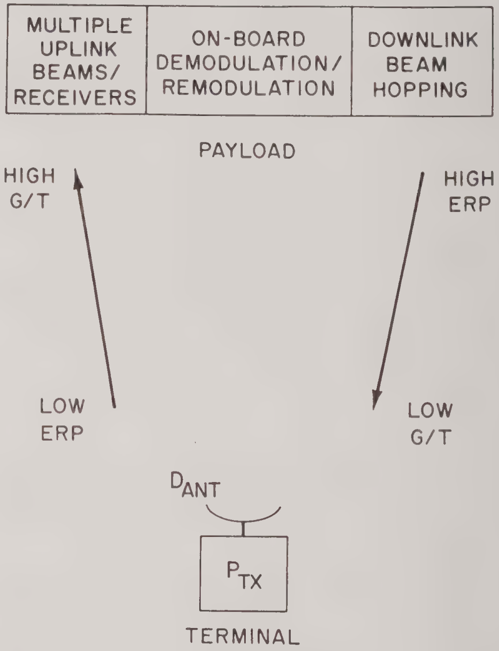

Fig. 4. System Approach

The spacecraft configurations considered in this paper all provide earth coverage uplink service from synchronous-altitude deployments (i.e., a 17° field-of-view (FOV) for the satellite receiving antenna system). This coverage can be accomplished through a single shaped beam ($G_{min} \approx 18$ dB) or through multiple narrow beams which together cover the full FOV. This latter approach permits (EHF) uplinks to be closed to low-EIRP terminals. Consequently, the user antenna size and/or transmitter power requirements can be reduced. In addition, a multiple-beam satellite antenna provides inherent discrimination against interference sources which are not located in the same beam as the user of interest. The narrow spacecraft receive beams can be realized through a compact multiple-beam approach based on a cluster of elemental horns and a common lens aperture. Groups of the horns can be combined through a fixed beam forming network to realize the desired beam shapes with a flexibility dependent upon the total number of horns. As shown in Fig. 5 (for the specific case of seven uplink coverage zones), the resulting beams can be designed to overlap slightly to avoid holes in coverage. This overlap does not result in interference between users if frequency assignments are not reused between adjacent beams.

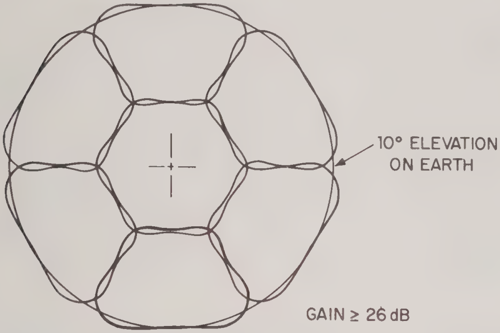

Fig. 5. Multiple Uplink Beams.

Multiple beam uplink coverage implies increased spacecraft complexity and size in both the RF and IF sections, since each beam must be provided a dedicated receiver* (Fig. 6). On the other hand, significant portions of the receiver chains, i.e., local oscillators and frequency synthesizers, need not be replicated in each individual receiver. To the fixed overhead payload weight and power consumption requirements of these shared components, one must incorporate allowances which increase as more beams are added to provide extra uplink receive gain. Consequently, the payload subsystem size increase due to a multiple beam uplink antenna and associated multiple RF/IF sections varies inversely with the required user terminal EIRP (i.e., as $P_{TX}^{-1} D_{ANT}^{-2}$). The specific receiver designs assumed here employ conventional waveguides and microwave components. The use of microwave integrated circuit (MIC) techniques should produce a considerable reduction in the size of multiple beam receivers.

Spacecraft on-board demodulation/remodulation processing decouples the design and performance of the up- and downlinks. As a result, the individual user terminals can benefit from full-duty-cycle uplink operation while several can simultaneously access the satellite with a frequency-division multiplexed (FDM) technique. On the other hand, maximum satellite power amplifier efficiency can be realized and intermodulation difficulties avoided by changing to a time-division multiplexed (TDM) signal format for the downlink. On-board processing to a channel bit stream also facilitates the implementation of features such as spacecraft message routing and data relay (e.g., the forming of composite data streams from several uplinks and/or crosslinks). In addition, it can provide the frequency and signal format changes between up- and downlinks which may be required for the direct interconnectivity of different terminal types.[2]

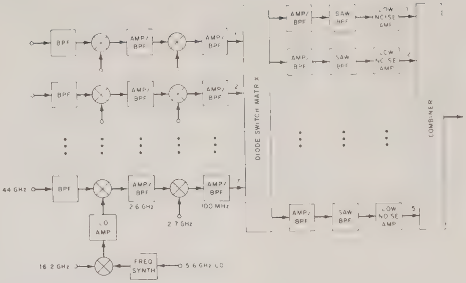

Fig. 6. Front-end and IF Section for Multiple Beams.

A noncoherent M-ary frequency shift keying (MFSK) uplink transmission format permits spectrum spreading via frequency hopping which can occur at rates faster than the rate of symbol transmission. If N users are frequency division multiplexed, a total of MN frequency slots are required, corresponding to a total bandwidth $B = MNf_s$ for a slot spacing f_s. Figure 7 depicts the behavior of this spread-spectrum signaling structure versus time for the specific case of 4-ary FSK. The M slots assigned to a user can be adjacent or can be pseudo-randomly chosen among the MN slots available, with the choices permuted from hop to hop. This latter feature permits each user to achieve an instantaneous spreading over the bandwidth B.

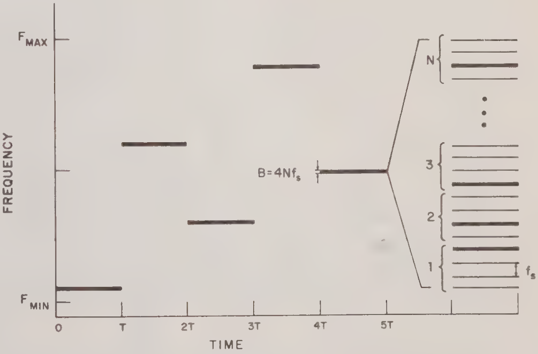

Fig. 7. Frequency-Hopping 4-ary - FSK.

---

* If the signals from the beams are combined into a common RF or IF bandwidth, the noise floor increase would negate the increased gain in each beam

The above uplink transmission format has been structured so that all users can be demodulated from the knowledge of the spectral energy distribution across the bandwidth $B = MHf_s$. If each chip received by the satellite is Fourier transformed, the information to demodulate all N channels will be obtained. Surface Acoustic Wave (SAW) technology provides a particularly power-efficient means of accomplishing this for large numbers of channels. In the configurations considered in this paper, the transforms are accomplished via chirp techniques which are implemented with reflective array compressors (RACs).[3]

The output of the SAW processor is sampled and A/D-converted so that subsequent digital processing, implemented with low-power T^2L, can be employed to combine chips, make M-ary symbol decisions, and construct a digital data stream for each user. These streams are buffered and then placed into the proper locations in the (beam-hopping) TDM downlink format. The routing control which directs this processing has the flexibility to either accept directions from the ground or to provide autonomous assignment of satellite resources upon user request.

The SAW demodulator incorporated in these configurations cannot be significantly reduced in size as the number of simultaneous channels decreases. For the large processing bandwidths associated with large number of users (e.g., >50), SAW technology is exceptionally power-efficient and has a distinct advantage over low-power T^2L digital processing in minimizing the overall impact on spacecraft weight. For fewer channels, the advantage of SAW technology is less distinct, but it remains competitive with T^2L for as few as ten channels.

The digital processing which operates on the output of the SAW demodulator and provides system routing control is closely related to the number of channels. Both the weight and power consumption of this digital processing are estimated to be linearly dependent on the number of channels, increasing in proportion to N_c after including an irreducible overhead.

The desires to serve terminals which have small antennas (i.e., upper-bounded values for D_{ANT}) and to provide large numbers of channels, N_c, both place a burden on a communication satellite's downlink, which in turn requires an EIRP proportional to $N_C D_{ANT}^{-2}$. The TDM format of this downlink permits the use of a narrow beam which is directed toward the user whose slot is being transmitted at the moment. When the next user slot occurs, the beam is redirected (i.e., "hopped") to cover the location of that user. In this way, the required downlink EIRP is realized largely through antenna gain rather than transmitter power, so that significant decreases in power consumption are possible. For example, if a 32-element phased-array is employed, the transmitter RF level can be reduced by ~ 15 dB, with a corresponding reduction in the transmitter power consumption. Although this advantage is offset somewhat by the power consumed by phase-shifters and beam-control circuitry and the increased weight and complexity of these components, the overall reduction in the total impact of the downlink system on the spacecraft weight is still impressive.

The particular technology for implementing a narrow hopped-beam at 20 GHz will be assumed to be a phased-array of earth-coverage horns, each fed by a small FET power amplifier preceded by a diode phase-shifter (Fig. 8). This approach avoids some of the inherent limitations on switching time and beam-hopping rate imposed by a more conventional design based on a TWTA feeding a ferrite-controlled antenna.

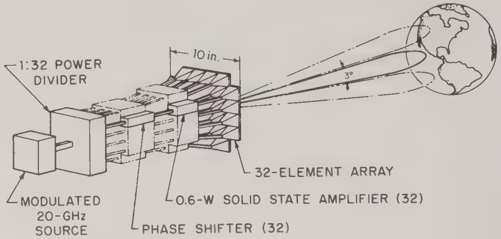

Fig. 8. Hopped-Beam Downlink Antenna

If the number of elements, N_e, in a downlink beam-hopping array is held constant, the EIRP provided by the downlink increases with the total RF power generated by the transmitters. Consequently, for constant N_e, the number of channels which can be supported by the downlink is linearly related to the array's power consumption and to its implied weight. However, N_e is in fact a design variable which can be chosen to minimize the impact of the beam-hopping system power and weight on the overall spacecraft weight. As can be seen in the examples in the next section, the result of such an optimization is that increased numbers of downlink channels can be supported with less than a proportionate increase in spacecraft size.

Additional details about the characteristics and potential advantages of multiple spacecraft receiver beams, on-board signal processing, and downlink beam-hopping techniques for EHF satellite communications systems to serve large numbers of mobile users are addressed in Refs. [4] and [5]. Also, some EHF spacecraft and terminal technology for a limited set of high-priority users has already been demonstrated with the LES-8/9 spacecraft in the Lincoln Experimental Satellite Program [6], [7], [8].

IV. SYSTEM CONFIGURATION CONSIDERATIONS

Some important system considerations involved in applying the above concepts to mobile-user EHF satellite communications can be illustrated by example configurations. Particular terminal and space-segment parameters affect the payload weight and power requirements, and these payload requirements imply an overall spacecraft weight which is typically indicative of the space-segment cost. In developing the examples in this paper, the parameters indicated in Table 1 have been held constant. The uplink and downlink transmission formats and the signal processing are flexible enough to operate at channel data rates which can range from 75 bps to 16 kbps. However, to be specific, the capacity of the payloads is given in terms of 2.4 kbps channels.

The overall spacecraft weight has been determined from the total payload weight and power requirements through an empirically-derived algorithm. The specific spacecraft assumptions which have been used in constructing the example configurations are summarized in Table 2. Although the particular concepts

TABLE 1

EXAMPLE EHF COMMUNICATION SYSTEM CHARACTERISTICS

Uplink Frequency - 44 GHz
Downlink Frequency - 20 GHz
Uplink Modulation - 4-ary FSK
Downlink Modulation - DPSK
Satellite Receiver System Temperature - 1800°K
Terminal Receiver System Temperature - 600°K
Terminal Radome Loss - 1 dB
Terminal Waveguide Loss Between Antenna and LNA - 1 dB

Terminal Tracking Loss
- Uplink - 2.0 dB
- Downlink - .5 dB

Terminal Antenna Efficiency

D_{ANT}	1 ft.	2 ft.	3 ft.
Uplink	55%	60%	65%
Downlink	45%	50%	55%

Elevation Angle Restriction $\geq 20°$

Margin for Atmospheric and Rain Attenuation
- Uplink: 12 dB (Worst Case), 16 dB (Representative)
- Downlink: 9 dB (Worst Case), 12 dB (Representative)

TABLE 2

SPACECRAFT ASSUMPTIONS

Orbit: Geostationary
Attitude Control System: 2-Axis Oriented Through Momentum Wheel
Reaction Control System: Pressurized Monopropellant Hydrazine System
Stationkeeping: East-West Only
Power Conditioning Efficiency: 85%
Mission Life: 7 Years

Solar Cells
- Current Technology: 20 W/KG
- Advanced Technology: 45 W/KG

Batteries
- Current Technology: NiCd
- Advanced Technology: NiH_2

Weight Contingency: 10%
Power Contingency: 10%

and technologies on which these examples are based can be applied to a wide variety of orbits, the particular results developed here are for the case of geostationary orbits. In addition, separate estimates for solar cells and battery requirements have been made for currently available technology and for corresponding technology projected as being available in 1985.[9]

The following communication system parameters are treated as variable in determining the spacecraft weight in the example configurations:

1) terminal antenna dish diameter, D_{ANT}
2) terminal transmitter power, P_{TX}
3) terminal waveguide loss, L_{WG}, between the transmitter and the antenna
4) number of channels, N_c, and
5) number of satellite receive beams, N_B, which together provide earth coverage.

Accordingly, Figs. 9, 10, and 11 give the overall satellite weight as a function of N_c for D_{ANT} values of 1 ft., 2 ft., and 3 ft., respectively. In each case, payload designs based on earth coverage through one beam ($N_B = 1$) and seven beams ($N_B = 7$) are shown. Furthermore, results are given for both current and advanced technology estimates.

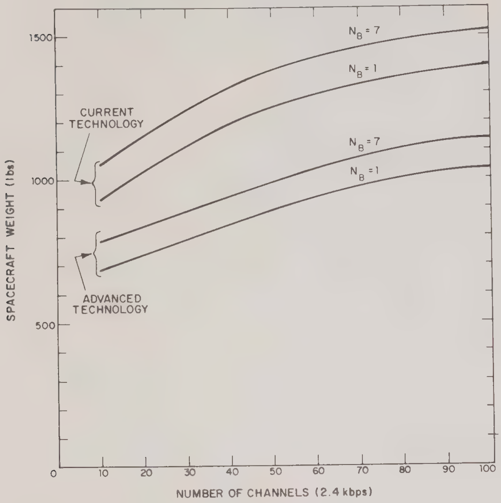

Fig. 9. Satellite Weight vs Communications Capacity: 1-ft. Terminals.

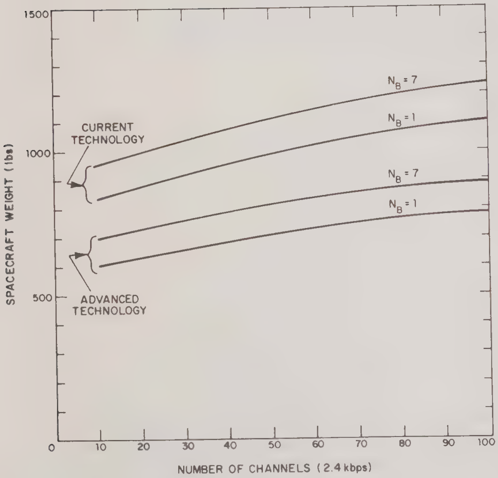

Fig. 10. Satellite Weight vs Communications Capacity: 2-ft. Terminals.

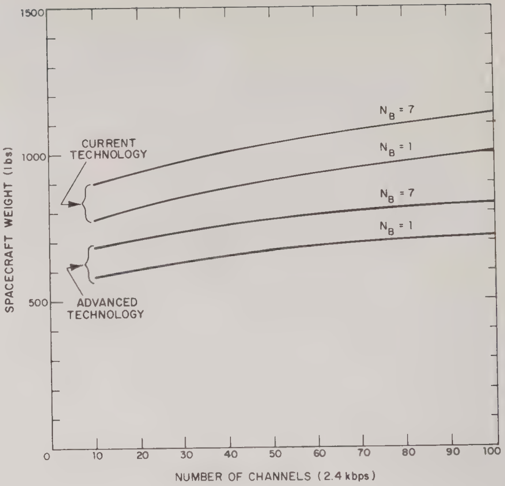

Fig. 11. Satellite Weight vs Communications Capacity: 3-ft. Terminals

For each specific choice of the parameters D_{ANT} and N_c, the EIRP required to close the downlink with the margin specified in Table 1 can be realized through various combinations of satellite antenna gain, corresponding to the choice of N_e, and satellite transmitter RF power, as discussed in the previous section. In the results presented here, N_e is an implicit variable which has been optimized in each case for minimum impact on spacecraft weight. For example, the least demanding downlink encountered here corresponds to $D_{ANT} = 3$ ft., $N_c = 10$ and is realized with minimum spacecraft impact for $N_e \approx 10$. The most demanding downlink encountered corresponds to $D_{ANT} = 1$ ft., $N_c = 100$ and is realized with minimum impact for $N_e \approx 90$.

In addition, each choice of D_{ANT} and N_B requires a specific RF power delivered at the terminal antenna in order to close the uplink with the margin given in Table 1. The transmitter RF power which this implies depends upon the waveguide loss between the transmitter and the antenna as shown in Fig. 12. Each choice of D_{ANT} and N_B in Figs. 9 through 11 has a corresponding curve in Fig. 12 which describes the associated terminal transmitter requirements.

The first three of these figures indicate that even with presently available spacecraft technology and the incorporation of performance-improvement features such as multiple-beam spacecraft receivers, extensive on-board signal processing, and hopped-beam downlinks, the weight of the resulting EHF satellite is still modest when compared to present military and commercial communications satellites. This weight is not a strong function of the total simultaneous capacity (over the decade considered here) due to the fixed overheads which dominate spacecraft structures and many subsystems, such as attitude control, stationkeeping, command/telemetry, uplink antennas/receivers, and frequency references. The largest variations (from maximum estimates of approximately 1000 lbs to about 1500 lbs) are associated with supporting 10-to-100 2.4 kbps channels to user terminals with 1-ft. apertures.

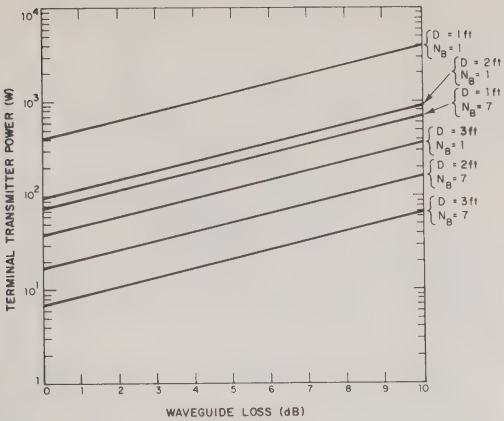

Fig. 12. Transmitter Requirements vs. Waveguide Loss.

For a given uplink margin, Figs. 9 through 11 also show that the use of seven receive beams reduces the user terminal EIRP requirements by at least 8 dB while adding only about 125 lbs to the satellite (i.e., $\leq$ 15%). In addition, the spacecraft size is not extremely sensitive to the terminal size (i.e., D_{ANT} values) in the range addressed. For example, 50 simultaneous 2.4 kbps channels* can be supported to 1-, 2-, and 3-ft. terminals by satellites which weigh approximately 1375, 1125, and 1025 lbs, respectively. Consequently, one can select terminal parameters in this range according to production costs and installation issues. The choices are not likely to cause significant negative space-segment impacts. Furthermore, the incorporation of projected (1985) solar cell and battery (NiH_2) technology reduces the satellite weight estimates by approximately 30%.

Figure 12 shows that the specific terminal configuration is an important factor in determining the final size of the required transmitter. If less than 1.5 dB of waveguide loss is present, then a 2-foot terminal with a 25W transmitter will provide the previously indicated uplink margins (Table 1) to an EHF spacecraft with seven uplink receive beams. However, if the transmitter must be installed some distance from the antenna, then a considerably more powerful (and perhaps more expensive) power amplifier would be needed.

V. CONCLUSIONS

The uplink antenna discrimination, on-board signal processing, and downlink beam-hopping satellite communications technologies discussed in this paper can be utilized to implement EHF systems which remove the present frequency congestion considerations and which provide increased capacities and (if desired) additional interference resistance. Only moderate size spacecraft are required to provide considerable simultaneous capacity to small, mobile user terminals. During the development of such systems, there will also be opportunities to select standard signal formats and basic terminal configurations which can serve a variety of requirements.

VI. ACKNOWLEDGMENT

The Space Communications Program at the M.I.T. Lincoln Laboratory is presently focusing on the development and demonstration of many of the advanced satellite communications technologies described in this paper. Consequently, the authors are indebted to their Lincoln colleagues for many of the concepts addressed here. We are pleased to present this material in their name.

REFERENCES

1. W. Cummings, P. Jain, L. Ricardi, "Fundamental Performance Characteristics that Influence EHF MILSATCOM Systems," IEEE Trans. on Comm., Vol. COM-27, No. 10 (October 1979), p. 1423.
2. L. S. Metzger, "On-Board Satellite Signal Processing," NTC, Birmingham, AL (December 1978).
3. R. R. Rhodes, "Use of Surface Acoustic Wave Reflective Array Compressors in Spectrum Analysis and Demodulation," EASCON, Washington, DC (October 1979).
4. R. E. Eaves, "EHF Satellite Communication Systems for Mobile Users," EASCON, Washington, DC (October 1979).
5. C. W. Niessen, "On-Board Processing for Resource Allocation in an EHF Military Satellite Communications System," ICC, Seattle, WA (To be presented, June 1980).
6. T. S. Seay, L. D. Collins, and J. I. Capetanakis, "LES-8/9 Communications System Design," AIAA 7th Communications Satellite Systems Conference, San Diego, CA (April 1978).
7. D. M. Snider and D. B. Coomber, "Satellite-to-Satellite Data Transfer and Control," AIAA 7th Communications Satellite Systems Conference, San Diego, CA (April 1978).
8. L. J. Collins, L. R. Jones, D. R. McElroy, D. A. Siegel, W. W. Ward, and D. K. Willim, "LES-8/9 Communications System Test Results," AIAA 7th Communications Satellite Systems Conference, San Diego, CA (April 1978).
9. R. L. Harvey, "The Critical Satellite Technical Issues of Future Pervasive Broadband Low-Cost Communications Networks," XXX Congress of the International Astronautical Federation, Munich, Germany (September 1979).

---

[*] With any of several near real-time demand-assignment multiple access (DAMA) techniques, this number of simultaneous channels can support the communications requirements of several hundred low-duty-cycle users.

80-0562

FLEET SATELLITE COMMUNICATIONS (FLTSATCOM) PROGRAM

P. S. Melancon
TRW Defense & Space Systems Group
Redondo Beach, California

R. D. Smith
Aerospace Corporation
El Segundo, California

Abstract

The FLTSATCOM satellite is the spaceborne element of a worldwide Department of Defense tactical communication system. The U.S. Navy, U.S. Air Force, and other DOD agencies are users, for which the system is satisfying Fleet Broadcast, Single Integrated Operating Plan, and Presidential support requirements. Two satellites are now operational with the third, fourth, and fifth satellite planned for launch in early 1980 to mid-1981. This paper will discuss the test program and explore test philosophy including the corrective action feedback process resulting from component failures. It will be shown that the total number of test discrepancies were small in number in relation to the complexity of the spacecraft.

I. Background

Program Description

The basic mission of the FLTSATCOM satellite is to provide communication capability to improve fleet communications and to make provision for operational use by priority DOD users. Worldwide tactical communications are provided in the UHF frequency band of 240 to 400 MHz, which is ideally suited to the mobile user. The terminals are relatively inexpensive and can operate with simple fixed antennas that do not require pointing.

TRW's program began in mid-1971 with pre-proposal work. The Request for Proposal was issued by SAMSO in February 1972. Following a series of negotiations in which proposal content and design approach were modified to better meet program requirements, a contract was awarded to TRW Defense and Space Systems Group on 9 November 1972.

In the initial design phase, program requirements were allocated to subsystems and preliminary designs were completed for all of the equipment. Upon approval of the concept at the Preliminary Design Review, the final design phase was initiated. In early 1974 communication subsystem tests indicated that, due to the large number of closely spaced transmit signals and the complex frequency plan, third and fifth order intermodulation products (IM's) were being generated which appeared in the receive channel bandwidth. These IM's were coupled into the receive system through the common transmit/receive antenna. This was a severe technical problem which was not anticipated during conceptual design phase. The culmination of the redesign effort was the addition of a second UHF antenna for receiving the uplink signals, thus separating the receiver input from the high power downlink signals. Design and process changes were instituted to produce hardware as free of IM generators as possible. The redesign necessitated changes to the transmit antenna, multicoupler filter, and the electrical integration units, relocation of components for balance, and redesign of the sun sensor to eliminate blockage from the receive antenna. A special test facility had to be designed and built to test the transmit antenna in an anechoic chamber under thermal vacuum conditions. The final design was completed in January 1975 and the Critical Design Review was closed out.

In late 1974 and throughout 1975, the spacecraft components were constructed and submitted to component qualification tests. The qualification program involved exposing each component to environments calculated to be in excess of those expected in operational use. Upon completion of the component tests, they were integrated into the qualification spacecraft which was then subjected to a series of tests to evaluate its performance under worse than expected environments. The qualification program was completed by the close of 1976.

Because of the intermodulation problem, start of manufacturing of flight units was delayed until September 1975. The first phase was to construct two spacecraft and later phases of the program added three more spacecraft. Two satellites presently in orbit at 100° west longitude and 23° west longitude were launched on 9 February 1978 and 4 May 1979, respectively. Performance of both satellites has been almost flawless to date. Flight 3 is scheduled for a January 1980 launch with the fourth and fifth satellite launches planned for late 1980 and mid-1981.

Mission Profile

Each satellite is injected into a near-geosynchronous equatorial orbit using an Atlas-Centaur launch vehicle and an apogee kick motor. The Atlas-Centaur places the satellite in elliptical transfer orbit. Following separation from the booster, the satellite is spun-up to approximately 60 rpm. On the fifth transfer orbit, the apogee kick motor is fired to place the satellite into a synchronous circular orbit. After despinning, the solar array panels and UHF antennas are deployed, and then the sun and earth are acquired to establish normal mode. Three-axis stabilization is maintained by thrusters and a reaction wheel to point the fixed antennas at the earth while the solar arrays track the sun line.

Satellite Description

The satellite, shown in Figure 1, consists of a payload module, spacecraft module, antennas, solar arrays, and apogee kick motor. In the pre-launch configuration it weighs 4173 pounds and 2273 pounds after AKM firing.

The satellite configuration consists of a hexagonal shaped structure to which payload and spacecraft equipment panels are attached. A main platform supports hydrazine tanks, solar array drives, reaction wheels, and electronic equipment, and provides an interface for the spacecraft and payload equipment panels.

Copyright © American Institute of Aeronautics and Astronautics, Inc., 1980. All rights reserved.

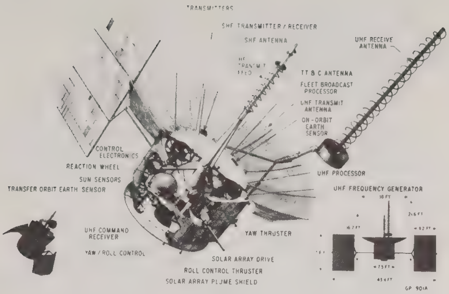

Figure 1. FLTSATCOM

The payload module equipments provide for:

a) One fleet-broadcast 25 KHz channel and SHF beacon
b) Nine fleet relay, 25 KHz channels
c) Twelve Air Force narrowband, 5 KHz channels
d) One DOD wideband, 500 KHz channel.

The payload equipment consists of (12) transmitters, UHF receiver subsystem, fleet broadcast processor, Air Force processor, SHF beacon and receiver, UHF command decoder, frequency generators and oven-controlled crystal oscillators, SHF antenna, multicoupler/filters, and UHF receive and transmit antennas.

In the fleet broadcast operation, the SHF uplink signal is received by the SHF antenna and SHF receiver. The processed SHF signal appears at an intermediate frequency, is amplified, filtered and limited, then upconverted, amplified through transmitter 1 and radiated.

The nine fleet relay channels (2 thru 10) receive, amplify, limit, and re-radiate UHF uplink signals through transmitters 2 thru 10 at different frequencies.

The 12 narrowband channel (11 thru 22) signals are preamplified and routed through separate paths of downconversion, limiting, and upconversion. These signals are then combined and amplified by transmitter 11.

The DOD wideband channel (23) utilizes a separate downconverter, intermediate frequency amplifier, limiter, upconverter, and transmitter 12.

The spacecraft module equipments provide for:

a) Telemetry, Tracking and Command (TT&C)
b) Attitude and Velocity Control Subsystem (AVCS)
c) Apogee Kick Motor (AKM)
d) Electrical Power and Distribution Subsystem (EPDS).

The TT&C consists of an S-band antenna, diplexer, command receivers, dual command unit, decrypters, dual encoder and telemetry transmitters. The S-band antenna receives uplink commands in the 1760 to 1840 MHz band and radiates telemetry in the 2200 to 2300 MHz band. Uplink commands are demodulated as three tones by two receivers tuned to separate frequencies. These tones are transformed to data bit outputs (S, 1 or 0) by the command unit. The decrypter unscrambles these data bits before the addressed user can execute them as discrete commands. The encoder accepts analog, digital, and bilevel data from all the subsystems and formats it into a pulse code modulated (PCM) bit stream which modulates a 1.024 MHz telemetry subcarrier in the transmitters. Each 2.5 watt transmitter provides telemetry at a different downlink frequency.

The AVCS consists of the reaction wheel, sun and earth sensors, control and actuation electronics, solar array drive assembly, thrusters and propellant lines and tanks. The AVCS provides satellite attitude data during transfer orbit and is used to reorient the satellite for firing the AKM at the proper attitude. Sun and earth sensor data are processed by the control electronics to automatically acquire the sun and earth. On orbit three-axis stabilization (normal mode) is achieved by the AVCS processing of earth sensor data to control the reaction wheel (pitch control) and fire hydrazine thrusters for roll control. Yaw control is achieved passively through gyroscopic coupling between the wheel momentum and the satellite angular momentum. The AVCS also provides the clocking of the solar arrays so they are always illuminated by the sun.

The EPDS consists of solar arrays, a power control unit, distribution electronics, three nickel cadmium batteries, and DC-to-DC converters. The solar arrays, consisting of 22,692 solar cells, generate 1574 watts at launch which guarantees at least 1210 watts at the end of the five-year mission life. Each battery consists of 24 cells, each automatically bypassed if any cell fails (open or short circuit). Three transmitter converters provide regulated 24 volts for transmitters 1 thru 10 and 12, a fourth converter provides 28 volts for transmitter 11. Three additional converters provide regulated power to remaining subsystem equipment.

Thermal control for spacecraft and payload modules is accomplished primarily by passive means. Multilayer aluminized Kapton insulation, second surface fused silica mirrors and thermal coatings are employed. Both commandable and thermostatically controlled heaters are used in selected locations to augment the passive system.

The apogee kick motor is a solid propellant engine which provides the delta velocity needed to inject the satellite into a synchronous equatorial orbit.

II. Operational Utilization

Navy Communication Service

Four FLTSATCOM satellites will provide the Navy with a worldwide communications system between the latitudes of 70° north and 70° south. Satellite No. 1 became operational on 4 April 1978, Satellite No. 2 on 15 July 1979, and Satellite No. 3 is scheduled for operational use in early 1980. Satellites No. 4 and No. 5 are scheduled to be operating in mid-1981. The location and coverage area for each satellite is shown in Figure 2. Satellite No. 5 may be an on-orbit spare.

The services provided by FLTSATCOM are shown in Figure 3. The Navy has a worldwide network of communications stations, five of which were selected as satellite terminal stations, and are located on Guam, Hawaii, Stockton, Norfolk, and Naples, Italy.

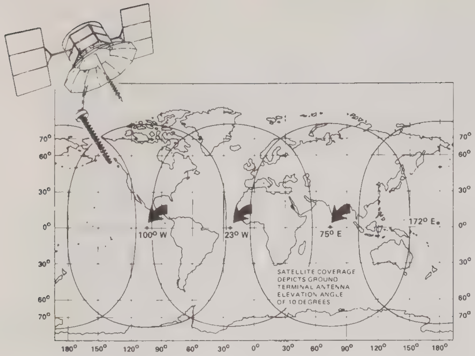

Figure 2. Coverage Areas

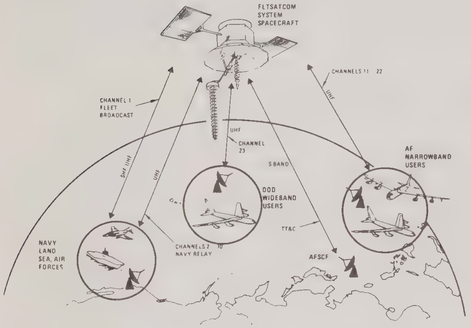

Figure 3. Communication Links

These stations are designated Communication Area Master Stations (CAMS) and manage the communication resources in their respective areas with the Stockton Station serving as a back-up for Hawaii and Norfolk.

The fleet broadcast channel (No. 1) is a one-way shore-to-ship channel with no report-back capability. This 25 KHz channel is a time-division, multiplexed broadcast at 1200 bps with 15 different data channels and a frame sync channel. Channel No. 2 can be used as a back-up for the fleet broadcast UHF downlink.

Channels 2 thru 10 all have a bandwidth of 25 KHz and are UHF uplink and downlink channels and are utilized as follows:

- Channel 2, when not being used for fleet broadcast back-up, is used for Automatic Secure Voice Communication (AUTOSEVOCOM) for coverage from one satellite area to another for ship-to-shore communication.
- Channel 3 and 9 are the Common User Digital Information Exchange System (CUDIXS) channels and operate with a data transmission rate of 2400 bps.
- Channel 4 is the Submarine Satellite Information Exchange Subsystem (SSIXS) channel and operates with a data transmission rate of 2400 bps.
- Channel 5 is the Tactical Data Information Exchange Subsystem (TADIXS) channel and is a dedicated communication link between Navy Fleet Command Centers (FCC) and Task Force Command Centers (TFCC).
- Channel 6 is the Tactical Support Center Information Exchange Subsystem (TSCIXS) channel and is designated to provide communications at a 2400 bps rate between patrol aircraft and Tactical Support Centers.
- Channel 7 serves the High Command Voice Network (HICOM) and Channel 8 serves the Netted Secure Voice (NSV) system. The system employs digitized voice and the RF transmission data rate is 2400 bps.
- Channel 10 is the Tactical Intelligence Subsystem (TACINTEL) channel and operates with a data transmission rate of 2400 bps.

FLTSATCOM is providing the Navy with a speedy and reliable message service to and from fleet units. Although on occasion there are problems of interference, multipath, and scintillation associated with the UHF spectrum, the overall performance has been excellent. There are presently over 600 terminals utilizing the FLTSATCOM system and the number will increase in the near future.

Air Force and Department of Defense Service

The AFSATCOM portion of FLTSATCOM consists of twelve 5 KHz channels. Channels 11 thru 17 are 75 bps, FSK (narrowband frequency-shift key modulated), teletype regenerative channels. Channels 18 thru 22 are non-regenerative repeater channels with channel 22 designated for system orderwire use for coordination and control purposes.

The 500 KHz Department of Defense (channel 23) wideband channel provides a maximum of 14 simultaneous 75 bps teletype accesses to AFSATCOM terminals using the Tactical Transmission System (TATS). The channel may be preempted by the Joint Chiefs of Staff and operated as a digital vocoder voice channel in support of presidential directed missions.

III. Acceptance Test Program

General

An effective acceptance test program is designed to uncover workmanship defects at the earliest possible detection point (and therefore the point of minimum cost of correction) while not subjecting the units under test to environmental levels severe enough to set up incipient failure and/or otherwise shorten the expected life of the unit.

In an attempt to design an effective acceptance test program for FLTSATCOM, particular attention was paid to test sequence, environmental levels, and test (pass/fail) criteria at all levels of assembly from component (black box) to all-up satellite.

Another important aspect of the FLTSATCOM test program involved the testing imposed on all units during manufacturing build-up. At the lowest testable level (board or subassembly), each element was subjected to a complete functional test followed by a temperature cycling test. This temperature cycling test consisted of nine non-operating hot and cold temperature cycles (at unit acceptance test extremes) and one cycle with unit operating. A full functional test was performed at each of the hot and cold levels of this powered tenth cycle. Since formal failure reporting was required from first power-on, it is easy to determine the effectiveness of this pre-screen as will be shown later. It is to be noted that the functional test was a full performance test to acceptance test criteria.

Component (Black Box) Acceptance Test Program

Each FLTSATCOM component was subjected to the following test program:

- Full functional test*
- Three-axis random vibration, operative and monitored
- Four cycles (hot and cold) of thermal-vacuum with full functional tests at each temperature extreme (total of eight)*
- Post-environmental full functional test*.

(* Tests on UHF receiver performed at subsystem level for first three subsystems.)

These environments and sequences are typical of most component acceptance tests. Differences for FLTSATCOM are test levels, operation during vibration, and test criteria.

The random vibration test was selected at three minutes per axis for a power-spectral density (PSD) that enveloped worst case expected launch vibration and acoustics. This resulted in approximately a 10.7 g's rms per axis. From previous experience, the vibration test was conducted operative (regardless of launch-operative status) and the unit monitored for "glitches" on its input and output functions.

From a detailed thermal analysis of the satellite for each of its operating modes, orbital conditions, and phase of operational life combined with worst case conditions and thermal control system degradations, came a prediction of the worst case hottest and coldest temperature each component would experience. This thermal model and its results were validated during the qualification test of the development phase of the program. High and low temperatures for thermal-vacuum component acceptance test were determined for each unit by adding (subtracting) 20°F to the hottest (coldest) temperature. The nominal range for most FLTSATCOM components is from 20°F to 160°F. The solar arrays are tested from -260°F to 260°F. During the thermal-vacuum test, transitioning from hot to cold and vice versa was controlled to avoid thermal shock and a stabilization period was included to insure the unit was at the proper temperature prior to the functional test.

The functional test design embraced two facets: the parameters to be measured and the pass/fail criteria for each measurement. To determine the parameters to be measured it was necessary to prepare a test verification matrix which correlated test parameters with component specification items.

In most cases the test parameters were a direct measurement of specification items and hence can be considered direct measurements. For those specification elements which could not be measured directly, the test verification matrix documented the analysis from which the specification requirements were inferred from test measurements. The establishment of test limits for each parameter required extensive analysis. Since each specification requirement represents minimum required performance throughout the mission, hence end-of-life (EOL), it was necessary to adjust each parameter to its beginning-of-life (BOL) value, therefore making acceptance performance more demanding than specification requirements. In addition to absolute criteria, trend performance was also a controlled parameter.

Satellite Test Program

The FLTSATCOM satellite is assembled in a fashion similar to component assembly; viz., components, structural elements and harnessing are integrated into a functionally testable element. Mechanical and DC electrical integration is performed to bring the satellite to the proper level for its acceptance test cycle.

This acceptance test sequence is governed by the following factors:

- Mission profile - from launch through on-orbit operations.
- Satellite assembly/disassembly sequence - to verify proper operations.
- Verification of satisfactory completion of an environmental test.
- Establishment of proper performance baseline and evaluation of performance trend data.

The environmental levels selected for the satellite acceptance were selected to envelop the expected launch and orbital operations with acceptable guard-bands as governed by worst case considerations. A similar philosophy to that of component level testing was applied at the satellite level.

Test (pass/fail) criteria were selected based on component level testing. BOL performance specifications based on EOL requirements were the principal test pass/fail criteria. In several cases a detailed analysis and allocation was performed to relate satellite performance to unit performance.

During satellite level testing it was important to keep in mind satellite configuration and relate it to reality since not all testing was an exact duplicate of the on-orbit configuration. For those select cases wherein the test configuration did not represent the final configuration, it was imperative that the test article/test conditions more than encompass the on-orbit condition.

The major milestones of the satellite acceptance test program for FLTSATCOM are described below.

- Module Integration - spacecraft and payload modules are mechanically and electrically in parallel operation.
- Module Mating - the two modules are mechanically and electrically combined.
- Comprehensive System Test (CST) No. 1 - a complete performance test of all satellite functions. Under computer control, it requires eight days, 24 hours/day, to make over 60,000 measurements and compare to test limits. All prime and redundant equipments are tested as well as two of the many possible cross-strap configurations. Establishes baseline against which all trend data is measured.
- System Thermal Test - spacecraft is installed in a thermal chamber and a CST performed at high and low acceptance temperatures.

- Antenna Installation - transmit and receive antennas installed.
- Alignments - detailed measurement and adjustment of all satellite alignments - thrusters, sensors, reaction wheels, and antennas. This is the baseline data for subsequent measurements.
- Pre-Environment Intermodulation Product Test - performed in an anechoic chamber - very sensitive test - verifies that entire system is at least 20 dB below specification requirement (approximately -154 dBm).
- Dynamics - sine vibration (0.45g zero-to-peak), acoustic (139 dB), and pyrotechnic shock tests - satellite in launch -electrically- operative configuration. Detailed inspection of solar arrays and thermal mirrors conducted after test sequence.
- Post-Dynamics Integrated System Test - functional test that is an abbreviated version of a CST. Verifies satellite performance following dynamics.
- Thermal-Vacuum - satellite installed in T/V chamber on thermal fixture. Fixture used to simulate seasonal and diurnal extreme conditions. Three CST's performed, one at equinox and one each at winter and summer solstice seasons.
- Post-Environmental Intermodulation Products Test - same as pre-environmental test. Verifies no degradation due to environments.
- Post-Environmental Comprehensive Systems Test (CST) No. 2 - same as CST No. 1. Verifies performance after environmental exposure.
- Final Alignments - repeat measurement of all alignment functions - test limits on absolute values and shifts due to environments.
- Mass Properties Determinations - spacecraft is spin-balanced, weighed, and moment-of-inertia measurements performed. As a result of comparison of MOI measured-to-calculated data on F-1 and F-2, MOI measurement deleted on subsequent satellites.

Acceptance Test Program Results

Table 1 is a summary of the results of the FLTSATCOM acceptance test program. As indicated, the quantity of failures decreased as the hardware progressed from board level to on-orbit, ending with exceptional performance; viz., no orbital failures in 25 months of orbital operation. Using the FLTSATCOM reliability assessment analysis model, which is based upon individual piece part failure rates, one would predict approximately six failures in this orbital time-frame.

In Table 1, the number of failures for board and subassembly levels are combined. It is to be noted that the 3700 boards and 1256 subassemblies are not separate entities. Most of the boards become a part of one of these subassemblies. These items and the 388 components represent the electronic hardware and reaction control system components but does not include structure, solar arrays, antennas, and DC and RF cabling. This quantity of boards, subassemblies, and components is the hardware required for four satellites.

Satellite integration refers to that phase of build-up encompassing the mechanical and electrical integration of the payload and spacecraft modules.

In reviewing these results, one can see that the test program has been very effective in two ways.

- The majority of failures were detected at a very low level of assembly.
- The satellites completing this acceptance test program have been failure-free on orbit.

Table 1. FLTSATCOM Failure Results

	QUANTITY OF HARDWARE	NUMBER OF FAILURES
BOARD AND SUBASSEMBLY LEVEL	3700 BOARDS/ 1256 SUBASSEMBLIES	192
COMPONENT ACCEPTANCE TEST	388	69
SATELLITE INTEGRATION	3	18
SATELLITE ACCEPTANCE TEST	3	12
SATELLITE LAUNCH OPERATIONS	2	1*
SATELLITE ON-ORBIT	2	NONE**

---

* Detected during launch operations, most probably manufacturing defect, not critical to launch, hence not reworked.

** Represents 25 months of orbital operation.

Although these results impressively validate the efficacy of the FLTSATCOM test program, it should be noted that on an absolute scale, for the very large amount of hardware involved for four spacecraft (240,000 piece parts, 3700 boards, 388 components), there have been relatively few failures. This performance is in no small way the result of the following:

- Rigorous design based upon proven electrical and mechanical design standards, part application and derating, worst case analyses.
- Very high quality piece parts - resulted from extensive program involving process controls, in-process inspection, electrical and mechanical screening, burn-in, destructive physical analysis and a control system for insuring that parts which did not meet all requirements did not end up on flight hardware.
- Controlled manufacturing processes implemented by qualified personnel. All fabrication and assembly operations are controlled by process specifications (which had to reviewed and approved by the Air Force) and all personnel involved were certified through training schools for their particular discipline.
- A comprehensive failure reporting and corrective action program. System required formal failure reporting, failure analysis, and corrective action beginning with first power-on at the lowest level of assembly. Extreme emphasis was placed on failure analysis and corrective action.

IV. Launch and Orbital Operations

Launch Operations

The satellite is shipped from Redondo Beach to the ESMC aboard a C-5A. It is transported in the launch configuration (solar arrays and antennas stowed) in a container that is pressurized and humidity controlled.

Upon arrival, the satellite is erected in an assembly building and a Systems Test performed. The complexity of this test approaches that of the Comprehensive Systems Test performed during satellite Acceptance Test. The purpose of this test is twofold: to verify that the satellite has survived the shipping environment and that it is still fully operable. Ordnance is installed upon completion of this test and a Compatibility Test is performed to verify that the Satellite Control Facility (SCF) in Sunnyvale, California, can command the satellite and receive telemetry data properly.

Final insulation installations are made and the satellite is then transported to the Satellite Arming and Encapsulation Facility (SAEF-2). The apogee kick motor is installed, hydrazine loaded, the satellite is transported to the launch complex and erected atop the Atlas-Centaur booster.

An On-Stand Functional Test is performed which principally validates attitude control, electrical power, and command and telemetry functions. This test is followed by a practice countdown, which is a real-time dry-run of the actual satellite portion of the countdown. The satellite is then powered down except for oven-controlled crystal oscillators (OCXO's) and battery trickle charge until the actual countdown sequence begins on launch day.

The period from satellite arrival to launch is approximately 31 calendar days. This allows for all operations with contingency time, periodic formal data review and readiness reviews, and is scheduled to mesh with the Atlas-Centaur launch preparation sequence.

The only problem experienced in the launch of F-1 and F-2 during the launch operations sequence was the discovery of a pair of shorted temperature indicators in an AKM harness on F-2. A detailed review indicated an omission in the procedures to measure actual resistance rather than simple continuity, in the harness fabrication cycle. Since these two functions were not critical-to-launch, and there were no deleterious side effects from this, the Flight 2 satellite was launched without repair.

Orbital Test Program

Upon completion of the ascent, deployment, acquisition and establishment of normal mode sequences (which take approximately five days), and prior to being placed in operational service, the satellite is subjected to an extensive on-orbit test program. This test program is 30-45 days in duration and is predominately a test of the communications system. (AVCS, TT&C, and EPDS are thoroughly exercised in getting the satellite to this orbital condition.)

Measurements are made of approximately 600 payload performance parameters in fourteen test categories. All channels are operated in prime, redundant, and cross-strap configurations, and many of the measurements are performed in each of the three frequency plans in which the satellite is designed to operate.

Power output tests included the measurement of EIRP for each of the channel transmitters. A power distribution test is performed for transmitter 11 which is shared by the AF channels. A spurious output search is made which also includes the EIRP measurement of IM products.

Sensitivity tests include carrier-to-noise ratios at specified uplink signal levels. Bit error rate tests are performed on channels 11 thru 22 over the lower end of the dynamic range.

Frequency measurements are performed on selected repeater channels only since a common OCXO is used for these channels. A separate measurement is made for each mark and space frequency used in the regenerative channels.

Bandwidth and ripple measurements are made for each channel by either direct measurement or calculated by bit error rate data.

Selected tests and results are shown in Table 2. Test results exceed specification requirements by the amount required for performance margin and for expected degradation throughout the satellite life.

Table 2. Selected In-Orbit Test Results for Satellites F-1 and F-2

TEST	CHANNEL	SPEC VALUE END-OF-LIFE	IN-ORBIT MEASURED VALUE (RANGE)*
EIRP	1-3,5,7-10	26.0 dBw	28.7 - 30.8 dBw
	4,6	28.0 dBw	31.1 - 32.9 dBw
	11-22	16.5 dBw	18.6 - 20.5 dBw
	23	27.1 dBw	31.0 - 31.6 dBw
CARRIER/NOISE	1	53.5 dB	56.2 - 59.1 dB
	2-10	2.9 dB	8.5 - 12.1 dB
	18-22	14.0 dB	20.8 - 23.2 dB
	23	0.9 dB	2.2 - 6.0 dB
BANDPASS RIPPLE	1-10	0.5 dB	0.2 - 0.5 dB
	18-22	0.4 dB	0.1 - 0.3 dB
	23	0.75 dB	0.3 - 0.7 dB
CARRIER/IM	11-22	23 dB in 120 Hz	27.7 - 32.7 dB
	23	N/A	NONE DETECTABLE

---

* This range represents the highest and lowest measurement values per channel group encompassing:

- two satellites
- prime, redundant, and cross-strap configurations
- multiple frequency plans.

Orbital Performance

The performance of F-1 and F-2 in the Orbital Test Program has been exceptional. All parameters met their test criteria and compare favorably with factory test data. As of this writing F-1 has been in orbit 22 months and F-2 for seven months. They have been providing high volume, uninterrupted communication service since initial on-orbit operation.

V. Conclusions

The FLTSATCOM Acceptance Test Program was well designed, and through its implementation sorted out workmanship problems in an effective way. Test criteria and sequences utilized in the program proved to be an excellent foundation for detection of workmanship problems. Sound satellite design and engineering practices evolved during the development of the qualification spacecraft. Also, comprehensive Design and Manufacturing Readiness Reviews were conducted on all hardware components to further enhance the integrity of hardware design prior to initiating the manufacturing phase. These management methods yielded an effective acceptance test program that detected workmanship problems/failures early in the manufacturing cycle.

References

1. "Fleet Satellite Communication Systems Description" prepared by Naval Ocean Systems Center, San Diego, California, for Naval Electronic Systems Command PME-106, Washington, D.C., January 1978

2. Friedenthal, M. J. and Heist, E. K., "Fleet Satellite Communications Spacecraft", presented at WESCON, Los Angeles, California, September 1976.

3. Becker, V. L., Hannemann, T. W. and Kindorf, S. D., "FLTSATCOM IM Problems and Solutions", presented at AFTRCC Spring Meeting, Las Vegas, Nevada, April 1975.

4. "FLTSATCOM - Flight 1 Communications Subsystem Orbital Test Report", 32141-350-004-01, prepared by TRW Defense & Space Systems Group for Department of the Air Force, Headquarters Space and Missile Systems Organization, June 1978.

5. "FLTSATCOM - Flight 2 Communications Subsystem Orbital Test Report", 32141-350-017-01, prepared by TRW Defense & Space Systems Group for Department of the Air Force, Headquarters Space and Missile Systems Organization, September 1979.

80-0563

NAVY MILITARY SATELLITE CONSIDERATIONS

R.E. Conley
Office of Chief of Naval Operations
Washington, D.C.

and

C.J. Waylan
Science Applications, Inc.
Falls Church, Virginia

Abstract

Today's U.S. Navy depends upon satellites for worldwide day-to-day and critical means of communications which support data, voice and message traffic. No other means is comparable in availability, reliability, capacity, etc., to the satellite channel for connectivity to globally dispersed, mobile platforms.

Throughout the past two decades, the Navy's commitment to communication satellites has increased. This has resulted in a capability for virtually all surface ships and submarines. The capability these satellite systems provide is unprecedented in Navy history. After nearly 10 years of operational experience the Navy has matured in its understanding of the advantages and disadvantages of this means of communications and is preparing for a next generation design to serve the needs of the 1990s.

History

In the early 1960s, the Navy became active in communication satellite programs to meet the unique needs of providing highly reliable communication between dispersed platforms. In August 1962 the USNS KINGSPORT became the first seagoing ship to operate with a communication satellite (SYNCOM II)[1]. In 1965 the USS MIDWAY and USS CANBERRA established the feasibility of ship-to-ship communication operating with SYNCOM II and III satellites and the AN/SSC-2 terminals. These systems employed Super High Frequencies (SHF) for uplinking and Ultra High Frequencies (UHF) for downlinking[2].

In July of 1967, the MIT Lincoln Laboratory experimental satellite LES-5[3], was used by Navy patrol aircraft (P-2V) to establish a communication link while in flight. The LES-5 employed Very High Frequency (VHF). In the same time frame a VHF satellite communications capability was demonstrated aboard a submarine platform.

The Initial Defense Communication Satellite Program (IDCSP)[4] of the Defense Satellite Communication System (DSCS) provided the space segment for use with SHF ground terminals including AN/SSC-3 shipboard terminals in the late 1960s and early 1970s. Currently the DSCS II[5] satellites support the needs of the commmunity with the DSCS III[6] scheduled to be available in the mid-1980s. This satellite generation operates at SHF.

The shipboard terminals in use today by the Navy with the SHF DSCS satellites are a few AN/SSC-6 terminals which were an outgrowth of the AN/SSC-3s. The AN/WSC-6 program (an outgrowth of the AN/WSC-2 program initiated in the late 1960s to provide very capable terminals on large Navy ships) will deploy within the next few years several dozen terminals on Navy flagships.

As a result of the experience gained in the 1960s, the Navy made a decision to operate at the VHF/UHF frequencies for the dominant satellite communications means. A principal reason for this was the relatively low cost associated with the ship, submarine and aircraft terminals compared to those using the SHF frequencies. The VHF/UHF band offered adequate capacity to support the foreseeable communications needs of the fleet, a substantially improved availability/reliability over the High Frequency (HF) band and terminal costs which would permit a fleetwide deployment.

The main terminals associated with Navy VHF/UHF band satellite communications are the AN/SSR-1 fleet broadcast receiver, the AN/WSC-3 ship and submarine transceiver, also used for ship-to-ship connectivity, and the AN/ARC-143B patrol aircraft transceiver.

The satellites which demonstrated the advantages of this frequency band for Navy use and an initial operational capability were the TACSATCOM I[7], and LES-6[3]. Based on these results and Naval Research Laboratory efforts to provide an anti-jam fleet broadcast capability, the FLEETSATCOM,[8] spacecraft was developed. As the schedule for this spacecraft, which also supported joint needs, drifted behind that of the terminals following the demise of TACSATCOM I, an interim leased capability was arranged for in March 1973 on the MARISAT space program. A portion of this space segment has been referred to as GAPFILLER[9] by the Navy.

Currently, virtually all surface ships and submarines are outfitted with satellite communications capability for use in the VHF/UHF band and development of patrol aircraft systems are being completed. Two of the FLEETSATCOM spacecraft have been successfully orbited and are providing exemplary service.*

Constraints

The constraints that are placed on future satellite systems for Navy applications are many in number, severe in nature and not widely understood. The mobile platforms (ships, submarines and aircraft) and their missions' nature (globally

---

*The third FLEETSATCOM spacecraft is scheduled for launch on 17 January 1980.

Copyright © American Institute of Aeronautics and Astronautics, Inc., 1980. All rights reserved.

dispersed and long in duration) present unique communication system challenges. Many of these characteristics are similiar for aircraft or ground mobile forces regardless of the service. They are emphasized however when applied to the Navy mix of units.

One of the foremost considerations in defining a future satelite communication system for this community is the necessary capability of the system. The capacity, coverage and connectivity which it must provide and the threats such as jamming (uplink and downlink) plus the desire to limit platform detection are the main elements of the desired capability. Some of the details relating to system design concerning jamming and detection are contained in reference 10. The principal conclusions are that the highest frequencies which technology, propagation and cost considerations permit should be employed and a processing space segment is required for the mobile users as a result of their limited antenna sizes.

The nature of the environment in which the terminals must perform is a major consideration as well. The competition for antenna placement on ships and aircraft is intense - weapons systems, navigation systems and communication systems designers all vie for a "top-of-the-mast" position. Equipment space and weight availability coupled with cooling and electrical power systems' limitations place similar constraints on system design.

In order to achieve the capability which is essential within the environment which must be tolerated and yet permit fleetwide deployment, the unit cost of the systems must be affordable. The large numbers of units involved which must have the capability described make the system unit cost of utmost importance.

A straightforward approach displays the importance of unit production cost graphically (Figure 1).

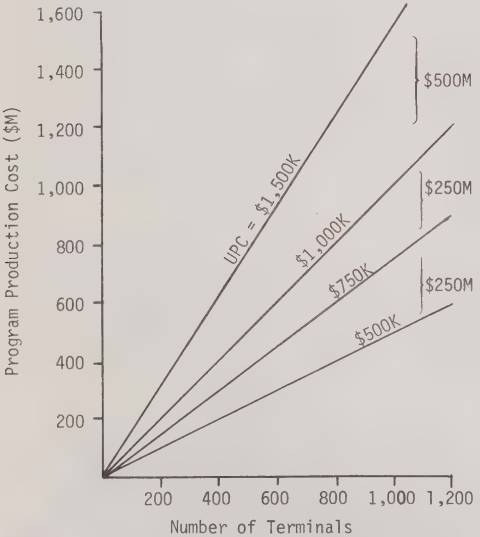

Figure 1. Program Production Cost Sensitivities

For example, if a unit cost of $750K is a target but $1M is achieved, the total program cost is increased by $250 million for a 1000 terminal procurement.

The system control to be incorporated is another consideration. As for all of the factors mentioned above, the control concept is a tradeoff. A centralized control approach, where a small number of key nodes control access and utilization of the system, tends to be in line with traditional military structure and organization constraints. It provides maximum visibility to system status and use to these key nodes. The main problems with this approach are the vulnerability which results from dependence upon the small number of key control points and the reduced flexibility and efficiency which a centralized control structure places on the system.

Any system striving to achieve utmost capability with state-of-the-art technology must seriously consider the "ilities". Military Combat System complexity and sophistication has grown at a much more rapid pace than the capability and availability of personnel to maintain them. The missions of Navy users tend to include long deployments to remote places with only limited personnel and spare parts available. Thus it is imperative that the communication system which is defined be highly reliable and when failures occur that they be repairable quickly and by personnel with a minimum of specialized training.

In defining a future system which will not be deployed for nearly a decade, designers must strive to be clairvoyant. In general, the technology which is employed must be as close to state-of-the-art as cost, reliability and maintainability considerations will permit. Most importantly, however, a design must be adaptable to accommodate changing requirements and threats and must admit to upgrading in an affordable way. These designs must also recognize the existing systems which must be supported during any transition period.

System Design

Efforts have been underway for some time to construct a satellite system which can be established within these constraints. The Military Satellite Communications Systems Office (MSO) has formulated a framework for military satellite communication systems which include the system for the mobile users addressed here.[11,12] Many of the initial conclusions concerning system design of the military satellite system which will accommodate Navy users are included in references 10, 13 and 14. Some of the key features of the system are that it will employ Extremely High Frequencies (EHF) where large bandwidths are available and utilize processing satellites.

A system definition effort to address surface ship, submarine and aircraft terminals, satellite payload design and control system and network philosophies has been underway since early 1979 by the Navy. It falls within the Navy Advanced SATCOM Program (NASP). This effort was succeeded by more than seven years of research and development work to determine the feasibility of the concepts involved as well as to advance and demonstrate the technology to support its early implementation.

Based upon the work which has been completed to date, it is instructive to identify which of the many elements of such a system are key in meeting the constraints which have been set forth above. In order to address this, consider Figure 2. It represents a generic one-way link from a transmit terminal through a satellite to receive terminal. Although in actuality, the system will accommodate multiple, simultaneous, duplex users, this single one-way link "snapshot" is adequate to make the desired analysis.

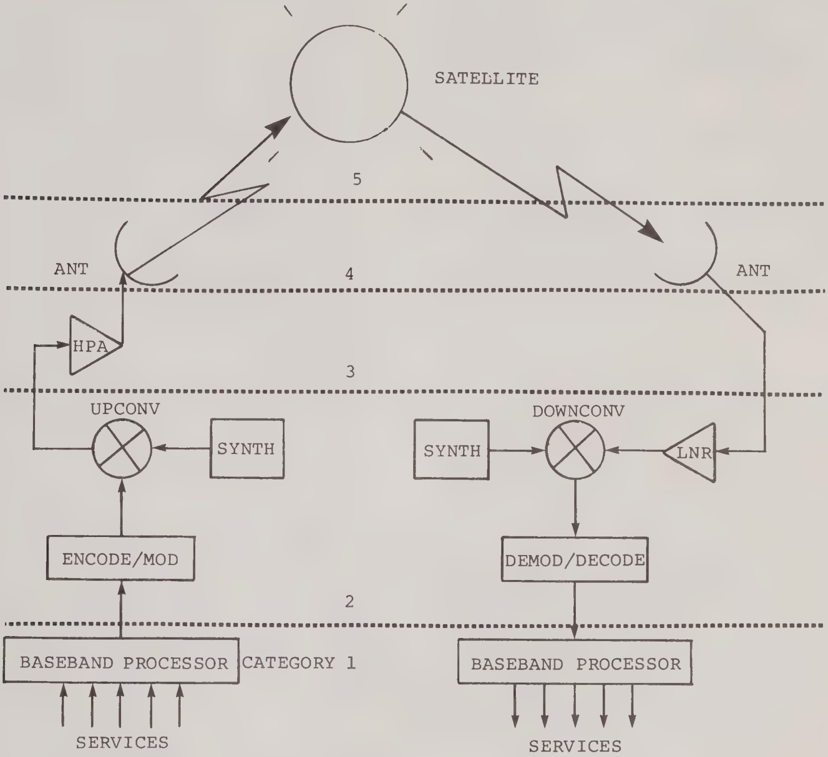

Figure 2. Generic One-Way Link

The subsystems in Figure 2 have been categorized to permit an orderly examination of the factors most influential in meeting the system constraints. We will address each constraint identified previously and discuss which categories of subsystems are key in meeting the constraint and why.

System capability which includes capacity, anti-jam and low detectability characteristics and coverage/connectivity, is the constraint which has most impact upon system design. The RF waveform of the system is a major factor in determining its capability. The impacts on category 2 subsystems by this constraint include timing and doppler sensitivity, bandwidth and settling time of components, etc.

The high power amplifier (HPA) and antennas influence capability rather directly. The bandwidth of the HPA and the RF power it delivers to the antenna, along with antenna size and efficiency are the principal factors determining transmitter effective isotropic radiated power (EIRP). Both capacity and anti-jam depend directly upon EIRP, thus the system capability required has a direct impact on sizing the HPA and antennas.

The satellite system employed is perhaps the most influenced by the required system capability. The coverage/connectivity achieved are largely dependent upon satellite orbit selection, antenna design and onboard processing complexity. The system waveform directly impacts satellite design, particularly in the case of extensive onboard processing such as spectrum despreading, demodulation, decoding, switching of antennas, etc.

The environment which surrounds the terminals will impact the terminal equipment size and weight, particularly the HPA and antennas. The cooling technique selected for the HPA will depend upon the availability of cooling water, etc., and the other uses of the space it occupies.

The environment in which the satellite must operate is a very important constraint on its design as well. Levels of radiation (natural or manmade), host satellite limitations and launch vehicle capabilities also constrain satellite design.

System cost or affordability is the next, and perhaps most important, constraint. The major terminal techniques affecting cost are the HPA and antennas. An EHF HPA utilizing a traveling wave tube (TWT) with several hundred watts RF power capability can represent 30% or more of the total terminal cost. A surface ship antenna installation with dual, $1m^2$ effective aperture antennas will represent at least 30%, if not more, of the total terminal cost.

The constraint placed upon the satellite subsystem by total system cost limitations is more difficult to come to grips with because replenishment costs can be so great and are so dependent upon the fortunes of launch vehicles, etc. Generally, satellite constellations are small enough to largely invalidate statistical methods for their predicted lifetimes, including launch. Suffice it to say here that total system costs can be a significant constraint on the satellite portion of the system.

As a survivability measure, a decentralized system control concept is most likely. This has significant effect on the satellite system, particularly constellation size, orbit selection and antenna design. The terminals are also affected by having substantially increased responsibility in knowing which satellite to access and what relay points to go through to establish the required links.

In the area of reliability and maintainability virtually all active elements of the terminals as well as the satellite are impacted. The most impacted elements of the system are those which preclude maintenance due to inaccessibility for extended periods. Examples include submarine antennas and hardware located in a submarine periscope or external to an aircraft. Satellites, of course, for the foreseeable future must be designed for no human maintenance, although techniques such as fault-tolerant computers and self-repairing hardware are being explored.

Finally, the need to be adaptable to upgrading as well as compatible with existing systems is of major concern in a military satellite system. A key factor in accommodating this constraint is the philosophy of transitioning to all-digital systems. This permits much easier interfacing of existing systems with a follow-on without too great an impact on the replacement system's capability or cost.

One could also place satellite design in the category of being constrained by the ability to upgrade in an affordable way. In the sense being utilized here, however, since one expects to replace satellites significantly more frequently than terminals, they are upgraded through total replacement rather than modification.

Table 1 summarizes what has been discussed relative to the categories of system elements impacted by the design constraints which have been imposed. Xs have been placed in the matrix at those points where greatest impact is expected. An apparent conclusion one can reach is that the terminal HPAs and antennas and the satellites are impacted by nearly all of the constraints and thus would be expected to received most attention in system design.

Table 1.
Key Factors in Meeting Design Constraints

Category	System Elements	CAPABILITY	ENVIRONMENT	AFFORDABILITY	SYS. CONTROL	"ILITIES"	UPGRADING
1	Baseband Processors						X
2	Modems, CODECS, up & down conv., synth, LNR	X				X	X
3	HPA	X	X	X		X	X
4	Antennas	X	X	X	X	X	
5	Satellite	X	X	X	X	X	

Technology

In order to permit the anticipated wide deployment of EHF satellite communication terminals into mobile platforms such as surface ships, submarines and aircraft, the technology at these frequencies must be adequately mature. A significant amount of effort over the past 5-10 years has been expended on advancing the state-of-the-art of the essential elements of EHF satellite systems. References 15, 16 and 17 represent a recent assessment of the states of some of this technology.

Keyed to the categories of the system established in Figure 2, equipment in category 1 and the coding and modem portion of category 2 are essentially insensitive to the frequency of operation. Technology exists now to support the development of these elements and IF amplifiers (not shown on the abbreviated figure) for the required terminals.

Technology will currently support low-noise-amplifiers for the low-noise-receiver (LNR) in category 2 with quite acceptable noise temperatures. FETs with 500-1000K temperatures can be built now at 44GHz and their temperature may be lowered to 300-600K[15] in time for deployment of the system under consideration. Schottky diodes and varactors[18] can be built now to provide the down- and up-converting function required in category 2.

In order to provide the level of anti-jam and low detection probability of a satellite system for this application, the frequency synthesizers, also in category 2, will likely be required to frequency hop at relatively rapid rates. Thus, switching and settling times are of concern. Technology is well in hand for this function with less than 1 usec switching times routinely possible. The synthesizer complexity, and thus reliability, is the main concern for this application.

Category 3 contains only the terminal HPA. Since it represents a major fraction of terminal cost and is such an important factor in determining capability, it is a critical element in assessing the ability of technology to support the required characteristics.

The terminal HPA may be a traveling wave tube (TWT) or a solid-state device. For the EHF frequencies being considered for the mobile terminal uplink (44GHz), coupled cavity TWTs instead of the helix TWTs used at microwave frequencies are required[16]. This technology has been demonstrated, however, the inherent large size and weight, the cooling requirements and the reliability limitations are disadvantages of TWTs. Although solid-state devices within the state-of-the-art cannot match the RF power, efficiency or bandwidths of TWTs at EHF, their substantially reduced size and weight and potentially increased reliability permits their location much closer to the antenna than possible with TWTs. This reduces the waveguide loss of the transmit system significantly. Improved performance of the individual devices, coupled with combining of these devices[16] to obtain increased overall HPA output power, represents one of the areas of potentially greatest reward in advancing the state-of-the-art of EHF technology for this application.

Category 5 contains the terminal antennas. Reference 19 addresses many of the considerations to be taken into account in designing the EHF antennas for this application. Current technology will readily support the construction of the antennas. The antenna pointing and tracking subsystem and radome implications represent the most uncertainty at this time. Since antennas are one of the most costly elements of the system, as well as one of the most influential factors governing capability, the various terminal antennas represent another area where potentially significant rewards can be achieved through continued research.

The final category consists of the total space segment of the system. EHF spaceborne technology has progressed at a comparable rate with terminal technology. The LES 8 and 9 spacecraft[20,21] demonstrated, interalia, EHF spaceborne technology at 36-38 GHz. The satellites employ EHF receivers and downconverters which contribute to total system noise temperatures equal to or less than 1750K. The EHF transmitters utilize IMPATT diodes to generate about .5W RF power. These receivers and transmitters are also alternatively used for a satellite-to-satellite crosslink.

Since an uplink EHF frequency band of 43-45 GHz and downlink frequency bands of 20.2-21.2 GHz and 40-41 GHz are the favored bands of operation for the user class being addressed[22], specific space qualified RF components must yet be developed. However, the current technology base will support this development.[15,16,23] The greatest potential rewards in advancing technology again lie in the power amplifier and antenna subsystems. Reference 14 explores some advanced concepts for uplink and downlink spacecraft antennas in this application.

The required onboard processing of the spacecraft in a system of this type is substantial. The main thrust is to maximize the number of simultaneous voice and data users with the necessary anti-jam and low detection probability while maintaining reasonable weight and power requirements for the space payload. Some applicable technology has been demonstrated with the LES-8 and 9 satellites[20], but significant current effort is underway to develop new technology to improve this aspect of the system. Some potentially applicable work is discussed in references 14 and 24.

Conclusions

Some of the considerations were give that are important in introducing a new communications satellite system for military application. This introduction is more complicated when there exist large investments in other military satellite communication systems, in established ways of information exchange, and in future demands which will exist in the 1990s.

A major, and perhaps most important consideration, is how will the system increase the capability over existing systems. In short, "What is the requirement for the system?" and "How will the system be used?".

The capabilities promised by the frequency range and the technology which supports it are electronic survivable communications platform to platform, reliable connectivity over broad ocean areas (which does not incumber the operational deployment of forces) and resistance to detection by enemy sensors unless they are well within detection range by other means. These attributes are attractive, needed, and are sufficient to support development leading to an operational system. An area requiring further investigation is consideration of how such a system will be operationally employed and what are the tradeoffs available in cost and complexity.

To conclude, there are a number of variables to be considered in the new designs. The applicable technology is in hand and system candidates have been proposed, but the most critical area requiring definition is the consideration of network needs and implementation. This definition must occur prior to any substantial investment.

References

1. "USNS KINGSPORT-Satellite Communications Ship", AIAA Annual Meeting, Paper Nr. 64-417, 30 June 1964.

2. "NASA Compendium of Satellite Communications Programs", NASA Report NASA-TM-X-70435, June 1973.

3. MacLellan, D.C., et.al.: "Lincoln Experimental Satellite 5 and 6", AIAA Third Communication Satellite Systems Conference, Los Angeles, California, April 1970, DDC-AD707475.

References (Cont'd)

4. Dwyre, D.G.; "The IDCSP Satellite - Concept and Performance", AIAA Paper Nr. 70-492, ibid., A70-25449.

5. Wright, I.C. and P. McLellan; "The Defense SATCOM System, Phase II - An Operational System", Proc. ICC-77, pp. 281, June 1977.

6. Weinrich, A.W.; "The DSCS III Communication Satellite Performance", ibid., pp. 291.

7. Brandes, R.D.; "The Tactical Communications Satellite", IEEE Trans. AES, Vol. AES-6, Nr. 4, July 1970.

8. McCartney, F.S. and E.K. Heist; "FLTSATCOM Program Review: Requirements, Design and Performance", Proc. EASCON 78, pp. 442, September 1978.

9. Coffman, W.R.; "Navy Leased Satellite Service", Proc. NTC 76, pp. 43.2-1, November 1976.

10. Waylan, C.J. and G.M. Yowell; "Considerations for Future Navy Satellite Communications", Proc. EASCON 79, pp. 623, October 1979.

11. Rosen, P.; "Military Satellite Communications Systems: Directions for Improvement", Signal magazine, pp. 33, Nov/Dec 1979.

12. Tuck, J.S.; "Military Satellite Communications Systems Architecture", Proc. EASCON 79, pp. 612, October 1979.

13. Ricardi, L.J.; "Some Factors That Influence EHF SATCOM Systems", ibid., p. 617.

14. Eaves, R.E.; "EHF Satellite Communication Systems for Mobile Users", ibid., p. 630.

15. Okean, H.C.; "Small Signal Amplifiers and Converters for Millimeter Wave SATCOM Systems", Proc. NTC-79, pp. 49.1.1, November 1979.

16. Kramer, N.B.; "High-Power Solid-State and Traveling-Wave Tube Sources for Millimeter-Wave Satellite Communications", ibid., pp. 49.2.1.

17. Frediani, D.J.; "Technology Assessment for Future MILSATCOM Systems: The EHF Bands", MIT Lincoln Laboratory Report DCA-5, April 1979.

18. Okean, H.C., et.al.; "Octave Input, S-to-Q-band Large Signal Upper Sideband Varactor Upconverter", 1979 IEEE-MTT Symposium Digest, pp. 134, May 1979.

19. Varley, R.F., R.F. Tucker and C.C. Chen; "Characteristics and Requirements of Millimeter Wave Communication Antennas", Proc. NTC-79, pp. 49.4.1, November 1979.

20. Sarles, F.W., et.al.; "The Lincoln Experimental Satellites LES-8 and 9, Proc. EASCON 77, pp. 21-1A, September 1977.

21. Ward, W.W.; "Developing, Testing and Operating Lincoln Experimental Satellites 8 and 9 (LES-8/9)", MIT Lincoln Laboratory TN 1979-3, 16 January 1979.

22. Jain, P.C.; "Use of EHF Frequency Bands in Future Military Satellite Applications", Proc. ICC-79, pp. 33.4.1, June 1979.

23. Swartley, R.H.; "High Performance Multi-Channel Transponder for the 30/20 GHz Band", Proc. EASCON 79, pp. 279, October 1979.

24. Rhodes, R.R.; "Use of Surface Acoustic Wave Reflective Array Compressors in Spectrum Analysis and Demodulation", ibid., pp. 283.

80-0566

SATELLITE DISTRIBUTED BROADCAST SERVICES AT WESTERN UNION

J. T. Ragan
Vice President-Broadcast Services
The Western Union Telegraph Company

Abstract

A review of Western Union's video and audio program distribution services provided by the company's Westar domestic communications satellite system. Traces growth of Westar Broadcast Services from 275 hours in 1975 to over 48,000 hours in 1979. Discussion of Western Union's program of testing small aperture terminals, which resulted in satellite distribution of 15-Khz commercial audio programming for first time in 1976. Current list of broadcast customers is reviewed, and future developments in broadcast distribution, including shared use facilities, are discussed. Figures for terrestrial vs. satellite distribution of programming material compared, supporting satellite implementation. Projected figures of earth stations using Westar system by end of 1980 estimated at 1,300.

The Western Union Telegraph Company is a full service common carrier that offers a wide range of voice, data, video and facsimile communications services to business, government and the general public. Its basic transmission system consists of three in-orbit domestic communications satellites, a 9,000-mile nationwide microwave system and extensive local distribution facilities within most major metropolitan areas.

The Westar satellite system, together with our landline facilities, offers wideband transmission coverage to major business and population centers throughout the U.S. Recently, as you know, Fairchild Industries and Continental Telephone joined together with us for joint ownership and use of the Westar system.

Here, I would like to discuss Western Union's broadcast services as they relate to video and audio program channel distribution via satellite.

Broadcast services generally may be characterized as any point-to-multipoint communications service, and include television and radio program distribution as well as a variety of special purpose data transmission services. These are provided either wholly via satellite, or by a combination of satellite and terrestrial facilities.

Introduction

Western Union was the first company in the U.S. to establish a domestic communications satellite system. Our satellite service was inaugurated in 1974 with the launching of Westar I and Westar II. Prior to that, conventional distribution of broadcasting programming depended primarily on AT&T's landline facilities and various video and audio tape distribution schemes.

The economics were such that real time nationwide, and often regional, program distribution was only within the reach of the major commercial networks. While service standards were high and performance generally good, the mere complexity and number of repeaters required for nationwide distribution resulted in a noticeable signal degradation at the end terminals. Also, certain system capacity constraints inhibited competition and program diversity in a number of major broadcast markets.

Satellites have changed all of that. Because satellites are distance insensitive (the same rates apply whether a program is being transmitted 500 or 2500 miles away) distance is no longer a pricing factor. The resulting economies have opened the door to a number of programming entrepreneurs heretofore excluded from the market.

With only a single repeater in space -- the satellite itself -- universally consistent, high-quality signal performance can be obtained at all points on a communications network. The constraints of limited capacity, and, in the case of radio, limited bandwidth, have been eliminated, and the industry is now faced with the welcome problems of increased program diversity, improved quality and opportunities for economical growth.

Western Union introduced its video distribution service in July 1975. From a modest beginning of only 275 hours of video transmission that year, service has grown to approximately 20,000 hours during 1979. If the PBS program service is included, that figure more than doubles.

In 1976, the concept of using Small Aperture Terminal (SAT) earth stations, with antenna diameters of 10 feet or less for receiving audio programming was introduced by Western Union during an extensive field test and evaluation program. This project led to the introduction of satellite distributed 15-Khz audio program channel service to the radio industry as a result of proven nationwide distribution and improved signal reproduction.

Copyright © American Institute of Aeronautics and Astronautics, Inc., 1980. All rights reserved.

The Westar System-Today and Tomorrow

The Present

Western Union's backbone transmission system, illustrated in Exhibit 1, consists of three Westar satellites, transmit/receive earth stations near New York, Chicago, Los Angeles, San Francisco, Seattle, Dallas and Atlanta, (where there are two earth stations, one full service and one dedicated to video) with Television Operation Centers in each of those cities and an interconnecting 9,000-mile microwave network.

The Westar satellites are spin stabilized, using a despin antenna system, with a primary payload of a 12-channel broadband communications repeater. The communications transponder consists of redundant wideband (500 Mhz) linear receivers and transmitter drivers; input multiplexers, 12 transmitters (power amplifiers) and output multiplexers. Each output filter has a useful bandwidth of 40 Mhz and modest out-of-band rejection.

Expected satellite performance for video and audio program channels are:

Video

Bandwidth	4.2 Mhz
Peak Frequency Deviation (760 Khz, 1 volt p-p sineware, no pre-emphasis)	12.0 Mhz
Pre-emphasis advantage	13.0 dB
Noise Weighting advantage	13.0 dB
Peak to peak picture to RMS weighted noise ratio	65.2 dB

Audio (Program Channel)

Peak frequency deviation of main carrier by sub-carrier	±1.5 Mhz
Sub-carrier to noise ratio	21.0 dB
Audio Bandwidth	15.0 Khz
Audio peak deviation	250.0 Khz
Pre-emphasis advantage	9.0 dB
Noise weighting - flat	0.0 dB
Test tone to noise ratio	76.0 dB

Western Union's primary earth stations have two 15.5 meter antennas (three at New York and Los Angeles), plus fully redundant, full-service terminals with high quality microwave systems that interconnect with the metropolitan areas they serve. At Atlanta, a single steerable antenna is employed for the dedicated video earth station while in Seattle a fixed single antenna station is used. Both are fully redundant stations with full service capability.

The Television Operation Centers are equipped with video and audio monitors, network switching matrices and audio and video controls for signal optimization.

Western Union's backbone system described above is, however, only a part of the total system capability and capacity. There are no 47 earth stations in service, or on file with the FCC, owned by independent or network-affiliated television stations which routinely access Westar for video programming.

Broadcast Services Users

A large number of TV broadcasters transmit video programming via Westar, including PBS, CBS-TV, Hughes Television, Robert Wold Co., and the Spanish International Network.

The Public Broadcasting Service (PBS) has in place an interconnected system consisting of more than 150 earth stations that uses the Westar system for programming distribution. CBS began satellite distribution of its sports programming, news and occasional live broadcasts via Westar in 1975, while Wold and Hughes act primarily as brokers, reselling their satellite time as part of their broadcast production and transmission business.

The Spanish International Network (SIN) is the only TV network in the U.S. that broadcasts Spanish language television programming exclusively. Currently, SIN transmits about 100 hours of weekly programming to 31 TV and cable affiliates, and reaches an estimated 12-to-20 million Hispanic Americans.

The Westinghouse Broadcasting System (Group W) is implementing a planned system whereby Westinghouse and Western Union will share Western Union existing ground facilities plus Westinghouse earth stations in Pittsburgh, Philadelphia and Baltimore. The system will be used by Westinghouse to transmit programs among its various TV stations as well as to distribute syndicated programs produced by Group W to other TV stations. Using its Television Syndication Center production facility at Pittsburgh, Westinghouse will offer satellite distributed video services to other program producers and syndicators.

Developments in distributing radio programming via satellite, while starting later than video, have closely paralleled television. The National Public Radio (NPR), Mutual Broadcasting System, RKO Radio Network, AP Radio, the Physicians Radio Network, ABC, CBS and NBC radio networks all use Westar.

Mutual, which is installing receive-only earth stations in the top 200 radio markets, expects to transmit to dozens of stations early this year and to have 650 stations in service by 1981. NPR, which has been transmitting to approximately 20 affiliates since October of last year, plans to have 150 receive-only stations and 17 uplinks by May 1980.

RKO and AP Radio have an agreement to share earth stations and satellite time on Westar by broadcasting their programming to 15-foot antennas in 50 cities. RKO has been broadcasting newscasts since last October to 12 of its own radio stations and plans to have over 100 affiliates in its radio network by the end of 1980.

The Future

The total video and audio distribution capacity represented by the combined Western Union and customer owned earth station networks described above provides satellite distributed broadcast services to all of the major broadcast markets in the contiguous United States, Hawaii, Alaska, Puerto Rico and the Virgin Islands.

To meet the increasing demand for service, in addition to the normal expansion of its existing earth station capacity. Western Union has developed a number of plans to enhance its direct distribution capability for Broadcast Services, including:

- A decision to emphasize broadcast services in the assignment of present and future satellite capacity, including capacity on the Advanced Westar system.
- After FCC action, implementation of a plan for shared use of the Public Broadcasting Service earth stations, and development and implementation of a similar plan for shared use of National Public Radio earth stations.
- Also subject to Commission action, implementation of a plan for joint use of the earth stations to be installed by Westinghouse (Group W).
- By the end of 1980, more than 1,300 earth stations will be using Westar on a full time basis.

During the next twelve to eighteen months, Western Union will have direct satellite distribution capability for video and audio program channel services in all or nearly all of the top 100 broadcast markets in the United States.

Service Options

The service and service options available are almost unlimited. The Western Union pricing approach recently filed with the FCC permits customers to tailor a service or combination of services to meet their specific requirements.

- There are three categories of transponder leased service, with appropriate pricing differentials, for users who are only interested in space capacity for interconnection with their own earth stations. On request, Western Union will furnish uplink and/or downlink service for use with leased transponders.
- For the occasional user, options include a total Western Union end-to-end service; a service employing only customer-owned earth stations; and any combination of Western Union and customer-owned facilities. Special rates are available to the high-volume user.
- Similar service options are available to the program channel user. Since the space segment rates are predicated on the percentage of transponder bandwidth and power required, customers can determine for themselves the optimum space segment and earth station configuration needed, based on trade-offs between the satellite power required and earth station antenna and LNA costs.

The versatility, economy of operation, and technical superiority of the satellite over conventional terrestrial distribution systems have been amply proven and widely accepted. The explosive growth of the earth station population, matched by an equally impressive growth in program material, virtually assures substantially increased program diversity and improved signal quality for our most important user - the audience.

Signal Quality and Performance

A performance standard for satellite distributed audio program channel service has not yet been established. Moreover, with each user effectively "customizing" his service by selecting earth stations with antenna diameters of 6', 10', 15' or larger, with attendant reduction in satellite power required, each system will have its own performance characteristics.

Commonly, however, a studio-to-studio peak program level-to-noise ratio exceeding 58 dB may be expected and significant improvement may be obtained with the use of companders.

Exhibit 2 describes video performance expectations for various combinations of earth stations. For end-to-end service provided by Western Union, the RS 250B standard is met or exceeded. When customer-owned earth stations are used, either wholly or in part (assuming that they are designed to meet broadcast standards), the recommended NTC-7 performance levels will be met.

Economics

Most audio program channel terrestrial systems are in 3.5 Khz, 5 Khz and 8 Khz bandwidths; no nationwide 15 Khz service is currently available comparable to that provided via satellite. Depending on the power required, typical space segment charges per channel, per month are in the range of $11,000-to-$16,000. Additional charges of $3,000-$5,000 per month would apply when company-furnished uplinks are required.

A coast-to-coast (New York-Los Angeles) video service of one hour during prime time would cost $1,839 on a landline system; $580 via satellite to an occasional user, and $390 to a high-volume user. Some typical multipoint distribution charges are as follows:

One Hour Prime Time

	Terrestrial	Satellite
Top 25 ADI Markets	$ 4,590	$1,136
Top 50 ADI Markets	6,318	1,800
Top 100 ADI Markets	15,714	3,100

Conclusion

Satellite technology has proven to be a highly reliable and economical medium for broadcast services applications. The implementation of earth station networks already committed, as well as those in the planning stages, and the deregulation of receive-only earth stations will contribute to the continued growth and development of satellite distributed broadcast services.

Western Union is committed to maintaining and strengthening its leadership role in satellite services to the broadcast industry.

Western Union's landline—satellite wideband transmission network.

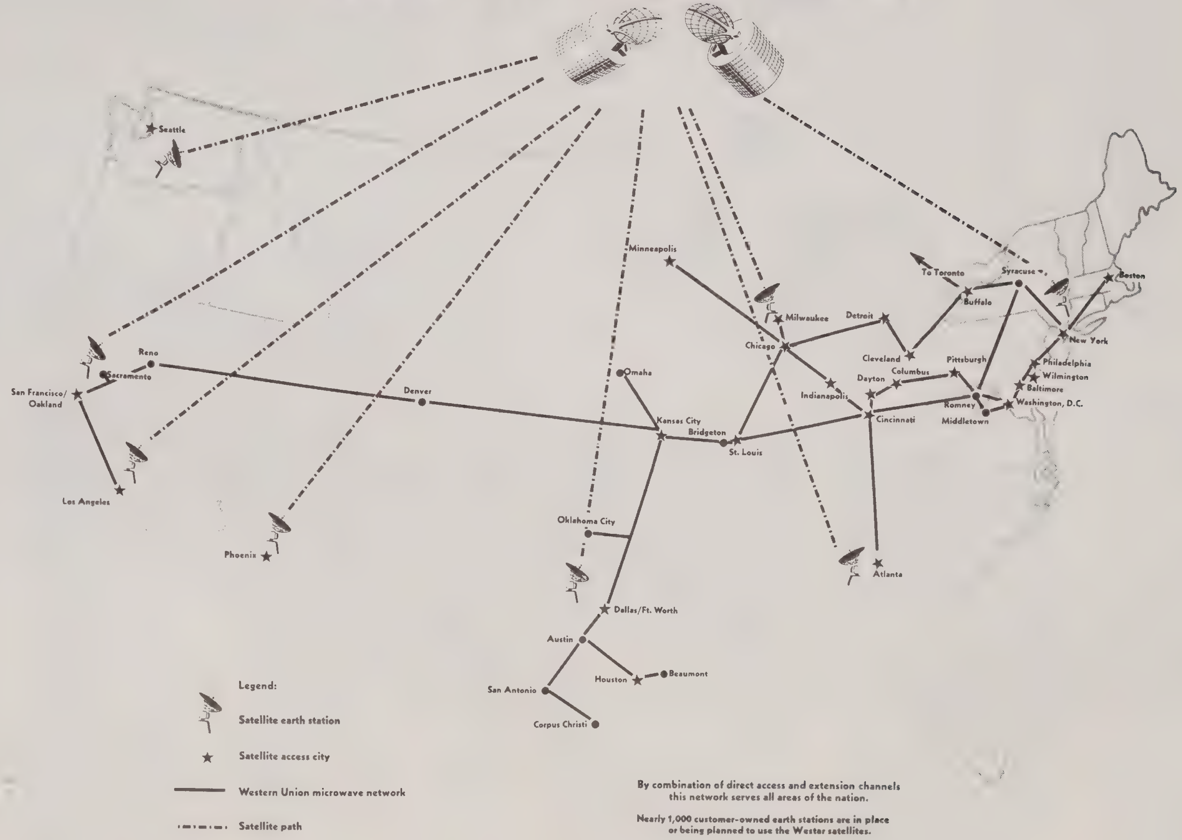
Seattle
San Francisco/ Oakland
Sacramento
Reno
Los Angeles
Phoenix
Denver
Minneapolis
Omaha
Kansas City
Bridgeton
St. Louis
Oklahoma City
Dallas/Ft. Worth
Austin
San Antonio
Corpus Christi
Houston
Beaumont
Milwaukee
Chicago
Detroit
Indianapolis
Dayton
Columbus
Cleveland
Cincinnati
Atlanta
Pittsburgh
Romney
Middletown
To Toronto
Buffalo
Syracuse
Boston
New York
Philadelphia
Wilmington
Baltimore
Washington, D.C.
Legend:
Satellite earth station
Satellite access city
Western Union microwave network
Satellite path

By combination of direct access and extension channels this network serves all areas of the nation.

Nearly 1,000 customer-owned earth stations are in place or being planned to use the Wester satellites.

80-0567

THE INTELPOST SYSTEM

Helmo Raag*
Communications Satellite Corporation
Washington, D.C. 20024

Abstract

INTELPOST is an experimental international electronic message system which COMSAT has been developing for the United States Postal Service. The INTELPOST system design is based on the use of high-speed digital document facsimile scanning and printing equipment which is interfaced to minicomputers for store-and-forward operation. The INTELPOST systems forms an intercontinental packet switched network.

Introduction

International Electronic Post (INTELPOST) is an experimental international electronic message system. The INTELPOST concept is illustrated in Figure 1. Since March 1978, COMSAT has been planning, designing and implementing the INTELPOST system for the United States Postal Service (USPS). The Postal Administrations of a number of countries have decided to implement similar INTELPOST installations, and have agreed with the USPS to conduct demonstrations and a field trial of the INTELPOST system.

The INTELPOST system has been designed to provide an international electronic message service between end users. It has been designed to be a postal service. This means that in addition to the technical design of the system, other INTELPOST service features, including message collection and delivery procedures as well as other message handling details, have been planned and coordinated between the participating Postal Administrations and are being implemented. This paper discusses mainly the more important technical features of the INTELPOST system.

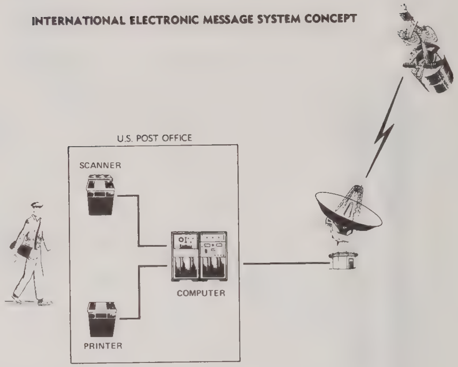

Figure 1.

System Design

The more important INTELPOST system features are:

Network Approach

All INTELPOST sites are intended to be interconnected to form a network, instead of being implemented as a series of separate point-to-point links. The network enables the routing of messages between any of the sites in the network. Each site can act as a source or a destination of a message. In addition, commensurate with the throughput capacity of the site, each site can act as a transit center for messages of other sites when the necessary transmission facilities are installed and the necessary routing instructions are included in the computers of the sites.

The advantages of the network approach to INTELPOST system design parallel those in telecommunication networks. The amount of scanning and printing equipment required at the various sites is minimized, system utility is maximized, network topology and the use of transmission facilities according to traffic requirements can be optimized, and alternative routing paths between sites can be provided.

---

*Director, Electronic Mail Systems
Member of AIAA

The views expressed herein are those of the author, and do not necessarily represent the views of the Communications Satellite Corporation or the United States Postal Service.

Copyright © American Institute of Aeronautics and Astronautics, Inc., 1980. All rights reserved.

The INTELPOST network has been designed as a packet switched network using an end-to-end communication protocol. This provides for considerable flexibility for accommodating changes in network topology and for supporting network expansion.

The initial implementation of the INTELPOST network resulted from a series of bilateral agreements between the USPS and the participating foreign Postal Administrations. This determined the star configuration of the initial network as shown in Figure 2.

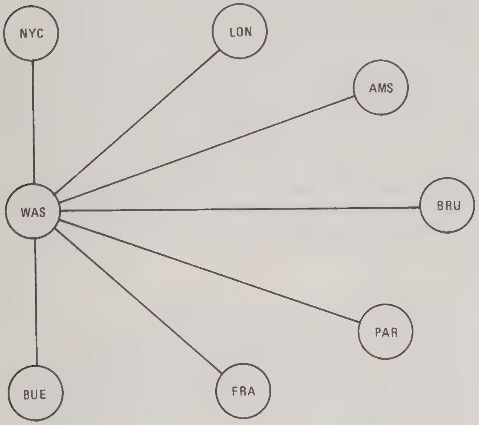

Figure 2.

Store-And-Forward Operation

The INTELPOST system equipment configuration is shown in Figure 3. It includes a minicomputer with disk storage for store-and-forward operation. All messages are stored on disk after scanning and before being transmitted to distant sites. Similarly, all received messages are stored on disk before printing. Thus the scanning and printing operations are separated from the message transfer procedures between sites. This provides a number of advantages. The transmission data rates to different INTELPOST sites are determined on the basis of traffic volume requirements and may vary (e.g., 9.6 kbs or 50 kbs). Store-and-forward operation provides transmission data rate buffering of the printers and scanners to the transmission lines. The disk storage allows for message load buffering both for incoming and outgoing message traffic. INTELPOST is intended to be an international system with sites in widely different time zones. It is not expected to have operating personnel at all sites, 24 hours a day, at least unitially. Store-and-forward operation allows unattended reception and storage on disk of incoming messages as well as unattended transmission of stored messages to distant sites. In the initial INTELPOST equipment configuration up to about 1000 pages can be stored on disk at a site at any one time. Store-and-forward operation allows to separate the transmission error control procedures from the scanning and printing operations, and it allows to retain the stored message on disk at the originating site until the receiving site notifies that it has received the entire message without errors.

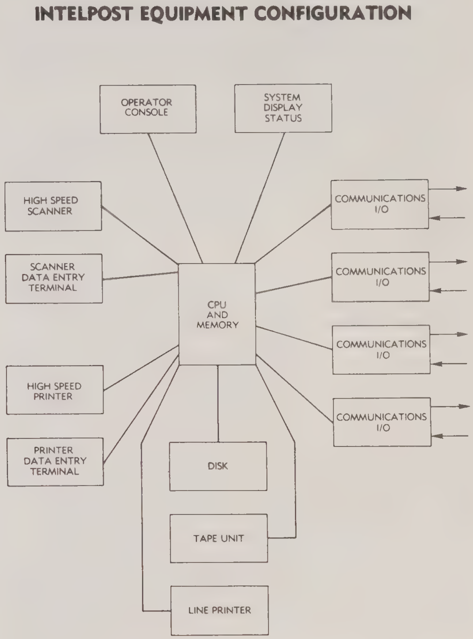

Figure 3.

High-Speed Scanning and Printing

High-speed facsimile scanning and printing equipment is important mainly for two reasons. First, it provides for operator convenience and secondly, it enhances system throughput capability. The facsimile data in the INTELPOST system conforms to the format of CCITT Draft Recommendation T.4. The specified resolution is 7.7 lines/mm and data compression is according to the modified Huffman run-length code specified in Rec. T.4. These parameters determine that a scanned page results in about four million bits uncompressed, and, on an average, about half a million bits compressed.

The facsimile scanners and printers in the present INTELPOST equipment implementation operate at about 10 - 12 seconds per page. The data compression and expansion is accomplished in the scanner and printer, respectively. Thus the transmission data rate to/from the computer is 50 kbs.

Message Control

In a postal electronic message system, message control is one of the fundamental and more important requirements. It is essential that no message or part of it be lost or misrouted. Measures must be included in the system design to keep a record of the scanning, transmission and printing times of messages along with other data although it is equally important that the contents of a message be not retained in the system for longer than to assure that the message has been successfully transmitted and printed.

Message control measures in the INTELPOST system are visualized to evolve in a phased manner. In the early phases of INTELPOST implementation, postal operators play a significant role in message control. Later, the use of more automated measures is visualized.

Message control in the INTELPOST system is exercised at present through the following system features. Each message to be transmitted is assigned an identification number which includes the originating site identity and a six digit assignable alphanumeric code. Each message is accompanied with a transmittal sheet where the sender's and addressee's names and addresses are included, the number of pages in the message, the destination site identity, the message identification number, the delivery method from the receive site to the addressee, etc. The scanner operator enters the required information (message identification number, destination, priority level and number of pages in the message) into the computer through an interactive data and display terminal.

The system keeps track of the message flow from the originating site to the receiving site through a series of updates of the "Document Information Block" (DIB) which is assigned in the originating computer to each message when the scanner operator enters the previously described data into the computer. The same information is transferred to and stored also in the receiving computer. The DIB is kept updated in both the originating and receiving site computers and it contains the time of message scanning, whether the message is in the transmission queue, time of transmission, time of printing and other information in addition to the data entered by the scanner operator. All times are recorded in GMT with resolution of one minute. Through the system operator interactive data entry and display terminal, and using the document identification number, it is possible to inquire about the current status of any message to be transmitted or received by that site.

The printer operator interacts with the computer also through an interactive data entry and display terminal and he can instruct the computer and the printer what document to print, what acknowledgement to send to the originating site (printed OK, rescanning required, etc.) and so on.

At the originating site, a confirmation label is printed in duplicate for every transmitted and printed message which includes the message identification number, the destination, the priority level, the scanning time at the originating site and the printing time at the receiving site. The confirmation lable is affixed to a copy of the transmittal sheet which is kept at the originating site as a record of the message handling.

Message control is exercised also as part of the message transmission procedures disk at the originating site until the receiving site signals to the originating site that the entire message has been received correctly. Similarly, the message is retained on disk at the receiving site until the printer operator acknowledges via the data entry terminal that the message has been properly printed.

Error Control

To protect against transmission errors, an error detection and retransmission scheme has been included on end-to-end basis. That is, the destination INTELPOST computer checks the received packetized data for errors in the individual packets and acknowledges all correctly received packets. The intermediate or transit sites do not perform such checking. The originating INTELPOST computer waits for the acknowledgements to arrive for all transmitted packets, and after a preset time, retransmits only the unacknowledged packets.

System Implementation

Since INTELPOST is an experimental system, an important requirement is that the system is flexible for accommodating changes in equipments as well as in operating features. At the same time, to permit its implementation in a relatively short time, the demonstration system was designed to include only the necessary basic system features which would allow a meaningful demonstration of system operation, and an initial evaluation of system operation and performance. The demonstration system was implemented with the following fundamental criteria in mind:

- Low cost
- flexibility for expansion
- nonredundant equipment configuration
- basic software

The INTELPOST systems have been implemented at present by all participants using RAPICOM 500T and 500R high speed facsimile scanners and printers and Digital

Equipment Corporation PDP 11/34 minicomputers. As the system evolves, implementations using other equipment can also be expected. The scanners and printers employ a specially designed computer interface. The minicomputer provides for modular system construction, for connection of different facsimile, character recognition or other terminal equipments, or for changes in INTELPOST network topology. Finally, the system software is also designed for implementation in a modular manner so that changes and additions of system features can be accomplished relatively easily.

The initial INTELPOST system implementation and operation have proved the soundness of the basic system design. During the field trial and for an operation system various system hardware and software enhancements are visualized. Among the more important intended improvements are the following:

- inclusion of additional scanners and printers and additional computer modules to increase system reliability as well as to increase system capacity;

- improve system monitoring, control, fault handling requirements and to provide for local options;

- provision of features for gathering system performance and traffic statistics, gathering accounting and billing data, message encryption, and dynamic traffic routing.

The star configuration of the initial INTELPOST network is not optimum for an operational system. Studies are currently underway to define a network configuration which provides for increased reliability, meets the varied traffic demands of the various sites and optimizes the use of transmission facilities. Figure 4 shows a mesh network of the same INTELPOST sites as in Figure 2. A meshed network can be engineered to provide the cited advantages over a star network.

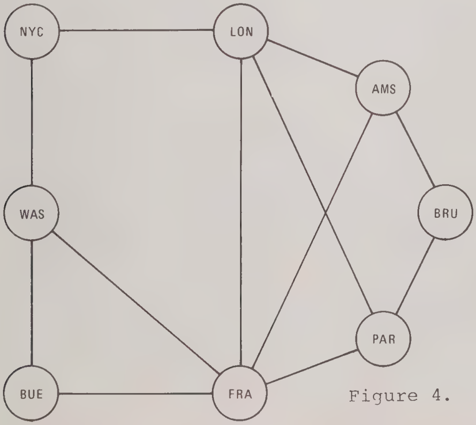

Figure 4.

The INTELPOST system is also particularly well suited for implementation as network through the use of satellite TDMA technology. The facsimile raster scanning and printing approach results in a relatively large amounts of data to be transmitted or received per message as compared with alpha-numeric transmission. This, together with the requirement to be able to transmit messages quickly in time windowns constrained by large intercontinental time zone differences and mail cutoff times for letter carrier delivery schedules, makes the use of high data rate circuits attractive. The use of the needed transmission capacity of a communications satellite provides connectivity between all sites, allows to allocate transmission capacity on demand, and to dimension the transmission system to meet the traffic and delivery time requirements.

80-0568

DIGITAL FACSIMILE COMMUNICATION OVER SATELLITE LINKS

Naohiko Hattori
Kokusai Denshin Denwa Co., Ltd. (KDD)
2-3-2, Nishi-Shinjuku, Shinjuku-ku
Tokyo 153, Japan

Abstract

This paper describes the correlation between the characteristics of digital facsimile transmission and those of the satellite links now operating as a main transmission means for international communication, combined with the recent increase in demand for new and improved functions.

The paper reports on the results obtained from testing the high-speed digital facsimile equipment developed by KDD on the practical international transmission channels over the satellite links and also describes functions necessary for maritime digital facsimile transmissions over their links. The paper is also to report the expected functions of international facsimile transmission service.

Lastly, the paper forecasts traffic characteristics of the digital facsimile and the new visual communication service over satellite links and then gives a description of the theme for future study.

1. Introduction

Demand has increased sharply in the facsimile communication as effective means to compensate characteristics of the communication media such as existing telegraph, telephone, and telex service. This trend has been also recognized in international communication.

Facsimile is a type of visual communications with an exceedingly high transparency for the recording information, and its characteristics offer great potential and possibility to be used for business in a briskly expanding economy and the information society as well. These will be pointed out, for example: the particulars can be transmitted accurately to a place so intended irrespective of how characters, figures and drawings come in configuration; documents already recorded can be transmitted straight without retyping; a high reliability of communications which is one of the features with recording communication can be expected; a high-speed transmission can be realized; the equipment can be obtained at a reasonable price; the operation is simplified.

In addition to the above-mentioned features, the digital facsimile described in this paper is conceived to have many factors available for the facsimile communication media. The digital facsimile has an enough affinity with the technique on digital information processing which is highly developed. With its affinity accordingly with the public digital data network now under way throughout of the world, something may be left available both in operation of the equipment for common use and in application of the technique for transmission, exchange, processing, terminal equipment, etc., thus leaving a potentiality of applying the digital facsimile for various scopes. That the equipment can be obtained at low cost compared with ones in the past as the result of remarkable technological innovations in solid state optical scanning and recording techniques, microprocessor, electrostatic reproduction technique, etc. and that a high-speed MODEM with the automatic line equalizer was recommended by CCITT and is now ready for supply very cheaply through LSI technique — these can be pointed out as influential factors to have accelerated development of the digital facsimile.

This paper is hence to give a description of a correlation between characteristics of the satellite link and functions to substantialize characteristics of the digital facsimile, when operating the digital facsimile communication expected as one of the important international communications in the future over the satellite link working influentially as an international main transmission means along with the submarine cable circuits.

The paper further particularizes "Quick-FAx", a high-speed digital facsimile equipment which was subjected to a field test on actual international transmission channels over the satellite link with its test result and then reports on various technical problems settled for the maritime satellite communication and the "Maritime Quick-FAx" also under development.

The paper refers moreover to a report on; the main traffic characteristic of digital facsimile telegram introduced as an international facsimile telegram service based upon the above test result; an introduction of the result obtained through analyzing the traffic characteristics, between countries with time difference; time of the international telex service which is operated at present for business as a one-way recording communication very close and similar characteristics to facsimile. The paper also estimates the traffic characteristics of the future international digital facsimile in view of its being a common base as one-way recording communication used for business, and then intends to give data which are useful to design facsimile communication systems for the purpose of using effectively international transmission circuits.

Copyright © American Institute of Aeronautics and Astronautics, Inc., 1980. All rights reserved.

2. International Digital Facsimile Communications and Satellite Links

International communications have achieved a remarkable upswing through the two major transmission media of communication satellite circuits and submarine cable circuits, on which the majority of communication services depend at present.

International facsimile communication is also performed through these transmission lines, and in Japan the international voice-grade leased circuits, the international DATEL and the international facsimile telegram service are used for international facsimile communications. On the other hand, maritime satellite DATEL through MARISAT has been in service since September 14, 1979, thereby enabling facsimile communications between ships and land subscribers.

Generally, the feature of the satellite circuits come in the following:

1) A propagation delay of 600 ms in reciprocation is caused due to a long transmission path.
2) The circuit characteristics have not close relations with physical ground distances.
3) A wide band transmission line of high quality can be offered.
4) The circuit configurations are provided in principle with a pluralism.

The transmission line which is characterized as above has something to do with the following for the international facsimile communication:

1) With reference to the propagation delay time on the transmission path, the problems on how efficiently to send signals within a short time and also on how to operate in consequence will be correlated.

(a) In case the public switched telephone network is used for transmission line for the international DATEL circuit, a function (echo suppressor) to control the echo arising mainly on the four-wire/two-wire conversion and another function (tone disabler) to stop the above function for a time will have to be taken into consideration for transmission and operating method of the facsimile signal.

(b) Next, in the case of digital facsimile, transmission errors will have to be taken into consideration for how to control it, which is classified roughly into transmission control procedure and that of processing it with the terminal function, both of these being combined where necessary.

2) For the circuit characteristics, stable and high quality circuits have been supplied at present over the satellite. The 1-hop and 3-hop international digital facsimile transmission tests were finished successfully over INTELSAT-IV Satellite between Japan (Tokyo), U. S. A. (New York) and Australia (Sydney) in January to February 1977.

3) and 4) An attractive characteristics may be emphasized, which is expected fruitfully to plural future services like international teleconference service.

3. High-Speed Digital Facsimile Equipment "Quick-FAX" and "Maritime Quick-FAX"

The efficient transmission of information is the most important technical theme in international facsimile communication.

To cope with the above requirement the high-speed digital facsimile equipment "Quick-FAX" was developed in September 1975, and an international transmission test was successfully carried out between Japan and U. S. A. by combining various physical circuits including INTELSAT-IV Satellite link. This equipment was introduced as a practical one to operate for the international facsimile telegram service on March 1, 1978.

In addition, the development of a maritime high-speed digital facsimile equipment "Maritime Quick-FAX" complying with the maritime satellite communication service (MARISAT SYSTEM) for vessels of various countries in the world on the Atlantic and Pacific Oceans was begun in July 1976, and will be tested in the first quarter of 1980. This equipment is expected to be effective for the maritime DATEL service in operation by KDD since September 14, 1979 and the maritime communication satellite service by INMARSAT.

3.1 High-Speed Digital Facsimile Equipment "Quick-FAX"

An ISO-A4 size document has about 2M bits picture elements in standard resolution and about 4M bits picture elements in high resolution. As will be described hereinafter, facsimile is utilized for the purpose of transmitting the multi-documents for more than 60 percent. Thus the facsimile communication must handle much information for transmission, which is conceived to give a different nature from general data transmission.

Shortening of the transmission time through coding technique and employment of a control procedure for efficient transmission will be needed for the international digital facsimile, thereby lowering the transmission cost.

In 1975 was developed Quick-FAX employing a line-by-line sequential two dimensional coding scheme available as a technique to curtail the redundancy of picture information and High Level Data Link Control (HDLC) Procedure for transmission control.

For evaluation of technical characteristics of the equipment and improvement for practical application and also for looking into potential demand for the international facsimile service, a field test and a demonstration were carried out as mentioned. As a result, Quick-FAX is proved to be a terminal of an international facsimile service transmitting documents of high quality and at high speed as the equipment has been improved for higher-speed operation since then and is now in commercial use. The specific features of the equipment are shown in Table 1 and outside view of the equipment is shown in Photo 1.

Table 1 Specification of Quick-FAX

Size of document	ISO A-4 size (210 mm × 297 mm) Letter size (216 mm × 279 mm)
Picture element density	Horizontal scanning 8 picture elements/mm (1728 pels / 215 mm) Vertical scanning 7.7 or 3.85 pels/mm (switchable)
Reading method	Flat-bed scanning system using CCD (Charge Coupled Device)
Vertical-scanning speed	Maximum 200 pels/sec
Recording system	Electrostatic recording system
Coding scheme	One-dimensional coding scheme (MH) and Two-dimensional coding scheme (READ) (switchable)
Data signalling rate	9600 bps (based on CCITT Rec V. 29) 4800 bps (based on CCITT Rec V. 27 ter) 2400 bps (based on CCITT Rec V. 27 ter) (switchable)
Transmission control procedure	Based on high-level data link control procedure (HDLC)
Operation mode and error control	Full duplex : Automatic error correcting system by repeat Half duplex : Automatic error correcting system by repeat or a system for replacing error scanning lines with right preceding scanning lines without correcting control
Operation of transmission and reception	Continuous automatic transmission & reception (for maximum 30 copies) Unattended reception Distant operator calling function
Others	Built-in test facilities Built-in fixed equalizers (for subscriber's line and delay distortion)

Photo 1 Transmitter(right)and receiver of Quick-FAX

According to the coding system employed for this equipment, the original information having scanned a document can be compressed to about 1/20 number of bits, and the bit number can be curtailed to about 1/2 of the coding bits according to one dimensional run-length coding system. For transmission of one sheet of document in ISO-A4 size, for example, the transmission time which used to take 14 minutes for the original information at the rate of 4800 bps can now be curtailed to about 30 seconds with high resolution (7.7 lines/mm).

3.2 Maritime Quick-FAX

A maritime satellite DATEL service using maritime satellite has been available as a service to satisfy one of the latest facsimile demands.

Shipboard subscribers can be connected with Japanese Datel subscribers or overseas ones by means of international communication circuits which are able to transmit facsimile messages for the new service.

For such high-speed digital facsimile equipment, the development of a mechanism capable of protecting against severe environmental conditions such as strong shocks, tilting, high temperatures, and dampness and the reproducing method, a function to prevent impulse noises from arising on the frequency demodulating unit described hereinafter, a function to ensure compatibility with the ground terminal equipment, and further an easy-maintenance arrangement necessary due to servicing being difficult on the sea — these will be claimed as particularly important matters in comparison with the ground facsimile equipment. Maritime Quick-FAX solved these technical problems and will subject it to a field test toward the first quarter of 1980.

To cope with the above conditions, this equipment employs a thermal recording system ; The data signalling rate, 4800 bps/2400 bps/1200 bps can be selected in accordance with the circuit condition.

To cope then with impulse noises arising in the voice band after frequency modulation (FM) is demodulated at ship station or shore station, the bit error rate has been greatly improved by employing smear/desmear filters applying digital filter technique. Furthermore, according to keep the compatibility between the shipboard facsimile equipment and the landboard facsimile equipment, a buffer memory is provided to adjust effectively the difference between the transmitting speed and the reproducing speed at the receiver.

4. Satellite Link Characteristics and Digital Facsimile Function

For high-speed digital facsimile Quick-FAX, a data link control procedure must be employed to transmit visual signals by way of such circuit as will require to have the signal propagated for long distance like the satellite link.

4.1 Frame Structures and Transmission Control Procedures

In this equipment a conception of the frame structures has been introduced for the transmission of facsimile signals, and thus an automatic retransmission error control is operative against picture signal transmission errors not only in the full duplex circuits but also in the half duplex circuits. Fig. 1 shows a frame structure, wherein (a) is a controlling frame, FIF (Facsimile Information Field) coming in 0 bit or 24 bits in this case. Then, (b) is a frame for picture signals, FIF coming in 2040 bits, fixed; (c) indicates a frame structure when transmitting documents only using one dimensional run-length coding scheme (MH); (d) indicates a frame structure when transmitting positively documents by means of two-dimensional coding. The frame structure is still the same in case of combining the one-dimensional coding and two-dimensional coding.

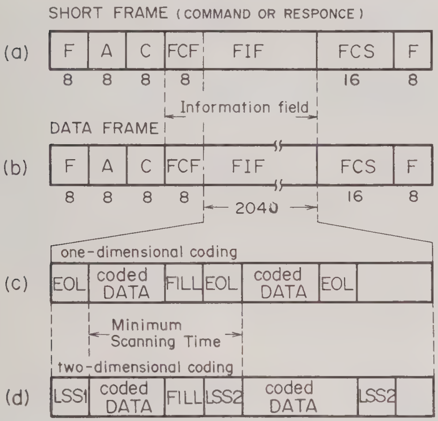
SHORT FRAME (COMMAND OR RESPONCE)
(a)
F A C FCF FIF FCS F
8 8 8 8 16 8
Information field
DATA FRAME
(b)
F A C FCF FIF FCS F
8 8 8 8 16 8
2040
one-dimensional coding
(c)
EOL coded DATA FILL EOL coded DATA EOL
Minimum Scanning Time
two-dimensional coding
(d)
LSS1 coded DATA FILL LSS2 coded DATA LSS2

Fig. 1 Frame structures and contents

Since a buffer memory except for the error control system is not arranged between the transmitting equipment and the receiving equipment, where the signal bit transmission time after one scanning line of picture information is encoded is less than the minimum scanning time specified on the equipment, a fill bit will be installed. Consequently in the case of the rate 4800 bps transmission of ground facsimile equipment the bit number decided by the minimum scanning time will be inserted so as to have come over 24 fill bits since the minimum scanning time is 5 ms.

Figures 2 and 3 show a normal sequence of control signals when using the full duplex circuit and the half duplex circuit each. In each case, the system is such that upon detection of a transmission error in each frame at receiving side through FCS (Frame Check Sequence), a repeat of those coming after the erroneous frame will be requested to the transmitting side.

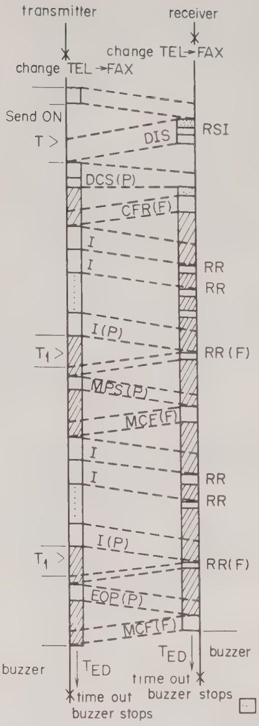
transmitter
receiver
change TEL→FAX
change TEL→FAX
Send ON
T >
RSI
DIS
DCS(P)
CFR(F)
I
I
RR
RR
I(P)
T1 >
RR(F)
MPS(P)
MCF(F)
I
I
RR
RR
I(P)
T1 >
RR(F)
EOP(P)
MCF(F)
buzzer
TED
TED
buzzer
time out
buzzer stops
time out
buzzer stops

Fig. 2 Signalling sequence in full-duplex mode

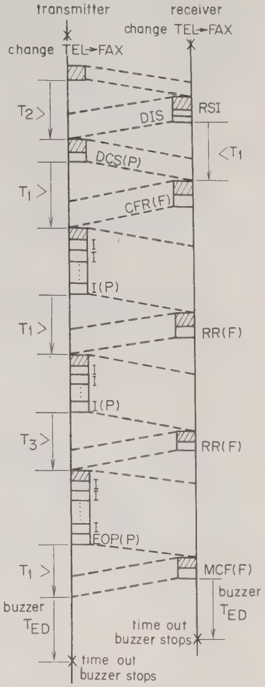
transmitter
receiver
change TEL→FAX
change TEL→FAX
RSI
T2 >
DIS
<T1
DCS(P)
T1 >
CFR(F)
I
I
I(P)
T1 >
RR(F)
I
I
I(P)
T3 >
RR(F)
I
I
I
EOP(P)
MCF(F)
T1 >
buzzer
TED
buzzer
TED
time out
buzzer stops
time out
buzzer stops
☐ Training signal
▨ Continuous Flags

Fig. 3 Signalling sequence in half-duplex mode (in case of automatic error correcting mode)

In the case of full duplex circuit structure, the receiving side reports, as receiving the frames to come, the detected errors, if any, and frame number to request next to the transmitting side. Therefore, in case a transmission error arises, the loss time from delay in the signal transmission is minimized.

However, in the case of half duplex circuit structure like that of Fig. 3, an influence of the loss time in reciprocating signals cannot be disregarded for ensuring at every constant frames even where no signal transmission error occurs.

A correlation between the frame length at using the full duplex circuit and the transmission efficiency η will be given, when assuming as follows, by the equation below (1), wherein B is a frame length (bits), R a control bit in the frame (bits), D one-way signal delay time (msec.) through transmission line (sec.). T a transmission rate (bits/sec.) and E a bit error rate.

In assumption, these are taken into consideration: (a) the frame length is fixed, (b) bit errors occur at random, and (c) the transmission error of command frame and the length of the response frame will be disregarded.

$$\eta = \frac{(1-E)^B (B-R)}{(B-X)(1-E)^B + X}$$

$$(\text{where } X = 2B + 2TD + R) \qquad (1)$$

The correlation between frame length and transmission efficiency is shown in Fig. 4 with the transmission rate and the bit error rate taken as parameter.

In the case of satellite links, it is considered that $D = 0.3$, $E = 1 \times 10^{-5}$ or so, and hence an optimal transmission frame length will be 2,000 bits or so.

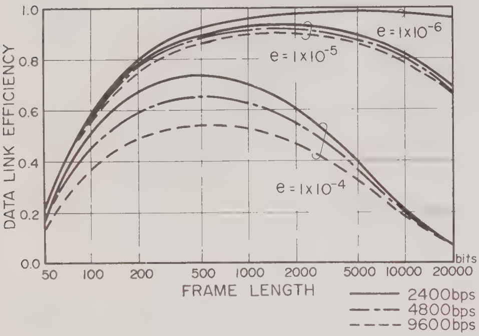

Fig. 4 Data link efficiency vs. frame length

4.2 International Field Tests over Satellite Links

For the first international transmission test, INTELSAT communication satellite, US domestic Satellite System (AMERICOM), Trans Pacific Submarine Cable and transcontinental land line were used in combination. During the test Australia was also connected over the satellite link, which was subjected to the test for 1 Hop through 3 Hops.

The test has proven that Quick-FAX is reliable enough for use internationally and thus was evaluated for high-speed operation function and high quality as well. The data relating to satellite links which were obtained through the test are shown in Table 2.

Many international field tests have been carried out with European countries since then. The automatic retransmission error control function has been found most effective in the full duplex circuit mode in 4-wire system and also very effective in the half duplex mode, if the circuit is kept within the range that the automatic equalizer of MODEM functions.

Table 2 Bit and block error rate (4,800 bits/sec.)

circuit	TOKYO → NY			TOKYO ← NY		
	total bits transmitted	number of errorneous bits	number of errorneous blocks	total bits transmitted	number of erromeous bits	number of errorneous blocks
		bit error rate	block error rate (10^3 bits/block)		bit error rate	block error rate (10^3 bits/block)
satellite (one-hop)	8.64×10^6	0		1.73×10^7	0	0
		$<1.2 \times 10^{-7}$			$<5.79 \times 10^{-8}$	$<5.79 \times 10^{-5}$
satellite (two-hops)	2.16×10^7	28		2.59×10^7	12	2
		1.29×10^{-8}			4.63×10^{-7}	7.71×10^{-5}
TPC	4.00×10^7	0		4.75×10^7	17	3
		$<2.5 \times 10^{-8}$			3.58×10^{-7}	6.31×10^{-5}

4.3 Maritime Satellite Communication and Digital Facsimile

For facsimile service by means of maritime satellite communication, a frequency modulation system is used at present to effect transmissions.

In FM system there exists some threshold level (Fig. 5) for the input level (C/N) to the frequency discriminator, and where it comes lower than that, the broad-band gain which is one of the features with FM system will be lost and S/N will deteriorate quickly. When coming near to the improvement threshold, impulse noises will come out at FM demodulation.

In coping with noise, KDD developed a smear filter (SF) and desmear filter (DSF) consisted of digital filter, provided with the characteristics shown in Fig. 6. This technique is intended to lessen errors by diffusing to the time base not only those arising at FM demodulation but also impulsive noise energy mixed in through the transmission line.

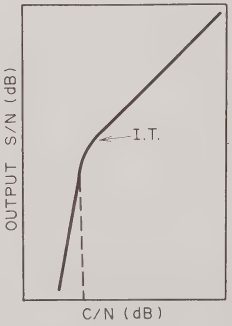

Fig. 5 Improvement threshold of FM demodulation

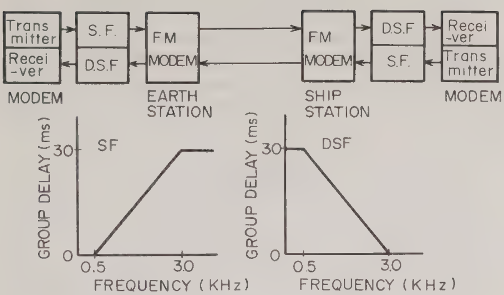

Fig. 6 Characteristics of SF and DSF

The RF band of MARISAT is 28 kHz; the noise level (C/No) per unit frequency is 50.4 dBHz circuit design value. The actual value is conceived to work at 53 dBHz or so. An improved effect of the filters by using the Simulator of maritime satellite communications system is shown in Figs. 7 and 8. There may be some difference in how Bit Error Rate (BER) is improved according to signal level and modulation system, however, an improvement at least in 1/10 to 1/100 is expected and thus the effectiveness has been ensured. The system then enjoys a big feature that it is effective to instantaneous impulsive noises mixed into the transmission line.

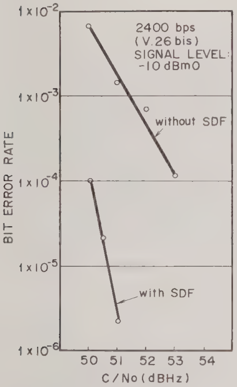

Fig. 7 C/No - BER
(Modulation : 4 ϕ PSK)

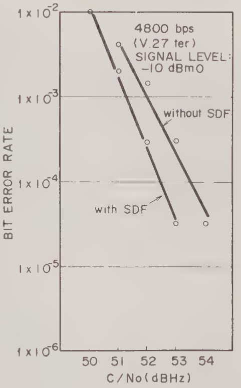

Fig. 8 C/No - BER
(Modulation : 8 ϕ PSK)

4.4 Interconnection of "Maritime Quick-FAX" and "Quick-FAX"

Employing the thermal recording system, scanning speed of the Maritime Quick-FAX is 10 ms/line which is twice of that of the ground Quick-FAX. Therefore, an influence to the recording speed at mutual communication through connecting both the two is as follows :

That the longer recording time at receiver on the ship is influential comes in the case where fill bit is inserted to cover the transmission time of the sum of encoded signals and line synchronization code.

The appearance order of the line encoded bit number on the picture and the frequency are correlated consequently. However, in case the line synchronization code does not come in, the data on an average transmission time for 8 sheets of documents of CCITT indicate that the transmission time is 6.2 percent incremental at standard resolution and 8.2 percent incremental at high resolution compared with land communications.

Therefore, even from coping with the terminal equipment working at 10 ms/line in recording time, the circuit holding time will increase 9 percent or below, little and thus an increase in the holding time is so limited in view of the general inclination of documents.

On the other hand, a receiving buffer memory to secure the above operation may be necessary for the equipment on ship side. Let minimum scanning speed of the terminal equipment on the land side be t (ms), that of the terminal equipment on the ship side t' (ms), transmission rate of MODEM V (bps) and the line number per picture ℓ, then the memory capacity S (bits) necessary at least for the receiving side can be expressed as follows :

$$S = t\ell(1 - \frac{t}{t'}) V \times 10^{-3} \qquad (2)$$

5. Traffic Characteristic of International Digital Facsimile

The international facsimile telegram service by means of high-speed digital facsimile equipment Quick-FAX was first commenced between Japan (KDD) and U. S. A. (RCA Globcom) on March 1, 1978, then with ITT Worldcom on October 1, 1978 and with WUI on February 5, 1979. From its being characteristic of high quality and high speed, the service for customer's convenience sake including an expansion of the area and an introduction of the consigning service are also under planning.

Figs. 9 and 10 show results obtained through analyzing the facsimile traffic handled on the international facsimile telegram during the six months from March 1, 1978.

The figures indicate that about 57 percent of all the messages were documents typed in Lathen alphabet but some of them included additional handwriting such as signature, corrections and the like. More than 90 percent of these messages were copies of the latest publications or originals of some sort of formal business documents.

Messages containing drawings, tables, signatures, etc., occupied some 60 percent of all the messages. None of them can be sent by communication media other than facsimile.

It is also interesting to note that 65 percent of all the messages consisted of multi-page documents. There were even some messages of over 100 pages long sent in one batch to the same addressee. Only less than 5 percent of all the messages were purely alphanumeric correspondences that could be sent by telex or telegram.

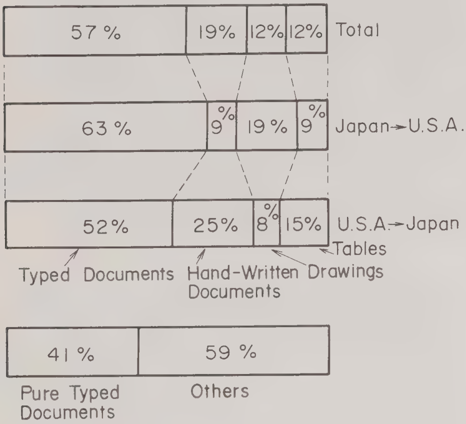

Fig. 9 Percent share of each type of documents

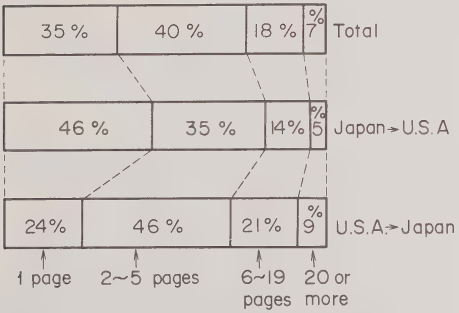

Fig. 10 Percent share of message size

It can be understood from the result that facsimile has been used as a very effective means for compansiating the existing service for business.

In assumption that the international facsimile communication is provided with a one-way transmission characteristic and is featured of recording the business documents, it is interesting to see the traffic characteristics of international telex service suggesting the future traffic characteristics of facsimile communications similar to the recording communication provided with a one-way transmission characteristics in business orientation, even though the contents of transmission are variant in field according to each communication means.

Fig. 11 shows a change in distribution of traffic volume and time difference where communication is made to the country with time difference through international telex service. A daily change in communication (transmission) can be expressed in the sum of the three normal distributions. A conversational communication mode through international telex service is below 10 percent. The way of sending from the calling side is a big factor to determine the traffic characteristics, and has been found relating largely to the flow of business through analysis. Namely, the service is utilized as a communication to leave the record in well consideration of the time difference at the called party's, and the transmission traffic is controlled to take a serious view of having the message delivered simultaneously with the commencement of business activity by the called party.

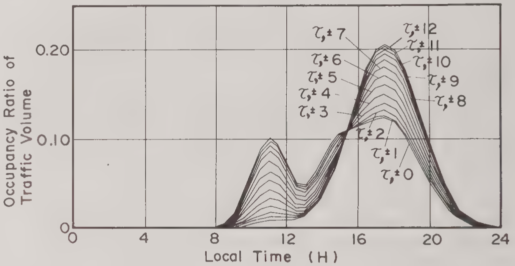

Fig. 11 Theoretical traffic intensity distribution vs. Time difference of INT TLX (outgoing)

Fig. 12 shows theoretical distributions of traffic volume with time difference as a parameter, of international telex, international telegram and international telephone services. The traffic distribution of the future international facsimile communication is forecasted to be similar to that of the international telex from the reason given above. These characteristics will be useful for the design of facsimile information processing and exchanging systems on international communication.

6. Conclusion

This paper has described the relation between characteristics of the international digital facsimile using mainly the voice-grade circuit and those of the satellite link operating as its transmission line.

Considering that the international digital facsimile is highly compatible with the public digital data network currently under construction by various countries and needing to cope with requirements for the diversified service, it is presumed that there is much potential demand for these data networks.

The facsimile itself will then not only retain in the area of merely transmitting documents but also be the support and driving force of the new international picture transmission service partly through combining organically with other communication means and information processing by computer, thus increasing the traffic volume in satellite links.

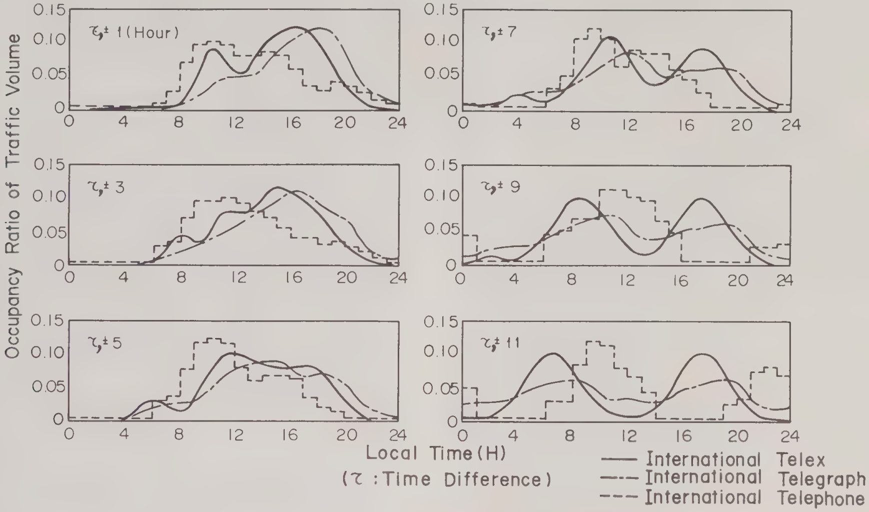

Fig. 12 Theoretical total distributions of international public communication systems (outgoing and incoming), $\tau = \pm1, \pm3, \pm5, \pm7, \pm9, \pm11$

7. Acknowledgement

The author wishes to acknowledge continuous guideance and kind suggestions of Dr. S. Oshima former Executive Vice President of KDD, Mr. Y. Matsumoto Vice President and Managing Director of KDD, Dr. Y. Nakagome Director R & D Labs., Dr. S. Watanabe, Director, Visual Comms. Planning Office. The author also wishes to acknowledge useful suggestions made by Dr. H. Teramura Deputy Director R & D Labs., Mr. K. Kobayashi Deputy Director, General Planning Office, Engineering Planning Department.

Application is also expressed to Dr. K. Kawai, Manager 1st Special Lab., R & D Labs. and the members of development group of the Maritime Quick-FAX for the useful discussion and comments on the subject of this paper.

8. References

1. H. Teramura, Y. Yamazaki, T. Isago, S. Yamamoto: Field Trail for the Digital Facsimile Service over the Satellite Circuit. (1978 DIGISAT)

2. K. Kobayashi: The Technical and Application of High-Speed Digital Facsimile. (March 1979 SGI Symposium)

3. Y. Nakagome, H. Teramura, N. Hattori: Digital Processing and Switching Facsimile Signals. (Oct. 1975 World Telecom. Forum)

4. N. Hattori, K. Nakao, Y. Yamazaki, H. Teramura: Experimental Digital Facsimile Switching System. (Dec. 1976 JEES SE-76-65)

5. Y. Wakahara, S. Yamamoto, N. Hattori, H. Kaneyasu, S. Uchiyama: Procedure Control and Signal Processing of Digital Facsimile Switching System. (Dec. 1976 JEES SE-76-66)

6. N. Hattori, K. Yamada: Traffic Characteristics of the International Telex Calls. (ITC-7, June 1973 No. 443)

7. T. Ohta: Telecommunication Traffic Influenced by Time Difference. (Dec. 1967 JEES)

80-0569

EXPERIMENT RESULTS OF JAPANESE BSE PROGRAM IN THE FIRST YEAR

Nobuo IMAI
Radio Research Laboratories, Ministry of Posts
and Telecommunications
Koganei-shi, Tokyo 184, Japan

Shoji SONODA
Nippon Hoso Kyokai (NHK: Japan Broadcasting Corporation)
Jinnan, Shibuya-ku, Tokyo 150, Japan

Yoh ICHIKAWA
National Space Development Agency of Japan
Hamamatsu-cho, Minato-ku, Tokyo 105, Japan

Abstract

The Japanese Medium-scale Broadcasting Satellite for Experimental Purpose (BSE) was launched successfully on April 8, 1978 JST. BSE was stationed on April 26 at the predetermined geostationary orbit position, 110 degrees east longitude. After the initial check of the satellite function, various kinds of satellite broadcasting experiments started on July 20, 1978. The experiments will be conducted for three years in order to obtain the technical data necessary for establishing future operational domestic satellite broadcasting systems. Most parts of experimental items planned in the BSE program have been carried into operation. This paper will present the results of BSE experiments which have been obtained heretofore along with a brief description of future experiment plan.

1. Introduction

The Japanese Medium-scale Broadcasting Satellite for Experimental Purpose (BSE) was launched successfully on April 8, 1978 JST from the Eastern Test Range of USA, using a Delta 2914 launch vehicle. After several precession maneuvers, Apogee Kick Motor (AKM) was fired at the third apogee and put into the drift orbit.

On April 26, BSE was stationed at the predetermined geostationary orbit position, 110 degrees east longitude. The BSE is held within the accuracy of ± 0.1 deg. and ± 0.2 deg. in orbit position and antenna beam pointing respectively.

The BSE is a three-axis stabilized spacecraft weighing about 350 Kgs in orbit.

It has two sets of Ku-band (14/12 GHz) transponders with 100 watt output power, and a uniquely shaped beam paraboloidal antenna for color TV broadcasting.

On July 20, 1978, the Radio Research Laboratories (RRL) of the Ministry of Posts and Telecommunications (MOPT) and the Nippon Hoso Kyokai (NHK: Japan Broadcasting Corporation) started various kinds of satellite broadcasting experiments. The experiments will be conducted for three years in order to obtain the technical data necessary for establishing future operational domestic satellite broadcasting systems. NASDA is responsible for the control and maintenance of the BSE during the experimental period.

The earth terminals which participate in the BSE experiments are Main Transmit and Receive Station (MTRS), two types of Transportable Transmit and Receive Stations (TTRSs, Type A and B), three types of Receive Only Sations (ROSs), and many Simple Receive Equipments (SREs).

Since the beginning of experiments, most parts of experimental items planned in the BSE program have been carried into operation.

Main experimental items of the BSE program are experiments on the evaluation of broadcasting service area, experiments on TV signal transmission, experiments on radio wave propagation, experiments on frequency sharing, experiments on satellite broadcasting signal reception, experiments on control and operation of satellite broadcasting system, and so on.

Details of results of these experimental items will be described in the following sections.

2. Experiments on the evaluation of broadcasting service area

The service area can be evaluated by measuring the field strength and received TV signal quality at many places throughout Japan. The satellite antenna has a suitable radiation pattern for providing high quality color TV broadcasting services to the whole Japan territory. Fig. 1 shows the BSE antenna radiation pattern and locations of the various earth terminals which participate in the BSE experiments, plotted on a map of Japan.

The Main Transmit and Receive Station (MTRS) is located in Kashima, which provides not only TV signal transmission and reception, but also Ku-band TT&C operation for experimental purposes. The receiving stations (ROSs and SREs) usually receive TV signals which are transmitted from MTRS or TTRSs. For TV-reception tests, additional SREs of about thirty are further incorporated.

The measurements of the received carrier level, video signal-to-noise ratio, and TV signal quality assessment have been carried out by MTRS, TTRSs, ROSs and SREs. One example of measurement results is shown in Table 1.

3. Experiments on TV signal transmission

3.1 Satellite transponder characteristics

To measure initial performance and time variation of satellite transponder characteristics, the initial check and periodical checks per every half year have been performed. Measured items are input-output characteristics (linearity, AGC characteristic, etc.), output characteristics (intermodulation, mutual modulation, spurious emission, etc.), amplitude characteristics, delay characteristics, frequency stability, noise characteristics, and so on.

Copyright © American Institute of Aeronautics and Astronautics, Inc., 1980. All rights reserved.

The measurement results of all these characteristics were satisfactory. Fig. 2 shows the variation of satellite output power from July 1978 to March 1979. The output level of satellite was obtained by converting the receiving level at MTRS. Each point gives a monthly average of every day values which are measured in a fixed measurement method at the same time in the morning.

As a whole, level variation of ± 0.5 dB is observed.

3.2 Standard TV signal transmission

(1) Radio frequency transmission characteristics

To clarify the RF transmission characteristics of satellite transmission links, various characteristics have been measured at the main station. They are level diagram of satellite links, transmitting power and its variation in up and down links, C/N and S/N in up, down and overall links, frequency characteristics (amplitude, delay, DG, DP), transponder input-output and frequency stability, spurious and intermodulation characteristics, and so on.

Here several representative characteristics will be described. As level diagrams are the most fundamental characteristics, they have been measured from the initial check period up to the present.

An example of radio frequency link levels between the MTRS and the BSE is shown in Table 2. The results show good correspondence with calculated design values.

At the main station, C/N is usually very high compared with other satellite links. So C/N can be measured over very wide range in the BSE links. Fig. 3 gives measurement results of C/N in up and overall links. C/N in uplink can be estimated from EIRP of the main station, and also from telemetry data of the satellite. Both estimated C/N values coincide within tolerances of 1 to 2 dB which correspond to telemetry quantization errors.

Fig. 4 gives the relation between C/N and S/N. Measured values coincide fairly well with calculated curves, and the improvement effect by emphasis (2.9 dB) is also apparent.

Using LCE (Level Control Electronics) settings as parameters, C/N in up, down, and overall links were measured to get noise figures of transponder with varying EIRP of the main station. Fig. 5 gives noise figures for channel A1 transponder. The noise suppression effect caused by HL-TWT's (100 W TWTA) nonlinearity is apparent.

It is fundamental to examine the frequency characteristics of amplitude, delay, differential gain (DG) and differential phase (DP) to know the satellite links characteristics for transmitting FM television signals.

In the satellite loop-back measurements, characteristics of both the satellite transponder and the earth station are mixedly measured. The characterisics of satellite transponder are obtained by subtracting the characteristics of earth station from the characteristics measured in satellite loop-back.

To transmit FM television signals faithfully, it is necessary to have flat amplitude and delay characteristics in pass-band. Fig. 6 shows measured amplitude and delay characteristics of overall link. Equalizers in the main station are effective in improving overall amplitude and delay characteristics. Fig. 6 gives the measurement results in March 1979, showing little change from the characteristics measured in July of 1978.

Fig. 7 shows DG and DP characteristics of overall link, which were measured at the same period as Fig. 6. It is seen from these measurement results that the BSE links have excellent RF transmission characteristics as television transmission links.

(2) Baseband transmission characteristics

Measurements of baseband transmission characteristics have been performed for many items. For video signals, they include modulation characteristics, amplitude and delay characteristics, waveform distortion, linearity (DG,DP), S/N and subjective assessment of picture quality. For sound signals, they are modulation characteristics, emphasis characteristics, frequency characteristics, distortion, S/N, and subjective assessment of sound quality, and so on. The BSE experiments have been conducted under the same parameter setting, assuming FM transmission of conventional NTSC-M color television signal as standard. Since January of 1979, dispersal signal has been added.

It is seen from these measurement results that baseband characteristics are almost determined by those of the main station, and are scarecely influenced by the satellite transponders.

3.3 Advanced TV Broadcasting system

Various kinds of signal transmission experiments have been carried out with the purpose of developing advanced TV Broadcasting technique or new application of satellite broadcasting system. Among them are PCM-TV transmission, ranging system using TV synchronous signal, standard time and frequency dissemination system via satellite, high-definition TV transmission and so on.

(1) High-definition television transmission

A high-definition television system parameter tentatively specified by NHK Technical Research Laboratories is shown in Table 3.

Fig. 8 shows the experimental system for the high-definition TV transmission with the BSE. A unique feature of this system is that the luminance (Y) and chrominance (C) signals are transmitted through the separate radio frequency channels. Necessary RF band widths is 80 MHz and 25 MHz for Y and C signals, respectively. Major advantage obtained by the Y/C separate transmission over the conventional composite color signal transmission is a great improvement, approximately 10 dB, of the signal to noise ratio. In other words, the satellite transmitting power can be decreased to 1/10 of that required for the conventional transmission method.

In November 1978, the first transmission experiment through the BSE was carried out at NHK Technical Research Laboratories for four days. As the signal sources, a color print of landscape scene and a strip from a 70 mm movie were picked up by the return beam Saticon camera and the special telecine equipment, respectively. Quality of the received picture was quite satisfactory so that one can hardly tell the degradation after the satellite transmission except a very slight increase of noise. Table 4 shows the carrier-to-noise ratio (CNR) measured on the Y and C channels. Also an average picture SNR is shown in Table 5. At the second transmission experiment held in March 1979, a high-definition TV reception was successfully demonstrated at the Ministry of Posts and Telecommunications down town in Tokyo.

The channel plan to be applied to the 12 GHz broadcasting satellite system operated in the ITU

Regions 1 and 3 has been decided by the World Administrative Radio Conference held in 1977 (WARC-BS). Since the plan is based on the conventional TV system such as NTSC, PAL or SECAM, it is evident that the high-definition TV described here does not conform with the technical standards specified by the plan. From the technical point of view, however, the experiment still remains to be meaningful because the effectiveness of the Y/C separate transmission method is proved through the actual satellite path, in considering its application to the 22 GHz and higher frequency bands allocated to the broadcasting service.

(2) Preliminary experiment on the dissemination of time and frequency

The dissemination of time and frequency standard by means of TV signals from a broadcasting satellite has a great advantage in the point that one can utilize such a system at any place throughout the country, using a simple receiving system with the same type of calibrating apparatus. But such system suffers from the frequency doppler shift due to the satellite orbital position variation. It is, therefore, necessary to take some preventive measures against this sort of frequency shift in order to disseminate the highly precise frequency standard.

In the doppler shift measurement system. Rb (rubidium) and Cs (cesium) atomic frequency standards were installed respectively at the BSE main station (at Kashima) and the RRL headquarters (at Koganei), about 100 Km apart each other. The two frequency standards are precisely synchronized in frequency to 1×10^{-12}, via TV synchronizing signals in the terrestrial TV signals. At both places the same type frequency synthesizers (HP 5100A) are used to generate reference color subcarriers. At Koganei, a simple receiving equipment with 1 mϕ antenna was used, and received composite video signal was used to "GENLOCK" a sync-generator, of which 3.58 MHz output signal was used to measure the frequency doppler shift averaged over 10 minutes by way of reading the phase comparison record.

The experimental result is shown in Fig. 9. Curve a gives measured doppler values at Koganei, together with calculated ones at Kashima which were estimated from predicted orbital values. Measured values coincide with calculated ones fairly well within the measurement error of 10^{-11} in the phase difference recording, although the doppler shift amounts to $\pm 4 \times 10^{-9}$ which is comparatively large value due to the fact that the measurement period was just before BSE orbital correction maneuvers, and also just at a new moon time meaning much influence of heavenly bodies.

Curves b and c show respectively the values of doppler shift, relative to the value at Kashima, at Wakkanai and Okinawa, the farthermost locations in the country. These two curves show variation amplitudes of $\pm 2 \times 10^{-10}$. This means that it is possible to receive standard frequency with the error within 2×10^{-10}, everywhere in the country if some measures are taken to cancel the doppler shift as received in Tokyo area. That will be realized by the phase (frequency) control of the transmitter by use of the prediction value or the servo control loop.

Further, it can be expected to get precision better than 10^{-11} by the method of averaging over 24 hours or utilizing zero doppler shift time calculated from orbital prediction value.

As for the influence of transmission path, there was little influence on the phase comparison even in the hard rain time. So it is thought that 12 and 14 GHz propagation characteristics do not give any severe influence on the time and frequency dissemination.

(3) Multi-channel still picture broadcasting system

Experiments on the transmission of approximately 50 still picture signals each consisting of a series of still color picture accompanied by digitally coded sound signal were conducted using one television channel exclusively.

The basic transmission parameters of the still picture broadcasting system such as the very low frequency transient characteristics and the pulse code transmission characteristics were measured by the transmission test via satellite.

From these test results it was concluded that the still picture broadcasting system could be realized which is compatible with the satellite broadcasting of standard television system.

(4) Multi-channel sound multiplexed television system

The sound multiplexing system was designed to transmit several sound signals using two sub-carriers 4.5 MHz and 5.0 MHz. The 4.5 MHz sub-carrier which carries main sound signal is compatible with the terrestrial television broadcasting. The 5.05 MHz sub-carrier is capable of transmitting up to four 5 KHz signals.

As a result of transmission test via satellite, the compatibility with the standard transmission system was confirmed and the cross talks between each sound channels and the cross effect from sound channel to video channel were found to have no major problems.

(5) PCM-FM sound transmission

The purpose of the experiment is to provide data to establish sound program broadcasting as a means of broadcasting high quality stereophonic or multi-channel sound programs.

The experiment was conducted with PCM transmission of stereo sound signals of 1.544 M bit/s using four phase PSK modulator.

As a result of experiment, the relation between C/N and the Bit Error Rate was quantatively cleared and the result was very near to that of theoretical value.

(6) Digital TV transmission

To search the possibility of digital TV broadcasting, a series of experiments on the digital transmission of TV signals have been conducted in both MTRS and TTRS of type B.

Measurements were performed to obtain fundamental data such as transmission characteristics of satellite link, Bit Error Rate characteristics for 4- or 8-phase PSK transmission in satellite links, 4-phase PSK transmission of DPCM coded color TV signals.

4. Experiments on radio wave propagation

The frequency band of 12 GHz allocated to satellite broadcasting has been applied to the down-link in this experiment, together with 14 GHz to the up-link. Since these frequencies are more easily affected by rainfall and snow than 4/6 GHz of the C-band, it is necessary to investigate propagation characteristics in various kinds of climate in Japan, in order to know how much percentage of time is guaranteed for the satellite broadcasting.

Here several propagation characteristics obtained at various locations in Japan, cocerning 14 and/or 12 GHz along the satellite-earth path for periods up to about one year will be described.

4.1 Data acquisition and processing

The locations of the stations concerned with the propagation measurements are already shown in Fig. 1. At the MTRS, the K-band beacon level (11.7 GHz) is received for measuring rain attenuation and depolarization. The other stations usually receive the TV signal which is transmitted from the MTRS or TTRSs.

The measured data at the MTRS are processed and edited by an on-line computer. In parallel with the measurement of radio signal from the satellite, several kinds of observations have been conducted in the MTRS, using a network of rainguages, a rain radar of the C band and others.

Concerning with NHK, the transmission of data measured and temporarily memorized at the TTRS and ROSs is performed daily through telephone lines or via the BSE in-band talk channel, and finally the data are edited on MTs.

One of the most important points of processing is how accurately and efficiently to extract additional attenuation due to rainfall from given data. The received power can be fluctuated with influence of such factors as attitude and orbital position of the satellite and pointing error of a receiving antenna. The computer processing procedure to eliminate the influence of other factors than rain was devised and it oprates fairly well.

4.2 Results

In Fig. 10 is shown an example of comparison between rain attenuations of the up- and down-links on a rainy day at Kashima. The plotted data are scattered a little for small attenuations. The ratio of attenuation of the up- to the down-link in decibel is about 1.4 which is almost equal to the theoretical value. As this relation was kept for other various rain events, it is possible to convert the statistics of the down-links to the ones for the up-links.

Fig. 11 shows cumulative distribution curves of attenuation of the BSE beacon signal (11.7 GHz) as well as the ones from the propagation experiment with the Engineering Test Satellite type II (ETS-II), which was performed during May 1977 to April 1978 using 11.5 GHz. As the frequency in the ETS-II is near the one in the BSE, the statistical curve of the ETS-II can be applicable also for the down-link of the BSE.

Fig. 12 presents cumulative distributions of rainfall rate at the main station. Correlation between the curves in Fig. 11 and those in this figure are not good. Because the distribution of rainfall covers 100 % of the time and that of rain attenuation covers only about 70 % due to various troubles of the system.

These statistics have to be taken at various locations and then receiving system parameters such as antenna size can be determined, required for practical service, when a certain amount of rain attenuation is given for a specified percentage of the time.

Cumulative distributions of rain attenuation and rainfall rate were derived from the data obtained at the ROSs and the TTRS during August to December, 1978. In Fig. 13 are shown the distributions for two typical locations, Owase and Kesennuma where the maximum and minimum rainfalls occurred respectively during the observation. In Table 6 rain attenuation and rainfall rate are given for 1 and 0.1 % of the time at each location, which were read from the above-mentioned distributions, together with the corresponding observed time. The observation of attenuation has been limited due to the cease of transmission on Saturday and Sunday, besides at nighttime in the beginning of the measurements. The rainfall rates in Table 6 are different from the one to be read in Fig. 13, because the rainfall data in the figure are employed only during the observation of attenuation.

In Fig. 14 are plotted points at which attenuation and rainfall rate occurred for the same percentage of time. From the figure, effective path length is about 5 km, which is almost coincided with the one in CCIR Report 564-1 and the result by the ETS-II. Effective path lengths were also derived from the measurements at the ROSs, of which the values for typical locations are given in Table 7. In comparison with the above-mentioned value at Kashima and the ones quoted in the same table from the CCIR Report, the values in the table are considerably shorter for severe rainfall rates. Although this may be ascribed to difference of meteorological conditions between the measuring locations, more data are needed to draw a conclusion.

The analysis of the propagation measurements has revealed preliminary but interesting results on statistics of rain attenuation at various locations of Japan, which would lead to final fruitful results at the end of the experiment for the expected full three years, besides an efficient method for eliminating non-propagation effects from obtained data.

5. Experiment on frequency sharing

In order to lay down basis for sharing criteria between up-links to broadcasting satellite (BS) and between up-links to BS and to communication satellite (CS) using the same frequency band at around 14 GHz, experiment on evaluation of interference criteria was carried out using the BSE.

In this experiment, interferences between the following simulated links have been considered.

[1] BS (FM-TV) → BS (FM-TV)
[2] BS (FM-TV) → CS (FM-TV)
[3] CS (FDM-FM) → BS (FM-TV)
[4] BS (FM-TV) → CS (FDM-FM)

Transmission parameters used for each uplink are shown in Table 8.

The TTRS type B was transported to be used mainly as interfering station at the Kashima Branch of the RRL where the MTRS is located, to eliminate error to be generated by satellite attitude drift.

5.1 Evaluation of intereferncе to the wanted FM-TV signals from the FM-TV and FDM-FM signals (cases [1] ∿ [3] above)

Subjective assessment of the wanted FM-TV signal interfered with FM-TV and FDM-FM signals, by varying an offset angle of unwanted station antenna, was conducted to obtain protection ration required and various margin which might need to compensate the difference between theoretical and actual values.

Tables 9 and 10 contain results obtained from experiment. Viewing condition used for this experiment is so different that viewers stand in front of picture monitor to facilitate them to detect interference to obtain protection ratio for high picture quality, which may be applied for up-link interference evaluation.

Although additional experiment is required, the following preliminary conclusion could be derived:

- ° BS/FM-TV → BS/FM-TV: protection ratio = 38 dB
- ° BS/FM-TV → CS/FM-TV: " " = 31 dB
- ° CS/FDM-FM → BS/FM-TV: " " = 35∿32dB (60∿972ch)

5.2 Interference from broadcasting satellite service (earth to space) earth station into fixed service satellite

Interference from FM-TV into FDM-FM was measured using the 14 GHz band for up-links, changing various parameters such as the ratio of disired-to-undesired signal power (DUR), TV video signals (color bar or color test chart), energy dispersal (with or without) and frequency deviation. The signal-to-interference noise ratio was proportional to D/U as shown in Table 11 and was not affected by TV video signals and energy dispersal.

The signal-to-noise ratio was also measured, changing the antenna direction angle of BSE earth station. Experimental results agree with the calculated values as shown in Fig. 15.

6. Experiments on satellite broadcasting signal reception

6.1 Received power and its stability

It has been confirmed by the measurements carried out simultaneously at 39 locations all over Japan that received powers were generally coincided with the corresponding predicted ones as shown in Fig. 16. Deviation of the received powers from the prediction were within 1 dB for 75 % of the measurements.

Comparatively long term variations of received power were measured at the ROSs. At the beam edge of the satellite transmitting antenna, where the ROSs situated on the isolated islands, the variation showed a maximum and reached up to about 5 dB, which included pointing error 2 dB inevitable to the simple tracking antenna equipped there.

Quality of received picture has been assessed subjectively, which was almost excellent at each location, using color-bar and specially prepared VTR signals.

From the TV-reception tests, an antenna size has been derived which was required to obtain weighted SN ratio of picture of more than 45 dB for 99 % of the time at each location. The required diameter is about 1 m around the center of the beam of the transmitting antenna, about 1.6 m for the fringe area of the mainland and 2.8 m to 4.5 m for the isolated islands. These meet approximately the initial design specification.

By the TV-reception tests, it has been confirmed that received power was generally coincided with the predicted values and also that excellent quality of picture was obtained at each location all over Japan. Influence of snow, especially fall of wet snow on a receiving antenna causes severe degradation of reception. It is needed keenly to clarify its mechanism and statistics and to develop a method for improvement.

The field tests in the urban and rural areas have also been conducted to investigate the influence of buildings and topography. The influence of high-ways, rapid railways, and airports, etc. on the reception quality of TV signals from the BSE have been investigated.

6.2 Solar noise interference

The solar noise interferences were measured after the autumnal equinox in 1978 and before the vernal equinox in 1979 in many earth terminals.

It is well known that the sun transits in a beam of a ground receiving antenna toward the vernal and autumnal equinoxes, if the antenna points to the geostationary orbit. A harmful interference can be happened to reception of satellite broadcasting at that case. Increase of noise was measured at several locations with antennas of different diameter.

Fig. 17 shows increase of noise power due to the solar noise interference at a receiver, of which noise temperature is about 600 K.

Fig. 18 shows duration time of the possible solar interference per day and number of days of its occurrence. In comparison of these results with the rain attenuation statistics, it is understood that the solar noise interference affects satellite broadcasting service only for much smaller percentage of the time than rain attenuation does, and moreover occurrence time and intensity of the interference can be predicted with practical accuracy. The solar noise interference was realized to affect satellite broadcasting service only for much smaller percentage of time than rain attenuation does.

7. Experiment on control and operation of satellite broadcasting system

7.1 Range measurement of broadcast satellite utilizing television sync-pulse

The range between the ground transmit and receive station and the satellite can be measured using the television sync-pulse.

TV Ranging Equipment was developed to evaluate the accuracy of the system with the BSE and TTRS Type A.

The expected error has -1.0 m mean and 0.56 m standard deviation. This value comes mainly from round-off error and high signal to noise ratio causes only 0.3 m error component.

Fig. 19 shows the change of the range in a short span. The residual fitting with first order function is 0.72 m in this case, and this value is a little greater than expected. The evaluation in a long span is achieved using a high accurate orbit elements, and it was concluded that the error is less than few meters that is enough for orbit determination.

7.2 Automatic television signal quality assessment (VITS measurement)

Transmission characteristics measurement equipment including VITS (Vertical Interval Test Signal) inserter and digital data processor was developed to measure and examine the stability of TV signal transmission.

An example of the received television signal characteristics is shown in Table 12.

7.3 Access to the satellite from the multiple ground stations

Program switching tests were performed via satellite between the MTRS and the TTRS moving around Japan using multiple-access control equipment fitted with propagation time dissolution logic.

As a result of subjective evaluation test, the switching function was found to be smooth and to have no visual problems.

8. Conclusion

The BSE experiments have been conducted favourably since July 1978. Most of experimental items planned in the BSE program have been carried into operation. But there are several experimental items which ought to be conducted hereafter, such as the investigation of scattering phenomena especially in the up-link path of 14 GHz, the regular experiments on standard time and frequency signals dissemination by means of TV signals, the experiments on simultaneous amplification of multiple sound signals for the purpose of sound broadcasting, and so on. They will be conducted in the latter half experimental period. It is expected that all the experiments in the BSE project will be performed with satisfactory results.

The operational broadcasting satellite BS-2 is now under consideration. It is expected to be launched in 1983 fiscal year with an on-orbit spare satellite.

According to the proposal, the BS-2 and its spare satellite will be similar to the present BSE satellite with respect to their scale and functions. The experimental results of the BSE program will be reflected to the system configuration of both space and ground segments.

The experimental results described in this paper are due to the endeavours made by many people who participated in the BSE experiments.

The authers wish to express their sincere thanks to the persons concerned of RRL, NHK, and NASDA. Also particular thanks are due to the staff of MOPT for their guidance in the BSE program.

References

(1) H. Kaneda et al., "Experiments with the Japanese BSE Program" AIAA Paper 78-753, April '78.

(2) K. Tsukamoto et al., "Technical Aspects of the Japanese Broadcasting Satellite Experiments" IEEE Trans. Broadcasting, vol BC-24, No. 4, Dec. 1978

(3) N. Imai et al., "Experimental Results of the Japanese BSE Program" IAF Paper IAF-79-F-280, Sept. 1979

(4) T. Ishida et al., "Present Situation of Japanese Satellite Broadcasting for Experimental Purpose", IEEE Trans. Broadcasting, vol BC-25, No. 4, Dec. 1979

(5) Y. Otsu et al., "Propagation Measurements and TV-Reception Tests with the Japanese Broadcasting Satellite for Experimental Purposes", IEEE Trans. Broadcasting, vol BC-25, No. 4, Dec. 1979

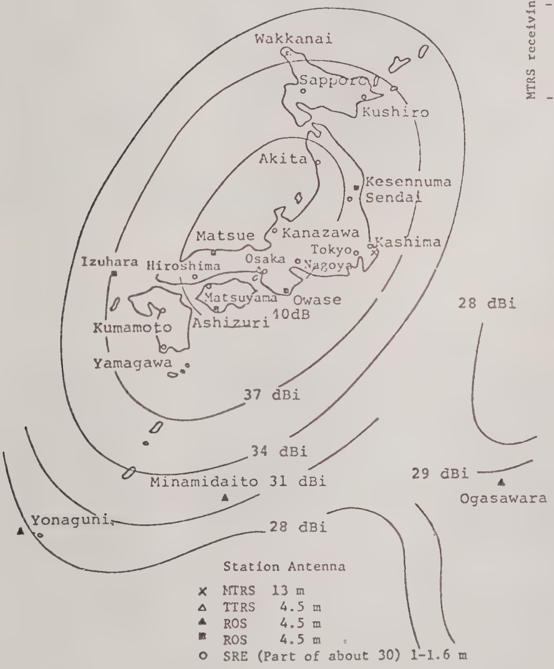
Wakkanai
Sapporo
Kushiro
Akita
Kesennuma
Sendai
Matsue
Kanazawa
Kashima
Tokyo
Izuhara
Hiroshima
Osaka
Nagoya
Matsuyama
Owase
10dB
28 dBi
Kumamoto
Ashizuri
Yamagawa
37 dBi
34 dBi
Minamidaito 31 dBi
29 dBi
Ogasawara
Yonaguni
28 dBi
Station Antenna
× MTRS 13 m
△ TTRS 4.5 m
▲ ROS 4.5 m
■ ROS 4.5 m
○ SRE (Part of about 30) 1-1.6 m

Fig. 1 The BSE antenna radiation pattern and ground station location

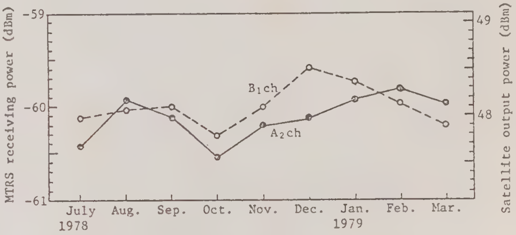

Fig. 2 Variation of satellite output power

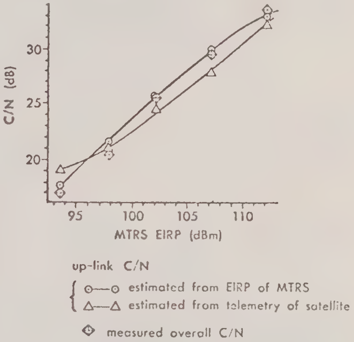

Fig. 3 C/N measurement result

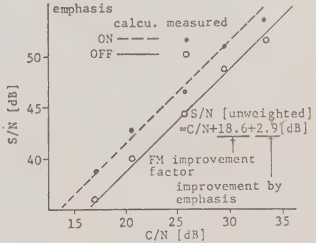

Fig. 4 Relation between C/N and S/N

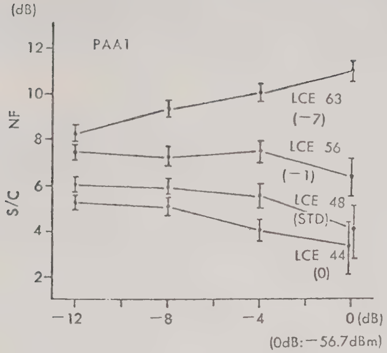

Fig. 5 NF characteristics of transponder

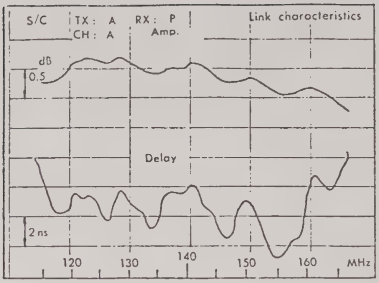

Fig. 6 Amplitude and delay characteristics of link

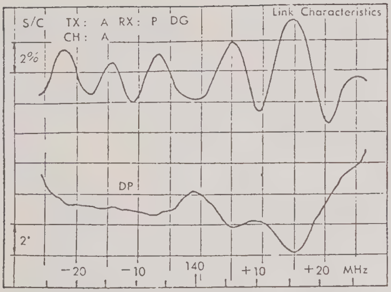

Fig. 7 DG and DP characteristics of link

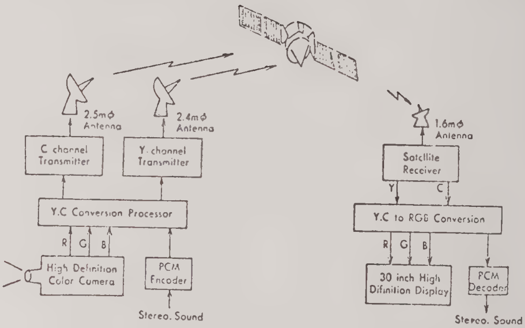
2.5mϕ Antenna
2.4mϕ Antenna
1.6mϕ Antenna
C channel Transmitter
Y channel Transmitter
Satellite Receiver
Y.C Conversion Processor
Y
C
Y.C to RGB Conversion
R
G
B
High Definition Color Camera
PCM Encoder
Stereo. Sound
30 inch High Difinition Display
PCM Decoder
Stereo. Sound

Fig. 8 High-definition TV experiment system with the BSE

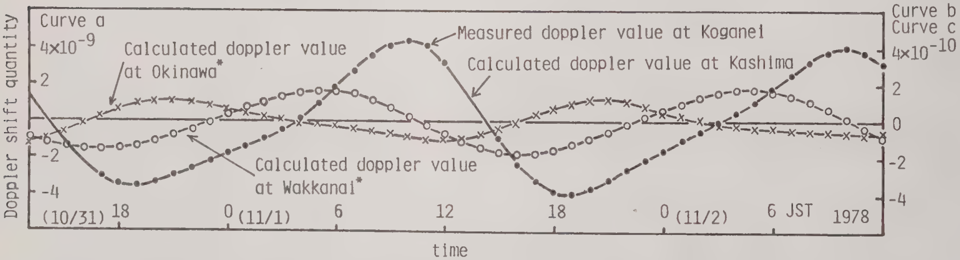

*: Calculated freq. shift when compensated at the transmitting side so as to cancel doppler shift at Koganei calculated by orbit determination program

Fig. 9 Doppler frequency by BSE

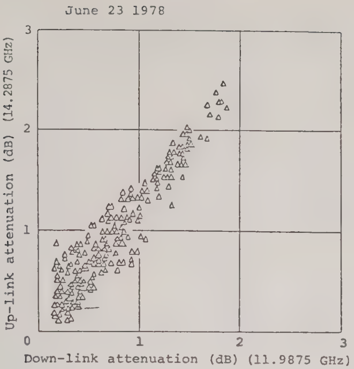

Fig. 10 Relation between measured attenuations of up and down links at Kashima

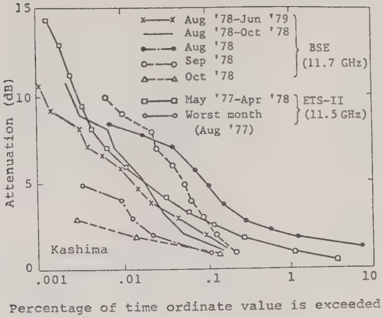

Fig. 11 Measurements of rain attenuation at Kashima

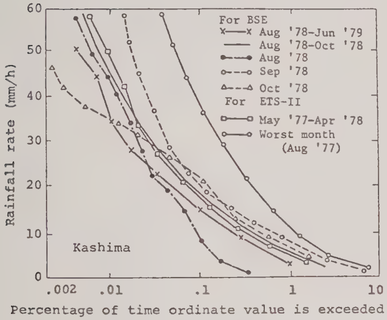

Fig. 12 Measurements of rainfall rate at Kashima

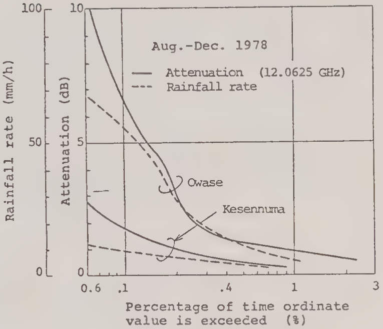

Fig. 13 Measurements of rainfall rate and attenuation at rainy and dry locations

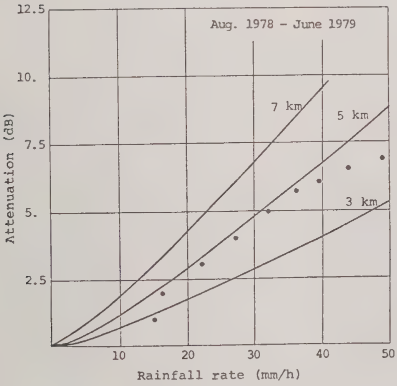

Fig. 14 Effective path length obtained at Kashima

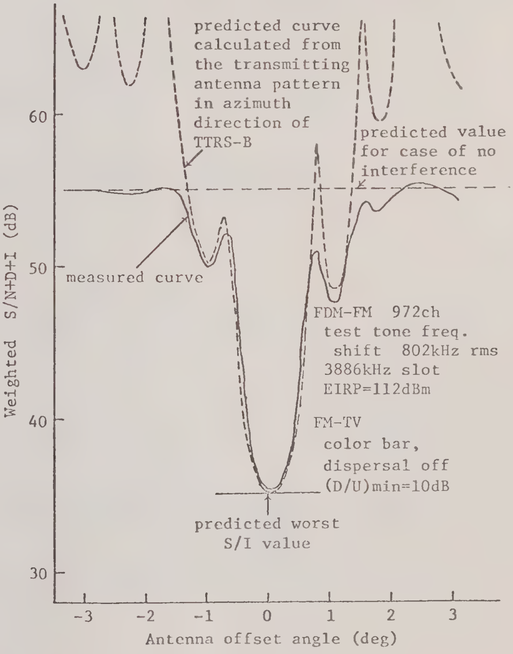

Fig. 15 Weighted S/N measured in changing MTRS antenna direction

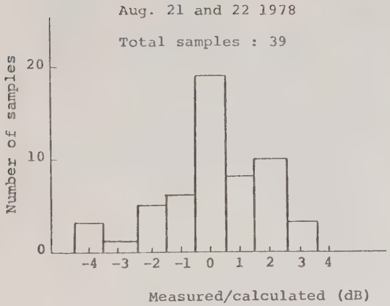

Fig. 16 Deviation of received power from calculated value

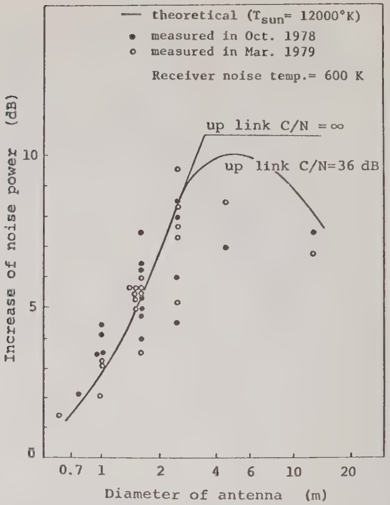

Fig. 17 Increase of noise at receiver input due to solar noise interference

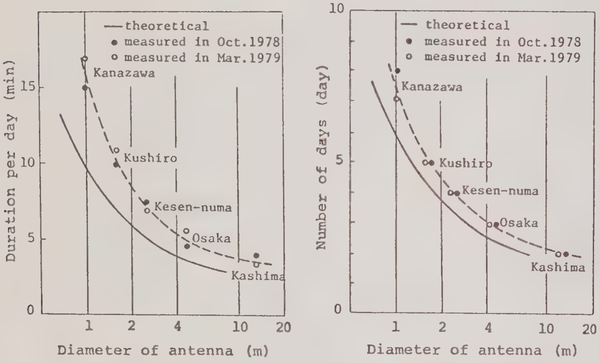

(a) Duration per day

(b) Number of days

Fig. 18 Duration and occurrance of solar noise interference

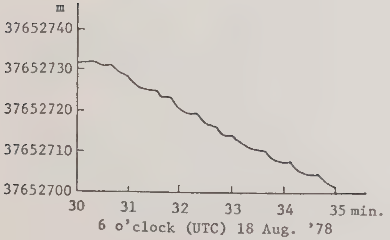

Fig. 19 Range change in a short span

Table 1 Measurements of Received Television Signal Characteristics

Location	Station	Antenna Diameter	Received Carrier Level		Weighted S/N
			Calculated	Measured	
Kashima	MTRS	13 m	-59.9 dBm	-59.8 dBm ∿ -60.2	59 dB
Osaka	TTRS A-type	4.5	-66.7	-63 ∿ -64.5	58
Tokyo	TTRS B-type	2.5	-74.0	-73 ∿ -74	54
Wakkanai	ROS	2.5	-75.9	-77.5 ∿ -81.2	47
Kesennuma	ROS	2.5	-72.8	-72.8 ∿ -74.4	48
Owase	ROS	2.5	-71.2	-72.4 ∿ -74	50
Matsue	ROS	2.5	-70.6	-72 ∿ -73	49
Ashizuri	ROS	2.5	-70.6	-69.7 ∿ -71.3	54
Izuhara	ROS	2.5	-73.1	-75.4 ∿ -76.2	49
Ogasawara	ROS	4.5	-75.3	-78.6 ∿ -81.6	45
Yonakuni	ROS	4.5	-79.1	-77.5 ∿ -79.5	48
Minami Daito	ROS	4.5	-74.2	-73.5 ∿ -74	51
Hachijo	ROS	1.6	-80.7	-81 ∿ -83.3	45

Table 2 BSE link budget

		MTRS	Mainland	Remote islands
Up-link (MTRS to BSE)				
MTRS, E.I.R.P.	(dBm/ch)	112.2		
Free space loos	(dB)	-207.4		
Rx. antenna gain	(dB)	38.1		
Noise power	(dBm/25 MHz)	-92.9		
Up-link C/N	(dB)	35.8		
Down-link Service area		MTRS	Mainland	Remote islands
Antenna of Rx.	(m)	13.0	1.6	4.5
Tx. power	(dBm/ch)	50.0		
Tx. feeder loss	(dB)	-1.7		
Tx. antenna gain	(dB)	37.6	37.0	28.0
Free space loos	(dB)	-205.9	-205.8	-205.4
Rx antenna gain	(dB)	61.9	43.0	53.5
Rcved carrier power	(dBw)	-58.1	-77.5	-75.6
Noise power	(dBm/25 MHz)	-96.4	-97.3	-96.6
Down-link C/N	(dB)	38.3	19.8	21.0
Total C/N	(dB)	33.9	19.7	20.9
TV signal quality				
FM improvement factor	(dB)	18.6		
Emphasis improvement factor	(dB)	2.9		
Unweighted S/N	(dB)	55.4	41.2	42.4

Table 3 Provisional standard of high-definition TV

Number of scanning lines	1125
Aspect ratio	3 : 5
Line interlace	2 : 1
Field repetition frequency	60 Hz
Video frequency bandwidth	
Luminance (Y) signal	20 MHz
Chrominance (C) signal	0.5 MHz*

* Line sequential

Table 4 Carrier-to-noise ratio for Y and C channels

Date. (Nov. 1978) Time (hours)	8th 15:40	9th 10:00	13th 15:40	15th 15:40	Mean
CNR (dB)					
Y ch.	16.7	—	16.4	16.6	16.6
C ch.	21.7	21.2	23.2	22.7	22.2

Table 5 Picture signal-to-noise ratio for Y and C channels

	Y ch.	C ch.	Remarks
CNR (dB)	16.6	22.2	mean
SNR (dB)	40.6	49.2	unweighted

Table 6 Measurements of attenuation and rainfall rate at ROSs and TTRS
(12.0625 GHz, August to December 1978)

Item / Location	Attenuation exceeded for given % (db)		Rainfall rate for given % (mm/h)		Observation Time (1000 min)	
	1	0.1	1	0.1	Attenuation	Rainfall
Ogasawara	/1)	1.1	3	19	29	82
Minamidatio	0.8	2.3	6	15	37	98 2)
Yonaguni	2.3	5.5	6	39	34	59
Kesennuma	0.3	1.7	4	12	38	160
Owase	0.8	6.5	13	52	41	164
Matsue	1.2	3.0	7	15	40	162
Ashizuri	1.2	3.3	6	28	39	162
Izuhara	/1)	/1)	7	20	32	161
Osaka	1.6	3.9	5	12	34	165

Note 1) No significant data due to trouble of equipment.

2) Observation time becomes shorter due to failure of rainguage.

Table 7 Effective path length obtained at rainy and dry locations

Location	Effective path length for given rainfall rate (km)		
	10 mm/h	25 mm/h	50 mm/h
Owase	4.3	3.2	2.6
: rainy	(5.3)	(4.7)	(3.8)
Ashizuri	5.0	2.9	2.6
: rainy	(5.1)	(4.5)	(3.7)
Kesennuma	6.8	/	/
: dry	(6.3)		

Note The values in ( ) are derived from Fig. 2 of CCIR Rep. 564-1 (Tokyo area)

Table 8 Transmission paramaters of up-link signal

BS/FM-TV	video signal deviation emphasis energy dispersal	12MHz CCIR Rec. 405-1 600kHz
CS/FM-TV	video signal deviation emphasis energy dispersal	21.5MHz CCIR Rec. 405-1 1MHz
CS/FDM-FM	noise-loaded with the following test-tone deviation 972ch ; 802kHz/ch 60ch ; 270kHz/ch	

Table 9 Protection ratio required for interference from FM-TV signal

wanted	unwanted	antenna offset method	laboratories test
BS/FM-TV	BS/FM-TV	35dB	37.8dB
BS/FM-TV	CS/FM-TV	29.3dB	31dB

(test picture : color bar)

Table 10 Protection ratio required for interference from FDM-FM signal

wanted	unwanted	antenna offset method*		laboratory test	
		60ch	972ch	60ch	972ch
CS/FDM-FM	BS/FM-TV	26.4dB	23.9dB	35.5dB	32.4dB

(test picture : color bar)

* : values were limited by signal-to-noise ratio of received signal

Table 11 Interference from FM-TV into FDM-FM in the same frequency channel

capacity	S/I*	d/U**	test condition
972ch	43dB	17.5dB	with the parameters for the Intelsat
	50dB	24.5dB	972-channel carrier
	60dB	34.5dB	FM-TV (color bars) without energy dispersal
60ch	43dB	8.5dB	test-tone deviation 270kHz rms
	50dB	16.0dB	emphasis off
	60dB	26.5dB	FM-TV (color bars) without energy dispersal

* : signal-to-interference noise ratio in the worst channel due to interference from an analogue FM-TV transmission

** : the ratio of wanted-to-unwanted signal power at the satellite input

Table 12 Example of VITS automatic measurement

```
08/31        15:14

        LEVEL(IRE)  PICTURE          SYNC           BURST
                      99              42              40

        FREQ.(MHZ)    0.50     1.00     2.00     3.00     3.58     4.20
              (DB)  - 0.2    - 0.3     0.1      0.5      0.6    - 3.7

        DISTORTION  LUM.BAR(%)  2T/BAR RATIO(%)  2T OVERSHOOT(%)
                      0.1             1.3            - 3.6

        C/L         C/L GAIN(DB)  L-C DELAY(NS)  STREEKING(%)
                      1.0            43             - 1.0

        S/N         S/N (DB)         DG(%)           DP(DEG)
                      49              1.4             2.0
```

80-0570

SYSTEM DESIGN AND TECHNOLOGY OF THE GERMAN DIRECT TV BROADCASTING SATELLITE

H. Kellermeier* and D.E. Koelle**
MBB Space Division, Ottobrunn / Germany

Abstract

The Federal Republic of Germany has started the development of a dedicated Direct TV-Broadcasting Satellite in mid-1979.

The paper describes the requirements and the design history and rationale for the selected concept. It is a three-module 1000 kg spacecraft, to be launched by the ARIANE in 1983 but also compatible with the SHUTTLE/SSUS-A.

Specific technology developments had to be performed during the past five years in order to prepare the development and to fulfill the performance requirements. This specific technology is described in more detail, as there are - the unified propulsion system, - the ULP solar array, - the RITA ion thruster units, - TWTA`s, - CFC antennas, and attitude control components.

It is shown that an optimized system design and the use of advanced technology leads to a very cost-efficient operational TVBS service.

I. History, Requirements

At the beginning of the nineteen-seventies the German Federal Post and Telecommunications Ministry assigned already high priority to direct satellite TV broadcasting in the 12/14 GHz frequency range,and encouraged the Ministry of Research and Technology to initiate developments of the respective communications technology in several German companies.

From 1972 to 1976 system studies of a direct TV broadcasting satellite system were performed in parallel by two German teams:

> One was headed by Siemens company with MBB responsible for the satellite design. The other lead by AEG/Telefunken company assisted by ERNO and DORNIER Systems for the spacecraft part.

The satellites at that time had to be designed for an ATLAS/CENTAUR launch, 4 to 5 channels with 400 to 700 W RF each and DC power requirements between 5 and 7 KW at end of mission. FIG. 1 shows the "Hochleistungssatellit" concept of a German TVBS as proposed by MBB/Siemens in 1974/75. It is characterized by three-axis stabilization at geosync. orbit after a spin-stabilized transfer and injection, deployable rigid solar arrays sun-oriented by a drive mechanism, and a modular spacecraft design existing of

- the steerable transmitt antenna (2.5 x 1.4 m)
- the repeater module with four redundant channel sections
- the satellite platform (service module) with the ultra lightweight solar array (ULP)
- and a solid apogee motor mounted into the central tube structure

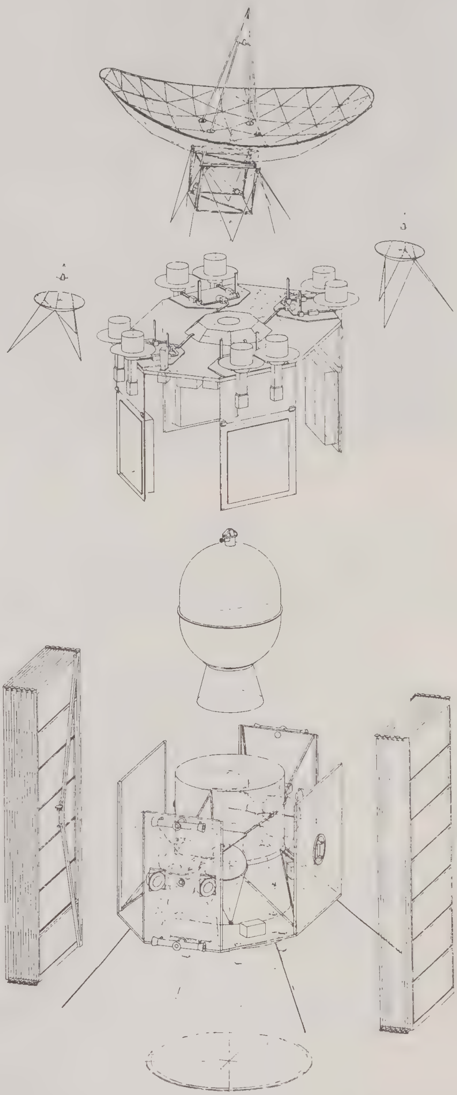

FIG. 1 Early German TVBS concept ("Hochleistungssatellit") by MBB 1975

---

* Head, Space System Studies
**Mgr., Advanced Systems and Technology Development

Copyright © American Institute of Aeronautics and Astronautics, Inc., 1980. All rights reserved.

This first attempt of a modular TVBS design was constraint by both the CENTAUR shroud diameter of only 2.7 m and the central tube structure carrying the 700 kg apogee solid motor load at launch. Hence the four channelized sections with the redundant TWTA`s mounted on heat radiators formed an octagonal satellite body with limited heat radiating surfaces.

Increase of this surfaces is only possible by increasing the satellite height. The instability during spin-transfer had to be compensated by active nutation damping which becomes rather difficult by increasing satellite height.

The main spacecraft requirements were

- a high antenna pointing accuracy of ± 0.1° for pitch and roll (± 1° yaw)
- RF output power of 4x320 W
- Stationkeeping ± 0.1° for N/S and E/W
- No TV-operation during eclipse and between 1°°h to 5°° h a.m.
- Design Lifetime 7 years
- Usable Lifetime 8 years with $R_{Sat.} \geq 60$ % for 3 out of 4 channels
- Transfer Mass 1745 kg (ATLAS CENTAUR)

New technology has been required in several areas like TWTA`s antenna,solar array, attitude and orbit control etc. to fulfill these requirements.

The Ministry for Research and Technology (BMFT) has supported the development of direct TV-broadcasting satellite technology in Germany since 1973. In 1978/79 the comprehensive and detailed definition of the satellite concept was performed for the BMFT/DFVLR by MBB supported by AEG-Telefunken, Dornier-System, ERNO and SEL.

The paper summarizes the results of the Phase B study completed in June 1979 in the following.

The legal and administrative basis for TVBS in Europe has been created by the WARC 77 in Geneva, allocating 5 channels to each country in Europe and defining the antenna beams and main parameters. For Germany these parameters are as follows

- TV-channels	2,6,10,14,18 (11.7-12.5GHz
- EIRP	65,5 dbW (260 W TWTA output)
- Satellite Position	19° West (+ 0.1)
- Antenna Beam	0.72x1.62 deg (cf.FIG.2)
- Polarisation	left-hand
- Cross Polar Pattern	-33 dB (-40 dB at boresight)

The uplink frequency will only be defined by the WARC 79, probably in the 19 GHz band. Until to the allocation by WARC 79 an uplink frequency range from 18.3 to 19.1 GHz has been chosen as baseline.

FIG. 2 shows the illumination area of the German TV-SAT from its orbital position above the equator. With larger ground antennas it will be possible to receive the German TV broadcasting also in Rome, Paris, London and Stockholm, thus paving the way for a real selection among European TV programmes from various countries.

The launch of the first socalled preoperational TV-SAT (A3) is planned for mid 1983. Two years later the first operational spacecraft (A5) shall allow the start of the operational TV broadcasting service for the Federal Republic of Germany.

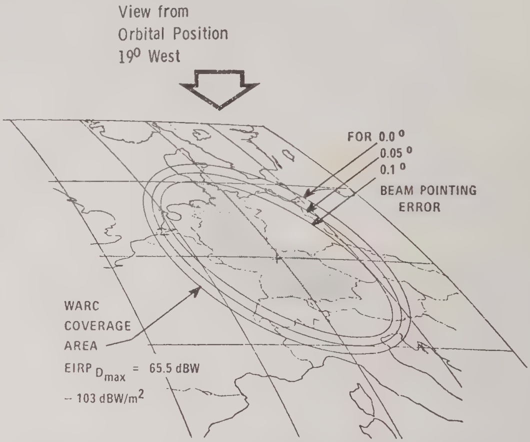

FIG. 2 Antenna Coverage Area for the FRG as Defined by WARC 1977

2. TVBS Technology

The 260 TWT required to make full use of the WARC figure of 103 dBW/m^2 at the edge of the coverage zone is an outgrowth of the 200 W TWT under development by AEG-Telefunken since many years (FIG.3).

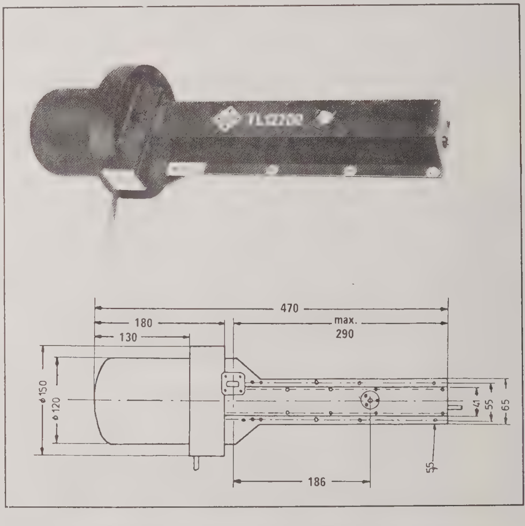

FIG. 3 260 Watt TWT Dimensions and 200 Watt TWT Hardware

The pre-developments comprise helix type TWT`s from 20 W (applied in the OTS-satellite) up to 260 W which is about the technological limit. For higher powers a coupled cavety type TWT of 450 W has been pre-developed.

For the beam coverage of FRG 12 GHz antenna reflectors made of carbon fibre with an aperture diameter of 2 m have been pre-developed by MBB (in mesh technology) and DORNIER Systems (rigid reflector). FIG.4 shows the rigid reflector made of Al-honeycomb core and carbonfibre pre-preg as used on TV-SAT.

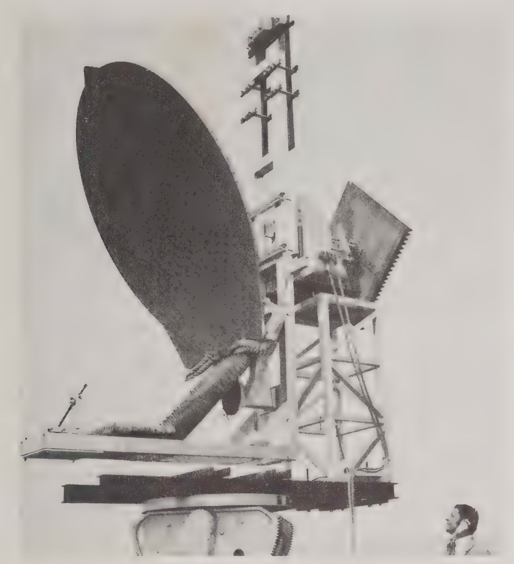

FIG. 4 12 GHz Carbonfibre Antenna Test

The ULP solar array technology represents a major improvement in performance as shown in FIG. 5, both with respect to the specific power (Watt per kg) as to the power range of 2 to 20 kW.

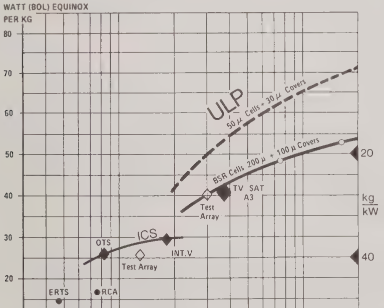

FIG. 5 ULP Performance Diagram

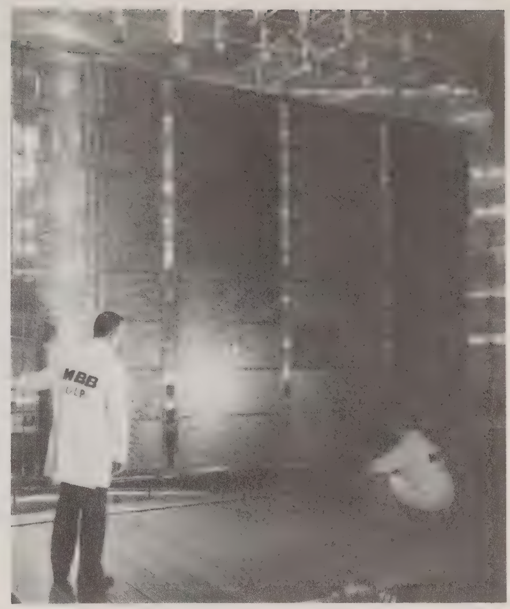

FIG. 6 The ULP Solar Array Test Wing

A ULP test array with four panels (each 3.3 x 1.1 m) has been built in flight configuration and hardware under BMFT/DFVLR-Contract with support from INTELSAT. The array has successfully performed an extensive series of qualification tests. FIG. 6 shows the array after a deployment test.

The unique technology applied uses rigid carbonfibre CFC frames and flexible pretensioned blankets. The AEG 2x4 cm BSR-cells will be used with 0.1 mm cerium-doped cover glasses to provide an output BoM of 310 to 350 W per panel (depending on the launch date or solar incidence conditions), and 242 to 260 W after 10 years in orbit. The panel size is 117 x 335,5 cm with a total number of 25 x 144 (3600) cells. Power capacity in transfer orbit is 200 Watt. The spring-actuated and controlled deployment system is the same as has been successfully used on the OTS solar array.

The solar array drive motor and power transfer assembly has been developed by Dornier-System (FIG. 7) and will be flown also on the NASA Space Telescope. The step-size for array adjustment is 0.15 deg.

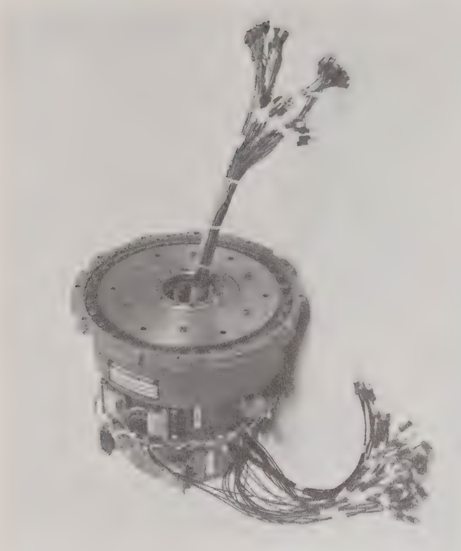

FIG. 7 Solar Array Drive Motor

The use of bi-liquid propellants (MON-1 and MMH) for apogee injection and orbit and attitude control provides an excellent opportunity for unification of both functions in one unified propulsion system UPS, which, for reasons of redundancy and modularity has 4 propellant tanks pressurized by He -gas of some 230 bar.

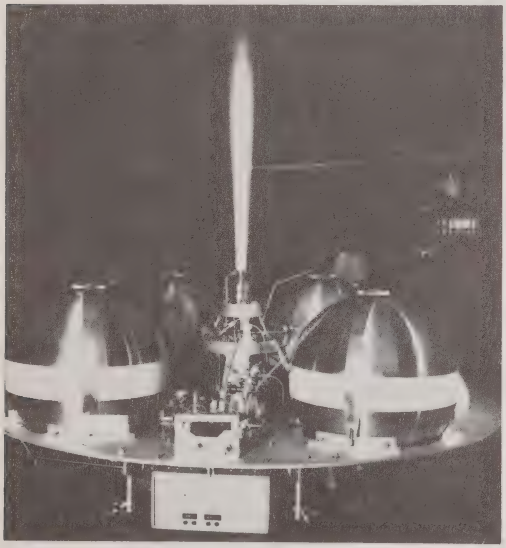

FIG. 8 a 4 Tank Test Model of UPS with 400 N Apogee Engine

FIG. 8 a shows a ground test of a functional UPS model with the MBB 400 N engine. The engine is now improved for the GALILEO mission in lifetime and performance and provides for an Isp = 309 sec nominally. 10 N thrusters (FIG. 8 b) as also used in the GALILEO RPM provide for the attitude and orbit control of the satellite.

The UPS provides (in contrast to solid ABM + hydrazin AOCS) outstanding flexibility in adaptation of propellant mass to different launch vehicles, extension of orbital life by fill-up to the max. tank capacity at the launch pad as well as unsymmetrical propellant loading if required.

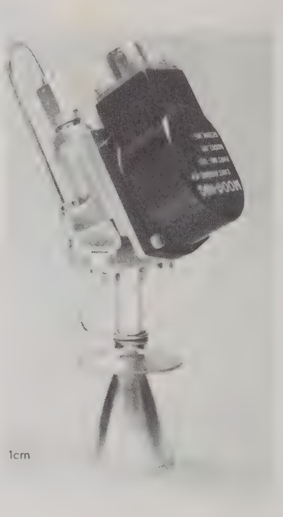

FIG. 8 b 10 N Bipropellant Thruster

For the preoperational TV-SAT A3 the electrical thruster package RITA-1 is foreseen for N/S-stationkeeping (FIG.9). However, since it is the first use of this new ion thruster system, chemical propellants are available as backup for the full 5 years period. However, this is not feasible for the operational satellite (A5) with its higher payload and power requirement over 10 years. In this case the fully redundant operational RITA-2 system is required for orbit control or the spacecraft lifetime in orbit is limited to some 6 years (with an according increase in number of spacecraft and launches required for a long-term program).

RITA-1 and -2 are autonomous units, mounted externally onto the propulsion module E-W-sidewalls. The engines with 10 mN thrust level have to operate two hours per day and require only 2 kg mercury per year as propellant, i.e. only one tenth of a bipropellant engine system.

In case of RITA-2 N/S and E/W orbit control up to 8 years can be performed and chemical thruster operation is required for the last 2 years only. A mass saving of about 100 kg chem. propellant is thus achieved for a1000 kgspacecraft in geosync. orbit.

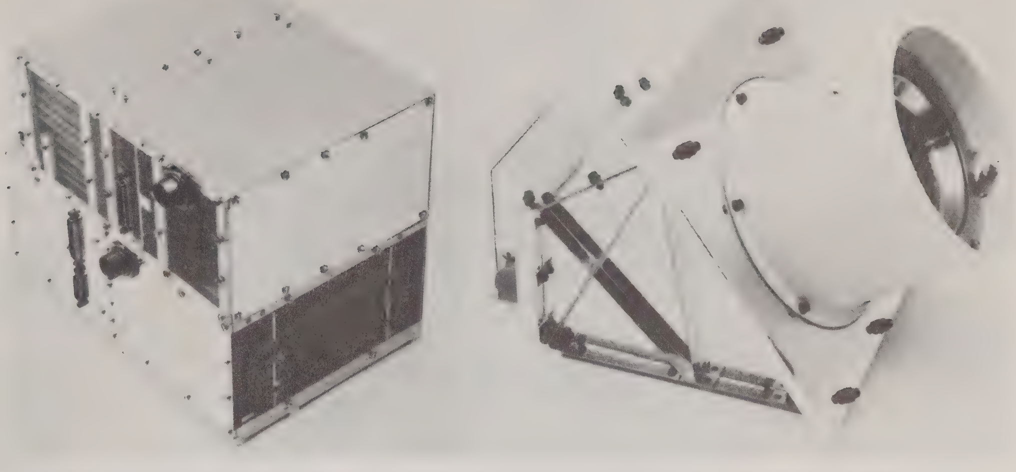

FIG. 9 RITA–1 Electric Propulsion System consisting of the 10 mN Radiofrequency Ion Thruster plus Power Supply

3. Spacecraft System Design

The German TV-SAT is the first of a new generation of satellites characterized by a high power demand (3 to 10 kW) and large antennas.

One basic requirement is the satellite compatibility with both of the two launch systems ARIANE and SHUTTLE/SSUS-A. The capability of both vehicles is marginal for a fully operational TV-SAT for Germany with five redundant TV-channels of 260 W each.

For the first satellite however, the socalled pre-operational TV-SAT A3, the launch capability is sufficient since the payload comprises only 3 operational plus 2 spare channels (non-redundant) and the lifetime in orbit is only 5 years.

The selected spacecraft configuration is a compromise from ARIANE and SHUTTLE requirements, however, taking into account the later extension to the fully operational version without greater modifications.

The TV-SAT spacecraft are characterized by the following specific design features (FIG.10):

(1) Subdivision in three separate modules

CM = Communication Module with repeater and antenna system

SM = Service Module with the spacecraft subsystems, and

PM = Propulsion Module with the spacecraft propulsion systems.

(2) Application of the bipropellant Unified Propulsion System (UPS) for apogee injection, orbit and attitude control

(3) Application of three-axis stabilized transfer from low Earth orbit (LEO) to geosync.orbit(GEO).

(4) Use of electric propulsion (ion thrusters) for orbit control (RITA).

(5) Use of the modular lightweight semi-rigid ULP solar array (for power ranges of 2 to 10 kW).

(6) Increased spacecraft bus redundancy and capacity for 10 (12) years operational lifetime in orbit, subdivided into a 5-6 year standby period and a subsequent 5-6 year operational period for maximum economy (minimum space segment cost).

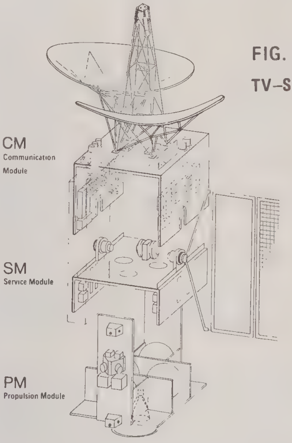

FIG. 10
TV–SAT Concept and Modularity

The satellite design is shown in FIG.11 and 12. Spacecraft main data are given in Table 1.

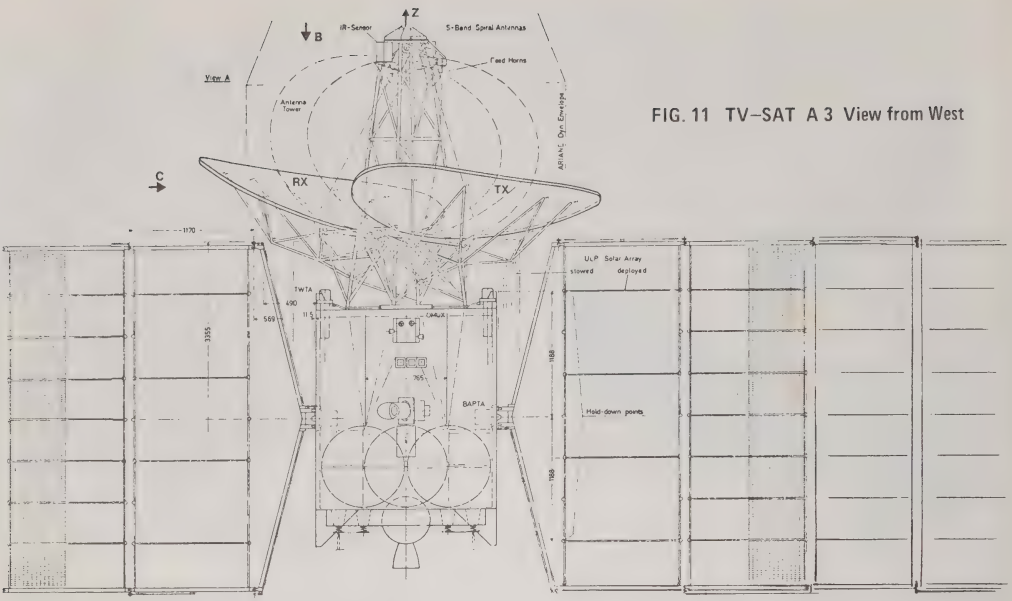
Z
B
IR-Sensor
S-Band Spiral Antennas
Feed Horns
View A
Antenna Tower
ARIANE Dyn Envelope
C
RX
TX
1170
ULP Solar Array
stowed
deployed
TWTA
490
115
569
OMUX
3355
765
1188
BAPTA
Hold-down points
1188

FIG. 11 TV–SAT A 3 View from West

TABLE I TV–SAT A3 SYSTEM CHARACTERISTICS

PAYLOAD	3 + 2 (spare) channels with 260 W TWTA s. Separate transmit and receive antennas		
	Total Mass	167.3	kg
	Power requirement	2 238	Watt
	Reliability (5 years)	0.930	
SPACECRAFT	Power BoM/EoM 5 y	3 400 / 2 850	W
	System reliability (5 y)	0.837	
	Bus reliability (10 y)	0.800	
	Payload Module mass	280.0	kg
	Service Module mass	300.0	kg
	Propulsion Module mass	210.0	kg
	Propellant for transfer, apogee maneuver and acquisition ARIANE: 693 kg,	Shuttle: 825.0	kg
	Propellants for attitude and orbit control	95 (max. 150)	kg
	Mercury for ion thrusters	10.0	kg
	Total mass after separation from		
	ARIANE	1 712.0	kg
	Shuttle + SSUS–A	1 880.0	kg
	Total length with extended arrays	19.25	m
SUBSYSTEMS	Antenna system with two deployable CFC dishes and central tower	56.7	kg
	Repeater with 5 TWTA' s of 260 W	110.7	kg
	Power subsystem (50 V bus)	59.5	kg
	ULP solar array	93.5	kg
	Array drive assembly (BAPTA)	14.4	kg
	Data system (TT&C, data handling)	24.9	kg
	Attitude/orbit measurement & control	48.5	kg
	Unified propulsion system	91.5	kg
	RITA–1 electrical thruster package (2)	32.6	kg
	Structure (excl. adapter)	144.7	kg
	Thermal control hardware	63.5	kg
	Bus harness, pyrotechnics	26.4	kg
	Balance mass, miscellaneous	5.0 (A) to 30 (S)	kg

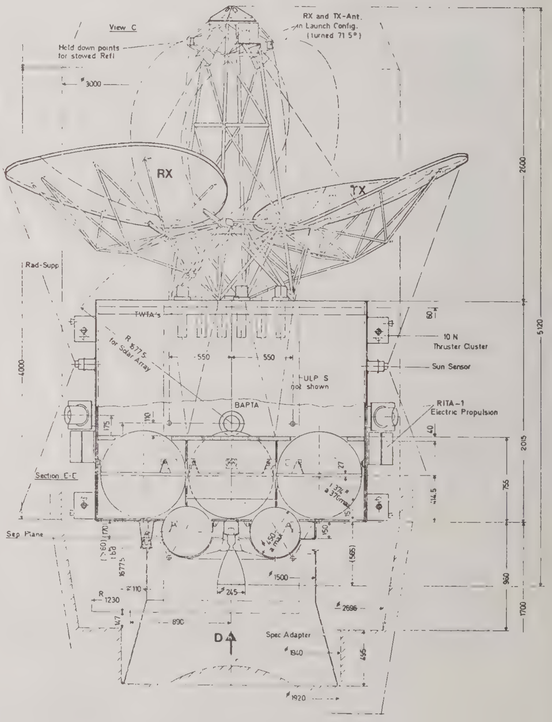
View C
Held down points for stowed Refl
RX and TX-Ant. in Launch Config. (turned 71.5°)
3000
RX
TX
2600
5120
Rad-Supp
TWTA's
R 16775 for Solar Array
550
550
ULP S not shown
60
10 N Thruster Cluster
Sun Sensor
4000
BAPTA
RITA–1 Electric Propulsion
110
175
40
2015
Section E-E
27
1374 a 376 max
414.5
755
Sep Plane
150
450 a max
(565)
1500
245
960
R 1230
110
2696
1700
147
890
D
Spec Adapter
1940
455
1920

FIG. 12 TV–SAT A 3 View from North

3.1 Communication Module

The payload consisting of repeater and antenna system is mounted on a U-shaped structure. This solution (conceived by MBB in 1974) has proven to be the most effective solution due to its large North-South areas for equipment mounting and thermal radiation. It has been implemented since for INTELSAT V and ECS. (FIG. 13).

New is the partially external mounting of the TWT`s with free radiating of the collector heads which have an operating temperature of some 300°C.

The overall design has already been made for the operational A 5 satellite version (with 10 TWTA`s), FIG.14a, including a structure-integrated heat-pipe network for equal heat distribution, FIG. 14b.
The total mass of the Communication moduleis 280 kg.

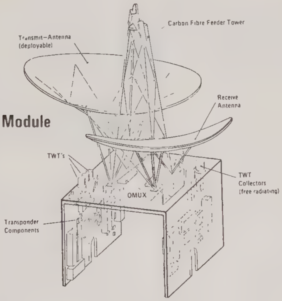
Carbon Fibre Feeder Tower
Transmit-Antenna (deployable)
Receive Antenna
TWT's
OMUX
TWT Collectors (free radiating)
Transponder Components

FIG. 13 Communication Module

The single conversion repeater comprises a full set of the 5 German channels, however, without redundancy. Only 3 are required to operate over 5 years, with two as spare channels.

The antenna system comprises two equal-sized elliptical CFC-reflectors (250x170cm) which are folded up during launch. Due to the higher uplink-frequency (18 to 19 GHz) the receive beam is smaller than the transmit beam. The transmit antenna has a gain of 40.6 dB; the EIRP is 62.5 dBW.

Since WARC 77 requires a high beam pointing accuracy of ± 0,1°, the reflectors as well as the tower are made of carbon fibre material (CFC), to keep thermal distortions as low as possible (~0.02° to 0.03°).

The antenna tower carries the Tx and Rx feed horns and waveguides, the S-band TM/TC antenna and the redundant infrared sensors. The sensor system will be improved by a radio frequency (RF) sensor in the operational A5 version.

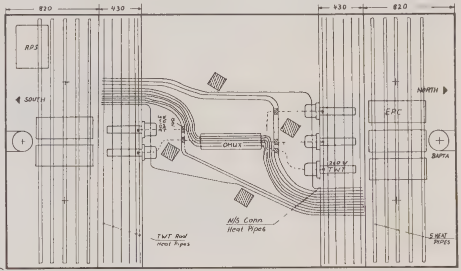
820
430
430
820
RPS
SOUTH
NORTH
EPC
OMUX
TWT
BAPTA
TWT Rad Heat Pipes
N/S Conn Heat Pipes
5 HEAT PIPES

FIG. 14b
CM Integrated Heat Pipe Concept (DS)

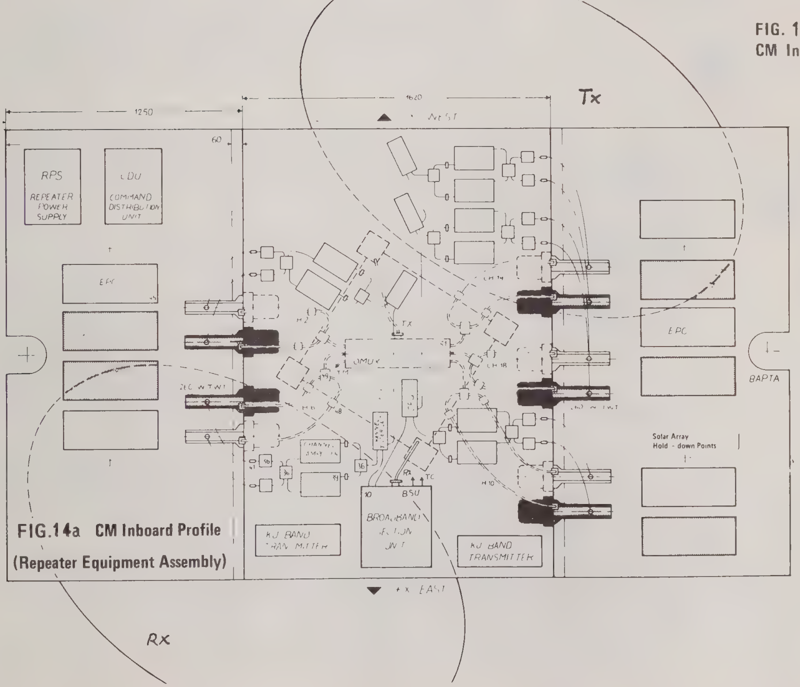
Tx
1250
1620
WEST
60
RPS
REPEATER POWER SUPPLY
CDU
COMMAND DISTRIBUTION UNIT
EPC
TWT
OMUX
TX
TM
CH 18
CH 14
BSU
BROADBAND RECEIVER UNIT
KU BAND TRANSMITTER
KU BAND TRANSMITTER
EPC
BAPTA
Solar Array Hold - down Points
+X EAST
Rx

FIG.14a CM Inboard Profile
(Repeater Equipment Assembly)

3.2 Service Module

The Service Module comprises all the spacecraft subsystems required for the satellite and payload operation (except propulsion).

The basic structure is U-shaped to provide (small) N/S thermal radiation surfaces for the major heat dissipating electronics and the battery.(FIG. 15). The total mass is 300 kg.

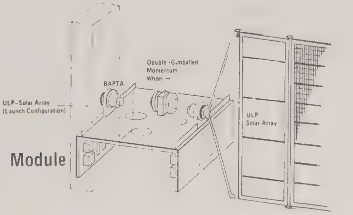
Double-Gimballed Momentum Wheel
BAPTA
ULP-Solar Array (Launch Configuration)
ULP Solar Array

FIG. 15 Service Module

FIG. 16 shows the lay-out of the service module (view from inside the satellite to Earth).

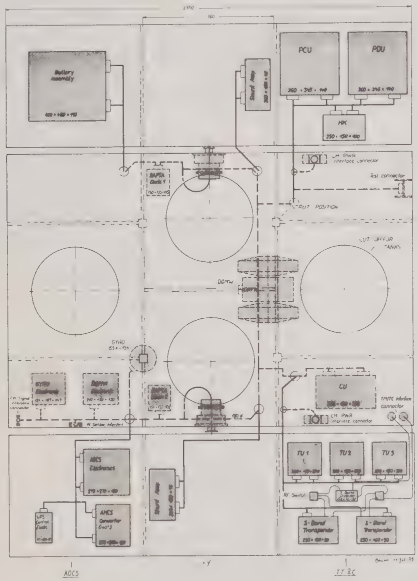
Battery Assembly
Shunt Assy
PCU
PDU
MX
BAPTA
SM PWR interface connector
Test connector
STRUT POSITION
OUT OFFSOR TANKS
DGMW
GYRO
GYRO Electronics
DGMW Electronics
CU
TM/TC interface connector
SM PWR interface connector
TU 1
TU 2
TU 3
AOCS Electronics
AOCS Converter
Shunt Assy
RF Switch
S-Band Transponder
S-Band Transponder
AOCS
TT&C

FIG. 16 SM Inboard Profile (Subsystem Equipment Assembly)

The power subsystem comprises power control, conditioning and protection circuits as well as the battery system. It is a regulated 50 V ± 2% single bus system. Each subsystem has its own power converter. The NiCd battery has a capacity of only 600 Wh because no eclipse operation of the repeater is required. Components for the power subsystem are under development at AEG-Telefunken and Dornier-System.

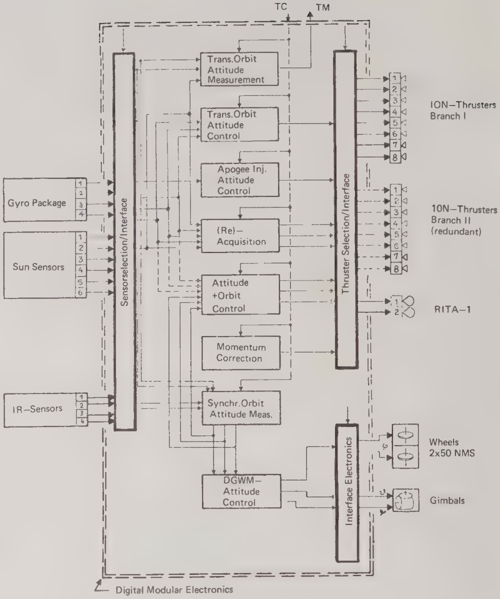
TC
TM
Trans.Orbit Attitude Measurement
Trans.Orbit Attitude Control
Apogee Inj. Attitude Control
(Re)-Acquisition
Attitude +Orbit Control
Momentum Correction
Synchr.Orbit Attitude Meas.
DGWM-Attitude Control
Gyro Package
Sun Sensors
IR-Sensors
Sensorselection/Interface
Thruster Selection/Interface
Interface Electronics
ION-Thrusters Branch I
10N-Thrusters Branch II (redundant)
RITA-1
Wheels 2x50 NMS
Gimbals
Digital Modular Electronics

FIG. 17 Attitude and Orbit Measurement and Control System Schematic

The power source for TV-Sat is the ULP modular lightweight array, developed by MBB and AEG-Telefunken in the past years specifically for this application.

The attitude and orbit control system (FIG. 17) allows for an antenna beam pointing accuracy of ± 0.14° in pitch and roll axis by means of an improved IR-sensor for TV-SAT A3. An RF-sensor is foreseen for the operational A5 version allowing to meet the specified ± 0.1°.

Together with the control thrusters it will furthermore provide for a station keeping accuracy (N/S and E/W) of ± 0.1° at the satellite`s orbital position of 19° West. The system comprises a double gimballed momentum wheel (developed by Teldex) for 3-axis control in the geosync. orbit. Attitude measurement for pitch and roll at this phase is performed by an IR-sensor (redundant). The yaw attitude is achieved by a special roll/yaw control law.

For 3-axis stabilized transfer and orbit injection a gyro package is used as reference, updated by the IR- and Sun-sensors signals and controlled by the 10 N thruster pulses. 6 digital Sun sensors provide the reference during S/C acquisition.

The control electronics include a double-redundant and programmable processor and memory and is under development at Dornier-System.

The spacecraft data system comprises the S-Band TM/TC system for the transfer phase and as back-up, the S-band antenna system and the Ku-Band transmitter. Further the decoder/encoder, bus controller and the subsystem terminals (interface units), as developed by SEL.

The capacity is for 370 telemetry channels and 280 command signals. The S-Band uplink frequency is 2 110 MHz, the downlink frequency 2 290 MHz.

3.3 Propulsion Module

One of the specific features of TV-SAT is the separable propulsion module with the Unified Propulsion System (UPS), based on the outstanding SYMPHONIE bipropellant technology.

The propulsion module also comprises the RITA ion thruster packages for orbit control. The module structure serves not only as mounting device for the complete propulsion system but also as the backbone of the whole spacecraft structure. The total PM dry mass is 210 kg.

Furthermore some 20 kg He and propellant residuals will remain with the UPS at EoM (End of Mission).

The UPS is a derivate of the Propulsion Module under development at MBB for the NASA Galileo Jupiter Orbiter. It uses the same tanks, engines and control hardware. The four spherical tanks provide a maximum capacity of 978 kg N_2O_4 and MMH, to be used for apogee injection , orbit and attitude control. A total of 16 small 10 N thrusters (FIG. 19) is foreseen, subdivided into two independent branches, as well as one 400 N thruster for the apogee maneuver. The extended nozzle of this engine will allow for 307 sec specific impulse. The tanks are equipped with capillary devices to ensure operation under weightless conditions.

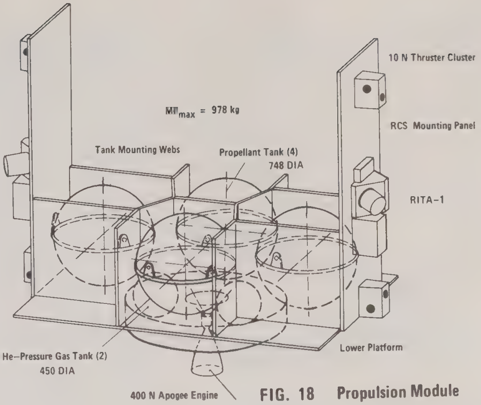
10 N Thruster Cluster
$\overline{M}_{max}$ = 978 kg
RCS Mounting Panel
Tank Mounting Webs
Propellant Tank (4)
748 DIA
RITA-1
He-Pressure Gas Tank (2)
450 DIA
Lower Platform
400 N Apogee Engine

FIG. 18 **Propulsion Module**

The apogee injection maneuver, requiring 682 kg of the propellants in case of an ARIANE launch (and 825 kg in case of a Shuttle/SSUS-A launch from KSC) is performed under controlled tank pressure of230 bar while the subsequent operation of the small thrusters is done in the blow-down mode.

The RITA electric propulsion as part of the propulsion module leads to a considerable mass saving in the operational TV-SAT A5 with N/S and E/W station keeping performed over 70% of the lifetime. Since RITA is operated by the solar array surplus power the mass saving increases with higher design lifetime of the satellite bus and total mass in geosync. orbit as shown in FIG. 20.

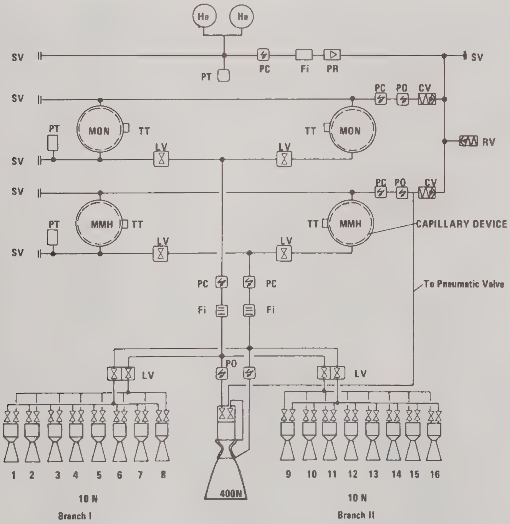
He
He
SV
PT
PC
Fi
PR
SV
SV
PC PO CV
MON
TT
TT
MON
PT
RV
SV
LV
LV
SV
PC PO CV
MMH
TT
TT
MMH
PT
CAPILLARY DEVICE
SV
LV
LV
PC
PC
Fi
Fi
To Pneumatic Valve
LV
PO
LV
1 2 3 4 5 6 7 8
400N
9 10 11 12 13 14 15 16
10 N
Branch I
10 N
Branch II

FIG. 19 **UPS Schematic**

Legend:

PO	Pyro Valve normally opend
PC	Pyro Valve normally closed
SV	Service Valve
Fi	Filter
PR	Pressure Regulator
RV	Relief Valve
CV	Check Valve
LV	Latch Valve
EV	Engine Valve
PT	Pressure Transducer
TT	Temperature Transducer

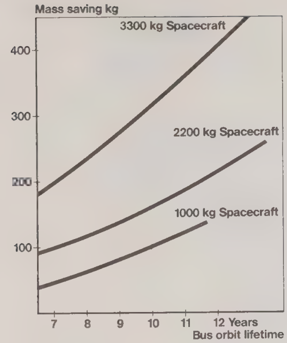

FIG. 20 Mass Savings by RITA–2 N/S and E/W Orbit Control

4. TVBS Operational Economics

From the very beginning, i.e. during the early design studies, economic optimization as required for an operational TV-broadcasting satellite system has been persued.

Cost minimization for the space segment is of increasing importance since the cost for each flight unit of these high-power satellites are relatively high, and - in addition - a standby spacecraft is required to avoid the risk of program interruption (requirement from the Post Administration).

Therefore, an extensive economic analysis was performed taking into account

- spacecraft bus design reliability vs. time with single and double redundancy
- payload design reliability vs. time with 1 of 2 TWT's and 2 of 3 TWT's
- power and stationkeeping propellant mass requirements vs. time with and without electric propulsion (ion thrusters)
- spacecraft mass and cost vs. lifetime

Fig. 21 shows the resulting reliability model curves. By going to double redundancy in critical areas as these are

- command receiver
- attitude control electronics
- data handling unit
- battery system

with the resulting increase in mass and cost, the same design reliability can be achieved for 10 years compared to 7 years with single redundancy.

As payload the German 5 channel TVB-system has been used, designed by AEG-Telefunken.

A total spacecraft mass limit of 1000 kg had to be observed, compatible with the ARIANE and SHUTTLE/SS US - a launch vehicles. This makes the use of electric propulsion mandatory for operational lifetimes of more than 7 years.

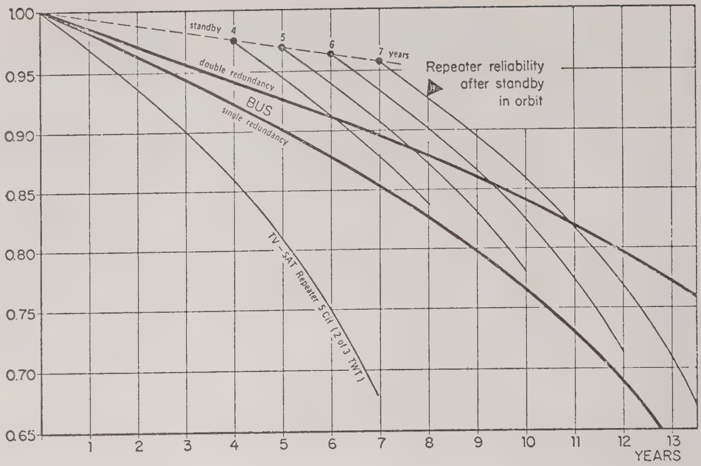

FIG. 21 Reliability Model Curves for Communicat. PL and Spacecraft Bus

To define the most cost-efficient solution the following formula has been established:

C^* = Cost per TV Channel and Year

$$C^* = \frac{C_S + C_L}{l \cdot n \; (R_{LV} \cdot R_{PL} \cdot R_{Bus})}$$

C_S = spacecraft recurring cost (Flight unit cost, 100 to 138 mio DM)
C_L = launch cost (ARIANE, 85 mio DM)
l = operational transponder lifetime
n = number of TV-channels per satellite (=5)
R_{LV} = launch vehicle reliability (ARIANE, 0.9)
R_{PL} = comm. payload reliabilty (Fig. 21)
R_{Bus} = spacecraft bus reliability (Fig. 21)

The results for a 1000 kg TV-SAT type satellite are depicted in Fig. 22 a and 22 b. Fig. 22 a shows the specific cost for the conventional approach of a satellite (+ standby) where comm. payload and bus have the same lifetime. This means that without a failure in the operating satellite the standby satellite also would be expended after the nominal lifetime (because of fuel depletion), without ever been used.

A much more efficient philosophy is to design the bus for twice the lifetime of the repeater (which fits better with the relevant reliability vs. time characteristics, see Fig. 22 b).

This means that each spacecraft after launch is first serving as the standby for 5 (6) years until the repeater is switched on for an operation over 5 (6) more years.

FIG. 22a
Average Annual Space Segment Cost (BUS=PL Lifetime)

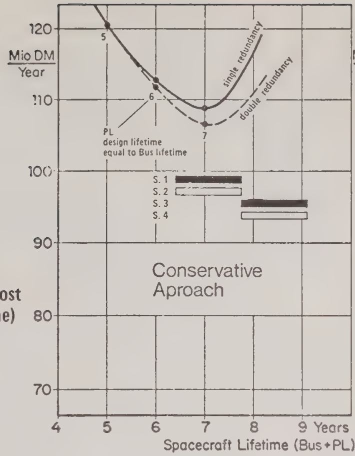

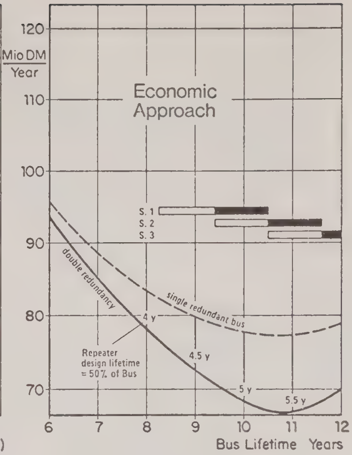

FIG. 22b
Average Annual Space Segment Cost (BUS Lifetime twice as PL-Lifetime)

By this new economic approach a cost saving for the German 5-channel TVBS-System of 40 Mio. DM per year is feasible.

According to Fig. 6 for an optimized German TVBS the program distribution cost will be as low as 15 Mio. DM per channel.

The cost for central ground station for the uplink and spacecraft operations on ground have to be added, however, this must be compared with the present cost of TV programs' ground distribution which amounts to over 150 Mio. DM per channel.

This example shows that direct-TV-broadcasting is a very cost-efficient means of program distribution.

The German TV-SAT will pioneer direct TV broadcasting to individual users in the middle eighties. The definition of the first spacecraft is based on technological components which have been developed and tested since several years. The satellite design combines high performance and reliability with acceptable development risks and cost. (Fig.23)

The expected fact that a direct TV-broadcasting system will require much lower investment and operations cost than a large network of ground transmitters certainly will be a major argument for a wide future use of such systems.

FIG. 23 On–Orbit Configuration of TV–SAT A3

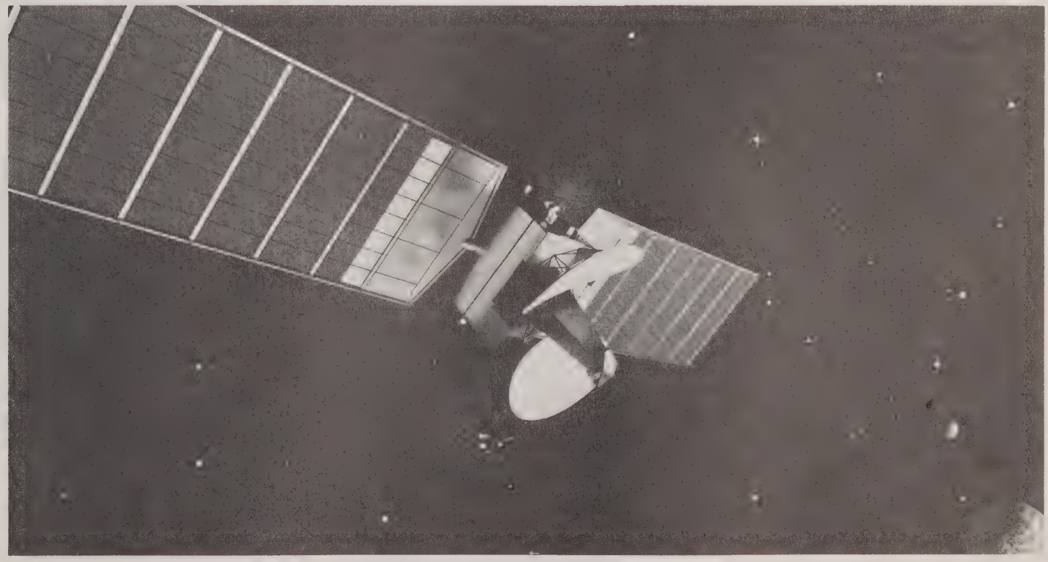

80-0571

FRENCH SATELLITE BROADCASTING SYSTEM

J.F. Arnaud, Télédiffusion de
France
C. Derieux, A. Pouzet, Centre
National d'Etudes Spatiales,
Paris - France

Abstract

The paper gives a preliminary description, of the preoperational French satellite broadcasting program (mission and spacecraft), decided in October 1979. Some of the specifications were fixed by Warc 1977.
Others characteristics are given in the paper such as the number and the nature of TV channels, the coverages, the service quality, the service availability. The anticipated satellite technical characteristics and technologies, resulting from a definition study, are described.

French Satellite Broadcasting System

If official texts were to be trusted, in this case the Final Acts of the World Administrative Radio Conference of 1977, whose purpose was to draw up a plan for broadcasting on 12 GHz from satellites, for Africa, Asia and Europe, then one would be tempted to believe that the Old World was planning well ahead of the New World in that field. Actually, the Final Acts were intended primarily to delimit the new service and to specify the bands of frequencies and the parts of the stationary orbit to be reserved for other services. Thus, when the broadcasting service of a country comes to consider the adoption of this new means of broadcasting programmes, it discovers that it is restricted by constraints in the form of maximum values, tolerances and limits with which it is obliged to comply. In addition, it has to define its project under all the following headings : -

(i) the number and nature of the programmes,
(ii) the areas to be served,
(iii) the quality of the service, in association with the hypothetical reference receiver, and
(iv) the continuity of the service.

The first two parameters will be defined by political decisions within the limits specified in the Final Acts of the Conference, whereas the last two fall within the competence of the broadcasting organisation concerned. As a consequence, it is upon these latter that we shall more particularly dwell in the first part of this discussion; the second part will be devoted to a description of the satellite itself, that is to say, to the platform and the payload.

Part One : The project

1.1. The number and nature of the programmes.

It was during the course of 1979, that the French government decided to establish a pre-operational direct satellite broadcasting system. In October 1979, French and German governments have decided to undertacke a cooperative program for development, fabrication and launch of two broadcasting satellites, one over French coverage and the other German coverage. The project defines indeed a system, because it will cover, in addition to the satellite and its ground facilities, an Earth-station for transmitting, up to the satellite, the sound and vision signals to be broadcast, as well as the receivers for the public.
It is to be borne in mind that, according to the terms of the Radio Regulations (RR), broadcasting is intended to be received directly by the general public (RR Nº 3040).
In the first phase, which will be of an experimental and pre-operational nature, only three television programs will be broadcast, although five per country were authorised by the 1977 Conference. Their program content is beyond the scope of this discussion, but it is nevertheless to be hoped that at least one of them will be attractive enough to persuade the general public to equip itself for the reception of the new service and thereby bear witness to the justification of the service. At this point, a word should be said about the sound signal; without doubt it is to the sound signals that reference should be made, because it is highly probable that two of them will be broadcast per channel, either to provide an additional sound component in a foreign language or to render stereophonic sound a possibility.

1.2. The area to be served

The area to be served is very strictly a function of the planning data adopted by the Conference, which define, among other parameters, the maximum aperture of the beam, assumed to be of elliptical cross-section, radiated by the satellite-borne antenna. It is evident that, as a consequence, there must inevitably be some departure from the formal aim of broadcasting on these frequencies, which is in principle strictly national, but is is recognised that it is impossible to confine the irradiation precisely within the frontiers of a country, which cannot be defined in any simple geometric fashion (Fig. 1).

Copyright © American Institute of Aeronautics and Astronautics, Inc., 1980. All rights reserved.

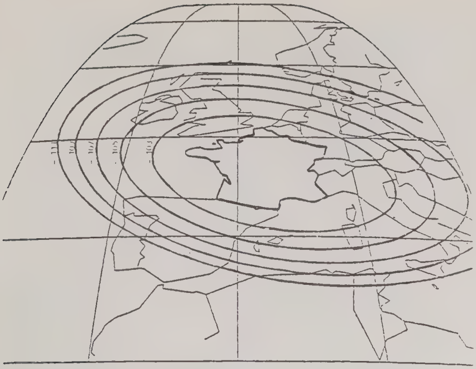

FRENCH COVERAGE

POWER FLUX DENSITY)

Curves - 103, - 105, - 107, - 109, - 111 dBW/m²

- FIG. 1 -

As a result, what are termed inevitable overspills into the neighbouring countries will be tolerated, overspills which will manifest themselves in all cases, except in the case of very isolated islands. France is a country having sufficiently small dimensions for it to be possible to cover it by means of a single beam and with a power within the range that can be radiated on 12 GHz from a satellite in the geostationary orbit, but, because of the irregular shape of the country and, in particular, because of the eccentric location of Corsica, any ellipse encompassing the whole of France encroaches considerably on the neighbouring countries, to the extent even of including the whole of Switzerland, Belgium and Luxembourg, as well as considerable areas of the United Kingdom, the Netherlands, the Federal Republic of Germany, Italy and Spain. The 1977 Plan is such that it provides for good reception, free of perceptible noise and interference, throughout the nations territory, provided that the receiving installations comply with certain minimum characteristics. It is in no way excluded that, by using a more efficient installation - for example, one incorporating a larger antenna, or by accepting from time to time some slight degradation of the quality - viewers in other countries might be able to obtain a sufficiently strong and adequately interference-free signal, to enable them to obtain acceptable pictures with which they would presumably readily be satisfied, bearing in mind that every broadcasting organisation is very well aware that the public tolerates, in programs coming from abroad, faults that would give rise to indignant reaction if they were to occur in the national programs. Thus, by means of receiving installations having about six times the sensitivity of the standardised reference receiver, the French programs could, il is hoped, be receivable as far as Denmark, Scotland and the coast of Algeria (Fig. 1). Nevertheless, it would not be wise to allow too little margin around the territory of France, for example, by insisting that the ellipse be tangential to the most westerly point of Britanny and the southern extremity of Corsica. In practice, no satellite in orbit is absolutely stable, and its residual movements, must allow an overall beam pointing accuracy of 0,1° in any direction apart the nominal axis and a maximum rotation of the beam of ± 2° around the nominal axis. This entail some global displacement of the ellipse which must, as a consequence have dimensions slightly greater than the theoretically necessary minimum, if the more remote parts of the national territory are never to be missed.

1.3. The receiving installation and the quality of the service

The ideal objective would be to provide the viewers with the additional programs without their having to modify their receiving installations in any way, but unfortunately that is a goal that is for many reasons quite unattainable. In the first place, apart from the fact that the radio-frequencies allocated to broadcasting in the VHF and UHF bands are already totally occupied by existing or reserved for planned transmitters, such low frequencies would require transmitting antennae too large to install on the satellite, if the radiation were to be concentrated within a country of average size. It was, therefore, necessary to move into the SHF bands, and it is in the neighbourhood of 12 GHz that the RR have reserved a band for services of the kind under discussion here (there is also an allocation at 2600 MHz, but that is not suitable for individual, as distinct from community, reception, because of the limits imposed on the power flux density).It will, therefore, be necessary to add a frequency-changing stage to the ordinary television receiver. Moreover, it is not practicable to install in a satellite a transmitter rated at several tens of kilowatts, which would in fact be the power necessary to serve France, even assuming that the receiving installations were provided with parabolic antennae of diameter 900 mm. The only way to get around this difficulty is to have recourse to frequency modulation, which has never yet been used for the vision signal in direct television broadcasting to the public, but only for the sound signal; this implies a further complication in the receiving arrangements. The RF characteristics adopted for the radiated signal are summarised in the Appendix.
Thus, it is convenient to make a distinction between the two sections of the receiving installation (Fig. 2) : namely the section comprising the circuits for processing the video-frequency and audio-frequency signals, with which are associated the display tube and the loudspeaker, and the radio-frequency section which comprises :

a) for receiving the terrestrial programs, the usual Yagi antenna and the tuning and demodulation circuits appropriate to the local terrestrial television standards, and

b) for receiving the satellite programs, a parabolic antenna, to which are connected a first frequency-changer and the tuning and demodulation stages appropriate to the satellite standards.

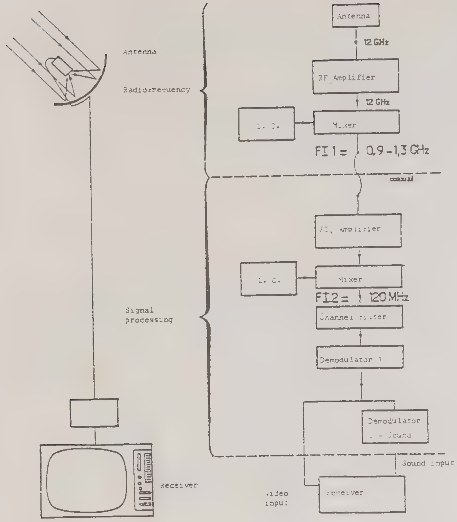

BROADCASTING RECEIVER - FIG. 2 -

It is not intended, in practice, other than in exceptional circumstances, to feed the 12-GHz radio-frequency signal into the viewers' homes, because at that frequency any reasonably-priced coaxial cable would introduce too much loss, and consequently the first frequency-changer must be installed in very close proximity to the parabolic antenna. A second frequency-change is in some cases necessary, depending upon the type of the demodulation that is to say, whether it is of the conventional type or of the threshold extension type.

The whole system has been dimensioned as indicated above, to ensure a service of good technical quality, but that statement needs a certain amount of explanation. In the case of the terrestrial networks, the quality of the sound and pictures depends to a large extent on the distance of the receiver from the transmitter. As seen from the satellite, on the contrary, all the receiving locations are more or less equivalent; between the most favoured location, that on the centre-ligne of the beam, and the most eccentric location, the difference is no greater than 3 dB. It is, therefore, easy to determine a power budget for the link, taking, of course, into account the effects of rain, and to calculate with precision the radiated power required. For a country like France, 350 watts are required - except during the most violent rainstorms, assumed to occur for less than 0,1 % of thetime - for the received pictures to be good, the power flux density attaining then at least - 103 dB (W/m^2), or 43 dB ($\mu V/m$), at all receiving locations, compared with some 65 to 70 dB ($\mu V/m$) for territorial UHF television. It should perhaps be recalled at this point that the purpose of the satellite is to serve all the viewers and that its characteristics are, therefore, defined on the basis of the simplest receiving installation. Nevertheless it must be borne in mind that, at the present time, cable-television and community-reception systems having multiple outlets are becoming more numerous. Such networks serve from fewer than ten to several thousands of connected households, and it would, therefore, seam reasonable to ask such communities to make a greater global financial effort. Whereas the average cost of adapting a domestic television receiver for individual reception from a satellite has been estimated at 3000 French francs (≈ US $660), the equipment necessary at the head-station of a community network could quite probably cost five or six times that amount. Moreover, it would benefit from a larger antenna, amplifiers of superior quality and larger bandwidth, because three programs have to be distributed. Thus, evidently, the possibility exists of reception outside the nominal service area mentioned in Section 1.2. What will in due course be the relative distribution in France of individual and collective installations for satellite reception remains to be seen; it will be difficult to determine the respective figures. Unfortunately, from the broadcasting point of view, France is a country having a dispersed population, of which a very substantial fraction lives in communities fo fewer than 2000 inhabitants. On the basis of the approximately fifteen million television receivers at present in use in France, it has been estimated that, to adapt all of them, about five million antennae would be required. That is the figure that is the most important, when it is desired to evaluate the market. Any estimate has its risk, but, without claiming any particular precision, a capital expenditure by the public amounting to about 20 000 millions French francs (≈ US $4.5 thousand millions) may be suggested, that is to say, about ten times the global cost of the satellite system over ten years. It is this consideration which, at the time of the conception of the system, urged the simplification of the receiving installation, at the expense of the satellite. A saving of FF 80 (≈ US $18) on each receiving installation on the ground would pay for one more satellite, launching and insurance included.

1.4. The continuity of the service

This is a notion which is familiar to every broadcasting organisation, as indeed it is also to every telecommunication engineer, but here it will be approached from a rather different standpoint. In practice, a terrestrial television network comprises a large number of transmitters and the failure of any one of them, which may have a local cause (breakdown of the transmitter itself) or an extraneous cause (failure of the public power supply or of the radio-relay chain supplying the program signals), gives rise to a local interruption which it is almost always possible to clear in a fairly short period of time. The satellite, on the other hand, is subject to fewer hazards, but any defect in its functioning has more serious consequences. In effect, a complete breakdown deprives a whole country of its programs and a repair is not in general possible. Only a reserve satellite already in orbit enables a quick restoration of the service to be effected. In the absence of such an immediately available reserve,

it would be necessary to wait several months before a new space-craft could be put in position. A failure of only one program channel is more tolerable, but in this case also, a reserve satellite must be available without too much delay.
Up to the present time, only complete breakdowns caused by the failure of a transmitter or the serious destabilisation of the platform, have been envisaged, but whereas a terrestrial transmitter made to function at half-power satisfies the greater part of its normal service area, a corresponding power reduction in a satellite transmitter jeopardises the picture quality over virtually the whole of the territory, particularly where the rainfall is heavy, so that redundancy at the level of the power amplifier should also be considered, a serious attitude error which dangerously reduces the energy received on the ground in the vicinity of certain frontiers or coastlines also demands an immediate remedy.
It is for this reason that, at the time of the definition of the satellite, great precautions were taken, both at the 1977 favourable conditions listed herebelow occur simultaneously, that the picture quality is degraded :

(i) the satellite is getting close to the end of its estimated life,
(ii) it is as far away as authorised from its correct bearing,
(iii) the receiving location is in the most eccentric part of the service area,
(iv) it is precisely at that location that the heaviest rain occurs.

In these circumstances, the received field-strength will no longer be adequate, and the functioning of the receiver will be affected corresponingly.

Part Two : The Satellite

The requirements of the project discussed in Part One point to certain specific characteristics for broadcasting satellites. These relate, in particular, to the high emitted power, demanding sources of electrical energy very much more powerful than those of communication satellites and also demanding power-output stages having the highest possible efficiency; even under those conditions, the problems of heat dissipation are still difficult. They relate also, in view of the international regulations, to the precision of maintenance of orbital position and attitude, as well as of the pointing of the antennae, all of which demand very sophisticated technology. Furthermore, the notions of service continuity and reliability appropriate to a broadcasting service influence the redundancy plans, above all as regards the output stages of the satellite-borne transmitters.
In general, the satellite comprises a platform, which should be as polyvalent as possible, combining the functions of the satellite : structure, power supply, thermal control, attitude and orbit control, apogee motor and TT and C; the satellite comprises also a payload specific to the project to be implemented, combining the receivers, transmitting antennae, channel-selective amplifiers output amplifiers and the like.

The satellite will, therefore, be designed in a modular fashion, resulting from the association of the platform and the payload.

The French decision of 1979 to establish a pre-operational system was preceded by a large number of studies undertaken in close collaboration by the Centre National d'Etudes Spatiales (CNES) and Télédiffusion de France (TDF) with assistance at the industrial level by the Société Nationale Industrielle Aérospatiale (SNIAS) and by the Thomson-CSF company. The technic studies led to an initial definition of the satellite, some features of which are discussed below.
At this point, it is appropriate to recall what was said in Part One, namely that the satellite is required to broadcast in three channels, in conformity with the stipulations in the Final Acts of the World Administrative Radio Conference on Satellite Broadcasting (WARC-SB, Geneva 1977); at the same time, attention was given to the possibility of increasing the capacity, at the having a shroud of useful internal diameter of three metres. The probability of satisfactory functioning of the three channels at the end of five years was taken as 0.75, the useful life of the satellite (specified as the time during which the satellite can be can be maintained in its orbital position) being taken as seven years.
In that initial definition made in 1979, the technical choices, although being based on existing technologies, might nevertheless have recourse to the most recent developments, provided that they were compatible with the first satellite launch in 1983.

2.1. The geometrical configuration

The satellite (Fig.3) has the now conventional configuration of three axis stabilisation and a heliotropic north-south solar generator.

The geometrical configuration was determined by a trade off involving the following parameters :

- the dimensions of the shroud of the launcher,
- the radiating areas necessary for the payload,
- the area reserved for the accomodation of the equipment,
- the flexibility for the arrangement of the antennae,
- the space necessary for stowing the solar generator,
- the minimum mass of the structure,
- the minimum length of the feeders between the power-amplifier and the antennae.

The body of the satellite has the form of a rectangular parallelepiped fo about 1.65 long in the "north-south" sense, 2.1 m wide in the "est- west" sense and 3 m high. In its launch configuration, the reflectors of the antennae are folded on one another on the opposite side to the plane of attachement to the launcher; as soon as the satellite is in position in orbit, a rotation of about 180° is made around an axis substantially parallel to the pitching plane, in order to bring them into their final configuration. The solar generator of the rigid type (RSG) consists of panels stowed along the north and south sides, and unfolded as soon as the operational orbital position is reach.
In its orbital configuration, the satellite has a spread of either 28.5 m (in the three-channel variant) or of 35.4 m (in the five-channel variant); The side presented toward the Earth is the side that carries the apogee motor.

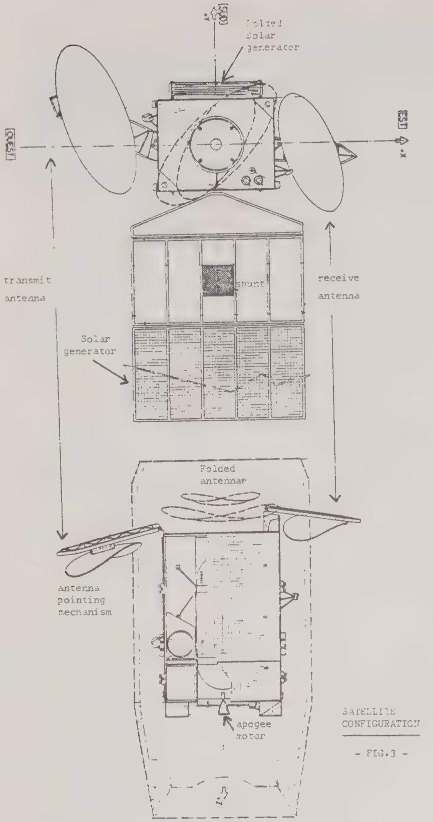

SATELLITE CONFIGURATION

- FIG.3 -

The modular design (Fig. 4) of the satellite was adopted in expansion and adaptation to a variety of projects.

2.2. The platform sub-systems (propulsion and service modules)

2.2.1. Structure

The modular design adopted has a central support structure comprising three modules, namely the payload module, the service module and the propulsion module. From considerations fo the strength of the materials, the structure consists of a "primary" structure and a "secondary" structure.

The primary structure is intended principally to pass on the launching stresses and to distribute them in the satellite; it consists (Fig.4) of a central tube, a central plate, four reinforcement gussets under the central plate and two reinforcement gussets above that plate, attached to the central tube.

The secondary structure consists essentially of the panels for supporting the equipment or for acess, and the backing struts for the central points of attachment of the solar generator.

The material used is in most cases either aluminium or carbon fibre.

2.2.2. Thermal control

The principal problems raised are those inherent in the very high and very concentrated power of many of the components of the payload, in the complete interruption of the functioning of that equipment during the eclipses, and in the very narrow range of conditions for the correct functioning of some items of the equipment (multiplexer), as well as the triaxial mode of stabilisation in the transfer phase.

The thermal control proposed is based on a passive design, supplemented by constant-conductance heat-pipes (for the radiators and the supplies for the travelling-wave tubes), or variable-conductance types (for the transfer phase and during the eclipses). All the heat-dissipating items are attached to the north and south sides, which constitute radiators receiving only a small amount of solar irradiation (as for the radiant collectors of the TWTs, they are located on the east and west sides); 9 m^2 are available, where the three-channel variant requires about 4 m^2 and the five-channel variant about 7 m^2. These areas are clad with silvered silicon mirrors. All the external surfaces that are not utilised as radiators are clad with superinsulation of high efficiency.

2.2.3. Power supply : solar generator and power distribution

The rigid solar generator comprises six sections per wing for the three-channel variant (ten sections for the five-channel variant); each section

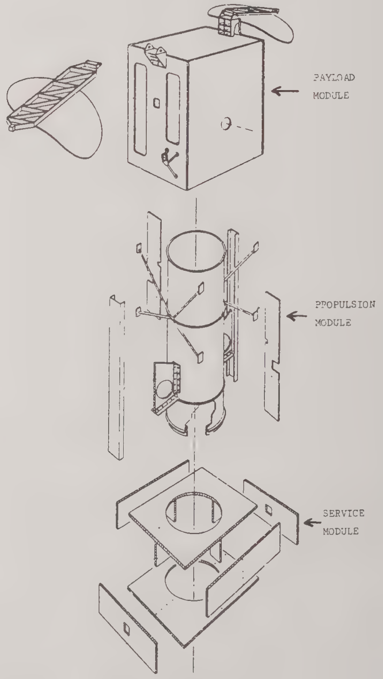

EXPLODED SATELLITE VIEW - FIG.4 -

contains thirty chains in parallel, each consisting of 156 cells in series grouped in three electrically independent units (the electrical arrangement of the external panels used in the transfer orbit is different); Each wing, of dimensions 12.1 m x 3.1 m (for three channels) comprises a yoke structure linked with the drive mechanism (SGDM) and delivers 1.8 kW at the end of its useful life.

The distribution of the energy is effected on two nominally separate bus-bars, from the two wings of the solar generator and from a group of two 32-cell nickel-cadmium batteries.

Under solar irradiation, the bus-bar voltages are regulated to 50 V by two linear and sequential shunts, each associated with one of the wings of the solar generator.

During eclipses, each of the two batteries is connected through a group of diodes to a service bus-bar supplying the energy needed, at a nominal voltage of 38.5 V.

Individual regulators adapt the bus-bar voltage to the requirements of the various items of equipment.

2.2.4. Attitude and orbit control and propulsion system

The control of the attitude and the orbit position must satisfy the demands of the broadcasting project, one fundamental stipulation of which is that the satellite-borne transmitting antenna must be pointed toward the area to be served with a precision of 0.1°. The solution adopted is that depicted in Fig. 5, which enables the complexity and thereby the cost of the platform to be reduced (by reduction of the number of gyroscopes and the use of infrared sensors). The main reflector of the transmitting antenna is mounted on a mechanical pointing device, which allows it a certain independence of movement relative to the body of the satellite; thus, although the precision of pointing of the antenna necessitates the use of a radio-frequency sensor detecting a beacon on the ground, the satellite piloting system can be simplified, because the platform then no longer needs such a high precision of stabilisation (0.2° to 0.4°, depending upon the axis) as that of the transmitting antenna. A system for detecting the attitude errors employing optical sensors and a drive no degree of liberty, that is to say with a fixed kinetic momentum, then complete the device for the precise pointing of the precise pointing of the antenna itself.

For the reaction sub-systems, the bi-ergol technology was adopted, as its specific impulse (285 s), being higher than that of hydrazine (220 s), allows a certain gain on the level of the mass. The bi-ergol technology was adopted also for the apogee motor (thrust : 400 N), thus a unified propulsion system, with tri-axial stabilisation during the transfer phase and the functioning of the apogee motor. The control of the attitude and the orbit position throughout all the phases of the project is thus effected by means of sixteen 10-N thrusters. It is estimate that the gain in mass is 50 kg, compared with the solution based on systems of separate thrusters and stabilisation by rotation during transfer. Furthermore, the constraints of inertia ratio and dynamic balancing are obviated.

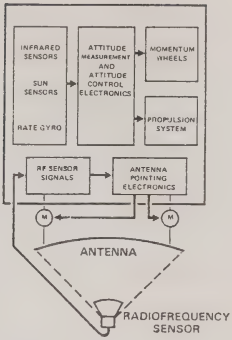

ATTITUDE AND ORBIT CONTROL - FIG.5 -

2.2.5. Tracking, Telemetry and Command

The telemetry function is effected during the transfer and positioning phases in the 2.2 - 2.29 GHz band and thereafter, in normal operations, in the broadcasting service band; the 2.2 - 2.29 GHz band can then be used as back up. The same principle has been adopted for the command, using first the 2.025 - 2.110 GHz band and then the service band. The tracking function is effected in the 2.2 - 2.29 GHz and 2.025 - 2.110 GHz bands during the transfer phase and in back-up mode by means of coherent transponders and by measuring the phase difference of tones modulating the carrier; in normal operations, the distance measurement is made on the television signal (sync.lines).

2.3. The payload sub-systems

The principal technical hypotheses adopted for the payload in the preliminary study assumed a configuration comprising a transponder having two frequency-changes, two separate antennae for transmission and reception and a frequency band between 15 and 18 GHz for the up-link (the WARC 1979 has since allocated the band 17.3 - 18.1 GHz).

2.3.1. The transponder

The transponder provided for the transmission of the three carriers for the television signals has the principal function of receiving those carriers from the ground by means of the receiving antenna, of separating them in order to amplify them individually and then or recombining them, to transmit them back to the ground by way of the transmitting antenna. The general schematic diagram is given in Fig.6.

The receiving function is effected by a wide-band receiver comprising two redundant chains. Each chain consists of an input filter, a receiving frequency-changer (18 - 3.5 GHz), an intermediate-frequency amplifier, a transmission frequency-changer (3.5 - 12 GHz) and a local oscillator.

The separation of the channels is effected by a demultiplexer consisting of filters coupled by circulators.

The channel amplification is carried out by solid-state gain-amplifiers, each of which consists of two redundant chains each comprising eight stages of amplification using field-effect transistors.

The power-amplifier design is based on the use of travelling-wave tubes (TWTA) rated at 220/230 W radio-frequency, each consisting of a brazed-helix TWT, of which the multi-stage collector is designed to get rid of the heat by radiating it into space, and of its power supply which provides the required voltages from the primary 50-V source.

The RF power required at the output of the power-amplifiers (350 W) being greater than the power that can be obtained from a helix TWT, it is necessary to combine the power of two TWTAs, by means of a T-circuit, as indicated in Fig. 7. At the input, the power supplied by the normal or reserve gain-amplifier is shared between the two TWTAs, by a power divider.

The initial phase balance and its rebalancing in flight is effected by ajustment of the helix voltages fo the TWTs, carried out by remote control.

The combination of the channels at the output is effected by means of a reflection multiplexer which regroups the three channel signals on a single feed to the antenna.

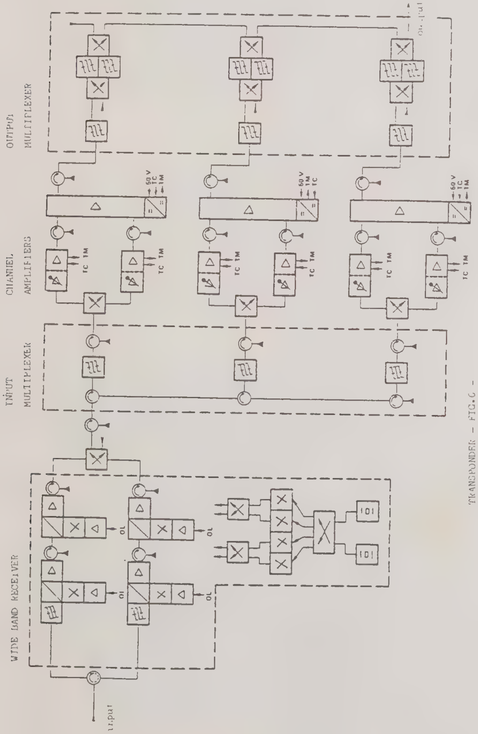

TRANSPONDER - FIG.6 -

In the preliminary study, the failure of one of the two TWTAs was taken account of by installing a third TWTA in spare, the inputs and outputs being switchable by change-over switches with two inputs and two outputs. Further devices which might ensure improved reliability are under study; for example, two redundant general-purpose power chains which could be substituted for any one of the three normal chains, thus obtaining a probability of good functioning of 0.86 for the three channels at the end of seven years (taking into account only the reliability of the TWTAs of 3500 fits), compared with 0.81 for the original configuration.

This option necessitates one additional TWTA (ten, instead of nine) and the change-over switches in cascade and might pose some heat problems; it is, therefore, at present undergoing complementary studies, in order to verify its greater benefit.

2.3.2. The antennae

The antenna sub-system comprises the following principal elements :

- a high-gain 12 GHz antenna for transmission and station-keeping,
- a high-gain receiving antenna,
- a mechanism for pointing the antenna (APM) and the station-keeping receiver associated with the transmitting antenna.

For the high-gain antenna for transmission and RF tracking, the solution based on multiple sources and an overdimensioned reflector (2.7 m x 1.06 m) was examined in the preliminary study, taking into consideration the advantages in gain and in conformity with the WARC tolerances, that could be expected of it. In that configuration, the reflector of pseudo-elliptical cross-section is illuminated directly by an eccentric primary source.

The primary source consists of nine horns, arranged in a diamond pattern and excited by a transmission circuit and by a circuit for producing the independent radio-frequency sensing signals. The expected gain advantages not having yet been confirmed by measurements, the study of the single-source solution with the reflector of normal dimensions is continuing (although that solution poses some problems regarding the purity of the polarisation), in order to be able to compare their radio and mechanical features and to decide in due course on the technology to be chosen for the satellite.

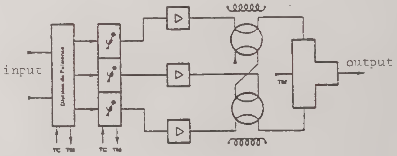

HIGH POWER AMPLIFIER

FIG. 7

The antenna-pointing mechanism allows an overall precision of ± 0.05°; it is slaved to the elevation and azimuthal coordinates provided by the tracking receiver, although ot can also be actuated by remote control. The mechanism employs magnetic bearings instead of ball-bearings, thus eliminating frictional and wear effects.
The tracking receiver is of the single-channel type, the "sum" channel being modulated by the two "difference" channels in time-division duplex, with square-law demodulation.
For the receiving antenna, it has been assumed a priori that it would be of the same type as the transmitting antenna. In the study, the use of 15 GHz was assumed, which would lead to an antenna of suitable dimensions for mounting on the satellite (reflector fo 2.24 x 0.9 m). Now, according to WARC 1979 results, an up-link in the 17,3 - 18,1 GHz band is assumed.

2.4. Mass & power budgets

Power budget

	Orb. Transfer	3 channels Eclipse	Summer solstice (7 years)	5 channels Summer (7 years)
PLATFORM				
Attitude and orbit control	46	38	38	38
BAPTA	32	22	70	70
House keeping	32	2	130	223
TTC	37	45	45	45
Thermal control	20	20	40	40
TOTAL	135	127	323	416
PAYLOAD				
Low-power chain		5	50	60
High-power chain			3000	5300
Antenna pointing			32	32
Thermal control	120	180		
TOTAL	120	185	3082	5392
Satellite total	255	312	3405	5808
Availability (SG)	311		3662	6148
Margin/extent of discharge	23 %	49 %	7.5 %	6 %

Mass budget

	3 Channels	5 Channels
Structure	165	165
Thermal control	55	75
AOCS	43.9	43.9
Propulsion	120	120
Solar generator	166.8	247
Power supply	63	77
TTC	28.8	28.8
Harness	25	25
Miscellaneous	10	10
RITA + Hg	/	/
Sub-total	677.5	791.7
Payload	183.5	267
Margin	109	88.1
Mass of satellite	970	1146.8
Ergols + pressurant	980	1153.2
Total at launch	1950	2300

Appendix 1

Specification

Colour-television system : 625 lines, L-SECAM C.C.I.R.
Base-band (including sound) : 6.5 MHz
Radio-frequency bandwidth : 27 MHz
Energy dispersal (deviation) : 600 kHz, 25-Hz triangular signal
Video pre-emphasis : to C.C.I.R. Recommendation 405.
Max. deviation for 1 V video at the reference frequency : 13.5 MHz
Modulation polarity : negative frequency deviation for sync. pulses
Sound-sub-carrier frequencies : 5.5 and 5.755 MHz
Max. sound-sub-carrier deviation : ± 100 kHz, peak to peak
Max. deviation of the carrier by a sub-carrier : ± 2.8 MHz
Sound pre-emphasis : 50 μ s

Quality parameters

Vision : Signal-to-unweighted ratio greater than 33 dB
for a carrier-to-noise ratio of greater than 14 dB
for 99 % of the least favourable month.
Differential-gain distortion : less than 10 %
Differential-phase distortion : less than 5°.

Luminance/chrominance gain inequality :
less than 10 %
Luminance/chrominance delay inequality :
less than 50 ns

Sound : Signal-to-weighted-RMS-noise ratio
(C.C.I.T.T.) : at least 60 dB
Signal-to-weighted-quasipeak-noise ratio
(C.C.I.R.) : at least 51 dB
Pass band : 40 - 15 000 Hz.

80-0573

PERFORMANCE OF THE TELESAT REAL-TIME STATE ESTIMATOR

F.C. Kes,* R.G. Lagowski,** A.J. Grisé†
Telesat Canada
Ottawa, Ontario

Abstract

Telesat has implemented an economical mission software system which runs entirely on in-house Hewlett-Packard 1000 F-Series minicomputers. The system supports all mission phases of the ANIK satellites, including transfer orbit. During routine stationkeeping operations, the orbital elements and the attitude vectors of all ANIK satellites are estimated in real time by an extended Kalman filter. Results based on more than two years of operation show that, in conjunction with other mission software elements, the real-time process not only reduces operating costs, but also improves the accuracy of the state estimates, especially when frequent satellite maneuvers are required.

Introduction

Telesat currently operates four geostationary satellites, providing a variety of satellite communication services to Canadian customers. Three of these satellites (designated ANIK A1, A2 and A3) are dual-spin satellites with twelve 6/4 GHz channels, while the fourth (ANIK B) is three-axis stabilized with twelve 6/4 GHz and six 14/12 GHz channels. Stationkeeping parameters for these satellites are summarized in Table 1. Three additional satellites (two 14/12 GHz and one 6/4 GHz) are scheduled for launch in 1981 and 1982.

The ANIK satellites are remotely monitored and commanded from the Satellite Control Centre (SCC) in Ottawa, which is linked to Telesat's main tracking station at Allan Park, Ontario, as shown in Fig. 1. All data, including telemetry and tracking data, is routed to the SCC and the adjoining Computer Centre where it is displayed, stored, and made available to real-time and batch users.[1]

Until 1976, the Telesat mission software[2,3,4] operated on a UNIVAC 1108 owned by a local computer utility, and accessed by Remote Job Entry. Another UNIVAC 1108, used as a backup during transfer orbit missions, was located in Oakland, California. The mission software comprised a set of independent programs which performed the following functions:

- mission design;
- transfer orbit navigation and control;
- synchronous orbit acquisition;
- post-flight analysis; and
- stationkeeping.

After the launch of ANIK A3 in 1975, it became clear that computer utility charges would continue to rise with each satellite launched (projected to about $400,000 per year after the launch of ANIK B). Moreover, additional time would be spent during the work week in estimating the orbital elements and attitude of the in-orbit satellites, leaving less time for maneuver planning or software development and maintenance.

Table 1 Stationkeeping Parameters

	ANIK A1	ANIK A2	ANIK A3	ANIK B
Launch date	Nov 1972	Apr 1973	May 1975	Dec 1978
Longitude	104° W ± 0.10°	106.5° W ± 0.10°	114° W ± 0.05°	109° W ± 0.05°
Inclination	< 0.10°	< 0.10°	< 0.05°	< 0.05°
Attitude[a,b]	< 0.15°	< 0.15°	< 0.15°	< 0.40°

[a] Relative to orbit normal vector.

[b] The ANIK B attitude is controlled on board.

---

[*] Supervisor, Mission Software and Stationkeeping Section, Satellite Control Systems Division.

[**] Lead Analyst, Mission Software Development, Satellite Control Systems Division.

[†] Lead Analyst, Orbit and Attitude Determination, Satellite Control Systems Division.

Copyright © American Institute of Aeronautics and Astronautics, Inc., 1980. All rights reserved.

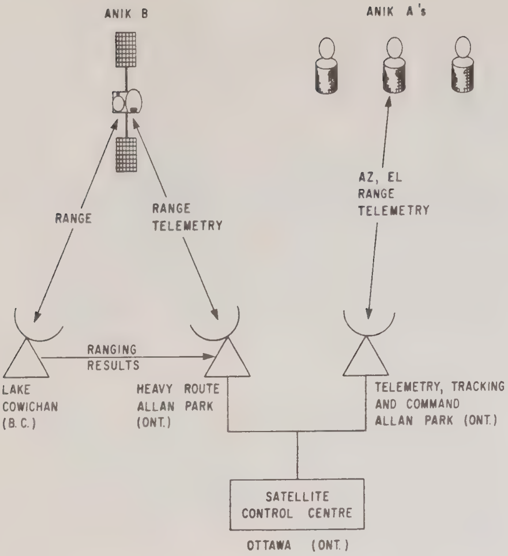
ANIK B
ANIK A's
RANGE
RANGE TELEMETRY
AZ, EL RANGE TELEMETRY
RANGING RESULTS
LAKE COWICHAN (B.C.)
HEAVY ROUTE ALLAN PARK (ONT.)
TELEMETRY, TRACKING AND COMMAND ALLAN PARK (ONT.)
SATELLITE CONTROL CENTRE
OTTAWA (ONT.)

Fig. 1 Satellite Control System.

At this time, Telesat was in the process of updating its Hewlett-Packard (HP) 2116 Data Processing System with HP 21MX's. Since these machines were found to have sufficient capability and capacity for scientific applications, it was decided to redesign and implement the mission software to run in house, reducing computer charges to about $15,000 per year. The software system was designed around a real-time Kalman filter which would simultaneously estimate both orbit and attitude states for all Telesat satellites.

The main objectives of the filter design were that it should:

- satisfy Telesat stationkeeping accuracy requirements;
- account for satellite maneuvers;
- remain stable for long periods of time;
- require little intervention by analysts;
- routinely provide solutions to off-line software; and
- report on its own performance.

The sections which follow describe the environment surrounding the filter (the computers and the mission software), the filter itself, and the results obtained.

The Telesat Computer System

As shown in Fig. 2, the Data Processing System currently includes three HP 1000 F-Series minicomputers under control of the RTE IVB operating system. These machines contain 384K words of 16-bit memory, as well as double-precision (64-bit) hardware and extensive firmware. The Data Storage Computer is dedicated to activities such as data acquisition and storage, historical data plotting, and real-time orbit and attitude determination. The Data Processing Computer is a general-purpose machine available for transfer orbit and stationkeeping activities, in addition to software development. The Utility Computer is used for dumping satellite data to long-term tape, and serves as a backup to the other two CPU's. Each computer is capable of assuming all functions. During transfer orbit, a fourth computer is available in an adjacent building, in case of a catastrophic failure in the Computer Centre.

Two identical sets of discs provide on-line and backup mass storage of 95M bytes each; 15M bytes may be accessed simultaneously by all three computers, and are used primarily for short-term (two weeks) storage of satellite data, and for real-time files used by the Kalman filter.

Users normally access the computers via one of four CRT terminals. They may submit batch jobs and converse interactively with text or data editors. Hardcopy output is sent to a 300 lpm printer, using HP-supplied spooling software.

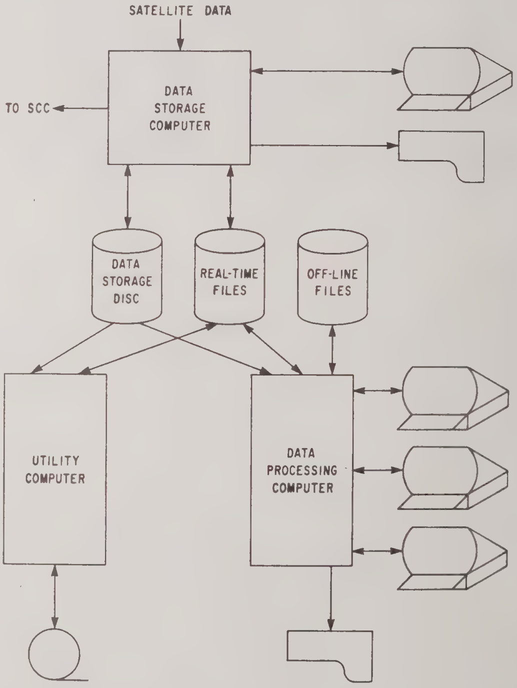
SATELLITE DATA
TO SCC
DATA STORAGE COMPUTER
DATA STORAGE DISC
REAL-TIME FILES
OFF-LINE FILES
UTILITY COMPUTER
DATA PROCESSING COMPUTER

Fig. 2 Data Processing System.

Mission Software

The Mission Software System carries out tasks such as weighted least squares estimation of satellite dynamics, ephemeris generation, eclipse prediction, planning and evaluation of satellite maneuvers, launch window analysis, apogee burn planning, and station acquisition preparation. These off-line tasks are integrated with the real-time function of the Kalman filter to support the analysts in all mission activities.

The software was designed and implemented in modular form, in order to make efficient use of computer memory partitions.* This technique also permitted the development, modification, and testing of program modules independently of each other. Each component has a specific local function, such as satellite telemetry data retrieval, propagation of satellite states, or computation of satellite maneuvers. An executive program is responsible for reading and decoding the task definition input, choosing the proper module execution sequence, and executing each module in turn. It also checks for module errors, and passes relevant information to each module.

A typical ANIK A stationkeeping maneuver task is executed within four minutes, and consists of the following components:

- summarize the current state;
- produce an 80-day satellite ephemeris by propagating the current state;
- generate an 80-day ephemeris of mean orbital elements;
- compute the maneuver parameters; and
- produce a maneuver message for the SCC in terms of number of thruster pulses and firing time.

The effects of maneuvers are assessed using an ephemeris generation task which typically takes less than three minutes to do the following:

- summarize the current state;
- generate a 45-day satellite ephemeris; and
- print and plot the appropriate ephemeris parameters.

The total CPU time for these two tasks is 2 1/2 minutes. Integration accuracy can be quoted in terms of a position vector error of about 20 meters per 100 days.

Extensive use is made of external mass storage disc files for a permanent data base, intermediate storage of results for inter-module communication, and storage of final task results. The permanent off-line files contain satellite mass properties and jet calibration data, satellite maneuver parameters, and tracking system coordinates. The temporary files contain current estimates of orbit and attitude state vectors, maneuver parameters, satellite ephemerides, and data residuals and partial derivatives for least squares state estimation. Real-time data files are used by the Kalman filter to store estimation results, and to communicate with the off-line system. These include a state file, an event file, and a solar and lunar ephemeris file. Interactive editors are available to initialize, modify, or list both the off-line and real-time data files.

Real-Time Orbit and Attitude Estimator

The extended Kalman filter performs the orbit and attitude determination by predicting the system state, and correcting it to conform to the observed tracking and attitude sensor data.[5,6,7] In addition to corrupting the orbit and attitude covariance matrices with white noise to account for mismodelling, these matrices are augmented to account for expected errors in RCS maneuvers, thruster misalignment, and center of gravity errors. The errors associated with the observations are assumed to be Gaussian with zero mean.

The orbit state contains the inertial position and velocity vectors, a correction to the solar radiation force model, and tracking antenna biases. The attitude state (only for dual-spin satellites) contains the spin axis attitude vector, a correction to the solar radiation torque model, and sensor geometry biases. State files containing current filter status information are stored on the real-time disc area for each satellite.

The interaction of the Kalman filter with the data flow is indicated in Fig. 3. Before being stored on disc, all real-time data is queued for transmission to the Kalman filter. When the operating system senses an entry in the real-time queue, it automatically schedules the Kalman filter. The data storage queue will store four sensor records or all tracking records, until retrieved by the Kalman filter. An internal data queue also stores up to 15 records if the filter is occupied. The program averages the incoming data pulse, propagates the approximate satellite state and covariance matrix, and computes the expected data values. If the observation residual is greater than four times the square root of the predicted variance error, the data is rejected; otherwise, the observation is filtered, and the state and covariance updated. The state is automatically stored on disc every second day for up to six weeks.

---

*Originally 12K words, partition sizes have been increased to 21K words.

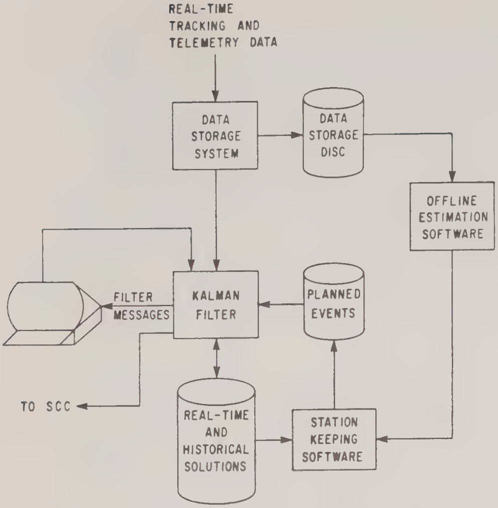

Fig. 3 Mission Software System.

Normally, analysts do not intervene in the operation of the filter. Maneuvers are entered in the Kalman filter event file by the off-line stationkeeping software; at the event time, the Kalman filter updates the state and covariance to reflect the expected maneuver performance. Computer Centre operators perform all routine housekeeping functions, such as execution control and report printing, using an interrupt command system. The set of interrupts consists of:

- include or exclude a particular satellite from the filter process;
- close current print spool file, and open a new one (each satellite has its own);
- search event file for newly inserted event;
- set trace mode on or off;
- display current state on the analyst's terminal; and
- display data rejection summary on the analyst's terminal.

Information is sent to four remote locations:

- Print spool file—all interrupt commands and events; state file summaries at the start and end of the spool file, after each tracking pulse, before and after each maneuver, and at specified regular intervals; data filtering summaries; error messages.
- Analysis Centre terminal—responses to interrupt commands; filter activity summary in trace mode; tracking data filter summaries; error messages.
- Computer Centre console—print spool file information; replies from data control program; error messages.
- SCC terminal—tracking data quality messages.

The Kalman filter is the primary method of state estimation used for stationkeeping purposes. In order to provide a method of reprocessing historical data and testing new software, a program is available to retrieve data for one satellite at a time from the Data Storage System for non-real-time estimation by the Kalman filter. In addition, the current filter solution may be verified by examining automatically produced observation residuals for up to 14 days of historical data (Fig. 4), and for three days of attitude sensor data. This procedure also predicts longitude, inclination, and orbit normal deviation of the attitude for the previous week and the next four weeks.

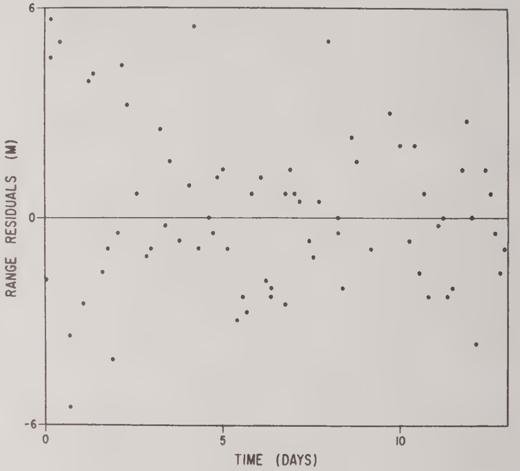

Fig. 4 ANIK A1 range residuals.

Results

The Telesat Kalman filter became operational in April 1977. Since this installation, all stationkeeping constraints for the ANIK A satellites have been met. In addition, the filter has permitted accurate stationkeeping of ANIK B, even before the satellite RCS system had been fully categorized (such as during North/South maneuvers[8] when plume impingement on the North solar array panel contributes a significant and, as yet, unpredictable inplane velocity). Figures 5 and 6 show the longitude cycles for a period of six months for ANIK A3 and ANIK B.

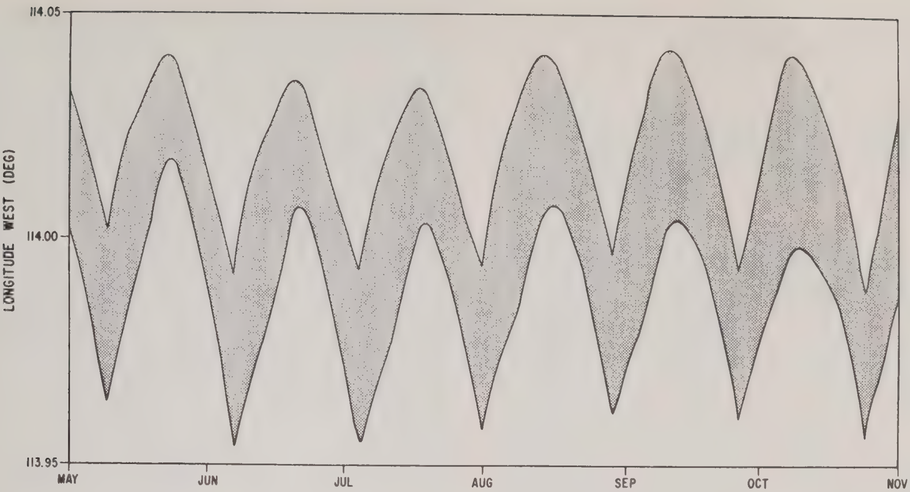

Fig. 5 ANIK A3 longitude history (1979).

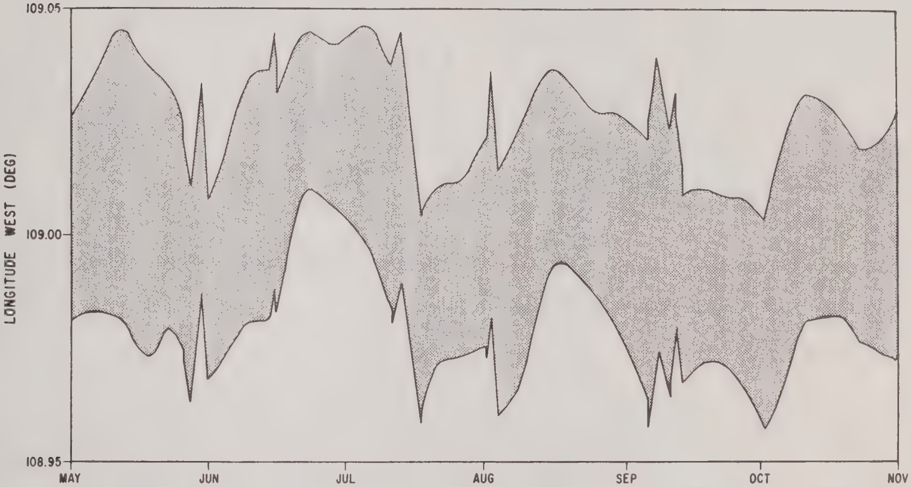

Fig. 6 ANIK B longitude history (1979).

Historical residual comparisons during the two years of operation consistently show that the latest solution always agrees with the observations for periods up to two weeks. As a result, no filter restarts have been required over this period. The main reasons for this stability are:

- the estimated states include stochastic parameters such as solar radiation force and torque corrections to built-in models, tracking azimuth and elevation biases and attitude sensor biases;
- the introduction of small corruptions of the covariance matrix during propagation to account for modelling errors; and
- the corruption of the covariance matrix to account for random maneuver parameter errors.

Because range biases tend to drift, the biases for the two-station ranging system of ANIK B must be periodically re-estimated (every four months) via weighted least squares. The Kalman filter adjusts its internal values for these biases from entries in the event file. The state file editor may be used to adjust antenna and attitude sensor biases for changes which are too sudden to be tracked by the filter. Table 2 presents the steady-state errors obtained by the Kalman filter system.

Table 2 Steady-state errors (3σ)

	Tracking system	
	One station	Two stations
Semi-major axis (m)	6.	4.
Eccentricity	0.000002	0.0000004
Inclination (deg)	0.0009	0.0003
Longitude (deg)	0.0002	0.00009
Drift rate (deg/day)	0.00009	0.00006
Attitude cone angle (deg)	0.006	0.006

Since the filter's states include radiation force and torque corrections to built-in models, its solutions can be used to improve the models while simultaneously helping to provide accurate orbit and attitude solutions. Conversely, weighted least squares estimation of the solar radiation torque is impractical since very long data arcs are required for accurate solutions, during which the torque value is not constant. On the other hand, the Kalman filter follows this parameter stochastically at each attitude observation. Figure 7 displays the results of the solar radiation torque for ANIK A3 over a period of two years.

As indicated previously, the filter is able to process both orbit and attitude maneuvers. By examining the output from the filter, the performance of a maneuver may be obtained within a few hours, compared to several days using weighted least squares. Since the filter provides early warning of abnormal maneuver performance, investigative or corrective action can be taken immediately. Figure 8 demonstrates the performance of the filter after a series of ANIK B stationkeeping maneuvers. Note that, because of the unknown drift rate after the North/South maneuver due to plume impingement, a relatively large 1σ drift error of 0.003° per day is assumed by the filter. However, even with this significant error, the Kalman filter converged to a steady state within 15 hours. Because of this rapid convergence, action can be taken to prevent unsatisfactory maneuvers from causing violations of stationkeeping limits.

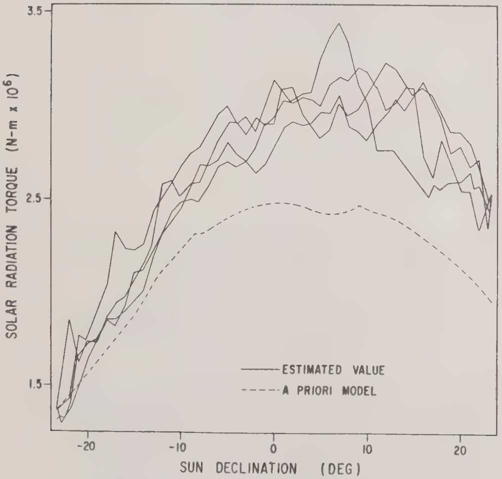

Fig. 7 ANIK A3 solar radiation torque measurements.

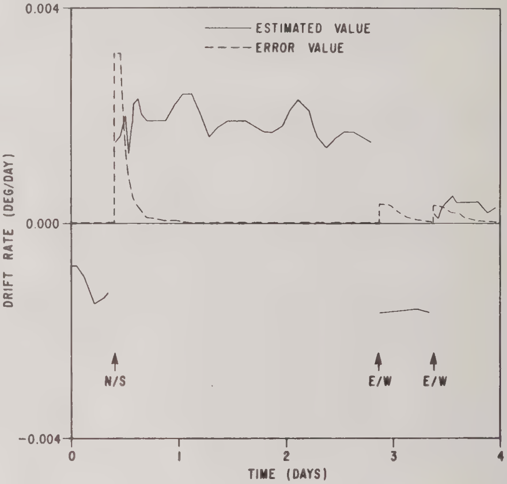

Fig. 8 ANIK B drift rate.

Since the Kalman filter automatically reports excessive ranging errors to the SCC, the satellite controllers can repeat the ranging process. This feature has significantly improved overall data quality.

The ability of reprocessing historical data in non-real time by the Kalman filter has provided an excellent backup to the real-time system. The backup system is required in case of:

- computer failure;
- human error (i.e., not informing the real-time filter of a maneuver);
- last-minute cancellation of a planned maneuver;
- bias changes; and
- abnormal maneuver performance.

In addition, the backup system may be used to test new versions of the Kalman filter program.

The stationkeeping operation of four satellites has been made routine and elegant because of the Kalman filter system. At the beginning of each work week, automatically produced data residuals and ephemeris predictions, based on current filter solutions, are available for study by the time analysts arrive. The states are entered in the logbook, the previous week's maneuvers are calibrated, and the current week's maneuvers are planned. Then, the Kalman filter is informed of the proposed maneuver. Typically, all maneuvers can be planned on the first working day of the week. During the week, for a few minutes each day, the printed output from the Kalman filter is analyzed to check on the filter's performance. If, for some reason (e.g., the sun shining in the earth sensor field-of-view) bad data is collected, corrective action can be taken immediately.

Conclusions

Aside from the long-term economic advantages of using minicomputers for mission applications, in-house computers provide extremely fast turnaround, easy access to the real-time data base, and greater influence over modifications to the computer system. The current generation of minicomputers offers powerful operating systems, virtually unlimited resources, and a large number of instructions, including vector operations; in-house minicomputers are highly competitive with traditional large-scale scientific machines.

The use of a real-time Kalman filter for state estimation is far superior to classical weighted least squares, although least squares methods should be available to support the filter. As well as the technical advantages mentioned earlier, the low-key nature of real-time estimation significantly reduces the manpower required for stationkeeping operations, and it is not affected by additional satellites; more time is available for software development and maintenance, and for maneuver planning.

The integrated modular design of the overall mission software system (including transfer orbit software) has improved maintainability and efficiency. Carefully designed input formats and parameter defaults of batch and interactive programs have largely eliminated jobs wasted due to input errors—a common occurrence with the original UNIVAC software.

In conclusion, the overall attractiveness of the in-house concept in general, real-time estimation in particular, and the lower operating costs, far outweigh the development cost of such a system.

References

[1] Kowalik, H., "Telesat Satellite Control System," Progress in Astronautics and Aeronautics, Vol. 42 (Communication Satellite Developments: Technology), edited by W.G. Schmidt and G.E. LaVean, Cambridge, Mass.: The MIT Press, 1976, p. 183.

[2] Domb, U., Grisé, A.J., and Kes, F.C., "The Orbit Determination System of Telesat Canada," The Journal of Astronautical Sciences, Vol. XXIII, No. 3, July-September 1975.

[3] Lagowski, R.G., "Attitude Determination for the ANIK Satellites," Canadian Aeronautics and Space Journal, Vol. 23, No. 2, March/April 1977.

[4] Wright, W.H., and Anzel, B.M., "Telesat Stationkeeping Methods and Performance," AIAA 5th Communications Satellite Systems Conference, Los Angeles, April 1974, AIAA Paper No. 74-452.

[5] Kalman, R.E., "On a New Approach to Filtering and Prediction Problems," Paper No. 59-IRD-11, The American Society of Mechanical Engineers, New York, N.Y., February 24, 1959.

[6] Rogers, C.E., "The Extended Kalman Filter Applied to the Determination of the Orbital Parameters of a Passive Earth Satellite," Paper No. AD-730 158, Air Force Institute of Technology, Wright-Patterson Air Force Base, Ohio, June 1971.

[7] Sage, A.D., and Melsa, J.L., "Estimation Theory With Applications to Communications and Control," McGraw-Hill Book Company, New York, N.Y., 1971.

[8] Cenker, R.J., "Pulsed Modulation of Orbit Adjust Thrusting to Simultaneously Control Roll and Yaw Attitude," AIAA Mechanics and Control of Flight Conference, Anaheim, Calif., August 1974, Paper No. 74-924.

80-0574

THREE-AXIS ATTITUDE CONTROL ACQUISITION RESULTS AND REGULAR OPERATIONAL STATUS OF BSE

Sachio SHIMOSEKO, Katsuyoshi ARAI and Hiroshi MATSUMOTO

National Space Development Agency of Japan
Hamamatsu-cho, Minato-ku, Tokyo 105, Japan

Abstract

The Japanese Medium-scale Broadcasting Satellite for Experimental Purpose (BSE) was planned by the Ministry of Posts and Telecommunications (MOPT) and developed by the National Space Development Agency of Japan (NASDA) since 1974. The BSE is the tiny step for future operational broadcasting satellite.

The BSE was successfully launched on April 8, 1978 JST and the attitude control mode transition was performed perfectly from spin to three-axis attitude control stabilization.

NASDA is responsible for the satellite housekeeping operations, and the Radio Research Laboratories (RRL) of MOPT and Japan Broadcasting Corporation (NHK) are responsible for experiments utilizing the BSE.

This paper will mainly explain the results of three-axis attitude control acquisition, regular operations and spacecraft status.

Introduction

The Japanese Medium-scale Broadcasting Satellite for Experimental Purpose (BSE) has two main features as follows,

[1] Three-axis zero momentum attitude control.
[2] Two sets of 14/12 GHz transponders with a shaped beam parabolic antenna for experimental TV broadcasting.

The BSE was successfully launched into the transfer orbit from the United States Eastern Test Range (ETR) using the Delta 2914 launch vehicle on April 8, 1978 (JST). It was named YURI (Lily) after being launched.

After several precession maneuvers in the transfer orbit, the Apogee Kick Motor (AKM) was fired at third apogee (nominal point) and the satellite was injected into the drift orbit.

In the drift orbit, attitude control mode transition from spin stabilized to three-axis zero momentum attitude control was performed and BSE was placed into a nominal geostationary orbit above the equator at 110 degrees East longitude on April 26, 1978.

The initial operation and check-out of the bus and the mission equipments of BSE was performed for three months by NASDA. The result of the check-out was satisfactory for all equipments of BSE.

On July 20, 1978 RRL and NHK started various kinds of experiments using the satellite. It has now been about two years since BSE launch, and the on-board equipments have accomplished their purpose during that period.

This paper mainly describes the results of BSE three-axis attitude acquisition in detail and those of the regular operation about one year after launch.

Fig.1 BSE Sequence of Events
— AMF to Three-axis Acquisition

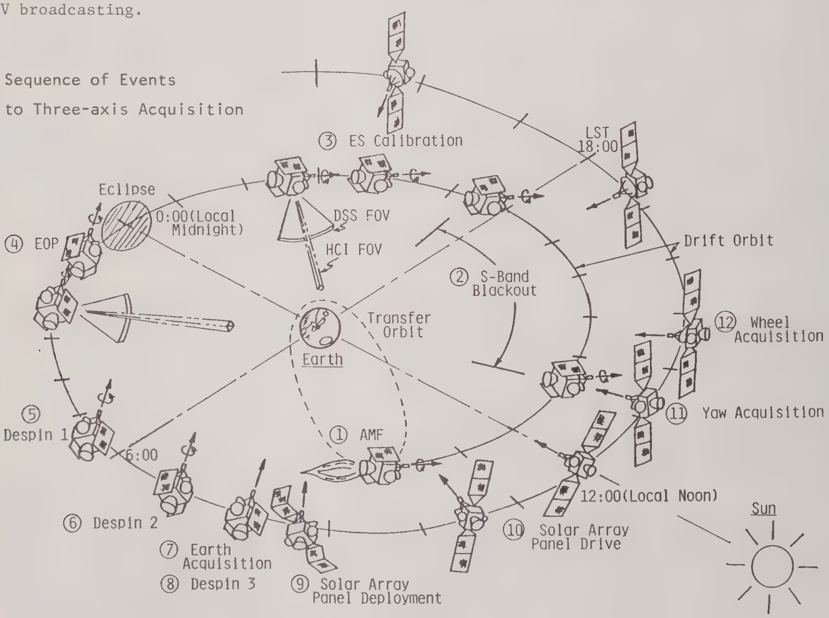

Copyright © American Institute of Aeronautics and
Astronautics, Inc., 1980. All rights reserved.

Summary of Launch-to-Orbit Operations

The BSE was successfully launched from ETR at 7:01 on April 8 (JST)[17:01 on April 7 (EDT)] by No. 140 Delta vehicle. It was injected into the transfer orbit of 35,844.4 Km apogee, 167.0 Km perigee, 27.28 deg. inclination and 631.6 minutes orbit periods at 7:25 am on April 8 (JST). The spin rate of BSE was 61.22 rpm.

On the transfer orbit, after attitude precession maneuvers were carried out four times to get the Apogee Motor Fire (AMF) attitude (net precession angle 134.69 degrees), the apogee motor was fired at near 140.1 degrees East longitude over the equator near third apogee at 9:33 on April 9 (JST). Then BSE was injected to the drift orbit of 35,660.8 Km apogee, 35,115.5 Km perigee, 0.1 degree inclination, 1,415.8 minutes orbit periods and 5.1 deg./rev. eastward drift rate. These parameters were very close to the scheduled orbit.

On the drift orbit, three-axis attitude was established at 13:40 on April 10 (JST) as shown in Fig. 1.

After three-axis attitude acquisition, orbit positioning control was performed nine times. Then BSE was placed into the scheduled geostationary orbit (110 degrees East longitude over the equator) at 20:22 on April 26 (JST).

Results of Three-axis Attitude Control Acquisition

Mode transition sequence of events from spin-stabilized to three-axis attitude control are shown in Fig. 1.

Detail of the events and their results will be explained in the following paragraphs.

(1) Apogee Motor Fire (AMF)

On April 9, the apogee motor was fired at third apogee. The following facts indicated the successful firing ; AKM case temperature rise, doppler frequency change (see Fig. 2), the amplitude variation of Digital Sun Sensor (DSS) output signals (see Fig. 3). The velocity increment of about 1.8 Km/sec was calculated from the orbit elements of pre- and post-AMF. Spacecraft nutation angle produced by AMF was about 2.0 degrees (max.) and its decay time was about 20 minutes (see Fig. 3).

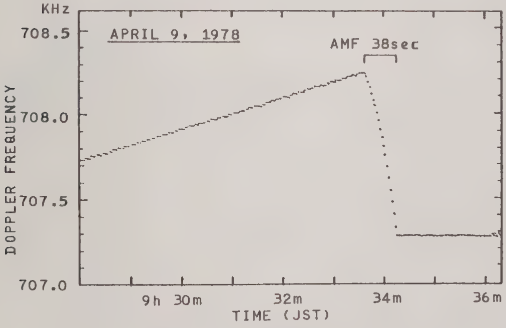

Fig.2 Doppler Frequency Shift at AMF
(Okinawa Station)

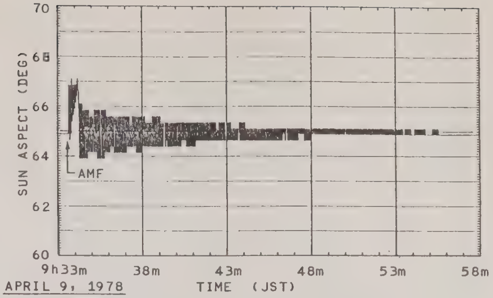

Fig.3 DSS Aspect Angle Output at AMF

(2) S-Band TT&C Blackout

BSE S-band TT&C antenna has not a perfect omnidirectional pattern and hid behind the spacecraft body away from the earth due to the spacecraft attitude after AMF. The ground station could not contact the spacecraft for 4 hours, which was called the S-band TT&C blackout. The estimated downlink level and actual data taken at the Okinawa tracking and data acquisition station are shown in Fig. 4. The obtained data are just on the estimated line.

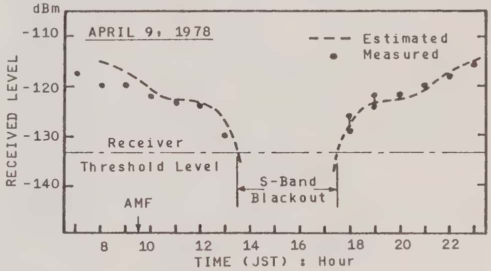

Fig.4 S-band Received AGC Level at Okinawa
Station (near Blackout)

(3) Earth Sensor Calibration

After the S-band TT&C blackout, the static infrared Earth Sensor (ES) pointed to the universe in which there were no objects producing infrared radiation. In this condition, pitch and roll bias between ES and Attitude Control Electronics (ACE) were evaluated. The measured bias values are 0.0 deg. for pitch, + 0.07 deg. for roll.

The attitude data for the Earth Orient Precession (EOP) maneuver was collected through DSS's and Horizon Crossing Indicators (HCI) including the redundant sensors.

(4) Earth Orient Precession (EOP)

Passing through the first eclipse in the drift orbit, an EOP maneuver of about 67 degrees was conducted so as to orient the spin axis (+ yaw axis) to the center of the earth at 8:10 Local Sun Time (LST). This EOP was so perfect that an additional vernier maneuver was not needed.

(5) Despin 1

Despin is the first step to the three-axis attitude control acquisition. Spin rate reduction is performed by a pair of negative yaw thrusters in continuous firing, of a duration commanded by the ground controller.

Despin 1 is the spin rate reduction from nominal spin rate to 35 rpm. From the sensor telemetry data, the actual spin rate was reduced from 59.41 rpm to 36.76 rpm. However, since the expected performance did not agree with on-line flight data, a additional calibration despin was conducted for ascertaining whether the function of the despin subsystem was correct or not. The calibration despin showed that the ACE worked properly and that the maneuver check sheet had been revised properly.

(6) Despin 2

The sequence of events from Despin 2 to solar array panel deployment had a lot of command operations and go or no go decisions in a short time.

Despin 2 is the second spin rate reduction to make the spacecraft acquire the earth. Sensor data showed the actual spin rate became 1.44 rpm by Despin 2.

Fig. 5 shows the relationship between thruster firing time and measured spin rate. The non-linear region of Despin 2 in Fig. 5 would be caused by the time difference between the telemetry and sensor data output sampling.

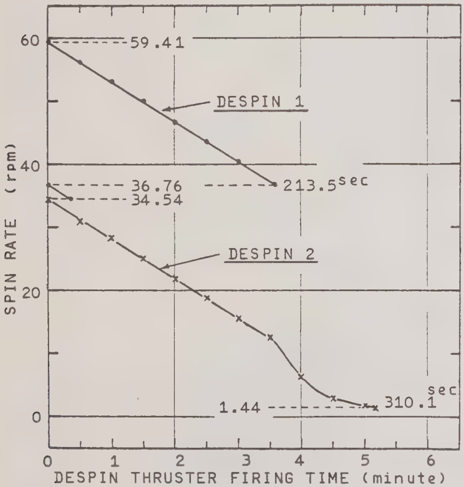

Fig.5 Relation between Despin Thruster Firing Time and Spin Rate Reduction

(7) Earth Acquisition

With the spacecraft turning around at 1.44 rpm about the yaw axis, the earth came into the earth sensor Field of View (FOV) automatically. From the ES information, it was verified that the + yaw axis (spin axis) of the spacecraft oriented almost to the center of the earth having no residual nutation caused by the EOP maneuvers. At this acquisition, the pitch and the roll thrusters were used and the ES was selected as the source of pitch and roll attitude information. Under the spacecraft dynamic condition (spin rate 1.44 rpm), the spacecraft could catch the earth using the pitch and the roll thrusters continually firing by ACE drive signals. In this condition, the yaw axis always oriented to the earth by the thruster control.

Fig. 6 shows the ES detectors configuration and the earth image. Fig. 7 shows the integrated ES pitch and roll attitude error signals during the earth acquisition. It can be seen that roll control is the same as pitch control with rotation around the yaw axis. Fig. 8 shows the ES pitch and roll error at earth acquisition.

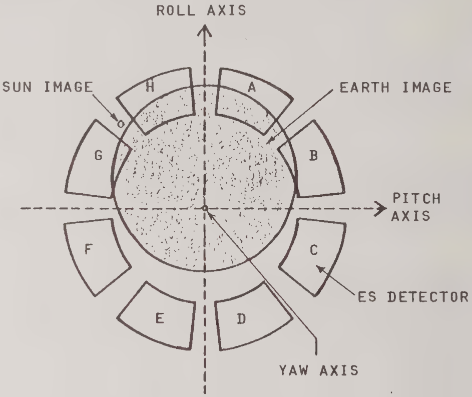

Fig.6 ES Detectors Configuration and Earth Image

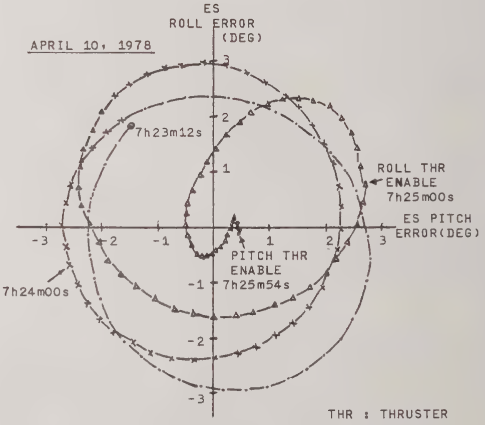

Fig.7 ES Integrated Pitch and Roll Error during Earth Acquisition

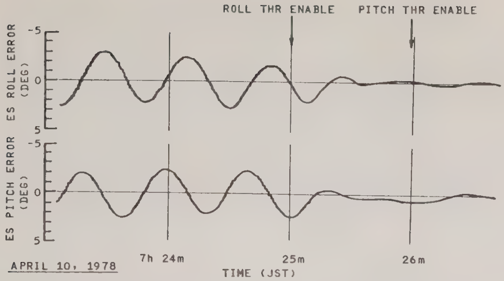

Fig.8 ES Errors during Earth Acquisition

(8) Despin 3

Despin 3 is the final despin, whose target is to make the spin rate 0 rpm. Execution of Despin 3 reduced the spin rate down to 0.5 deg./sec and no tumbling in any axis occurred.

(9) Solar Array Panel Deployment

Solar array panel deployment had to be done within 6 minutes after Despin 3 because of the thermal requirement for the array deployment mechanism. First, the north solar array panel and then the south solar array panel were deployed by firing electro-explosive device. Successful deployment was verified by the following facts;

- ° Yaw Rate Gyro (YRG) output + 0.5 deg./sec → + 0.2 deg./sec,
- ° Temperature rise of solar array panel,
- ° Increased shunt drive voltage.

It was estimated from the YRG output signal that the solar array panels were deployed within 30 seconds. As the deployed solar array generated enough power, required thermal control heaters were enabled (i.e. battery heater, transponder heaters).

Fig. 9 shows ES and YRG data during Despin 3 and Solar Array Panel Deployment. ES roll error suddenly increased over + 5.0 deg. just after solar array panel deployment by tumbling, but proper thruster firing controlled roll attitude within ± 1.0 degree.

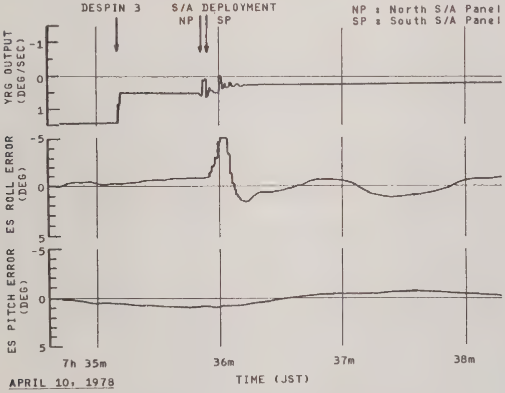

Fig.9 YRG and ES Output Signals during Despin 3 and Solar Array Panel Deployment

(10) Solar Array Panel Drive

Before yaw acquisition, the Sun Sensor Assembly (SSA) was selected for yaw axis control and the solar array panel started to be driven at nominal orbit rate (0.00417 deg./sec).

(11) Yaw Acquisition

The SSA could properly detect yaw axis attitude about a hour after local noon. Before yaw acquisition, the yaw axis had rotated at about + 0.2 deg./sec. Yaw acquisition was performed with the SSA and through yaw thruster firing by ACE control signals. At first the yaw rate was accelerated about 1 deg./sec by the + yaw thruster. When yaw attitude came into the limit cycle, the yaw rate was negatively accelerated and the yaw attitude was kept within the limit cycle by thruster control. After accomplishment of yaw acquisition, the spacecraft attitude was controlled by the thrusters in all axes.

Fig. 10 indicated YRG output and estimated yaw attitude during yaw acquisition.

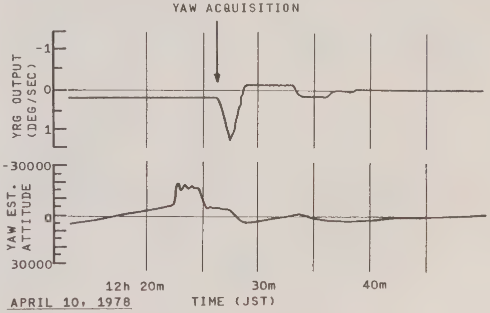

Fig.10 YRG Output and Yaw Attitude during Yaw Acquisition

(12) Wheel Acquisition

After yaw acquisition, three-axis zero momentum attitude control was performed by firing the required thrusters. But it was necessary to change control from the thruster control mode to the nominal reaction wheel control mode. The control range of the ACE had been changed to be so narrow that the momentum could get ± 10 % of wheel momentum capability. Three reaction wheels were enabled and control mode transition from thrusters to wheels was performed.

Results of Regular Operation

This chapter explains results of regular operation for one year since the successful launch. NASDA is responsible for the three-axis attitude control, North-South (N-S) and East-West (E-W) stationkeeping, housekeeping and operation in eclipse during the experimental period of three years. These operations have been successfully carried out so far.

Fig. 11 shows the past event history, failures and anomalies of on-board equipments. These failures and anomalies do not interfere with carrying out mission experiments owing to the redundancy.

Routine operations shown in Fig. 12 are needed in order to keep the beam pointing accuracy of the 12 GHz TV downlink within 0.2 degrees. In addition to the operations in Fig. 12, stationkeeping is periodically required to keep BSE within the orbit positioning requirements (i.e. inclination less than 0.1 deg., 110° ± 0.1°East longitude).

These operations are explained in the following paragraph.

(1) Wheel Unloading

Three reaction wheels which are orthogonally aligned with each of spacecraft axes are driven to eliminate attitude error and to keep system momentum zero. But a reaction wheel cannot keep spacecraft attitude within the required range if its momentum exceeds ± 80 % of wheel capability, so wheel unloading is needed to keep wheel momentum within bounds. Wheel unloading is wheel momentum dumping to less than ± 10 % of wheel capability utilizing thruster firing. The disturbance torque which works on BSE is mainly that of solar pressure. This torque tends to change due to the sun declination change.

The wheel momentum variation near the summer solstice and autumnal equinox are shown in Fig. 13.

It can be seen that pitch momentum is almost periodic, but that roll/yaw momenta grow faster as time passes and that the amplitude of the momentum variation in the summer solstice is larger than that of the autumnal equinox. So momenta of the roll/yaw wheels are unloaded daily in the summer and weekly in the autumn, while pitch unloading is performed every two weeks. In addition to the above unloading, pitch unloading is required to return the pitch momentum to the original momentum after orbit maneuvers because of the narrow control range of the ACE during the maneuver.

(2) Eclipse Operation

Since the solar array does not generate power in eclipse, the BSE configuration is changed to eclipse mode in which 100 W output transponders consuming high power are turned off and only the neccessary minimum equipment is turned on so as to keep the Battery Depth of Discharge (DOD) to less than 60 %. After passing through the eclipse time, the spacecraft is set to its normal configuration by the ground controller. These pre- and post-eclipse operations are carried out every day in eclipse periods.

Two eclipse seasons have been experienced since launch and the Battery DOD was 42 % for autumn equinox and 40 % for vernal equinox.

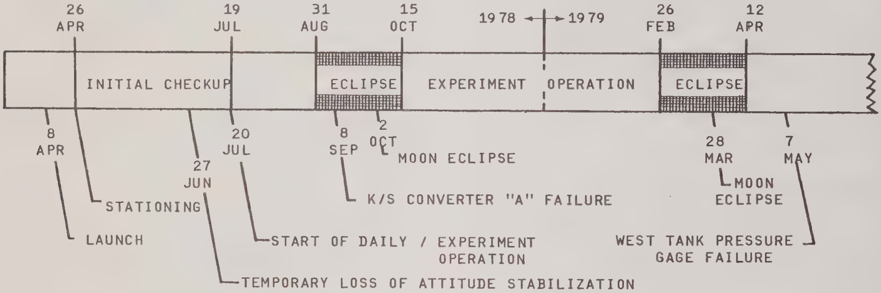
26 APR
19 JUL
31 AUG
15 OCT
1978 ← → 1979
26 FEB
12 APR
INITIAL CHECKUP
ECLIPSE
EXPERIMENT OPERATION
ECLIPSE
8 APR
27 JUN
20 JUL
8 SEP
2 OCT
MOON ECLIPSE
28 MAR
7 MAY
MOON ECLIPSE
STATIONING
K/S CONVERTER "A" FAILURE
LAUNCH
START OF DAILY / EXPERIMENT OPERATION
WEST TANK PRESSURE GAGE FAILURE
TEMPORARY LOSS OF ATTITUDE STABILIZATION

Fig.11 BSE Past Event History

Fig.12 BSE Routine Operations Schedule

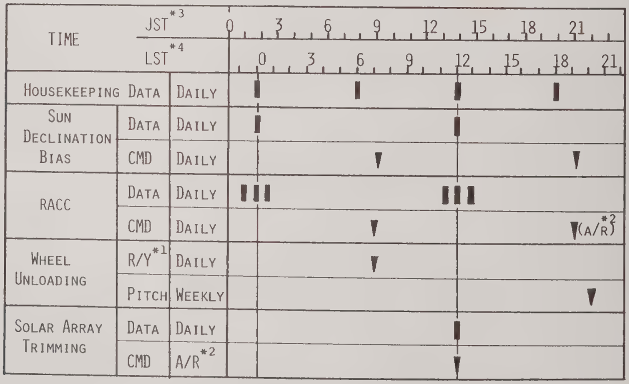

*1 Roll & Yaw
*2 As Required
*3 Japanese Standard Time
*4 Local Sun Time

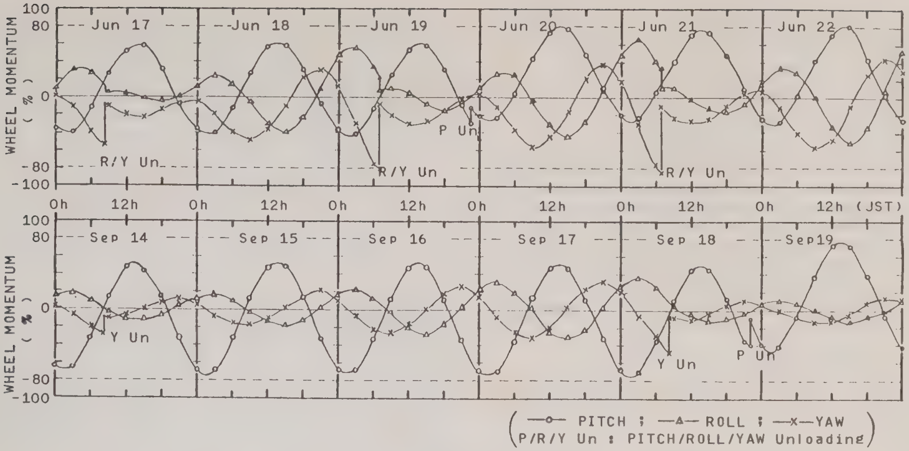

Fig.13 Wheel Momentum Variation in Summer and Autumn

Two times of eclipse due to the moon have also been experienced as shown in Fig. 11. In this case, it was necessary to turn the transponders off and set the spacecraft to the reduced power mode as for an eclipse due to the earth.

(3) Stationkeeping Operation

(a) North-South Stationkeeping (N-S ΔV)

Due to the luni-solar gravity influence, BSE orbit inclination increases as time passes. To satisfy the inclination requirement, N-S ΔV maneuvers are required with yaw pair thrusters in continuous firing for about 20 minutes. The BSE attitude is automatically controlled within the requirement by the attitude control thrusters during ΔV maneuver.

One example of a N-S ΔV maneuver on June 29, 1978 is shown in Fig. 14. It can be seen that all the attitude is kept within a small range and ACE controls perfectly all the axes.

All the N-S ΔV maneuvers have been successfully performed except for a south ΔV on June 27, 1978. At that time, temporary loss of the three-axis stabilization occurred because the roll disturbance torque produced by thruster plume impingement exceeded the thruster control torque. So the spacecraft rotated around the roll axis and lost stabilization. Restabilization was performed, which was almost the same as the sequence of the initial acquisition. The BSE acquire normal three-axis

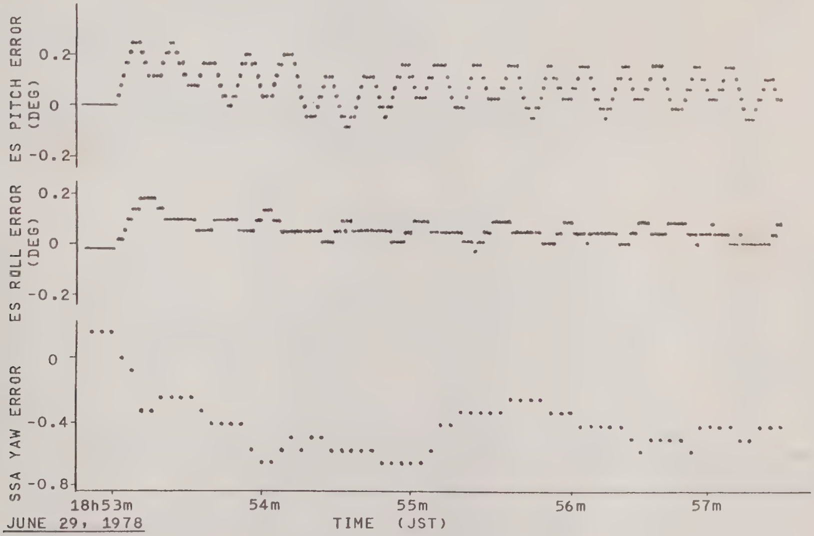

Fig.14 BSE South ΔV Maneuver Attitude Data

stabilization after 14 hours. As the new maneuver procedure, which provides larger control torque, was adopted after reacquisition of the attitude, following N-S ΔV maneuvers have been successfully conducted (see Fig. 14).

(b) East-West Stationkeeping (E-W ΔV)

Due to the two factors, the earth triaxiality and the large area of the solar array panel, E-W ΔV maneuvers are generally more frequent than for other spacecraft. The earth triaxiality makes the spacecraft move westward and the large solar array makes the eccentricity increase. The various kinds of error (i.e. error of control and orbit determination) and control margine have to be considered at maneuver planning. The E-W ΔV cycle pattern is shown in Fig. 15. Thruster firing time is much less than for N-S ΔV maneuvers and their duration is always less than 30 seconds. An additional E-W ΔV maneuver is always required after a N-S ΔV maneuver, because attitude control thruster firing affects not only the attitude but also the orbit.

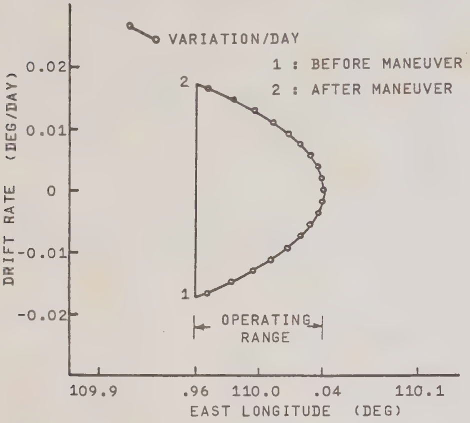

Fig.15 BSE E-W Maneuver Cycle Pattern

Spacecraft Subsystem Status

BSE experiments have been performed by RRL and NHK. They get valuable data from experiments. In this section, subsystem status will be explained.

The temperature of some components exceeded their expected values in summer and winter. But it was verified that their temperatures were less than the qualification temperature range and the components worked properly. In winter, temperatures of components which are located on the south housekeeping panel have a tendancy to exceed the expected values (i.e. battery, monopulse, earth sensor). In summer, the north transponder panel temperature tends to exceed the expected value.

S- and K- band command execution, telemetry data and ranging data acquisition have operated normally.

Broadcasting Satellites have to be controlled to fine attitude accuracy due to the antenna pattern and to obtain good individual reception. The BSE attitude is always stable and is kept within the requirement (12 GHz band beam pointing error < 0.2 deg.). One example of antenna beam pointing error and rotation which was calculated from the telemetry data is shown in Fig. 16. It can be seen that rotation is controlled within 0.2 deg. and pointing error is less than 0.12 deg.. However, pitch error exceeds 0.2 deg. when pitch wheel momentum crosses the zero point. Because wheel momentum which is

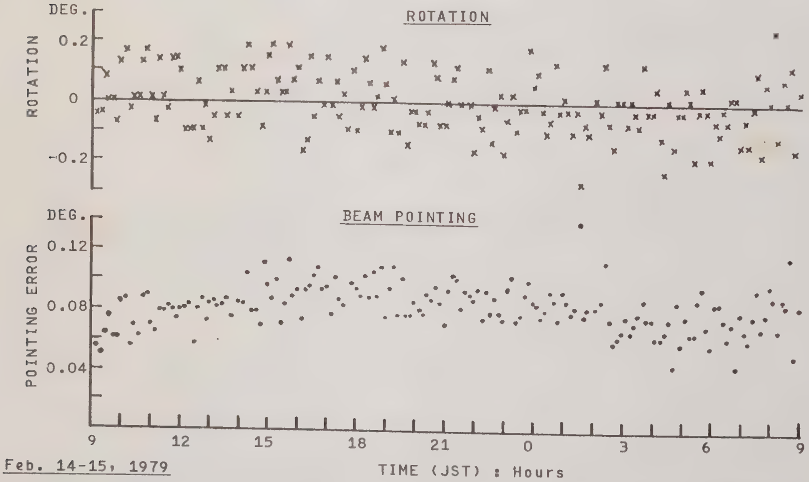

Fig.16 Antenna Beam Rotation and Pointing Error

Sensor Combination

Pitch & Roll : ES

Yaw : MECO (Monopulse & ES Combination)

less than ± 2 % wheel capability is in the uncontrolled region and zero crossing point is the largest solar disturbance torque and moreover the pitch axis is apt to rotate three times as other axis due to the moment of inertia. When the SSA is selected for yaw axis control, Roll Acceleration Control Command (RACC) is used for yaw axis control near local noon and local midnight. But RACC control sometimes exceeds the pointing error limit (0.2 deg.), especially in winter when RACC control is not as good as was expected.

Conclusion

The BSE is the first broadcasting satellite in the world, and also the first three-axis attitude control spacecraft in Japan.

The experiments and the operations of the BSE have been very satisfactory to all concerned. The results of the BSE mission will be reflected in future operational satellite designs.

References

(1) T. Ishida, et al. : "Medium-scale Broadcasting Satellite for Experimental Purpose", 6th AIAA Satellite Communication Systems Conference, Montreal, Canada, April 1976.

(2) Y. Ichikawa : "The Results of Initial Checkup of Japanese Broadcasting Satellite for Experimental Purpose", IEEE Trans., Vol. BC-24, No. 4, Dec. 1978, pp. 74-80.

(3) Y. Ichikawa and K. Arai : "The Japanese Medium-scale Broadcasting Satellite for Experimental Purpose", 11th International Television Symposium, Montreux, Switzerland, May 1979.

(4) N. Imai, et al. : "Experimental Results of the Japanese BSE Program", IAF Paper IAF-79-F-280, Sept. 1979.

(5) T. Ishida, et al. : "Present Situation of Japanese Satellite Broadcasting for Experimental Purpose", IEEE Trans., Vol. BC-25, No. 4, Dec. 1979, pp. 105-112

80-0575

MULTIPLE SATELLITE OPERATIONS AND MANAGEMENT

F.W. Weber
Deputy Director, Space Segment Implementation
Communications Satellite Corporation
Washington, D.C.

Abstract

This paper will discuss INTELSAT in-orbit experience and the operational procedures employed for management of the INTELSAT space segment based on over nine years in-orbit experience with the INTELSAT IV and IVA satellites. The INTELSAT space segment network consists of seven INTELSAT IV and five INTELSAT IVA satellites ranging in age from two to nine years. These satellites have various operational roles such as full time international traffic, leased domestic services and in-orbit spare.

Background

COMSAT has been deeply involved in launch, control and operation of multiple satellite communications systems for over 15 years. The majority of this effort was performed in establishing the global communications network for the International Telecommunications Satellite Organization (INTELSAT) while serving in various roles as Manager, Management Services Contractor, and presently as Technical Services Contractor to INTELSAT. COMSAT has also provided technical support to COMSAT General Corp., a subsidiary of COMSAT, in the implementation and control of the COMSTAR domestic satellite system and the MARISAT global maritime system.

To date COMSAT has launched a total of 33 satellites: 27 satellites for INTELSAT in the INTELSAT I, II, III, IV and IVA series; six satellites for COMSAT General, including three MARISAT and three COMSTAR satellites. Fourteen of the launches were INTELSAT IV and IVA satellites, two of which were lost due to launch vehicle failures and the remainder of which are in operation providing service in the INTELSAT global satellite system. All six of the COMSAT General satellites are still in service. The satellites range in age from two to ten years and have various operational roles. Experience has shown that each series of satellites has its own unique characteristics and imposes special control and operational procedures, while individual satellites in any series may develop anomalies which require special management techniques to achieve the design lifetime.

Introduction

This paper concentrates on the operational philosophy and management of the INTELSAT space segment and in particular, the in-orbit experience with the INTELSAT IV and IVA satellites over the past nine years. The INTELSAT space segment presently consists of seven INTELSAT IV and five IVA satellites ranging in age from two to nine years and serving in various operational roles for full time international traffic, leased domestic services, and in-orbit spares. The INTELSAT network has grown from a single INTELSAT I with a capacity of 240 two-way voice channels or one television channel serving the Atlantic Ocean Region to the present multiple satellite global system of 12 satellites distributed over the three ocean regions with a total global capacity of approximately 58,000 two-way voice channels plus 24 television channels. The INTELSAT IV is capable of carrying 4,000 two-way voice channels plus two TV channels and the INTELSAT IVA has a capacity of more than 6,000 two-way voice channels plus two television channels. Beginning in 1980 when the INTELSAT V will be launched with a capacity of 12,000 two-way voice channels plus two television channels[1], the in-orbit resources will grow to 18 satellites of three different series. Each series of satellites has its own unique characteristics and imposes special monitoring and management requirements on the control network.

Earth Segment

The INTELSAT tracking, telemetry, command and monitoring (TTC&M) network used in the management of the system consists of nine antennas located at eight earth stations around the globe and is directed from the INTELSAT Satellite Control Center in Washington, D.C. The TT&C facilities are located at:

Facility	Antennas	Visibility
Andover, Maine	1	AOR
Paumalu, Hawaii	1	POR
Fucino, Italy	2	AOR/IOR
Pleumeur Bodou, France	1	AOR/IOR
Tangua, Brazil	1	AOR
Yamaguchi, Japan	1	POR/IOR
Carnarvon, Australia	1	POR/IOR
Zamengoe, Africa	1	AOR/IOR

Copyright © American Institute of Aeronautics and Astronautics, Inc., 1980. All rights reserved.

All the TT&C facilities are collocated with communications earth stations and are full performance antennas with a G/T of 32.5 capable of supporting transfer and synchronous orbit operations. Two of the antennas are high performance 30 meter antennas with a G/T>41.0 and are also used for in-orbit performance verification testing of newly launched satellites to insure that they survived the launch and transfer orbit environment without degradation.

Space Segment

The INTELSAT satellite complement consists of seven INTELSAT IV's which were launched during the period January 1971 through May 1975 and five INTELSAT IVA's launched during the period September 1975 through March 1978. The satellites were launched on an Atlas-Centaur vehicle and weighed approximately 1400 kg at launch and more than 700 kg after apogee motor fire. The satellites are dual spinners with the solar array, apogee motor, batteries, stationkeeping and other ancillary functions contained in the spinning portion of the spacecraft. The communications equipment (antennas, wideband receivers and channelized transponders) is mounted on the platform comprising the despun section. The attitude determination and despin control system consists of the despin motor, a despin control electronics, three earth sensors and two sun sensors. Despin control can be referenced from any of the three earth sensors (one each screening the northern hemisphere, the equator, and the southern hemisphere) or by the sun sensor corrected for apparent motion by a time-of-day clock. An additional despin mode is available where the despin timing pulses are transmitted from the ground.[2]

The INTELSAT IV consists of 12 active transponders (plus redundancy), horn antennas for earth coverage and two parabolic antennas for 4½° spot beams with mechanical steering of the reflector so that one satellite design can be reconfigured in orbit to serve any of the three ocean areas. On-board switches allow certain transponders to be placed in either spot or global beam coverage mode. The seven year end-of-life power available from the solar array is approximately 450 watts at solstice and the redundant power systems include nickel cadmium batteries with a measured capacity of about 20 amp hours for eclipse operation.

The greatest difference between the INTELSAT IV and IVA series is in the communications equipment.[3] While the total spacecraft weight has remained nearly constant, the circuit capacity was increased one and one-half times by exploiting advanced technology to reduce the weight of many components. Twenty 36 MHz transponders (and redundancy elements) are available on each spacecraft. Beam separation (spatial frequency reuse) and polarization diversity permit 16 transponders to occupy the spectrum of eight. The total spectrum provided by one INTELSAT IVA satellite is about 800 MHz. The antenna mast supports global horns for the four earth coverage transponders and one 900 cm square reflector for reception and two 1300 cm square reflectors for transmission. More than 100 feeds are used with these three reflectors to produce sophisticated shaped beams. The power system on the INTELSAT IVA was improved to provide an end-of-life power of 525 watts and the battery size was increased to a measured capacity of more than 26 amp hours to handle the increased current load without increasing the depth of discharge.

Control and Operations Philosophy

Control of the satellites and management of communications subsystem are the key elements in the ability of the system to achieve the mission goal and minimize interruptions in service. Effectiveness of the satellite control procedures directly reflects on the quality and availability of communications services. Since these satellites provide commercial communications services, maintaining a high quality and insuring continuity of service is essential. These goals led to the development and evolution of the INTELSAT control and operations philosophy. Early recognition of performance trends with appropriate adjustments to the operations plan and quick response of the control network is essential in maximizing the quality and continuity of service. Accordingly, the INTELSAT operation philosophy requires continuous full-time monitoring of each satellite throughout its lifetime. At separation from the Centaur launch vehicle when the spacecraft is first powered up, the INTELSAT Control Center in Washington, D.C., assumes control of the satellite and, using the global TTC&M network, guides the satellite through the transfer orbit to the final on-station emplacement. From separation from the launch vehicle throughout the operational life of the satellite, all telemetry information is routed to the Control Center and all command instructions originate and are directed from the Control Center. The control network continuously monitors the health of each satellite, measures the orbital parameters, and provides a means of controlling the various subsystems on board the spacecraft. Each satellite is under the constant surveillance of either a dedicated TT&C antenna or communications antenna. From launch until retirement of the satellite, every word of every frame of telemetry data is continuously monitored, limit checked and representative samples are stored for historical purposes. The telemetry provides a continuous and real time measure of the satellite's configuration, health, and orbital attitude. Each parameter (temperature, voltage currents and attitude data) is limit checked against the expected value and if an out-of-limits condition is detected, an alarm is sounded in the Spacecraft Control Center in Washington, D.C., requiring operator action to assess the situation and initiate corrective action if appropriate. The alarm indicates to the operator what parameter is out of limits, what it read prior to going out of limits, the present value, and how long it has been out of limits. The alarm is repeated until acknowledged by the operator.

Every aspect of satellite control incorporates redundancy. A satellite is always within view of at least two TT&C antennas and, to insure that no data goes unchecked in the event of a line interruption to the Control Center or equipment failure in the Control Center, responsibility for a particular satellite or pair of satellites is assigned to each of the nine TT&C earth stations. In parallel with transmission of the data to Washington, earth station computer equipment processes the telemetry data and performs the same limit checks and recording of data as performed at the Control Center. In addition to the real time processing of the data, every word of every frame on each telemetry beacon from each satellite is recorded for future use. All of this data is always available for the previous ten days while earlier historical data is available in a sampled fashion at one frame every seven minutes for the past 60 days, and one frame every hour from launch until retirement of the satellite. The performance of each subsystem is continuously assessed to recognize performance trends such that operation plans can be adjusted or workarounds developed to change the communications carrier parameters, satellite gain or other operating parameters to compensate for changes in performance or operational difficulties encountered with the satellite.

Spare or contingency satellites must be treated exactly the same as operational satellites such that they are ready to instantly restore service as required. If a satellite emergency, system failure, or system interruption occurs that cannot be resolved in a short time, earth station antennas are pointed over to a spare satellite for restoral service. The configuration and operating parameters of the spare satellite must be continually adjusted to exactly duplicate the performance characteristics of the in-service satellite. A spare or contingency satellite requires the same level of surveillance and represents the same workload to the control network as the in-service satellite.

Communications System Monitoring

Quality of communications service is directly dependent upon maintaining discipline in the system, proper communications subsystem configuration, insuring proper earth pointing of the antennas, and maintaining the satellite orbital attitude and position. Discipline is maintained in the communications system by monitoring the RF carriers to insure that all transmission parameters are within acceptable limits, thus precluding interference with other communications carriers on the same satellite. An operations center is in contact with every earth station and directs each station in the adjustment of uplink carriers as required to maintain acceptable quality in all circuits. This operations center can receive on request in real time measurements of any or all communications parameters to investigate interference problems and correct them as quickly as possible. Communications carrier parameter measurements are performed by a network of eleven sets of custom designed communications system monitoring equipment located at the TTC&M stations and selected communications earth stations. The data on all carriers on all satellites is transmitted to data processing equipment in the Operations Center in Washington to provide real time data to maintain the required discipline in the global communications network.

In-Orbit Experience

Interaction with the Orbital Environment. Continuous monitoring and instant response capability of the control network is further necessitated to respond to in-orbit anomalies or satellite emergencies. The mass properties of the spin stabilized INTELSAT IV and IVA satellites are such that the stability margin is relatively small. Two passive nutation dampers based on the pendulous single axis eddy current design are located high on the antenna mast to provide nutation damping and insure the stability of the satellite. However, due to the dynamics, particularly in the case of the INTELSAT IVA, the damper is narrowly tuned and insures stability only if proper despin is maintained. As a result, in the event of despin control system malfunction or anomaly, the satellite can become unstable within a short time leading to catastrophic loss of the satellite or consumption of an excessive amount of fuel which would reduce the satellite's useful lifetime. On several occasions INTELSAT satellites have suffered a loss of despin control which on at least one occasion nearly resulted in a satellite going into a flat spin. These problems have not been due to equipment failures but rather due to interaction of the satellite with its orbital environment resulting in anomalous performance. This phenomenon has been experienced or evidenced on nearly all geosynchronous satellites and results when solar activity changes the local environment by distoring the earth's magnetosphere at synchronous orbit altitudes. Such disburbances are described as magnetospheric substorms. During enhanced levels of substorm activity a distortion of the magnetosphere through synchronous altitude results in an influx of high energy electrons which can differentially charge the satellite. Photo emission from the sun lit portions of the satellite bleed off this charge while it accumulates on the darkened portions of the satellite. When the charge (potential difference) is high enough, arcing can result affecting thermal surfaces or changing the state of spacecraft digital equipment.[4] In the INTELSAT IV the despin control electronics is the unit most susceptible to these transients. On numerous occasions in orbit and verified by ground test simulating charging of the spacecraft, the energy discharge or arcing resulted in a change of state of a flip-flop in the digital despin control electronics leading to disruption in the despin system causing communications outages. This problem was first encountered on the INTELSAT III series and, when experienced in the early days of INTELSAT IV, emergency procedures were developed to assure the safety of the satellite and maintain a positive stability margin in the event of a despin subsystem disruption. Since all the elements of the despin system (control electronics, reference sensor and motor drive) are initially suspect in the event of a loss of despin, control is switched to a complete set of redundant units. The execution of these emergency procedures in response to out-of-limits alarms has resulted in limiting interruptions in service to between five and ten minutes. To insure a minimum response time, an alert system has been established. A teletype in the Control Center receives real time data from magnetometer stations located at high latitudes. These stations detect variations in the earth's magnetic field indicative of enhanced magnetospheric substorm activity. Experience has shown that when disturbances reach a threshold level at selected magnetometer sites (e.g., K indices of five and six at Goosebay and Loring), satellite anomalies may occur. Accordingly, when the threshold levels are reached, the Control Center and earth stations go on an "alert" status and are ready to respond to an anomaly should it occur.

Various satellites respond differently to these effects with anomalous performance in different subsystems while some satellites do not appear to respond at all. All of the INTELSAT IV series have evidenced degradation in the optical solar radiators (OSR) on the sun shield. The data shows that while the absorption coefficient, alpha, is predicted to change from 0.08 to 0.085 over the seven-year lifetime, the value of 0.17 was measured after only about four years and increases to 0.21 after seven years. This degradation is believed to be due to crazing of the OSR quartz surface and depletion of the aluminized reflective surface due to arcing. The thermal margin on the spacecraft is such that this has caused no problem even after nine years. Later INTELSAT IV spacecraft and all INTELSAT IVA spacecraft were modified to desensitize some electronic circuits and to ground all floating conductors and thermal blankets to minimize the susceptibility to differential charging and arcing.

Communications Receiver Problems. Other problems encountered with the INTELSAT IV and IVA series involved the communications and power systems. Communications system monitoring equipment (CSM) provides data for subsystem performance evaluation and permits early recognition of performance trends. Based on this data, satellite operating parameters are adjusted and/or the operational plans are revised to compensate for changes in performance. The primary data used for the subsystem performance evaluation is transponder gain (including receiver gain) and output TWT e.i.r.p. Prior to launch it was recognized that the resistive bias network for the tunnel diode amplifier in the front end of the receiver absorbed moisture and during the drying-out process in the early months in orbit would exhibit a decrease in gain on the order of 3 dB. The CSM data did indeed show that during the initial six weeks to three months operation, gain on the various receivers decreased 1½-3 dB as predicted. However, after several more months operation a further decrease in transponder gain was noted. The gain would begin decreasing at a rate of 1 dB per month for several months and then the rate increased to about 3 dB per month until the transponder gain no longer met specification and it was necessary to switch on a redundant unit to maintain satisfactory performance. Special tests were conducted which showed that the decrease in gain was in the receiver and further identified the driver TWT as the cause of the problem. The driver TWT was of an advanced design to provide a low noise figure and incorporated two types of processes for fabrication of the cathode and application of the oxide coating.

Operational experience coupled with special ground tests showed that the receivers were suffering from a generic problem with all receivers exhibiting similar gain degradation characteristics, although there were different time constants associated with the two types of driver TWT cathodes. While the design parameters of the TWT were all within the accepted range of design values, and no single one should have resulted in the observed performance, the particular combination, aggravated by operation at the high end of the normal range of cathode temperatures, resulted in a decrease in lifetime for the TWT design. The two types of receivers exhibited average useful lifetimes of about 12 and 22 months. This receiver problem complicated operations since periodically the transponder gain had to be adjusted to optimize traffic as the receiver gain decreased. In addition, operational planning in the deployment of satellites had to take into consideration remaining useful receiver lifetime so that the satellites could be assigned and reassigned operational roles which would allow for turning off receivers in the contingency satellites to extend the usable lifetime of the satellite. In this manner, coupled with a receiver redundancy level of four for one, it was possible to utilize the satellites such that all the INTELSAT IV's could achieve the design life of seven years with usable receivers still available. In this case, early recognition of the performance trends allowed development of a work-around plan to insure the availability of the required number of satellites with sufficient communications capacity in accordance with the operation plans throughout the designated satellite lifetime dictated by the operational traffic plans.

Power Subsystems-Batteries. In the latter years of the INTELSAT IV lifetime, similar operational constraints were imposed by the performance exhibited by the batteries which power the satellites during eclipse. Experience in orbit with various satellite series has shown power system management to be evolutionary requiring continual adjustment in response to observed performance. The INTELSAT IV batteries were no exception with the charge/discharge ratio, reconditioning procedures, post eclipse charging procedures requiring close and continual monitoring and frequent adjustment to optimize battery end-of-discharge voltage performance. Performance during the 10th and 11th eclipse season was marginal under full load and indicated that the battery would be incapable of supporting a full load with acceptable end-of-discharge voltage during the 12th and subsequent eclipse seasons. As a result of this and the receiver constraints, the older INTELSAT IV satellites were deployed as contingency satellites and the output TWT's turned off during eclipse season to reduce the load and extend the cycle life of the batteries. The last two INTELSAT IV's launched contained the high capacity INTELSAT IVA type battery (26 amp hours vs. 20 amp hours) greatly reducing the depth of discharge and exhibited the expected improved voltage performance.

Output TWT Failure. Adjustment of the power loads to increase the cycle life on the batteries contributed to the only other operational problem encountered with the INTELSAT IV series satellites. While the majority of output TWT's exhibited a graceful slow degradation, significant changes were noted after TWT's were turned off during eclipse season. Of the more than 40 TWT's stored in the "off" condition for several months after several years (something more than 25,000 hours) of operation, approximately 40% failed shortly after turn-on. Prior to turn-off, input current and gain were found to be essentially normal. After "turn-on", input current and gain were again found to be normal but quickly degraded leading to failure of the tube over approximately a four-week period. (Failure of a tube is defined as loss of 6 dB in gain or 2 dB in e.i.r.p.) With a 2:1 redundancy scheme, failure of the output TWT's did not impact communications capacity although operational plans had to be adjusted to minimize cycling of older tubes and adjusting current loads by turning off only young tubes or tubes which had been previously cycled. On the older INTELSAT IV satellites serving in contingency roles, power loads are kept to a minimum of four operating TWT's to satisfy thermal constraints while minimizing the stress on the batteries.

By employing close surveillance and adjusting the operational plans and satellite control and deployment strategy in response to performance trends, coupled with adequate satellite subsystem redundancy, to date it has been possible to satisfy all the mission requirements projected for the INTELSAT IV series of satellites. The INTELSAT IVA series while very similar to the INTELSAT IV did not suffer from the receiver degradation problems. Minor changes in the design of the battery coupled with increased capacity and optimized power system management techniques has resulted in improved performance of the INTELSAT IVA batteries relative to those of the INTELSAT IV to date. The majority of the output TWT's on the INTELSAT IVA are a different design than those utilized on the INTELSAT IV and have not yet exhibited anomalous performance after more than four years in service.

Transition from One Satellite Series to the Next.

As satellite technology improves, operational procedures and control techniques can be enhanced using the increased flexibility and capabilities of the newer satellites. Periodically, as traffic in a region grows, satellites must be replaced with newer higher capacity satellites. Recognizing that introduction of the INTELSAT V would involve a complex and lengthy transition phase, techniques were developed to minimize traffic interruptions and operational impact and further, significantly reduce the transition period.

Transition is an involved procedure since a traffic plan suitable for one series of satellites cannot be used on the new satellite and therefore a transition phase is required. In the past, transition from one series of satellite to the next has been accomplished by locating the new satellite approximately three degrees from the operating satellite (sufficient distance to preclude interference) and the traffic plan adjusted until a carrier configuration is achieved which will provide communications upon pointover to the new satellite. The first step in such a transition is to offload traffic in the various transponders and adjust the RF parameters to be compatible with the new satellite transponder performance characteristics. When the communications on the operating satellite has been reconfigured such that the new satellite could carry the new traffic, all earth stations are instructed to pointover to the new satellite and the carriers are again adjusted to meet the performance characteristics of that satellite. Then the remainder of the carriers which had been offloaded are brought into service. Adjustment of all the carriers is then required to optimize the overall system performance. Such a transition consumes a period of several months. The first few months are required to revise the operations plan and reconfigure carriers while the actual pointover, restoral of all the communications carriers and final adjustment is performed during the final month. With the introduction of the INTELSAT V, which takes advantage of four times frequency reuse by both polarization isolation and beam separation isolation and the addition of the 14/11 GHz frequency band, the transition from the INTELSAT IVA series satellite will be a much more complex procedure, consuming several more months and involving a temporary assignment of communications carriers to a third satellite. In order to minimize traffic interruptions during the transition from the INTELSAT IVA to INTELSAT V satellites, the feasibility of a new transition technique was demonstrated during the Indian Ocean Region transition from the INTELSAT IV to INTELSAT IVA satellites. Two satellites were collocated such that their stationkeeping limits of ± 0.1 degree overlapped by 0.05 degree. It was demonstrated that phase maneuvering within these stationkeeping limits could be executed to maintain a maximum of 0.05 degree separation between the two satellites such that both satellites would be within the operating beamwidth of the communications antennas permitting dual-illumination. This requires extremely tight stationkeeping tolerances to limit daily motion eccentricity about the mean to less than 0.02 degree. Plane separation of the two satellites has to be maintained less than 0.01 degree. Stationkeeping within these limits was complicated by the fact that ranging information was available for only one satellite since only one satellite could be operated at a time or multipath interference of the communications carriers would occur. Accordingly, orbit determination for the operating satellite was performed in a routine manner utilizing earth station aspect angles and range information. Orbit determination of the other satellite had to be performed using the angle track data from two geographically well separated earth stations. Success of extended collocation stationkeeping is critically dependent upon the quality of range and angle measurements used to determine orbit for maneuver planning and evaluation. An orbit determined with range and angle data is quite tolerant to angle data errors and even provides accurate unambiguous estimates of the mean angle measurement biases. Therefore, the two stations providing only angle track data had to have accurate angle measurement biases established by angle and range tracking on a third satellite with a known orbit. (During the INTELSAT IVA to V transition, range data will be available for both satellites.) The demonstration of collocation was successful and simplified the transition from the INTELSAT IV to INTELSAT IVA. The communications carriers were reconfigured as discussed above over a period of four to five months and pointover was then accomplished by turning off the receiver on the operating satellite and activating the receivers on the higher capacity INTELSAT IVA satellite. The total elapsed time from turn-off of the receivers until the traffic was restored on the new satellite was 19 seconds and restoration and realignment of the operations plan was accomplished in approximately another month.

Using this collocation technique during the transition from the INTELSAT IVA to the INTELSAT V satellite will reduce the required transition time by allowing dual-illumination. The flexibility in the INTELSAT IVA and INTELSAT V satellites will allow operation of specific transponders in both satellites simultaneously such that transition can be accomplished on a transponder-by-transponder basis eliminating extended interruptions in service and relocation of various earth station carriers.

Conclusion

Operational procedures developed and experience gained during the INTELSAT IV, IVA era will be applied to the follow-on series forming the basis of the operational philosophy for the INTELSAT V. The ability to demonstrate and refine new operational procedures with the in-orbit satellites ensures a smooth and efficient introduction of the INTELSAT V. The proven control, data processing, and communications management techniques will provide a firm foundation to ensure high quality and maximize continuity of communications service.

References

1. Fuenzalida, J., Rivalan, P., and Weiss, H. (1977) Summary of the INTELSAT V communications specifications. COMSAT Tech., Rev. 7.

2. Owens, J.R. and Morgan, W.L. (1977) In-Orbit Operation 6 Experience with INTELSAT Satellites. ACTA ASTRONAUTICA Vol. 5, No. 3-4, March-April 1978, p. 151-171.

3. Dicks, J. and Brown, M., Jr. (1975) INTELSAT IV transmission system design. COMSAT Tech. Rev. 5. 73-104.

4. Muelenberg, A., Weber, F.W., and Westerlund, L. (1975) Spacecraft Electrostatic Charging Phenomena, COMSAT Labs Technical Memorandum CL-34-74.

80-0577

OPERATIONAL EXPERIENCE ON OTS-2

A. S. Fagg and J. B. MacLauchlan
European Space Operations Centre
Darmstadt, West Germany

Abstract

This paper outlines briefly the primary objectives of the OTS-2 mission and describes the means by which these objectives were successfully accomplished in terms of facilities and organisation between interested parties. The paper then concentrates on orbit and attitude control aspects of OTS-2 describing the orbit and attitude control subsystem, its operation and its role in ensuring the very high availability of OTS for its communication mission. Station-keeping strategies are presented with details of implementation and some of the results obtained.

Introduction

OTS-2, the Orbital Test Satellite of the European Space Agency (ESA), was launched on 11th May, 1978. OTS-2 is a communications satellite in the 11 and 14 GHz bands and the forerunner of the European Communications Satellite (ECS) system, which will become operational in 1982. The OTS mission is primarily one of a test satellite to assess the satellite technology and communications concept which will be used in the operational system.

Mission Objectives

The specific objectives of OTS may be listed as follows:-

i) an in-orbit demonstration of the operational capabilities of the satellite and its constituent subsystems;

ii) experimental validation of the communications concepts (re-use of the spectrum based on polarisation discrimination, digital transmission and speech interpolation, time division multiple access) and the propagation assumptions;

iii) to study the technical problems arising from the utilization of the system on a pre-operational basis.

To assess the degree to which OTS would meet its objectives, an Orbital Test Programme (OTP) was established. This comprised a series of test activities designed to evaluate the essential characteristics of the technology and communication techniques adopted in the satellite design.

Mission Description

OTS is a three-axis stablised satellite situated at 10°E and maintained within ±0.1° of that position in both east-west and north-south directions. A general impression of OTS may be found in fig. 1. Six repeater channels are carried, two each of 5 MHz, 40 MHz and 120 MHz bandwidth. This is shown diagramatically in fig. 2. The corresponding communication coverage zone is given in fig. 3.

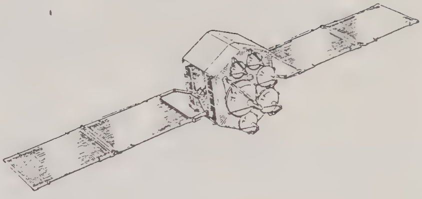

Fig. 1 - OTS in orbital configuration

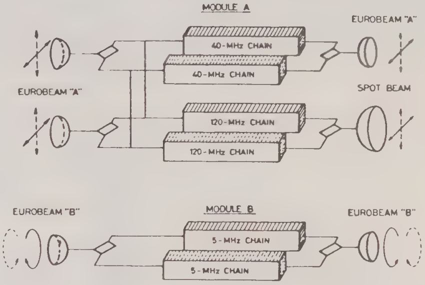

Fig. 2 - Communications payload of OTS

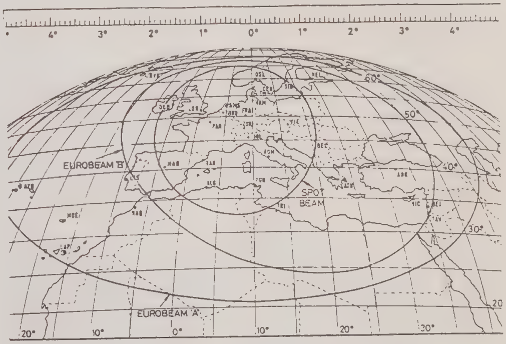

Fig. 3 - Coverage zones of the OTS antennas

The satellite is controlled from the European Space Operations Centre (ESOC) at Darmstadt, West Germany via the TTC station located at Fucino, Italy. Large earth stations involved in the OTP are located at Bercenay-en-Othe, France, Goonhilly, U.K., Usingen, West Germany and Fucino, Italy. In addition, some 40 stations throughout Europe are involved in propagation measurements.

The Orbital Test Programme incorporates those tests performed both by ESA and by Interim Eutelsat, who represent the European PTT Administrations, and who

Copyright © American Institute of Aeronautics and Astronautics, Inc., 1980. All rights reserved.

are the ultimate users of the ECS system. The OTP was, in general, divided into two parts - an ESA test period and a EUTELSAT test period - although there was and remains a degree of interspersing of tests from both authorities throughout the mission. The ESA tests, which were essentially completed in 1978, consisted of technological tests and a series of classical RF tests. Subsequently, the majority of satellite utilisation has been by EUTELSAT with a comprehensive programme of communication tests ranging from relatively simple transmission tests to TDMA, television and traffic, etc.

To ensure an efficient programme of tests, a management structure was established which may be found in fig. 4. Overall plans and broad schedules were drawn up by the executive bodies of the two organisations. Detailed implementation of this overall schedule was conducted by the appropriate coordinator. Subsequent to this scheme, a formal agreement between ESA and Interim EUTELSAT for the utilisation of OTS has been established. The utilisation programme is planned by a liaison group consisting of members of each organisation.

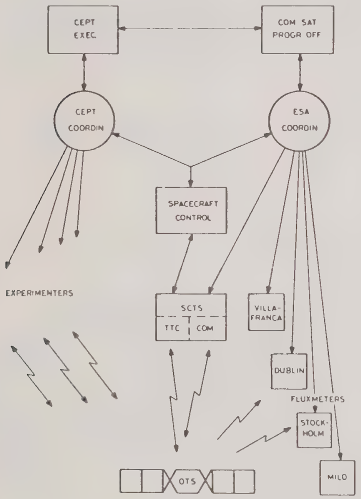

Fig. 4 - The OTP management structure

Operations

Routine support of OTS is not operationally demanding, consisting primarily of station-keeping manoeuvres, thermal control and power management during eclipse seasons. However, due to the nature of the OTS mission, a large number of OTP activities, requiring active satellite operations were necessary. The majority of these tests involved special operation of the attitude and orbit control system (AOCS). The following may be used to illustrate this type of operation:

Antenna pattern measurement

To determine the actual in-orbit antenna pattern, it was necessary to slew the satellite in a raster scan formation to enable measurements to be made by the European ground stations. This was achieved by "rolling" OTS about ±2° to shift the coverage area north and south and, maintaining the selected roll position, to perform an east-west scan of similar magnitude.

Slew manoeuvres

Repointing OTS to a predefined point (again within a square of about 2° N-S/E-W) was utilised on several occasions

- calibration of ground stations
- transmission of TV signals from Europe to a 3 metre dish in, for example, Cairo, Egypt or Rabatt, Morocco.

Solar sailing

This technique of using the solar arrays to provide a controlled disturbance torque on OTS was found to be most successful. Roll/yaw control was disabled and control about these axes was performed by periodic adjustment of the solar array axes with reference to the satellite body (reference 1).

The Attitude and Orbit Control Subsystem

The Attitude and Orbit Control Subsystem (AOCS) provides the following functions:-

Attitude control and manoeuvring capability during the transfer orbit to geosynchronous orbit altitude and for the transition from spin stabilisation to a three axis stabilisation configuration.

Attitude and orbit control of the spacecraft in the three-axis stabilised configuration so that the pointing accuracy requirements of ±0.08° in roll and pitch and ±0.35° in yaw are maintained.

Description of equipment and use

To maintain three-axis stabilisation, the subsystem uses a fixed momentum wheel (FMW) to provide control torques about the pitch axis and gyroscopic stability about roll and yaw axes. A two axis infra-red earth sensor (IRES) provides roll and pitch attitude references and this sensor can be biased by ground command by up to ±2° about both axes. In normal mode operation, control torques about the roll/yaw axes are provided by hydrazine thrusters aligned so that roll and yaw errors are reduced simultaneously. There is no yaw attitude reference in this mode; yaw errors translate into roll errors due to orbital motion. The threshold on the roll loop is set at ±0.042° which results in about 5 thruster actuations per day.

For station-keeping manoeuvres when large attitude disturbance torques may occur due to thruster misalignment or mismatch, dedicated station-keeping control loops are provided which maintain roll and yaw pointing via hydrazine thrusters. Pitch control remains with the FMW. The attitude reference for pitch and roll is again the IRES but for yaw a Rate Integrating Gyro is brought on-line and stabilised before manoeuvres.

All equipment is redundant. As part of the test and evaluation objectives of OTS, the two IRES are made by different manufacturers (Sodern and Galileo) as are the two FMWs (Philips and Teldix). There are two complete sets of thrusters. Fig. 5 shows the sensor and thruster layout.

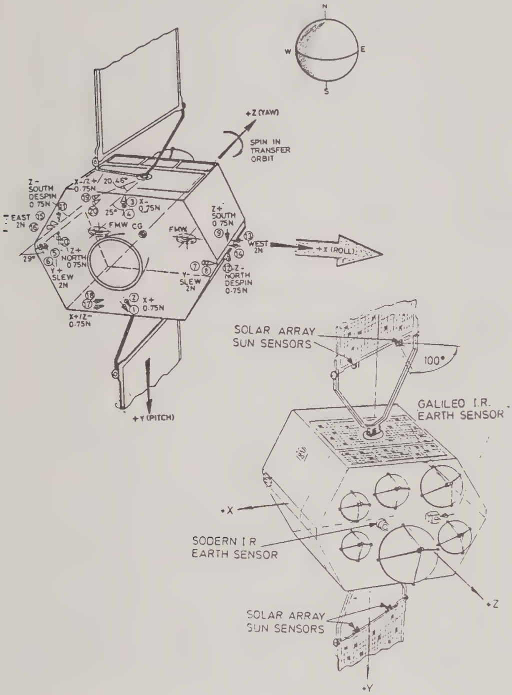

Fig. 5 - OTS-2 Thruster and Sensor Layout

A number of special operations required depointing of the spacecraft by up to 2.0° in pitch and roll. This was achieved by first disabling the roll/yaw thruster control loop and then pulsing yaw thrusters by ground command to rotate the momentum vector about the roll axis. Initially the achieved offset in roll was maintained by biasing the IRES by the achieved roll angle and re-enabling the roll/yaw loops. However, the translation of the roll error into yaw due to orbital motion resulted in an inordinate number of thruster pulses with a consequent effect on the orbit and disruption of east-west station-keeping. When this was realised, the procedure was modified to rely upon the gyroscopic stiffness to maintain the roll offset for the period of the operation, normally less than 2 hours. Offset angles in pitch are easily achieved by biasing the IRES. The pitch control loop via the FMW immediately provides the required offset.

On-board protection electronics

In addition to the equipment for normal mode and station-keeping attitude control, there are electronics for on-board contingency protection. This protection operates at two levels. At the first level, detection of a potentially serious loss of pointing or an AOCS power supply anomaly will result in a switch from prime to redundant FMW, IRES and control electronics plus disabling of the prime thruster branch by closing the main valves. Earth pointing is maintained and therefore full payload operation continues uninterrupted while diagnosis of the problem and subsequent reconfiguration takes place. This is known as the Automatic Reconfiguration Mode (ARM). The second level of protection is automatically implemented if this first level fails to maintain Earth pointing. After a pause of 15 minutes, all normal AOCS units are switched OFF and a basic sun acquisition loop is enabled with the redundant thruster branch to point the roll axis towards the sun. In this mode, known as Emergency Sun Acquisition (ESA), payload operation is, of course, interrupted until a suitable point in the orbit is reached for re-acquisition of the 3-axis stabilised configuration.

The naturally confident opinion prior to launch was that these electronics would never actually be used, and indeed a special OTP test was planned for the end of life to check their operation. However, in fact ARM was achieved 9 times and ESA twice in the first year of operation!

Some of the anomalies that led to these incidents are discussed in the following section. It is important to note that, except for the 1st and 8th ARM, which were followed by ESA, operation of the payload continued without interruption and recovery to the normal configuration was straightforward.

Problems

There is always interest in problems. Fortunately, on OTS there have been few and none which have seriously interfered with the routine operation of the spacecraft, which continues to be very straightforward. The problems which have affected operations concern the IRES and the hydrazine thrusters.

Initially, the Galileo IRES was on-line. However, this sensor was found to be susceptible to random, internal switching between its four bolometers, due both to electromagnetic interference and internal reflections of the sun's rays at certain times of the year. The sensor thus gave apparent depointing signals to the control logic which caused switching to the redundant equipment via the ARM on-board protection electronics. For these reasons the Sodern sensor was brought on-line and, although it is potentially less accurate than the Galileo, it has performed quite satisfactorily. It has been found, however, to be more sensitive than expected to the seasonal variations in the earth's infra-red profile, which introduces error about the roll axis as shown in Fig. 6. This error was detected by the unexpectedly large number of the roll/yaw thruster actuations which suggested that the spacecraft momentum vector was not perpendicular to the orbit plane. The solution has been to use the IRES bias unit to inject a correcting signal.

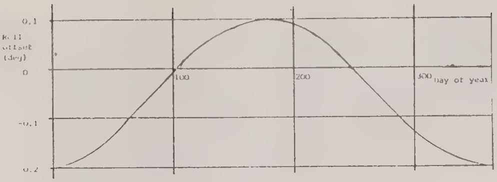

Fig. 6 - Seasonal variation of roll offset - SODERN Sensor

A second problem with this IRES is that when one of the four bolometers comprising the sensor has to be inhibited to prevent serious depointing when the sun or moon appears in its FOV, a large offset sometimes greater than 0.05° is apparent. The roll/yaw control loops are inhibited to prevent the actual roll attitude being affected but, in pitch, there is no such solution and the pitch attitude will suffer an actual offset for the period, about 2 hours.

The hydrazine thrusters have exhibited two types of anomalous behaviour. The first is the apparent generation of gas in the flow control valves and tubing close to the thruster. This is attributed to the interaction of the hydrazine with the materials used in the valve construction and has been repeated in the laboratory. The result is 'missing pulses' or degraded performance when the thruster is operated after a period of inactivity and is of particular consequence for station-keeping manoeuvres (see below).

The second thruster anomaly has been on a yaw thruster on the prime thruster branch. This has produced an impulse where none has been commanded which has, on several occasions, resulted in significant depointing, sufficient to cause reconfiguration via the ARM protection logic. This is tentatively attributed to a faulty valve seat allowing hydrazine to trickle into the catalyst bed. If the catalyst is then heated via the thruster heaters, the absorbed hydrazine suddenly decomposes, producing the observed impulse and corresponding depointing. The anomaly is still under investigation but in consequence, all manoeuvres have now to be carried out using the redundant thruster branch unless it is an operation where heating of the suspect thruster can be avoided.

Finally, a phenomenon which is not in fact anomalous but certainly causes problems, is the unexpectedly large pitch torques produced by thruster exhaust plume impinging on the solar arrays during North-South station-keeping manoeuvres. How this is dealt with is described more fully below.

East-West Station-Keeping

Strategy

The strategies developed to counteract the two significant perturbing effects for East-West station-keeping of the Earth's triaxiality (J_{22} harmonic) and solar radiation are well known. A summary of the strategy applied for OTS follows.

The objectives of the strategy are to minimise propellant consumption and frequency of manoeuvres while maintaining the longitude within the required 10°E ± 0.1° deadband. The driving perturbation is the triaxiality effect and at a longitude of 10°E this requires a single prograde ΔV increment of about 0.07 m/sec once every 3 weeks or so. To minimise the effects of solar radiation pressure which could result in a large eccentricity building up if uncontrolled, the nominal strategy is to time the application of the velocity increments required for the triaxiality correction to maintain an eccentricity of about 0.00025 and the perigee of the orbit orientated towards the sun. With the area/mass ratio of OTS-2, the eccentricity then does not vary very much from the value of 0.00025 during the interval between manoeuvres while the drift of the perigee away from the sun line is corrected by the manoeuvre. Control of both perturbing forces is therefore achieved with a single burn every 3 weeks or so, although occasionally a double burn manoeuvre is required to restore the situation after it has been upset by some external disturbance (i.e. a North/South manoeuvre or excessive roll/yaw thruster pulses). The 0.00025 eccentricity results in a daily longitude oscillation of amplitude 0.02°.

This strategy works well with OTS and, with the available orbit determination accuracy of about 0.003°/1σ, the longitude deadband could easily be reduced to ±0.05° without additional propellant usage. The achieved longitude history to date is shown in fig. 7. However, the achievement of a regular three week cycle has not proved practical due to normal mode thruster actuations, which have a significant ($\sim$10% of the J_{22} effect) but unpredictable effect on E-W drift rate and due to the periodic North-South manoeuvres which have an in-plane effect two or three times that of an East-West manoeuvre, albeit mostly radial.

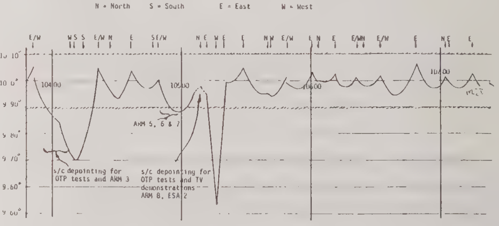

Fig. 7 - Longitude history - 1st year

Early in the mission, the ±0.1° longitude deadband was overrun on three separate occasions; on two of them 9.7°E longitude was reached before corrective action reversed the drift. The main reasons for these occurrences were the initial lack of appreciation of the effect the normal mode thrusters had on the orbit during the tests, which required depointing of the spacecraft, and the failure to allow sufficient time for orbit determination following either such manoeuvres or the occurrence of other events (ARM, ESA) involving thruster actuation. Since this time, a daily check of longitude is made via antenna azimuth and elevation measurements independently of the weekly orbit determination and possible effects on the orbit of any tests involving thruster actuation are considered carefully before the tests are implemented. The longitude has been maintained well within the deadband since November, 1978.

TABLE 1 - Orbit Determination Accuracy

a) Measurement accuracy

Tracking Station	Measurement Type	Accuracy at 1σ		Frequency of Measurement
		bias	noise	
Fucino, Italy lat., long. 41.98°N,13.60°E	range (m) azimuth (°) elevation (°)	~0 0.01 0.03	4 0.002 0.006	every 4 hours or every 2 hours for 2 days following a S/K manoeuvre
Villafranca, Spain lat., long., 40.44°N, 3.95°W	range (m)	~0	10	3 times daily during normal working hours, 2 hours apart. Monday to Friday only.

b) Position determination accuracy

	Accuracy, 1σ
Range	0.06 km
East-West	2.8 km = 0.0038° longitude
North-South	2.8 km = 0.0038° latitude

Orbit Determination

Orbit determination calculations are made weekly using measurements made from the Fucino station in Italy (SHF tone ranging, azimuth and elevation) and from the Villafranca station in Spain (SHF tone ranging only). Measurement frequency is broadly every 2 hours for the 2 days following a station-keeping manoeuvre and every 4 hours at other times. The accuracy achieved is summarised in Table 1.

Thruster Performance

Up to July, 1979, twenty-seven manoeuvres have been performed. Most of these manoeuvres used the East thruster on the 'B' branch of thrusters. In general, performance of these 2 N thrusters is predictable and close to pre-launch predictions. Table 2 summarises the burns and relative performance.

Thruster	Branch	No. of manoeuvres	Total burn time (secs)	Mean % error
East	prime	6	181	-2%
West	prime	5	51	no data
East	redundant	12	344	-1%
West	redundant	4	158	no data

TABLE 2 - East-West Thruster performance

Implementation

The implementation of the East-West manoeuvres has developed through several stages. Pre-launch predictions of thruster misalignment torques required a cautious approach at first. To be sure of maintaining roll and yaw control, manoeuvres were implemented with the station-keeping control loops on-line and burns were limited to a duty cycle of 1 sec every 30 seconds to avoid large pitch overshoots. However, it became apparent that the thruster misalignments were, in fact, very small and, following some checks it was found feasible to dispense with the station-keeping loops and implement the manoeuvres in normal mode. Burn sizes of about 10 seconds cause a small increase in nutation, which is quickly damped out and a virtually indistinguishable pitch transient. Thus, East-West manoeuvres are now extremely straightforward. In addition, it has recently been possible to use the 'A' branch thrusters for East manoeuvres as the Z-thruster on this branch, suspected of spurious operation, is not used and furthermore, need not be heated.

North-South Station-Keeping

Strategy

The strategy adopted to counteract luni-solar perturbations and maintain a ±0.1° latitude deadband (i.e. inclination less than 0.1°) is to correct only for secular effects and to ignore cyclic effects. This strategy requires burns in a north (or south) direction at a satellite Right Ascension with respect to the 1st point of Aries of between 270° and 279°, depending on the year (90° to 99° for south burns).

The problem with the Z-thruster on the prime thruster branch has meant that these manoeuvres are constrained to using the redundant thruster branch. The thrusters on this branch are north pointing producing a velocity increment in a northerly direction. Because of this and because the manoeuvres have developed into a very complex operation, they are performed only once every 6 weeks or so and are timed to occur some 4 - 5 days before the next East-West manoeuvre becomes necessary. This timing allows any in-plane cross coupling of the impulse to be corrected by the East-West manoeuvre.

The strategy enables the inclination to be maintained at less than 0.07° throughout the year and for one third of the year it is, in fact, kept less than 0.05°. If the requirement existed, the orbit determination accuracy is good enough to permit maintenance of inclination at less than 0.05° throughout the year.

The North-South deadband of ±0.1° latitude has not been transgressed throughout the mission.

Thruster performance

Accurate assessment of the thruster performance is complicated by the fact that the two yaw thrusters used to implement the burn are naturally also used for yaw control. Prior to a burn, they are pulsed to maintain the limit cycling between the ±0.1° yaw thresholds set in the station-keeping control loops. These pulses should therefore be added to the programmed impulse of the burn itself. During a burn, yaw pointing is maintained by interrupting the continuous operation of one of the two thrusters. These 'off modulation' pulses are therefore lost pulses which need to be subtracted from the programmed burn. Thus, the number of pulses used for yaw control has to be known in order to estimate the actual performance.

In general, the resolution of the RIG telemetry is sufficient to do this and the results obtained are certainly within the accuracy obtained for the estimation of the achieved impulse from orbit determination. Table 3 summarises these results and shows that the achieved thrust levels were approximately 10% below pre-launch predictions. This deficiency is currently unexplained.

Yr/day	Direction	Corrected burn time secs.	Δ Z	Error	In-plane	components
			m/s	%	Radial m/s	targential m/s
78/198	S	2000	4.35	-28	-0.200	-0.035
78/229	N	1267	3.17	-12	-0.150	-0.018
78/252	S	816	2.04	-10	-0.076	-0.018
78/290	N	1878	4.83	- 6	No	data
78/341	N	2535	6.44	- 7	-0.274	0.035
79/015	N	1688	4.08	-11	-0.249	-0.011
79/050	N	1428	3.49	- 8	-0.205	-0.002
79/113	N	2105	4.94	-12	-0.193	0.043
79/153	N	2406	5.80	- 8	-0.193	0.048
79/190	N	1745	4.13	- 9	-0.118	-0.001

TABLE 3 - North-South manoeuvre performance

Implementation

The implementation of the North-South manoeuvres is achieved as for East-West manoeuvres, with the station-keeping control loops enabled to provide thruster control of the roll and yaw axes and the FMW providing pitch control via the normal mode control loop. The required North-South impulse is achieved by firing the two yaw control thrusters simultaneously.

It was envisaged that burns of up to 2,000 secs would be required and these would be executed as a single continuous firing. However, on the first attempt at such a manoeuvre, a dramatic increase in FMW speed occurred with the upper tolerance limit for the FMW being reached after less than 60 secs into the firing and the manoeuvre was abandoned. Initially it was suspected that this was the result of a pitch torque induced by badly misaligned thrusters. However, subsequent manoeuvres demonstrated that it was due to 'plume impingement', i.e. the thruster exhaust plume hitting the solar array panels producing a pitch torque. This had not been considered during planning of these operations as it was thought to be negligible. The magnitude of the plume impingement torque is proportional to the orientation of the solar array panels relative to the thruster plumes and varies sinusoidally as illustrated in Fig. 8.

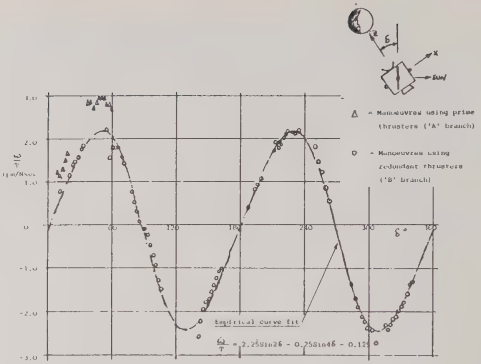

Fig. 8 - Variation of FMW speed per N.sec of impulse with solar array orientation

The operational procedures have therefore been changed to accommodate these plume impingement torques. In the first place the planned firing has to be split into several shorter burns so that the FMW speed change is kept within the ±10% operating limits. Secondly, a momentum offloading manoeuvre has to be introduced after each burn to return the speed to a suitable starting value for the following burn and so on. At the times of year where the plume impingement torque is maximum, as many as 10 shorter burns have to be implemented. In addition, the timing of each burn has to be very carefully planned so that the centroid of the separate burns is the same as the centroid of the continuous firing in order to achieve the required effect on the orbit plane.

These manoeuvres are further complicated by the problem of 'missing pulses' in the attitude control thrusters, particularly the roll axis control thrusters, in conjunction with the seasonal offset apparent on the Sodern sensor roll output. As mentioned above, this offset is corrected in normal mode control by injecting a seasonally varying bias voltage into the control loop. Unfortunately, this bias is not also fed to the station-keeping control loops with the result that when these loops are switched on, they immediately see a large roll error (maximum 0.2°) and thrusters are pulsed to reduce this to within the +0.05° threshold. The resulting overshoots in the situation where a thruster fails to respond, i.e. only gas is expelled, could be large and have, on one occasion, come very close to the ARM threshold of 0.4°.

The solution to this problem has been to prime the thrusters some time before the manoeuvre, i.e. pulse them until a repeatable impulse is obtained and secondly, to remove the roll error by open loop pulsing of the yaw thrusters before enabling the control loop. Thus the roll rate at first crossing of the threshold is low and the resulting limit cycling is relatively gentle. The pitch thrusters which are to be used for momentum offloading during the manoeuvre are also primed in the same way.

The manoeuvres are currently implemented as described without difficulties. However, it can be seen that the whole operation is a great deal more complex than originally envisaged. It is also time consuming both in preparation and execution.

In-plane coupling of impulse

The North-South manoeuvres are executed a few days before a necessary East-West manoeuvre, so that any cross-coupling of the North-South manoeuvre impulse into the East-West direction can be determined and then allowed for in planning the East-West manoeuvre.

In-plane coupling has several sources, all connected with the firing of the thrusters. These are:-

- Misalignment of the North-South facing thrusters;
- Spacecraft attitude errors relative to the orbit plane;
- Roll thruster actuations for attitude control during the manoeuvres;
- Pitch thruster actuations necessary for momentum offloading to balance plume impingement torques.

Of these sources, the contribution from the roll and pitch thrusters have proved to be most significant (ref. 2). The roll thrusters produce a thruster component directed radially inwards towards the Earth. The magnitude of the resulting velocity increment is typically 0.1 m/sec for 1,000 seconds of burn, which is larger than a normal velocity increment for an East-West manoeuvre but, being radial, affects only the orbit eccentricity and argument of perigee. The pitch thrusters produce a radial and an along-track velocity increment respectively about 0.02 m/sec and +0.01 m/sec per 1,000 secs of burn at the time of maximum plume impingement torque. The along-track component can be significant in its effect on the longitude drift rate. Table 3 includes the observed radial and along-track components for each manoeuvre. The resulting effect on longitude drift rate has been counteracted without problem at the execution of the East-West manoeuvres. It has, however, meant that a 2-burn manoeuvre is required occasionally and there can be some disruption of the East-West strategy.

Conclusions

OTS has made a convincing demonstration of fulfilling all its mission objectives and is continuing to do so. In particular, the integrity of the design concept has been clearly proven with respect to the spacecraft availability for communications traffic; this is apparent when it is noted that in over 18 months of routine operation the total outage of the spacecraft has been 6 hours - an availability of 99.96%.

Experience with OTS has shown a few areas where small improvements in design to upgrade unit performance or to permit operational simplification could be considered for incorporation on the future operational ECS spacecraft. The OTS mission continues to provide a platform for advanced communication experiments. The remaining consumables are such to allow full mission capability until at least mid-1984 - three years more than the originally planned mission duration.

Acknowledgement

The OTS mission has been supported in different ways by many people. The authors are grateful for the cooperation received from many areas within ESA, from MESH (the spacecraft contractors) and from EUTELSAT.

References

1. Attitude Control by Solar Sailing - A Promising Experiment with OTS-2.
   U. Renner, ESA Journal, 1979, Volume 3.

2. OTS Operations Report no. 1. 'In-plane velocity components resulting from North-South station-keeping manoeuvres'. A. S. Fagg

80-0578

HERMES SATELLITE (CTS): PERFORMANCE AND OPERATIONS SUMMARY

H.R. Raine and J.S. Matsushita
Department of Communications
Communications Research Centre
Ottawa, Ontario, Canada

Abstract

The Communications Technology Satellite, named Hermes, was the first to demonstrate high power 12 GHz transmissions from a satellite. The three-axis stabilized satellite was operated in geostationary orbit for nearly four years. The satellite design and performance and the operational features of the mission are outlined in this paper. Emphasis is placed on the novel operational requirements which arose during this experimental mission.

I. Introduction

General

The experimental Communications Technology Satellite, named Hermes, was designed and built in Canada under a joint program of the Canadian Department of Communications (DOC) and the United States National Aeronautics and Space Administration (NASA). The European Space Research Organization (now the European Space Agency) also was a participant under an agreement with Canada and provided certain spacecraft components including 20W TWT's, a parametric amplifier and development of the solar array blanket. The principle objectives of the program were to develop and flight test:

(1) a high-efficiency travelling-wave-tube amplifier having a saturated power output of greater than 200 Watts at 12 GHz;

(2) a lightweight extendible solar array with an initial power output greater than 1 kilowatt;

(3) a 3-axis stabilization system required to maintain accurate antenna boresight positioning on a satellite with flexible appendages;

(4) and to conduct satellite communications systems experiments using the 12 and 14 GHz bands and low-cost transportable ground terminals.

Hermes was launched in January 1976 on a Thor Delta 2914 launch vehicle. Hermes was designed for a mission life of two years but as a result of the experienced gained with operations during this period, and a continuing demand by users to conduct communications experiments, the mission was extended for a further two years[1]. The satellite was maintained in geostationary orbit at 116°W longitude for 3½ years and moved to 142°W for the last 5 months of operation. East-west station-keeping was initially maintained within ±0.2°; however, to economize on fuel, the station-keeping requirement was relaxed to ±0.3° after the move. Maintenance of 0° orbit inclination was not part of the mission plan, although a reduction in inclination was made in preparation for the extended mission. The satellite ceased operation in November 1979.

Satellite Description

The launch weight of the spacecraft was nominally 1,490 lbm and the initial on-orbit weight was 780 lbm. After placement in the geostationary orbit by firing the solid fuel Apogee Kick Motor (AKM), the spinning satellite was drifted to 116°W, despun, and 3-axis stabilized. The spacecraft was 3-axis stabilized using a fixed axis momentum wheel and low thrust hydrazine thrusters, so that the front panel supporting the SHF antennas continually pointed toward the earth.

During launch, the flexible arrays were stored against the north and south panels of the spacecraft body. The arrays were extended to the flight (operational) position as shown in Fig. 1, perpendicular to the orbit plane, during the attitude acquisition manoeuvre. Each of the two flexible solar sails had a length of 21.3 feet. The solar arrays, which provided more than 1,300 watts at the beginning of life, tracked the sun and rotated once per day with respect to the spacecraft body.

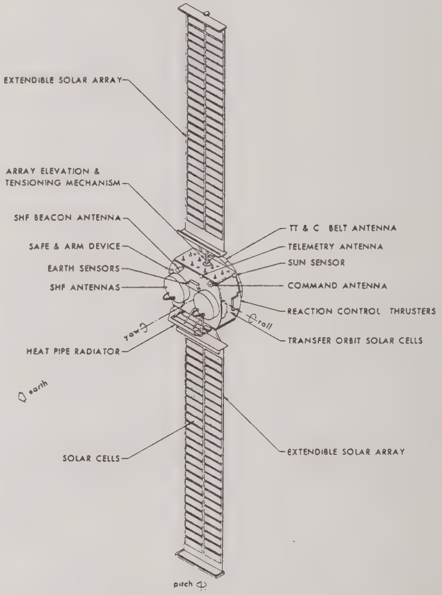

Fig. 1 Hermes Satellite In-Orbit Configuration

The two SHF communications antennas were independently steerable via ground command toward any location on the surface of the earth visible from the satellite. The spot beams had half power beamwidths of 2½°. The SHF transponders provided two radio frequency (RF) channels each having a bandwidth of 85 MHz. One channel used a 200 Watt TWT to produce a boresight EIRP of 59 dBw; the other channel used a 20 Watt TWT to give an EIRP of 48 dBw. The primary receiver used a parametric amplifier with a noise temperature of about 1000 K.

Copyright © American Institute of Aeronautics and Astronautics, Inc., 1980. All rights reserved.

Consistent with the experimental nature of the project and weight limitations imposed by the launch vehicle, only essential housekeeping functions were provided during the solar eclipses. Redundancy was incorporated to the extent practicable into the various subsystems.

II. Operational Phase

General

While each phase of the mission placed demands on both the satellite and ground segments, only the on-orbit phase is addressed in this paper. The highlights of the early phases of the mission are described elsewhere[1,2,3].

As a result of the nominal performance of the launch vehicle and apogee motor, the hydrazine consumed to bring the satellite on station was substantially below that budgetted (see Table 1), leaving an additional 10 lbm of hydrazine available for other activities as noted in the following sections.

Table 1 Hydrazine Fuel Budget

ITEM	BUDGET LBM		ACTUAL LBM	
	ALLOWANCE	REMAINDER	USAGE	REMAINDER
At Launch	0.0	54.7	0.0	54.7
Pre-Apogee Motor Firing Manoeuvres	5.0	49.7	5.0	49.7
Post-Apogee Motor Firing Manoeuvres	1.4	48.3	1.3	48.4
Station Acquisition Firings to 116°W	24.8	23.5	14.9	33.5
Attitude Acquisition Sequence	2.1	21.4	1.5	32.0
Normal On-Orbit Operations (1976-1977)	9.9	11.5	2.7	29.3
Orbit Inclination Change (0.8° to 0.1°)	0.0	11.5	19.1	10.2
Normal On Orbit Operations (1978-1979)	0.0	11.5	2.6	7.6
Relocation to 142°W	0.0	11.5	3.5	4.1
Decomposition Allowance*	0.0	11.5	0.8	3.3
Unuseable Residual*	0.0	11.5	0.8	2.5
Uncertainties*	0.8	10.7	2.4	0.1

* Estimated Value

A simplified mission timeline is shown in Fig. 2. Generally, any anomalies encountered were accommodated without difficulty, and had little or no impact on ensuing operations. Indeed, as already noted, the mission was extended to almost twice its planned life. There were, however, five malfunctions or failures which affected the experimental program and/or operations significantly. These malfunctions and their impact are discussed later in the paper.

Check-out Phase

The check-out phase immediately followed the attitude acquisition. During the two month period, satellite health and the prime operating configurations were checked by a team of spacecraft specialists including at least one engineer knowledgeable with the behaviour of each subsystem. A small team of dynamicists were retained over this period to develop non-standard procedures related to the operation of the attitude control system. Considerable contractor consultation support was utilized during this learning period.

The hour-by-hour control of the satellite was achieved with a total of five Duty Controllers, one of whom was on shift at all times, supported by an equipment operator. A minicomputer was used in the control station for controlling the satellite, formatting commands and logging data. Software prompts were provided to the Duty Controller by subroutines applying limit checks, timing and scheduling messages, etc. The central computer at the Communications Research Centre (CRC) was used for offline work in processing telemetered satellite data, processing orbit data for orbit determination and predicting events such as eclipses and sun and moon interferences.

The knowledge gained during this period resulted in changes to the standard operating procedures; the important ones are described in the following sections.

On-Orbit Operations Phase

Following the check-out period, the satellite entered the routine on-orbit operations phase which continued until the end of the mission. This phase included a number of special operations. A few anomalies occurred; these will be discussed separately.

Organization

The Space Communications Program Office (SCOPO) was formed at CRC (see Fig. 3) to manage the Hermes Project, as well as to continue the operation of the Alouette and ISIS satellites and to engage in other communications satellite experiments and projects. Approximately 12 people were responsible for routine control centre operations associated with Hermes. Four engineers drawn from the prelaunch integration, mission and attitude acquisition teams were responsible for the day-to-day monitoring of the satellite health, devising new procedures and conducting special operations. Over a dozen more specialists were available for part-time consultation and/or special operations support in such areas

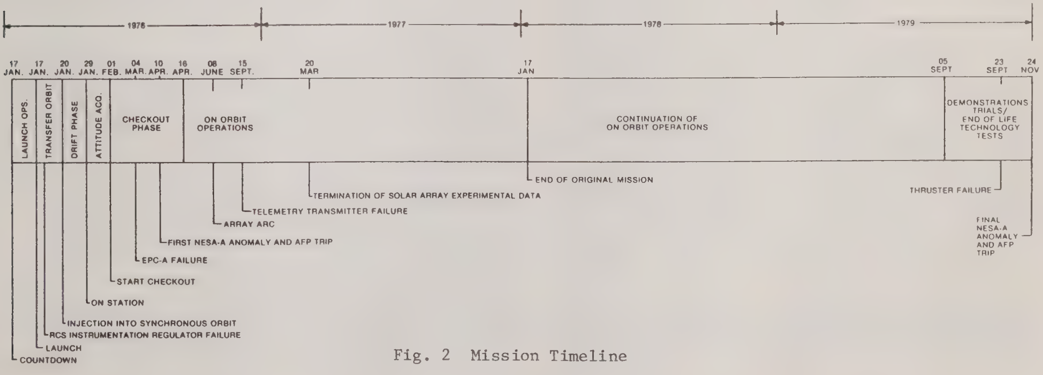
1976
1977
1978
1979
17 JAN.
17 JAN.
20 JAN.
29 JAN.
01 FEB.
04 MAR.
10 APR.
16 APR.
08 JUNE
15 SEPT.
20 MAR
17 JAN
05 SEPT
23 SEPT
24 NOV
LAUNCH OPS.
TRANSFER ORBIT
DRIFT PHASE
ATTITUDE ACQ.
CHECKOUT PHASE
ON ORBIT OPERATIONS
CONTINUATION OF ON ORBIT OPERATIONS
DEMONSTRATIONS TRIALS/ END OF LIFE TECHNOLOGY TESTS
END OF ORIGINAL MISSION
TERMINATION OF SOLAR ARRAY EXPERIMENTAL DATA
TELEMETRY TRANSMITTER FAILURE
ARRAY ARC
FIRST NESA-A ANOMALY AND AFP TRIP
EPC-A FAILURE
START CHECKOUT
ON STATION
INJECTION INTO SYNCHRONOUS ORBIT
RCS INSTRUMENTATION REGULATOR FAILURE
LAUNCH
COUNTDOWN
THRUSTER FAILURE
FINAL NESA-A ANOMALY AND AFP TRIP

Fig. 2 Mission Timeline

as spacecraft charging, battery management, attitude recovery, thruster behaviour, circuit analysis and thermal trend analysis, throughout the mission. Other staff within SCOPO were responsible for scheduling and controlling experiments, installing and operating experimental communications earth terminals.

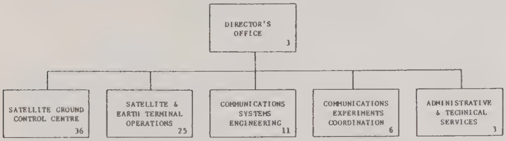
DIRECTOR'S OFFICE
3
SATELLITE GROUND CONTROL CENTRE
36
SATELLITE & EARTH TERMINAL OPERATIONS
25
COMMUNICATIONS SYSTEMS ENGINEERING
11
COMMUNICATIONS EXPERIMENTS COORDINATION
6
ADMINISTRATIVE & TECHNICAL SERVICES
3

Numbers indicates total staff

Fig. 3 Space Communications Program Office

Daily Routine

Daily routine satellite commands were typically related to battery charging, heater control, and antenna steering for SHF communications experiments. During the first 3 years of the mission, the high voltage supplies of the 200W TWTA were switched off and the cathode heater switched to half power during idle communication periods in order to conserve cathode life. In the last 5 months of operation, this precaution was removed in order to accumulate more life data on this tube.

Immediately after deployment of the arrays, the on-board clocked stepping system was activated to maintain the face of each array toward the sun. Since the clock source exhibited minor thermally-induced departures from the desired frequency, small angular errors were accumulated. A daily resetting of the array position was introduced therefore as a routine operation.

Tracking, Telemetry and Command (TT&C)

In addition to the daily execution of commands and receipt of data, routine operations also involved biweekly ranging measurements using the coherent S-Band TT&C transponder. Measurements were typically made at 2 hour intervals over a 24-hour period at the CRC ground station. After filtering, ranging accuracies of better than 10 metres were achieved, thus permitting excellent orbit determination. Predictions of events, such as eclipses and sun and moon interferences to the Non Spinning Earth Sensors (NESA's), were consistently accurate to better than 5 seconds in time throughout the mission, except during special dynamic events. Since there was no redundancy of the 10 metre TT&C antenna system at CRC, the agreement with NASA provided for support by NASA Spaceflight Tracking and Data Network (STDN) for 2-3 hours per week while routine maintenance was performed on the CRC equipment. During these periods, telemetry data was routed from the selected STDN station to Goddard Space Flight Center, then to the CRC ground station. Command signals generated within the CRC ground station were issued to Hermes in the reverse direction during these maintenance periods and directly from CRC to the satellite at other times.

Non-spinning Earth Sensors (NESA's)

The NESA's provided the primary attitude pointing information to the on-board attitude control system (ACS). Each NESA was designed to provide control error signals for each of two axes (see Fig. 4). In the initial mission planning, NESA-B alone was to be used, while retaining NESA-A in reserve as a spare and for those occasions when sun or moon interferences to NESA-B required that it be switched off. Detailed planning however indicated that an inordinate amount of switching would be required during the mission (see Table 2) to accommodate all the interference events. Consequently both NESA's were operated simultaneously to control their respective scan axes except during particularly severe interference conditions.

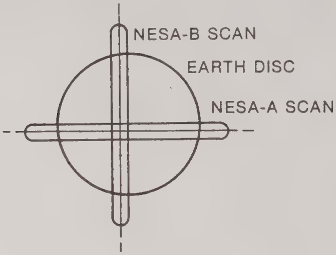

Fig. 4 NESA Geometry

A technique was devised in the first month of operations to inhibit the thruster action of the roll/yaw control loop during all NESA-B interferences, thereby eliminating the need for NESA-B switching for the rest of the mission.

Table 2 Frequency of Interference Events

INTERFERENCE	DURATION	OCCURRENCE
Sun to NESA-B	≈15 minutes	≈100 days/year
Moon to NESA-B	≈12 minutes	≈ 12 days/month
Sun to NESA-A	≈ 3 hours	≈ 12 days/equinox
Moon to NESA-A	≈ 3 hours	≈ 3 days/month

No analogous capability was possible to overcome the effects of the interferences to the NESA-A. In view of the experimental nature of the mission and other side-effects of NESA-A switching described later, it was decided to allow the satellite to "ride through" NESA-A moon interference events resulting in occasional pitch errors of up to 1½°, each lasting for several minutes. It was necessary however to switch NESA-A off for the sun interference events. NESA-A switching was, as a result, limited to 5 or 6 times during each equinox season.

Telemetry Degradation

One particular satellite anomaly, namely a degradation of the telemetry transmitter, so pervaded the operation that virtually every procedure and routine was affected. This anomaly started in the first year of the mission. Plans and procedures were introduced to cope with decreasing availability of telemetered data. Arrangements were made to obtain support from NASA STDN 26-metre stations as the signal level fell below the CRC station PCM threshold. Since the output power was time and temperature dependent, data availability varied according to time of day, season of the year, operating mode of the satellite and time in the mission. During the summer of 1979, as a worst case, data were obtained about 60% of the time, frequently with a bit error probability $\approx 10^{-1}$, using the 26m

STDN stations.

In the planning for possible zero telemetry operations, the following guidelines were established:

1. Full utilization of experience with previous satellite subsystem behaviour.

2. Full utilization of the characteristics of all r.f. transmissions from the satellite including the S-band carrier, the SHF CW Beacon, a CW spurious signal in the 200 watt channel, and a SW spurious signal in the 20 watt channel.

3. Simplification of command operations to reduce the possibility of mistakes.

The guidelines were never fully implemented since sporadic telemetered data continued to be available through the mission. However, several procedures were implemented as a result:

1. Computer controlled command groups were developed to include in each at least one command (whenever possible) which affected the presence or amplitude of an SHF signal to provide independent evidence that the commands were in fact executed by the satellite.

2. The fluctuations in the amplitude of the spurious signals in either SHF channel were monitored to permit verification of thruster firing. This was done during operations to dump energy from the momentum wheel by determining the satellite body nutation period. Assuming all rates except the wheel speed are known, the momentum wheel speed could be calculated within an accuracy of 1% by the relationship:

$$\dot{\theta}_w = \frac{2\pi\sqrt{I_x I_z}}{I_w T} \qquad (1)$$

where:

I_w is the Moment of Inertia (MOI) of the wheel,
I_x is the MOI about the roll axis,
I_z is the MOI about the yaw axis,
T is the nutation period, and
$\dot{\theta}_w$ is the wheel speed.

3. During idle periods between SHF experiments, the SHF antennas were aimed to either side of Ottawa and the received signals in the two channels were monitored for evidence of attitude anomalies. Computer monitoring of the SHF beacon was provided, to assure the Duty Controller of normal satellite pointing conditions and power subsystem behaviour. The CTS Project Office at the NASA Lewis Research Center also monitored the SHF signals as a part-time backup to the CRC capability.

4. The operating mode of the solar array tracking was changed from the clock mode described earlier to an automatic sun tracking mode; thus the daily reorientations were no longer required and the arrays would automatically track the sun in the case of loss of attitude control.

5. Ranging measurements for orbit determination originally carried out using the failing S-Band system were transferred to the SHF subsystem with no loss of accuracy.

Special On-Orbit Operations

General

In addition to the day-to-day routine operations, there were other more specialized events carried out periodically. For these events, one or two people were added to the operational roster, usually involving a person from the spacecraft health team and a specialist in whatever area was involved to assess data in real time, and to authorize deviations from the procedures as required. Formal procedures were developed for these events.

Eclipses

The spacecraft batteries were sized to carry only the housekeeping load of up to 100W through eclipses. It was planned therefore that the experiments bus would be switched off at entry and on again at exit of each eclipse. Provision had been made to do this switching automatically. Before flight, it had been expected that the solar array voltage would decrease monotonically at eclipse entry and that the cold arrays would generate high voltages as the satellite exited from each eclipse. This voltage, it was expected, would decrease to nominal values as the cells became warmer. After the first two full eclipses, it became evident that the solar cells were cooling before the illumination fell to zero, causing the voltage to increase (unexpectly) just before eclipse entry thus causing an overvoltage tripoff. It is suspected that this abnormal switching cycle was partially responsible for a subsequent experiments' bus relay malfunction, which destroyed the primary experiment power converter. Following this failure, the main communications equipment was left off for the remainder of the 1976 spring eclipse season while the problem was analysed, and the eclipse procedures were revised. The automatic circuits were disabled, and all bus switching was commanded from the ground for all subsequent eclipses. The communications equipment was switched off during the 1976 autumnal eclipse season as well, as a precautionary measure.

Approaching the end of the spacecraft mission, the batteries degraded to a point where they could no longer support the housekeeping load for the longest eclipses. Procedures were instituted to progressively reduce the load by turning off nonessential items in a priorized order designed to minimize risk to the spacecraft. The load was limited to 60 watts (average) for parts of the 1979 autumnal eclipses.

East-West Station-keeping and Relocation

In order to maintain the position within 0.2° of the nominal station, a station-keeping manoeuvre was required approximately once each month. The time of day at which the thrusters were fired was selected to be as near the orbit apogee or perigee as possible to help control eccentricity, consistent with maintaining reasonable thermal conditions for the thrusters. A typical station-keep required a velocity change of 4 cm/sec at 116°W and 16 cm/sec at 142°W.

Because of the possible immediate consequences of thruster malfunctions and the degrading quality of the telemetered data, it was arranged that a

Reaction Control System (RCS) specialist be present for all thruster firings.

The major relocation undertaken to move the satellite to 142°W for communications with Eastern Australia was an extension of the regular East and West Station-keeping manoeuvres. West engine firings accelerated the spacecraft until a drift rate of 1¼° per day was achieved. The East engine was then used to decelerate the spacecraft. The manoeuvre was completed in just over a month, as planned.

Momentum Dumping

The momentum wheel speed was kept within its operating range of 4300 to 3800 rpm by periodically firing the appropriate pitch thruster to speed up the wheel. This manoeuvre was performed every two weeks, on a regular basis to minimize disruption to other activities. Normally, the attitude disturbance caused by the thruster firings was unnoticed by the communications experimenters. As noted earlier, thruster firings produced a distinctive motion from which detailed ACS/RCS performance could be ascertained using either telemetered data or observed SHF signal fluctuations.

North-South Station-keeping (NSSK)

There was no provision made for NSSK in the design of the spacecraft since it was intended to bias the initial inclination to 0.75°, then allow the inclination to drift through zero again to 0.75° during the two year mission. When the mission stretched beyond two years, the growing inclination became objectionable, requiring frequency repointing of the experiments' communications earth terminals. Since there was surplus fuel available, it was decided to reduce the orbit inclination from 0.8° to 0.0° from November 1977 to June 1978. The method involved firing a yaw thruster pair (see Fig. 5), in a manner such that the N-S components of thrust added while the E-W components and attitude torques cancelled.

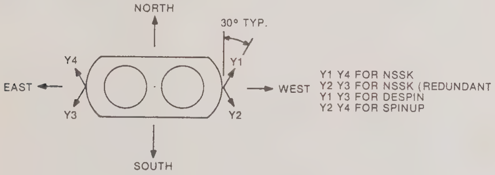

Fig. 5 Yaw Thruster Layout

Because of thrust level variations from pulse to pulse, the torque cancellation was not complete and measurable attitude errors resulted. Consequently the on-board roll control, which had been designed with a response appropriate for the normal disturbances encountered in the mission, was inhibited during these firings, and a specially-designed controller in a ground-based computer was used to control the yaw thruster firings as well as monitor and maintain roll control. The control of pitch was retained on board the satellite[9,17].

Battery Reconditioning

Immediately preceding and following each eclipse season, the batteries were subjected to one or more reconditioning cycles, with discharges carried down to about 0.9V per cell. In conducting this operation, the regular operating staff was augmented by a battery specialist and a spacecraft health team member. The battery specialist determined in real time the termination point of the discharge and, from the end voltage and discharge rates, calculated the recharge required. The spacecraft health monitor concentrated primarily on the thermal conditions, particularly in the discharge resistor area, and on the quality of the telemetered data.

Simulations and Training

Training of staff and debugging of programs prior to launch made use of a real-time interactive computer model resident in the central CRC computer. This model accurately reflected the kinematics and dynamics of the satellite as a rigid body through all phases of the mission following apogee motor firing. The model also simulated the satellite in regard to its reponse to commands and the transmission of telemetry data, simplified thermal responses, S-Band and SHF antenna patterns, etc. It was interfaced with a minicomputer which operated in real time for commanding and providing displays in the ground control station. It became a standard training tool throughout the mission for checkout of new procedures, training of dynamicists and duty controllers, etc.

Technology Tests

As part of the advanced technology experiments, certain operations involved non-standard attitude control conditions in order to investigate the flexibility of the solar array and the performance of the Attitude Control System. The experiments included firing of thrusters to excite various flexible body resonances; operating the momentum wheel outside its normal range and inhibiting the offset thrusters for long periods at different times of year to measure the structural damping and disturbing torques[11]. For these tests, formal procedures were generated, and checked with the real-time simulation before being used with the spacecraft. For all critical periods during the tests, extra coverage was provided by dynamics specialists and a spacecraft health team member.

Shutdown Configuration

Following a NESA-A anomaly described in a later section, all r.f. transmitters were automatically switched off after the arrays ceased tracking the sun and the battery voltages collapsed. The momentum wheel speed fell to zero, and within two weeks the satellite nutated into a flat spin, rotating at about 72° per minute. Owing to the low electrical dissipation it is estimated that the average internal satellite temperature fell below -75°C. This configuration is essentially identical to that planned for the end of the mission with the exception of the opening of a few additional relays as an added precaution against reactivation of the transmitters.

Major Malfunctions

General

The following malfunctions are addressed specifically in view of their impact on the Hermes operations and/or because of their important generic implications.

Failure of the Experimenters' Power Converter (EPC)

Four days into the first eclipse season, the EPC failed shortly after exit from an eclipse. It was concluded by a Materials Review Board that the failure occurred in the "fold-back" input current limiter due to a transient overstress condition. The transient was caused by one of the two series connected bus relays unaccountably opening and closing.

It was decided not to risk a switch-on of the redundant experiments power converter and its associated bus relays until after the investigations were complete, and at least until after the eclipse season was over. The first season was completed using the still-operative prime bus relays. Since the prime converter was inoperative, the SHF transponder and beacon were inactive during the remainder of the season. As mentioned previously, the operations at eclipse entry and exit were also modified to open and to close the bus relays by ground command.

Shortly after the 1976 spring eclipse season, the redundant power converter and the bus relay switches were commanded on successfully, and experimentation resumed. Entering the fall eclipse season, it was decided not to risk daily switching of the redundant converter and relays, so operations reverted to the mode used during the spring eclipse season. For the remainder of the mission, however, the redundant converter and relays were utilized. They operated satisfactorily throughout the following six eclipse seasons.

NESA-A

An anomaly of the NESA-A caused loss of satellite attitude pointing on seven occasions during the mission. The initial anomaly occurred during switch on of NESA-A following a sun interference, abruptly producing a full scale error signal. This output initiated an Automatic Failure Protection (AFP) mode which caused a 3° per minute rotation about the pitch axis and a moderate nutation cone. Manual firing of thrusters was required to re-orient the satellite, followed by a reconfiguration of the ACS/RCS system to re-activate the automatic on-board pitch and roll/yaw control loops. Since NESA-A was needed during periods of interference to NESA-B by the sun or moon, its use was continued in spite of its potential anomalous behaviour while minimizing the number of switchings.

Later in the mission, five spontaneous NESA-A anomalies of the same kind occurred when no switching was involved. Although the main RCS valves were automatically closed by AFP, pressurized gas remained in the hydrazine lines and the NESA-A abnormal output would, within 1-5 minutes after the anomaly, cause thruster firing as the pressure fell to zero. These firings caused nutation cones of up to 50° (25° half angle) and rotation about the mean pitch axis with rates up to 20° per minute. Recovery sequences involved commanded nutation damping, precessions, reduction of pitch rates, and ACS/RCS reconfiguration.

The fifth spontaneous NESA-A anomaly on 24 November 1979 introduced a 40° cone and a pitch rate of greater than 12° per minute. The direction of the cone and the sun declination angle were such that the field of view of the sun sensors on the solar arrays was exceeded. Consequently the arrays ceased tracking the sun and power was lost to the satellite, causing switch off of all of the SHF signals. With the feeble telemetry signals, it was impossible to obtain sufficient information to effect a recovery before the batteries discharged. Within hours after anomaly, the telemetry transmitter automatically switched off as the degraded batteries were completely discharged. At this point, the momentum wheel despun and no further control was possible since the satellite body rate increased to 720° per minute. Thereafter, the satellite motion finally transferred to a flat spin about the yaw axis with a rate of approximately 72° per minute.

Telemetry Transmitter

The Tracking, Telemetry and Command (TT&C) system S-Band transponder is described elsewhere[4]. Due to the vital nature of the TT&C, virtually complete redundancy was designed into the system, including the transmitters. Telemetered data however were not completely redundant between the two encoders, in order to obtain more data with the given encoder capacity. Transmitter A (Tx A) was used in the mission until completion of the attitude acquisition phase, and Tx B was planned for use throughout the on-orbit phase. About 4 months after launch, the output r.f. power level of the Tx B began to fall, although the effects were not obtrusive until 6 months into the mission. As the signal strength slowly decreased, continuous availability of telemetry data received directly at CRC from the satellite became questionable. In September 1976, it was decided to switch back to the previously-satisfactory Tx A to ensure reception of data throughout the eclipses. Unfortunately, Tx A failed completely after some further 30 hours of operation, forcing return of operations back to the degrading Tx B.

Subsequently, Tx B continued to degrade by about 3 dB each year, possibly because of surface radiation damage in the transistors of the output stages. Investigations suggest an interstage electrical connection also may have degraded due to thermal cycling, causing severe impedance mismatch. This degradation caused loss of drive to the transmitter output stages. It is possible this latter problem was responsible for the demise of Tx A.

Solar Array Implementation

During the third eclipse season it became impossible to switch on the Solar Array Technology instrumentation. Consequently some flexible solar array data such as temperatures, test cell voltages and currents, etc., were no longer available and satellite control loop experiments, planned to be conducted late in the mission, could not be carried out. A transient event counter, used for monitoring electrical transients such as might be caused by the discharge of static voltages on the satellite was also taken out of service by this problem. Fortunately sufficient data had been collected in over a year of operation to characterize the array behaviour for operational purposes.

Transmitter Experiment Package (TEP)

Twice during each of the first two eclipse seasons, while the SHF transponder was in use (i.e. 1977) temperatures in the TEP showed sudden abnormal increases which continued until the r.f. power output of the tube was decreased. An investigating board concluded that the temperature increases were due to depriming of arteries in the heat pipe thus drastically reducing the capability of the heat pipes to conduct heat away from the TEP[5]. The depriming was caused at least in part by freezing of the working fluid (methanol) due to shadowing of the heat pipes along the radiation fin by the spacecraft itself. Although the thermal design had taken into account shadowing during the solar eclipses, near the equinoxes, shadowing by the spacecraft body produced a much longer period without sunlight on the pipes.

There were no lasting effects observed and the heat pipes continued to reprime and function properly after each event. The effect on operations was to place a constraint on the power output of the TEP when telemetry data were not available. Since the pipes in the deprimed condition could still conduct away enough heat to maintain satisfactory temperatures if the r.f. output power did not exceed 115W, this limit was imposed during equinox periods when the anomaly was likely to occur. Subsequent to the institution of the operating constraints, no further thermal anomalies were observed.

III. Spacecraft Performance Summary

A complete summary of the first year's performance of Hermes is given by Raine[1]. Additional data obtained since the first year are presented here, and reference will be made to other publications which contain more detailed information.

Telemetry, Tracking and Command

The telemetry and tracking portion of this system already has been mentioned in the previous sections.

As for the command portion of the system, it has performed flawlessly throughout the mission. There were no verified incidents of commands not being executed when received by the satellite; or being executed when not required.

Thermal

There is some evidence of very minor degradation of thermal control surfaces. Quantitative data are difficult to extract because the heat dissipations are so dependent on the mode of operation, and because of lack of continuous data. Generally, in the areas controlled by second surface mirrors, the temperature excursions increased by 2° to 3°C, primarily over the last two years of the mission.

Power

The prime power sources behaved much as expected. The batteries performed adequately for the two year mission, but this resource had to be husbanded very carefully during the extended mission. Fig. 6 indicates the capacities obtained at the beginning of the reconditioning cycles. The solar arrays degraded predictably, with one exception, as shown in Fig. 7[7,8]. The sudden drop of 15% early in the mission was attributed to damage to wiring leading from several solar cell panels, possibly due to arcing arising from charge buildup on the array blanket. However the arrays were sized originally to provide power for additional experimental equipment that was not incorporated on the flight spacecraft due to weight constraints. Consequently, this loss had no impact on operations throughout the extended mission.

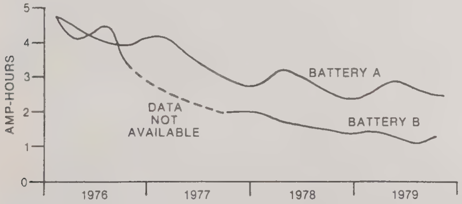

Fig. 6 Battery Capacity to 26.2 Volts

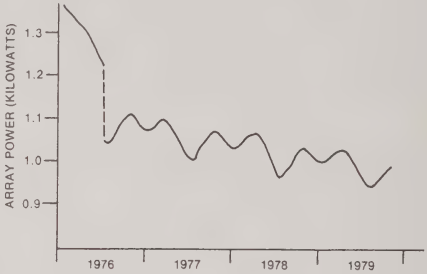

Fig. 7 Total Solar Array Power

Attitude Control System/Reaction Control System

A complete account of the performance history of the RCS, including the performance during the NSSK manoeuvres is described elsewhere[3,9]. Table 1 provides a summary of the fuel usage during the other major events. The ACS performance is described in other papers[1,10,11].

The prime pair of offset thrusters were used from the start of the mission until late in 1979, when one thruster stopped functioning. Gaps in the telemetered data made it difficult to assess the day-to-day performance. When switchover to the redundant pair of offset thrusters was made, the effects were immediately noticeable, since the numbers of daily thruster firings fell substantially.

Throughout the mission, thrust effectiveness of the low thrust engines appeared to degrade, with performance as poor as 50% of nominal, especially during the first few pulses after a period of inactivity. This effect has been attributed to entrapment of the nitrogen pressurant after it permeated through the tank diaphrams as the mission progressed or, to the presence of decomposed hydrazine. This underperformance was accommodated during the momentum dumps, moves, etc., by merely increasing the number of firing pulses; the on-board roll/yaw system automatically accommodated underperformance, by increased pulsing.

SHF System

The performance of the SHF transponder has been described previously[6,12,13]. Over the 3½ years, the nominal design limit of antenna steering of 13,300° was nearly reached on one antenna in one axis only, with no apparent degradation of the steering capability (see Table 3). After 20,000 hours of operation, 200W TWT performance continued to be nominal[13].

Table 3 Accumulated Antenna Steering

DIRECTION	200 WATT BEAM	20 WATT BEAM
East-West	12,400°	9,000°
North-South	4,600°	3,000°

The transponder remained essentially unchanged after 31,000 hours of operation. At the end of the mission, some of the redundant equipment was switched on, and the performance is summarized below:

a) Redundant 20W TWT - The performance was essentially unchanged after the 3½ years of storage in space. Both tubes exhibited similar anomalous trip-off characteristics following turn-on. The frequency of the trip-offs decreased with time, e.g., the redundant tube had 11 trip-offs in its two months of operation, seven of those in the first week.

b) Redundant SHF Receiver - This receiver had a conventional tunnel diode amplifier in the front end rather than the parametric amplifier of the prime receiver. Noise measurements confirmed the expected 3 dB difference in noise figure. The local oscillator in the redundant unit operated within 20 kHz of the frequency of the prime unit, after nearly four years of storage in space.

IV. Communications Experiments

Hermes was shared equally between DOC and NASA on an alternate day basis to permit communications experiments in the respective countries. The experimental programs in both Canada and the U.S. were completed on 30 June 1979. Canada continued with communications demonstrations until the end of the mission.

During the mission, a total of 38 experiments were performed in Canada. In addition, many demonstrations were conducted domestically while some involved other countries. Twenty-one transportable earth terminals ranging in size from 0.6m to 3m, as well as a fixed 9m terminal at CRC, were used in Canada, with the satellite. The types of experiments are indicated in Table 4. These experiments and the results are examined in more detail in other papers[13,14,15]. An early summary of the CTS U.S. experiments is also provided elsewhere[16].

Table 4 Canadian Hermes Communications Experiments

38 EXPERIMENTS	
23 SOCIAL	15 TECHNICAL
7 Tele-Education	3 Terminal Evaluation
3 Telemedicine	4 Data Modems
5 Community Interaction	2 Multiple Acces
4 Administration	1 Propagation
3 Radio/TV Broadcast	4 Precision Measurements
1 Direct TV Broadcast	1 Computer Communications

The Canadian experimenters were allocated use of the satellite transponders and a number of ground terminals for an agreed period of time by the experiments coordination group. In general, several experimenters shared the use of the transponders on any day. At the end of each scheduled experiment period, the corresponding experimental network was shut down and another experimental network in another part of the country was activated within the half hour allocated for satellite antenna steering, attenuator changes and ground terminal readiness checks. A wide variety of signal types such as TV, voice, data or high speed digital data were employed each day. To minimize the amount of antenna steering required to accommodate the various experimental scenarios, the daily program was arranged typically to "walk" westerly across the North American continent in general accordance with the time zones.

V. Conclusions

An outline of the Hermes mission has been described in which several of the operational problems have been outlined and their implications discussed. In general, the level of redundancy designed into the satellite was satisfactory and indeed many of the redundant circuits were never used. There are some areas where design improvements are indicated for future satellites in such areas as improved operational flexibility of control modes for the ACS, heater control, battery charge/discharge management, etc. However for Hermes, operational work-arounds were successfully devised to satisfy operational needs. The mission was terminated during a final communications demonstration. Owing to the advanced age of the satellite at that time, this was not unexpected.

With only one or two notable exceptions over limited periods, such as the EPC-A and TEP thermal anomalies, effects of anomalies on the satellite behaviour and its operational control were essentially unnoticed by the communications experimenters. As a result, there was a continuing demand to use Hermes for as long as possible. With the invaluable assistance of the NASA STDN network, these demands were met and the mission life almost doubled over the initially-planned period. Consequently, increased confidence has been gained in the use of 14/12 GHz communications systems and many user groups have gained experience in the application of this new technology.

Acknowledgements

The authors wish to acknowledge the significant contributions made by NASA toward the successful flight operations of Hermes. In addition, as is common with similar projects, a substantial team effort was required to ensure the success of the mission. This effort is gratefully acknowledged, with particular note of the support provided in battery management by J. Lackner of the Defence Research Establishment in Ottawa; by Dr. F. Vigneron and his team of dynamicists at CRC; and by SED of Saskatoon for operational assistance.

References

1. H.R. Raine, "The Communications Technology Satellite Flight Performance", Paper IAF 76-223, International Astronautical Federation, 27th Congress, Anaheim, California, 10-16 October 1976.

2. D.A. Bennett, "Ground Controlled Conversion of Communications Technology Satellite (CTS) From Spinning to Three-Axis Stabilized Mode", Paper 76-1928, AIAA Guidelines and Control Conference, San Diego, 16-18 August 1976.

3. V.J. Sansevero Jr. and H. Garfinkel, "Flight Performance of the Hydrazine Reaction Control Subsystem for the Communications Technology Satellite", AIAA/SAE 12th Joint Propulsion Conference, Palo Alto, California, 26-28 July 1976.

4. C. Baxter, "Design of an S-Band Transponder Providing Command, Telemetry Ranging and Range Rate Functions for Scientific Satellites", AIAA/CASI 6th Communications Satellite Systems Conference, Montreal, 8 April 1976.

5. R.E. Alexovich and A.N. Curren, "Thermal Anomalies of the Transmitter Experiment Package on the Communications Technology Satellite", NASA Technical Paper 1410, April 1979.

6. R.E. Alexovich et al., "Performance of the 12 GHz, 200 Watt Transmitter Experiment Package for the Hermes Satellite", Proc. of the 20th Symposium of the Royal Society of Canada, Ottawa, 29-30 November, 1 December 1977.

7. J.V. Gore, "The Flight Performance of the CTS Body Mounted and Deployable Solar Arrays", Baton Rouge Photovoltaic Specialists Conference, 15-19 November 1976.

8. T.D. Harrison, et al., "In-Orbit Characteristics of the Communications Technology Satellite Deployable Solar Array", Inter-Society Energy Conversion Engineering Conference, Tahoe, 12-17 September 1976.

9. V.J. Sansevero Jr., H. Garfinkel and S.F. Archer, "On Orbit Performance of the Hydrazine Reaction Control Subsystem for the Communications Technology Satellite", AIAA/SAE 14th Joint Propulsion Conference, Las Vegas, 25-27 July 1978.

10. F.R. Vigneron and R.A. Millar, "Flight Performance of the Stabilization System of the Communications Technology Satellite", Journal of Guidance and Control, Vol. 1, November-December 1978, pp 404-412.

11. F.R. Vigneron, "Dynamics, Control and Structural Flexibility Results from the Hermes Mission", in Astronautics for Peace and Human Progress, Acta Astronautica, Pergamon Press, 1979, pp 397-411.

12. W. Greiner and R. Bonhomme, "Implementation and In-Orbit Evaluation of a 14 GHz Parametric Amplifier", AIAA 7th Communications Satellite Systems Conference, San Diego, 23-27 April 1977.

13. R.W. Huck and J.W.B. Day, "Experience in Satellite Broadcasting Applications with CTS/Hermes", XIth International TV Symposium, Montreux, 27 May-1 June 1979.

14. N.G. Davies, J.W.B. Day, D.H. Jelly and W.T. Kerr, "CTS/Hermes - Experiments to Explore the Applications of Advanced 14/12 GHz Communications Satellites", in Astronautics for Peace and Human Progress (Acta Astronautica), Pergamon Press, 1979, pp 319-336.

15. N.G. Davies, "Communications Technology Satellite (Hermes) Experiments and ANIK-B Pilot Projects", Australian/Canadian Communications Satellite Workshop, Canberra, 22-24 August 1979.

16. P.L. Donoughe and H.R. Hunczak, "CTS (Hermes) - United States Experiments and Operations Summary", Proc. of the 20th Symposium of the Royal Society of Canada, Ottawa, 29-30 November, 1 December 1977.

17. E.A. McPherson, W.B. Graham and T.D. Harrison, "Design and Flight Performance of a Ground-Based Attitude Controller for North South Stationkeeping", Paper 14.2, Proceedings of the Canadian Conference on Automatic Control, Montreal, 23-25 May, 1979.

80-0580

30/20 GHz FIXED COMMUNICATIONS SYSTEMS SERVICE DEMAND ASSESSMENT

M. Westheimer*, R. B. Gamble*,
K. M. Speter*, and H. R. Seltzer**

International Telephone and Telegraph Corporation
New York, N.Y.

Abstract

This paper, based on a telecommunications traffic study performed by ITT for NASA, presents projections of voice, video and data traffic for the 1980-2000 time period. The projections are presented in terms of source-oriented units, peak hour traffic carried over long distance facilities, and traffic estimated to use satellite facilities. The volume of telecommunications traffic transmitted over long distance facilities is predicted to increase by a factor of five over the period studied. Traffic carried by satellite will increase at an even faster rate. Voice services will continue to account for the largest part of the overall demand for telecommunications services. However, due to economical and technical factors, the voice, video and data traffic carried over satellite facilities will all be of the same order of magnitude in the 1980-2000 time period. While none of the three services will dominate satellite transponder use, the relative mix will vary somewhat, with plurality of transponder use shifting from data services in 1990 to voice services in 2000. Based on projections of C and Ku band satellite system capacities, the satellite traffic demand may well exceed capacity by the end of the 1980s, necessitating implementation of 30/20 GHz satellite systems. An assessment is made of the demand elasticity as a function of availability and response time.

1. Introduction

This paper summarizes the results of a telecommunications traffic demand projection to the year 2000 performed by ITT for the NASA Lewis Research Center. The study is part of the initial phase of a five year NASA program to support communication satellite technology development, so that emerging telecommunications demands can be met.

Accordingly, particular emphasis is placed on long distance communications, on that portion of the demand suitable for satellite delivery systems, and on the potential role of 30/20 GHz systems in meeting the anticipated growth of demand.

2. Methodology

To establish a basis upon which voice, video and data traffic projections could be made in a clear and meaningful manner these three major service categories were further subdivided as shown in Table 1.

Table 1 - Service Categories

VOICE	VIDEO	DATA
Message Toll Service	Network TV (NTV)	Message Traffic
Business	Cable TV (CATV)	TWX/Telex
Residential	Videoconferencing	Facsimile
Wide Area Toll Service	Educational Video	Electronic Mail
Private Line Services	Health & Public Affairs	Character Oriented
Point-Point/Multipoint		Image Oriented
Switched		Computer Traffic
Foreign Exchange (FX)		Terminal/CPU
Telpak		CPU/CPU
		Narrowband Teleconfg.
		Image Mode
		Character Mode
		Freeze Frame TV

The resulting subcategories reflect technical and operational similarities and are compatible with usual groupings of market and traffic data presentation.

In the voice categories, Private Lines include foreign exchange (FX) lines, private switched networks such as Common Control Switched Arrangements (CCSA), and bulk point-to-point channel offerings such as Telpak.

Narrowband teleconferencing, including freeze-frame video service, was grouped under Data since, it can be carried over ordinary voice equivalent lines, digital or analog. Videoconferencing was assumed to involve full motion. Slow motion video was not considered as a viable offering.

Traditional facsimile traffic, while technically part of electronic mail, was grouped separately because of current baseline data availability.

---

* Advance Planning Department, U.S. Telephone and Telegraph Corporation, a subsidiary of ITT, New York, N.Y.

** ITT Telecommunications Technology Center, Stratford, CT.

Copyright © American Institute of Aeronautics and Astronautics, Inc., 1980. All rights reserved.

Baseline traffic demand within these groups was obtained from a large variety of sources in the public domain, including FCC and other government publications, industry association data, educational institution statistics, business travel statistics and corporate annual reports. Study reports, market research reports and internal ITT information were reviewed and analyzed to establish a 1976-1980 baseline and short term traffic projections. These efforts were supplemented by several hundred interviews within user groups, industry and trade associations, government and regulatory agencies and market research firms.

For the more mature services (primarily the voice services) an analysis was made of demographic, economic and traffic data to establish valid correlation factors. Correlating demographic and economic trends were then used to project telecommunications traffic. These projections were adjusted for the impact of regulatory trends such as those emphasizing the growing use of private leased lines and networks.

For newly developing services and those undergoing rapid functional and technical changes, projections were adjusted for the impact of such business factors as document flow, travel replacement and the growing substitution of electronics for the filing and transmitting of hard copy.

For all service projections, the impact of technological trends on the nature of services offered and on traffic volume was considered.

The voice, video and data traffic projections presented in this paper are given at three levels:

1. Source Traffic, representing the volume of unprocessed, voice, video and data information. Given in units applicable to the terminal used.

2. Long Distance Traffic, representing the traffic transmitted 200 miles or more in the busy hour of the day. Given in terms of the total bit rate which must be handled by the long distance facilities in the busy hour.

3. Satellite Traffic, representing that portion of Long Distance Traffic estimated to use satellite facilities. Given in busy hour bit rate and equivalent digital transponders.

The first level of traffic projections (Source Traffic) is given in terms of user oriented units. For the voice services, call volume and the number of private lines serve as basic units. For the video services, channels irrespective of channel bandwidth are used where these are dedicated (e.g. Network and Cable TV, Educational Video). Where usage is shared (e.g. Videoconferencing, Health and Public Affairs) total annual usage rather than channels is the measure employed. For the data services, yearly bit volume generated at the source terminal is used as the traffic measure. This is derived from estimates of terminal population and usage factors.

For all three services a distance factor is used to eliminate the short haul portion of the traffic which is generally not a candidate for satellite transmission.

At the second level of traffic projections, (Long Distance Traffic) transmission efficiency factors, signal coding and compression and other means of concentration are applied to the source traffic to obtain the traffic carried over long distance facilities. Since, during the time frame of this forecast the current analog transmission and switching facilities will be increasingly replaced by those using digital techniques, a conversion to common units, terabits (10^{12} bits) per year is made to permit a comparison of the various segments of traffic based on the amount of transmission capacity they require.

Because transmission channel requirements are based on maximum (peak) traffic rather than yearly volume, peak factors are applied to give busy hour traffic in terms of terabits/second in the peak hour.

At the final level, (Satellite Traffic) the share of traffic using the satellite medium is estimated. Satellite transponder requirements are projected, assuming the use of digital transponders throughout the forecast period, and taking into account improvements in information bits per analog spectrum bandwidth (bits/Hz) of digital satellite transponders during the time frame of this study.

The estimates of C and Ku band satellite systems capacity are based on most likely orbital spacings and antenna beamwidth for satellites operating in these bands. The time frame when a new generation of Ka band satellites must be introduced to satisfy the traffic demand is obtained by a comparison of the demand in terms of satellite transponders with the projected capacity of C and Ku band systems.

3. Traffic Projections

Source Traffic

Voice

The growth in voice traffic is shown in Table 2. The values shown include an allowance for traffic generated by unsuccessful call attempts. Average call holding time increases with time and is of the order of 6 minutes for Message Toll Service (MTS) and 7 minutes for Wide Area Toll Service (WATS).

Table 2 - Voice Service Demand - Basic Units
(Greater than 200 Miles)

	1980	1990	2000
MTS Residential (call-sec. x 10^9)	634	1540	2950
MTS Business (call-sec. x 10^9)	686	1800	3920
WATS (call-sec. x 10^9)	1250	2880	4470
Private Lines (duplex lines x 10^3)	57	150	357

Average annual growth in long distance MTS usage is projected at approximately 10% in the first projected decade, and 8% in the second. Although residential telephones exceed business telephones, business accounts for the larger share of MTS LD calls.

WATS message growth of approximately 9% in the first decade and 4% in the second and the nearly 10% average annual growth for private lines reflect a shift from shared to leased facilities.

MTS accounts for 51% of non-private line voice services in 1980, 54% in 1990 and 61% in 2000. The increased MTS share in 2000 is due primarily to greater use of leased line services at the expense of WATS.

Video

Video service projections are shown in Table 3.

Table 3 - Video Service Demand - Basic Units
(Greater than 200 Miles)

	Units	1980	1990	2000
Network TV	Video Channels	10	12	16
CATV	Video Channels	35	50	60
Videoconferencing	Videoconference-Hrs. per year	10 x 10^3	1660 x 10^3	6200 x 10^3
Educational Video	Video Channels	15	165	500
Health & Public Affairs	Video Channel-Hrs per year	0	52 x 10^3	104 x 10^3

In 1980, Network TV (NTV) and Cable TV (CATV) are the largest users in the group. Whereas NTV and CATV can be considered mature services with a moderate annual growth rate, a much more rapid growth rate is foreseen for Videoconferencing and, to a lesser degree, Educational Video and Health & Public Affairs. NTV, CATV and Educational Video channels generally use dedicated facilities, whereas Videoconferencing and H&PA are characterized by random or occasional usage, subject to peaking during busy period. Annual channel demand is therefore given in terms of "video channels" (without specific bandwidth connotation) in the first group and channel usage time in the second. By 1990 Videoconferencing and Educational Video will be the most important video services with Health & Public Affairs showing substantial growth as well. This trend is seen to continue to 2000.

Data

Projections for data traffic generated by the terminals are shown in Table 4 in terms of terabits (10^{12} bits) per year.

Table 4 - Data Services Traffic Demand - Base Units
(Bits per Year x 10^{12}, 200 Miles or More)

	1980	1990	2000
MESSAGE TRAFFIC			
TWX/Telex	0.7	0.7	0.4
Facsimile	40	351	1092
Electronic Mail-Image	0	2700	2520
Elect. Mail-Character	0	180	672
TOTAL MESSAGE TRAFFIC	41	3232	4284
COMPUTER TRAFFIC			
Terminal/CPU	165	530	1360
CPU/CPU - Distrib. Proc.	8	70	680
CPU/CPU - E.F.T.	1	12	23
TOTAL COMPUTER TRAFFIC	175	612	2063
NARROWBAND CONFERENCING			
Image Mode	1	42	104
Character Mode	Negl.	0.2	1.8
Freeze Frame TV	8	320	968
TOTAL NARROWBAND/ TELECONFERENCING	9	362	1074
TOTAL TRAFFIC DEMAND	224	4206	7421

Baseline data is obtained in terms of the quantity of information to be transferred (for example, by estimating the number of documents to be transferred by electronic mail and the number of bits necessary to accomplish this transfer by image and character mode transmissions). Projections are then made using a variety of techniques specific to each of the categories and subcategories investigated.

From the source traffic point of view, image-oriented electronic mail predominates in 1990 and 2000, followed by computer traffic, particularly terminal/CPU traffic. The decline of image-oriented electronic mail traffic in the last decade represents a shift to character-oriented electronic mail and to improved coding techniques.

For a valid interpretation of the share of the total data traffic represented by each of the data services shown in Table 4, it must be remembered that the figures represent bits generated at the source, and do not include the inefficiency inherent in most forms of data transmission. The appropriate correction for this inefficiency is considered at the next level of projections given below.

Long Distance Traffic

The traffic carried over long distance transmission facilities may differ in form and quantity to that generated at the user terminal. The long distance traffic is therefore determined by applicable adjustments for analog/digital conversion, compression due to coding, concentrating and multiplexing, or, in the case of data terminals, expansion due to the inefficiency of operating key terminals on dial-up voice lines. In addition, the source traffic, given in yearly volume is converted to peak hour traffic at this level since transmission facility requirements are dictated by peak rather than average traffic.

Long distance traffic, whether analog on digital at the source, is presented in equivalent digital form, conforming with the trend towards digital transmission and switching techniques.

Voice

Duplex circuits required to carry the MTS, WATS and private line traffic volume are shown in Table 5.

Table 5 - Voice Service Demand - Millions of Peak Hour Duplex Circuits (Greater than 200 Miles)

	1980	1990	2000
MTS Business & Residential	0.11	0.28	0.59
WATS	0.18	0.41	0.63
Private Line	0.06	0.15	0.36
TOTAL	0.35	0.94	1.58

Annual traffic is converted to peak hour traffic using peak/average ratios of 3.1 for MTS and WATS. Private lines must be available to carry traffic at all times and are therefore assigned a peak/average ratio of 1.0. Circuit requirements are obtained using a grade of service (share of unsuccessful calls, excluding customer busy) of .003 for toll trunks, equivalent to an end-to-end grade of service of .01. The equivalent digital peak hour traffic, obtained by assuming a 64 Kilobits/Second (Kbps) voice digitization rate, is shown in Table 6. This rate is standard in the digital T-carrier equipment in growing use today. The same standard was assumed for the entire time period of this study.

The total voice data and video traffic during the business peak hour (day time) exceeds that which occurs in the residential peak hour (evening). Therefore the residential traffic component shown in Table 6 is that which occurs during the business peak hour.

Table 6 - Busy Hour Voice Traffic

	Traffic Rate During Busy Hour - Megabits/Second		
	1980	1990	2000
MTS Business	12,600	33,000	72,000
MTS Residential	1,100	2,700	5,300
WATS	23,000	53,000	82,100
Private Lines	7,300	19,200	45,700
TOTAL	44,000	107,900	205,100

Video

The analog spectrum bandwidth or the equivalent digital bit rate required to represent a full motion color video image varies considerably with the quality of the received image and the degree of sudden motion to be transmitted. Because of the generally low sudden motion content of video scenes, standard transmission of such scenes includes a substantial amount of redundant information. The 6 Megahertz (MHz) analog bandwidth or its equivalent digital 42 Megabits/Sec. (Mbps) rate can therefore, in most cases, be reduced without unacceptable loss of quality.

To compute the peak hour digital traffic contributed by the five video services shown in Table 3, compression ratios based on current and projected technology and shown in Table 7 are applied to the basic digital rate of 42 Mbps per video channel.

Table 7 - Projected Video Compression Ratios(1)

Service	1980	1990	2000
Network TV	1:1	1:1	2:1
CATV	1:1	2:1	3:1
Videoconference	1:1	6:1	7:1
Educational Video	1:1	6:1	6:1
Health and Public Affairs	1:1	5:1	7:1

(1) Relative to a basic rate of 42 Mbps for a simplex full video channel.

Some of the values shown, represent weighted average mixes of various quality requirements. The highest compression taken as part of this mix is 14:1, representing a nominal 3 Megabits (Mbps) per second digital rate, which can be carried over two T1 lines of 1.544 Mbps each.

In addition, peak factors of 2.66, representing the peaking of traffic during certain hours due to operational factors and time zone differences are applied to the Videoconference and Health & Public

Affairs services. The remaining video services are considered to operate over leased or private channels, available on demand. The peak factor for these services is therefore 1.0.

The resulting peak hour video traffic demand is shown in Table 8.

Table 8 - Busy Hour Video Traffic

	Traffic Rate During Busy Hour - Megabits/Second		
	1980	1990	2000
Network TV	400	500	300
CATV	1,500	1,000	800
Videoconference	400	10,300	33,000
Educational	600	1,200	3,500
Health & Public Affairs	0	200	300
TOTAL	2,900	13,200	37,900

Network and Cable TV, predominant in 1980, account for only 12% of the total digital peak hour demand in 1990, and, because of slow growth relative to other services and application of compression techniques, 3% in 2000. Videoconferencing emerges as the dominant video service with 78% of the total peak hour video demand in 1990 and 87% in 2000. Without the effect of peaking during the busy hour, i.e. on an annual traffic volume basis, videoconferencing accounts for 49% of the annual video demand in 1990 and 64% in 2000. The fact that videoconferencing represents such a high share of the annual and peak hour video LD traffic in spite of the high degree of compression highlights its importance as a major video service in the 1990-2000 period.

Data

Since the information carried by data traffic is inherently in digital form, conversion of source traffic to LD traffic requires only that appropriate efficiency factors be applied. These factors, accounting for the ratio of the amount of information to the communications capacity required to transfer that information, will differ for each of the data services and are shown in Table 9.

In many cases, particularly those involving keyboard terminals accessing computers through dialup voice lines, the efficiency is quite low because of human interaction times. Thus communication links capable of transferring thousands of bits per second may actually transfer information at rates averaging only a few bits per second because the channel is usually reserved full time for the period of the session whether or not data is actually being transferred. The consequent very large multiplication of the service demands due to this inefficiency has been reflected in the 1980 demand estimates.

Table 9 - Data Services Efficiency Factors

Service	1980	1990	2000
TWX/Telex	.01	.1	.2
Fascimile	.15	.2	.25
Electronic Mail-Image	---	.5	.5
Electronic Mail-Character	---	.4	.4
Terminal/CPU	.0015	.002	.0035
CPU to CPU-Dist. Proc.	.007	.01	.02
CPU to CPU-EFT	.1	.2	.4
Teleconference-Image	.25	.25	.25
Teleconference-Character	.25	.25	.25
Freeze Frame TV	.5	.5	.5

Recent techniques such as packet switching, can improve efficiency by factors on the order of 100 to one. By 1990 an estimated one-third of the terminal/CPU applications will benefit by such highly efficient facilities and an estimated 60% by the year 2000. Even with such substantial use of packet switching, or other relatively efficient means, the overall efficiency of data traffic remains low throughout the forecast period.

The annual long distance data traffic, obtained by applying the efficiency factors to the source traffic of Table 4 is shown in Table 10.

Table 10 - L.D. Data Traffic (Greater Than 200 Miles)
Thousand of Terabits Per Year

	1980	1990	2000
MESSAGE TRAFFIC			
TWX/Telex	Neglig.	Neglig.	Neglig.
Fascimile	0.3	1.7	4.4
Electronic Mail	*	5.9	6.7
TOTAL MESSAGE TRAFFIC	0.3	7.6	11.1
COMPUTER TRAFFIC			
Terminal/CPU	110.0	265.0	389.0
CPU/CPU	1.2	7.0	34.1
TOTAL COMPUTER TRAFFIC	111.2	272.0	423.1
NARROWBAND TELECONFERENCING			
Image & Character Mode Support	Neglig.	0.2	0.4
Freeze Frame TV	Neglig.	0.6	1.9
TOTAL NARROWBAND/TELECONFG.	Neglig.	0.8	2.3
TOTAL DATA TRAFFIC DEMAND	112	280	437

* 1980 Electronic Mail included in other traffic subcategories.

Because of the inefficiencies inherent in terminal/CPU/voice grade line operation, the computer traffic category becomes the dominant component of annual LD data traffic. The fact that Message Traffic, which at the source data traffic level represents 77% of data traffic generated in 1990 and 58% in 2000 represents less than 3% of LD data traffic in that time period, is indicative of the effect of packet switching and similar techniques on network utilization.

Table 11 shows the data traffic rate during the busy hour.

Table 11 - Busy Hour Data Traffic

	Traffic Rate During Busy Hour-Mbits/Sec.		
	1980	1990	2000
MESSAGE TRAFFIC			
TWX/Telex	13	1	21
Facsimile	49	325	809
Electronic Mail - Image	*	500	467
Electronic Mail - Character	*	52	104
TOTAL MESSAGE TRAFFIC	62	878	1,401
COMPUTER TRAFFIC			
Terminal/CPU	20,400	49,100	72,000
CPU/CPU - Distrib. Proc.	164	972	4,720
CPU/CPU - EFT	1	6	5
TOTAL COMPUTER TRAFFIC	20,565	50,078	76,725
NARROWBAND TELECONFERENCING			
Teleconference Support - Image	1	35	87
Teleconference Support - Character	21	21	1
Freeze Frame TV	4	148	449
TOTAL N.B. TELECONF. TRAFFIC	26	204	537
TOTALS (rounded)	20,600	51,100	78,800

*Included in other components of data traffic.

Peak factors in the data services vary from the 2-3 range in those generally low urgency services, such as CPU/CPU, which are frequently able to utilize communications factilities outside of normal business hours, to the 4-5 range in those services in which demand inherently peaks due to working hour and time zone factors. Although the Terminal/CPU peak hour traffic share drops from 99% in 1980 to 91% in 2000 it is clear that network sizing and channel requirements are practically determined by Terminal/CPU traffic considerations only.

Satellite Traffic

The source traffic demand and busy hour LD traffic represent total demand for long distance communications in the United States. This traffic will be carried over many types of terrestrial and satellite facilities.

For the purpose of projecting satellite market penetration percentages it is assumed that satellite system cost and reliability compare favorably with those of terrestrial modes of long distance communications. As part of the overall K_a satellite program, NASA has awarded system study contracts to investigate the cost and reliability problem further.

Although the large investments in existing terrestrial plant facilities tend to slow the widespread utilization of satellite communications, the projected quintupling of total demand over the next two decades cannot be accommodated without making substantial use of the high capacity potential and flexibility of demand assignment available through satellites.

The demand pressure, and the distance insensitivity of satellite communications which opens the possibility of pricing strategies very attractive to certain classes of users, generally encourage satellite transmission and favor increased capture of communications traffic by this transmission mode. However, with respect to each of the services discussed in this paper, the satellite medium presents special characteristics, some favorable and some unfavorable, which influence the fraction of total traffic likely to be sent over satellite facilities. These special characteristics are reflected in arriving at the estimated capture ratios shown in Table 12.

Table 12 - Percent Capture By Satellite

	1980	1990	2000
Voice	2	15	25
Video	50	60	60
Data	1	50	60

These capture ratios are applied to the peak hour traffic shown in the first column of Table 13 to obtain the peak hour satellite traffic rate shown in the second column of the table.

Projections of digital throughput rate for transponders with an equivalent spectrum bandwidth of 36 MHz are shown in the third column of Table 13. The 1.2 bits/Hz represented by the 1980 value represents a conservative current state-of-the-art estimate, with improvements to 2 bits/Hz in 1990 and 3 bits/Hz in 2000 expected to be feasible through the use of advanced modulation techniques. The resulting projection for equivalent digital transponders is given in the last column.

Table 13 - Required Satellite Capacity

	Busy Hour Traffic Rate Mbits/Second Total	Busy Hour Traffic Rate Mbits/Second Satellite	Transponder Throughput Capacity (Mbits/Sec.)	Required Equivalent Digital Transponders
1980				
Voice	44,000	880	42	21
Video	2,900	1,450	42	35
Data	20,600	210	42	5
TOTAL	67,500	2,540	42	61
1990				
Voice	107,900	16,190	72	225
Video	13,200	7,920	72	110
Data	51,100	25,550	72	355
TOTAL	172,200	49,660	72	690
2000				
Voice	205,100	51,280	108	475
Video	37,900	22,740	108	210
Data	78,800	47,280	108	438
TOTAL	321,800	121,300	108	1,124

The projected total satellite demand, superimposed on a plot of projected available C and K_u band orbital transponder capacity shown in Figure 1, indicates a capacity problem by 1989. If the improvements in transponder digital throughput rate shown in Table 13 fail to materialize, the most probable year in which C and K_u band systems will become saturated advances to 1987. For either event, the need for new satellite technology prior to the decade of the 1990s is evident.

Fig. 1 - Required Transponders vs. C and Ku Capacity

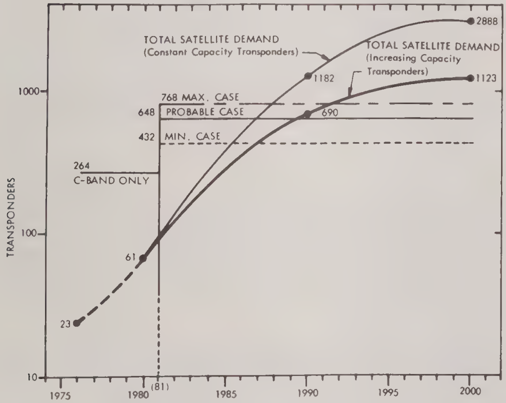

4. Availability and Delay Impacts

K_a band satellite systems offer a potential solution to the transponder saturation problem. However, K_a systems would present substantial rain outage problems. For this reason the impact of circuit availability and delay factors on demand was considered in the present studies. The ranges of availability investigated relate to expected 30/20 GHz satellite link performance and are shown in Table 14.

Table 14 - Typical Reliability Performance

Availability (Percent)	99.99	99.9	99.5	99.0
Aggregate Outage (Hours per Year)	0.9	9	44	88
Typical Frequency (Outages per Year)	11	35	105	175
Typical Duration (Minutes)	5	15	25	30

Availability

The investigations show that for all three service groups a fairly clear dividing line exists at the 99.9% availability level as shown in Table 15. Whereas in 1990 and 2000 89% of users questioned will accept the service at "same cost" i.e. at cost comparable to other transmission modes, 96% would accept it at a lower cost. At 99.5% availability the service is virtually unacceptable with acceptability of only 7% at same cost rising only to 22% given a lower cost for the K_a service.

Table 15 - Summary
Percent Acceptable vs. Availability

	Demand Terabits/Yr.	99.99% Same Cost	99.99% Less Cost	99.9% Same Cost	99.9% Less Cost	99.5% Same Cost	99.5% Less Cost	99.0% Same Cost	99.0% Less Cost
1980									
Voice	559,000	100	100	96	100	6	23	0	10
Video	83,000	82	90	38	55	2	13	0	0
Data	112,000	99	100	70	90	20	30	0	20
TOTAL	754,000	98	99	86	94	8	23	0	8
1990									
Voice	1,401,000	100	100	96	100	6	23	0	10
Video	171,000	91	94	57	69	2	14	0	0
Data	280,000	100	100	71	90	21	31	2	21
TOTAL	1,852,000	99	99	89	96	8	23	3	11
2000									
Voice	2,893,000	100	100	95	100	5	22	0	10
Video	418,000	97	98	65	76	3	16	0	0
Data	437,000	99	100	71	90	20	30	1	20
TOTAL	3,748,000	99.5	99.8	89	96	7	22	1	10

The availability requirements for video appear to be somewhat more stringent than those for voice and data, as shown in the table.

Real Time vs. Delayed Delivery

Because rain outages may force delays in delivery of nonreal time traffic carried over K_a band systems, the percentages of real time and deferred demand for the three categories was investigated (see Table 16). As expected, voice demand is virtually 100% in the real time category. Only 7-8% of the video demand would tolerate outages of the order of hours and 13-16% would tolerate one-day delays. The outage tolerant traffic represents primarily the off-line video program transmission market.

Table 16 - Summary
Percent Real-Time vs. Deferred Traffic Demand

	Demand Terabits/Yr.	Real Time	Deferred		
			Minutes	Hours	One-Day
1980					
Voice	559,000	100	0	0	0
Video	83,000	53	0	14	33
Data	112,000	60	20	20	0
TOTAL	754,000	89	3	5	4
1990					
Voice	1,401,000	100	0	0	0
Video	171,000	76	0	8	16
Data	280,000	59	20	20	1
TOTAL	1,852,000	91	3	4	2
2000					
Voice	2,893,000	100	0	0	0
Video	418,000	80	0	7	13
Data	437,000	58	20	20	2
TOTAL	3,748,000	93	2	3	2

COSTS DECREASE →

In the data category slightly less than 60% of the requirements are real time, 20% can tolerate delays of minutes, and 20% delays of hours. Delays of one day are acceptable to a negligible percentage of individuals interviewed.

5. Conclusions

Demand for telecommunications in general, and for satellite communications in particular, will increase by substantial factors over the next two decades. Voice services over this period will continue, by wide margins, to account for the largest part of overall demand for telecommunications services. However, due to economic and technical factors, the satellite captured demand for voice, video, and data services will all be of similar magnitude in the 1980 to 2000 time frame.

New communications facilities should be designed to achieve levels of reliability at least equal to typical present day facilities, but need not be appreciably better in order to be effective. While some traffic can be deferred to off-peak hours, the bulk of the traffic projected will require real-time transmission capabilities and future designs should reflect this division of traffic.

The capacity of the C and K_u satellite bands to handle the projected demand is limited and is likely to be exceeded by the 1990s. Steps necessary to introduce new satellite technology, and to develop the 30/20 GHz band for commercial transmission, should be taken in time to respond to the emerging demand forecast in this study.

It should be noted that the saturation time frame for C and K_u band facilities is sensitive to a number of variables which require close monitoring. Among these are:

- Actual growth in numbers and bit rate capacity of C and K_u transponders.
- Growth of packet switch plant as it affects efficiency of data traffic.
- Fiber-optics technology.
  - (a) As a means of extending, trunking satellite systems to users.
  - (b) As an alternative to long haul satellite transmission.
- Growing sophistication of voice encoding equipment.
- Availability of low-cost echo cancellers.
- Energy shortage impact on travel.
- Frequency re-use technology for C and K_u band systems.

80-0583

MULTIGIGABIT SATELLITE ON-BOARD SIGNAL PROCESSING*

W. Morris Holmes, Jr.
Advance Systems Engineering Director
for Communication Systems
Space Systems Division
TRW Inc.

Abstract

The satellite communication system described provides communications for very small and very large (trunking) users. Independent combinations of FDMA and TDMA are used in the uplink and downlink designs to minimize terminal costs. Signal routing for small users is accomplished by a digital store-and-forward technique which greatly simplifies the terminal receiver, compared to satellite-switched TDMA. Different processing techniques are used for very high data rate users, but complete interconnectivity between all users is maintained. This avoids double-hop routing with excessive transmission delays.

Introduction

A NASA LeRC funded 30/20 GHz Mixed User Architecture study has resulted in a baseline system design for cost-effective communications in the years 1990 to 2000. Generation of a useful mixed user TDMA architecture has required a broad overview of system characteristics.

The TRW 30/20 GHz Baseline System consists of a synchronous orbit satellite, 18 large trunking terminals with 12 meter apertures and 10 km space diversity, 25 to 30 small trunking terminals with 6 meter apertures and 10 km space diversity, several thousand inexpensive customer-premises-services (CPS) terminals, and a master control station with at least one alternate master control station.

The CPS terminal low-cost design offers the greatest challenge in the 30/20 GHz communication system. Since the number of CPS terminals is very large, the terminal direct cost is a large (perhaps the largest) element of system cost. The CPS terminal performance drives the satellite design, and hence determines a second major system cost element. Because the CPS system is able to avoid using terrestrial signal distribution and routing, and the charges associated with these functions, the CPS system also represents the largest economic value element of the system.

Discussion

A previous paper (Reference 1) presented the system overall concepts, and described the on-board routing and fixed beam antenna coverage. This paper will present some additional features which make the system especially efficient in serving the CPS terminals.

The satellite (Figure 1) is a 6000 pound, 4500 watt, 3-axis stabilized synchronous-orbit-design. This is large, but well within projected launch vehicle capabilities for the operational time period. A major feature of this system design is a maximum capability satellite to allow minimum requirements in the CPS terminals. This is a clearly cost-effective approach in a system with several thousand CPS terminals.

Several techniques are used to simplify the ground terminal. These include:

1. Provide high satellite EIRP and G/T to minimize terminal EIRP and G/T requirements.

2. Provide adaptive independent uplink and downlink error-correction coding to further reduce terminal EIRP and G/T requirements by 10 dB.

3. Provide satellite on-board routing supported by a master control station to efficiently utilize system capacity without complex hardware at the CPS terminals.

4. Provide external logic support to CPS terminals for operation and maintenance with infrequent scheduled visits by maintenance personnel.

5. Provide a standard 24-voice-channel DS-1 interface with individual channel routing within the system.

The satellite uses twelve-foot aperture antennas. These are close to the maximum size that can be stowed inside the Shuttle bay using a solid reflector. This is not a hard limitation since we have demonstrated the ability to deploy larger antennas with adequate surface accuracy on the TDRSS program, but twelve-foot diameter is also considered a good choice for reasonable system complexity. The full antenna gain capability of the large reflectors is utilized both at 30 and 20 GHz for uplink and downlink respectively. A fixed beam system described in Reference 1 covers high density areas and scanning beams cover the remaining areas in the forty-eight contiguous states. Separate fixed spot beams may be used for Hawaii and Alaska coverage.

The system block diagram (Figure 2) is relatively complex. Satellite Switched Time Division Multiple Access (SSTDMA) is used for routing trunking users. The SSTDMA switch, upconverters, downconverters, preamplifiers, and RF power amplifiers associated with the SSTDMA service are at the top of the block diagram.

The processing section in the lower two-thirds of the block diagram consists of preamplifiers, downconverters, FDM demultiplexers, demodulators, buffers, a processor, modulators, FDM multiplexers, and RF power amplifiers. There is also a box in the lower right-hand corner labeled "Adaptive FEC coding and decoding." FEC stands for forward-error-correction. This box reduces terminal EIRP and G/T requirements by 10 dB, by providing 10 dB better uplink and downlink performance independently when rain occurs at a CPS terminal.

---

*This paper reports work contracted under Contract NAS3-21933 sponsored by NASA Lewis Research Center.

Released to AIAA to publish in all forms.

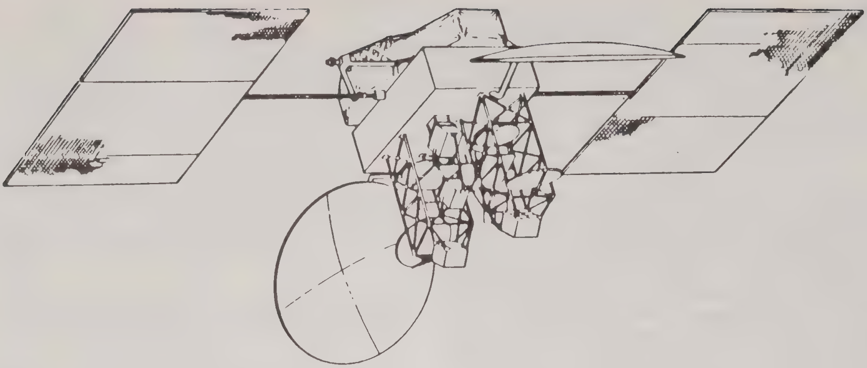

Figure 1. Satellite Design

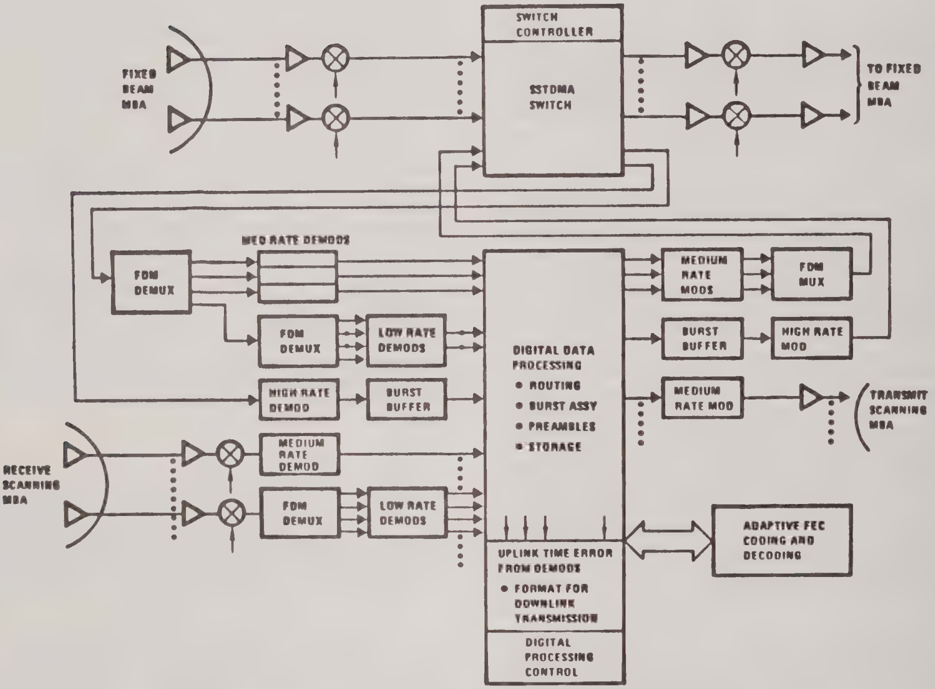
SWITCH CONTROLLER
FIXED BEAM MBA
SSTDMA SWITCH
TO FIXED BEAM MBA
MED RATE DEMODS
FDM DEMUX
MEDIUM RATE MODS
FDM MUX
FDM DEMUX
LOW RATE DEMODS
BURST BUFFER
HIGH RATE MOD
DIGITAL DATA PROCESSING
• ROUTING
• BURST ASSY
• PREAMBLES
• STORAGE
HIGH RATE DEMOD
BURST BUFFER
MEDIUM RATE MOD
TRANSMIT SCANNING MBA
MEDIUM RATE DEMOD
RECEIVE SCANNING MBA
FDM DEMUX
LOW RATE DEMODS
ADAPTIVE FEC CODING AND DECODING
UPLINK TIME ERROR FROM DEMODS
• FORMAT FOR DOWNLINK TRANSMISSION
DIGITAL PROCESSING CONTROL

Figure 2. Satellite Communication Subsystem Block Diagram

The 10 dB coding improvement actually consists of 5 dB increase in channel Eb/No due to changing to a rate 1/3 coding format without changing channel signaling rate, and 5 dB of coding gain. Individual terminals require rain protection very seldom, provided that several dB of clear-weather system margin is provided. Furthermore, rain protection requirements at different terminals are generally uncorrelated statistically, since large RF rain-loss conditions are caused by physically-small intense rain cells.

Since rain protection is used infrequently, the average channel signaling rate need not be increased. When a terminal requires rain protection the burst length for that terminal is increased by a factor of three on both the uplink and downlink. This requires revision of the system TDMA burst allocation plan, and perhaps revision of the beam scanning plan. This is not considered a problem since flexibility and rapid revision capability are already required for rapid demand channel routing. The factor-of-three burst-length increase provides 10 log (3) or 4.8 dB better ability to combat channel degradation.

Soft-decision Viterbi-algorithm decoding provides another 5.2 dB coding gain for a complete 10 dB channel degradation capability. The CPS terminal downlink decoder need only operate on the buffered data intended for that terminal. This will usually be about 1.0 Mbps or less. The satellite uplink decoder is more difficult since it must handle TDMA bursts from several terminals and store intermediate results while time-sharing between data streams.

One other concern that must be addressed is the circuit delay introduced or removed when switching to and from coded operation. On some circuits (voice) this may be accepted as a "glitch" since it will occur very infrequently. On critical circuits with very low error rate requirements either buffer delay-compensation or burst outage restoration coding may be needed.

While independent uplink and downlink adaptive FEC coding will represent a difficult technical task, the payoff of 10 dB reduction in both EIRP and G/T for several thousand DTU terminals makes it very attractive.

Satellite on-board routing utilizes a one-frame store-and-forward algorithm to provide complete routing flexibility for each of the 30,000 sixty-four kilobit channels in the processing data throughput (Reference 1). The on-board routing algorithm is supported by a master control terminal computer which modifies the algorithm to meet routing requirements on a demand basis. Figure 3 is a timeline for establishing a new channel between any two operating terminals in the system. Less than 1.5 seconds are required, allowing individual channels to be requested by an individual telephone ultimate user without noticeable delay from the satellite demand allocation process.

Terminal timing is fully synchronous. This is a departure from current satellite TDMA system design that is made attractive by the satellite demodulation and remodulation process. Since there is only one downlink carrier and data clock, that derived from the satellite frequency standard, the CPS terminal can use simple narrowband phase-lock-loop (PLL) techniques rather than high bandwidth rapid-acquisition demodulators currently required. This directly reduces terminal receiver costs.

The downlink singal from the satellite modulator and frequency standard also provides the CPS terminal with system frequency and time, preturbed only by downlink doppler and range variation. Figure 4 describes the process used to calculate the downlink

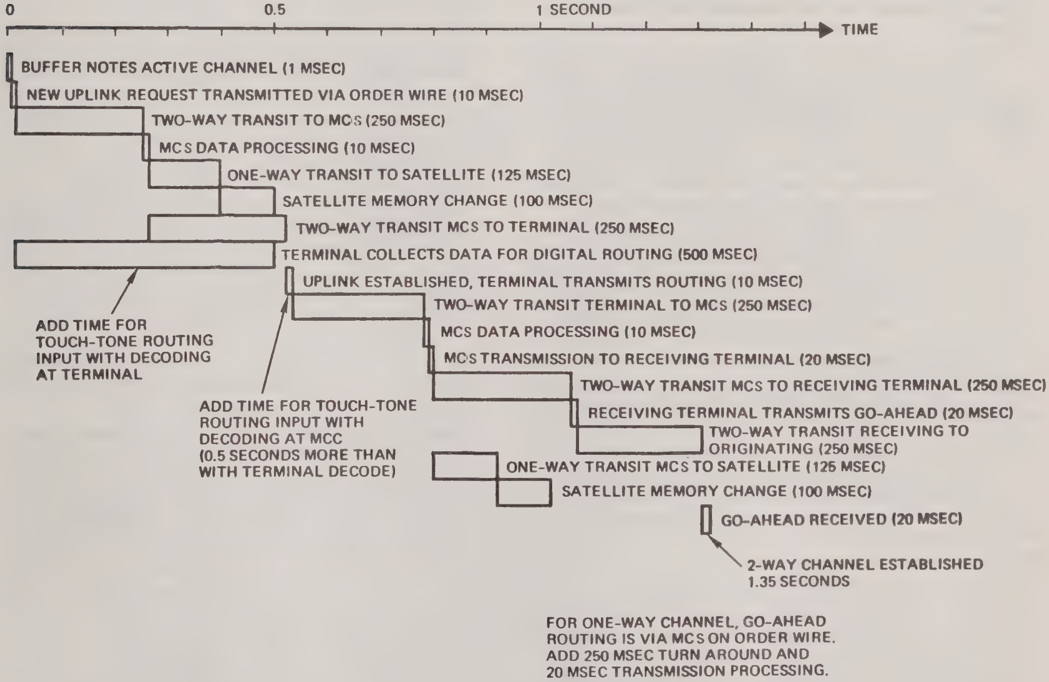
0
0.5
1 SECOND
TIME
BUFFER NOTES ACTIVE CHANNEL (1 MSEC)
NEW UPLINK REQUEST TRANSMITTED VIA ORDER WIRE (10 MSEC)
TWO-WAY TRANSIT TO MCS (250 MSEC)
MCS DATA PROCESSING (10 MSEC)
ONE-WAY TRANSIT TO SATELLITE (125 MSEC)
SATELLITE MEMORY CHANGE (100 MSEC)
TWO-WAY TRANSIT MCS TO TERMINAL (250 MSEC)
TERMINAL COLLECTS DATA FOR DIGITAL ROUTING (500 MSEC)
UPLINK ESTABLISHED, TERMINAL TRANSMITS ROUTING (10 MSEC)
TWO-WAY TRANSIT TERMINAL TO MCS (250 MSEC)
MCS DATA PROCESSING (10 MSEC)
MCS TRANSMISSION TO RECEIVING TERMINAL (20 MSEC)
TWO-WAY TRANSIT MCS TO RECEIVING TERMINAL (250 MSEC)
RECEIVING TERMINAL TRANSMITS GO-AHEAD (20 MSEC)
TWO-WAY TRANSIT RECEIVING TO ORIGINATING (250 MSEC)
ONE-WAY TRANSIT MCS TO SATELLITE (125 MSEC)
SATELLITE MEMORY CHANGE (100 MSEC)
GO-AHEAD RECEIVED (20 MSEC)
ADD TIME FOR TOUCH-TONE ROUTING INPUT WITH DECODING AT TERMINAL
ADD TIME FOR TOUCH-TONE ROUTING INPUT WITH DECODING AT MCC (0.5 SECONDS MORE THAN WITH TERMINAL DECODE)
2-WAY CHANNEL ESTABLISHED 1.35 SECONDS
FOR ONE-WAY CHANNEL, GO-AHEAD ROUTING IS VIA MCS ON ORDER WIRE. ADD 250 MSEC TURN AROUND AND 20 MSEC TRANSMISSION PROCESSING.

Figure 3. New Voice Channel Establishment Timeline

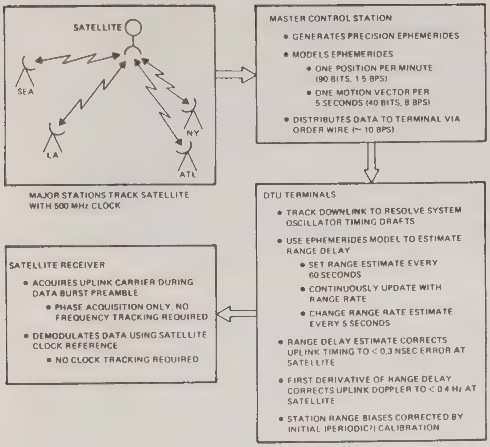
SATELLITE
SEA
LA
NY
ATL
MAJOR STATIONS TRACK SATELLITE WITH 500 MHz CLOCK
MASTER CONTROL STATION
• GENERATES PRECISION EPHEMERIDES
• MODELS EPHEMERIDES
• ONE POSITION PER MINUTE (90 BITS, 1.5 BPS)
• ONE MOTION VECTOR PER 5 SECONDS (40 BITS, 8 BPS)
• DISTRIBUTES DATA TO TERMINAL VIA ORDER WIRE (~ 10 BPS)
DTU TERMINALS
• TRACK DOWNLINK TO RESOLVE SYSTEM OSCILLATOR TIMING DRAFTS
• USE EPHEMERIDES MODEL TO ESTIMATE RANGE DELAY
• SET RANGE ESTIMATE EVERY 60 SECONDS
• CONTINUOUSLY UPDATE WITH RANGE RATE
• CHANGE RANGE RATE ESTIMATE EVERY 5 SECONDS
• RANGE DELAY ESTIMATE CORRECTS UPLINK TIMING TO < 0.3 NSEC ERROR AT SATELLITE
• FIRST DERIVATIVE OF RANGE DELAY CORRECTS UPLINK DOPPLER TO < 0.4 Hz AT SATELLITE
• STATION RANGE BIASES CORRECTED BY INITIAL (PERIODIC?) CALIBRATION
SATELLITE RECEIVER
• ACQUIRES UPLINK CARRIER DURING DATA BURST PREAMBLE
• PHASE ACQUISITION ONLY, NO FREQUENCY TRACKING REQUIRED
• DEMODULATES DATA USING SATELLITE CLOCK REFERENCE
• NO CLOCK TRACKING REQUIRED

Figure 4. Terminal Timing Control

and uplink effects. Known effects restrict the uplink frequency and timing accuracies to 0.4 Hz and 0.3 nanosecond respectively at the satellite. The system requirements can be made much less severe (20 Hz and 4 nanoseconds) to reduce the requirements placed on terminal hardware. Other timing approaches are available and are also being explored.

The CPS terminal receiver and transmitter block diagrams of Figures 5 and 6, respectively, are compatible with the system operation concepts described above. They are reasonably self-explanatory with Figure 4 and the narrative description above.

The system approach described departs from conventional communication practice in several areas. The satellite has several features that will require significant design and development efforts. Some of the concepts need experimental validation before the risks associated with them become acceptable for a commerical communication system. NASA Lewis Research Center has started a program to develop advanced concepts into usable system concepts. Satellite communications technology has advanced in terms of reliability and reduced costs over the past few years, but has not fully utilized the technological advances that are available today.

With the leadership of a strong NASA communications technology development effort, we may be on the threshold of a large quantum jump that will bring the benefits of satellite technology to the small user.

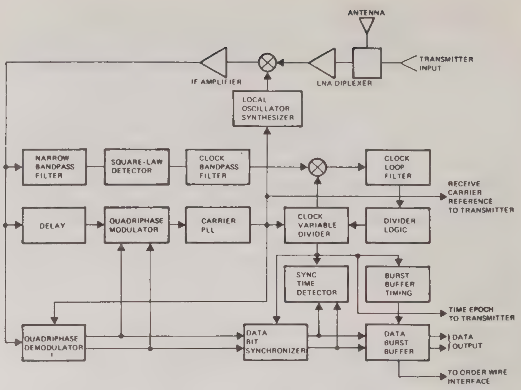
ANTENNA
TRANSMITTER INPUT
IF AMPLIFIER
LNA DIPLEXER
LOCAL OSCILLATOR SYNTHESIZER
NARROW BANDPASS FILTER
SQUARE-LAW DETECTOR
CLOCK BANDPASS FILTER
CLOCK LOOP FILTER
RECEIVE CARRIER REFERENCE TO TRANSMITTER
DELAY
QUADRIPHASE MODULATOR
CARRIER PLL
CLOCK VARIABLE DIVIDER
DIVIDER LOGIC
SYNC TIME DETECTOR
BURST BUFFER TIMING
TIME EPOCH TO TRANSMITTER
QUADRIPHASE DEMODULATOR
DATA BIT SYNCHRONIZER
DATA BURST BUFFER
DATA OUTPUT
TO ORDER WIRE INTERFACE

Figure 5. Terminal Receiver Block Diagram

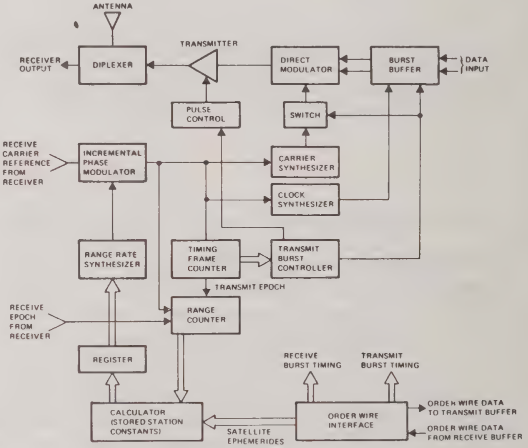
ANTENNA
TRANSMITTER
RECEIVER OUTPUT
DIPLEXER
DIRECT MODULATOR
BURST BUFFER
DATA INPUT
PULSE CONTROL
SWITCH
RECEIVE CARRIER REFERENCE FROM RECEIVER
INCREMENTAL PHASE MODULATOR
CARRIER SYNTHESIZER
CLOCK SYNTHESIZER
RANGE RATE SYNTHESIZER
TIMING FRAME COUNTER
TRANSMIT BURST CONTROLLER
TRANSMIT EPOCH
RECEIVE EPOCH FROM RECEIVER
RANGE COUNTER
REGISTER
RECEIVE BURST TIMING
TRANSMIT BURST TIMING
CALCULATOR (STORED STATION CONSTANTS)
SATELLITE EPHEMERIDES
ORDER WIRE INTERFACE
ORDER WIRE DATA TO TRANSMIT BUFFER
ORDER WIRE DATA FROM RECEIVE BUFFER

Figure 6. Terminal Transmitter Block Diagram

References

1. W. Morris Holmes, Jr., "Multigigabit On-Board Signal Processing," International Telemetering Conference, November 1979, San Diego, CA.

2. Herbert G. Raymond and W. Morris Holmes, Jr., "An Advanced Mixed User Domestic Satellite System." This conference, session on Digital Satellite Systems.

80-0584

DIRECT ACCESS SATELLITE COMMUNICATIONS USING SS-FDMA

John D. Kiesling*
General Electric Space Division
Philadelphia, Pennsylvania 19101

Abstract

Direct to user systems using so-called "roof top" antennas are attractive because they avoid the use of terrestrial facilities with their concommitant performance limitations and costs and enable the carrier to provide a fully switched system for maximum user flexibility. Such systems now existing as minor services offered by satellite carriers are not attractive because of high costs and limitations in data and voice transmission caused by the long satellite delay. While the latter effects are being overcome, it is doubtful whether a really competetitive direct user system can be accomplished without a fresh approach. The paper identifies earth station cost as the most critical direct-to-user enabling technology and concludes that a low-cost cost-effective simple earth station based on SCPC/DAMA (e.g. FDMA) is achievable provided certain added complexities in the space segment can be tolerated. These complexities include high eirp, accomplished by the use of higher power, or multiple beam antennas, or both, and the use of on-board switching to control the signal routing. The technology for accomplishing this higher performance design, and also methods for overcoming the effects of precipitation attenuation in single earth station antenna systems with availabilities approaching 0.9999 are described. Finally, an inquiry is made into the relative merits of terrestrial systems, direct access satellite systems and satellite trunking systems (involving traffic concentration). In addition, a system is hypothesized and costed to support the analysis. It is concluded that substantial limitations are imposed on the existing trunking systems by the access links and that the opportunities for improved economic viability are limited particularly for telephone and data application. On the other hand, the direct access system, though presenting substantial technology challenges, does offer the possibility for a high performance, flexible and reliable service, including the provision of new services difficult to provide by terrestrial facilities at user costs which are attractive visa-vis terrestrial facilities even for short breakeven distances and low data rates.

Introduction

Direct access communications whereby customer premises earth stations communicate directly via a communications satellite, without the aid of any terrestrial facilities is an attractive communications medium. The principle deterrent to economic viability vis-a-vis alternative means is earth station cost. The earth station is simplest, and lowest in cost when configured for operation in the Frequency Division Multiple Access (FDMA) mode, using SCPC/DAMA or Single Channel Per Carrier equipment, with Demand Assigned Multiple Access. If the satellite has high EIRP, by virtue of multiple, narrow spot beams, or high power transponders, or both, the earth station antenna, amplifier and receiver cost can be minimized. On board switching used in conjunction with multiple beam antennas can provide the system routing flexibility while minimizing satellite power and cost. In fact, the two characteristic disadvantages of FDMA, lack of routing flexibility, and poor power utilization due to amplifier linearization can be overcome so that an efficient, flexible satellite design can be accomplished. The resulting direct access system is cost effective compared to both terrestrial facilities and existing and planned satellite trunking facilities (based on FDMA or TDMA), and over very short paths. The achievement of attractive economic features requires a new approach to the design of both the earth station (with regard to cost) and its complementary satellite. With regard to earth stations, the simplicity of an FDMA earth station combined with a standardized design, (including the signalling and switching subsystems) enables a maximum application of Microwave Integrated Circuits (MIC), and LSI, utilizing super components (filter, HPA, up-converter, IF as an example), high production, standardized factory tests and simple installation and checkout procedures, in order to achieve acceptably low costs, nominally $20,000 per station. The analysis to date indicates that a standard 32 KbPS MODEM can handle signalling including network control requirements, and all data rates (perhaps multiplexed) up to 32 KbPS, or voice. Higher data rates, multiple voice channels and multiple simultaneous destinations also can be accommodated. The satellite makes use of a multiplicity of on-board crosspoint switches and channel filters all of a new design, to accomplish routing flexibility. The satellite also is high powered in order to permit low earth station EIRP and G/T, e.g., small antennas. A concommitant benefit of FDMA operation is the ability to provide high continuity of service-approaching 0.9999 - with single antenna earth stations, despite fading due to precipitation attenuation. This is accomplished by "power sharing" in the satellite, between carriers experiencing fading and those which are not - essentially balancing the carrier to noise ratios in the total system. Another benefit of FDMA operation is that the transponder power is proportional to the traffic demand, hence antenna beams having disparate traffic also can have disparate transponder powers. This minimizes the total satellite solar array power. In addition for solar eclipse operation, the satellite battery system can be sized for the actual traffic during the eclipse period, which is considerably less than that for the busy hour. These functions are accomplished by variable power transponders.

System Concept

Use of a multiple beam satellite requires a method for satellite routing of the FDMA signals. There are N^2 possible routes (including the possibility for communications within a beam), for N contiguous beams covering the service area. In TDMA at least N^2 switches are required to perform the routing. This is acceptable because the time allotted to each user can be dynamically

---

* Manager, Domsat Programs

Copyright © American Institute of Aeronautics and Astronautics, Inc., 1980. All rights reserved.

varied according to the traffic demand in each beam. In FDMA the bandwidth per route is dynamically varied according to the traffic demand. Figure 1 depicts the basic satellite arrangement for "N" beams. The FDMA Routing Network contains the frequency converters, channelization and switching to accomplish the routing. The routing is in the form of RF "Paths" traversing the satellite uplink and downlink beams, e. g. , the satellite is a "bent pipe". This concept is illustrated in Figure 1 showing an example of routes from uplink beam "i" to the other "n" beams. The traffic is contained within defined RF bandwidths or "paths", using wideband (WB) paths, say 36 MHz and narrowband (NB) paths, say 5 MHz. Each path can contain single or multiple carriers, with digital or analogue modulation. The bandwidth allocation per route is changed by adding or subtracting these standardized bandwidths by on-board switching.

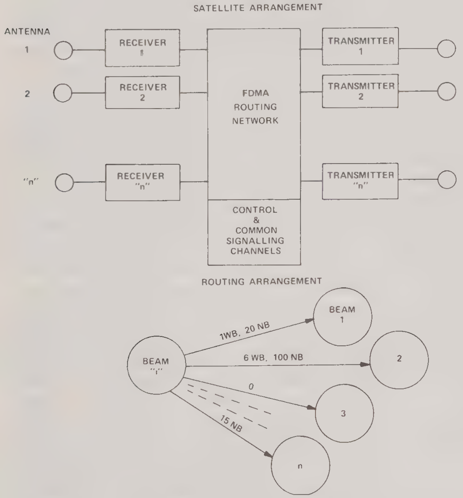

Figure 1. Satellite Arrangement for SS-FDMA

Since an important application for SS-FDMA is for direct to user services (customer premises terminals), the traffic transmitted from a typical earth station is expected to be at relatively low data rates, e. g. , several tens of kilobits of throughput for voice and/or data. This traffic accesses the satellite by being assigned frequencies within the bandwidth of the "path" having the proper destination. This is accomplished within the earth station by a conventional SCPC/DAMA signalling and switching system with centralized control. No demodulation or decoding is necessary in the satellite; this would be overwhelmingly complex because of the relatively low data rate per user. Consequently, it is a misnomer to think of SS-FDMA as a "switch board in the sky" because the actual signalling and switching system is embodied in the terrestrial centrally controlled SCPC/DAMA System. The satellite switch network merely emulates the required busy hour traffic, and is not normally used in setting up calls. The advantages of SS-FDMA are:

1. Earth station costs are low, e. g. , the earth station contains simple signalling, switching and modulation equipment, and the antenna and HPA performance requirements are minimal.

2. Flexible routing is available, on demand, and the system does not require specific modulation and coding methods - it is transparent.

3. Large aggregate traffic can be achieved even though individual user demands are small.

4. SS-FDMA is compatible with any of the frequency bands now allocated to communication satellites; Ku and Ka band, however, are better for direct access because there are no significant limitations on satellite power flux density or minimum earth terminal antenna diameters.

5. User costs are low.

6. Use of FDMA has several key system advantages: the switch design tolerates failures because many different switches are involved in setting up parallel paths; the many carriers offer statistical advantages for power sharing, e. g. , dynamically balancing thermal noise of faded and unfaded carriers to minimize the impact of fading due to precipitation attenuation; availabilities of 0. 9999 can be achieved with single antennas at Ka Band. The transponder power per beam, and the total battery energy per eclipse can be sized for the actual traffic expected, through the use of multi-level amplifiers (or switched amplifiers), thus minimizing the imact of power and batteries to the satellite design, (in TDMA each transponder and earth station must always transmit the burst power).

Use of SS-FDMA also has disadvantages. One is the complexity of the satellite channelization and switching, however, this paper describes recent developments which minimize these constraints. Also, FDMA requires output amplifier linearization, usually by backoff, (all in all FDMA turns out to be more efficient than TDMA despite backoff, if the items of 6 above are implemented).

In essence, SS-FDMA reverses the present trend in communication satellite design by placing more complexity in the satellite in order to achieve greater simplicity and therefore lower cost in the earth stations. It is shown later that this added satellite complexity does not significantly impact user costs, but that the earth station cost is the systems principle economic "driver".

Dynamic margins are used to provide high availabilities to single antenna Ka Band earth stations using SS-FDMA. In essence, the thermal noise and intermodulation noise of the unfaded and faded carriers are balanced through control of the earth station HPA levels via the network control center (the satellite transponder has constant gain and is linearized). Attenuation is measured and alarmed through measurement of a downlink pilot carrier at each earth station. The overall carrier to noise ration γ at any station is

$$\gamma = \gamma_O \gamma_F K_O = \frac{1}{\frac{1}{2.5\,\gamma_I} \times \frac{1}{\gamma_{CD}} \times \frac{1}{\gamma_{CU}} \times \frac{1}{\gamma_{ND}} \times \frac{1}{\gamma_{NU}}}$$

where γ_O is the minimum acceptable CNR

γ_F is the fixed margin; if this is exceeded, the network will respond by changing signal levels in that link*

K_O = sky noise ratio

γ_I = carrier to intermodulation ratio

γ_{CD} = antenna system downlink interference due to side lobes and orthogonal polarization

γ_{CU} = antenna system uplink interference due to side lobes and orthogonal polarization

γ_{ND} = downlink carrier to noise ratio

γ_{NU} = uplink carrier to noise ratio

The coefficients of equation 1 are selected to satisfy the link requirements under various conditions of uplink and downlink fading. Hence, the network responds to fading conditions by changing the earth station HPA levels; the intermodulation noise in the satellite amplifier and the antenna interference also change dynamically. The results are shown in Figure 2 in terms of the required uplink or downlink carrier to thermal noise ratio plotted versus the fixed margin, for various values of antenna interference and intermodulation noise, for the idealized case of 1000 carriers per transponder. Fixed margins of about 2 dB are indicated, with thermal CNR's of about 25 dB. Since the downlink and uplink attenuation values are assumed to be 20 dB and 30 dB, respectively for 0.01% (typical of mid-Atlantic region), provision of a fixed margin only, (with antenna and intermodulation noise values of 30 dB) would require thermal carrier to noise ratios of 37 dB. Thus a considerable savings in satellite power is accomplished. Figure 2 also shows that it is desirable to achieve antenna isolation and intermodulation noise interferences of 30 dB (no copolarized beams are assumed, thus even in cases of severe attenuation when orthogonality is impaired, there is still side lobe isolation). The antenna isolation can benefit a little from interstitial spacing of carriers, particularly in the regions of filled or saturated beams.

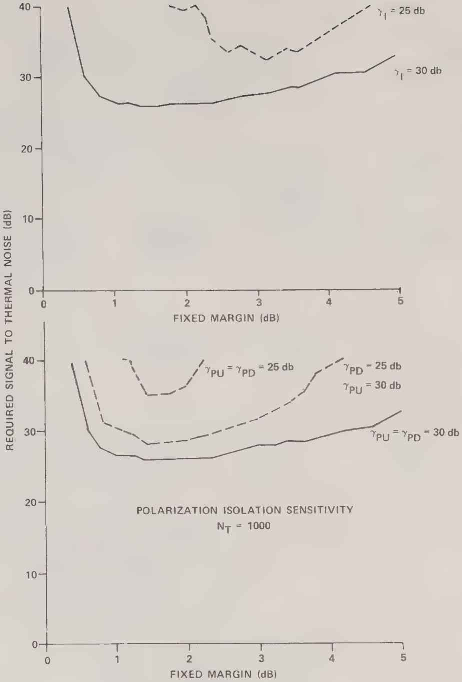

Figure 2. Required Signal to Thermal Noise Ratio vs. Fixed Margin for Various Carrier to Intermodulation Ratios and Various Antenna Carrier to Interference Ratios.

Satellite Design

A simplified diagram of a satellite SS-FDMA network is depicted in Figure 3, consisting of frequency converters, channel filters (to identify each "path") and a crosspoint switch. The multiplicity of filters and switches in SS-FDMA requires that great pains be taken to minimize their impact on satellite mass and power. This is accomplished by converting the FDMA bands to low frequencies; this enables implementation of channel filters by way of Surface Acoustic Wave (SAW) filters or similar devices and large scale switch arrays by way of LSI. In particular, at this stage of technology, CMOS, silicon on saphire is particularly attractive. The reader is referred to Reference 1 for additional information on this technology.

Figure 4 depicts a ten beam coverage plan for the 48 states. By estimating the population within each of the beams a hypothetical traffic matrix can be constructed illustrating typical beam and route utilization. The results in MHz are shown in Table 1, assuming 2500 MHz as the frequency allocation, and of this, 833 MHz is available in each beam. Total bandwidth per beam shows a variation of 20:1 in capacity between the highest capacity beam and the lowest capacity beam. The upper left corner depicts heavy routes (> 50 MHz), and the

---

*The average link margin is considerably greather than this value.

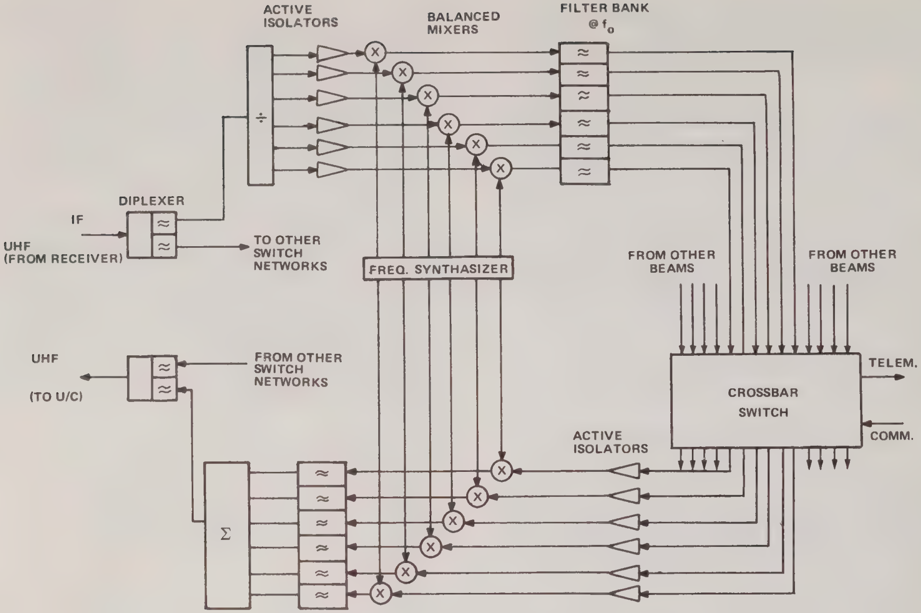
ACTIVE ISOLATORS
BALANCED MIXERS
FILTER BANK @ f_0
DIPLEXER
IF
UHF (FROM RECEIVER)
TO OTHER SWITCH NETWORKS
FREQ. SYNTHASIZER
FROM OTHER BEAMS
FROM OTHER BEAMS
UHF
(TO U/C)
FROM OTHER SWITCH NETWORKS
CROSSBAR SWITCH
TELEM.
COMM.
ACTIVE ISOLATORS
Σ

Figure 3. Example of Typical Switch Network

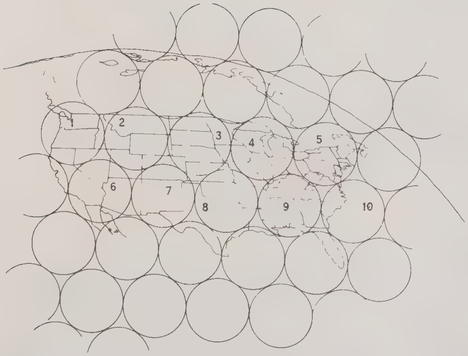
1
2
3
4
5
6
7
8
9
10

Figure 4. Example of Typical 10 Beam Coverage Plan

lower right corner, light routes. The objective of the SS-FDMA switch design is to provide the desired routes, while maintaining efficient spectrum utilization and while providing the flexibility of allowing for substantial changes in the routing. For example, route 10-7, requiring no satellite capacity might in the future have to provide a 36 MHz path on demand to accommodate a new requirement for interactive TV teleconferencing. While the switching design is very complex, an example of a switch network meeting these requirements is given in Table 2. A combination of preassigned 36 MHz routes, and fully switched 36 MHz and 10 MHz routes are provided for flexibility. In addition, "pooled" switch networks also are used; ten additional 36 MHz routes can be added to eight of the beams, but no more than four to beam ten, no more than two to beam 2, etc., twenty additional 10 MHz routes can be added to all ten beams,

Table 1. Ten Beam Traffic Matrix in MHz

BEAM	1	2	3	4	5	6	7	8	9	10	
1	196	192	150	92.5	53.4	49.8	35.6	32.0	21.4	10.7	833.4
2	192	185	146	89.0	53.4	49.8	35.6	32.0	21.4	10.7	814.9
3	150	146	113.9	74.8	42.7	39.2	28.5	24.9	14.2	7.1	641.3
4	93.6	89.0	74.8	46.3	24.9	24.9	17.8	14.2	10.7	3.6	398.8
5	53.4	53.4	42.7	24.9	14.2	10.7	10.7	10.7	7.1	3.6	231.4
6	49.8	49.8	39.2	24.9	10.7	10.7	7.1	7.1	7.1	3.6	210.0
7	35.6	35.6	28.5	17.8	10.7	7.1	7.1	7.1	3.6	0	153.1
8	32	32	24.9	14.2	10.7	7.1	7.1	7.1	3.6	0	138.7
9	21.4	21.4	14.2	10.7	7.1	7.1	3.6	3.6	3.6	0	92.7
10	10.7	10.7	7.1	3.6	3.6	3.6	0	0	0	0	39.3
											3553.6 MHz or 1.42 reuses

but no more than eight to beam ten and no more than four to beam two, etc. The "pooled" switch networks offer the possibility of additional bandwidth in unfilled beams while reducing the switch complexity, e. g., reducing the number of switches needed.

Table 2. Example of Switch Matrices Capable of Satisfying the Requirement of the Traffic Matrix of Table 1.

		36 MHz		10 MHz		10 MHz	36 MHz
		PREASS	SWITCHED	PREASS	SWITCHED	POOLED	POOLED
BEAM	1	10	8		8	4	0
	2	10	8		8	4	0
	3	9	7		10	4	2
	4	4	4		14	4	2
	5	2	2		8	6	2
	6	1	2		11	6	2
	7	1	1		10	6	4
	8	1	1		10	6	4
	9	0	0		10	8	4
	10	0	0		6	8	4
SWITCH MATRIX			33x33		95x95	56x20x56	24x10x24
NUMBER OF SWITCHES		1089		9025		5600	480

Even so, the number of switches is formidable - requiring implementation in LSI to reduce weight, (the reader is referred to Reference 1 for design examples of switch matrices suitable for this application.) The resulting spectrum plan for several of the beams is illustrated in Figure 5, showing RF paths provided by preassignment, full crosspoint switching and partial ("pooled") crosspoint switching. Note that a significant reserve capacity is available in each beam, particularly unfilled beams. For example, the traffix matrix identifies a need for only six 10 MHz paths in beam 10, yet four 36 MHz paths and eight 10 MHz paths can be added.

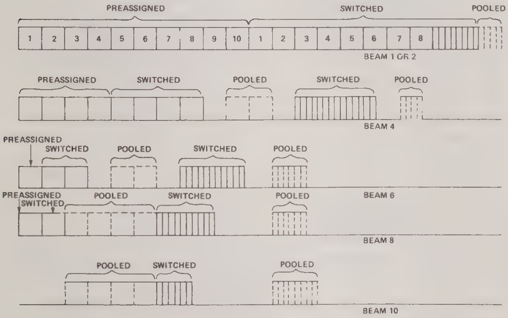

Figure 5. 10 Beam Satellite Channel Allocation

Estimates of KaBand satellite weight and power based on the use of 1 meter 2 meter and 3 meter earth station antennas are given in Table 3. The communications payload is dominated by the high power transponder amplifiers. The principle reason for the large power is the small earth station antennas needed for direct user service (to get low earth station cost and hence low service cost). However, operation at Ka Band where equipment performance is poorer, and where additional power is needed to overcome the effects of fading, (as well as multiple beam antenna interference and transponder linearization), also add to the power requirements.

The SAMSO (Aerospace) cost model [2] and other models [3, 4] can be used to estimate the cost of SS-FDMA satellites. This is described fully in Reference 1 wherein satellite non-recurring costs and recurring costs are converted to annual costs by considering:

- 10% interest for satellite construction
- launch costs
- costs for 3 satellites, 2 launch vehicles
- launch and on-orbit insurance
- O&M for satellite control
- 10 years depreciation
- return on investment = 15%

In addition, the satellite "fill" factor is assumed to be 58% (15% growth in traffic for 10 years). The resultant recurring and non-recurring costs and annual costs are displayed in Figure 6 as a function of satellite weight. Two prime powers were considered to examine the impact of high satellite power. The 10 beam satellite capacity is 74, 000 preassigned 32KbPS (2 way) trunks.

Table 3. Spacecraft Characteristics for 10 Beam Satellite as a Function of the Earth Station Antenna Diameter

	1M	2M	3M
COMMUNICATIONS PAYLOAD WEIGHT, LBS	3584	1702	937
ARRAY WEIGHT, LBS	1315	356	178
BATTERY WEIGHT LBS	407	159	123
SUBTOTAL	5299	2217	1238
SPACECRAFT WEIGHT, LBS*	11776	4927	2751
PRIME POWER, KW	19.7	5.3	2.6

*BEGINNING OF LIFE IN SYNCHRONOUS ORBIT

Earth Stations

Direct user terminals must be cost effective at low data rates and modest service requirements if they are to find wide applicability.

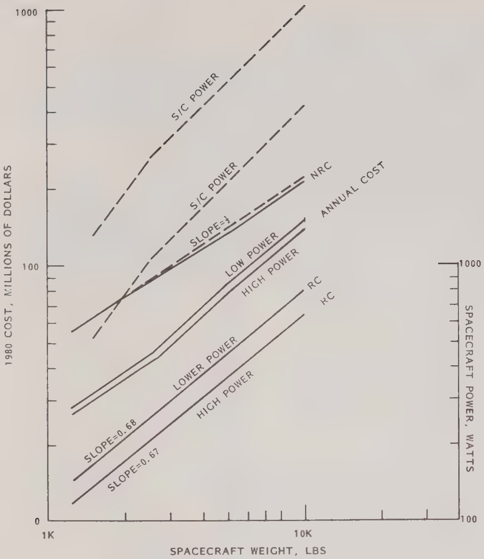

Figure 6. Space Segment NCR, RC and Annual Costs (1980 Dollars)

FDMA earth stations are the most attractive for direct to user service because they are lowest in cost. Low cost stems from simplicity. The MODEMS are low speed and operate in the continuous (non-bursting) mode, coding implementation is simple, the HPA power is minimal because the bandwidth is minimal and signalling and switching costs for centralized SCPC/DAMA also are minimal. In addition, there is no need for satellite drift correction or rapid switching or framing of data. The complexity is all in the satellite. For applications with one MODEM, the MODEM can provide both signalling and communications (not at the same time). Multiple data inputs can be time multiplexed at the interface and AVD modes are permissible. Single and multi-destination carriers can be provided. As additional capacity and flexibility is required, additional MODEMS can be added and the HPA power increased accordingly (now linearization will be needed). Such stations can provide all services and flexibility needed for direct to user services. Even so, Reference 1 indicates that single MODEM earth station acquisition costs should be in the range of $10, 000 to $30, 000 in order to compete effectively with terrestrial facilities. Somewhat higher costs are permitted as the service (aggregate data rate) increases. Even with simple FDMA terminals with 2 meter antennas and 5 watt solid state HPA's, these low costs will be hard to achieve. In addition to simplicity of configuration, these terminals also must benefit from a maximum of integrated circuit design (including the microwave subsystems), standardization and high production. Easy installation, checkout and simple O&M procedures also are important. References 1 and 5 provide ample evidence that the range of costs are achievable, so that this subject will not be discussed further here. Two earth stations are defined, however, to enable computation of user costs. One has a single 32 KbPS MODEM and the other 2 64 KbPS and 1032 KbPS MODEMS with a range in cost of $30, 000 to $50, 000.

User Costs

End-to-end user costs can be computed for the two earth station types and the 10 beam satellite capable of 74, 000 preassigned 32KbPS trunks. This is accomplished by multiplying the earth station acquisition cost by a factor of . 33 (. 22852 capitol recovery factor at ROI = 20% for 10 years, and the remainder for O&M) and adding to this the average satellite trunk charge, either preassigned, or demand assigned (a factor of 20:1 is calculated as a use factor for DAMA). Thus, the end-to-end cost is representative of a carrier tariff. The results in 1980 dollars are shown in Figure 7 versus earth station antenna diameter for the single MODEM earth station, over a range of earth station costs from $10, 000 to $30, 000. The low slope indicates that earth station antennas in the range of 1 meter to 3 meters minimize user costs. DAMA, with a 20:1 cost factor has little influence on user costs - these are dominated by the earth station costs; e. g. , earth station costs are the primary economic driver in this system. This supports the original SS-FDMA contention that increased satellite complexity is acceptable and desirable if it simplifies and reduces the cost of the earth station. Actually, if R&D is completed, the increased cost of on-board FDMA switching increases satellite system costs by only a few percent; (the greatest satellite complexity is caused by the higher power requirements of the direct-to-user service).

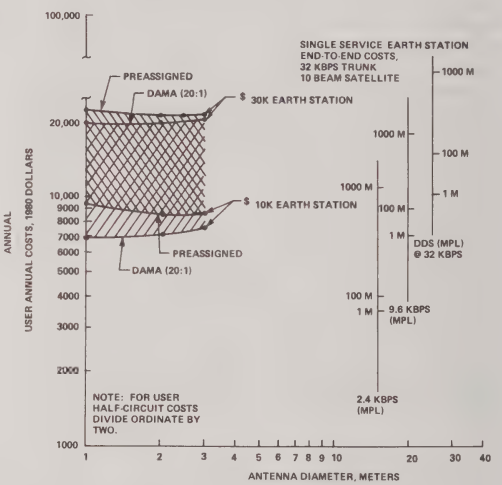

Figure 7. Single Modem Earth Station Costs

Figure 7 indicates a range of user costs from $7500 per year to approximately $20, 000 per year. The cost/mileage MPL terrestrial traffic including termination costs for 2. 4KbPS, 9. 6KbPS and 32KbPS (prorated 56KbPS DDS) are plotted on the right of Figure 7. A comparison of costs shows the need to drive earth station costs below $20, 000. If an earth station cost of $10, 000 can be attained, the satellite service competes favorably with the terrestrial system and provides a viable terrestrial alternative even at short distances. Wideband data, e. g. , 9. 6KbPS and above, are very attractive by satellite. Results for the multi-

MODEM earth station for a range of earth station costs between $30,000 and $50,000 are given in Figure 8 in terms of costs per "MODEM" (earth station costs are prorated by data rate). Economic benefits accrue because certain earth station costs, such as antenna, LNR, converters, HPA are shared amongst the 12 services. Now user annual costs range between $1500 and $5000. The negative slope for preassigned service indicates in this case that the satellite charge is relatively large and therefore larger earth station antennas are needed to reduce its effect. However, with DAMA, the satellite charges are again reduced, and the zero slope condition indicates again that earth station antennas in the range of 1 meter to 3 meters are optimum. Comparison with terrestrial facilities shows that the satellite system compares favorably even at a 2.4KbPS data rate (in the calculation 2.4KbPS is buffered to 32KbPS for transmission through the satellite), and at very short distances. Of course, this earth station (with 12 MODEMS and 448KbPS of total service capability) is suitable for use only by large communications users. The majority of users will have requirements for earth stations which are in between the two cases studied. However, it should be noted that most direct to user applications would be satisfied by earth stations with only a few MODEMS.

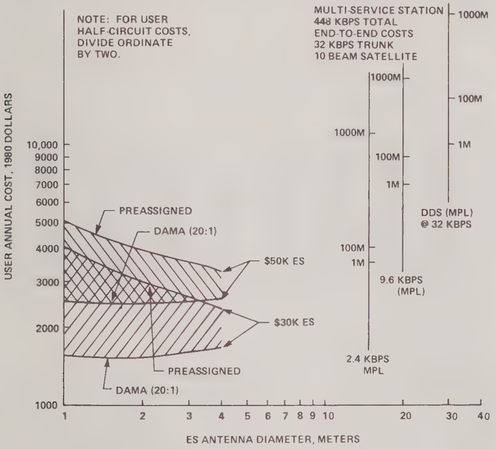

Figure 8. Multi-Modem Station Costs

Conclusions

The Study [1] results shows that a direct access system based on SS-FDMA can provide flexible service, at user costs which are very attractive compared to existing tariffs and at lower costs than conventional trunking satellite systems (except for very long routes). Operation at Ka Band, using carrier power sharing, attractive with FDMA, permits single earth station antenna operation (no antenna diversity) with high service availability. Thus flexibility, including complete signalling and switching capability, (including a TELCO interface if necessary), low cost and high reliability is achievable. Similar results are achievable at Ku Band. The system design, in essence reverses current trends in satellite communications by placing more technology in the satellite to simplify the earth station configuration and thus reduce overall cost.

Access directly to satellite completely avoids performance and cost limitation of terrestrial loops and interconnects and offers new versatility - bandwidth on demand - for system users.

1 Satellite Systems Based on SS-FDMA, NAS 3-21745
2 Unmanned Spacecraft Cost Model, 4th Edition, February, 1978 (SAMSO)
3 Communications Satellite Modeling Technique; Comsat Technical Review, Vol. 2, No. 1, Spring, 1972
4 Space Transportation System Reimbursement Guide TCS-11802
5 Communications Systems Technology Assessments Study, Vol. 2, NASA CR 135224

80-0585

20/30 GHZ SATELLITE BUSINESS SYSTEM IN GERMANY

D. Otto, W. Kriegl, H. M. Braun
Space Programme Department
Dornier System GmbH, Postfach 1360
7990 Friedrichshafen, Germany

Abstract

Like other nations, Germany is considering the use of the 20/30 GHz bands for future satellite business systems (SBS). There are, however, some differences in the applicability of an SBS to German telecommunication services compared with other European countries such as Italy. To illustrate these reasons, a survey of the present situation in telecommunications is presented together with forecasts for the existing and potential new services, and for the latter the likelihood of their being implemented in the near future. It is concluded that in Germany a Satellite Business System is primarily of interest for new broadband services such as video and high speed data transmissions, especially when the implementation of a switched broadband system is considered. For narrowband services and their expected growth rates the existing network, with its projected extensions, will be sufficient for the next decade. Finally preliminary results of the lay-out for a German SBS are given.

Introduction

In all parts of the world the telecommunication traffic is increasing and individual nations are facing the problems of satisfying their demands. To achieve these, the existing networks and the services need to be extended.

One possible solution seems to be the implementation of new microwave links, but as the presently assigned frequency bands are nearly completely filled, the only possibility is to move to higher frequencies. Here, however, the atmospheric attenuation is very high so that a large number of relay stations is needed, which in turn is very expensive and lacks versatility.

Another possibility is the use of cables, where the frequency choice is nearly arbitrary and the only requirement for the future is the selection of a broadband one. The best choice in this case might seem to be the glass fibre cable, but only at first glance since it is only suitable for short distances. For long distance traffic, however, the attenuation effect is too high. The same is also true for circular waveguides, the development of which has now been stopped due to the better performance characteristics of the glass fibre cable. The only practical cable for long distances is the coax cable which is already widely used. But like the microwave links, all cable systems also lack versatility and need a long time for their introduction and implementation.

A satellite system working in the 20/30 GHz bands which are especially assigned to satellite services, would largely avoid the disadvantages of terrestrial cable and microwave systems and seems to offer a cost effective solution for future services. Several industrialised nations are therefore already planning operational systems in these bands, and the purpose of this paper is to show the possibilities for and main characteristics of a German Satellite Business System (SBS). The results were obtained mainly within a study titled "20/30 GHz Utilisation for Satellite Communications in Germany" funded by the German Ministry of Research and Technology.

Present Telecommunication Situation in Germany

Telephone: This is the most important and most common communication system, but still has not reached the same significance as in other countries with a similarly high GNP. Although Germany is in 7th place regarding the absolute number of phones, it is only in 14th place when phone density i.e. the number of phones per inhabitant, is considered. Fig. 1 shows the development of phone density from 1970 to 1977, from which it can be seen that the rate of growth has remained constant during this period. This appears to be slower than might have been expected since the German telephone network is one of the more advanced in the world. However, the latest trends indicate that a breakthrough has now arrived and the phone will soon be a greater mass communication means in Germany.

Telex: This basic communication service for industry is most extensive in Germany mainly because of its high industrialisation level. Regarding the number of users, the German Federal Republic owns the largest network in the world. Nevertheless, the traffic is still increasing, an observation which has also been made in countries where the saturation level for phones has nearly been reached. Fig. 2 shows the increase in the telex traffic to foreign countries in minutes

Copyright © American Institute of Aeronautics and Astronautics, Inc., 1980. All rights reserved.

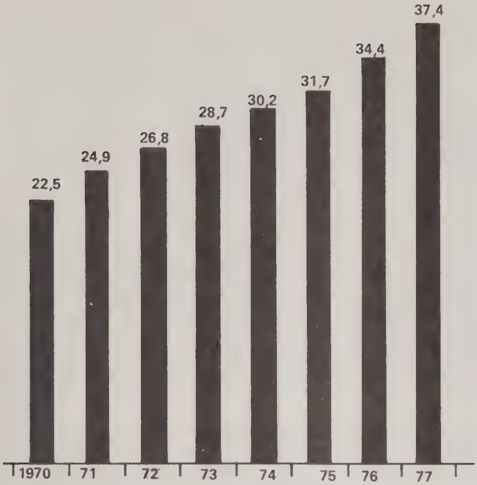

Fig. 1 Number of Phones per 100 inhabitants

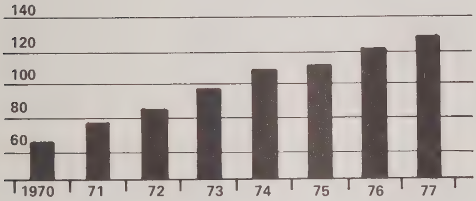

Fig. 2 Telex Traffic to Foreign Countries in Million Minutes

Data Transmission: After a slow start a rapid growth occurred in the mid 1970's (Fig. 3). The figure reflects the increasing use of electronic data processing by German companies. The trend was especially assisted by the development of powerful and cost effective terminals for smaller and medium sized users. Furthermore the users were provided with efficient transmission schemes with partly decreased tariff structures for some systems. The introduction of the so-called "Integrated Telex and Data Network" (IDN), with speeds of 200, 600, 1200 and 2400 bps, which covered the majority of user demands, provided one of the major incentives of this growth. For higher speeds, up to 48 Kbps with fixed connections only are available at present.

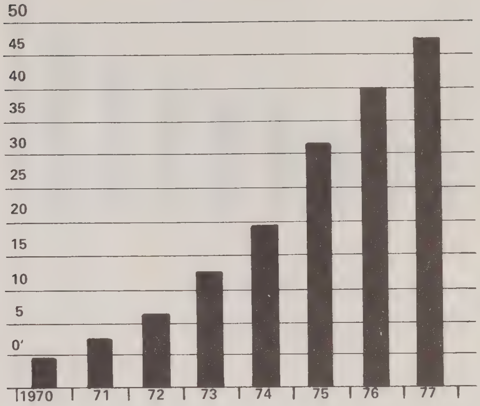

Fig. 3 Data Terminals in Thousands

TV-transmission: This network is the least developed one. Although the German Federal Republic has about 56,000 line kilometers for TV transmissions, nearly all realised as microwave links, they serve only to interconnect the different studios and to bring the German TV programmes to the transmitting stations. Private TV lines such as cable TV do not exist in Germany due to government restrictions.

Forecasts for the Extension of Existing Services

Telephone: The present goal is to have one telephone connection in each of the 24 million households in Germany by 1985. Regarding the above mentioned breakthrough in this field it is expectedthat this goal will be reached earlier. While the increase in phones per inhabitant as shown in Fig. 1 will have reached saturation by then, the traffic is nevertheless expected to increase even further, in particular in the number of long-distance calls. It is just these types of call which are of the most concern from the standpoint of the transmission technique. So it can be concluded that the trend shown in Fig. 4 will continue. One stimulus to strengthen this trend is the charges policy of the German government. Also other influences, such as the introduction of new services or the energy shortage will possibly lead to an even bigger shift to phone channel communications than expected.

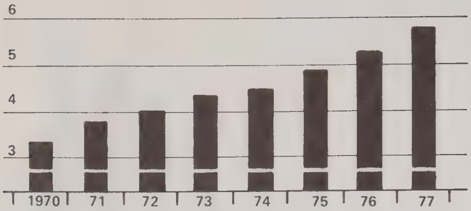

Fig. 4 Long Distance Calls in Billions

Telex: The telex business is also showing a strong growth rate. However, it cannot be excluded that in future it will slow down because of competing new services such as office telex and remote copying. For the transmission technique, however, the choice is only of minor interest, for telex and the new services all occupy similar narrow frequency bands.

Data Transmission: Here the clear indications is that the increase in traffic and terminals will continue. This will imply an extension in the IDN network and may provide the first big challenge for the implementation of a German SBS, especially when there are requirements for high speed data transmissions.

TV transmission: The existing TV network is already nearly fully extended and because of the political considerations the future for other TV transmissions, such as private (or commercial), local and pay TV is still open. If there is a positive decision in future, Germany will face the challenge to introduce a broadband long distance network as quickly as possible.

New Communication Services and their Chances

For ease of understanding the services are here divided into narrowband and broadband ones. Narrowband services are those whose occupied bandwidth is similar to that of a phone channel, and broadband services are those for which the bandwidth corresponds to the magnitude of a TV channel.

Narrowband Services

Office telex: This is a combination of telex and typewriting, but six times faster than telex and with more characters. The advantage of office telex is that its terminals can be decentralised in contrast to the present telex machines. Presumably office telex will be introduced during the next few years in Germany and a wide spread usage can be expected.

Video text: Text information and simple figures can be received and made visible on an ordinary TV set with a special decoder. In contrast to other new services this one does not need an additional bandwidth, as the signals make use of the redundancy in a TV signal. The information is inserted in the video blanking interval and so this service is part of broadband communications.

Screen text: This can be regarded as a duplex version of video text where the return channel is a simple telephone channel connected to a central computer. An experiment with 6,000 participants is starting in 1980 and if the result is encouraging this new service can be introduced by 1982.

Remote copying: This represents an addition to office telex, for transmitting the contents of the original documents. Until recently the lack of standardisation has restricted its use, but as these problems have now been solved, a rapid growth can be expected.

Facsimile Newspaper: A special case of remote copying. However, according to the present market situation, the high costs for the terminals required and the inconveniences for the customers, such as the buying of special paper and maintaining the supply of it to the terminal, the facsimile newspaper will have little chance in the near future to achieve a major breakthrough.

Video single picture: This is the transmission of single pictures in series via existing TV channels. Probably this service will also use the video blanking interval and hence needs no extra bandwidth. So it is not of interest here. The service itself will not become one of great importance.

Phone single picture: Similar to video single picture. The only difference is the use of telephone instead of video channels, which results in a transmission time of about one minute for one picture. Because of this long time and the required additional storage devices, it is not expected that this service will gain much interest in the near future.

Remote controlling: In many industrial application remote controlling is already used on special links. There are no indications yet that remote controlling could be offered as a public service with success.

Electronic mail: A combination of office telex and remote copying, where the letters are transmitted electronically from the forwarding post office to the receiving one. The delivery, however, is still made by postmen. Perhaps this service might have a chance to be introduced in international mail services. For Germany's internal services it is not of particular interest as the mail delivery is normally very quick.

Broadband Services

Cable TV: As stated in the previous section the future for TV transmissions is still open. Nevertheless it is necessary to be prepared if a decision to allow them arrives. Furthermore as other nations are using cable TV, it seems likely that Germany will finally introduce this new medium as well.

Picture phone: Because of the present technological level, and the very high costs for the implementation and for the terminals, the picture phone will not be introduced in the near future. This holds for both the 1 MHz and th 5 MHz versions.

Video conferencing: To save time and money the introduction of a service allowing video conferences has been proposed. Experiments have revealed, however, that this service was not well accepted by the participants and the costs are still too high. So this service will have only a small chance to be implemented as a new service.

High speed data transmission: As the low and medium speed data transmissions are showing a very rapid growth rate, the high speed data transmission is expected to have the best chance for implementation as a broadband system.

Possibilities for an Operational German SBS

Presently and in the next few years the growth of the exisiting and the most likely new narrowband services can be handled by the German terrestrial telecommunication network and its projected extension. So there will be no need for a German SBS which supports those services, at least not for the next decade. The picture is quite different, however, when considering broadband services. Presently only non-commercial broadband services exist, and there is no public network available yet nor in the foreseeable future which might be able to handle these signals. But it is very likely that soon there will be a demand for broadband systems, particularly when they become operational in other countries. Germany, as a highly industrialised nation, cannot afford to lag behind in the development of this new field without risking a setback in its technology and services. Germany must therefore decide how to implement such a network, either terrestrially with coax cable or with a communication satellite system. First studies on this subject have revealed that the latter appears to provide the most versatile, cost effective and fastest solution to implement. This far it can be concluded that the German SBS would be realised primarily to offer new broadband services and not to support the terrestrial narrowband systems. To be as versatile as possible the German SBS would incorporate switching matrices to interconnect different users at different locations.

Preliminary Lay-Out of the Space Segment

The German SBS will use 30 GHz for the uplink and 11 GHz or 18 GHz for the downlink, depending on the CCIR recommendation. At present the use of the 18 GHz band has been assumed. Clearly the areas with the greatest amount of traffic are the big cities, so the use of spot beams to serve these areas seems to be the best solution. Fig. 5 gives an indication of the required antenna gain and antenna diameter to achieve a certain coverage area in Germany. As can be seen a trade off between the antenna diameter and the coverage area on ground is necessary. Normally coverage areas of 30 to 50 km are desirable, which would result in antenna diameters of 22m to 13m, respectively. Such an antenna size has a strong implication for the accuracy of the antenna pointing control, for it has a very narrow beamwidth, as illustrated in Fig. 6. As the pointing accuracy normally should be better than the beamwidths by one order of magnitude, the attitude control is one of the most important subsystems. To form the spot beams and a beam covering whole Germany the use of an offset cassegrain antenna with a switchable feed cluster is foreseen. This design ensures maximum versatility.

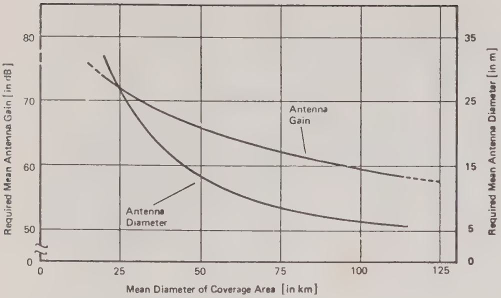

Fig. 5 Required Antenna Gain for a given Coverage Area

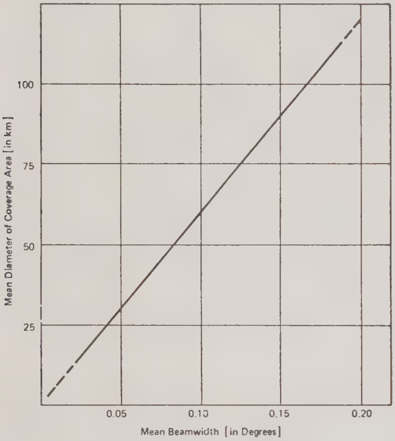

Fig. 6 Resulting Beamwidth

A straightforward system lay-out would require more than 20 dB margin due to weather effects for one single receiver station. For two stations spaced about 30 km and working in space diversity, this margin is reduced to 13 dB, but is still too high. Keeping this fact in mind, strategies were considered for controlling these fadings. The boundary condition set was to transmit a certain data rate independent of the weather condition, and so the following solution was derived.

For modulation, 8-phase-CPSK is selected when the weather is good. When it is bad, the system steps down to 4 or 2-phase-CPSK, and when it is raining very hard a 2-phase CPSK with rate 3/4 convolutional coding can be selected. In this way it is possible to compensate for attenuations of up to 14 dB. To maintain the same bit rate a TDMA system with variable burst lengths is necessary. The burst lengths are:

	T_O	for 8-phase-CPSK
	$3/2\ T_O$	for 4-phase-CPSK
	$3\ T_O$	for 2-phase-CPSK
and	$4\ T_O$	for 2-phase-CPSK with "rate-3/4 convolutional coding"

The burst lengths are modified by demand assignment.

So, for n participating stations, the frame length T_F must be

$$T_F = n \cdot T_N,$$

where T_N is the burst length for normal (good weather) conditions. As the switchover to a smaller number of phase states is a rare event, a system lay-out with a frame length of

$$T_F = 1.2 \cdot n \cdot T_N$$

was felt to be sound.

Additional measures to improve the signal for distortion ration are

- control of the uplink transmission power to decrease the distortion in neighbouring channels,
- predistortion of the polarisation in the ground stations to compensate for the depolarisation effects of the atmosphere and
- application of a regenerative transponder.

For the system outlined above, link calculations were made and it was found that a minimum data rate of about 100 Mbps under worst case conditions with small earth terminals is feasible.

Conclusion

Marketing studies and trend analyses reveal the growing demands for the existing services and indicate good prospects for some additional new services. However, the German telecommunication network and its projected extension has already reached such a high level that all narrowband services can be handled by it, at least for the next decade. Broadband systems which are likely to come, e.g. high speed data and video transmissions, in contrast, cannot use this network for at present it is only laid out for narrowband services. Thus the demand for broadband services can only be satisfied by an implementation of a special new network. For long distance traffic the best solution is a German SBS. The preliminary lay-out indicates the use of a large offset cassegrain antenna fed by a feed cluster to produce spot beams which cover all major German cities. To compensate for rain attenuations the use of CPSK with different phase states is foreseen. To achieve the same data throughput independent of the weather, TDMA with different burst lengths and space diversity is applied, along with some additional techniques to increase the signal to distortion ratio.

80-0586

AN EXPERIMENTAL 20/30 GHz COMMUNICATIONS SATELLITE CONCEPTUAL DESIGN EMPLOYING MULTIPLE-BEAM PARABOLOID REFLECTOR ANTENNAS*

ALFRED M. GOLDMAN JR.**

Jet Propulsion Laboratory
California Institute of Technology
Pasadena, California

Abstract

This paper describes an experimental 20/30 GHz communications satellite conceptual design employing multiple-beam paraboloid reflector antennas coupled to a Time Division Multiple Access (TDMA) transponder. The satellite employs solid state GaAs FET Power Amplifiers and Low Noise Amplifiers. Signal processing and switching takes place on-board the spacecraft.

The area to be served by this satellite would be the Continental United States plus Alaska, Hawaii, Puerto Rico, and the Virgin Islands. In addition, part of Southern Canada plus Mexico City would be served. The feeds for the paraboloid reflectors produce 32 narrow beams. The narrow beams use geographic and polarization diversity to obtain eight-fold frequency reuse.

Up-link and down-link data rates are 100 Mbps for each of the 32 beams. Spectrum-efficient QPSK modulation is used. The combined link performance provides a bit error rate between 10^{-6} and 10^{-9} depending upon the presence or absence of precipitation in the link.

The earth stations have 4.6 meter diameter paraboloid antennas, uncooled GaAs FET Low Noise Amplifiers and TWTA transmitters. The earth stations are designed to be low cost.

1.0 Introduction

A major thrust of the National Aeronautics and Space Administration communications satellite research and development program is the pursuit of the technology necessary for a wideband communications satellite operating at frequencies near 20 GHz for the down-link and 30 GHz for the up-link. Key technologies to be developed include: solid-state satellite transmitters and low-noise amplifiers; techniques for spectrum conservation through multiple frequency reuse; on-board switching and signal processing; consideration of lens antennas, phased arrays, or paraboloid reflectors with feeds which generate multiple, narrow beams; and satellite compatibility with earth stations of moderate size and cost (1,2).

NASA could decide to launch an experimental satellite to further advance the technology prior to industry undertaking development of an operational 20/30 GHz satellite system. In that event, NASA would have to select a technical approach that would give valuable information for subsequent commercial designs by industry. It is likely that a single configuration will be synthesized from previously proposed conceptual designs. The challenge will be to maximize the technology development return from that configuration.

1.1 Background

Currently, domestic and international Fixed Service Satellites (FSS) provide point-to-point service at 4/6 GHz (C-band) or 12/14 GHz (Ku-band). Both of these bands provide 500 MHz of available spectrum for both the up-link and down-link. C-band transmissions are relatively immune to atmospheric water vapor, oxygen, and ozone absorption; Ku-band transmissions are only moderately affected. However, only a limited number of desirable synchronous equatorial orbital slots exist over the Atlantic Ocean, with its heavy traffic load, and over North, Central, and South America and the Caribbean, where many domestic systems operate today. Long before the year 2000, the available orbit slots and spectrum at 4/6 GHz and 12/14 GHz will be consumed through the growth in telecommunications traffic. Also, these bands are shared with many terrestrial services which complicate spectrum management to ensure that satellite and terrestrial systems do not interfere unacceptably with each other. Thus, the 20/30 GHz Ka-band is a likely candidate for commercial satellite service.

In order for this to occur, technology development must begin now. The principal advantage to the use of Ka-band is the availability of 2.5 GHz of spectrum for commercial use for both the up-link and down-link. This is five times the spectrum available at C-band or Ku-band. The principal disadvantage is the sharply increased atmospheric attenuation at 20 GHz and, particularly at 30 GHz, especially when rain lies in the path between the satellite and an earth station. Another disadvantage is the current relatively high cost of earth station 20 GHz receivers and 30 GHz transmitters. The twin challenges to the satellite system designer are to penetrate the atmospheric attenuation with a strong enough signal to provide a specified service (data rate and bit error rate) between 99.50 to 99.99% of the time, and to put enough performance into the satellite in order to moderate the cost of earth station equipment. Many workers in the field have studied 20/30 GHz satellite communications as indicated by the following references 3 through 14.

---

* This paper presents one phase of research conducted at the Jet Propulsion Laboratory, California Institute of Technology under contract No. NAS-7100 sponsored by the National Aeronautics and Space Administration.

** Member Technical Staff at JPL and Associate Fellow AIAA.

Copyright © American Institute of Aeronautics and Astronautics, Inc., 1980. All rights reserved.

2.0 Market To Be Served By The Satellite

A rationale must be developed for the size and distribution of the market to be served by the satellite. A 20/30 GHz commercial satellite will be used to interconnect large metropolitan areas which generate significant volumes of intercity message and data traffic. From a list of Standard Metropolitan Statistical Areas (SMSA's), 32 metropolitan areas were selected, based largely upon population as shown in Table 1. The 32 up-link and down-link beams from the paraboloid reflector antennas were directed at specific latitudes and longitudes within a given SMSA. Note that some beams will cover more than a single SMSA, as borne out by the population figures in the table. The New York, Chicago, and Los Angeles beams cover the largest populations within the Continental United States (CONUS). The 27 largest SMSA's in CONUS are served. Three smaller U.S. SMSA's are also served: Anchorage, Honolulu, and San Juan. In addition to providing atmospheric propagation data at high and low latitude earth stations, these beams also will test the performance of an off-set fed paraboloid reflector antenna at very large scan angles in terms of beamwidths. The 30 beams which are directed at U.S. cities, will cover more than 100 SMSA's larger than 150,000 population and more than one-half of the total U.S. population.

The Seattle beam includes Vancouver, B.C. The Buffalo beam includes Toronto. An individual beam is pointed at Montreal, in order that Canada's three largest cities will be covered. Also, as a means of sharing satellite technology on a neighborly basis, a beam is pointed at Mexico City, which is to become the world's largest SMSA.

Figure 1 shows a mercator projection of 30 of the 32 beams onto the surface of the Earth. The satellite is located on the equator at 95 deg. W. longitude. Each beam is conical with a 0.333 deg. half-power beamwidth. Notice that as the latitude and longitude of beam pointing directions departs further and further from the sub-satellite point, the intersections of the conical beams with the spherical Earth appear as distorted ellipses on this mercator projection. Notice that the beams are equally divided between vertical and horizontal polarization to reduce interference between nearby beams operating at the same frequency. Verification of the effectiveness of polarization isolation will be a part of the experimental satellite program. Figure 2 is a perspective view from the satellite at synchronous altitude. The projections of all 32 narrow conical beams retain their circular cross section in this figure.

3.0 Systems Considerations

The following sub-sections will discuss various systems considerations, requirements, or trade-offs that had significant impacts on the conceptual design of the satellite or the earth stations.

3.1 TDMA And FDMA

A commercial 20/30 GHz satellite may use either Time Division Multiple Access (TDMA) with on-board demodulation, digital data processing at baseband, satellite switching (SS), frequency translation and remodulation in a transponder or Frequency Division Multiple Access (FDMA) without on-board demodulation in a transponder. The conceptual design discussed in this paper employs an SS-TDMA rather than an FDMA transponder primarily to save weight, particularly with respect to the filters.

Preliminary results of the market studies commissioned by NASA Lewis (8) indicate that the intercity message and data traffic would not be evenly distributed among the 496 possible SMSA pairs in Table 1. In fact, the New York beam will generate or receive much more traffic than any other beam. The Chicago and Los Angeles beams also will be heavily loaded. It would appear that an even distribution of 100 MHz of spectrum for each of the 32 SS-TDMA beams would lead to situations where a few SMSA pairs (e.g. New York - Chicago) would be under-served, and many SMSA pairs (e.g. Anchorage - San Juan) would be over-served for the traffic generated. Rather than complicate the SS-TDMA transponder by requiring dynamic allocation of spectrum and transmitter power according to data rate demand, a uniform allocation of 100 MHz of spectrum and 4 watts of transmitter output power was made for each beam. Dynamic allocation of spectrum and transmitter power will await a second-generation SS-TDMA system.

3.2 Frequency Reuse And System Capacity

The pair of 20 and 30 GHz paraboloid reflector antennas are sized such that they both produce narrow beams with 0.333 degree half-power beamwidths. Each antenna has 32 off-set feeds that produce 32 narrow beams. The 32 down-link (20 GHz) beams cover the same areas as the 32 up-link (30 GHz) beams. Half of the up-link and down-link beams are vertically polarized, and half of the beams are horizontally polarized. This dual polarization coupled with the narrow beams and geographic separation permits eight-fold frequency reuse. The data rate in each up-link and down-link beam is 100 Mbps. Spectrum efficient QPSK modulation is used, so the bandwidth allocated to each beam is 100 MHz. The vertical and horizontal polarizations permit two-fold frequency reuse. However, due to geographic separation of the beams, the same bandwidth and frequencies can be reused four more times. This is illustrated in Table 1. Therefore, although the capacity of the TDMA paraboloid reflector system is 3.2 Gbps, only 400 MHz of spectrum near 20 and 30 GHz is required.

3.3 Single Beam TDMA Data Rate Selection

The 32 beam paraboloid reflector antennas will provide $(N^2-N)/2 = 496$ possible connections between SMSA's using the Satellite-Switched Time Division Multiple Access (SS-TDMA) scheme. Each of the 32 up-link or down-link beams will provide a data rate of 100 Mbps and, by using spectrum-efficient QPSK modulation, occupy 100 MHz of bandwidth. Each beam will provide 32 channels of digital data at a rate of 1.544 Mbps; each of these 32 channels corresponds to a standard DS-1 circuit. In addition, each beam will carry a shared, single channel of digital data at a rate of 44.736 Mbps which corresponds to a standard DS-3 circuit that has sufficient bandwidth for video signals. The total data rate for the 32 DS-1 circuits and the single DS-3 circuit is 94.144 Mbps. When the TDMA frame overhead is added, the required data rate for each beam approaches 100 Mbps.

3.4 Solid State Vs Traveling Wave Tube Amplifiers

A major objective is to eliminate, if possible, all Traveling Wave Tube Amplifiers (TWTA's) from the satellite, primarily in order to save weight. Gallium Arsenide Field Effect Transistors (GaAs FET's) are employed as Power Amplifiers (PA's).

GaAs FET's also can be used as Low Noise Amplifiers (LNA's). Thus, we have an all solid-state GaAsFET PA and LNA combination in the satellite which has modest power requirements and is light weight. This also makes it easy to physically separate transmitting and receiving subsystems in the satellite.

3.5 Trunking Or Direct-To-User Service

Most of the commercial C-band Fixed Satellite Service today is provided through trunking. Telephony, television, facsimile, and data are concentrated,primarily using telephone company facilities, which interface with a large, relatively costly earth station for transmission to or reception from a satellite with relatively modest performance. Both American Satellite Corporation and Satellite Business Systems are pioneering in providing direct-to-user commercial services where smaller, lower-cost earth stations located on the customer's premises are used, and, in the case of SBS, a higher performance, Ku-band (12/14 GHz) satellite. The 20/30 GHz satellite conceptual design discussed in this paper will provide trunking services relative to today's level of high-rate digital transmission while employing direct-to-user-cost-class earth stations for the up-link and down-link.

3.6 Service Availability Or Reliability

If it never rained, and the skies were not cloudy all day, the telecommunications link service availability or reliability could approach 100%. Also, the data rates could be very high using spectrum efficient modulation such as QPSK, and the bit error rate (BER) could be very low. However, all of this becomes technically very difficult and economically very costly when rain enters the picture, particularly for the 30 GHz up-links.

Generally, service availability or reliability goals are set at 99.50% to 99.99% of the time with bit error rates between 10^{-5} and 10^{-9} depending upon whether direct-to-user or trunking service (approximately respectively) is under consideration.

3.7 Link Performance And Service Availability Trade-Offs

Generally, there are two brute force methods of maintaining a given service availability for a given data rate and BER. First, the earth station 30 GHz up-link transmitter could have an auxillary, high-power mode for use when rain degrades the link performance. Similarly, the satellite 20 GHz down-link transmitter could have a commandable high-power mode. Both of these options add weight, complexity, and cost to the system. In the interest of economy, both the TDMA satellite transponder and the earth station transmitters will operate with a single, moderate power mode.

Antenna aperture size and, hence, gain could be increased either on-board the satellite or at the earth stations were it not for the following factors.

The size of the satellite paraboloid reflector antennas is set by the operating frequency and a desire to produce narrow beams of only 0.333 degree half-power width. The use of narrower beams (requiring larger antennas) could result in very large antenna beam pointing losses if the spacecraft attitude control system could not maintain an antenna pointing accuracy of 0.1 degrees.

The earth station paraboloid reflector antenna diameter is 4.6 meters which is representative of relatively low-cost direct-to-user stations. At 30 GHz, the narrow beamwidth will provide adequate discrimination between nearby satellites operating at the same frequency in synchronous orbit.

The use of cooling to reduce either the satellite or earth station receiver equivalent thermal noise temperatures has been avoided in order to keep system complexity, weight, and cost low in this area. Uncooled GaAs FET LNA's are used in both the satellite and earth station receiver front ends to provide relatively low noise temperatures at moderate cost.

Another technique that may increase service availability is the use of site diversity. Within a given narrow beam or SMSA service area, two identical earth stations, separated by 8-16 kilometers, are provided. At least one of the two stations should have a relatively weather-free link to the satellite at all times. The two stations are connected by a terrestrial microwave link operating at a lower frequency than 20 or 30 GHz that would not be severely affected by precipitation. However, the use of site diversity would double the number and, therefore, the total cost of the earth stations. A limited introduction of site diversity would be in keeping with the experimental nature of this satellite system. The approach used in this conceptual design is 1) to use conservative parameter assumptions in the telecommunications link design, and 2) to provide adequate up-link and down-link rain attenuation margins to assure a 99.5% service availability to all sites at 100 Mbps with a BER of 10^{-6}. In other words, a BER of 10^{-6} would be exceeded only 0.5% of the time or only 1.78 days in a year at any site. On days when there was very little water vapor in the atmosphere, the 100 Mbps data rate could be provided with a BER of 10^{-9} or less.

4.0 Telecommunications Link Performance

Table 2 presents a summary of telecommunications performance. The 30 GHz up-link, the 20 GHz down-link, and the combined link are detailed in the table.

The up-link and down-link data rates are 100 Mbps. Spectrum-efficient QPSK modulation is used, so the corresponding bandwidth is 100 MHz. The system was designed with generous up-link and down-link allowances for rain attenuation (without site diversity) to assure 99.5% service availability throughout six climate zones comprising the CONUS. Additional allowances were made for miscellaneous link losses due to spacecraft antenna surface roughness, microwave plumbing losses, and carrier interference from unwanted signal sources. The combined rain attenuation and miscellaneous link loss allowances are -20 dB for the 30 GHz up-link and -15 dB for the 20 GHz down-link.

The combined link performance, including attenuation, provides a link margin in excess of 3 dB relative to an energy per data bit to noise spectral density ratio, $E_b/N_o = 10.53$ dB, which corresponds to a QPSK BER = 10^{-6}. Without rain attenuation, the link margin exceeds 12 dB relative to E_b/N_o=12.55 dB, which corresponds to a QPSK BER = 10^{-9}.

4.1 Communications Subsystem Design

Figure 3 presents the TDMA frame format. The total time span of the frame is 32768 microseconds. At the beginning of each frame are two 64 microsecond periods that are used for central and local timing references and synchronization for the entire TDMA subsystem. The remainder of the frame is divided into 32 periods of 1020 microseconds with one such period for each of the 32 possible SMSA destinations. At the beginning of each 1020 microsecond period is a preamble consisting of a guard time, a carrier and clock recovery time, and a burst start identification code word, each of which lasts 4 microseconds. The data packet itself lasts 1000 microseconds. This is followed by an 8 microsecond postamble. Each of the 32 up-link or down-link beams will support a data rate of 100 Mbps. Therefore, each complete TDMA frame will contain 32 x 1000 x 10^{-6} sec x 10^8 bits/sec = 3.2 megabits of digital data. Also, the frame overhead will be (32 x 20 + 2 x 64)10^{-6} sec/ (32 x 1000) 10^{-6} sec = 2.4%. In one second, there could be as many as 32/0.032768 = 976 switches between beams.

Figure 4 presents the SS-TDMA satellite transponder. Carriers from the 16 vertically and 16 horizontally polarized up-link beams between 29.6 and 30.0 GHz enter one of eight geographically segmented combiner filters which are followed by low-noise GaAs FET preamplifiers. With the aid of local oscillators and 400 MHz bandwidth amplifiers, each group of four carrier frequencies (F1, F2, F3, and F4) is down-converted to 6 GHz. A bank of 100 MHz bandwidth filters (excluding guard bands to be determined during detailed filter design) separates the individual beam carriers prior to demodulation of the QPSK 100 Mbps data stream and entry into a data register. Data routing control and switching occur at baseband with up to 976 switches per second. The switching may be altered by command from a Telemetry, Tracking, and Control (TT & C) central system earth station if desired. Leaving the switch, the data stream again enters a data register, is QPSK modulated, and, with the aid of a local oscillator, is up-converted to the down-link frequency. Each data stream passes through a 4 watt GaAs FET power amplifier, enters one of eight geographically segmented multiplexers, and becomes one of the 16 vertically or 16 horizontally polarized down-link beams between 19.8 and 20.2 GHz.

Figure 5 diagrams one of the 32 TDMA earth stations. Thirty-two channels of 1.544 Mbps data plus one channel of 44.736 Mbps data from local telephone company digital concentrators enters a bank of input/output buffers. The data stream is now under the supervision of a demand access processor/ controller, which meters the data into a time division multiplexer/demultiplexer, where the TDMA frames are either made up or broken down. For the up-link, the data enters a QPSK modulator at 100 Mbps. A local oscillator up-converts to the 30 GHz carrier frequency. The transmitter uses a 100 watt TWTA. A satellite TDMA frame timing monitor directs the transmitter power into the diplexer and thence to be radiated from the 4.6 meter diameter paraboloid antenna. If the satellite TDMA frame timing monitor senses that data is to be received, the down-link data stream passes through the antenna, through the diplexer, and into a low-noise GaAs FET amplifier with a bandwidth of 100 MHz. With the aid of a local oscillator, the 20 GHz carrier frequency is down-converted and demodulated by the receiver. The 100 Mbps data stream is then demultiplexed and sent to the buffer for distribution to local telephone company circuits. In this TDMA subsystem, the up-link and down-link data rates are both 100 Mbps. The subsystem operates continuously. Therefore, there is no need to burst the data on the up-link at higher data rates.

4.2 Telecommunications Link Parameters

There are two commonly used expressions for computing antenna gain for a paraboloid of 54% efficiency as chosen in this study (see "ITT Reference Data for Radio Engineers"). $G = 27000/\theta^2$ or $G = 59.1\ d^2f^2$, dimensionless, where θ = antenna 3 dB beamwidth = 21.35/df, degrees, d = antenna diameter, meters, f = frequency, GHz. Of course, these expressions are equally applicable to receiving or transmitting antennas. Also, the gain may be expressed in decibel form. In the case of the 20 and 30 GHz spacecraft paraboloid reflectors, the beamwidth, θ = 0.333 deg. for both antennas. Therefore, the product df = 64, and the antenna diameters are 3.2 meters and 2.13 meters, respectively. Also, the gain for the antennas is $G = 27000 \div (1/3)^2$ or 53.85 dB at both 20 and 30 GHz.

The earth station antenna is a paraboloid reflector with a diameter of 4.6 meters. At 20 GHz, the gain is $G = 59.1(4.6)^2(20)^2$ or 57.00 dB. At 30 GHz, the gain is $G = 59.1(4.6)^2(30)^2$ or 60.52 dB.

The transmitters for each of the 32 narrow beams from the paraboloid reflector are composed of GaAs FET Power Amplifiers with an output of 4 watts. (Smaller GaAs FET's may have to be combined in parallel in order to provide a 4 watt output at 20 GHz for each narrow beam.)

International Radio Regulations limit the power flux density (PFD) on the surface of the earth in the band from 17.7-22.0 GHz to -115 dBW/m^2 in any 1 MHz band for angles of arrival between 0 and 5 degrees above the horizontal plane (under assumed free-space propagation conditions). This can be expressed as follows:

$$\text{PFD}, \frac{\text{Watts}}{\text{m}^2} = \frac{\text{sat. EIRP, Watts}}{\text{sat. transponder BW, MHz}} \; \frac{1\ \text{MHz}}{4\pi R^2, \text{m}^2}$$

This can be re-written in terms of the maximum allowable satellite EIRP as:

$$\begin{aligned} \text{EIRP}_{\text{max}}, \text{dBW} &= -115 \frac{\text{dBW}}{\text{m}^2} + 162.07\ \text{dBm}^2 + \text{BW dBMHz} \\ &= 47.07\ \text{dBW} + \text{BW dBMHz} \end{aligned}$$

For this satellite, each of the 32 TDMA beams is allocated a portion of the bandwidth of the transponder. BW = 100 MHz = 20 dBMHz for the 20 GHz down-links. This means that the satellite EIRP of 59.87 dBW is within the allowable EIRP_{max} = 67.07 dBW.

There are no limits on earth station EIRP provided that the antenna elevation angle is at least 5 deg. above the local horizontal. For the earth stations, a Traveling Wave Tube Amplifier (TWTA) with a power output of 100 watts at 30 GHz is specified. This is well within current technology.

The free-space loss is specified for the slant range from the satellite to the center of the area to be served, i.e., 37.5 deg. N. latitude and 95 deg. W. longitude. This gives $R = 3.74 \times 10^7$ meters (instead of $R = 3.58 \times 10^7$ meters at the sub-satellite point on the equator).

Both the earth station receivers and the satellite receiver use GaAs FET Low Noise Amplifiers (LNA's) which are uncooled. They are assumed to have equivalent thermal noise temperatures of 316 K or 25 dBK, and 1000 K or 30 dBK, respectively. The satellite receiver has a higher temperature because the spacecraft antennas point towards the 293 K earth.

5.0 General Satellite Configuration Description

Figure 6 presents a proposed satellite conceptual design which employs a pair of multiple-beam paraboloid reflector antennas. The larger antenna is for the 20 GHz transmitting down-link, and the smaller antenna is for the 30 GHz receiving up-link. The antennas are cantilevered from one face of the spacecraft bus, which is a 152.5 cm cube. The antennas fold up for launch. The antennas themselves do not fold; they are merely hinged at the cantilever points. The paraboloid reflectors have circular cross-sections when viewed from the front with diameters of 3.2 m and 2.13 m. The paraboloid reflectors use off-set feed arrays each of which is supported by three struts (that do not fold for launch). The paraboloid reflector antennas have an f/d equal to 2/3. Also, the off-set angle of the feed array is 20.55 deg. with respect to the paraboloid axis of symmetry in order to reduce aperture blockage.

The spacecraft derives its electrical power from roll-out solar arrays. The arrays are comprised of flexible solar cells mounted to a thin substrate that is initially rolled inside two cannisters, which are 30.5 cm in diameter and 152.5 cm long, prior to deployment at geosynchronous altitude. As the solar arrays deploy, tapered, telescoping, articulating booms, which are initially stored inside two cannisters, which are 30.5 cm in diameter and 61 cm long, also are deployed. The articulating booms enable the solar arrays to track the sun (in an East-West sense) as the geosynchronous spacecraft orbits the Earth. The array and boom cannisters are mounted on the sides of the spacecraft bus as shown in Figure 6. When the solar arrays are fully deployed, their active areas total 21.38 sq. m. With the solar arrays deployed, the maximum spacecraft dimension is 16.77 m.

5.1 Off-set Feeds For Paraboloid Reflector Antennas

Figure 7 shows the front of the feed array assembly for the paraboloid reflector antennas. The feeds consist of small horns with openings of dimensions $\lambda \times \lambda$ arranged in a mirror image pattern of the 32 independent beams to be generated. At frequencies of 20 and 30 GHz, the wavelengths are 15 mm and 10 mm, respectively. Thus the dimensions of the front of the rectangular feed array assembly are 16λ by 40λ . The feed assemblies are assumed to be 15 cm deep. This should permit the inclusion of Gallium Arsenide Field Effect Transistor (GaAs FET) Power Amplifiers (PA's) and the multiplexers within the 20 GHz feed assembly or GaAs FET Low Noise Amplifiers (LNA's) and the combiner filters within the 30 GHz feed assembly. This provides an all-solid-state system with physical separation between the transmitting and receiving feed assemblies. Half of the horns are polarized vertically, and half are polarized horizontally to assist in isolating nearby beams. Dual polarization plus the combiner filters and multiplexers which geographically segment the feeds permit eight-fold frequency reuse. The isolation between adjacent beams is desired to be at least 25 dB.

5.2 Attitude Control And Paraboloid Antenna Pointing Loss

The attitude control system stabilizes the spacecraft about all three principal axes. A monomethyl hydrazine gas jet system is used for initial orientation and spacecraft positioning upon reaching GEO. The jets will be used for East-West(longitudinal) and North-South (plane change) station-keeping. The bulk of the propellant will be used to overcome plane changes due to orbit perturbations by the Sun and the Moon. A three-axis system of momentum wheels will be required to assure that the spacecraft and, therefore, the antenna beams can be pointed to within 0.1 deg. of the desired direction (15). When the momentum wheels become saturated, the gas jets will be used to unload the wheels. Lastly, accurate Sun and Earth-limb sensors will be required for spacecraft pointing references.

The paraboloid reflector antennas and their offset feeds produce narrow beams with half-power, or -3 dB, beamwidths, $\theta = 0.333$ deg. at both 20 GHz and 30 GHz. Thus, a 0.1 deg. total spacecraft attitude control pointing capability corresponds to a $0.3\ \theta$ antenna pointing error. Both paraboloid antennas have diameter-to-wavelength ratios $d/\lambda = 213$. This enables the computation of an antenna pointing loss of 1.10 dB for either reflector antenna.

5.3 Paraboloid Antenna Surface Roughness Loss

For a paraboloid reflector with an f/d ratio equal to 2/3, the loss, L, will be 0.41 dB, due to an RMS surface roughness, σ, if we assume that the surface roughness-to-wavelength ratio, $\frac{\sigma}{\lambda} = 0.0254$.

For frequencies of 20 and 30 GHz, the corresponding RMS surface roughness, σ, would be 0.381 mm and 0.254 mm, respectively.

For both paraboloid reflectors, the ratio of diameter to RMS surface roughness $\frac{d}{\sigma} = 8400$ which is well within current industry manufacturing capability (16).

5.4 Launch Vehicle And Upper Stage Considerations

When the spacecraft is ready for launch with its antennas folded up, it could be enclosed in a cylindrical volume of radius 1.92 m and length 6.1 m. This does not include an allowance for an apogee kick motor (AKM) to circularize the orbit and to make the necessary plane change after the spacecraft reaches apogee on its transfer ellipse. Also, an allowance for a perigee kick motor (PKM) to transfer the spacecraft from low earth orbit (LEO) to geosynchronous earth orbit (GEO) is not included. In view of the volume of the spacecraft, the use of expendable launch vehicles such as the Delta, Atlas/Centaur, Japanese "N" vehicle, or the ESA Ariane would be precluded. This is primarily due to the desire to have large, high-gain antennas that produce narrow beams. Therefore, the Space Transportation System (STS) will be used. The Shuttle orbiter payload bay volume is a cylinder 4.57 m in diameter and 18.29 m long. If the weight of the spacecraft plus AKM can be limited to 2000 kg, the Spin Stabilized Upper Stage or SSUS-A may be used as the PKM. The SSUS-A stage weighs 4890 kg. The Shuttle plus the SSUS-A is equivalent to the Atlas/Centaur for this mission.

5.5 Spacecraft Electrical Power

The spacecraft derives its electrical power from roll-out solar arrays. Nickel-Cadium storage batteries will be used during the semi-annual solar eclipse periods which may last up to 72 minutes. The battery capacity will be defined by the reduced demands during roughly 10:00 P.M. to 2:00 A.M., local time, in the areas served by the satellite. Also, Ni-Cad batteries, which undergo many cycles, should not be discharged to less than 50% of their rated capacity.

The active area of the deployed solar arrays is 21.38 sq. m. If we assume that the satellite will survive for about seven years, the solar cell output will degrade (non-linearly) about 25% from the beginning of life (BOL) to the end of life (EOL) due to radiation damage. Also, the articulating booms only remove the East-West component of the solar incidence angle with respect to the solar arrays. A factor of cos (23.5 deg) will compensate for the maximum North-South motion of the sun relative to the solar panels during the year. We will assume that operation of all spacecraft subsystems will require 50% of the power at EOL and a solar incidence angle of 23.5 deg. This will leave 50% of the power for operation of the spacecraft transmitters that are in use at that time. All transmitters are assumed to be Gallium Arsenide Field Effect Transistors (GaAs FET's) which are assumed to be 20% efficient in converting input power to RF output power at 20 GHz in the early 1980's. Assume that the solar array output at BOL will be 87.14 watts/sq. m. Thus, at EOL we will be able to generate approximately: 21.38 sq. m. x 87.14 watts/sq. m x (1.00 - 0.25) x 0.917 x 0.5 x 0.20 = 128 watts of RF output power at 20 GHz (17).

6.0 Conclusions

This paper has described an experimental 20/30 GHz communications satellite conceptual design employing multiple-beam paraboloid reflector antennas coupled to a Time Division Multiple Access (TDMA) transponder.

The area to be served by this satellite would be the CONUS, plus Alaska, Hawaii, Puerto Rico, and the Virgin Islands. In addition, part of Southern Canada plus Mexico City would be served. The feeds for the paraboloid reflectors produce 32 narrow beams directed at selected Standard Metropolitan Statistical Areas. The narrow beams serve more than one-half of the United States population. The narrow beams use geographic and polarization diversity to obtain eight-fold frequency reuse amongst themselves.

The telecommunications link performance is presented. The up-link and down-link data rates are 100 Mbps for each of the multiple narrow beams from the paraboloid antennas coupled to a TDMA subsystem. Spectrum-efficient QPSK modulation is used. The combined link performance provides a BER = 10^{-6} with the presence of rain in the link. In clear weather, the combined link performance provides a BER less than 10^{-9}.

The satellite employs solid state GaAs FET Power Amplifiers and uncooled Low Noise Amplifiers. The 20 GHz transmitting and 30 GHz receiving system elements are physically separated in this configuration. Signal processing and switching takes place on-board the spacecraft bus. The spacecraft is three-axis stabilized and has roll-out solar arrays which produce 1860 watts of power at the beginning of the mission. The spacecraft would be launched using the Space Transportation System.

The earth stations have 4.6 meter diameter paraboloid antennas, uncooled GaAs FET Low Noise Amplifiers, and TWTA transmitters. The earth stations are designed to be low cost.

7.0 References

1) "Technical Priorities for Future Satellite Communications", Satcom Technology Study Team - J.H. McElroy, Study Manager, Office of the Director, Goddard Space Flight Center, July, 1978.

2) "NASA's Role in Satellite Communications R & D", Communications Division, Office of Space and Terrestrial Applications, NASA Headquarters, Washington, D.C., February 7-8, 1979.

3) Advanced Satellite Communications Systems Using the 20-30 GHz Bands", Proceedings of a Symposium held at Genoa, Italy, 14-16 December 1977, European Space Agency, ESA SP 138.

4) "Japan Bids for Leadership in Space Communications", C.L. Cuccia, "Microwave Systems News", March, 1978.

5) "Expanding Broadband Switched Communications Networks", David H. Staelin, "Satellite Communications", January, 1979.

6) "Meeting the Twin Challenges of Demand and Conservation of Spectrum and Orbit Through Technology", David Jarett, IEEE EASCON-77 RECORD, Arlington, Virginia, September 26-28, 1977.

7) "On Several Communications Satellite Designs Using Large Space Antennas",Alfred M. Goldman, Jr. and Robert Edelson, Pacific Telecommunications Conference, Honolulu, Hawaii, January 8-9, 1979.

8) "Determining Potential 30/20 GHz Domestic Satellite System Concepts and Establishment of a Suitable Experimental Configuration", Grady H. Stevens and Godfrey Anzic, International Telecommunication Exposition, Dallas, Texas, February 26 - March 2, 1979.

9) "The DSCS III Satellite - A Defense Communication System for the '80's", I.S. Haas and A.T. Finney, AIAA 7th Communications Satellite Systems Conference, San Diego, California, April 24-27, 1978.

10) "Big Comsats for Big Jobs at Low User Cost", Ivan Bekey, "Astronautics and Aeronautics", February, 1979.

11) "A Scanning Spot-Beam Satellite System", D.O. Reudink and Y.S. Yeh, "Bell System Technical Journal", October, 1977.

12) "A Rapid Scan Area-Coverage Communication Satellite", D.O. Reudink and Y.S. Yeh, AIAA 7th Communications Satellite Systems Conference, San Diego, California, April 24-27, 1978.

13) "Spot Beams Promise Satellite Communication Breakthrough", D.O. Reudink "IEEE Spectrum", September, 1978.

14) "Imaging Reflector Arrangements to Form a Scanning Beam Using a Small Array", C. Dragone and M.J. Gans, "Bell System Technical Journal", February, 1979.

15) Federal Communications Commission - Docket No. 20271 Report and Order released December 21, 1978, page A-238.

16) "Industry Capability for Large Space Antenna Structures", R. E. Freeland, Jet Propulsion Laboratory Report 710-12, May 25, 1978 (Internal Document).

17) "Aviation Week and Space Technology", January 15, 1979 issue, page 47 plus private communication with Larry Chidester of Lockheed Missiles and Space Company.

TABLE 1. POPULATION SERVED BY 32 FIXED BEAMS

BEAM	POPULATION SERVED	BEAM POLARIZATION	BEAM FREQUENCY
New York NY; Philadelphia, PA; Newark, NJ	20,641,900	H	F1
Nassau-Suffolk, NY; Hartford, CN	5,469,100	V	F4
Boston, MA	6,713,100	H	F3
Washington, D.C.; Baltimore, MD	6,778,300	V	F2
Pittsburgh, PA; Cleveland, OH	6,286,100	V	F3
Cincinnati, OH; Indianapolis, IN	3,654,300	V	F4
Columbus, OH	2,310,100	H	F1
Detroit, MI	6,428,200	V	F2
Buffalo, NY; Toronto, ONT	5,558,100	H	F4
Montreal, QUE	2,798,000	V	F1
Chicago, IL: Milwaukee, WI	9,474,300	H	F4
Minneapolis - St. Paul, MN	2,010,800	V	F3
St. Louis, MO	2,548,900	H	F3
Kansas City, MO	1,481,100	V	F1
Atlanta, GA	1,776,000	H	F2
Tampa - St. Petersburg, FL	2,070,400	V	F1
Miami, FL	2,656,300	H	F3
San Juan, P.R.	707,275	H	F2
New Orleans, LA	1,497,400	H	F4
Houston, TX	2,746,400	V	F3
Dallas-Ft. Worth, TX	2,652,900	H	F1
San Antonio, TX	1,368,500	V	F2
Denver-Boulder, CO	1,684,300	H	F2
Phoenix, AZ	1,605,700	V	F4
San Diego, CA; Riverside, CA	2,731,900	H	F3
Los Angeles, CA; Anaheim, CA	9,354,800	V	F2
San Francisco, CA; San Jose, CA	6,189,600	H	F1
Portland, OR	1,518,100	H	F2
Seattle, WA; Vancouver, B.C.	2,931,000	V	F3
Anchorage, AL	148,800	V	F1
Honolulu, HA	691,200	H	F4
Mexico, D.F.	11,943,050	V	F4

Beam Polarization: H - Horizontal, V - Vertical
Beam Frequency:

F1 - 19.8-19.9 GHz or 29.6-29.7 GHz
F2 - 19.9-20.0 GHz or 29.7-29.8 GHz
F3 - 20.0-20.1 GHz or 29.8-29.9 GHz
F4 - 20.1-20.2 GHz or 29.9-30.0 GHz

TABLE 2. TELECOMMUNICATIONS LINK PERFORMANCE SUMMARY (SINGLE BEAM)

UP-LINK (f=30 GHz, λ=10mm)	
Earth station transmitting antenna gain	60.52 dB
Earth station transmitter output power (100 watts)	20.00 dBW
Satellite receiving antenna gain	53.85 dB
Boltzmann constant, 1/k	228.60 $\frac{\text{dBW}}{\text{KHz}}$
Free Space Loss (R=37400 km)	-213.44 dB
Satellite receiver temperature (T=1000K)	- 30.00 dBK
Bandwidth, B = 100 MHz, equivalent to data rate = 100 Mbps	-80.00 dBHz
Allowance for rain attenuation	-15.00 dB
Miscellaneous additional up-link losses	-5.00 dB
$(S/N)_{up}$ including rain attenuation	19.53 dB
$(S/N)_{up}$ without rain attenuation	34.53 dB
DOWN-LINK (f=20 GHz, λ= 15mm)	
Satellite transmitting antenna gain	53.85 dB
Satellite transmitter output power (4 watts per beam)	6.02 dBW
Earth station receiving antenna gain	57.00 dB
Boltzmann constant, 1/k	228.60 $\frac{\text{dBW}}{\text{KHz}}$
Free space loss (R=37400 km)	-209.92 dB
Earth station receiver temperature (T=316K)	-25.00 dBK
Bandwidth, B=100 MHz, equivalent to data rate = 100 Mbps	-80.00 dBHz
Allowance for rain attenuation	-10.00 dB
Miscellaneous additional down-link losses	-5.00 dB
$(S/N)_{down}$ including rain attenuation	15.55 dB
$(S/N)_{down}$ without rain attenuation	25.55 dB
COMBINED LINK	
$(S/N)_{comb}$ including rain attenuation	14.09 dB
link margin relative to E_b/N_o =10.53 dB and BER = 10^{-6}	3.56 dB
$(S/N)_{comb}$ without rain attenuation	25.04 dB
link margin relative to E_b/N_o = 12.55 dB and BER = 10^{-9}	12.49 dB

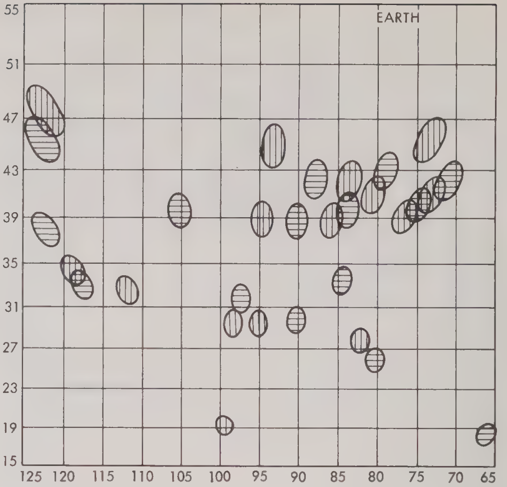

SATELLITE LOCATED ON EQUATOR AT 95 deg WEST LONG.

Figure 1. Mercator Projection of 0.333 Deg. Beams from paraboloid reflector antennas

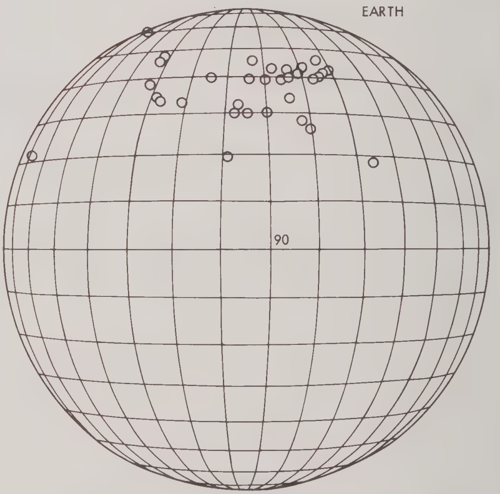

SATELLITE LOCATED ON EQUATOR AT 95 deg WEST LONG.

Figure 2. Perspective view from the satellite showing 0.333 Deg. beams from paraboloid reflector antennas.

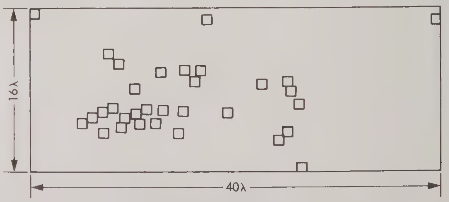

Figure 7. Off-set feed assembly for 20 GHz or 30 GHz paraboloid reflector antennas.

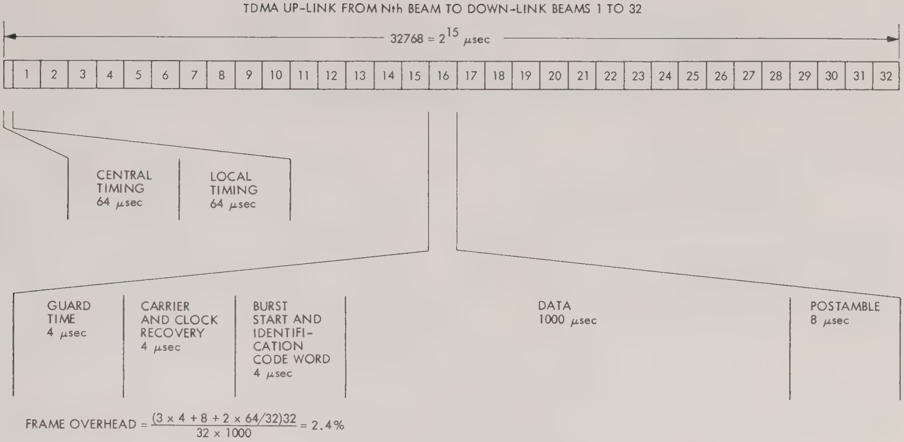
TDMA UP-LINK FROM Nth BEAM TO DOWN-LINK BEAMS 1 TO 32
32768 = 2^15 μsec
1 2 3 4 5 6 7 8 9 10 11 12 13 14 15 16 17 18 19 20 21 22 23 24 25 26 27 28 29 30 31 32
CENTRAL TIMING 64 μsec
LOCAL TIMING 64 μsec
GUARD TIME 4 μsec
CARRIER AND CLOCK RECOVERY 4 μsec
BURST START AND IDENTIFICATION CODE WORD 4 μsec
DATA 1000 μsec
POSTAMBLE 8 μsec
FRAME OVERHEAD = (3 x 4 + 8 + 2 x 64/32)32 / 32 x 1000 = 2.4%

Figure 3. TDMA Frame Format

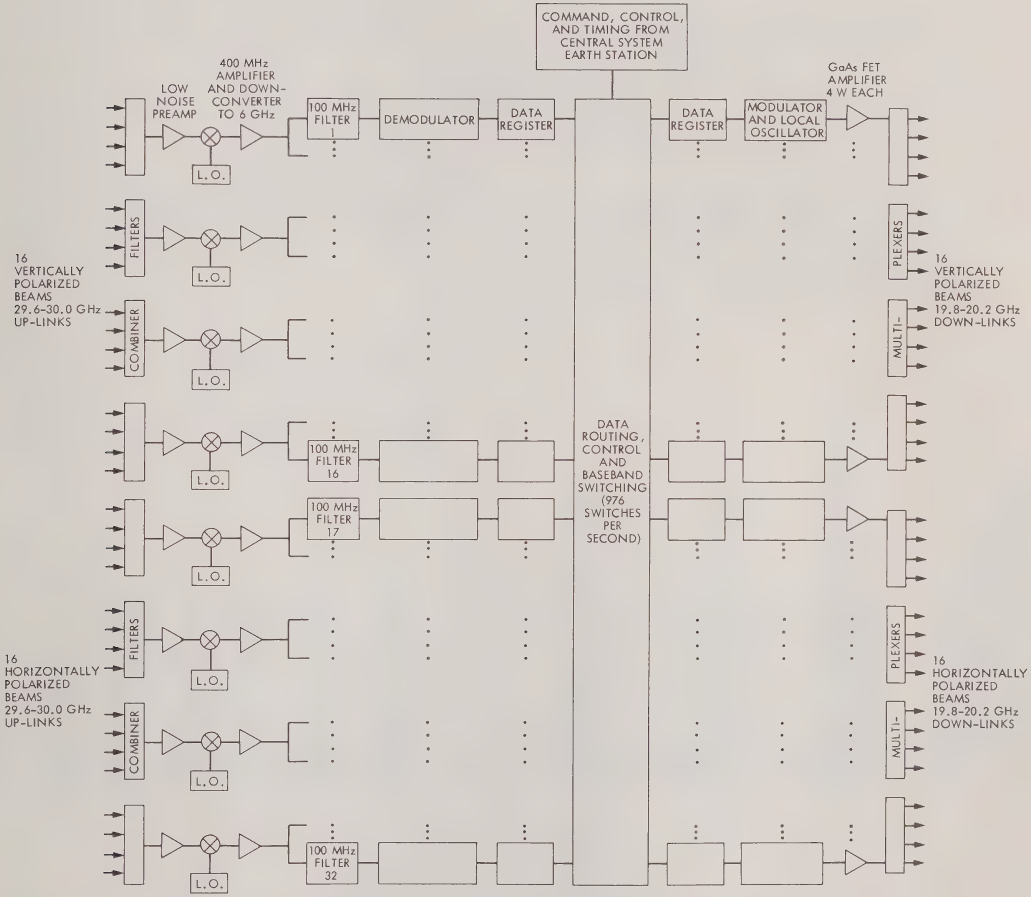
COMMAND, CONTROL, AND TIMING FROM CENTRAL SYSTEM EARTH STATION
LOW NOISE PREAMP
400 MHz AMPLIFIER AND DOWN-CONVERTER TO 6 GHz
100 MHz FILTER 1
DEMODULATOR
DATA REGISTER
DATA REGISTER
MODULATOR AND LOCAL OSCILLATOR
GaAs FET AMPLIFIER 4 W EACH
L.O.
FILTERS
COMBINER
16 VERTICALLY POLARIZED BEAMS 29.6-30.0 GHz UP-LINKS
PLEXERS
MULTI-
16 VERTICALLY POLARIZED BEAMS 19.8-20.2 GHz DOWN-LINKS
100 MHz FILTER 16
100 MHz FILTER 17
DATA ROUTING, CONTROL AND BASEBAND SWITCHING (976 SWITCHES PER SECOND)
16 HORIZONTALLY POLARIZED BEAMS 29.6-30.0 GHz UP-LINKS
16 HORIZONTALLY POLARIZED BEAMS 19.8-20.2 GHz DOWN-LINKS
100 MHz FILTER 32

Figure 4. SS-TDMA Satellite Transponder (on-board data processing and switching at baseband).

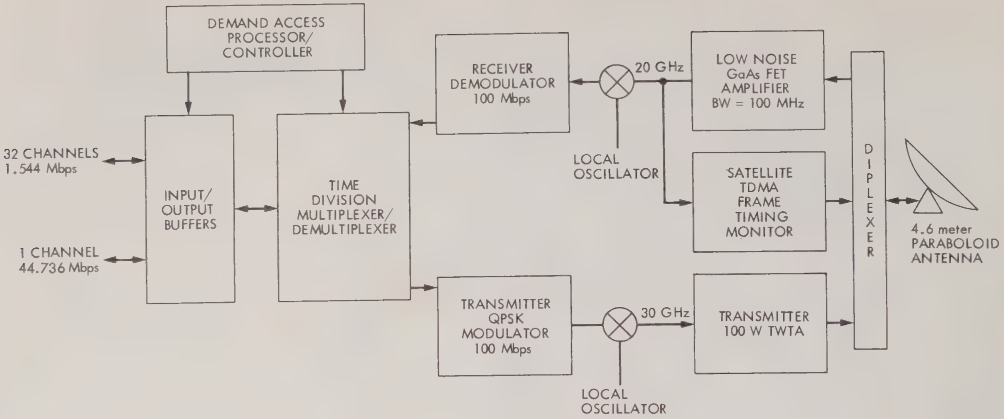
DEMAND ACCESS PROCESSOR/ CONTROLLER
RECEIVER DEMODULATOR 100 Mbps
20 GHz
LOW NOISE GaAs FET AMPLIFIER BW = 100 MHz
32 CHANNELS 1.544 Mbps
LOCAL OSCILLATOR
SATELLITE TDMA FRAME TIMING MONITOR
DIPLEXER
INPUT/ OUTPUT BUFFERS
TIME DIVISION MULTIPLEXER/ DEMULTIPLEXER
4.6 meter PARABOLOID ANTENNA
1 CHANNEL 44.736 Mbps
TRANSMITTER QPSK MODULATOR 100 Mbps
30 GHz
TRANSMITTER 100 W TWTA
LOCAL OSCILLATOR

Figure 5. TDMA Earth Station

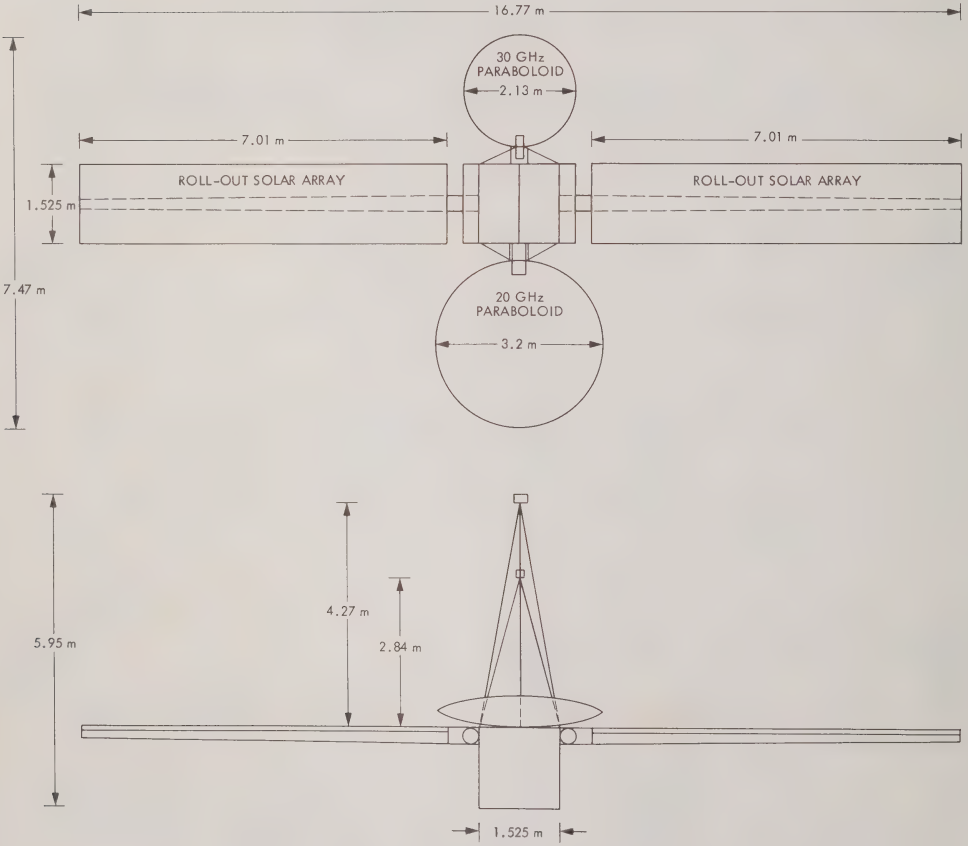
16.77 m
30 GHz PARABOLOID
2.13 m
7.01 m
7.01 m
ROLL-OUT SOLAR ARRAY
ROLL-OUT SOLAR ARRAY
1.525 m
7.47 m
20 GHz PARABOLOID
3.2 m
5.95 m
4.27 m
2.84 m
1.525 m

Figure 6. Satellite Configuration

80-0588

ARIANE PERFORMANCES AND COST FOR COMMUNICATION SATELLITE LAUNCHES

Brian STOCKWELL
Deputy Head, Ariane Program Office
European Space Agency (ESA)
Paris, France

Abstract

The paper describes the genesis of the Ariane program, the developmental activities of the past years, and the test results that have been achieved so far. In particular, the results of the first qualification launch will be described.

The paper then goes on to describe the planning for the completion of the qualification launches, and for the series of committed operational launches through 1985.

The performance of Ariane 1 will be given in detail, together with the projected performances of Ariane 2 and Ariane 3.

The commercial basis of the Ariane launch Service will be described and technical interface, performance, and cost data will be given.

Introduction

The Ariane launch vehicle development program was agreed in 1973 by the Member States of the European Space Agency, and the aim of that program was to provide an independent launch capability for European and other users for geostationary payloads in the 1,000 kg class. This aim is close to fulfillment and Ariane will be available to the world market for the provision of launch services at the end of 1980.

Development Program

The Ariane design is based upon proven technology, and draws much from previous European launcher programs. The storable first and second stages are directly derived from the developments of the French National program (which successfully produced the Diamant satellite launcher), while the cryogenic third stage derived its technology from major preceeding developmental efforts.

The development effort has proceeded successfully, and the fourth and final qualification flight will occur on schedule in 1980. The total European investment in the program at that time will exceed 900 million US dollars at current rates.

As an additional development and demonstration aid, it is intended to use the second, third, and fourth qualification flights in order to orbit real payloads. The second flight will carry the Max Planck Institute Firewheel and amateur radio Amsat spacecraft, the third flight will carry the ESA Meteosat, plus the Apple spacecraft from India; the fourth flight will carry the ESA Marecs-A maritime communications spacecraft.

Thus, at the end of 1980, Ariane will be able to provide a thoroughly proven launch service to all potential users. The place that Ariane occupies in the launch service spectrum is shown in fig.1, with the range of performances given for Ariane corresponding to the improvements expected by the time of the later production launches.

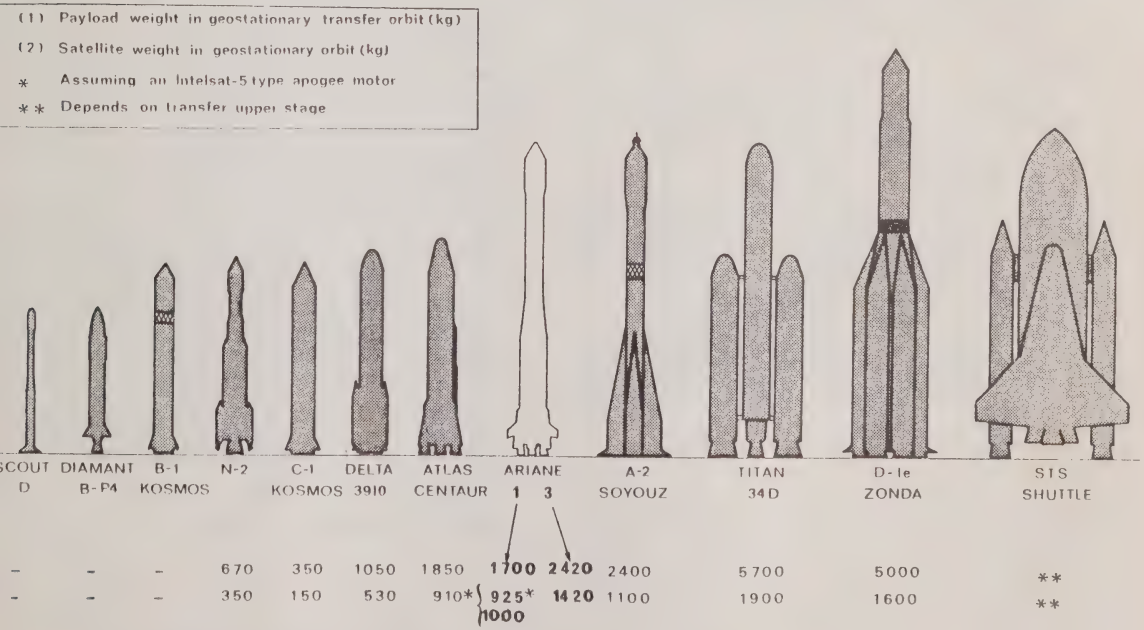

Released to AIAA to publish in all forms.

Operational Program

The first batch of six operational vehicles is in full production, and a follow-on batch of five has now been committed.

Currently Ariane is committed to provide launch services for the ESA maritime mission (at least two launches), for the ESA Sirio-2 project, for the ESA scientific mission Exosat, for Intelsat-5 (one firm launch and two options), for the European fixed services PTT Eutelsat System (at least four launches), for the French domestic Telecom fixed services system (at least two launches), and for the French Spot Earth Observation satellite. Other firm users are in immediate prospect, including an operational European Meteorological System, an eventual European Remote Sensing program, and several experimental and operational direct television broadcast systems.

In addition Ariane has been offered in support to the Arabian Regional System, to Indonesia for the Palapa-B system, and to Canada for Anik-D, and overall the market for Ariane is seen as large and expanding.

The performance of the initial production version of Ariane is such that nominally 1,700 kg can be placed in the geostationary transfer orbit corresponding to approximately 925 kg in geostationary orbit - the transfer orbit from the European launch site in French Guyana being such as to considerably improve injection efficiency in comparison with launches from Florida in the USA. In fact the performance of Ariane is such that already some 1,800 kg into transfer orbit is possible, while growth versions of Ariane already in hand will bring this to over 2,400 kg.

The current overall Ariane performance, on the conservative basis of the 1,700 kg baseline, is given in fig.2 for a variety of possible missions. The currently available shroud volume is depicted in fig.3.

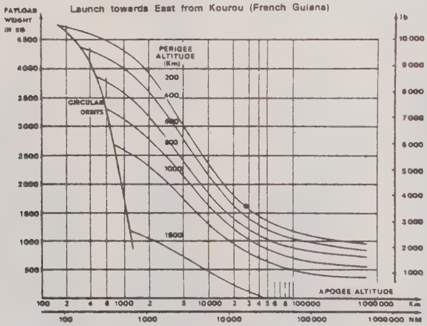

Fig.2 - General Performance of Ariane-1

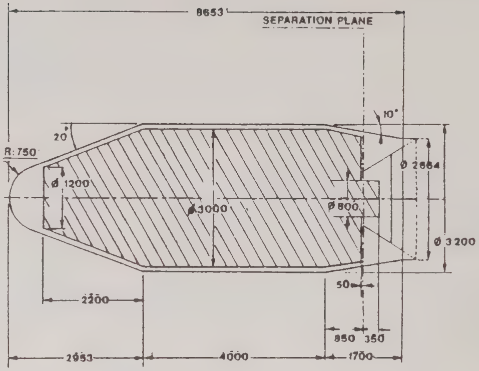

Fig.3 - Fairing envelope and payload free volume

Performance Improvements

A performance improvement program is currently in hand. This will lead to the flight in 1982 of the first uprated version of the basic launcher. The improvements that are in hand include the addition of two seven-ton strap-on solid boosters, the uprating of the Viking engines of the first and second stages (via a 10% pressure increase), the stretch of the third stage so as to increase propellant capacity from 8 to 10 tonnes, the improvement of the third stage motor, and an increase in the shroud length. These various modifications will bring the performance into transfer orbit up to 2,400 kg. At this payload level the particularly demanding missions expected in the mid "80"s (including the direct TV Broadcast mission) can certainly be met, fig.4

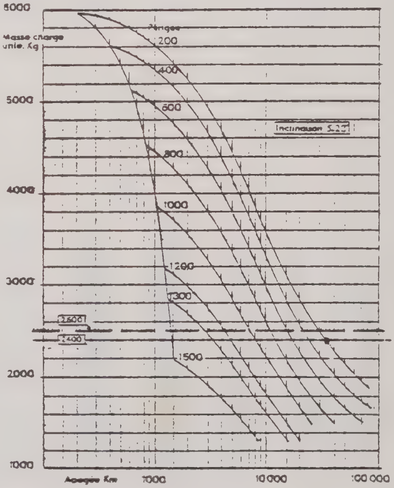

Fig.4 - Performance of Ariane-3

As a separate matter, the development is also in hand of a dual launch system (SYLDA), allowing Ariane to carry two payloads independently but simultaneously, (fig.5).The capability will become operational with the combined Sirio-2/Marecs-B launch in April 1981, and will initially allow the simultaneous launching of two spacecraft corresponding to a 3910/PAM class vehicle plus a 2914 class vehicle (these being the Delta equivalents). With the advent of Ariane-3 both spacecraft can be of the STS/PAM class.

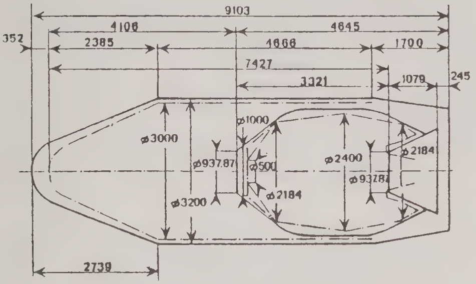

Fig.5 - Configuration Ariane 3-SYLDA growth version

The Ariane Launch Service

It is the policy of the Agency to offer Ariane in support to all peaceful missions and systems, be they European or not, and at prices and on terms that are intended to be competitive with other launch services that may be offered to the world market.

The development costs of the Ariane program have not been and will not charged to operational users.

The Ariane launch service is available on a commercial basis to all appropriate civilian entities. The conventional nature of the Ariane vehicle, the well-established manufacturing and operational infrastructure, and the firm commitments of European and non-European users for missions running into the mid 80"s together allow a very precise definition of cost (and performance) into the future. It is therefore possible to offer guaranteed maximum prices years ahead without risk of the customers in terms of either technical performance or cost.

The price of a full Ariane launch, with all the performance improvements currently under way included, will not exceed the equivalent of 160 million French Francs ('78'). The price of a shared Ariane launch for a payload of the Delta class will not exceed the equivalent of 80 million French Francs ('78'), again including the performance improvement. These price indications include all associated launch services and include the necessary down-range facilities.

The payment schedule for an Ariane launch is set as :

20% at -36 months
20% at -30 "
20% at -24 "
15% at -18 "
10% at -12 "
10% at - 6 "
5% at launch

The payment of earnest money of $ 100,000 is required prior to significant commitment (this amount would be deducted from the first progress payment against a firm order, and if no order was subsequently placed would be subject to deduction of actually incurred expenditure).

Options are offered on the understanding that the option holder has the right of first refusal, but in case where a firm customer requests the launch slot concerned then the option holder must either take up on relinquish the slot. The former case requires signature of a contract and payments following the standard schedule; in the latter case best efforts would be made to find an acceptable alternative slot. Relinquishment entitles the option holder to the return of any payments made, subject to deduction of any expenditure actually incurred, and subject to what obligations the provision and acceptance of a re-scheduled slot might imply. The normal price for an option is 1% of final price per month of option, with 50% of the option payments made being credited towards purchase should the option be exercised. Cancellation of the option without further commitment means that any monies paid are forfait.

These conditions are standard and indeed the most stringent conditions to be applied and each user will be considered separately in light of the particular circumstances that may rule.

Further, it is probable that a user requiring only half the Ariane capability could be accommodated at relatively short notice, as a number of "half-passenger" launches are to be expected where space exists for a second passenger.

Technical Characteristics

The technical characteristics of Ariane are indicated in fig.6 through 10. Further details, including an overall system description, are to be found in the conference brochure "ARIANE".

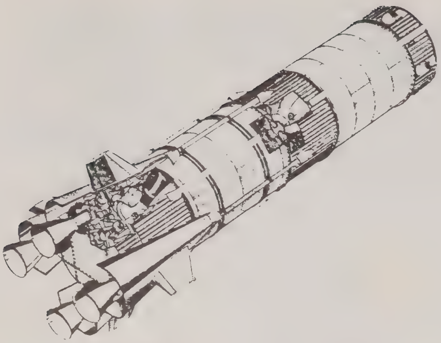

Total weight of structures	13.270	kg
Total weight of stage at liftoff	159.550	kg
Height	18.4	m
Diameter	3.800	m
Thrust at sea level	2.445	kN
Thrust in vacuum	2.745	kN
Specific impulse at sea level	248.6	s
Specific impulse in vacuum	281.3	s
Flight burn time	145	s

Fig.6 - First stage L.140

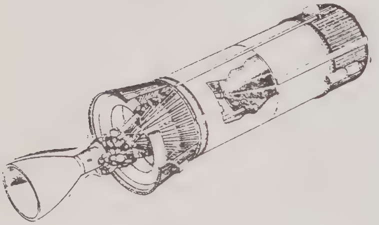

Total weight of structures	3.285	kg
Total weight of stage at liftoff	36.790	kg
Height	11.505	m
Diameter	2.600	m
Thrust in vacuum	709	kN
Specific impulse in vacuum	292.3	s
Burn time	132	s

Fig.7 - Second stage L.33

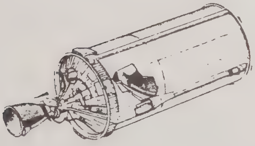

Total weight of structures	1.157	kg
Total weight of stage at liftoff	9 387	kg
Height	9.080	m
Diameter	2.600	m
Thrust in vacuum	60	kN
Specific impulse in vacuum	431	s
Burn time	570	s

Fig.8 - Third stage H.8

Total weight	300	kg
Height without adaptor : (external cylindrical part)	0.300	m
Height with adaptor	1.150	m
Diameter	2.664	m
Diameter at the payload interface	1.200	m

The functional systems are:

- inertial guidance and control system,
- sequencing system.
- telemetry,
- telecommand,
- tracking.

Fig.9 - Equipment Bay

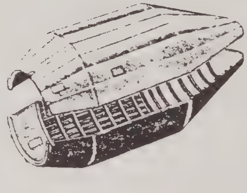

Total weight	810	kg
Height	8.653	m
Maximum diameter	3.200	m

Fig.10 - Fairing

80-0589

IUS - A KEY TRANSPORTATION ELEMENT FOR COMMUNICATION SATELLITES

Denton R. Hanford,* Manager
Orbital Transportation Systems, Boeing Aerospace Company
P. O. Box 3999 - M/S 82-36, Seattle, Washington 98124
Phone: (206) 773-0172

Abstract

The Inertial Upper Stage portion of the Shuttle Space Transportation System is described in this paper. The vehicle, its sub-systems and its integration into the orbiter are detailed along with the resulting capabilities. Ground, pre-flight and orbital operations are described.

The many services to the spacecraft provided by IUS are presented including the interfacing with the STS system, the provision of power if desired, on-orbit checkout, communication, thermal control, and discrete commands during orbit transfer operations.

Status of the IUS program is summarized including development, production and current flight schedules. Finally the paper describes potential options for either more or less capability than the baseline IUS.

Introduction

The Inertial Upper Stage (IUS), Figure 1, is under joint development by the United States Air Force and NASA as a key element of this nation's Space Transportation System. The primary objective of the IUS design was to provide an upper stage approximately three times less likely to fail and with greater payload capability than current upper stages for expendable launch vehicles flying geosynchronous missions. Solid propellant was chosen to simplify interfaces and integration into the shuttle, and the IUS's interfaces with the spacecraft were intended to ease the transition from current launch vehicles to the Space Transportation System. The resulting vehicle and its capabilities are described in this paper.

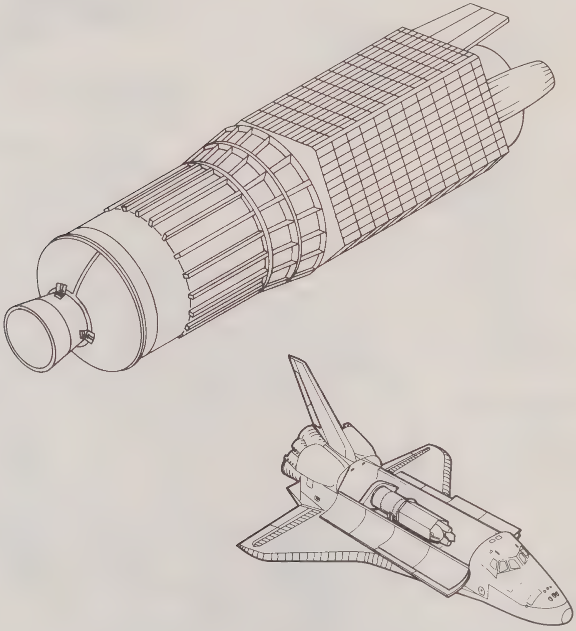

Fig. 1 The Inertial Upperstage Launching Tracking and Data Relay Satellite

---

* Member AIAA

Copyright © American Institute of Aeronautics and Astronautics, Inc., 1980. All rights reserved.

IUS System Description

The Inertial Upper Stage has a variety of diverse missions to perform. It is therefore not a single vehicle but a family of vehicles as shown in Figure 2. The family however is made up of nearly identical active components and vary primarily only in their structure and number or size of solid rocket motors. Main propulsion is provided by two primary motor sizes. The larger of the two motors employs 21,400 pounds of propellant, whereas the smaller of the motors contains 6,000 pounds. The avionics components and reaction control system components of all three vehicles are virtually identical, differing only slightly depending on civilian or military communications or where the planetary 3-stage configuration employs some unique avionics associated with the spinning third stage.

The workhorse of the family is the basic 2-stage vehicle. It performs approximately 90% of the missions anticipated over the next 10 years. The cutaway of Figure 3 shows that it is made up of one large motor for the perigee burn of a typical geosynchronous orbit transfer and a small motor for the apogee burn. The equipment is mounted around the smaller of the two motors, and its arrangement is illustrated in Figure 4. The 2-stage IUS is capable of placing over 5,000 pounds of spacecraft weight in the final geosynchronous orbit when deployed from the Shuttle Orbiter. The total weight of the system as it is installed in an orbiter is given in Figure 5. The major portion of the actual vehicle weight is made up of solid propellant. The motors can be offloaded to any value of propellant down to 50% of the designed load. This feature can reduce the shuttle usage charge for spacecraft lighter than the 5,000 pound design weight.

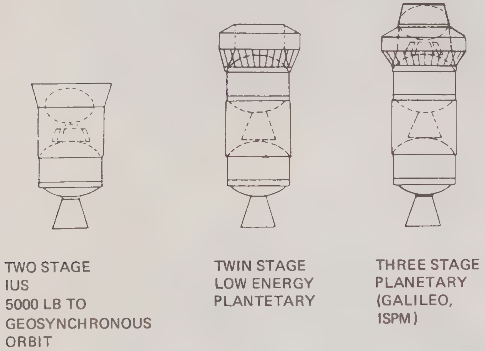
TWO STAGE
IUS
5000 LB TO
GEOSYNCHRONOUS
ORBIT
TWIN STAGE
LOW ENERGY
PLANTETARY
THREE STAGE
PLANETARY
(GALILEO,
ISPM)

Fig. 2 IUS Family

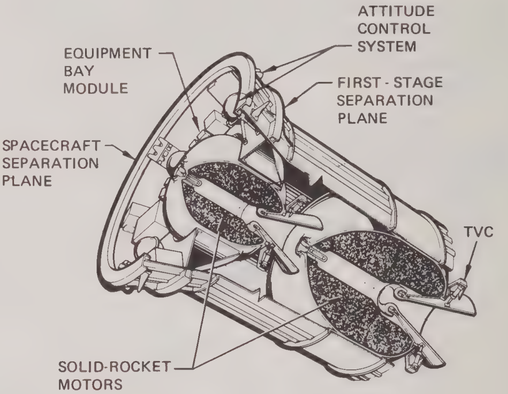
ATTITUDE
CONTROL
SYSTEM
EQUIPMENT
BAY
MODULE
FIRST - STAGE
SEPARATION
PLANE
SPACECRAFT
SEPARATION
PLANE
TVC
SOLID-ROCKET
MOTORS

Fig. 3 Basic IUS Two-Stage Vehicle

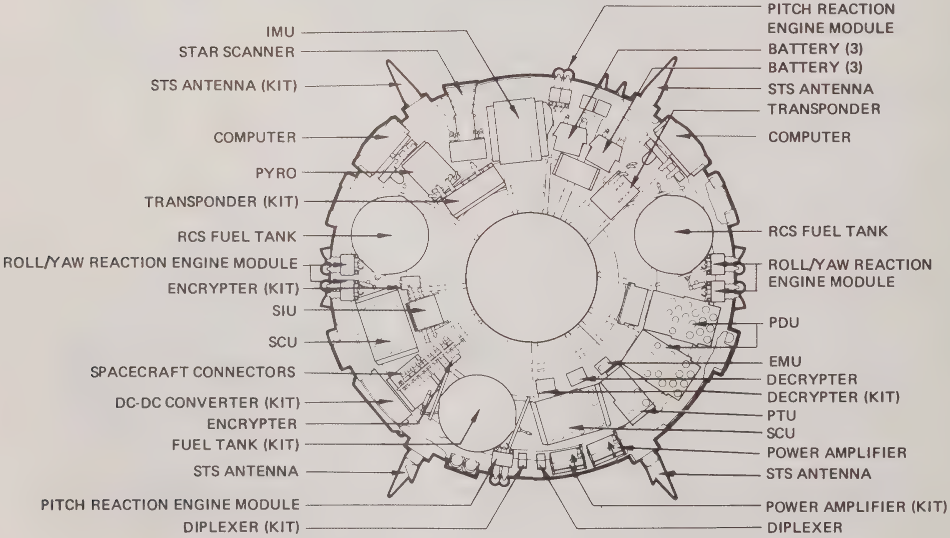
IMU
STAR SCANNER
STS ANTENNA (KIT)
COMPUTER
PYRO
TRANSPONDER (KIT)
RCS FUEL TANK
ROLL/YAW REACTION ENGINE MODULE
ENCRYPTER (KIT)
SIU
SCU
SPACECRAFT CONNECTORS
DC-DC CONVERTER (KIT)
ENCRYPTER
FUEL TANK (KIT)
STS ANTENNA
PITCH REACTION ENGINE MODULE
DIPLEXER (KIT)
PITCH REACTION
ENGINE MODULE
BATTERY (3)
BATTERY (3)
STS ANTENNA
TRANSPONDER
COMPUTER
RCS FUEL TANK
ROLL/YAW REACTION
ENGINE MODULE
PDU
EMU
DECRYPTER
DECRYPTER (KIT)
PTU
SCU
POWER AMPLIFIER
STS ANTENNA
POWER AMPLIFIER (KIT)
DIPLEXER

Fig. 4 IUS Equipment Support Section Arrangement

FLIGHT VEHICLE	32,377	
STAGE 1		
STRUCTURE & INSULATION		716
AVIONICS & POWER		305
SRM @ BURNOUT		1,313
MAIN PROPELLANT		21,404
EXPENDED INERT		99
WEIGHT GROWTH ALLOWANCE		97
LOADED		23,934
STAGE 2		
STRUCTURE		545
AVIONICS & POWER		896
RCS		340
SRM @ BURNOUT		535
MAIN PROPELLANT		6,002
EXPENDED INERT		36
WEIGHT GROWTH ALLOWANCE		89
LOADED		8,443
AIRBORNE SUPPORT EQUIPMENT	9,187	
BOEING FURNISHED ASE		6,933
GOVERNMENT FURNISHED ASE		1,504
SPACECRAFT ASE		750
PAYLOAD	5,033	
TOTAL STS PAYLOAD UP	46,597	

REF. MASS PROPERTIES REPORT # 37

Fig. 5 IUS Weight Summary for 5000 LB Payload

Since qualification of all the hardware is not complete, a weight growth allowance of 4% of the dry weight is included in the weight statement. This allowance provides confidence that the performance will be achieved when the operational flights take place.

A major weight element of the IUS system is the Airborne Support Equipment (ASE). The ASE, illustrated in Figure 6, provides all structural, electrical, command and data interface functions between the IUS/Spacecraft combination and the Orbiter. The ASE incorporates a low-response spreader beam and torsion bar which reduces spacecraft dynamic loads to approximately one-third of that experienced without this system. The ASE also provides power to the IUS and spacecraft during orbiter operations and transmits data to and from the orbiter and IUS/Spacecraft. On-orbit checkout is accomplished while still attached to the ASE prior to deployment. The ASE can withstand all loads including abort landings, and like the IUS itself provides redundant power and data capability.

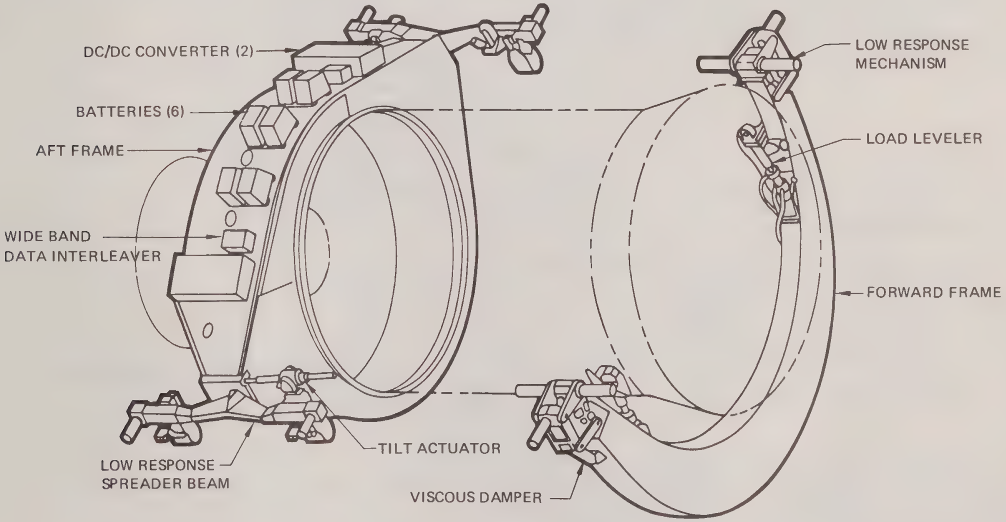

NOTE: PURGE DUCTS AND UMBILICAL TRAYS NOT SHOWN

Fig 6 IUS Airborne Support Equipment

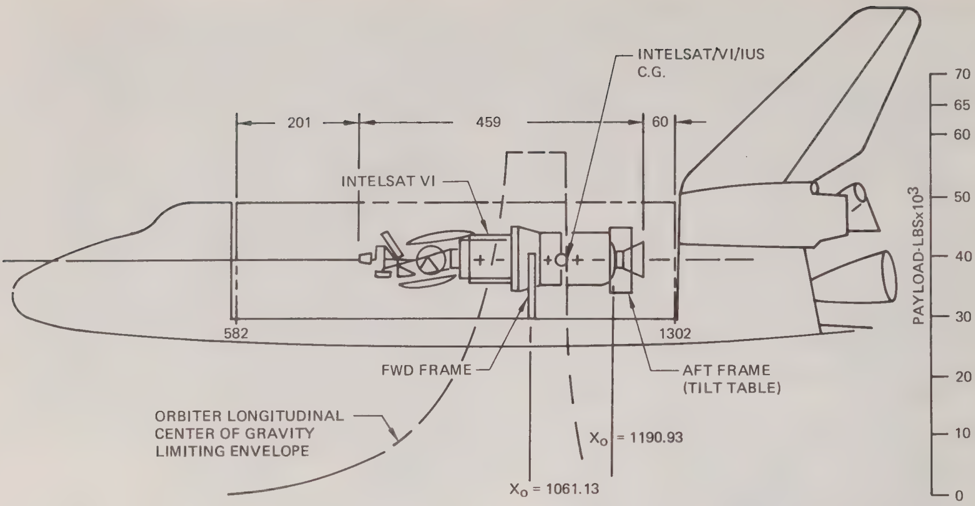
INTELSAT/VI/IUS
C.G.
201
459
60
INTELSAT VI
582
1302
FWD FRAME
AFT FRAME
(TILT TABLE)
ORBITER LONGITUDINAL
CENTER OF GRAVITY
LIMITING ENVELOPE
X_o = 1190.93
X_o = 1061.13
PAYLOAD-LBSx10^3
70
65
60
50
40
30
20
10
0

Fig. 7 Intelsat VI/IUS Installation

A typical installation of the IUS and a communication satellite in the payload bay is illustrated in Figure 7. The placement as shown is selected in order to keep the center of gravity within shuttle limits. If another payload is sharing the shuttle flight and is mounted forward of the IUS, the IUS can be shifted aft much closer to the rear bulkhead of the shuttle payload bay. In fact, two IUS's can be carried on a single shuttle flight, each with room for a 10- to 12-foot long spacecraft, Figure 8. Such an arrangement requires spacecraft lighter than the 5,000 pound design in order to stay within shuttle cargo weight limits.

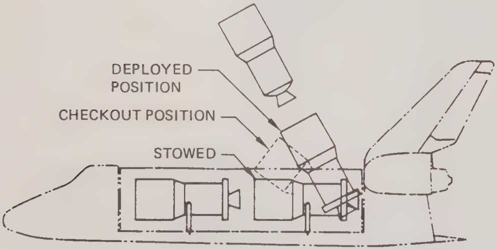
DEPLOYED
POSITION
CHECKOUT POSITION
STOWED

Fig. 8 Tandem IUS Arrangement

The ability of the IUS to provide for shuttle payload sharing is an important feature. In addition to tandem arrangements, the 5,000 pound IUS capability can be used to advantage by mounting multiple spacecraft on a single upperstage. The first flight of the IUS is expected to carry two communication satellites for the Department of Defense, namely a DSCS II and a DSCS III, Figure 9. This IUS will fly atop a Titan Launch Vehicle.

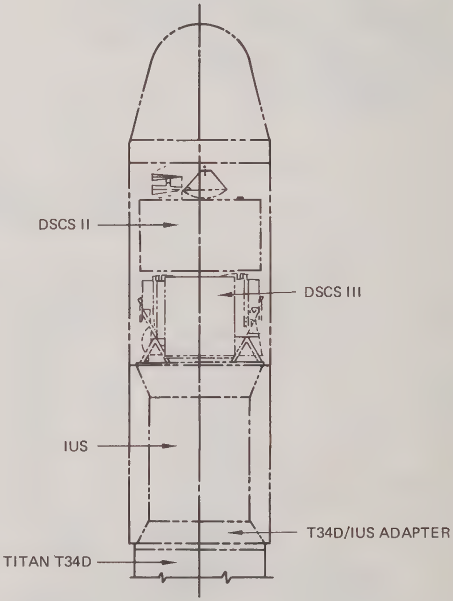
DSCS II
DSCS III
IUS
T34D/IUS ADAPTER
TITAN T34D

Fig. 9 DSCS II/III Arrangement

The IUS provides some other unique capabilities in addition to its payload capability to geosynchronous orbit. Its guidance system is capable of correcting for a wide range of mission uncertainties. It does, of course, provide the velocity correction after each burn of the SRM's to make up for the statistical uncertainty of the solid rocket motor performance. It also, however, will correct for a variety of mission delays including launch, deployment, and other on-orbit delays. These capabilities are summarized in Figure 10. The result is a system capable of placing a spacecraft within very tight injection accuracy requirements with no post-launch input required from the ground.

The avionics system should have unparalleled reliability in performing these functions. Each avionics component is built and tested to the highest standards yet imposed on the industry. In addition there are no catastrophic single point failure modes possible in the entire avionics or control system. The system redundancy schematic is illustrated in Figure 11. The two single string functions of the tracking, telemetry and command and Star Scanner are not mandatory for successful mission operation; therefore, all mission critical functions are redundant with the exception of the solid rocket motors and the structure.

INPUTS	GAMMA GUIDANCE	OUTPUTS
● MISSION TYPE ● EARTH ORBITAL PLANETARY ● VEHICLE TYPE ● STAGES OFFLOAD ● PAYLOAD TYPE ● WEIGHT ● TRAJECTORY CONSTRAINTS	● ENERGY MANAGEMENT ● POST DEPLOYMENT TARGETING ● CLOSED LOOP GUIDANCE ● MID COURSE UPDATES	● THRUST STEERING DIRECTIONS ● IGNITION TIMES ● VERNIER BURN TIMES

FEATURES

- ADAPTABILITY - ACCOMMODATES
  - LAUNCH DELAYS
  - DEPLOYMENT OR ON-ORBIT DELAYS
  - OFF NOMINAL ORBIT
- AUTONOMY - ON BOARD COMPUTATIONS
- EXPLICIT GUIDANCE - INDEPENDENT OF REF TRAJECTORY

Fig. 10 Adaptive Guidance Flexibility

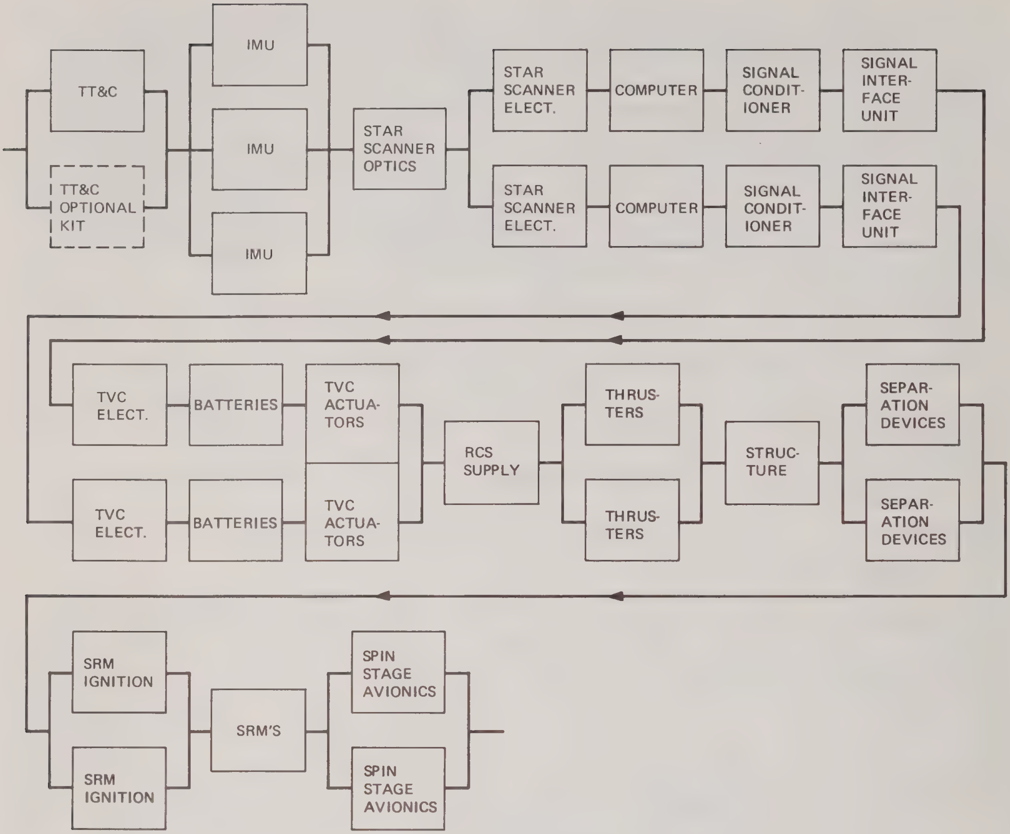
TT&C
TT&C OPTIONAL KIT
IMU
IMU
IMU
STAR SCANNER OPTICS
STAR SCANNER ELECT.
COMPUTER
SIGNAL CONDIT-IONER
SIGNAL INTER-FACE UNIT
STAR SCANNER ELECT.
COMPUTER
SIGNAL CONDIT-IONER
SIGNAL INTER-FACE UNIT
TVC ELECT.
BATTERIES
TVC ACTUA-TORS
TVC ELECT.
BATTERIES
TVC ACTUA-TORS
RCS SUPPLY
THRUS-TERS
THRUS-TERS
STRUC-TURE
SEPAR-ATION DEVICES
SEPAR-ATION DEVICES
SRM IGNITION
SRM IGNITION
SRM'S
SPIN STAGE AVIONICS
SPIN STAGE AVIONICS

Fig. 11 Redundancy is a Significant Feature of the IUS Avionics System

The IUS/Spacecraft physical interface is the forward face of the Equipment Support Section. The structural attachments consist of 8 points located in a circle of approximately 112 inches in diameter. Interface details can be found in reference 1.

All key elements of the IUS system have undergone successful developmental testing, and most elements are well into qualification testing. Development tests have indicated that all specification requirements will be met. Figure 12 summarizes some of the key results of the testing in each of the three major IUS subsystems. The current resulting predictions of the IUS systems capability are illustrated in Figure 13. Note that the injection accuracy is nearly twice as good as that required by the specifications.

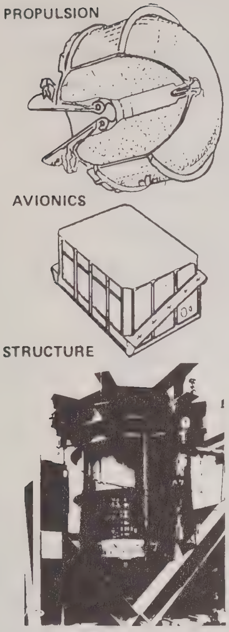

ELEMENT	MINIMUM REQUIRED	DEMONSTRATED
● TWO LARGE & TWO SMALL MOTOR TESTED AT FULL DURATION		
● LARGE MOTOR – 152 SEC BURN	291.6 ISP	293.3 ISP
● SMALL MOTOR – 98 SEC BURN	284.5 ISP	286.9 ISP
● SMALL SPIN MOTOR –	70 RPM @	71 RPM @
● RCS TESTED TO OVER 3 TIMES FLIGHT DUTY CYCLE AND BETTER ISP		
STEADY STATE ISP (SEC)	229 ISP	233 ISP
● GUIDANCE		
GYRO DRIFT	0.009 DEG/HR MAX	0.007 DEG/HR
● FAILURE DETECTION & RECONFIG.		
SWITCH TIME	200 MS MAX	144 MS
● RF OUTPUT POWER	20 WATTS	23 WATTS
● ALL AVIONICS LRU'S TESTED IN FUNCTIONAL EQUIV. CONFIG. - OVER 70% TESTED IN PRE-PRODUCTION CONFIGURATION		
● KEVLAR MOTOR CASE SKIRT TEST EXCEEDS LOADS	3,024 LB/IN	3,560 LB/IN

Fig. 12 Subsystem Hardware Development Status

PARAMETER	REQUIREMENT	CURRENT VALUE	MARGIN
DELIVERY CAPABILITY			
PAYLOAD			
STS 2-STAGE GSO	5,000 LB.	5,033 LB.	+33 LB.
INJECTION ACCURACY - 2-STAGE GSO (STS)			
POSITION	92 N.M.	48 N.M.	+ 44 N.M.
VELOCITY	78 FPS RSS	32 FPS	+ 46 FPS
INCLINATION ERROR	0.12°	0.047°	+ 0.073°
CONTROL/STABILITY MARGIN - GSO			
RIGID MODE GAIN	6 dB	7.4 dB	+1.4 DB
RIGID MODE PHASE	30°	33.8°	+ 3.8°
FLEXIBLE MODE GAIN	10 dB	80 dB	+ 70 dB
DOWNLINK POWER MARGIN - DOD	6 dB	6.7 dB	+ 0.7 dB
ANTENNA COVERAGE - DOD	90% @ GSO	93.9%	+ 3.9%
MISSION RELIABILITY - GSO	0.96	0.976	+ .016

Fig. 13 Status of Key Requirements

Integration of the IUS into the space shuttle system has turned out to be one of the more significant efforts required during the IUS developmental phase. This is one of the key advantages that IUS can offer to a user of the shuttle. An IUS user will avoid duplicating this effort since all interfaces with the shuttle are provided by the IUS, namely mechanical, electrical and data or commands. As illustrated in Figure 14, this effort is considerable; and it is approximately 80% complete for IUS. Not only does it include the interfaces in the orbiter payload bay, but the IUS system provides all of the equipment, procedures, and operations necessary to attach, checkout and install the IUS and spacecraft at Kennedy Space Center. Aside from the Airborne Support Equipment, 168 separate items of support equipment were designed and fabricated. The three major Interface Control Documents (ICD's) and innumerable test and operational planning documents represent thousands of pages, all requiring coordination with multiple organizations. Considerable test and checkout software is also being developed.

Operations and Services

The IUS system fabrication and assembly takes place in Seattle. All equipment is installed in the equipment support section and acceptance tested in Boeing's Space Chamber at the Kent Space Facility. At this point inert motors are used to support the acceptance testing. Motor processing and assembly takes place at the Chemical Systems Division's plant of United Technologies Corporation in Sunnyvale, Caifornia. The IUS without motors is shipped to the Eastern Launch Site (ELS). The motors are shipped directly from CSD. Final assembly and checkout of the IUS takes place at ELS.

AIRBORNE SUPPORT EQUIPMENT DESIGN & FABRICATION
GROUND HANDLING EQUIPMENT DESIGN & FABRICATION
ASSEMBLY AND CHECK-OUT
CARGO INTEGRATION IN VPF FACILITIES & EQUIPMENT
- FACILITIES & EQUIPMENT ICD'S
- INTERFACE VERIFICATION & INTEGRATED TEST PROCEDURES

PAD OPERATIONS
- LAUNCH PREPARATION IN RSS
  - FACILITIES & EQUIPMENT ICD'S
  - INTERFACE VERIFICATION
  - INTEGRATED TEST PROCEDURES, ETC.
- IN-ORBITER OPERATIONS
  - FACILITIES & EQUIPMENT ICD'S
  - INTERFACE VERIFICATION
  - INTEGRATED TEST PROCEDURES, ETC.

FLIGHT CONTROL TO INJECTION
- FLIGHT DESIGN
- CREW & FACILITIES PREPARATION (PIP ANNEXES, ORD ANNEX, INTEGRATED SIMULATIONS, ABORT PLANNING ETC,)

Fig. 14 Integration Tasks

The flow of operations at ELS are illustrated in Figure 15. The IUS is mated to the Airborne Support Equipment and is completely checked out prior to mating with the spacecraft. The spacecraft for non-DOD applications is mated to the IUS in the Vertical Processing Facility. Spacecraft-provided test equipment is used to verify spacecraft readiness for interface verification. A functional test is performed to verify the adequacy of the spacecraft to IUS interface which supports data and command flow across the IUS to orbiter umbilical and across the IUS spacecraft interface connecter.

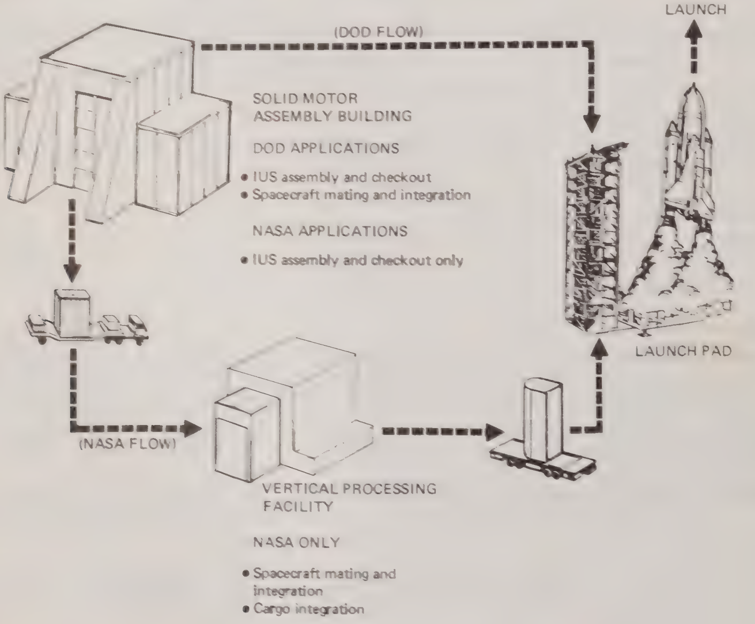
LAUNCH
(DOD FLOW)
SOLID MOTOR ASSEMBLY BUILDING
DOD APPLICATIONS
• IUS assembly and checkout
• Spacecraft mating and integration
NASA APPLICATIONS
• IUS assembly and checkout only
LAUNCH PAD
(NASA FLOW)
VERTICAL PROCESSING FACILITY
NASA ONLY
• Spacecraft mating and integration
• Cargo integration

Fig. 15 ELS Ground Operations Concept

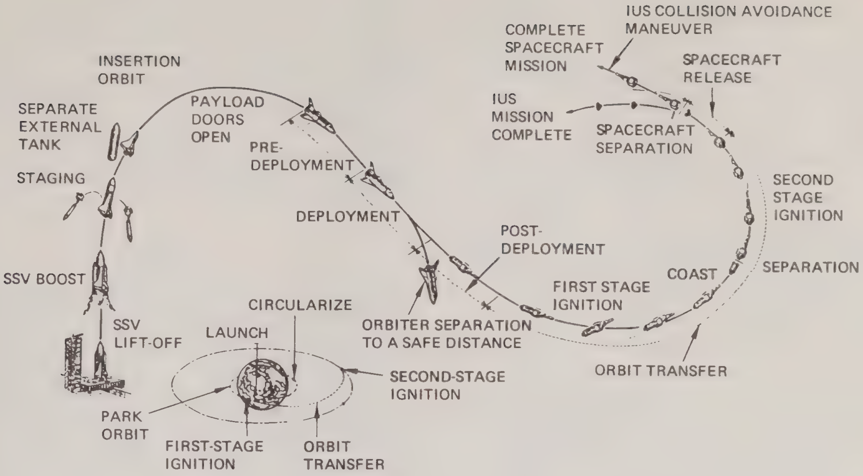
INSERTION ORBIT
SEPARATE EXTERNAL TANK
STAGING
SSV BOOST
SSV LIFT-OFF
PAYLOAD DOORS OPEN
PRE-DEPLOYMENT
DEPLOYMENT
POST-DEPLOYMENT
ORBITER SEPARATION TO A SAFE DISTANCE
CIRCULARIZE
LAUNCH
SECOND-STAGE IGNITION
PARK ORBIT
FIRST-STAGE IGNITION
ORBIT TRANSFER
COMPLETE SPACECRAFT MISSION
IUS COLLISION AVOIDANCE MANEUVER
SPACECRAFT RELEASE
IUS MISSION COMPLETE
SPACECRAFT SEPARATION
SECOND STAGE IGNITION
SEPARATION
COAST
FIRST STAGE IGNITION
ORBIT TRANSFER

Fig. 16 Sequence of Events for Typical Geosynchronous Mission

The ability of the spacecraft to operate on simulated orbiter or IUS power is verified during this test. The IUS and spacecraft are inspected, cleaned and installed on the mobile payload ground handling mechanism in preparation for transport to the pad. The NASA payload canister transportation system is used for transportation. The canister transporter provides environmental conditioning and monitoring of the transportation environment during movement to the pad. Department of Defense payloads do not use the Vertical Processing Facility and are integrated with the IUS in either the solid motor assembly building or at the pad.

The flight operations of the IUS can be completely autonomous. A typical geosynchronous orbit mission (Figure 16) requires approximately 10 hours. Shortly after the shuttle achieves orbit, the payload bay doors are opened. With the payload bay doors open, attitude constraints are provided to avoid overheating of both spacecraft and IUS avionics due to direct overexposure to sunlight. Deployment is via springs which are attached to the aft airborne support equipment frame which has been tilted up for clearance from the payload bay. The IUS reaction control system is activated when the IUS is approximately 200 feet from the orbiter, and the IUS is armed for the first motor ignition after the IUS has achieved approximately a 10-mile separation from the orbiter. The transfer to the geosynchronous altitude takes approximately five hours during which the IUS maneuvers to preprogrammed attitudes selected for spacecraft communication or thermal control operations. Interruptions occur only for brief periods immediately prior to and following the main IUS motor burns during which IUS attitudes take precedence and also at IUS staging during which the RCS is inhibited. The first stage and the spent first stage motor is retained until near the apogee motor firing. Staging is followed shortly thereafter by the circularization burn of the second stage motor. After final orbit correction using the IUS reaction control system, the spacecraft then provides the final separation of the IUS second stage and equipment support section. The IUS then performs a collision avoidance maneuver completing the IUS operations.

POWER	110 AMP HOURS 28 ± 4 VOLTS
DISCRETES TO SPACECRAFT	8 REDUNDANT
DOWNLINK TELEMETRY	16 Kbps
ATTITUDE CONTROL	
ATTITUDE HOLD (EACH AXIS)	± 0.5 DEGREES
RATE (PITCH, YAW AXIS)	± 0.1 DEG/SEC
RATE (ROLL AXIS)	± 0.3 DEG/SEC
ATTITUDE PROFILE	MEET SPACECRAFT COMMUNICATION AND THERMAL REQUIREMENTS

Fig 17 IUS Provides Many Services To Spacecraft

During flight operations the IUS provides a variety of services to the spacecraft. These are summarized in Figure 17. While in the payload bay, the IUS can transmit orbiter power to the spacecraft, and also has the capability to provide power to the spacecraft throughout IUS operations to the point of separation from the spacecraft. One hundred and ten amp hours at a nominal 28 volts is available. Eight separate functional discrete commands can be provided to the spacecraft. The commands are also redundant. Spacecraft data can be transmitted throughout IUS operations up to 16,000 bits per second. As previously noted, communication coverage is very close to 100%; however, the IUS can also reorient its attitude so that the spacecraft might communicate directly if desired. Attitude maneuvers may also be provided for spacecraft thermal control.

Potential Improvements to Improve Performance

Although the IUS provides more payload weight capability to geosynchronous orbit than previous geosynchronous launch systems, there have been projections of even greater requirements in the late 1980's. The current family of IUS's includes a 3-stage configuration currently designed for interplanetary missions. This configuration, however, has a performance capability in excess of 7,000 pounds to geosynchronous orbit. The third stage of the current design is spin stabilized. The first two configurations of Figure 18 are currently under contract and as previously discussed are well on the way to development. Timing of the 3-stage configuration is tied into requirements of the International Solar Polar and Galileo Planetary Missions.

A potential growth configuration is shown dashed in, in 1985. This configuration is made up of three large and one small motor and must be placed into orbit by two space shuttle flights. Such a configuration could perform all of NASA's planetary requirements through the year 1991 (provided the Solar Electrical Propulsion System is also developed). This same configuration can place very large payloads to geosynchronous orbit as indicated. Such a vehicle may satisfy some of the geosynchronous communications platform requirements currently under discussion. Acceleration levels during operations with this vehicle are also relatively low, on the order of 2.2 G's maximum. Instead of the normal two-burn transfer to geosynchronous, this vehicle would perform the transfer in either three or four burns resulting in intermediate orbits between the shuttle orbit and geosynchronous. The schedule for this vehicle's availability will be dependent upon when it receives developmental funds. A 1985 operational capability would require preliminary design studies to commence this year.

Summary

IUS program objectives of providing a flexible and reliable upper stage with ample services to the spacecraft are being met. In 1981 the IUS will demonstrate its capability with the first launch of the tracking and data relay satellite system from the shuttle. This will be the largest spacecraft ever placed in geosynchronous orbit. The capabilies of the IUS extend even beyond that and should meet the communications industry's needs and keep pace with this rapidly expanding field throughout the 1980's.

References

1. "IUS Spacecraft Accommodations Guide," Boeing document D290-10543-1, dated Feb. 1980.

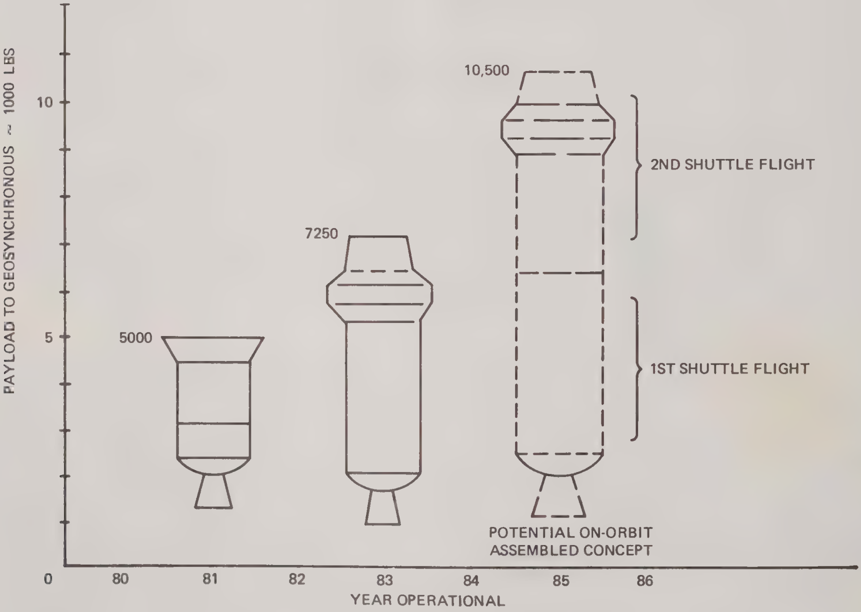

Fig. 18 The IUS Offers the Opportunity for Significant Communications Satellite Growth

80-0592

ASCENT PROPULSION STUDY FOR INTELSAT VI

Marshall H. Kaplan*
The Pennsylvania State University
University Park, Pennsylvania

and

William W. Dorsey+
International Telecommunications Satellite Organization
Washington, D.C.

Abstract

Results of a six-month study to investigate the trade-offs for a propulsion system which can provide the ascent requirements for a new generation of international communications satellites are presented. An initial on-orbit mass of between 1500 and 2000 kg is assumed. A variety of propulsion options were considered, including liquid bipropellants, solids, and combinations of these. Both integrated and separate propulsion stages have been reviewed. Ascent stabilization effects are also included. Cost and schedule aspects have been considered for a first launch in 1985. Thrust and impulse ranges are given, options are narrowed, and specific recommendations are offered.

Introduction

It appears that INTELSAT VI may be the biggest commercial communications satellite ever launched. In addition, it is likely to be launched by the Space Shuttle. These two factors lead to unique problems of ascent staging and spacecraft design. However, these satellites provide an opportunity to apply the latest developments in propulsion to the problem of providing staging to reach geosynchronous orbit. Ascent scheme from the Space Shuttle has a major impact on spacecraft design and the selection of the control system. Many factors come into play in selecting a staging subsystem or other means of providing the ascent velocity increments. Several organizations have already studied the ascent problem to geosynchronous orbit for a variety of reasons and payload sizes. Hughes Aircraft Company recently did a study of Multimission Modular Spacecraft (MMS) Applications for geosynchronous spacecraft.[1] This study examined the applicability of the MMS to a large class of synchronous altitude missions, and more specifically, to commercial communications satellites. These represent the greatest share of the potential market for this particular orbit. In its conclusions, the Hughes study indicated that the MMS has some application for geosynchronous spacecraft programs. These are, however, limited primarily to single spacecraft or large payload programs. It appears that INTELSAT VI will be a large spacecraft, but a number of these vehicles will be built. Furthermore, as more and more optimized stage designs mature the advantages of using the MMS are eroded. Thus, the possibility of using an MMS for INTELSAT VI has not been considered here.

Ford Aerospace and Communications Corporation (FACC) has studied a spacecraft perigee[2] subsystem for use with INTELSAT V. This stage incorporates a liquid bipropellant system and is spin stabilized. It is intended to replace the McDonnell Douglas Payload Assist Module-Atlas Centaur class (PAM-A) stage on the basis of cost effectiveness. Although it can handle larger payloads, it is restricted to spin stabilized ascent and provides only the perigee velocity increment. Thus, the FACC study does not take into account all possible options for staging from the Shuttle to geosynchronous orbit. Nevertheless, some of the concepts are useful in evaluating potential stage designs.

The Communications Satellite Corporation has recently completed a study of shuttle geosynchronous propulsion systems for INTELSAT VI size spacecraft.[3] This study includes a preliminary look at the conceptual options and lists the advantages and disadvantages of each one. A preliminary comparison of a solid propellant stage and a liquid bipropellant stage is presented. Some of the implications of spin or three-axis stabilization during transfer orbit are identified. A limited preliminary cost comparison of different systems is also provided. The work reported here is the next step, which is to take a more quantitative look at many of the parameters and costs effecting the selection of the staging option for INTELSAT VI.

Three types of options exist during the selection process for INTELSAT VI. Firstly, propulsion options include liquids, solids, and combinations of these. The propulsion stages can be separated or integrated into the spacecraft system. Thus, the stage design can be separate, integrated, or a hybrid design. Ascent guidance and stabilization method also effect the selection for staging. For example, the spacecraft may be spin-stabilized, or it may be three-axis stabilized using an inertial reference system. Thus, the on-orbit configuration is greatly influenced by the selection of the ascent guidance and staging system.

The objectives of this spacecraft propulsion system study have been pursued via a six-month effort involving industry surveys, analysis and simulations related to performance, and reviews of costs and concepts. Important performance parameters and relationships have been identified, including error sources and mass property effects. Follow on efforts have been recommended in order to develop a rationale which will converge to a selection process for the INTELSAT VI spacecraft.

Assumptions have been made regarding spacecraft mass and power, launch vehicle and date, and ascent sequence. The Space Shuttle will take INTELSAT VI into a circular orbit at 296 km with an inclination of 28.5 deg. The satellite will have

---

This paper is based upon work sponsored by the International Telecommunications Satellite Organization (INTELSAT). Views expressed in this paper are not necessarily those of INTELSAT.

* Professor of Aerospace Engineering, Associate Fellow, AIAA

+ Technical Planning Section, Member AIAA

Copyright © American Institute of Aeronautics and Astronautics, Inc., 1980. All rights reserved.

a 10-year life with an initial mass of 1500 to 2000 kg. The first launch will take place in 1985.

The Options

Spacecraft propulsion system options have been classified according to engine type, satellite interface, and ascent guidance used. Rocket motors can be solid or liquid and sometimes used in combinations. Propulsion stages can be separate or integrated in the spacecraft. Ascent guidance can incorporate a spinning or inertially guided vehicle. However, the selection of an option may influence the remaining options, e.g., an integrated solid motor usually requires a spinning vehicle.

Propulsion Equipment

The propulsion equipment category includes a variety of thrust devices which have promise and will be available. Only chemical propulsive devices have been considered here. Electric devices would take too long for orbit raising using the spacecraft power source. Solid propellant rocket motors and liquid bipropellant engines seem to represent the only viable options. Hydrazine monopropellant cannot provide competitive performance for large velocity increments.

Solid propellant motors are relatively simple, but have certain undesirable qualities. They produce high acceleration loads and limited mission flexibility. However, they have been very successful and are in wide use. Specific impulses of the order of 2900 N-s/kg are readily available. In many cases offloading can provide customized impulses. When used in a stage such as the Inertial Upper Stage (IUS), which provides its own guidance and control system, spin stabilization is not necessary. However, when used as a simple kick motor, spin through the burn is required.

Liquid bipropellant engines use a fuel and an oxidizer which burn in a combustion chamber. Specific impulses of up to 3000 N-s/kg are possible with storable propellants such as MMH and N_2O_4. Thrust levels are lower than for solids. Thus, finite burn times at lower acceleration must be assumed. Bipropellant usage has not been extensive, but this should change in the shuttle era. Liquids have higher dry weights, but better propellant usage. For large Δv maneuvers of large spacecraft, they dominate over solids in terms of overall weight, versatility, and injection velocity accuracy. The possibility of using cryogenic propellants exists, because the Centaur upper stage is being considered for Shuttle launch of interplanetary spacecraft. This uses liquid oxygen and liquid hydrogen, with a specific impulse of up to 4300 N-s/kg. However, cryogenics are very difficult to handle and are not storable. Thus, only storables are seriously considered for the INTELSAT VI time frame.

Perigee and apogee burns are separate and distinct. Each may be carried out by a solid or liquid rocket. In fact, one ascent sequence could incorporate a solid perigee motor and a liquid apogee rocket (e.g. Hughes' Leasat). Another possibility is to supplement a solid perigee burn with a liquid rocket which is also used for the apogee injection. This last scheme permits an existing solid motor to inject more mass into the transfer orbit.

Stage Design Choices

Ascent stages can be thought of as separate or integrated. For example, if the Two-Stage IUS is used, this is a separate stage for both perigee and apogee burns. PAM-A is only a separate perigee stage. A liquid bipropellant system which provides stationkeeping on orbit after apogee injection is an integrated stage.

A separate stage would have certain accessories associated with it. For example, the PAM stages have active nutation dampers and some structure in addition to the kick motor. The IUS is essentially a spacecraft whose payload is another spacecraft. An integrated stage would consist of a minimal amount of equipment. For example, an integrated bipropellant stage might consist of a rocket engine, added propellant and a limited number of hardware scale ups in the satellite. A separate stage that is already available (e.g., IUS) has an advantage in that development costs are already taken care of. Only the recurring costs would be significant. On the other hand, the development of an integrated stage could be largely absorbed in the costs of the whole spacecraft, and recurring costs could be lower.

Ascent Guidance and Stability

Another key option in the selection of an ascent system is the guidance and stabilization approach. There are basically two choices: spinning and three-axis oriented. A spinner takes advantage of gyroscopic stiffness to eliminate effects of perturbation torques. Thus, the angular momentum vector wants to remain in an inertial orientation. However, the body naturally wants its maximum moment of inertia axis aligned with the momentum vector. Ideally, the spin axis is this maximum inertia axis. Then disturbances which create transverse motion are ineffective over short periods of time, i.e., during perigee or apogee burn. If the spin axis is not the "major" axis, then it must be the axis of least inertia in order to preserve any gyroscopic stiffness. In such a case, "active" or controlled nutation damping is required to maintain stability. It is entirely possible that during a perigee or apogee burn, a transformation of inertia axes could take place. For example, the spin axis could change from the minor axis to the major axis due to propellant depletion. This would be desirable if the transformation took place quickly, i.e., the inertia ratio jumped from less than 1.0 to at least 1.05. At a value of 1.0 tumble is likely (nutation frequency and damping go to zero). Thus, such transformations, if done, are deliberate and instantaneous.

Spin is common when solid rockets are used. The only exception is IUS, which is relatively expensive and complex. Liquid motors can be used easily in either a spin or non-spin mode. However, an inertia ratio of less than 1.0 may not be acceptable due to potentially high dissipation from fuel slosh. This in combination with low thrust could result in excessive active damping requirements. Low thrust does permit a non-spinning perigee and apogee burn because disturbing torques are small.

Guidance during ascent is dependent upon stabilization technique used. A spinning ascent is simpler because gyroscopic stiffness is used. Non-spinning schemes require an inertial reference system and active attitude control. This approach is particularly advantageous when the satellite already has an inertial system on board. However, a primary advantage for a liquid, non-spinning ascent is the possible early deployment of antennas and solar arrays.

Trade-Off Parameters

A study of propulsion options, when coupled with a complicated set of constraints, must consider the interplay of a large number of parameters. The selection of a single hardware element or technique affects many other aspects of the system. Mission requirements and STS constraints have been established to the extent necessary to carry out this work. The stage options are clearly limited to those already mentioned. Ascent stabilization options include only the two distinguishable choices: spinning or nonspinning. Propulsion performance is measured by parameters like specific impulse, thrust, total impulse, mass fraction, dimensions, and costs. Design parameters deal with STS utilization, sensors, etc. Hardware development is primarily concerned with propulsion system availability in the desired time frame.

Basic Mission Constraints

The starting point for this trade-off study is a set of expected specifications relevant to INTELSAT VI. The communications payload is assumed to have a mass of 350-400 kg and requires 1.5 to 2.0 kW. The bus or total spacecraft in geosynchronous orbit should have a wet mass of 1500 to 2000 kg with an end-of-life (EOL) power of 2.5 to 3.0 kW. A useful life of 10 years is assumed here. In its stowed configuration with ascent propulsion, the configuration should be optimized for the Space Shuttle, which provides transportation to a 296-km circular orbit at an inclination of 28.5 deg with the first such launch in 1985.

The beginning-of-life (BOL) propellant load on the spacecraft in geosynchronous orbit is essentially a function of useful life and propulsion type. As a first estimate assume a hydrazine stationkeeping system with I_{sp} = 2,156 N-s/kg. The well known rocket equation gives the relationship between propellant mass fraction, velocity increment, and specific impulse,

$$\frac{M_p}{M_{s/c}\ (\text{wet})} = 1 - \exp(-\Delta v/I_{sp})$$

where M_p = propellant mass, Δv = velocity increment, and I_{sp} = specific impulse in N-s/kg. The velocity increment is primarily influenced by stationkeeping requirements and perturbations. For example, inclination control requires 40.2-51.3 m/s/yr varying over a nine-year cycle. Take an average of 45.7 m/s/yr. Longitudinal drift requires up to 2 m/s/yr. A single longitudinal shift of 120 deg in 50 days is anticipated to move a spare satellite into position, requiring 27.1 m/s. Thus, for 10 years, this totals 504.1 m/s, which leads to a propellant mass fraction of 20.85 percent of the initial mass. Therefore, the dry mass has a range of 1,187 to 1,583 kg.

An optimized impulsive perigee burn raises the apogee to an altitude of 35,786 km and reduces inclination by 1.5 deg. The associated impulsive velocity increment is 2,438 m/s. The following impulsive apogee burn circularizes the orbit and reduces inclination to zero, requiring a velocity increment of 1,802 m/s. There are a number of potential variations on this ascent profile. For example, lower thrust devices require a finite burn time to impart large velocity increments. Multiple burns can be used at perigee and/or apogee with some penalties in time and propulsion utilization efficiency. Another possibility is to use multiple apogees (bielliptic transfer), intermediate to the final altitude. In any case, the final inclination would probably be biased to take advantage of the natural inertial direction of inclination build up. This would delay the first required inclination correction burn.

Launch windows may be important, depending on ascent guidance technique used.[4] For example, a sun sensor used for yaw control would require the relative sun position to be favorable. This, in turn, influences launch constraints.

Return now to the problem of finite burn times. The use of liquid bipropellants for the perigee burn requires such a consideration along with the use of multiple burns to establish a proper transfer orbit. During a finite burn of several minutes, the thrust vector may be inertially oriented or steered to maintain the flight path direction. If the vehicle is spinning, the first option is much easier to implement. In either case, there will be some increase in velocity increment required when compared to impulsive burns. The orbital rate in a 296-km orbit is 3.98 deg/min. For example, a 10-minute perigee burn is associated with an orbital arc of about 40 deg. To minimize propellant penalties the pitch of the spacecraft would remain constant in the orbital frame. This would require an inertial pitch rate of about 3.98 deg/min. However, a spinning ascent may preclude this type of attitude maneuver to maintain simple guidance logic and minimize ascent hardware. Thus, the effects of single or multiple zero-pitch-rate burns on propellant and orbital altitude were evaluated to determine the feasibility of a finite burn time. Considerations included aerodynamic effects on apogee altitude with associated propellant penalties. As an alternative, an induced pitch rate of 3.98 deg/min via a precession thruster is possible. A computer simulation was used to integrate the equations of orbital motion during perigee burns. Its output consists of propellant penalties associated with zero and nonzero pitch rates for given thrust levels. In all cases, a 296-km parking orbit was assumed as the starting point for a GEO transfer sequence.

The digital simulations accurately computed finite perigee burn effects for both zero-pitch-rate and precession cases. The program calculates the number of burns and total Δv required to achieve a geosynchronous transfer orbit for a given initial spacecraft mass, fixed thrust level, and corresponding burn time. The equations of motion for the orbit are integrated directly throughout the arc of the burn where thrust and drag forces are present. At the termination of the burn the altitude is high enough to neglect aerodynamic drag. At that point Keplerian orbital elements are determined and conditions at the beginning of the next burn are calculated analytically. This procedure was repeated in each case until an apogee with geosynchronous altitude was achieved.

Two distinct scenarios were used. The first assumed that thrust was maintained tangential to the flight path at all times by pitch precession control. Two initial mass values were considered: 7,275 kg (corresponding to a GEO satellite in the 1,500 kg class) and 9,700 kg (a 2,000 kg class satellite). The two primary outputs of this simulation are the excess velocity increment (Δv loss) and the time from initiation of the first perigee burn until reaching the first geosynchronous apogee. This program includes a sophisticated atmospheric density profile set by the Jacchia 1970 model[5] with solar conditions corresponding to September 1979, i.e., above average levels. A drag coefficient of 3.0 and reference area of 5.0 m^2 were assumed.

Results for the controlled pitch precession cases are presented graphically in Figs. 1 through 4. In each case 3, 5, and 7 perigee burns were assumed. It is apparent that for three or more perigee burns at thrusts of at least 4,000 N, the losses due to finite burn time and drag are less than 5.5 percent. For example, the larger spacecraft using five burns with 8,000 N of thrust has a 1 percent propellant penalty and takes 21 hours to reach the first correct apogee. For the cases with zero pitch rates (inertial pointing) losses were considerably greater. Figs. 5 through 8 illustrate these results. Again, 3, 5 and 7 burns were assumed. Losses can be as high as 19.3 percent, which requires an equivalent expenditure of 2,908 m/s rather than 2,438 m/s. The loss for four burns at 4,000 N is estimated from Fig. 7 as 11 percent with a time to first apogee of about 16 hours.

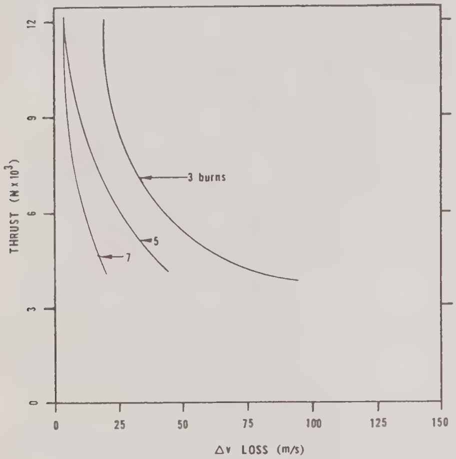

Fig. 1 Finite perigee burn penalty for an initial mass of 7275 kg with controlled pitch rate

During an inertially oriented burn, some altitude drop occurs at the beginning. For large burn arcs, the altitude drop is severe. Table 1 lists a number of minimum altitudes for different thrust levels and number of burns. Any case in which the minimum altitude is below about 200 km is probably unacceptable.

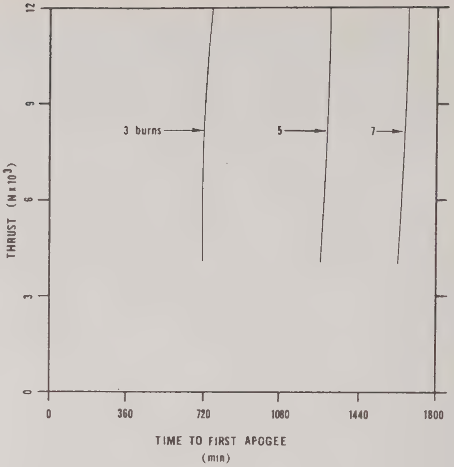

Fig. 2 Time to first synchronous apogee for an initial mass of 7275 kg with controlled pitch rate

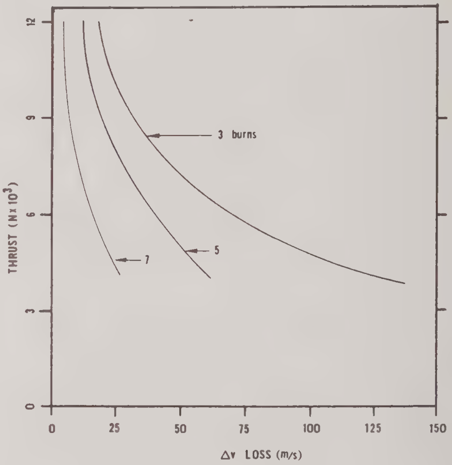

Fig. 3 Finite perigee burn penalty for an initial mass of 9700 kg with controlled pitch rate

Propulsion Stage Performance

In order to determine the mass of the vehicle which leaves the Orbiter, every kilogram of satellite injected into geosynchronous orbit must be multiplied by a mass factor. This is a function of the ascent design (integrated or separate stages), propulsion system performance, and transfer orbit parameters. As a basic example, assume an impulsive transfer from the basic Shuttle orbit to geosynchronous orbit via a two-burn Hohmann-plus-plane-change sequence. This is a "conventional" transfer orbit. Two burns yield velocity increments of 2,438 m/s and 1,802 m/s for perigee and apogee, respectively. The mass ratio between STS throw weight and BOL weight is obtained by the following chain of terms for a separate ascent state design:[1]

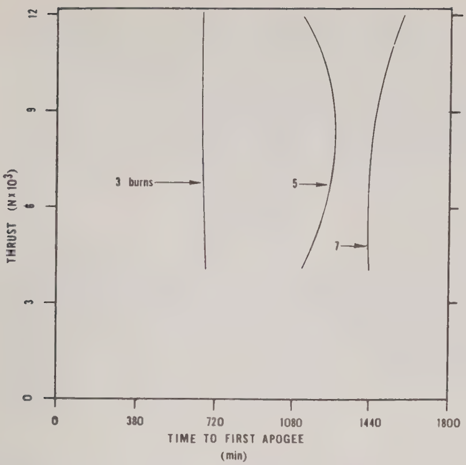

Fig. 4 Time to first synchronous apogee for an initial mass of 9700 kg with controlled pitch rate

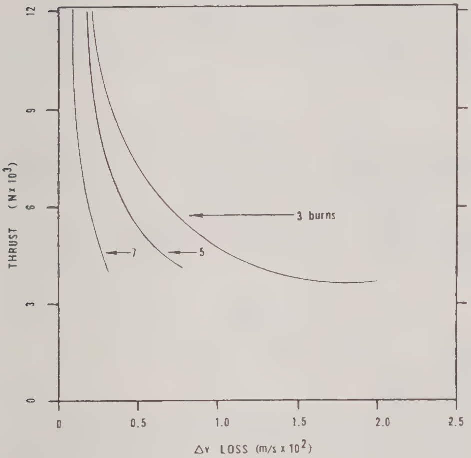

Fig. 5 Finite perigee burn penalty for an initial mass of 7275 kg with inertial pitch maintained

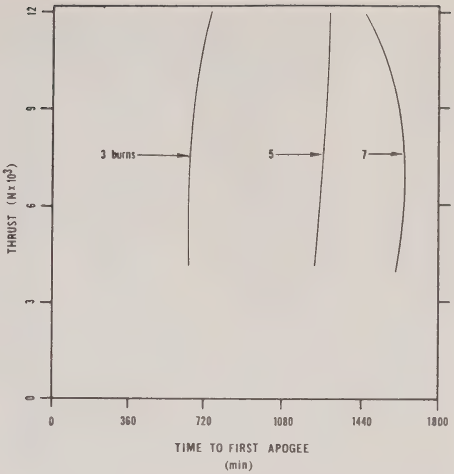

Fig. 6 Time to first synchronous apogee for an initial mass of 7275 kg with inertial pitch maintained

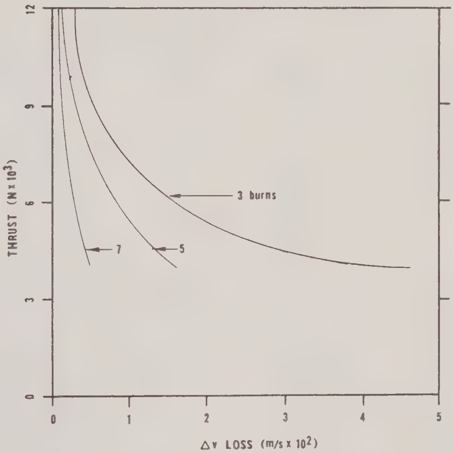

Fig. 7 Finite perigee burn penalty for an initial mass of 9700 kg with inertial pitch maintained

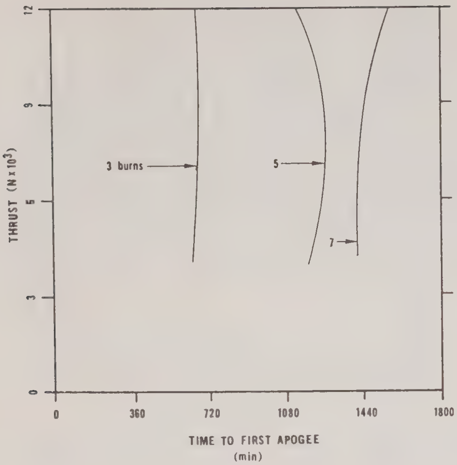

Fig. 8 Time to first synchronous apogee for an initial mass of 9700 kg with inertial pitch maintained

Table 1. Minimum altitudes for inertially oriented thrust*

Mass	Thrust	No. of Burns	Minimum Altitudes
7,275	12,000	3	294.33
7,275	12,000	5	294.33
7,275	12,000	7	294.33
7,275	8,000	3	294.51
7,275	8,000	5	294.89
7,275	8,000	7	294.89
7,275	4,000	3	254.67
7,275	4,000	5	290.07
7,275	4,000	7	295.37
9,700	12,000	3	294.75
9,700	12,000	5	294.75
9,700	12,000	7	294.75
9,700	8,000	3	288.72
9,700	8,000	5	295.17
9,700	8,000	7	295.17
9,700	4,000	3	137.96
9,700	4,000	5	274.18
9,700	4,000	7	293.82

* Initial circular altitude of 296.0 km.

$$\frac{M_{STS}}{M_{BOL}} = \left(\frac{M_{BOL} + M_{AMCA}}{M_{BOL}}\right) \times \left(\frac{M_{XFR}}{M_{BOL} + M_{AMCA}}\right) \times \left(\frac{M_{XFR} + M_{PMCA}}{M_{XFR}}\right) \times \left(\frac{M_{STS}}{M_{XFR} + M_{PMCA}}\right)$$

where M_{STS} = Orbiter throw out mass
M_{BOL} = BOL mass in geosynchronous orbit
M_{AMCA} = AKM case and adaptor mass
$M_{XFR} = M_{BOL} + M_{AMCA} + \text{AKM}_{\text{propellant mass}}$
M_{PMCA} = PKM case and adaptor mass

There is still another mass factor which relates the Orbiter cradle and other bay support equipment to the throw mass, M_{STS}. This is estimated as

$$\frac{M_{LAUNCH}}{M_{STS}} = 1.1$$

i.e., 10 percent of the launched mass remains in the Orbiter. For the example case at hand, assume AKM and PKM both have specific impulses of 2,891 N-s/kg. This immediately leads to

$$\frac{M_{XFR}}{M_{BOL} + M_{AMCA}} = 1.864$$

and

$$\frac{M_{STS}}{M_{XFR} + M_{PMCA}} = 2.323$$

For the Two-Stage IUS, the apogee motor case and adaptor, and the equipment bay module have a total mass of 965 kg. The perigee motor case and interstage structure have a total mass of 1,097 kg. To obtain the ratio M_{STS}/M_{BOL} for the IUS, multiply 965 by 1.864, then that by 2.323, and add this mass to 1,097 times 2.323. Then the overall throw mass is

$$M_{STS} = 4.330\ M_{BOL} + 6{,}727\ \text{kg}.$$

Note that the IUS cradle and other Orbiter equipment have a fixed mass of 4,276 kg.

For a PAM perigee stage with integral apogee motor there is no extra mass for AKM case and adaptor, i.e.,

$$\frac{M_{BOL} + M_{AMCA}}{M_{BOL}} = 1.00$$

For the perigee stage, assume

$$\frac{M_{XFR} + M_{PMCA}}{M_{XFR}} = 1.21$$

This leads to a throw mass of

$$M_{STS} = 5.239\ M_{BOL}$$

For the integrated perigee and apogee stages, assume

$$\frac{M_{BOL} + M_{AMCA}}{M_{BOL}} = 1.00$$

$$\frac{M_{XFR} + M_{PMCA}}{M_{XFR}} = 1.12$$

which leads to

$$M_{STS} = 4.85\ M_{BOL}$$

Table 2 summarizes the throw mass range and options based on the above calculations.

Table 2. Launch and throw mass range

	For M_{BOL} range of 1500-2000 kg.	
Ascent Option	M_{STS} (kg)	M_{LAUNCH} (kg)
IUS	13,222-15,387	17,498-19,654
SSUS	7,859-10,478	8,644-11,526
Integrated	7,275-9,700	8,003-10,670

Potential solid propellant kick motors are selected on the basis of thrust and total impulse. Usually, thrust is scaled up with spacecraft mass, keeping the acceleration within acceptable bounds. The more important parameter here is total impulse. This is calculated by

$$\text{Impulse} = I_{sp} \, M_p$$

where I_{sp} = specific impulse

M_p = propellant mass

Using the rocket equation and I_{sp} = 2,891 N-s/kg, the propellant mass fractions are

$$\frac{M_p(\text{AKM})}{M_{BOL}} = 0.864$$

for AKM, and

$$\frac{M_p(\text{PKM})}{M_{XFR} + M_{PMCA}} = 1.323$$

for PKM. Therefore, the range of AKM propellant mass is 1,296-1,728 kg, and for PKM this is 4,477-5,969 kg. The total impulse required of the AKM is in the range

$$3.75 \times 10^6 - 5 \times 10^6 \text{ N-s } (8.42 \times 10^5 - 1.12 \times 10^6 \text{ lb-s})$$

and for the PKM,

$$1.29 \times 10^7 - 1.73 \times 10^7 \text{ N-s}$$
$$(2.91 \times 10^6 - 3.88 \times 10^6 \text{ lb-s})$$

As a point of reference, the IUS large motor carries up to 9,777 kg of propellant with I_{sp} = 2,874.3 N-s/kg, corresponding to an impulse of 2.81 x 10^7 N-s. By offloading, this may be sized to accommodate the perigee requirements of a spacecraft with the mass of interest here.

Hardware Survey

Suppliers

There are many potential propulsion hardware suppliers for an INTELSAT VI staging system. Availability and cost are critical for a 1985 launch date. Both solid and liquid rocket suppliers were surveyed. Table 3 summarizes solid propellant motor possibilities at present. Only motors which might satisfy perigee or apogee impulse requirements are listed. Many smaller motors are available and might be considered for perigee useage if combined with liquid boosters or used in a bielliptic transfer.

Table 3. Solid propellant space motors

Source	Designation	Impulse (10^6 N-s)	I_{sp} (N-s/kg)	Status
Thiokol	Star 62	7.82	2857	In house development
Thiokol	Star 75	13.27	2907	Study
Thiokol	Star 31	3.74	2876	In qualification
Thiokol	Star 37XE	3.76	2822	In qualification
Thiokol	Star 48	5.70	2835	In qualification
CSD*	IUS Large	27.94	2871	In development
CSD*	IUS Small	7.72	2862	In development
Aerojet	62-KS-33,700	9.31	2803	Minute Man 3
Aerojet	66-KS-60,000	17.60	2813	Minute Man 3

* Chemical Systems Division of United Technologies.

Table 4 lists a variety of MMH, N_2O_4 bipropellant motors in development or use. All those shown will satisfy thrust requirements for perigee staging. There are several smaller engines available with thrust levels of around 400 N. Although these are too small for perigee applications, apogee thrust can be considerably lower without appreciable penalties. For example, if a solid is used for perigee kick, then a small liquid engine could provide apogee impulse. Since a Centaur stage is being considered for a Shuttle launch, the eventual acceptance of other cryogenic stages with specific impulses near 4250 N-s/kg cannot be ruled out. However, the ascent propulsion stage timing is such that cryogenics should not be available for a 1985 launch date.

Table 4. Liquid bipropellant space engines

Source & Model	Nom. Thrust (N)	I_{sp} (N-s/kg)	Status
Marquardt: R-40A	4,005	2930	Shuttle RCS engine
Bell	4,210	2832	Competed for Shuttle RCS engine
Rocketdyne	4,005		Experimental
Rocketdyne	7,120		Experimental
Rocketdyne	11,125		Experimental
Rocketdyne	1,335	2813	In use

To summarize the sources of properly sized staging rockets, it would appear that Thiokol, CSD, and Aerojet might provide solid motors for perigee and/or apogee burns. Liquids bipropellant engines could be provided by Marquardt, Bell, or Rocketdyne.

Spacecraft Interfaces

Separate ascent stages would require the least interfacing with the satellite, and have a minimal design impact. Integrated stages would lead to a major impact with many interfacing problems. During perigee and apogee burns, high heat transfer rates must be avoided to protect satellite subsystems. Engine supports must be insulated. Power requirements are discrete, i.e., valve opening and closing. Forces due to thrust must be transmitted to the structure. Propellants tanks will be large and will have a major impact on mass properties and energy damping. Attitude control is needed during non-spinning ascent. RCS thrust size and location would have to satisfy ascent requirements. Engine exhaust plume problems are usually solvable through conventional design methods. Telemetry and command functions may be minor or major depending on the degree of autonomy of the ascent guidance.

An integrated system would probably be tied into the on-orbit system. On-orbit propulsion systems currently under development are either monopropellant or bipropellant types. The monopropellant system is simply an upgraded version of standard hydrazine systems which have been used over the past 15 years. This upgrading includes the use of "high performance" thrusters for large impulse maneuvers, such as N-S stationkeeping. Bipropellant systems are lower thrust versions of the N_2O_4-MMH engines being considered for perigee and apogee burns.

One hydrazine system now being developed achieves high performance by electrically augmenting the decomposition process in a second stage vortex chamber.[6] This thruster will be used on INTELSAT V. The other type of system being developed uses low thrust bipropellant engines. The INSAT satellite will use such a system. This is the first U.S. application of small bipropellant engines for satellite on-orbit control. Apogee injection is accomplished with a 445-N thruster. The European Symphonie satellite uses a similar system. Primary reasons for use of these systems include high performance (i.e., specific impulses up to 3038 N-s/kg) and the ability to combine on-orbit hardware with orbit insertion tankage and related components.

Hardware Status

Tables 3 and 4 give some insight into the status of solid and bipropellant engines for possible use on ascent stages. In general solid motors will be available in a large range of impulses. Additionally, IUS could be used for staging. Bipropellant engines offer fewer sizes, i.e., in the 4000, 7000, or 11,000-N range.

The Two-Stage IUS will deliver up to 2325 kg to GEO with a position accuracy of ±170 km (RSS), a velocity accuracy of 24 m/s, inclination error limit of 0.12 deg. Subsystems include two solid rocket motors, avionics, and structure.[7] The first Shuttle-launched IUS is scheduled for the TDRSS, probably in 1981. In 1980 or 1981, a Titan will launch an IUS/DSCS payload. The cost for a baseline IUS is estimated to be $10.3 million for each of the five units, including launch operations, satellite integration, adapter, etc.

Other solids are available for use in spinning ascent schemes. For example, Table 3 lists several potential perigee and apogee motor choices. A typical perigee motor has an estimated maximum cost of $3.1 million for each of five units, including development costs. The IUS motor is developed and should cost under $1.5 million per unit. Apogee motors are also available. For example, one design could be developed and obtained for a maximum of $2.1 million for each of five. Other choices may not need development, thus, the cost per unit could be below $1.0 million. In summary, the cost of a two-stage spinning solid ascent system without avionics should be below $10.2 million. This anticipates $2.2 million for the structure and other support devices, and $5.0 million for the first S/C integration and $2.0 million for each succeeding one.

Liquid bipropellant engines being developed or under consideration will have thrust levels of 4000, 7000, or 11,000 N, as noted in Table 4. Estimated development cost of a complete system with one engine, four propellant tanks and four pressurization bottles is $16 million, and each system would cost about $1 million. A structure must be added to this, and there are the usual costs for launch operations, satellite integration, and ASE refurbishment. Some savings will be realized in STS launch costs with an integrated propulsion system because of its length.

Conclusions and Recommendations

The work presented in this report represents an early evaluation of propulsion options for INTELSAT VI. These options have been presented and some of the consequences of each have been identified. Many basic assumptions have been made and initial requirements have been specified. Some of the important propulsion parameters and performance relationships have been presented and certain restrictions identified.

Solid propellant ascent stages are available in two types. The IUS is a non-spinning, complex two-stage device which can place up to 2,325 kg into GEO. However, each such unit will probably cost over $10 million. Another solid propellant option is a two-stage spinning configuration upon which is attached the spacecraft. Such a configuration could be relatively simple and inexpensive. Two existing solid rockets could be used at a minimum of development costs. Such an ascent approach should be less expensive than the IUS. It is conceivable that a solid spinning two-stage device could carry a cost of about half that of IUS.

Another option permits the use of a completely integrated bipropellant liquid rocket system. This will incorporate ascent engines with at least 4,000 N thrust. Such an integrated system, including development costs, could be near or below the cost of a solid rocket ascent stage. Options involving combinations of liquids and solids are also potential choices. The most obvious one is the use of a perigee solid rocket motor with an apogee liquid bipropellant system. Such a system is to be used on Leasat. However, the application of this combination to a 2,000 kg spacecraft which might be three-axis stabilized has not been shown to be an optimum result.

In summary, there is just not sufficient data available to make a definitive choice of ascent propulsion combination. Therefore, several activities are recommended to arrive at a meaningful choice of options. Firstly, detailed designs should be developed for a spinning ascent stage, a bipropellant integrated liquid system, and a combination solid perigee motor and liquid apogee motor. The spinning stage would use relatively inexpensive solid rocket motors and could be simple compared to IUS. The integrated bipropellant system could be non-spinning and make use of the spacecraft guidance system. Another bipropellant option would use spin stabilization during ascent and again use the spacecraft guidance system. This latter case would allow the spacecraft to have a simpler avionics package. Finally, a combination solid perigee motor and a liquid apogee system would require spinning ascent at least through the first burn. Since the apogee stage would be an integrated system, it would use the spacecraft guidance system and could be spinning or three-axis stabilized. The IUS option should be retained, at least until cost comparisons have been completed.

Along with the effort to develop the designs the development of a decision schedule and scenario should be laid out for the acquisition of a propulsion system. This should be in phase with INTELSAT VI plans. Part of the development of the ascent stage design should include simulations which give effects of errors on ascent performance. Another area to be studied is the use of autonomous versus ground commanded ascent schemes. Finally, the problem of Shuttle integration of spacecraft appears to be quite complex and some work on related problems appears appropriate.

Based on the limited data available on schedules and costs, a range of prices for an ascent system can be only roughly estimated at this time. Either an integrated bipropellant liquid stage or a solid rocket system would cost between $5 and 11 million (in 1979 dollars). A combination system such as one with a solid perigee motor and a liquid apogee system will probably have a cost in this same range. Included in these costs is the expense of launch operations, satellite integration, an adaptor, and a variety of other minor costs. Of course, the basic Shuttle launch cost is not included.

References

[1] "Multimission Modular Spacecraft (MMS) Applications for Geosynchronous Spacecraft," Hughes Aircraft Co., Report No. 86302, March 29, 1978.

[2] Johnson, J. T., "Satellite Propulsion Module and Optimized Concept," Ford Aerospace and Communications Corp., 1979.

[3] "Shuttle Geostationary Propulsion System Study," Communications Satellite Corp., Contract INTEL-052, September 1979.

[4] Wright, W. H., "Launch Window for a Shuttle-Based Geosynchronous Orbit Mission," Journal of Spacecraft and Rockets, Vol. 16, No. 6, Nov.-Dec. 1979, pp. 439-441.

[5] Justus, C. G., Woodrum, A. W., Roper, R. G. and Smith, D. E., "Four-D Global Reference Atmosphere Technical Description," Part I, NASA TMX-64871, Sept. 1974.

[6] Sackheim, R. L., Fritz, D. E. and Macklis, H., "The Next Generation of Spacecraft Propulsion Systems," AIAA Paper 79-1301, presented at the AIAA/SAE/ASME 15th Joint Propulsion Conference, June 18-20, 1979, Las Vegas, Nevada.

[7] Hanford, D. R., "IUS--A Key Transportation Element for Communications Satellites," AIAA Paper No. 80-0559, presented at the AIAA 8th Communications Satellite Systems Conference, April 20-24, 1980, Orlando, Florida.

80-0593

FORWARD ERROR CORRECTION FOR SATELLITE TDMA IN THE INTELSAT V ERA*

John S. Snyder
COMSAT Laboratories
Clarksburg, Maryland

Takuro Muratani
KDD Research and Development Laboratories
Tokyo, Japan

Abstract

Incorporating forward error correction coding in an INTELSAT V satellite TDMA system requires careful system analysis. Several approaches are presented including those employing both block and convolutional codes. Block codes are shown to be preferable for high-speed TDMA applications. A recommended approach is discussed in which unique word detection is employed for carrier phase ambiguity resolution. A hardware model of a (128,112) BCH block codec operating at 120 Mbit/s is described. Measured data are compared with both computer simulation results and an easily calculated performance approximation.

Introduction

The INTELSAT V satellites will reuse the 6/4-GHz transmission bands with spatially isolated antenna beams and orthogonal circular polarizations.[1,2] In the Atlantic Region this will involve two hemispheric beams (Figure 1), the western antenna pattern covering North and South America, and the eastern one including Europe and Africa. Northern coverage of each hemispheric beam will include an oppositely polarized zonal beam sharing the same frequency band. INTELSAT V will also reuse the 14/11-GHz bands through spatial isolation. In the Atlantic Region a western spot beam will cover a portion of the U.S. and Canadian coast, while an eastern spot beam will cover most of western Europe.

Investigations[3] of 120-Mbit/s time-division multiple-access (TDMA) operation with quaternary phase shift keying (QPSK) modulation in such an environment have identified various potential transmission impairments, including rain attenuation and co-channel interference from beam depolarization, as well as interference from other systems. Briefly, these investigations have shown that forward error correction (FEC) coding is desirable to achieve bit error rate (BER) objectives, and that the greatest BER improvement is required for the 6/4-GHz paths.

This paper is based upon a recent study[4] and subsequent hardware implementation dealing with the application of FEC coding to a 120-Mbit/s TDMA system operating via INTELSAT V. The results show that block codes are preferable to convolutional codes for high-speed TDMA applications because the latter require additional complexity to terminate the code at the beginning and end of each burst. Furthermore, unique word detection is recommended for carrier phase ambiguity resolution to obtain the lowest bit error rate while minimizing overall system complexity.

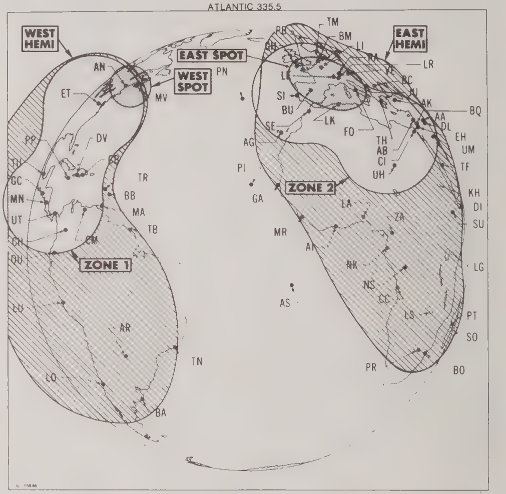

Figure 1. Atlantic Ocean Region Coverage of INTELSAT V [from Reference 2 by permission]

Since many links require coding and since all requirements can be met with a high-rate code and moderate codec complexity, one code and one decoding method are recommended for use throughout the system. A single codec operating in a burst mode may be used to process all the bursts in a frame. Hardware testing confirms that a (128,112) BCH block code meets BER objectives with a comfortable margin.

Performance objectives are first outlined, and the interrelationships between the FEC codec and other components of the system are examined. This is followed by a discussion of potentially useful block and convolutional codes. A recommended coding approach is then presented, accompanied by theoretical analysis and hardware test results.

---

*This paper is based upon work performed at COMSAT Laboratories under the sponsorship of the International Telecommunications Satellite Organization (INTELSAT).

Copyright © American Institute of Aeronautics and Astronautics, Inc., 1980. All rights reserved.

Performance Objectives

Studies of anticipated INTELSAT V TDMA system performance[3] have generally employed as objectives the provisional recommendations of a 1976 CCIR draft document[5] which indicate that BER should not exceed:

a. 1 in 10^6 10-minute mean value for more than 20 percent of any month;
b. 1 in 10^4 1-minute mean value for more than 0.3 percent of any month;
c. 1 in 10^3 1-second mean value for more than 0.01 percent of any year.

The ranges of uncoded BER at the demodulator which are of primary interest in evaluating candidate FEC techniques for INTELSAT V use were determined from these studies. These ranges are shown in Table 1, where they are compared with coded BER objectives.

Table 1. Demodulator Bit Error Rates vs BER Objectives

	Clear Sky Cases	Interference-Limited Cases	Thermal-Noise-Limited Cases
Uncoded (Input) BER	4.5×10^{-6} to 7.0×10^{-5}	1.5×10^{-3} to 3.0×10^{-3}	5.5×10^{-4} to 1.4×10^{-3}
Coded (Output) BER Objective	$\leq 10^{-6}$	$\leq 10^{-3}$	$\leq 10^{-3}$

System Aspects

The FEC codec is not an independent building block which may simply be added to a system as needed. Effects of the codec upon the system and the impact of the system upon the codec must be carefully considered. For example, the codec changes the system's data rate because parity bits are inserted by the encoder and deleted by the decoder; altering the error statistics by differential encoding is an example of system impact upon the codec. Thus, a systems approach to the incorporation of FEC coding in a TDMA system is necessary.

Ambiguity Resolution Factors

Systems tradeoffs are most evident in the area of carrier phase ambiguity resolution. The use of differential decoding to resolve phase ambiguity not only doubles the BER but also causes errors to occur in pairs. Although a special convolutional code has been designed for use with paired errors,[6] its performance does not meet the objectives of Table 1.

If FEC decoding is performed after differential decoding, a simple bit interleaver may be employed to split the paired errors between the P and Q channels.[7] In this case, a separate FEC codec is required for each channel. Alternately, a more complex interleaver may be used to disperse errors over more than one code block, permitting the use of a single FEC codec. In either event, the simplicity of ambiguity resolution by differential coding is countered by additional hardware complexity elsewhere in the TDMA system. Moreover, the second approach is not suitable for burst mode operation.

If, instead, FEC decoding is accomplished prior to differential decoding, the decoder is not affected by paired errors, although it must contend with phase ambiguity. In this situation, a code transparent to phase ambiguity may be utilized with separate codecs for each of the P and Q data channels.[7,8]

With a transparent code, the complement of a codeword is also a codeword. At the end of a TDMA burst, however, a shortened block may be used with block codes to avoid transmitting dummy information bits to complete the code block. Unfortunately, the complement of a shortened codeword may not be a shortened codeword. Inversion of data due to phase ambiguity may be detected and corrected before FEC decoding, however, by adding approximately nine polarity indicating (PI) bits per channel to the preamble. Polarity inversion may be determined by a majority decision of the PI bits in a channel.

With a transparent convolutional code, the PI bits are needed to provide both correct dummy bits to complete decoding at the end of a burst and correct decoder initialization at the beginning of a burst. As with a block code, the alternative is to transmit additional data bits.

A special block code devised by Nakamura[9] to be transparent to both bit inversion and channel reversal permits the use of a single transparent FEC decoder prior to the differential decoder. The Nakamura decoder is more complex than decoders for alternative block codes and requires the transmission of dummy information bits to complete the last code block in a burst or the use of PI bits.

Possible channel inversion over the whole burst may be corrected with PI bits, permitting the use of a pair of nontransparent block or convolutional decoders prior to the differential decoder. If the function of the PI bits is extended to include correction of channel interchange as well as inversion, only a single FEC codec, which could be nontransparent, would be required. Since the PI bits would then be accomplishing the complete ambiguity correction function, differential coding could be eliminated. Moreover, the ambiguity resolving function of the PI bits could be assumed by the unique word (UW) detector.[10]

Placing the differential decoder after the FEC decoder approximately doubles the low BER of the error correction decoder output rather than the higher channel BER, which reduces degradation in terms of E_b/N_o. A modem cycle slip, however, results in a transient burst of errors until the transparent decoder is filled with new data. This process consumes the balance of the current code block for transparent block codes and one complete constraint length for transparent convolutional codes. For nontransparent codes, reliance on PI bits in the preamble to remove inversion can cause incorrect decoding of the portion of the burst following the slip.

Cycle slipping should not be overemphasized as a system consideration, since the modem should be designed to perform satisfactorily in all respects under the anticipated operating conditions. It would appear desirable, however, to specify cycle slipping performance. The worst-case error rates of Table 1 require a narrower bandwidth in the demodulator's carrier recovery circuit for a given slip probability than would be needed with a lower BER. Narrowing the bandwidth increases demodulator acquisition time, necessitating an increase in the carrier and bit timing recovery sequence from the 30 symbols employed in previous INTELSAT TDMA system proposals[11] to more than 70 symbols. In addition, a UW length of 10-11 symbols would be needed if UW detection were used for ambiguity resolution. If differential coding were employed, 18 symbols would be required due to the doubling of channel errors.

Phase ambiguity may be resolved by using a syndrome synchronizer,[7] as well as by either differential coding or UW detection. The syndrome synchronizer recognizes when the FEC decoder is attempting to correct at an excessively high rate. Attributing this to phase ambiguity, the synchronizer sequentially tries all possible combinations of channel reversal and inversion until the correction rate drops below an acceptable level. The long search times involved generally make this method of ambiguity correction unsatisfactory for TDMA operation.

TDMA Ambiguity Resolution Summary

Of these ambiguity resolution techniques, those applicable to TDMA are (in order of decreasing decoded BER):

a. differential decoding before FEC decoding,
b. differential decoding after FEC decoding, and
c. UW detection.

Although employing differential decoding before FEC decoding performs ambiguity resolution with a minimum of hardware, this is accomplished at the expense of other system components. For TDMA applications, two FEC codecs are required. As with any differential coding approach, the UW detector must process a sequence which is over 50 percent longer than would otherwise be required. Since the relationship between input and output BER for typical double-error-correcting (DEC) codes is generally $BER_{OUT} = K(BER_{IN})^3$, doubling the channel error rate by differential decoding results in a final error rate approximately eight times larger than that without differential coding.

Differential decoding after FEC decoding is a viable alternative for an essentially continuous channel, even though the final error rate is approximately doubled and two FEC codecs are required. For burst mode operation, however, PI bits are required to avoid the transmission of dummy terminating bits. Since the function of the PI bits may be accomplished by the UW and differential coding thereby eliminated, this configuration reduces to that of UW detection. Thus, differential decoding after FEC coding is of questionable utility in TDMA applications unless the dummy bits are transmitted.

Use of the UW for ambiguity resolution requires a more complex UW detector than is necessary for system synchronization alone. This is because each half of the UW must be recognized in either channel in true or complemented form. The extra complexity is partially compensated for by the use of a much smaller UW length. This method requires only a single FEC codec and achieves the lowest BER.

Soft Decisions

The use of a soft-decision decoding technique would require that the FEC codec be located near the modem, since elsewhere the TDMA system is only able to handle binary quantities. Furthermore, the use of soft decisions would have significant impact upon modem design, regardless of the method used to obtain the soft output. A conventional PSK detector could be employed until the hard decisions were made. High-speed analog-to-digital conversion would then be necessary to obtain 2- or 3-bit quantization in each of the two channels.

Alternately, a soft-decision demodulator employing a multi-phase detector could be used. In this case, the received signal for each of the two channels would be coherently demodulated by multiple reference carriers. A logical conversion would then map the multiple phase detector outputs into the corresponding soft output vectors. The advantage of the second method is its insensitivity to level variations in the received carrier, which reduces AGC requirements.

Clocking and Timing

The data rates at the input and output of an FEC codec differ because the uncoded data stream consists only of information bits while the coded data contain additional parity bits. A phase-locked loop is often employed for clock rate conversion; the codec inputs and outputs then interface with the rest of the system as continuous bit streams. This approach is inappropriate for TDMA application primarily because it requires 2-speed operation of the TDMA terminal and additional multiplexer/demultiplexer complexity.

In the recommended approach (Figure 2), the uncoded data stream at the terrestrial side of the FEC codec is operated with an intermittent clock, while coded data at the satellite side are processed with the continuous terminal clock. The intermittent clock is obtained from the terminal clock by providing gaps corresponding to parity bit locations. This approach has two advantages; existing compression and expansion buffers, rather than additional memory, are used to provide the bit rate conversion, and only the terminal clock is required to drive the timing and data gating control units.

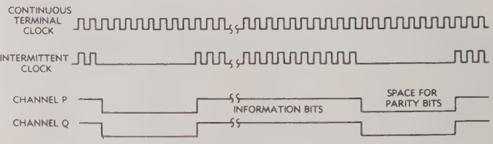

Figure 2. Intermittent Clocking

For convenience in generating timing signals, it is preferable that all gating lengths be increments of four symbols. Block codes must be modified so that the parity and information symbols are each in multiples of four. For a rate k/n convolutional code, data are clocked in increments of 4k information symbols followed by 4(n - k) parity symbols. This requires a small amount of additional memory in the convolutional codec for format conversion.

An elastic buffer is required in the terminal to interface with the data and clock signals from the demodulator, which are asynchronous with the terminal clock. This buffer also provides a symbol clock to the FEC decoder which continues after the end of a burst to allow completion of the decoding. It may be designed to reposition an incoming burst so that the inter-burst gap is a multiple of four symbols. This prevents conflict at the FEC decoder between the timing signals associated with the incoming burst and those associated with the burst already in the decoder, which may otherwise restrict the spacing between bursts.

Burst Termination

In general, the data portion of a burst will not be an exact multiple of the code block length. However, completing the last block with dummy information bits is not necessary when a block code is used because dummy zeros are presumed to have preceded the short data block. Since preceding zeros would not affect the encoder, they would also not affect the decoder and need not be inserted when decoding the short block.

This does not apply to a convolutional code, however, since decoding the last information bit requires knowledge of parity bits extending one constraint length beyond the last information bit. These final parity bits must be flushed from the encoder at the end of the burst, although they may be compressed for transmission without actually being accompanied by the corresponding dummy information bits. However, the dummy information bits must be inserted by the decoder at the end of the burst. Since high-rate convolutional codes have quite long constraint lengths, the need for dummy bits results in significant decoding delay at the end of a burst. In many cases, this may require spacing the coded portions of adjacent bursts by more than the length of the preamble, thereby increasing guard time requirements. Furthermore, processing the compressed parity bits requires maximum system speed (120 Mbit/s) from portions of the encoder and decoder which ordinarily operate at a much lower rate.

Code Considerations

General Requirements

The primary performance objectives of Table 1 may be summarized as follows:

a. to improve a raw channel BER of 3×10^{-3} under cochannel interference conditions arising from rain induced depolarization to better than 1×10^{-3}; and

b. to improve a raw channel BER of 7×10^{-5} under clear sky conditions to better than 1×10^{-6}.

Errors produced in the case of interference were concluded to be sufficiently random to permit the use of random-error-correcting codes to achieve the desired performance goals. This was subsequently confirmed during hardware testing of the codec models.

For commercial service, a high-rate code will most efficiently utilize the channel. For rates below 7/8, decoders can be rather simple, but efficiency deteriorates significantly because of the additional percentage of parity bits. Changing the code rate from 3/4 to 7/8 increases efficiency almost 0.7 dB. Less than 0.6 dB of further improvement is available in the limit as a code rate of unity is approached, of which only 0.1 dB would be obtained with a rate of 9/10. While efficiency improves only slightly for rates above 7/8, decoding complexity increases enormously. A code rate of 7/8 appears to represent a nearly optimum tradeoff between efficiency and decoder complexity.

Similarly, a marked improvement in performance is obtained with a DEC code rather than a single-error-correcting (SEC) type. Error-correcting ability refers to the number of errors in one code block which a block code is guaranteed to correct, or the number of errors in one constraint length which a convolutional code will correct. A significant additional improvement is obtained with a triple-error-correcting (TEC) code, although the incremental improvement is not as great as in the former case. Furthermore, the TEC decoder is considerably more complex.

For DEC codes, the controlling objective is to improve a channel error rate of 3×10^{-3} to better than 10^{-3}; any DEC code satisfying this objective will easily meet the second objective of improving a BER of 7×10^{-5} to less than 1×10^{-6}. For SEC codes, the two objectives are approximately of equal difficulty.

Viterbi[12] and sequential[13] decoding were considered, since they offer potentially large coding gains both with and without the use of soft decisions. Viterbi decoding is not presently practical for code rates greater than 3/4 nor for data speeds of 120 Mbit/s. Sequential decoding is also impractical with high-rate codes and fast transmission speeds. Investigation of other soft-decision decoding methods proposed by Massey,[14] Forney,[15] Weldon,[16] Chase,[17] Sundberg,[18] and Hartman and Rudolph[19] indicated that they were inappropriate for high-speed operation and/or high-code-rate application. Moreover, the use of soft decisions adds complexity to the demodulator.

Concatenation of two FEC codes is a powerful error-correction method. Furthermore, a single high-rate code may be applied universally to all links, and the outer code applied selectively to links requiring additional improvement. The interleaver needed to disperse the error bursts resulting from the inner codec can be implemented by a slight modification of the TDMA expansion/compression buffers. While both interesting and practical, concatenation is unnecessary since a single high-rate code with hard-decision decoding can satisfy the performance objectives.

Candidate Coding Approaches

The performance of self-orthogonal convolutional codes with hard-decision threshold decoding was studied by computer simulation.[4] Single-, double-, and triple-error-correcting codes with rates up to and including 7/8 were examined.

The performance of BCH block codes surpassed that of threshold-decodable block codes. Moreover, computer simulation verified the superiority of BCH codes with even minimum distances over those with odd minimum distances.[4] A BCH code with even minimum distance is obtained by multiplying the generator polynomial of an ordinary BCH code by the term (x + 1), thereby increasing the number of parity bits by one. The additional parity bit provides an overall parity check on the code block. For even moderate block lengths, this only slightly reduces the code rate and can often be combined with the block size adjustment required for the information and parity portions to be in four symbol increments. The improved performance of the even minimum distance BCH codes occurs because these codes can detect t + 1 errors as well as correct t errors. Therefore, the number of decoder output errors is not increased due to false corrections when exactly t + 1 errors are present in a code block.

A number of potentially viable block and convolutional coding approaches are shown in Table 2. Only codes of high rate (approximately 0.875) which meet the primary objective of reducing a channel error rate of 3×10^{-3} to 1×10^{-3} are included. The (127, 12) BCH code clearly provides the most coding improvement and meets the maximum BER objective with the most margin. A table look-up decoder would require 14×2^{14} bits of memory.

Although the (63, 56) BCH code is well within the maximum BER objective without differential coding, there is less margin because its error rate is approximately three times greater than that of the (127, 112) code. Since this is an SEC code, performance at lower channel error rates

Table 2. Candidate TDMA Coding Approaches

Configuration	Basic Code	Basic Code Rate	Modified Code[a]	Modified Code Rate	Input BER[b]	Output BER[c]	No. of Codecs
No Differential Coding	(127,112) DEC/TED BCH[d]	0.882	(128,112)	0.875	3×10^{-3} 7×10^{-5}	1.5×10^{-4} 3.0×10^{-9}	1
	(63,56) SEC/DED BCH[e]	0.889	(64,56)	0.875	3×10^{-3} 7×10^{-5}	4.8×10^{-4} 3.0×10^{-7}	1
	7/8(384,336) DEC Convol.	0.875	7/8(384,336)	0.875	3×10^{-3} 7×10^{-5}	5.1×10^{-4} 7.0×10^{-9}	1
Differential Decoding After FEC Decoding (FEC inside)	(127,112) DEC/TED BCH	0.882	(128,112)	0.875	3×10^{-3} 7×10^{-5}	3.0×10^{-4} 6.0×10^{-9}	2
	(60,52) Approx. DEC Nakamura	0.867	(60,52)	0.867	3×10^{-3} 7×10^{-5}	4.2×10^{-4} 8×10^{-8}	1
	(63,56) SEC/DED BCH	0.889	(64,56)	0.875	3×10^{-3} 7×10^{-5}	1×10^{-3} 6×10^{-7}	2
	7/8(384,336) DEC Convol.	0.875	7/8(384,336)	0.875	3×10^{-3} 7×10^{-5}	1×10^{-3} 1.4×10^{-8}	2
Differential Decoding Before FEC Decoding (FEC outside)	(127,112) DEC/TED BCH	0.882	(128,112)	0.875	6×10^{-3} 1.4×10^{-4}	1×10^{-3} 2.2×10^{-8}	2

[a] The parameters of the modified code have been changed so that the information and parity bits in a code block are in multiples of four symbols.

[b] For differential decoding before FEC decoding, the input BER is given at the output of the differential decoder.

[c] For differential decoding after FED decoding, the output BER is given at the output of the differential decoder.

[d] DEC/TED means double-error-correcting/triple-error-detecting.

[e] SEC/DED means single-error-correcting/double-error-detecting.

will be orders of magnitude poorer than that of DEC codes. The advantage of the (63, 56) code is hardware simplicity. Only 6 x 2^6 bits of memory would be required in the decoder. Since the code length is small, shift register lengths would also be correspondingly small. Therefore, of the codes listed in Table 2, this is the simplest to decode. Since Table 2 was predicated upon the importance of high code rates, the hardware advantage of the (63, 56) code is obtained at the expense of error-correcting performance. Alternately, high performance and hardware simplicity may be attained by relaxing the code rate objective.

The rate 7/8 convolutional code performs similarly to the (63, 56) code at a channel error rate of 3×10^{-3}. However, since it is a DEC code, its performance more nearly approaches that of the (127, 112) code at lower input error rates. The amount of hardware required by the rate 7/8 code ranges between that needed by the two previous candidates. However, parity bits must be flushed at the encoder, dummy information bits inserted at the decoder, and additional system guard time provided.

The (60, 52) Nakamura code is well within the BER objective, with an error rate less than three times the best of the (127, 112) code (without differential coding) at a channel error rate of 3×10^{-3}. This special code permits the use of a single transparent FEC decoder followed by differential decoding. However, a more complex decoder than the one required with the (127, 112) code is needed. Furthermore, either dummy information bits must be used to complete the last data block at the decoder, or PI bits must be added to the preamble.

Universal application of a single code and decoding method throughout the TDMA system appears most advantageous, since numerous links can benefit significantly from coding, and requirements can be met with a high-rate code and a hard-decision codec of reasonable complexity. The BCH block codes offer better BER performance and shorter length than comparable threshold-decoded convolutional codes.

Recommended Approach

Block codes are more suitable for TDMA operation, since the extra complexity needed by convolutional codes to flush parity bits at the end of a burst is not needed. Also, the block decoder does not require the insertion of dummy information bits corresponding to the flushed parity bits. The time required to process the numerous dummy bits would restrict the minimum spacing of adjacent bursts with a convolutional decoder.

The resolution of phase ambiguity by UW detection is recommended to obtain the lowest BER, minimize overall system hardware and operating complexity, and maximize transmission efficiency. Placement of the FEC codec between the system multiplexer/demultiplexer and scrambler/descrambler permits a single codec operating in a burst mode to process all bursts. The intermittent clock approach described earlier simplifies TDMA terminal hardware.

The foregoing conclusions limit the alternatives to the (63, 56) and (127, 112) BCH codes. If anticipated channel conditions and BER objectives were unalterable and if minimization of FEC hardware complexity were an overriding consideration, the choice would clearly be the (63, 56) code. The safety factor offered by the (127, 112) candidate was considered important, however, in view of the potential for change in anticipated channel error rates and objectives, as well as the need to maintain an adequate system margin. Furthermore, this more powerful code offers significantly better performance at lower channel error rates. Therefore, the (127, 112) BCH code was chosen for hardware implementation.

Characteristics

The selected code has double-error-correcting/triple-error-detecting properties which are obtained by adding an overall parity check to a DEC (127, 113) BCH code and eliminating one information bit. Addition of the triple-error-detecting capability prevents false corrections when three errors are present in one code block, which would otherwise result in an average of four output errors. Thus output BER is only 0.75 that of the original DEC code. This improvement is obtained with a negligible increase in decoding hardware.

The generator polynomial of the selected code is obtained by multiplying the original code's polynomial by the term (x + 1), yielding

$$G(x) = (x + 1)(x^{14} + x^{12} + x^{10} + x^6 + x^5 + x^4 + x^3 + x^2 + 1).$$

This increases the number of parity bits per code block from 14 to 15. A dummy bit is added so that the parity and information bits are in multiples of four, resulting in a (128, 112) BCH code. A complete code block (Figure 3) contains 112 bits of information followed by 15 parity bits and a final dummy bit. Any polarity is acceptable for the dummy bit, whose only function is filling the parity symbol time slot.

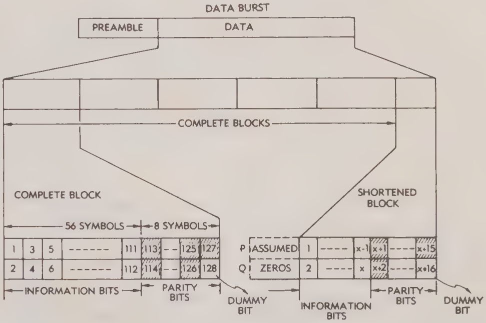

Figure 3. (128,112) BCH Code Block Structure

Since the data portion of a TDMA burst is not necessarily an exact multiple of 112 bits, the final code block in a burst will generally contain less than 112 information bits. In decoding, zeros are assumed to have preceded the data bits to complete the last block although the decoder does not take special action regarding these fictitious bits. The shortened block contains the normal complement of 15 parity bits plus one dummy bit.

Encoding is accomplished (Figure 4a) by dividing a block of 112 input bits by the generator polynomial. The remainder of this calculation forms the parity bits which are appended to the end of the data block.

As data enter the decoder data buffer (Figure 4b), the syndrome of the error pattern is simultaneously calculated. The syndrome is used to address a location in read-only memory (ROM) containing the positions of the error bits within the code block. The ROM output is compared with a counter which indicates bit position as data are shifted out of the data buffer. When a bit in error appears at the output of the buffer, the comparator's output is used to correct the error. Comparator action is inhibited when the overall parity check indicates three errors within a code block.

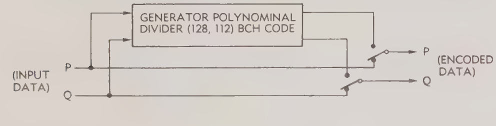
GENERATOR POLYNOMINAL DIVIDER (128, 112) BCH CODE
(INPUT DATA)
P
Q
P
Q
(ENCODED DATA)

a) Encoder

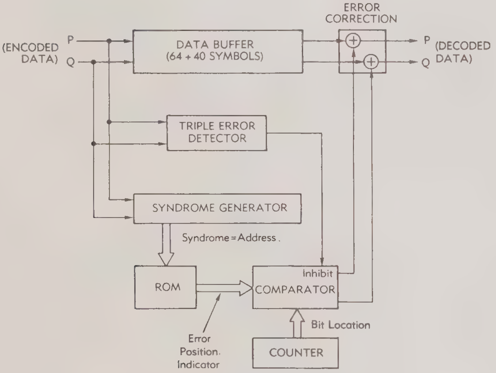
ERROR CORRECTION
(ENCODED DATA)
P
Q
DATA BUFFER (64 + 40 SYMBOLS)
P
Q
(DECODED DATA)
TRIPLE ERROR DETECTOR
SYNDROME GENERATOR
Syndrome = Address
ROM
Inhibit
COMPARATOR
Bit Location
Error Position Indicator
COUNTER

b) Decoder

Figure 4. High-Speed (128,112) BCH Codec

Bit Error Rate Performance

Each 1- and 2-bit error produces a syndrome pattern corresponding to a unique location in the ROM (Figure 5), permitting all such combinations to be corrected. Moreover, all triple errors in one block are detected, which prevents them from causing erroneous corrections.

Odd combinations of errors greater than three are also detected, except for those with syndrome patterns identical to single bit errors. In such cases, false correction of the impersonated bit occurs. When an even number of errors greater than two produces a syndrome identical to a 1- or 2-bit error pattern, erroneous 1- or 2-bit correction will also transpire. However, approximately half such even errors will generate one of the remaining syndrome combinations, resulting in no false decoder action. Table 3 summarizes decoder response for the various combinations of input errors.

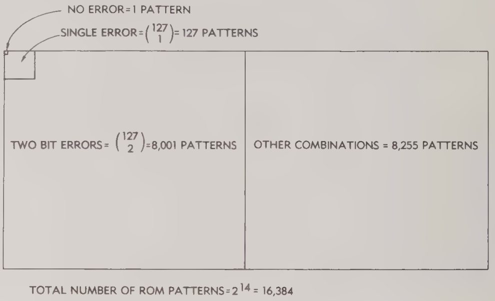
NO ERROR = 1 PATTERN
SINGLE ERROR = $\binom{127}{1}$ = 127 PATTERNS
TWO BIT ERRORS = $\binom{127}{2}$ = 8,001 PATTERNS
OTHER COMBINATIONS = 8,255 PATTERNS
TOTAL NUMBER OF ROM PATTERNS = 2^{14} = 16,384

Figure 5. Structure of ROM Look-up Table

Table 3. Output Error Characteristics

No. of Input Errors	Decoder Operation	Output Error Distribution	Mean No. of Output Errors
1	All corrected	0	0
2	All corrected	0	0
3	All detected	3	3
4	None detected	4 (prob ≃ 1/2) 6 (prob ≃ 1/2)	5 (approx)
5	Most detected	5 (approx)	5 (approx)
6	None detected	6 (prob ≃ 1/2) 8 (prob ≃ 1/2)	7 (approx)
7	Most detected	7 (approx)	7 (approx)
8	None detected	8 (prob ≃ 1/2) 10 (prob ≃ 1/2)	9 (approx)
9	Most detected	9 (approx)	9 (approx)

The probability of a block of N input bits containing exactly j errors is given[20] by

$$P[j] = \binom{N}{j} p_i^j (1 - p_i)^{N-j} \qquad (1)$$

where the errors are assumed to be both random and independent, and the channel error probability is p_i. The term $\binom{N}{j} = N!/(N-j)!j!$ represents the number of combinations of N bits taken j at a time, and the remaining terms give the probability of receiving a particular sequence of j erroneous bits and (N - j) correct bits. Although errors are assumed to be random and independent, no specific distribution is assumed for the channel noise amplitude.

For table decoding, each syndrome pattern corresponds to a specific error pattern, and feedback from the decoder output is not present to complicate the analysis. Thus, all j-bit input error sequences may be associated with an average number of output errors; the probability of an output bit error may be expressed by summing the contributions from all input sequences exceeding the error-correcting capability of the code (i.e., all sequences for which $j \geq t + 1$) to obtain

$$P_o = \sum_{j=t+1}^{N} \frac{e_j}{N} \binom{N}{j} p_i^j (1 - p_i)^{N-j} \qquad (2)$$

where

e_j = average number of output errors resulting from j input errors
t = error-correcting capability of the code
N = size of the code block.

A computer solution of equation (2) for values of j ranging up to and including 5 was completed as part of a computer simulation of the selected (128, 112) BCH code, resulting in the solid curve of Figure 6. The simulation results confirm the data of Table 3, since the values obtained for each e_j indicate that syndrome patterns are uniformly distributed over all possibilities for input error combinations of $j \geq 3$.

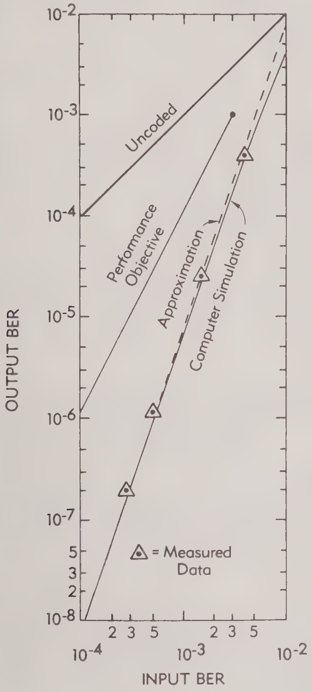

Figure 6. BER Performance of (128,112) BCH Code

A considerably simplified expression for output error probability may be obtained by observing that most decoder output errors are caused by (t + 1) input bit errors. Furthermore, the term $(1 - p_i)^{N-j}$ may be approximated by unity, except at the higher error rates. A DEC code would produce approximately four output errors for three input errors, since approximately half would result in two erroneous additional changes, and approximately half would be considered error free and passed unchanged. With triple-error-detecting ability, however, all 3-bit error combinations are detected, and only three output errors are produced. Therefore, equation (2) may be simplified to

$$p_o \simeq \frac{3}{N} \binom{N}{3} p_i^3 \qquad (3)$$

or

$$p_o \simeq \frac{(N - 1)(N - 2)}{2} p_i^3 \qquad (4)$$

Since N = 127 is the code block size, excluding the unused dummy bit, this may be expressed

$$p_o \simeq 7875 \, p_i^3 \qquad (5)$$

Equation (5), which is plotted as the dashed line in Figure 6, provides an easy-to-use approximation of error performance which is extremely good over most of the useful BER range.

Equation (3) shows that the triple-error-detection ability reduces the output error rate of the DEC code by 0.25. While this improvement is not dramatic, it is obtained with a minuscule addition to the decoding circuitry. Equation (4) is valid, not only for the full code block but also for shortened blocks; N represents the shortened block size including parity bits but excluding the final dummy bit. As N is reduced, equation (4) shows that the output error rate corresponding to a given input error rate also decreases. This is expected, since the assumed zeros preceding a short block are error free. Thus, the correctable number of errors in a full block may be compressed into a shortened block and still be corrected. The performance predicted by equation (4) has been experimentally verified for shortened blocks with N = 63 and N = 103.

The measured data points shown in Figure 6 were obtained using 120-Mbit/s QPSK modems looped back at their 140-MHz IF ports. Noise was introduced between the modulator and demodulator. The same data are replotted against E_b/N_o in Figure 7. Compared with theoretical uncoded PSK, the (128, 112) BCH codec provides coding gains of 1.8 dB at an output error rate of 1×10^{-4} and 2.6 dB at 1×10^{-6}.

Conclusions and Recommendations

Block codes are more suitable for TDMA, since, unlike convolutional codes, they do not require the additional complexity of termination at the beginning and end of a burst. BCH block codes are also shorter and perform better than threshold-decoded convolutional codes. Moreover, a code rate of 7/8 constitutes a good compromise between efficiency and decoding complexity.

Since many links require coding and all requirements can be fulfilled with a high-rate code and a hard-decision codec of moderate complexity, a single code and decoding method is recommended. One codec operating in burst mode may be located between the multiplexer/demultiplexer and scrambler/descrambler and used to process all bursts. Intermittent clocking is recommended to accommodate the difference in bit rates between the coded and uncoded data streams. Furthermore, UW detection is recommended for carrier phase ambiguity resolution to obtain the lowest BER while minimizing overall system complexity.

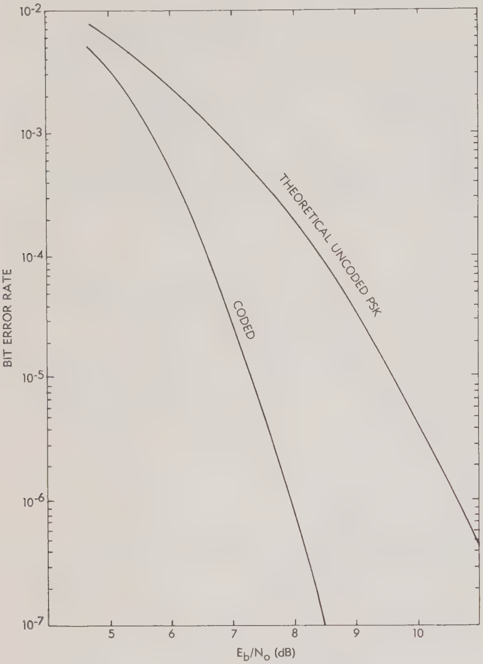

Figure 7. BER vs E_b/N_o for (128,112) BCH Code

A preferred (128, 112) BCH codec which corrects all double-bit errors in one code block and detects all triple-bit errors has been described. Hardware performance verifies the applicability of the recommended approach to incorporating error correction into the TDMA system contemplated for use with the INTELSAT V satellites of the 1980s. In particular, the practicality of employing a high-rate BCH code with a ROM look-up table decoder in a high-speed TDMA environment has been confirmed. The recommended approach will provide the coding gain needed to maximize data throughput while maintaining BER objectives for INTELSAT V TDMA.

The approach was selected because of the importance of a high code rate, minimum BER and minimum system complexity. When different objectives are stressed, other possibilities emerge. For example, an alternate (64, 56) BCH code was presented which offers less BER improvement, but much simpler decoding hardware. Both high performance and hardware simplicity are possible with a lower code rate.

If differential decoding after FEC decoding is preferred, two (128, 112) codecs may be utilized with a slightly higher decoded error rate. Alternately, a single (60, 52) Nakamura codec could be employed with an additional BER penalty. In either case, the differential codec's ability to correct ambiguity changes during a burst could be best utilized if system considerations would permit transmission of dummy information bits. If the achievement of the most rapid response to ambiguity changes is emphasized, differential decoding may be followed by a pair of (128, 112) codecs; however, this would result in the poorest decoded BER.

Acknowledgment

The authors wish to acknowledge the contributions of H. Saitoh, K. Koga, Dr. T. Mizuno and Y. Yasuda of KDD Research and Development Laboratories.

References

1. D. F. DiFonzo, "Antennas: Key to Communications Satellite Growth," Microwave Systems News, June 1978, pp. 83-91.
2. J. C. Fuenzalida, P. Rivalan, and H. J. Weiss, "Summary of the INTELSAT V Communications Performance Specifications," COMSAT Technical Review, Vol. 7, No. 1, Spring 1977, pp. 311-326.
3. C. Devieux, COMSAT Laboratories, Clarksburg, Md., Private Communication.
4. T. Muratani, H. Saitoh, K. Koga, T. Mizuno, Y. Yasuda, and J. S. Snyder, "Application of FEC Coding to the INTELSAT TDMA System," 4th International Conference on Digital Satellite Communications, Montreal, Canada, October 23-25, 1978, pp. 108-115.
5. "Systems in the Fixed-Satellite Service Using PCM for Telephony—Allowable Bit-Error Rates at the Output of the Hypothetical Reference Circuit," CCIR Draft Recommendation Document 4/147-E, 24 May 1976.
6. P. L. Chen and R. A. Rutledge, "Error Correcting Codes for Satellite Communications Channels," IBM Journal of Research and Development, Vol. 20, No. 2, March 1976, pp. 168-175.
7. Y. Tsuji, "Phase Ambiguity Resolution in a 4-Phase PSK Modulation System with Forward-Error-Correcting Convolutional Coding," COMSAT Technical Review, Vol. 6, No. 2, Fall 1976, pp. 357-377.
8. G. D. Forney, Jr., and E. K. Bower, "A High-Speed Sequential Decoder: Prototype Design and Test," IEEE Transactions on Communications Technology, COM-19, No. 5, October 1971, pp. 821-835.
9. K. Nakamura, "A Method for Constructing an Error Correcting Code Used in Differential Coding System," Annual Fall Conference Record of IECE, No. 13, Japan, September 1976.

10. E. R. Cacciamani, Jr., and C. J. Wolejsza, Jr., "Phase-Ambiguity Resolution in a Four-Phase PSK Communications System," IEEE Transactions on Communications Technology," COM-19, No. 6, December 1971, pp. 1200-1210.

11. G. Dill, J. Deal, and W. Maillet, "The INTELSAT Prototype TDMA System," 1975 IEEE Intercon Conference Record, Session Paper No. 29/3, April 8-10, 1975, pp. 1-8.

12. A. J. Viterbi, "Convolutional Codes and their Performance in Communication Systems," IEEE Transactions on Communications Technology, COM-19, October 1971, pp. 751-772.

13. J. M. Wozencraft and B. Reiffen, Sequential Decoding, Cambridge, Mass.: M.I.T. Press, 1961.

14. J. L. Massey, Threshold Decoding, Cambridge, Mass.: M.I.T. Press, 1963.

15. G. D. Forney, Jr., "Generalized Minimum Distance Decoding," IEEE Transactions on Information Theory, IT-12, April 1966, pp. 125-131.

16. E. J. Weldon, Jr., "Decoding Binary Block Codes on Q-ary Output Channels," IEEE Transactions on Information Theory, IT-17, November 1971, pp. 713-718.

17. D. Chase, "A Class of Algorithms for Decoding Block Codes with Channel Measurement Information," IEEE Transactions on Information Theory, IT-18, January 1972.

18. C. E. Sundberg, "One-Step Majority-Logic Decoding with Symbol Reliability Information," IEEE Transactions on Information Theory, IT-21, March 1975, pp. 236-242.

19. C. R. P. Hartman and L. D. Rudolph, "An Optimum Symbol-by-Symbol Decoding Rule for Linear Codes," IEEE Transactions on Information Theory, IT-22, September 1976.

20. M. Schwartz, Information Transmission, Modulation, and Noise, New York: McGraw-Hill, 1970, p. 314.

80-0594

A HIGH PERFORMANCE PROCESSOR CONTROLLED BPSK/QPSK MODEM FOR DATA RATES UP TO 4 MBPS

Woo Paik, Engineering Manager
Lindsay A. Weaver, Engineering Manager
Itzhak Gurantz, Senior Engineer
Ilan Peer, Engineer
LINKABIT Corporation
San Diego, CA

Abstract

This paper describes a high performance, full-duplex, BPSK/QPSK digital modem for data rates up to 4 MBPS. It uses newly designed digital algorithms for transmit filtering, receive carrier tracking, bit timing, and AGC. The performance of the modem is within 0.5 dB of theoretical coherent BPSK/QPSK at a BER of 10^{-7}. An internal multi-rate FEC convolutional encoder-decoder provides performance improvement as high as 6 dB at a BER of 10^{-7}. A general purpose microprocessor interfaces with the front panel, remote interface, modem I/O, redundancy control, and back-up memory. The microprocessor also provides on-line monitoring, self-test, and estimates of receive channel conditions.

INTRODUCTION

Introduction

The BPSK/QPSK modem described in this paper is a high performance full-duplex digital modulator-demodulator for operation at data rates up to 4.0 Mbps. The channel symbol rate ranges from 32 K baud to 2.0 M baud and is determined by a replaceable circuit board which contains baseband filters and clocks. The modem is a complete, self-contained unit including all necessary power supplies, timing and frequency synthesizers. To achieve high performance, newly conceived and designed digital signal processing algorithms have replaced the traditional analog building blocks. These include transmit filtering, receive carrier tracking, bit timing and AGC. An optional internal multi-rate FEC convolutional encoder-decoder provides for significant additional performance improvement. In order to support rate 1/2 coding the modem is designed to operate reliably at E_s/N_o as low as 0 dB. The unit is controlled from a serial remote interface or a front panel which contains digital displays of various modem and channel parameters, as well as pushbuttons and a keyboard for entering commands to the modem (see figure 1). Frequency acquisition-range, coding rate of internal FEC encoder-decoder, and QPSK/BPSK selection are front panel controllable. Incorporated into the modem is a general purpose microprocessor which is used to control and monitor such functions as front panel operation, remote interface, modem I/O and redundancy control. Additionally, the processor makes estimates of channel conditions for front panel display, carries out on-line monitoring of modem operation, and executes a complete off-line self test. Measured channel error rate (in coded mode), estimated E_b/N_o, signal level, and carrier offset can be displayed under front panel control. The modem also contains a built-in scrambler/descrambler and differential encoder/decoder.

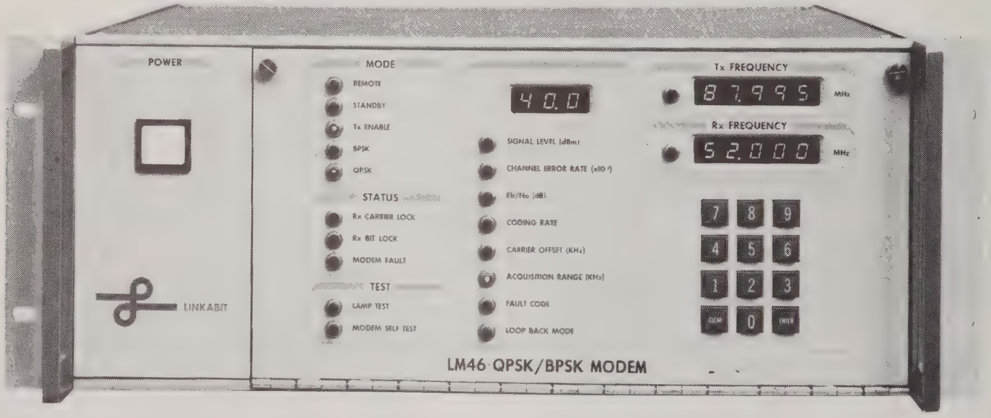
POWER
LINKABIT
MODE
REMOTE
STANDBY
Tx ENABLE
BPSK
QPSK
STATUS
Rx CARRIER LOCK
Rx BIT LOCK
MODEM FAULT
TEST
LAMP TEST
MODEM SELF TEST
40.0
SIGNAL LEVEL (dBm)
CHANNEL ERROR RATE
Eb/No (dB)
CODING RATE
CARRIER OFFSET (KHz)
ACQUISITION RANGE (KHz)
FAULT CODE
LOOP BACK MODE
Tx FREQUENCY
87.995 MHz
Rx FREQUENCY
52.000 MHz
7 8 9
4 5 6
1 2 3
CLR 0 ENTER
LM46 QPSK/BPSK MODEM

Figure 1. The LM46 Modem.

Copyright © 1980 by LINKABIT Corporation

Released to AIAA to publish in all forms.

Performance

Figure 2 shows bit error rate as a function of signal energy-to-noise density ratio. The solid curve is the performance of ideal BPSK and QPSK over infinite bandwidth, additive white Gaussian channel with matched filter detection [1, 2]. The measured bit error rate performance of the modem in the QPSK mode is indicated by circles. Notice that the performance is within .5 dB of theoretical at 10^{-5} bit error rate.

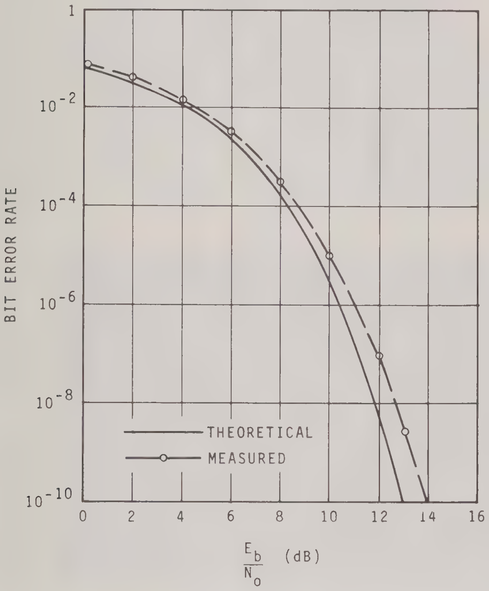

Figure 2. Uncoded Bit Error Rate Performance.

With an internal convolutional coder and sequential decoder operating at code rates of either 1/2, 3/4 or 7/8, additional performance improvements are achievable depending on data rate*. For a data rate of 200 Kbps and below, for these coding rates, the coding gain is on the order of 6 dB, 5 dB or 4 dB, respectively. The above coding gains are each reduced by about 1 dB for data rates on the order of 2 Mbps. Figure 3 shows measured bit error rate performance of the modem at channel symbol rate of 2.1 Msps, which corresponds to data rates of 1.029 Mbps, 1.544 Mbps and 1.801 Mbps, respectively, for the three coding rates.

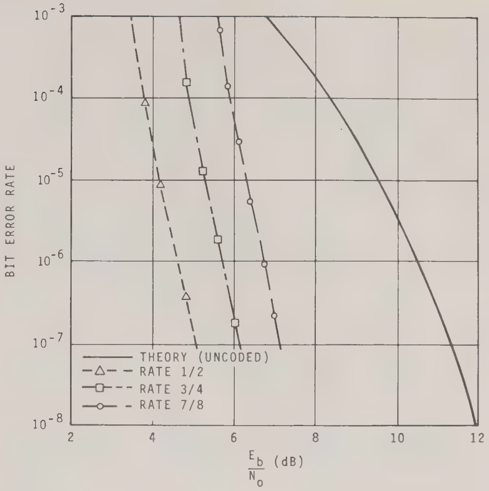

Figure 3. Coded Bit Error Rate Performance at 2.1 Msps (QPSK).

DESIGN FEATURES

Modem Structure

Figure 4 shows the block diagram of the modem. The TX data, after necessary scrambling and encoding, enter the modulator digital filters which are followed by D/A (digital to analog) converters and analog filters. The filtered I and Q data streams are up-converted to desired IF frequencies by a broadband quadrature modulator. The desired RX IF signal passes through an AGC attenuator, and then is down-converted to baseband by a broadband quadrature demodulator. The baseband I and Q signals are filtered by demodulator analog filters, and then digitized by A/D (analog to digital) converters. All the necessary tracking loops including carrier tracking loop and bit tracking loop are implemented in the digital processor which processes I and Q samples from the A/D converters. The RX data are obtained from the I and Q samples after necessary decoding and descrambling. Built-in digital, baseband, IF, and remote loop-back capabilities are provided for versatile self-error checking.

The modulator and demodulator frequencies can be independently set by a processor-controlled built-in synthesizer within the 52-88 MHz IF band in 5 kHz steps by front panel or remote control. The synthesizer is designed to have low phase noise characteristics, which is essential to high performance PSK modems. The direct conversion design with the broadband quadrature modulator and demodulator eliminates the need of channel filters and reduces spurious responses. Composite demodulator signal level can be as high as -5 dBm without causing performance degradation while nominal input level is -30 ±10 dBm.

---

*The performance of a sequential decoder improves for lower data rates due to the increase in the ratio of the decoder computation rate to the data rate.

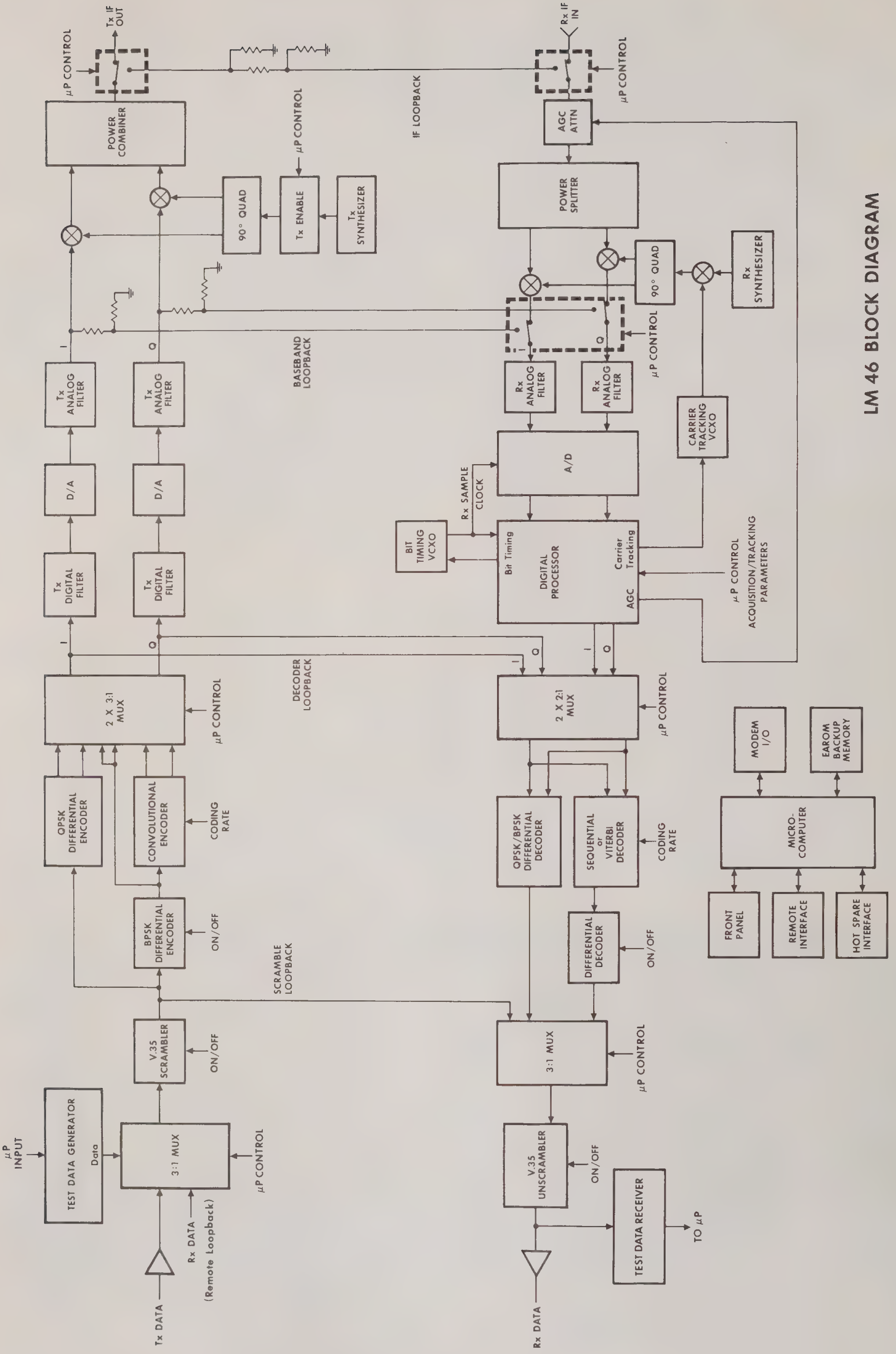

LM 46 BLOCK DIAGRAM
Tx DATA
Rx DATA (Remote Loopback)
μP INPUT
TEST DATA GENERATOR
Data
3:1 MUX
μP CONTROL
V.35 SCRAMBLER
ON/OFF
BPSK DIFFERENTIAL ENCODER
ON/OFF
QPSK DIFFERENTIAL ENCODER
CONVOLUTIONAL ENCODER
CODING RATE
2 X 3:1 MUX
μP CONTROL
I
Q
Tx DIGITAL FILTER
Tx DIGITAL FILTER
D/A
D/A
Tx ANALOG FILTER
Tx ANALOG FILTER
90° QUAD
Tx ENABLE
Tx SYNTHESIZER
μP CONTROL
POWER COMBINER
μP CONTROL
Tx IF OUT
IF LOOPBACK
BASEBAND LOOPBACK
DECODER LOOPBACK
SCRAMBLE LOOPBACK
Rx IF IN
μP CONTROL
AGC ATTN
POWER SPLITTER
90° QUAD
Rx SYNTHESIZER
I
Q
μP CONTROL
Rx ANALOG FILTER
Rx ANALOG FILTER
CARRIER TRACKING VCXO
A/D
Rx SAMPLE CLOCK
BIT TIMING VCXO
Bit Timing
DIGITAL PROCESSOR
Carrier Tracking
AGC
μP CONTROL ACQUISITION/TRACKING PARAMETERS
2 X 2:1 MUX
μP CONTROL
QPSK/BPSK DIFFERENTIAL DECODER
SEQUENTIAL or VITERBI DECODER
CODING RATE
DIFFERENTIAL DECODER
ON/OFF
3:1 MUX
μP CONTROL
V.35 UNSCRAMBLER
ON/OFF
TEST DATA RECEIVER
TO μP
Rx DATA
MODEM I/O
EAROM BACKUP MEMORY
MICRO-COMPUTER
FRONT PANEL
REMOTE INTERFACE
HOT SPARE INTERFACE

Figure 4. LM46 Block Diagram.

In the following sections we show how the extremely high performance was obtained. Careful design of baseband filters and digitally implemented tracking loops are two major contributing factors.

Baseband Filters

The demodulator filter is a 6-pole Butterworth active lowpass filter with a delay equalizer. The pole and zero locations of the delay equalizer were optimized to minimize the group delay variation over the passband. The demodulator filter was implemented using wideband operational amplifiers and fast buffers with gain-bandwidth products of over 100 MHz for accurate and reproducible filter response. Figure 5 shows measured frequency response of the demodulator filters. Group delay response also shows a similar match between I and Q channels. Figure 6(a) shows impulse response of the demodulator filter.

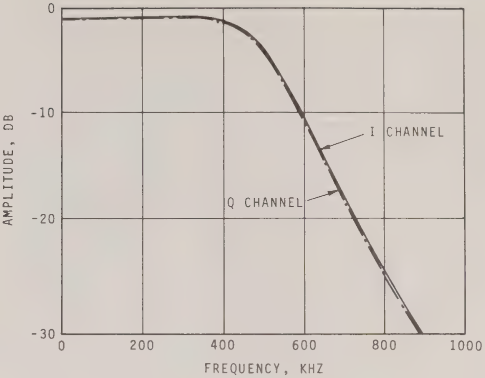

Figure 5. Frequency Response of the Demodulator Lowpass Filter.

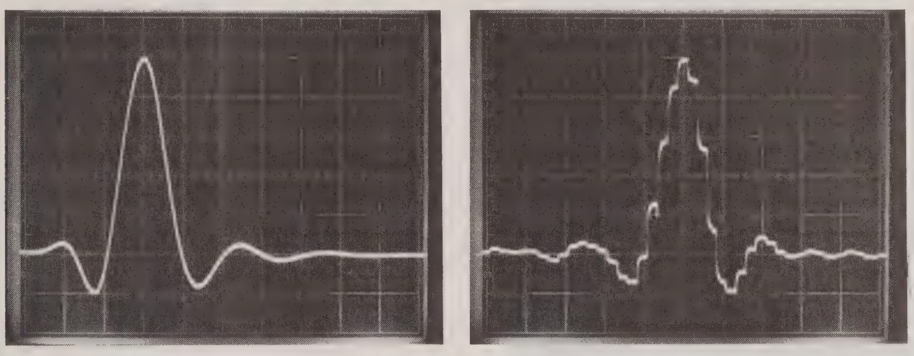

(a) Impulse response of the demodulator filter.

(b) Impulse response of the modulator digital filter.

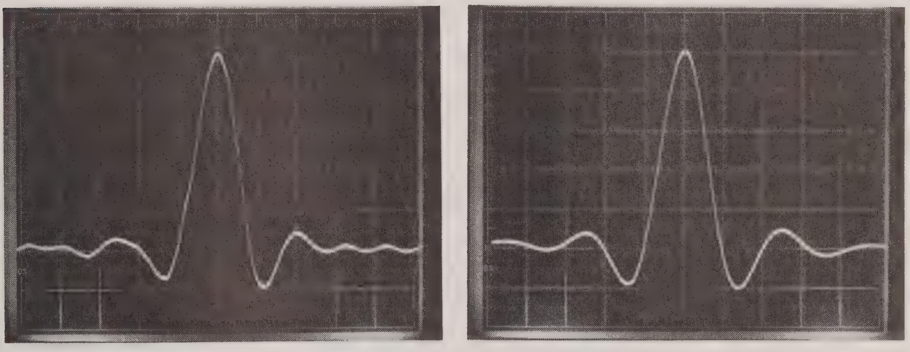

(c) Impulse response of the modulator digital filter followed by the smoothing analog filter.

(d) Combined impulse response.

In all figures, one horizontal grid segment corresponds to one symbol time.

Figure 6. Measured impulse response of baseband lowpass filters.

The demodultor filter is implemented by a digital filter which can be programmed for any desired finite impulse response. The modulator digital filter has been programmed to produce a time-reversed replica of the demodulator filter impulse response which realizes a nearly ideal matched filter to the demodulator filter. The output of the digital filter is further filtered by an analog filter to remove the spurious output components which are caused by the finite sampling rate of the digital filter. Figures 6(b) and 6(c) show the impulse responses of the modulator filter without the analog filter and with the analog filter, respectively. Notice that Figure 6(c) is a time-reversed replica of Figure 6(a).

The combined impulses response of the modulator and the demodulator filters is shown in Figure 6(d). Notice that the zero crossings of the combined response occur almost exactly at the sampling time. The resulting eye pattern (Figure 7) is nearly ideal and it contributes to the extremely high performance of the modem.

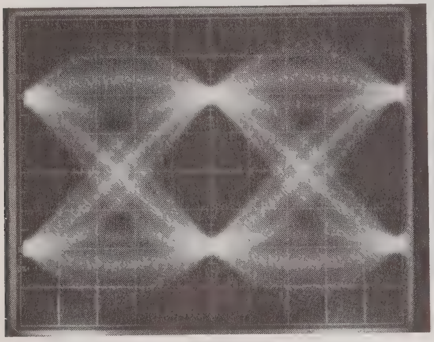

Figure 7. Measured Eye Pattern of the Modem.

Figure 8 shows the output spectrum of the modem (QPSK modulated by 4095 PN data at 2.06 M bits/second). Because of the clean output spectrum and narrow bandwidth, the modem is ideal for closely spaced FDMA (Frequency Division Multiple Access) satellite communication systems. Figure 9 shows measured bit error rate performance in the presence of adjacent channels of equal strength on both sides. The additional degradation due to adjacent channels is less than 0.3 dB with 1.2 Hz/baud channel spacing and less than 0.1 dB with 1.3 Hz/baud channel spacing at 10^{-3} bit error rate uncoded or 10^{-7} bit error rate with 7/8 coding.

Carrier and Bit Tracking Loops

Among the functions that a demodulator has to implement, one of the most important is that of signal acquisition and tracking. The performance of a modem can degrade rapidly if its synchronization is inadequate, particularly in QPSK modulated systems [By synchronization we refer to carrier phase and bit time synchronizations]. In the LM46 modem, special attention has been given to the design and implementation of the synchronization circuitry for operation over a wide range of E_S/N_O. Some of these features are described in this section.

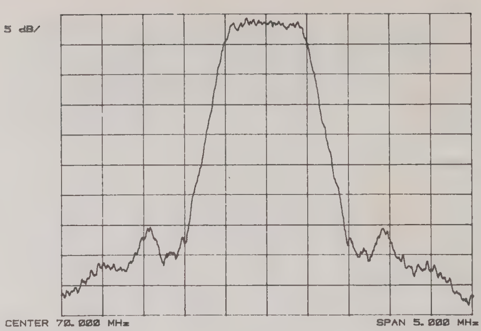

Figure 8. Output Spectrum of the Modem (QPSK with 4095 PN Data, 2.06 Msps).

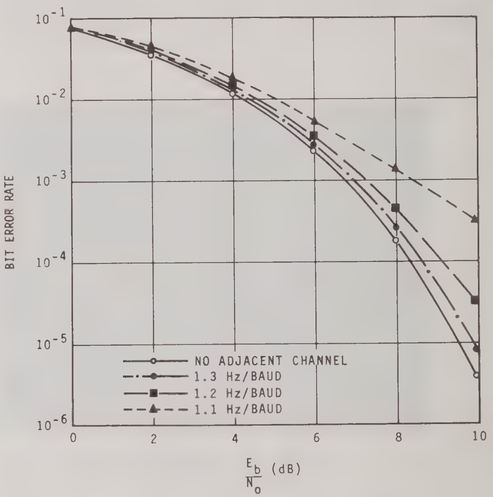

Figure 9. Bit Error Rate Performance with Adjacent Channels of Equal Strength on Both Sides (QPSK).

In general, synchronization circuits are implemented digitally using phase-locked loops. The loop error signals are obtained from the baseband signal, thus providing maximum control sensitivity. The use of read-only memory (ROM) allows for the implementation of almost arbitrary error functions required for near optimal loop control. Microprocessor control of all acquisition algorithms allows for a flexible acquisition procedure.

Carrier Acquisition and Tracking

A modified digital Costas Loop is used for carrier acquisition and tracking. An easily implemented Frequency-Phase detector is used for frequency acquisition. Several of its advantages are:

(1) No outside VCXO sweep is required; this reduces the acquisition range to half, on the average.

(2) Immunity to frequency false-lock provided the frequency uncertainty is less than one quarter of the baud rate. [More accurately, the frequency uncertainty has to be less than one quarter of the loop update sampling rate].

(3) Does not require a complete new acquisition procedure after temporary loss of carrier lock.

(4) Sweep rate is automatically determined by SNR conditions of the loop. Acquisition is fast for high SNR, but slows down for lower SNR.

(5) The AFC circuit has only minor influence on tracking performance; thus it does not require its disconnection following acquisition.

The loop can acquire and track carrier frequency offset of up to ±40 kHz at E_S/N_O as low as -2 dB. Figure 10 shows actual modem acquisition at different SNR levels. Phase tracking has been designed for a wide SNR range, so phase slip frequency is kept very low even at low SNR. In the QPSK mode, the probability of phase slip is less than one per $1\text{x}10^9$ bits at $E_S/N_O = 0$ dB and less than one per $3.6\text{x}10^{10}$ bits at $E_S/N_O = 3$ dB.

Bit Time Tracking

To achieve bit synchronization, the LM46 uses a second order loop controlled VCXO. This loop including the lock indicator has been carefully designed for low SNR operation, even in the presence of maximum carrier frequency offset. Thus, the bit lock indicator serves as a signal presence indicator. The loop can acquire and track bit frequency offset of up to ±100 p.p.m at E_S/N_O as low as -4 dB.

CONCLUSION

Conclusion

Design features and performance characteristics of a highly automated fully digital implementation of a BPSK/QPSK satellite modem have been presented. The high performance combined with narrow occupied bandwidth, automatic signal acquisition, and high flexibility makes the modem ideal for FDMA satellite communication systems. On-line fault monitoring including continuous channel error rate measurement provides additional reliability.

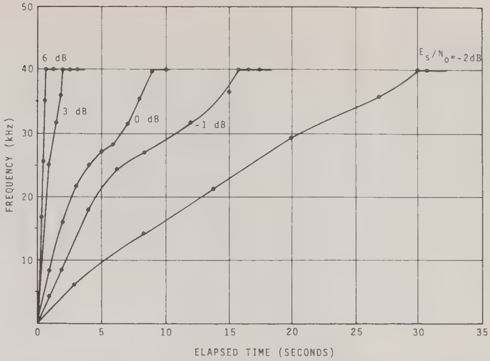

Figure 10. Acquisition Performance of the Modem (QPSK, 2.1 Msps).

Future Applications

The present design of the modem can be upgraded to approximately 10 Mbps data rates with relatively minor modifications. This will require a faster logic family (Schottky TTL instead of low-power Schottky TTL). A 30 Mbps high speed modem is now being developed using similar building blocks to those presented here. The digital processor-based implementation allows this type of modem to be easily modified for switched or burst transmission applications. Such a packet-switched modem is now being developed on an on-going project.

References

[1] Viterbi, A. J., Principles of Coherent Communication, McGraw-Hill Book Company, New York, 1966.

[2] Wozencraft, J. M., and Jacobs, I. M., Principles of Communication Engineering, John Wiley & Sons, Inc., New York, 1965.

[3] Paik, W. H., Gurantz, I., and Weaver, L., Carrier Tracking Loop with Digital Phase-Frequency Detector ... Analysis and Simulation, LINKABIT Tech. Note No. 7.136, LINKABIT Corp., San Diego, California, 1979.

[4] Heegard C., Heller J. A., Viterbi A. J., A Microprocessor-Based PSK Modem for Packet-Transmission Over Satellite Channels, IEEE Transaction on Communications, Vol. Com-26, No. 5, May 1978.

[5] Gilhousen, K. S., A Multi-Stack Microprocessor for Satellite Modems, National Telecommunications Conference Record, December 1974.

[6] Jacobs, I. M., Microcoding for a UHF Satellite Modem, International Conference on Communications Conference Record, June 1975.

80-0595

PREFILTERED QPSK - A BANDWIDTH EFFICIENT MODULATION

M. U. Chang and M. C. Austin
Hughes Aircraft Company
Space & Communications Group
El Segundo, California 90245

Abstract

Prefiltered QPSK is a QPSK-type modulation with sin(x)/x pulse shaping. Performance of this modulation through linear and nonlinear channels is studied. This modulation has a much narrower spectral main lobe than other QPSK type modulations and has little or no side lobes. The results are compared with QPSK, staggered QPSK (SQPSK), and MSK. Performance measurements of a laboratory modem breadboard were used to verify the results from computer simulation.

The major results of this paper indicate that under severe band limited nonlinear conditions, prefiltered QPSK outperforms QPSK, SQPSK, and MSK. The effect of phase equalization of the channel filter is also investigated. Phase equalization produces drastic improvement over non-equalized filtering when the channel bandwidth is fully utilized.

Introduction

Due to the increasing demands on satellite communications, more and more emphasis has been placed on bandwidth efficient modulation techniques. It is desirable to study the performance of these modulations under various channel conditions; i.e. bandwidth limitation, noise, modulation/demodulation distortion, nonlinearity, etc. The system under consideration can be depicted by Figure 1. Two independent data sequences are fed into two identical pulse shaping networks. For QPSK the pulse shapes are rectangular. With delay $\tau = T/2$ (T = symbol duration) on one of the data sequences, SQPSK results. If the shaping is half-cycle cosine and $\tau = T/2$, the modulation takes the form of MSK. For prefiltered QPSK, data sequences are shaped by truncated sin(x)/x waveforms. This modulation will be discussed in detail in Section II.

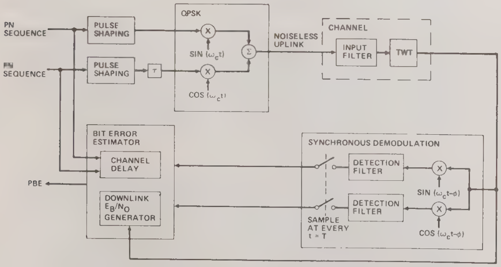

FIGURE 1. GENERAL PULSE SHAPING MODULATION BLOCK DIAGRAM

The channel used in this investigation consists of a channel filter and a TWT nonlinearity. The two channel filters used were a 7-pole Chebyshev design with a bandwidth of 56 MHz and a 56 MHz self-equalized filter. The 56 MHz self-equalized filter was constructed having an amplitude response similar to the unequalized filter but with much less group delay variations (see Figure 2). The nonlinear element in the channel is a space qualified Hughes Ku band TWT. It has a bandwidth much wider than the signal bandwidth.

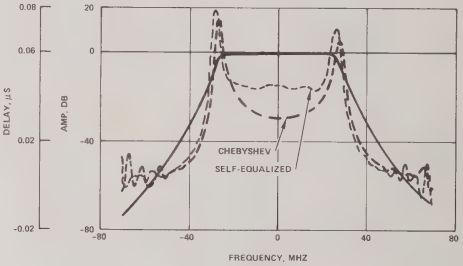

FIGURE 2. CHANNEL FILTER AMPLITUDE AND GROUP DELAY RESPONSES

Both hardware experiments and computer simulations were employed in evaluating the system. A high quality, flexible 80 Mbps laboratory modem capable of operating with a 1.5 GHz carrier was developed [1]. The 80 Mbps rate was selected because it is both low enough to allow accurate distortion measurements/modeling and high enough to evaluate performance at low error rates. To ensure modulation format differences are not masked by hardware implementation, extensive effort was given to the construction of nearly ideal performing transmitters and receivers.

For the computer simulation, a sample data simulation language structure called SYSTID [2,3] was used. SYSTID allows the user to describe the signal flow in a topological block diagram form, and generates specific FORTRAN programs for subsequent linkage to the model library and execution of the simulation. The SYSTID model library contains a large number of models commonly found in communication system. SYSTID allows the user to specify input sequences, modulator type, modulator imperfections, filter types and parameters, nonlinearities, noise sources, demodulator implementa-

Copyright © American Institute of Aeronautics and
Astronautics, Inc., 1980. All rights reserved.

tion and imperfections. System calibration models such as noise bandwidth, group delay, power measurements, and others that expand the direct applicability and flexibility of the software system as a whole are included in the SYSTID model library. Nonlinear transfer characteristics are modeled by their AM/PM and AM/AM characteristics. The channel filter transfer function are obtained from point-by point automatic network analyzer measurements of the actual filter.

Outstanding agreement between breadboard meausrements and computer simulations have been achieved [1]. As an example, Figure 3 shows the bit error rate comparisons of measured and simulated performances for MSK. Note the improvement between the 56 MHz nonequalized and self-equalized channel filters. In the remainder of this paper, the simulated performance of prefiltered QPSK is presented. The results are compared with those of QPSK, SQPSK, and MSK.

Prefiltered QPSK

From Fourier transform theory, an ideal low-pass filter (LPF) with cut off frequency at ω radians/sec has an impulse response of $\sin(\omega t)/\omega t$. The nulls occur at $\omega t = \pm n\pi$, $n = 1,2,3,\ldots$, or at $t = \pm n/2f$. The term 2f, called Nyquist rate, represents the ideal signaling rate at which impulses can be transmitted through this LPF without any intersymbol interference (ISI) if the output of the LPF is sampled exactly at $t = \pm n/2f$. Equivalently, if $\sin(\omega t)/\omega t$ shaped pulses (called Nyquist pulses) are transmitted at a rate of 2f, the signal spectrum is rectangular with width ω (i.e., $-\omega/2$ to $\omega/2$) and no ISI results if the waveform is sampled at $t = \pm n/2f$. This modulation achieves bandwidth efficiency of 2 bit/sec/Hz. Since the $\sin(x)/x$ waveform is nonrealizable, the term "prefiltered" thus involves pulse shaping to a finite approximation of $\sin(x)/x$ to achieve a nearly rectangular signal spectrum.

The two PN sequences referred to in Figure 1 are rectangular pulses of duration T and take on values of ± 1. The pulse shaping network is implemented analytically via discrete linear convolutions of discrete-time impulse trains and time truncated samples of the Nyquist pulse contained in the finite length shift register. This pulse shaping network then produces samples of truncated $\sin(\pi t/T)/(\pi t/T)$ for each +1 or -1 pulse. Figure 4(a) shows the pulses generated for +1, +1, and -1 data pulses. Figure 4(b) shows the composite waveform. In addition to the truncation, an extra weighting of sinusoidal roll-off is imposed. The so called cosine-roll-off is given by

$$\frac{\sin(\omega t)}{\omega t}\;\frac{\cos(\psi t)}{1-(2\psi t/\pi)^2}$$

where $\omega = \pi/T$ and $\psi/\omega \cdot 100\%$ is the cosine-roll-off percentage [4]. This type of roll-off has the advantages that it retains all the

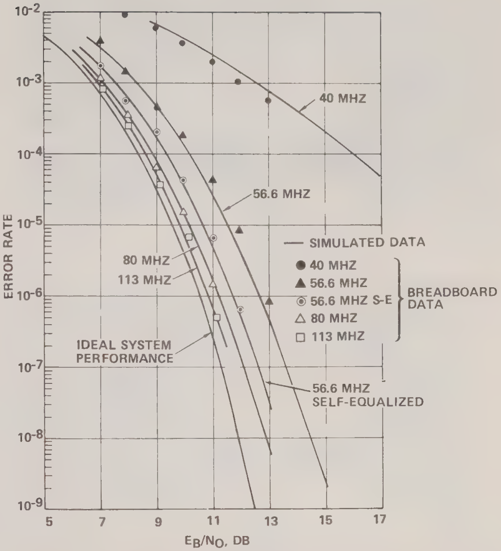

FIGURE 3. MEASURED AND SIMULATED BER PERFORMANCE FOR MSK AND TWO-POLE BUTTERWORTH DETECTION FILTER (BW = 21.5 MHZ)

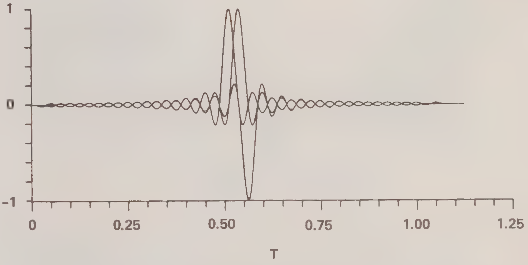

a) ISOLATED PULSES

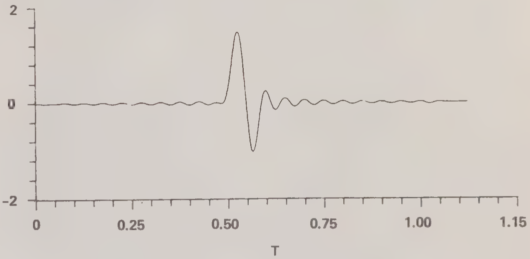

b) COMPOSITE WAVEFORM

FIGURE 4. OVERLAPPING SIN (X)/X PULSES

spectral nulls (additional nulls may be added), has distortionless peak amplitude points and half amplitude points, and it suppresses the oscillatory tails of the original sin(x)/x waveform at the expense of a wider spectrum. It should be apparent that ISI due to sampling time error (i.e, sampling at $t = n/2f \pm \zeta$) is reduced. As a matter of fact, if the pulses are not truncated, the overlapping tails of sin(x)/x form a divergent series. The series converges, however, with the sinusoidal roll-off. Figure 5(a),(b), (c) show the effect of various roll-off percentages.

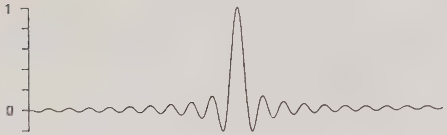

a) 0% ROLL-OFF

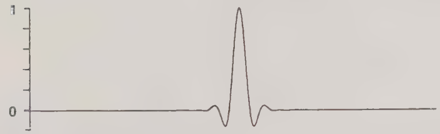

b) 40% ROLL-OFF

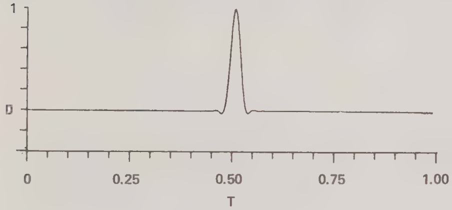

c) 100% ROLL-OFF

FIGURE 5. ROLL-OFF EFFECT

A regular QPSK modulator with amplitude and phase imbalance is used in the simulation to modulate the prefiltered waveforms. The output of the channel is synchronously demodulated and filtered. An analytical bit error estimator calculates probability of bit error by generating noise variances of appropriate E_b/N_o and averaging inverse error functions over entire input sequences. Several types of detection filters were used in the study, including non-realizable brickwall filters (ideal low pass filters) and third order Butterworth filters. Without ISI and without channel distortion, the brickwall filter with bandwidth (baseband) -bit time product (BT) of 0.5 is the optimum filter for the original $\sin(\pi t/T)/(\pi t/T)$ Nyquist pulses. However, for practical cases the brickwall filter is not optimum due to the truncations, sinusoidal roll-off, modulator imperfections, nonlinearity of the channel, and bandwidth limiting. By varying the detection filter bandwidth, the optimum value of BT has been found for each detection filter type and for each of the data rates investigated.

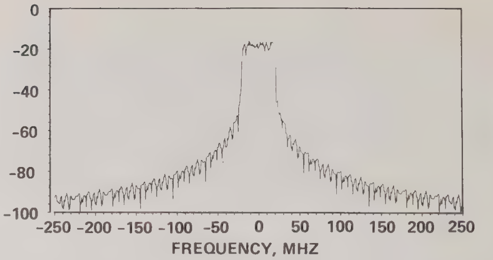

a) 0% ROLL-OFF

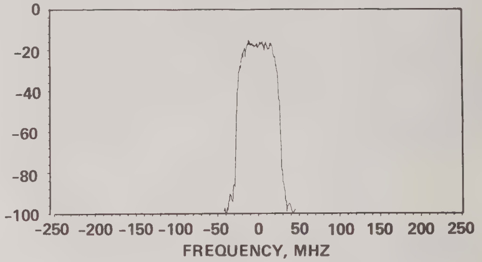

b) 40% ROLL-OFF

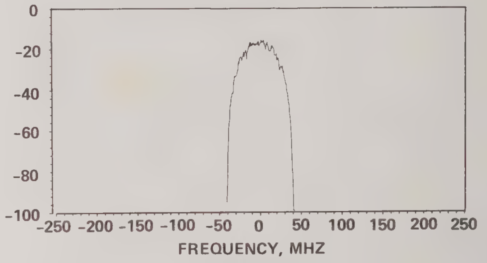

c) 100% ROLL-OFF

FIGURE 6. POWER SPECTRA OF MODULATOR OUTPUT

Discussion of Results

Several simulation runs were performed to determine the proper truncation lengths and the optimum roll-off factor. It is obvious from Figure 5 that with roll-off, a truncation length of ±4T is sufficient. It turns out that even with zero percent roll-off, ±4T does not degrade the bit error rate performance significantly when compared with a truncation length of ±10T. Figure 6 shows the power spectra of modulated signal with zero percent, forty percent and one hundred percent roll-off. Note that the main lobe widens from half to the full width of the main lobe of a QPSK spectrum with the same data rate (bit rate is 80 Mbps) as the roll-off factor increases. However, the side lobes of the spectrum are reduced with larger roll-off percentages. Later results will show that some amount of roll-off is a must to achieve better overall performance. For the remainder of the paper, forty percent roll-off and a truncation length of ±10T are used unless specified otherwise. Figure 7 shows the signal phasor diagrams as the modulated signal passes through the filter and the TWT. Since the filter bandwidth (56 MHz) is approximately the same as the signal bandwidth (see Figure 6b), little filtering effect can be seen. The channel TWT is driven to saturation. The amplitude limiting effect of the TWT is clear. Figure 8 and 9 show the respective eye patterns and power spectra. The estimated TWT output spectrum gives some measure of side lobe regeneration.

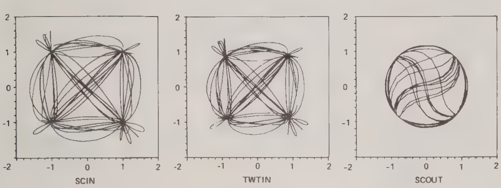

a) MODULATED SIGNAL b) AFTER FILTER c) AFTER TWT

FIGURE 7. SIGNAL PHASOR DIAGRAMS

Figure 10 shows the performance of prefiltered QPSK as a function of increasing data rate for both brickwall and third order Butterworth detection filters. Performance degradation is referenced to ideal QPSK for a bit error rate of 10^{-5}. Again, the bandwidths of the detection filters are optimized for each of the data rates. It becomes clear that the Butterworth filters are better "matched" filters than the brickwall filters when the nonlinear TWT is present. Also the self-equalized channel filter improves the performance when the data rate approaches the channel bandwidth. The performance of prefiltered staggered QPSK, using Butterworth detection filters, is summarized in Figure 11. Nyquist pulse shaping results in a highly nonconstant envelope modulation for both staggered and non-staggered cases. Although the envelope of the staggered case does not have sharp nulls as does the non-staggered case, it has larger amplitude fluctuations. This is suspected to be the major contributor to the excessive degradations when the channel is nonlinear. To reconfirm the earlier conclusions on the roll-off and truncation effects, Figure 12 shows the degradation curves with various roll-off factors and truncation lengths. As one would expect, since a larger amount of roll-off results in a wider signal bandwidth, the degradation increases faster as the data rate approaches the channel bandwidth. In addition, Figure 12 also shows that some amount of roll-off is essential. The performance comparisons of Nyquist pulse shaping with QPSK, SQPSK, and MSK are shown in Figure 13 and 14 for the equalized and nonequalized channel filters. These figures indicate that prefiltered QPSK performs better than the others under severe band limited conditions. The detection filters used for QPSK, SQPSK, and MSK are second order Butterworth filters with optimum BT products. Past results indicate that this simple second order Butterworth yields excellent performance.

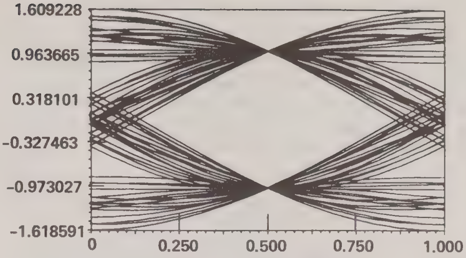

a) MODULATED SIGNAL

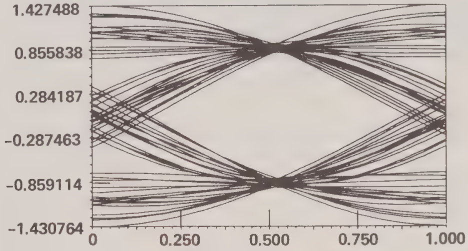

b) AFTER FILTER

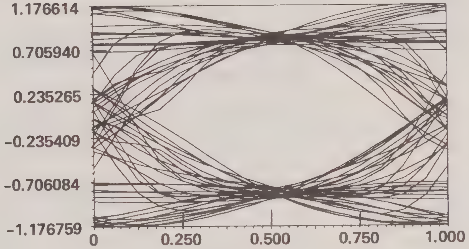

c) AFTER TWT

FIGURE 8. EYEPATTERNS

Conclusions

Although the Nyquist pulse shaping does not achieve 2 bit/sec/Hz as the theory predicts, its performance warrants serious consideration as a viable modulation scheme. With some amount of roll-off, its signal energy is concentrated in a main lobe that is narrower than any of the QPSK type modulations. This narrow-spectrum/low-side-lobe modulation has potential application in FDMA multi-carrier per channel situations. Although several types of detection filters other than Butterworth and Brickwall were investigated, an additional effort remains of searching for a better detection filter. In general, modulation formats that produce a constant signal envelope tend to be compatible with high efficiency power amplifiers (e.g., TWTs driven into saturation).

An important observation is that for all the constant envelope modulation formats (e.g., QPSK, SQPSK, or MSK), the signal envelope is no longer constant when it reaches the saturating amplifiers because of the bandlimiting by the channel filter. Prefiltered QPSK is an example of a non-constant envelope modulation that shows very promising performance in a bandlimited nonlinear channel.

One question that has not been addressed here is the carrier recovery problem. Synchronous demodulation was assumed in all the computer simulations; although static detection phase error of 3 degrees was incorporated in all the results. Further investigation in the general area of detection techniques, including the various detection filter types and carrier recovery, are planned.

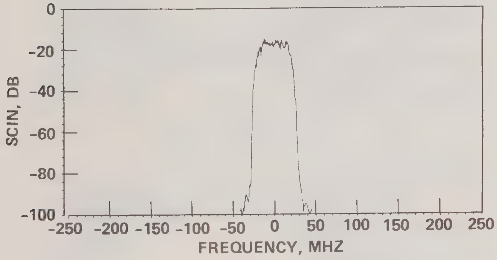

a) MODULATED SIGNAL

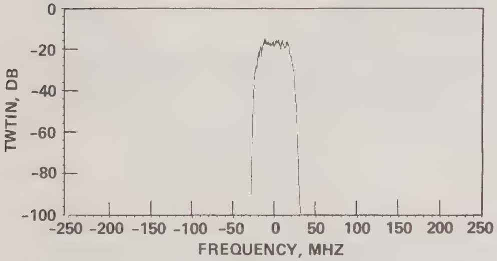

b) AFTER FILTER

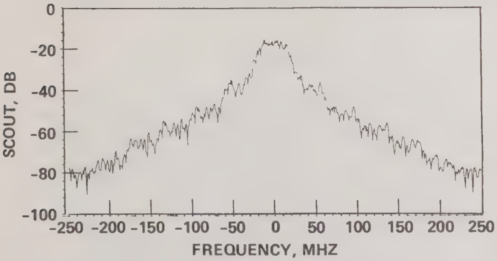

c) AFTER TWT

FIGURE 9. POWER SPECTRA ALONG SIGNAL PATH

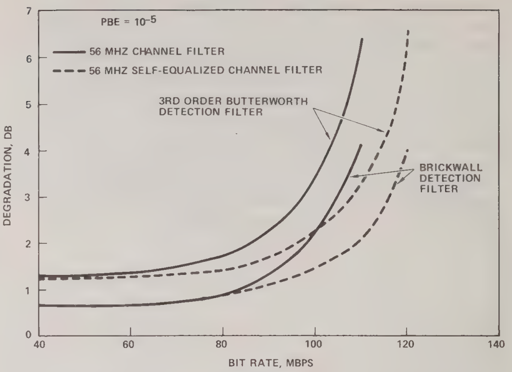

a) LINEAR CHANNEL

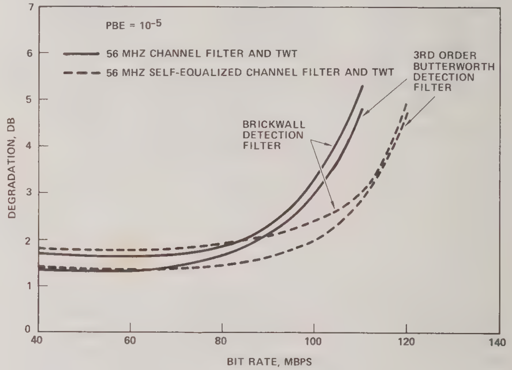

b) NONLINEAR CHANNEL

FIGURE 10. COMPARISON OF DETECTION FILTERS AND CHANNEL EQUALIZATION FOR PREFILTERED QPSK

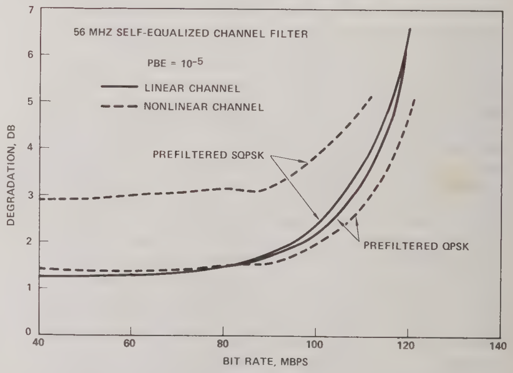

FIGURE 11. COMPARISON OF PREFILTERED QPSK AND PREFILTERED SQPSK PERFORMANCE

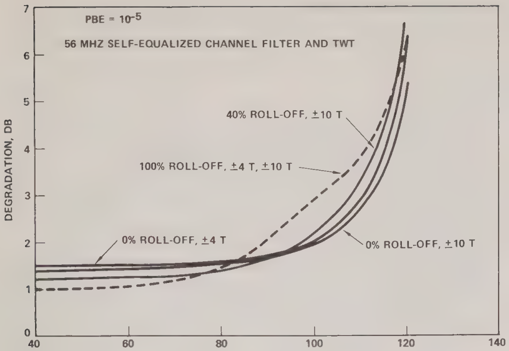

a) LINEAR CHANNEL

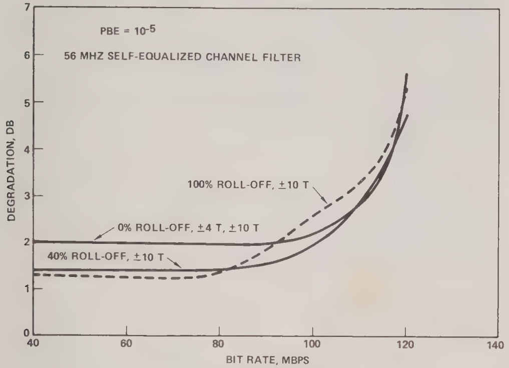

b) NONLINEAR CHANNEL

FIGURE 12. ROLL-OFF AND TRANCATION EFFECTS ON PREFILTER QPSK PERFORMANCE

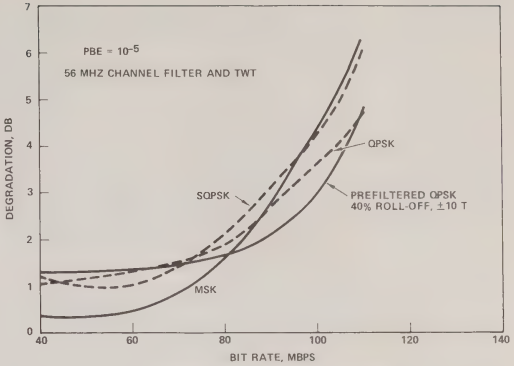

a) CHANNEL WITHOUT PHASE EQUALIZATION

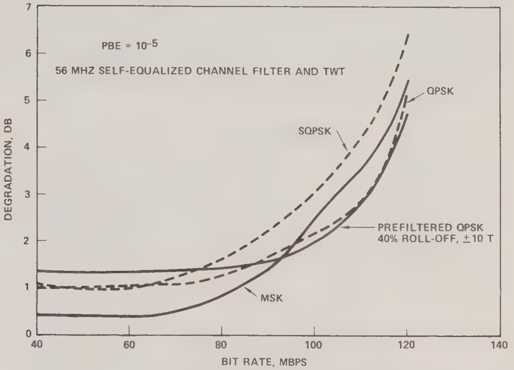

b) CHANNEL WITH PHASE EQUALIZATION

FIGURE 13. E_B/N_O DEGRADATIONS OF QPSK, SQPSK, MSK AND PREFILTERED QPSK FOR BAND LIMITED NONLINEAR CHANNEL

References

[1] Horwood, D. F., Austin, M. C., and Angello, P. S., "Comparative Evaluation of MSK and QPSK in Band and Amplitude Limited Channel," Proc. 1978 International Telemetry Conference, pp. 531-544, Nov. 1978.

[2] Fashano, M., and Austin, M. C., "A Flexible User Oriented Approach to Communications Systems Simulation," Proc. International Telemetry Conference, Vol. 14, pp. 629-638, Nov. 1978.

[3] Tranter, W. H., Zeimer, R. E., and Fashano, M., "Performance Evaluation Using SYSTID Time Domain Simulation," International Conference on Communication, Paper 20a, June 1975.

[4] Bennett, W. R., and Davey, J. R., Data Transmission, McGraw-Hill, 1965.

[5] Chethik, F., "Bandwidth Efficient Modulation and Detection," Canadian Conference on Satellite and Power Systems," pp. 147 -150, Montreal, 1976.

[6] Murakami, S., Furuya, Y., Matsuo, Y., and Sugiyama, M., "Modulation Scheme Comparative Study for Nonlinear Satellite Channels," International Conference on Communication, pp. 19.2.1-19.2.5, June 1978.

80-0596

DIGITAL CHIRP MODULATION: OPPORTUNITIES FOR LOWER COST AND HIGHER PERFORMANCE IN MOBILE-SATELLITE COMMUNICATION

P. K. Lee, J. M. Ruddy, B. E. White
The MITRE Corporation
Bedford, MA 01730

Abstract

Linear frequency (chirp) modulations implemented with surface acoustic wave (SAW) devices are suggested to provide improved digital satellite communications for mobile terminals. Technical characteristics of digital chirp such as cross-correlation coefficient and bit error rate (BER) performance in additive white Gaussian noise (AWGN) are discussed. Digital chirp with large time-bandwidth product has coherent performance nearly equivalent to orthogonal signals. Several technological opportunities for digital chirp are surveyed including variable data rates, frequency hopping hybrids, and lower power flux densities. Design constraints, technical performance enhancements, and potential cost reductions for two categories of mobile-satellite communications terminals are identified.

Introduction

Communications satellites offer the unique capability to provide timely and reliable connectivity between any two points on the globe. This is invaluable for long range mobile communications and indispensable for modern military communications, command and control.

Communication among widely dispersed mobile terminals at super high frequencies (SHF) and above is likely to be limited by the satellite downlink power. Other pertinent factors include excessive path loss and a small G_r/T_e ratio of antenna gain to receiver noise temperature. It is possible to alleviate this problem by increasing the satellite effective isotropic radiated power (EIRP) by means of narrow beam, high gain satellite antennas and larger transmitters. This may not be permissible if the maximum power flux densities (PDFs) imposed by the International Telecommunications Union (ITU) are exceeded. Fortunately, practical modulation schemes with the same power but substantial bandwidth expansion can be used to stay within the ITU regulations.

Digital linear frequency modulation, long employed for radar signaling, is one such scheme. Chirp also has outstanding protection against Doppler frequency shift(1), multipath fading(2), impulsive noise, and wideband AWGN. Chirp can easily be implemented by surface acoustic wave (SAW) devices, allow variable data rates without feedback, and combine with frequency hopping (FH) to achieve signal processing gains unattainable by pure spread spectrum techniques. Some of these advantages also accrue to other attractive modulation schemes such as continuous phase FSK(3,4).

Systematic information needed to characterize chirp modulation is summarized in the next section. The penultimate section presents two system applications and the last section contains conclusions.

Digital Chirp Modulation

Linear frequency modulation (FM) or chirp modulation is a well known spread spectrum technique(5). Unlike other modulations, such as pseudonoise (PN) and FH, which have been widely accepted for digital communications systems(6), chirp has been almost exclusively employed by peak-power limited radars to extend range and improve resolution. This paper advocates more serious consideration of chirp for digital communications.

Though PN modulation exhibits performance comparable with digital chirp in several areas, chirp may be preferable for mobile-satellite communications. This is due primarily to excellent immunity to impulsive noise, Doppler frequency shift, and short channel interruptions(7). Ease of implementation and rapid signal synchronization may be attributes shared by chirp and PN realized by SAW devices(8-10).

This section summarizes a literature review of digital chirp. Topics are presented in the following order: signal characteristics, performance in AWGN, implementation by SAW devices, combined FH and chirp, variable data rates, and multiple access.

Signal Characteristics

An elementary down-chirp modulated signal can be expressed as

$$s(t) = \begin{cases} A\cos(\omega_2 t - mt^2/2), & 0 \leq t \leq T \\ 0, & \text{elsewhere} \end{cases} \qquad (1)$$

where $mT \leq \omega_2$, and

A = signal amplitude
ω_2 = angular carrier frequency (rad/sec)
T = duration of the chirp signal (sec)
m = rate of radian frequency sweep (rad/sec^2)
mT = swept spectrum (chirp) bandwidth (rad/sec)
mT^2 = time-bandwidth product or processing gain (rad).

For optimum detection of the signal, a matched filter with the impulse response

$$h(t) = K\cos(\omega_2(t-T) + m(t-T)^2/2), \quad 0 \leq t \leq T \qquad (2)$$

can be used. By requiring a matched-filter output of unity at t=T, one obtains $K=2/(AT)$ and an ideal matched-filter output

$$g(t) = \frac{\sin m(T-t)t/2}{m(T-t)T/2}\cos\omega_2(T-t), \qquad (3)$$
$$0 \leq t \leq 2T.$$

In practice, the received signal may be distorted by frequency or time shift. If the amount of Doppler shift ω_d is a small percentage of signal bandwidth and if the time shift τ is small compared to signal duration, as is true for most applications, there is very little deterioration in

Copyright © American Institute of Aeronautics and Astronautics, Inc., 1980. All rights reserved.

the shape and peak amplitude of the matched-filter output. Fig. 1 shows decline and relative time shift of the peak amplitude as a function of $|\omega_d|/mT$.

Performance in AWGN

The BER performance of a digital communication system in AWGN is not dependent on the fine structure of the elementary signal waveforms but on the receiver structure (e.g., coherent vs. noncoherent) and the signal-space distance between the waveforms. This distance is proportional to $\sqrt{1-\rho}$, where ρ is the cross-correlation coefficient of the two signals. In AWGN a binary coherent receiver typically performs about 1 dB better than a noncoherent receiver, and antipodal signals ($\rho = -1$) as in binary phase shift keying (PSK) perform 3 dB better than orthogonal signals ($\rho = 0$) as in binary frequency shift keying (FSK). However, in trading link performance for less equipment complexity and reduced synchronization (timing and frequency accuracy) requirements, a noncoherent receiver and orthogonal signals are commonly proposed for mobile-satellite links.

It has been shown that binary chirp can be superior to PSK and FSK in partially coherent and fading channels(12). This is only partially due to the negative values of $\rho \geq -0.6$ possible for binary chirp signals since $\rho = -1$ for binary PSK. Evidently, the frequency diversity nature of chirp is advantageous in real time-dispersive channels.

As shown in the Appendix, binary chirp yields

$$\rho \approx \frac{1}{G}\left(\cos(\tfrac{\pi}{2}P^2)\int_P^{G+P}\cos(\tfrac{\pi}{2}u^2)\,du + \sin(\tfrac{\pi}{2}P^2)\int_P^{G+P}\sin(\tfrac{\pi}{2}u^2)\,du\right) \qquad (4)$$

where

$$P = (\omega_1 - \omega_2)/\sqrt{2\pi m} \qquad (5a)$$

$$G = \sqrt{2m/\pi}\ T \qquad (5b)$$

and where ω_1 and ω_2 are the initial chirp frequencies, m is the magnitude of the slope of an elementary chirp in rad/sec^2, and T is the duration. Note that P in (5a) can be either positive or negative. Practically, a negative P is preferred for conserving the system bandwidth as fig. 2 shows using (A-2).

Expression (4) was computed for $-10 \leq P \leq 10$, and $0.5 \leq G \leq 10$ and displayed in three dimensions as in fig. 3 for $P \geq 0$. It is found that $|\rho|$ is bounded by 0.15 for chirp signals with $|P|\,G$ larger than 16. Based on these graphical results and the Appendix, ρ is essentially zero for large time-bandwidth signals. Hence, wideband binary chirp has nearly the same BER as binary FSK in AWGN.

Implementation by SAW Devices

Since chirp and other modulations can be implemented by SAW devices of potentially low cost, a brief description of these electro-acoustic devices is appropriate.

Practical SAW devices include delay lines, filters, convolvers, correlators, etc. They are typically constructed of thin sheets of crystalline piezoelectric material. An acoustic wave excited by signals applied to metal electrodes deposited on the top surface propagates along that surface accompanied by electric fields extending into the crystal. This provides access to the wave along its entire propagation path. Present technology permits surface waves to be excited in a frequency range of approximately 10 MHz to 1.5 GHz. The propagation speed is in the order of 3000 m/sec which provides delays of up to about 100 μsec with crystals no more than about one foot long. This implies a 10 kbps lower bound on baud rate.

Fig. 4 shows a pair of surface wave transducers configured to form a chirp filter. The input transducer has several constant overlap and periodic electrodes, but apodization (varying electrode overlap) is employed to control the tap amplitude weights in the chirped (non-periodic) output transducer. Reducing the overlap decreases the tap amplitude in two ways. First, the electrodes sample a smaller fraction of the incident acoustic beam, and second, reducing the overlap reduces the tap efficiency.

More advanced electro-acoustic devices are under various stages of development at the MIT Lincoln Laboratory, as reported in an excellent paper by Cafarella(14). These devices include a memory correlator which can serve as a programmable, asynchronous matched filter or as an analog signal memory. An integrating correlator capable of more than 50 dB of processing gain and integration times up to 10 msec is also in the offing.

Combined Frequency Hopping and Chirp

State-of-the-art SAW devices designed for chirp modulation possess a maximum processing gain of about 50 dB(15-17). In some military applications, higher processing gain may be required(18,19). A hybrid FH and chirp modulation scheme could meet that requirement as well as increasing Doppler shift resistance, decreasing cochannel interference, and simplifying implementation by relaxing specifications on synthesizers and filters, etc. An analysis of the component and total processing gains for the hybrid scheme follows.

Combinations of channel symbol interleaving and error correction coding techniques make tone jamming look essentially like wideband noise at a FH communications receiver. Thus, without losing much generality, it is assumed that the channel interference is AWGN.

Let $B \geq W_c$ in Hz, denote the instantaneous channel bandwidth plus guard band occupied by a chirp signal and its FH carrier. If the total hopping bandwidth is $W \gg B$, there are approximately W/B channels available. Let the chirp signal and detection bandwidths be, respectively, $W_c = mT/2\pi$ and $R = 1/T$, in Hz, where m is the chirp rate in rad/sec^2 and T is the chirp duration. Then the following signal processing gains are obtained:

$$G_h \approx W/B = \text{number of hopping channels} \qquad (6a)$$

$$G_c = W_c/R = mT^2/2\pi = \text{chirp time-bandwidth product.} \qquad (6b)$$

The total processing gain of the combined scheme is thus

$$G_p = G_h G_c \approx (TW)(W_c/B). \tag{6c}$$

This gain is reduced from the overall time-bandwidth product, TW, by the guard band inefficiency, represented by the factor B/W_c but, otherwise, is theoretically equal to that of pure FH or pure chirp for the same total bandwidth W and elementary signal duration T.

Variable Data Rates

A variable data rate capability is desirable in a communications system which may encounter time varying channel disturbances caused by man-made or natural sources. Conventional approaches to variable data rate adaptability require a large buffer and a reliable feedback link(20) in contrast to the approach described below.

Moule, Newton and Paige(21,22) have demonstrated a variable slope chirp scheme with two dispersive filters having a cubic variation of phase with frequency, as configured in fig. 5. The overall frequency-time slope can be maintained linear within a fixed bandwidth, but varied over a range of time-bandwidth products from 0 to 100 (1000 forecasted) simply by changing an external local oscillator frequency. This inherent capability permits a receiver to automatically acquire and track a changing channel data rate.

Multiple Access

Chirp, like most other modulation schemes, can be employed in a frequency, time, or code division multiple-access mode for sharing a satellite transponder or processor, for example. Since digital chirp with a large time-bandwidth product occupies a much wider bandwidth than needed for transmitting information at a certain rate, spectrum utilization may be poor if one of these multiple-access techniques is employed. Fortunately, additional chirp users can be accommodated within the same time-frequency region by varying the FM slopes.

Cook(1) derived a general expression relating the number of useful signals N, a crosstalk measure X^2, and the time-bandwidth products T_iW_i of the signal sets. Only results relevant to an asynchronous communications mode are presented. If both positive and negative FM slopes are employed in a set of chirp signals equally spaced in time-bandwidth product (with spacing $1/X^2$), Cook showed that the number of usable signals is

$$N = 2X^2((TW)_{max} - (TW)_{min}) + 2 \tag{7}$$

where

$(TW)_{max} = \max_i T_iW_i$

$(TW)_{min} = \min_i T_iW_i$

X^2 = peak power response of a matched filter to a chirp signal of adjacent FM slope of the same sign.

More precisely, X is defined as

$$X = 1/\sqrt{|m_j/m_i - 1|\, T_iW_i} \tag{8a}$$

where

$$m_i = 2\pi W_i/T_i \tag{8b}$$

is the FM slope of the ith chirp signal of time-bandwidth product T_iW_i, and where m_j is the FM slope of the same sign from an adjacent chirp closest in time bandwidth product to T_iW_i. As an example, if the maximum crosstalk level is -20 dB, i.e., if $X^2 = 0.01$, there will be N = 32 usable signals with $TW_{max} = 2000$ and $TW_{min} = 500$, from (7).

System Applications

The feasibility of applying chirp to SHF and VHF/UHF mobile-satellite communications is discussed in this section. Special attention is given to military aircraft applications.

SHF Satellite Communications to Airborne Terminals

The design of airborne satellite terminals is severely constrained by limitations on cost, weight, aircraft space, and aerodynamic effects. In particular, an airborne antenna must be physically small. It is desirable to employ antennas which can be flush-mounted to minimize air drag and that do not require an expensive pointing and tracking subsystem. Unfortunately, this generally implies a lower antenna gain which means that the ratio of receiving antenna gain to effective receiver noise temperature, G_r/T_e, is bound to be smaller than that achievable with a ground terminal.

The capacity of a downlink depends on satellite EIRP and terminal G_r/T_e according to the relation

$$R(E_b/N_o) \leq P_r/N_o = (EIRP)\ (G_r/T_e)/kL \tag{9}$$

where

R = data rate (bps)
E_b/N_o = receiver output signal-to-noise ratio
P_r = received power (W)
N_o = single-sided noise power spectral density (j)
G_r = receiver antenna gain
T_e = effective receiver noise temperature (°K)
k = Boltzmann's constant, 1.38×10^{-23} j/°K
L = total link loss factor.

If G_r/T_e is reduced, the EIRP must be increased to provide the same communications performance. Unfortunately, high EIRP may cause interference to other terrestrial systems sharing the same band. To mitigate such interference, the ITU has specified limits on power flux density (PFD) at the earth's surface. If the downlink bandwidth is fixed, this implies a minimum G_r/T_e to support communications of an acceptable quality.

The PFD Φ, usually expressed in dBW/m^2, at the earth's surface over a fixed specified bandwidth B_o is given by

$$\Phi = \left(\int_{B_o} E_s(f)\, df\right)/4\pi r^2 \tag{10a}$$

where $E_s(f)$ is the transmitted signal energy or power spectral density at frequency f, and r is a given satellite-terminal range; EIRP in the signal bandwidth B_s can be expressed as

$$\text{EIRP} = \int_{B_s} E_s(f)\, df. \tag{10b}$$

For a given EIRP and B_s, suppose Φ would exceed a specified PFD limit Φ_{max} by a factor $\beta = \Phi/\Phi_{max} > 1$. Then this PFD limit can be met by distributing the same EIRP over a wider signal bandwidth $B_s' > \max\{B_s, B_o\}$ using a spread spectrum modulation scheme, i.e., from (10)

$$\begin{aligned} 4\pi r^2 \Phi &= 4\pi r^2 \beta \Phi_{max} = \beta \int_{B_o} E_s'(f)\, df, \quad \beta \geq 1 \\ &= \int_{B_s'} E_s'(f)\, df = \text{EIRP}, \end{aligned} \tag{11a}$$

$$B_s' \geq \max\{B_s, B_o\}.$$

If the PFD limit is not exceeded for a given EIRP and B_s, then from (10)

$$\text{EIRP} = \alpha 4\pi r^2 \Phi \tag{11b}$$

where $\alpha \geq 1$ for $B_s \geq B_o$ and $\alpha \approx 1$ for $B_s < B_o$.

Relation (9) will now be rewritten in terms of Φ to highlight the minimum G_r/T_e required to support a data rate R at a given E_b/N_o. The loss factor L can be expressed as

$$L = (4\pi r/\lambda)^2\, L_r L_t \tag{12}$$

where

λ = wavelength (m)
L_r = rain attenuation loss factor
L_t = tilt differential loss factor (due to off-boresite terminal/satellite pointing angles).

Substitution of (11) and (12) into (9) yields

$$G_r/T_e \geq R(E_b/N_o) L_r L_t\ 4\pi k f^2/(c^2 \alpha \Phi) \tag{13}$$

where $c = \lambda f \approx 3 \times 10^8$ m/sec.

Limits of PFD specified by ITU for frequency bands in the SHF range are shown in table 1(23). These limits were established at the World Administrative Radio Conference for Space Telecommunications (WARC-ST) in 1971. Since there has been controversy regarding whether the PFD limits are too conservative, they were subject to revision at the 1979 WARC. Available information on any revisions will be included in the oral presentation of this paper. For the purposes of the following example, however, the 1971 WARC limits will be employed to ascertain the minimum G_r/T_e required for an airborne terminal.

For these calculations it is assumed that $R = 4$ kbps, $E_b/N_o = 12$ dB, $L_t = 3$ dB and $\alpha = 1$ in (13). Four generic center frequencies 4, 7.5, 11, and 18.7 GHz are selected along with appropriate rain margins to permit airborne terminals to be operated on the ground. The ITU PFD limits, defined along the main beam axis of a satellite antenna, for satellite look angles or terminal elevation angles of 5° or less are employed from table 1 to find the worst-case minimum G_r/T_e required. Then the implied terminal antenna diameter D is computed assuming $T_e = 360$°K and a 50% aperture efficiency, i.e., $G_r = 4\pi A_e/\lambda^2 = (\pi D/\lambda)^2/2$, where A_e is the effective antenna aperture. Results are summarized in table 2.

A given downlink has margin, even with less than a 5° elevation angle, if the corresponding terminal G_r/T_e exceeds the minimum value shown in table 2, e.g., 18.4 dB/°K for f = 7.5 GHz. The G_r/T_e for existing military airborne terminals in this downlink band is only about 7 dB/°K. Hence, performance would be inadequate, even at elevation angles exceeding 25° where Φ_{max} is 10 dB larger, if conventional narrowband modulation were employed instead of the actual PN spread spectrum scheme. As already pointed out, smaller terminals could be used with additional bandspreading while satisfying the PFD limits.

VHF/UHF Extender

The performance of military mobile-satellite communications in the VHF/UHF bands could be enhanced by extending the bandspread signaling concept beyond the presently contemplated spectral allocations(24). Desirable signal design attributes of this extension would be minimum crosstalk interference to users sharing the same spectrum, maximum anti-jam (AJ) protection, and variable data rate. As mentioned previously, digital chirp is a potential candidate for providing these capabilities.

One or more new antennas and additional RF hardware, waveform generators, frequency synthesizers, and digital control circuitry may be required to cover the extended band. Since VHF/UHF frequency bands are allocated to mobile radio, television, etc., mobile-satellite terminals might radiate in the extended band only in stressed modes. Experiments to determine the feasibility of such operation on a non-interfering basis would be worthwhile.

New antennas for an airborne UHF extender might be mounted on top of the aircraft fuselage to provide upper hemispherical coverage and to permit extra protection both from and to ground systems. Tests for UHF (225-400 MHz) city noise showed that top-mounted antennas are well protected against interfering signals from the ground at altitudes of at least 5000 feet(25). From reciprocity considerations, it could be inferred that when the top-mounted antenna is transmitting at a comparable power, similar protection can be realized for ground users. Nevertheless, interference to ground systems from such an aircraft to satellite uplink will be examined below from a PFD point of view. In contrast to the uplink, a typical satellite to aircraft downlink transmission should not significantly interfere with ground systems because of the path loss difference.

There seems to be no existing comprehensive information on the acceptable PFD levels for extended VHF/UHF bands. Partial reference data in the 1971 ITU recommendation on broadcasting satellite service covering 620 to 790 MHz is given by(23)

$$\Phi_{max}(\text{dBW/m}^2) = \begin{cases} -129, & \theta \leq 20° \\ -129 + 2(\theta-20)/5, & 20° < \theta \leq 60° \\ -113, & 60° < \theta \leq 90° \end{cases} \tag{14}$$

where θ is the satellite look angle. Although not stated explicitly by the ITU, it is assumed that the bandwidth is 4 kHz for this specification, as it usually is at frequencies below 15 GHz.

Now suppose an aircraft flying at about 10 km (32,800 ft) is banking and causing the top-mounted antenna to radiate as much as $\theta = 6°$ below the local horizontal reference surface to a ground location approximately 10 km/tan $6° \approx 95$ km (59 mi) from the sub-aircraft point over a line-of-sight distance $r \approx 10$ km/sin $6° \approx 95.7$ km. If the aircraft radiates 100 W with 3 dB of antenna gain in that direction, then from (11a) and (14),

$$\beta = \mathrm{EIRP}/(4\pi r^2 \Phi_{max}) \approx 23 \text{ dBW} - 110.6 \text{ dB/m}^2 + 129 \text{ dBm}^2/\text{W} \approx 13{,}800.$$

Assuming uniform signal energy densities and an original signal bandwidth of $B_s = B_o = 4$ kHz for simplicity, a bandspread to $B_s' = \beta B_s \approx 55$ MHz with an associated energy density scaling of $E_s'(f) = E_s(f)/\beta = \mathrm{EIRP}/B_s'$ is required to meet the PFD limit.

Summary

Digital chirp modulation has been studied for its potential performance enhancement and cost reduction, especially for airborne-satellite communications.

When realized with SAW devices, chirp and PN modulations can offer comparable advantages in AWGN performance, ease of synchronization, and spread spectrum signaling. Chirp is superior to PN in the presence of Doppler shifts and over fading, time dispersive channels; chirp may also be simpler to implement. In AWGN the performance of chirp signals of opposite slope and large time-bandwidth product is nearly equivalent to orthogonal binary FSK.

New technological opportunities now available through the employment of digital chirp modulation include combined FH and chirp, adaptive variable data rates without feedback, and low crosstalk multiple access schemes. ITU PFD limitations were taken into account as link design constraints, and spread spectrum signaling was advocated to improve the utility of VHF/UHF and SHF military airborne satellite terminals.

References

1. Cook, C.E., "Linear FM Signal Formats for Beacon and Communication Systems," IEEE Trans. Aero. Elect. Syst., July 1974, pp. 471-478.
2. Gott, G.F., and Karia, A.J., "Differential Phase-Shift Keying Applied to Chirp Data Signals," Proc. IEE, Sept. 1974, pp. 923-928.
3. Amoroso, F., and Kivett, J.A., "Simplified MSK Signaling Technique," IEEE Trans. Comm., April 1977, pp. 433-441.
4. Smith, W.R., "SAW Filters for CPSM Spread Spectrum Communication," Proc. Ultrasonic Symposium, 1977, pp. 524-528.
5. Cook, C.E., and Bernfeld, M., Radar Signals, New York: Academic Press, 1967.
6. Dixon, R.C., Spread Spectrum Systems, New York: Wiley, 1976.
7. Holland-Moritz, E.K., Dute, J.C., and Brundage, D.R., "Swept Frequency Modulation," Proc. Nat. Elect. Conf., 1966, pp. 469-474.
8. Grant, P.M., et al., "Fast Synchronization for Spread Spectrum Communications by Correlation in Surface-Acoustic-Wave Devices," Proc. Ultrasonics Intern. Conf., 1975, pp. 146-151.
9. Griffiths, A.S., and Smith, W.H., "FM Chirp Communications: An Easy-Demonstrated Multiple-Access Modulation Form for Dispersive Channels," Intern. Conf. Comm., 1967, p. 32.
10. Unkauf, M.G., "Surface Wave Devices in Spread Spectrum Systems," Surface Wave Filters: Design, Construction, and Use, H. Matthews, ed., New York: Wiley, 1977.
11. Berkowitz, R.S., ed., Modern Radar-Analysis, Evaluation, and System Design, New York: Wiley, 1965.
12. Berni, A.J., and Gregg, W.D., "On the Utility of Chirp Modulation for Digital Signalling," IEEE Trans. Comm., June 1973, pp. 748-751.
13. Gerard, H.M., "Surface Wave Inter-Digital Electrode Chirp Filters," Surface Wave Filters: Design, Construction, and Use, H. Matthews, ed., New York: Wiley, 1977.
14. Cafarella, J.H., "Acoustoelectric Surface Wave Devices for Programmable Signal Processing," 11th Proc. IEEE Intern. Symp. Circuits Systems, 1978.
15. Bristol, T.W., "SAW Devices and Applications - A Status Report," Microwave Journal, Dec. 1977, pp. 16, 19, 20, 22, 30.
16. Ralston, R.W., et al., "A New Signal Processing Device, the Integrating Correlator," Proc. Ultrasonics Symposium, 1977, pp. 623-628.
17. Webb, D.C., "SAW Filters Simplify Signal Sorting," Microwave System News (MSN), Sept. 1978, pp. 75, 77, 78, 81, 83, 84.
18. Haggarty, R.D., Palo, E.A., and Bridge, W.M., "SAW Processors vs. Competing Technologies for Spread Spectrum Data Link Applications," MTP-195, The MITRE Corporation, Bedford, MA 01730, November 1978; also, 1978 IEEE Ultrasonics Symposium, Cherry Hill, NJ, 25 - 27 September 1978, pp. 567-572.
19. White, B.E., Wilson, Q.C., and Kota, S.L., "Satellite Communications System Netting Concepts for Mobile Terminals," Nat. Telecomm. Conf., 1978, pp. 28.2.1-28.2.5.
20. Covers, J.K., and Lee, S.K., "A Simple Buffer Control for Variable - Rate Communication Systems," IEEE Trans. Comm., Sept. 1976, pp. 1045-1048.
21. Moule, G.L., Newton, C.O., and Paige, E.G.S., "Performance of a Surface Acoustic Wave Variable Slope Chirp Filter," Proc. Ultrasonic Symposium, 1977, pp. 611-614.
22. Newton, C.O., and Paige, E.G.S., "Surface Acoustic Wave Dispersive Filter with Variable, Linear, Frequency Time Slope," Proc. Ultrasonic Symposium, 1976, pp. 424-427.
23. Final Acts of the World Administrative Radio Conference for Space Telecommunications, Geneva: International Telecommunication Union, 1971.
24. Private communications, Brandon, W.T., The MITRE Corporation, Bedford, MA 01730.

References (Concluded)

25. Lebow, I.L, Jordan, K.L., and Drouilhet, P.R., "Satellite Communications to Mobile Platforms," Proc. IEEE, 1971, pp. 139-159.

Appendix

Derivation of Cross-Correlation Coefficient

For binary elementary signals $s_1(t)$ and $s_2(t)$ of equal energy E and duration T, the cross-correlation coefficient ρ is defined as

$$\rho = \frac{1}{E}\int_0^T s_1(t)s_2(t)dt \qquad \text{(A-1a)}$$

where

$$E = \int_0^T s_i^2(t)dt,\ i = 1,2. \qquad \text{(A-1b)}$$

For the chirp signal set

$$\left.\begin{aligned} s_1(t) &= \sqrt{\frac{2E}{T}}\ \cos(\omega_1 t + mt^2/2) \\ s_2(t) &= \sqrt{\frac{2E}{T}}\ \cos(\omega_2 t - mt^2/2) \end{aligned}\right\}, \quad 0 \leq t \leq T \qquad \text{(A-2)}$$

and assuming that $\omega_i \gg mT$, $i = 1,2$

$$\begin{aligned} \rho &\approx \frac{1}{T}\int_0^T \cos[(\omega_1 - \omega_2)t + mt^2]dt \\ &= \frac{1}{T}\, R_e\left\{\exp(-jw^2/4m)\int_0^T \exp(j[\sqrt{m}t + w/2\sqrt{m}]^2)dt\right\} \end{aligned} \qquad \text{(A-3a)}$$

where

$$w = \omega_1 - \omega_2. \qquad \text{(A-3b)}$$

With the change of variable

$$\sqrt{m}t + w/2\sqrt{m} = \sqrt{\pi/2}u \qquad \text{(A-4)}$$

and letting

$$P = w/\sqrt{2\pi m} \qquad \text{(A-5a)}$$

$$G = \sqrt{2m/\pi}\ T \qquad \text{(A-5b)}$$

the approximation of (A-3a) becomes

$$\rho \approx \frac{1}{G}\Big[\cos(\tfrac{\pi}{2}P^2)\int_P^{G+P} \cos(\tfrac{\pi}{2}u^2)du + \sin(\tfrac{\pi}{2}P^2)\int_P^{G+P} \sin(\tfrac{\pi}{2}u^2)du\Big]. \qquad \text{(A-6)}$$

Using standard notation for the Fresnel integrals

$$C(x) = \int_0^x \cos(\tfrac{\pi}{2}u^2)du \qquad \text{(A-7a)}$$

$$S(x) = \int_0^x \sin(\tfrac{\pi}{2}u^2)du \qquad \text{(A-7b)}$$

and noting that the integral arguments are even functions of u, and that G is non-negative, (A-6) can be rewritten as

$$\rho \approx \frac{1}{G}\left[\left\{\begin{matrix} C(G+P) + C(P) \\ -C(G+P) + C(P) \\ C(G+P) - C(P) \end{matrix}\right\} \cos(\tfrac{\pi}{2}P^2) + \left\{\begin{matrix} S(G+P) + S(P) \\ -S(G+P) + S(P) \\ S(G+P) - S(P) \end{matrix}\right\}\sin(\tfrac{\pi}{2}P^2)\right],\quad \left\{\begin{matrix} G+P \geq 0,\ P \leq 0 \\ G+P < 0,\ P \leq 0 \\ P > 0 \end{matrix}\right\}. \qquad \text{(A-8)}$$

In the special case where the system bandwidth equals the chirp bandwidth (cf. fig. 2)

$$-w = \omega_2 - \omega_1 = mT$$

$$G+P = -P = \sqrt{m/2\pi}\ T$$

and (A-8) reduces to

$$\begin{aligned} \rho &\approx \frac{2}{G}[C(P)\cos(\tfrac{\pi}{2}P^2) + S(P)\sin(\tfrac{\pi}{2}P^2)] \\ &= \frac{1}{\sqrt{TW_c}}\ [C(\sqrt{TW_c})\cos(\tfrac{\pi}{2}TW_c) + S(\sqrt{TW_c})\sin(\tfrac{\pi}{2}TW_c)] \end{aligned} \qquad \text{(A-9a)}$$

where

$$TW_c = mT^2/2\pi \quad \text{(cycles)} \qquad \text{(A-9b)}$$

is the time-bandwidth product in cycles. Since $C(\infty) = S(\infty) = 1/2$, $\rho = O(1/\sqrt{TW_c})$ for large time-bandwidth products. Since the sum frequency term, not shown in (A-3a),

$$\begin{aligned} \frac{1}{T}\int_0^T \cos(\omega_1 + \omega_2)t\ dt &= \frac{\sin(\omega_1 + \omega_2)T}{(\omega_1 + \omega_2)T} \\ &= \frac{\sin(2\omega_1 + mT)T}{(2\omega_1 + mT)T} = O(1/TW_c) \end{aligned} \qquad \text{(A-10)}$$

approaches zero with increasing TW_c faster than the difference frequency term of (A-3a), (A-9a) is an excellent approximation to ρ for large time-bandwidth products even when ω_1 is not much larger than mT.

Table 1

1971 Limits of ITU Power Flux Density

Frequency Range (GHz)	PFD Limit Φ_{max} (dBW/m^2) in Any 4 kHz		
	θ = satellite look angle		
	$\theta \leq 5°$	$5° < \theta \leq 25°$	$25° < \theta \leq 90°$
1.670 - 1.710 1.770 - 1.790 2.200 - 2.300 2.500 - 2.535	-154	$-154 + (\theta - 5)/2$	-144
2.5 - 2.69	-152	$-152 + 3(\theta - 5)/4$	-137
3.4 - 4.2 7.25 - 7.75	-152	$-152 + (\theta - 5)/2$	-142
8.025 - 8.5 10.95 - 11.2 11.45 - 11.7	-150	$-150 + (\theta - 5)/2$	-140
12.5 - 12.75	-148	$-148 + (\theta - 5)/2$	-138
17.7 - 19.7 21.2 - 22.0	-139 -115	$-139 + (\theta - 5)/2$ (based on equivalent specification $-115 + (\theta - 5)/2$ in any 1 MHz)	-129 -105

Table 2

Example Terminal Sizes Implied by PFD Limits

f (GHz)	4	7.5	11	18.7
L_r (dB)	4	5	7	12
Φ_{max} (dBW/m^2)	-152	-152	-150	-139
$(G_r/T_e)_{min}$ (dB/^{o}K)	11.9	18.4	21.7	20.3
D (ft)	8.3	9.3	9.3	4.7

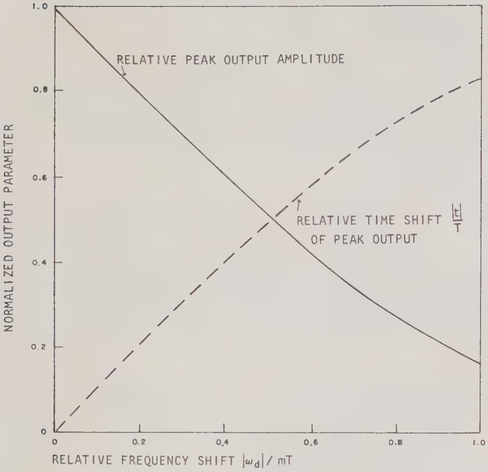

Figure 1. CHIRP MATCHED-FILTER OUTPUT PARAMETERS(11)

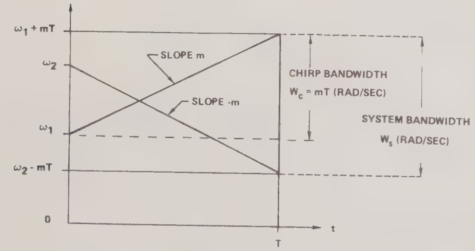
$\omega_1 + mT$
ω_2
ω_1
$\omega_2 - mT$
0
SLOPE m
SLOPE -m
CHIRP BANDWIDTH
$W_c = mT$ (RAD/SEC)
SYSTEM BANDWIDTH
W_s (RAD/SEC)
T
t

$$W_s = \begin{cases} 2mT - (\omega_2 - \omega_1), & mT \geq \omega_2 - \omega_1 \\ \omega_2 - \omega_1, & mT < \omega_2 - \omega_1 \end{cases} \quad \omega_2 \geq \omega_1$$

$$ 2mT - (\omega_2 - \omega_1), \quad \omega_2 < \omega_1$$

TIME BANDWIDTH PRODUCT

$TW_c = mT^2$ (RAD)

Figure 2. CHIRP AND SYSTEM BANDWIDTH DEFINITIONS FOR THE BINARY CASES

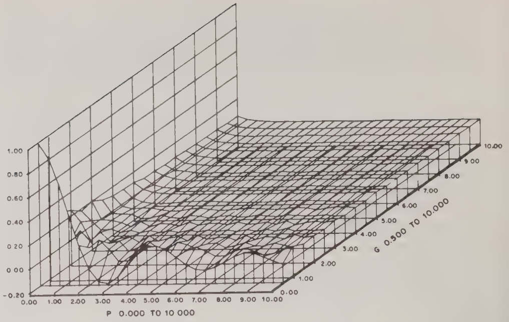

Figure 3 CROSS-CORRELATION COEFFICIENT FOR CHIRP SIGNALS, POSITIVE P

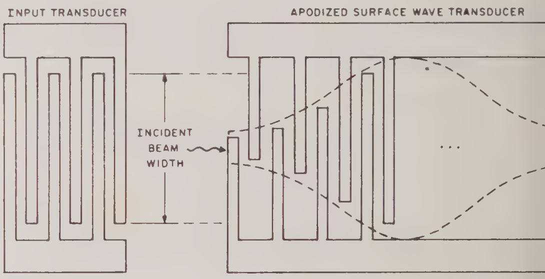
INPUT TRANSDUCER
APODIZED SURFACE WAVE TRANSDUCER
INCIDENT
BEAM
WIDTH
...

Figure 4. BASIC TRANSDUCER CONFIGURATION OF SURFACE ACOUSTIC WAVE CHIRP FILTER(13)

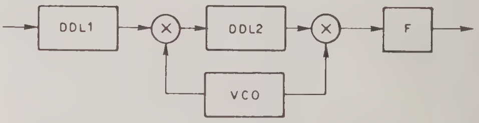
DDL1
DDL2
F
VCO

DDL1, DDL2	SAW DISPERSIVE DELAY LINES WITH CUBIC PHASE CHARACTERISTIC
VCO	VOLTAGE CONTROLLED OSCILLATOR CONTROLLING DISPERSIVE SLOPE
F	FILTER TO REJECT MIXER SIDEBAND

Figure 5. ARRANGEMENT FOR VARIABLE SLOPE DISPERSION(22)

80-0597

APPLICATION OF SATELLITE DEMAND ASSIGNMENT IN TELEPHONE NETWORKS

John M. Fraser*
Hughes Aircraft Company
El Segundo, California

Abstract

Judicious use of demand assignment multiple access (DAMA) systems by national telephone system planners can result in major savings by eliminating the need for installation or expansion of terrestrial switching and trunking facilities while continuing to achieve a desired grade of service. Examples of DAMA applications are drawn from the Indonesian Palapa system and the Satellite Integrated Telephone System (SITS). A brief description is given of the network management and traffic measurement capabilities provided by DAMA. Finally, there is a discussion of new single channel per carrier (SCPC) equipment suitable for DAMA.

Introduction

Although a DAMA system has been used by Intelsat for many years,**this international application is different from the use of DAMA in a national telephone system. This paper concentrates on the use of DAMA as an integral part of a national telephone system.

DAMA provides a satellite telephone circuit between ground stations only when a telephone call is in progress. Figure 1 illustrates the use of DAMA to set up circuits between ground stations without traversing any intervening switches or terrestrial links. Thus, it can be seen that DAMA provides switchable direct trunks on demand between any switching centers associated with DAMA ground stations.

Telephone planners can regard the DAMA system as a new tool in improving their trunking and switching plans. The judicious use of DAMA can postpone or eliminate the need for installation or expansion of terrestrial switching and trunking facilities resulting in major system savings. DAMA is not a panacea for all network problems, however. Its economic use in a specific network depends on such factors as the degree of overbuild, terrain, and time required to provide services. Each network must be evaluated individually.

This paper also describes possible applications of DAMA and savings in trunk and terminal equipment that can be achieved by its incorporation into a national telephone network. The Indonesian Palapa DAMA and the SITS, the latest Hughes DAMA system, are discussed. In the SITS the local exchange switch is located in the ground station and is controlled by the DAMA microprocessor in the ground station. The billing functions and information and intercept operators are housed in the centralized master control station (MCS).

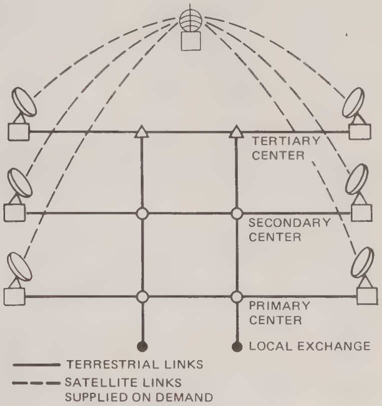

Fig. 1 Demand assignment multiple access system as part of switching hierarchy.

This DAMA can, therefore, be regarded as a complete telephone system from telephone set to telephone set. Network management and traffic measurement functions incorporated in DAMA systems are also discussed. In addition, a brief description is given of the latest generation of SCPC equipment suitable for DAMA systems.

DAMA Efficiencies

Any system that assigns satellite circuits only on demand must use the circuits more efficiently than if the circuits were permanently assigned (PA). Several cases have been examined (see Table 1) to illustrate that DAMA requires not only fewer satellite circuits, but also fewer SCPC voice channel units at each terminal. The network of Figure 1 was the model for these calculations. For illustrative purposes, it was assumed that it was necessary to interconnect completely the six switching centers of Figure 1 with equal size trunk groups ranging in size from 1 to 20 trunks. The information in the first two columns of Table 1 was assumed. The results of the calculations for permanently assigned and DAMA trunks are shown in the other columns. Table 1 shows that significantly fewer circuits and modems are required for DAMA, even with 20 circuits per node pair.

Figure 2 shows that when the number of nodes is increased, the differences between DAMA and permanent assignment become very large. Figure 2 shows this effect, assuming systems of different numbers of nodes with 1 percent blockage and 1 erlang between each pair of nodes. In a 40 node network, the initial size of the Indonesian Palapa network, DAMA provides a 4.6 satellite circuit improvement and a 3.6 demand assignment (DA) modem improvement.

*Project Manager, Commercial Systems Division, Hughes Aircraft Company.

**"Demand Assigned Service for INTELSAT Global Network," Spectrum, January 1971.

Copyright © American Institute of Aeronautics and Astronautics, Inc., 1980. All rights reserved.

Table 1 Circuits and modems required with PA and DAMA in 6 node network

System Blockage*	PA Circuits per Node Pair	Erlangs per Node Pair	Number of Satellite Circuits		Number of Modems	
			PA	DAMA	PA	DAMA
0.01	1	0.01	15	3	30	12
0.01	2	0.15	30	9	60	30
0.01	10	4.46	150	91	300	210
0.01	20	12.03	300	217	600	468
0.03	1	0.03	15	4	30	12
0.03	2	0.28	30	11	60	30
0.03	10	5.53	150	105	300	228
0.03	20	14.00	300	241	600	504

*90% of blockage was assigned to modems and 10% to satellite circuits.

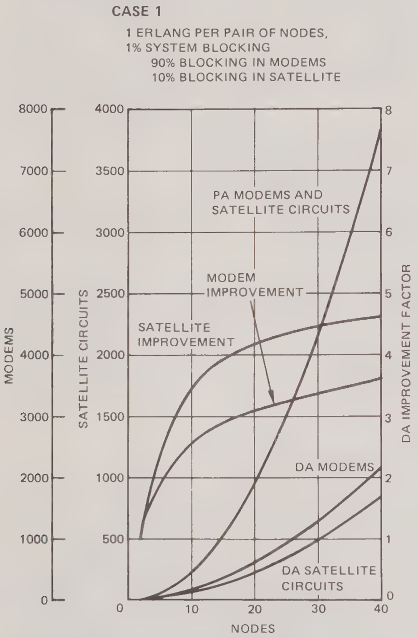

Fig. 2 DAMA and permanent assignment differences related to number of nodes.

If the traffic between each pair of nodes in this 40 node network is 0.1 of an erlang, the approximate satellite circuit improvement is 15 and the modem improvement is 7.

Assigning 90 percent of the blockage to the modems and 10 percent to the satellite circuits was somewhat arbitrary. Other allocations could be used to change the relative savings in modems and satellite circuits because the trade between satellite circuits and modems depends on the number of stations in a system. For a small number of stations, the addition of modems at each station is cheaper than the addition of satellite circuits to achieve a certain grade of service. For a large number of stations, however, the cost of adding modems at each station becomes much greater; it becomes reasonable, therefore, to allocate higher blocking in the modems and achieve the desired grade of service by reducing satellite blocking. In addition, allocating a large part of the blockage to the modems permits the telephone administration to easily decrease the system blockage by increasing the number of modems at each station if traffic is higher than predicted.

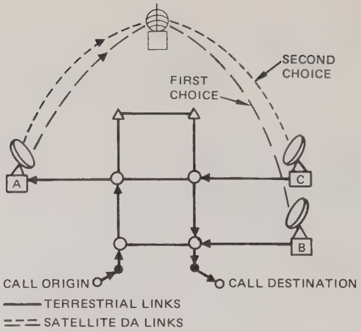

Fig. 3 DAMA alternate routing.

Routing Strategies

At present, the Indonesian Palapa DAMA system provides direct trunks on demand between 50 ground stations without using any of the alternate routing provisions in the DAMA system. However, since DAMA is a computer controlled switching system, fairly sophisticated routing strategies can be incorporated. One form of alternate routing that could be implemented in DAMA is shown in Figure 3. In this example, the call routed to ground station A would first be routed by the DAMA MCS to ground station B, which is closest to the call destination. If the call were blocked by lack of modems at B, DAMA would automatically reroute it to ground station C and the call routing would be completed over terrestrial links. To prevent a double hop, the terrestrial switch associated with C must be structured so that the call coming from C is not routed by the switch back out to C, which might be able to complete the routing via a satellite circuit to B.

The above example illustrates only one method of DAMA's application in routing strategies. Many more sophisticated routing rules could be incorporated, depending on network needs and the logic of the terrestrial switches.

Palapa DAMA System Overview*

Palapa incorporates a DAMA system employing centralized control. The DAMA system provides automated telephone connections between ground stations by digital control of the SCPC equipment and assignment of satellite frequencies when a given telephone circuit requests a connection.**

*J. Sutanggar Tengker, "Indonesian Domestic Satellite System," presented at EASCON, 21 to 29 September 1976, New York, NY.

**Any of 12 transponders on the satellite can ultimately provide nominally 1000 SCPC channels or 500 two way circuits.

On demand, the centralized control system incorporated in the MCS in Jakarta assigns a transmit/receive frequency combination to the requesting station and the converse frequency pair to the destination station. At the conclusion of the call, the circuits are released and the pair of frequencies is available to central control for reassignment.

The control system must first sense that a ground station is initiating a call. Then it must find out to which other ground station the call is directed, determine the availability of circuits both in the satellite and in the destination station, assign a frequency pair to the two stations involved, and thus let the two ground stations access each other through the satellite. The DAMA control system also determines when a call is completed so it can release the circuit returning the pair of frequencies to the pool, thus making them available on demand to a new caller.

Principal elements of the DAMA system are the remote units at the ground stations and the master control equipment. A remote unit consists of a microcomputer, control data link modem, and DAMA signaling units. The microcomputer provides a command processing from the master computer and logic control of the telephone interface in response to line signals. The control data link modem provides communication with the MCS through dedicated satellite SCPC channels. The DAMA signaling unit provides detection and orginization of seize, release, and blocking of telephone line signals. Figure 4 is a simplified system block diagram.

Palapa Operational Sequence

The Palapa system can operate with decadic dialing and semiautomatic or automatic switching. The following description is for automatic operation.

To establish the status of each ground station, the DAMA control system polls each station sequentially by broadcasting a polling signal through the satellite at a dedicated frequency to each station once every second. This polling operation is shown schematically in Figure 5. Each station is addressed individually by its ground station code incorporated in the polling data stream.

The polling command triggers a response (at a dedicated frequency) from the remote unit in each ground station as shown in Figure 6. However, this response is triggered only from a station that has experienced a seize or release since the last poll. Each ground station responds in time sequence, identifying itself and giving changes in circuit seize or release status. Each ground station indicates whether it wants to initiate a call, or whether a call has just ended, and which modem number it is using. The modem information is necessary because the central control computer keeps track of all the busy modems in each ground station.

Upon receipt of ground station seizure signal (call-initiate response), the central control computer assigns two frequencies through the central control link to the originating modem. After

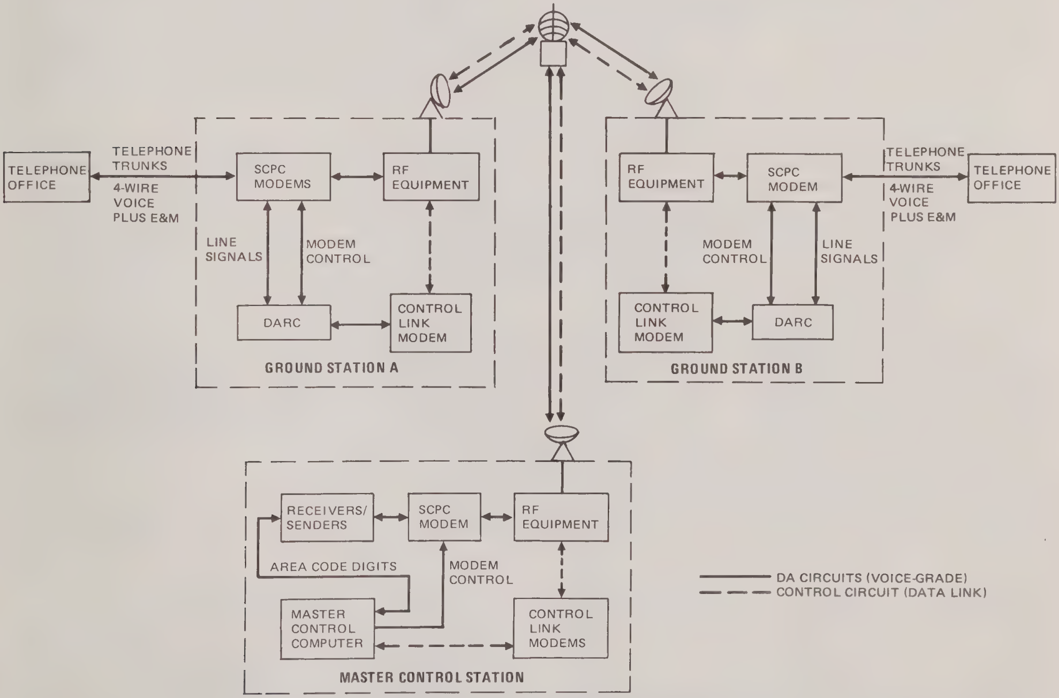
TELEPHONE OFFICE
TELEPHONE TRUNKS
4-WIRE VOICE PLUS E&M
SCPC MODEMS
RF EQUIPMENT
LINE SIGNALS
MODEM CONTROL
DARC
CONTROL LINK MODEM
GROUND STATION A
RF EQUIPMENT
SCPC MODEM
TELEPHONE TRUNKS
4-WIRE VOICE PLUS E&M
TELEPHONE OFFICE
MODEM CONTROL
LINE SIGNALS
CONTROL LINK MODEM
DARC
GROUND STATION B
RECEIVERS/ SENDERS
SCPC MODEM
RF EQUIPMENT
AREA CODE DIGITS
MODEM CONTROL
MASTER CONTROL COMPUTER
CONTROL LINK MODEMS
MASTER CONTROL STATION
DA CIRCUITS (VOICE-GRADE)
CONTROL CIRCUIT (DATA LINK)

Fig. 4 Demand assignment system.

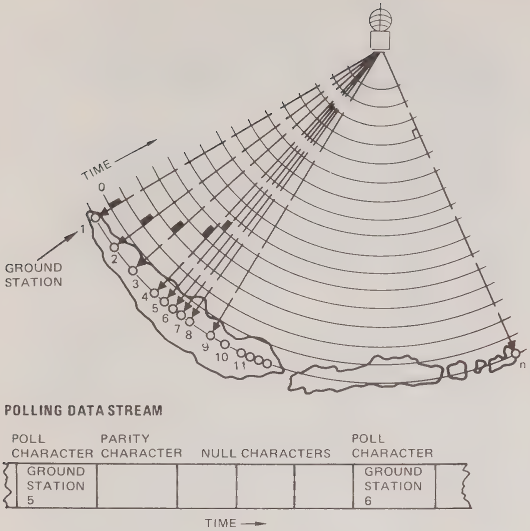

Fig. 5 Polling by satellite.

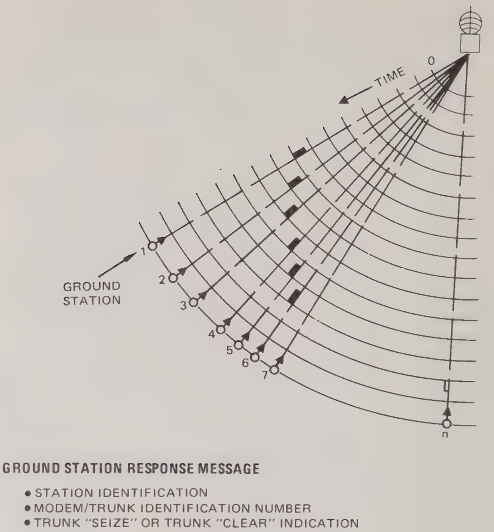
TIME
0
1
2
3
4
5
6
7
n
GROUND STATION
GROUND STATION RESPONSE MESSAGE
• STATION IDENTIFICATION
• MODEM/TRUNK IDENTIFICATION NUMBER
• TRUNK "SEIZE" OR TRUNK "CLEAR" INDICATION

Fig. 6 Ground station response to polling command.

receipt of the frequency assignments, the originating ground station and master control equipment tune their respective modems to the assigned frequencies. Thus, a connection is made between the originating ground station and the master control equipment in the MCS via a voice grade telephone circuit (see Figure 7a). This connection involves the same frequencies that will be used subsequently to connect the requesting station with the destination station.

The area code, stored in the switching machine at the telephone office, is now transferred through the requesting ground station via this voice grade link to the master control computer. Central control determines the destination station from the area code and the availability of modems at that destination. If a modem is available, the frequency assignment (the reverse of transmit/receive assigned to the requesting station) is sent through the control data link to the destination station.

Now, both requesting and destination station modems are tuned to the frequencies assigned. The MCS relinquishes its voice grade circuit to the requester by deactivating its modem, and the two remote stations are now connected via the circuit assigned them (Figure 7b). After this, the MCS is no longer involved in the connection. The requesting telephone office forwards the subscriber number stored in the switching machine through the satellite system to the destination telephone office, and the call now proceeds in a normal manner as it would via a terrestrial system.

The MCS continues to poll each station to determine new requests or completions of calls, i. e., seizes or releases.

SITS Description

In rural areas, telephone administrations conventionally provide a small switching machine or switchboard to interconnect phones in the same village or to connect them to a long distance trunk. When long distance service is provided by domestic satellite, the ground station is often purchased as a separate package from a supplier. The existing telephone office and the new ground station are then interconnected by buried cable pairs or other means (see Figure 8). If frequency congestion exists, the ground station must be located away from the village and may be connected to the telephone office by a microwave link. Whether the ground station is close or remote, an operator is required at the telephone central office for billing of satellite calls.

Hughes has determined through studies conducted at the company in 1977 that economic and system advantages accrue by locating the local telephone switch in the satellite ground station and combining the local switching functions with the DAMA system. SITS is of interest for rural locations with no existing telephone switching facilities or for locations with outdated or rudimentary equipment in need of replacement.

The Hughes studies clearly indicated that major economies would accrue from a significant reduction in the number of parts required; the reduction also improves reliability. A comparison of Figures 8 and 9 reveals the advantages of combining the telephone office and ground station:

- Only one power system is required.
- The multipair VF cable link connecting the central office to the ground station is eliminated.
- A single building houses both ground station and telephone office.

In addition, the SITS approach permits the billing procedure to be automated at the MCS. Instead of having operators at each rural office, fewer operators may be located at the MCS, only for information and intercept functions.

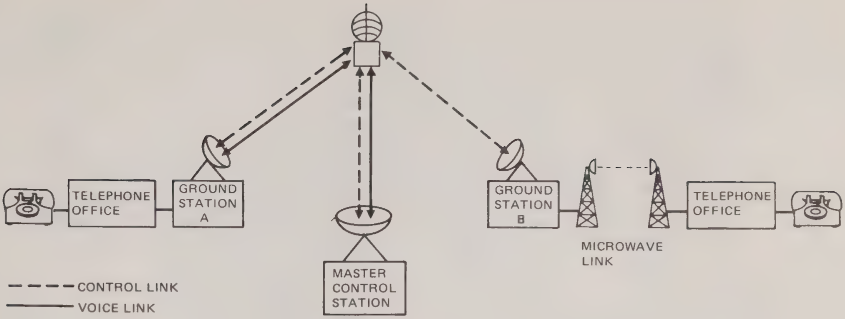
TELEPHONE OFFICE
GROUND STATION A
MASTER CONTROL STATION
GROUND STATION B
MICROWAVE LINK
TELEPHONE OFFICE
CONTROL LINK
VOICE LINK

a) GROUND STATION A SETS UP VOICE LINK WITH MCS; AREA CODE TRANSMITTED TO CENTRAL COMPUTER.

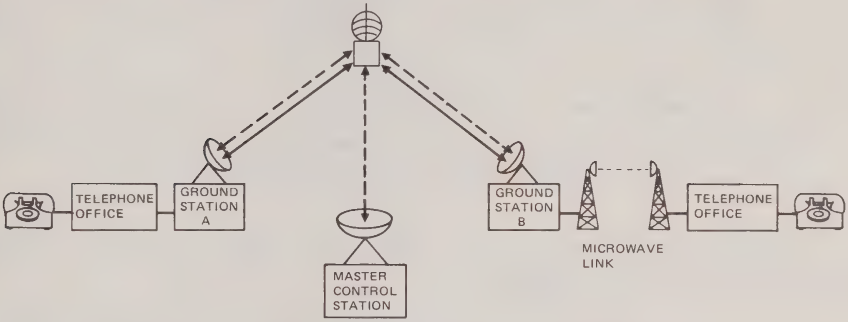
TELEPHONE OFFICE
GROUND STATION A
MASTER CONTROL STATION
GROUND STATION B
MICROWAVE LINK
TELEPHONE OFFICE

b) MCS NOTIFIES B OF CIRCUIT REQUEST AND STATIONS A AND B ARE LINKED DIRECTLY.

Fig. 7 Demand assignment sequence.

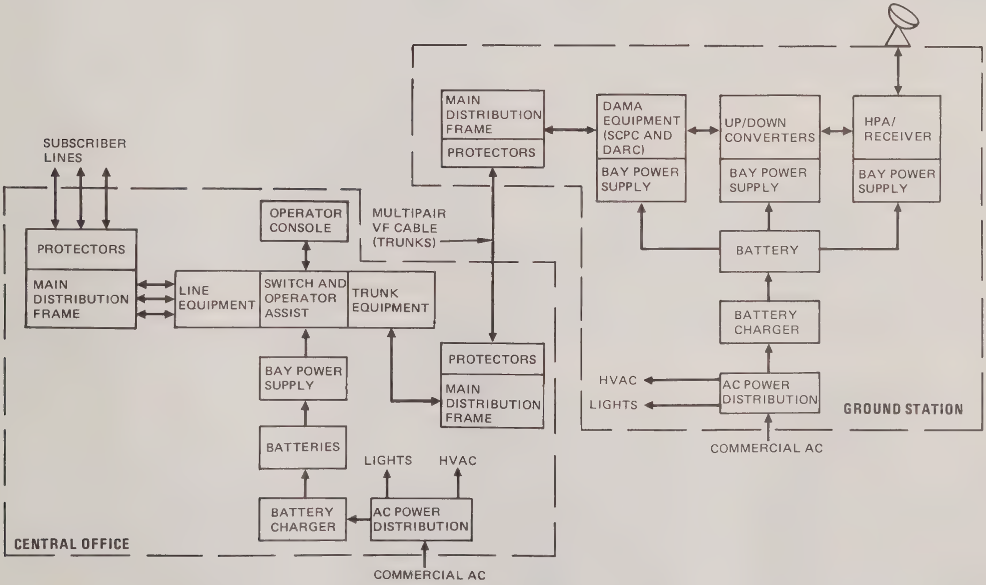
SUBSCRIBER LINES
PROTECTORS
MAIN DISTRIBUTION FRAME
LINE EQUIPMENT
OPERATOR CONSOLE
SWITCH AND OPERATOR ASSIST
TRUNK EQUIPMENT
MULTIPAIR VF CABLE (TRUNKS)
BAY POWER SUPPLY
BATTERIES
BATTERY CHARGER
AC POWER DISTRIBUTION
LIGHTS
HVAC
COMMERCIAL AC
PROTECTORS
MAIN DISTRIBUTION FRAME
CENTRAL OFFICE
MAIN DISTRIBUTION FRAME
PROTECTORS
DAMA EQUIPMENT (SCPC AND DARC)
BAY POWER SUPPLY
UP/DOWN CONVERTERS
BAY POWER SUPPLY
HPA/ RECEIVER
BAY POWER SUPPLY
BATTERY
BATTERY CHARGER
HVAC
LIGHTS
AC POWER DISTRIBUTION
GROUND STATION
COMMERCIAL AC

Fig. 8 Satellite telephone system (separate locations).

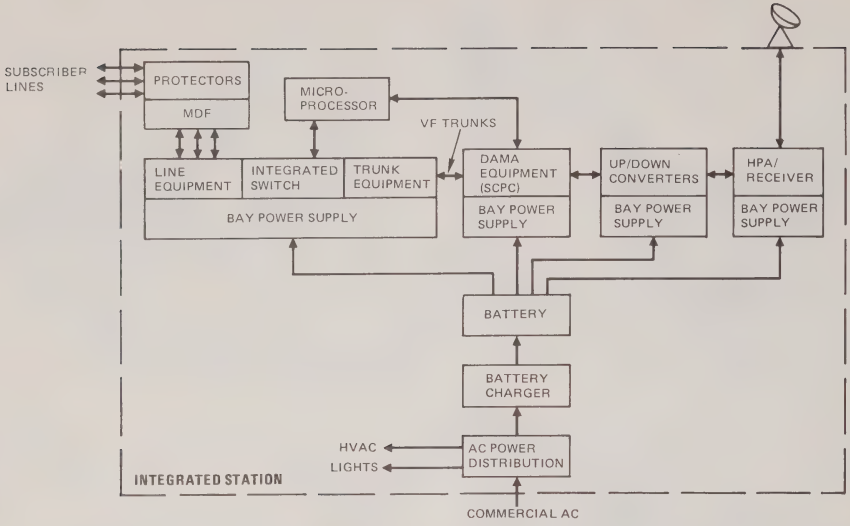

Fig. 9 Satellite integrated telephone system.

Frequency congestion is unlikely in the rural environment that SITS is aimed for; however, the SITS ground station could be located away from interference by extending the subscribers' lines.

To achieve the ultimate potential advantages of the SITS concept, Hughes designed and developed the integrated switch shown in Figure 9. Table 2 shows a comparison between SITS and the Indonesian system. For an administration, the salient differences are that SITS provides centralized billing and centralized operators at the MCS.

The following describes the placement of a telephone call between two remote stations.

SITS Local Calls

A subscriber wishing to make a local call waits to hear a dial tone and then dials the prescribed number of digits (possibly four). The microprocessor operates on this information to cause the switch to make the proper connections between the two local subscribers for the duration of the call. For billing purposes, the microprocessor counts the number of local calls completed by a subscriber station and transfers the count to the MCS over a data channel on command of the MCS.

SITS Long Distance Calls

For long distance calls, a form of common channel interoffice signaling (CCIS) is used over a dedicated 4800 bps data channel which transfers information between ground stations and the MCS. In the Indonesian system, the digital channel was used only to receive seizure, release signals, and tune the station modems. An analog voice frequency circuit was set up between the originating ground station and the MCS to receive the address information of a call. In SITS, this same channel is used to transmit and receive all the information to set up a call. In addition, this data channel is a nonpolled channel with adequate provision to safeguard against the problems of contention.

To make a long distance call through the satellite, the subscriber at the originating ground station A waits for a dial tone and dials a selected digit (say 1), to indicate that it is a long distance call, followed by up to a 10 digit address for the distant subscriber. If the microprocessor at the originating station finds a free modem, it commands the switch to connect the subscriber to the modem. If there is no free modem, the subscriber gets a congestion tone. The complete address information plus the calling party number is transmitted to the MCS over the data channel as a stream of digits as shown in Figure 10a. Other information, such as station and modem (not shown in Figure 10), are also transmitted as part of this initial address message. In many smaller systems, it will not be necessary to transmit 10 digits to identify the called party; however, the system is designed for this capacity. In addition, provisions would be made to transmit and receive station signals (to determine, for example, whether a subscriber is allowed long distance calls).

After the MCS computer analyzes the address information, it transmits the necessary information over the data channel to the called ground station B (Figure 10b). At the distant ground station the modem is tuned and the microprocessor determines

Table 2 Comparison with Indonesian system

Function	SITS	Indonesia
Data channel	4800 bps – nonpolled	1800 bps – polled
Signaling	Digital	Analog
Seizure, release, tuning	Data channel	Data channel
Address	Data channel	Analog on VF circuit
Billing information	Collected at MCS	Not handled
Operations	At MCS	Dispersed

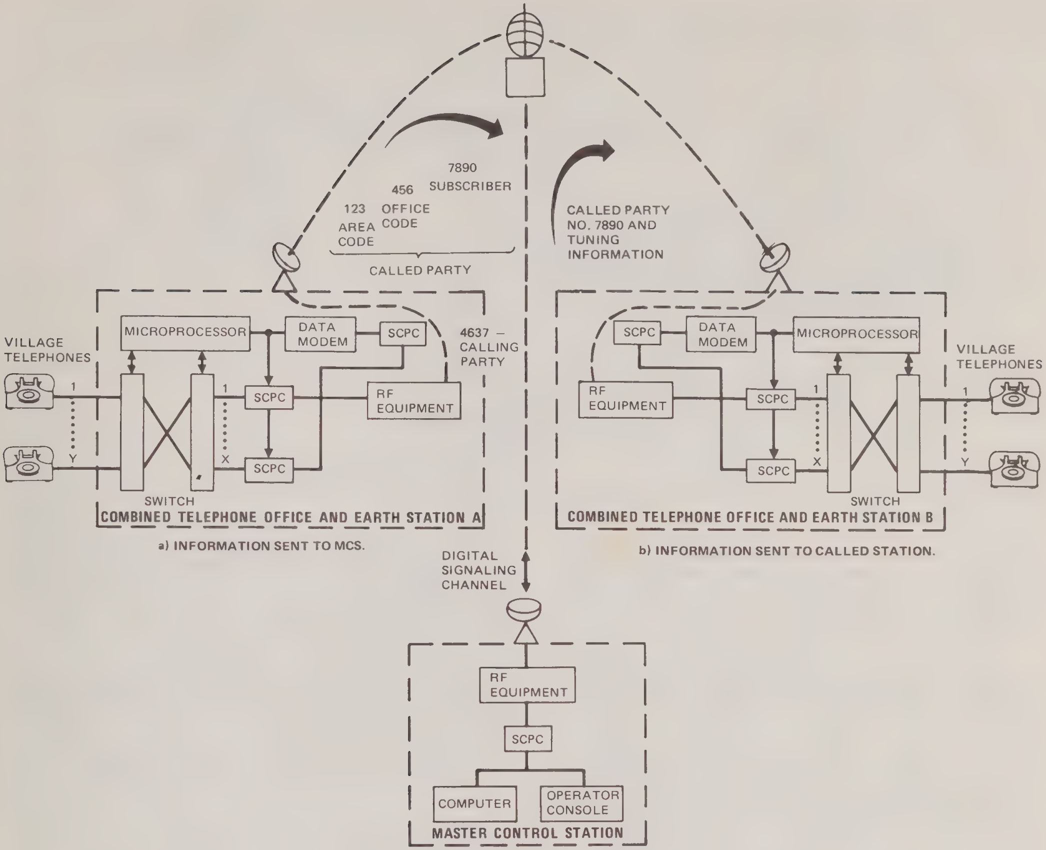
7890
456 SUBSCRIBER
123 OFFICE
AREA CODE
CODE
CALLED PARTY
CALLED PARTY
NO. 7890 AND
TUNING
INFORMATION
4637 – CALLING PARTY
VILLAGE TELEPHONES
MICROPROCESSOR
DATA MODEM
SCPC
SCPC
SCPC
RF EQUIPMENT
1
Y
1
X
SWITCH
COMBINED TELEPHONE OFFICE AND EARTH STATION A
SCPC
DATA MODEM
MICROPROCESSOR
VILLAGE TELEPHONES
RF EQUIPMENT
SCPC
SCPC
1
X
1
Y
SWITCH
COMBINED TELEPHONE OFFICE AND EARTH STATION B
DIGITAL SIGNALING CHANNEL
RF EQUIPMENT
SCPC
COMPUTER
OPERATOR CONSOLE
MASTER CONTROL STATION

a) INFORMATION SENT TO MCS.

b) INFORMATION SENT TO CALLED STATION.

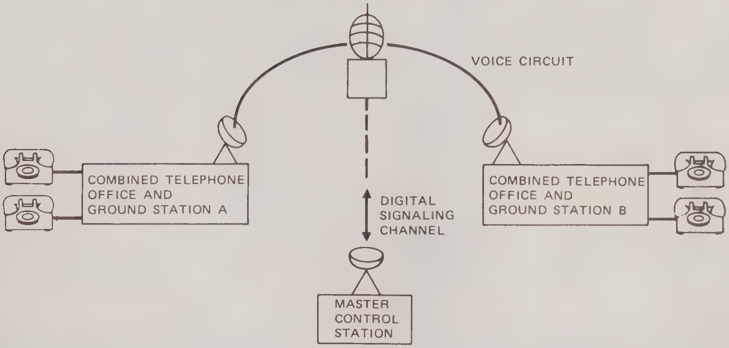
VOICE CIRCUIT
COMBINED TELEPHONE OFFICE AND GROUND STATION A
COMBINED TELEPHONE OFFICE AND GROUND STATION B
DIGITAL SIGNALING CHANNEL
MASTER CONTROL STATION

c) VOICE CIRCUIT CONNECTION ESTABLISHED

Fig. 10 Call setup.

whether the called party is busy and, if not, signals the MCS. The MCS meanwhile has sent a tuning command to the A station. The B station microprocessor commands the local switch to connect the called party to the tuned modem and to provide ringing signals to the called party. When the called party answers, an answer signal is sent to the MCS, which inserts the time of day in the billing information. This completes the call setup as shown in Figure 10c. At the completion of the call, release signals are sent to the MCS, the modems are detuned, and the pair of frequencies returned to the DAMA frequency pool.

Calls can also be set up between rural stations and gateways to the terrestrial telephone network. At the gateway the CCIS is converted to the national signaling system as shown in Figure 11.

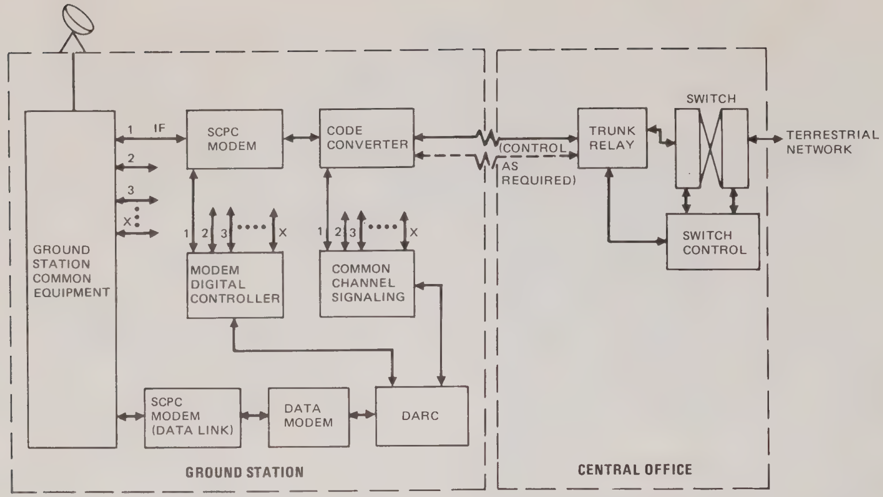

Fig. 11 Gateway station.

Since the MCS has billing information on each call (Table 3), it can provide a tape which can be processed to prepare subscriber bills. The MCS computer has look-up tables for different rates for different times of day.

If subscriber dials 0, a voice frequency connection is set up directly between the subscriber and an information and service operator in the MCS. Likewise, if a subscriber dials a wrong number or a "no such" number, a direct connection is made to an intercept operator at the MCS. These operator positions will be equipped to set up a call by dialing directly into the computer.

Network Management and Traffic Measurement

Inherent in centrally controlled DAMA SCPC telephone networks are a potentially powerful planning capability, i.e., the ability to collect comprehensive nationwide traffic data at a single monitoring point. Instead of planning from the basis of limited samples collated from many locations at different times, the DAMA system enables an administration to collect traffic statistics on every call placed in the DAMA system.

Both day to day network management and longer range growth planning may be based on a detailed history of system usage rather than broad extrapolations from a few limited traffic measurements.

Figure 12 depicts the functional interfaces of the process of DAMA traffic statistics collection. A descriptive record of each call is written on magnetic tape by the control computer each time a call is completed in the DAMA system. In the Indonesian system, the information in each call record includes the originating station, the destination station, and duration of the call. SITS includes, in addition, the originating subscriber's number and the called party's number.

Table 3 Billing information

Type of Signal	Function
Called party answer	Time start of call
Calling party number	Identify calling party
Called party number	Identify called location
Release	Time end of call

Subsequent processing of this call transaction tape on a backup computer permits the computation of statistics such as:

1) Total network point-to-point busy hour traffic matrices
2) Circuit activity versus time of day
3) Call blockage summaries
4) Call holding time distributions
5) Circuit utilization summaries (erlang/circuit ratios)

for each station individually

6) Billing information from SITS data

Results from these calculations are presented in graphic as well as tabular formats.

Centralized Maintenance

A centralized DAMA can transmit maintenance status data from each ground station periodically to the MCS. These data could include low/high voltage alarms, fuel measurements, temperature, and security alarms. The MCS could request these data be sent during nonbusy hours or override capability could be included in event of catastrophic failures. Armed with status data from each ground station, skilled technicians at the MCS could determine the health of each station and the cause of any failures or potential failures. Less skilled people could then be dispatched to a ground station with the appropriate plug-in mod-

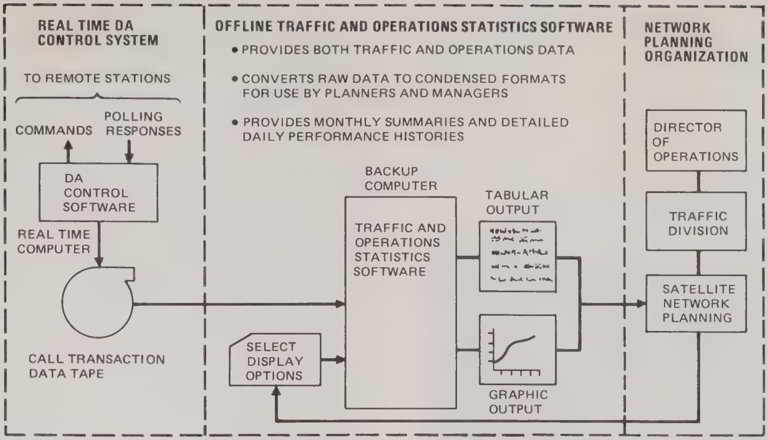

REAL TIME DA CONTROL SYSTEM
TO REMOTE STATIONS
COMMANDS
POLLING RESPONSES
DA CONTROL SOFTWARE
REAL TIME COMPUTER
CALL TRANSACTION DATA TAPE
OFFLINE TRAFFIC AND OPERATIONS STATISTICS SOFTWARE
• PROVIDES BOTH TRAFFIC AND OPERATIONS DATA
• CONVERTS RAW DATA TO CONDENSED FORMATS FOR USE BY PLANNERS AND MANAGERS
• PROVIDES MONTHLY SUMMARIES AND DETAILED DAILY PERFORMANCE HISTORIES
BACKUP COMPUTER
TRAFFIC AND OPERATIONS STATISTICS SOFTWARE
TABULAR OUTPUT
GRAPHIC OUTPUT
SELECT DISPLAY OPTIONS
NETWORK PLANNING ORGANIZATION
DIRECTOR OF OPERATIONS
TRAFFIC DIVISION
SATELLITE NETWORK PLANNING

Fig. 12 DA traffic functional interfaces.

ules and instructions. Correction of a fault at a ground station will immediately be reflected in the status data at the MCS. If needed, further diagnostics can continue over the order wire while the technician is at the ground station.

New SCPC Equipment

As a result of the successful operation of the Indonesian system, Hughes developed a new generation of SCPC equipment as part of a continuous effort to improve the technical performance and economical operation of small ground stations. Actually, the new equipment is the third generation of SCPC equipment developed and has been sold commercially.

The first generation of Hughes SCPC equipment was used in the first thin route telephony ground stations, operating in conjunction with the Canadian Anik satellites. These small ground stations are used to serve isolated regions of Canada and remote oil drilling sites above the arctic circle. The second generation SCPC equipment, designated HS 732, is used throughout the Indonesian Palapa system. The third generation, HS 732A, improves on the successful architecture of the HS 732 equipment by incorporating simplified advanced circuitry and repackaging. Thus, it makes the equipment more compact and more accessible while reducing the number of internal connections and components, improving power efficiency, and increasing mean time between failures.

Each generation of SCPC equipment provides toll quality telephone service in synchronous satellite communications systems, using highly reliable equipment of simple design. The HS 732A system uses analog FM with voice operated carriers, syllabic companders, pre-emphasis, and special deisgn features to reduce intrinsic noise contributed by intermodulation and local oscillators. It can operate with the various signaling systems used throughout the world and is designed for easy integration into DAMA operation. A brief description of the advanced HS 732A system is presented herein. A more detailed description is given in another paper.*

The HS 732A system is a complete satellite ground station electronics package interfacing between voice frequency signals and single channel slots in the 6 and 4 GHz band. The system consists of common equipment which includes power supplies, reference oscillators, up/downconverters, and IF summing and splitting equipment in addition to individual channel modem modems.

The basic building block of the advanced SCPC subsystem is the shelf which is 10.5 inches high. As Figure 13 shows, a single shelf can hold from 1 to 12 modems along with associated distribution equipment. The same type of shelf is used to contain other modules to provide functions that may also be required such as reference signal generation, frequency translation, orderwire service, and demand assignment remote control. Connections to all units within a shelf are from the front, which simplifies installation alignment, and maintenance.

Either ac or dc power can be specified as the prime power source. Such designation allows operation either in conventional ground stations, which employ commercial or locally generated ac, or in the telephone plant, where dc is typically available. The prime power consumption per SCPC modem is quite low; a full rack of 84 channels requires only about 1500 watts which is one-half to one-third the amount required by earlier equipment designs. Although air conditioning is recommended, the equipment can operate without it in a wide range of temperature and humidity conditions and only requires protection from condensation and contamination.

---

*John M. Fraser, Egli, and Elbert, "A New Generation of Single Channel Per Carrier (SCPC) Equipment", presented at EUROSPACE Conference, Naples, Italy, September 1978.

The advanced design of the modems and compact packaging permit a large channel capacity to be contained in a small space, necessitating only convection cooling to maintain operation during varied environmental conditions.

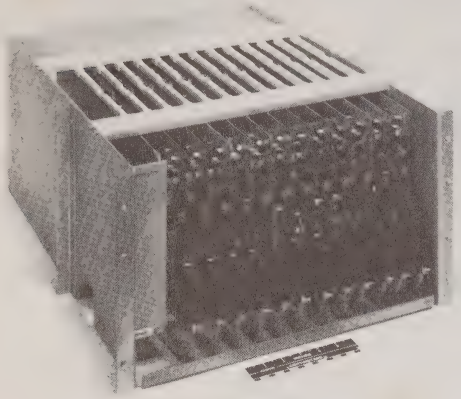

Fig. 13 Shelf construction.

HS 732A Single Board Modem

The main elements of the single board modem used in the HS 732A system (Figure 14) are the signal interface unit, modulator/transmitter, channel synthesizer, receiver/threshold extension demodulator (TED), and command and status unit. A block diagram of this modem also appears in Figure 14. All baseband processing is done in the signal interface unit. In the modulator/transmitter, the baseband signal frequency modulates the carrier and translates the carrier to IF. The channel synthesizer provides the local oscillator for proper IF frequency selection. The receiver/TED selects and demodulates the desired IF carrier. Finally, the command and status unit receives commands from and returns status information to the separate modem digital processor. Table 4 provides a more comprehensive list of the functions of the modem elements.

The advanced SCPC equipment provides a level of performance, summarized in Table 5, which meets the needs of modern transmission networks. This equipment conforms to applicable International Telephone and Telegraph Consultative Committee and International Radio Consultative Committee recommendations and permits a wide range of services to both large and small ground stations. Transmission parameters, including channel spacing and deviation, can be selected to

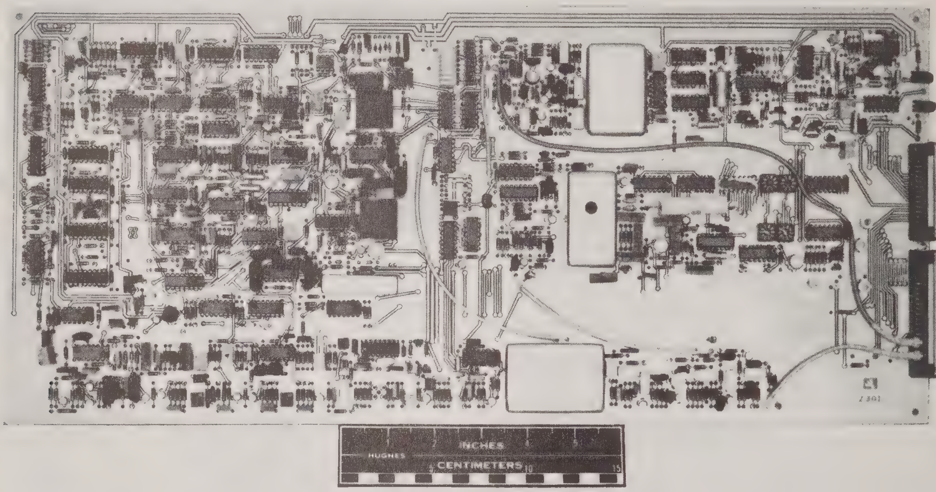
INCHES
HUGHES
CENTIMETERS

a) MAIN ELEMENTS

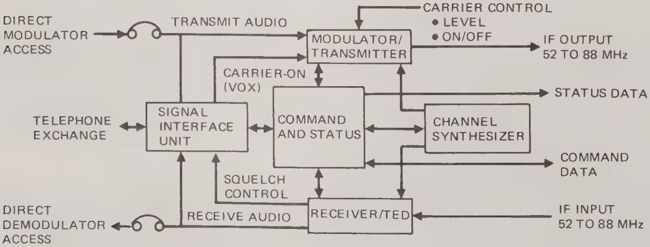
CARRIER CONTROL
• LEVEL
• ON/OFF
DIRECT MODULATOR ACCESS
TRANSMIT AUDIO
MODULATOR/ TRANSMITTER
IF OUTPUT 52 TO 88 MHz
CARRIER-ON (VOX)
STATUS DATA
TELEPHONE EXCHANGE
SIGNAL INTERFACE UNIT
COMMAND AND STATUS
CHANNEL SYNTHESIZER
COMMAND DATA
SQUELCH CONTROL
DIRECT DEMODULATOR ACCESS
RECEIVE AUDIO
RECEIVER/TED
IF INPUT 52 TO 88 MHz

b) BLOCK DIAGRAM

Fig. 14 Main elements and block diagram of single board modem.

Table 4 Modem element functions

Signal interface unit	Interfaces modem with telephone exchange
	Provides all baseband processing including companding, speech detection (VOX). AGC, squelch, and other options
Modulator/transmitter	Generator pre-emphasized FM carrier
	Provides energy dispersal
	Translates carrier to selected channel frequency at IF
	Controls transmit carrier (on/off level)
Channel synthesizer	Generates local oscillator signal for translation of FM carrier to and from IF
Receiver/TED	Selects desired receive carrier from IF range
	Demodulates information from FM carrier
	De-emphasizes baseband
	Provides squelch control
Command and status unit	Provides remote control interface
	Provides mutual frequency input if desired

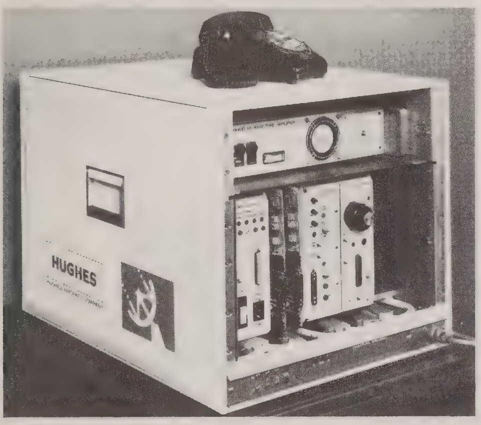

Fig. 15 Nonredundant two channel small terminal assembly.

Table 5 SCPC telephone service performance summary

Modulation	Companded FM with pre-emphasis
Channel spacing	22.5, 30, 45, or 60 kHz (strappable)
Test tone deviation (30 kHz spacing)	5.65 kHz peak (1 kHz at 0 dBMO)
Deviation limit	+3.4 dBMO, with AGC
Two-tone IM distortion	$<$-30 dB, with each tone at -1 dBMO
C/N_0 for equivalent 10,000 pWOp (S/N_W = 34 dB)	55 dB-Hz
Threshold C/N_0	51 dB-Hz
Transmit frequency stability at 6 GHz	±1 kHz
Transmit level at 6 GHz	-10 dBm total of all carriers
Transmit level stability at 6 GHz	
Versus time/temperature	±0.5 dB per 90 days
Versus frequency (over 36 MHz)	±1 dB
Spurious and intermodulation products	$<$-40 dB/4 kHz

optimize the network for maximum transponder capacity (22.5 kHz spacing), minimum ground station cost (30 or 45 kHz spacing), or maximum baseband bandwidth (60 kHz or greater spacing).

Rural Terminal

An example of a nonredundant two channel terminal complete with 40 watt TWTA is shown in Figure 15. This small terminal would be suitable for rural applications. The standard design 10.5 inch shelf can be seen just below the TWTA within the portable container. The modems in this case operate on permanently assigned frequencies since no modem digital processor or DAMA equipment is included. This equipment can be added at any time to upgrate the terminal for full DAMA service.

A station with three modems and nonredundant common equipment resembles the station in Figure 15. A six modem station would require the addition of another shelf and would be packaged similarly.

80-0480

HIGH-SPEED SATELLITE DATA TRANSMISSION OF MARITIME SEISMIC DATA

by

Thomas O. Calvit
COMSAT Corporation

Lynn B. Heitman
Texas Instruments Incorporated

Abstract

Maritime communications in the form of telex, telephone and voice grade data are now a reality on many seismic vessels. These services are being provided by MARISAT — a communications satellite system developed for the maritime industry. Data transmission at higher speeds has recently been demonstrated with MARISAT. An experiment has been conducted in which test data are transmitted at an effective rate of 56 kilo-bits per second from an operational seismic vessel. Both the bit-error-rates and the channel availabilities measured over a wide range of vessel motion conditions indicate that acceptable service can be provided.

The availability of a high-speed data channel direct from a vessel to a user's computer facility offers a new dimension in data collection services. Low volume data such as navigation, gravity, and magnetics can be transmitted on a daily basis and the analysis and display of the data can be accomplished while the vessel is still on the prospect. Selected seismic lines can be transmitted and used to determine proper processing parameters before the total volume of prospect data arrives at the computer center. Enhanced quality control and improved vessel and processing productivity can be attained from these capabilities.

The cost of high-speed data service is tied to three major system components: 1) MARISAT system usage costs, 2) earth station to user circuit costs, and 3) shipboard and shore-based terminal costs. The costs related to item 2) can be minimized by taking advantage of the lower cost and convenience of domestic satellite circuits that are currently available. The total projected incremental cost of the service appears to be acceptable for transmission of selected seismic data and all of the low volume data.

The technical outlook for this service is good and the remaining problems can be solved with available technology. The final cost of the service will be determined by both tariff and regulatory issues.

Introduction

It has long been apparent that the introduction of the MARISAT system would lead to many new communications applications for the maritime community. One application, recognized at an early date, is to provide ship-to-shore, high-speed, data transmission service.

In another technical arena, seismic exploration continues after many years to prove its value in the location and development of offshore petroleum deposits.

The past decade has witnessed remarkable strides in these two separate and highly specialized technologies. Over the past two years, however, studies and tests have indicated the possibility of an application of marine satellite technology which could significantly improve the speed with which the seismic survey industry delivers its product.

This paper addresses the possibility of a satellite service to transmit seismic data from a survey vessel to shore-based computing facilities and technical personnel. The technical feasibility of 56-KBPS data transmission has been tested and the results of those tests are summarized. A system operational analysis is presented and the estimated production speed and service costs are discussed.

Overview of Seismic Survey Technology

The petroleum industry has, for many years, employed seismic exploration methods in the location and development of offshore petroleum deposits. In the past, two-dimensional seismic methods have been used extensively and they continue to be of proven value. Three-dimensional seismic methods have been introduced in recent years as an advanced tool for use in the precision mapping of developing offshore fields. The petroleum industry relies on this information in making decisions concerning the allocation of their development resources.

Timely decisions must be made and, therefore, a usable seismic product is needed as quickly as possible. Unfortunately, the rigors of seismic data collection, the resulting data volume and the complexity of computer processing all tend to lengthen the turnaround time.

Traditionally, marine seismic exploration consists of an offshore data collection cycle followed by a shore-based processing cycle. Results are not generally processed and interpreted until after the vessel has left the prospect area. Occasionally, this delay results in vessels being forced to make long and expensive return voyages to resurvey prospect areas which had originally yielded erroneous or inadequate results. This situation creates a need for intermediate results which can be made available in parallel with the data collection activity.

Two potential alternatives could reduce turnaround time and provide valuable intermediate results:

(1) Place computing capability and technical support personnel aboard the seismic vessel,

or

(2) Transmit the data to shore-based computer facilities and technical personnel.

There are limitations on the physical size and processing power of computer systems capable of operation aboard a seismic survey vessel. There are also limitations on the technical personnel that can

Copyright © American Institute of Aeronautics and Astronautics, Inc., 1980. All rights reserved.

be accommodated on these ships and it is increasingly difficult to attract individuals willing to ride seismic vessels. The problem is particularly acute in the case of the geophysicists required to make data processing interpretations and decisions.

MARISAT Overview

The MARISAT communications satellite system was developed specifically for two separate and distinct users — the U.S. Navy and maritime industry.[1] The three geostationary satellites in the system were launched in 1976 and are positioned such that they cover the Atlantic, Pacific, and Indian Ocean regions. U.S. ground stations at Southbury, Connecticut, and Santa Paula, California, operate with the Atlantic and Pacific satellites respectively. The ground station for the Indian Ocean satellite is in Yamaguchi, Japan. A number of approved shipboard terminals are available and typically they consist of two separate units — an above-deck complement including RF high-power amplifier, low noise receiver and a 4-foot-diameter parabolic antenna that is compensated for ship motions. The necessary electronics for modulation, access, control and frequency conversion are located below decks. Worldwide telephone, voice-grade data, and telex services are provided through each MARISAT ground station which interconnects with both domestic and international common carriers. The coverage of the MARISAT satellite and the location of the U.S. ground stations are shown in Figure 1.

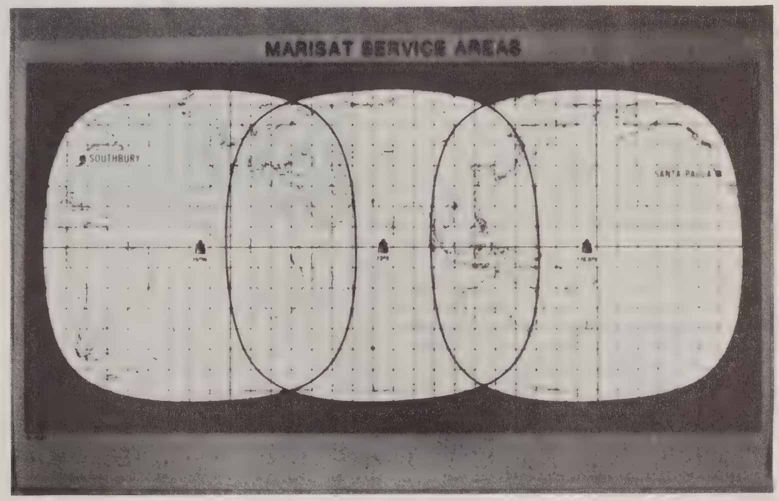

Fig. 1

About 300 MARISAT ship terminals have been installed. Approximately 10% of these terminals are on seismic data collection vessels and this represents about 30% of the industry's worldwide fleet. High-quality, reliable voice circuits offer a measure of privacy not previously available in marine communications. Telex is the international standard 50-baud service that is compatible with current worldwide systems. Data may be transmitted over the MARISAT voice circuit at rates up to 2400 BPS. Distress signals are supported by the system and are automatically relayed to the U.S. Coast Guard or the proper foreign authority.

Presently, data services are limited to those possible over a voice-grade terrestrial telephone circuit. Data transmission at speeds above 2400 BPS is not currently available with the MARISAT system. Due to ship terminal receiver limitations and the relative sizes of the mobile shipboard antenna and the ground station antenna, more communications capacity is available in the ship-to-shore direction than in the opposite direction. Higher satellite power levels are required for transmission to the small diameter shipboard antenna systems than to the larger ground station antennas.

Discussions with potential users led to the decision to consider 56-KBPS data transmission as an initial service application. It was decided that a feasibility test and demonstration should be conducted at sea to evaluate the performance possible from the system.

Feasibility Test

Arrangements were made to conduct a feasibility test[2] in the North Sea aboard the M/V J.E. Jonsson, a seismic exploration vessel operated by Geophysical Service Inc. The ship is 168 feet long and displaces 1,008 gross tons. It is equipped with a Scientific-Atlanta Model SA-3055 MARISAT terminal. Modulation and Forward Error Correction (FEC) equipment elements augmented the existing terminal equipment on the ship and at the shore station. Rate one-half convolutional encoding was built into the Quadriphase Phase Shift Keyed (QPSK) modulator used on the ship and the input data stream to the coder/modulator was provided by a bit error rate tester operating at 56 KBPS.

Existing laboratory equipment was redesigned to operate at an effective data rate of 56 kilobits and the package was mechanically modified to be suitable for the anticipated shipboard test environment. Tests of the modified equipment with the MARISAT simulator at COMSAT laboratory and via the MARISAT satellite demonstrated the expected performance of the test components in a static environment.

Test Equipment Description

Figure 2 is a block diagram of the equipment tested. A Bit Error Rate test set was used to generate an input pseudorandom sequence at 56 KBPS (kilobits per second). This data stream was then encoded at 1/2 rate to provide FEC. The encoded data stream entered the QPSK modulator at a rate of 112 KBPS and with an IF frequency of 90.8 MHz which was compatible with the MARISAT terminal used. This signal was upconverted to a frequency of 1640.8 MHz by the terminal, transmitted to Atlantic MARISAT satellite and relayed to the Atlantic ground station in Southbury, Connecticut.

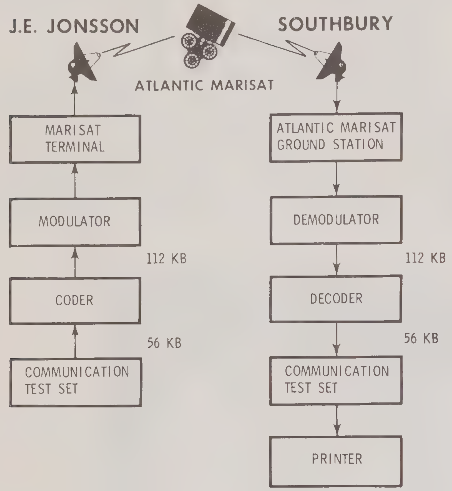

Fig. 2

At Southbury, the received signal was filtered and demodulated to a digital data stream at a rate of 112 KBPS. This data stream was then decoded to detect and correct data errors and provide an output at 56 KBPS which went to a data test set of the same model as used on the shipboard system. The test set at the ground station checked each received bit against an identical internally generated pseudorandom sequence. Each errored bit was counted by the test set and printed on an attached printer.

The shipboard test equipment was packaged in a separate rack located to the left of the MARISAT terminal as shown in Figure 3. The equipment drawer with the combined coder and modulator is located on the top and the communication test set is at the bottom of the rack. A chart recorder, meters, and a coaxial switch are located in the center of the rack. The switch is used to select either a normal MARISAT voice channel or a test data channel as input to the MARISAT terminal.

The request for start-up of operations was coordinated through the MARISAT operator using normal telephone service. Support personnel at the ground station provided the required circuit patch and monitored the operation of the shore-based test equipment. Simplex shore-to-ship voice or teletype was available after the ship terminal equipment had been switched to transmit data; and it was used to feed pertinent details of the test in progress back to the operators aboard the vessel. Test runs were set up to continue for several hours at a time depending upon existent ship motion conditions, circuit availability, and support personnel schedules.

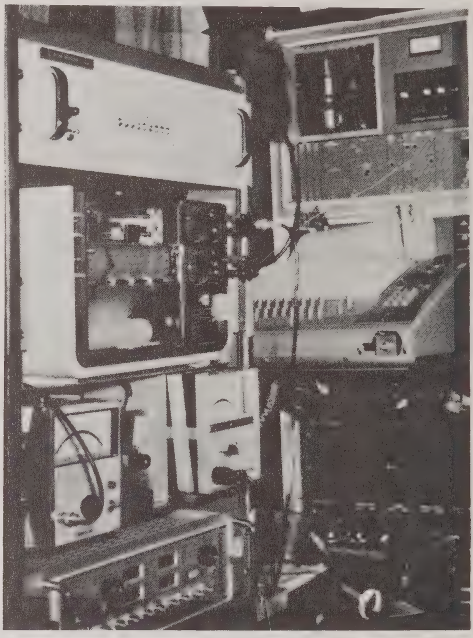

Fig. 3

During the test period, a wide range of environmental and ship operational conditions were encountered. The elevation angle from ship to satellite was about 17° as the ship operated in Storfjorden Fjord in Norway (62.5°N, 7°E) and was approximately 23° when the ship was in the Moray Firth in Scotland (58°N, 3°W). The typical link budget of Table 1 shows that with expected atmospheric and propagation losses, an energy per bit of 12.2 dB to 14.0 dB could be provided. Prior to the shipboard tests, laboratory assembly tests were performed and they indicated that the shore station, soft-decision-decoding/QPSK modulation equipment would provide a Bit-Error-Rate (BER) of better than 1×10^{-5} at E_b/N_o above 5 dB to 6 dB. This theoretically calculated performance was confirmed during the shipboard tests with shore station measurements.

Test Results

Over a two-week test period, there were approximately 136 hours of experimental tests. Tests were initiated any time the shipboard motion permitted work activities (characteristically, for continuous ship rolling motion of less than 10°). During those test periods the link "Availability"

Table 1

UPLINK			
Ship Transmitter Power		(watts)	37.2
Diplexer/Feed Loss		(dB)	0.6
Ship Antenna Gain		(dB)	23.5
Ship EIRP		(dBW)	38.6
FSL*		(dB)	188.6
Losses		(dB)	
Wet Radome	0.5		
Polarization Coupling	0.2		
Atmospheric Absorption	0.4		
Satellite G/T		(dB/°K)	-15.9
C/No			
Without Losses		(dB-Hz)	62.7
With Losses		(dB-Hz)	61.6
Flux Density			
Without Losses		(dBW/m^2)	-124.3
With Losses		(dBW/m^2)	-125.4
Saturation Flux Density		(dBW/m^2)	-100.6
Input Backoff			
Without Losses		(dB)	23.7
With Losses		(dB)	24.8
DOWNLINK			
Satellite Saturation EIRP		(dBW)	20.5
Carrier Output Backoff**			
Without Losses		(dB)	17.5
With Losses		(dB)	18.5
Carrier EIRP			
Without Losses		(dBW)	+3.0
With Losses		(dBW)	+2.0
FSL ***		(dB)	196.9
Losses		(dB)	
Atmospheric Absorption	0.3		
Rain Attenuation	0.5		
Polarization Coupling Loss	0.4		
Rain-Induced Sky Noise	1.2		
Shore Station G/T		(dB/°K)	33.0
C/No			
Without Losses		(dB-Hz)	67.7
With Losses		(dB-Hz)	64.3
C/Io **			
Without Fade		(dB-Hz)	81.7
With Fade		(dB-Hz)	83.3
TOTAL LINK			
C/No			
Without Losses		(dB-Hz)	61.5
With Losses		(dB-Hz)	59.7
Eb/No			
Without Losses †		(dB)	14.0
With Losses ‡		(dB)	12.2

* Elevation Angle = 23°, 1640.5 MHz (Ship in Moray Firth, Scotland).

** Assumes 3 to 6 voice carriers.

*** Elevation Angle = 15°, 4197 MHz (Southbury Shore Station).

† Assumes 56-KBPS Data Rate.

‡ MARISAT F-1 operating L-Band Receiver 1, C-Band TWT 1.

was defined as that percentage of time, after initial carrier acquisition, when carrier lock was accomplished and data were being received. The minimum time period for loss of acquisition under this definition was 1 second because of test equipment limitations. The BER was also recorded and is defined as the ratio of bits in error to the total number of bits transmitted during a period of availability.

A summary of the test results is presented in Table 2. The test results are divided into five separate sequential test periods covering locations along the route of the vessel. Figure 4 illustrates the test route with vessel locations marked at 6-hour periodic time intervals. The first test period extended over two days while at dockside in Middlesbrough, Endland. A total of 29.7 hours of test data was collected without a circuit dropout (100%) availability) and the average bit error rate measured was 2.1 x 10^{-8}. This rate is roughly equivalent to 1 error for every 50 million transmitted bits assuming the errors to be uniformly distributed with time. At a data rate of 56 KBPS, this equates roughly to 1 errored bit every 15 minutes or 120 errored bits over the 30-hour test period. The errors occurred in bursts of about 40 bits or less and a peak error rate of 1.5 x 10^{-10} was observed

Table 2

DATES	LOCATION	TOTAL TEST HOURS	AVAIL-ABILITY (PERCENT)	BER	SEA ENVIRONMENT AND VESSEL MOTION
11/15 THRU 11/16	DOCKSIDE MIDDLESBROUGH	29.7	100.0	2.1×10^{-8}	QUIESCENT
11/17 THRU 11/19	ENROUTE ENGLAND TO NORWAY	32.5	97.2	1.8×10^{-7}	HIGH WIND AND WAVES; SHIP ROLL TO 20°
11/20 THRU 11/23	OPERATING IN STORFJORDEN FJORD	17.8	98.4	7.4×10^{8}	CALM WATERS; NEGLIGIBLE SHIP MOTION
11/23 THRU 11/24	ENROUTE NORWAY TO SCOTLAND	6.2	92.4	5.3×10^{-8}	VERY HEAVY SEAS; WINDS TO 40 KNOTS; WAVES TO 20 FEET; PITCH ANGLES AS LARGE AS 20°
11/25 THRU 11/29	OPERATIONS IN MORAY FIRTH	50.2	95.6	1.6×10^{-6}	CLOUDY AND RAINY; SOME HEAVY SEAS; RAPID PITCH MOTIONS PEAKING AT ABOUT 12°; OCCASIONAL ROLL TO 10°

during one 13-hour period. These bit error rates compare quite favorably to terrestrial and other satellite communication circuits.

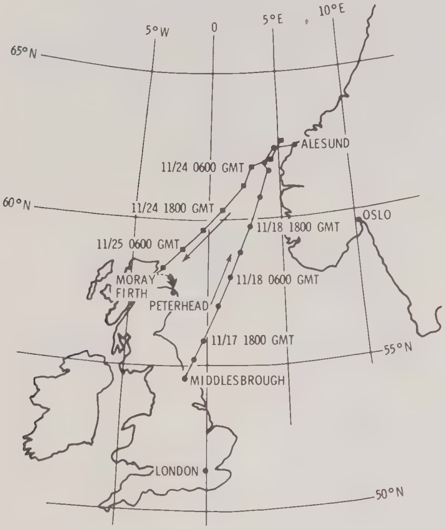

Fig. 4

The start of the sea test was delayed for a day due to severe weather conditions in the area. Soon after embarking on the journey from Middlesbrough to Alesund, Norway, the remnants of this storm were encountered. High winds and waves produced peak ship rolls in excess of 20° during the test, but 32.5 hours of data were recorded during the 2-1/2 days required to cross the North Sea. Circuit availability dropped to 97.2% and the average bit error rate observed was 1.8×10^{-7}. Tests had to be completely suspended at times due to extreme ship motion when the vessel was rolling beyond 30°.

While operating in the Storfjorden Fjord near Alesund over a 3-1/2-day period, both the circuit availability and bit error rates improved. The waters were relatively calm in the fjord; however, some signal degradation was noted when the vessels periodically made rapid heading changes.

Very heavy seas, high winds and waves, and peak pitch angles to 20° were observed on the return voyage from Alesund to northern Scotland. Only 6 hours of data were collected during the 45 hours required for crossing the North Sea. It was not possible to collect additional data due to physical conditions. The measured circuit availability was the lowest recorded during the test. The antenna stabilization system on the Jonsson's terminal was designed to operate at pitch angles of less than ±7.5° and with pitch motion periods of 2π seconds or greater. These specifications were frequently exceeded during this part of the voyage; however, the bit error rate was better than expected for the prevailing conditions.

The final tests were performed in Moray Firth off the coast of northern Scotland. This series of tests involved the greatest number of test hours and operation in a variety of weather and sea-state conditions. Ballasting of the seismic streamer and related preparations for data collection were accomplished early during this period; however, the high sea states generated noise conditions which delayed effective seismic data collection for several days. Rapid pitch motion, peaking at about 12°, caused the highest average bit error rates which were observed during the tests. However, this 1.6×10^{-6} bit error rate is adequate for high data transmission efficiency if the proper protocol and blocking techniques are chosen.

The test allowed performance evaluation over a wide range of operational extremes for the seismic vessel. Measured bit error rates actually exceeded the predicted value of 10^{-6} for much of the time. Circuit availability in the upper 90% range is typical for most of the test, and this exceeds the expected results. The performance data show that the circuit is suitable for data transmission and the relatively trouble-free operation of the equipment indicates the potential for good system reliability.

Domestic Interconnect Circuit

The test results demonstrate the feasibility of transmitting and controlling data between an operational seismic vessel and a MARISAT shore station. An additional circuit is required to complete the data transmission path between the shore station and the user's computer facility; and suitable duplex channels can be provided either by domestic satellite or by terrestrial links. Terrestrial links display distinctly shorter propagation delay time compared to satellite links. With the geostationary altitude of 22,600 miles, a signal relay through the satellite between earth stations requires approximately 0.25 second. Via terrestrial facilities, the same signal could travel across the country in about 0.01 second. While these are extremely short intervals, the additional delay in satellite propagation time can be a significant factor in the efficiency of the data transmission if appropriate communication protocols are not used. Protocol considerations will be discussed in a later section of the paper.

Satellite links also have advantages over terrestrial links, the more significant being cost and reliability. The benefit of lower cost satellite links is just beginning to be realized by U.S. users who are utilizing new services offered by U.S. domestic satellite suppliers. American Satellite Corporation (ASC) first introduced a low-cost, customer premises private earth station (PES) that allows users to establish direct 56-KBPS satellite links. The service utilizes transponder capacity on the WESTAR satellite and is billed at a flat monthly rate for each PES and each satellite duplex channel. This arrangement results in substantial cost savings in the case where a PES supplies several wide-band circuits. Additional domestic satellite services have been approved by the Federal Communications Commission and announced by RCA (via the SATCOM satellite) and by AT&T (via the COMSTAR satellite); and it is possible that Satellite Business Systems (SBS) will also offer such services via their own satellites.

Improvements in satellite circuit reliability and quality compared to terrestrial links result in large part from the smaller amount of equipment involved in supplying the circuit. Terrestrial circuits employ cables, microwave links, and various monitoring and control offices — often, all in tandem. Local telephone companies are also involved since they must supply tail circuits between the long lines office and the user's facility. Satellite circuits employing PES terminals avoid this equipment and the related problems. PES stations with automatic 100% back-up for all systems and emergency power are quoted with reliability of better than 99.95%!

The advantages of satellite over terrestrial circuits force an obvious choice for the interconnect circuit between the MARISAT shore station and the user's computer facility. Figure 5 illustrates the network configuration which would probably be used for this service during the early 1980's. Ocean coverage is limited to Atlantic and Pacific satellites at elevation angles above 10°. Use of the Indian Ocean satellite service is not immediately planned due to the need for a triple satellite-hop to effectively serve locations in the central part of the U.S. The Atlantic and Pacific MARISAT satellites serve most of the regions of present interest to the seismic industry with one major exception being the western Gulf of Mexico area.

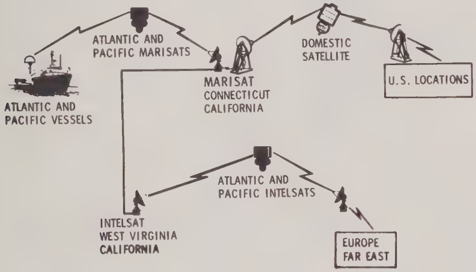

Fig. 5

Interconnects to U.S. locations are assumed to be via a domestic satellite. Exceptions would be those cases where the user's facility is near the MARISAT shore station. Vessels operating in the Atlantic will transfer their data through the Southbury, Connecticut, shore station and co-located PES will route the data via the domestic satellite to the user computer facility. Pacific vessels will pass data through the Santa Paula, California, shore station in a similar manner. Data transmissions to Europe, the Far East and other served countries will be accomplished via an INTELSAT satellite. In Figure 5, the solid line between the MARISAT shore stations and the INTELSAT stations is a terrestrial link. This link eliminates a triple, satellite-hop delay. Tail circuits from the INTELSAT stations in the served countries and the user's facility are also assumed to be terrestrial.

A new, international maritime satellite organization, INMARSAT, came into existence in July 1979, with the signing of an agreement by nations representing more than 95% of the eventual investment capital. Coordination efforts now underway will assure a smooth operational transition from MARISAT to INMARSAT.

INMARSAT is scheduled to be in operation in 1982 and additional shore stations are planned worldwide. This development should allow worldwide coverage and could provide for direct interconnect of INTELSAT stations with INMARSAT stations.

Communication Protocol

To efficiently use the data transmission circuits between the user and an operational seismic vessel, it is necessary to provide a control scheme or protocol for the communication circuit. As mentioned previously, the major disadvantage of a satellite circuit is the propagation delay. The seismic service circuits will generally involve two satellites resulting in a double-hop delay. The propagation delay for each satellite-hop is approximately one quarter of a second, therefore, the total time for data to propagate over two satellite links and for control characters to be returned to the originating end is approximately 1 second. (Additional delays are encountered for propagation through computers, modems, and related communications equipment.)

Data are normally divided into fixed length blocks with identification, source and destination, error control, and other overhead data appended. Control characters are used to establish communication between two processors over a link and also to signify when data are received and to indicate various error conditions. In the event of an error, a block or packet of data is retransmitted until received correctly.

A simple protocol method involves waiting for each block of data to reach its destination and then signaling the source to send the next block. This method results in poor efficiency over satellite circuits due to the magnitude of the propagation delays. More advanced methods involve continuously transmitting blocks of data until an error is detected and then either 1) selectively retransmitting the errored block out of sequence and reinserting it (replacing the errored block) in a buffer at the receiving end, or 2) backing up to the block detected in error (Go-back-N), retransmitting this and all successive blocks. Either scheme involves buffer memories at both sending and receiving terminals.

Figure 6 illustrates the comparison of these two methods of control protocol. Channel throughput efficiency is plotted versus bit error rate for a fixed block size of 9000 bits and 48 overhead bits.

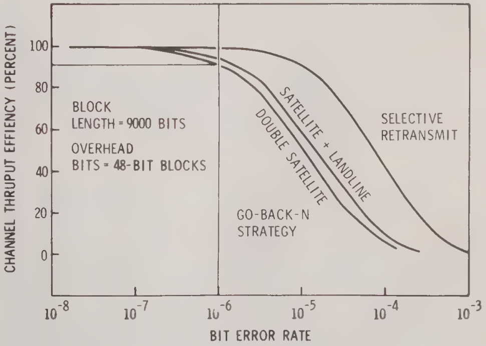

Fig. 6

For bit error rates less than 10^{-6}, either method will provide more than 90% throughput efficiency. The selective retransmit strategy becomes more beneficial at higher bit error rates. The feasibility sea test indicated that the bit error rate should typically be less than 10^{-6} and that errors would have a bursty rather than a uniform distribution.

Selective retransmission strategy is much more complex than Go-back-N, and no standard protocols have been defined for this strategy. Systems do exist that use selective retransmission protocol[3/] at these speeds, but they are not directly compatible with other communication networks. HDLC/X.25[4/] is a standard system and communication protocol that uses the Go-back-N strategy and it is compatible with current and planned systems.

Operational Utilization

A marine seismic survey is a data intensive operation. Significant numbers of data tapes are collected and normally stored aboard the vessel until it either reaches port or a data drop can be arranged. Table 3 illustrates the expected data volumes for combinations of sample rates and number of channels. A productive seismic vessel will commonly ship several thousand 2400-foot reels of 1600-bpi tape to a computing center every two or three weeks. Significant increases in data volume will occur as the number of channels recorded in marine work continues to rise. Nonseismic data including navigation, gravity and magnetic data, and other types of prospect data are typically of low volume compared to those of the seismic data. Table 4 summarizes the volume of nonseismic data that would be created for the same operational assumptions depicted in Table 3. The number of traces and sample rates has a negligible effect on this data volume. The number of equivalent tapes created between port calls is extremely small when compared with the seismic tape volume.

Table 3

	NUMBER OF TRACES/SAMPLE RATE		
	48/2 OR 96/4	96/2 OR 192/4	240/2 OR 480/4
BITS/RECORD (10^6)	3.0	6.0	14.6
BITS/KM (x 10^6)	120.0	240.0	585.6
KM/TAPE	3.0	1.5	0.6
AVERAGE NO. TAPES/DAY	33	67	167
TAPES/PORT CALL	660	1340	3333 853 AT 6250 BPI

ASSUMPTIONS: SEG B DFS V/VI. 6-SEC RECORDS; 25-M SHOTPOINTS; VESSEL SPEED, 10.8 KM/HR (6 KNOTS); 2400-FT TAPES AT 1600 BPI; VESSEL DURATION, 20 DAYS BETWEEN PORT CALLS

Communication costs and data transmission speeds (for current technology; satellite systems) both preclude the transmission of all the data collected by a productive seismic vessel; however, a selectively employed 56-KBPS data service could be used to reduce turnaround time for seismic products and to allow the provision of intermediate processed and interpreted results in parallel with ongoing survey work. Currently, a mismatch of about seven to one exists between the seismic data collection rate and the 56-KBPS transmission rate assuming the 48-trace, 2-millisecond or the 96-trace, 4-millisecond combination as described in Table 3. Therefore, to achieve the maximum benefit, it is necessary to select the correct type of data for transmission.

Table 4

- PROSPECT INFORMATION
- NAVIGATION DATA
  - PRIMARY NAVIGATION SYSTEM
  - SECONDARY NAVIGATION SYSTEMS
  - STREAMER TRACKING SYSTEM
- PROCESSING PARAMETERS
  - DFS-RELATED DATA
  - WATER DEPTH, STREAMER DATA, AIRGUN ARRAY DATA, OFFSET
- GRAVITY/MAGNETICS
  - ASSUMPTIONS: 25-M SHOTPOINTS; VESSEL SPEED, 10.8 KM/HR (6 KNOTS); TAPE DENSITY, 1600 BPI; TAPE LENGTH, 2400 FT

BITS/SHOTPOINT x 10^6 = 0.005
BITS/KM x 10^6 = 0.2
KM/TAPE = 1600
TAPES/PORT CALL = 1.25

Total turnaround time for the seismic product has to be measured from the moment the seismic data are collected (when the first shot is fired) until the final maps and sections are delivered to the individual responsible for exploration decisions. Delays in storing the data aboard the vessel are compounded by transportation and often, export and import delays. Most seismic computing centers are set up for the barrage of data that comes with the arrival of a marine shipment. Provisions are made for rapid cataloging and input of the raw data. Much of the processing must proceed sequentially and cannot be overlapped due to data dependence. This sequential processing creates a significant portion of the turnaround delays. Intermediate displays must be produced for input crew analysis and decision-making between processes. The successful completion of processing tests at an early stage is the key factor in maintaining the flow of seismic data through the processing sequence. The navigation data postprocessing is essential to the completion of a 3D analysis. The interdependence of key sequential processes is illustrated in Figure 7 for a typical marine 3D process sequence.

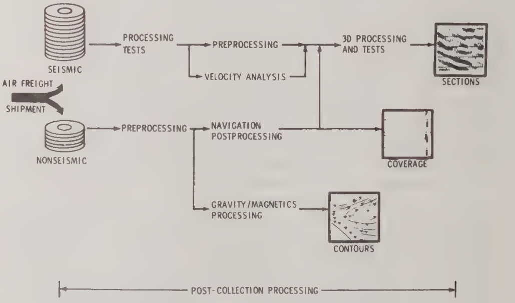

Fig. 7

Intermediate processed and interpreted results have not been generally available while a vessel was still on the prospect. The obvious exception was a large prospect requiring an extended period for the vessel to collect all data. Even in this case, time delays can still create difficult problems.

A strategy for the use of high-speed data transmission, illustrated in Figure 8, would achieve maximum impact with a limited volume of data transmission and related costs. All nonseismic data would be transmitted due to the low volume and the need for the navigation data to allow completion of 3D processing. Navigation data would be processed in parallel with data collection and 3D coverage would be determined before the vessel leaves the prospect area. Selected seismic data would be transmitted to allow processing tests and creation of intermediate interpreted displays. Based upon these tests, processing parameters would be determined and evaluated before the vessel leaves the prospect area. Optional data transmissions (indicated by dashed lines in Figure 8) could be deferred until the exploration decision-maker deems them necessary and prudent.

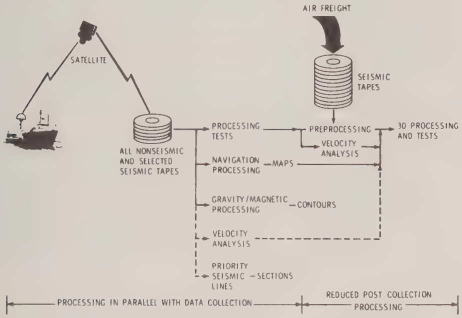

Fig. 8

The majority of the seismic data would still be air-freighted to the processing center where completed processing tests and preselected parameters would allow a reduced post-collection processing sequence and a reduced product turnaround time.

Estimated Costs and Transmission Time

Assuming the technical and operational feasibility of high-speed data transmission, the following 3D prospect example uses typical values of data volumes, transmission times, and costs to examine economic practicality.

An assumed 8- by 10-kilometer prospect area with 100-meter seismic grid line spacing and 25% crosslines will necessitate the collection of 1000 kilometers of data. If shotpoints are spaced at 25-meter intervals and 96 traces are recorded at a 4-millisecond sample rate (6-second records using an SEG-B recording format),[5] 40,000 shotpoints will be collected and the total seismic data volume will be 1.2×10^{11} bits. The total nonseismic volume is assumed to be 2×10^{8} bits. Transmission at 56 KBPS with 90% efficiency will result in a data rate of 1.8×10^{8} bits per hour. Converting this back to kilometers of seismic data transmitted per hour results in a figure of 1.5 kilometer per hour or about 7 times slower than the data collection data rate.

Figure 9 illustrates the incremental cost to transmit various recommended data sets versus the 56-KBPS communication tariff (cost for one hour of satellite data transmission in U.S. dollars). The incremental (added) costs are expressed as a percent of the total prospect data collection plus data processing costs. The fixed costs (indicated in the shaded area) represent the allocated costs of domestic satellite interconnect circuit, and the vessel and shore-based data transmission terminals. In today's dollars, the fixed costs would amount to about 1.25% of the example prospect's total cost. Nonseismic data would add a negligible percentage to this basic cost. The cost to transmit 1% of the seismic data for processing tests would range from a negligible percentage to an additional 0.8% and the cost to transmit 10% of the seismic data (required for velocity analysis) could cost up to an additional 8%. Total additional costs could be as high as 10.2%.

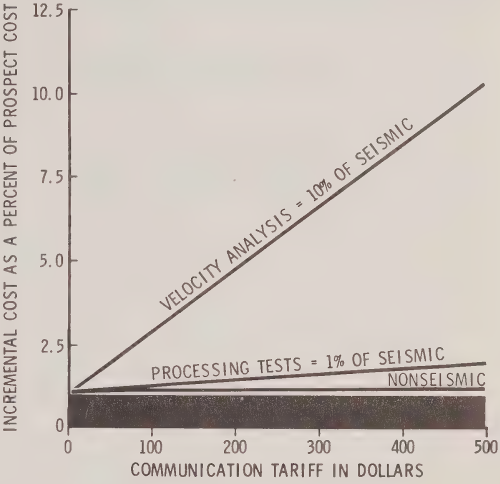

Fig. 9

Current thinking on the MARISAT tariff ranges toward the upper extreme of the scale. However, the volume of data that the seismic and other industries would like to transmit and hence the number of hours of utilization will undoubtedly influence the level of the final tariff. The use of terrestrial circuits for the interconnect between the customer facility and the MARISAT shore station, or the use of INTELSAT via international common carriers will increase the fixed costs above those shown (which assume a domestic satellite). The terminal equipment costs assumed in the fixed costs estimated may also vary with the manufacturer.

It would require 1.1 hour to transmit all the nonseismic data for the prospect. A total of 6.6 hours would be required to transmit 1% of the seismic data and 66.6 hours for 10% of the seismic data. Almost three days of transmission time would be required to send all the data described in Figure 9.

Conclusions

It has been demonstrated that 56-KBPS data transmission is both technically and operationally feasible between seismic vessels and shore-based computer facilities. Furthermore, this capability appears to be a viable alternative to on-board data processing. An acceptable tariff and use with selected data, should lead to a cost-effective and beneficial service for the seismic exploration industry.

References

1/ Lipke, D.W., et al, "MARISAT — A Maritime Satellite Communications System" COMSAT TECHNICAL REVIEW, Vol. 7, No. 2, Fall 1977.

2/ Calvit, T.O., "A MARISAT 56 KBPS Ship-To-Shore Data Service" Presented at the 1979 San Francisco RTCM Assembly Meeting, April 23-26, 1979.

3/ Martin, James, "Future Developments in Telecommunications, Chapters 29 and 33, Prentice-Hall, Englewood Cliffs, NJ. 1977.

4/ Gilbert, D. and Perry, J., "The Significance of X.25" Mini-Micro Systems Magazine, September 1979.

5/ Society of Exploration Geophysicists (SEG), "SEG B tape format specification", P.O. Box 30987, Tulsa, OK, 74101.

80-0525

RCA SATCOM SYSTEM EXPANSION

W. BRAUN[*] AND J.E. KEIGLER[**]
[*]RCA American Communications, Inc., Piscataway, N.J.
[**]RCA Astro Electronics, Princeton, N.J.

Abstract

The continuing rapid increase in channel demands on the RCA Americom domestic satellite communications system has resulted in a planned system expansion both in the number of satellites and in the traffic capacity per satellite. Following a modest up-rating of the next several Delta-launched spacecraft, a larger second generation satellite design will be introduced in the mid-'80's that exploits the launch economy and payload capacity of the space shuttle. System profitability studies have concluded that this expanded domestic network should remain at C-band (6/4 GHz), with traffic capacity per satellite increased by a combination of higher EIRP, improved filter characteristics, and terrestrial equipment advances. Satellite life and reliability will be extended by the combination of increased propellant capacity, additional component redundancy, and greater power system capacity. Earth station improvements to complement these spacecraft features and so realize a doubling of per channel capacity include both the rf stages and more efficient modems. The resultant lower annual cost per channel will allow Americom to offer new services as well as continue to expand the present customer base.

I. Introduction

With the high utilization of the first two 24 channel RCA Satcom satellites during their four years of service, RCA had planned a third satellite for service in early 1980. This F-3 satellite retained the same channelization and EIRP as the first two but incorporated four spare TWTAs and higher capacity batteries to achieve improved reliability over the eight year design life; unfortunately it never attained operational status, being destroyed as a result of malfunction of the apogee motor. The fourth and fifth satellites of this series are now in production for launch in 1981 to replace the unsuccessful F-3 and to provide additional capacity with a four spacecraft system. Minor modifications have been incorporated to extend the orbit life to ten years with improved communications and attitude control performance.

Planning for replacement of the first two satellites in 1983-4 plus expansion of the satellite constellation, Americom has selected a second generation spacecraft design with higher traffic capacity yet lower annual cost per channel. Like the original series, the Satcom II satellites will be designed, fabricated, and controlled into orbit by RCA Astro Electronics. These new spacecraft will exploit the launch economy plus the weight and volume capability of the NASA space shuttle to provide increased in-orbit payload, life, and reliability. Corresponding improvements in ground station and signal processing equipment are planned to complement these satellite characteristics so that system traffic capacity and profitability may be maximized.

II. System Requirements

The RCA Americom system serves four distinct domestic communications traffic markets: commercial, government, video/audio, and Alaska.(1) Commercial Communications Services provides private leased channels for voice, data, and facsimile traffic via major RCA earth stations near New York, Chicago, San Francisco, Houston, Atlanta, Los Angeles, and Denver plus several smaller stations on off-shore drilling platforms. Growth in this traffic since 1977 and forecasts through 1982 are shown in Figure 1. Government Communications Services provides voice, video, and high speed data services to federal agencies (NASA, DoD, NOAA, etc.) via twenty-five RCA-owned earth stations located on various government installations; government traffic has more than doubled in the last two years and is projected to multiply by factor of three in the next three years. Video and Audio Services provides point-to-point transmission and multipoint distribution of television and radio news service to broadcasters, cable TV operators, and publishers. Expansion has been most rapid in the network of receive-only stations owned and operated by the CATV industry, with approximately 1500 such stations now being served by the RCA Satcom satellites and 1300 more scheduled by the end of 1980. Alascom Services provides long distance message toll service to Alaska Communications, Inc., the common carrier for both intra- and inter-state message and TV traffic in Alaska, whose demand for transponder channels has increased from 9 in 1977 to 16 in 1979 and is expected to grow to approximately 20 in 1982.

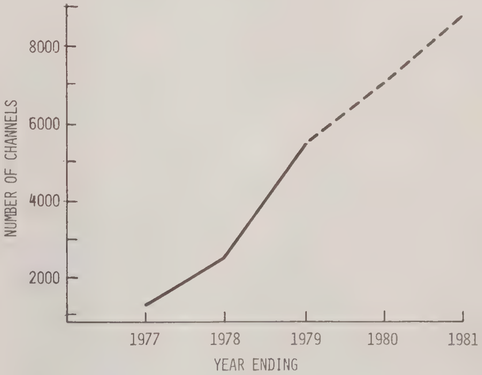

Figure 1. Private Leased Channel Traffic Growth on the Americom System

---

** Associate Fellow AIAA

Copyright © American Institute of Aeronautics and Astronautics, Inc., 1980. All rights reserved.

Expansion of the RCA Americom system to serve the growth of these four business sectors must satisfy the criterion of commercial viability. To this end, technological enhancements are measured against the twin benchmarks of performance improvement and return on investment. Primary objectives of the system expansion are increased traffic capacity per satellite, longer satellite life with improved reliability, and compatibility with existing terrestrial and space facilities. Applying the above criterion of profitability to these objectives has resulted in a system expansion plan which is primarily a product enhancement rather than product innovation. This decision to expand the system via product improvement was the result of two major technical/economic trade-offs: specialized vs. general purpose satellite design and C-band (4/6 GHz) vs. K-band (12/14 GHz) service.

Selection of specialized satellite and earth station types for each of the four classes of traffic carried by the Americom system offers the advantage of optimized configurations, thereby permitting competitive advantage within a given market. For example, in cable television, the transponder bandwidth could be reduced by one-third to allow 50% more channels within the allocated 500 MHz bandwidth, yielding a lower cost per channel and more channels per spacecraft. However, such a specialized design for this one type of traffic poses great difficulties in service restoration and adds costs to CATV systems for modification of the many existing stations. Furthermore, large investment in a specialized system is only appropriate for a market that is stable, mature, and predictable in its behavior, scarcely the case for commercial satellite communications where new technologies, services, and markets appear constantly. Conversely, new satellites and earth stations that are compatible with existing facilities obviate plant modification costs and simplify service restoration in event of catastrophic failure, a feature of great significance to satellite users. Satellite design decisions to ensure this compatibility with the large existing network include the choice of frequency band, transponder channelization, polarization, interconnectivity, and power levels.

Evaluation of K-band operation for the Americom system, either in lieu of or in addition to C-band (that is, either dedicated or hybrid satellites), focused on two key questions: would K-band enable RCA to penetrate and develop profitable communications markets not otherwise accessible, and is K-band necessary to accommodate the forecasted growth of the four Americom business centers? While K-band station locations are not limited by RFI congestion of terrestrial microwave networks, frequency coordination for C-band stations has become less formidable with precise on-site measurement of interference levels and the judicious use of natural or artifical screening. The K-band appeal of customer rooftop antennas is already being realized at C-band in numerous major business and government facilities which are located in suburban areas remote from metropolitan RFI congestion. While K-band has no proscribed downlink flux density limits, the C-band limit is on flux density per 4 KHz; therefore adaptive energy dispersal in which the energy spreading waveform is inversely proportional to the signal level can be used to meet this limit without sacrificing a constant fraction of the frequency deviation (and hence S/N) for dispersal purposes. In addition, the large downlink margins required at K-band to overcome the deep fades due to precipitation in the transmission path dictate high power transmitters that will necessarily be TWTAs for the next decade, while lower power C-band amplifiers can employ the more reliable solid state technology of GaAs FETs. Lastly, the economic attraction of a hybrid satellite with greater spectral capacity diminishes with the practical difficulties of orbit slot limitations, due to different spacings for C and K-band satellites as well as to restoration costs and operational complexity when partial failures occur.

RCA Americom has concluded from these studies that their traffic markets for the next decade can most profitably be served by concentrating current investment in upgrading the C-band system by earth station improvements together with a second generation satellite of increased capacity. Overall traffic projections can be accommodated at C-band by a system design which doubles per transponder capacity and deploys additional satellites into unused orbit locations.

III. Spacecraft Design

With the economic analysis of the total Americom network having determined that 24 channel, frequency reuse, C-band satellites comprise the most profitable approach to the mixed types of service provided, the design criterion for the second generation of satellities is again maximum communication capacity per unit cost. Maximizing this ratio entails a system design which both increases the traffic capacity and availability of each channel and reduces the life cycle costs based upon spacecraft hardware development, launch charges, and average satellite life. Availability of the space shuttle as the standard (and only U.S.) launch vehicle by the mid-80's time frame of Satcom II deployment introduces new factors, and concommittant design influences, into the equation.

Shuttle Launch Constraints

Utilization of the space shuttle vehicle represents constraints that are both physical and financial. Physically, the total payload characteristics of STS are well known, namely a cargo bay 15 feet in diameter and 60 feet long, with a maximum weight capacity into earth parking orbit of 65,000 pounds if optimally distributed. Dividing this capacity among the several payloads to be carried into orbit on a particular flight, each with its peculiar shape, mass, and ejection schedule, will generally result in a total cargo bay weight less than the 65,000 pound limit. NASA's announced pricing policy for STS payloads accounts for this inefficiency by a formula based upon the greater of the volume or weight fractions of total cargo bay capacity multiplied by 1.33 times the reimbursable cost per flight.(2) Thus the cost to each user is calculated as the larger of:

$$C_W = \frac{W}{65} \times \frac{4}{3} \times 31x10^6 = \$634x10^3\ W$$

or

$$C_V = \frac{L}{60} \times \frac{4}{3} \times 31x10^6 = \$689x10^3\ L$$

where

W = payload weight in thousands of pounds

L = payload length in feet

For these calculations each payload weight includes any recoverable cradle and airborne support equipment required in addition to the actual deployed parking orbit payload, and the payload length is the total of separation allowances plus the actual hardware length.

This pricing formula has led to some arguments that the optimum design for shuttle launched spacecraft should equalize the weight and volume fractions of shuttle capacity, or W = 1083 L pounds per foot. However, for a given communications satellite traffic capacity and mission life time, such an equal length and weight solution is neither necessary nor sufficient for lowest system costs. Rather, it is the sum of spacecraft cost plus the launch cost by the above NASA formula which is to be minimized. Basing the launch cost on the larger of shuttle weight or length fractions has resulted in the current trend to minimize the cargo bay length of the individual payloads. Horizontal, SSUS-A type installations are eschewed by competitive commercial users, and the now-standard SSUS-D installation is vertical rather than the original inclined concept. Alternately, the full-diameter, short length cylindrical type payload services some applications. The Satcom II design will employ the vertical installation approach to achieve maximum communications subsystem weight and power capability per launch cost. Table 1 summarizes the salient characteristics of the spacecraft design.

Table 1 RCA Satcom II Characteristics

Launch Vehicle	STS/PAM
Transfer Orbit Weight	3050 lbs.
Mission Life	10 yrs.
Transfer Orbit Stabilization	Spin
Synchronous Orbit Control	Stabilite®
End of Life Array Power	1000 W
Battery Capacity	80 A-hr.
Operating Transponder Channels	24
Spare Power Amplifiers	8
Receive Frequency Band	5.925 to 6.425 GHz
Transmit Frequency Band	3.7 to 4.2 GHz
EIRP Per Channel	34.5 dBw
G/T	-3.5 dB/K
Minimum Polarization Isolation	33 dB

Spacecraft Configuration

While the Satcom II spacecraft will be significantly larger and heavier than the original RCA Satcoms now in service, it will retain the basic features of its predecessors, namely three-axis body stabilization, sun-oriented solar panels, and cross-gridded antenna reflectors for frequency reuse, as shown in Figure 2. Propellant supply, power system capacity, and component reliability/redundancy will be sufficient to ensure ten years continuous operation of all channels. To realize higher traffic capacity of the 24 C-band transponder channels, each of the major communications subsystem elements will incorporate technological advances over the present designs: a shaped beam antenna increases gain over the coverage areas; a low-noise receiver further increases uplink carrier-to-noise; sharper multiplex filters decrease crosstalk and distortion interference; and higher power amplifiers of improved linearity increase signal-to-noise, reduce FDM interference, and increase capacity. The highly successful attitude and velocity control systems of Satcom will be up-rated for the larger structural configuration as will the array size and battery capacity for the higher power payload.

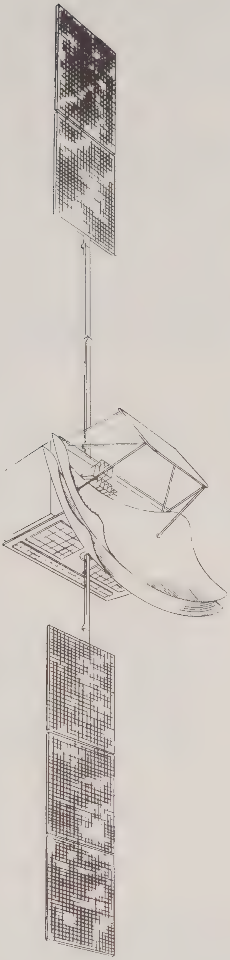

Figure 2. Satcom II Spacecraft Configuration

The tentative selection for the perigee stage is the up-rated SSUS-D (McDonnell-Douglas PAM), with its transfer orbit payload capacity of 2750 to 3100 pounds.

Communications Subsystem

Although the geographical areas of the expanded Americom network to be served by the Satcom II series are identical to those presently covered, namely CONUS, Alaska, and Hawaii, the antenna design will be more sophisticated to achieve higher gain over those areas as well as adapt to the relatively wide spacecraft longitude range to be accommodated. Shaping the antenna beam pattern to approximate the coverage area entails an oversized antenna reflector together with multiple feed horns whose size, location, power division, and relative phasing are the design variables to achieve the desired beam contour. For the wide longitude range to be spanned by the several spacecraft of the Satcom II series, different beam shapes are desired as illustrated in Figure 3 to optimize beam gain rather than employ a larger, lower gain beam that encompasses the sum of the coverage areas as seen from the several longitude stations. Pre-launch adjustment of the feed power-splitting and phasing network for a specific beam shape is planned, as the orbital station will be pre-assigned; however, some degree of in-orbit reconfiguration is also being evaluated to compensate for subsequent relocation of a spare satellite.

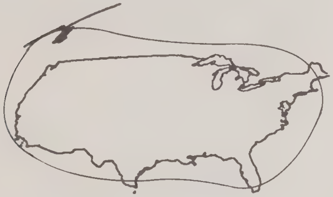

Figure 3a. Antenna Beam Coverage from 83W

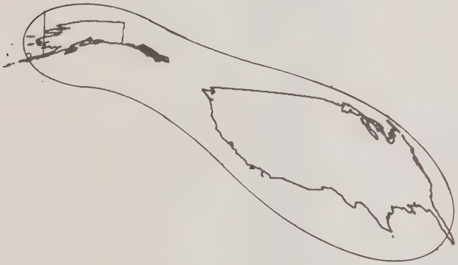

Figure 3b. Antenna Beam Coverage from 140W

Packaging the necessarily long focal length, multiple feed antenna within the limited height and volume between the vertically mounted spacecraft body and the shuttle orbiter bay doors precludes the conventional design of a front-fed antenna with an upright feed tower as used on Satcom I. The folded-optics approach illustrated in Figure 4 achieves the equivalent of the front-fed, off-set feed within this restricted volume with a rigid mechanical design that avoids mechanism and misalignment risks of a deployable design. As on the current Satcom satellites, the reflector is comprised of overlapped, cross-gridded surfaces to achieve the two orthogonal linear polarizations, with the vertical separation of the two surfaces providing a corresponding separation of their focal points that accommodates the two sets of feedhorns.

Each element of the Satcom II transponder incorporates design improvements that together with the higher antenna gain double the traffic capacity above the current satellite performance. The receivers use GaAs FETs in both the 6 GHz pre-amplifier and 4 GHz driver sections to achieve a 3 dB improvement in noise figure. Sharper channel band edge attenuation with lower in-band gain slope (and thus reduced cross-talk) is realized by advanced multiplex filter designs, with six-pole equalized-elliptic function characteristics for the input filters and four pole, elliptic function response for the output filters.

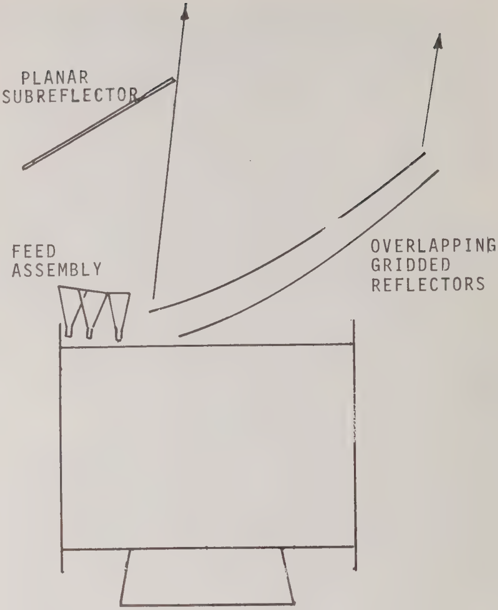

Figure 4. Folded Optics Antenna Concept

Both performance and reliability of the power amplifier will be significantly improved by the use of all solid state GaAs FET amplifiers in lieu of TWTAs(3). Figure 5 compares the linearity of an 8.5 watt RCA SSPA (solid state power amplifier) with that of the 8.5 watt TWTA to be flown on F-5 of the current Satcom series in 1981; Table 2 summarizes the resultant increase in channel capacity with this improved linearity. Elimination of the hot cathode life limitation and high voltage converter complexity of TWTAs will greatly increase the probability of amplifier survival for the full ten year mission. Transponder reliability is

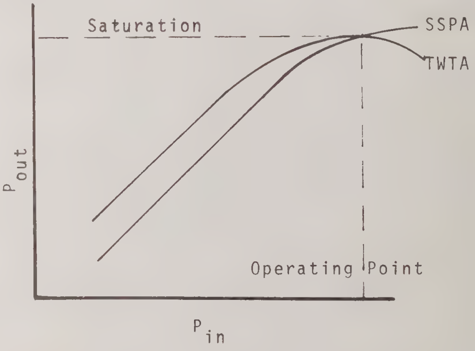

Figure 5. Power Amplifier Linearity Comparison

Table 2. Increase in Channel Capacity with Power Amplifier Linearity

Traffic Mode	Channel Capacity Increase, SSPA to TWTA
FDM Single Saturated Carrier	4%
FDM-FDMA	
Two Carriers	10%
Six Carriers	25%
SCPC	50%

also increased by installing two spare SSPAs for each of the four groups of six channels; the improvement in availability of all 24 channels throughout the mission life is illustrated in Figure 6 for this 4x(8 for 6) arrangement compared to the 4x(7 for 6) used in the current F4, and also compared to the 12x(3 for 2) arrangement used on some other spacecraft. For reference, the availability of all 24 channels if TWTAs were used in the same 4x(8 for 6) is also plotted.

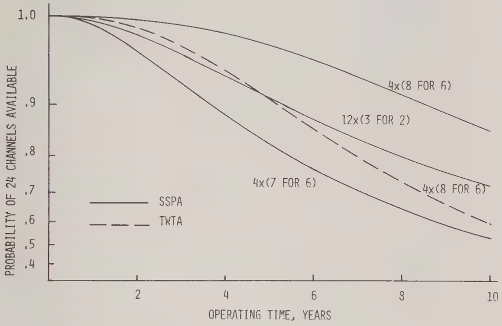

Figure 6. Power Stage Reliability Comparison

Power Supply

Increases in the mission life, from eight to ten years, and in the transmitter power of each channel necessitate an uprating of the basic RCA Satcom power system of single-axis drive solar array and three independently charged batteries. For the total communications payload plus spacecraft bus dc power, including battery recharging, of 1000 watts, the total array area is 120 square feet, comprised of five panels of high efficiency, thin junction cells. Continuous operation of all 24 transponder channels throughout the maximum 72 minute eclipse is supplied by 150 pounds of NiCd batteries; NiH_2 cells continue to be evaluated at RCA and elsewhere, but they do not have the statistical data base of NiCd. As demonstrated on RCA Satcom F1 and F2, now over four years in orbit, the proper combination of cell design, depressed operating temperature, full discharge reconditioning, and trickle charge can provide long life with NiCd.

As on flights 1 and 2, maximum reliability and minimum weight are achieved in the power system by eliminating any central regulator or battery boost voltage circuitry. Distributed regulation is performed by the various subsystems, all of which contain dc-dc converters for their particular requirements. Hence the bus voltage ranges from a maximum of 35.5v, when power is supplied by the array, to a minimum of 24v at the end of maximum eclipse with full 24 channel load.

Attitude Control

Precision three-axis body stabilization will again be accomplished with the basic RCA Stabilite ® design of fixed pitch momentum wheel together with autonomous magnetic torquing for maintenance of the angular momentum vector to the orbit normal. (4), (5) North-south station-keeping maneuvers are simplified with the solar-array shaft through the on-orbit center-of-mass; since the orbit inclination control thrusters are displaced symmetrically about the shaft, roll and yaw disturbance torques due to thruster plume imprignement on the array are minimized, and firing can occur at all array positions throughout the day.

Except for the initial phase of deployment from the space shuttle, the spin-stabilized transfer orbit sequence will be unchanged, including the dual-spin turn prior to three-axis transition. Spacecraft logic and thrusters will be used for active nutation control when the combined spacecraft and PAM is nutationally unstable during the interval from STS ejection until PAM firing.

Reaction Control

Transfer orbit attitude torquing and synchronous orbit velocity control will be supplied by the same fully redundant, twelve thruster, four tank configuration monopropellant system (6). The integral blowdown tanks containing surface tension fuel management screens will be sized for the ten year mission and greater spacecraft mass. Similarly, larger thrusters will be used to assure sufficient throughput capacity for the ten year fuel budget.

A Thiokol STAR-30 solid rocket motor has been tentatively selected for the apogee motor.

Structural and Thermal Control

The rectangular box with its central thrust column containing the apogee motor and large north-south panels for equipment mounting and thermal radiators will be expanded to accommodate the increased weight, volume, and thermal dissipation of the subsystem components. As indicated in Figure 7, this expansion will be primarily in the lateral direction to take advantage of the greater volume within the shuttle envelope, while the vertical dimension is restricted to provide the maximum height for the primary communication antenna. The folded solar arrays again cover the thermal radiators in their stowed, transfer orbit position, maintaining thermal as well as power balance throughout the transfer orbit.

IV. Terrestrial Network Enhancement

With the improvements in satellite EIRP, amplifier linearity, and channel response described above, concommitant enhancement of terrestrial equipment characteristics will be implemented to realize the objective of doubling the traffic capacity per standard 40 MHz transponder channel. A critical component of system capacity is the G/T of the receiving earth stations in the system.

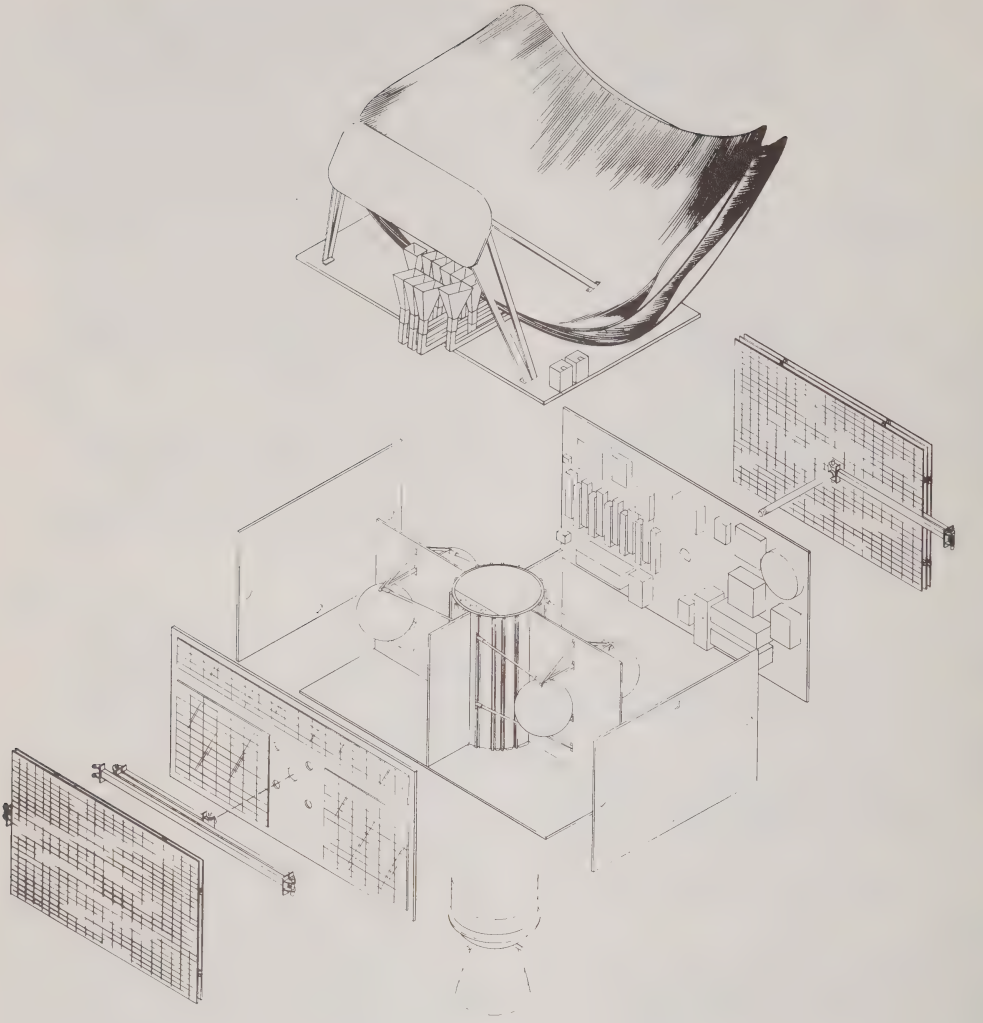

Figure 7. Spacecraft Structural Arrangement

Americom has under way a program to upgrade this figure of merit via the use of recently available Low Noise Amplifiers providing noise temperature performance on the order of 35°K. These, when mounted immediately behind the feed system of the antenna, will result in an average G/T improvement of 1.4 dB over the 55°K units now installed. Cryogenically cooled amplifiers which held sway for so long in satellite communications systems are giving way to uncooled units of this kind because of the inherent reliability and reduced maintenance expense of the uncooled amplifier.

In addition to greater receiver sensitivity, the existing capacity of FDM/FM carriers will be increased from 1000 to 2000 circuits by compandors which compress the dynamic range of a voice signal prior to transmission through the satellite channel and then expand it to its original range at the receiver. A signal-to-noise improvement is attained by the attenuation of channel noise during idle periods which contain no voice activity, resulting in a net compandor improvement of about 12 dB including the increased loading effect of higher average channel level on the baseband. This signal-to-noise improvement can then be reduced to the original S/N level (51 dB earth station to earth station) by decreasing the per channel FM deviation, thereby allowing more channels to be added to the FDM baseband. Together with the reduction in distortion and increase in bandwidth achieved by the elliptic function filters in the satellite transponder, these ground station enhancements comprise a system potential of 3000 one-way voice circuits per transponder channel.

To improve signal quality and user satisfaction, RCA is implementing adaptive echo cancellers on its private leased channel services. These devices have been found to be significantly superior to conventional echo suppressors because of their ability to estimate the echo on a path (via digital signal processing) and then subtract it out. Tests performed by the RCA Laboratories indicate that an echo canceller makes a satellite channel perform as well as a terrestrial channel. The adaptive nature of echo cancellers permits them to compensate for a wide variety of circuit conditions, thus overcoming customer resistance to satellite voice channels.

Expanding upon the voice, data and TV services presently being provided by the Americom system, RCA is planning future service offerings which will expand and diversify its role in the telecommunications market. Wideband data communications service between customer locations, to be known as "56 Plus", will be provided by the installation of dedicated 5-meter duplex earth stations located at the customer's offices. These stations will be remotely monitored and controlled from a master station in RCA's commercial earth station system. All data carriers are error-correction coded by a rate 7/8 convolutional encoder and threshold decoder to conserve transponder power. The wideband digital carrier(s) can either be a single wideband data carrier of 56 Kbps, or a time division multiplexed digital carrier consisting of any combination of lower data rates, or two delta modulation voice-grade channels with rf transmission via binary phase shift keying. Standard performance for this service is a bit error rate of 1×10^{-7} at an availability of 99.95%. This availability is achieved by full redundancy of all electronic subsystems with automatic switching to "hot standby" back up units.

A Selective Multiple Address Radio & Television System (SMARTS) is Americom's latest innovation in the video and audio telecommunication market. Americom will install at existing network radio or TV affiliates' studios a receive-only earth station for reception of syndicated programming that has been scrambled for security prior to transmission. The control system automatically controls remote station access and establishes billings based on usage.

In the realm of audio broadcasting and distribution, RCA will be offering a system capable of providing direct distribution of high quality audio signals and high speed data (56 kbps) to various end users and network affiliates. All incoming subscriber signals will be converted to digital format and Time Division Multiplexed into a single saturating/BPSK carrier, the most efficient form of transponder utilization since no intermodulation products are generated in the spacecraft. The signal will be received by small aperture receive-only earth stations installed directly on customer premises and the appropriate portion of the composite carrier stripped off and demodulated. The system is designed to have greater dynamic range, lower distortion, and superior baseband frequency response than is available on terrestrial facilities.

Digital transmission is used because of its superior immunity to terrestrial microwave systems thereby increasing the likelihood of co-locating a receive-only earth station on a customer premise without the need for artifical shielding or other devices. An important design constraint which is also satisfied is that the system not introduce undue levels of interference into adjacent satellite systems, present or future. Digital signal processing techniques are now well developed and permit scrambling of the signal to prevent piracy and give great flexibility. Audio bandwidths from 5 kHz to 15 kHz are available.

V. Conclusions

Although the total traffic demand of the Americom network will continue its rapid growth over the next decade, that growth can be satisfied by expansion and improvement of C-band facilities which maintain compatibility with existing installations. Taking advantage of the launch economy and large payload capacity of the space shuttle, the second generation Americom satellite will retain the current 24 channel, polarization reuse frequency plan, but with the traffic capacity per channel more than doubled by a combination of higher EIRP, better linearity, and sharper frequency response. The additional spacecraft weight available by means of the shuttle will also permit the incorporation of sufficient propellant, power margin, and component redundancy to ensure a ten year mission life, thereby further decreasing the average circuit cost per year. With an increase in the number of such second generation satellites plus the several terrestrial installation improvements, the expanded Satcom network will both accommodate the growth of the four present traffic centers and introduce new types of services.

References

1. J. Christopher and J.E. Keigler, "The RCA Americom Satellite Communications Systems". IAF Paper 79-267, Munich, FRG. September 1979.

2. "Reimbursement for Shuttle Services Provided to Non-US Government Users", NASA Management Instruction 8610.8, January 21, 1977 (subsequently incorporated in the Code of Federal Regulations as 14CFR 1214.1).

3. F. Drago, J. Hawley, H. Huang, and F. Sechi, "C-Band FET Power Amplifier for TWTA Replacement", IAF Paper 79-310 Munich, FRG, September 1979.

4. R. Cenker, "Pulsed Modulation of Orbit Adjust Thrusting to Simultaneously Control Roll and Yaw Attitude", AIAA Paper 74-924. Anaheim, California, August 1974.

5. G. Schmidt, "The Application of Magnetic Attitude Control to a Momentum Biased Synchronous Communications Satellite", Boston, Massachusetts, August 1975.

6. D. Balzer, Y. Brill, W. Scott, and P. Sing, "The Monopropellant Hydrazine Reaction Control System for the RCA Satcom Satellite", AIAA/SAE Propulsion Conference, Palo Alto, California, July 1976.

80-0535

EXPERIMENTS IN SATELLITE COMMUNICATIONS WITH SMALL EARTH TERMINALS†

J. Kaiser*
COMSAT Laboratories
Clarksburg, Maryland 20734

Abstract

From January 1976 to June 1979, COMSAT participated in experiments using the Communications Technology Satellite (CTS), a joint undertaking between the United States (NASA) and Canada (CRC). The CTS was launched into a geostationary orbit at 116° west longitude; it had two transponders of 85-MHz bandwidth and operated in the 12/14-GHz frequency bands. The maximum e.i.r.p. was 49 dBW in one transponder and 59 dBW in the other, making it the most powerful communications satellite on orbit at the time.

COMSAT's experiments focused on the use of very small and highly transportable earth terminals that could be used for emergency communications in the event of natural disasters. For this purpose COMSAT joined with the American National Red Cross in disaster communications exercises and two real disaster situations. Other experiments included demonstrations of applications of business communications with satellite earth terminals situated directly at the customer's premises. Still other experiments used the wide bandwidth and high e.i.r.p. of the CTS for experiments in digital television and data transmissions. One novel experiment involved simultaneous interpretation for a United Nations conference in Buenos Aires, Argentina, from the U.N. building in New York City via satellite.

Introduction

COMSAT participated in experiments using the CTS from January 1976 until June 1979. The original COMSAT experiment (No. 6) was designed to explore the feasibility of providing communications via satellite in disasters or emergencies when normal communications are disrupted. The experiment was later expanded to explore other uses of small transportable earth terminals for a variety of communications.

COMSAT designed and constructed a number of earth terminals for these experiments. The two basic terminals consisted of a transportable terminal with a 1.2-m antenna and a fixed terminal with a 4.6-m antenna located at Clarksburg, Maryland. Two fully self-contained road transportable terminals with 2.4-m antennas were also constructed for an experiment in business communications jointly conducted by COMSAT and Satellite Business Systems (SBS). The electronics for the 1.2-m terminal were also used with antennas having 2- and 2.4-m diameters for special applications. In addition, a small horn antenna with an aperture of 17 cm x 20 cm was built to receive FM sound directly via satellite.

The experiments in disaster communications were conducted in conjunction with the American National Red Cross, which provided simulated disaster scenarios in several locations. The earth terminals were also used in two real disaster situations.

Other experiments exploited earth terminal transportability to demonstrate applications to business communications via satellite directly from the user premises. These communications included live color TV for two-way video conferences, reduced bandwidth freeze frame color TV for slide presentations, and various digital computer and facsimile transmissions.

Experiments were made in wideband digital TV and data transmissions. Another involved the simultaneous interpretation for a United Nations conference in Buenos Aires, Argentina, from the United Nations Building in New York City via satellite. An experiment in clock synchronization via satellite was performed between master clocks at the National Bureau of Standards in Boulder, Colorado, and the Naval Observatory in Washington, D.C.

The CTS Spacecraft

The CTS (called HERMES in Canada), a joint undertaking by the United States (NASA) and Canada (CRC), was launched into geostationary orbit at 116° west longitude in January 1976. It was 3-axis stabilized and carried two 85-MHz-bandwidth communications transponders operating in the 12/14-GHz frequency bands. Figure 1 shows the frequency plan for the CTS, and Figure 2 is a simplified schematic of the two transponders. Each transponder was connected to one antenna so that both antennas were required for a complete transmit and receive path. The CTS transmitted an unmodulated beacon from an earth coverage circularly polarized antenna with 100 mW of power, resulting in an e.i.r.p. of about +8 dBW as viewed by a linearly polarized earth terminal antenna.

---

*Manager, Small Terminal Development Project.

†This paper is based upon work performed at COMSAT Laboratories under the sponsorship of the Communications Satellite Corporation.

This paper is declared a work of the U.S. Government and therefore is in the public domain.

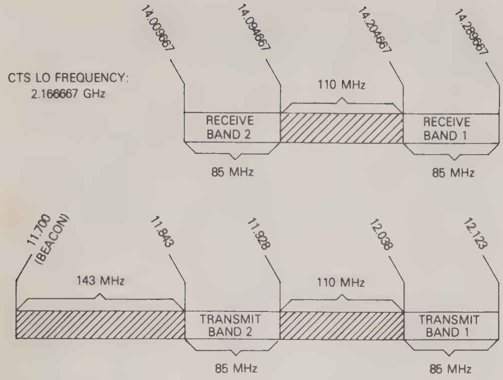

Figure 1. CTS Frequency Plan

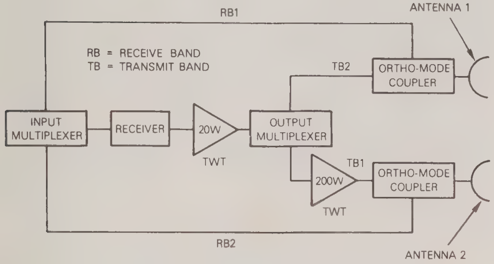

Figure 2. CTS 12/14-GHz Communications Transponder Schematic

Approximately 30 U.S. experimenters and an equal number of Canadian experimenters used CTS on a scheduled basis.[1,2] The U.S. experimenters had access to the spacecraft on alternate days, and each experiment was allocated a fixed time period, allowing 15 minutes to point the spacecraft antennas to the requested locations. CTS transponder No. 1 (TB-1), connected to a 200-W TWT, had a maximum e.i.r.p. of 59 dBW; and TB-2, connected to a 20-W TWT, had a maximum e.i.r.p. of 49 dBW. The signal in TB-1 also passed through the 20-W TWT of TB-2, causing a suppression of the signal in TB-1 by a signal in TB-2 when the latter was near saturation. The receiver used a parametric amplifier at 14 GHz with a noise temperature of 1350 K, resulting in an on-axis G/T of 6.4 dB/K. This relatively high G/T permitted small low-power earth terminals to access the CTS.

Since the CTS was originally designed to operate for approximately one year, there were no plans for north-south stationkeeping. It was launched with an inclination of -0.6°, which drifted through zero about midyear 1976 and then increased. A stationkeeping maneuver was eventually performed, and the inclination was maintained to less than about 1.3° for the entire experimental period. There was no operation during the eclipse periods.

Earth Terminal Design

The original purpose of the COMSAT experiment, to devise small, highly transportable earth terminals for emergency communications, required only a simple, unsophisticated earth terminal design. It was realized early in the design phase that the wide bandwidth (85 MHz) and high e.i.r.p. (59 dBW) of the CTS would permit a variety of transmission modes. Therefore, the design resulted in a terminal far more sophisticated than that required for emergency communications; however, the necessary transportability and field operability were maintained. A considerable amount of baseband equipment was available at COMSAT Laboratories to interface the IF systems at 70 MHz. Thus, for the CTS experiment frequency conversion was provided between 70 MHz and 12/14 GHz.

The design philosophy for the earth terminals was keyed to the integration of both existing and advanced design equipment into the required subsystems, since there was insufficient time for a completely new and unified design. The resulting transmitter, receiver, and up/down-converter subsystems, common to all of the earth terminals, could accommodate a large variety of system configurations required by the diverse experiments. The basic design of the electronics incorporated a double frequency conversion system from 12 GHz to 1.5 GHz to 70 MHz, and from 70 MHz via 1.5 GHz to the transmit band at 14 GHz.

It was realized at the outset that the ability to select any receive and/or transmit frequency within the 85-MHz bandwidth of the transponders would permit COMSAT and other experimenters to share CTS, particularly since the footprint of the CTS coverage was quite large. Thus, the up/down-converter was designed with the capability to select any frequency in either 85-MHz band in steps of 0.25 MHz. Fixed frequency oscillators were incorporated into the receiver (10.4115 MHz) and the transmitter (12.578167 GHz) for the first conversion to a nominal 1.5 GHz. Frequency selection was accomplished in the up/down-converter by using synthesizer-driven cavity-tuned local oscillators followed by switchable 85-MHz filters. Figure 3 is a schematic of the up/down-converter, and Figure 4 is a photograph. This unit, though relatively simple in the diagram, had some design problems. The synthesizer-controlled local oscillators produced many spurious signals and exhibited less than the expected phase noise purity. The first problem was resolved by carefully routing all wires and using semirigid cables for interconnections. The second problem required an increase in the frequency step size of the synthesizer from 0.25 to 2.5 MHz for some of the narrowband digital transmission experiments. This was accomplished by removing a "divide by ten" step in the synthesizer.

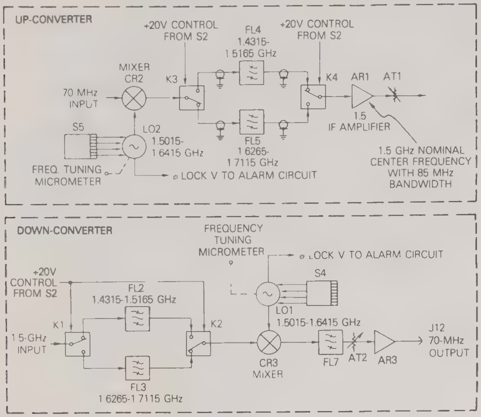
UP-CONVERTER
+20V CONTROL FROM S2
FL4 1.4315-1.5165 GHz
+20V CONTROL FROM S2
MIXER CR2
K3
K4
AR1
AT1
70 MHz INPUT
S5
LO2
1.5015-1.6415 GHz
FL5 1.6265-1.7115 GHz
1.5 IF AMPLIFIER
1.5 GHz NOMINAL CENTER FREQUENCY WITH 85 MHz BANDWIDTH
FREQ. TUNING MICROMETER
LOCK V TO ALARM CIRCUIT
DOWN-CONVERTER
FREQUENCY TUNING MICROMETER
LOCK V TO ALARM CIRCUIT
+20V CONTROL FROM S2
S4
FL2 1.4315-1.5165 GHz
LO1 1.5015-1.6415 GHz
K1
K2
J12 70-MHz OUTPUT
1.5-GHz INPUT
CR3 MIXER
FL7
AT2
AR3
FL3 1.6265-1.7115 GHz

Figure 3. Up/Down-Converter Schematic

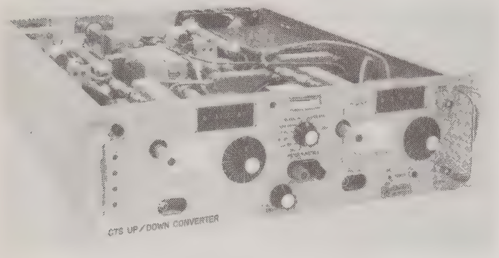
CTS UP/DOWN CONVERTER

Figure 4. Up/Down-Converter

The transmitters for the transportable terminals were based on Varian 20-W TWTs; the fixed terminal had a 200-W TWT. In each case, the input to the transmitter was via coaxial cable at the 1.5-GHz IF. The TWT with its LO, mixer, filter, circulator, load, and cooling fans was mounted near the antenna and connected to the associated high-voltage power supplies by a 6-m cable. This arrangement permitted the transmitters to be mounted in relatively small and lightweight weatherproof containers close to the feed flange. This reduced the length of the flexible waveguide required between the TWT and feed, thereby reducing losses and minimizing reliability problems with the flexible waveguide. The high-voltage cables caused no problems, even in heavy rain, after the original connectors were replaced by special Mil Spec units. All transmitters covered the 14.0- to 14.3-GHz band. The high gain of the TWTs (59-dB small signal and 53-dB saturated) and the special high output mixers made it possible to drive the TWTs directly from the output of the up-converters with up to 10-m of RG 214 cable without a driver amplifier at 14 GHz.

The receiver units consisted of one parametric amplifier built to COMSAT specifications by LNR Inc. and three FET units integrated by COMSAT. The FETs were designed for this purpose by AMPLICA. Figure 5 shows the schematic applicable to all receiver units; the parametric amplifier replaces the FET for the LNR unit. Figure 6 is a photograph of an FET receiver. The parametric amplifier had a noise temperature of 260 K and the FET 330 K with an RF to IF gain of 50 dB. All units covered the 11.7- to 12.2-GHz frequency band.

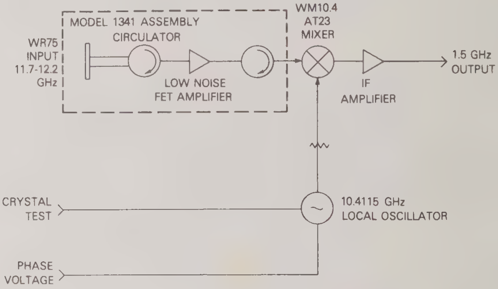
MODEL 1341 ASSEMBLY
CIRCULATOR
WM10.4
AT23
MIXER
WR75 INPUT 11.7-12.2 GHz
LOW NOISE FET AMPLIFIER
1.5 GHz OUTPUT
IF AMPLIFIER
CRYSTAL TEST
10.4115 GHz LOCAL OSCILLATOR
PHASE VOLTAGE

Figure 5. Receiver Schematic

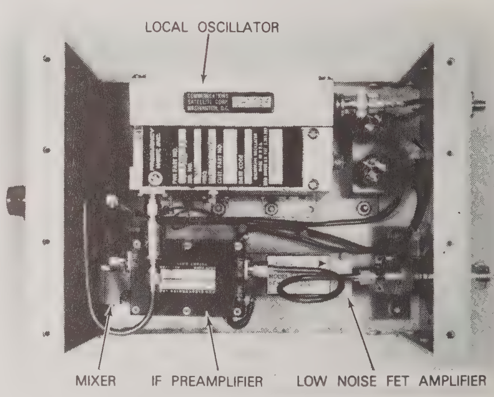
LOCAL OSCILLATOR
MIXER
IF PREAMPLIFIER
LOW NOISE FET AMPLIFIER

Figure 6. FET Receiver

Each terminal was supplied with an antenna, feed and mount, and baseband equipment suitable for the particular applications. Tables 1-4 summarize the terminal characteristics. Figures 7-9 show the 1.2-m terminal in its emergency communications configuration, the road transportable terminal, and the 4.6-m terminal, respectively.

Table 1. 1.2-m Terminal Characteristics

Antenna	1.2-m diameter, fiberglass
Feed	Dual linearly polarized, Cassegrain
Mount	Tripod, hand pointing 0°-75° el, all azimuth
Antenna Gain	
Transmit	42 dB
Receive	40.5 dB
TWT Transmitter	20 W maximum
Low-Noise Rcvr	260 K paramp
Maximum e.i.r.p.	55 dBW
G/T	15.5 dB/K
Shipping Weight	Approx. 250 kg (whole terminal)
A/C Power	110 VAC (1.5-2 kW)
Communications	3 two-way channels, 3-kHz baseband width each. These can carry voice, facsimile, and full duplex 300-wpm teletype messages.
Alternate Capability	Receive only TV with two program audio channels and the above transmit and receive capability.

Table 2. 2-m Terminal Characteristics

Antenna	2-m diameter, metal
Feed	Dual linearly polarized, front feed
Mount	Elevation over azimuth
Antenna Gain	
Transmit	46 dB
Receive	44.5 dB
TWT Transmitter	20 W maximum
Low-Noise Rcvr	FET 330 K
Maximum e.i.r.p.	59 dBW
G/T	18.5 dB/K
Shipping Weight	Approx. 350 kg (whole terminal)
A/C Power	110 VAC (1.5-2 kW)
Communications	Transmits video in CTS band No. 1 (high-power TWT) with 3 program audio channels. Receive video in band No. 1 or No. 2.

Table 3. 2.4-m Terminal Characteristics

Antenna	2.4-m diameter, fiberglass
Feed	Dual linearly polarized, front feed
Mount	Elevation over azimuth, motor driven, azimuth ±75° from trailer rear, elevation 5° to 75°
Antenna Gain	
Transmit	48.5 dB
Receive	47.2 dB
TWT Transmitter	20 W maximum
Low-Noise Rcvr	FET 330 K
Maximum e.i.r.p.	61.5 dBW
G/T	21.4 dB/K
Weight of Trailer	4100 kg
Tow Vehicle	Van, weight 2700 kg
A/C Generator	5 kW (Onan)
Communications	Two-way video with 3 program subcarriers or digital bit stream up to 10 Mbit/s and 3 SCPC audio channels

Table 4. 4.6-m Terminal Characteristics

Antenna	4.6-m diameter, fiberglass
Feed	Dual linearly polarized, Cassegrain
Mount	Elevation over azimuth, motor driven
Antenna Gain	
Transmit	54 dB
Receive	53 dB
TWT Transmitter	200 W maximum
Low-Noise Rcvr	330 K FET
Maximum e.i.r.p.	76 dBW
G/T	27.5 dB/K
Communications	Full color, analog TV, wideband digital TV voice, data

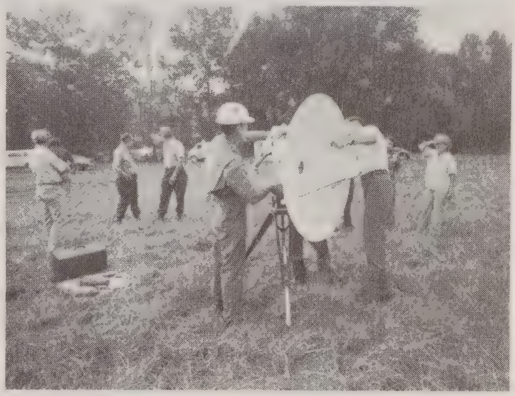

Figure 7. 1.2-m Terminal in Emergency Communications Configuration

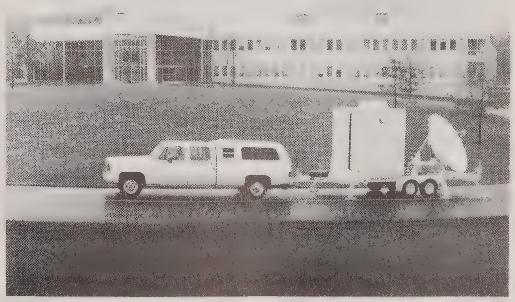

Figure 8. 1.2-m Transportable Earth Terminal

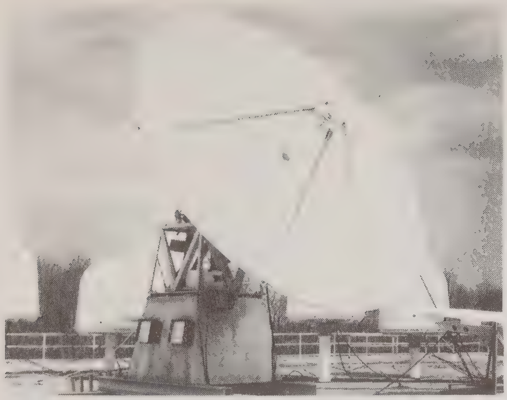

Figure 9. 4.6-m Earth Terminal

Emergency Communications Experiments

A number of simulated disasters and two real disaster situations were used to determine the feasibility of satellite communications for emergencies. These experiments were conducted with the assistance of the American National Red Cross, which decided on the type of exercise and its location and also provided the users of the communications channels. These exercises were usually held in conjunction with planned regional Red Cross disaster exercises. The inputs to the communications channels consisted of simulated emergency traffic, situation reports, requests for supplies and emergency relief personnel.

In each case, the 1.2-m terminal was transported to the disaster site by appropriate means and connected via the CTS to the 4.6-m terminal in Clarksburg, Maryland. Three voice grade full duplex channels were provided between the two terminals; two of these were then connected to the public switched network in Clarksburg, where echo control equipment was also added. This permitted a call to be originated at the emergency site by direct dialing of the desired number after a line had been obtained through an access code. A call directed to the emergency site was made by dialing a given number at Clarksburg, from which it was routed by an operator to the emergency site. Thus, the link from the disaster site was fully automatic and had operator assistance inbound. This arrangement proved to be well suited to the emergency communications situations.

Forest Fire Emergency Exercise

On July 29, 1976, a simulated forest fire emergency communications exercise was held at the Washington National Forest in Luray, Virginia. The principal purpose of this test was to demonstrate that the small terminal could be deployed at an unprepared site to furnish emergency communications to a headquarters location in the event of a major forest fire. As a companion effort, the Red Cross headquarters in Washington, D.C., was connected to the small terminal via the CTS using voice and teletype circuits. The terminal was transported to the site in a small van with an AC generator towed behind. It was set up within a half hour at an unprepared site, and communications were successfully completed as planned. Figure 10 shows the terminal in the field, and Figure 11 shows the teletype terminal at the Red Cross headquarters.

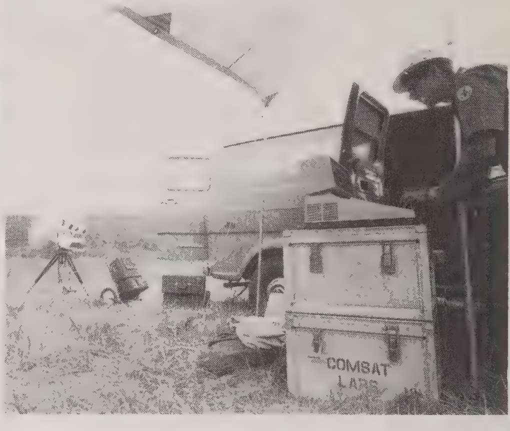

Figure 10. 1.2-m Terminal in the Field

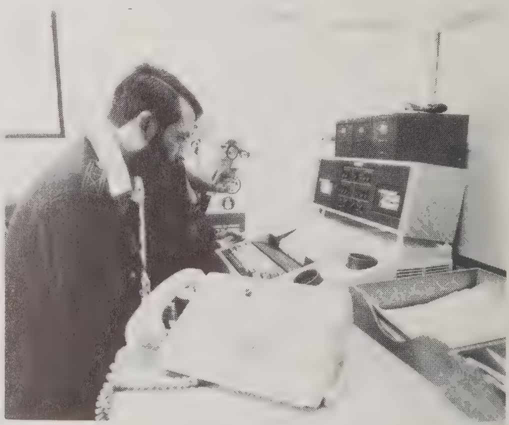

Figure 11. Teletype Terminal at Red Cross Headquarters

Flood Watch

In a similar exercise in Cincinnati, Ohio, the small terminal was transported in a small U-haul trailer towed by a station wagon. This exercise simulated a flood disaster along the Ohio River. Communications were established to the Red Cross disaster coordination center in Alexandria, Virginia, and other points. The exchanged information included status reports and requests for aid and emphasized teletype messages so that hard copy for files and records could be produced.

Johnstown Flood Disaster

While a hurricane watch exercise was being conducted in Texas, a real flood emergency occurred in Johnstown, Pennsylvania. The 1.2-m terminal was shipped by commercial airliner in the baggage compartment to Pittsburgh and then taken by small van to Johnstown, where it was installed at the disaster site.

Again, two voice circuits were made available to the Red Cross relief team at Johnstown via the CTS and the 4.6-m terminal at Clarksburg, Maryland. The satellite link proved to be very valuable, and at one time was the only means of communications in or out of the flood-stricken area. Messages transmitted included casualty reports, requests for equipment and personnel, and sketches of major damage areas transmitted by facsimile. For this real emergency, the CTS was preempted from use by other experimenters for about two days.

Tornado Disaster

The 1.2-m terminal was deployed for a tornado emergency at Wichita Falls, Texas, in May 1979. However, normal communications were restored rapidly and the need for satellite communications was eliminated.

Business Communications Experiments

The 2.4-m transportable terminals were used in a number of business communications experiments conducted with SBS. These experiments, called Project Prelude, demonstrated satellite communications of interest to the business community that would be available in the 1980's. The communications channels for these experiments consisted of two-way, full-motion color TV with three audio subcarriers for teleconferencing and, as an alternate mode, a digital bit stream up to 1.5 Mbit/s using a Harris Corp. variable data rate modem with three audio channels on SCPC. These modes could be selected rapidly during the presentations. The digital data were used to transmit computer data, freeze frame TV, and facsimile.

Several companies representing business machine manufacturers participated in these experiments together with host companies where the demonstrations were held. Figure 12 is a schematic of the equipment connected to the earth terminals, which were located near a host company's plant or office and connected to the conference room with cables up to 300 m long. Table 5 lists the participating companies and the equipment used. The Harris modems were operated in the two-phase PSK mode. A complete report on Project Prelude is available from SBS.[3] The experiments in general were well received by the participants; they showed that an earth terminal located at a user's premises can handle a variety of business communications from teleconferencing to data retrieval. Figure 12 shows the multitude of connections for a typical business communications demonstration.

Table 5. Project Prelude Participants

Host Company	Terminal Locations
Rockwell International Co.	Pittsburgh, Pa., Los Angeles, Ca.
Texaco	Harrison, N.Y., Houston, Texas
Montgomery Ward & Co. Inc.	Chicago, Ill., Baltimore, Md.
Equipment	Manufacturer
Large Screen Color TV	Advent Corp.
TV Freeze Frame Storage	Arvin/Echo
High-Speed, High-Resolution Facsimile Terminal	Dacom/Rapidfax
High-Speed "Any Datarate" Modem	Harris Corp.
Computer System Data Processing Network	Hewlett-Packard Co.
Color TV Cameras	Ikegami Electronics (U.S.A.) Inc.
Color Freeze Picture Transmission System	NEC America Inc.

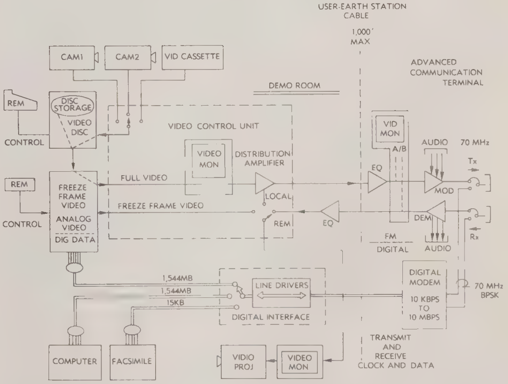
USER-EARTH STATION CABLE
1,000' MAX
CAM1
CAM2
VID CASSETTE
ADVANCED COMMUNICATION TERMINAL
DEMO ROOM
REM
DISC STORAGE
VIDEO DISC
CONTROL
VIDEO CONTROL UNIT
VID MON
AUDIO
70 MHz
A/B
Tx
VIDEO MON
DISTRIBUTION AMPLIFIER
EQ
REM
FULL VIDEO
FREEZE FRAME VIDEO
ANALOG VIDEO
DIG DATA
LOCAL
MOD
FREEZE FRAME VIDEO
DEM
CONTROL
REM
EQ
Rx
FM
DIGITAL
AUDIO
1,544MB
1,544MB
15KB
LINE DRIVERS
DIGITAL INTERFACE
DIGITAL MODEM
10 KBPS TO 10 MBPS
70 MHz BPSK
TRANSMIT AND RECEIVE CLOCK AND DATA
COMPUTER
FACSIMILE
VIDIO PROJ
VIDEO MON

Figure 12. Schematic of Earth Terminal Equipment

Wideband Communications

COMSAT Laboratories and NASA Lewis Research Center collaborated in an experiment in wideband digital TV and data transmission, DICE (digitally implemented communications experiment). This experiment employed COMSAT-developed digital video equipment operating at a nominal bit rate of 49 Mbit/s through a 4-phase DPSK modem also developed by COMSAT.[4,5] The transmission consisted of a full duplex digital bit stream supporting 60 voice grade telephone channels and one data channel. The telephone channels were multiplexed at about 1.5 Mbit/s onto the horizontal synchronization interval of the TV.

The operation of the DICE equipment required a C/N_0 of 94 dB (Hz), or approximately a 19-dB C/N in the 33-MHz RF bandwidth needed for the 49-Mbit/s 4-phase DPSK signal. A rate 7/8 forward error correction code was used to achieve an error rate of 10^{-7}. To obtain the up-link noise performance required in the link, it was necessary to insert both the 4- and 5-dB attenuators into transponders No. 2 and 1, respectively.

This system was demonstrated at the 7th AIAA Conference in San Diego, California, in June 1978. The NASA transportable earth terminal (TET) with a 2.4-m antenna was located in San Diego; the fixed terminal at Clarksburg was the other end of the link. The DICE system allowed two authors (one in San Diego, the other in Maryland) to present a joint paper to two audiences in a video conference mode, complete with two-way questions and answers from the audiences.

Miscellaneous Experiments

The transmission of color TV from remote locations using small antennas was demonstrated on two occasions. At the request of the NBC TV network, a 2-m terminal was taken to Yellowstone National Park and full color TV with three audio channels was transmitted via the CTS to the NASA receiving station in Cleveland, Ohio, and then sent via cable into New York for the "Glorious Fourth" telecast of July 4, 1976. The following week, the same 2-m terminal was used to transmit the Scottish Games from Grandfather Mountain, North Carolina, to the Southeastern Communications Association TV studio in Columbia, South Carolina, where the 1.2-m terminal was set up in the parking lot in a receive only mode. The program was then sent to 277 public TV stations.

Perhaps the smallest antenna ever used for direct broadcast reception from a satellite was a horn antenna with an aperture of 17 cm x 20 cm. It was used to receive standard commercial quality FM sound directly via the CTS at the Voice of America engineering building in Washington, D.C. Figure 13 shows the antenna and a small FM battery operated receiver for the FM music. Figure 14 is a block schematic of the receiving system. It should be noted that the signal at 12.08 GHz received from the CTS was fed directly to a mixer and converted to about 100 MHz, amplified, and sent to the FM receiver antenna. The transmission format was standard FM broadcast quality with a baseband from 30 Hz to 15 kHz, a modulation index of 5.0, and a bandwidth of 180 kHz.

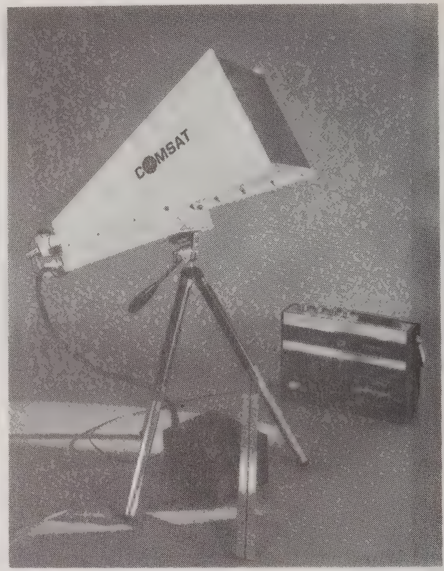

Figure 13. Small Horn Receiver Antenna

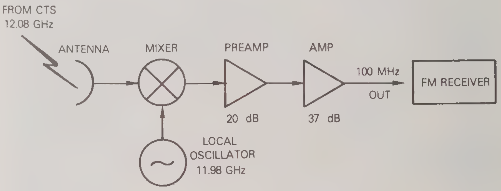

Figure 14. Receiver Schematic

A demonstration of this receiver in an urban environment showed that the technology exists for using very small, inexpensive earth terminals for direct FM reception via satellite. It is clear that, in this case, a large portion of the CTS resources were used for one FM sound channel, and that a calculation of the economics would show that such use is not justified at this time for a commercial system.

In connection with a United Nations multilingual meeting in Buenos Aires, Argentina, the feasibility of simultaneous language interpretation via satellite was investigated. The 2-m terminal used for the Yellowstone TV transmission was taken to Buenos Aires with the 200-W TWTA from the 4.6-m terminal. NASA placed a transportable earth terminal next to the United Nations building in New York. The simultaneous interpretation for a part of the conference in Buenos Aires was performed in New York and returned via the CTS to the conference.

The baseband equipment, constructed specifically for this experiment, consisted of an 8-channel Lenkurt multiplex system and a Farinon TV modulator and demodulator. Figure 15 is a block schematic of the system.

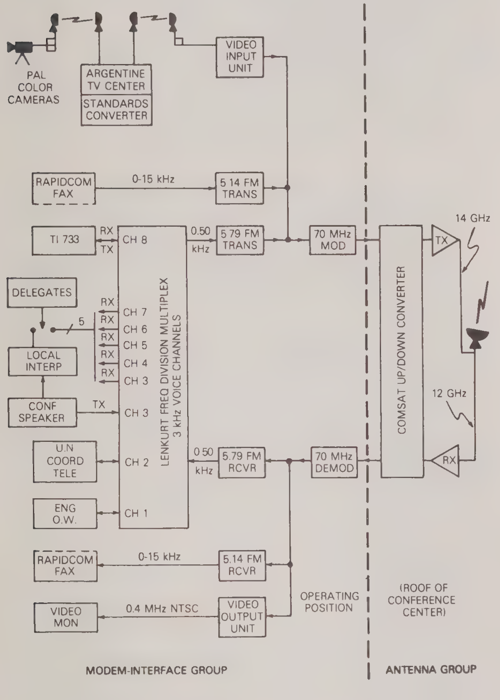
PAL COLOR CAMERAS
ARGENTINE TV CENTER
STANDARDS CONVERTER
VIDEO INPUT UNIT
RAPIDCOM FAX
0-15 kHz
5.14 FM TRANS
TI 733
RX
TX
CH 8
0.50 kHz
5.79 FM TRANS
70 MHz MOD
DELEGATES
5
CH 7
CH 6
CH 5
CH 4
CH 3
LOCAL INTERP
CONF SPEAKER
U.N COORD TELE
CH 2
ENG O.W.
CH 1
LENKURT FREQ DIVISION MULTIPLEX 3 kHz VOICE CHANNELS
0.50 kHz
5.79 FM RCVR
70 MHz DEMOD
COMSAT UP/DOWN CONVERTER
14 GHz
TX
12 GHz
RX
RAPIDCOM FAX
0-15 kHz
5.14 FM RCVR
VIDEO MON
0.4 MHz NTSC
VIDEO OUTPUT UNIT
OPERATING POSITION
(ROOF OF CONFERENCE CENTER)
MODEM-INTERFACE GROUP
ANTENNA GROUP

Figure 15. Teleinterpretation System Schematic

The transmission system provided full color TV (NTSC) with one 15-kHz audio channel, an engineering order wire for use by the earth station operations, a coordination circuit for the United Nations experiment coordinators, five channels of voice grade audio for the interpretation, and one channel for a high-speed teletype machine operating at 300 bauds. The TV audio circuit was also used for a high-speed facsimile transmission (Rapicom). The 70-MHz IF interface was separated from the up/down-converter by about 300 m of RG 58 cable. The antenna unit was placed on top of the 14-story conference building.

The TV signal originating at Buenos Aires was in the PAL format. It was first transmitted to a conversion center in midtown Buenos Aires and returned in NTSC format via microwave link; then it was transmitted via CTS to New York.

Experimental results showed that remote interpretation is technically feasible. A teleconference held at the conclusion of the experiment between the interpreters in New York and Buenos Aires concluded that voice circuit quality is important in the interpretation process, whereas the delay introduced by the satellite link presents no problem. Documents were transmitted using the Rapicom facsimile machines modified for 4-wire operation. Documents prepared by a Chinese language typewriter in Buenos Aires were transmitted at the medium speed of the Rapicom machine (approximately 50 s per page) and were considered of adequate quality for translation.

The 2.4-m transportable earth terminals were used for an experiment in clock synchronization between the primary time standards at the U.S. National Bureau of Standards in Boulder, Colorado, and the U.S. Naval Observatory Time Service in Washington, D.C., and the 7.0-m terminal at the Canadian National Research Council (NRC) in Ottawa, Canada.

Prior to COMSAT's participation, this experiment had used earth stations located away from the primary time standards, with attendant problems in logistics and accuracy in transporting cesium beam clocks from one location to another. The 2.4-m terminals were set up at Boulder and Washington, sufficiently close to the primary time standards to permit a direct short cable connection to these facilities.

The clocks are synchronized by transmitting time pulses in both directions via CTS from two locations. Station A transmits a pulse, which starts a counter. This counter is then stopped by the receipt of the time pulse from the distant station B. The information thus obtained at stations A and B is then processed by computer to remove time ambiguity and path length changes.

The clock synchronization experiment was conducted in three modes:

a. A 1-pulse-per-second (pps) time signal was impressed on a standard video modulator and sent as an FM analog video signal via CTS with a nominal RF bandwidth of 20 MHz.

b. A modem developed by NRC impressed a 1-MHz signal derived from the 1-pps clock pulse on the FM modulator.

c. COMSAT designed an interface unit for the Harris modem for the time transfer application. This unit received a 1-MHz signal and a 1-pps signal from the cesium beam master clock. These inputs were used to coherently produce a 100-pps data stream, clocked at a 25-kbit/s rate, which was then transmitted via CTS in the form of a 25-kbit/s BPSK signal. Thus, the RF bandwidth used in this mode is compatible with the bandwidth required for a standard 56-kbit/s QPSK data transmission.

The standard deviation of the measurements obtained from the three modes was on the order of 10 ns. These tests demonstrated that satellite communications can be used to synchronize clocks with high precision and at a small cost of satellite resources, i.e., a modest channel bandwidth, requiring perhaps only one or two 15-minute transmissions per week.

Conclusions

The experiments discussed in this paper show that technology exists for a variety of communications via satellite using small transportable earth terminals.[6] The use of the 11/14-GHz frequency bands avoids interference with ground-based communications systems and simplifies the placement of terminals at customer premises. Transmission impairments due to rain, though not discussed in this paper, must be considered when link margins are allocated for operating systems.

The design of the earth terminal equipment proved that components are available for these frequencies, and that the equipment reliability is quite good. Some failures were experienced in an early version of the TWT high-voltage power supplies, but there were no TWT failures in over three years of operation. Oscillator stability for the up/down-conversion becomes significant for the 12/14-GHz frequencies. Solid-state, low-noise receivers using FETs are available at a low cost compared to parametric amplifiers, and the availability of high-gain TWTAs ranging from 20 to 200 W makes economically viable earth terminals possible for many of the described communications modes. The design of the CTS, with its high G/T and e.i.r.p., indicates that such parameters should be attainable in future satellites. The concept of "scheduled" satellite communications between many users at prearranged times rather than continuous availability may be included in a future design.

References

1. NASA TM-X-71824, CTS Reference Book, NASA Lewis Research Center, Cleveland, Ohio, October 15, 1975.
2. "HERMES (The Communications Technology Satellite), Its Performance and Applications," Proceedings of the Twentieth Symposium of the Royal Society of Canada, Vol. 3, November 29--December 1, 1977.
3. "Prelude, Communications of the 80's," Evaluation Report on Project Prelude, Experiment No. 26, in the CTS Program, Satellite Business Systems, 8003 Westpark Drive, McLean, Virginia 22101, May 1978.
4. A. G. Gatfield, H. G. Suyderhoud, and C. J. Wolejsza, Jr., "System Design for the Digitally Implemented Communications Experiment (DICE)," International Conference on Communications, Chicago, Illinois, June 12-15, 1977.
5. C. J. Wolejsza, D. Chakraborty, and V. Uzunoglu, "A Universal Modem Design for Digital Satellite Communications," International Conference on Communications, Philadelphia, Pennsylvania, June 14-16, 1976, Conference Record, Vol. I, pp. 3-12-3-18.
6. J. Kaiser, L. Veenstra, E. Ackermann, and F. Seidel, "Small Earth Terminals at 12/14 GHz," COMSAT Technical Review, Vol. 9, No. 2, Fall 1979.

80-0560

SPACE LASER COMMUNICATIONS SYSTEMS FOR THE EIGHTIES*

M. Ross[†], J. D. Wolf[‡], R. M. F. Linford, J. L. Abernathy
McDonnell Douglas Astronautics Company
Box 516, St. Louis, MO 63166

Abstract

The evolution of laser communications technology is traced, from component development in the early seventies, to field tests of complete systems late in the decade. Development of critical components for high data rate, satellite-to-satellite cross-links led to the demonstration of acquisition, tracking and 1Gbps communications in laboratory experiments, under simulated satellite dynamic conditions. These experiments were extended to ground-to-ground tests over several kilometers at White Sands, New Mexico in 1979, and an air-to-ground experiment will be conducted in 1980. The feasibility of low data rate, aircraft-to-satellite laser communication links is to be demonstrated with a payload to be launched in 1982 on board the Air Force P80-1 spacecraft. These experimental systems are described. Advanced component developments for long-life and multi-gigabit laser systems are discussed, and a range of potential systems for operational aircraft-to-satellite and satellite-to-satellite lines are illustrated.

1.0 Introduction

Since inception of the laser as a communications carrier, its inherent characteristics of high data-rate capacity, jam-resistance, privacy, EMI-resistance, small antenna size and survivability have been widely recognized as potential assets for military communication systems. The evolution of user requirements for aircraft-to-satellite and satellite-to-satellite communication links with these very requirements has driven both Government and Industry to sponsor the necessary technology research and development. Throughout the last decade laser communications (Lasercom) has progressed from key component developments, via engineering model hardware, to field-tested experimental system. It is now anticipated that, during the 1980's, this maturing Lasercom technology will evolve into operational systems, to meet future military and civilian communication needs.

The progress of Lasercom is illustrated in Figure 1-1. Early development activity addressed critical component technology for neodymium-YAG laser systems operating at 1.06 and 0.53 microns. As illustrated in Figure 1-1, all the necessary goals for a 1Gbps satellite-to-satellite system were met or exceeded, proving that the application of Lasercom would not be limited by component technology. The component phase was followed by the successful demonstration of an Engineering Feasibility Model (EFM) System in the laboratory, in which both hardware design and system performance were verified. More recently, in the field at White Sands, New Mexico, communications at 1Gbps with less than 10^{-6} bit error rate, automatic acquisition, and microradian tracking have been demonstrated in ground-to-ground tests from the building shown in Figure 1-2. These tests were conducted over a short path (2 km), and the atmospheric scintillations were significantly more severe than are anticipated for operational links exiting or outside most of the atmosphere. Nevertheless, through use of direct detection, non-coherent techniques, these distortions by the atmosphere were accommodated by the system.

DEVELOPMENT OF CRITICAL LASERCOM TECHNOLOGIES

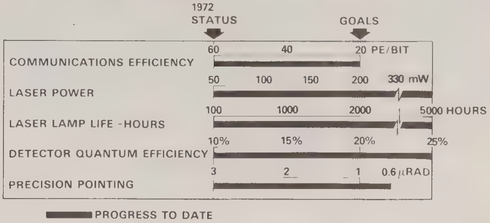

FIGURE 1–1

LASERCOM GROUND STATION BUILDING AT WHITE SANDS

FIGURE 1–2

Two significant Air Force experimental system programs to be completed in the early 1980's are important stepping stones toward space deployment later in the decade. The first is the Airborne Flight Test Systm (AFTS) program which will conduct two-way laser communications experiments from aircraft-to-ground starting in August 1980. Section 2.0 of this paper discusses that activity in detail. A second experimental program will launch and test a Lasercom Space Measurement Unit (LSMU) as a secondary payload on the P80-1 (Teal Ruby) satellite in 1982. This activity is discussed in Section 3.0. Advancements in the base technology continue, and Section 4.0 summarizes the state of development of very long life, reliable solid-state laser pump sources, and device technology for operation up to 4 Gbps. Section 5.0 gives examples of system utilization, and summarizes the applicability of hardware developed for the AFTS and LSMU experiments to these uses.

---

*Work conducted in part under Air Force contract F33615-76-C-1002

[†] Senior Member, AIAA

[‡] Member, AIAA

Copyright © American Institute of Aeronautics and Astronautics, Inc., 1980. All rights reserved.

2.0 Airborne Flight Test System

As an important first step towards reducing the risk of deploying operational Lasercom systems, the Airborne Flight Test System program will demonstrate several key areas of component and system technology.

The experiment concept is illustrated in Figure 2-1. A high-data-rate laser transmitter is to be installed in an Air Force EC-135 as the source of a 1 Gbps, 0.53μm Lasercom downlink. This transmitter will acquire, track and communicate with a receiver at White Sands Missile Range (WSMR), New Mexico. The receiver will also transmit 100bps and 20kbps data streams on pulsed 1.06μm beams, which will be used both as tracking beacons and as low data rate communication uplinks.

AIRBORNE FLIGHT TEST SYSTEM

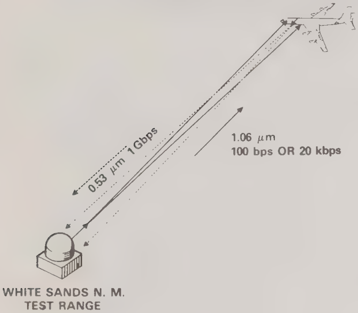

FIGURE 2–1

The objectives of the flight tests include:

- Demonstration of 1 Gbps communications over long range (up to 100km)
- Dynamic acquisition and tracking in the laser far field
- Evaluation of jam-resistance and covertness of Lasercom
- Verification of space-applicable transmitter hardware design

The program is divided into ground-to-ground and air-to-ground phases. The ground-to-ground tests are completed and the air-to-ground tests are being conducted in two stages: (a) Acquisition handover in December 1979, and (b) Two-way communications in August 1980.

Ground-To-Ground Test

During the fall of 1978 and spring of 1979, laser communications equipment was installed at Cowan Site, White Sands Missile Range (WSMR) and tests were conducted over a 1.3 mile (2.1km) path. These tests were designed to demonstrate the performance of a 1 Gbps laser communications system through the atmosphere, and provide design information for the aircraft flight test. The transmission path was to and from a 24-inch mirror situated 1.05 kilometers north of the site on a tower structure, as shown in Figure 2-2. The equipment used for these tests consisted of previously developed hardware from the Engineering Feasibility Model (EFM) program, and new hardware developed especially for this program. The more important ground-to-ground test results are summarized below.

AFTS REMOTE MIRROR AT WHITE SANDS

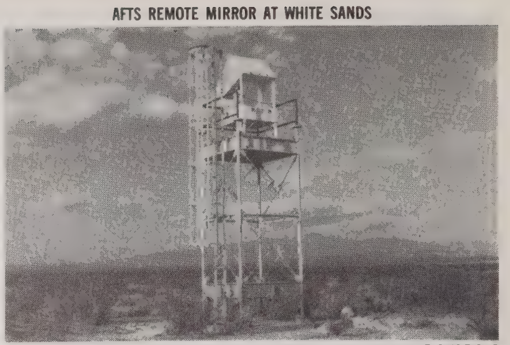

FIGURE 2–2

Acquisition Time Measurements. Results of acquisition time tests are illustrated in Figure 2-3. The transmitter acquisition time was consistently less than 2 seconds, consistent with previous laboratory measurements in spite of atmospheric variations. The receiver terminal was evaluated in a similar manner and an acquisition time of 0.5 sec was obtained.

EXAMPLE OF ACQUISITION SEQUENCE DURING GROUND-TO-GROUND TESTS

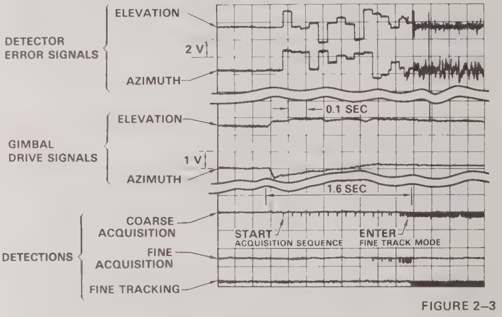

FIGURE 2–3

Cooperative Fine Tracking Tests. Fine tracking measurements were made to determine the stability of the cooperative tracking system in the presence of atmospheric perturbations. Data was taken for day, dusk, and night atmospheric conditions. The results for the tracking tests are summarized in Table 2-1.

TABLE 2–1

RESULTS OF COOPERATIVE FINE TRACKING TESTS

	TRANSMITTER			RECEIVER	
	PEAK TRACKING ERRORS			PEAK TRACKING ERRORS	
	AZIMUTH	ELEVATION	SCALED*	AZIMUTH	ELEVATION
TRACKING DAYTIME 1/31/79-1430 HRS.	11.6 μrad	5.02 μrad	1.6 μrad	7.4 μrad	11.2 μrad
TRACKING DUSK 1/31/79-1630 HRS.	3.4 μrad	2.6 μrad	0.6 μrad	5.5 μrad	4.7 μrad
TRACKING NIGHT 1/30/79-2200 HRS.	10.0 μrad	2.2 μrad	1.3 μrad	6.9 μrad	6.3 μrad

* SCALED FOR SPACE-APPLICABLE SYSTEM, RSS OF AZIMUTH AND ELEVATION VALUES.

Both terminals performed as expected in these tests. The receiver terminal tracking errors (4.7 to 11 μrad) compare favorably with AFTS tracking budget of 9.9 μrad to point a 100 μrad beam. These results also scale with aperture size to the accuracies required in a typical space-to-space or space-to-ground application. Using the dusk data as most like space conditions, the receiver terminal can support a 20 μrad beamwidth ($1/e^2$ diameter) in the tracking mode.

The transmitter terminal tracking error (2.2 µrad to 11.6 µrad) must also be scaled, to account for the geometry of the field test, to compare system performance for the AFTS and space applications. When this is done, the tracking errors scale to between 0.6 to 1.6 µrad, compared to 1.0 to 2.0 µrad required for a typical high data-rate space system, and to the 0.6 µrad measured in the laboratory.

Communication Tests. The 1Gbps communications system performed at near-laboratory levels over the test range. The system was operated with various modulation formats and power levels and the bit error rate was measured. Figure 2-4 shows a comparison of data taken inside the building over a short path (6m) and data taken over the 2.1 kilometer path. The system performed very well in spite of frequent variations in received power due to atmospheric scintillation.

1 Gbps COMMUNICATION DATA FROM GROUND-TO-GROUND TESTS

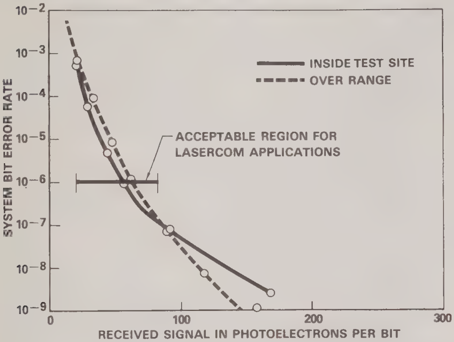

FIGURE 2–4

Air-to-Ground Tests

The features of the AFTS System are illustrated in Figure 2-5 and key specifications are summarized in Table 2-2.

AFTS SYSTEM BLOCK DIAGRAM

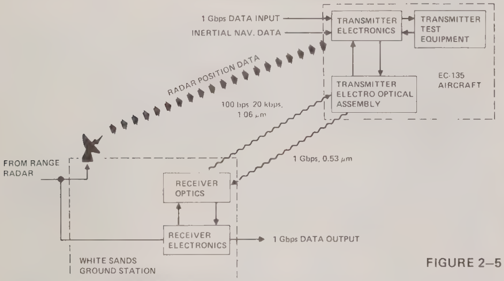
1 Gbps DATA INPUT
INERTIAL NAV. DATA
TRANSMITTER ELECTRONICS
TRANSMITTER TEST EQUIPMENT
RADAR POSITION DATA
TRANSMITTER ELECTRO OPTICAL ASSEMBLY
EC-135 AIRCRAFT
100 bps 20 kbps, 1.06 µm
1 Gbps, 0.53 µm
FROM RANGE RADAR
RECEIVER OPTICS
RECEIVER ELECTRONICS
1 Gbps DATA OUTPUT
WHITE SANDS GROUND STATION

FIGURE 2–5

TABLE 2–2

AFTS SYSTEM SPECIFICATIONS

PARAMETER	AIRBORNE TRANSMITTER		GROUND RECEIVER	
	(a)	(b)	(a)	(b)
LASER – WAVELENGTH	0.532 µm		1.064 µm	
– OUTPUT	150 mW		5W	4W
– PULSE RATE	500 Mpps		10pps	3kpps
OPTICAL APERTURE (DIA)	20cm	5cm	2.5cm	35cm
BEAM DIVERGENCE	5-25µrad	100µrad	12.4mrad	1mrad, 100µrad
TRACKING DETECTOR				
– WAVELENGTH	1.064µm		–	0.532 µm
– ACCURACY	0.6µrad	5µrad		12.5µrad
COMMUNICATION DETECTOR	AVALANCHE PHOTODIODE		DYNAMIC CROSSED FIELD PMT	
COMMUNICATION FORMATS	1 Gbps PQM, 500 Mbps PDBM 500 Mbps PPBM		100 pps PIM , 20 kbps PIM	

The flight hardware installation is shown in Figure 2-6. The electro-optical assembly is shown behind the cargo door, which has been modified to mount a 0.75m optical window for transmission and reception. The electro-optical assembly is mounted on an isolation-support structure, which uses a shock mount to eliminate linear vibration inputs, and a single point rotary joint for the optical assembly attachment. The environmental enclosure provides both protection against contamination, and temperature control during aircraft ground operations. The transmitter electronics and associated test equipment are located in shock-mounted racks installed parallel with the center line of the aircraft.

AFTS TRANSMITTER INSTALLATION IN THE EC-135 AIRCRAFT

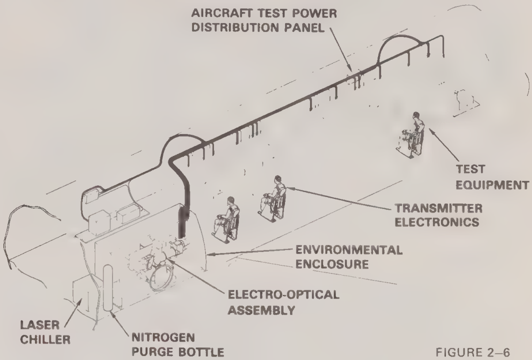
AIRCRAFT TEST POWER DISTRIBUTION PANEL
TEST EQUIPMENT
TRANSMITTER ELECTRONICS
ENVIRONMENTAL ENCLOSURE
ELECTRO-OPTICAL ASSEMBLY
LASER CHILLER
NITROGEN PURGE BOTTLE

FIGURE 2–6

The installation, shown in Figure 2-6, includes only a few transmitter equipment items that have been developed to space prototype levels. These include the laser, modulator, imaging optics and telescope. Figure 2-7 illustrates the latter two items in a compact subassembly that has a 20 cm (8 inch) aperture and weighs only 22kg (48lb), including the acquisition and tracking detectors.

SPACE-APPLICABLE IMAGING OPTICS AND TELESCOPE USED IN AFTS AIRBORNE TRANSMITTER

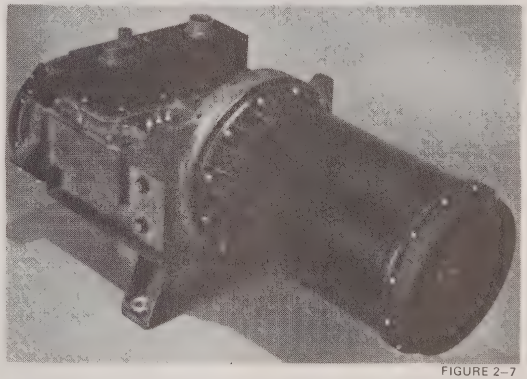

FIGURE 2–7

During the airborne tests the aircraft will fly a circular trajectory around the ground station at slant ranges up to 100 km. The high-data-rate transmitter will acquire and track the 1.06 µm beacon beam to obtain line-of-sight pointing information to the ground station for the high-data-rate transmitter. The high-data-rate transmitter will then acquire, track and transmit a narrow (100 μrad) 0.53 μm beam with 1 Gbps Pulse Quaternary Modulation (PQM). Instrumentation will be provided on the aircraft and at the ground station to measure acquisition and tracking times, tracking accuracies, and communication error rates, to infer slant path atmospheric effects, and to make direct measurement of far field patterns by scanning the transmitted beams.

3.0 LSMU Experiment

The use of Lasercom for aircraft-to-spacecraft uplinks requires that the spaceborne receiver provide wide area coverage while restricting access to only valid (i.e. friendly) users. These features are basic to either low-data-rate Report Back, or for Call-Up as a first step in establishing a high-data-rate reconnaissance relay link. These apparently conflicting requirements are provided by the Multiple Access Receiver (MAR). The field of view of the MAR is segmented into up to 100 elements, providing 100 separate and independent communication channels. Each channel can handle up to 30 simultaneous valid user transmitters, and the receiver can accept a total of 200 simultaneous users across the full aperture. Both by virtue of the element-to-element isolation and by the use of encoding techniques, the receiver can operate at full capacity in the presence of severe jamming.

The feasibility of the MAR and its use in aircraft-to-space uplinks is soon to be demonstrated in an experimental program with a near-earth-orbit satellite. The Lasercom Space Measurement Unit (LSMU) Experiment will consist of a laser transmitter at a ground station at White Sands Missile Range (WSMR), which will communicate with a MAR on board the Air Force P80-1 spacecraft. An artist's concept of the spacecraft and a visualization of the infrared laser uplink are shown in Figure 3-1. An optional airborne transmitter is also being considered.

LASERCOM EXPERIMENT WITH THE AIR FORCE P80-1 SATELLITE

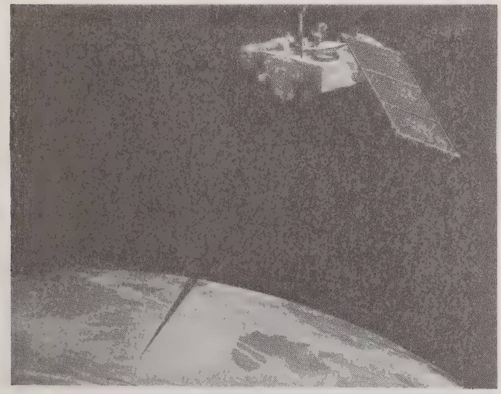

FIGURE 3–1

Details of the lasercom links are illustrated in Figure 3-2. The prime uplinks are the 100 bps channels utilizing 5W, 10pps Nd-YAG laser transmitters operating at 1.06 μm. Also included in the ground station is a 4W, 3kpps laser transmitting at 20 kbps to the spacecraft. An 800 bps downlink using a gallium arsenide transmitter (0.9 μm) in the spacecraft is also shown in Figure 3-2.

LSMU EXPERIMENT CONCEPT

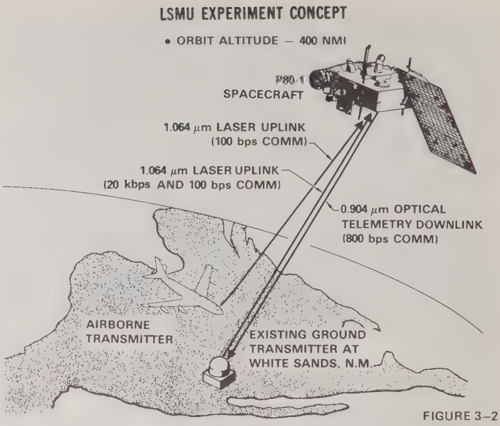
• ORBIT ALTITUDE – 400 NMI
P80-1
SPACECRAFT
1.064 μm LASER UPLINK
(100 bps COMM)
1.064 μm LASER UPLINK
(20 kbps AND 100 bps COMM)
0.904 μm OPTICAL
TELEMETRY DOWNLINK
(800 bps COMM)
AIRBORNE
TRANSMITTER
EXISTING GROUND
TRANSMITTER AT
WHITE SANDS, N.M.

FIGURE 3–2

The objectives of the experiment include the following:

- Demonstration of low data rate laser communications with the spaceborne MAR including:
  - Validated access to a wide field of view, multi-channel receiver.
  - 100 bps Report-Back communication.
  - Call-up initial acquisition sequence.
  - 20 kbps communications applicable to secure voice.
  - Transmitter-beacon tracking by the receiver.
- Demonstration of open-loop pointing of an airborne laser transmitter toward a spaceborne optical receiver (experiment option).
- Verification of the design and perfromance of key components of an airborne transmitter and a spaceborne receiver.
- Evaluation of the effect of atmospheric parameters on laser communications.
- Demonstration of an optical telemetry downlink.

Experiment Description

The functions of the experiment are illustrated by the block diagram in Figure 3-3.

LSMU EXPERIMENT FUNCTIONAL BLOCK DIAGRAM

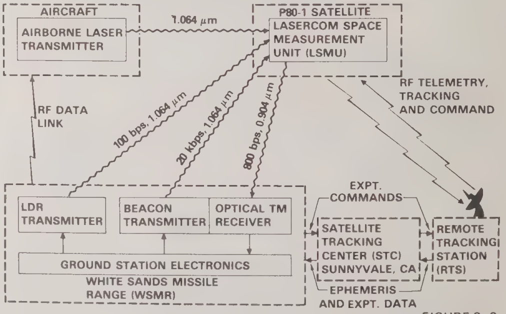
AIRCRAFT
AIRBORNE LASER TRANSMITTER
1.064 μm
P80-1 SATELLITE
LASERCOM SPACE MEASUREMENT UNIT (LSMU)
RF TELEMETRY, TRACKING AND COMMAND
RF DATA LINK
100 bps, 1.064 μm
20 kbps, 1.064 μm
800 bps, 0.904 μm
LDR TRANSMITTER
BEACON TRANSMITTER
OPTICAL TM RECEIVER
GROUND STATION ELECTRONICS
WHITE SANDS MISSILE RANGE (WSMR)
EXPT. COMMANDS
SATELLITE TRACKING CENTER (STC) SUNNYVALE, CA
REMOTE TRACKING STATION (RTS)
EPHEMERIS AND EXPT. DATA

FIGURE 3–3

The LSMU will be integrated into the P80-1 spacecraft, utilizing the location vacated by another payload. The spacecraft will be launched by the Space Shuttle and then inserted into a 400 nmi, 72.5° inclination orbit. As shown in Figure 3-4, the receiver will be accessible from the

COMMUNICATION ENVELOPE AROUND WHITE SANDS

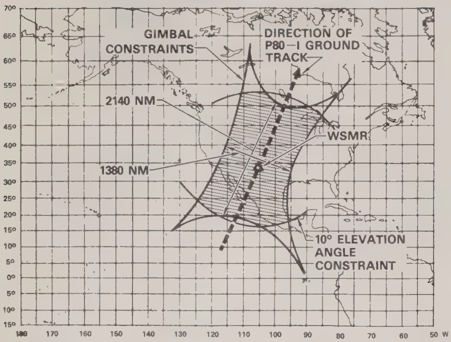

FIGURE 3–4

ground station at WSMR over a large area of the western United States, and contact times of up to 10 minutes will be available twice each day.

If the optional air-to-space experiment is conducted, the airborne laser transmitter will be used to transmit data to the LSMU, while the ground station will serve as a second simultaneous user, and as a would-be jammer.

As illustrated in Figure 3-3, ephemeris data provided by the Air Force Satellite Control Facility (SCF) will be used to open-loop point the LSMU, the Ground Station gimballed optics, and the airborne transmitter optics. LSMU gimbal commands and other experiment commands will be generated at WSMR and transmitted to SCF for subsequent uplink to the P80-1 spacecraft on a pass over a Remote Tracking Station (RTS) prior to the WSMR experiment pass. These operational commands will be stored in the LSMU Control Unit. During the experiment pass over WSMR, the LSMU module will be operated autonomously, using the spacecraft only to provide power and an initiate command, and to record the output data for subsequent transmission via the spacecraft telemetry to an RTS.

Experiment data relayed from the RTS, via the SCF to the experiment ground station at White Sands, will arrive in delayed time. Some real-time telemetry via the Vandenberg Tracking Station may be available, but only on a limited number of passes. To overcome the difficulties of operating an experiment under these conditions the optical telemetry link is included. Using a 100 pps, 400W peak, gallium arsenide source, the link will carry 800 bps, including the 100 bps Report-Back data and a variety of health and status parameters.

The LSMU has self-test capabilities which will be utilized to assess experimental status, for anomaly diagnosis and to assess the long term effects of the space environment on system operation. The experiment will also be operated at other locations around the world to measure the background optical radiation. In this mode, the LSMU will point at predetermined locations on the earth, to measure the effects of different background conditions on space laser communications.

Payload Characteristics

The LSMU experiment module is illustrated in Figure 3-5. The electronic and electro-optical components are all mounted in a cylindrical enclosure that interfaces directly with the spacecraft. A spring-loaded cover closes one end of the enclosure to protect the optical surfaces during all phases prior to initialization in the operational orbit. This cover will be released by a hot wire initiator 2-4 weeks after insertion. The aft end of the enclosure is protected by a cover which also acts as a thermal radiator.

LASERCOM SPACE MEASUREMENT UNIT FLIGHT MODULE

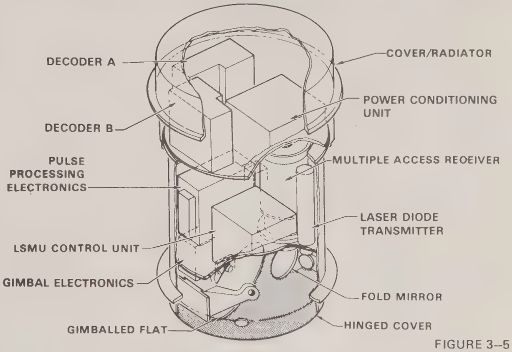

FIGURE 3–5

The gimballed mirror is used to point the field of view of the Multiple Access Receiver and the optical telemetry transmitter at the WSMR ground station. Gimbal pointing commands will be transmitted on the command uplink from SCF, and provided to the LSMU Electronics via the spacecraft Command Distributor. In certain experiment modes, the gimbal control will be augmented by error signals from the Multiple Access Receiver.

Communication data on the laser uplink will be detected by the Multiple Access Receiver, validated by the Decoder, and then relayed to the spacecraft telemetry for recording or real-time transmission to a tracking station.

Mission Schedule

The space-flight hardware is currently under development, will be ground-tested in late 1980, and will be delivered for spacecraft integration in March 1981.

The launch of the P80-1 spacecraft is currently scheduled for November 1982 and experiments are planned for the following 12-month period.

4.0 Advanced Component Development

The success of the system tests that have been described in the previous sections is based on the development of key components in prior years. With future operational systems in mind, new component developments are in progress, amongst them a diode pump source for Nd:YAG lasers and a modulator for 4 Gbps.

Diode Pump Source

The 500 Mpps Nd:YAG laser used in the AFTS 1 Gbps transmitter is pumped by a potassium arc lamp specially developed for this application. As a result of several design iterations, the operating lifetime of these lamps exceeds 5000 hours, an adequate life for many applications. However, in systems requiring very long life, continuous operation, or where the lamp power consumption is unacceptable, the injection laser diode is a very attractive alternate pump source. As illustrated in Figure 4-1, the output of a GaAlAs diode doped to lase at 808 nm is an excellent match to the 810 nm pump band of Nd:YAG. In excess of 60% of the diode output is absorbed.

ABSORPTION OF LASER DIODE OUTPUT AT 810 nm PUMP BAND OF Nd-YAG

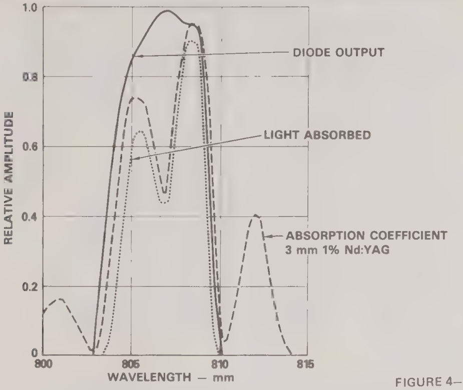

FIGURE 4–1

Several years of development effort at MDAC-St. Louis have effectively solved most of the material and fabrication problems. In accelerated life tests, operational lifetimes of in excess of 100,000 hours have been extrapolated. Diode arrays with up to 10% efficiency have been demonstrated which could lead to a diode-pumped laser requiring only 40W input, compared to 250W required by the equivalent lamp-pumped version. A concept for such a laser is illustrated in Figure 4-2.

CONCEPT FOR DIODE-PUMPED LASER

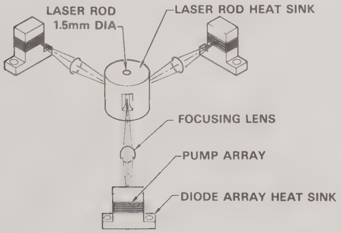

FIGURE 4–2

4 Gbps Modulator

Possible requirements for lasercom systems transmitting data rates in excess of 1 Gbps have led to the development of a traveling wave modulator. The capacitance of lumped-element modulators used at 1 Gbps for AFTS, and the transit time through the length of the crystals, limit the modulation bandwidth. The capacitance problem is overcome by incorporating the modulator crystal in a traveling wave structure. This structure can also be designed so that the switching voltage travels at the same velocity as the optical beam, thus solving the transit time problem.

Such a traveling wave modulator has been designed (Figure 4-3) and successfully tested up to 2 Gbps (Figure 4-4). The device is believed to be readily scalable to 4 Gbps.

VELOCITY MATCHED TRAVELING WAVE MODULATOR

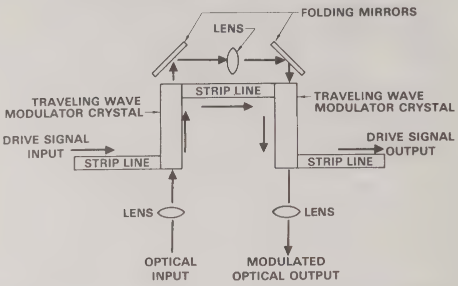

FIGURE 4–3

OUTPUT OF 2 Gbps TRAVELING WAVE MODULATOR

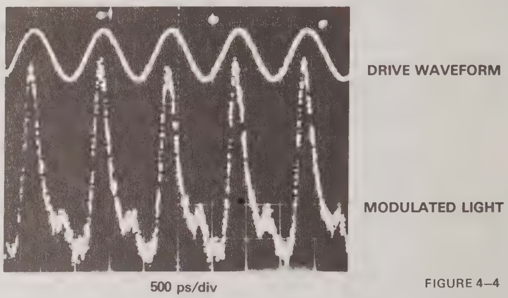

FIGURE 4–4

5.0 Future Application of Laser Communications

Technology and systems have evolved to such a level that application of laser terminals to specific links is now possible. Those applications most suitable for employment of the laser are aircraft-to-space and space-to-space links.

Small airborne terminals with miniature antennas can relay real-time wideband data from distant locations around the world to the Continental United States through satellites, uninhibited by interference, and with a high degree of privacy. For example, an airborne transmitter terminal and satellite receiver can be constructed to uplink up to 1 Gbps data, and simultaneously downlink command and control information at 20 kbps, as illustrated in Figure 5-1. Terminal characteristics for such a link are given in Table 5-1.

Hybrid systems utilizing laser uplinks from earth-to-space and space-to-space with a RF downlink, are generally most attractive due cloud effects on laser downlinks. However, although significant penetration of clouds is not possible at data rates above about 10kbps, space-to-ground laser linking can achieve high availability via several small optical collectors located in areas with statistically independent weather patterns.

AIRCRAFT-TO-SATELLITE HIGH DATA RATE LINK

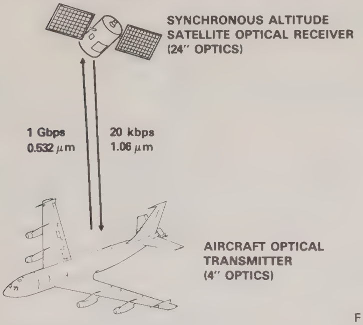

FIGURE 5–1

TABLE 5–1

AIRCRAFT-TO-SATELLITE TERMINAL CHARACTERISTICS

PARAMETER	AIRCRAFT TRANSMITTER	SATELLITE RECEIVER
ANTENNA DIAMETER	10 cm (4 in.)	60 cm (24 in.)
LASER	0.53 μm, COMMUNICATIONS	1.06 μm, BEACON
LASER POWER (DIODE-PUMPED)	0.2W	0.1W
BEAMWIDTH	7μrad	100μrad
POINTING & TRACKING ERROR	2.5μrad	35μrad
MODULATION FORMAT	PULSE QUATERNARY	PULSE INTERNAL, M = 6
OPTICAL TRANSMISSION	0.25	0.34
DATA RATE	1 Gbps	20 kbps
BIT ERROR RATE	10^{-6}	10^{-6}
MARGIN	8 dB	8 dB
WEIGHT	160 kg (350 lb)	155 kg (340 lb)
POWER	310W	300W

As shown in Figure 5-2, a satellite transmitter with 8" optics, and a 3.5 μrad beam can provide a satellite-to-satellite crosslink at 1Gbps over a 81,000 km distance, utilizing the same receiver characteristics given in Table 5-1.

SATELLITE-SATELLITE CROSSLINK 81,000 km DISTANCE

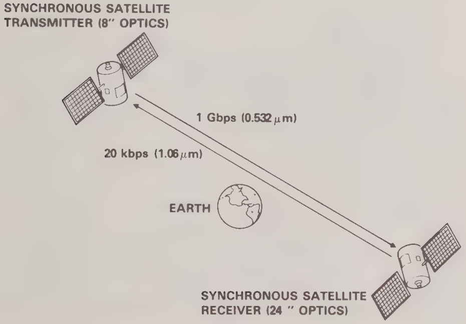

FIGURE 5–2

Needs for very long distance crosslinks are being defined for survivable satellite systems. The immunity of the optical transmission to nuclear disturbances, and the inherent jam-resistance make the laser system a strong candidate for such a need. As shown in Figure 5-3, a full duplex 10kbps link can be configured with only 6" optics. Estimated terminal weight is 200 lbs, and estimated power is 150W.

Fabrication and experimental field tests, of the major system elements which comprise high-data-rate transmit and receive terminals, are being accomplished by the Airborne Flight Test System and LSMU programs discussed above. Tables 5-2 and 5-3 compare the required operational elements with the current experimental programs, showing that the significant steps in the development of these elements are occurring.

LONG DISTANCE CROSSLINK 200,000 km DISTANCE

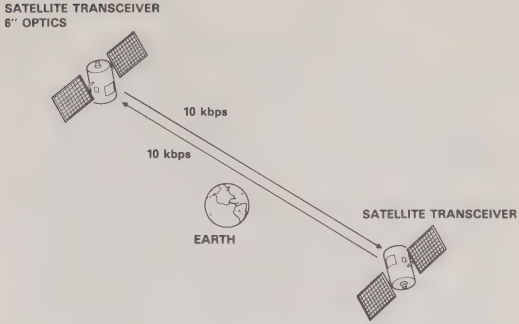

FIGURE 5–3

TABLE 5–2

CONTRIBUTION OF EXPERIMENTAL PROGRAMS HIGH DATA RATE TRANSMITTER DEVELOPMENT

ELEMENT	OPERATIONAL TERMINALS		EXPERIMENT SYSTEMS	
	SPACE TRANSMITTER	AIRCRAFT TRANSMITTER	AFTS	LSMU
TELESCOPE	8" CASSEGRAIN	4" REFRACTIVE	8" CASSEGRAIN	2.5" REFRACTIVE
OPTICS	TRACKING, POINT AHEAD, AUTO-ALIGNMENT	TRACKING, POINT-AHEAD, AUTO-ALIGNMENT	TRACKING, POINT-AHEAD, AUTO-ALIGNMENT	TRACKING
DETECTORS	AVALANCHE PHOTODIODE (APD)	APD	APD	APD
LASERS	0.532 μm SUN-PUMPED OR DIODE-PUMPED	0.532 μm LAMP-PUMPED	0.532 μm LAMP-PUMPED	0.804 μm DIODE ARRAY
MODULATOR	PULSE QUATERNARY (POLARIZATION & DELAY)	PULSE DELAY	PULSE QUATERNARY (POLARIZATION & DELAY)	PULSE INTERVAL
DATA RATE	1 Gbps, 20 kbps	1 Gbps, 20 kbps, 100 bps	1 Gbps, 20 kbps, 100 bps	20 kbps, 100 bps
COMMUNICATION ELECTRONICS	BASEBAND MULTIPLEXED	BASEBAND MULTIPLEXED	BASEBAND MULTIPLEXED	
ACQUISITION & TRACKING ELECTRONICS	ANALOG DRIVE & DIGITAL PROCESSOR	ANALOG DRIVE & DIGITAL PROCESSOR	ANALOG DRIVE; DIGITAL PROCESSOR	ANALOG DRIVE; DIGITAL PROCESSOR
JAM RESISTANCE ACQUISITION		CONVOLUTIONAL ENCODER	PIM ENCODER	CONVOLUTIONAL ENCODER

TABLE 5–3

CONTRIBUTION OF EXPERIMENTAL PROGRAMS TO HIGH DATA RATE RECEIVER DEVELOPMENT

ELEMENT	OPERATIONAL TERMINAL SPACE RECEIVER	EXPERIMENT SYSTEMS	
		AFTS	LSMU
TELESCOPE	24" CASSEGRAIN	14" CASSEGRAIN	14" CASSEGRAIN
OPTICS	TRACKING, SCANNING, ALIGNMENT	TRACKING, SCANNING, ALIGNMENT	TRACKING, SCANNING, ALIGNMENT
DETECTORS	APD, IMAGE DISSECTOR	IMAGE DISSECTOR	APD QUADRANT
LASER	1.06 μm SUN-PUMPED OR DIODE-PUMPED	1.06 μm LAMP-PUMPED	1.06 μm LAMP-PUMPED
MODULATOR	PULSE INTERVAL	PULSE INTERVAL	PULSE INTERVAL
DATA RATE	1 Gbps, 20 kbps	1 Gbps, 20 kbps, 100bps	20 kbps, 100 bps
COMMUNICATION ELECTRONICS	BASEBAND DEMULTIPLEXED	BASEBAND DEMULTIPLEXED	–
ACQUISITION & TRACKING ELECTRONICS	PROCESSING, LOOP COMPENSATION, MODE LOGIC	PROCESSING, LOOP COMPENSATION, MODE LOGIC	PROCESSING, LOOP COMPENSATION
JAM RESISTANCE ACQUISITION	MULTIPLE ELEMENT RECEIVER, CONVOLUTIONAL DECODER	MULTIPLE ELEMENT RECEIVER, PIM DECODER	MULTIPLE ELEMENT RECEIVER, CONVOLUTIONAL DECODER

6.0 Summary

The near-term experimental systems, AFTS and LSMU, are expected to demonstrate that all the key technologies and system design parameters have matured to the point that operational systems can be developed with minimal technical risk. Advance technology developments and operational system studies are paving the way for Laserccom to assume a vital role in the communication systems of the 1980's.

80-0558

SHAPED-BEAM, FREQUENCY-REUSE FEED ARRAYS FOR OFFSET-FED REFLECTORS

E. C. Nygren
Ford Aerospace and Communications Corporation
Western Development Laboratories
Palo Alto, California

Abstract

Shaped-beam, frequency-reuse feed arrays for offset-fed reflector antennas are now under production at Ford Aerospace and Communications Corporation for the INTELSAT-V spacecraft. The array-reflector combinations, which operate in the 4 GHz and 6 GHz frequency bands, generate shaped multiple beams with low sidelobes and low cross-polarization levels, thereby providing frequency reuse via both sidelobe and cross-polarization isolation. The feed arrays are comprised of clusters of closely-packed square waveguide elements which are located at the optimum reflector scan plane. Each feed element consists of a septum polarizer with dual input (output) ports which provide for both senses of circular polarization and a stepped aperture transformer. The arrays are fed by air strip-line power distribution networks which feature low RF losses, arbitrary amplitude and phase coefficients, no conventional connectors and interconnecting cables, and a lightweight construction.

I. Introduction

The growth in global communications traffic has increased the demands placed upon satellite channel capacity, which is limited by available frequency bands. In order to meet these increasing demands, two alternate approaches can be taken: 1) develop systems which utilize bands in higher frequency ranges; 2) develop techniques for increasing the capacity of existing communication bands (4 GHz downlink and 6 GHz uplink). Although the former approach is currently a reality and its further development is inevitable, the dual aspects of a mature technology and immense capital investments in equipment for the 4 GHz and 6 GHz frequency bands provide the impetus to pursue the latter alternative as a primary goal.(1) The successful increase in channel capacity within the existing bands can primarily be credited to recent advances in antenna technology which have made polarization and spatial frequency reuse a reality.

The INTELSAT-V spacecraft will be the first to employ an antenna system which provides both means of frequency reuse. At 4 GHz and 6 GHz, as shown in Figure 1, there are two hemispheric (hemi) beams for eastern and western coverage which both utilize the same frequency band. Superimposed on each of those beams is an oppositely polarized smaller (zone) beam which occupies the same frequency band and is isolated from the hemi-beam by polarization orthogonality. Thus, each complete antenna system produces four independent shaped beams from a single array-reflector combination, with stringent sidelobe interference requirements, high polarization purity demands, and the need for patterns with sharp roll-offs.(2)

Specifically, axial ratios must be less than 0.75 dB within the coverage areas, sidelobe and cross-polarization isolation between beams must be at least 27 dB, and the maximum gain slope is 1.2 dB/0.4°. The feed array developed for INTELSAT-V has made it possible to meet those requirements.

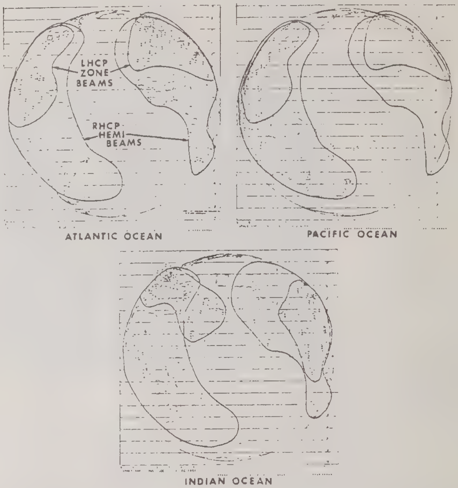

Fig. 1 Hemi/Zone Shaped-Beam Patterns

The complete INTELSAT-V antenna system is shown in Figure 2. In addition to the 4 GHz and 6 GHz hemi-/zone offset-fed reflector antennas, there are movable 14/11 GHz East and West spot beam antennas, 4 GHz and 6 GHz earth coverage antennas, and a beacon antenna(3). A block diagram of the hemi/zone antenna system is shown in Figure 3. Each hemi/zone antenna feed array consists of a closely packed array of square waveguide feed horns which are fed by the power-division and phasing networks. The feed elements feature stepped aperture transformers, septum polarizers, and dual end-launch coax-to-waveguide transitions.

The zone systems include switches which provide for the selection of one of two possible beam configurations, one of which is optimum for the Atlantic and Pacific Ocean orbits, and the other for Indian Ocean coverage. Certain feed elements are common in the formation of both beams and are fed by a network cluster which in turn is fed by the output of a fixed power divider. The second port of the power divider is attached to the switch which selects the input to the appropriate feed cluster power divider.

The excitation coefficients (amplitude and phase) required to achieve the desired radiation patterns are determined by using computer optimi-

Copyright © American Institute of Aeronautics and Astronautics, Inc., 1980. All rights reserved.

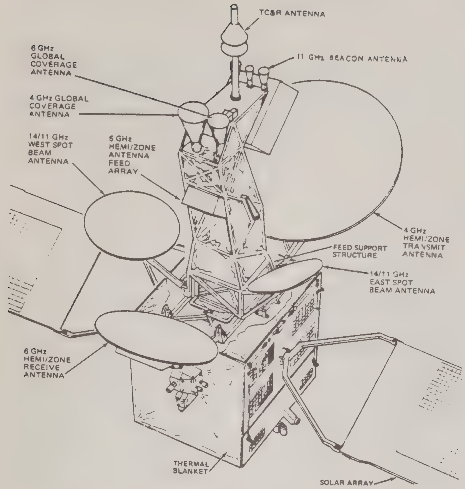
TC&R ANTENNA
6 GHz GLOBAL COVERAGE ANTENNA
11 GHz BEACON ANTENNA
4 GHz GLOBAL COVERAGE ANTENNA
14/11 GHz WEST SPOT BEAM ANTENNA
6 GHz HEMI/ZONE ANTENNA FEED ARRAY
4 GHz HEMI/ZONE TRANSMIT ANTENNA
FEED SUPPORT STRUCTURE
14/11 GHz EAST SPOT BEAM ANTENNA
6 GHz HEMI/ZONE RECEIVE ANTENNA
THERMAL BLANKET
SOLAR ARRAY

Fig. 2. INTELSAT-V Antenna System

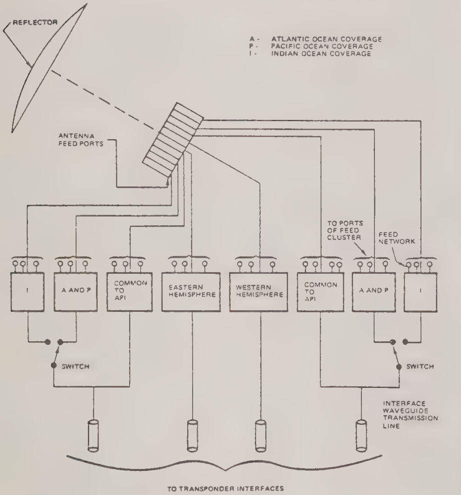
REFLECTOR
A - ATLANTIC OCEAN COVERAGE
P - PACIFIC OCEAN COVERAGE
I - INDIAN OCEAN COVERAGE
ANTENNA FEED PORTS
TO PORTS OF FEED CLUSTER
FEED NETWORK
I
A AND P
COMMON TO API
EASTERN HEMISPHERE
WESTERN HEMISPHERE
COMMON TO API
A AND P
I
SWITCH
SWITCH
INTERFACE WAVEGUIDE TRANSMISSION LINE
TO TRANSPONDER INTERFACES

Fig. 3. Hemi/Zone Antenna System Block Diagram

zation procedures. These values are then modified as required on an experimental antenna system which includes variable controls in order to modify the phase and amplitude coefficients in order to meet the beam-shape and sidelobe requirements. These experimentally optimized coefficients then become the design goals for the feed network designers.

A 4 GHz feed array is shown in Figure 4, a 6 GHz array system in Figure 5, and a set of hemi receive circuit boards and upper ground plane in Figure 6. The transmit array utilizes 79 active elements; and the receive, 82. The feed networks are located directly behind the feed array polarizers in a plane parallel to the antenna aperture, with the hemi network closest to the polarizers

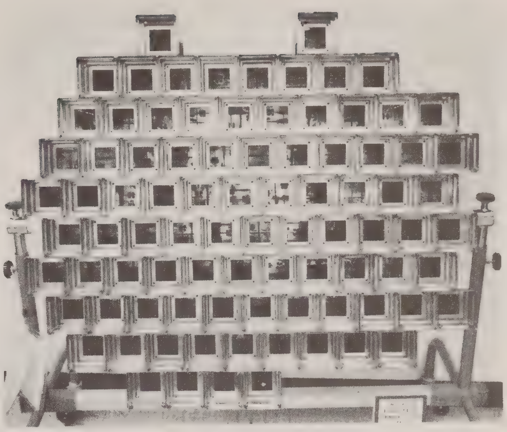

Fig. 4. Transmit Feed Array

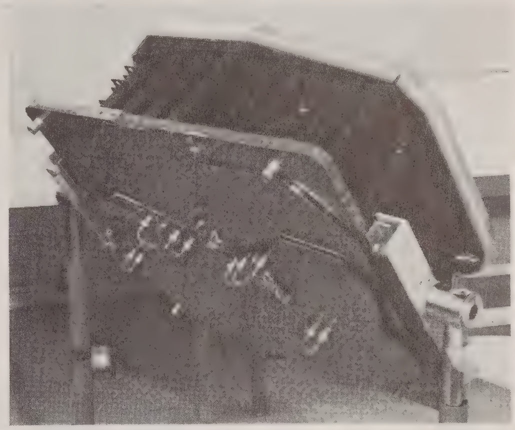

Fig. 5. Receive Feed Array System

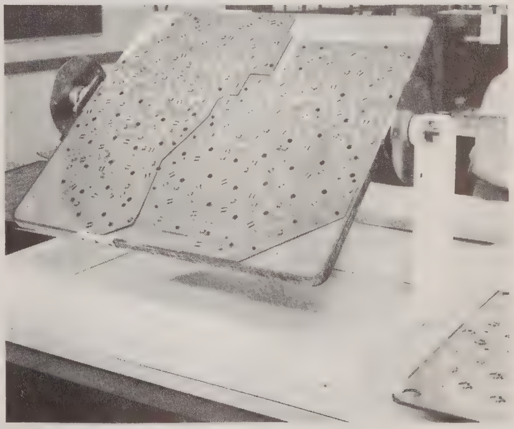

Fig. 6. Hemi Receive Circuit Boards and Upper Ground Plane

and the zone networks stacked on top of the hemi layer. Feed network outputs lie directly behind the appropriate polarizer inputs and connection is made through a short side-launch coaxial section, which is at right-angles to the plane of the air stripline network. The septum polarizer divides the square radiators into two rectangular waveguide sections, one for each sense of circular polarization. Each rectangular section, as shown in Figure 7, is fed through a hook-coupler to either a hemispherical-coverage or a zone-coverage feed network. The polarizer-feed-element units are plugged directly into the feed network package and are locked into place. The entire transmit feed array weighs 17.7 Kg; and the receive, 9.42 Kg.

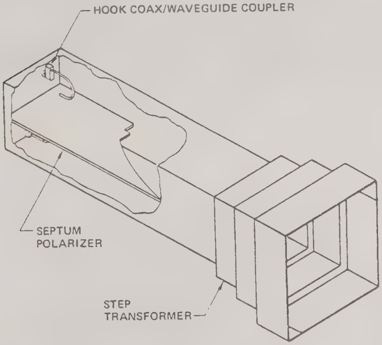

Fig. 7. Array Feed Element

II. Array Design

The antenna system shaped radiation patterns are formed by the summation of the individual illuminations from the feed elements which are fed by the beam-forming networks with the proper excitation coefficients.(4) The performance of a shaped-beam frequency-reuse offset-fed reflector system will to a great extent, be determined by its feed array. The array is comprised of many individual radiators, layed out on a regular grid pattern, each capable of simultaneously radiating (or receiving) two oppositely polarized beams. By properly designing the array, feed elements, and feed networks, the antenna system can generate shaped, multiple beams with low sidelobe and low cross-polarization levels.

The reflector geometry is determined on the basis of the requirements for shaped-beam roll-offs, sidelobe levels, isolation between coverage regions, and spacecraft physical constraints. Since an offset parabolic reflector does not produce cross-polarization for circularly polarized waves, the feed array itself controls the cross-polarization performance of the antenna system. Thus, the feed array active element pattern should have a very low cross-polarization response and the selection of a feed element type will be very strongly influenced by this factor. The size of the element will depend on the maximum allowable gain ripple and the reflector F/D ratio, but primarily its size must be such that it intrinsically exhibits low cross-polarization in the array environment and minimizes the deleterious effects of mutual coupling.

The feed element E- and H-plane patterns should be equalized to obtain low circular cross-polarization active element patterns. In addition, the active element pattern should have a well-defined phase center within a prescribed conical region around the forward direction and have a sufficient amplitude taper. It is also important to assure that undesirable higher order modes in the feed aperture, if excited by the element, are negligibly small.

In the case of an infinite array, a computer analysis can be used to design an array which displays low-cross-polarization characteristics. However, for a finite array of irregular shape, the mutual coupling between elements is very difficult to predict and will be different for each element. These mutual coupling differences will cause the axial-ratio patterns to be unbalanced and may increase average cross-polarization levels over the feed-reflector subtended angle. However, for a large array (50 or more elements), the active patterns are nearly the same for all elements except for those at the edge of the array. Thus, for the INTELSAT-V shaped-beam antenna analysis, an infinite array was assumed.

Two basic waveguide elements were considered for the feed array analysis: square waveguide and circular waveguide. The square elements were selected primarily for mechanical considerations. Theoretical studies of several cases with different array lattices and guide dimensions were conducted for a rectangular waveguide in an infinite planar array excited by a circularly polarized field. Since the cross-polarization isolation requirement is extremely stringent, the axial ratio of the feed array over the reflector substanded angle was the most important factor in selecting the feed cluster design.

The optimized array has an element spacing of 1.130 wavelengths at the low end of the frequency band and 1.243 wavelengths at the high end (10% bandwidth, transmit). These element spacings result in low cross-polarization levels, but lead to the generation of grating lobes, which for the present design, will be stronger at the high frequency where the element spacing is larger. However, the six grating lobes exist well outside the region subtended by the reflector and do not cause a significant spillover loss, since in the worst case, the element pattern is 16 dB down from the peak.

The total number of elements and the overall shape of the array is determined by the shaped-beam coverage and sidelobe isolation requirements. Whereas most of the feed elements contribute to forming the desired far-field radiation contours, some are included for the purpose of cancelling sidelobes in order to meet the beam-to-beam isolation requirements. The final transmit (4 GHz) array design consists of 88 square waveguide elements, 79 of which are active, whereas the receive (6 GHz) design employs 90 elements, 82 of which are active. The inactive elements are included near the central portions of the array (where they are not needed for beam shaping) in order to maintain continuity and each is terminated with a matched load.

The feed array design requires an efficient technique for determining the number of elements, the shape, and the excitation coefficients (both amplitude and phase) in order to obtain the proper coverage contours from the antenna system (5). However, a discussion of the beam-shaping and optimization procedure is beyond the scope of this paper.

III. Feed Element

Frequency-reuse circularly polarized feed elements must exhibit extremely low axial-ratios over the angular region subtended by the reflector. The feed must be relatively small (about one wavelength) in order to radiate low cross-polarized energy over the reflector surface. Also, mutual coupling between elements must be reduced and their E- and H-plane patterns equalized. In addition, the impedance of each element must be carefully controlled, both at the aperture and at the feeding network interface, since for a circularly-polarized feed, reflections from the feed aperture and terminals can produce cross-polarization. Finally, the polarizer itself must produce extremely low axial ratios.

The INTELSAT-V Hemi/Zone feed elements feature square waveguide radiating apertures that utilize a series of steps for impedance matching, a septum polarizer, and dual coax-to-waveguide transitions. A considerable effort was invested in the development of the feed element in order to produce extremely low levels of cross-polarization.

Polarizer

It is necessary to select a polarizer design which will not only produce the required electrical performance, but will also be suitable for use in an array and must be compact and of light-weight construction. These considerations, in addition to the frequency reuse requirement, limit the number of suitable condidates. The design selected for the INTELSAT-V application, the septum polarizer, is a compact waveguide device which produces both right-hand and left-hand circularly polarized waves. It has a square cross-section waveguide at the aperture end and a sloping curved septum which divides the guide into two rectangular cross-section waveguides with a common broadwall. One section corresponds to the RHCP port and the other to the LHCP port. Thus, the septum polarizer performs the function of an orthomode transducer in separating the two orthogonally-polarized signals.

In order to obtain approximately 90° of phase shift over the operating frequency band, the shape as well as the total length of the septum is critical. Also, the size of the square waveguide should be selected so it is well above cutoff at the lowest frequency of interest and slightly below the cutoff for the next higher mode at the high frequency. The INTELSAT-V septum polarizer was designed such that a -90° phase response occurs twice within the desired frequency band. This "balanced phase" response yields a lower axial ratio over a broader bandwidth than do other candidates considered, which have monotonically increasing phase functions.

The septum polarizer was optimized in a closed waveguide system with a precision rotating section which permitted a probe to be easily rotated to any position. The performance of the final design is summarized below.

Frequency, GHz	3.7-4.1
Maximum Axial Ratio, dB	0.16
Insertion Loss, dB	0.08
Return Loss, dB	28
Isolation, dB	32

The operating temperature range for the entire feed system is -90°C to +55°C and the axial-ratio of the polarizer must not exceed 0.2 dB at its worst condition over this range. The feed element (shown in Figure 8) is a graphite reinforced plastic (GRFP) structure with copper plating on the inside surfaces and weighs 55 gm and 35 gm for transmit and receive respectively. The differential spacing between opposite walls of the polarizer body must remain within 0.2 to 0.3 mil over the temperature range to meet the axial ratio requirement. In order to meet axial ratio and isoiation requirements, tuning devices are employed. Primary tuning is achieved by adjustment of three screws opposite the curved edge of the septum to provide the best axial-ratio performance; and if a slight out-of-square condition exists, small corner clips may be added for compensation.

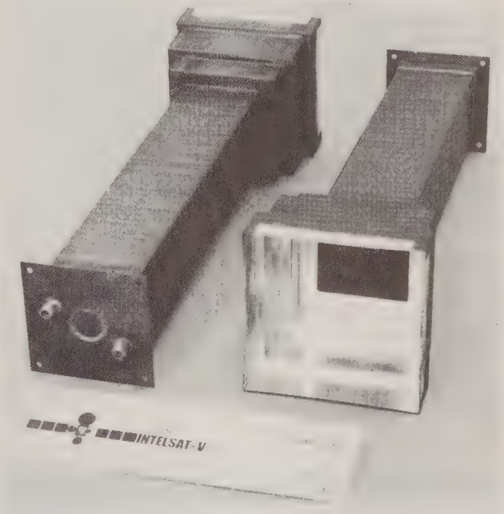

Fig. 8. Graphite-Epoxy Feed Element

Aperture Steps

The first goal for the feed element design was to match the feed element aperture to the polarizer. A stepped rather than tapered transition was selected in order to minimize the overall feed element length. Matching was accomplished by using a central array element which was fitted with variable sliding sections, resulting in a worst case measured VSWR of 1.17:1 for the optimized stepped aperture.

Feed Element Aperture

Next, in order to reduce the cross-polarization of the feed element to acceptable levels, two modifications were implemented at the aperture. The first reduced mutual coupling between elements and the second equalized the E- and H-plane beamwidths. A 6 GHz 7-element array consisting of a central element surrounded by a ring of six others was used to experimentally accomplish the objective of optimizing the feed aperture in the array environment. Before installing the central element in the array, its septum polarizer was pretuned for a minimum axial-ratio. Then, small hook-like metal tabs, which were empirically designed, were placed in the aperture to reduce mutual coupling from about -30 dB to more than -43 dB throughout the operating band. The tabs reduce mutual coupling to the same amount for every element in an array and make it possible to essentially treat every feed as a single, isolated element.

The 7-element feed array was then moved to an antenna test range where active element axial ratio patterns could be measured. Additional "equalizer" tabs were added to the aperture in order to approximately equalize the E- and H- planes.

Feed Element Rotation

The element design features which were established on the 7-element array were incorporated into a 48-element feed array. Upon examining initial measurement results, it was decided that the polarization ellipses of the individual elements were all oriented in the same direction. In order to obtain some cancellation between ellipses, every other element was rotated 90° with a resultant slight improvement within the entire frequency band. The final shaped-beam pattern of the 48-element array and offset reflector exhibited a maximum axial ratio of 0.6 dB and a typical value of 0.25 dB.

Coax-to-Waveguide Coupler

The tightly packed waveguide feed elements, each with two inputs, require end-on collinear waveguide coaxial transitions. After examining various concepts, a hook-type coupler was selected. The coupler, shown in Figure 7, is simple and displays a maximum VSWR of 1.07:1 over the required frequency band.

IV. Feed Network

The INTELSAT-V shaped-beam antenna system presented a unique challenge to the feed network designer: Given a large, tightly-packed array of radiating apertures, design a feed network system that would provide two independent sets of complex output coefficients. Because of the tightly-packed array geometry, both of the polarizer inputs require coax-to-waveguide transitions which enter from the rear of the element, thereby precluding waveguide network systems. To answer the INTELSAT-V challenge, a high-performance feed network system was developed. It features a thin, low-loss, air stripline geometry which allows it to mate directly to the feed radiators without conventional RF connectors and interconnecting coaxial cables. Complex, arbitrary feeding coefficients are produced by the networks, some of which have dozens of output terminals, and each with only a single input.

The transmit and the receive feed systems each include six separate feed networks: Western and Eastern Hemis, Western and Eastern Atlantic/Pacific Zones, and Western and Eastern Indian Ocean Zones. The Eastern and Western Hemi circuit boards are supported between common ground planes, as are the Eastern and Western Zone boards. The entire transmit feed network package has 120 output ports; and the receive, 126. The overall size of the transmit network package is about 3 feet by 4 feet and the receive unit is about two-thirds as large. The dielectric circuit boards, which occupy about 12% of the region between ground planes, consist of a teflon impregnated fiberglass cloth with etched copper traces on both sides.

The network achieves the desired power distribution through the use of unequal impedances at matched, cascaded junctions, whereas the relative phases are realized through the use of differential line lengths. The requirement that the phase and amplitude of each output be arbitrary, imposes the condition that the path from the network input to every output is geometrically different from all other paths. Thus, there is no symmetry and the exact characteristics of each path must be carefully analyzed to maintain tight phase tolerances. The behavior of the power-division elements, transmission line bends, mismatch effects, etc., must be considered in detail.

To ensure that accurate differential phases are obtained, all line lengths were mathematically calculated and optimized through the use of a computer-graphics system. The power-division element characteristics were experimentally determined and the phase characteristics of bends in the air stripline were measured. The computer-optimized line lengths and measured power division junction performance characteristics were fed into a network analysis program which determines output amplitudes, phases, and the VSWR at each terminal. Based upon the computer analysis, necessary design changes were determined and applied to the theoretical design. When the network line lengths were finalized, the computer-graphics system produced the program through which negatives suitable for circuit-etching were obtained.

Before designing the complete feed networks, each factor contributing to the electrical performance was individually investigated. Studies included the properties of air stripline, power division elements, side-launch transitions, circuit-to-circuit isolation, bends and network tuning. The final network design procedure then accounts for each contributing factor in order to obtain high-performance networks from the first etching.

Air Stripline

Impedance and Phase Velocity. The dielectric-supported air stripline (shown in Figure 9) consists of two parallel center conductors attached to a thin dielectric support substrate. Ground planes parallel to the center conductors complete the balanced transmission line for TEM-mode propagation. By making the dielectric substrate thickness small with respect to the stripline height, most of the fields will be concentrated in the air-filled (or vacuum) region, thereby minimizing the dissipation loss due to the dielectric material.

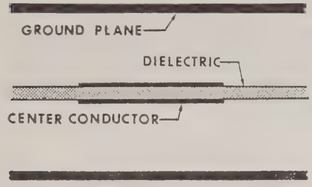

Fig. 9. Dielectric-supported Air Stripline Geometry

The inhomogeneous nature of the transmission media, however, causes difficulties in calculating the characteristic impedance and phase velocity of dielectric-supported air stripline. A variational method of analysis has been employed by Gish and Graham (6) to analyze this stripline configuration in the presence of sidewalls and for a zero-thickness center conductor. A computer program which uses a modified version of the Gish and Graham method was used to determine the air stripline parameters.

Attenuation. Only a small portion of the field lines will pass through the dielectric substrate due to fringing. Thus, the attenuation in air stripline is due primarily to the conductor losses. In order to experimentally determine the attenuation, a meandering 50 ohm line was tested with copper-plated aluminum ground plane with 0.25" spacing between ground planes. For this geometry, the measured loss was 0.108 dB per foot at 4 GHz.

Power Division Elements

Network power division elements with geometries suitable for printed circuit techniques were selected for experimental studies. These elements all have outputs which are isolated from each other and the input impedance of each is matched when looking into any arm when the other arms are terminated by matched impedances. Additionally, the power incident upon the input of each is, in general, divided unequally between the outputs.

Several three and four-port devices were potential candidates for use as dividing elements and could be fabricated in air stripline. However, after considerable development, it was concluded that only the ring-hybrid and symmetrical directional coupler configurations were suitable for the current application.

Ring Hybrids. Ring hybrids with both circular and elongated geometries were utilized. The desired power-split ratios of experimental hybrids deviated somewhat from theoretical predictions for unequal-split elements. This was due primarily to junction effects and to the fact that the phase velocity of air stripline is different for each impedance and thus, quarter-wave lengths also are different for each section. In order to generate design curves for the hybrids, compressed rings with power ratios of 1.0:1 to 5.5:1 and circular rings with power ratios of 1.0:1 to 3.5:1 in ratio increments of 0.5 were constructed and tested. The curves correcting for the deviation between measured and theoretical power-split ratios were incorporated into the hybrid-ring design computer program.

Since as many as six power-division elements were cascaded in the feed networks, it was imperative that each junction mismatch be minimized in order to avoid VSWR build-ups at the output terminals. Thus the electrical performance of each test hybrid was improved by experimentally adding matching tabs near the junctions.

Broadside Directional Coupler. For junctions which require large power division ratios, hybrid-ring and compressed hybrid-rings cannot be used. Symmetrical directional couplers, on the other hand, are generally useful for large power division ratios, but not for low ratios, because of the small gap spacings required. For these cases, couplers were designed which had the dielectric material removed on either side of the coupling section and the edges copper-plated to simulate rectangular rod conductors.

Side-Launch Transitions

Three major problems were encountered in employing conventional side-launch transitions at C-band frequencies:

1. The side-launch transition geometry presents a discontinuity in the non-homogeneous air-stripline transmission line, which can launch parallel plate modes causing mismatches, phase deviations and losses at various points within the frequency band of interest.

2. The side-launch transition also can generate trapped modes between the strip conductors within the dielectric support, which also manifest themselves in the form of mismatches, phase deviations, and losses at various points within the frequency band of interest.

3. All known side-launch transition geometries in air-stripline presented fairly high voltage standing wave ratios to the output ports at C-band frequencies.

The side-launch transition, shown in Figure 10, was developed to overcome all three problems, and, in addition, provide support for the circuit board. In order to eliminate the parallel plate moding, the U-shaped "dam" section was used. To eliminate the deleterious "trapped" mode, the dielectric is removed for a small distance along the center conductor strip. The side of the strip is then plated with metal in order to simulate a short section of rectangular conductor, which will not launch the mode.

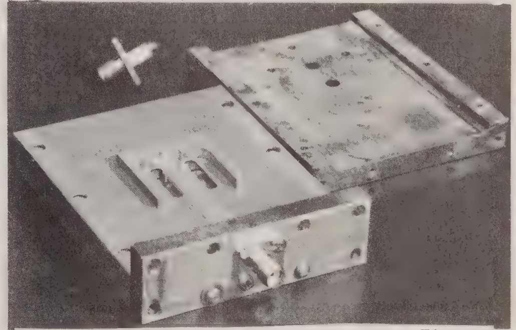

Fig. 10. Side-Launch Transition in Test Fixture

The U-shaped dam consists of two sections, one above the circuit board and one below it, providing support at every output. A time-domain reflectometer was employed during the transition development so that the final version was broadband. Within the transmit band (3.7-4.2 GHz), and the receive band (5.9-6.4 GHz), the measured VSWR was below 1.05:1 and no extraneous modes were present.

Circuit-to-Circuit Isolation

Since there are many transmission line paths in close proximity with each other, it is of interest to know what minimum spacing can be tolerated in order to avoid coupling between adjacent lines. To answer that question, isolation was measured for parallel lines with several spacings separating them. The length of the line in the coupling region was about a quarter of a wavelength within the frequency band of interest. The test results indicated that for coupling to be less than -30 dB, the separation must be at least 75% of the ground plane spacing.

Bends

The feed networks include several bends in each path and in order to determine their properties, test circuits with mitered bends of various angles were tested. The bends exhibited shorter RF paths than the physical centerline paths would indicate and corrections were used for the network layouts. For example, the phase through a 90° bend was about 6° shorter than that calculated on the basis of the center-line path length. Since there may be 20 or more bends in a given input-to-output path, it is essential that they be accounted for.

Stub-Tuners and Phase Shifters

The network design goal for the output VSWR was a maximum of 1.25:1 within the frequency band and the phase accuracy goal is for the worst case to be within ± 20°. To meet these goals, tuning and phase shifting devices were developed which would improve performance after the network had been initially tested. To accomplish this goal, networks are first assembled with non-locking fasteners and tested. Based upon the test data, stub tuners and phase shifters are then added to the network boards as required, prior to assembly with locking hardware.

Network ports with VSWR levels exceeding 1.25:1 are tuned using 0.005 inch thick stubs soldered to the circuit lines which emanate from the side-launch transitions. The lengths and locations of the tuning stubs are determined from the impedance measurements made on the Automatic Network Analyzer (ANA).

Phase shifters are installed on the circuit boards in order to compensate for errors greater than ± 20° (including relative line length phase dispersion). A reliable, low VSWR and low-loss phase shifter was obtained by using 0.025 inch thick Epsilam-10* material. The dielectric is clad with copper on one side and a copper-to-copper bond is obtained with the 50 ohm air stripline circuit traces. To maintain air stripline symmetry, identical strips are bonded to both sides of the circuit board and the phase shifter length is set at approximately half a wavelength in order to maintain a good impedance match. Phase shift increments are obtained by varying the width of the phase shifter (i.e., the fraction of the 50 ohm trace it covers) and phase shifts of up to 20° can be obtained for a single section.

Multipactor and High-Power Tests

Multipactor and high-power breakdown tests were conducted on key components. Testing was conducted in a thermal/vacuum chamber which was evacuated to a pressure of 3×10^{-5} Torr. Visual observation through a window in the chamber was used during testing to detect multipactor breakdown, and incident and reflected power were also monitored. None of the components exhibited either form of breakdown during the tests.

V. Array Measurements

Each antenna feed array is thoroughly tested before installation on the spacecraft antenna tower with its associated offset reflector. Before the array is assembled, all feed elements and distribution networks are individually tested and optimized. The entire array is electrically tested, vibrated, and then temperature cycled ten times over the operating range (-90°C to +55°C), during which time, electrical measurements are periodically performed.

The performance of the feed array is characterized by phase and amplitude errors, VSWR, and by RF losses. Theoretical and experimental studies led to the conclusions that the following performance limits should be satisfied for the array feed elements:

Phase Error, Max.:	± 20°
Amplitude Error, Max.:	± 0.6 dB
VSWR, Max.:	1.28:1

Only a small number of feed elements would approach the limit extremes and most would display far superior performance levels.

The complete array is tested by employing "sniffer"** elements which are used to measure the relative amplitude and phase, isolation and VSWR at each element aperture.

An automatic network analyzer is used to record and analyze the measured data and to provide printouts of the phase and amplitude error† at each port, the VSWR for each port, network loss, and average phase and amplitude errors for the network.

---

* 3M Company dielectric with relative dielectric constant = 10.

** A "sniffer" is an element which is identical to the feed element under test except that it does not have the stepped section, so that it can mate directly with the first square guide section which includes the polarizer.

† Errors are defined as any deviation from the center frequency design goals and include the inherent frequency dispersion of the differential line lengths, power-division junctions, etc.

As an example of the measured performance of an entire feed array, consider that portion of the receive (6 GHz) system which forms the Western Hemispherical beam. Forty-two of the array feed elements are fed from a single air stripline distribution network. The pertinent parameters, which were measured by utilizing the "sniffer" technique, are listed below for several frequencies.

Receive Hemi Array Performance

Freq. GHz	Loss dB	Average ± Error Amplitude dB	Phase DEG	Average VSWR
5.9	1.12	0.18	4.9	1.18
6.0	1.12	0.22	4.0	1.17
6.1	1.13	0.21	3.7	1.16
6.2	1.18	0.19	3.9	1.15
6.3	1.18	0.18	4.6	1.17

Average cross-polarization (swept) = 35 dB

Temperature tests indicated that some amount of dielectric circuit support warpage took place when the networks were brought up from the cold extreme to ambient. Rather than adding many additional spacers to support the board, a low dielectric constant foam was sandwiched between the circuit board and each ground plane. The foam accounts for about 0.2 dB of the feed network loss.

Each feed array is enclosed in a specially constructed foam thermal test chamber and then cycled through the temperature extremes 10 times. RF measurements are conducted at various temperatures by inserting metalized foam plugs into all feed apertures and then utilizing the "sniff test" technique to obtain the VSWR, amplitude, and phase of each feed. The foam plugs provide temperature insulation and their metallization serves as waveguide aperture extensions which enable tests to be conducted at temperature extremes. In addition to the temperature workmanship test of each array, a separate transmit feed system will be designated as the Life-Test unit and will be cycled 200 times, during which time measurements will be recorded at periodic intervals in order to verify the in-orbit integrity of the feeds. In addition, the feed system will be subjected to vibration and acoustic tests.

VI. Antenna System Performance

Although it is beyond the scope of this paper to discuss the overall antenna system performance, a comparison of predicted and measured pattern contours is presented in Figures 11 and 12. In Figure 11, the calculated West Hemi Receive coverage contour is shown for the case of 6.130 GHz and for comparison, the measured contour at 6.129 GHz is given in Figure 12. Each antenna coverage is evaluated in terms of five primary parameters: minimum gain/coverage (dBi); gain slope (dB/0.4^{o}); axial ratio (dB); sidelobe isolation (dB); and cross-polarized isolation. To obtain the cross-polarized isolation, contours similar to those given are obtained for the opposite sense of circular polarization from that of the antenna of interest. All other parameters are either directly measured, or obtained from the contour plots. As may be noted from a comparison of Figures 11 and 12, excellent correspondence between predicted and measured performance has been obtained.

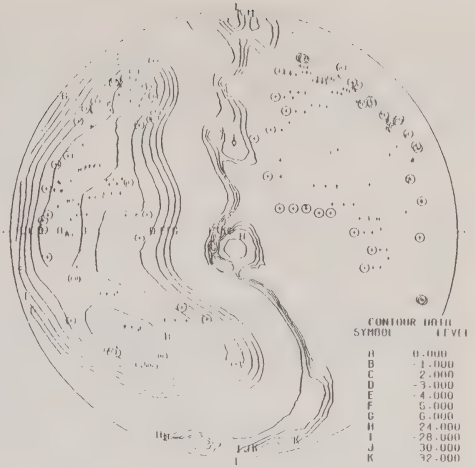

Fig. 11. Calculated West Hemi Receive Coverage Contour For 6.130 GHz

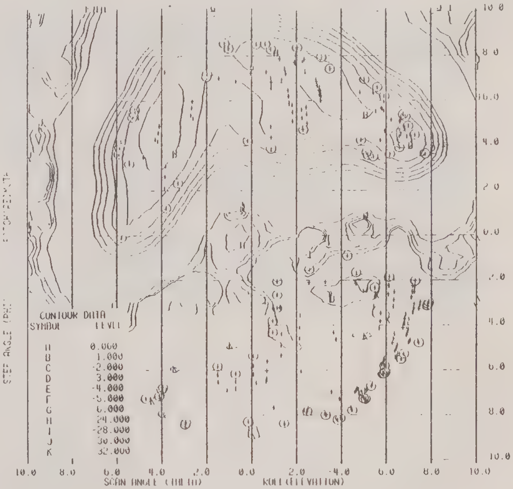

Fig. 12. Measured West Hemi Receive Coverage Contour For 6.129 GHz

VII. Summary and Conclusions

The feed array concept which was developed for the INTELSAT-V Hemi-Zone antennas has made it possible to meet the stringent requirements imposed upon the shaped-beam frequency-reuse systems for the ground stations within coverage regions. These include axial ratios of less than 0.75 dB within the coverage areas and sidelobe and cross-polarization isolation between beams of greater than 27 dB. The feed array system, which features septum polarizers and air stripline distribution networks, was analytically optimized and then experimentally refined in order to meet electrical requirements. The phase errors were within ±20^{o}; the amplitude errors, less than ± 0.6 dB; the VSWR levels, less than 1.28:1; RF losses were low. The mechanical design includes the selection of graphite-epoxy feed elements and honeycomb feed network ground planes.

Acknowledgement

The work described in this paper was performed by many individuals, including the author. A partial list includes Dr. C. C. Han, Dr. S. W. Lee, Paul D. Frank, Gary H. Schennum, Harry J. Gould and Dr. E. W. Matthews.

References

1. D. F. DiFonzo, "Introduction to Commercial Communications Satellite Systems", Communication Satellite Antenna Technology, Short Course, Boston University, Oct. 31-Nov. 4, 1977.

2. C. C. Han, "A Multifeed Offset Reflector Antenna for INTELSAT-V Communication Satellite", Seventh European Microwave Conference, Bella Center, Copenhagen, Denmark, Sept. 5-8, 1977.

3. V. J. Jakstys and H. T. Ward, "INTELSAT-V Spacecraft Antennas Subsystem", Technical Conference and Exhibit by International Foundation for Telemetry, presented at Los Angeles Airport Hyatt House, Nov. 11, 14, 15 and 16, 1978.

4. E. W. Matthews, C. L. Cuccia, and M. D. Rubin, "Technology Considerations For The Use of Multiple Beam Antenna Systems in Communication Satellites", 1979 MTT Symposium, Orlando, Florida, April 30-May 4, 1979.

5. C. C. Han, A. E. Smoll, H. W. Bilenko, C. A. Chuang, and C. A. Klein, "A Beam-Shaping Multifeed Offset Reflector Antenna", paper 76-249, AIAA/CASI 6th Communications Satellite Systems Conference, April 5-8, 1976, Montreal, Canada.

6. D. L. Gish and P. Graham, "Characteristic Impedance and Phase Velocity of a Dielectric-Supported Air Stripline With Side Walls", IEEE Transactions, MTT, March 1970.

80-0526

THE IMPACT OF SATELLITE TECHNOLOGY ON RURAL TELEPHONE SYSTEM PLANNING

Bruce B. Lusignan, Mousa M. Mousa
Mohammed K. Samarkandy and Ching C. Han
Communications Satellite Planning Center
Stanford University
Stanford, California 94305

Abstract

Telecommunication system planning and development for rural areas is instrumental in the advancement and modernization of developing countries. There are many practical communication facilities that can be employed to implement a telecommunication system. The maturity of satellite technology in the 1980's will definitely have a strong costing and technical influence in implementing the architecture of such a system. This paper conducts trade-offs among various technologies such as radio telephone, cable, UHF/VHF radio, switches and satellites for various geographical environments. It then assesses the state and impact of satellite technology in relation to supplementing the existing telephone networks and/or planning a new rural telephony network.

I. Introduction

The rapid improvement in satellite and ground technology in recent years and expected advancement in the 1980's have greatly reduced the cost of satellite communications, especially for national telephony, television and data interconnection services. A number of nations, such as Brazil and Saudi Arabia have national services based on the INTELSAT system. Some nations such as the United States and Canada have domestic satellite services to supplement national telephony networks. It is expected that the role of satellite systems will grow in implementing a rural telephony network, both where there are existing facilities and where totally new networks are needed.

The expanding use of satellites results in part from cost reduction brought about by technical advances. Today, a simple TV reception station can cost as little as $7,000 and a small two-way telephone station can cost as little as $40,000. Practical national networks using satellite technology have appeared almost overnight. The very rapid reduction in ground station cost, from $8 million to $40,000 in about eight years, presents national planners with the need to review their telecommunications investments.

The attractiveness of satellites for many countries has also improved as a result of reduced technical domination. The European Space Agency, People's Republic of China and Japan will follow the United States and the Soviet Union in establishing a proven capability to launch satellites into synchronous orbits. A number of industrial nations have already developed the capability to construct satellites and their associated subsystem components.

This paper will review the different classes of satellite ground stations with special emphasis on the small stations suited to national telephone networks. Following that, a review of other technologies will be presented showing how satellites compete with radio relay, cable, small switches and radio telephone technologies. Emphasis will be placed on rural telephone applications where there are advances in all these areas.

II. Low Cost "Domestic" Satellite Ground Station

Satellite ground station cost, a vital factor in determining the advantage of satellites relative to terrestrial facilities, has been reduced drastically in recent years. This has been a known fact in complex INTELSAT type stations employed to handle heavy international telephone traffic. But most significant of all, is the introduction in the early 1970's, of the so called "Domestic" stations. These stations are used extensively in the United States, originally for rural telephone service in the state of Alaska, and then widely for television and radio distribution and data interconnection throughout the rest of the country. They are also used with the Canadian and Indonesian satellite systems. There are well over a thousand of these stations in use today and will be most important to developing countries in the future.

The low cost of the "Domestic" station is made possible by reduction in the diameter of the ground antenna and reduction in the sensitivity of the ground receiver. The "Domestic" station uses an antenna of 4 to 5 meters in diameter and an LNA temperture of 120° K. The standard INTELSAT A and B stations use much larger antennas (10 to 30 meters) and more sensitive LNA's (about 60° K). Because of their smaller antennas and less sensitive receivers the "Domestic" stations have a smaller "Figure-of-Merit". With the "Domestic" stations it appears that there would be a major penalty in cost of satellite power. Fortunately, satellites for national or domestic service such as for Canada, Indonesia and the United States, cover a smaller area with highly efficient shaped beam antenna. The improvement in satellite coverage antenna gain has increased the strength of the signals almost 10 times, making up for almost half of the "Figure-of-Merit" differences between "Domestic" and standard "A" stations. Although the later INTELSAT satellites are also equipped with shaped beam antennas, but as yet developing nations have not taken advantage of this improvement. Another means in compensating for the lower "Figure-of-Merit" is the use of sophisticated modulation techniques in the "Domestic" station. The standard "A" and "B" stations use either FDM-FM or PCM-SCPC, two fairly old and only moderately efficient modulation techniques. The "Domestic"

Copyright © American Institute of Aeronautics and Astronautics, Inc., 1980. All rights reserved.

stations use either CVSDM-SCPC or amplitude compandored FM-SCPC with Voice Activation. These sophisticated new techniques, which use less than a tenth as much power from the satellites as the earlier techniques, in combination with shaped beam satellite antennas, completely compensate for the difference of "Figure-of-Merit" between standard "A" and "Domestic" stations. The size of the ground antenna can then be determined by a cost trade-off between ground antenna size and satellite power. For a typical application, where 1,000 stations are assumed to provide 3 to 4 telephone channels, each to meet a typical rural telephony need, the optimum ground station size turns out to be around 4.5 meters.

There is another important factor in the cost of "Domestic" stations known as "Transponder Gain". For telephone service the station transmits the signals up to the satellite. They are received by the satellite, amplified in the transponder, and re-transmitted back to earth to the desired receiving station. The Transponder Gain determines how strong the signals received by the satellite have to be in order to transmit sufficient signal strength back to the ground. If the Transponder Gain is too small excessive power will be required from the ground station transmitter. Choosing correct Transponder Gain also guarantees that interference to other satellites is minimized. With correct Gain the "Domestic" stations meet all International recommendations for adjacent satellite protection.

National or regional satellites must have higher power radiation (32 dB to 35 dB per transponder). They also must provide a Transponder Gain which is sufficient to give the ratio of $(S/N)_{down}$ to $(S/N)_{up}$ at about 7 to 10 dB for a "Domestic" station. With such satellites, the "Domestic" stations can have a variety of applications, including television reception for local redistribution by cable or by low power transmitter to conventional TV sets.

The focus of this paper is on telephone services. Here the "Domestic" satellite stations offer very attractive solutions for bringing services to remote towns. The stations can be installed in about one week by a crew of four or five technicians. A station is easily transported to the site by truck, and once erected it operates unattended. However, the satellite systems are not the best for all service requirements, but rather a mix of the available technologies.

III. Radio, Radio Telephone, Cable and Switches

The other technologies which are available to provide telephone service to rural areas include radio, cables, and a new technology radio telephone. Each of these technologies, as described briefly below, can be used in conjunction with local small switches. Together with the satellite stations described previously these technologies make up the building blocks of the rural telephone network.

A. Switches

Small rural switches, also called PABX (Priate Automatic Branch Exchange) or concentrators, connect the personal telephones to the equipment carrying the calls over the long distance. Their basic cost advantage is that they allow a number of long distance circuits, this substantially cuts down the cost of the long distance equipment. The typical cost of small switches (concentrators) is from $400 to $600 per telephone. A small switch would allow 30 to 40 telephones to share 3 or 4 long distance circuits.

B. Open-Wire or Buried Cable

Wire and cable are used to connect the subscribers lines to the nearest location with switching capabilities or to interconnect switching equipment. In some systems, amplifiers (repeaters) are installed every 2 to 5 Km to maintain signal quality. The cable can be run either long distance into more centralized offices, or to intermediate small switches or concentrators. The switches reduce the number of lines needed between the concentration points and the central offices. With concentration, the number of channels required depends on the calling rate and the desired grade of service.

C. VHF or UHF Radio

Radio is also used to provide communications in rural areas. The VHF or UHF terminal equipment consists of a directional antenna, an antenna tower (10m - 90m), modem, multiplexer, and power supply. The subscribers at one location can each use a dedicated channel, or a group of subscribers can share a channel, providing the subscribers' lines are first connected to a concentrator. Implementing VHF or UHF radio for distances beyond the horizon (usually 20 to 30 Km) requires the installation of a radio repeater. The cost of a repeater is substantial, making this technology fairly unattractive for paths requiring a number of repeaters. The VHF-UHF radio system cost varies with the number of channels, the antenna gain, tower height and transmitter power, depending on the distance of the link and on the geographic features. Typical VHF and UHF installations cost $54,000 plus $1,000 per channel. Repeaters may cost $43,000 plus $3,600 per channel.

D. Radio Telephone

Radio Telephone technology is another means by which to serve rural areas. This type of communication technology is important where a number of small communities fall within the radio coverage area of a central point. Each subscriber in this system is equipped with a telephone set, VHF-directional antenna, duplex radio and a logic unit for control. Subscribers are controlled by a central base station. This base station is equipped with a number of duplex radio channels, omnidirectional antenna, power supply and a switch control system. The major cost for the subscriber's unit is contributed by tower, duplexer and transmitter power requirement. The signal level required at different distances from the base varies; this makes the radio telephone cost vary with distance. Station cost is contributed by the switch, controller, antenna tower and transmitter. Typical base stations may cost $10,000 plus $2,500 per channel.

IV. Methodology of Cost Comparison and Sensitivity Analysis

A computer program based on a modified infinite search procedure has been used to compare the various technologies in providing rural telephone services. This program gives not only an optimized combination of technologies, but also a year by year installation plan to meet budget limitations and to serve the greatest number of people in each year. Population and geographic location are two parameters which are used in projecting the expected telephone service demand over the planning period which is usually 15 years. Capital costs, installation, expansion, and maintenance costs describe the available technologies. All possible combinations of interconnections and technologies are tested by the program to find the least cost solution. Cost comparison is based on the present value of the expenditure over the total study period.

A number of cases were analyzed for the same area having 28 communities with populations ranging from 500 to 2,500 people to assess the role of the different technologies by restricting the solutions of particular combinations. The total system cost and the amount of each technology used in the network depends on the costs assumed. It is important for both equipment manufacturer's and for buyers to be aware of how different technologies compete with each other in rural applications. It is difficult in planning to obtain competive comparisons between similar equipment manufactured by different companies. It is even more difficult to obtain guidance on selecting between dissimilar equipment.

In order to show how one equipment type competes with others in rural applications this study employed a base case where all technology are allowed for an optimum interconnection of the 28 communities. One by one, each technology is raised and lowered 50% in price, keeping the prices of the others constant. The resulting change in selection of that technology is a measure of market price elasticity for the technology. How much can its price be raised before the sales drop seriously? How much increase in sales will result from price reductions? The analysis also gives information on the sensitivity of overall network costs to changes in costs of one technology. The results of this study have revealed the following interesting points:

1. Most clearly "Domestic" satellite stations compete directly with VHF or UHF radio links. If there is a direct line-of-sight link between two towns, the VHF or UHF radio will be less expensive than "Domestic" satellite stations, at the nominal costs. If the VHF or UHF radio goes very much up in price, or the satellite down, then VHF or UHF radio is eliminated. If the VHF or UHF radio decreases in price, or the radio telephone increases, then radio telephone can be less expensive even when one repeater is required between towns. Satellites may still be suited where two radio repeaters would be needed (over 50 Km) but this remoteness would be rare in most countries.

2. Secondly the role of cables is constrained to distances up to about 5 to 8 Km. Over this distance VHF or UHF radio is less expensive. The "Break Even" distance varies somewhat with numbers of lines required and with prices of cable and radio, but pretty much stays within this range.

3. The radio telephone application is shown most clearly when these cost comparisons are studied together with other data. These show radio telephone to be most useful in areas with a number of small communities, 20 to 200 people separated by small distances, 2 Km to 10 Km. Such distributions are found in the farming areas of most developing countries. In this kind of region, family groups or very small towns are spread out over the arable land to be near their individual farms. It is much less expensive to provide telephone service to them by radio than by cable or any other means.

V. Conclusions

If care is taken in the specification of satellites and ground stations, the new technology can be of great use to developing countries. The satellite power level must be correct and its Transponder Gain be appropriatly set to serve the small "Domestic" class ground stations.

The satellite technology then can take its proper role along side the older technologies of VHF or UHF radio, cables, small switches, and the newer technology of trunked radio telephone. The appropriate combination of all these technologies can reduce the cost of telephone service to rural areas by a factor of about five over what it has been in the recent past. With this reduction in cost, many countries can now consider providing rural telephone service where previously such services were unaffordable.

Bibliographies

1. M. Mousa, "Role of Trunked Radio Telephone Technology in Rural Communication Networks", Ph.D. dissertation, Communication Satellite Planning Center, Stanford University, in preparation.

2. J. J. Ginty,"An Analysis of Domestic and Foreign Small Earth Station Markets". O. T. Report 76-3.

3. M. K. Samarkandy, "The Small Earth Terminal, Design Considerations and Cost Analysis", Communication Satellite Planning Center, Stanford University, June 1978.

4. John D. Von Bergen, "Maintenance and Operations Engineering Considerations in Developing Nations" INTELCOM 79, Dallas, Feb. 26-Mar. 2, 1979.

5. "Plan Rector Para El Desarrallo de la Telefonia Rural", Datas Basic Laboratorio de Telecommunicationes C.I.C.E.S.E., Ensenada B.C., Mexico Junio de 1979.

6. S. G. Pitroda, "State of Telecommunications in Developing Countries-An Overview", IEEE Trans. Commun., Vol. Com-24, July 1976.

7. F. J. D. Taylor, "Domestic Satellite Systems for the Lesser-developed Countries", Telecommun. J., Vol. 44, 11/1977.

8. CCITT, editorial Working Party on Rural Telecommunications, "Single Channel Radio System in Rural Telephony", a draft of Chapter 2, see 5.5.2 of Radio-Transmission and Distribution, June, 1976.

9. W. Carl Mitchell, "The Use of Satellites is Meeting the Telecommunication Needs of Developing Nations", Ph.D. dissertation, Satellite Communications Planning Center, Stanford University, June 1975.

10. Panjuna Gurg Sharma, "Rural Communication Planning Methodology for Integrating Satellite and Terrestrial Facilities", Ph.D. disseration Communication Satellite Planning Center, Stanford University, December, 1976.

80-0495

INTERNATIONAL AND MOBILE SATELLITE SYSTEMS AFTER WARC-79

David J Withers
The Post Office, London, England

Abstract

International satellite systems tend to have heavy traffic with fast growth. These traffic demands lead to frequency re-use or duplicated satellites and earth terminals or more sophisticated transmission techniques. The additional bandwidth allocated by WARC-79 at L-band, 4/6 GHz and 11/14 GHz will provide a fourth option, and one that INTELSAT, INMARSAT and EUTELSAT, for example, will surely use in the 1980s.

The use of intersatellite links to convert two satellites, neighbours in orbit, into a single interconnected network is a further option, particularly of interest for INTELSAT, and its realisation has been brought nearer by the intersatellite allocations made by WARC-79 at 23 and 32 GHz.

It is impossible to guess now the impact on an organisation like INTELSAT of the forthcoming WARC on guaranteed orbital access.

I International fixed-satellite systems

WARC-79 approximately doubled the bandwidth available for international fixed-satellite systems at 6 and 4 GHz and also doubled the bandwidth available for them at 14 and 11 GHz. In many countries the same bands will be available also for domestic satellite networks, but it is the international networks that will derive most direct benefit from this WARC-79 outcome.

All commercial fixed-satellite networks currently in regular service use a bandwidth of 500 MHz for up-links at 6 GHz and a corresponding down-link band at 4 GHz. Most operate at 5925-6425 MHz and 3700-4200 MHz. Traffic tends to increase as time passes and satellites eventually fill. The system management is then typically faced with a choice; another similar satellite may be brought into use at a different orbital location to take off some of the traffic or the system may be changed to make the same satellite, or a single replacement for it, capable of handling more traffic. The former is usually the quicker and often the cheaper solution. However, parts of the geostationary orbit are getting rather crowded and it is not always easy to find a suitable slot for a new satellite.

This problem of saturation is particularly difficult for the INTELSAT global system, for four reasons:-

a. its traffic is exceptionally heavy, particularly in the Atlantic Ocean Region, and is growing fast,

b. for geographical reasons only limited ranges of orbital location are acceptable.

c. coordination of global-coverage satellites with other satellites is particularly difficult, since the option of using satellite antenna directivity to reduce interference may not be available, and

d. unlike a typical domestic satellite system, the INTELSAT global network is one whole. The split into three ocean regions is unavoidable for obvious reasons, but any further subdivision of the network between different satellites is a serious disadvantage causing substantially increased earth segment costs.

In this last respect we can compare INTELSAT with a typical domestic satellite network which, from the communication standpoint, can be more accurately regarded as a group of several or many independent networks which happen to make use of the same spacecraft. The continued association of these networks in a new common spacecraft of higher capacity after the old spacecraft can no longer absorb the growth of traffic may or may not reduce space segment costs, but it has virtually no earth segment impact.

Notwithstanding these disadvantages, when INTELSAT first exhausted its 500 MHz of bandwidth in the Atlantic, using an INTELSAT III satellite, at the end of 1969, the only solution available was to split the traffic between two INTELSAT III satellites. The use of a 'Major Path' satellite to relieve the 'Primary' satellite of some of its traffic has been a regular feature of the Atlantic Ocean Region for most of the time since then. Soon afterwards the two INTELSAT IIIs gave way to one, then two, INTELSAT IVs; this new satellite generation had twelve 6-watt TWTs and high gain transmit antennas instead of two 10-watt tubes and

Copyright © American Institute of Aeronautics and Astronautics, Inc., 1980. All rights reserved.

a global antenna, allowing it to carry twice as much traffic. Even so, the INTELSAT IVs had to be phased out, starting in 1976, being replaced by INTELSAT IVAs. These new satellites provided a further doubling of capacity through satellite beam frequency reuse. Both INTELSAT IVAs were fully loaded in 1979 and were due for replacement by INTELSAT Vs. However, INTELSAT V is overdue, as a result of which it has been necessary to bring a third satellite into use. The first INTELSAT V is expected in service in mid- to late-1980; it should provide yet one more doubling of the per-satellite capacity and it would provide this by dual polarisation over most of bandwidth and by use of additional transponders operating in a new pair of frequency bands, located at 14 and 11 GHz.

The newly introduced third Atlantic satellite is to continue in service. Even so, traffic is growing so fast that the region will be saturated again by about 1984, or perhaps sooner if the development of the system does not go to plan; for example if existing earth station antennas fail after retrofitting to attain the required standard of polarization purity or if earth station owners are slow to build the new earth stations that are needed.

INTELSAT has already put several years study into what it should do next to cope with all this growth. Final decisions have not been taken yet, but the most cost effective solution is likely to involve the introduction of Time Division Multiple Access, (TDMA) on a substantial scale in the early 1980s and the introduction of new satellites about 1984/5 with a larger degree of satellite antenna beam frequency re-use and dual polarization across the board at 6/4 GHz. TDMA is a relatively new method of multiplexing and multiple access which can make more efficient use of the available bandwidth.

However, all these new techniques for increasing the transmission capacity of a single satellite, desirable as they are from an abstract consideration of efficient use of the satellite medium, raise major technical and corporate problems for INTELSAT. Satellite beam frequency reuse and dual polarisation introduce new interference paths which cannot be accurately quantified in advance and are difficult to allow for economically in the network transmission plan. They also increase the complexity of the satellite, seen as a network of input and output ports linked by an interconnection field; with the relatively rigid interconnection facilities of today's networks this is a source of significant loss of capacity. Any change in the system that calls upon earth station owners to install new kinds of equipment creates difficulties and uncertainties in a loosely-knit collaborative body like INTELSAT. For all these reasons, any new option that would give the next generation of satellites more capacity without more complexity would be a boon.

The new bandwidth at 6 and 4 GHz is bound to be an important factor in the development of the INTELSAT system in the mid 1980s. My own expectation is that its chief importance will be to give much-needed turn-around capacity to facilitate the introduction of TDMA. However, increased exploitation of the higher frequencies raises two kinds of problem for INTELSAT. Firstly, earth station owners in general have proved to be rather reluctant to build 14/11 GHz earth terminals; this attitude may change when the pioneers have proved designs in service and have acquired direct experience of propagation degradations at these frequencies. Secondly, the higher down-link rain margin required at 11 GHz makes operation with wide satellite beams costly in terms of satellite payload, and the alternative of using multiple high gain beams may save payload but it creates system problems. For these reasons I expect INTELSAT to treat the new spectrum at 14 and 11 GHz as just one option among several which are available for long term development.

On the other hand, for an international system with limited geographical coverage like the European Communication Satellite (ECS) system, to be operated by EUTELSAT, the 14 and 11 GHz bands are quite suitable. This system is scheduled to enter service in 1982/3 using TDMA and the existing 500 MHz bandwidth allocations with full dual polarization. EUTELSAT expects to run out of bandwidth towards the end of the 1980s, and the extra bandwidth allocated by WARC-79 will allow second generation spacecraft to have twice as much capacity without satellite beam frequency re-use.

II Intersatellite links in international satellite networks

Another option for increasing the satellite capacity available to a single earth station antenna which INTELSAT has considered from time to time is to use intersatellite links to convert two or more conventional satellites, a few degrees apart in orbit, into what is in effect a single compound satellite. For inter-satellite links, WARC-71 had allocated bands in the absorption lines due to the atmospheric gases in order that there could be frequency sharing without interference between such links and any likely service o operated on the earth's surface. However, none of these bands is below 54 GHz; INTELSAT has shrunk so far from the cost of developing and space-proving hardware so far in advance of the state of the art.

However, WARC-79 allocated new intersatellite bands at 23 and 32 GHz, where development costs would be less. The allocations are not ideal. At 23 GHz, half the band is shared with satellite broadcasting in ITU Regions 2 and 3, and this will clearly pose sharing problems when this broadcasting band is exploited. At 32 GHz, the band is shared with terrestrial radionavigation, and this may limit the intersatellite service to links between nearby satellites. Nevertheless, these bands should provide a viable medium for "compounding" nearby satellites pending the development and space-proving of 60 GHz hardware, providing INTELSAT with an interesting additional option.

III Satellite systems for mobile users

In recent years satellite services for ships and aircraft have received a lot of attention. The intensive study of aeronautical systems that was a feature of the first half of the seventies has come to nothing for the moment, but corresponding activity in the maritime field has led to two important results; the MARISAT system, American-owned, is now in business and is already serving several hundred ships, and an international maritime satellite organisation, INMARSAT, came into being last year to establish and manage a world system.

INMARSAT has studied the traffic load that its system will probably be carrying within 20 years and has concluded that the 7.5 MHz of bandwidth allocated in 1971 for links between ships and satellites will not be enough; double that amount will be needed. WARC-79 was not able to find 15 MHz, but it increased the existing bandwidth to 14 MHz each way for ships, leaving 14 MHz each way for aircraft, still preserving a 1 MHz band for satellite Search and Rescue operations involving any kind of vehicle. An additional 5 MHz was allocated undirectionally for the ship-to-satellite direction, intended for real-time transmission of seismic data from sea-bed exploration craft to shore

Mobile-satellite systems use fixed-satellite frequency bands for the links between the satellite and fixed earth stations, and no doubt INMARSAT will use parts of the 6 and 4 GHz bands, like MARISAT.

The technical requirements of land-transportable earth stations are broadly similar to those of fixed earth stations and the same frequency bands are often used for both applications, some appropriate coordination procedure being used where there are terrestrial allocations in the same band. With this in view, WARC-79 made mobile-satellite allocations in the 7, 8, 14, 20 and 30 GHz bands. In addition various new footnote allocations were made for mobile satellite services at lower frequencies around 2.6 GHz, 900 MHz and 400 MHz, mostly subject to geographical limits and subject to potentially difficult problems of coordination with terrestrial services using the same bands. It seems to me likely that the main use for these latter allocations will be for links which can be quickly set up to stationary land vehicles operating in out-back territories, but the possibility of service to moving road vehicles may also emerge.

IV The planned mid-eighties WARC on orbit-spectrum access

One of the most cherished principles governing the use of space is that it should be available for the peaceful use of all nations. There are some arcs of the geostationary orbit which are already showing signs of crowding by fixed-satellite networks. Some countries are concerned that there may not be orbit/spectrum space for their use, particularly in the more desirable frequency bands, in the not-too-near future when they will be ready to exercise their rights, because the first-comers will have blocked them out.

It is not difficult to find technical grounds for arguing that this view is pessimistic, but the concern is very understandable. Several administrations proposed to WARC-79 that the problem be solved by international planning of the use of orbit and spectrum. These proposals generated extensive discussion. "Planning" was not defined in these documents but it could cover a wide range of activities, and at one end of this range is the rigid kind of orbit/spectrum planning that was used for the satellite broadcasting service at 12 GHz in Regions 1 and 3 by WARC-77, a process that would be very inefficient in the fixed-satellite service.

In the end, WARC-79 resolved to have a further conference in the mid-80s to decide what means, planning or otherwise, should be adopted to ensure that all countries were indeed able to exercise their right to equitable access to space and spectrum. Clearly, the outcome of this mid-80s conference could have great significance for international fixed-satellite services.

V Acknowledgement

Acknowledgement is made to the Director, International Network of the British Post Office for permission to publish this paper.

80-0514

TRENDS IN MILITARY SATELLITE COMMUNICATION NETWORKS

I. M. Jacobs
E. V. Hoversten
C. R. Moore
LINKABIT Corporation
San Diego, California

ABSTRACT

Military satellite communication network evolution will be driven by a growing need for survivable, antijam communications. Major changes will result from the shift to EHF frequency bands, satellite on-board processing, switchable high gain antennas, and cross-links. These changes will include packet oriented demand assigned multi-access for voice and low rate data networks serving a large set of small users. Jamming protection and encryption for all users will be provided.

Network concepts will incorporate priority access disciplines and an absolute preempt capability consistent with the variability of military needs. A variety of network protocols will be used to support peculiar needs for specific users, but there will be a continuation of the trend toward having some modes of interoperability among the services. Cross-linked satellites will support true worldwide communications networks.

INTRODUCTION

The major characteristic of future military networks that will distinguish them from their commercial counterparts is that they will support antijam communications. While there are other significant differences--rapid changes in the user population, tolerance for asset outage, the worldwide nature of some nets, and centralized network configurations are examples--the dominant differences result from the AJ nature of the networks. Many trends will be established by EHF frequency band occupancies, by the drive to attain low cost terminals using new processing capabilities of satellites, and by multiple satellite networks. Each of these topics will be discussed from the point of view of the implication of antijam processing.

While much of the military communications will follow the form of commercial networks for peace-time operation of the three services, the antijam networks will be significantly different, since in an antijam environment the satellite itself is the primary target for attack. Antijam systems tend to be uplink power limited rather than downlink power limited as is the case in many commercial systems. Finally, one of the most dominant characteristics of a commercial channel, the number of bits of information supported per Hertz, is not relevant in an antijam communication system since the bandwidth required to support the antijam capability is orders of magnitude greater than the information rate. In the antijam situation the parameter of Eb/No dominates and must be evaluated, not simply in the white Gaussian noise background, but against an environment of interference designed to specifically attack the characteristics of the network involved.

Since military systems take seven to ten years to deploy, the terrestrial equipment that supports a communication network must have a legacy from one satellite constellation to the next. As satellite technology improves, and since antijam communications is primarily a technological battle, there are significant increases in performance from one satellite generation to the next. The terminals to be developed and the networks and operational disciplines that these terminals support, must have the legacy to be either transparent or easily updated with changes in satellite environment.

Copyright © American Institute of Aeronautics and Astronautics, Inc., 1980. All rights reserved.

The Military Traffic

There are several characteristics of the user population in the military environment that affect the overall network configuration. First, there are a large number of users. Sets of networks that are interoperable and can be varied in their interconnection numbering up to a thousand users are not uncommon. The number of users active at any one time is quite volatile and because of the nature of military activities, the rate of entry of terminals at a critical time may be quite high. Military networks are often judged by the speed with which they can react to changes rather than their carrying capacity in a steady-state mode. Terminals must be deployed and set up in new areas and be brought either into existing or newly defined networks in a very short period of time. Often this start-up problem is not restricted to a single or a small set of terminals, but may involve the entire network, as might be exemplified by a fleet of aircraft responding to an alert and wishing to enter a communication network almost simultaneously.

Antijam communication nets will support digital data, in the form of low rate message traffic, computer-to-computer activities, and voice. A number of different connectivities are required to support military needs, the most typical are shown in Figure 1. Typically, the voice information will not be transmitted at the toll grade 64 Kbps data rate seen in the commercial environment, but rather at a vocoded 2400 bps rate supportive of military communications. The computer-to-computer activities that will be supported involve many individual systems, both old and new, having no consistent protocol in their communications. The terminals will thus have to interface with a wide variety to data rates, timing standards, framing techniques, and character/field standards.

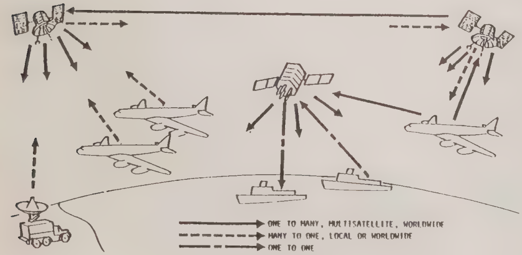
ONE TO MANY, MULTISATELLITE, WORLDWIDE
MANY TO ONE, LOCAL OR WORLDWIDE
ONE TO ONE

Figure 1. Typical Military Networks Configuration

A final characteristic that determines the form of networks in the military environment is the requirement for priority and for preempt. While military communications have varying delay requirements similar to those experienced in the commercial environments, the concept of priority and of preempt capability is even more strongly defined in the military. There will exist, in most cases, a rigid discipline of message structures to which there are assigned absolute priorities that can be given the capability of preempting existing transmissions. In the end, an absolute preempt capability will be reserved in these networks so that some centralized decision making entity can take over the net for a new set of uses.

These traffic requirements point to the priority oriented demand access (PODA) concepts that are presently being developed by DARPA and deployed in some military networks in a non-antijam basis. These techniques will be extended to antijam networks through the development of integrated control schemes which allow a mix of distributed and central control to support a mix of terminal capabilities and degraded environmental conditions (e.g., rain induced fading) at specific terminals, and efficient network entrance techniques.

The Military Satellite

A large number of satellite constellations have been used and are being proposed for use in military communications. They range from dedicated satellites having substantial capability in terms of processing, transmitted power, and directive antennas, to small satellites where communication packages are in fact secondary pay-loads on satellites whose primary mission is other than communications. The former obtains the antijam performance desired primarily through the sophistication of the technology and processing provided. The later provides immunity through the proliferation of satellites, thus requiring the jammer to cover a large number of targets rather than dedicating his energy to a single dedicated satellite. In either case, cross-links may interconnect the satellites and either allow hidden operation or provide means of establishing worldwide networks without multiple terrestrial relays.

In many proposed military networks, the communications are, multi-band; operation can be at EHF, SHF or UHF, with the same information often being distributed in more than one band simultaneously. The satellites also operate in a multi-mode capacity where different data rates are supported under different levels of stress and, finally, the networks are often supported by a multiplicity of satellites so that a terminal may expect to have access to a number of satellites during normal operations.

Future satellites will employ some form of the processing shown in Figure 2. An array of narrow beam antennas will provide both gain and spatial discrimination for the uplink transmissions. Steerable nulls may also be employed to enhance suppression of jamming signals. The on-board signal processing will include frequency hopping, full demodulation and decoder/deinterleaving processes. In the transmit chain, the converse of these processes will be performed, but the antenna will probably not be a multi-beam antenna, but will be a single beam capable of being switched rapidly to support time division multiplexing of the downlink transmission.

The access control on the satellite can consist of something as straight forward as earth commanded crossovers between channels of different frequencies and different uplink receivers, or it can provide the full DAMA control. Processing capability will be such that the access algorithms can be performed in the satellite so that all real-time DAMA control is exercised by the satellite. In this case, terrestrial units would only command mode changes and initiate preempt in extraordinary circumstances.

Frequency division multiplex will be used on the uplinks as long as the terrestrial transmitters are peak power limited. For spacecraft transmitter efficiency, however, a TDM downlink will most likely be employed. Both of these transmissions will employ GHz spreads in their frequency hopping modulation at EHF bands.

Military Terrestrial Terminals

Drivers for change in military networks involve both an increased need for secure communications in support of modern weapons systems and the need to reduce the actual costs of both the initial acquisition and of the operation of the terminals. As weapons systems proliferate, terminals that have the capability of providing cheap, variable interfaces that allow the network to operate independently of the existing constraints of terrestrial communications systems and, thus, translate between the network format and the constraints of existing systems will become more and more valuable.

The low cost terminals of the future will provide the antijam capability from both the frequency hopping processing and the directional antenna capability shown in Figure 3. To support these two capabilities, an

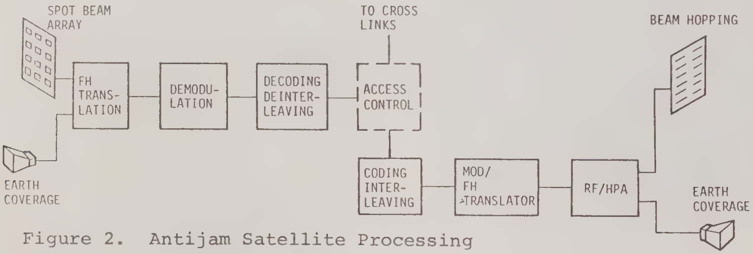
SPOT BEAM ARRAY
TO CROSS LINKS
BEAM HOPPING
FH TRANSLATION
DEMODULATION
DECODING DEINTERLEAVING
ACCESS CONTROL
CODING INTERLEAVING
MOD/ FH TRANSLATOR
RF/HPA
EARTH COVERAGE
EARTH COVERAGE

Figure 2. Antijam Satellite Processing

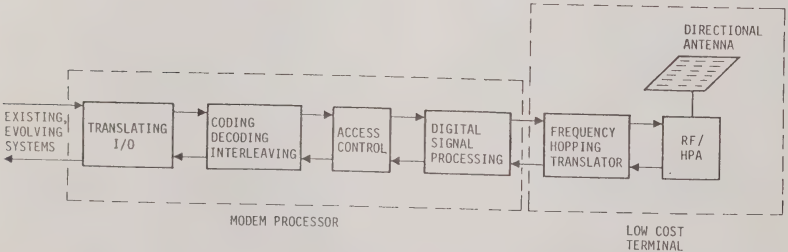
DIRECTIONAL ANTENNA
EXISTING, EVOLVING SYSTEMS
TRANSLATING I/O
CODING DECODING INTERLEAVING
ACCESS CONTROL
DIGITAL SIGNAL PROCESSING
FREQUENCY HOPPING TRANSLATOR
RF/ HPA
MODEM PROCESSOR
LOW COST TERMINAL

Figure 3. Terrestrial Terminal For Military Networks

extensive digital processing capability will be employed. The digital processing of the signal, access control, coding and decoding, interleaving, and the I/O translation will be a portion of every terminal.

The I/O translation will mate the network transmission format to the I/O formats employed in the external communications systems. These communications systems will support existing systems as well as evolving systems. The translating capability will eliminate unnecessary content, reduce the message to the minimum required for transmission and then restore the original format at the receiving end.

Conclusion

DAMA systems incorporating the PODA concept are being deployed in the military now although they have no significant antijam capability. Future systems will emphasize this latter capability and will extend the DAMA concept through the use of processing satellites and narrow-beam antennas to establish worldwide networks both through the use of cross-links and through a proliferations of satellite assets.

80-0539

CRYPTOGRAPHIC TECHNIQUES FOR SATELLITE NETWORKS*

Lin-Nan Lee
COMSAT Laboratories
Clarksburg, Maryland 20734

Abstract

Cryptography has received much attention during the past few years because of public awareness of the need for communications security. This paper examines a few new cryptographic techniques which may satisfy various security needs of satellite communications networks, and discusses both the unique properties of satellite networks with respect to communications security and future technological trends.

Introduction

During the past decade, rapid advances in telecommunications and computer technologies have led to a so-called "information age." Large amounts of information can be collected, stored, transmitted, and disseminated in split seconds at relatively low cost with today's technology. Since telecommunications and data processing are experiencing almost unlimited growth, communications and data security has been widely recognized as an important issue. Use of cryptography as a principal means to provide communications and data security is no longer limited to the military and diplomatic communities. In the U.S., the Privacy Act of 1974 and the establishment of the Data Encryption Standard (DES) in 1977 have been two major milestones promoting public use of cryptographic techniques.

The unique characteristics of satellite communications networks present certain advantages and disadvantages with respect to communications security. For example, an earth station with adequate G/T is normally required to intercept the network communications. The earth station is considerably more expensive than the equipment needed to intercept a terrestrial microwave link. However, because the earth station can be located anywhere within the coverage of the satellite antenna, it is difficult to ensure communications security through physical security measures. Thus, cryptography plays an essential role in providing communications security in satellite communications networks.

A number of cryptographic schemes which are very attractive for use in satellite communications networks have been developed recently. Among the most interesting are public-key cryptosystems and digital signatures,[1,2] one-time pad techniques with current solid-state technology,[3] the incorporation of cryptography with multiplexing[4,5] or forward error correction coding,[6,7] and an analog scrambling technique which operates without bandwidth expansion.[8,9] This paper will highlight these new developments and discuss their impact on the design of security systems in satellite communications networks.

A Scrambling Technique Without Bandwidth Expansion For Analog Signals

Since the eavesdropper in the satellite communications network generally possesses an earth station, he can probably afford the equipment necessary to defeat traditional analog scrambling techniques such as frequency inversion and band splitting. It has generally been assumed that the only way to encrypt an analog signal successfully is to sample and quantize the signal and to encipher it digitally. However, sampling and quantization usually imply expanded signal bandwidth. The new scrambling technique proposed by Wyner[8,9] seems to offer good potential for analog encryption.

Wyner's technique is based on the existence of a set of orthonormal band-limited functions $\{f_0, f_1, \ldots\}$ which may be used as a set of bases to "support" the band-limited signal. Any band-limited signal $\underline{s}$ can be uniquely expressed as a linear combination of the orthonormal bases, i.e., $\underline{s} = \Sigma_i s_i f_i$, where s_i are real numbers. That is, the signal can be considered as a vector $\underline{s} = [s_0, s_1, \ldots]$. The scrambler is a unitary transformation represented by a square matrix $A = \{a_{ij}\}$. The output of the scrambler $\underline{s}' = \underline{s} \cdot A$ is another signal, limited within the same band, which is a linear combination of the base functions $\underline{s}' = \Sigma_i s_i' f_i$, where

$$s_i' = \sum_j s_j a_{ij}$$

The descrambler is simply represented by the transpose of A. Since $A A^T = I$, the identity matrix, the original signal can be recovered by multiplying A^T by the scrambled signal, i.e., $\underline{s}' A^T = \underline{s} \cdot A A^T = \underline{s}$.

In Wyner's paper, a set of prolate spheriodal functions was suggested as a set of good band-limited base functions. Matrix A is considered as the encryption key and must be kept secret. It must be significantly different from the identity matrix so that the scrambled signal is substantially different from the original

---

*This paper is based upon work performed at COMSAT Laboratories under the sponsorship of the Communications Satellite Corporation.

Copyright © American Institute of Aeronautics and Astronautics, Inc., 1980. All rights reserved.

signal. The security of the scheme is obviously dependent on the size of matrix A. However, as in many other encryption schemes, a large key size does not necessarily guarantee the security strength of the system. In this case, the size of the set of base functions, which determines the dimension of matrix A, is a tradeoff between implementation complexity and signal distortion. To be acceptable to the user, the descrambled signal must contain almost all the components of the original signal. Incorrectly adding or removing certain relatively insignificant signal components definitely degrades the signal quality, but may not render the signal totally unintelligible. This seems to offer an opportunity for cryptanalysts.

In summary, since it is anticipated that satellite communications systems will continue to carry a significant amount of analog traffic in the next decade or so, Wyner's scheme may offer a solution for privacy protection.

Public-Key Cryptosystems

One of the principal advantages of a time-division multiple-access (TDMA) satellite network is the ability of each earth station to communicate with any other station in the network. However, if communications privacy must be protected, the terminal at each earth station must maintain n - 1 secret encryption keys to retain the full network connectivity offered by a TDMA network of n earth stations. If the enciphering and deciphering procedures are performed either at or inboard the TDMA terminal, the terminal or the cryptographic device must be capable of changing keys dynamically as each TDMA subburst is transmitted or received. Furthermore, for a large network, key distribution and management are very complicated, since a total of n(n - 1)/2 keys must be distributed and kept secret.

The public-key cryptosystem concept was first proposed by Diffie and Hellman.[1] Instead of identical keys to encipher and decipher messages at the transmit and receive ends, two different keys, related by a so-called "trapdoor" one-way function, are used. Calculation from one key to the other is simple with the "trapdoor" information, but extremely difficult without this information. (In some cases, the trapdoor information can be the deciphering key itself.)

A user selects the trapdoor information (usually the values of some variables), selects a deciphering key, and calculates the enciphering key. The enciphering key is announced to the public and stored in a public file maintained by all earth stations. To send information, a user obtains the destination's enciphering key from the public file and uses it to encipher the message. As indicated above, calculation of the deciphering key from the enciphering key without the trapdoor information is computationally infeasible. Only the destination with the secret deciphering key can decipher the message.

Although the TDMA terminal must still maintain a file of enciphering keys, the task is considerably simpler since no privacy protection is required. The encipherer must still change the enciphering key dynamically based on the destination of the messages. The TDMA terminal must maintain a secret deciphering key, and the entire network must maintain n enciphering keys and n deciphering keys. Thus, the public-key cryptosystem substantially reduces the key distribution and key management problem in a large network.

The use of a single key to decipher messages from all sources in the network is particularly attractive if traffic analysis is a concern. For example, in a random multiple-access network, using a conventional cryptosystem, at least the source address of the received packet is required to decipher the message with the correct key. On the other hand, since a public-key cryptosystem uses a single key to decipher all messages destined to a particular station, the source as well as destination address can be encrypted.

Most of the public-key cryptosystems known to date are based on the difficulty of factorizing a product of two large primes or solving a general knapsack problem. The scheme by Rivest, Shamir, and Adelman (RSA) uses the factorization of the product of two distinct primes as the trapdoor information, e.g., $r = p_1 p_2$. Let e and d be two integers related by

$$ed = 1 \quad \mathrm{mod}[(p_1 - 1)(p_2 - 1)]$$

The user chooses d as his secret deciphering key and announces the enciphering key, e, to the public. The enciphering algorithm simply raises the message, m, to the eth power in the ring of modulo r, i.e.,

$$x = m^e \quad \mathrm{mod}\ r,$$

where x is the cryptogram, or the enciphered message. Upon receiving x, the user raises the cryptogram to the dth power modulo r to recover the message,

$$m = x^d \quad \mathrm{mod}\ r.$$

Without the trapdoor information (p_1 and p_2) or d, recovery of m is generally very difficult.

Most of the known public-key cryptosystems have some deficiencies. The RSA scheme requires exponentiation in the enciphering and deciphering process, and thus a relatively large number of computations. The Merkle Hellman scheme requires bandwidth expansion and a large key size. Most importantly, it can be shown that if the key parameters are not chosen properly, none of the schemes are secure.[10,11] Even with properly chosen key parameters, the security strength of these schemes is subject to further study. Nevertheless, the concept of the public-key cryptosystem is exciting and offers great potential.

Digital Signatures

An interesting possibility proposed by Diffie and Hellman[1] is the use of public-key cryptosystems for digital signatures. If the enciphering and deciphering procedures of a public-key cryptosystem commute, a user can "sign" his message with his own secret deciphering key and anyone can use the enciphering key from the public file to verify his signature. As an example, for the RSA scheme, the signed message from the user may take the form

$$y = m^d \mod r.$$

To verify the signal using e from the public file, anyone may obtain

$$m = y^e \mod r.$$

Since only the user knows d, only the user knows how to produce y such that m can be recovered from y by raising y to the eth power modulo r. The concept of the digital signature is extremely useful in electronic funds transfer and similar business activities. It also has potentially interesting applications to a number of satellite communications networks.

A better known example is SALT verification.[12] Each country included in the treaty is allowed to plant seismic sensors in the other country and to transmit seismic data back to verify compliance with the treaty. The transmitted data must be processed so that the other country cannot forge them; however, it must be able to verify that the transmission contains only the seismic data. The digital signature concept offers a unique opportunity to meet these two potentially conflicting requirements.

Another possible application of digital signatures is in the area of automatic network control. A network control message may be broadcast to all earth stations. In some cases, it is extremely desirable that each earth station be able to verify the authenticity of the control message. A possible approach is to encrypt the control message to each individual earth station with conventional cryptosystems. This would generally require n separate transmissions if n earth stations are involved. However, to exploit the broadcast property of the satellite, the control center can "sign" the control message with a digital signature scheme and broadcast only once. Every earth station can verify the authenticity of the control message with the key in the public file, whereas no one can produce a fake control message because only the control center has the secret key.

Digital signatures are not necessarily derived from commutable public-key cryptosystems. Shamir[13] has recently proposed a simpler digital signature scheme which cannot be used as a public-key cryptosystem. As in the case of the public-key cryptosystems, the security strength of digital signatures needs to be investigated further before they can be used with confidence.

One-Time Pad With Solid-State Technology

The one-time pad is one of the oldest cryptographic techniques and is unbreakable in theory as well as in practice. Basically, both the transmit and receive sides have an identical key pad. The sender exclusive-ORs the information with unused bits of the key stream, and sends the result as the cryptogram. The recipient uses the same key bits from the key pad to recover the information. Since each key bit is used only once, the size of the key pad is the same as the amount of information to be protected. Although this feature makes the system secure in theory, it is also a major drawback in terms of key distribution. However, rapid advances in solid-state technology have simplified the key distribution problem considerably. For example, a single chip of 65-kbit programmable read-only memory (PROM) may store as much information as a total of 100 computer cards, or 80 feet of paper tapes.

Recently, the size of PROMs has quadrupled every two years. Although it is still far from practical to encrypt digitized voice with the one-time pad, it is now very practical to use a one-time pad with PROM key pads in certain low-duty-cycle, low-data-rate applications. For example, for a 100-bit-per-day data collection platform, a single 65-kbit/s PROM may be used for two years, and for certain remote controlled devices, a few PROM chips may be sufficient for the entire design life of the device.

Each byte of the PROMs can be individually addressed, hence simplifying the synchronization problem which exists in a traditional one-time pad system. Because the application is restricted in low-duty-cycle, low-data-rate situations, the starting address of the key stream can normally be transmitted with the cryptogram to provide the necessary cryptosync.

Combination of Multiplexing and Cryptography

Messages to different destinations multiplexed together in a seemingly random manner can be difficult to interpret without precise knowledge of the multiplexing procedure. It is intuitively possible to provide privacy protection in a high-data-rate digital link by properly multiplexing the traffic to different destinations. This leads to the multiple-destination cryptosystem proposed by Lee and Lu.[4] (At about the same time Davida[5] proposed the same concept independently for data base security.) This scheme is based on the Chinese Remainder Theory and the computational difficulty of factoring products of large primes.

Let $P = \Pi_i p_i$, $d_i = P/p_i$, $c_i = d_i(d_i^{-1} \bmod p_i)$. Given p_i and m_i, $0 \leq m_i < p_i$, the Chinese Remainder Theory provides a method of constructing x, $0 \leq x < P$, such that $m_i = x \bmod p_i$ for all i. That is,

$$x = \left(\sum_i m_i c_i\right) \bmod P$$

If m_i is the message to destination i and p_i is the secret deciphering key for destination i, the transmit side (with c_i, the enciphering key for destination i) can encipher its messages to all destinations $\{m_i\}$ by computing x, and can transmit x as the multiplexed cryptogram. At the receive side, station i can recover its message with its deciphering key p_i to obtain

$$m_i = x \bmod p_i.$$

It cannot recover messages to other destinations because it has only its own deciphering key. Figure 1 illustrates the situation at the transmit and receive stations.

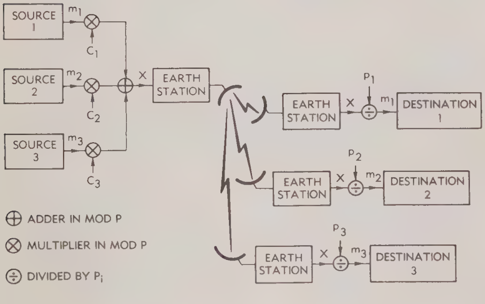
SOURCE 1
m_1
C_1
SOURCE 2
m_2
C_2
SOURCE 3
m_3
C_3
X
EARTH STATION
EARTH STATION
X
P_1
m_1
DESTINATION 1
EARTH STATION
X
P_2
m_2
DESTINATION 2
EARTH STATION
X
P_3
m_3
DESTINATION 3
⊕ ADDER IN MOD P
⊗ MULTIPLIER IN MOD P
⊕ DIVIDED BY P_i

Figure 1. Simplified Block Diagram of a Multiple-Destinational Cryptosystem

This scheme has negligible bandwidth expansion. For example, if each message, m_i, is a 100-bit number, each p_i is probably a 101-bit number. To multiplex n messages, P is at most a 101n-bit number, and the bandwidth expansion is no more than 1 percent. This scheme is not a public-key cryptosystem because p_i can be derived from c_i and P, and the transmit side must keep c_i secret. If the opponent obtains a few plaintext and cryptogram pairs, this scheme in its basic form cannot resist known plaintext attack. However, with a slight bandwidth expansion, the transmit side may attach a small random number to each m_i before enciphering to defeat such attacks.

The multiple-destination cryptosystem proposed by Lee and Lu is inherently secure against traffic analysis because messages to each destination cannot be singled out without the deciphering key. It is also more difficult to cryptanalyze messages between a particular source-destination pair because all messages from the source must be recorded and analyzed. Figure 2 compares the TDMA burst format with a conventional encryption and multiple-destination cryptosystem. Furthermore, since the deciphering keys, p_i, can be products of large primes themselves, the same multiple-destination cryptosystem can be used at different levels of multiplexing and fits easily into the network hierarchy as shown in Figure 3.

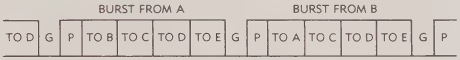
BURST FROM A
BURST FROM B
TO D
G
P
TO B
TO C
TO D
TO E
G
P
TO A
TO C
TO D
TO E
G
P

a. Conventional Encryption Techniques (individual subbursts are clearly visible)

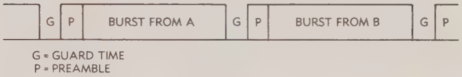
G
P
BURST FROM A
G
P
BURST FROM B
G
P
G = GUARD TIME
P = PREAMBLE

b. Multiple-Destinational Cryptosystems (bursts appear as single entities)

Figure 2. TDMA Format

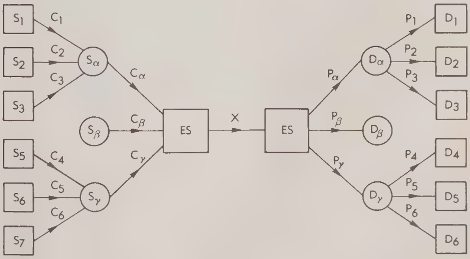
S_1
C_1
S_2
C_2
C_3
S_α
S_3
C_α
S_β
C_β
ES
X
ES
P_α
D_α
P_1
D_1
P_2
D_2
P_3
D_3
P_β
D_β
S_5
C_4
S_6
C_5
S_γ
C_6
S_7
C_γ
P_γ
D_γ
P_4
D_4
P_5
D_5
P_6
D_6

Figure 3. Multiple-Destinational Cryptosystem Used at Different Levels of Network Hierarchy

Combination of Forward Error Correction and Cryptography

The use of forward error correction coding techniques for privacy protection was first proposed by McEliece.[6] His original intention was to build a public-key cryptosystem based on forward error correcting coding techniques. His scheme is based on the fact that decoding a general block code is a complicated mathematical problem, but that decoding a well-structured Goppa code is computationally feasible. It is also straightforward to convert a well-structured Goppa code by a simple linear transformation. Therefore, McEliece proposed the secret linear transformation as the trapdoor information to convert an encoder for the Goppa code to a general encoder.

In McEliece's scheme, the general encoder is announced to the public as the enciphering key. A user looks up the destination's enciphering key and encodes his message. Before transmission, artificial noise within the error-correcting capability of the Goppa code is added to the encoded message. This noise is necessary to prevent the cryptanalyst from directly inverting the encoding process which is in the public file. At the destination, the receiver first converts the receive block by the inverse transformation of the secret linear transformation, and then decodes it with a decoder for the Goppa code.

Since a sequential decoder for long convolutional codes is much simpler to implement than a Goppa code with about the same error-correcting capability (particularly in high-speed applications), Lu, Lee, and Fang[7] proposed a similar scheme based on the computational cutoff property of sequential decoding. Since information can be transmitted very reliably at a rate slightly below, but not above, the computational cutoff rate, R_{comp}, it may be possible to build a cryptosystem so that the transmission rate appears to be above R_{comp} for opponents without the key information, and below R_{comp} for legitimate receivers with key information. As shown in Figure 4, such a concept involves a secret expansion function F, which expands the bandwidth of the original signal somewhat before it is encoded by a convolutional encoder. As in the case of McEliece's scheme, artificial noise is added to the encoded message before transmission.

The destination receives a sequence corrupted by channel noise and attempts to decode the sequence with a sequential decoder for the convolutional code equivalent to the combined effect of the expansion function, F, and convolutional code, G. If the rate of the convolutional code is r_c, the rate of the equivalent code is r_e ($r_e < r_c$) and the artificial noise is adjusted so that the overall channel, including the effect of both channel noise and artificial noise, has a cutoff rate

$$r_e < R_{comp} < r_c.$$

The legitimate receiver with the knowledge of F can decode the information successfully. For an opponent without knowledge of F, analyzing the transmission is difficult.

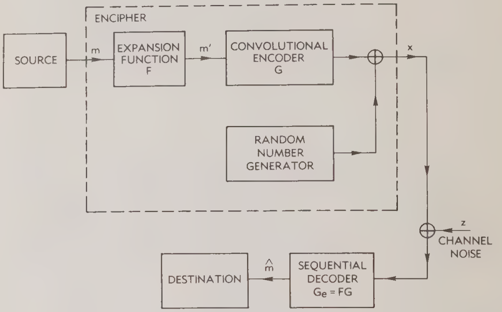

Figure 4. Cryptosystem Based on Error Coding for Simultaneously Achieving Secure and Reliable Communications

In this case, channel noise actually strengthens the communications security. In fact, it is often cost-effective to trade the signal power with moderate bandwidth expansion by means of forward error correction coding, even if communications privacy is not essential. In this particular example, it would be meaningless to reduce the channel noise to a level which is relatively insignificant compared to the artificial noise. The artificial noise, however, cannot be eliminated totally because the opponent may have an earth station with considerably better G/T, and therefore less channel noise. Proper balance of the channel noise and artificial noise is the key to a secure and cost-effective system in this case. Since the complexity of a sequential decoder is usually a weak function of the code complexity, it seems reasonable that the price for communications privacy in a convolutionally coded, sequentially decoded, satellite communications system may be very low.

Conclusion

Cryptography has been the subject of extensive investigation during the past five years. Public-key cryptosystems and digital signatures will have a significant impact on the implementation of satellite network security. The one-time pad with VLSI PROMs is a good example of how modern technology revitalizes previously "impractical" techniques. The incorporation of cryptography into multiplexing and forward error correction coding illustrates the concept of integrated system design with potential cost savings. Wyner's technique for analog signal scrambling is also a milestone in the development of voice scrambling techniques.

In addition to these schemes, other major developments include the more celebrated, somewhat controversial, Federal Data Encryption Standard (DES), which is intended for privacy protection of all non-military government data. It is expected that the DES may also be used in some of the satellite networks, particularly in conjunction with the Diffie and Hellman public-key distribution scheme[1] as being demonstrated by the MITRE Corporation.[14]

As satellite technology evolves, some of the unique characteristics of present satellite networks may change. On the one hand, the trend of greater effective isotropic radiated power (e.i.r.p.) on future satellites implies less expensive receivers and greater availability to the general public. On the other hand, the broadcast capability of the satellite may be traded for multiple-beam frequency reuse, which makes it practically impossible for any opponent outside the beam coverage to intercept the communications. However, it is expected that the characteristics unique to present satellite networks will most likely remain unchanged in the forseeable future. The cryptographic techniques which appear attractive in conjunction with these characteristics will most probably remain attractive. As the advance of solid-state and digital processing technologies continues, these techniques are expected to find application in future satellite networks.

References

1. W. Diffie and M. Hellman, "New Directions in Cryptography," IEEE Transactions on Information Theory, Vol. IT-22, No. 6, Nov. 1976, pp. 655-664.
2. R. Rivest, A. Shamir, and L. Adleman, "A Method for Obtaining Digital Signatures and Public Key Cryptosystems," Communications of ACM, Vol. 21, No. 2, Feb. 1978, pp. 120-126.
3. R. Fang and S. Lu, "Authentication over Low-Data-Rate Channels with Feedback," COMSAT Technical Review, Vol. 9, No. 1, Spring 1979, pp. 1-14.
4. L. Lee and S. Lu, "A Multiple-Destinational Cryptosystem for Broadcast Networks," COMSAT Technical Review, Vol. 9, No. 1, Spring 1979, pp. 25-36.
5. G. Davida, D. Wells, and J. Kam, "A Data Base Encryption System with Subkeys," Technical Report TR-CS-78-8, Department of Electrical Engineering and Computer Science, University of Wisconsin-Milwaukee, August 1978.
6. R. McEliece, "A Public Key Cryptosystem Based on Algebraic Coding Theory," JPL DSN Progress Report, 1978.
7. S. Lu, L. Lee, and R. Fang, "An Integrated System for Secure and Reliable Communications over Noisy Channels," COMSAT Technical Review, Vol. 9, No. 1, Spring 1979, pp. 49-60.
8. A. Wyner, "An Analog Scrambling Scheme Which Does Not Expand Bandwidth, Part I: Discrete Time," IEEE Transactions on Information Theory, Vol. IT-25, No. 3, May 1979, pp. 261-274.
9. A. Wyner, "An Analog Scrambling Scheme Which Does Not Expand Bandwidth, Part II: Continuous Time," IEEE Transactions on Information Theory, Vol. IT-25, No. 4, July 1979, pp. 415-424.
10. G. Simmon and J. Norris, "Preliminary Comments on the MIT Public Key Cryptosystem," Cryptologia, Vol. 1, No. 4, Oct. 1977, pp. 406-414.
11. T. Herlestam, "Critical Remarks on Some Public-Key Cryptosystems," BIT, Vol. 18, 1978, pp. 493-496.
12. G. Simmons, "Cryptology: The Mathematics of Secure Communications," The Mathematical Intelligencer, Vol. 1, No. 4, January 1979, pp. 233-246.
13. A. Shamir, "A Fast Signature Scheme," Department of Mathematics MIT, Cambridge, Mass., May 1978.
14. S. Berkovits, J. Kowalchuk, and B. Schanning, "Implementing Public Key Scheme," IEEE Communications Magazine, Vol. 17, May 1979, pp. 2-3.

80-0591

AN ITALIAN UPPER STAGE TO INJECT LOW TO MEDIUM WEIGHT SATELLITES IN ORBIT

Giangrande Barresi (°)
Carlo Carnebianca

Compagnia Nazionale Aerospaziale
Via Salaria km 9,300
Rome - Italy

Abstract

In Italy is now ready to start, in the frame of the national space program, the development of a Spinning Solid Upper Stage for light weight spacecraft, named IRIS, with energy requirements beyond the Shuttle basic capability.

The IRIS system consists of:

- the expendable stage, which is the portion deployed from Shuttle Orbiter, composed of a solid motor and of the subsystems required for the connected services (See Fig. 1).
- the reusable airborne support equipment intended to provide check-out and control capabilities before deployment
- ground support equipment to support, handle, transport, assembly, test and check out the system from the integration up to launch preparation.

This paper illustrates the basic design approach and possible future improvements of the IRIS program.

Keywords: Spinning Solid Upper Stage; Solid Rocket Motors; Avionics.

Introduction

During these last years the Italian space industry made a very important effort in the development of apogee solid propellant motor systems to inject spacecraft into a geosynchronous orbit.

These systems have been successfully employed in the geostationary orbital operations in the ESA Satellite GEOS 1 and 2, and in the italian SIRIO-1 telecommunication satellite.

To expand their capabilities in the space propulsion systems, the italian industries will develop in the frame of the governmental five year national space plan a research and development program named IRIS Project (Italian Research Interim Stage), with the following aims:

a) to continue the successful cooperation with NASA, by establishing a scientific and technical interest in the field of the recoverable launch vehicles, developping an upper stage for lightweight payloads.

b) to substantially exploit the know-how and the experience acquired by the italian space industry in the field of space propulsion, by the development and the accomplishment of the IRIS system to be launched by NASA STS. This system will have the capability to cover a range of missions with energy requirements below those foreseen by the SSUS presently under development in USA.

For such range of missions the U.S. upper stages could lead to a not-optimized system.

I - IRIS baseline

IRIS nominal mission description

For a nominal geosynchronous mission, the Shuttle Orbiter places the payload into a 296. Km circular orbit inclined at 28.5° degrees (see Fig. 2).

After check out, the IRIS/spacecraft assembly is spun up and deployed by the orbiter. Initial attitude, spin up and perigee velocity are obtained from the orbiter.

Spin capability of up to 100 rpm for IRIS is available from the airborne support equipment spin up mechanism.

After the IRIS spacecraft is released, the orbiter maneuvers to a safe distance.

IRIS and the orbiter coast in the parking orbit for approximately 45 minutes until the appropriate crossing of equator occurs.
At this time the IRIS stage solid rocket motor (SRM) fires and injects the IRIS stage/spacecraft assembly into a geosynchronous transfer orbit with a perigee altitude of 296. Km and an apogee altitude of 35,788 Km.

The velocity increment required to accomplish the nominal mission, considering 2 degrees maximum correction of transfer plane inclination is:

$$V = 2{,}450.\ \mathrm{m/s}$$

The sequence of major events for a geostationary mission from lift-off through S/C separation and tumble of IRIS expended hardware are:

- Nutation control enabling-desabling
- Solid motor ignition
- IRIS/Spacecraft separation
- Tumble system release

The major error sources affecting inclination and apogee altitude dispersions are the attitude error and the impulse error during the IRIS solid rocket motor burn.

(°) Member AIAA

Copyright © American Institute of Aeronautics and Astronautics, Inc., 1980. All rights reserved.

Performance

Fig. 3 synthesizes the low energy capability of IRIS system as spacecraft mass versus velocity increment and apogee altitude.

The area named "no plane change" is referred to all elliptic orbits which can be achieved from the shuttle parking orbit by firing the IRIS solid rocket motor with the thrust aligned to local velocity of parking orbit.

The reference nominal mission is characterized by the following parameters:

Velocity increment = 2,450. m/s

Apogee Altitude = 35,788. Km

Useful Payload= 600. Kg

with a maximum of 2 degrees of orbit inclination correction.

Fig. 4 shows the IRIS performance capability for geosynchronous transfer orbits as spacecraft mass versus plane orbit inclination relevant to the equatorial plane.

Configuration description

IRIS stage

The IRIS stage is composed of a solid rocket motor for perigee velocity increment, a payload attach fitting, to interface with the spacecraft, an electrical sequencing subsystem for control of the stage operations after its deployment, a telemetry subsystem, which provides transmission of stage performance data to the orbiter, wiring for spacecraft functions while in the orbiter, separation subsystem and a tumble subsystem for spacecraft separation and an active nutation control subsystem to damp out coning during the coasting phase.

The solid rocket motor (SRM)

The solid rocket motor design will exploit the experience acquired in the previous successful projects in order to improve reliability and reduction costs.
The grain technology allows suitable propellant offloading to meet user specific mission requirements.
Table I summarizes the SRM characteristics.

Payload Adapter

The payload adapter is a cylindrical structure providing support and separation interface to the spacecraft.

On the external wall of the adapter are installed the mechanical and electrical equipment required for stage operations.

Sequencing subsystem

Physical separation of the IRIS stage from the orbiter initiates sequencing subsystem operation leading to the following major events:

- Nutation control enabling-desabling
- Solid rocket motor ignition
- Spacecraft separation
- Tumble weight development

The actuating and monitoring devices, including power batteries and timers, are redundant (Fig. 5).

Nutation control subsystem (NCS)

During the 45 minutes of the coasting phase, inherent dynamic instability of IRIS/Spacecraft assembly requires damping of nutation, as it builds up. This task is achieved by means of the NCS which includes an accelerometer (to sense nutation), an electronic logic (housed on the adapter) and propulsion elements.

Separation subsystem

The first separation is performed between the airborne support equipment and IRIS stage/spacecraft assembly which has to be deployed from the orbiter.

The second separation is performed between the spacecraft and IRIS stage after perigee motor burn-out.

The separation is achieved by:

a) activation of two bolt-cutters releasing a marman clamp band, which tightens two properly shaped mating flanges of the two bodies to be separated

b) release of four separation springs which impart a relative velocity of 1-2 m/s between the two separated bodies.

Tumble subsystem

It consists of an expendable weight connected to the IRIS motor case and a steel wire wound around it.

The tumble weight, once deployed after spacecraft separation, causes a dynamic unbalance with the aim of avoiding any possible recontact which might occur due to motor thrust residuals.

Telemetry Subsystem

Information on vehicle performance data are obtained by means of an S-band PCM/PM RF system.

IRIS Airborne support equipment

The subsystem consists of the equipment necessary to support, control and monitor the IRIS stage and spacecraft, while in the orbiter cargo bay.
Moreover, it incorporates a spin mechanism to perform a spin-up maneuver of the IRIS stage/spacecraft assembly prior to deployment.

The support structure possesses sufficient strength and rigidity to be compatible with the critical loading conditions in the STS Orbiter.

IRIS weight preliminary breakdown

a) Expendable hardware

Payload attach fitting (Structure & Avionics)	75. Kg
Solid Rocket Motor and associated hardware contingency	1,100. Kg

b) Airborne support equipment (Structure & Avionics)	1,100. Kg
c) Installed weight in orbiter Cargo Bay (Payload excluded)	2,275. Kg

Environment

The IRIS system will be designed to withstand the STS imposed thermal and dynamic environment during all phases of shuttle oprations including an emergency landing of the orbiter.

Program description

The first launch of the IRIS is envisaged by the end of 1983.

The IRIS development schedule is shown in Fig. 6.

II - IRIS Future Growth

The development of IRIS system will provide a solid spinning upper stage for the market of the light weight spacecraft with low energy mission requirement basis.

An improved version of IRIS is foreseen to satisfy the italian national space program needs (see Fig. 7).

Moreover derivatives of the highly reliable solid rocket motor of IRIS baseline can be used as apogee booster motors to place up to 2,000 Kg of payload into a geosynchronous orbit.

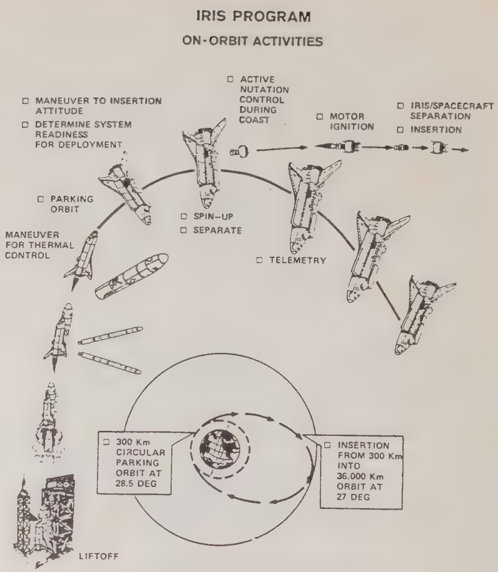
IRIS PROGRAM
ON-ORBIT ACTIVITIES
☐ MANEUVER TO INSERTION ATTITUDE
☐ DETERMINE SYSTEM READINESS FOR DEPLOYMENT
☐ ACTIVE NUTATION CONTROL DURING COAST
☐ MOTOR IGNITION
☐ IRIS/SPACECRAFT SEPARATION
☐ INSERTION
☐ PARKING ORBIT
MANEUVER FOR THERMAL CONTROL
☐ SPIN–UP
☐ SEPARATE
☐ TELEMETRY
☐ 300 Km CIRCULAR PARKING ORBIT AT 28.5 DEG
☐ INSERTION FROM 300 Km INTO 36.000 Km ORBIT AT 27 DEG
LIFTOFF

FIG. 2 - Sequence of events for geosynchronous mission

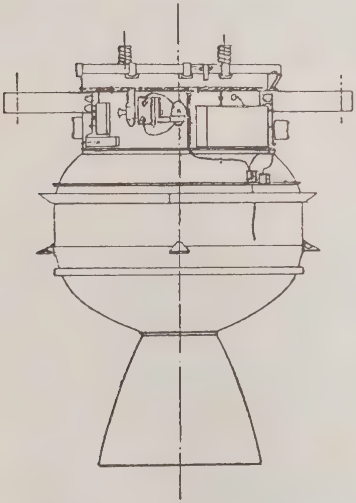

FIG. 1 - IRIS stage baseline configuration

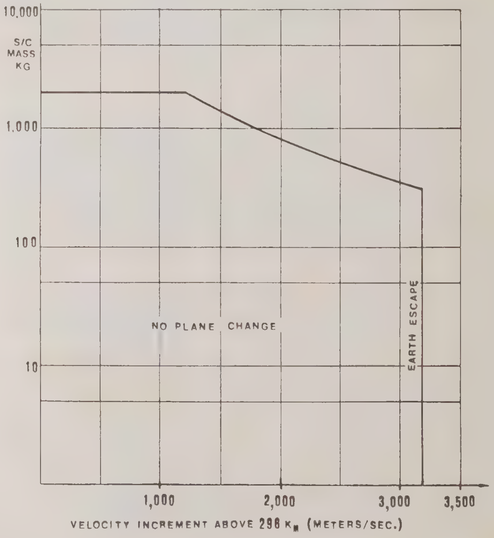

FIG.3 IRIS performance envelop

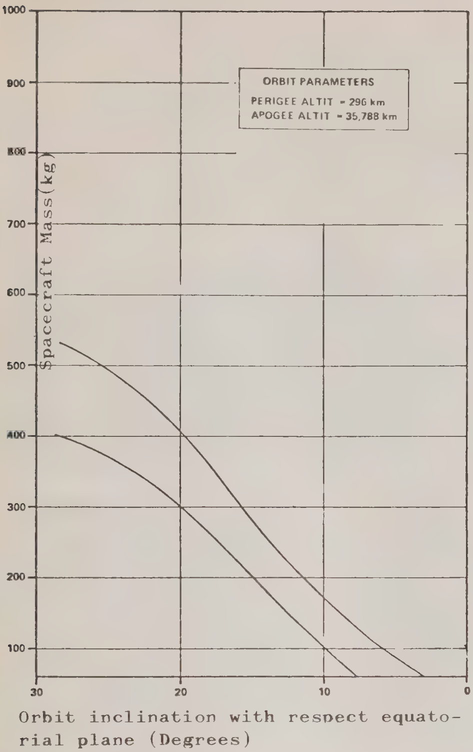

FIG. 4 - IRIS geosynchronous transfer orbit capability

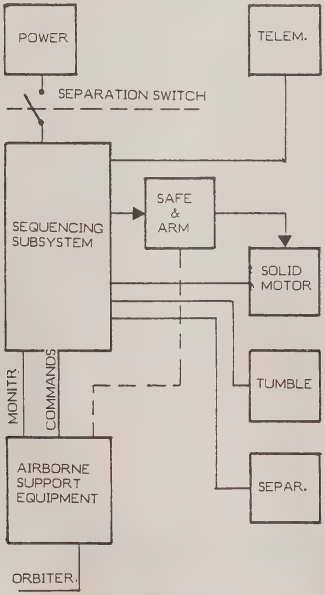
POWER
TELEM.
SEPARATION SWITCH
SEQUENCING SUBSYSTEM
SAFE & ARM
SOLID MOTOR
TUMBLE
SEPAR.
MONITR.
COMMANDS
AIRBORNE SUPPORT EQUIPMENT
ORBITER

FIG. 5 - Stage block diagram

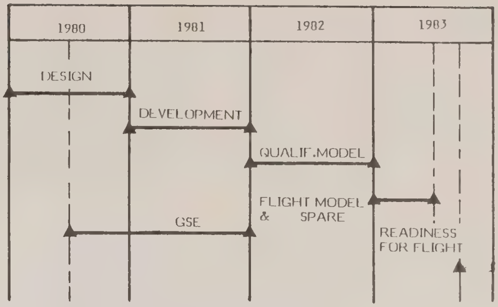
1980
1981
1982
1983
DESIGN
DEVELOPMENT
QUALIF.MODEL
FLIGHT MODEL & SPARE
GSE
READINESS FOR FLIGHT

FIG. 6 - IRIS program milestones

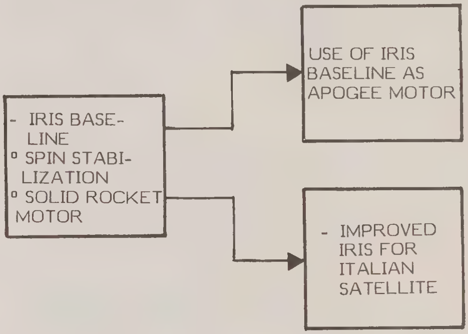
- IRIS BASELINE
○ SPIN STABILIZATION
○ SOLID ROCKET MOTOR
USE OF IRIS BASELINE AS APOGEE MOTOR
- IMPROVED IRIS FOR ITALIAN SATELLITE

FIG. 7 - IRIS program growth

PARAMETER	MOTOR PERFORMANCE	
	Loading 100%	Loading 81,5%
Total impulse (kg x sec)	278,000	226,500
Total weight (kg)	1,059	881
Max. thrust (N)	4,985	6,463
Max.accelerat. (g)	5.2	7.6
Tot.burn time (sec.)	72.9	48.6
Specific impul. (sec)	293	293

TABLE I - Candidate solid motor characteristics

80-0496

SATELLITE SYSTEMS FOR INDUSTRIALIZED NATIONS - AFTER WARC '79

Perry G. Ackerman*
Howard L. Weinberger**
Space & Communications Group
Hughes Aircraft Company
El Segundo, California

Abstract

The need for orbital capacity is foreseen as being greatest in the arc serving the industrialized nations of North America. This paper describes the applications requiring orbital capacity and a series of technological developments which can provide major increases in that capacity. The conclusion is derived that even in this highly developed industrialized nation, advanced technology will continue to provide all of the necessary communications capacity.

The last year has seen a rapid acceleration both in the use of existing communication satellite capacity and in commitments for future satellites. Although not limited to North America, it is here that the proliferation of new systems and applications are likely to be most extensive.

Concern has been expressed in many quarters about an anticipated disparity between available orbit capacity and the needs of would-be users, specifically developing countries. For the foreseeable future, however, the real squeeze will be in those portions of the orbit used by the developed countries, of which the prime example is the arc serving North America.

While current applications involve principally private line services and TV program distribution, a host of new requirements has surfaced. One class involves sophisticated users whose requirements include computer-to-computer links for businesses, large cross-section links for transcontinental backbone service, and facsimile and television conferencing for business and government users. The second class is characterized by the use of large numbers of small earth terminals, served by high-EIRP satellites. Typical applications will be for service to remote communities, interactive instruction, and broadcasting direct to the home. The aggregate orbit requirements for these new systems, when added to the steady growth of existing systems, would seem sure to exhaust the available orbit capacity within 10 to 20 years if it were not for a variety of techniques that exist for either reusing the available bandwidth, or reducing the bandwidth required for a given type of transmission.

The WARC has made important additions to the communications capacity of the orbit. These result from: a) increased frequency allocations, including bidirectional operation in certain bands (Figures 1 through 4); b) a tighter stationkeeping accuracy requirement (± 0.1° instead of ± 1°); and c) elimination of restrictions on use of the orbit in Region 2 near 12 GHz*. In addition, proposals were rejected that would have inhibited the use of small earth terminals by restricting their use to narrow bands in undesirable portions of the spectrum.

In spite of these factors which will tend to increase its orbital capacity, occupancy of the orbit will inevitably become more concentrated with the introduction of new networks. Sooner or later it will be necessary to call on new technology to provide additional orbit slots as needed. One example of such technology would be new earth terminal antenna techniques which provide a major reduction in sidelobe levels, thus permitting closer satellite spacing for a given level of inter-system interference. Results of work with offset-fed reflector antennas indicate that, in many cases, the required spacing can be reduced to between one-half and one-third of what is now required.

Reuse of the allocated frequency bands has already been achieved to some extent, and will become more prevalent. For example, dual polarization appears to have been adopted more or less universally in new satellite designs (Intelsat V, Comstar, Satcom, Advanced Westar (K-band), Westar IV, Anik D, and Palapa B). Frequency reuse by means of multiple satellite antenna beams represents a potentially more powerful approach than dual polarization. It is already used in Intelsats IVA and V, and will be used in Advanced Westar (K-band) and Anik C. Perhaps the most ambitious planning to date is being done by ATT, whose advanced system concepts call for U.S. domestic coverage using a multiplicity of beams. Frequency reuse by means of multiple antenna beams can be accomplished either with multibeam satellites, or with several independent satellites which serve different geographic areas, for example, the U.S. and countries in South America, from a common orbit location. The latter arrangement will be more widely used, particularly in the near term.

---

*Manager, Systems Engineering Laboratory
Associate Fellow, AIAA

**Sr. Scientist, Commercial Systems Division

*Broadcasting Satellite Service restricted to 75° - 100° and 140° - 170° W. Longitude, and Fixed Satellite Service excluded from these orbit areas.

Copyright © American Institute of Aeronautics and Astronautics, Inc., 1980. All rights reserved.

A variety of signal processing techniques have been developed which provide a large increase in the channel capacity (voice or TV) per unit bandwidth. Most of this work has been confined to the laboratory or to limited feasibility testing because there has been adequate orbit/spectrum available to meet requirements with techniques that are less efficient, but simpler and cheaper. This situation has now begun to change rapidly as unused transponder capacity shrinks, and as the desirable portions of the orbit become congested. In addtion, system operators are finding that they may be able to accommodate traffic growth most economically by measures which do not require additional satellites--and earth terminal antennas. Finally, solid-state developments, exemplified by the great variety of new special purpose IC chips, have made possible major simplifications in advanced signal processing hardware, thus mitigating what were once considered unacceptable cost problems.

The performance of a number of bandwidth-efficient signal processing techniques is summarized in Figure 5. For example, TDMA with PCM voice channels provides about double the transponder capacity of the currently widely used FDMA mode, and has recently been approved for use in the Intelsat network. It will be used to extend the life of the Intelsat V design, and to reduce the number of orbit locations that would otherwise be required for future generations of satellites. TDMA is also in the process of being implemented by at least one domestic carrier, in order to avoid having to lease additional transponders to handle traffic growth.

Speech interpolation permits the number of voice circuits that can be handled by a satellite link to be doubled, as a minimum and can be employed together with TDMA to provide a capacity increase of about four times. By using delta modulation with syllabic companding for encoding of voice channels, a further factor of two capacity increase can be achieved.

Speech interpolation and syllabic companding can also be applied to analog communication links. The capacity improvements are of the same order as in the digital case. Except for companding with FM/SCPC channels, neither technique has yet been exploited in a major way in satellite networks. However, recent announcements by two domestic satellite carriers of substantial compandor purchases, and by ATT relative to the future use of speech interpolation in the long distance network, suggest the possibility of important future applications.

Demand assignment is a process by which satellite capacity is allocated dynamically to earth terminals. In applications involving low-capacity terminals, it is possible to take advantage of call arrival statistics to increase the effective satellite capacity, relative to the case in which channels are preassigned to terminals. A capacity increase of up to five times is possible, depending on the traffic per terminal, and the number of terminals. Demand assignment networks have been implemented in Indonesia and Algeria.

Although it is doubtful that any future satellite networks will make use of all capacity improvement techniques that have been outlined here, it is of interest to note that the SBS network is designed to employ TDMA, speech interpolation, delta modulation, and demand assignment.

A number of successful efforts have been made in recent years to reduce the bandwidth required for video transmissions by taking advantage of the redundancy built into the signal format. Equipment is now on the market which permits two analog video signals to be interleaved on a single carrier. In this way, four video signals have been sent over two carriers in a single 40 MHz transponder. Other equipment is available which uses a digital transmission format. Depending on the degree to which rapid motion must be reproduced, from 3 to 20 video signals can be multiplexed together and transmitted over a single transponder. Although the equipment required for video bandwidth compression is expensive, the potential saving in transponder lease costs is large, and there are certain to be future applications where the technique is economically viable. As a result, the current capacity of one video transmission per transponder in domestic service and two in international service will increase, on the average, if not in all cases.

It is of interest to make an approximate estimate of the communications capacity of the orbit, based on the improvement techniques that have been described. Figure 6 lists a "reasonable" set of assumptions, and the resulting calculated telephone and TV capacities. It would appear that these values (millions of telephone channels and tens of thousands of TV channels) greatly exceed any requirements estimates that have been made for the rest of this century. As can be seen, the assumptions which were used are far from being the most optimistic that could have been employed, even based on today's technology. In the event that even greater capacity should be required, more extensive application of the available technology would be possible. In addition, technology which is now under development, for example, in the areas of speech bandwidth reduction and exploitation of higher frequency bands, should provide for further major increases in orbit capacity.

Looking yet further ahead, methods are being studied for increasing orbit capacity by sharing the same orbit location among satellites in properly phased, slightly inclined, geosynchronous orbits.

To summarize, new technology which has been demonstrated, but not yet used widely, provides the capability of increasing the communication capacity of the geostationary orbit by a very large factor relative to what is now being achieved. This capacity increase is over and above what will result from the new satellite frequency allocations agreed to at the WARC. Of course, new technology will tend to be adopted only as required to meet the objectives of individual network operators. One of the key questions to be answered over the next few years is whether this voluntary process can be depended on to keep orbit capacity ahead of demand. If not, special regulatory measures may have to be considered. Such measures might apply to the domestic arena alone, or could be required on an international basis also. What can be stated with certainty now is that there are a wide variety of measures available which can provide a vast increase in orbit capacity. Even in the intensively used portion of the orbit serving North America, adequate capacity can be made available, both to meet anticipated growth requirements, and to provide for new services, such as broadcasting to the home and TV teleconferencing, which are now at the point of becoming a reality.

FIGURE 1. FIXED SATELLITE SERVICE DOWNLINKS BELOW 10 GHz

	Region 1	Region 2	Region 3
3400–3600	Radio Location Primary in Denmark, Norway, United Kingdom	Radio Location Primary	
		After 1985 all Administrations Urged to Cease Radio Location Operations or to Protect FSS	
3600–3700		Radio Location Removed	
3700–4200		Existing Allocation	
4500–4800		Allocation Changed from Uplink to Downlink	

1100 MHz

- Agreement by United States, Canada, United Kingdom, Netherlands, Belgium, Australia not to block use by INTELSAT of any allocations for space segment or of 4500-4800 anywhere other than in Belgium, Norway, Netherlands, and United Kingdom, "Reasonable effort" to accommodate FSS, consistent with footnotes.

FIGURE 2. FIXED SATELLITE SERVICE UPLINKS BELOW 10 GHz

	Region 1	Region 2	Region 3
5850–5925	Existing	Radio Location Removed	Existing
5925–6425		Existing Allocation	
6425–7075		New Allocation	

1225 MHz

FIGURE 3. FSS AND BSS DOWNLINKS 10 TO 13 GHz

	Region 1	Region 2	Region 3
10.7–10.95		FSS – New Allocation	
10.95–11.20		FSS – Existing Allocation	
11.20–11.45		FSS – New Allocation	
11.45–11.7		FSS – Existing Allocation	
11.7–12.1	BSS Existing Allocation	FSS – Existing Allocation BSS (53 dBW Limit)	BSS Existing
12.1–12.2		FSS/BSS	
12.2–12.3			FSS – New Allocation Dom and Subreg
12.3–12.5		BSS – New Allocation FSS – Permitted	
12.5–12.75	FSS Existing		BSS – New (51 dBW) FSS Existing

- 1983 RARC decides FSS/BSS split in 12.1 to 12.3.
- ARC segmentation – No longer required in 11.7 to 12.1; not required in 12.1 to 12.3 after RARC.
- Existing FSS in 12.1 to 12.2 shall not restrict BSS plan.
- RARC should take into account existing FSS in 12.1 to 12.2 if in accordance with 1977 BSS WARC ARC segmentation.
- At least 4 BSS channels per country in Region 2.

FIGURE 4. FSS AND BSS UPLINKS 10 TO 20 GHz

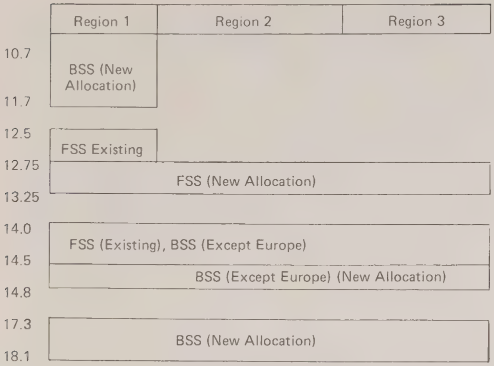
Region 1
Region 2
Region 3
10.7
BSS (New Allocation)
11.7
12.5
FSS Existing
12.75
FSS (New Allocation)
13.25
14.0
FSS (Existing), BSS (Except Europe)
14.5
BSS (Except Europe) (New Allocation)
14.8
17.3
BSS (New Allocation)
18.1

FIGURE 5. COMMUNICATIONS CAPACITY OF FREQUENCY SPECTRUM

Service	Operating Mode	Capacity per 40 MHz Transponder	Capacity per 500 MHz (Dual Polarization)
Telephone	FDMA	500	12,000
	TDMA	1,000	24,000
	TDMA-Companded or DSI	2,000	48,000
	TDMA-Companded-DSI	4,000	96,000
Television	Analog	2	48
	Analog-"Strap" Multiplexing	4	96
	Digital-Compressed (Broadcast Quality)	3	72
	Digital-Compressed (Teleconference Quality)	10	240

FIGURE 6. COMMUNICATIONS CAPACITY SUMMARY

Coverage Area Dimension, mi.	Satellite Spacing, deg	Total Telephone Circuits	Total TV Channels
2,000	10	2×10^6	6,000
2,000	5	4×10^6	12,000
1,000	10	9×10^6	27,000
1,000	5	18×10^6	54,000

- INTELSAT traffic forecast for 1981 is 25,000 telephone circuits (1990 extrapolation is 15% per year = 88,000 circuits).

Assumptions

- Dual polarization.
- Three frequency bands (1500 MHz total).
- Each frequency band accommodates 12, 40 MHz transponders,
- Each 40 MHz transponder accommodates 2000 telephone channels or 3 television channels.

80-0502

THE INTELSAT V NICKEL-HYDROGEN BATTERY SYSTEM

G. Van Ommering, C. W. Koehler, and D. C. Briggs
Ford Aerospace & Communications Corporation
Western Development Laboratories
Palo Alto, California 94303

ABSTRACT

The first nickel-hydrogen battery for a long-life synchronous satellite application is being developed by Ford Aerospace & Communications Corporation under contract with INTELSAT. It is intended for possible incorporation into the later spacecraft in the INTELSAT V series. This new energy storage system promises to significantly extend spacecraft life expectancy while providing other benefits, including mass reduction and battery state-of-charge telemetry.

The characteristics and design of the INTELSAT V nickel-hydrogen battery are described and compared with those of the nickel-cadmium battery. Full compatibility with the spacecraft and interchangeability of the two battery systems are major design requirements. The background of the nickel-hydrogen technology is discussed, and a projection is made of the capabilities of future batteries using optimized cell designs.

INTRODUCTION

The INTELSAT V satellites are currently being built by Ford Aerospace & Communications Corporation under contract to the International Telecommunications Satellite Organization (INTELSAT). These active repeater communications satellites are designed for use in a synchronous equatorial orbit. A single satellite design provides INTELSAT communications requirements of the Atlantic, Pacific, and Indian Ocean regions. Communications frequency bands utilized by these satellites are 6/4 GHz and 14/11 GHz.

The fifth spacecraft in the INTELSAT V series is planned to be the first long-life synchronous operational satellite relying on the nickel-hydrogen ($Ni\text{-}H_2$) battery for energy storage. This advanced battery system is being developed by FACC under contract with INTELSAT to utilize the improvements and advantages this system has demonstrated on previous INTELSAT development programs. Upon successful completion of the qualification effort, the flight production phase is expected to provide $Ni\text{-}H_2$ batteries for all future INTELSAT V spacecraft.

The INTELSAT V $Ni\text{-}H_2$ battery has been designed to be completely interchangeable with the Ni-Cd system and to minimize impact on all other spacecraft systems. The constraints and the required design concepts are described in this paper. The electrical, thermal, and mechanical design considerations, as well as performance data, are discussed and a projection is made of the characteristics of optimized batteries using the same design principles.

SATELLITE POWER SUBSYSTEM DESCRIPTION

The INTELSAT V satellite, shown in Figure 1, is three-axis stabilized with a rectangular body measuring 1.65 x 2.01 x 1.77 meters. Solar array wings extend approximately 7.0 meters each side of the spacecraft.

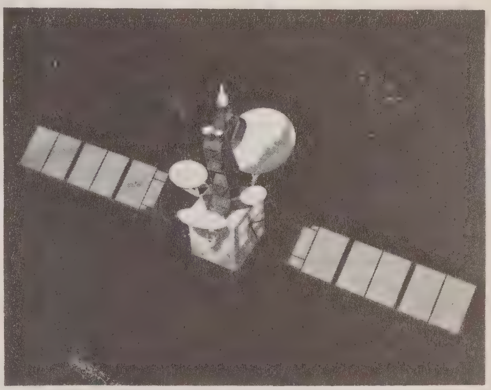

Figure 1. INTELSAT V Spacecraft

The power subsystem utilizes a single-axis tracking solar array as a primary power source with batteries for energy storage (1). One solar array wing and one battery are dedicated to each of two independent primary power buses. This power subsystem has been designed to provide continuous power to each satellite subsystem over a 7-year orbital lifetime. A direct energy transfer topology was selected for the INTELSAT V power subsystem to enhance system efficiency and minimize weight. The voltage of the two primary power buses during sunlight operation is limited by sequential linear partial shunt regulators. The primary bus voltages during solar eclipse are controlled by the battery voltages. The batteries are interfaced to their respective buses through redundant discharge diodes. DC/DC converters, integrated within using subsystems, are designed to accommodate the bus voltage range between sunlight and solar eclipse operation with margin. The major elements of the INTELSAT V electrical power subsystem (EPS) are interconnected as shown in Figure 2.

*This paper is based upon work performed under the sponsorship of the International Telecommunications Satellite Organization (INTELSAT). Views expressed are not necessarily those of INTELSAT.

Copyright by Ford Aerospace & Communications Corporation 1980.

Released to AIAA to publish in all forms.

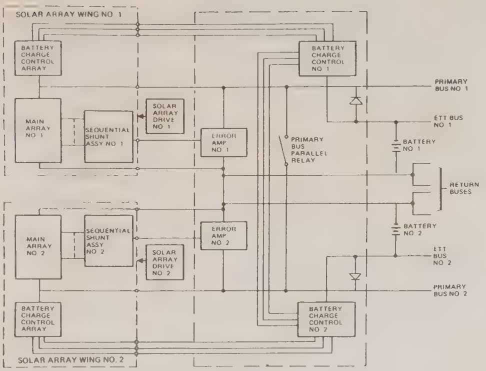

Figure 2. INTELSAT V Simplified Electric Power Subsystem Block Diagram

BATTERY TECHNOLOGY BACKGROUND

Nickel-cadmium (Ni-Cd) batteries have been the only type of energy storage device used to date in communications spacecraft. For long-term applications, however, Ni-Cd batteries have demonstrated certain limitations. In order to achieve the required lifetime the depth-of-discharge (DOD) must be controlled and careful thermal and recharge management is required. The known principal degradation modes are hydrolysis and oxidation of the nylon separation material, cadmium migration, and electrolyte redistribution. The first two degradation modes are primarily time and temperature dependent and thus can be partially retarded by proper thermal control. The electrode changes which cause electrolyte distribution problems appear to be primarily DOD dependent. Experience has shown that the Ni-Cd batteries can be a major life-limiting subsystem (2).

The $Ni\text{-}H_2$ battery system, under development since 1971 (3,4), is expected to provide continuous energy storage for orbital missions in excess of 10 years. $Ni\text{-}H_2$ cells have no cadmium electrodes and no nylon separators and therefore suffer no apparent time and temperature dependent degradation. The platinum catalyzed hydrogen electrodes undergo no significant changes with time or cycles. The fuel cell asbestos separator material is much more stable in KOH electrolyte than is nylon. Electrochemically impregnated nickel electrodes are being introduced into space use with the $Ni\text{-}H_2$ system. These electrodes permit higher active material utilization than do conventional vacuum-impregnated types, and thus can provide high performance with less active material, reducing electrode expansion and pore-size changes (5). This electrode stability, coupled with the high electrolyte affinity of the asbestos separator, strongly retards electrolyte distribution problems. Thus $Ni\text{-}H_2$ batteries are expected to have a considerably longer operational life than Ni-Cd batteries when used at the same DOD, and could operate at a higher DOD for similar life requirements. Additionally, the indifference to reversal of $Ni\text{-}H_2$ battery cells permits deep discharging without risk of permanent damage to the battery. Utilizing the deep-discharge capability of $Ni\text{-}H_2$ batteries, significant mass savings can be realized over equivalent Ni-Cd systems. A further potentially important feature is that the state of charge of a $Ni\text{-}H_2$ cell can be directly sensed through its internal pressure. This is a useful diagnostic and potential charge management tool.

The data obtained on $Ni\text{-}H_2$ cells have demonstrated excellent cycle life performance. Under high-rate, high-overcharge cycling at 60 percent DOD 6000 cycles were achieved, and at 80 percent DOD in excess of 4000 cycles at room temperature. Flight quality lightweight cells have demonstrated over 3 years of real-time cycling and over 4000 cycles at 60 percent DOD in continuing tests at COMSAT Laboratories.

Two flight demonstrations of the $Ni\text{-}H_2$ technology have been undertaken. The first (6,7), on the Navigation Technology Satellite 2 (NTS-2), involved a 35-Ah battery using 14 cells (8) provided by INTELSAT and built by Eagle-Picher Industries. The launch took place in June 1977 and the battery has performed very well to date (9). A 3-year-old NTS-2 prototype battery on test at FACC shows no degradation when compared to a new INTELSAT V Ni-Cd battery under identical conditions, as shown in Figure 3. The second flight experiment involved a battery built by Eagle-Picher for a U.S. Air Force/Lockheed spacecraft in low earth orbit and was reportedly quite successful (10). The successful flight experience and excellent laboratory performance prompted the current development of $Ni\text{-}H_2$ batteries for INTELSAT V.

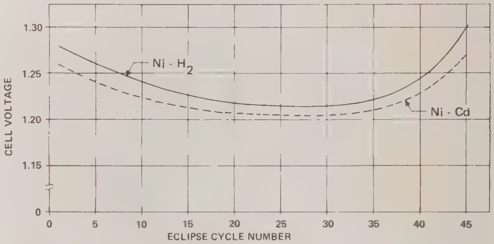

Figure 3. End-of-Discharge Voltages During Simulated Eclipse Season for 35- Ah $Ni\text{-}H_2$ and Ni-Cd Batteries

BATTERY DESIGN REQUIREMENTS

The batteries on the INTELSAT V spacecraft are required to supply power for spacecraft operation during solar eclipses and to support the electrothermal thruster (ETT) firings used for north-south stationkeeping, as well as other peak power demands. Eclipse requirements consist of 616 charge/discharge cycles over the 7-year spacecraft design life, with a discharge load of 480 watts per battery for up to 1.2 hours. ETT firings are estimated to occur approximately 175 times over the spacecraft life, with varying load and duration requirements.

The INTELSAT V spacecraft design incorporates electrical power (1) and thermal control subsystems compatible with the 34-Ah Ni-Cd battery which is the baseline energy storage system for early flights. The $Ni\text{-}H_2$ battery design was required to be compatible with these subsystems to maintain interchangeability of the two battery types and to minimize changes to the spacecraft. In addition, various spacecraft dimensional constraints must be accommodated. A further requirement is that incorporation of $Ni\text{-}H_2$ in place of Ni-Cd batteries must not upset spacecraft mass balance.

A principal consideration guiding $Ni\text{-}H_2$ battery design was that, where appropriate, existing technology should be applied with minimal changes in order to ensure successful performance of the flight hardware. The INTELSAT $Ni\text{-}H_2$ cell design was used with only minor changes since this design has the most extensive and successful orbital experience.

BATTERY DESIGN

The battery design developed in accordance with the above requirements is described in the following subsections. A summary of $Ni\text{-}H_2$ battery performance characteristics, along with those for the NiCd system, is given in Table 1. Figure 4 shows the Engineering Model $Ni\text{-}H_2$ battery.

Table 1. INTELSAT V $Ni\text{-}H_2$ and Ni-Cd Battery Performance Characteristics

Characteristics	$Ni\text{-}H_2$	Ni-Cd
ELECTRICAL		
Configuration (2 batteries/ spacecraft)	27 cells each	28 cells each
Nominal Battery Capacity	30 Ah	34 Ah
Maximum Depth of Discharge*		
Nominal, BOL	57%	49.5%
Nominal, EOL	60%	52.5%
Worst Case, EOL	64.5%	56.0%
Charge Rates, EOL		
Full	C/25	C/28
Intermediate	C/44	C/50
Trickle	C/73	C/83
Telemetry		
Battery Voltage	1	1
Battery Current	1	1
Cell Voltages	27	28
Cell Pressure/State-of-Charge	1	N/A
Battery Temperature	2	2
THERMAL		
Temperature Range	0 to 25°C	0 to 25°C
Qualification Range	-6 to 36°C	-6 to 36°C
Heater Power	28 W	28 W
Thermal Mass	1047 J/kg°C	940 J/kg°C
MECHANICAL		
Footprint	52x52 cm	47x34 cm
Height	22 cm	13 cm
BATTERY MASS	30.15 kg	32.50 kg
MASS BREAKDOWN		
Cells	24.03 kg	28.71 kg
Structural Hardware and Thermal Cover	4.23	2.02
Connectors, Heaters, Thermistors	0.13	0.13
Strain Gages and SGE	0.13	
Diode Assemblies	0.96	1.04
Wire, Epoxy and Miscellaneous	0.67	0.60

*EOL = End-of-Life; BOL = Beginning-of-Life

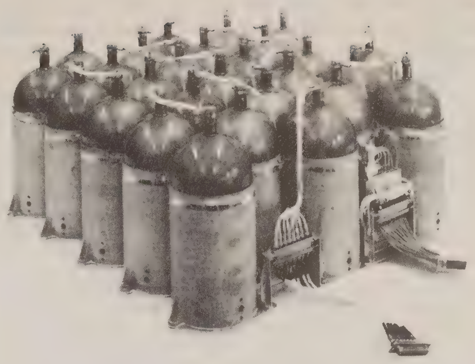

Figure 4. INTELSAT V $Ni\text{-}H_2$ Engineering Model Battery

Battery Cells

The $Ni\text{-}H_2$ cells for the INTELSAT V program are similar to the NTS-2 cells and are manufactured by Eagle-Picher Industries, Inc. of Joplin, Mo. The basic INTELSAT cell design is shown schematically in Figure 5. Each cell consists of a cylindrical pressure vessel with hemispherical end domes, a cylindrical stack of electrodes, and associated support hardware. Hydrogen gas pressure increases to approximately 38 atm (560 psi) during charge. The pressure is a near linear function of available capacity.

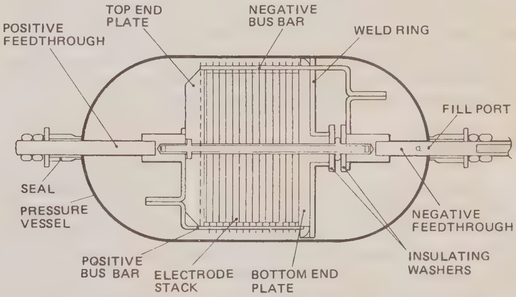

Figure 5. INTELSAT V $Ni\text{-}H_2$ Battery Cell Design Schematic

The cells are fabricated to the same quality standards as applied to INTELSAT V Ni-Cd cells. Areas receiving particular attention are the electrodes and the pressure vessel which undergo qualification testing for each lot. The pressure vessels are made of two hydroformed parts of age-hardened Inconel 718, typically 0.50 mm thick. These parts are electron-beam welded to an Inconel 718 weld ring which supports the electrode stack. Each domed end has a Ziegler plastic compression-type electrical feedthrough. Qualification testing on each pressure vessel lot includes coupon tensile tests on the material and burst and fatigue tests on complete vessels. One vessel is burst tested as fabricated; measured burst values range from 157 to 184 atm (2300 to 2700 psi). A second vessel is fatigue tested by subjecting it to 30,000 pressure cycles; subsequent burst pressures measure 177 to 225 atm (2600 to 3300 psi). All cells are subjected to a 68 atm (1000 psi) acceptance test, as well as helium leak tests prior to final closure and hydrogen leak tests after final closure.

The nickel electrodes are fabricated by electrochemical impregnation in Eagle-Picher's batch version of the process developed by Bell Laboratories. The electrodes are sampled frequently; chemical and electrochemical analyses are performed to verify proper active material loading level, absence of corrosion and excessive carbonate contamination, level of cobalt additive, capacity, and active material utilization. The hydrogen electrodes are fabricated by screening a platinum-teflon mixture onto a photo-etched, teflon-backed nickel substrate, followed by sintering. They are tested for proper platinum loading and polarization performance.

Following preliminary acceptance tests at the vendor, a series of tests performed at FACC characterizes cell voltages, capacity, and charge retention at 0, 10, and 20°C. This information is entered in a computer program which selects a group of cells with optimally matched characteristics for use in one battery.

Qualification of the cells includes several life tests. An accelerated test is underway on 25 Engineering Model cells, and is intended to demonstrate in less than 1 year the capacity delivery equivalent to more than 10 years of orbital operation. A second test consists of semi-accelerated eclipse cycling on one qualification battery. In this test, the solstice seasons will be reduced to 14 days. On the second qualification battery, a real-time synchronous orbit simulation will be performed.

Electrical Design

The battery charging electronics are designed to provide a maximum charge voltage compatible with a 28-cell Ni-Cd battery. Since Ni-H_2 cells exhibit somewhat higher (approximately 20 mV) charge voltages, a 27-cell Ni-H_2 battery is required to maintain charge voltage compatibility. Because the discharge voltage is also somewhat higher, the impact on the power system is minimal during all operational modes.

The Ni-H_2 battery capacity is rated at 30 Ah, while the actual capacity at 10°C is approximately 32 Ah. The rated DOD with a nominal average voltage of 1.25 volts per cell will be 57 percent. At end-of-life, the worst case average discharge voltage is assumed to be 1.18 volts per cell, leading to an estimated end-of-life DOD of 60 percent. With a one-cell open-circuit failure, this would increase to approximately 64.5 percent, which is well within the system's projected capability and INTELSAT's specified limit of 70 percent.

The battery design incorporates individual cell bypass circuitry to protect against an open-circuit failure. Other reliability features include cell interconnection by two parallel redundant wires and the connection between the ends of the cell series string and the battery power connector with four redundant wires.

A wide range of current levels is available for battery charging, but three primary rates, full, intermediate, and trickle, are planned for actual use. These average rates correspond to C/21, C/38, and C/63, respectively, at beginning-of-life, degrading to approximately C/25, C/44, and C/73 at end-of-life when sequenced on a 50 percent duty cycle.

The spacecraft system is designed to telemeter 28 cell voltages per battery. The voltage channel left vacant by the use of only 27 cells has been assigned to carry an amplified signal of a strain gage bridge which senses the pressure of one cell. A strain gage electronics package is an integral part of the battery and is discussed later.

Mechanical Design

In order to achieve complete interchangeability with the Ni-Cd battery, the INTELSAT V Ni-H_2 battery was required to be compatible with existing spacecraft dimensional constraints. In addition, it must withstand the anticipated launch environment while maintaining cell accelerations at acceptable levels. These requirements were to be met in the most mass- and cost-efficient manner and permit straightforward battery assembly operations.

The structural design satisfies these requirements. The basic feature of the design is the support of each battery cell in a cylindrical aluminum sleeve. These sleeves are arranged in a hexagonal close-packed pattern, as shown in Figure 4. This configuration reflects the dimensional constraints imposed by the spacecraft panel dimensions and the presence of an alignment hole in the panel, which must remain unobstructed.

A cylindrical cell mounting sleeve is clamped around each insulation covered cell. Diodes are installed on an integral bracket in the lower part of each sleeve. Twenty-seven sleeves are assembled in the hexagonal close-packed arrangement and attached to each other near their bases and top edges. These mechanical interconnections limit cell motion during launch and facilitate handling of the battery assembly. A baseplate, which primarily serves a thermal purpose, is riveted to the bottom of the sleeves.

The cell mounting sleeves are thermally and mechanically optimized structures, fabricated by investment casting of high-strength aluminum alloy. Successful, reproducible casting of this relatively complicated part, with a very thin wall, has been a significant factor in the achievement of a low-mass and cost-efficient structural design. The castings are made with universal mounting feet and other brackets and are machined to obtain the required sleeve configuration.

The structure was first proven by vibration tests of single cell/sleeve assemblies and of a full structural model of the battery using simulated cells. Both assemblies withstood the qualification level environment, including sine vibration at 20 g to 100 Hz, and at 5 g to 2000 Hz, as well as random vibration at 22.6 g (rms). The Engineering Model battery then verified the design at the same vibration levels without difficulty. Dimensional and mass properties data for the Ni-H_2 and Ni-Cd batteries are included in Table 1.

Thermal Design

The thermal design of the $Ni\text{-}H_2$ battery was subject to the same requirements applying to the Ni-Cd battery, and was required to maintain battery interchangeability. Design temperature limits are 0° and 25°C. Other battery design requirements were the minimization of heater usage and of radiative heat transfer to and from other spacecraft components. The thermal design objectives were to be achieved in the most mass- and cost-efficient manner possible.

The optical solar reflector (OSR) is sized for the Ni-Cd battery. Since no changes to the size or emittance of the OSR were allowed, a $Ni\text{-}H_2$ baseplate design was developed to conduct heat effectively from all cells to the OSR area. Local conductance of this plate is controlled by the presence or absence of lightening holes. With an optimized hole diameter and plate thickness, the baseplate gradient is predicted to be 3.1°C under worst-case trickle charge conditions.

Computer simulations of transient temperature performance of the $Ni\text{-}H_2$ battery have been performed during an eclipse cycle with 1.2 hour discharge. Figure 6 shows typical results indicating that the temperature range is well within the 0° to 25°C design requirement under typical operating conditions. One important temperature gradient is that between the cell electrode stack and the cell wall. The maximum gradient between these points should never exceed 9°C in order to avoid water loss from the stack by vapor transport. Computer simulations indicate a worst-case gradient of 2.5°C, which provides a significant safety margin.

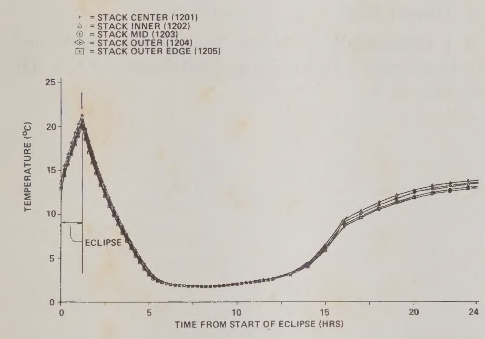

Figure 6. Simulated Eclipse Cycle Temperature Performance for the INTELSAT V $Ni\text{-}H_2$ Battery

An important feature of the thermal design is the low emittance treatment of the battery surface, which radiatively decouples the battery from other spacecraft components. A low-emittance ultra-lightweight shield is mounted over the exposed battery cell domes to provide an emittance of less than 0.1. The sides of the battery are wrapped with aluminized mylar.

In addition to the passive means of thermal control described above, charge control and heaters are used. Charge control may be utilized for high temperature thermal control, particularly at equinox and during ETT firing cycles. When the battery reaches full charge (concurrent with elevated battery temperature), the charge rate is decreased to the intermediate or trickle charge rate, reducing dissipation. At the low battery temperatures, the passive battery thermal control is augmented by 1-watt heaters on each cell. The heaters are thermostatically activated at +2°C and deactivated at +3°C. Thermistors are used to automatically control the heaters (ground command override is provided) and for battery temperature telemetry. Table 1 includes comparative thermal data for the $Ni\text{-}H_2$ and Ni-Cd batteries.

Pressure Monitoring

One cell in the battery has a strain gage bridge bonded on its pressure vessel. The bridge transmits a signal proportional to the internal cell pressure and, consequently, to the available cell capacity. Since the cells in a battery are well matched, this will provide a reasonable estimate of battery state-of-charge. In future batteries, the strain gage signal might be used as part of an automatic charge control system, but its current function is primarily to provide diagnostic information.

The bridge consists of four strain gages. Two are active and bonded directly to the pressure vessel; the other two are bonded to a small piece of Inconel 718 alloy mounted onto a silicone rubber pad on the vessel. The properties and thickness of the rubber are selected so that the gages are exposed to the vessel temperature, but not to the stress in the wall. The result is a bridge with excellent temperature compensation and high signal output.

Power for excitation of the bridge is derived from the battery terminals and conditioned in the Strain Gage Eletronics (SGE) Assembly mounted on the battery. The SGE also amplifies the bridge output to a value similar to a battery cell voltage for telemetry via the 28th cell-voltage channel. In addition to the power supply and amplification functions, the SGE provides adjustment for the zero-offset of the bridge and for the gain, so that nearly identical output vs capacity characteristics can be obtained on all batteries.

SAFETY CONSIDERATIONS

An important concern with the $Ni\text{-}H_2$ battery cells, as with all pressure vessels used on spacecraft, is the safety of personnel exposed to the pressurized equipment. The California Code requires a safety factor of 4:1 during personnel exposure and 2:1 at all other times. NASA requirements, including those for equipment onboard the Space Shuttle, specify a 2:1 safety factor.

In order to comply with these codes, modified procedures are being adopted to positively ensure the required safety margins. Batteries and cells are not to be handled in a charged condition, and a protective cover is used when a battery is being operated with personnel nearby. These procedures are used in spite of the demonstrated 4:1 safety factor. Further protection derives from leak and proof testing of all cells and leak testing of assembled batteries. Also, all ungrounded battery surfaces are conformal coated with polyurethane to protect against accidental shorting.

FUTURE NICKEL-HYDROGEN BATTERIES

The advantages of $Ni\text{-}H_2$ over Ni-Cd batteries in terms of life expectancy and long-term performance are generally accepted; however, the mass savings projected early in the development of the $Ni\text{-}H_2$ technology have not been fully realized and battery envelope volume, while usually not critical, is significantly larger than that of the Ni-Cd system. FACC has performed a critical analysis of the basic design approaches of $Ni\text{-}H_2$ cells and batteries, and certain areas with high potential for mass improvement have been identified. Consideration also is given to the impact of cell design on battery packaging weight. These improvements are projected to ultimately yield mass savings of approximately 11.5 kg for an INTELSAT V sized battery system which now weighs 60.3 kg. Increasing the DOD to the 70 percent level would yield an additional 3 kg savings. It can therefore be projectd that an advanced optimized $Ni\text{-}H_2$ battery system suitable for a 1 kW synchronous spacecraft would weigh about 46 kg. (The current best mass-optimized Ni-Cd battery system of this size is the INTELSAT V unit weighing 65 kg.) This design improvement could simultaneously yield a 50 percent reduction in battery envelope volume.

CONCLUSIONS

The INTELSAT V nickel-hydrogen program has demonstrated that a full sized battery can be built which meets all operational and environmental requirements for synchronous orbit communication spacecraft in general, and specifically for the INTELSAT V spacecraft. The $Ni\text{-}H_2$ battery achieves a higher life expectancy and a lower mass than the current INTELSAT V Ni-Cd battery. The $Ni\text{-}H_2$ battery potentially offers a convenient method for determining the battery state-of-charge using strain gages. The battery mechanical and thermal design concepts are readily adaptable to different capacity, voltage, and footprint requirements. Projected further improvements in mass (20 percent) and volume (50 percent) efficiency appear possible by using optimized cell designs.

REFERENCES

1. H. N. McKinney and D. C. Briggs, "Electrical Power Subsystem for the INTELSAT V Satellite," Proc. 13th Intersoc. Energy Conversion Engineering Conf., 1978, p. 47.

2. J. D. Dunlop, M. W. Earl, F. W. Weber, and D. B. Cooper, "INTELSAT IV Ni-Cd Battery Orbital Performance", Proc. 28th Power Sources Symposium, Atlantic City, N.J., 1978.

3. J. F. Stockel, G. Van Ommering, L. Swette, and L. Gaines, "A Nickel-Hydrogen Secondary Cell for Synchronous Orbit Application," Proc. 7th Intersoc. Energy Conversion Engineering Conf., 1972, p. 87.

4. J. Giner and J. D. Dunlop, J. Electrochem, Soc. *122,* 4 (1975).

5. G. Van Ommering and A. J. Appleby, Electrochemical Society Fall Meeeing, 1977, Extended Abstracts, Vol. 77-2, p. 117.

6. J. D. Dunlop, G. Van Ommering, and M. W. Earl, in "Power Sources 6," D. H. Collins, ed., London, Academic Press, 1977, p. 231.

7. F. Betz, J. F. Stockel, and A. Gaudet, "Nickel-Hydrogen Storage Battery for Use on Navigation Technology Satellite-2," Proc. 11th Intersoc. Energy Conversion Engineering Conf., 1976, p. 510.

8. G. Van Ommering and J. F. Stockel, "Characteristics of Nickel-Hydrogen Flight Cells," Proc. 27th Power Sources Symposium, Atlantic City, N.J., 1976, p. 124.

9. Personal communication, J. F. Stockel, COMSAT Laboratories, January 1980.

10. D. J. Smith and L. E. Miller, "Nickel-Hydrogen Battery Space Experiment," Air Force Technical Report AFAPL-TR-78-43, July 1978.